TRANSACTIONS

OF THE

AMERICAN INSTITUTE OF MINING AND METALLURGICAL ENGINEERS

(INCORPORATED

Volume 167

IRON AND STEEL DIVISION 1946

TECHNICAL PAPERS, DISCUSSIONS AND SYMPOSIA PRESENTED BEFORE THE DIVISION AT MEETINGS HELD AT CLEVELAND, OCTOBER 16-18, 1944, NEW YORK, OCTOBER 25-26, 1945, AND CHICAGO, FEBRUARY 25-28, 1946; ALSO THE HOWE LECTURE SCHEDULED FOR THE NEW YORK MEETING, FEBRUARY 1945, WHICH WAS CANCELED.

PUBLISHED BY THE INSTITUTE

AT THE OFFICE OF THE SECRETARY

29 WEST 39TH STREET

NEW YORK 18, N.Y.

Notice

This volume is the nineteenth of a series containing papers and discussions presented before the Iron and Steel Division of the American Institute of Mining and Metallurgical Engineers since its organization in 1928; one volume each year, as follows:

1928, Iron and Steel Technology in 1928 (later listed as Volume 80 of the Transactions); 1929 (vol. 84), 1930 (vol. 90), 1931 (vol. 95), 1932 (vol. 100), 1933, 1934, 1935, 1936, 1937, 1938, 1939, 1940, 1941, 1942, 1943, 1944, 1945 and 1946, Transactions of the American Institute of Mining and Metallurgical Engineers, Iron and Steel Division.

This volume contains papers and discussions presented at the meetings at Cleveland, Oct. 16–18, 1944; New York, Oct. 25–26, 1945 and Chicago, Feb. 25–28, 1946; also the Howe Lecture for the New York Meeting, February 19–22, 1945, which was canceled.

Papers on iron and steel subjects published by the Institute prior to 1928 are to be found in many volumes of the Transactions of the Institute; in Vols. 37 to 45, inclusive; 47, 50 and 51, 53, 56, 58, 62, 67 to 71, inclusive; 73 and 75. Vol. 67 was devoted exclusively to iron and steel.

Iron and steel papers published in the Transactions before the year 1936 may be found by consulting the general indexes to Vols. 1 to 35 (1871–1904), Vols. 36 to 55 (1905–1916), Vols. 56 to 72 (1917–1935), and Vols. 73 to 117 (1926–1935).

COPYRIGHT, 1947, BY THE

American Institute of Mining and Metallurgical Engineers (Incorporated)

PRINTED IN THE UNITED STATES OF AMERICA

Ent. Egin Driet 8-20-47 23043

FOREWORD

It is a privilege, as Chairman of the Iron and Steel Division, to preface this 167th volume of the Transactions A.I.M.E. and the 19th consecutive annual volume of the Division. The technical sessions and papers of the period covered by the volume were of high order, and the work of the various committees in the selection and preparation of material is highly commendable. In addition to this volume the National Open Hearth Steel Committee, Electric Furnace Steel Committee and the Blast Furnace and Raw Materials Committee each conducted independent programs and have published in separate volumes all papers and discussions pertinent thereto. These volumes are of particular value to those closely connected with the operation of steelmaking and preparation of materials.

During the past year the Division executive committee has been particularly grateful for the work of the Physical Chemistry of Steelmaking Committee under the chairmanship of T. S. Washburn; to the Division's Publications Committee, of which C. M. Loeb, Jr., was the Chairman; and to the Programs Committee, of which J. S. Marsh was the Chairman. The high degree of excellence of the papers presented and the wide scope of coverage bespeaks much commendation for their efforts and careful selection.

To comment particularly on the subject matter of this volume would require considerable space, but I cannot help but point to the very well chosen paper presented by Dr. T. L. Joseph as the 23rd Howe Memorial Lecture, on "The Blast-furnace Process and Means of Control." This is the first time that the blast-furnace process has served as the subject of the Howe Memorial Lecture, two other papers on pig iron having been previously presented. Dr. Joseph's work in blast-furnace and raw-materials research is outstanding, and the lecture herein contained does much to provide a clearer understanding and working knowledge of the blast-furnace process.

Although belonging to the previous year, this volume contains the 22nd Howe Memorial Lecture, by Marcus A. Grossmann, on "Toughness and Fracture of Hardened Steels," which marks an additional milestone in the somewhat slow progress toward an understanding of the reasons for the rather unpredictable property of steel known as "toughness."

W. E. Brewster, Chairman, Iron and Steel Division.

CHICAGO, ILLINOIS September 23, 1946

A.I.M.E. OFFICERS AND DIRECTORS

For the year ending February 1947

PRESIDENT AND DIRECTOR LOUIS S. CATES, New York, N. Y.

PAST PRESIDENTS AND DIRECTORS
CHESTER A. FULTON, Baltimore, Maryland
HARVEY S. MUDD, Los Angeles, Calif.

TREASURER AND DIRECTOR
ANDREW FLETCHER, New York, N. Y.

VICE-PRESIDENTS AND DIRECTORS

H. J. Brown, Boston, Mass. John L. Christie, Bridgeport, Conn. Erle V. Daveler, New York, N. Y. D. H. McLaughlin, New York, N. Y. Leo F. Reinartz, Middletown, Ohio J. R. Van Pelt, Jr., Columbus, Ohio

DIRECTORS

RAYMOND F. BAKER, New York, N. Y.
C. H. BENEDICT, Lake Linden, Mich.
W. E. BREWSTER, Chicago, Ill.
MILTON H. FIES, Birmingham, Ala.
J. C. KINNEAR, McGill, Nev.
A. B. KINZEL, New York, N. Y.
PHILIP KRAFT, New York, N. Y.
D. D. MOFFAT, Salt Lake City, Utah
W. E. WRATHER, Washington, D. C.

ROBERT H. MORRIS, Ansted, W. Va. J. C. NICHOLLS, Toronto, Ont., Canada RUSSELL B. PAUL, New York, N. Y. W. B. PLANK, Easton, Pa. JOHN R. SUMAN, HOUSTON, TEXAS ROBERT W. THOMAS, Ray, Ariz. CLYDE E. WEED, New York, N. Y. EUGENE A. WHITE, Tacoma, Wash.

DIVISION CHAIRMEN—Directors Ex-officiis

L. W. KEMPF (Institute of Metals), Cleveland, Ohio H. F. BEARDMORE (Petroleum), Tulsa, Okla. W. E. BREWSTER (Iron and Steel), Chicago, Ill. H. F. HEBLEY (Coal), Pittsburgh, Pa. J. R. CUDWORTH (Mineral Industry Education), Tuscaloosa, Ala. OLIVER C. RALSTON (Industrial Minerals), Washington, D. C.

SECRETARY
A. B. PARSONS, New York, N. Y.

STAFF IN NEW YORK

Assistant Secretaries EDWARD H. ROBIE E. J. KENNEDY, JR. E. O. KIRKENDALL WILLIAM H. STRANG Assistant Treasurer
H. A. MALONEY
Advertising Manager
"Mining and Metallurgy"
WHEELER SPACKMAN

CONTENTS

Foreword by W. E. Brewster. A.I.M.E. Officers and Directors. Iron and Steel Division Officers and Committees. Howe Lectures and Lecturers. Photograph of T. L. Joseph, Howe Lecturer 1946. Photograph of Marcus L. Grossmann, Howe Lecturer, 1945.	3 4 7 10 14 38
TECHNICAL PAPERS AND DISCUSSIONS	
Howe Lecture	
The Blast-furnace Process and Means of Control. By T. L. Joseph. (Metals Tech., April 1946,	
T.P. 2021). Toughness and Fracture of Hardened Steels. By Marcus A. Grossmann. (Metals Tech., April 1046, T.P. 2020)	15
1946, T.P. 2020)	39
Steelmaking	
A Radiation Pyrometer for Open-hearth Bath Measurements. By H. T. CLARK and S. FEIGEN-	0-
BAUM. (Metals Tech., June 1946, T.P. 2031)	
T.P. 2004). With discussion	93
By Theodore B. Winkler and John Chipman. (Metals Tech., April 1946, T.P. 1987). Sulphur Equilibria between Liquid Iron and Slags. By Nicholas J. Grant and John Chip-	111
MAN. (Metals Tech., April 1946, T.P. 1988). With discussion.	
Properties of Metals; Sponge Iron	-04
Anelasticity of Metals. By Clarence Zener. (Metals Tech., Aug. 1946, T.P. 1992). With	
discussion	
Elastic After-effects in Iron Wires from 20° to 550°C. By WILLIAM A. WEST. (Metals Tech.,	
Aug. 1946, T.P. 1993). With discussion	192
Tech., Feb. 1946, T. P. 1973)	
Grain-growth Inhibitors in Steel. By JAMES W. HALLEY. (Metals Tech., June 1946, T.P. 2030).	
With discussion	
The Low-temperature Gaseous Reduction of Magnetite Ore to Sponge Iron. By O. GEORGE	
Specht, Jr. and Carl A. Zapffe. (Metals Tech., June 1946, T.P. 1960). With discussion.	237
Stainless Steel and Iron-silicon Alloys	
A Test for Hydrogen Embrittlement and Its Application to 17 Per Cent Chromium, 1 Per cent	
Carbon Stainless-steel Wire. By CARL A. ZAPFFE and M. ELEANOR HASLEM. (Metals	
Tech., Jan. 1946, T.P. 1954). With discussion.	
A Precipitation-hardening Stainless Steel of the 18 Per Cent Chromium, 8 Per cent Nicke Type. By R. Smith, E. H. Wyche and W. W. Gorr. (Metals Tech., June 1946, T.P.	
2006). With discussion.	
Constitution of Commercial Low-carbon Iron-silicon Alloys. By R. L. RICKETT and N. C	
Fick. (Metals Tech., Feb. 1946, T.P. 1966). With discussion	
Ferrite, By C. G. Dunn. (Metals Tech. Aug. 1946, T.P. 1990). With discussion Some Aspects of Crystal Recovery in Silicon Ferrite Following Plastic Strains. By C. G.	357
Dunn (Metals Tech. Aug. 1946, T.P. 1991)	

	The Solubility of Hydrogen in Molten Iron-silicon Alloys. By Hung Liang, Michael B. Bever and Carl F. Floe. (Metals Tech., Feb. 1946, T.P. 1975). With discussion	
	Transformation of Austenite	
	Some Factors Affecting Edgewise Growth of Pearlite. By W. H. Brandt. (Metals Tech., Dec.	
	1945, T.P. 1857). With discussion	405
	Anisothermal Decomposition of Austenite. By J. H. Hollomon, L. D. Jaffe and M. R. Nor-	403
	TON. (Metals Tech., Aug. 1946, T.P. 2008). With discussion.	410
	Relationship between Transformation at Constant Temperature and Transformation during	4-9
	Cooling. By G. K. Manning and C. H. Lorig. (Metals Tech., June 1946, T.P. 2014). With	
	discussion	442
1	The Temperature Range of Martensite Formation. By R. A. GRANGE and H. M. STEWART	
	(Metals Tech., June 1946, T.P. 1996). With discussion	467
1	Hardenability Effects in Relation to the Percentage of Martensite. By J. M. HODGE and M. A.	
	OREHOSKI. (Metals Tech., April 1946, T.P. 1994). With discussion	502
	Equilibrium Relations in Medium-alloy Steels. By Clarence Zener. (Metals Tech., Jan.	
	1946, T.P. 1856). With discussion	513
	Phase Boundaries in Medium-alloy Steels. By W. A. West. (Metals Tech., Jan. 1946, T.P.	
	1924). With discussion	535
	Kinetics of the Decomposition of Austenite. By Clarence Zener. (Metals Tech., Jan. 1946,	
	T.P. 1925). With discussion	550
	SYMPOSIA	
	Symposium on Hardenability	
	Introduction. By M. A. GROSSMANN	599
	The Hardenability Concept. By JOHN H. HOLLOMON and L. D. JAFFE. (Metals Tech., Jan.	
	1946, T.P. 1926). With discussion	601
	Hardenability and Quench Cracking. By L. D. JAFFE and JOHN H. HOLLOMON. (Metals	
		617
	Relationship between Hardenability and Percentage of Martensite in Some Low-Alloy	
	Steels. By J. M. Hodge and M. A. Orehoski. (Metals Tech., Sept. 1945, T.P. 1800).	
	With discussion.	627
	Determination of Most Efficient Alloy Combinations for Hardenability. By H. E.	
	HOSTETTER. (Metals Tech., Sept. 1945, T.P. 1905). With discussion.	043
	An Appraisal of the Factor Method for Calculating the Hardenability of Steel from Com-	
	position. By G. R. Brophy and A. J. MILLER. (Metals Tech., Oct. 1945, T.P. 1933).	
	With discussion	054
	J. GARDNER BROOKS. (Metals Tech., June 1946, T.P. 2029). With discussion	670
	Addition Method for Calculating Rockwell C Hardness of the Jominy Hardenability	0,0
	Test. By Walter Crafts and John L. Lamont. (Metals Tech., Oct. 1945, T. P. 1928)	
	With discussion	
	The Influence of Titanium on the Hardenability of Steel. By G. F. Comstock. (Metals	
	Tech., Sept. 1945, T.P. 1904). With discussion	719
	Symposium on Hot-working	
	A Laboratory Evaluation of the Hot-working Characteristics of Metals. By C. L. CLARK	
	and J. Russ. (Metals Tech., Dec. 1945. T.P. 1839)	736
	Effect of Various Elements on the Hot-workability of Steel. By HARRY K. IHRIG. (Metals	
	Tech., Oct. 1945, T.P. 1932)	749
	Discussion	777
	Contents Volume 166, Institute of Metals Division, 1946	791
	Index	793

IRON AND STEEL DIVISION

Established as a Division February 22, 1928 (By-laws printed in the 1939 Transactions Volume of the Division)

Officers and Committees for Year ending February 1947

W. E. Brewster, Chairman, Chicago, Ill.
E. G. Hill, Past Chairman, Wheeling, W. Va.
P. F. Dolan, Vice Chairman, Sparrows Point, Md.
C. D. King, Vice Chairman, Pittsburgh, Pa.
GILBERT SOLER, Vice Chairman, Canton, Ohio
Ernest Kirkendall, Secretary, 29 West 39th Street, New York 18, N. Y.

Past Chairmen

	Past Chairmen	
RALPH H. SWEETSER, 1928 G. B. WATERHOUSE, 1929 W. J. MACKENZIE, 1930 F. M. BECKET, 1931 F. N. SPELLER, 1932 JOHN JOHNSTON, 1933	L. F. REINARTZ, 1934 A. B. KINZEL, 1935 C. E. WILLIAMS, 1936 FRANCIS B. FOLEY, 1937 J. T. MACKENZIE, 1938	J. Hunter Nead, 1939 Frank T. Sisco, 1940 C. H. Herty, Jr., 1941 E. C. Smith, 1942 H. W. Graham, 1943 W. A. Haven, 1944 Erle G. Hill, 1945

Executive Committee

	Discoult o Committee	
Until 1947	Until 1948	Until 1949
G. R. BROPHY	K. L. FETTERS	M. GENSAMER
H. J. FORSYTH	J. S. Marsh	H. E. PHELPS
A. P. MILLER	C. E. SIMS	H. K. WORK

Blast Furnace and Raw Materials

A. J. BOYNTON, Chairman

T. B. COUNSELMAN, Vice Chairman	
B. W. NORTON, Vice Chairman	
T. F. PLIMPTON, Secretary	
H. W. JOHNSON	I. C. MURRAY
T. L. JOSEPH	L. F. SATTELE
C. D. KING	I. H. SLATER
C. H. LENHART	G. E. STEUDEL
R. A. LINDGREN	H. A. STRAIN
H. E. McDonnell	B. M. STUBBLEFIELD
an an areas variables	C. L. WYMAN

Open Hearth Steel

A. P. MILLER, Chairman,
L. F. REINARTZ, Past Chairman
E. L. RAMSEY, Vice Chairman
FRANK T. SISCO, Secretary-Treasurer
H. M. GRIFFITH
W. C. KITTO
L. A. LAMBING
A. E. REINHARD

Francis L. Toy G. L. VonPlanck D. N. Watkins T. T. Watson W. H. Yeckley

W. E. Brewster P. F. Dolan P. G. Harrison

W. A. HAVEN G. W. HEWITT C. F. HOFFMAN

Bessemer Steel

H. C. DUNKLE G. M. YOCOM
K. L. FETTERS

H. W. GRAHAM F. L. Toy

Electric Furnace Steel

Executive Committee
C. W. BRIGGS, Chairman
H. W. McQuaid, Past Chairman
FRANK T. Sisco, Secretary
H. E. Phelps
W. J. Reagan
C. A. Scharschu

H. A. SCHWARTZ GILBERT SOLER E. A. WALCHER

A. L. FEILD JOHN JUPPENLATZ T. J. McLOUGHLIN

Conference Committee
W. J. REAGAN, Chairman
J. B. CAINE, Vice Chairman
R. C. GOOD
R. K. KULP

F. B. RIGGAN
C. E. SIMS
C. C. SPENCER
N. I. STOTZ
A. C. TEXTER

SAMUEL ARNOLD III
R. E. BIRCH
W. M. FARNSWORTH
R. H. FRANK
S. D. GLADDING

Physical Chemistry of Steelmaking

G. A. LILLIEQVIST CHARLES LOCKE

B. M. Larsen, Chairman W. O. Philbrook, Secretary J. J. Golden T. L. Joseph L. A. Lambing J. S. Marsh Shadburn Marshall

D. L. McBride
C. E. Sims
Gilbert Soler
C. R. Taylor
Michael Tenenbaum
T. S. Washburn

H. B. EMERICK K. L. FETTERS C. R. FITTERER A. G. FORREST

M. B. BEVER

JOHN CHIPMAN

Metallography and Heat Treatment

F. M. Walters, Jr., Chairman M. Gensamer J. T. Norton Howard Scott

G. V. SMITH G. A. TIMMONS CYRIL WELLS

WALTER CRAFTS J. T. EASH SAMUEL EPSTEIN

Membership

NORMAN F. TISDALE, Chairman H. E. JOHNSON C. L. LABEKA J. C. MURRAY W. E. REMMERS

C. E. SIMS J. M. STAPLETON M. J. UDY S. P. WATKINS

R. H. ABORN

O. E. CLARK P. F. DOLAN J. W. HALLEY J. E. JACOBS

Mining and Metallurgy A. B. Kinzel, Chairman

T. S. FULLER

J. H. HALL

Howe Memorial Lecture W. E. Brewster, Chairman C. H. Herty, Jr. J. T. MacKenzie

E. C. SMITH

Robert W. Hunt Medal and Prize W. E. Brewster, Chairman J. H. Nead H. A. Strain

H. K. WORK

K. C. McCutcheon

C. G. HOGBERG

J. E. Johnson, Jr. Award Carl F. Hoffman, Chairman T. L. Joseph L. F. Sattele

J. M. STAPLETON

Programs

J. S. Marsh, Chairman W. O. Philbrook Gilbert Soler

MICHAEL TENENBAUM F. L. TOY F. M. WALTERS, JR.

Publications

F. B. FOLEY, Chairman G. R. BROPHY

R. K. KULP B. M. LARSEN

Nominating

E. G. HILL, Chairman W. A. HAVEN FRANK T. SISCO

E. C. SMITH

H. W. GRAHAM

J. B. AUSTIN

GERHARD DERGE

R. J. Allen Janet Z. Briggs

H. B. EMERICK

The Howe Memorial Lecture

The Howe Memorial Lecture was authorized in April 1923, in memory of Henry Marion Howe, as an annual address to be delivered by invitation under the auspices of the Institute by an individual of recognized and outstanding attainment in the science and practice of iron and steel metallurgy or metallography, chosen by the Board of Directors upon recommendation of the Iron and Steel Division.

So far, only American metallurgists have been invited to deliver the Howe lecture. It is believed that this lecture would gain in importance and significance were it possible to include metallurgists from other countries, but the Institute has not yet been able to do this on account of lack of special funds to support this lectureship.

The titles of the lectures and the lecturers are as follows:

- 1924 What is Steel? By Albert Sauveur.
- 1925 Austenite and Austenitic Steels. By John A. Mathews.
- 1926 Twenty-five Years of Metallography. By William Campbell.
- 1927 Alloy Steels. By Bradley Stoughton.
- 1928 Significance of the Simple Steel Analysis. By Henry D. Hibbard.
- 1929 Studies of Hadfield's Manganese Steel with the High-power Microscope. By John Howe Hall.
- 1930 The Future of the American Iron and Steel Industry. By Zay Jeffries.
- 1931 On the Art of Metallography. By Francis F. Lucas.
- 1932 On the Rates of Reactions in Solid Steel. By Edgar C. Bain.
- 1933 Steelmaking Processes. By George B. Waterhouse.
- 1934 The Corrosion Problem with Respect to Iron and Steel. By Frank N. Speller.
- 1935 Problems of Steel Melting. By E. C. Smith.
- 1036 Correlation between Metallography and Mechanical Testing. By H. F. Moore.
- 1937 Progress in Improvement of Cast Iron and Use of Alloys in Iron. By Paul D. Merica.
- 1938 On the Allotropy of Stainless Steels. By Frederick Mark Becket.
- 1939 Some Things We Don't Know about the Creep of Metals. By H. W. Gillett.
- 1940 Slag Control. By C. H. Herty, Jr.
- 1941 Some Complexities of Impact Strength. By Alfred V. de Forest.
- 1942 Time as a Factor in the Making and Treating of Steel. By John Johnston.
- 1943 The Development of Research and Quality Control in the Modern Steel Plant. By
 Leo F. Reinartz.
- 1944 Gray Iron-Steel Plus Graphite. By J. T. MacKenzie.
- 1945 Toughness and Fracture of Hardened Steels. By Marcus A. Grossmann.
- 1946 The Blast-furnace Process and Means of Control. By T. L. Joseph.

TECHNICAL PAPERS AND DISCUSSIONS



T. L. JOSEPH

Henry Marion Howe Memorial Lecturer, 1946

The Blast-furnace Process and Means of Control

By T. L. JOSEPH,* MEMBER A.I.M.E. (Henry Marion Howe Memorial Lecturet)

It is a distinct privilege to participate in this meeting convened to honor the memory of Henry Marion Howe, a distinguished scientist and metallurgist. Many have added to our rapidly growing fund of metallurgical knowledge but few have made the unique contribution of formulating basic concepts essential to an over-all comprehensive view of the subject of metallography.

Of those previously selected to deliver this lecture, several have added a personal touch to their discourse because they were able to refer to their associations with Dr. Howe. It was not my good fortune to know him or to enjoy his inspiring influence. Like most of you, my contact has been with his published works, which are outstanding in that they provide lucid, detailed expositions of the nature and behavior of metals and alloys. His deep understanding and clarity of expression have greatly accelerated our progress in metallography and in the use of metals.

The degree to which a man's thinking, experimentation and writing contribute toward an understanding of basic laws and phenomena determines whether his life's work is of transitory or permanent value. This occasion appropriately recognizes the fundamental importance of Dr. Howe's pioneer work in the field of metallurgy.

On two former occasions, gray iron was selected as a subject for discussion. The fact

that the production of pig iron has not been discussed before does not reflect any lack of interest on the part of Dr. Howe or former lecturers in the process that underlies the production of steel.

Although Dr. Howe's work in his later years centered around metallography, his earlier publications show a considerable interest in the production of iron and steel. He recognized that in the ascending spiral of metallurgical advancement we are not winding a single thread but are weaving a complex fabric.

Specific evidence of his interest in the production of pig iron may be found in his book on The Metallography of Cast Iron and Steel. In explaining why blast furnaces have been in constant use for about 600 years, he says: "The process is economical because it utilizes with extraordinary completeness the calorific power of the coke due to the thorough transfer of heat from the gaseous products of combustion to the charge." This emphasis on heat transfer, overlooked in many more extended and more recent discussions of the blast-furnace process, illustrates Professor Howe's ability to see the essentials. Other distinct advantages of the blast furnace, such as the removal of much of the sulphur and practically all of the oxygen, were mentioned. It was also stated that although the blastfurnace process is complex in nature, its outward form is comparatively simple, thus permitting large-scale production at small labor costs. All who contemplate the production of metallic iron from its ores by any other process might well consider the

Manuscript received at the office of the Institute March 14, 1946. Issued as T.P. 2021 in METALS TECHNOLOGY, April 1946.

Professor of Metallurgy, Minnesota School of Mines and Metallurgy, Minneapolis, Minnesota.

[†] Presented at the Chicago Meeting, February 1946. Twenty-third Annual Lecture.

¹ References are at the end of the paper.

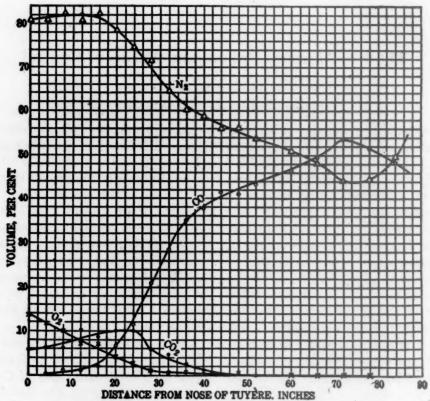


Fig. 1.—Tuyere-gas analyses: average of results from thirteen furnaces (Kinney2).

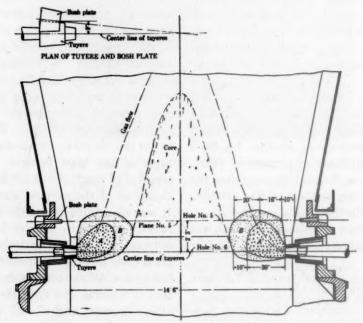


FIG. 2.—COMBUSTION ZONES AND INACTIVE CENTRAL CORE (Kinney2).

advantages of the blast furnace emphasized by Dr. Howe.

POSTWAR SHIFTS IN EMPHASIS

During the war, the output of pig iron was of paramount interest while fuel economy, uniformity of operation, and close control of the process were of secondary importance. In the postwar period, there will be a shift of emphasis toward closer control over practice and toward more efficient operation. This will be a natural result of a more competitive market for steel. Output per unit will not, however, be neglected, because large furnaces offer economiès in reduced costs above raw materials. The fact that unit capacity has been more than doubled in the last 25 years is good evidence that large furnaces offer definite advantages. These advantages have not, however, come in the form of fuel economy, and there is some question as to whether somewhat better control over large units is due entirely to an increase in furnace size or partly to the combined effects of a quarter of a century's progress in several directions.

BASIC FEATURES OF SMELTING PROCESS

An examination of some of the basic features of the smelting process and some of the major difficulties probably is the best means of determining how we can improve furnace practice. Operators are doing a remarkable job in furnace control, considering the difficulties inherent in the raw materials and some features of furnace practice. They could, however, do a much better job in controlling the composition of the iron if more attention were given to the size preparations of raw materials, particularly the ore.

The major obstacles to greater efficiency and closer control center around the problem of obtaining a more ideal counterflow of gases and solids. Because it is possible to achieve a fair degree of control by maintaining a certain pattern of gas flow does not mean that this is a correct pattern or that we are taking full advantage of the principle of counterflow. The problem

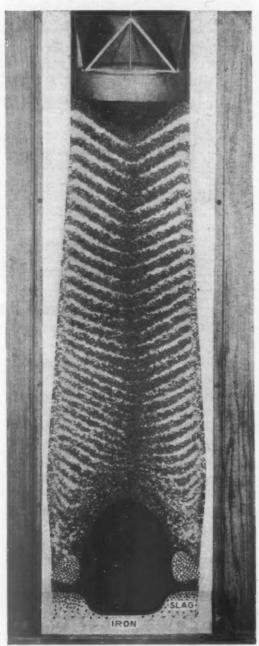


FIG. 3.—ARRANGEMENT OF MATERIALS IN FURNACE MODEL.

is difficult to resolve because there is considerable conjecture in any attempt to get a picture of conditions inside the furnace.

Ample evidence is available, however, to show that conditions are far from ideal. The work of Kinney² for the Bureau of Mines has provided pertinent information readily through the central area at the tuyere level but tend to follow the periphery of the bosh. The inevitable result is a much lower temperature in a relatively inactive

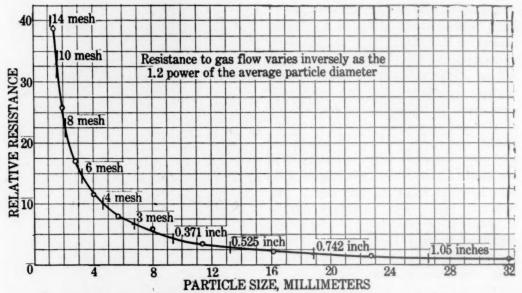


FIG. 4.—RELATION BETWEEN PARTICLE SIZE AND RESISTANCE TO FLOW OF GASES.

on the extent of the combustion zones and also in conditions in the shaft.

As a result of this work, it is now generally recognized that combustion is confined to rather small zones adjacent to the tuyeres.

Tuyere-gas analyses of Kinney,2 reproduced in Fig. 1, show that under average conditions the oxygen content drops immediately from 21 per cent to about 14 per cent, and then decreases gradually to about 1 per cent at 30 in. from the nose of the tuyere. Beyond 50 in. the gas is composed largely of CO and N2, showing that combustion is confined to small areas. Attention is called to the fact that toward the center of the furnace the carbon monoxide increases to about 50 per cent whereas the nitrogen undergoes a large drop, from about 80 per cent to less than 50 per cent. This dilution of nitrogen by carbon monoxide formed with oxygen from the charge shows clearly that the gases from the small combustion zones do not flow central core (Fig. 2). Although no combustion can occur beyond about 50 in. from the tuyeres, we do not know how sharply the temperature or the effectiveness for smelting decreases toward the center. It seems quite clear, however, that the modern 27-ft. hearth has a relatively large inactive core at the tuyere level and probably is more active along the periphery of the entire furnace.

ARRANGEMENT OF MATERIAL IN FURNACE

Although we have no precise information, the general arrangement of the material inside the furnace is believed to be similar to that shown in Fig. 3, which is a picture of a half-section model. In producing the layered arrangement shown, the model was first filled with coke, which was then removed through six areas corresponding with the pear-shaped combustion zones, in which substantially all of the heat and reducing power for the process are released.

As the material was removed, charges were dumped from the bell to maintain a constant level of the stock. For purposes of reproduction, limestone was used to The layers of comparatively finely divided ore are thickest at the walls and taper to a point short of the center. Conversely, the coke layers are thinnest at the walls

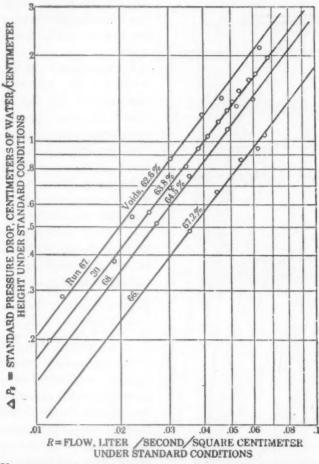


Fig. 5.—Variation of pressure drop with degree of packing (Furnas7).

simulate ore charges between the dark layers of coke.

It is not likely that the layered arrangement is preserved in the lower part of furnaces to the degree shown in this model. Mixing of layers probably occurs in the lower part of the shaft. However, the strong tendency for the layered arrangement to persist in the model leaves some doubt as to where mixing begins. In the upper part of the furnace, the materials assume the general arrangement shown in the model, which affords an insight into the distribution according to particle size.

and thickest near the center. This particular arrangement of the layers is due to the difference in particle size and the resulting angle of repose. The position assumed by the ore and the distance it extends toward the center will depend upon its volume and angle of repose. For the ore layers, the angle of repose will average about 34° compared with 27½° for the coke. This difference in the angle of repose of ore and coke has a pronounced effect upon the particle size distribution and the relative permeability of the stock column. Although the high permeability of the central area

is largely due to the absence of ore, large pieces of all raw material tend to roll to this part of the furnace.

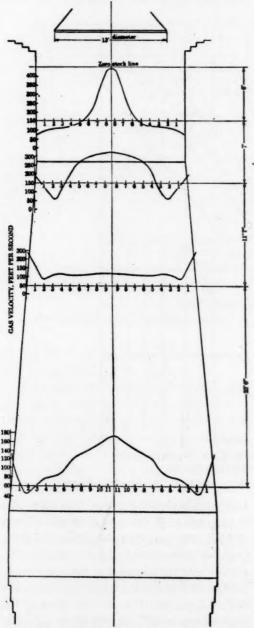


Fig. 6.—Gas velocity at various planes (Kinney8).

As long as the materials exist as separate and distinct layers, large pieces of coke free from fines will promote permeability in the central area and throughout the coke layers. Since the coke occupies about 60 per cent of the volume, more permeable coke layers will reduce the pressure drop through the furnace and hence promote smooth operation. When mixing of ore and coke occurs, the beneficial effects of properly sized coke are lost, as will be brought out later (Fig. 20).

Comparatively thick ore layers and relatively thin coke layers suggest high resistance to gas flow next to the walls. This is not true, however, because the furnace batter and a somewhat faster travel of stock result in a loose packing of the charge and high gas velocities next to the inwall. With present raw materials, uniform gas flow is impossible. All we can hope for is a workable distribution to fit existing raw materials. A current job of all operators is to maintain at all times a proper balance between the gas moving up the center and along the walls.

PATTERNS OF GAS DISTRIBUTION INHERENT TO PRESENT RAW MATERIALS AND CHARGING METHODS

The path of the gas stream above the tuyeres is determined by the relative resistance of the charge in various parts of the furnace. Particle size and the degree of packing are predominantly important in determining the resistance to gas flow. When the size of particle falls below 3/2 in., the resistance increases rapidly, as shown in Fig. 4. Since the central portion of the charge contains little ore and large pieces of coke and stone, the inevitable result is an open, permeable center. In sharp contrast with this condition, the ore layers that are relatively thick next to the walls contain material predominantly smaller than 36 in. Were it not for the looser packing of the stock next to the walls, the resistance to gas flow would be high. However, as may be seen in Fig. 5, the resistance to gas flow changes sharply with variation in voids. The lower line represents an increase in voids of only 4.6 per cent but the resistance

to gas flow as measured by the pressure drop through the bed is reduced to about one-half. With R equal to 0.03, the pressure drop falls from over 0.8 to about 0.4. This seems incredible unless we keep in mind that only 10 to 15 per cent of the total cross-sectional area is effective for gas flow. An increase of only 4.6 per cent voids may accordingly produce a large change in the resistance to gas flow.

Although work on experimental furnaces had indicated wide variations in the velocity of the gas moving through various parts of the charge, it was not until Kinney's surveys of industrial furnaces became available that we knew with certainty that the radial distribution of the gases in the upper shaft is far from uniform. Variations in gas velocities across four planes are shown in Fig. 6. In the straight section near the stock line, where the ore layers are not subjected to the loosening effect of inwall batter, the velocities are very high in the center, with no wall effect. The effect of the large coke particles and the absence of small ore in the center is reflected in a central velocity of 480 ft. per sec. compared with 80 ft. at the wall. This observed variation in gas velocity indicates an average particle size of about 0.5 in. near the walls and 4.5 in. in the center of the furnace.

Across a plane just below the straight section where the inwall batter is 1 in. per foot, there is a pronounced wall effect. The gas velocity at this level is comparatively high at the walls and reaches a low of about 50 ft. per sec. some 30 in. from the inwall. In the area beyond about 3 ft. from the wall, the thick ore layers are not subjected to the loosening effect of the batter.

This effect of inwall batter may become so pronounced as to produce a periphery with less resistance than the center of the furnace. Under these conditions the highest gas velocities would be at the wall, with a gradual reduction toward the center. Areas of high gas velocity are at relatively high temperatures, particularly in the

center of the furnace, where the heat capacity of the stock is low because coke weighs only about 30 lb. per cu. ft. In this par-

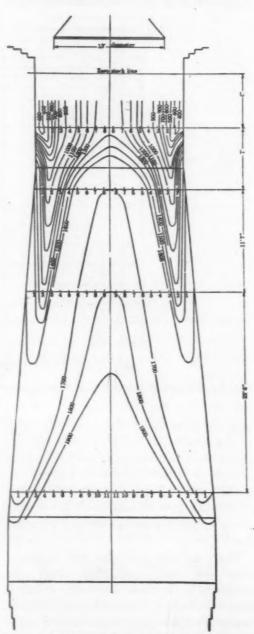


Fig. 7.—Isotherms in blast-furnace shaft (Kinney⁸).

ticular case, the temperature was as high in the center of the furnace, 6 ft. below the stock line, as it was 2 ft. from the inwall at a level about 10 ft. above the mantle. In the regions of excessive gas flow the transfer of heat is not efficient because the temperature of the stock is relatively high, to the point where it will settle regularly without some innovation such as high-top pressure. It would not, in other words, be feasible to operate the furnace if the ore

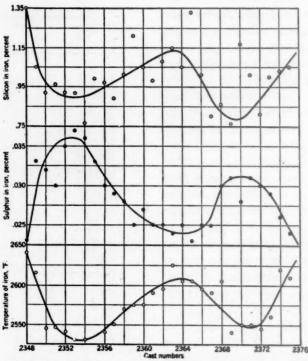


Fig. 8.—Relation between silicon and sulphur and the temperature of consecutive casts.

thus reducing the temperature differential or the driving force for heat transfer between the gas phase and the solid phase. Just as it is not possible to capture the sensible heat of the gases by the charge, there is also poor utilization of the reducing power of the gas in the areas of high gas flow.

These differences in gas flow, temperature, and gas composition from the periphery to the center may vary in degree from one furnace to another but irregularities are always present when fine ore is used. The use of good metallurgical coke modifies these conditions but does not eliminate them. At normal rates of blowing with fine-ore charges, areas of high gas flow must be established in some parts of the charge to reduce the pressure drop through the stock

layers were of uniform thickness across the furnace because the pressure drop through the stock would reach the point where the stock would not settle. However, the necessity of having areas of high permeability creates a problem in maintaining a proper balance between the flow of gas along the walls and up through the center.

GREATER PERMEABILITY NEEDED IN AREA BETWEEN WALLS AND CENTER

What seems to be needed is an effective means for opening up the area between the walls and the open center. Because of restricted gas flow, the temperature in this part of the furnace is relatively low, as indicated by the isotherms in Fig. 7. In other words, the area of low gas flow and low temperatures, as shown by the V-shaped dips in the isotherms, is not being used effectively. The solution to the probTEMPERATURE VARIATIONS IN SHAFT INFLUENCE HEARTH TEMPERATURES

Normally the hot blast is uniformly distributed to the various tuyeres so that the

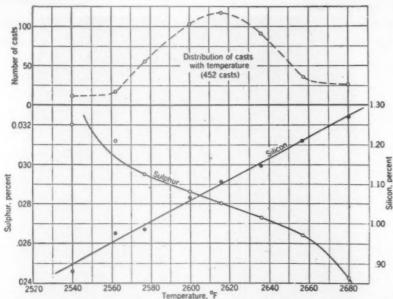


Fig. 9.—Average relation between temperature of pig ipon and silicon and sulphur.

lem requires an increase in the relative permeability of the area between the periphery and the center. This can be accomplished most effectively by size preparation of the ore charge, which would eliminate the great disparity in this size of the ore and the coke. Aside from the problem of increasing the efficiency by utilizing the shaft more effectively, such a change would make it much easier to maintain smooth operation and closer control over the analysis of the iron.

An excess of gas along the periphery carries off a large amount of dust, raises the temperature of the inwall and thus increases the heat losses from the shaft and the wear on the lining. Although a large excess of gas through the center may relieve dust losses and lining wear, and permit more uniform peripheral distribution of the gas, it results in a loss of efficiency, because there is little ore in this part of the furnace to absorb heat and to utilize the reducing power of the gases.

heat of combustion is uniformly liberated. However, the amount of heat carried back to the crucible depends upon a balanced flow of gas. With efficient heat transfer, less heat is lost in the top gas and the charge carries more heat to the hearth. A balanced gas flow also results in less gasification of carbon above the tuyeres, which has a direct bearing upon hearth temperatures and iron analysis. Sudden changes in the pattern of gas flow accordingly may result in wide fluctuations in hearth temperature and in iron analysis.

IRON ANALYSIS VARIES WITH TEMPERATURE

Careful measurements show that temperature exerts a predominating influence upon the reduction of silica and desulphurization. A drop in the temperature of the iron means a drop in silicon and a rise in sulphur as shown by variations from cast to cast in Fig. 8, and by average data in Fig. 9. It is difficult to control iron analysis

because it is difficult to control shaft temperatures and in turn hearth temperatures. A number of expedients are available for changing the pattern of gas flow but the small ore charges would widen the area containing nothing except large pieces of coke, and thus permit more gas to flow through the center of the furnace. Another

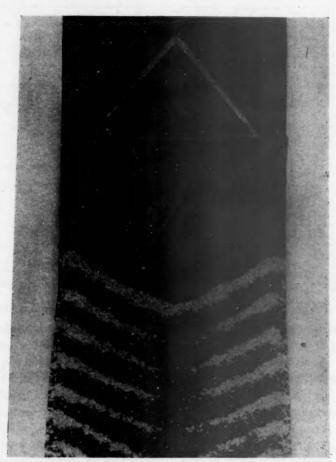


FIG. 10.—POSITIONS OF LARGE ORE CHARGE AND CHARGES OF NORMAL SIZE.

operator is always at a loss to know conditions as they exist.

MEANS FOR CONTROLLING GAS FLOW

Large ore charges that extend all across the furnace at the stock level introduce more resistance to gas flow in the central portion and thus divert more gas to the walls. Periodic use of these large charges, shown in Fig. 10, furnishes one means of controlling the radial distribution of the gases or a properly balanced flow in the center and along the walls. Conversely,

expedient for increasing the flow in the central area is to increase the resistance at the walls by lowering the stock line. As indicated in Fig. 11, the ore layers formed when the stock line is low are unusually thick next to the walls and act to blanket the flow of gases through this area. Other factors—speed of bell drop, bell clearance, and the arrangement of stock on the large bell—affect the radial distribution of the stock and in turn the path of the gas. Ore charges that do not move off the large bell readily and uniformly are deposited unevenly, as shown in Fig. 12. In this case,

the charge was finely divided and stuck to one side of the bell.

PARTIALLY FLUIDIZED STOCK AND CHANNELING

The securing of a properly balanced gas flow is complicated by the fact that tendency of smaller particles to lift. However, when the flow exceeded this rate, fine particles were lifted and danced in the gas stream, resulting in a sharp decrease in the pressure drop through the bed. Experimental points fall below an extension of the curve that shows the relation



FIG. 11.—THICKER ORE CHARGES NEXT TO WALL AS RESULT OF LOW STOCK LINE.

inequalities are self-aggravating, particularly at high blowing rates. The energy of the gas stream tends to lift small particles and to keep them in suspension between larger particles, which act to some extent as a retaining screen. As shown in Fig. 13, the pressure drop through the bed decreases sharply once this lifting velocity is reached. At rates of flow up to 0.03 liters per sec. per sq. cm., the bed was static with no

between flow and pressure drop before lifting; in other words, after lifting began the pressure drop increased more slowly as the rate of flow increased. Once the lifting of particles has slightly fluidized the bed, it is interesting to note that a much higher rate of flow can be maintained for the same pressure drop through the bed. For example, the flow is about three times as great after lifting for a

FIG. 10.—POSITIONS OF LARGE ORE CHARGE AND CHARGES OF NORMAL SIZE.

operator is always at a loss to know conditions as they exist.

MEANS FOR CONTROLLING GAS FLOW

Large ore charges that extend all across the furnace at the stock level introduce more resistance to gas flow in the central portion and thus divert more gas to the walls. Periodic use of these large charges, shown in Fig. 10, furnishes one means of controlling the radial distribution of the gases or a properly balanced flow in the center and along the walls. Conversely, expedient for increasing the flow in the central area is to increase the resistance at the walls by lowering the stock line. As indicated in Fig. 11, the ore layers formed when the stock line is low are unusually thick next to the walls and act to blanket the flow of gases through this area. Other factors—speed of bell drop, bell clearance, and the arrangement of stock on the large bell—affect the radial distribution of the stock and in turn the path of the gas. Ore charges that do not move off the large bell readily and uniformly are deposited unevenly, as shown in Fig. 12. In this case,



FIG. 11.—THICKER ORE CHARGES NEXT TO WALL AS RESULT OF LOW STOCK LINE.

inequalities are self-aggravating, particularly at high blowing rates. The energy of the gas stream tends to lift small particles and to keep them in suspension between larger particles, which act to some extent as a retaining screen. As shown in Fig. 13, the pressure drop through the bed decreases sharply once this lifting velocity is reached. At rates of flow up to 0.03 liters per sec. per sq. cm., the bed was static with no

between flow and pressure drop before lifting; in other words, after lifting began the pressure drop increased more slowly as the rate of flow increased. Once the lifting of particles has slightly fluidized the bed, it is interesting to note that a much higher rate of flow can be maintained for the same pressure drop through the bed. For example, the flow is about three times as great after lifting for a

pressure drop of 0.2 through the bed. After the particles begin to lift, the pressure drop increases more slowly with increased rate of flow. This tendency to lift_is not

properly balanced flow is maintained, gassolid contact is not sacrificed and much is gained from this partly fluidized condition in a more uniform stock descent, as a result

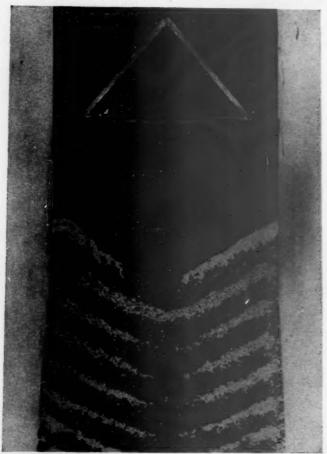


FIG. 12.—UNBALANCED ARRANGEMENT DUE TO IRREGULAR MOVEMENT FROM THE BELL.

uniform throughout a bed, however, and small inequalities may start a channel, which enlarges quickly.

Lifting of particles by the gas stream occurs in blast furnaces as normally operated, particularly in areas of high gas velocity along the periphery and in the center of the furnace. High blast pressures immediately after cast, and the apparent tightness of the stock column often manifest at this time, show that it takes a little time to get the column partly fluidized after the blast is reduced and the column has assumed a denser packing. If the lifting is uniform throughout whole areas and a

of the decrease in pressure drop through the furnace. It is very difficult, however, to fluidize the stock uniformly and to prevent channeling and high dust losses. Fines in the ore and fast rates of blowing aggravate channeling. Two degrees of channeled flow are shown in Figs. 14 and 15. Small inequalities in resistance start channeling, which carries over dust and creates a looser packing, thus ultimately producing a bad channel. Some localized channeling no doubt occurs in the ore layers, but the most difficult type seems to result from unequal peripheral gas flow.

PERIPHERAL DISTRIBUTION OF THE GAS

By means of surveys on a level about 10 ft. below the stock line, and from continuous records of inwall thermocouples,

slight differences in the permeability of the stock start a vicious cycle. A small channel is further aggravated by the lifting of particles of progressively increasing size.

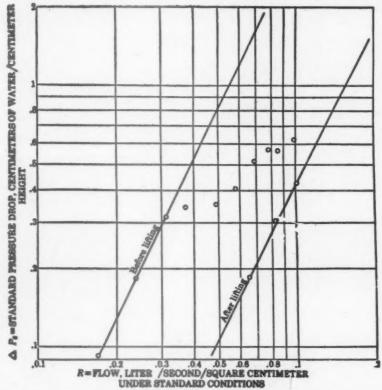


FIG. 13.—EFFECT OF LIFTING OF FINE PARTICLES UPON THE PRESSURE DROP IN A BED (Furnas7).

Johnson³ found gross irregularities in the temperatures around the furnace. In the inwall temperature was high, surveys extending inward about 4 ft. showed that this whole side of the furnace was relatively hot. A condition of unbalanced temperature, such as that shown in Fig. 16, resulted from a badly balanced distribution of the gases. Time will not permit the detailed discussion this work deserves, but it should be mentioned in passing that poor peripheral gas distribution occurred at times on several furnaces normally worked to maintain a high degree of uniformity in the analysis of the iron. Unbalanced conditions appeared for no apparent reason, persisted for a time, then disappeared. The only explanation seems to be that

An unbalanced peripheral distribution of the gas stream leads to unbalanced temperatures in the shaft, which persist to the crucible. Variations in hearth temperatures thus produced cause variations in the composition within a single cast and from one cast to the next. Furnace production and efficiency also suffer when the peripheral gas flow is unbalanced or the gases channel up one side of the furnace. The presence of fine ore in the charge restricts the gas flow in areas intermediate between the wall and the center, thus tending to increase the velocity of the gas along the walls and the likelihood of channeling. Elimination of fines from the ore burden, or some change in operation to reduce the velocity of the gas and the pressure drop



Fig. 14.

Fig. 15.

Fig. 15.

Fig. 15. PERMEABILITY AND MODERATE GAS VELOCITIES.

FIG. 15.—CONDITION OF BED WITH RELATIVE HIGH GAS VELOCITIES AND EXCESSIVE CHANNELING.

through the bed, are needed to improve efficiency, uniformity of operation and uniformity of iron. If mechanical difficulties can be solved so as to make it practicable to rob the process of heat, the coke rate, according to Rice,⁴ has increased with furnace size as shown in Fig. 17. If larger furnaces require more coke in spite of lower

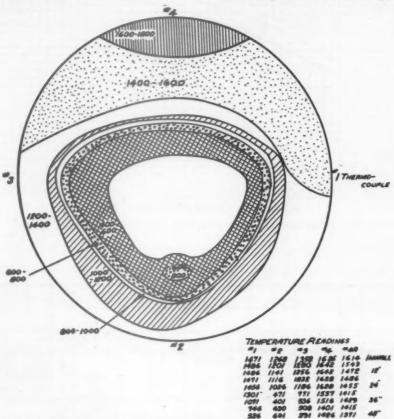


Fig. 16.—Temperature surveys made during poor peripheral gas distribution (Johnson³).

to operate blast furnaces at elevated top pressures, a means will become available for greatly reducing gas velocities, channeling, and the pressure drop through the stock column. This innovation would permit the movement of a larger mass of gas through the charge at lower velocities by reason of a denser gas.

WILL LARGE FURNACES SOLVE EXISTING PROBLEMS?

While large furnaces offer economical advantages, they have not shown any great promise for overcoming the conditions that limit tonnage, efficiency and control. In spite of proportionately less exterior area heat losses, they must have some features that tend to reduce their efficiency.

There are good indications that the entire furnace volume is not used as effectively in the larger furnaces. McKee⁵ and Rice⁴ have examined data from furnaces with varying hearth diameters, to determine whether the larger furnaces are burning coke and producing iron in proportion to their size. As shown by the lower curve in Fig. 18, the amount of coke burned per minute per square foot of total hearth area has steadily decreased as the hearth diameter has increased. This is not surprising in view of the fact that the inactive central core at the tuyeres has increased substantially.

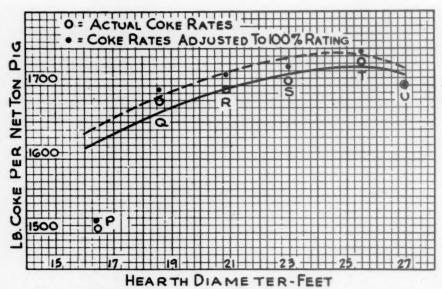


FIG. 17.—RELATION BETWEEN FURNACE SIZE AND COKE RATE (Rice4).

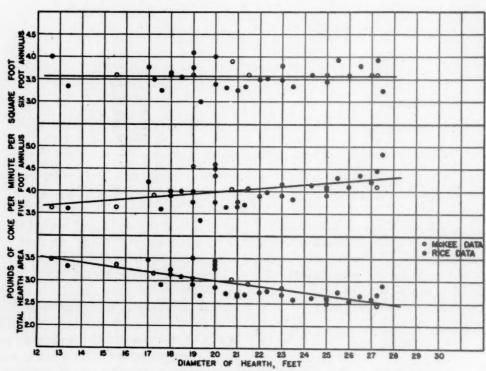


FIG. 18.—RELATION BETWEEN HEARTH DIAMETER AND COKE BURNED.

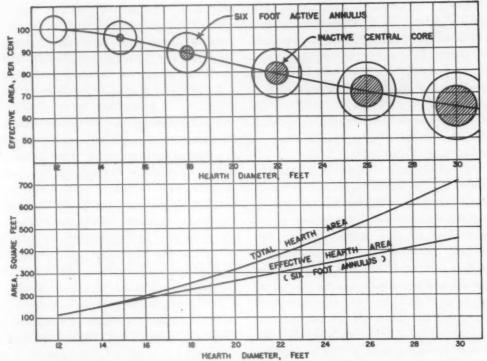


FIG. 19.—CHANGES IN EFFECTIVE HEARTH AREA AS FURNACE SIZE INCREASES.

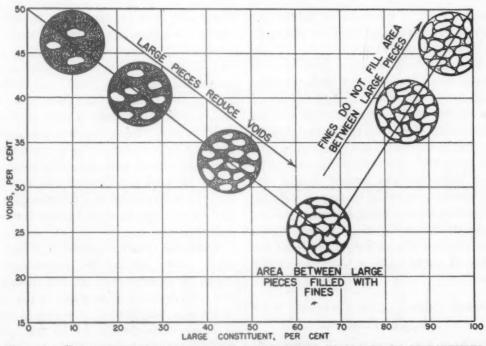


FIG. 20.—EFFECT UPON VOIDS OF ADDING LARGE PIECES TO BED OF SMALL PARTICLES.

Actually, the ability of a furnace to take blast and burn coke is not fixed by hearth conditions but by conditions in the shaft that govern how much gas can be handled without encountering high dust losses and periodic hanging. Any furnace dimension that provides a yardstick of potential output must, therefore, be related directly or indirectly to the ability of the shaft to handle gases effectively.

The middle curve shows that a 5-ft. annulus is too small to be an index of effective furnace volume. As the hearth diameter has increased, the coke burned per square foot of this active annulus has increased. However, the coke burned per square foot of a 6-ft. annulus has held more constant as the furnace size has increased from 12 to 28 ft. It appears, therefore, that with typical raw materials, the 6-ft. annulus as suggested by Rice4 gives a rough index of the volume of gases that can be handled and the amount of coke that can be consumed. For example, the straight line indicates that under average conditions about 3.6 lb. of coke can be burned per minute, or about 5200 lb. per day per sq. ft. of effective hearth area.

The experimental points show a wide spread in all three curves because variations in raw materials affect the ability of the furnace shaft to handle gases without encountering irregular operation. If more gas can be handled in the shaft, more coke can be burned. The indications seem to be that large furnaces cannot handle gas volumes in proportion to over-all volume. Extending this reasoning a step farther, we reach the conclusion that the gas stream does not flow as uniformly throughout the shafts of larger furnaces as in the smaller ones.

INACTIVE CENTRAL CORE INCREASES WITH HEARTH DIAMETER

Using a 6-ft. annulus as a measure of effective hearth area, it becomes evident that there is an inactive core of substantial

size in a 27-ft. hearth (see Fig. 10). This raises the question as to whether we are not reaching the point of diminishing returns in enlarging the hearth to get greater output. A broad study of furnace performance will also show that large furnaces have not produced in proportion to total working volume. Although we have no extensive furnace surveys to guide us, it appears that the larger furnaces work more along the walls or periphery throughout their entire height. This explains why additional furnace height has been more effective in the larger furnaces. Faster stock travel in the outer area and a tendency for more gas to follow the periphery has reduced the time of gas-solid contact, which has been partially corrected by additional height.

It appears, therefore, that we cannot look to furnace size as a means of removing the major obstacles to closer control and greater efficiency. The use of sized ore and agglomerated fines has led to record tonnages and smooth performance because such a practice gets at causes for unbalanced gas flow, poor heat transfer, poor reduction, variations in hearth temperature and iron analysis. In the past, the structure and size of the coke have been emphasized in controlling gas flow and maintaining smooth and efficient operation. No one will question the merits of good coke but the difficulty in fixing standards for quality indicates that we are trying to accomplish too much with the coke alone. The disparity in size between metallurgical coke and fine ore creates a problem as a consideration of the voids or passageways for gas flow will indicate.

Additions of large pieces to a bed of small pieces reduces the percentage of voids. As shown in Fig. 20, this reduction in voids continues up to about 65 per cent of the large constituent, or as long as there is ample fines present to fill the space between the large pieces. Up to this point, large pieces form areas of zero voids and accordingly act as single solid obstructions

n

e t so

e al ne en en

k

he er g-

es

as

n,

on nd

in ng

ne

ut

ity

ish

ine

of

will

of of

ion

ent

nere

ace

int,

and

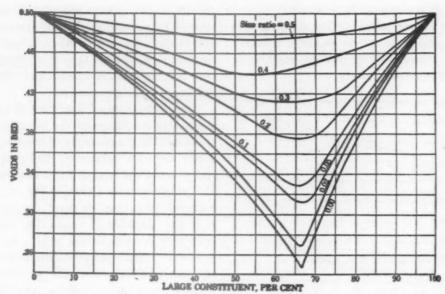


Fig. 21.—Maximum reduction of voids and maximum size ratio in two-component systems (Furnas⁷).

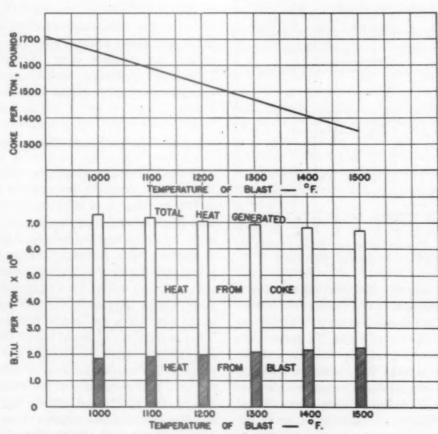


FIG. 22.—COMPARISON OF HEAT FROM BLAST, HEAT FROM COKE, TOTAL HEAT AND COKE RATE.

to the flow of gases. Beyond about 65 per cent of coarse material, the openings between the large pieces become effective because there is an insufficient quantity of fine particles to fill them.

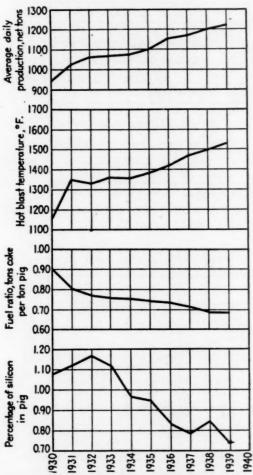


FIG. 23.—EFFECT OF BLAST TEMPERATURE ON FURNACE PRACTICE (Hoffman⁶).

It so happens that the large pieces of coke occupy about two thirds of the furnace volume and thus when mixed with fine ore give a minimum of voids. We prevent the mixing by charging the ore and coke in separate layers. The value of properly sized coke, accordingly, comes mainly from its effect in promoting the permeability of the well-preserved coke layers or in the central area where there is little if any ore. At any rate it appears that there are

definite limitations on what can be accomplished by changes in the physical properties of the coke and that other steps such as size preparation of the ore are needed to give a more positive control over the distribution of the gas stream.

sh

The elimination of fine sizes of ore by agglomeration increases the percentage of voids and the permeability of the ore layers where they are relatively thick, and the resistance of the stock column as a whole is at a maximum. As shown in Fig. 21, sized material, be it large or small, contains the maximum number of voids. The greatest reduction in voids occurs when very large and very small particles are mixed. As the two fractions approach the same size there is comparatively little reduction in voids.

Aside from opening up the densest part of the stock column thus facilitating a balanced gas flow, more effective use of shaft, and closer control, sized ore would reduce the pressure drop through the furnace and thus open the way to higher blowing rates and or higher blast temperatures.

IMPORTANCE OF BLAST TEMPERATURE

High blast temperatures contribute to the smelting process in two ways, as shown in Fig. 22. More heat units are introduced with the blast and there is some reduction in the total heat required for a fixed amount of smelting work. About 1.8 million B.t.u. is introduced with 1000°F. blast, compared with about 2.3 million for a temperature of 1500°F. This increase in the heat content of the blast for a 500° rise in temperature is not as large as one might expect because of a substantial reduction in coke and blast volume. The combined effects of reducing the total heat required plus the additional heat in the 1500° blast reduces the heat supplied by the coke by about one million B.t.u., which is equivalent to about 300 lb. of coke.

These relationships are not rigid but can be calculated with sufficient accuracy to show the general effect and the relative importance of blast temperature. The

POTENTIALITIES OF BENEFICIATED RAW' MATERIALS

Better size preparation of the ore will improve the gas distribution, heat transfer,

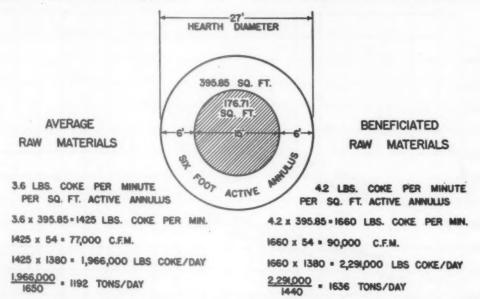


Fig. 24.—Comparison of wind volumes, coke rates, and tonnages on hypothetical furnace.

entire generalized diagram is based upon the premise that only that fraction of the carbon charged which is burned at the tuyeres supplies heat. Comparatively small amounts of heat are released outside the tuyere zones from which hot gases carry heat and reducing power preferentially to the most permeable areas of the stock.

The effect of high blast temperatures on production, fuel ratio and silicon in the iron are shown in Fig. 23, taken from Hoffman's⁶ report covering a decade's practice on imported ores. An increase in blast temperature of 380°F, over the period 1930 to 1939 was accompanied by a decrease of 436 lb. in the coke rate and an increase of 275 tons in average daily production. No change was made in furnace dimensions, and no mention was made of marked changes in raw materials so that the improvement in practice can be largely attributed to the increase in blast temperature.

and decrease the pressure drop through the furnace, which in turn will open the way for higher blast temperatures and faster blowing rates. The combined effects of lower coke rates and somewhat faster blowing will raise the tonnage level substantially.

An attempt is made in Fig. 24 to compare the tonnage level, using typical raw materials and beneficiated raw materials in a furnace with a 27-ft. hearth. As shown earlier, we can expect to burn 3.6 lb. of coke per min. per sq. ft. of active annulus when using typical raw materials. This will amount to 1425 lb. per min., and a blast volume of 77,000 cu. ft. per min. Assuming 60 min. of lost time, 1,066,000 lb. of coke will be burned per day, producing 1192 tons at a coke rate of 1650 pounds.

With beneficiated raw materials, we can reasonably expect to raise the coke-burning rate to 4.2 lb. per min. per sq. ft. of active hearth area. Extending this value, we arrive at 1660 lb. coke per min., 90,000 cu. ft. per min., 2,291,000 lb. of coke per day, or

1636 tons of iron per day on 1440 lb. of coke per ton of iron.

Applying these two rates of combustion to furnaces of varying size, we arrive at naces should be considered in the light of what can be accomplished by providing better facilities for both chemical and physical beneficiation of raw materials.

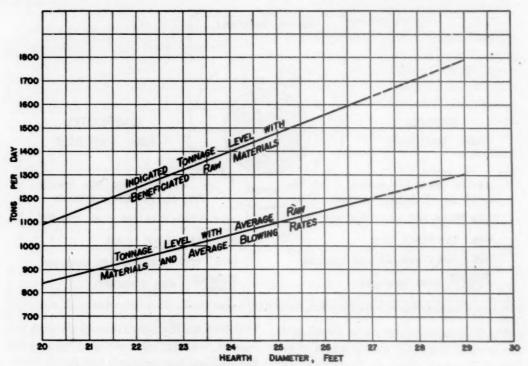


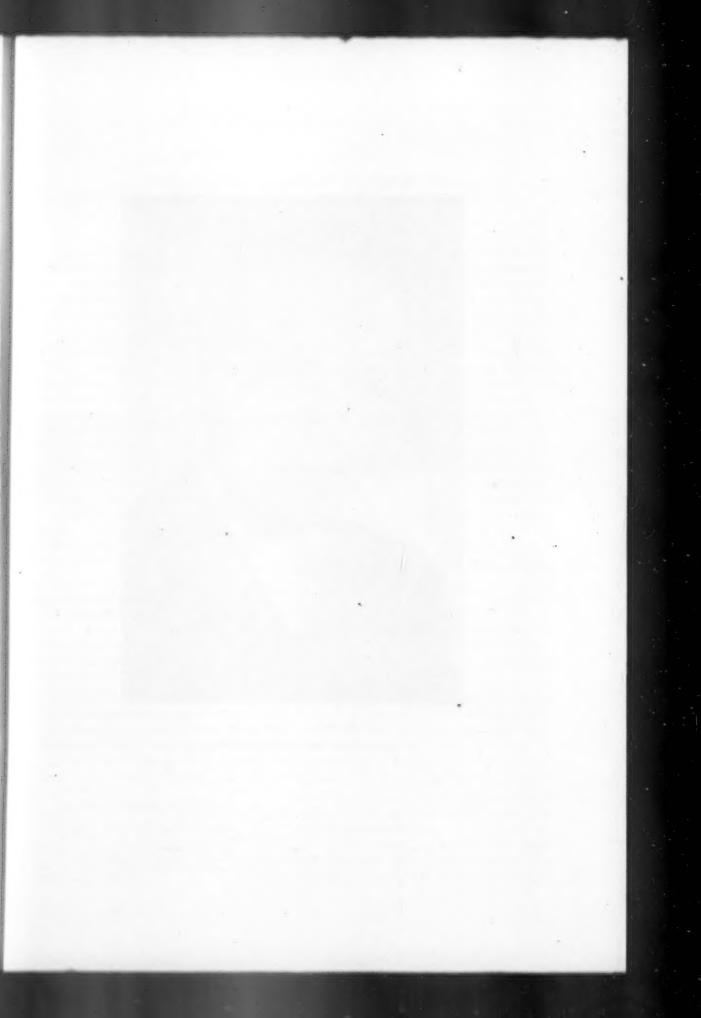
FIG. 25.—POTENTIAL TONNAGES WITH BENEFICIATED RAW MATERIALS.

comparative tonnage levels for typical and for beneficiated raw materials, as shown in Fig. 25. With a 20-ft. hearth, we may expect 840 tons with typical raw materials and about 1100 tons with beneficiated raw materials. On a 27-ft. hearth, we can move up from about 1200 tons to over 1600 tons by improving raw materials.

Whether we advance along the lower line by increasing furnace size or along the upper line by the beneficiation of raw materials, or somewhere in between, will depend upon costs. However, the possibilities of better control, increased efficiency, lower coke rates, and higher tonnages through beneficiated raw materials deserve careful study in formulating plans for expansion and development as well as in the current operation of existing units. Capital expenditures for additional fur-

REFERENCES

- Henry Marion Howe. The Metallography of Cast Iron, 25. New York, 1916. McGraw-Hill Book Co.
- S. P. Kinney, P. H. Royster, and T. L. Joseph: Iron Blast Furnace Reactions. U. S. Bur. Mines Tech. Pub. 391 (1927)
- H. W. Johnson: The Peripheral Distribution of Gases in the Blast Furnace. Yearbook Amer. Iron and Steel Inst. (1038) 07-158.
- O. R. Rice: Three Blast Furnace Questions. Blast Furnace and Steel Plant (Dec. 1945) 33, 1523-1528.
- 5. A. G. McKee: Results of Enlarging Furnaces From 20 to 25 Peet and Probable Future Developments. *Proc.* Blast Furnace and Raw Materials Conference, A.I.M.E. (1942) 125-132
- C. F. Hoffman: Manufacture of Low-silicon Pig Iron Using High Blast Temperatures, Proc. Open Hearth Conf., A.I.M.E. (1940) 146.
- C. C. Furnas: Flow of Gases through Bed of Broken Solids. U. S. Bur. Mines Bull.
- 8. S. P. Kinney: The Blast-Furnace Stock Column. U. S. Bur. Mines Tech. Paper 442 (1929).





MARCUS A. GROSSMANN
Henry Marion Howe Memorial Lecturer, 1945

Toughness and Fracture of Hardened Steels

By Marcus A. Grossmann,* Member A.I.M.E.

(Henry Marion Howe Memorial Lecture†)

THE Institute has established this lectureship to honor the memory of a great American metallurgist, one whose fame has continued long after his passing. As one scientist recently stated it, "All metallurgical texts gradually become outdated and outmoded, except those of the great Henry Marion Howe." It seems fitting, then, that, once every year, we should review, in his honor, some aspects of the science in which he was such a distinguished leader, and also discuss any new data that may help to clarify our concepts. It is my privilege, for which indeed I express the deepest appreciation to this Institute, to offer for consideration a few thoughts on the toughness and fracture of hardened steels.

Before proceeding to the data, I wish to express my great indebtedness to many associates whose stimulating discussions, generous contributions of data and cooperation in experiments are gratefully acknowledged. (But I wish to absolve them of any blame that may arise from the way in which their discussions and data have been used!) First, Dr. Edgar C. Bain, Vice President, Carnegie-Illinois Steel Corporation, whose amiable but merciless criticisms and always constructive and thoughtful suggestions help unfailingly to guard against pitfalls. Then to associates at Gary Steel Works, especially Mr. H. B.

Wishart, Mr. W. K. Smith and Mr. V. Elliott, for great assistance in securing data. Also to Col. C. H. Greenall, Director of Laboratories, Frankford Arsenal, and his metallurgical staff, including Messrs. J. K. Desmond, H. Markus, D. F. Armiento, H. Rosenthal and Henry George, for numerous data and illustrations. Further to Dr. J. R. Low and Dr. M. Asimow, for helpful discussions of effects of states of stress during deformation and rupture, to Mr. J. M. Hodge for discussions and data, to the staff of the U.S. Steel Corporation Research Laboratory for advice and data, and to the Metallurgical Staff at Duquesne Steel Works. The individual acknowledgments will also be found under illustrations. Acknowledgment is also due to Mr. S. C. Snyder for incredibly meticulous scrutiny of manuscript. To all of these, grateful thanks.

INTRODUCTION

The discussion to be offered here will deal with quench-hardened steels only, and may perhaps be considered under three headings:

r. It was found that, when ferrite was precipitated in the (prior austenite) grain boundaries of hardened steel, the notchbar toughness was much less than in pieces fully hardened. The fracture took place in the ferrite, and the loss in toughness is attributed to the lower cohesive (cleavage) strength of the ferrite, as compared with martensite.

 When notch-bar impact test pieces of quenched and tempered steels were examined as to their mode of fracture, it

Manuscript received at the office of the Institute Jan. 21, 1946. Issued as T.P. 2020 in METALS TECHNOLOGY, April 1946.

^{*} Director of Research, Carnegie-Illinois Steel Corporation, Chicago, Illinois.

[†] Twenty-second Annual Lecture. Scheduled for the New York Meeting, February 1945, which was canceled.

was found that the fracture ranged from predominantly intergranular (characterized by bright facets) to predominantly transgranular (characterized by dull fracture). The mode of fracture is influenced not only by composition and grain size, but also by tempering temperature. The intergranular type tended to be more extensive when the tempering temperature was raised from 400°F. or lower, to 500°F. or higher.

3. The well-known loss in toughness when the tempering temperature is raised from 400° to 500°F. appears to bear a relation to the change in mode of fracture, because of a loss in cohesive (cleavage) strength. This viewpoint is suggested by the mechanism of tempering, and is analogous to the above-described loss in toughness when ferrite is precipitated in martensite grain boundaries.

TOUGHNESS OF HARDENED STEELS

The search for "toughness" is never ending, though some may wish to paraphrase C. Hartly Grattan's remark¹ and say: "If all the persons who seek high hardness without sacrifice of toughness were laid end to end, it would be a good thing." Nevertheless, the problem has been subjected to scrutiny by many experimenters, in the hope of explaining certain anomalous behaviors.

The term "hardened steels" in the title of the paper refers to steels that, having been hardened by quenching, are then tempered but moderately if at all, so that their hardness is still high. The toughness of such steels may be measured in several ways, but our data have to do mostly with the notch-bar impact test.

EFFECT OF SHAPE OF TEST PIECE

The fact that we shall deal mostly with the notch-bar impact test means that the observed trends might differ, in degree even if not in kind, if a different form of

test piece had been used. As is well known, the "toughness" (energy absorbed in the breaking) of a notched bar depends on the temperature at which the test is carried out, the values being low (brittle behavior) when the testing temperature is sufficiently low, and high (tough behavior) when the testing temperature is high. However, Heindlhofer2 long ago pointed out that the temperature at which a piece becomes brittle depends on the shape and the manner of testing of the test piece. Asimow³ says simply: "Plasticity is a relative behavior, depending on the system of stresses imposed on the material." Or, as Bain4 says, colorfully: "Metals are not brittle; shapes are brittle."

als

at

ar

tic

To obtain some data on the effect of shape of piece and of testing temperature in the specific type of steel to be discussed here, a WD4150 steel of the following composition

P	ER CENT	4.	PER	CENT
C	0.52	Cr		1.01
Mn	0.85	Mo		0.20
P	0.016	Cu		0.14
S	0.023	Ni		0.06
Si	0.24			

was tested in three different forms of test piece, having been hardened by heating to 1600°F. and quenching in oil, followed by tempering at 400°F. The three forms are illustrated in Fig. 1, and were characterized by: (1) narrow notch, (2) largeradius notch, and (3) absence of notch. (Notches were ground after quenching and tempering.) Fig. 1 shows that in the absence of a notch the piece was toughest at about o°F.; with the large-radius notch it needed to be warmed to at least 212°F. to reach maximum toughness; and with the narrow notch it needed to be warmed to 500°F. or more to be tough (meaning that the 400° temper could not even be so tested). The narrow notch, of course, represents a relatively higher degree of triaxial stress under the notch. The chart

¹ References are at the end of the paper.

also shows that, with this narrow notch and at these high hardnesses, the energy values are not particularly sensitive to small variations in testing temperature near room behavior easier, a larger grain size was provided by heating the steels to a much higher temperature than usual prior to quenching. We were at the time examining

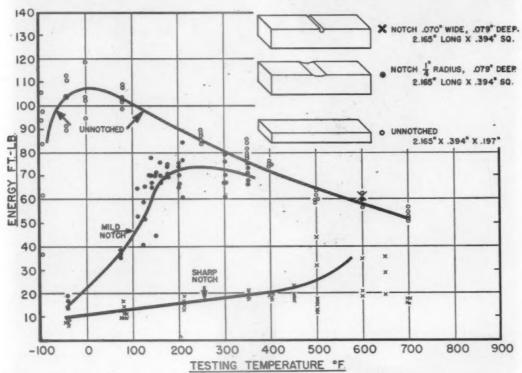


FIG. 1.—Effect of shape of piece and of testing temperature on energy absorbed in breaking (Armiento).

temperature, at which temperature the tests in the remainder of the paper were made.

FRACTURE AT GRAIN BOUNDARIES

In such quenched steels, certain observed fracture behaviors had suggested that fracture took place in grain boundaries, even when the steel had been tempered. To ascertain whether this was so, attempts were made to fit together the two halves of broken notch-bar pieces or tensile pieces, so that the junction could be studied microsopically, after sectioning, but, with our technique at least, these attempts were uniformly unsuccessful when the grain size was fine, as is ordinarily the case. In order to make examination of the grain

tensile-test bars of a chromium-molybdenum 4150 steel containing 0.57 per cent C, o.90 Mn, o.021 P, o.030 S, o.26 Si, 0.00 Cr, 0.21 Mo, and the coarser grain size was provided by raising the heating temperature from the usual 1500° up to 2100°F. The pieces after quenching in oil were tempered at about 800°F. and the tensile piece pulled to fracture, whereupon the two halves were fitted together for examination. As anticipated, microscopic examination showed that fracture occurred in the grain boundaries, as illustrated in Fig. 2. This was very bad, as we did not realize that this was a special case. Instead. like all good metallurgists, we were satisfied with having proved a preconceived notion! Furthermore, there was nothing very

or ar ca fr



FIG. 2.—OCCURRENCE OF FRACTURE IN GRAIN BOUNDARIES OF QUENCHED AND TEMPERED STEEL. X 100. (R. Swanson.)

"Sensitive tint" illumination.

FIG. 3.—FRACTURE OF COARSENED LOW-METALLOID IRON: a, × 100; b, × 75.

Transgranular path indicated by arrows.

original about the finding, because Bain and Vilella⁵ had already shown, for the case of coarsened high-carbon steel, that fracture occurred in the grain boundaries when the hardened steel was untempered.

This is not to say, of course, that fractures in all steel were suspected of being in the grain boundary. For example, in coarsened "low-metalloid" iron the fracture is transgranular. A material was at hand of the following approximate composition: C, 0.05 per cent; Mn, 0.05; all other elements low. It was coarsened by heating to 2400°F. followed by cooling in the furnace. Its hardness was Rockwell B-28 and it was quite brittle for such a material, showing Charpy values of 13 to 16 ft-lb. Both on the main fracture and in the small branch fractures, the path of fracture was quite clearly across the grains, as indicated by the arrows in Fig. 3.

mium-molybdenum steel was available, but of somewhat lower carbon content, S.A.E. 4140, of the following composition: C, 0.42 per cent; Mn, 0.70; P, 0.020; S, 0.010; Si, 0.27; Cr, 1.00; Mo, 0.21. This was low enough in carbon to provide considerable precipitation of ferrite in the grain boundaries when suitably treated, so for coarse grain size the steel was heated at 2000°F. in CO atmosphere for 11/2 hr.; then, to precipitate ferrite (after equalizing the temperature at 1500°F.), it was cooled to 1300°F. and held there for the number of minutes indicated, then quenched in cold water and tempered at 400°F. The pieces had been made oversize, so that they could be ground to 10 mm. square to remove decarburized metal, and finally were notched by grinding with a narrow cutoff wheel to a depth of 2 mm. When broken as notch-bar impact tests, they showed energy values as given in Table 1.

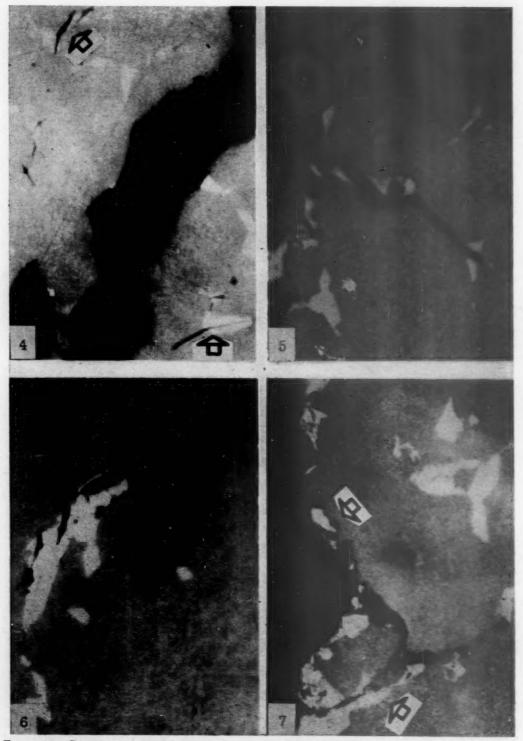
TABLE 1.—Effect of Ferrite Precipitated in Grain Boundaries on the Energy Absorbed in Notch-bar Impact Tests, SAE 4140 Steel (W. K. Smith).

	Perrite		
Time at 1300°F.,)	Time at 1300°F., 1 Min.	Time at 1300°F., 15 Min.
	9.5 Izod G ^a 7.8 Izod G ^a 9.2 Izod G ^a 11.7 Izod G ^a 14.3 Charpy G ^a 10.0 Charpy G ^a 8.0 Charpy F ^a 11.3 Charpy F ^a	11.2 Izod G 14.4 Izod G 10.2 Izod G 13.4 Izod G 15.4 Charpy G 15.5 Charpy G 10.5 Charpy F	3.5 Izod G 4.7 Izod G 3.1 Izod G 4.3 Izod G 3.2 Izod G 5.4 Charpy G 5.8 Charpy G 4.6 Charpy G 5.3 Charpy P
Average	10.2	12.9	6.3 Charpy F 7.0 Charpy F
		Average	4.8

[•] The designations Charpy and Izod do not refer to shape of notch, since all notches were of the shape ground by a thin abrasive wheel to a depth of 2 mm. The designations Charpy and Izod refer to the manner of placing in the testing machine—Charpy horizontal, struck at center; Izod clamped vertically, struck on protruding end. G means, broken at Gary; F, broken at Frankford.

Nevertheless, our test led to an experiment that really did yield an interesting fragment of information. Since fracture in the hardened steel occurred in the grain boundaries, curiosity was aroused as to what the mechanical properties would be if the grain boundaries were occupied by thin layers of ferrite. A similar chro-

The pieces with ferrite in the grain boundaries were consistently and strikingly more brittle than those without ferrite—that is, fewer foot-pounds were absorbed in breaking. Since the energy absorbed corresponds to the amount of deformation prior to rupture, it appears that when ferrite was present the piece needed to be



Figs. 4-7.—Rupture in ferrite, in grain boundaries of hardened SAE 4140 steel. \times 250. (Rahrer.)

bent only a little to reach the rupture strength of the ferrite, whereas with the normal structure the piece bent much farther (more energy absorbed) before the rupture strength was attained. That the rupture in the ferrite-containing pieces did actually occur in the ferrite regions is amply attested in the appearance of the fractured pieces in the microscope. Figs. 4 to 7 illustrate behaviors in 4140 steel after a variety of treatments, all involving however a heating to a high temperature followed by holding at 1300°F. for stated times to precipitate ferrite. Thus in Fig. 4, near the main fracture, the incipient fractures are seen to occur most frequently in or adjacent to patches of ferrite, as indicated by the arrows. In Fig. 5, a branch rupture is seen to occur mostly through patches of ferrite. In Fig. 6, several ruptures began in a single large patch of ferrite. In Fig. 7, arrows point to patches of ferrite in the main path of fracture as well as branch fractures through ferrite islands.

An entirely analogous behavior was observed in SAE 2345, 3.5 per cent nickel steel, of the following composition: C, 0.45 per cent; Mn, 0.72; P, 0.016; S, 0.029; Si, 0.24; Ni, 3.58; Cr, 0.03. When samples were heated to 2100°F. for 20 min., quenched directly in oil, tempered at 400°F., and prepared with a ground notch as described previously, they showed an average Charpy value of 24 ft-lb., but when the 2100° treatment was followed by isothermal precipitation of ferrite at 1160°F. (followed by oil quench and the 400°F. tempering), the average Charpy value was only 6 ft-lb. and the rupture was again observed to be in the ferrite areas.

The conclusion thus seems inescapable that the contribution (if it can be called that) of the ferrite lies in its low fracture strength. Evidently there is no opportunity for the ferrite to flow (in shear), a behavior we are prone to associate with so soft a material as ferrite. Had the ferrite

been able to flow, it would have absorbed energy in the flow process, and consequently would have contributed to greater toughness, rather than brittleness. In considering the stress situation in this case, it is to be remembered that there are relatively large volumes of a very hard material, martensite with a Brinell hardness of perhaps 500 to 550, bonded together by thin layers of a very soft material, ferrite with a Brinell hardness of possibly 80 or 100. The ferrite consequently has no opportunity to flow, since it is bonded, as a thin layer, between hard masses of martensite.

Curiosity is aroused therefore as to how thick the layers of ferrite would have to be, before conditions would permit shear flow, with its resultant toughness; or, stated in more general terms, how great must be the proportion of soft material (in the presence of these hard masses) to permit shear flow and to cause toughness. Accordingly, pieces of the same 4140 steel were caused to transform for successively longer times at 1300°F., the last pieces after 6 hr. being completely transformed. The results are shown in Table 2. All pieces were austenized at 2100°F., then allowed to transform at 1300°F. for the times stated, quenched in oil, tempered at 400°F. and finally notched.

TABLE 2.—Effect of Proportion of Soft Structural Constituent on Notch-bar Toughness of Hardened 4140 Steel (W. K. Smith).

Time at 1300°F.	Hardness, Rockwell C	Energy, Ft-lb.	Proportion of Ferrite (plus Pearlite), Per Cent
None (direct quench) o to 1 min 5 min 10 min 20 min 40 min 1 hr 2 hr 6 hr	51 51 50.5 47 47 42 19 (7 RC) (88 RB)	17, 10 16, 9 5, 5, 5 5, 5, 5 4, 4, 4 4, 4, 4 4, 4, 4 7, 7, 6 35, 34, 39	None None 1 2 5 F (+P) 18 F + P >50 F + P 100 F + P

As expected, the now familiar loss of toughness was thus observed when small amounts of ferrite were present in the grain boundaries. The surprising feature was to a considerable proportion of isothermally transformed ferrite and pearlite, are shown in Fig. 9 in their undeformed state.

That the behavior with relatively large



FIG. 8.—RUPTURE IN PEARLITE. \times 250. (Smith.) 4140 steel partially transformed to ferrite and pearlite, balance martensite. $R_{\rm C}=19$. Ft-lb. = 7.

the fact that the steel had to be transformed (to ferrite and pearlite) to the extent of 50 per cent of its volume before even a small recovery of toughness was found. At this point the over-all hardness had dropped to 19 R_C, surely a rather soft material, and yet the toughness (ft-lb.) had not even attained the value of the original ferrite-free hard material (hardness 51 R_C). As was to be expected in view of this behavior, the path of rupture was in the soft (low-strength) constituents, as illustrated by the rupture through the pearlite in Fig. 8. Micrographs of four typical samples, ranging from a very small

amounts of ferrite and pearlite associated with hard martensite is probably typical of steels of this type was indicated by a similar test on a nickel-chromium S A E. 3140 steel. Samples were prepared from a heat of the following ladle analysis: C, 0.38; Mn, 0.74; P, 0.018; S, 0.026; Si, 0.27; Ni, 1.39; Cr, 0.76. The samples were heated at 2100°F. for 20 min., transferred to a salt bath at about 1240°F. (slight temperature fluctuations noted), held for the times indicated, quenched in water and finally tempered at 400°F. for one hour. All notches were then ground as before, and the specimens were

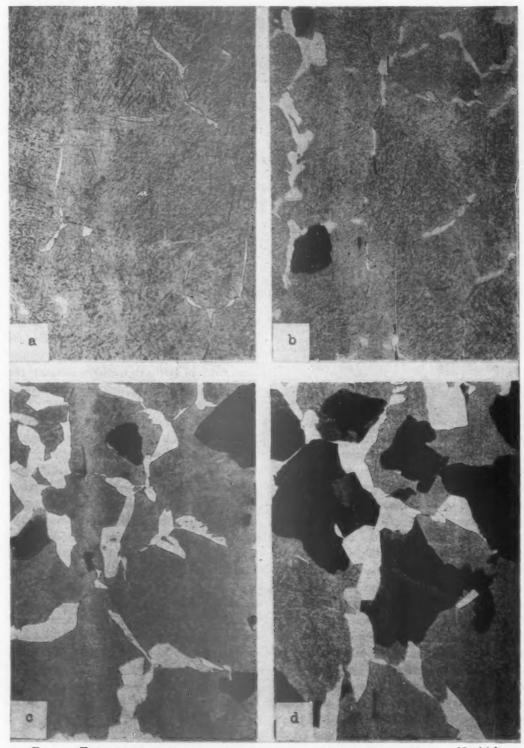


FIG. 9.—FOUR STRUCTURES SHOWING BRITTLE NOTCHED-BAR BEHAVIOR. \times 100. (Smith.) 4140 steel transformed at 1300°F. isothermally: a, 10 min.; b, 20 min.; c, 1 hr.; d, 2 hr. (see Table 2).

broken as Charpy pieces. Table 3 shows for each treatment the average Rockwell C hardness, the energy absorbed (ft-lb.) and the observed microstructure; and shows that here again, with as much as 30 per cent of soft constituents, the pieces were still brittle.

Table 3.—Effect of Proportion of Soft Structural Constituent on Notch-bar Toughness of Hardened SAE 3140 Steel. (W. K. Smith)

Time at 1240°F.	Average Hardness, Rockwell C		Proportion of Ferrite (Plus Pearlite)
None (direct (quench).	53.3	28, 39, 18	Very slight trace of ferrite
I min	53.2	32, 25, 32	Very slight amount of ferrite
5 min	53.3	9, 10, 9	
10 min	52.5	5. 5. 5	Considerable ferrite, small spots pearlite
30 min	38.7	6, 4, 5	
1 hr	18.2	42, 40, 41	About 75 per cent transformed

At any rate, it is clear from these tests that the presence of a small amount of ferrite, say 2 to 5 per cent in the grain boundaries of these hardened steels, leads to brittleness.

As to the reason for the brittleness, it may be pointed out that much greater amounts of soft constituent (at least 30 to 50 per cent) had to be present before these soft regions could flow (in the notched bar) and the piece consequently become tough. This behavior emphasizes the thought that there was no possibility of any substantial amount of flow (in shear) of the ferrite when its amount was small, of the order of 2 to 5 per cent, when the rest of the steel was hard. Consequently, it is suggested that the embrittling effect of the ferrite is due to its weakness, its low disruptive strength in triaxial stress.

This concept, that brittleness is some-

times due to weakness, should perhaps be emphasized, because it must not be considered to contradict the more familiar experience that brittleness is a characteristic associated with hardness and strength. Consider the general stress situation when gradually increasing load is applied to a notched bar (resulting in a condition of triaxial stress under the notch). The following sequence obtains: (1) the stress increases, (2) the yield point is reached and the metal begins to flow, (3) work-hardening progresses as the flow proceeds, (4) eventually the metal is strengthened by work-hardening sufficiently to support (without flow) the stress necessary to produce rupture, so that (5) rupture results.

If the metal is hard and strong, its yield point in step 2 is already high, so that very little flow in steps 3 and 4 is needed to reach the rupture strength, even though that rupture strength be high. Hence there is but little plastic deformation before rupture, and the piece is "brittle." This is the mechanism involved in the familiar experience that brittleness is an accompaniment of hardness and strength.

On the other hand, suppose there are planes of low rupture strength. In that case, even though the yield strength is lower than in the case described previously it would take only a little of the deformation in steps 3 and 4 to reach the postulated lower rupture strength. Hence in this case too there would be but little plastic deformation before rupture, and the piece would be "brittle." This is the mechanism involved in the concept that brittleness is sometimes due to "weakness." Let us therefore inquire a little into the question as to which areas are weakest when steel is fractured.

POSITION OF WEAKEST PLANE IN STEEL

Let us consider it to be obvious that when load is applied to a notched bar of steel the initial rupture occurring in the region of greatest stress will occur in the plane of most pronounced weakness. True, the state of stress is not uniform in all directions, so that the aspect of unfavorable placing of the plane of weakness should be recognized—but in a piece of steel the grains are so numerous that there will always be a substantial number of grains whose weakest planes are placed unfavorably in relation to the stress, so that these would constitute the position of potential first rupture.

We must now consider some evidence that the crystallographic position of the weakest plane in hardened steel is by no means fixed and constant but is rather fugitive and variable, being different in different steels and being affected also by the tempering treatment.

Some curious evidence made its appearance in examination with a binocular microscope, of fractures of a nickelchromium-molybdenum NE 8640 steel of the following composition: C, 0.39 per cent; Mn, o.89; P, o.014; S, o.023; Si, 0.32; Ni, 0.56; Cr, 0.51; Mo, 0.26. Preliminary observations had suggested that the fracture appearance was different with different grain sizes, and also varied as a result of tempering treatments. Consequently, a series of grain sizes was imparted to the steel by heating samples to 2000°, 2100°, 2200° and 2300°F., followed by quenching in oil. For each heating temperature, samples were left untempered, and others were tempered at respectively 400°, 500° and 700°F. The pieces were then notched and fractured and the fractures examined with the binocular microscope.

To aid in documenting the appearances observed, the reader is first invited to examine Figs. 10 to 14, which are representative of the several samples of coarsest grain size (quenching temperature 2300°F.) as observed with the binocular microscope. (Directions for viewing these stereoscopic micrographs are given under Fig. 10.)

Fig. 10 shows the fracture of the hardened steel, as quenched, without tempering. The fracture shows an interspersing of rough areas and smooth areas, and there is moderately good evidence that the rough areas represent fracture across the grains (transgranular), and that the smooth, shiny facets represent grain-boundary surfaces (intergranular). By contrast, as an example of smooth, shiny facets, one may observe the character of the fracture in Figs. 12 and 13, where practically all of the grain facets are shiny. As to the belief that the smooth, shiny facets represent grain boundaries, one may refer to the early work of Bain and Vilella.5 They showed, in micrographs of coarsened highcarbon, plain-carbon steel, that the fracture was in the grain boundaries. The fractured surface of such steel, when the grains are coarse, generally shows only shiny facets under a binocular microscope. Our own micrographs, including Fig. 1 in this paper, merely duplicate the evidence of Bain and Vilella that shiny facets represent grainboundary fracture. Incidentally, at adequate magnification on the binocular microscope, the surfaces of the individual grains are seen to exhibit the slightly curved appearance known to be characteristic of grain surfaces when masses of metallic grains are separated along their grain boundaries, corresponding to the slightly curved grain boundaries of a plane section viewed on the metallurgical microscope. A corroborative item, indicating that each individual facet represents a single grain, is the circumstance that occasional shiny fracture facets show the parallel striations characteristic of twinning, and that each individual manifestation of twinning extends across a single facet only. (The twinning of the parent austenite grain of course has often been observed in coarse martensite in polished and etched plane sections viewed on the microscope.) This view, that the shiny facets (in hardened steel fractures) repre-

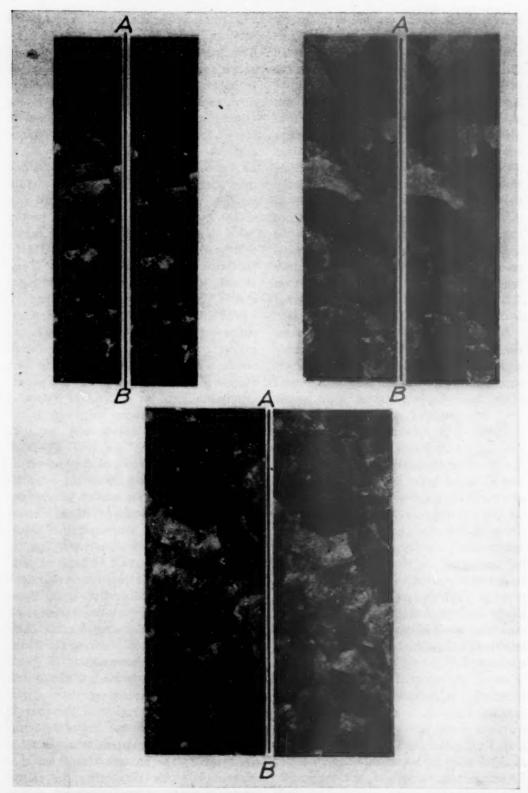


Fig. 10.—Fracture of hardened 8640 steel as quenched, without tempering. Stereoscopic. \times 24. (*H. George.*)

sent individual grain-boundary surfaces, received support in many observations of fractures under the binocular microscope and of polished and etched sections of the

quench crack), and a rough transgranular break is visible in Fig. 11. The best that can be said is that, in view of such evidence as is available, it has seemed clear

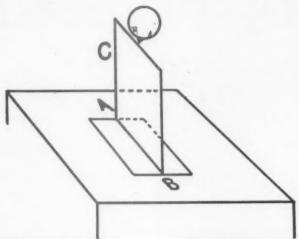


FIG. 10a.—DIRECTIONS FOR VIEWING STEREOMICROGRAPHS.

After a little practice, the stereoscopic micrographs of Figs. 10 to 14 may be caused to appear

in relief without the use of a stereoscope.

As in the drawing herewith, each illustration consists of two views (slightly different) of the same field, separated by a line AB as in the drawing. The illustration is placed flat on the desk, a piece of cardboard C is set vertically on line AB, and the observer views the illustration from the end of the cardboard. In this way the left eye sees the left-hand illustration only, and the right eye the right-hand illustration only.

An 8 by ro-in. cardboard is usually a convenient size. An observer wearing bifocal glasses should of course use the "reading" portion. The illustration should be so placed in relation to lighting (window, etc.) that the two portions are illuminated equally, avoiding shadows from

cardboard C.

Fig. 10 consists of three illustrations, of different widths. As pointed out by F. Seitz, the closer together the two portions are placed, the easier does the stereoscopic viewing become. However, close placing means that the field of view common to the two portions is narrower. Hence, the easiest illustration to see stereoscopically is the narrowest one in Fig. 10, but the

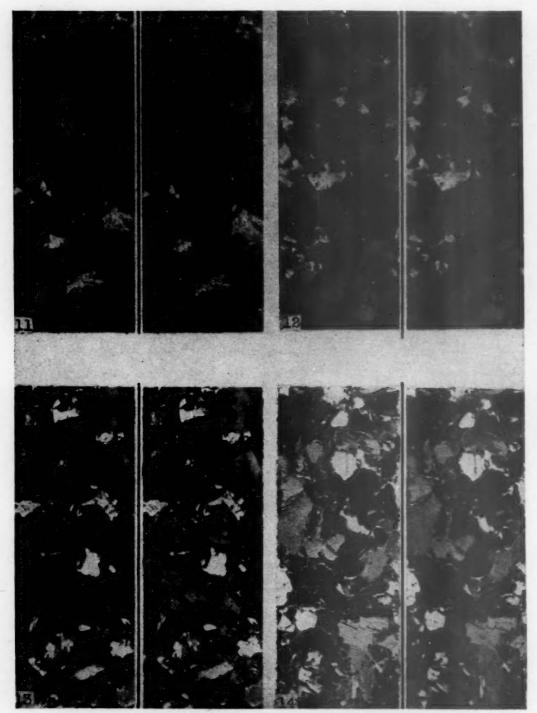
field is the most limited.

Having placed the illustration and cardboard as described, the observer should look at the narrowest illustration (both eyes open, of course) until the stereoscopic effect appears. With most observers, it will be necessary to continue looking for a period of time during which the image will continue to look "flat," and then the stereoscopic effect will suddenly appear. In a group of observers of these illustrations, the time from first observation to stereoscopic appearance (in this narrowest illustration) varied from a few seconds to five or six minutes. (This has nothing to do with "good eyesight," but involves "stereopsis.") Once the stereoscopic effect has appeared on the narrowest illustration, the observer should proceed to the next wider one, and when this has been observed stereoscopically should proceed to the widest one. Here again observers differ, as some who quickly observed the narrowest one took longer time for the wider ones, and vice versa. In observing Figs. 11 to 14, Fig. 10 may of course be used for practice.

usual type in the course of the present work. Somewhat less clear is the evidence that the rough appearances in the fracture represented transgranular fracture, but Fig. 15 shows a typical partially transgranular fracture as observed on a sectioned plane of a piece as quenched (a quenched steel but tempered at 400°F.

to us that the bright facets represent pure grain-boundary separation, and that rough fractures do not and are probably transgranular.

On this basis, let us examine Fig. 11, which is representative of the same



Figs. 11, 12 and 13.—Fractures of Quenched and Tempered 8640 Steel.
Fig. 11, tempered 400°F.; Fig. 12, 500°F.; Fig. 13, 700°F.
Fig. 14.—Fracture of coarsened low-metalloid iron. All stereoscopic. × 24. (H. George)
For viewing directions, see Fig. 104.

The fracture is still (on the basis above) partly grain-boundary and partly transgranular. Contrasting with this is the appearance in Fig. 12, representing steel

While the fractures of Figs. 10 to 13 are characteristic of steels quenched and tempered, needless to say other types of fractures may be encountered in ferrous



FIG. 15.—FRACTURE OF HARDENED 4150 STEEL. X 100.

Partially transgranular break indicated by arrows: (a) as quenched (quench crack); (b) quenched and tempered (fracture on bending notched bar).

tempered at 500°F. In this the facets are almost entirely bright and are characteristic of grain-boundary fracture throughout. Further, in Fig. 13, when the steel was tempered at 700°F., the facets are bright, the fracture is thus presumably entirely in the grain boundaries, and the appearance is quite like that when the tempering was at 500°F. This bright fracture appearance persists up to tempering temperatures of at least 800° or 900°F., and often higher.

materials. As an illustration, the fracture of the low-metalloid iron of Fig. 3 is recorded in Fig. 14.

Postponing temporarily any discussion as to the reasons for the rough or the shiny modes of fracture in Figs. 10 to 13, one is impressed by the mere fact of the profound change in nature of the fracture, when comparing the steels tempered below 400°F. with those tempered above that temperature. Further, as stated previously, there had been indications that the fracture

changed with the grain size. Therefore we should now record the observations on the NE 8640 steel with its variety of treatments mentioned previously (quenching temperatures, 2000° to 2300°F.; tempering, none to 700°F.).

As a basis for tabulating the appearances of the various fractures, let us merely recognize that in a fracture we may see the two types of appearance: (1) the shiny facets, and (2) the rough areas. Further, since these are the only two types observed in such hardened steels, the classification of the fracture may state solely what percentage of its area consists of bright facets, the balance being understood to be the rough areas. The appearances of the fractures of the NE 8640 steel may consequently be classified as in Table 4.

TABLE 4.—Proportion of Bright Fracture in Fractured Surfaces

		Of Total Fractured Area, Following Proportion was Estimated to Consist of Bright Facets, Per Cent					
Quenched in Oil from	Temper- ing	Viewed with Unaided Eye	Viewed in Binocular Micro- scope, X 30	Average			
2300°F.	None 400° 500°	50 50 100	50 50 100	50 50 100			
2200°F.	700° None 400° 500° 700°	100 20 20 100 100	98 50 15 98	99 35 18 99			
2100°F.	None 400° 500° 700°	10 10 90	5 3 97	8 7 94			
2000°F.	None 400° 500° 700°	90 5 5 80 80	95 2 5 80 85	93 4 5 80 83			

Table 4 emphasizes strongly a feature already observed in Figs. 10 to 13; namely, the difference in mode of fracture in all samples tempered at 400°F. and below, when compared with those tempered at 500°F. and above. This difference is most striking in the pieces quenched from 2100°

and those from 2000°F. In these cases the pieces tempered at 400°F. and below showed only about 5 to 10 per cent shiny facets (o5 to oo per cent rough), whereas those tempered at 500°F. and above showed 80 to 95 per cent shiny facets (only 20 to 5 per cent rough). We shall presume to speculate a little about this behavior presently. We have used the phrase "400°F. and below" because the mode of fracture found in any steel after a 400°F, tempering has been found (in tests of numerous steels) to be quite characteristic of lower tempering temperatures as well; for example, 300° or 350°F. We have used the phrase "500°F. and above" because, as indicated previously, the mode of fracture observed after a 500°F. tempering was characteristic also of tempering temperatures up to 800° or 900°F., and in some cases even 1000° or 1100°F.

Another feature appearing in Table 4, considering now the tempering temperatures 400°F. and below, is the fact that, when the grain sizes were finer as a result of lower heating temperatures prior to quench, the proportion of shiny facets decreased (proportion of rough fracture increased). The grain sizes ranged from 0, for the 2300° quench, down to about 2 to 3 for the 2000° quench. Thus the first feature found to affect the mode of fracture was the tempering temperature, and now the second feature found to affect it is the quenching temperature, the latter involving a change in grain size.

A third feature that affects the mode of fracture is the composition of the steel. As mentioned previously, Bain and Vilellas showed that, in hardened high-carbon, plain-carbon tool steel, coarse grained and untempered, the fracture takes place in the grain boundaries. Their work was done on the Shepherd and Jernkontoret fracture standards. Examination of the coarser fracture standards, with the binocular microscope, usually showed 100 per cent shiny facets. This compares with only

50 per cent shiny facets in the NE 8640 steel, at even the coarsest grain size, and of course even less at the finer grain sizes. Anent this trend with grain size in the NE 8640 steel, a similar trend was observed in the carbon tool steel, for whereas the coarser grain sizes showed 100 per cent shiny facets, the finer grain sizes showed appreciable proportions of rough fracture.

This suggested an obvious little experiment. Since the tool-steel fracture standards not only showed a range of grain sizes, but were found to vary in their mode of fracture as well, it seemed probable that a person reading fractures would inevitably be swayed by roughness of fracture as well as by grain size. Consequently, a mere change in mode of fracture might mislead a person into thinking that a change in grain size was necessarily involved. For example, Table 4 shows that tempering above 500°F. provides a mode of fracture different from tempering below 400°F. Could this mislead an expert reader of fractures? A test was made, using the four samples of NE 8640 steel quenched from 2000°F. Since all were quenched from the same temperature, they all had the same grain size; they varied only in tempering temperature, but this influenced the mode of fracture. The fractures were judged with the unaided eve independently by two expert fracture readers, who had no prior knowledge of the thoughts or experiments described here. As far as they knew, these were simply four samples of which they were asked to judge the grain size. Their readings are given in Table 5.

TABLE 5.—Grain-size Readings, N.E. 8640 Steel, Quenched from 2000°F.

Tempering, Deg. P.	Reader A	Reader B
None	4½ (few 3's)	51/2
400	4 (few 3's)	434
500	194	23/2
700	132	2

The rougher fracture of the pieces tempered at 400°F. or below thus misled these experts into assigning a much finer grain size than was present in reality, for microscopic examination showed that all samples were about alike, as follows:

Tempering Grain Size

None 2½ with few 1's
700°F. 2 to 3 with few 1's

In other words, when judging the NE 8640 fractures by comparison with the tool-steel fracture standards, the expert readers agreed that the samples tempered below 400°F. apparently had a grain size about No. 5, whereas they actually had a grain size about No. 2, but this real grain size became apparent only when the pieces were tempered above 500°F.

These findings raise disquieting questions about the rating of grain size by the use of a single set of fracture standards:

- r. Must there be a separate set of fracture standards for each different composition of steel (or group of compositions)? This question is raised because we have seen that, when the tempering temperature was 400°F. or below, the mode of fracture of N.E. 8640 steel was quite different from that of the standard high-carbon tool steel, resulting in incorrect estimates of grain size.
- 2. If pieces to be judged as to grain size have been tempered, must there also be standards that have been tempered at corresponding temperatures? This question is raised because of the profound change in mode of fracture when comparing pieces tempered below 400°F. with those tempered above 500°F.
- 3. Would fracture grain-size readings be more reliable if it were specified that all pieces (both sample and standards) be tempered at 500°F. or above? This question is raised because it would offer a partial solution, though an imperfect one.

The variations in mode of fracture described have now been observed in numerous carbon and low-alloy steels, and, in view of the findings, the whole scheme of rating fracture grain sizes from a *single* set of fracture standards seems called in question.

On the other hand, this should not be construed as any criticism of (or as casting any doubt upon) the use of the Shepherd or Jernkontoret fracture standards for judging the grain size of carbon tool steels. Those fractures were standardized for use with carbon tool steels; they are themselves made of carbon tool steels, their mode of fracture is the same, and for their intended purpose they are entirely reliable. (Metallurgists proceeded, perhaps incautiously, to apply these standards to other steels, so that if there was any lack of caution, it should be charged to the metallurgists and not to the tool-steel fracture standards!)

RELATION OF VARIATIONS IN MODE OF FRACTURE TO VARIATIONS IN MECHANICAL PROPERTIES

The foregoing discussion has commented on certain variations in the mode of fracture of hardened steels. Inevitably the question arises, are these variations in fracture appearance associated with any variations in mechanical properties? Consequently, it is of interest to record certain data on the "toughness" of such steels as measured by the notch-bar impact test.

Behaviors typical of the low-alloy steels were found in five heats of WD 4150 steel of which the compositions are given in Table 6.

TABLE 6.—Compositions of W.D. 4150

Steels Tested

PER CENT

Steel	С	Mn	P	S	Si	Cr	Mo	Ni	Cu
-	-	-	-	-		-		-	-
A	0.48	0.82	0.015	0.014	0.25	0.96	0.21	0.08	0.02
CDE			0.016						
D	0.54	0.78	0.018	0:023	0.18	0.98	0.21	0.09	0.14
E	0.48	0.75	0.026	0.021	0.20	0.98	0.24	0.09	0.04
G	0.52	0.85	0.020	0.024	0.27	1.01	0.20	0.04	0.12

In the prior processing, bars of about 3-in. diameter were forged to small bars about 1/2 in. square, from which were cut standard size Charpy bars, which were left unnotched. The pieces were heated, quenched and tempered, the notch being cut after all heat-treatment was completed. (The notch was ground with a thin abrasive wheel, as described earlier, about 1/6 in. wide, 0.079 in. deep.) The heating temperature in various tests ranged from 1475° to 1600°F., and the quench ranged from oil to 10 per cent brine. In this group of steels, there was no detectable variation due to heating temperature in this range. or to change in quenching medium, compared to a recognizable variation due to change in steel and the marked variation due to change in tempering temperature. The tempering range was from no tempering to 600°F. The average change in notch-bar breaking energy with change in tempering temperature is recorded in Table 7 and plotted in Fig. 16.

Table 7.—Effect of Tempering Temperature on Notch-bar Toughness of Five Heats of WD 4150 Steel

Steel	Poot-pou	nds after F	ollowing To	empering
Steel	None	400°F.	500°F.	600°F.
A	4.8	26.5	18.2	20.9
CDEG	2.2	16.2	14.9	16.6
P	2.6	11.9	10.7	13.5
G	3.5	17.6	14.7	14.1

Table 7 and Fig. 16 show that these steels follow the familiar pattern of low-alloy steels, in that the notch-bar toughness increases at first as the tempering temperature is raised, up to a temporary maximum when the tempering is at about 400°F., followed by a falling off to a new minimum at about 500° to 600°F. This is followed finally by a sharp increase when the tempering is at still higher temperatures, such as 800° to 1100°F., not shown here.

It seems of interest to speculate about the reason for the decrease in notch-bar toughness, when the tempering temperature is raised from 400°F. to about 500° or 600°F.

than the internal stress is dissipated. The present work happens to deal with other aspects of the situation, so that no actual data became available in regard to this

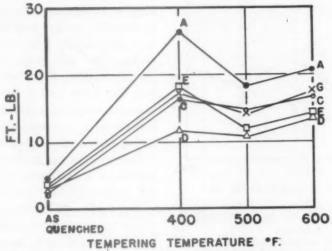


FIG. 16.—NOTCH-BAR TOUGHNESS OF FIVE HEATS OF WD 4150 STEEL (Armiento).

This behavior, widely experienced but still unexplained, is anomalous in that, over most of the tempering range, when a piece is softened by tempering and thus acquires a lower yield point, its toughness increases. Such behavior is normal, and is understandable according to present concepts. But in raising the tempering temperature from 400°F. to 500° or 600°F., although the steel is softened and the yield point decreases, the notch-bar toughness decreases.

Various possible explanations have been suggested for this behavior. The present author long ago ascribed the loss in toughness to the decomposition of retained austenite, since the retained austenite is decomposed in this range of temperature. To his embarrassment, he now finds that position scarcely tenable, in the light of experiments presently to be described. Bain suggests that another possibility presents itself for consideration; namely, that if one attributes low plasticity to the presence of internal stress, one might reason that the strength falls off faster

hypothesis. Such data are much needed and ought to be forthcoming. Hodge⁷ suggests that the phenomenon is somehow associated with precipitation of carbides. In a very special sense, the present data seem to support the idea that this behavior plays a part, as will presently appear.

Before discussing the metallurgical behaviors, let us consider the mechanism of notch-bar breakage as to path or position of breakage, because any proposed metallurgical explanation must of course be consistent with the observed path of breakage. In experiments already described, it was shown that, when ferrite was precipitated in the prior-austenite grain boundaries, the toughness was decreased and the path of rupture was in this ferrite in the grain boundaries. It seems most reasonable to ascribe this behavior to the lower cohesive strength (lower disruptive strength) of the ferrite. In other words, the toughness was decreased because of weakness introduced at the grainboundary regions. Proceeding now to

normally quenched steels, considering Figs. 10 to 13 and the data of Table 4, it was observed that in this steel, when the tempering temperature was 400° F.

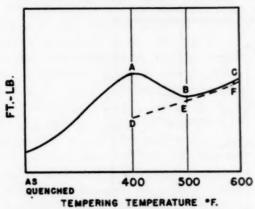


FIG. 17.—HYPOTHETICAL EFFECT OF RE-FRIGERATION, IF RETAINED AUSTENITE IS RESPONSIBLE FOR ANOMALY.

Solid line, quenched and tempered. Broken line, quenched, refrigerated and

tempered.

or lower, the fracture appearance was partly or largely rough, with strong indications that the rough appearance represented transgranular fracture whereas when the tempering temperature was 500°F. or higher, the fracture surface consisted largely or almost entirely of bright facets, with quite valid evidence that these facets represent fracture in the grain boundaries. It scarcely seems too venturesome, then, to state rather definitely that, in proceeding from a tempering temperature of 400°F. to one of 500°F. or higher, the character of fracture changes from one that is partly or largely transgranular to one that is largely in the grain boundaries, at these large grain sizes in this steel at least. But we have also seen that, in raising the tempering temperature from 400°F. to 500° or 600°F., we encounter a loss in toughness. Are these two phenomena related? It would appear that they could well be, if we consider the hypothesis of weakness at the grain boundaries.

When the pieces were tempered at 400°F. or below, the fracture was partly or

largely transgranular, hence it is obvious that the weakest regions at the moment of fracture were the transgranular paths. But when the pieces were tempered at 500°F. or above, the path of fracture was largely or almost entirely in the grain boundaries, so that now the grain boundaries are weaker than the transgranular paths. Are the grain boundaries now actually weaker than before, or are they only relatively weaker because the transgranular paths became stronger? It seems justifiable to conclude that they actually are weaker, on the following basis:

Referring to the experiments on loss of toughness when ferrite was precipitated in the grain-boundary regions, it was concluded that toughness was decreased because of weakness introduced at the grain-boundary regions. Analogously, in going from 400° to 500°F. tempering temperature, we observed (Table 7) that the toughness was decreased, and we have seen that with this increase in tempering temperature the grain boundaries became at least relatively weaker. Consequently, because there is a decrease in toughness in spite of the lesser hardness (lower yield point), we conclude that the grain boundaries became actually weaker.

Any proposed explanation for the decrease in toughness, when going from a tempering temperature of 400°F. to 500° or 600°F., must in our view take into account the weakening of the grain boundaries. Let us therefore now examine proposed metallurgical explanations.

EFFECT OF RETAINED AUSTENITE

What experiments can be devised to evaluate the effect of retained austenite? The most direct test, of course, would be to compare a steel containing retained austenite with the same steel free of retained austenite. A way to do this is provided by the fact long known, and more recently explored by Cohen and associates, that if a quenched steel is refriger-

ated to very low temperatures its retained austenite is *more or less* completely decomposed. Consequently, for our purposes we may 'examine the toughness of steels duced here, that the retained austenite has been eliminated by the tempering at 500°F. But we may also practically eliminate the austenite by refrigeration, and then

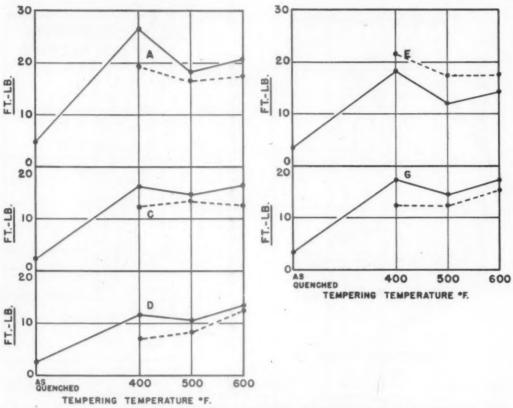


Fig. 18.—Effect of intervening refrigeration in Quenched and tempered WD 4150 steels of Fig. 16 (Armiento).

Solid lines, quenched and tempered.

Broken lines, quenched, refrigerated and tempered.

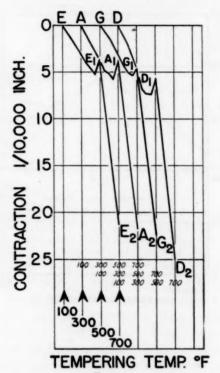
quenched and then tempered directly with that of the same steels quenched and then refrigerated before tempering. Before we examine the data, we may speculate a little as to what we should expect to find if decomposition of retained austenite is the sole reason for the loss in toughness.

In view of the data in Table 7 and Fig. 16, we recognize that a normal behavior for quenched and tempered steels of this type is as shown by the solid line in Fig. 17. Consider position B, representing a tempering temperature of 500°F. We know, from much evidence of earlier investigators and other evidence to be ad-

temper at 500°F., resulting again in a steel free of austenite and tempered at 500°F. The steel, therefore, should exhibit about the same toughness as the steel at B, under our assumption that the retained austenite was the sole influencing factor. Consequently, in Fig. 17 we plot the conjectured toughness of the refrigerated and 500° tempered steel at point E. Further, under our assumption that the retained austenite is the sole reason for the anomalous behavior, we should expect the refrigerated steel (with its freedom from retained austenite) to respond to tempering in the normal manner: i.e., it should be

tougher than at point E when tempered above 500°F.—for example, as at point F for 600°F.; and be *less tough* than at point E when tempered below 500°F.—for ex-

intervening refrigeration are shown in the dotted lines. It is seen that only one of the steels, namely steel D, fulfills both of the conditions anticipated in case retained



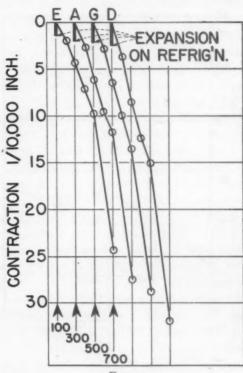


FIG. 19.

FIG. 20.

FIGS. 19 and 20.—CONTRACTION ON TEMPERING OF QUENCHED WD 4150 STEELS. ALL MEASUREMENTS AT ROOM TEMPERATURE AFTER TEMPERING (Rosenthal).

(Note shift of abscissa for each steel, to avoid overlapping.)

Fig. 19, quenched and tempered; Fig. 20, quenched, refrigerated and tempered.

ample, as at point D for $400^{\circ}F$. To summarize, if retained austenite is the sole factor in the anomaly, then, if a quenched steel is refrigerated before tempering, it should behave according to the dotted line D E F in Fig. 17, and the product tempered at $400^{\circ}F$. should be markedly less tough (point D) than when tempered without refrigeration (point A).

Let us see what actually happened. The five steels of Table 7 and Fig. 16 were quenched, refrigerated in liquid nitrogen and then tempered. The results are plotted in Fig. 18, one chart for each of the five steels, the full line representing the steel quenched and then tempered directly (same data as Fig. 16), while the data for

austenite was the sole factor in the anomaly, in that it was less tough than the normally treated steel after a 400°F. temper, and was also progressively tougher after higher tempering temperatures.

These data certainly indicate that retained austenite is not the sole factor in the anomaly, unless the refrigeration failed to remove the austenite in some of the steels. To test this point, recourse was had to a study of volume changes as indicated by length measurements. Cylinders of steels A, D, E and G were prepared, about 1-in. diameter and about 2½ in. long; these were hardened by quenching, the ends were ground parallel and length measurements were made. The cylinders

for the first series were then tempered without intervening refrigeration over a range of temperatures, the length being measured after each tempering, and the sion upon tempering. The data for the second series, involving refrigeration, are shown in Fig. 20. The expected expansion upon refrigeration was observed, as indi-

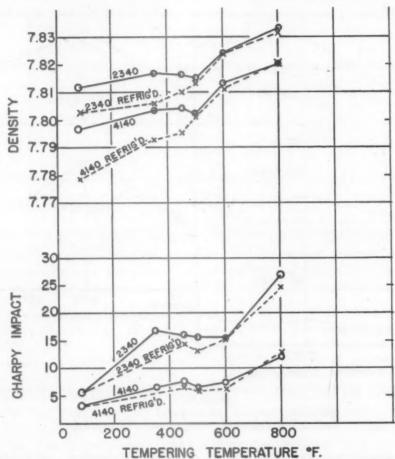


Fig. 21.—Changes in notch-bar toughness and in density upon tempering SAE 2340 and SAE 4140 steel (Darken).

results are shown in Fig. 19. As has been shown so often before, there is contraction up to about 400° F. due to tempering of martensite, then at 500° F. an expansion is indicated at points E_1 , A_1 , etc., due to a predominating conversion of austenite to alpha iron (or 500° bainite) and thereafter a contraction due to further tempering of martensite as to points E_2 , A_2 , and so forth.

If the austenite is previously transformed by refrigeration, the refrigeration should be accompanied by an expansion, and thereafter there should be no 500° expancated, and there was little if any indication of any change at 500°F. (only a slight change in slope and certainly no rise as before). The only slightly curious situation is in the amount of expansion upon refrigeration. Steel E, which departed most (Fig. 18) from the hypothesized Fig. 17, had the least expansion upon refrigeration, and steel D, which conformed rather well to Fig. 17, expanded the most. There seems to be no doubt that the retained austenite was quite thoroughly transformed. (These expansion tests on

cylinders were checked on specimens of Charpy size, and the results were substantially the same.)

The point was also tested by making

in the regularly quenched and tempered steel; the refrigerated steel, while less tough than the unrefrigerated steel at 400° to 450°F., nevertheless also shows a reduced

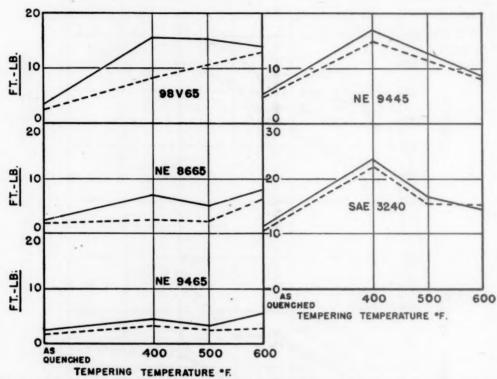


Fig. 22.—Effect of intervening refrigeration in five quenched and tempered steels (Armiento).

Solid line, quenched and tempered Broken line, quenched, refrigerated and tempered

density measurements and notch-bar tests on two steels, an SAE 2340 steel and an SAE 4140 steel, as shown in Fig. 21. Again there is the localized minimum in density in the regularly quenched and tempered steels at 500°F., with absence of such a minimum in the steel with intervening refrigeration in liquid nitrogen. Attention is called to the rather pretty concordance in density of the pieces tempered at 500°F.; the density was the same whether the austenite was destroyed by the 500°F. tempering alone or by the prior refrigeration followed by tempering. In the Charpy test, there is a zone of reduced toughness at 500° to 600°F. toughness at around 500°F. tempering when compared with 400° tempering.

Notch-bar tests were also made on the five lots of steel listed in Table 8.

These steels were heat-treated in the normal manner and tested after notching as previously described, and were also heat-treated with a refrigeration in liquid nitrogen intervening between the quenching and the tempering. The values are shown in Fig. 22, and again it is seen that the data are equivocal as far as deciding the role of austenite is concerned: i.e., in some steels there was resemblance to the postulates of Fig. 17 and in others there was not. (It will be understood, of

course, that, since each "type" of steel in Fig. 22 is represented by only a single heat, the behaviors are not necessarily characteristic of the several types. The the austenite is still present) are generally at least a little tougher than the refrigerated pieces (in which the austenite has been transformed), the difference being some-

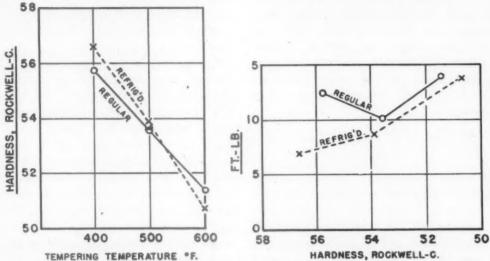


FIG. 23.—Development of hardness by refrigeration and its relation to notch-bar toughness.

recognizable variations within a single type, as exemplified in Figs. 16 and 18, illustrate this point.)

These examinations of 12 lots of steel, of various low-alloy compositions, raise a question as to whether austenite plays any role. On the one hand, we may surely conclude that austenite is not the main factor in the loss of toughness around 500° to 600°F., because breakdown of the austenite (by refrigeration) rarely if ever eliminates this loss of toughness. On the other hand, if we compare the two treatments after tempering at only 400°, we observe that the regular pieces (in which

times rather marked and sometimes only very slight. This suggests that austenite may play a part (or do we detect here merely a reluctance to abandon the austenite theory!).

In connection with the lesser toughness of the refrigerated steels, a question might be raised as to whether the modest increase in hardness, to be expected when the retained austenite is transformed by refrigeration, would account for the lessened toughness. It seems definite that it does so in certain marginal instances, but that it is by no means always responsible is indicated in Fig. 23. Hardness measure-

TABLE 8 .- Steels Shown in Figure 22

				Compos	ition, Per	Cent			
Type	С	Mn	P	S	Si	Ni	Cr	Мо	v
08V65	0.60	0.98	0.014	0.008	0.14	1.04	0.87	0.28	0.08
NE 8665 NE 9465	0.62	1.22	0.014	0.014	0.30	0.59	0.51	0.09	
NE 9445 SAE 3240	0.49	0.46	0.023	0.025	0.53	1.65	0.35	0.11	

ments were made on selected broken notch-bar pieces of steel D of Fig. 18, the selection being made on the basis that their behavior was typical. The hardness readings at the left show the relative hardnesses in the two sets of samples when tempered as shown. At the right, the notch-bar values are plotted against hardness (instead of against tempering temperature), showing that there are features in the behavior other than hardness.

Decrease in Cohesive (Cleavage) Strength

A lesser "toughness" implies in these cases a lesser cohesive strength in the path of fracture. Consider the two cases: (1) in the case of the anomalous falling off in toughness, at around 500°F. tempering, any explanation must take into account the accompanying weakening, particularly at the grain boundaries; (2) in comparing steels tempered at only 400°F., some steels are tougher than others—for instance, steel A compared with steel D in Fig. 16—and a steel with normal quenching and tempering may be more tough than when the same steel is treated with intervening refrigeration; e.g., steel D in Fig. 18.

Consequently in case 1, if retained austenite is involved, (a) it must have been present in the grain boundaries, and (b) its 500° decomposition product (lower bainite) must have lower cohesive strength than austenite. As to a, it is known that most of the retained austenite occurs as small polyhedra within the grain, and not at the grain boundaries; as to whether even small regions of austenite are present at grain boundaries, microscopic appearance suggests that little or none is present. As to b, whether austenite has a higher cohesive strength than lower bainite, evidence is lacking.

With reference to case 2, involving steels tempered at only 400°F., the path of fracture is generally transgranular.

If retained austenite has a favorable effect, it could presumably do so only if its cohesive strength is greater than that of tempered martensite, and here again evidence is lacking. Further, there was no evidence that the tough steel A of Fig. 16 had more retained austenite than the less tough steel D.

To summarize then, we may say that retained austenite (and its decomposition) cannot be the feature responsible for the loss in toughness when raising the tempering temperature from 400°F. to 500° or 600°F., and further data will be needed before it can be decided whether it is responsible even in part. Additional data are also needed mainly to decide whether the austenite that is still present after a 400°F. tempering plays a part in the degree of toughness found after such 400°F. tempering.

PRECIPITATION OF CARBIDES

The idea that the 500° loss in toughness might be due to precipitation of carbides seemed worthy of investigation because of two circumstances; namely, (1) Antia, Fletcher and Cohen9 produced evidence strongly supporting earlier evidence that the precipitation of iron carbides begins only when a tempering temperature of 400°F. has been exceeded; (2) precipitation and agglomeration of carbide would of course establish a larger "mean free ferrite path," shown by Gensamer, Pearsall, Pellini and Low10 to reduce the "crack strength." A lower crack strength would result in less toughness by the same mechanism as was shown to operate in the case of ferrite precipitated in martensite grain boundaries because of the correspondingy lower cohesive (cleavage) strength of the ferrite.

Since the grain-boundary cleavage, in going from 400° to 500°F. tempering, became prominent particularly with rather coarse grain size, and since microscopic evidence would presumably be clearer

at coarse grain sizes, the possibilities were investigated by coarsening a series of steels and observing their appearance at a series of tempering temperatures. As will presently be shown, agglomeration of carbides, with resultant more pronounced ferrite, did indeed appear to be observed at grain boundaries, upon tempering. A group of samples of a heat of 4150 steel was heated to approximately 2000°F. for ½ hr. and quenched in water. The samples were tempered as follows:

"No draw"
300°F.
400°
500°
600°
800°
1000°

(The sample designated "no draw" was actually tempered for a few minutes at about 250°F. because of mounting in Bakelite, but in microscopic appearance it was quite indistinguishable from other samples completely untempered.)

The untempered pieces showed unexpectedly, in the grain boundaries, a series of unetched or only lightly etching areas, possibly best described as spear-shaped masses, often but not always with serrated edges. A variety of typical shapes are shown in Fig. 24. The edges were not always sharply defined, as they sometimes merged imperceptibly into the body of the adjacent martensite grain. Except for their peculiar shape, they seem to have the characteristics of martensite needles and may perhaps be described as "martensite spines."

These spines occupy positions unmistakably in the grain boundaries of the parent austenite grains.

After tempering at 300°F., they etched more slowly than the body of the grain, so that at low magnification on the micro-

scope they clearly delineated the grain size by means of white outlines around darker etching martensite grains, as in Fig. 25A. Tempering at 400°F. caused them now to etch more rapidly than the bodies of the martensite grains, so that now the grain size was delineated by the darkened constituent surrounding lighter martensite grains, as in Fig. 25B. After tempering at 600°F., they again etched more slowly than the bodies of the grains, so that the grain size was delineated by lightetching areas surrounding the darker grains, as in Fig. 25C. It was an entertaining circumstance that, within a tempering range of 300°F., the grain delineation changed from light to dark and back again to light.

Of more importance possibly than the entertaining feature of these observations was the need for interpreting the phenomenon. It would appear that, except for their occurrence as relatively large masses in the grain boundaries, the behavior of these spines accords entirely with the tempering of martensite. The appearances at somewhat higher power are shown in Figs. 26 to 29. After 300°F. tempering, the spines still etched but slowly, as represented by the light areas in Fig. 26. After tempering at 400°F., the spines now etched rather rapidly, resulting in the dark appearance in Fig. 27. This is believed to be the typical dark-etching martensite, before any significant precipitation of carbide. After tempering at 600°F., the structure now etches but slowly, as in Fig. 28, and is believed to consist of ferrite containing the finely agglomerated carbides. Tempering at still higher temperature causes no significant change in this appearance, although it must be concluded that the carbides have probably agglomerated somewhat further. For example, Fig. 20 shows the structure after tempering at 1000°F., and this structure is typical of both lower and higher tempering temperatures such as 800° and 1200°F.

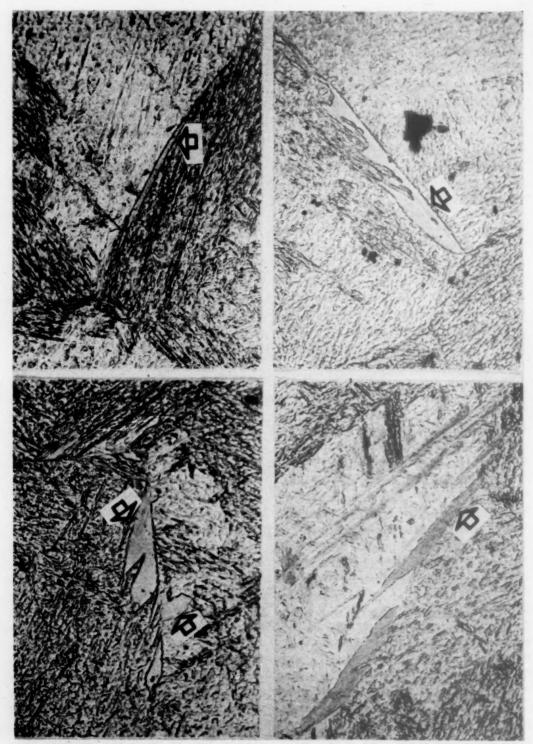


Fig. 24.—Typical shapes of "martensite spines" in grain boundaries of coarsened SAE 4150 steel. Picral etch. \times 650.

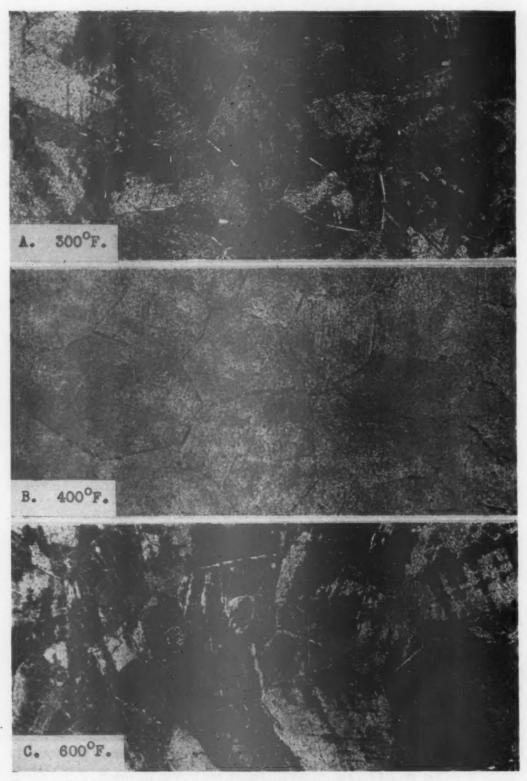
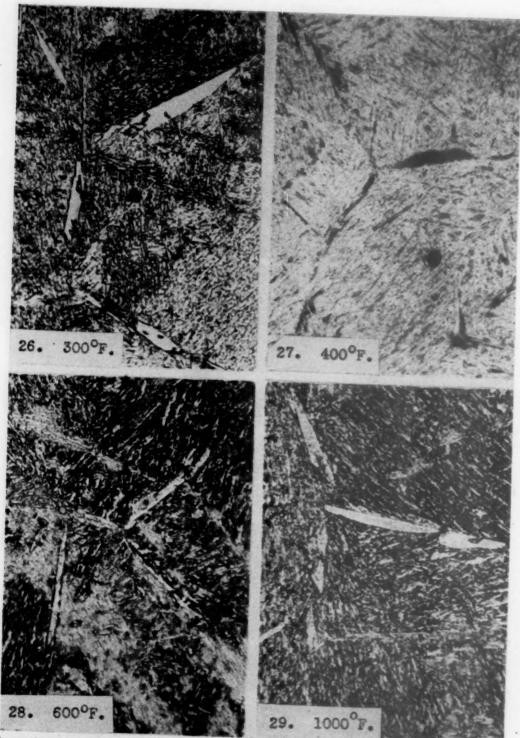


Fig. 25.—Delineation of grains by constituent whose etching characteristics change with tempering temperature. All picral etch. \times 100. A, 300°F.; B, 400°F.; C, 600°F.



Figs. 26-29.—Etching characteristics of grain-boundary constituent, after different tempering temperatures. All pickal etch. × 650. Fig. 26, 300°F.; Fig. 27, 400°F.; Fig. 28, 600°F.; Fig. 29, 1000°F.

A tempering at 500°F, happened in this case to be just at the point where the transition from the 400° appearance to the 600° appearance could be observed. Fig.

because of the occurrence of massive grainboundary "martensite spines."

If the precipitation and agglomeration of carbide begins at about 500°F. (as

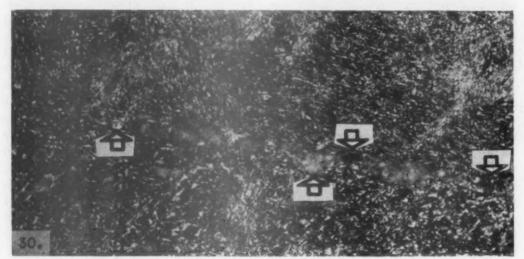


Fig. 30.—Appearance of grain-boundary constituent after tempering at 500°F. Picral etch. × 1000.

Upper arrows point downward to regions etching dark; lower arrows point upward to regions etching light.

30 shows spines that evidently are just in the process of transition, since the upper arrows point to regions that are still rather dark etching and resemble the 400° product, whereas the lower arrows point to regions that already have begun to take on the lighter etching characteristics of the 600° product. In general, it is difficult to find grain delineation in the 500° samples, because the grain-boundary spines are often at the stage where they are etching just about as rapidly as the body of the grain, being neither dark etching like the 400° product.

RELATION OF MARTENSITE TEMPERING TO MECHANICAL PROPERTIES

The foregoing observations lead to what seems to be a quite justifiable inference: that the loss in toughness upon tempering at 500°F. is a result of the normal process of the tempering of martensite, shown in this case particularly in the grain boundary

seems to be the case and as shown by Cohen et al. and others) there would begin at this temperature a weakening of the cohesive (cleavage) strength of the tempered martensite.

It appears that the relatively thick grain-boundary "martensite spines" create a situation in which each spine, after sufficient tempering, constitutes a relatively thick region of ferrite with embedded carbide. Because of the agglomeration of carbide, there would be a larger "mean free ferrite path," using the concept and terminology of Gensamer, Pearsall, Pellini and Low.10 In proceeding therefore from a 400° tempering to a 500° to 600° tempering, there would be a change from the 400° condition, where carbides are not yet precipitated and there cannot be said to be any "mean free ferrite path," to the 500° to 600° condition, where carbides would be precipitating and agglomerating. resulting in a probably very small but nevertheless effective mean free ferrite path, with a consequently lowered cleavage strength. This lower cleavage strength would lead to lower notch-bar toughness by the same mechanism as is found in the introduction of ferrite in the martensite (prior austenite) grain boundaries, by isothermal precipitation as described earlier.

In such coarse-grained material at least, where the "martensite spines" are found in the grain boundaries, the weakness at the grain boundaries (after 500° or higher tempering) causes the breakage of notchbar specimens to take place predominantly at the grain boundaries. Thus it appears that the martensite spines as quenched are strong (high cleavage strength), and retain their high strength when tempered at any temperature up to about 400°F. Consequently, in this grade of steel at least, there is no pronounced weakness at the grain boundaries when tempering at 400°F. or below, and the fracture is only partially in the grain boundaries. By contrast, when these spine regions are tempered at 500°F. or above, they become not only weaker than the spines tempered at 400°F. but also even relatively weaker than the remainder of the grain, so that the fracture takes place preferentially in the grain boundaries. (The extent of grain-boundary weakness, at tempering temperatures below 400°F., as pointed out earlier, varies with the composition of the steel as well as with grain size, so that some grades of steel at some grain sizes may fracture in the grain boundary even at tempering temperatures below 400°F. An example is coarsened high-carbon tool steel. No evidence is available as to the reason for this phenomenon.)

Other steels were then examined to ascertain the possible prevalence of the grain boundary behavior, as encountered in this 4150 steel. Steels of the compositions shown in Table 9 were at hand.

Samples were heated to 2100°F. to provide coarse grain size, quenched in water and specimens from each steel

tempered respectively at 350°F. and 1000°F. In Figs. 31 to 36, each figure represents a single steel, showing the structures after tempering at 350° and at 1000°, at low and at high magnifications for each. The compositions in Table o are arranged in the order of increasing carbon contents, regardless of the alloy composition, and the corresponding figures showing the microstructures are arranged in the same order. Viewing the micrographs in this order, the following circumstance may be observed. Examining the structures after the 1000° draw, it is seen that in the steel of lowest carbon content (0.25 per cent C.) there is no appreciable outlining of grains by tempered "martensite spines"; that at the highest carbon content (0.61 per cent

TABLE 9.—Steels Examined for Grainboundary Fracture

No.	Steel	Composition, Per Cent							
No.	Type	С	Mn	Si	Ni	Cr	Mo		
1	8630	0.25	0.83	0.22	0.48	0.51	0.19		
2 3 4 5 6	4135	0.34		0.25	0.16	0.98	0.20		
3	T1335	0.36	1.97	0.29		0.09	0.00		
4	4340	PO.38	0.90				0.22		
5	1345	0.45	1.08	0.32	0.16	O.II	0.07		
0	8660	0.61	1.25	0.24	0.60	0.55	0.12		

C) the outlining of grains by tempered "martensite spines" is quite definite; and that, between the two extremes of carbon contents, the degree of definiteness of grain-boundary delineation by tempered "martensite spines" increases fairly regularly with the carbon content. Here again the relationship of grain-boundary fracture in the notch-bar test to grain boundary tempered "martensite spines" in the microstructure came into evidence. The broken notch bars, from which the micrographs of Figs. 31 to 36 were prepared, were examined as to prevalence of bright facets, which (as described earlier in the paper) are believed to represent fracture in the grain boundaries. The pieces examined were the ones tempered at

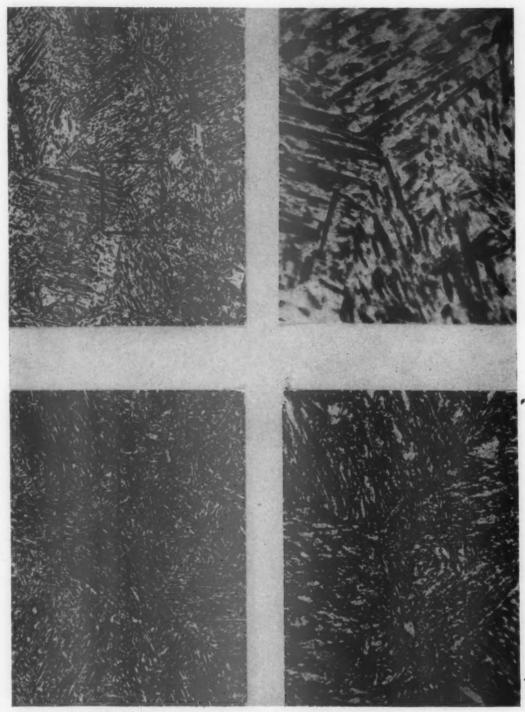


Fig. 31.—Steel No. 1. Heated to 2100°F., Quenched in water, tempered at 350°F. and at 1000°F., respectively.
Tempering: Upper two, 350°F., lower two, 1000°F.
Magnification: Left, × 160; right, × 700.

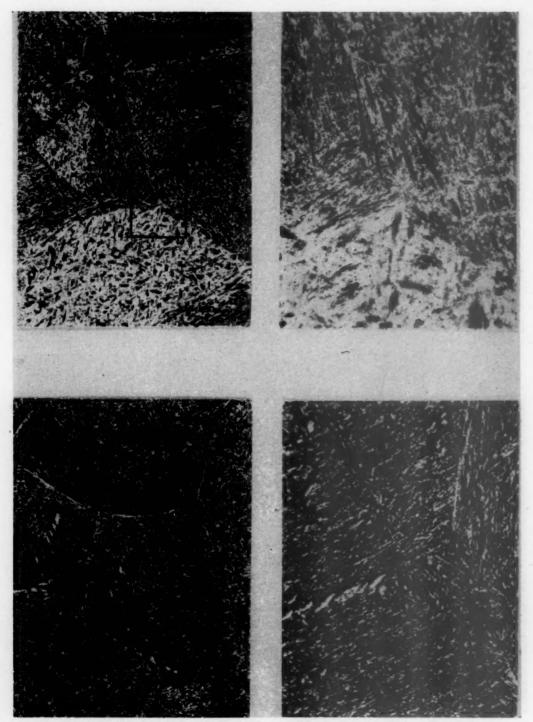


FIG. 32.—Steel No. 2. TREATMENT SAME AS STEEL IN FIG. 31.

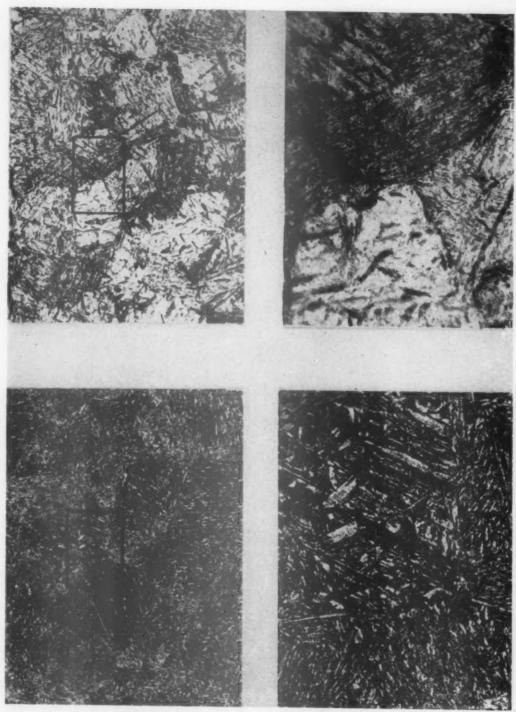


Fig. 33.—Steel No. 3. Treatment same as steel in Fig. 31.

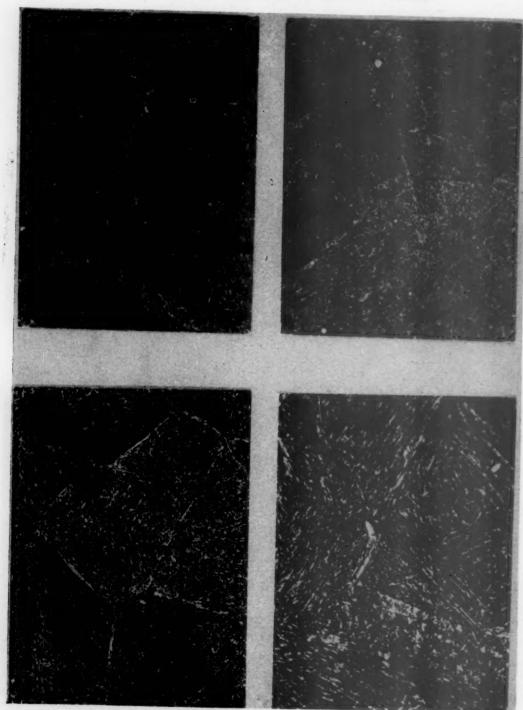


Fig. 34.—Steel No. 4. Treatment same as steel in Fig. 31.

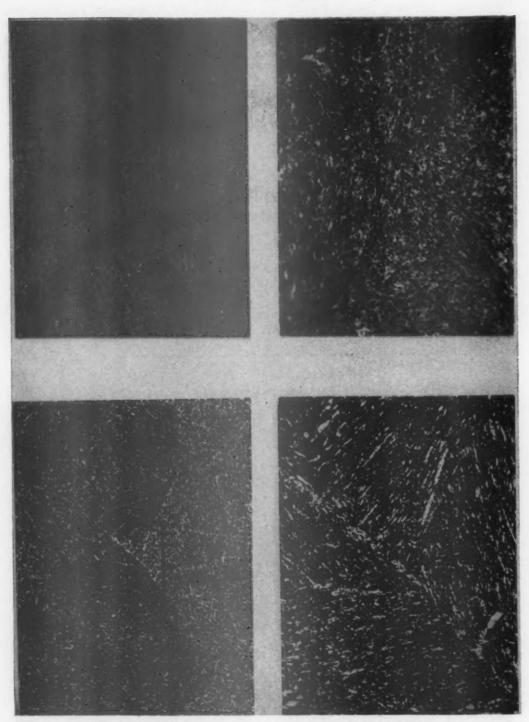


Fig. 35.—Steel No. 5. Treatment same as steel in Fig. 31.

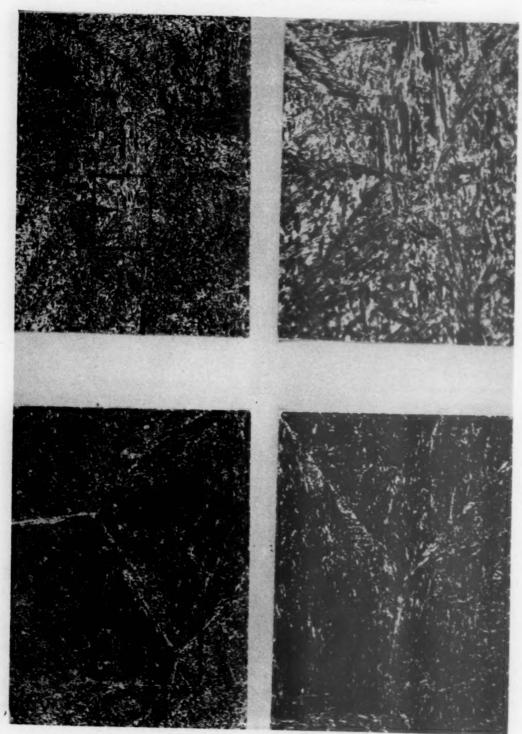


Fig. 36.—Steel No. 6. Treatment same as steel in Fig. 31.

1000°F. When arranged in the order of increasing proportion of bright facets, the order was found to be almost precisely in the order of increasing appearance of grain-

occurrence of the tempered "martensite spines" is merely a circumstance in coarsened high-carbon steels, which circumstance made it possible to draw certain

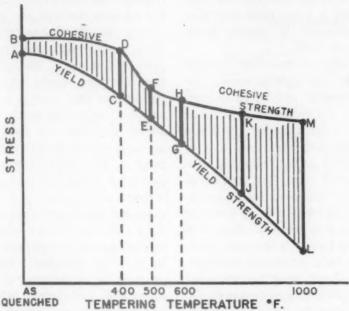


Fig. 37.—Relation of yield and fracture strengths upon tempering a quench-hardened steel.

boundary tempered "martensite spines," which, as stated, was about the same as the order of increasing carbon content.

Consequently, one is led to conclude that the formation of "martensite spines" in the grain boundaries seems more likely to occur with higher carbon contents. However, this does not imply that the tempering mechanism in itself in the low-carbon steels differs from that in the high-carbon steels. It means merely that the weakened tempered martensite positions are now within the grains without any preferential occurrence in the grain boundaries. Consequently the fracture in low-carbon steels takes place through the grains, as observed in the series just described. Hence any reduced toughness after 500° to 600° tempering (as compared with 400° tempering) is presumably due to the same mechanism of tempering as in the case of the higher carbon steels. In short, the conclusions as to the mechanism of tempering as related to the loss in toughness after 500° tempering. It is to be inferred, therefore, that the loss in toughness after tempering at 500°F. is due to the same mechanism, even in the lower carbon steels. Furthermore, the observations recounted here have embraced only the steels in the coarsened condition, to facilitate microscopic examination. No data are at hand, as yet, as to the behavior in the fine-grained condition, which obtains in steels as ordinarily heat-treated from normal lower quenching temperatures. But it is likewise to be inferred that the 500° loss in toughness is due to the same type of mechanism, even though the grain-boundary occurrence of "martensite spines" may be much more limited at the lower quenching temperatures. In brief, whether the fracture takes place in the grain boundaries or within the grains, it seems

justifiable to conclude that the loss in toughness after 500° tempering (as compared with 400° tempering) is due to agglomeration of carbides leaving ferrite with its consequent relative weakness, and that, as Bain phrased it upon reviewing these data, the phenomenon is inherent in the tempering process itself.

It may be noted further that, as tempering proceeds, the carbides would continue to agglomerate and hence increase the "mean free ferrite path." This would result in still lower cohesive (cleavage) strength. Contrasting with this, it is of course known that as the tempering temerpature is raised from, say, 600°F. to say 1000°F., the notch-bar toughness increases, rather than decreases, as would be expected if cohesive strength alone were the determining factor. It is known, however, that the yield point also decreases, and consequently it must be concluded that the yield point falls more rapidly (so to speak) than does the cohesive strength. As pointed out by many and as described above, the "toughness" in a notch-bar test is a measure of the amount of flow from yield point to fracture. Consequently it must be concluded that even though the cohesive strength decreases, the yield point decreases still more rapidly, as the piece is tempered; in other words, the interval between yield point and cohesive strength increases as the tempering temperature is raised, so that the amount of flow (and consequently the energy absorbed in breaking) increases as the tempering temperature is raised beyond 600°F.

One may therefore conceive a general picture of the effects of the tempering process on the toughness of steel. The quenched steel, before tempering, has a high yield strength, so that when the notched bar is stressed beyond the yield strength it very soon reaches the cohesive strength (only a little deformation) and the piece is brittle. When it is tempered lightly, up

to 400°F., the yield strength becomes lower whereas the cohesive strength falls but little if at all; consequently, when the metal is stressed beyond the yield strength, it deforms somewhat more before reaching the cohesive strength, and consequently is a little "tougher" than before tempering. Upon raising the tempering temperature from 400° to 500°F., the cohesive strength now falls more rapidly than does the yield strength, so that there is less deformation and the steel is less tough. Thereafter, as already described, the yield strength falls the more rapidly so that the steel becomes tougher. The effect of tempering in the case of a notch-bar test may therefore perhaps be pictured in a possibly oversimplified but nevertheless suggestive diagram (Fig. 37). Stress is plotted vertically and tempering temperature horizontally. In the "as quenched" state, the yield point A is very close to the cohesive strength B, and there is little plastic flow before rupture, the extent of flow being represented by the interval AB. At a tempering temperature of 400°F. the yield strength has fallen appreciably, as to point C, while the cohesive strength has fallen but little if at all, as to point D. The amount of flow is therefore represented by the greater interval CD and the steel is tougher than at AB. After tempering at 500°F., the yield point has fallen further. but the cohesive strength has fallen even more markedly, so that the interval EF is less than CD at 400°F. After 600° tempering, the interval GH is usually again a little greater than EF, so that the steel after 600° tempering is a little tougher than the 500° product. However, the relationship is sometimes such that the 600° product is less tough than the 500°, so in that case GH would be less than EF. Thereafter, as the tempering temperature is raised, the toughness becomes increasingly greater, as represented for example by the increasing lengths of intervals such as JK and LM.

PROBLEMS

Even though the conclusions drawn here should prove to be valid, the data that have been presented serve only to raise many more questions.

Is the inference actually warranted, as seems permissible, that the behaviors described for coarsened grains represent the behavior of steels in the normal uncoarsened, fine-grained condition?

What shall be done about grain-size fracture standards?

Why do quenched steels (without tempering) tend to break more pronouncedly in the grain boundaries when the grain size is coarse?

Why do steels of different compositions,

and especially of different carbon contents. display different tendencies to break in the grain boundaries, (1) when tempered, (2) untempered?

REFERENCES

- I. C. H. Grattan: Harper's Magazine (June
- 1945) 190, 577. 2. K. Heindlhofer: Trans. A.I.M.E., Iron and
- Steel Div., (1935), 116, p. 232.

 3. M. Asimow: Personal communication.

 4. E. C. Bain: Personal conversation.

 5. J. R. Vilella and E. C. Bain: Metal Progress
- J. R. Vilella and E. C. Bain: Metal Progress (1936) 30, 39-45.
 E. C. Bain: The Alloying Elements in Steel, 285. Amer. Soc. for Metals, 1939.
 J. M. Hodge: Personal conversation.
 P. Gordon and M. Cohen: Trans. Amer. Soc. for Metals (Sept. 1942) 30, 569.
 Antia, Fletcher and Cohen: Trans. Amer. Soc. for Metals (New York) 2000.

- Soc. for Metals (1944) 32, 290.

 10. Gensamer, Pearsall, Pellini and Low:

 Trans. Amer. Soc. for Metals (Dec. 1942), 30, 983.

A Radiation Pyrometer for Open-hearth Bath Measurements

BY H. T. CLARK* AND S. FEIGENBAUM, † MEMBERS A.I.M.E.

THE importance of measuring the temperature of molten steel in the open-hearth furnace has been recognized for many years. Poor temperature control may be costly to steelmaking operations and lead to a lowered quality of the steel. Low or excessive temperatures may shorten the life of the furnace, ladles and molds. Rates of reactions in the furnace and efficiencies of deoxidizers are known to change materially with a change in the temperature of the metal and slag. Ladle skulls and mold and stool stickers cause steel to be scrapped instead of being converted into useful products. Finally, the structure, segregation and surface condition of ingots are affected by the teeming temperature.

Mill investigations of the effect of bath temperature upon steelmaking operations have been largely qualitative in character, based upon observations by practical melting men. The physical chemist has used the empirical information available and has reached reasonable and useful conclusions with respect to the various melting processes. The introduction of a reliable direct-reading pyrometer will permit accurate quantitative evaluation of the effects of temperature and should furnish a more rational basis for study of the thermochemistry of steelmaking.

The problem is not merely one of making a small number of temperature measurements in the open-hearth furnace. This has been done by several methods to a degree of precision that was apparently satisfactory. Considerable effort by a number of investigators has been directed rather to the development of an openhearth bath pyrometer that would be both accurate and practical for routine measurements. To be practical, the pyrometer should be inexpensive to operate; that is, the installation, operating and maintenance costs should be exceeded by the tangible benefits to the open-hearth operator.

Temperatures from 2800° to 3100°F. are encountered in the open-hearth furnace. The surface of the molten metal is covered by several inches of slag, which prevents direct observation of the metal surface for optical or radiation measurements. Both slag and metal are highly reactive at these temperatures and will attack to a greater or lesser extent any material immersed in them. Adequate protection of thermocouples, which of necessity must be brought to the temperature of the bath, has generally resulted in a large, heavy assembly made up of brittle materials, unsuited for handling on the open-hearth floor. The life of the equipment was short and maintenance was an important consideration.

EARLIER WORK

Any one of a number of physical properties of liquid steel could conceivably be used as a basis for temperature measurement. Efforts to the present time, however, have been confined largely to measuring either the thermal electromotive force generated between two dissimilar materials immersed in the steel or the intensity of radiation from the surface of the steel. These

Open Hearth Proc., 1946.
† Open-hearth Metallurgist, Jones and Laughlin Steel Corporation, Aliquippa, Pennsylvania.

^{*}Assistant Manager, Research and Development, Jones and Laughlin Steel Corporation, Pittsburgh, Pennsylvania. Issued as T.P. 2031 in METALS TECHNOLOGY, June 1946; also in Open Hearth Press, 2006.

employ one of the various forms of thermocouple or some type of radiation-measuring device such as an optical pyrometer, photoelectric cell or thermocouple radiation pickup element.

A tungsten-molybdenum thermocouple was used by B. Osann and E. Schroder, G. Leiber, and S. Fornander and T. Omberg in electric and open-hearth furnaces. The elements were encased in protection tubes to prevent attack by slag, metal and furnace atmosphere. From three to six readings could be taken without changing the thermocouple and the immersion time in the furnace for each reading was two to three minutes.

The tungsten-graphite thermocouple, proposed by H. L. Watson and H. Abrams,4 and further developed by F. Holtby,5 uses the graphite as one of the elements and. in the conventional assembly, as a protection tube for the tungsten. In a later paper, Holtby6 describes a divided thermocouple of small heat capacity, which completed the hot junction through the molten metal. This thermocouple may be used in molten iron or steel but in the latter the elements will dissolve quickly if not protected by an outer refractory tube. Different lots of tungsten and of graphite will vary somewhat in calibration and compensation is required in order to obtain reliable temperature values.

The carbon-silicon carbide thermocouple was developed by G. R. Fitterer⁷ and has been used to measure molten iron and steel temperatures. The silicon carbide element is enclosed in a graphite sheath, which, as in the tungsten-graphite thermocouple, is both the other element and the protection tube. The electromotive force generated by this thermocouple is exceptionally high—nearly ½ volt at 3000°F.

The platinum-platinum rhodium thermocouple, because of the careful standardization of the thermoelectric properties of the A few years ago English metallurgists, seeking to take advantage of the standardized elements of the platinum-platinum rhodium thermocouple, worked out a technique¹⁰ using a single thin-walled quartz tube as protection for the thermocouple. This method has now been employed in this country by Weitzenkorn¹¹ and in Canada by Freeman.¹² The advantages lie in rapid measurements, lower maintenance costs and more reliable readings.

Radiation methods include as a measuring device the optical pyrometer, which is found in practically every open-hearth shop; its use has been described by Blaurock,13 Cook,14 and Wenzl and Morawe.8 The last named investigators report that only a small correction is required to make the results comparable to readings with the platinum thermocouple when the optical pyrometer is sighted on the bright areas of the stream of molten metal. Various modifications using an optical pyrometer, a photoelectric cell or a total radiation element have been suggested to make possible temperature measurements of the molten metal itself in the openhearth furnace.

One of these modifications is the openend tube, immersion pyrometer described in this paper. Its principle is based on Patent No. 2020019, granted to Collins and Oseland; its use as a photoelectric pyrometer has been discussed by Sordahl and Sosman^{15,16} and as a total radiation

wires, has been generally accepted as the standard pyrometer for measuring steel temperatures, and a number of investigators^{8,9} refer to its use and to comparisons with other pyrometers they were investigating. In this instrument the elements must be protected against attack by reducing gases, and hence require a gastight inner protection tube. This tube in turn is protected normally by an outer tube having greater resistance to attack by molten slag and metal.

¹ References are at the end of the paper.

pyrometer by Bradley¹⁷ and Martin.¹⁸ The manner in which the open-end tube pyrometer is used is illustrated in Fig. 1. The steel tube, with an orifice in the front of the steel rather than of the slag surface or back wall of the furnace and may be readily charted by means of a high-speed, automatic recorder.

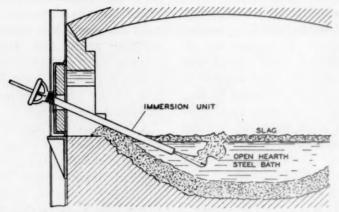


FIG. 1.—Position of open-end tube, immersion pyrometer, while a reading is being taken in the open-hearth furnace.

end, is thrust through the slag into the liquid steel. A continuous flow of air keeps the molten slag and metal from entering the tube and opens a cavity into which the radiation-sensitive device is sighted. Used originally with an optical pyrometer sighted through a glass window at the rear end of the tube, it was later adapted to operate with pickup elements, the outputs of which could be permanently recorded.

DEVELOPMENT OF THE PYROMETER

The present paper describes a modified form of this pyrometer, using a total radiation element, that has performed satisfactorily in extended tests. The openend tube has several features that make it particularly attractive as a means of measuring liquid-steel temperature. Unlike the thermocouple, no part of the pyrometer attains the temperature of the steel; this simplifies the design, since refractory materials are not required and the maintenance problem is materially lessened. The choice of a suitable radiation element is dictated by requirements of mechanical ruggedness and electrical and thermal stability. Temperatures obtained are those

The work described by Bradley17 and Martin¹⁸ on this pyrometer seemed to offer promise if sufficient development were carried out on the instrument, and Iones and Laughlin approached the Leeds and Northrup Co., offering plant and research facilities for this work. The equipment was set up at Aliquippa and a series of readings was taken. The direction that the development work should take so that the instrument would be suitable for routine temperature measurements in the openhearth bath quickly became apparent. Several major changes were made over a period of time and these have all contributed to the present form of the pyrometer.

A high-speed recorder, the Speedomax, was substituted for the standard recorder in order to decrease to a minimum the time of immersion necessary to obtain a flat-topped temperature record. The Speedomax reaches a steady state somewhat more rapidly than the standard Rayotube when the latter is exposed suddenly to a constant source of radiation. Therefore, attention was directed to making the Rayotube as fast as is consistent with ruggedness and reproducibility

of readings. Speed of response is extremely important, since excessive heating of the tube may occur with even a few additional seconds immersion. Important also for

A reliable and simple means of checking the immersion unit is essential to the successful mill application of an openhearth pyrometer. The total radiation

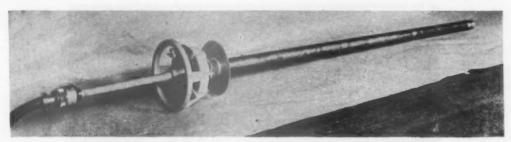


Fig. 2.—Immersion unit, showing outer steel pipe for protection of Rayotube control head, and special connector for air line and electrical leads. (Courtesy of Leeds and Northrup Company.)

reproducibility of readings was the arrangement of the Rayotube in the immersion unit to prevent errors due to: (1) a gradual change in the size of the outer orifice, (2) occasional freezing of steel around its periphery, or (3) to any slight shift in the position of the Rayotube relative to the outer orifice.

An improvement of a major nature was the change in location of the Ravotube from the rear of the immersion tube to a position within a few inches of the front orifice. Readings taken with the Rayotube in the former position were affected by the straightness of the tube and, since the pipe may warp during the course of an immersion, there was always some uncertainty as to the reliability of any reading. In addition, the solid angle of radiation viewed by the Rayotube was increased materially when it was moved to the forward position so that a faster response could be obtained with sufficient sensitivity. The design of a radiation pickup element to withstand the temperatures encountered in the present pyrometer and to give readings that are virtually unaffected by the rapid changes in ambient temperature involved, represents a most important contribution to this development.

elements are not particularly sensitive to visible radiation and hence a standard lamp cannot be used. Small furnaces equipped with thermocouples were tried but the temperatures easily attained are rather low and the setting of the pyrometer could not be checked readily in the steelmaking range. A method of comparing the output of the immersion unit with that of a similar unit reserved for checking purposes was therefore tried and proved successful. The flame or backwall of the open-hearth furnace itself was used as the source, hence the check was made at approximately the same temperature as that encountered in the molten steel.

As a result of these several changes, the reproducibility of the readings increased and the pyrometer gradually assumed its present form.

PRESENT FORM OF INSTRUMENT

The pyrometer assembly consists of the immersion unit, the checking unit with built-in galvanometer, the recorder and an air-flow regulator and air filter.

The immersion unit shown in Fig. 2 houses the Rayotube assembly and is made up of a 7-ft. length of pipe, fitted on the one end with a ½-in. orifice, and on the other with a head containing the

necessary control equipment. The immersion unit weighs 60 lb. and is regularly handled by one operator. The outer pipe is in three sections welded together. The tip

potentiometer dial in the head and this is adjusted during the checking operation to obtain a null galvanometer reading. A receptacle for the lead wires from the check-

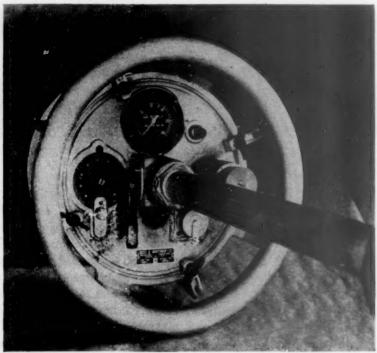


FIG. 3.—CIRCULAR CONTROL PANEL EQUIPPED WITH PUSH-BUTTON SWITCH, CALIBRATING DIAL, CALIBRATING SWITCH, AIR VALVE, AND PRESSURE GAUGE. (Courtesy of Leeds and Northrup Company.)

is bored to provide the orifice and the socket for the inner assembly; the middle section, 2 ft. long, is of heavy-walled (0.250-in.) tubing; and the remainder is standard 2-in. pipe. All the parts are made of low-carbon steel and several hundred immersions can be made before the pipe is discarded. In no instance to date has the inner assembly suffered damage.

A pressure gauge and an off-on valve on the air line are essential for safe and convenient operation. The control head is depicted in Fig. 3. A push-button switch is installed in the Rayotube circuit so that readings are taken only while the unit is immersed in the steel. The output of the Rayotube is regulated by means of a ing unit and a short length of r-in. pipe to bring in the air and shielded cable complete the equipment mounted on the head panel. Release of four clamps permits removal of this panel and of the entire inner immersion assembly as a single unit.

The Rayotube is mounted inside a double-walled pipe approximately 10 in. long, for protection from radiation and mechanical damage, as shown schematically in Fig. 4. Part of the air is deflected to flow between the walls to aid in cooling while the main portion flows between the outer wall and the outside tube. A collecting lens is mounted at the front end of the pipe. A thin glass window protects this lens from occasional sparks. A hole of 44-in. diameter in the front end of the

Rayotube assembly serves to define the useful radiation, and this inner orifice is only % in. from the front end of the outer pipe. The arrangement places the

of the inner assembly and also permits considerable latitude in the size of the front aperture.

The electric leads to the immersion unit

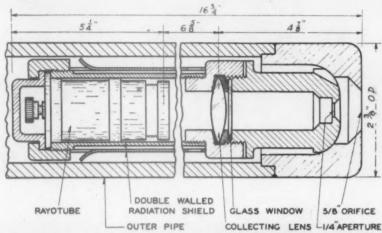


Fig. 4.—RAYOTUBE IN RELATION TO INNER AND OUTER ORIFICES, SHOWING RADIATION SHIELDS AND PATHS OF AIR FLOW.

sensitive element of the Rayotube less than 13 in, from the molten steel and permits the use of a solid angle of 17°.

The inner assembly (Fig. 5) is connected to the panel in the head of the immersion unit by means of a length of ½-in. pipe that also shields the lead wires from

are located inside the air hose, to prevent damage and wear. A covered receptacle in the shop floor houses the air regulator and filter and a combined air-electric connector for the flexible hose. Provision is being made to accommodate the complete immersion assembly in this space

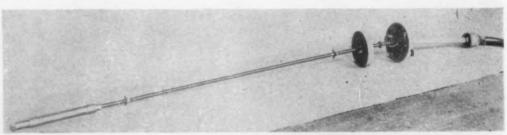


FIG. 5.—INNER ASSEMBLY OF IMMERSION UNIT. (Courtesy of Leeds and Northrup Company.)

radiation. A compression spring back of the panel holds the inner assembly against the end of the outer immersion tube while lugs at intervals keep it in a coaxial position. The use of the inner orifice, which is fixed relative to the Rayotube, makes unnecessary painstaking positioning when it is not in use. Shielded leads extend beneath the shop floor to the recorder mounted in the furnace-control house.

The checking unit in Fig. 6 is similar in design to the immersion unit except that the outer pipe serves merely as mechanical protection for the Rayotube and does not extend back beydon this point. A clamp is provided to mount the

mounted on the back end of the small pipe and an electrical plug connects the two Rayotubes in opposition through the

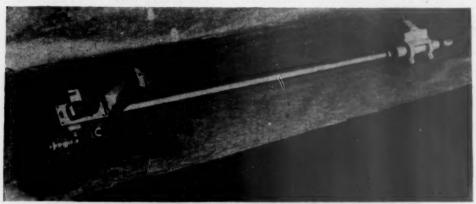


Fig. 6.—CHECKING UNIT, USED FOR CALIBRATION. (Courtesy of Leeds and Northrup Company.)



FIG. 7.—IMMERSION UNIT BEING STANDARDIZED BY MEANS OF CHECKING UNIT AT OPEN-HEARTH FURNACE.

checking unit on the side of the immersion unit so that the two fields of view are coincident in a plane a few feet from the orifices. A sensitive galvanometer is

galvanometer. No air is required during the checking operation, since the front ends of the two units are merely rested in the wicket hole so that there is an unobstructed view of the interior of the furnace. The setting of the immersion unit is adjusted until the null point is attained and the immersion unit is then identical effort has been made, therefore, to reduce. this possibility. In Fig. 8 the pyrometer is shown in operation in a 150-ton openhearth furnace.



Fig. 8.—Temperature reading being taken in large tilting open-hearth furnace at Aliouippa.

in output with the checking unit. Fig. 7 is a plant photograph of the pyrometer being checked at the open-hearth furnace.

The air used during an immersion is first filtered to remove oil, water or dirt that might deposit on the window. It then passes through the flow regulator, which supplies a substantially uniform flow regardless of reasonable changes in pressure. This arrangement makes unnecessary any manual adjustment of the air flow and permits the use of an on-off valve in the head of the immersion unit. The only likely cause of damage to the unit is that the air may be insufficient to keep steel out of the tube. Considerable

The recorder is a standard Speedomax, range 1400° to 3200°F., and chart speed, when energized, of 2 in. per minute. The scale in the upper temperature range is about one inch per hundred degrees Fahrenheit. One recorder has been used successfully for two furnaces, contact being made with either of the furnaces through a shielded switch. Other contacts on this switch may be used to light a signal lamp on the open-hearth floor, corresponding to the furnace in the recorder circuit.

OPERATION OF THE PYROMETER

Much of the development work has been done on tilting, basic open-hearth furnaces producing a high proportion of duplex heats, for which the refining period is relatively short. The first reading on such a heat is usually taken soon after the last hot-metal addition and readings are taken at intervals until the heat is ready to block or tap. The number of readings taken during a heat will depend on furnace conditions and the grade of steel. It has been established that readings can be taken at 10-min. intervals without excessive heating of the radiation element. This interval may be somewhat reduced if a greater volume of air is allowed to flow through the pipe between readings.

pipe was overheated and warped at the conclusion of the second immersion but straightened as it cooled.

The air pressure maintained in the pyrometer during an immersion is not critical but must be sufficient to keep molten metal out of the orifice. Occasionally at normal pressures, high-velocity sparks pass the inner aperture and strike the thin glass window protecting the lens. The resultant loss in response of the Rayotube, caused by the pitted window, is compensated for by adjustment of the potentiometer circuit when the unit is checked. The damaged window can be

TABLE 1.—Readings Taken with the Immersion Pyrometer on a Number of Heats during the Refining Period

	Fir	st Readi	ng	Seco	nd Read	ding	Th	ird Read	ing	Final Reading			
Heat No.	Per Cent C	Min- utes to Tap	Temperature Deg. F.	Per Cent C	Min- utes to Tap	Temperature, Deg. F.	Per Cent C	Min- utes to Tap	Temperature, Deg. F.	Per Cent C	Min- utes to Tap	Tem- pera- ture, Deg. F.	
9038	0.58	68	2015	0.45	48	2920	0.38	38	2950	0.34	28	2960	
9054	0.18	60	2930	0.21	27	2930	0.17	10	2965	0.10	5	2965	
9061	0.44	45	2880	0.28	25	2915	0.23	15	2920	0.18	5	2940	
9062	0.23	62	2910	0.18	52	2920	0.12	22	2955	0.08	2	2970	
9068	0.54	61	2960	0.35	31	2995	0.31	21	2980	0.20	3	3000	
9074	0.33	65	2935	0.29	45	2980	0.18	20	2995	0.15	IO	3005	
9082	0.32	47	2945	0.26	27	2960	0.18	17	2965	0.12	2	2975	
9128	0.75	100	2840	0.45	50	2925	0.37	40	2950	0.30	30	2960	
9141	0.38	40	2900	0.32	25	2935	0.20	10	2980	0.19	2	2970	

The temperature of the Rayotube rises to about 175°F. immediately following a normal immersion. A comparison of check readings taken when the pyrometer is warm and others taken after it has cooled to room temperature indicates that variations in temperature of the radiation element do not affect the values obtained for the bath temperature. The unit was subjected to a severe test when two readings were taken in rapid succession through the same door of the furnace. The second reading was within 10°F. of the first and the unit remained in calibration after cooling, as indicated by checks made before and after the test. The outer replaced when the unit is taken apart for routine cleaning and inspection. At a gauge pressure of 10 lb., approximately 90 cu. ft. of air per min. passes through the bath. The gauge pressure will increase several pounds at the time of the immersion, owing to an increased back pressure. Nominal variations in the amount of air used seem to have little effect on the temperature readings; however, tests have indicated that excessive amounts of air tend to give high values.

It is recognized that the temperature may vary considerably in different parts of the bath; this is particularly true of a quiet bath in a large furnace. The present design of pyrometer is not suitable for exploring the conditions within a furnace, but, if desired, the immersion unit could be lengthened for this purpose without temperatures for any given emissivity value, provided the temperature is established by an independent method.

In the plant work with the open-end

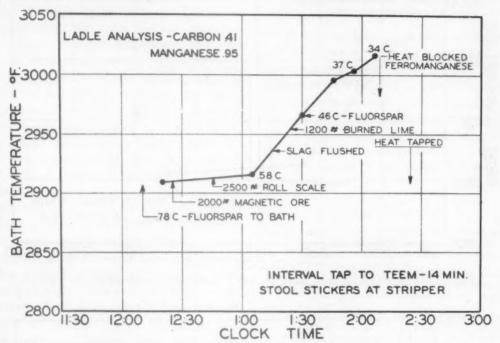


FIG. 9.—TEMPERATURE-TIME DATA ON HEAT THAT TEEMED WITH INGOT STICKERS.

affecting the basic dimensions. In actual practice, readings are taken at a standard location in the furnace. Local agitation of the bath by the air stream tends to reduce possible temperature variations due to stratification. Finally, the degree of activity of medium and low-carbon basic heats, during the refining period, seems adequate to ensure a representative temperature reading at this critical time.

The output of a radiation pyrometer is maximum for a radiating surface having an emissivity of unity. The cavity opened up in the steel by the air stream is not strictly a black body because of the presence of the cold end of the immersion tube. Hence, the emissivity is less than one and the temperature reading is lower than that for a black body at the same temperature. The setting of the recorder can be adjusted so that the pyrometer will read correct

tube pyrometer, the temperature scale was tentatively set some time ago on a basis of optical pyrometer readings taken at tapping of the heat. These relative values are now being modified to conform with platinum-platinum rhodium thermocouple readings and indications are that those reported below are somewhat high. The calibration of the immersion unit by means of the checking unit is independent of the recorder setting.

Examples of the changes in temperature during the working of individual heats are shown in Table 1 and illustrate a practical use of the pyrometer. Fig. 9 presents graphically the bath temperatures taken during the refining of an intermediate carbon, killed steel. The final readings indicated that the temperature of the steel was excessive, verified by the occurrence of stool stickers even though the

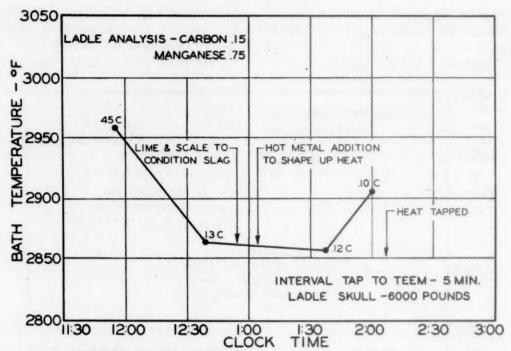


FIG. 10.—TEMPERATURE-TIME DATA ON HEAT WITH 6000-POUND SKULL IN LADLE.

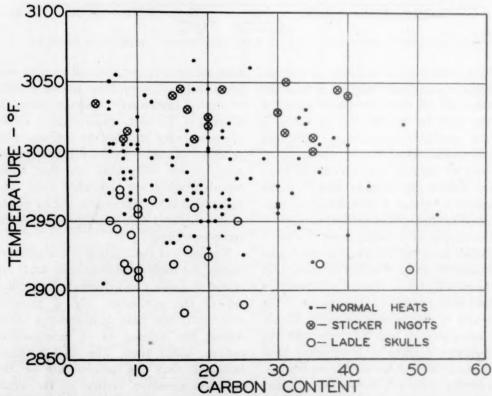


FIG. 11.—HEATS WITH STICKER INGOTS AND LADLE SKULLS IN RELATION TO NORMAL HEATS.

heat was held in the ladle for 14 min. It can be noted that the temperature increased rapidly as the bath became more active following the slag flush and that it continued to increase until the heat was blocked. Fig. 10 is a record of a heat made under abnormal furnace conditions resulting from fuel difficulties. The melter was unable to obtain adequate steel temperature during the major portion of the refining period. Although the conditions improved before tap, the temperature was insufficient for steel of this grade and the heat teemed with a 6000-lb. skull.

The occurrence of ladle skulls and of "sticker" ingots is essentially a steel-temperature problem although the temperature of the ladle, the rate of tap, the holding time in the ladle, etc., exert an influence on the results. Fig. 11 shows the incidence of these teeming irregularities for a large number of heats on which temperature observations were taken. Heats that gave pronounced difficulty due to sticker ingots had high bath temperatures while those with skulls were below normal. The effect of carbon content of the steel on ingot stickers and skulls is shown by the graph.

Many heats below or above the most desirable temperature can be teemed satisfactorily. Temperature control of the steel in the furnace, however, can do much toward reducing teeming difficulties.

SUMMARY

A radiation pyrometer, which offers certain advantages with respect to ease of operation, maintenance and reliability, has been developed and tested extensively under plant conditions. The instrument employs a radiation device, mounted inside an open-end steel tube, sighted on the liquid steel. Compressed air keeps the orifice free from molten slag and steel. In the course of the work, a convenient method was devised for standardizing the pyrometer to ensure continued accuracy

in mill use. Mill tests indicate that the instrument is a practical pyrometer for measuring bath temperatures in the openhearth furnace.

ACKNOWLEDGMENTS

The authors take pleasure in according public recognition to the members of the Leeds and Northrup Co. who have cooperated in this joint project. They also wish to acknowledge the assistance of their associates at the Jones and Laughlin Steel Corporation; in particular, Dr. H. K. Work, who suggested this project and has shown a continued interest in the development.

REFERENCES

 B. Osann and E. Schroder: Temperaturmessungen mit Wolfram-Molybdan-Thermoelementen. Archiv Eisenhuttenwesen (1933) 7, 89-94.

 G. Leiber: Temperaturmessungen im Stahlbade des basischen Siemens-Martin-Ofens. Archiv Eisenhuttenwesen (1937) 11, 63-66.

3. S. Fornander and T. Omberg: Temperature Measurements of Liquid Steel in the Basic Open-hearth Process. Jernkontorets Ann. (1939) 123, 527-544.

Ann. (1939) 123, 527-544.

4. H. L. Watson and H. Abrams: Thermoelectric Measurement of Temperatures above 1500°C, Trans. Amer. Electrochem. Soc. (1928) 54, 19-36.

5. F. Holtby: Rapid Temperature Measure-

5. F. Holtby: Rapid Temperature Measurements of Cast Iron with an Immersion Thermocouple. *Trans.* Amer. Foundrymen's Assn. (1939) 47, 854-871.

men's Assn. (1939) 47, 854-871.
6. F. Holtby: Rapid Temperature Measurements of Molten Iron and Steel with an Immersion Thermocouple. Trans. Amer. Soc. for Metals (1941) 29, 863-875.

7. G. R. Fitterer: Pyrometry of Liquid Steels and Pig Irons. Temperature, Its Measurement and Control in Science and Industry. Amer. Inst. of Physics (1941) 946-957.

946-957.

8. M. Wenzl and F. Morawe: Temperaturmessungen von flussigem Gusseisen,
Thomasroheisen and Stahl. Stahl und
Eisen (1927) 47, 867-871.

Eisen (1927) 47, 867-871.

9. T. L. Joseph: Oxides in Basic Pig Iron and in Basic Open-hearth Steel. Trans.

A.I.M.E. (1937) 125, 204-245.

A.I.M.E. (1937) 125, 204-245.

10. F. H. Schofield: First Report on Proposed "Quick Immersion" Methods of Measuring the Temperature of Steel in the Open-hearth Furnace. Seventh Rep. on Heterogeneity of Steel Ingots, Iron and Steel Inst. (1937) 222-238.

on Heterogeneity of Steel Ingots, Iron and Steel Inst. (1937) 222-238.

II. L. F. Weitzenkorn: A Method for Determination of Bath Temperature. Proc. Electric Furnace Steel Conf. A.I.M.E.

(1944) 2, 143-149.

12. R. W. S. Freeman: High Temperature Measurements of Liquid Steels Using the Quick Immersion Thermocouple Technique. Canadian Metals and Metal-

Technique. Canadian Metals and Metallurgical Industries (1944) 7, 23-25.

F. Blaurock: Beitrag zur optischen Temperaturmessung von flussigem Eisen und Stahl. Archiv Eisenhuttenwesen (1934-35) 8, 517-532.

14. E. Cook: Open-Hearth Temperature Control. Trans. Amer. Soc. for Metals (1936) 24, 649-678.

 (1936) 24, 649-678.
 15. L. O. Sordahl and R. B. Sosman: Measuring Open-hearth Bath Temperatures. Instruments (1940) 13. 127-130.

16. L. O. Sordahl and R. B. Sosman: The Measurement of Open-hearth Bath Temperature. Temperature, Its Meas-urement and Control in Science and Industry, Amer. Inst. of Physics (1941) 927-936.

17. M. J. Bradley: Measuring Temperature Beneath Surface of Molten Metal. Proc. Open Hearth Conf., A.I.M.E. (1939) 22, 192-198.

18. E. D. Martin: Plant Test and Use of Equipment for Measuring Moltenmetal temperature. Proc. Open Hearth Conf., A.I.M.E. (1939) 22, 199-201

The Boron-oxygen Equilibrium in Liquid Iron

By Gerhard Derge,* Member A.I.M.E.

(Chicago Meeting, February 1946)

METALLURGISTS have used borax as a fluxing agent traditionally, but until recently elemental boron' has played an insignificant role as an alloying element. Neither the metal nor its compounds have been regarded as important metallurgical materials and there is a surprising lack of knowledge concerning their metallurgical behavior. The new applications to steelmaking of both boron and borates, which arose in part from wartime incentives and restrictions, have been seriously handicapped by this lack of data. For example, rasorite, a naturally occurring sodium borate, has been shown to be an effective substitute for aluminum as a ladle deoxidizer in rimming steels.1 Likewise, the effectiveness of boron as an alloying agent has been demonstrated,2,3 giving deep hardening when used in restricted amounts. The exploitation of both of these uses has been retarded by the difficulty of attaining suitable metallurgical control. Recognizing that the most important information required was a knowledge of the equilibrium between boron and oxygen dissolved in liquid iron, Gurry⁴ calculated this relation from the best thermal data available. However, estimates of the entropy of melting of boron, the activity coefficient of boron in liquid iron and the

activity coefficient of B₂O₃ in slag were involved, and experimental work on this problem was obviously desirable.

The experiments to be described were planned to establish the boron-oxygen relations in liquid iron and to demonstrate at the same time the ferroborate slag compositions in equilibrium with various amounts of oxygen in liquid iron. Accordingly, slags containing varying proportions of iron and boron oxides were held in contact with molten iron, and samples of both slag and metal were analyzed. The limitations upon the accuracy of the data will be considered, but in a practical sense the oxygen levels that can be attained in iron by iron borate slags, and the amounts of boron in iron at these oxygen levels were established.

EXPERIMENTAL PROCEDURE

No entirely suitable refractory was found for the mixtures of iron oxide and boron oxide used as slags. Crucibles of silica, magnesia, Ramix, beryllia, and zirconia were all tried unsuccessfully. The most satisfactory method discovered for handling them was the rotating-crucible technique, which creates a parabolic crucible of liquid iron.5,6 Even this was not entirely successful, for at steelmaking temperatures (1600°C.) the slags had such a low surface tension that they crept up to the refractory and slowly dissolved it. These difficulties made it impossible to maintain a constant slag composition for an unlimited period of time. However, by using the rotating technique, short runs could be made in

Manuscript received at the office of the Institute Dec. 21, 1944; revised Jan. 10, 1946. Issued as T.P. 2004 in METALS TECHNOLOGY, August 1946.

August 1946.

* Member of the Staff, Metals Research
Laboratory, and Associate Professor, Department of Metallurgical Engineering, Carnegie
Institute of Technology, Pittsburgh, Pennsylvania.

¹ References are at the end of the paper.

both silica and magnesia crucibles. Silica crucibles gave the least experimental trouble and most of the work was done with these. Since the slags picked up silica

> . 00 0

FIG. I.—SCHEMATIC DIAGRAM OF APPARATUS.

- 1. Gas inlet.
- 2. Peephole cover.
- 3. MgO brick.
- 4. Dowel connection.
- 5. Copper furnace coils.
- 6. Silica tube.
- Stovepipe crucible. 7. Stovepipe cruci.
 8. Transite frame.
- 9. Refractory packing.
- 10. Transite.
- 11. Picein.
- 12. Wooden base.
- 13. Turntable.

from the crucible, and since some silicon was introduced into the metal from this source, several heats were made in magnesia crucibles to avoid difficulties in interpretation that might arise from the presence of silicon. These experiences with

slags containing only iron and boron oxides must not be interpreted as precluding the use of borates in commercial operations because they will destroy the refractories. Many satisfactory runs have been made in magnesia crucibles with simulated open-hearth slags containing up to 10 per cent of B2O3.

The apparatus used is shown schematically in Fig. 1. Heating was by means of a 35-kva. induction furnace 5. A section of stovepipe 7 was crimped in at the base and the space between it and the silica tube 6 was packed with silica or magnesia sand o. The iron charge was placed in the stovepipe and the inner surface of the refractory packing was sintered during the melting. A loose-fitting magnesia brick cap 3 was placed over the collar of the quartz tube 6 during this period. A neutral gas (see Table 1) was passed through a quartz tube I in this brick to minimize oxidation. When the 1600-gram metal charge was completely melted, rotation was started at 190 r.p.m. and the previously mixed slag ingredients were added slowly through a funnel in the cap. After about 10 min., metal samples were taken by suction into a 5-mm. quartz tube 7 and the power was turned off; samples of both slag and metal were also taken from the solidified material.

Temperatures were observed with an optical pyrometer corrected for the emissivity of iron, and the power input was adjusted to maintain a constant temperature before the slag constituents were added; no further temperature measurements were made, owing to the unknown emissivity of the slag. The last temperature reading prior to slag addition was recorded as the temperature of the heat. The data from a series of runs made at 1560° and 1660°C. show no significant differences and therefore are combined and reported as representing conditions at 1600°C. For this reason it is not felt that the calculation of a temperature coefficient is justified, but it would appear to be very small.

The slags were prepared by mixing varying amounts of Fe₂O₃ and B₂O₃. Since ingot iron is highly oxidized, the final slag compositions were always much lower in B2O3 than the initial mixture owing to pickup of iron oxide from the metal. Normally no other additions were made. so any deoxidation of the metal which occurred during the heat was accomplished through reaction with the slag, and any boron found in the metal was reduced from the slag. In these heats equilibrium in the metal was approached from the highoxygen low-boron side. In the few special cases noted in Table 1 ferroboron was added to the melt before any slag additions were made. In these heats equilibrium was approached from the opposite side; i.e., low-oxygen, high-boron.

The sampling of these small heats during rotation was difficult. Samples were taken periodically in heats 31 and 32 to establish operating conditions but subsequently one molten sample was sucked into a quartz tube just before the power was turned off and samples were also taken from the solidified ingot and slag The samples taken by suction were erratic and frequently contained slag; they were generally higher in boron and oxygen than samples cut from the ingot. The ingot samples, solidified in the crucible, actually froze within about one minute of the time the power was turned off. The data from these ingot samples are regarded as the most reliable because they contained no entrapped slag, and they are used exclusively in the discussion to follow.

The metal samples were analyzed for oxygen by vacuum fusion. The boron in the metal was determined by a modified Chapin distillation-titration method⁸ and the procedure was checked with Bureau of Standards samples. Silicon was determined also, for reasons that will become

apparent. The conventional fluoride volatilization method¹³ was used for silicon. The slags were analyzed for B₂O₃ by a modified Chapin method, for silica by fluoride volatilization, and for total iron (reported as FeO) by the Zimmermann-Reinhardt method.¹⁴

EXPERIMENTAL DATA

The data from all satisfactory runs are listed in Table 1. In many cases the total slag analyses are considerably less than 100 per cent, and a few slags total slightly more. The results in the table all represent averages of duplicate analyses in good agreement with each other. Some of the deviations may be accounted for by the fact that the iron was all reported as FeO while actually some Fe₂O₃ was probably present. Complete analyses for the other normal slag constituents: CaO, MgO, Al₂O₃ did not account for the discrepancies found and it must be admitted that some of the discrepancies are larger than might be expected. The analytical procedures were all reviewed carefully and checked with standard samples. It may be that they can be explained by some unknown complex of iron and boron oxides. Heats that were used solely for the purpose of establishing sampling techniques, or which were interrupted by such uncontrollable causes as crucible failure, have been omitted. In the following treatment only analyses from the metal and slag that froze in the crucible have been used and no distinction has been drawn between heats made at different temperatures. The reasons for this have already been outlined.

In Fig. 2 the data for percentage of boron in iron have been plotted against percentage of B₂O₃ in slag for the heats made in silica crucibles. The slags contained 2.4 to 49.1 per cent silica and will be referred to as silicate slags. This plot shows that it is possible to introduce from zero to slightly more than 0.1 per

LABLE 1.

er C
SiO ₂ FeO Fer Cent
\$6.30
48.34
49.25
27.65 34.27
31.64 58.36
23.76 53.74
10.89
38.42 61.47
35.71 18.33
15.69 41.33
38.32 52.79
9.1 40.04
2.39 25.18
22.86 71.60
26.79 64.1
27.04 62.53
24.98 54.23

Nitrogen Slag-rosorite as	Helium Helium	Ferroboron	Ferroboron Helium	Ferroboron	Ferroboroa		Nitrogen	Nitrogen	Nitrogen	Nitrogen	Helium	Helium	Helium	Helium	Helium	Helium	Niteogen	TARRES OF THE PARTY OF THE PART	Nitrogen	(Not included in	Helium Ferroboron	Helium	Ferroboron
36.08	49.18	8.29	10.02	12.81	19.36		1.23	O.SII	30 H	0.73	15.04	12.61	10.8	1	90.00	3.03	0.20	12.25	370.5	5,934.0		0.711	132.7
1,13	0.934	1.00	0.408	0.585	3.66		0.389	0.881	10.50	1.16	4.64	4.38	5.14	4	0.10	0.00	0.28	4.50	314.0	2,525.0		117.0	22.16
0.022	0.004 0.005 0.005	0.051	0.032	0.032	0.003	BLES	0.150	0,165	0.158	0.138	0.115	0.161	0.131		0.114	0.065	0.074	0.141	0.026	0.0036	0.013	0.081	0.080
0.008	0.054	0.008	0.015	0.0119	0.006	PART BMgO CRUCIBLES	0.005		0.007		0.008		0,000					0.0005				0.0073	0.003
0.0311	0.3351 0.2320 0.2280 0.0931	0.0083	0.0485	0.00220	0.0037	PART B	0.0028	0.0005	0.0019	0.0013	0.0003	0.0007	0.0000	2000	0.0801	0.00100	0.0094	0.0000	0.0004	0.0092	0.2837	0.0004	0.0045
19.94	19.94	54.67	57.52	50.78	54.59		91.23	92.93	. 93.40	95.93	02.78	93.66	95.77		80.24	68.75	92.03	95.73	00.53	93.37		95.45	80.87
36.63	19.95	36.36	11.25	23.86	38.45		0.5	0.7	1.13	1.37	0.55	0.33	0.31		0.33	0.23	0.47	0.13	0.27	1.45		01.0	4.73
30.23	52.68	7.61	24.56	21.89	7.29		3.16	0.58	0 77	0.63	3.24	2.88	3.11	-	(34.57)	22.47	0.81	2.72	1.18	3.35		1.00	5.99
1-15 D-15	10-15 D-15 Id-15	20-30 D-30 10-10	2a 20 D-20 Ia-10	26-20 D-20	24-15 D-15		1-10 D-10	D-10	D-10	1-10 D-10	D-10	1-10 D-10	D-10	01-10	D-10 1-10	D-10	D-50	D-10	D-10	D- 5	14- 5	D-10 14- 5	2a-10 D-10
0091	1680	1660	1680	1660	2001		1590	1590	1590	1590	1600	1590	1580	1600	1600	1600	2777	1000	1660	1680	1700	1680	
74	79* 80*	9100	828	80000			50	22	53	54	5.5	57	00 .	65	09	29		70	11	78	416	046	

Time elapsed between final slag addition and taking of sample.
Equilibrium approached from high boron side.
Sufficient sample not available for check analysis.
D Sample frozen in crucible.

cent boron into the metal by increasing the B₂O₃ content of the slag up to about 50 per cent. The 0.003 per cent boron specified in most boron steels is in equilibrasorite can be used for control of oxygen in rimming steels.

The same data are plotted in Fig. 4 to show the relations between boron and

in metal

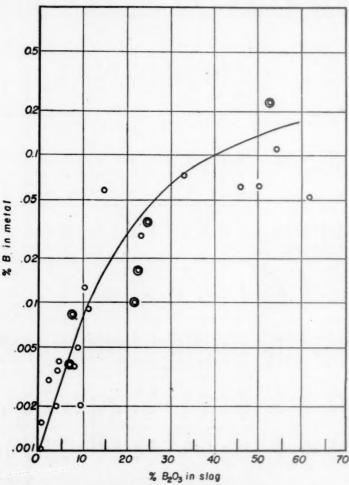


Fig. 2.—Percentage of B₂O₃ in slag vs. percentage of B in metal. Heats from silica crucibles, see Table 1, part A for heat data. The double circles indicate equilibrium approached from high-boron side.

rium with a slag containing only 5 per cent B₂O₃.

The data for percentage of oxygen in iron are plotted against percentage of B₂O₃ in silicate slags in Fig. 3, which shows that oxygen levels down to 0.02 per cent can be obtained by varying the slags from zero to 50 per cent B₂O₃. This curve provides experimental confirmation of the observation made in mill practice that

oxygen dissolved in liquid iron, and the familiar shape of a deoxidation curve is apparent. The position of this boron deoxidation curve is near that of silicon, 12 and since the bath was in contact with a silicate slag in a silica crucible it is advisable to consider the boron-silicon relations in these melts (see Fig. 5). In this plot no relation is shown between boron and silicon in the metal, and a wide range of

silicon values is associated with any given boron content, which indicates that in these experiments the oxygen was controlled by boron rather than by silicon. For example, in the three heats with a they were not saturated with silica—a condition that is required for application of such data¹²—quantitative consideration of the combined effects of boron and silicon would seem to be fruitless.

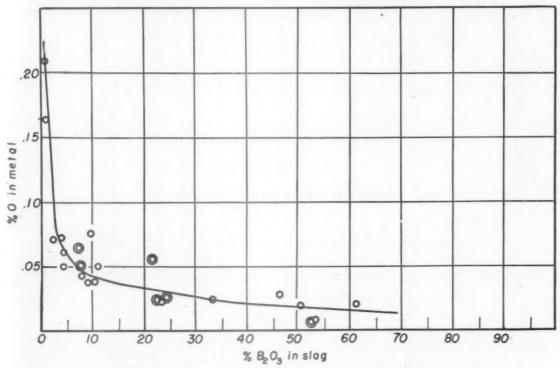
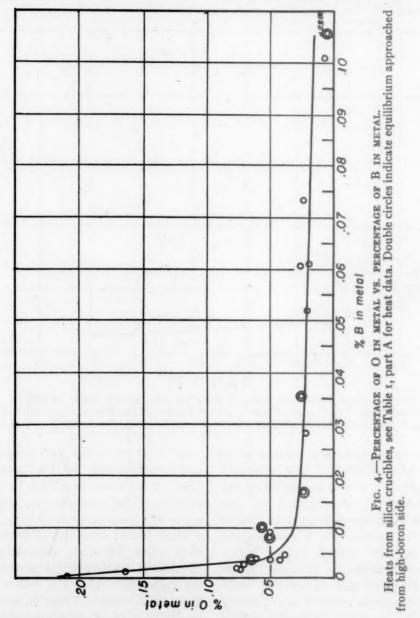


Fig. 3.—Percentage of B₂O₂ in slag vs. percentage of O in metal. Heats from silica crucibles, see Table 1, part A for heat data. Double circles indicate equilibrium approached from high-boron side.

boron content of about o.o. per cent boron the silicon was found to vary from o.or to 0.06 per cent silicon, but in Fig. 4 the oxygen for these same heats is between 0.050 and 0.056 per cent oxygen. Two of these heats started with a lower oxygen content and one started with a higher oxygen content. In this example, apparently the final oxygen content was determined by the boron rather than the silicon. One is thus forced to conclude that the consistent character of the boron deoxidation curve in Fig. 4 is due to boron. In view of the considerable range of reported values for the silicon deoxidation constant,11 and the fact that the range of silica analyses in the slags indicates that

In order to avoid any possible misinterpretation due to the presence of silicon, a few heats were made in magnesia crucibles. The resultant slags contained 0.1 to 4.73 per cent silica and the iron had a maximum of 0.000 per cent silicon. As with silica crucibles, equilibrium was approached from both the low-boron and the high-boron side. The values for the boron and oxygen found in these runs are shown in Fig. 6. These data show somewhat higher oxygen values than the data obtained from silica crucibles. The data are fewer than were obtained from silica crucibles. Greater experimental difficulties were encountered with the magnesia crucibles; these apparently were due to

the well-known high solubility of iron oxides in magnesia. Solution of iron oxide in the magnesia crucibles occurred during melting and the crucible then served as a skimming the initial slags and adding more B₂O₃. It is not believed that slagmetal equilibrium was approached as closely as in the runs made in silica

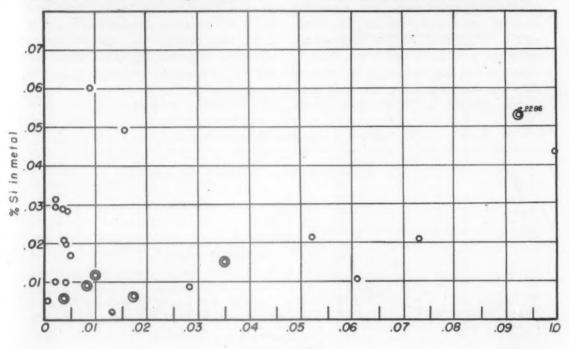


source of iron oxide to both slag and metal and made it difficult to attain a boron-oxygen equilibrium.¹⁶ Heats 60 and 63 finished with higher B₂O₃ content in the slag than the other magnesia-crucible heats. These slags were obtained by

crucibles. For these reasons, it is felt that although the data obtained with magnesia crucibles demonstrate qualitatively that boron oxide slags act as deoxidizers and that boron can be transferred from slag to metal at these oxygen levels, the quan-

titative data are not as reliable as those obtained with silica crucibles. These remarks are based on experimental ob-

of the data indicate that the amounts of boron found in the iron are not due to slag inclusions. Indeed, if the latter possibility



**B in metal

Fig. 5.—Percentage of B in metal vs. percentage of silicon in metal.

Heats from silica crucibles, see Table 1, part A for heat data. Double circles indicate equilibrium approached from high-boron side.

servations. The data will be considered statistically in the next section.

DISCUSSION OF DATA

Several of the solidified ingots were examined microscopically, to provide an additional check on the chemical analyses for oxygen and boron. Large slag inclusions were not observed, but the lowboron, high-oxygen samples showed structures typical of iron silicates that have separated during freezing (Fig. 7a). The intermediate boron samples showed fewer of these iron silicates and increasing amounts of the intergranular constituent commonly associated with high-boron steels (Fig. 7b); while the high-boron samples showed larger patches of this boron constituent (Fig. 7c, d, e, f). These observations and the general consistency were correct, the high-boron samples would then be high in oxygen, and this is not true.

It would thus appear that the data obtained from silica crucibles present an experimental study of the equilibrium for the reaction considered theoretically by Gurry:⁴

²B (% liquid Fe) + 30 (% liquid Fe)
=
$$B_2O_3$$
 (slag)

And making the conventional assumption that the activity of B₂O₃ (slag) is unity, one can evaluate the deoxidation constant:

$$K_{\rm B} = \frac{1}{\rm B^2(\% \ liquid \ Fe) \times O^3(\% \ liquid \ Fe)}$$

$$K_{\rm B} = 2.4 \times 10^8$$

This value of K_B is the average of the 24 heats that were made in silica crucibles.

The average for 14 heats made in magnesia crucibles is 34.7×10^8 , while the average for all heats is 14.3×10^8 .

In these experiments the convention of using unit activity for the B₂O₃ in the slag is not rigorous, for the slags are not saturated with B₂O₃, and it was thought that a better constant might be obtained by some other treatment. The most satisfactory solution found has been to use

molecular species in the slag are SiO₂, FeO, and B₂O₃. Another constant, $Km_{\%B_4O_6}$, was figured on the assumption that the molecular species are SiO₂, FeO, and B₄O₆. Still another constant, $Km_{\%B_4O_4} \times \text{Si}_2\text{O}_4$, was derived on the assumption that the slag contains Si₂O₄, FeO, and B₄O₆. The standard deviation σ and the coefficient of variation $\frac{\sigma}{\bar{k}}$ are shown for

TABLE 2.—Data from Different Crucibles

		a Crucib 19 heats			esia Cruc 14 heats	ibles,	Combined Data Silica plus Magnesia Crucibles, 33 heats			
-	Average K	Std. Dev.	Coef. Variation	Ř		<u>σ</u> <u>K</u>	Ř		- R	
		•	r K		σ	K	Α.	-	Ř	
$K\mathbf{B} = \frac{\mathbf{I}}{[\%\mathbf{B}]^2[\%\mathbf{O}]^3}$	2.32	2.56	1.70	34.7	82.9	2.38	16.08	56.3	3.51	
$KB_2O_3 = KB \times wt. \%B_2O_3$	29.38	22.46	0.77	49.3	98.4	2.00	37.4	67.6	1.81	
$Km\%B_2O_3 = KB \times m \%B_2O_3$ $(B_2O_4, FeO, SiO_2) \dots Km\%B_4O_4 = KB \times m \%B_4O_6$	30.3	26.1	0.86	5.8	8.8	1.5	19.9	24.3	1.2	
(B_4O_6, FeO, SiO_2) $Km_{\%}B_4O_6.Si_2O_4 = KB \times m$	18.60	18.39	0.99	3.21	5.11	1.59	12.07	16.24	1.35	
%B4O6 (B4O6, FeO, Si2O4)	21.82	19.78	0.91						-	

All values for \bar{K} and σ should be multiplied by 10°; i.e., $\bar{K}B = 2.32 \times 10$ °.

the weight percentage of B₂O₃ in the slag in the following equilibrium expression:

2B (% liquid Fe) + 3O (% liquid Fe)
=
$$B_2O_3$$
 (% slag)
 $K_{B_2O_3} = \frac{B_2O_3$ (% slag)
 B_2O_3 (% liquid Fe) × O_3 (% liquid Fe)
= $K_B \times B_2O_3$ (% slag)

The values for $K_{B_2O_2}$ are listed in Table 1, and a cursory examination indicates that this is a slightly better constant than K_B . Several other variations have been investigated, but none of these appears to have any advantage over the simple use of weight percentage B_2O_2 in the slag. The average values \bar{K} of some of these are included in Table 2. The values for $Km_{\%B_2O_2}$ were calculated using mol percentages, on the assumption that the

each treatment. The coefficient of variation probably affords the best means of comparison because the numerical values of the constants derived by different methods have varying orders of magnitude. In making these comparisons it was necessary to limit the calculations to the heats for which complete analytical data were available. These quantities are listed separately for the heats in silica and magnesia crucibles and for all heats combined. In considering the KB values for the various combinations of data it is evident from the σ values that the K_B value for silica crucibles is considerably better than for magnesia crucibles, or for the heats from all crucibles combined, and this is in accordance with observations made during the experiments. The same

statement can be made concerning $K_{B_2O_2}$. The comparisons between K_B , $K_{B_2O_3}$ and other constants can be made best by the coefficients of variation. For the heats from silica crucibles, the coefficients are nearly the same, but an advantage can be claimed for the treatment involving the percentage of B2O3 in the slag. The use of mol per cent is slightly better for magnesia crucibles. When the combined data from silica and magnesia crucibles are considered the coefficient is lower when the mol percentage of B2O2 in the slag is taken into account. The conclusion is that the most reliable data are from silica crucibles and that under these conditions we do not have sufficient knowledge of slag chemistry to benefit much by correcting for the B2O3 content of the slag; however, if all types of slag are to be considered, some advantage may be gained from this correction on the simplest possible molar basis.

For purposes of discussion, the metaloxygen data for carbon, manganese, silicon and aluminum as reported by the Physical Chemistry of Steelmaking Committee, are plotted in Fig. 8. (A log-log scale is used to include a wide range of compositions. 12,9,10) The experimental points for boron obtained with silica crucibles are shown with open circles and the dashed line represents the average for these points as calculated above;

$$K_{\rm B} = 2.4 \times 10^8$$

The solid circles represent the data obtained with magnesia crucibles. The band calculated by Gurry⁴ is also shown and the marked difference between this band and the experimental results is apparent. In considering this difference, the first question to be answered is whether or not equilibrium was attained in the experiments. Table 1 shows that most heats were sampled 10 to 15 min. after the final slag addition. These short times were necessary because of the experi-

mental difficulties, already pointed out. Slag attack on the crucible material made longer runs difficult. However, several heats were continued for 45 min. and No. 34

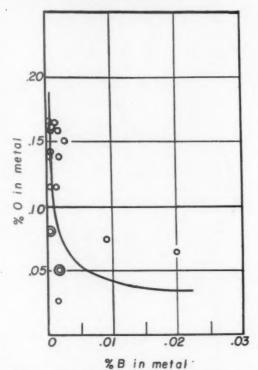


Fig. 6.—Percentage of B in metal vs. percentage of O in metal.

Heats from magnesia crucibles, see Table 1, part B, for heat data. Double circles indicate equilibrium approached from high-boron side.

ran 75 min. (Table 1.) The data from these longer runs are in satisfactory agreement with the data from 10-min. runs. There is every reason to believe that this was actually sufficient time to attain equilibrium. The experiences of Fetters and Chipman15 are typical of those reported in the literature; with a stationary induction furnace and a 65-lb. iron melt, they found that equilibrium was reached in 18 to 23 min. after any slag addition. The additional slag-metal interface and the added mixing obtained with the rotatingcrucible technique, and the small charge of only 31/2 lb., would all indicate that 10 to 15 min. should be sufficient time for a

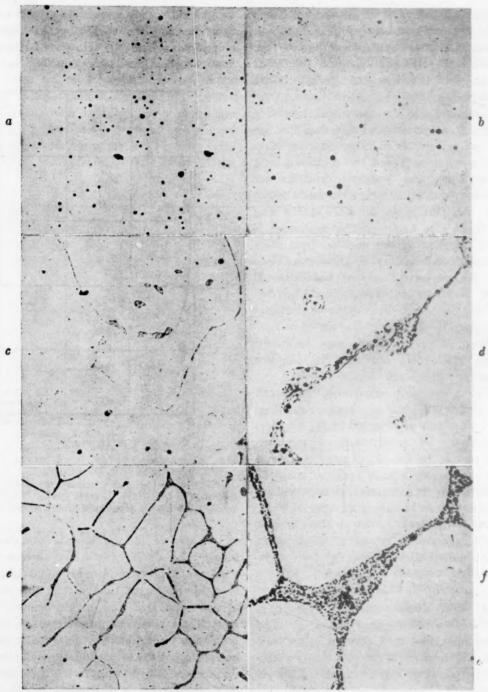


Fig. 7.—Micrographs of solidified ingots.

a. Heat No. 53; 0.00049% B (× 100).

b. Heat No. 29; 0.0049% B (× 100).

c. Heat No. 41; 0.06% B (× 100).

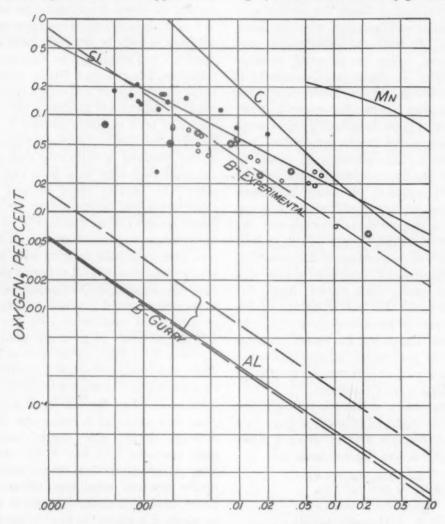
d. Heat No. 41; 0.06% B (× 100).

e. Heat No. 79; 0.23% B (× 100).

f. Heat No. 79; 0.23% B (× 500).

Original magnifications given; reduced about one fifth in reproduction.

close approach to equilibrium. Also, the data from all heats in both magnesia and silica crucibles are self-consistent, and the same final equilibrium was approached increase in oxygen with increase in boron. Furthermore, if the equilibrium curve is below the experimental curve shown in Fig. 8, the boron found at any given oxygen



ALLOYING ELEMENT, PER CENT

Fig. 8.—Combined deoxidation curves Mn, Si, C, Al, B-Gurry, B-Experimental.

o SiO2 crucibles.

SiO2 crucibles Equilibrium approached from high-boron side.

MgO crucibles.

from opposite directions. It has also been shown that the shape of the deoxidation curves in Figs. 4 and 6 establishes that the sampling was satisfactory and that increasing amounts of boron do not represent entrapped slag, for this would require an level represents a supersaturation of boron in the liquid iron and this does not seem likely, since in the heats that started on the high-oxygen side all the boron must enter the iron by reduction from slag at the slag-metal interface.

Since the experimental data represent a true equilibrium, the difference from Gurry's calculated value for KB should be analyzed. This difference is of the order of 105 for the case Gurry has selected with an activity coefficient of 0.02 for boron in iron. If both the experimental and theoretical values are accepted, a means is provided for calculating the activity of boron oxide in the slag, but in view of the uncertainties about the molecular constitution of these slags this operation seems meaningless. All simple assumptions lead to absurdly high activities. It should be pointed out that the limited data on hand made it necessary for Gurry to assume activities for boron oxide in the slag and boron in the metal, and to estimate the entropy of melting of boron. It is not clear how the differences between the theoretical and experimental values should be distributed among these various items, but it is not felt that the reliability of the calculation is great enough to discredit the experimental value. The experiments show that the deoxidizing power of boron in liquid iron is comparable to that of silicon rather than aluminum.

An indication of the general usefulness of this experimental constant is given by a magnesia-crucible heat in which a simulated open-hearth slag was used:

SLAG ANALYSIS, PER CENT

$$B_2O_3$$
 2.46

FeO 54.8

 SiO_2 7.0

 CaO 30.1

 MgO 4.8

$$\frac{CaO + MgO}{SiO_2} = 5$$

METAL, PER CENT

 $B = 0.0017$
 $O = 0.14$
 $K_B = 3.6 \times 10^8$
 $K_{B_2O_3} = 8.8 \times 10^8$

It is evident that even though this slag has markedly different chemistry from those in Table 1, equilibria in the metal and between slag and metal are of the same order as those in the simpler slags.

The implications of these data for steelmaking operations should be reviewed: Since oxygen levels comparable to those obtained with silicon can be reached under ferroborate slags, the deoxidation of lowcarbon steels by the use of borax-containing minerals, as rasorite, is a technically sound operation and should not be regarded with suspicion. The extensive fluxing powers of borax are well known and such a treatment might be expected to produce a very clean steel and be a desirable method for preliminary deoxidation. In these experiments, it was observed qualitatively that all of the slags used were very fluid even well below the melting point of iron. The experiments also indicate that by using proper oxygen control it should be possible to introduce a specified amount of boron into steel by a ladle reaction with borax, which would generally be a cheaper process than the use of expensive ferroalloys. Such a treatment would produce a ladle slag in substantial equilibrium with the steel and should result in good uniformity for the entire heat. Since the amounts of boron desired are extremely small, it seems likely that this method of control might be more satisfactory than the use of ferroalloys. Also, this means of lowering the oxygen activity of the slag should minimize ladle reactions with any easily oxidized alloy addition, such as chromium. The results reported would also indicate that boron can be eliminated about as easily as silicon if it enters the heat in the scrap. Conversely, the reduction of boron from a slag under only slightly oxidizing conditions, as after a furnace block on a highcarbon heat, or under a reducing slag in the electric furnace, may be expected to occur. Since such small amounts of boron are important in determining hardenability. these conditions should be checked carefully. Corbett and Williams¹⁷ made many observations on the high efficiency of boron recovery from boron compounds, which are also in line with these expectations. Such predictions require confirmation in practice but it is felt that the experiments provide some of the basic metallurgical data that must be considered if the use of borax and boron is to be fully exploited in steelmaking practice.

SUMMARY

1. The boron-oxygen relations in liquid iron have been determined experimentally by analyzing for these elements in melts made under slags containing varying amounts of iron and boron oxides, using crucibles of both silica and magnesia.

2. The results show that the deoxidizing power of boron is comparable to that of silicon and can be expressed by the constant

Kn

$$= \frac{1}{B_2(\% \text{ liquid Fe}) \times O^3(\% \text{ liquid Fe})}$$
$$= 2.4 \times 10^8$$

3. The results show that the amounts of boron of commercial interest can be introduced into steel from boron oxide compounds and that these amounts are subject to control by suitable oxygen control.

ACKNOWLEDGMENTS

This research was conducted as part of a project sponsored by the Pacific Coast Borax Co. in the Metals Research Laboratory at the Carnegie Institute of Technology.

The early heats in silica crucibles were made by Mr. Tom Omori. The bulk of the experimental work was done by Martha Messmer Helzel. The analyses of boron in iron were made by Dr. Margaret W. Kelly, of Connecticut College for Women.

REFERENCES

- F. G. Norris: Conservation of Aluminum. Open Hearth Proc. A.I.M.E. (1942).
- 25, 109. 2. T. W. Lippert: Boron. Iron Age (Nov. 19. 1942) 41.

- 3. M. A. Grossmann: Hardenability Calcu-
- lated from Chemical Composition.

 Trans. A.I.M.E. (1942) 150, 227.

 4. R. W. Gurry: The Relative Deoxidizing
 Power of Boron in Liquid Steel and the
- Fower of Boron in Liquid Steel and the Elimination of Boron in the Open Hearth. Trans. A.I.M.E. (1944) 158, 98.

 5. C. R. Taylor and J. Chipman: Equilibria of Liquid Iron and Simple Basic and Acid Slags in a Rotating Induction Furnace. Trans. A.I.M.E. (1943) 154.
- 6. E. P. Barrett, W. F. Holbrook and C. E. Wood: Induction Furnaces for Rotating Liquid Crucibles. Trans. A.I.M.E. (1939)
- T. Motock: Open Hearth Proc., A.I.-M.E. (1943) 26, 149.
 J. L. Hague and H. A. Bright: Determination of Boron in Steel and Cast Iron.
 Page Nat. Bur. Stds. (Aug. 1938)
- J. Chipman: Application of Thermo-dynamics to the Deoxidation of Liquid Steel. Trans. Amer. Soc. for Metals
- (1934) 22, 385. 10. J. Chipman: Chemistry at 1600°C. Trans.
- Amer. Soc. for Metals (1942) 30, 817.

 11. C. A. Zapffe and C. E. Sims: Silicon-oxygen Equilibria in Liquid Iron. Trans.
 A.I.M.E. (1943) 154, 192.

 12. Basic Open Hearth Steelmaking, 498. Phys.
- Chem. of Steelmaking Com., A.I.M.E.,
- 1944. 13. Scott's Standard Methods of Chemical
- Analysis, Ed. 5, 1.

 14. Treadwell-Hall: Analytical Chemistry, Ed.
- Iteauwan
 J. II.
 K. L. Petters and J. Chipman: Equilibria of Liquid Iron and Slags of the Systems CaO-MgO-PeO-SiO₂. Trans. A.I.M.E.
- (1941) 145, 95.
 16. J. S. Marsh: Slag-metal-oxygen Relationships in the Basic Open-hearth and Electric Processes. Trans. A.I.M.E. (1945) 162, 672. Also, Proc. Open Hearth Conf., 1944, A.I.M.E., 126.
 17. R. B. Corbett and A. J. Williams: Effects of Boron in Steel. U. S. Bur. Mines Reprint R. I. 3816.

DISCUSSION

(R. L. Forrest presiding)

N. F. TISDALE. *- This paper goes a long way to explain some hitherto unknown boron phenomena. With reference to analysis of boron, I am afraid that the author may get into trouble with some chemists in Pittsburgh who are regularly analyzing for boron on full heats of steel. There are several that claim to check in the third place, and plus or minus two in the fourth place. We ourselves use the spectrograph for determining boron and have developed an accurate method that compares favorably with the chemical methods.

^{*} Molybdenum Corporation of America, Pittsburgh, Pennsylvania.

The addition of boron oxide to the ladle or slag has been tried for a number of years, and it is known that boron is reduced to the metal. The part that is missing in the discussion is the uniformity of its effect in the form in which it is present. Some boron carbide has been found, and it could cause machining troubles.

Since such very small amounts of boron (0.003 per cent) are used to obtain the desired physical properties, and small extra amounts would ruin the steel. I do not believe that the reduction of boron from boron oxide is dependable enough to take a chance on producing off-grade steel by this method.

F. G. NORRIS. - This paper is a typical example of the results of an exchange of ideas. Observation of plant processes was discussed with a possible laboratory study in mind. The action of rasorite and other forms of borax had been observed in the shop, but not entirely understood.

Professor Derge was sufficiently interested in this subject to investigate it in a systematic way. His results seem to be entirely in accord with the use and also the misuse of borax for deoxidizing purposes.

Although outlined in general terms in the body of the paper, it may be profitable to describe in detail what happens in a ladle of steel containing say, 0.05 per cent O when about 50 or 60 lb. of rasorite is added. The rasorite is added during tapping and the usual amount of furnace slag covers the ladle. To what extent do the equilibrium studies apply to such a situation? What is a reasonable estimate of the oxygen content of the steel after such treatment?

J. C. SOUTHARD. †-It is interesting to have a direct determination of the boron-oxygen equilibrium in liquid steel and compare it with values calculated by Gurry¹⁸ from thermal data. The discrepancy is of considerable magnitude. A similar discrepancy exists in the aluminum-oxygen equilibrium between the calculated curve of Chipman19 and the experimental curve of Wentrup and Hieber. 20 The latter discrepancy has been ascribed by Chipman to the difficulty of obtaining complete separation of aluminum oxide crystals from liquid iron. In the present equilibrium this can scarcely be the explanation, for with the fluidity of boron oxide slags separation should be obtained quite easily. A discrepancy also exists in the titanium-oxygen equilibrium between the calculated values of Gurry18 and the direct determinations of Wentrup and Hieber²¹ although to a smaller degree. These discrepancies, all in the same direction, suggest that there may be something inherently wrong with the theoretical calculations and that the published18 deoxidation values for zirconium and vanadium also may be in error. It is the purpose of this discussion to examine the theoretical calculations in detail.

The calculated oxygen concentrations in liquid iron in the instances cited are based on calorimetrically determined values of the free energies of the various oxides of the various deoxidizing elements. These free-energy values apply to the conventional standard state of the pure substances at one atmosphere pressure. In steel deoxidation the oxygen, deoxidizer, and deoxidation product are not present as pure substances and the differences in the free energy between their actual state and the standard state must be determined, usually from the "activities" of the various substances. The activity of oxygen in liquid iron has been experimentally determined by Chipman, Vacher, and others, but the activities of most deoxidizing elements in steel and their oxides in slag are pure assumptions. Thus the sources of error in the calculated deoxidation values may be said to lie either in the calorimetric free energies or in the activities of the deoxidizing elements and their deoxidation products.

The magnitude of the possible error in the standard free energy will be examined first. This will be estimated from the equilibrium concentrations o.or per cent B and o.o36 per cent O as read from the author's Fig. 8 and Gurry's activity coefficient of 0.02 for boron. The latter gives the smaller discrepancy of the two activity coefficients assumed by Gurry.

^{*}Assistant Metallurgical Engineer, Wheeling Steel Corporation, Steubenville, Ohio.
† Metallurgist, Titanium Alloy Mfg. Co.,
Niagara Falls, N. Y.

18. W. Gurry: Trans. A.I.M.E. (1944) 158,

<sup>98-106.

19</sup> J. Chipman: In Basic Open Hearth Steel-

³⁰ H. Wentrup and G. Hieber: Archiv Eisen-

huttenwesen (1939-40) 13, 15-20.

1 H. Wentrup and G. Hieber: Archiv Eisenhuttenwesen (1939) 13, 69.

The activity of the B2O2 in the slag is a most certainly less than its mol fraction because of its well-known compound-forming tendencies. Since the average molar concentration of B₂O₄ in Derge's experiments is less than 0.13, the upper limit of the activity of B2O2 should be less than o.1. Lower values tend to make the discrepancy larger. The activity of oxygen corresponding to the 0.036 per cent is calculated as 1.44 × 10-6 from the H2/H2O equilibrium over molten iron as measured by Fontana and Chipman. 22 These activities yield a value of about minus 200,000 cal. for the free energy of formation of B2O3 from liquid boron and gaseous oxygen. Gurry18 calculated minus 254,600 cal. from thermal data. Thus the calorimetric quantities would have to be in error by some 54,000 cal. if Gurry is correct in his estimate of the activity of boron in steel.

By far the largest single calorimetric quantity entering into the calculation of the free energy is the heat of combustion of boron. The value used in the calculations was that of Roth and Borger.²³ Roth is a calorimetrist of wide experience. It would be a very exceptional circumstance (for instance, an extremely impure sample) that would lead to an error of 54,000 cal. His sample of boron was prepared by passing BCl₂ and H₂ over a glowing tungsten filament. Laubengayer, Hurd, Newkirk and Hoard24 report that this method yields very pure boron substantially free from hydrogen. Nevertheless, the heat of combustion of hydrogen is about minus 34,000 cal. per gram as compared with minus 16,100 cal. per gram for boron, and small amounts of hydrogen should materially affect the latter. But calculation shows that the sample would have contained over 12 per cent hydrogen to have led to an error of 54,000 cal. in the heat of formation of boron oxide. This seems to lie well outside the possible hydrogen content. Probably 10,000 cal. would be the limit of error from this source.

The uncertainty in the estimated entropy of fusion of boron mentioned by the author could scarcely be more than 2 cal. per degree,

which at steelmaking temperatures would be equivalent to about 7500 cal. Thus the maximum error in the calorimetrically determined free energy probably does not exceed 20,000 cal. which would account for less than 40 per cent of the discrepancy.

The second source of error, the activity of boron in liquid iron, must therefore be held accountable for the major part of the discrepancy. Calculations from Derge's data indicate that the activity coefficient of boron in liquid iron must be less than 0.001 and possibly as low as 0.0001, depending on how much error is assigned to the calorimetric free energy. Uncertainties in the activity of boron in the slag are in such direction as to require still lower activities of boron in steel.

The reasons for such low activity coefficients of boron form a source of speculation. It is assumed that the iron used in the author's experiments is virtually free from carbon, for boron probably forms a very strong carbide, which would in effect lower its activity in steel. Boron forms intermetallic compounds with iron in the solid state and some of this affinity probably carries over into the liquid state.

There is a strong implication that thermodynamicists have been estimating high values for the activity coefficients of deoxidizing elements in liquid steel. We should have more experimental data on this subject, not only for the liquid state, but also for the solid, inasmuch as the calculation of equilibria involving stabilization of carbon and nitrogen also depends on these activity coefficients.

J. CHIPMAN.*—I think it would be rather a pity to leave the discussion of this very good paper without some comment on the value and merit of the work done. This is a very good piece of work, which shows us a great deal more than we used to know about the chemistry of boron in steel.

G. Derge (author's reply)—The discussions of this paper have served to clarify some of the difficulties of experimentation and interpretation encountered by the author, and he is very appreciative of these remarks as well as the comments on the value of the results.

The determination of which analytical

³² M. G. Fontana and J. Chipman: Trans. Amer. Soc. for Metals (1936) 24, 313-336.

¹³ W. A. Roth and E. Borger: Ber. (1937)

⁷⁰⁻B, 791.

A. W. Laubengayer, D. T. Hurd, A. E. Newkirk and J. L. Hoard: *Jnl.* Amer. Chem. Soc. (1943) 65, 1924-1931.

^{*} Professor of Metallurgy, Massachusetts Institute of Technology, Cambridge, Massachusetts.

methods should be used for boron in the metal and slag was a difficult problem. The selection of a modified distillation titration for the slag analysis was quite obvious. Even though the exact problem had not been described in the literature, it did not appear likely that either colorimetric or spectrographic methods could hold much promise for the large amounts of boron oxide that were anticipated. Moreover, a high order of accuracy was not required. The selection of a method for boron in the iron was more difficult. At the time the work was started, off-the-record symposia were based on this very question and difficulties were reported on all methods; but the Chapin method seemed best established and best suited to the wide range of compositions expected. If this same work were being planned today, the analytical picture would be more as Mr. Tisdale has described it.

The possibility of influencing machinability adversely by introducing boron through a slag reaction is difficult to imagine. If a given steel composition exists in the ladle as a true homogeneous liquid, the distribution of boron between carbides and a solid iron phase will depend upon freezing processes only and not on the method by which the boron was introduced into the liquid. It is conceivable, however, that a boron-bearing ferroalloy may contain boron carbides that do not become molten in the ladle. These will survive in the poured ingot as a heterogeneous constituent. The use of boron oxide slags as a source of

boron seems to be the safest way to avoid this risk.

The review of the sources of error in thermodynamic data by Dr. Southard shows very clearly the importance of obtaining experimental values of deoxidation constants, the experiments simulating conditions to be encountered in actual practice. I would like to emphasize what he and many others have pointed out but very few have appreciated, that "these free energy values apply to the conventional standard state of the pure substances at one atmosphere pressure." This condition can very seldom be realized in any real case. Our experiments illustrate this point. Even when boron oxide was the only slag constituent added, the slag samples analyzed upward of 20 per cent iron oxide. Imagine what must happen in the problem proposed by Mr. Norris, in which only 50 lb. of rasorite is added to 100 tons of steel. I do not wish to avoid the issue presented by Mr. Norris, but I believe the basic slag described at the end of the paper shows that the experimental equilibrium constant can be used as a first approximation for predicting the oxygen level to be expected from this treatment. Beyond this, such mill variables as steel composition, slag composition, temperature, ladle size, and time in the ladle must cause deviations that must be determined for individual practices. It is my belief that these deviations will not be large, but this must be determined in the mill, and is beyond the scope of this paper.

An Equilibrium Study of the Distribution of Phosphorus between Liquid Iron and Basic Slags

BY THEODORE B. WINKLER, * JUNIOR MEMBER AND JOHN CHIPMAN, † MEMBER A.I.M.E. (Chicago Meeting, February 1946)

In order to understand more fully the complexities of the reactions occurring between the liquid steel and the slag in the basic open-hearth steelmaking furnace, investigations in this country and abroad have turned to laboratory equilibrium studies. This paper is one of a series of reports on investigations being conducted at the Massachusetts Institute of Technology. The experimental work was completed early in 1942:

The slag systems found in the basic open hearth are very complex, being made up of at least eight major components and as many others whose effect might be classified as minor. The first two papers of the series, by Fetters and Chipman, 1,2 as well as the paper by Taylor and Chipman.3 dealt with the simplest possible slag system that would resemble those found in the basic open hearth—the slag system consisting of CaO-MgO-SiO2-FeO. (Taylor's rotating induction furnace eliminated the necessity of contamination of the slag by MgO.)

Having arrived at some reasonable conclusions regarding the physical chemistry of the reactions between molten iron and the simple slags at equilibrium, the next step was to investigate more complex slag systems. The major purpose of the present investigation was to determine what factors control the distribution of phosphorus between molten iron and the more complex basic slags at equilibrium, and to what extent these factors are influential. The slags used contained CaO, MgO, SiO2, FeO, Fe2O3, P2O5, MnO, Al2O3 and CaF2, but not all of the slag samples contained all of these components at one time.

REVIEW OF LITERATURE

Although a number of interesting papers have been published on the subject of dephosphorization of an iron bath, there are as yet no results from laboratory studies that give thoroughly reliable information on the dephosphorization reaction. Even for the supposedly simple Fe-O-P system involving iron-phosphorus melts and iron oxide-iron phosphate slags, the experimental results are contradictory and no formulas have been established that adequately fit the equilibrium conditions. The Fe-O-P system has been studied by Schackmann and Krings,4 von Samson-Himmelstjerna,5 Oelsen and Maetz,6 Bischof and Maurer,7 Diepschlag and Schürmann,8 and Herty,9 and the results of their investigations appear in Table 1. A number of different equilibrium constants and distribution ratios

This paper is based upon a thesis submitted by Theodore B. Winkler in partial fulfilment of the requirements for the degree of Doctor of Science at the Massachusetts Institute of Technology. Manuscript received at the office of the Institute Nov. 3, 1945. Issued as T.P. 1987 in METALS TECHNOLOGY, April 1946.

* Graduate Student, Massachusetts Institute of Technology, Cambridge, Mass.;

tute of Technology, Cambridge, Mass.; now with Bethlehem Steel Co., Bethlehem, Pennsylvania,

[†] Professor of Metallurgy, Massachusetts Institute of Technology.

¹ References are at the end of the paper.

TABLE 1.—Previous Investigations of Fe-O-P System

Tempera-		tal		Slag			Equilibrium Constant
ture, Deg. C.	C. Per Cent	P.	PrOs. Per Cent	FeO, Per Cent	Impurity,	K_{P1}	or Ratio
Deg. C.	Per Cent	Per Cent	Per Cent		Per Cent		
				Herty*			
1510	Electro-	4.99	24.5	75.5 80.6	1	0.095	
1510	lytic iron	3.42	19.4	80.6		0.089	
1510 1510		3.04	21.7	78.3		0.074	
1510	1	3.87	22.5	77.5	1	0.097	
				lag and Sch	ürmann ⁸		
1570 1520	0.10	0.75	1.63	98.37		0.016	
1520	0.10	0.08	1.53	98.47		0.018	
1570	0.15	0.80	1.23	98.77	1	0.011	
1570	0.01	0.72	1.37	98.63	1	0.015	
			von San	nson-Himme	elstjerna*		77 - L
1550	Armeo	4.13	21.0	79.0		0.055	KP2 ⁶ 2.8 × 10 ⁻⁶
1550	iron	4.23	20.7			0.050	-3.I
1550	non	3.84	20.0	79.3 80.0		0.051	2.5
1550		2.77	12.8	87.2		0.023	3.4
1550		3.41	11.6	88.4		0.012	3.4
1550 .		3.4I 1.64	5.6	94.4		0.015	3.4
1550		1.79	4.5	95.5		0.0095	7.6
1550		4.37	16.6	83.4		0.020	8.2
1550	M	2.62	11.6	88.4		0.021	3.6
1550	1	2.16	5.2	94.8		0.0079	8.1
			Bisc	hof and Ma	urer [†]		
	1	1	1	1	1		KPs (%P2Os)/[%
1150		7.86	36.2	63.8		93.5	0.147 4.60
1150	0.55	7.05	35.1	64.9 72.8		21.2	0.252 4.97
1450	0.32	5.04	27.2	72.8		0.214	0.239 5.37
1500	0.07	8.35	36.0	64.0		63.3	0.140 4.31
1500 1574	0.20	9.05	34.8	65.2 89.1		0.035	0.132 3.84 0.601 5.76
13/4		1.09		rer and Bise	hof18	0.033	3.70
	1	1	Mau	tel and bise	SiO ₂	-	(# D.O.\ / [# D]
1525	Armco	2.05	10.86	88.71	0.36	0.014	(%P2Os)/[%P] 3.68
1535	iron	3.40	10.72	87 21	2.20	0.011	3.15
1540 1550 1540	non.	1 51	5 16	87.31 91.70	2 32	0.017	3.43
1540		1.51	5.16 8.98	89.20	2.32 0.68	0.023	4.75
1550		1.60	6.54	92.12	0.75	0.016	3.87
1530		6.14	22.24	75.28	1.18	0.039	3.63
1540		7.56	10.57	79.04	1.02	0.013	2.59
1550	1	3.34	10.10	87.24	0.95	0.010	3.00
			Schael	kmann and			
	1.	1	1	1	Al ₂ O ₃		KP4d
1450	Armeo	2.06	12.6	79.3	8.2	0.049	0.081
1450	iron	3.15	19.0	78.3	2.8	0.069	0.064
1450		3.46	23.6	73.7	3.8	0.178	0.043
1450		3.98	20.9	71.4	7.7 5.1	0.213	0.058
1450		4.95	25.7 26.7	65.2	8.1	0.263	0.058
1430		0.02	20.7		ZrO2	0.203	0.030
1450		7.95	33.8	64.5	1.7	6.82	0.043
1450		8.23 10.60	32.8	61.8	5.5	9.10	0.043
1450		10.60	33.8	61.1	5.1	18.3	0.058
1450		11.83	35.7	60.4	3.9	276.0	0.059
1450 1450		15.20	37.7	55.0	7.4		0.063
1450	1	19.50	44.3	50.6	5.1		0.053
1525		13.90	31.4	53.5	15.1	1.39	0.079
1525	1	12.00	27.8	57.I 66.I	15.1	0.706	0.093
1525		7.17	24.3 17.8	77.0	9.6	0.005	0.081
1525		5.80 4.87	17.6	77.0 69.1		0.0068	0.114
1525 1525			9.45	73.4	14.8	0.0008	0.212
1525		4.32	11.5	74.1	14.4	0.012	0.186
1525		3.81	6.25	75.7	14.4	0.0046	0.407
1525		3.70	4.60	75.7 75.8	19.6	0.0031	0.575
1525		2.52	3.44	79.3	17.1	0.0043	0.553
1525		1.43	1.27	77.3 86.8	21.4	0.0043	0.863
		0.93	1.64	86 8	11.5	0.012	0.478
1525 1525	1	0.64	0.73	83.2	16.1	0.012	0.720

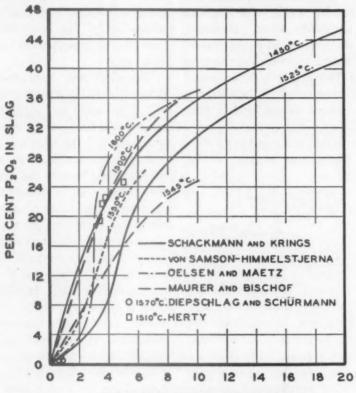
[•] Herty and Diepschlag and Schürmann: $K_{P1} = \frac{(3\text{FeO.P2O}_5)}{(\text{FeO})^5[P]^2}$ where (3FeO.P2O_5) , (FeO) = mol fractions, [P] = weight per cent.

b von Samson-Himmelstjerna: $KP_2 = \frac{(\text{FeO})^6 [\text{Fe}_3 P]^2}{[\text{Fe}]^{11} (3 \text{FeO}. P_2 O_5)}$ where all concentrations are expressed as mol

^{*} Bischof and Maurer: $K_{P_3} = \frac{(\text{FeO})^{\frac{4}{5}}[P]^2}{[\text{Fe}]^{\frac{4}{5}}(P_2O_5)}$ where all concentrations are expressed as mol fractions.

d Schackmann and Krings: $K_{P_4} = \frac{(\text{FeO})^{\frac{4}{5}}[P]^2}{[\text{Fe}]^{\frac{4}{5}}(P_2O_5)}$ where (FeO), (P₂O₅), [Fe] = mol fractions, [Σ P] = weight per cent phosphorus.

were devised by the different investigators, but for the sake of comparison, the one proposed by Herty was used to make calculations comparing the experimental plants were used in the evaluation of the various methods. Zea's summary table, which is reproduced in part below, indicates that the method of Schenck and Riess



PER CENT PHOSPHORUS IN METAL
FIG. 1.—PUBLISHED DATA ON Fe-O-P SYSTEM.

data collected by the various investigators. The data yield a "constant" that is far from constant (Table 1), for the values vary between 0.0031 and 276. To illustrate further the inconsistency of the data, a composite diagram of the data (Fig. 1) was made in which the value of percentage of phosphorus in the metal was plotted against percentage of P₂O₅ in the slag.

In a new publication, Zea¹⁰ makes an appraisal of the methods set forth by Whiteley, ¹¹ Herty, ⁹ Maurer and Bischof, ¹² and Schenck and Riess¹³ for predicting the phosphorus content of a steel bath in a basic open hearth. Slag and metal analyses collected in two British steel

gave the best results, but a maximum discrepancy between actual phosphorus and calculated phosphorus of 0.018 per cent is still too large to be of practical value.

Discrepancy between Calculated and Analyzed Percentage of Phosphorus, from Zea¹⁰

Investigator	Maxi- mum	Mini- mum	Aver- age	Num- ber of Sam- ples
Whiteley	0.020	0.003	0.010	29
	0.027	0.003	0.012	29
	0.019	nil	0.006	15
	0.018	0.001	0.005	29

Schenck and Riess¹⁸ developed a set of equilibrium diagrams by which it is

possible to evaluate the free CaO and free FeO contents of a slag if the temperature, total SiO2, total MnO, total Fe and the available lime (total lime minus lime combined with P2O5) of the slag are known. For the construction of this set of diagrams equilibrium constants were calculated, using weight per cent as the concentration values, to determine how much of the total CaO and total FeO are tied up in compound formation. By substituting in the following equation the proper values for free CaO and free FeO, obtained from the diagrams, as well as the temperature and total P2O5 content, the phosphorus content of the metal was calculated.

$$\log K_{\rm P}^{\rm IV} = \log \frac{[P]({\rm FeO})^{5} ({\rm CaO})^{4}}{(\Sigma {\rm P}_{2}{\rm O}_{5})} + {\rm o.o6o} (\Sigma {\rm P}_{2}{\rm O}_{5})$$

$$\log K_{\rm P}^{\rm IV} = -\frac{51,800}{T} + 35.05$$

McCance¹⁴ studied dephosphorization and showed that no practical amount of dephosphorization was accomplished by slags of less than 32 per cent CaO. Tenenbaum¹⁵ developed a constant to illustrate dephosphorization in the basic open hearth, but indicated that no dephosphorization could take place below a 2:1 lime-silica ratio.

On the whole, the information published on dephosphorization is either too general and qualitative to be of any practical use, or the information that is quantitative has too many limitations to be of any use to the steelmaker.

EXPERIMENTAL METHOD

The induction furnace and the experimental procedure used in making the experimental heats are essentially the same as described by Fetters and Chipman.¹ One significant change was made in the furnace; namely, the method of providing a source of heat for the slag, which is not accomplished by induction heating. The slag was kept molten by the radiant heat

from an arc drawn between two carbon electrodes suspended above the bath but within the furnace crucible (Fig. 2). The heat supplied was more intense than that furnished by the graphite slag heater previously used, and thus permitted the utilization of the more refractory highlime slags so important in a dephosphorization study.

The electrodes were made of 11/4-in. graphite rods, so arranged that the length of the arc could be controlled by rotating the vertical parts of the electrodes. Power was supplied through a resistor from a 230-volt line; an input of about 10 kva. was sufficient to heat the upper portion of the furnace to a temperature roughly approximating that of the metal. The electrodes normally lasted for about 8 hr. of continuous service before the tips became too short to strike an arc. No carbon pickup was observed in the metal as long as it was covered by slag. This was important, since a pickup of less than o.o1 per cent would have made accurate sampling impossible. It was not feasible to obtain exactly uniform temperature and in general it is probable that the slag was slightly hotter than the metal, thus reversing the gradient of former experiments in which an induction-heated block was suspended above the slag. It seems unlikely that the results are in any way vitiated by these irregularities. The heat transfer from metal to slag is quite good, by virtue of the rapid stirring in the metal. For this reason the slag layer next to the metal is always substantially at the temperature of the metal.

The experimental heats were made by melting a 65-lb. charge of Armco ingot iron in a magnesia crucible under a vacuum, to reduce the carbon content to below o.o. per cent. A mixture of oxides to provide a synthetic slag was added in sufficient quantity to cover the surface of the metal bath, and the slag heater was installed. A nitrogen atmosphere at a positive pressure was maintained within

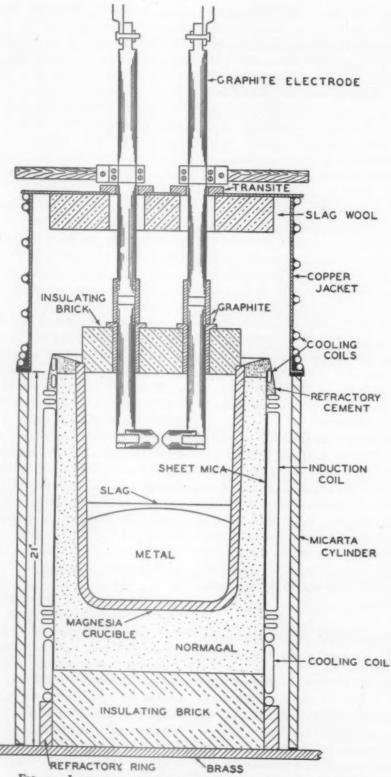


FIG. 2.—INDUCTION FURNACE WITH CARBON-ARC SLAG HEATER.

the furnace, so that the subsequent equilibrium between slag and metal would not be disturbed by the oxygen in the air. The temperatures were measured with tungsten-molybdenum thermocouples, using fused silica protection tubes and water-cooled or air-cooled thermocouple holders. The tungsten-molybdenum thermocouples were calibrated against platinum-platinum 10 per cent rhodium couples. and subsequent checks on the calibration curves were made with platinum couples under operating conditions. The accuracy of the temperature readings is at least within ±10°C. The samples were taken by the use of small split steel molds, which were dipped into the bath. The molds for the metal samples were smaller in diameter and of heavier wall thickness than the slagsampling molds, in order to provide rapid solidification of the metal and inhibit segregation within the sample. All the metal samples were sound and free from internal blowholes, a condition that is easily obtained when the carbon content is well below o.o. per cent.

The slag samples were analyzed by conventional chemical methods under carefully controlled conditions for the oxides contained; the reported values of the oxides being the result of check determinations. The metal samples were analyzed for phosphorus by conventional chemical methods and the total oxygen content by the vacuum-fusion method; again the results reported were obtained from check determinations.

USE OF RADIOACTIVE TRACER TO STUDY RATE OF ESTABLISHMENT OF EQUILIBRIUM

Since the data gathered in the investigation were to be treated as equilibrium data in applying thermodynamic principles to arrive at a solution for dephosphorization, it is obvious that it was necessary to be sure that equilibrium existed at the time of sampling and temperature measurement. It was necessary to ascertain how long a time was required for the slag and metal bath to return to equilibrium after the equilibrium had been disrupted by a slag or metal addition or a temperature change.

To arrive at the time interval needed to establish equilibrium, radioactive phosphorus was used. Anhydrous tricalcium phosphate that had been made radioactive was added to the bath after the bath had been adjusted to a constant temperature. After the addition, metal samples were taken every 5 min. for 40 min., after which the temperature was raised and samples were again taken every 5 min. The metal samples were exposed to a Geiger counter, which determined the relative amount of radioactive phosphorus in each sample. When the amount of radioactive phosphorus within successive metal samples reached a constant value as indicated by the Geiger counter, equilibrium had been re-established. As is clearly shown in Fig. 3, equilibrium was re-established within 15 min. in both tests. This experiment was carried out in two different heats, and the results were confirmative. In order to be on the safe side, at least 30 min. was allowed after a bath addition or a temperature change before a set of samples and a temperature were taken.

RESULTS

In the course of the investigation, 11 experimental heats were made and a total of 98 pairs of slag and metal samples were taken, each pair being accompanied by a temperature measurement. Space prohibits the publication of a detailed account of each of the experimental heats, but Table 2 shows the clock time at which each set of samples and temperature measurement were taken, with accompanying chemical analyses of both the slag and metal samples.

TABLE 2.—Chemical Analyses of Slag-metal Samples

Unach Mr.	Metal	Slag	Clock	Temper-		Steel Analy	Analysis, Per C.	Cent				Slag An	Analysis, 1	Per Cent			
ricat No.	Test	Test	Time	Deg. C.	Mn	w.	Δ	0	CaO	SiOs	Peo	FesOs	MgO	S	Ps08	MnO	CaF
E-29	H	e	11:26	1612	0	0.0195		0.153	22.II	II.60	52.44		5.71	0	0.07	0	
	6	105	IZ:II	191	0	0.019		0.176	23.01	10.86	50.59		5.78	0	I.90	0	
	00	200	12:43	IOSI	0 0	0.0195		0.100	22.84	10.84	50.53		2.90	0	I.80	0	
4	20	13	25.20	4000	00	0.030		0.150	24.21	00.00	40.40		5.20	0	4.03	0	
E-30	1	2 61	10:57	1576	00	0.0348		0.10	20.00	27.10	26 97		10.0	0.051	16.0	0 0	
	3	4	11:47	1597	0	0.036		0.143	26.66	25.54	26.74		12.07	0		0 0	
	100	9	12:40	1573	0	0.0375		0.132	26.07	26.00	26.30		12.84	0		00	
	2	00	1:23	1656	0	0.037		0.180	27.33	36.06	25.59		14.46	0	3.75	00	
	10	N. N.	23.55	1715	0	0.036		0.233	27.83	24.98	26.55		14.83	0	. 10	0	
	14	13	3:00	1715	0	0.0365		0.240	29.51	21.02	26.92		12.57	0		0	
11	PA (O	4:04	1008	0	0.0375		0.165	29.94	22.24	24.34		11.13	0	- 81	0	
	7.7	1.0	5:15	1000	00	0.0335		0.151	27.78	25.80	21.08		13.82			0	
W. 22	200	100	10.07 T	19191	0 000	0.0305		0.120	20.35	29.40	19.68		17.14	0	- 90	0	
200	i v	A	11:40	1640	0.144	0.083		200	0.3	A. 88	70.94		3.04	0.000	00	13.80	
	130	E3	2:14	1620?	0.100			0.175	0 0	0.86	66.27 27.20		200	0.137	00	20.00	
	1.4	15	3:31	16802	0.100	0.000		0.227	000	46.30	200		0.4	001.0	0 0	20.02	
	10	17.	4:00	16902	0.350	0.033	0	0.180	0.40	I. 74	86.30		2 . 44	0.112	00	20.00	
	19	20	4:43	1610	0.220	0.021	0	0. I30	0.32	2	27.03		200	0.120	00	22.07	
	21	23	5:14	1593	091.0	0.033	0	0.100	0.34	13.26	39.74		5.68	0.00I	0	37.80	
	23	24	5:45	1610	0.220	0.023	0	0.078	0.38	22.0I	24.47		12.46	0.064	0	39.24	
	NO CO	22	0:40	0191	0.195	0.030	0	0.095	0,38	22.12	26.81	00	12.76	0.057	0	36.47	
D-34	2 N	-	3000	1000	0.133	0.033	0.030	0. IIO	35.01	7.02	30.50	H (0.02	0.131	10.0	7.33	
	200	10	12:15	1647	0.142	0.030	0.030	0.057	41.00	27.06	8.70	0.00	0.03	0.114	2 30	7.48	
	a	TO.	I:33	1550	0.077	0.030	0.045	0.003	35.55	28.12	13.21	SI	0.75	0.034	3.43	7.02	
	II	E.Z.	1:52)	1.590	0.083	0.030	0.049	0.067	35.52	27.72	12.87	91.	9.77	0.034	3.85	7.68	
	13	14	2:27	1015	0.000	0.020	0.071	0.098	34.38	26.44	14.70		10.37	0.038	3.46	7.58	
	ES	07	3:43	1043	0.181	0.030	0.087	0.053	38.24	33.84	5.03		14.71	0.035	0.64	5.39	
	33	3.4	000	16660	0.157	0.030	0.130	0.045	30.11	33.04	141		14.97	0.033	1.35	0.33	
E-35	2 =	100	1:04	1530	0.33	0.00	0.139	0.0/3	24.50	38.87	00.00		20.52	0.030	1.13	10.0	
	4	69	1:37	1620	0.40	0.030	0.133	0.0038	30.67	34. 20	3.30	10	30.4	0000	0.10	22.7	
	0	00	2:03	1600	0.43	0.023	0.135	0.0041	31.24	39.14	1.16	. 22	26.20	0.002	0.035	I.O.I	
	1.5	91	3:36	1605	0.39	0.030	0.136	0.0053	28.81	40.34	0.68	. 23	16.02	0.046	0.00	1.71	
25 45	23	24	3:55	1010	0,18	0.037	0.130	0.032	34.95	36.90	5.33	. 33	23.74	0.017	0.16	6.87	
15-30	- 0	-	20:1	1025	0.000	0.033	0.082	0.073	34.03	33.04	9.35		17.38	0.000	0.03	3.38	
	2 14	*	2.02	15030	0.044	0.024	0.084	0.057	24.50	39.35	12.30	44	17.48		0.00	3.72	
	200	000	200	1608	0.038	0.023	0.070	9000	27.90	20.41	14.03		22.00	0.014	1.03	3.00	
	0	OI	2:54	1605	0.033	0.022	0.077	0.084	23.48	35.13	16.80		10.62	010	20.00	30.00	
	17	18	3:30	1612	0.015	0.023	0.033	0.138	28.05	24.34	28.70		11.50	0.020	2.23	2.80	
	61	20	4:21	1654	0.012	0.023	0.037	0.199	22.05	21.12	36.36		12.13	0.020	1.53	2.64	
	31	33	4:53	1595	0.000	0.022	0.030	0.160	20.76	20.50	38.86		10.51	0.130	1.67	2.51	
0	23	34	2:17	1635	00000	0.033	0.035	0.183	15.86	15.70	50.25		9.14	0.038	1.05	2.08	
2-37	4 0		10:55	1505	V0.003	0.032	0.017	0.105	35.80	29.18	18.00		11.05	0.037	1.18	1.18	
	200	4.	14:15	1000	200.00	0.021	0.012	0.113	34.34	28.03	19.34		II.45	0	60.1	1.18	
-	-	0	00:21	0001	00000		800	2001	20 AY	00	TO COL		NO X	e	7 0	0 0	

TABLE 2.—(Continued)

Heat No	Metal	Slag	Clock	Temper-	226	el Analy	oteel Analysis, Fer Cent	30				slag An	alysis, I	Slag Analysis, Per Cent			
near No.	Test	Test	Time	Deg. C.	Mn	so.	Д	0	CaO	SiO ₂	Peo 1	FesO.	MgO	S	P,04	MnO	CaP,
E-37	œ ;	7		1622	0.006	0.019	0.007			70	21.63	3.98	.56	0.38	1.14	1.25	
	13	0.5	1:50	1011	0.000	0.021	0.000	0.093	41.01	20.08	11.89	2,32	10.19	0.010	0.85	I. 18	
	12.	14		1501	0.003		0.008			100	10.44	2.33	100	030	0.00	1.00	
	61	18		1635	0.000	0.018	0.0095			80	17.03	2.71	54	010	0.48	1 1 200	
	12	20		1608			900.0			48	27.62	4.54	46	030	0.55	1.10	
E-38	0	4		1630	0.172		0.046	0.161		00	60.73	4.28	.62	146	0.077	29.08	
	ומו	00		1072	0.211	0.025	0.048	0.194		91.	60.26	3.57	. 55	136	0.058	29.58	
	- 0	0 0		1730+	0.234		0.040	0.225		8	58.50	3.25	83	112	0.058	30.86	
	2:	12		1730	0.314	0.025	0.040	0.225	43	74	58.81	2.97	8	118	0.050	30.84	
	12			1000	45.00		0.147	0.200	24	5.6	58.70	3.91	94	123	0.270	28.43	
	25	791		200	27.00		900	0.130	000	900	29.17	4.12	200	130	0.500	20.49	
		000		1636	200		200	0.110	200	300	51.70	2.5	000	144	50.2	13.01	
	10	30		1630	275		0.00	121	300	0 0	20.14	20.4			1.07	23.57	
	31	33		1613	0.370	0.032	0.082	0.007	3.4	10	22 13	20.00		441	200	29.07	
	23	24		1715	0.520	0. 4	0.104			2 8	200	200		1 2 2 2	25	34.31	
E-39		4		1618	0.238	0.015		084		100	10.24	_	200	020	70.0	200	
	100	9		1670	0.270	0.016	0.146	118		64	16.46	_	03		2	12.06	
	1-	80		1590	0.212	0.030		683		100	10.50	_	2 3	000	00	100	
	0	10	12:51	1635	0.228	0.031	0.120	960		00	13.66	_		1 344	1.77	10.60	
	II	12.		1644	0.254	0.031	0.180	920		73	10.90	-			3.12	10.52	
	13	14		1594	0.176	0.031	0.153	080		14	13.05	_		-	1.94	11.71	
	201	01		1015	0.103	0.033	0.008	.093		10	13.65	_		-	3.45	9.85	
	170	000	40	1703	0.238	0.032	0.005	_	38.58		17.09	3.00	6.73	1 160	2.74	9.33	
	100	2 2 2		1001	0.21	0.034	0.071	200		44	14.57	_	10	H 0	10.8	9.55	
	23	34		1670	0.166	0.033	0.048	IIA		100	24.00	-	3 6	1 223	10.0	0.70	
E-40	H	100		1530	0.086	0.030	0.200	041		43	IA	_	99	put	24	20.00	A. K
	4	9		1640	0.106	0.028	0.298	690		43	18	_	W:	0381	100	2.42	3.0
	7	6	2:23	1625	0.143	0.027	0.182	040		26	3.37	_	54	1001	71.17	1.33	10.2
	10	13	3:04	1615	0.162	0.025	0.130	038		30	74	14	00	148 1	7.73	1.37	16.40
	150	17	2:01	1595	0.080	0.033	0.0084	072		30	28	.40	55	941.	99.	3.28	17.59
	100	30	5:33	1583	0.043	0.023	0,0000	104		14	37	_	77	114	1.57	3.84	12.96
0, 0	100	13.3	5:52	1023	0.040	0.034	0.0003	120		54	43	II.	20	114	5.34	3.68	12.60
E-43	29 1	2	11:30	1005		0.047	0.174	132		03	13.93		200	034 1	1.77	1.83	AlgOs
	na	00	15:11	1592		0.077	0.151	120		40	13.83	_	OI	048 1	5.23	1.83	
	0 0	0.5	13:35	1570		0.000	0.150	004		00	9.84	_	IO	040 I	00.	I.60	
	07	N	10:1	1590		0.075	0.152	103		20	10.00		04	040	0.02	1.00	
	200	000	1.40	1030		0.074	0.149	_		000	10.30	_		.003 I	.33	1.40	
	100	3.6	20.0	1623		0.00	0.138	200		0 0	11.00		200	1 2/0.	.05	1.52	
	200	4 5 5	20.00	1000		0.00	0.110	601		900	08.	.65	70	1 400.	20.	N . S	
	200	10	20.0	407		40.0	100.0	000		00	000	45.	200	1 000	01.	1.00 x	
	n or	100	9 6	2620		0.000	0.000	000		000	20.	141	10.	1001	.93	1.50	
	31	223	2000	2007		0.07	0.000	000		200		000	0.75	1581.	.34	1.50	0.00
	24	300	20.00	1604		2000	2000	2000		2 4	000	22.	200	2600 1	51.	1.44	
	200	200	40.4	13004		00.0	0.032	200		200	13.38	15.	5.40	202	7 47	1.40	
	200		1 10.0	0074													

INTERPRETATION OF RESULTS

Having failed in numerous attempts at finding some simple correlation between a phosphorus distribution ratio and slag It is obvious from the chemistry of the process that dephosphorization cannor proceed to any useful extent without the presence of free or uncombined lime. If

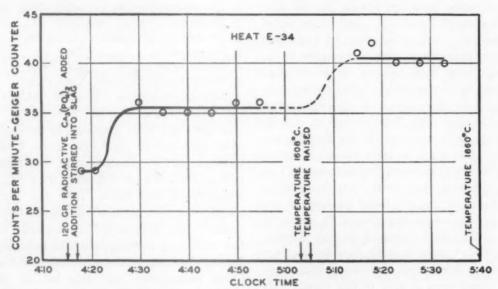


FIG. 3.—DETERMINATION OF EQUILIBRIUM BY USING RADIOACTIVE PHOSPHORUS.

composition, the authors decided to attack the problem by the more devious and complicated route of calculating an equilibrium constant for the dephosphorization reaction, which may be represented by the following chemical equation. The underlined symbols indicate the components dissolved in the metal phase and the parentheses designate slag components.

$$_{2}P + _{5}O + _{4}(CaO') \rightleftharpoons (_{4}CaO.P_{2}O_{5})$$
 [1]

The equilibrium expression for the chemical reaction takes the following form:

$$K_{\rm P} = \frac{(a_{\rm 4CaO.P_2O_5})}{[a_{\rm P}]^2[a_{\rm O}]^5 (a_{\rm CaO'})^4}$$
 [2]

In Eqs. 1 and 2 the parentheses indicate the concentration of the slag constituents and the brackets the concentration of the metal constituents; a indicates the activity; CaO' refers to free or chemically uncombined lime, but lime that is in solution.

no free lime were present to form a stable calcium phosphate, the P2Os or iron phosphate would be reduced by the metal bath and the dephosphorization could proceed only as far as the oxidation reaction would allow, which for the less strongly basic open-hearth slags is not far enough. It was necessary, therefore, to devise some reasonable measure of the free lime content of the slags involved in this investigation. It should probably be pointed out that the term "free lime" refers in this paper to lime that is in solution in the slag but that is uncombined in any way with any other substance, such as SiO2 or Fe2O2 or P2O5; it does not refer to undissolved lime, found in most basic openhearth slags.

Constitution of Liquid Slag

The controversial subject of the physical make-up of a liquid slag is a matter that is far from being settled to the satisfaction of all concerned. However, it is certain that there is some sort of attraction between the components of slag systems. Probably the most easily visualized, most widely and easily used hypothesis for the constitution of liquid slag, particularly where thermodynamic calculations are employed, assumes that the oxide components of the slags form more or less stable chemical compounds somewhat similar to the combinations that appear in the same slags in the solid state. Even though no definite compounds may form in the liquid state, the assumption at least affords a logical pattern for the attraction between the slag components that must exist in order to account for the slag-metal reactions in any metallurgical refining process. In preparing a quantitative measure of the dephosphorizing power of basic slags, the assumption of the existence of chemical compounds in liquid slags is used in this paper. This does not mean that the authors believe that such chemical species necessarily exist; the immediate usefulness of the assumption is not dependent on its ultimate truth. The concept of a simple liquid slag, in which all molecular species obey the laws of ideal solutions, has such advantages of simplicity that it might still be the most useful basis for numerical calculations even if it led to fictitious or improbable molecular formulas. Up to the present time, and in the calculations that follow, the assumption has been found to be a useful and sufficient basis for a physicochemical picture of slag behavior. It has not led to highly improbable formulas, although some of these do not correspond precisely with the more complex crystalline phases of the solidified slags.

After many other combinations of molecular compounds had been tried in a careful study of the experimental data, it was found that the behavior of liquid basic slag on the average conforms most closely to the ideal solution laws when it is considered as being made up of the following molecular species:

I.	Calcium orthosilicate	4CaO.2SiO2
2.	Calcium metasilicate	2CaO.2SiO2
3.	Free lime	CaO'
4.	Tetracalcium phosphate	4CaO.P2O6
5.	Ferrous oxide	FeO
6.	Monocalcium ferrite	CaO.Fe ₂ O ₂

7. Monocalcium aluminate. CaO.Al2O2*

8. A complex phosphate.... 4CaO.P2O6.CaF2

The MgO and MnO contained in the slags were assumed to have the same basic behavior as CaO, consequently they exist in the free state or combined with SiO₂, P₂O₅, Fe₂O₃, and Al₂O₃. They lose their identity in the calculations, since their molar values were added algebraically to that of lime. (It is recognized that assuming MnO to have the same basicity as CaO is a broad assumption, but this led to no inconsistencies in the results until the MnO content exceeded 12 per cent.)

Calcium orthosilicate and calcium metasilicate appear in the equations as double molecules, in the manner suggested by Taylor and Chipman.³ Without the use of the double molecule, the data could not be made to correlate properly. Preliminary calculations indicated that tetracalcium phosphate would fit better than tricalcium phosphate but either could probably have been used with satisfactory results. Since one of the assumptions, which will be fully explained later, accounts for the presence

^{*}The recent work of Grant and Chipman, 16 which was completed after the present paper was written, indicates the more probable existence of 2CaO.Al₂O₃. Such a formula would fit the data of this paper about as well as the one that was used. For purposes of calculations on the behavior of phosphorus in slags of ordinary alumina content, it is a matter of little consequence which formula is employed, and for this reason it has seemed unnecessary to recalculate the data of this paper. In the more important conclusion, that alumina behaves as an acid in basic slags, the two investigations are in full agreement.

of free lime in virtually all of the slags encountered in the investigation, it was assumed that the Fe₂O₃ found by chemical analysis existed in the liquid state as CaO.Fe₂O₃. Therefore, the term FeO in this paper refers only to ferrous oxide, not a total iron value calculated to ferrous oxide.

In a manner similar to that which led to the choice of tetracalcium phosphate, it was found that CaO.Al₂O₃ worked best for slags containing any alumina. It has been proposed by numerous investigators that fluorspar in basic slags forms an apatite compound; it was found here that the data for slags containing fluorspar fell in line with other fluorspar-free slags if the spar was assumed to form a complex molecule with lime and phosphoric oxide.

Calculation of Equilibrium Constants

Returning to the equilibrium equation for the dephosphorization reaction, Eq. 2 can be simplified by making substitutions for the chemical activities. The phosphorus in the metal phase probably occurs as Fe₃P, but as far as any thermodynamic calculations are concerned, the quantity may be expressed in the terms of elemental phosphorus. In dilute solutions, the percentage by weight of the solute so closely approaches the activity that ap may be substituted by percentage of phosphorus by weight. Similarly, it has long been known that the activity of oxygen may be expressed as per cent oxygen by weight. It has been assumed here that the metal and slag phases may be considered as ideal solutions; therefore, the activities of the slag components, namely, CaO' and 4CaO.P2Os may be expressed as mol fractions of those components. The equilibrium constant now takes the following form, in which the parentheses indicate mol fractions of the slag components and the brackets signify per cent by weight of the metal components:

$$K_{\rm P} = \frac{(4{\rm CaO.P_2O_6})}{[\%{\rm P}]^2[\%{\rm O}]^5({\rm CaO'})^4}$$
 [3]

The weight percentage values for phosphorus and oxygen were easily obtainable from analysis, but the mol fractions of free lime and tetracalcium phosphate presented quite another problem. In order to arrive at a mol fraction value of any of the slag components, it was necessary to establish a logical molten-slag constitution for the entire slag system similar to the one described in the preceding section.

The chemistry of dephosphorization as expressed in Eq. 1 shows that the reaction cannot proceed to any reasonable extent without the presence of free lime. It is widely believed that CaO has the greatest affinity for SiO2 of all the oxides present in the slag, and that there can be no CaO available for combination with any other oxides until the thirst for SiO2 has been satisfied. Dicalcium silicate has been generally conceded to be the most stable of the calcium silicates in basic open-hearth slags. Therefore, until a limesilica ratio in the slag of 2:1 has been exceeded in the normal process of the constantly increasing lime-silica ratio in the progress of an open-hearth heat, it is sometimes supposed that no lime is available to combine with P2O5 to promote dephosphorization. In direct contradiction to this hypothesis, the data collected for this investigation exhibit definite dephosphorization of an iron bath by basic slags having a lime-silica ratio below 2:1. Consequently, there must be some free lime available for combination with P2O5 in basic slags, that are more acid than a 2:1 lime-silica ratio.

Dicalcium silicate cannot then be as stable as has been so often proposed. It probably dissociates in some manner such as the following:

$$(4CaO.2SiO2) \rightleftharpoons (2CaO.2SiO2) + 2(CaO') [4]$$

The dissociation constant for the reaction is expressed as follows, in which parentheses indicate mol fractions of slag components:

$$K_D = \frac{(2\text{CaO}.2\text{SiO}_2)(\text{CaO}')^2}{(4\text{CaO}.2\text{SiO}_2)}$$
 [5]

When a value of CaO' can be determined that will satisfy Eq. 5, this value can be used in Eq. 3 to determine the value of K_P . As a first approximation in strongly basic slags, it was assumed that (CaO') is the mol fraction of lime remaining after all the acidic oxides have been satisfied (assuming dicalcium silicate as the only lime silicate present). In the more acid slags such an assumption is not allowable even as a first approximation. Under these conditions the value of (CaO') is quite small, and as a substitute the principal dephosphorization reaction may be considered to be the following:

$$2P + 5O + 2(4CaO.2SiO_2)
\Rightarrow (4CaO.P_2O_5) + 2(2CaO.2SiO_2)
K_{P'} = \frac{(4CaO.P_2O_5)(2CaO.2SiO_2)^2}{[\%P]^2[\%O]^5(4CaO.2SiO_2)^2}$$
[7]

By dividing $K_{\mathbf{P}}'$ by $K_{\mathbf{P}}$ and extracting the square root the value for $K_{\mathbf{D}}$ is obtained.

$$\sqrt{K_{P}'/K_{P}} = K_{D}$$
 [8]

To obtain numerical values for the three equilibrium constants involved a very tedious set of approximations with a picked group of data on slags containing only CaO, MgO, SiO₂, FeO, Fe₂O₃ and P₂O₅. Two groups of slag compositions were chosen, the basic group having a lime-silica ratio well above 2:1, thus ensuring

the presence of a relatively large amount of free lime; the acid group having a limesilica ratio below 2:1, thus ensuring the presence of a much smaller quantity of free lime. All the slag oxides as obtained from chemical analyses were calculated to mols per 100 grams of slag, as, incidentally, were the oxides for all the slags in the investigation. On an arithmetical basis the oxides of the slags in the basic group were divided into the molecular compounds listed earlier. All P2O5 was combined with lime as 4CaO.P2O5, all Fe2O3 as CaO.Fe2O3, all SiO₂ as 4CaO.2SiO₂, all remaining CaO as free lime (CaO'), and FeO as FeO; no 2CaO.2SiO2 appears in the first approximation for the basic group. This enabled the mol fractions of CaO' and 4CaO.P2O6 to be calculated and substituted with the values for %P and %O in Eq. 3, resulting in numerical values of KP for each slag sample. The values of $\log K_P$ were plotted against the reciprocal of the absolute temperature as is shown on Fig. 4 under the heading of First Approximation.

The same procedure was followed using the slags in the acid group. All P2O5 was combined with CaO as 4CaO.P2O5, all Fe₂O₃ as CaO.Fe₂O₃, all remaining CaO combined with SiO2 as 4CaO.2SiO2 and 2CaO.2SiO2, and FeO as FeO; no free lime (CaO') appears in the first approximation for the acid group. This in turn enabled the calculation of the mol fractions of 4CaO.-2SiO2 and 2CaO.2SiO2 for substitution in Eq. 7 along with the value of %P and %O resulting in numerical values for $K_{\mathbb{P}}'$. The values of $\log K_{\rm P}'$ were plotted against the reciprocal of the absolute temperature as is shown in Fig. 4. From the lines representing $\log K_P$ and $\log K_{P'}$ it was possible to calculate a line for the plot of $\log K_D$ versus 1/T, which also appears in Fig. 4 under the heading of First Approximation.

By making use of the first approximated value for K_D and the analyzed slag oxides as converted to mols per 100 grams of slag, it was possible to develop an algebraic

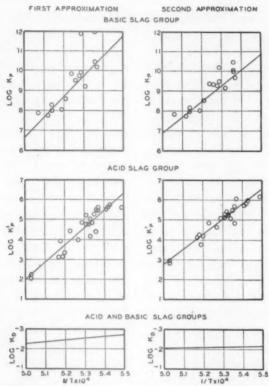


FIG. 4.—APPROXIMATIONS OF DISSOCIATION CONSTANT FOR DICALCIUM SILICATE.

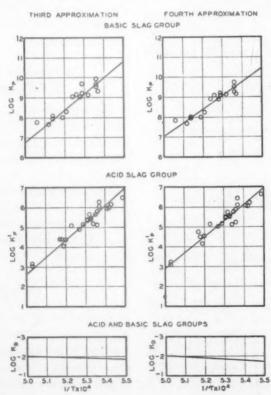


Fig. 5.—Approximations of dissociation constant for dicalcium silicate.

expression* by which the mol fractions of the liquid slag components were recalculated on the basis of the dissociation of dicalcium silicate. The use of this algebraic expression made it possible to arrive at a value for free lime for all of the slags, that value of free lime being used ultimately in the calculation of the phosphorus equilibrium constant K_P . The algebraic formula involves the use of the K_D term for its solution, but only an approximate value was available from the first approximation shown in Fig. 4. In order to make the formula usable, the value for K_D was made more exact by a tedious set of approximations making use of the algebraic expression and Eqs. 3 and 7. The course of the approximations is shown graphically in Fig. 4 under the heading of Second Approx-

* () indicates mols per 100 grams; () indicates mol fractions.

$$\frac{(C) = (CaO) + (MgO) + (MnO)}{-4(P_2O_4) - (Fe_2O_3) - (Al_2O_3)}$$

$$(C_2S_3) = (2CaO.2SiO_3)$$

 $(C_4S_2) = (4CaO.2SiO_2)$

 $\overline{(S_2)} = \frac{1}{2} (SiO_2)$ (Due to double silicate molecules)

 $(CaO') = (C) - 4(C_4S_2) - 2(C_2S_2)$

No = total number of mols per 100 grams

$$K_{D} = \begin{array}{l} \text{total number of mols per} \\ \text{of slag} \\ K_{D} = \frac{(2\text{CaO}.2\text{SiO}_{2})(\text{CaO}')^{2}}{(4\text{CaO}.2\text{SiO}_{2})} \\ = \frac{((\text{C}_{2}\text{S}_{2})/\text{N}_{e})((\text{CaO}')/\text{N}_{e})^{2}}{((\text{C}_{4}\text{S}_{2})/\text{N}_{e})} \end{array}$$

By suitable substitution this equation reduces to the following form:

$$x^{3} + ax^{2} + \frac{1}{4}bx - \frac{1}{4}c = 0$$
Where $x = (C_{2}S_{2})$

$$a = [(C_{1}) - A(S_{2})]$$

$$a = [(C) - 4(S_2)]$$

$$b = [(C) - 4(S_2)]^2 + K_D N_s^2 = a^2$$

$$+ K_D N_s^2$$

$$c = K_D N_s^2(S_2)$$

from which

$$\frac{(C_2S_2)}{\text{of slag.}} = x = \text{mols of } 2\text{CaO.}2\text{SiO}_2/\text{100 grams}$$

$$(C_4S_2) = (S_2) - x = \text{mols of } 4\text{CaO.}2\text{SiO}_2/100$$

$$\frac{\text{Grams of slag.}}{\text{CaO'}} = \frac{\text{grams of slag.}}{\text{CaO'}/\text{100 grams of slag.}} = \text{mols of}$$

In the expression above the only unknowns are $x(2\text{CaO}.2\text{SiO}_2)$ and N_s (total mols per 100 grams). The equation for each slag sample was solved by a series of approximations, using the value of N. from the previous solution of KP and KP' as the first approximation.

imation and in Fig. 5 under the heading of Third Approximation and Fourth Approximation. It is known that each approximation was an improvement over the preceding one because the spread of the individual data points about the lines for K_P and $K_{P'}$ became progressively smaller. Any additional approximations made no noticeable improvement in the spread of the points nor any substantial change in the value for K_D .

In the course of the approximations, the value for KD changed from one that increased slightly with increasing temperature to one that decreased slightly with increasing temperature. In neither case was the trend very marked and, since the heat of reaction is uncertain, it will be sufficient for our purposes to adopt a constant value independent of temperature. Since all of the approximated curves for log KD clustered about the value of

$$\log K_D = -2.0 \qquad [9]$$

the value of o.o. was chosen as the best estimate of the dissociation constant for dicalcium silicate.

Determination of Phosphorus Equilibrium Constant

Having arrived at numerical values for the mol fractions of free lime (CaO') and tetracalcium phosphate (4CaO.P2O5) by the use of K_D and the algebraic expression it was a simple matter to calculate the phosphorus equilibrium constant by substituting the values in the equation below along with the respective values for the percentage by weight of metal oxygen and phosphorus.

$$K_{\rm P} = \frac{(4{\rm CaO.P_2O_5})}{[\%{\rm P}]^2[\%{\rm O}]^5({\rm CaO'})^4}$$
 [3]

A tabulation of the resultant values for K_P converted to log K_P appear in Table 3 together with the accompanying values for the reciprocal of the absolute temperature. A plot of $\log K_P$ versus the reciprocal of the

Table 3.—Summary of Results $K_D = 0.01$

Heat	Slag Test No.	Oxygen Activity	Mol Fraction (FeO)	Log Kp	T × 104	(4CaO.P ₂ O ₅) [%P] ² at 1600°C.	Mol Fractio (CaO')
E-29	5	0.72	0.70	9.123	5.29	169	0.148
	7	0.69	0.70	8.952 9.579	5.28	97.3 94.0	0.147
	13	0.86	0.68	9.216	5.37	110	0.134
E-30	2	0.75	0.63	9.991	5.41	16.0	0.076
	6	0.63	0.54	9.820 10.112	5.35 5.42	10.6	0.074
	8	0.62	0.53	8.507	5.18	29.3	0.073
	II	0.63	0.52	7.250	5.03	56.5	0.127
	13	0.65	0.54	7.123 9.614	5.03	72.0	0.123
	18	0.66	0.47	9.167	5.34	16.1	0.071
	21	0.51	0.45	9.184	5.29	3.09	0.080
E-32	4	0.73	0.80		5.19		0.175
	13	0.70	0.69		5.23		0.276
	15	0.69	0.68		5.12		0.289
	17	0.55	0.60		5.09		0.378
	20	0.58	0.64		5.31		0.322
	24	0.32	0.48		5.31		0.246
7	27	0.40	0.51		5.31		0.219
S-34	I	0.37	0.44	7.753 8.010	5.12	385 230	0.410
	6	0.20	0.24	9.668	5.21	39.8	0.257
	10	0.34	0.32	10.546	5.49	5.08	0.158
	12	0.30	0.34	9.022	5.37	14.3	0.154
	16	0.19	0.18	9.331	5.22	4.50	0.205
	27	0.19	0.19	9.730	5.32	1.03	0.182
E-35	34	0.26	0.24	8.476	5.17	4.07	0.185
33	3 8	0.02	0.06		5.29		0.155
		0.02	0.04	. 4	5.34		0.185
	16 24	0.02	0.02		5.33		0.156
2-36	2	0.29	0.27	9.006	5.27	3.58	0.107
	4	0.33		0 -6 -	5.52		
	6 8	0.33	0.34	8.564	5.20	7.82	0.169
	10	0.36	0.39	9.566	5.33	1.13	0.090
	18	0.57	0.56	9.512	5.31	27.2	0.107
	20	0.70	0.62	9.192	5.19	37.8	0.123
	24	0.69	0.72	8.470	5.36	12.9	0.099
E-37	2	0.53	0.41		5.44		0.144
	5 5	0.49	0.44		5.34		0.131
	7	0.50	0.44		5.28		0.207
	9	0.39	0.35		5.31		0.150
	12	0.51	0.44		5.37 5.37		0.142
	18	0.45	0.41		5.24		0.129
2 -0	20	0.55	0.53		5.32		0.141
3-38	6	0.62	0.66	- 1	5.26		0.310
	8	0.59	0.61		4.49		0.326
	10	0.57	0.61		4.48		0.368
	12	0.62	0.61	5.674	5.09	0.740	0.360
	16	0.54	0.59	6.502	5.39 5.34	0.140	0.295
	18	0.52	0.54	6.438	5.27	3.70	0.365
	20	0.42.	0.48	6.276	5.25	4.31	0.441
	24	0.40	0.41	4.623	5.30	2.88	0.495
E-39	4 6	0.34	0.30	9.778	5.29	20.8	0.156
	8	0.39	0.38	8.028	5.14	56.8	0.246
	10	0.37	0.31	9.746 8.922	5.36	15.3 31.6	0.174
	12	0.28	0.27	8.245	5.21	11.7	0.208
	14	0.36	0.34	9.324	5.36	5.0	0.173
	16	0.38	0.36	9.470	5.29	28.6 266	0.173
	20	0.35	0.35	7.775 9.103	5.01	68.6	0.325
	22 24	0.36	0.42	9.113	5.32	135	0.367
			0.41	7.947	5.14	221	0.378

TABLE 3.—(Continued)

Heat	Slag Test No.	Oxygen Activity	Mol Fraction (FeO)	Log KP	$\frac{1}{T \times 10^4}$	(4CaO.P ₂ O ₅) [%P] ² at 1600°C.	Mol Fractio (CaO')
E-40	3	0.24	0.12	11.626	5.55	0.635	0.098
4-	3 6	0.25	0.19	10.048	5.23	10.7	0.122
	9	0.18	0.10	8.968	5.27	16.2	0.458
	12	0.16	0.10	9.216	5.30	23.I	0.587
	17	0.32	0.32	9.816	5.36	718	0.510
	20	0.48	0.46	9.465	5.39	707	0.418
	23	0.50	0.47	8.768	5.28	965	0.414
E-42	3	0.56	0.38	9.853	5.33	7.65	0.071
	6	0.56	0.39	9.847	5.36	8.03	0.082
	9	0.45	0.29	10.146	5.43	4.01	0.098
	12	0.45	0.32	10.313	5.37	7.52	0.081
	15	0.43	0.29	8.867	5.23	23.8	0.156
		0.40	0.29	9.275	5.28	15.7	0.148
	21	0.43	0.29	8.733	5.25	22.7	0.195
	24	0.37	0.28	9.186	5.30	22.5	0.204
	27	0.33	0.27	8.591	5.22	37.8	0.276
	30	0.33	0.28	8.947	5.25	68.8	0.298
	33	0.30	0.25	9.095	5.26	103	0.356
	36	0.27	0.24	9.231	5.26	177	0.431
	39	0.32	0.31	7.773	5.06	5050	0.441
	41	0.31	0.31	9.439	5.35	1455	0.442

TABLE 4.—Values of the Equilibrium Constants

Temperature, deg. C KP (Eq. 3) K _D (Eq. 5) KP' (Eq. 7)	5 X 1011	1550 4 × 10 ¹⁰ 0.01 4 × 10 ⁶	1600 3 × 10 ⁹ 0.01 3 × 10 ⁵	1650 4 × 10 ⁸ 0.01 4 × 10 ⁴	1700 4 × 10 ⁷ 0.01 4 × 10 ⁸
--	----------	---	--	--	--

absolute temperature appears in Fig. 6. The shaded points indicate the values in which the slag contained some fluorspar;

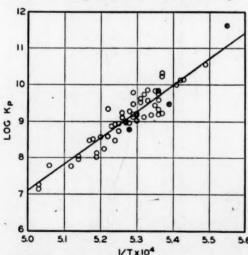


FIG. 6.—Effect of temperature on phosphorus equilibrium constant.

the equation of the line drawn through the points by the method of least squares is as follows:

$$\log K_{\rm P} = 71,667/T - 28.73$$
 [10]

The log K_P values for heat E-38 are lower than the rest of the data (Table 3), because MnO, which was between 25 and 35 per cent in this heat, has largely taken the place of CaO and the dephosphorization was done by MnO and MgO instead of CaO, MgO, and MnO. It may be concluded, then, that MnO is not as good a dephosphorizer as CaO. However, in amounts up to 12 per cent MnO in the slag, MnO may be added to CaO without disturbing the K_P relationship.

The fluorspar that is present in a few of the slags does not upset the dephosphorization constant if it is assumed to combine with the calcium phosphate. Apparently it does not improve dephosphorization, except by increasing the ability of the slag to carry more lime. The alumina within the limits encountered in the investigation does not interfere with the relationship if it is considered to form a calcium aluminate.

Values of the several equilibrium constants defined in Eqs. 3, 5 and 7 at several temperatures are shown in Table 4. It

should be emphasized that these constants are valid only in connection with the formulas that have been assumed for the slag compounds and the equations assumed for their reactions. They are not fundamental constants of nature and are useful only in supplying the numerical pattern for the picture of slag constitution presented. Some new picture may later appear more beautiful or more useful, and in this event these numbers will cease to be of interest.

Distribution of Iron Oxide between Slag and Metal

Raoult's law as applied to the distribution of iron oxide between the slag and the metal afforded a reasonably good and simple method for ascertaining the soundness of the calculated liquid slag constituents. Raoult's law implies that the mol fraction of iron oxide in the slag should be equal to the activity of iron oxide in the slag, and Nernst's law says that the activity of iron oxide in both slag and metal should be equal when the slag and metal phases are in equilibrium. The activity of iron oxide in the metal is easily computed by dividing the analyzed oxygen content of the metal by the saturation oxygen of the metal at the temperatures under consideration. The standard state, in which the activity of iron oxide is unity, is defined as the saturation value of oxygen in iron obtained by using essentially a pure iron oxide slag. Taylor and Chipman3 have published the most recent information regarding the saturation of iron with oxygen under an iron oxide slag and reported the following formula:

 $\log \text{ per cent oxygen} = -6320/T + 2.734$

By using saturation values from this formula, the oxygen activities for all the metal samples were calculated and plotted against the respective mol fractions of the slag iron oxide. The numerical values appear in Table 3, and the graph is shown in Fig. 7. The spread of points about the theoretical straight line may appear to be

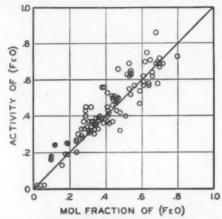


FIG. 7.—DISTRIBUTION OF IRON OXIDE, STRAIGHT LINE REPRESENTING RAOULT'S LAW.

excessive, but considering the complexity of the mol fraction calculations, the relationship is considered to be good.

In Taylor and Chipman's work³ the FeO of the slag was really total FeO, or the total iron of the slag converted to ferrous oxide. In this study, the FeO of the slag is expressed as true FeO, or only the ferrous iron content of the slag converted to the ferrous oxide. If Taylor and Chipman had used true FeO instead of total FeO in their determination of the solubility of iron oxide in the metal, they would have arrived at a slightly higher solubility value. Consequently, the oxygen activity values for this investigation should have been based on the slightly higher solubility value that they would have found had true FeO been used instead of total FeO. Actually then, the oxygen activity values in this paper should be lower than they are, which would make the points in Fig. 7 fit the theoretical line better than they do. It may also account for the discrepancy between the experimental points and the calculated line discussed in the following section.

Effect of Slag Composition on Oxygen Activity

Fig. 8 represents the effects of slag composition on lines of iso-oxygen activity in grouping indicates that CaO, MgO and MnO are considered here to be of equal basic strength. Since SiO₂ combines with CaO predominantly as dicalcium silicate

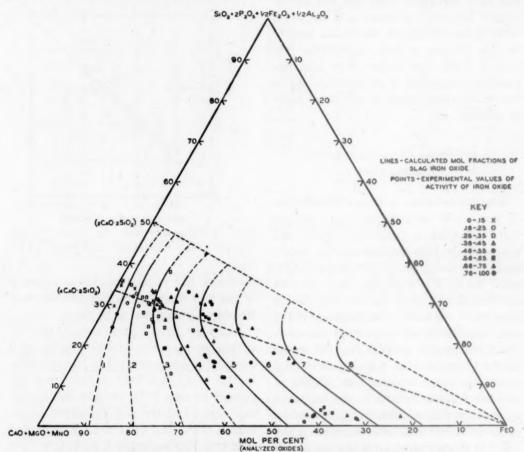


FIG. 8.—EFFECT OF SLAG COMPOSITION ON ACTIVITY OF IRON OXIDE.

the manner of similar diagrams drawn by Fetters and Chipman² and Taylor and Chipman.³ The ternary plot groups all the basic oxides of the slag in one corner, all the acid oxides in the second corner, and FeO in the third corner. In Fig. 8 the slag compositions are represented on the coordinates as mol fractions of the slag oxides as determined by *chemical analysis*. The basic corner consists of the mol fractions of CaO, MgO, and MnO; the acid corner of the sum of mol fractions of SiO₂, 2P₂O₅, ½ Fe₂O₃, and ½ Al₂O₃; and the oxide corner, the analyzed mol fraction of FeO. The

(4CaO.2SiO₂) and P₂O₅ with CaO as tetracalcium phosphate (4CaO.P₂O₅), P₂O₅ is considered to be equivalent to 2SiO₂. Similarly, since Fe₂O₃ and Al₂O₃ are assumed to form CaO.Fe₂O₃ and CaO.Al₂O₃, they are taken to be equivalent to ½ SiO₂. It must be understood that the mol fractions of these oxides were computed from chemical analysis data, not from the slagconstitution calculation involving the dissociation of dicalcium silicate. The points on the plot are actual values for the activity of iron oxide calculated from analyzed oxygen contents of the metal samples. The lines on the graph are theoretical calculated lines, which represent the mol fractions of slag iron oxide for the entire slag system as calculated from the compli-

tion on the free lime content. The diagram was drawn in the same fashion as Fig. 8, the oxygen activity plot, except that in Fig. 9 the lines represent constant values

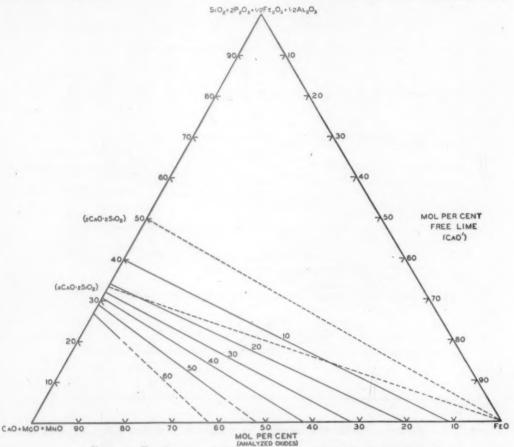


Fig. 9.—Effect of slag composition on free lime content.

cated slag-constitution computations. The points agree reasonably well with the lines except that the 0.6 experimental oxygen activity values fall more closely to the 0.5 calculated FeO line; this may be accounted for by the discussion on oxygen activity in the preceding section.

Effect of Slag Composition on Free Lime

Since this paper proposes the presence of free lime in virtually all the slag compositions encountered in basic steelmaking, it was considered advisable to include Fig. 9, a plot showing the effect of slag composiof mol percentage of free lime. At a given slag composition, temperature has little or no effect on the free lime content. It must be pointed out that the free lime values also include free MnO and free MgO, since for all the calculations MnO, MgO, and CaO were added together and the total of all these oxides were considered as so much CaO.

APPLICATION OF PHOSPHORUS EQUILIBRIUM CONSTANT

An expression for the dephosphorization simpler than an equilibrium constant is a phosphorus-distribution ratio. It was found that the ratio (4CaO.P₂O₅)/[%P]², where the slag component is expressed as the mol fraction, gave the best relationship with respect to slag composition. The ratio is a The effect of slag composition at constant temperature is more easily visualized in Fig. 11, a two-component diagram where the abscissa is the base-acid ratio and the

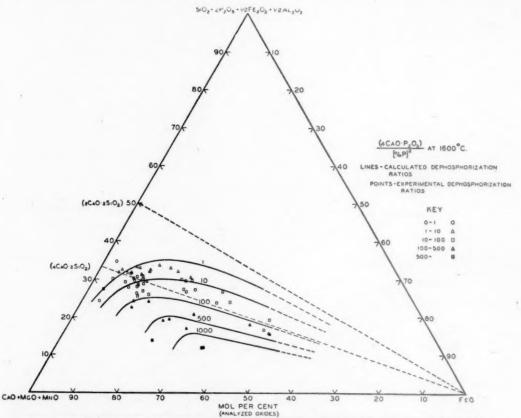


FIG. 10.—EFFECT OF SLAG COMPOSITION ON DEPHOSPHORIZATION RATIO AT 1600°C.

logical one, since it appears in the equilibrium constant.

To illustrate the effect of slag composition at 1600°C. on the dephosphorization ratio, a ternary diagram was made similar to those developed for oxygen activity and free lime. In Fig. 10, the lines represent constant dephosphorization ratios calculated from the K_P expression, the free lime and oxygen activity values having been picked from their respective ternary diagrams. The points on the plot are experimental values from the data collected from the experimental heats; the values of the ratios corrected to 1600°C. are listed in Table 3.

ordinate is iron oxide. The lines on this diagram are the same as those in Fig. 10 with some additions. Fig. 11 clearly shows that dephosphorization is favored by increased slag basicity and increased slag iron oxide. However, no benefit can be derived by increasing basicity above approximately a 3.0 basicity value; dephosphorization can then be improved only by increasing the iron oxide content of the slag. Likewise, after a 40 mol per cent iron oxide slag has been reached, dephosphorization can be improved only by a slag of higher basicity.

Since dephosphorization is improved by an increase in the base-acid ratio, it would appear that all the bases improve dephosphorization and that all the acids hinder dephosphorization. That is true as far as the bases are concerned, but it is not

MnO and about 20 MgO. In the calculations MgO and MnO were treated as lime, so if they had not aided dephosphorization in somewhat the same manner as

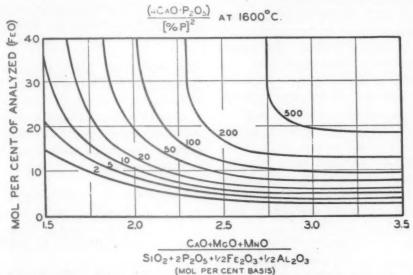


FIG. 11.—EFFECT OF SLAG COMPOSITION ON DEPHOSPHORIZATION RATIO.

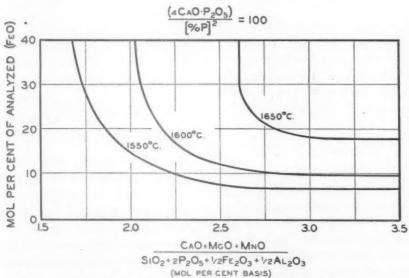


FIG. 12.—EFFECT OF TEMPERATURE ON DEPHOSPHORIZATION RATIO.

strictly true for the acidic oxides. Since all the experimental values of K_P line up in Fig. 6, the basic oxides MgO and MnO must improve dephosphorization as does CaO, for they were substituted for CaO in the slag in all proportions up to 12 per cent

lime, the data points representing high MgO or high MnO would have fallen below the rest. However, as was pointed out earlier, slags containing more than 12 per cent MnO do not conform, because the values of the phosphorus equilibrium con-

stant from these slags are lower than the other results. This means that above 12 per cent MnO, the dephosphorizing power of MnO is not as great as CaO would have been in equivalent concentration.

Since the acidic oxides use up the bases by combining with them, at first glance it might be assumed that all the acids hinder dephosphorization. This is entirely true where silica is concerned but it is not strictly so for Al₂O₃ and Fe₂O₃. Although both of these combine with CaO and thus deprive P₂O₅ of some lime, Fe₂O₃ and Al₂O₃ apparently have no adverse effect on dephosphorization provided there is undissolved lime available in the slag, because Fe₂O₃ and Al₂O₃ impart greater fluidity to the slag and enable the slag to take more lime into solution.

Since the data points for all slags containing fluorspar conform with all the other data points, it may be concluded that fluorspar also has no adverse effect on dephosphorization.

The temperature effect on dephosphorization is more easily visualized in Fig. 12, which shows that a decrease of 100°C. allows a much less basic slag and one that is lower in iron oxide to be used to obtain the same amount of dephosphorization.

SUMMARY

A series of experimental heats was made in an induction furnace to study the factors controlling the distribution of phosphorus between a molten iron bath and a basic slag at equilibrium. In order to determine the rate of establishment of equilibrium conditions within the furnace, radioactive phosphorus was introduced as a tracer. The results showed that 10 to 15 min. was required to reestablish equilibrium after it had been disturbed by a furnace addition or temperature change.

A liquid-slag constitution was developed, which included the following compounds:

- Dicalcium silicate..... 4CaO.2SiO₂
 Monocalcium silicate.... 2CaO.2SiO₂
- 4. Tetracalcium phosphate.. 4CaO.P2O6
- 5. Ferrous oxide..... FeO
- 6. Monocalcium ferrite.... CaO.Fe₂O₃
- 7. Monocalcium aluminate. . CaO.Al₂O₃
- 8. A complex phosphate.... 4CaO.P₂O₆.CaF₂

The MgO and MnO were treated as though they had the same basic behavior as CaO.

A value for the dissociation constant of calcium orthosilicate at steelmaking temperatures was determined according to the following expression:

$$(4\text{CaO}.2\text{SiO}_2) \rightleftharpoons (2\text{CaO}.2\text{SiO}_2) + 2(\text{CaO'})$$

$$K_D = \frac{(2\text{CaO}.2\text{SiO}_2)(\text{CaO'})^2}{(4\text{CaO}.2\text{SiO}_2)}$$

$$K_D = \text{o.o1} \text{ (independent of temperature)}$$

An equilibrium constant for the dephosphorization of molten iron by a basic slag was calculated. The expressions for the chemical reaction of dephosphorization and the dependence of the equilibrium constant on temperature are as follows:

$$\frac{2P + 5O + 4(CaO') \rightleftharpoons (4CaO.P_2O_5)}{K_P = \frac{(4CaO.P_2O_5)}{[\%P]^2[\%O]^5(CaO')^4}}$$

$$\log K_P = 71,667/T - 28.73$$

The effect of slag composition on the activity of slag iron oxides and on the free lime content of the slag is illustrated in ternary diagrams, which take into account all of the slag oxides.

Dephosphorization has been found to be improved by the following factors:

- 1. Decreased temperature.
- Increased iron oxide content of slag and metal.
- 3. Increased base-acid ratio of the slag:
 - a. Increased lime content of the slag.
 - b. Increased magnesia content of the slag.

- c. Increased manganese oxide content of the slag.
- d. Decreased silica content of the slag. .

Fluorspar additions to the slag have no adverse effect on the dephosphorizing power of the slag.

ACKNOWLEDGMENTS

The authors wish to express their thanks to their associates D. L. Guernsey, S. T. Yuan and N. J. Grant, for their assistance in carrying out the experiments. and in analyzing the slag and metal samples.

For the preparation of the radioactive tricalcium phosphate and the measurement of the metal samples with the Geiger counter, the authors thank Prof. Robley D. Evans and the Cyclotron Center at the Massachusetts Institute of Technology.

Further thanks are extended to the Open Hearth Committee of the American Institute of Mining and Metallurgical Engineers for a fellowship grant, which contributed greatly to the completion of this work.

REFERENCES

1. J. Chipman and K. L. Fetters: Trans Amer. Soc. for Metals (1941) 29, 953-

- K. L. Fetters and J. Chipman: Trans.
 A.I.M.E. (1941) 145, 95-112.
 C. R. Taylor and J. Chipman: Trans.
 A.I.M.E. (1943) 154, 228-247.
 H. Schackmann and W. Krings: The
 Fe-O-P System. Zisch. anorg. allge.
- Chem. (1933) 213, 161-179.
 5. H. P. von Samson-Himmelstjerna: Dephosphorization of a Steel Bath. Archiv
- Eisenhültenwesen (1932) 6, 471-475.

 6. W. Oelsen and H. Maetz: The Behavior of Fluorspar and of Calcium Phosphate in Relation to Ferrous Oxide in the Melt and Its Metallurgical Significance. Mitt. K-W-I. Eisenforschung (1941) 23, 195-
- 7. W. Bischof and E. Maurer: Distribution of Phosphorus between Iron and Iron Phosphate Slags Containing Lime. Archiv
- Eisenhüttenwesen (1932) 6, 415.

 8. E. Diepschlag and H. Schürmann: Investigation of the Dephosphorization of Iron by Oxidation. Angewandte Chem.
- of Manganese Carbon and Phosphorus in Basic Open-hearth Process. Trans.
- A.I.M.E. (1926) 73, 1107-1134. K. Zea: The Phosphorus Reaction in Basic Open-hearth Practice. Iron and
- Steel Inst. Preprint (April 1945).

 11. J. H. Whiteley: Proc. Cleveland Inst. Engrs. (1922-23) No. 2, 36-65.

 12. E. Maurer and W. Bischof: Distribution of Phosphorus between Metal and Slag in Basic Process of Steel Manufacture. Jnl. Iron and Steel Inst. (1935) 132,
- H. Schenck and W. Riess: Studies on Chemistry of Basic Open Hearth Process. Archiv Eisenhüttenwesen (1936) 9, 589-600.
- McCance: Application of Physical Chemistry to Steelmaking. Symposium on Steelmaking, Iron and Steel Inst.
- 15. M.
- (1938) 331.

 1. Tenenbaum: Proc., Open Hearth Conf., A.I.M.E. (1944) 27, 152-159.

 1. J. Grant and J. Chipman: Sulphur Equilibria between Liquid Iron and Slags. This volume, page 134.

Sulphur Equilibria between Liquid Iron and Slags

By Nicholas J. Grant,* Junior Member, and John Chipman,* Member A.I.M.E. (Chicago Meeting, February 1946)

A FULL understanding of the behavior of sulphur in the basic open-hearth process has been delayed by lack of dependable data covering a wide range of slag conditions in the absence of other complicating factors that are likely to be present under operating conditions. It has been generally accepted that strongly basic slags will dissolve more sulphur than will those in which the acidic and basic constituents are more nearly balanced. It has been known that both slag and metal would absorb sulphur from the flame when the sulphur content of the fuel is high. It has been generally believed that manganese assists in the transfer of sulphur from metal to slag. Almost nothing has been known of the effect of temperature upon desulphurization; the data have been conflicting and there has been a tendency to depend rather heavily upon analogy with the better understood desulphurizing reaction of the blast furnace.

Many attempts have been made to build up from open-hearth data a satisfactory theory of the chemical reactions involved in the process. That this has been an extremely difficult task is owing to two reasons that have been very generally recognized. The first is the parallel and simultaneous reaction of sulphur transfer between flame and bath. The second is the difficulty of distinguishing between the factors that ultimately limit the transfer from metal to slag-i.e., equilibrium conditions—and those whose influence is only upon the rate of transfer. It has been the object of the work here recounted to study the equilibrium distribution of sulphur between slag and metal in the absence of these complicating factors, with the hope that a better understanding of the equilibria involved would lead to a better control of the over-all process in the openhearth furnace.

A review of the literature on steelmaking reveals almost complete agreement with respect to the paramount importance of lime in promoting desulphurization. In expressing this effect in quantitative terms, however, and in formulating the relationships between the concentrations of other slag components and the desulphurizing power, there is little agreement. For instance, the "basicity" or basic strength of the slag is commonly measured by some kind of ratio of concentration of basic to acidic oxides. Of these, the following have been reviewed by Schenck:20

$$V \text{ ratio} = \frac{\% \text{ CaO}}{\% \text{ SiO}_2}$$

Körber and Oelsen's

$$V' = \frac{\% \text{ CaO}' \cdot 100}{\% \text{ CaO} + \% \text{ SiO}_2}$$

where $(\% \text{ CaO'}) = \% \text{ CaO} - 1.18\% \text{ P}_2\text{O}_5$. Herty's B ratio

=
$$\%$$
 CaO - (0.93 · $\%$ SiO₂)
- (1.18 $\%$ P₂O₅)

Among others there appear the following:

Manuscript received at the office of the Institute Nov. 20, 1945. Issued as T.P. 1988 in METALS TECHNOLOGY, April 1946. * Assistant Professor of Process Metallurgy and Professor of Process Metallurgy, respec-tively, Massachusetts Institute of Technology, Cambridge, Massachusetts.

²⁰ References are at the end of the paper.

Darken and Larsen's²⁶

$$L \text{ ratio} = \frac{(\text{CaO}) -_4 (\text{P}_2\text{O}_5)}{\text{SiO}_2}$$

$$(\text{in mols/100 grams slag})$$

$$R \text{ ratio}^9 = \frac{\text{CaO}}{(\text{SiO}_2 + \text{o.634 P}_2\text{O}_5)}$$

$$(\text{in mols/100 grams slag})$$

$$B/A \text{ ratio} = \frac{\text{CaO} + \text{MnO}}{_2(\text{SiO}_2) + _4(\text{P}_2\text{O}_5)}$$

$$(\text{in mols/100 grams slag})$$

There are other somewhat more complicated measures of basicity scattered throughout the literature.

In using these various ratios, it becomes evident that for individual shop practice all conditions of temperature, slag composition and time. Nor do these various ratios permit a comparison of data among shops using different practices or making different grades of steel.

In Table 1 are summarized the conclusions reached by a number of investigators on the effects of various slag and metal constituents and temperature. This table is not complete nor does it explain various limits set up in the literature. It does permit the following general summary:

1. Most investigators felt that temperature for one reason or another aids desulphurization in a secondary role.

TABLE 1.—Summary of Effect of Various Factors on Desulphurization of Low-carbon Steels and Pure Irons

		Effect on Desu	lphurization*	
Quantity or Constituent	Ai	ds	Hinders	No Effect
	Primary	Secondary	minders	No Elect
High temperature (CaO) slag	1, 3, 7, 8, 11, 13, 14, 15, 16, 17, 18, 20,	I. 3. 4. 6. 8. 18. 20 5. 12. 22	2, 24	9, 22, 26
MnO) slag. MgO) slag. Al ₂ O ₃) slag. Fe ₂ O ₃) slag. FeO) slag.		2, 3, 8, 12, 13, 15, 17, 23, 24, 26 8, 11, 24 1, 25	2, 4, 11, 24 11, 12 2, 5, 9, 12, 14, 16,	3, 4, 18, 20, 26 18, 20, 26 11, 20, 26 3, 4
CaF ₂) slag	21 4, 5, 12, 22, 23	1, 3, 5, 7, 12 1, 2, 3, 7, 8, 15, 17, 18, 24, 26	17, 18, 23, 24, 26	10, 11, 24, 26

· Numbers refer to references on page 149.

any one of them can tell a consistent story as long as conditions from heat to heat and from furnace to furnace do not vary. If the Al₂O₃ content does not vary outside the limits of 2 to 4 per cent, and if the MgO stays quite constant at, let us say, 4 to 6 per cent, etc., some one of these measures can be made to work fairly well. They all fail consistently to interpret the results under varying conditions, however; and, more important, their use does not permit one to attain a clear picture of the behavior of sulphur under

This opinion is not held by all, for several persons felt that high temperature was undesirable and three attributed no effect to it.

- 2. High lime is desired by all, but a minority feel that Mn in the metal and MnO play the more important role in desulphurization. The tendency has been to determine free or available lime as a measure of the desulphurizing power of the slag.
- Most investigators assign a secondary role to MnO.

4. The feeling appears to be that MgO is not effective as a desulphurizer but may play a weak secondary role if and when it is in solution in the slag.

5. There is general agreement that SiO₂ and P₂O₅ are acid constituents, which must be at least neutralized by bases before desulphurization can occur.

6. There is less agreement with regard to Al₂O₃, the split being quite equal in regarding it as a secondary aiding factor, a hindrance and a noneffective item. Several thought that Al₂O₃ has fluidifying properties, being able to take CaO into solution about as well as fluorspar does.¹

7. Almost everyone felt that FeO was detrimental, although one or two found FeO effective as a desulphurizer at very low basicity. 24 Diehl³ ascribed a "no-effect" role to it, as did Maurer and Bischof. 4

8. Many gave Mn in the metal the major credit in desulphurization; the rest agreed that its role as a secondary agent was important.

9. Disagreement on the role of fluorspar is evident, the split being fairly equal between those who feel that it plays a direct role as a desulphurizer and those who give it credit only as a fluidifying agent.

10. Previous data¹³ have indicated that higher carbon heats of the same basicity resulted in slightly higher sulphur ratios.

Two distinct mechanisms of sulphur removal had been advanced by various investigators. The first of these has been accepted by almost everyone up to the present; it is incorporated in the following reaction:⁸

$$\frac{\text{FeS} + \text{CaO}_{\text{(alag)}} = \text{FeO}_{\text{(alag)}} + \text{CaS}_{\text{(alag)}}}{\Delta F^{\circ} = +19,370 + 1.54T}$$

The second method has been upheld by those who believe that the manganese in the metal is the primary means of desulphurization.^{5,12,22,23} The CaO is held as a secondary force, which retains the sulphur in the slag and generally permits

MnO to remain free of FeO, so that MnO can be reduced to Mn to return to the bath, where it continues its desulphurizing work.

Still a third group subscribes to the belief that much of the sulphur is eliminated by means of the highly oxidizing flame sweeping over the slag surface. Calcium sulphate is supposedly formed, which on dissociation permits SO₂ gas to escape. The argument against the possibility of having the sulphate present is explained very well by Darken and Larsen. ²⁶ Since this paper is not concerned with the gas phase and has eliminated it as a variable, this item will not be discussed.

EXPERIMENTAL METHOD

The induction furnace and the experimental procedure used in making the experimental heats E-5 through E-22 are those used by Fetters and Chipman.9 The test results are taken from that study with the sole change that sulphur was reanalyzed more closely for the purposes of this paper. In heats E-20 through E-44 one significant change was made in the furnace setup; namely, the method of providing a source of heat for the slag, which is not heated by induction. The slag was kept moiten by the radiant energy from an arc drawn between two carbon electrodes suspended above the bath but within the furnace crucible as described more completely by Winkler and Chipman.29 The heat supplied by this method was much more intense than that furnished by the graphite heater used in the early heats.

The experimental heats were made by melting a 65-lb. charge of Armco ingot iron in a magnesia crucible under a vacuum to reduce the carbon content below 0.01 per cent to eliminate the carbon-oxygen reaction as a variable. A mixture of oxides to provide a synthetic slag was added in sufficient quantity to cover the surface of the metal bath, after which

the slag heater was installed. A nitrogen atmosphere at a positive pressure was maintained within the furnace to prevent any disturbance of equilibrium by oxygen from the air and also to prevent too rapid burning of the graphite electrodes. Iron sulphide was added in many of the heats to assure a sulphur content within the range of accurate analysis.

Temperatures were measured with tungsten-molybdenum thermocouples protected from the metal and slag by fused silica protection tubes. The assembly was rigged up in a water-cooled or air-cooled holder. The tungsten-molybdenum thermocouples were calibrated against a platinum-platinum 10 per cent rhodium couple with subsequent checks on the calibration curve made with platinum couples under operating conditions. The accuracy of the temperature readings is considered within ±10°C.

Samples were taken by use of a small split steel mold, coated with magnesia slip, by dipping into the metal bath and permitting the sample to freeze in the nitrogen atmosphere. The molds for the metal samples were smaller in diameter and of heavier wall thickness than the slag samplers, in order to obtain very rapid solidification of the metal and to inhibit segregation. The metal samples were all sound and free of internal blowholes, a condition that is easily obtained when the carbon content is well below o.o. per cent.

The slag samples were analyzed by conventional chemical methods under carefully controlled conditions for the oxides present. The metal samples were analyzed for phosphorus, manganese and sulphur by standard techniques while the oxygen determinations were obtained by vacuum fusion. Again all results were checked at least once.

EXPERIMENTAL RESULTS

In the course of the investigation, 15 experimental heats were made for a total

of 140 pairs of slag and metal samples, each pair being accompanied by a temperature measurement. In addition to this, 12 experimental heats for a total of 72 pairs of slag-metal-temperature tests were taken from the work done by Fetters and Chipman⁹ to get additional sulphur distribution points in the very simple slag compositions, as a double check on the method used in heats E-29 through E-44. With all these data it is not possible to list any more than the most necessary items, for the sake of brevity. More complete data on slag compositions are given in the papers cited. 9,29

Table 2 lists heats E-31, E-43 and E-44, which are not included in the phosphorus study by Winkler and Chipman.29 Heat E-31 was excluded in that study because the temperature measurements were of insufficient accuracy for determinations of phosphorus equilibria, but they were sufficiently accurate for the sulphur study to be included in Fig. 6 herein after it had been established that temperature was a very minor variable. The remainder of the heats in series E-20 to E-42 are completely listed in the above mentioned paper.29 The slag-metal tests from the paper by Fetters and Chipman are to be found in that paper. More accurate sulphur determinations resulted in the sulphur ratios shown in Table 3 for the tests that were used.

DISCUSSION OF RESULTS

Basicity Measurements

A close examination of Table 2 in this paper and Table 2 in that by Winkler and Chipman²⁹ indicates that the over-all study includes slag combinations of almost every conceivable sort. There are relatively simple slags composed only of the CaO-SiO₂-FeO-MgO constituents; there are lime-free slags with high MnO; there are slags free of P₂O₅ and others of inordinately high P₂O₅; there are slags essentially

free of Al₂O₃; others are free of SiO₂ and have Al₂O₃ as a substitute; there are high-FeO and low-FeO slags, etc. In general, it can be said with perfect safety that if any formula or any one given set of conditions can be made to correlate these highly irregular slag compositions with

R, etc., in itself proved to be the answer. Where slags approached quite closely fairly narrow composition limits typical of open-hearth slags, the agreement was only fair; otherwise the presence of not too large amounts of Al₂O₃, MnO, CaF₂, threw the points far off the scale. For example,

TABLE 2.—Chemical Analyses of Slag-metal Samples

Heat No.	Metal Test	Slag Test	Tem- pera- ture,	S	Per Ce		is,			Slag	Analys	sis, Pe	r Cent		
110.	1050	Test	C. Deg.	Mn	S	P	0	CaO	SiO ₂	FeO	Fe ₂ O ₃	MgO	S	P2O6	MnC
E-31	1 3 6 16 18 20	2 4 7 17 19 21		0.002	0.023 0.024 0.0225 0.023 0.023		0.271 0.359 0.331 0.243 0.211 0.216	0.12 <0.10 0.08 <0.10	0.48 0.58 0.58 1.42	89.96 89.13 88.56 79.28	3.42 3.20 4.16 5.44	5.98 6.73 6.45 5.42	0.062 0.069 0.0685 0.070 0.078 0.076		0.1:

Heat No.	Metal Test	Slag Test	Clock Time	Tem- pera- ture,	Steel Analysis, Per Cent			Sla	g Ana	lysis, P	er Cer	nt	*	
	1000	1000		Deg. C.	S	CaO	SiO ₂	FeO	Fe ₂ O ₃	MgO	S	P2O8	MnO	A12O
E-43	2.3	1	11:03	1520	0.196	18.71	11.58	36.80	5.81	6.37	0.20			19.8
	5.6	4	11:31	1638	0.191		10.76		3.46	10.89	0.21			20.2
	8.9	7	12:08	1670	0.193	23.94		33.10	5.94		0.23			20.6
	11.12	10	12:40	1608	0.196	21.83		37.41	5.76		0.22			17.8
	14.15	13	1:20	1537	0.189	21.89		45.67			0.44			12.3
	17.18	16	1:57	1635	0.163	29.34			11.92	5.84	0.61			9.2
	20.21	19	2:26	1580	0.170	26.37			10.48	5.98	0.66			9.6
	23.24	22	2:56	1628	0.165	24.20			10.66		0.63			7.3
		25	3:16	1655	0.167	28.82			10.80	5.89	0.68			7.5
E-44	29.30	1	3:51	1520	0.150	19.66		43.92	6.43		0.07	°	MnO	4.6
15-44	5.6	4	10:31	1605	0.152	18.68		44.77	6.00	6.10	0.22	04	A	23.2
	8.9	7	10:55	1661	0.139	30.59		34.58			0.37		-	15.4
	11.12	10	11:44	1596	0.128	26.47		39.48			0.39	No	No	16.7
	14.15	13	12:15	1686	0.128	25.64		39.94			0.35		-	15.5
	17.18	16	12:58	1649	0.080	31.56		32.85		7.76	0.36			15.2
	20.21	19	1:21	1594	0.139	17.49		44.91	5.80		0.18			21.0
	26.27	25	2:30	1573	0.128	33.53		34.17	10.06		0.52			13.4
	29.30	28	3:15	1590	0.107	36.53			12.02		0.64			9.5
	32.33	31	3:55	1625	0.102	38.94			9.33		0.54			9.6
	35.36	34	. 4:19	1610	0.107	38.44			10.47	5.42	0.61			9.9
	38.39	37	4:43	1565	0.107	36.97	4.24	31.90	10.68	6.13				9.0
	41.42	40	5:03	1644	0.104	38.01			11.45					7.4
	44.45	43	5:35	1647	0.107	39.50	4.22	31.16	12.40	5.94	0.64			8.8

Other heats in the series E-29 through E-42 appear in the paper by Winkler and Chipman,³⁰ and in the series E-5 through E-22 in the paper by Petters and Chipman.⁵

the sulphur distribution ratio, that formula will truly contain the basis for a satisfactory explanation of sulphur behavior.

As a preliminary check, all the various basicity measures appearing in the literature were tried as a gauge of the desulphurizing power of these complex slags. None of these various ratios, V, V', B, B/A, L,

Darken and Larsen's 26 L ratio failed to correct for any Al_2O_3 , higher MnO, CaF_2 , higher P_2O_5 and MgO. The same was true of the R ratio. The B/A ratio corrected for P_2O_5 in almost all ranges but threw high MnO slags very far out of line. With the B/A ratio the trend of the values was unidirectional but the spread was quite

severe, indicating insufficient correction for various items. The V' and B ratios were no better in explaining desulphurization.

From this preliminary work, however, it became evident that a more applicable set of rules could be worked out to correct properly for slag composition variables. The final set of conditions, which works extremely well, will be discussed below. The other attempts that were not as successful cannot be more than briefly mentioned, to conserve space.

All the data pointed without question to the fact that excess base appeared to be the main controller of the sulphur distribution between the slag and metal phases. The problem was to determine the most accurate measure of the excess base.

Constitution of Liquid Slag

Many interpretations of slags and their physical and chemical makeup at high temperatures have been advanced over many years. The classical theory interprets slag behavior strictly on the basis of the compounds represented by the phases present in the solidified slag, as determined by petrographic studies. Care must be exercised, however, in interpreting liquidslag behavior too literally from solid-slag appearances. Going a step further, some investigators ascribe various degrees of dissociation to suit the particular calculations. More recently compound formation has been looked upon simply as a convenient basis for numerical computations regarding slag behavior.

P. Herasymenko¹⁹ has advanced the hypothesis that liquid slags of steelmaking types are completely dissociated electrolytically and contain practically no neutral molecules. The difference between this concept and that of simple compound formation depends upon the degree of completeness of such reactions as the following:

$$_2\text{CaO} + \text{SiO}_2 = \text{Ca}_2\text{SiO}_4$$

$$= 2Ca^{++} + SiO_4^{----}$$

Substantial completeness of the first step

is an essential part of most explanations of basic slag behavior. Herasymenko presents good evidence that the second step occurs, but to what extent the data do not show. Recent studies of the distribution of iron oxide between slag and metal have not given support to the hypothesis of complete ionization. On the contrary, it is difficult to interpret the data on the basis of any ionic dissociation of FeO itself.

It was hoped originally that data on the distribution of sulphur between slag and metal might confirm or refute the ionization hypothesis, since the ionic concentrations would be small and the behavior of sulphur in the slag, therefore, should be that of a simple ion in dilute solution. It is found, however, that the results may be equally well explained with or without ionization. The method that has been found most satisfactory for graphical presentation of the results is one that could be used equally well whether the compounds of the slag are ionized or not. Thus while they do not confirm, the data at least admit the hypothesis of complete ionization.

The method of calculating the excess base or acid count used in this work was as follows. All slag analyses were converted first to mols and finally to mols per mol of slag. Combinations of base or acid for neutralization were taken as follows on a molar basis.

- 2 Base: 1 SiO2
- 4 Base: 1 P2O6
- 2 Base: 1 Al₂O₃
- 1 Base: 1 Fe₂O₈

FeO and CaF₂ were considered neutral species. CaO, MnO and MgO were considered as basic constituents of equal value mol per mol. According to this method of neutralization, it is possible to have excess acid available as a constituent in a slag. This does not necessarily mean "free" acid, since an excess of silica might simply convert an orthosilicate into a metasilicate

TABLE 3.—Summary of Calculations

Heat	Test	Temperature, Deg. C.	(S)/[S]	Excess Base	Excess Acid	Heat	Test	Temperature, Deg. C.	(S)/[S]	Excess Base	Excess Acid
E-29	2	1612	2.51	0.099		-E39	12	1644	1.84	0.070	
	5	1617	2.63	0.061		1139	14	1594	1.61	0.008	
	7	1621	2.51	0.058			16	1615	1.78	0.022	
	7	1594	2.65	0.053			18	1703	2.84	0.132	
		1590 1576	2.43	0.043			20	1703 1627	2.24	0.072	
E-30	13 2 4 6 8	1576	1.04	10	0.033		22	1605	4.90	0.194	
	4	1597	0.83		0.041		24	1670	3.70	0.198	
	6	1573 1656	0.72		0.041	E-40		1530	3.70 I.I7	0.190	0.016
		1656	0.76		0.020		3 6	1640	1.36		0.009
	II	1715	0.97		0.007		9	1625	3.70	0.142	
	13	4715	0.88	0.034			12	1615	5.92	0.219	
	10	1608	0.88		0.025		17	1595 1583	5.92 8.00	0.337	
	18	1600	0.78		0.036		20	1583	4.95	0.275	
17	21	1617	0.49 2.70 2.88		0.051	-	23	1623	4.75	0.274	
E-31	2	1796	2.70	0.078		E-42	3 6	1605	0.72		0.019
	4 7	1705	2,88	0.079				1592	0.62		0.023
	1 -7	1787	3.03	0.089			9	1570	0.61		0.020
	17	1750	3.04	0.082			12	1590	0.65		0.019
	19	1070	3.38	0.119			15	1638	0.84		0.000
E ac	21	1690	3.30 4.30 5.95	0.109			18	1623	1.00		0.019
E-32	I	1655	4.30	0.165			21	1632	1.22		0.005
	13	1640 1620	5.95	0.264			24	1614	1.22		0.002
	13	1680	5.40	0.272 0.271			27	1640	1.56		
	15 17 18	1690	5.00	0.271			30	1629	1.97	0.056	
	18	1700	5.31	0.353			33 36	1625	2.78	0.097	
	20	1610	5.31 5.31 6.19	0.330			30	1624	3.89	0.149	
	22	1503	3.96	0.154			39	1700	4.76	0.208	
	24	1593	2.78	0.077		E-43	42 I	1595	4.43 I.02	0.207	
	27	1610	2.78	0.057		13-43	4	1520	1.10		0.110
E-34	I	1680	6.00	0.260			7	1670			0.051
	4	1655	4.22	0.222			10		1.10		
	4	1647	1.38	0.039			13	1537 1635 1580 1628	2.32	0 052	0,000
	10	1550	1.17	0.039	0.006		13	1635	2 74	0.053	
	12	1590	1.14		0.006		19	1580	3 88	0.160	
	14	1615	1.31		0.000		22	1580 1628	3.82	0.102	
	14	1550 1590 1615 1643 1608	1.17	0.001		*	25	1588	4.07	0.149	
	27	1608	1.14		0.005		25 28	1655	7.25	0.294	
	34	1000	1.03		0.003	E-44	I	1520	1.67		0.008
E-35	2	1530 1620	4.60		0.041		4	1520 1605	1.45		0.000
	3 8 16	1620	4.50	0.096			7	1661	2.66	0.136	0,000
	8	1600	2.70		0.021		10	1596	3.04	0.154	
	16	1605	2.30		0.034		13	1686	2.74	0.184	
E-36	6 8	1535			0.102		16	1649	4.50	0.157	
	0	1050	0.61		0.004		19	1594	1.29		0.000
	8	1608	1.36	0.006			25 28	1573	4.06	0.181	
	10	1612	0.46		0.066			1590 1625	5.98	0.278	
	18	1013	1.13	- 1	0.016		31	1625	5.30	0.307	
	20	1654	1.24		0.007		34	1610	5.70	0.269	
		1595 1635 1565	1.35		0.012		37	1565	5.51	0.284	
3-37	24	1035	1.05		0.027		40	1644	5.29	0.310	
2-31	1 1	1600	1.36		0.017	E-5	43	1647	5.98	0.300	
	4	1666	1.05	0.035	0.019	E-5	6	1538	1.17		0.021
	2 4 5 7 9	1622	1.90	0.019			10	1593 1546	1.08		0.022
	6	1611	1.43	0.019	0.003		14	1575	1.13		0.019
*	11		45		0.001	E-6	3	1550	2.17	0.113	0.011
	12	1590	1.33		0.015	20-0	3 9 4 18	1604			
	14	1591	1.22		0.020	E-10	9	1565	1.29	0.116	0.018
-	16	1575	0.56		0.028	10-10	T8				
	18	1635	0.56		0.022	E-11	5	1577	1.40		0.006
	20	1608	1.50		0.001		12	1594	1.57		0.000
E-38		1630	5.40	0.281	0.002		21	1580	1.67		0.017
	4	1672	5.44	0.296			24	1637	1.65	0.017	0.017
	8	1730	4.48	0.331		E-12		1551	7.25	0.326	
	10	1738	4.71	0.340			8	1586	6.12	0.276	
	12	1738	5.35	0.334			10		4.60	0.167	
	14	1583	6.00	0.271			13	1605	4.10	0.141	
	14	1598	0.00	0.302			18	1607	5.48	0.264	
	18	1625		0.268			21	1590	3.40	0.345	
	20	1630	5.16	0.333		E-15	3	1652	1.60	1040	0.017
	22	1613	6.93	0.358			5	1678	2.30	0.061	
	24	1715	7.46	0.394			7	1641	2.41	0.050	
3-39	2	1615	1.81		0.033		9	1625	3.42	0.117	
		1615	2.40	0.006			11	1624	3.42	0.113	
	4	1671	2.40	0.083			13	1619	4.78	0.244	
	8	1590	2.00	0.015			15	1601	4.1-	0.278	
	10	1635	2.26	0.039			17	1632		0.347	

TABLE 3.—(Continued)

Heat	Test	Temperature, Deg. C.	(S)/[S]	Excess Base	Excess Acid
E-15	19	1640	8.05	0.362	
E-16	7	1636	3.18	0.054	
	9	1648	2.60	0.018	
	II	1660	1.67		0.027
	15	1597	1.20		0.061
	17	1616	1.29		0.073
E-18	19	1608	1.04		0.016
E-19	3	1628	2.23	0.019	0.010
2	5	1649	2.89	0.044	
	9	1719	2,30	0.069	
	II	1723	2.16	0.070	
	14	1624	2.40	0.023	
	18	1639	2.05	0.038	
	24	1623	1.33		0.008
12	29	1608	0.82		0.040
E-20	3	1593		0.065	
	5	1627	2.53		0,000
	7 9	1640	1.93		0.008
	II	1657	1.53		0.022
	14	1643	0.99		0.015
	19	1602	1.33		0.019
	22	1638	1.69	0.029	
	25	1610	2.15	-0.039	
E-21	3	1592			0.000
	5 8	1600	1		0.000
		1617	1	0.087	
	10	1619	4.00	0.154	
	13	1611	4.37	0.187	1
	15	1630	4.48	0.247	1
	19	1653	4.53	0.241	1 1
E-22	9	1602	5.40	0.169	
	10	1615	5.88	0.254	
	13	1596	6.88	0.297	
	15	1638	6.10	0.284	
	17	1665	1.33		0.001
	19	1596	0.88		0.035
	21	1586	0.68		0.054
	23	1604	1.15		0.044
	25	1590	1.92		0.029
	29	1604	1.73		0.013
	31	1598	1.48		0.058

or form a polymeric silicate ion such as $(Si_2O_7)^{-6}$. One exception was made in the grouping shown above. If, after neutralization of SiO_2 , P_2O_5 and Al_2O_3 , there was excess base available, ferrite was assumed to be capable of forming; however, Fe_2O_3 behaved as an acid only as long as there was base available. If all the base was consumed in handling the first three acid groups above, then Fe_2O_3 was considered simply as part of the FeO.

The results of these calculations are listed in Table 3.

Effect of Excess Base or Acid upon Sulphur Distribution

A large-scale plot was prepared, showing the distribution ratio (S)/[S] against

"excess base or acid." This plot contained all of the data on heats E-20 through E-42 except those containing Al₂O₃ or CaF₂, since the effects of these constituents were initially unknown. This plot showed the expected increase in the desulphurization ratio with increasing excess of base. It showed a totally unexpected lack of influence of FeO and of temperature. It was, in fact, possible to draw a very satisfactory normal line representing all the data within the ranges 3 to 70 per cent FeO and 1540° to 1660°C. This standard curve is shown in each of the Figs. 1 to 6 inclusive, which also demonstrate the effect of individual variables upon deviation from the normal.

Effect of MnO and CaF2

Fig. 1 shows how the high MnO points (up to 30 per cent MnO) in slags containing no lime fit the standard curve. This plot shows that MnO is indeed as good a desulphurizer on a mol per mol basis as CaO. Where both MnO and CaO were present in large quantities the effect on the sulphur distribution ratio is the same as though only CaO or only MnO were present.

Fig. 2 shows the desulphurization ratio for slags containing fluorspar. The points scatter themselves regularly about the standard line. The fit of the points is not as good as might be desired but is definitely sufficient to demonstrate that fluorspar is without effect on the sulphur distribution.

Effect of Al2O3

At first, in calculating excess base or acid, the Al₂O₃ content was ignored, since its strength as a base or acid was not known. The literature certainly did not offer a concrete suggestion. The resulting points, when the slags were uncorrected for Al₂O₃, fell on a line to the extreme right of the standard line of Fig. 3. This indicated that the calculated values were too basic and required some correction for Al₂O₃ as an

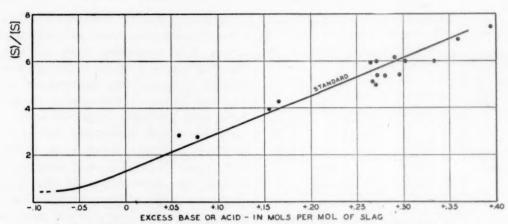


Fig. 1.—Effect of high manganese oxide on desulphurization ratio. Data on slags containing 13 to 39 per cent MnO and free of CaO.

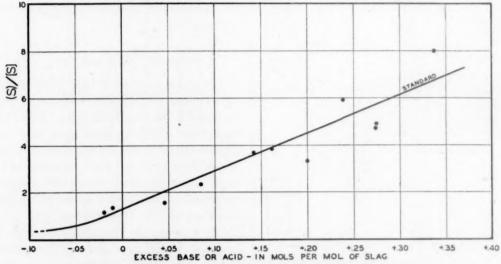


Fig. 2.—Effect of fluorspar on desulphurization ratio. Data on slags containing 4 to 17.6 per cent CaF₂.

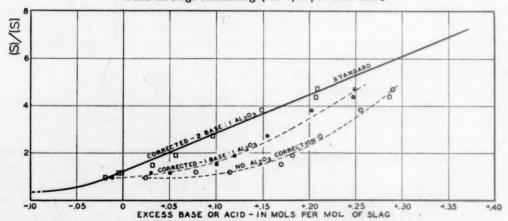


FIG. 3.—EFFECT OF ALUMINA ON DESULPHURIZATION RATIO.

Illustrating method of determining the behavior of alumina; data of heat E-42.

acid. Accordingly, one mol of base was used to neutralize one mol of Al₂O₃. The newly calculated points fell closer to the normal line now (Fig. 3) but still regularly

of the occurrence of any crystalline aluminates in the solidified slags.

Subsequently two additional heats were made, E-43 and E-44, wherein Al₂O₃ was

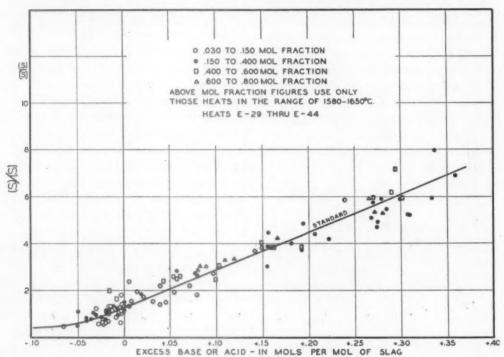


Fig. 4.—Effect of FeO on desulphurization ratio in the temperature range 1580° to 1650°C.

This plot shows all points used in establishing the standard line; data on slags from heats E-20 through E-44.

offset from it. In a second recalculation, two mols of base were used to neutralize one mol of Al₂O₃. The recalculated values now fell very regularly about the standard line, a line through them coinciding with the standard, showing that on a mol per mol basis Al₂O₃ is as much acid constituent as is SiO₂, requiring the same number of mols of base for neutralization. Fig. 3 is a very good example of how easy it is to study the behavior of unknown constituents in slagmetal work once a reasonable theory is worked out to give a standard reference line. It is also a good example of the method by which conclusions are reached regarding the nature of the compounds in liquid slag. It should be noted also that the validity of the conclusion is independent

substituted almost exclusively for SiO₂ (Al₂O₃ went up to 23 per cent while SiO₂ was down to 1 per cent). The values calculated by this method fall very regularly about the normal line as before and cannot be differentiated from the normal openhearth type alumina-free points.

The calculations of the preceding paper²⁹ were based in part upon the assumption that alumina forms such compounds as CaO·Al₂O₃. The precision of the data on phosphorus distribution was not sufficient to permit a decision between this and the formula here employed, 2CaO·Al₂O₂. Since the high-alumina heats E-43 and E-44 were not included in the phosphorus study, a recalculation of the data to the new

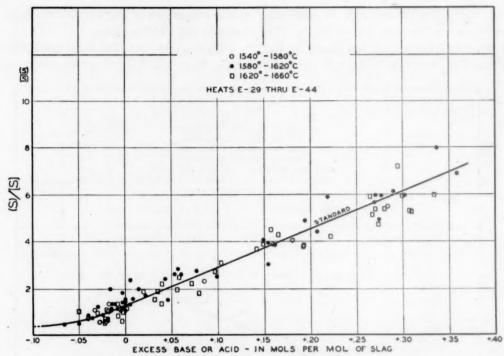


Fig. 5.—Effect of temperature on desulphurization ratio.

Data on slags from heats E-29 through E-44.

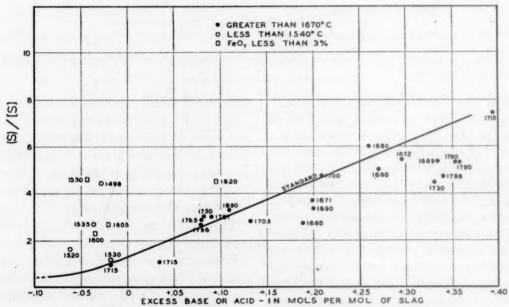


Fig. 6.—Effect of FeO and temperature extremes on sulphur ratio.

basis would not be expected to make a noticeable difference in the conclusions.

Effect of Slag FeO

All the slags in heats E-20 through E-44 were next plotted on one graph (Fig. 4). Only the slags in the temperature range 1580° to 1650°C. were included to eliminate temporarily any possible temperature effect. All slags in the range of 3 to 70 per cent FeO were includes, regardless of other composition variables. Fig. 4 shows without the question of a doubt that the equilibrium sulphur distribution ratio is a function only of excess base or acid. For a given value of excess base the distribution is independent of the FeO content of the slag. Four ranges of FeO are shown in the figure and the scatter of points around the line is about equal in each of the chosen ranges.

This does not mean that the addition of iron oxide to a slag is entirely without effect on the desulphurization ratio. An addition of iron oxide acts as a diluent to the acidic and basic components and thus decreases the excess base or acid count of the slag. Its effect on desulphurization is only that due to this dilution. This is a much smaller effect than would have been predicted on the basis of the reaction generally assumed:

$$CaO (slag) + FeS = CaS (slag) + FeO (slag)$$

If this were the controlling reaction, an increase in the mol fraction of FeO from o.1 to o.6, at constant CaO activity, should produce a sixfold decrease in the desulphurization ratio. Experimentally it is found that, at constant excess base, such a change in FeO content is without effect on the sulphur ratio. The two conditions are not identical and are not simply related. A constant value of excess base with slag FeO changing from 0.1 to 0.6 involves a decrease in activity of basic oxides of about 50 per cent which, on the basis of the equation, would approximately halve its desulphurizing power. Thus the equation would predict that an increase of FeO from 0.1 to 0.6 at constant excess base would reduce the sulphur ratio by a factor of 12. The fact that the ratio is not reduced at all (Fig. 4) may be regarded as strong evidence that the equation fails to represent the reaction by which sulphur is controlled in the basic open-hearth process.

To make this point clearer, let us select a pair of slags having about equal excess base and about equal sulphur ratios but differing widely in FeO content and see how they would compare with respect to a hypothetical equilibrium constant of the now discredited equation written above. The data for two such pairs are tabulated below, values for (FeO) and (CaO') being quoted from Winkler.²⁹

Sample No.	Excess Base	(S)/[S]	(FeO)	(CaO')	K
E38-14	0.271	6.0	0.66	0.295	14.9
E44-34 E32-22 E40-20	0.269 0.154 0.142	5.7 3.96 3.70	0.10	0.587 0.266 0.458	8.7

From this it is seen that K is not a constant at all and hence that equilibrium in the reaction as written has nothing to do with desulphurization by slags of this type.

This does not imply that this reaction is absent in the blast furnace or under reducing electric-furnace slags where the FeO content is much lower. A second argument that this is not the controlling reaction is found in the nearly complete absence of a temperature coefficient. The reaction as written is endothermic; hence, desulphurization should improve with increasing temperature (as it does in the blast furnace). However, in the next paragraph it will be shown that the temperature effect, if any, is in the opposite direction.

As an alternative mechanism, it is suggested that desulphurization takes place by reactions of which the following are typical: $\frac{\text{FeS}}{\text{MnS}} = \text{FeS (slag)}$ $\frac{\text{FeS}}{\text{MnS}} = \text{MnS (slag)}$

The dependence upon slag basicity is then ascribed to the effect of basicity upon physical characteristics of the slag, an effect that might be roughly summarized by the statement that sulphides become more soluble as the slag becomes more basic.

It is evident that this explanation requires also that the desulphurization ratio be affected by the alloy content of the bath, since different sulphides would possess different distribution ratios. It may be shown, however, that at the level at which manganese occurs in normal openhearth practice the MnS content of the metal is small compared with its FeS content.³⁰ The desulphurization ratio is thus mainly controlled by the distribution ratio for FeS.

Effect of Temperature

There remained only the need of determining the effect of temperature on the sulphur ratio for constant excess base or acid. Fig. 5 shows the point distribution for three temperature ranges, using again only the heats with more than 3 per cent and less than 70 per cent FeO. Essentially there is no temperature effect in the range 1540° to 1660°C. To determine whether extremes of temperature might show some effect, those points in the range 1670° to 1800°C. are plotted in Fig. 6.

Some of these extra high temperatures may be in error by some 20° to 30°C., but they all are above 1670°C. It appears from Fig. 6 that there is a very small temperature effect in the direction that increasingly high temperatures make desulphurization slightly worse. Several low-temperature points of equal uncertainty are also plotted. Some of these low temperature points are further complicated by being of very low FeO (less than 3 per cent). The latter points show that ex-

tremely low temperatures and/or low FeO favor desulphurization to a greater or lesser degree, combinations of the two factors producing a fairly large favorable effect.

Sulphur Distribution under Simple CaO-SiO₂-FeO Slags

It has been shown that the sulphur distribution ratio is controlled almost wholly by the excess base or acid present in the slag at equilibrium, the excess constituent being calculated by the method just described. These calculations had worked for slags of regular and extreme composition variations. There were available in addition a large group of slags in the CaO-MgO-SiO₂-FeO system, which had been investigated by Fetters and Chipman.9 Calculated by the method just described, the results are plotted in Fig. 7. For the sake of comparison, the standard line of the much more complex slags of heats E-29 through E-44 shown in Fig. 5 is also drawn in Fig. 7. The agreement is almost perfect, and the points from both groups of heats could readily be plotted together.

The spread in values shown in Figs. 5 and 7 can be attributed to several causes:

- Calculations in the mol and mol-fraction values and in the compound formations may contribute some small amount to the error.
- 2. Small errors in the analysis of sulphur can contribute quite largely to the spread; for example, an error of 0.002 per cent in the metal sulphur can cause a change of 0.5 or more in the sulphur ratio. If an additional error in the opposite direction was made in the slag sulphur, the error in certain cases can amount to between 0.5 to 1.0 in the sulphur ratio. This is not too unlikely with regard to sulphur determinations. On this basis it can therefore be concluded that the spread in the sulphur ratios for a given excess base value is

not severe at all, but is within the desired limits.

Practical Considerations

Until now the results from a precise equilibrium study in heats free of carbon method described in this paper, and the values are plotted in Fig. 8. It was necessary to discard three of Diehl's slag-metal sets that showed sulphur ratios of 9.4,10.6 and 10.9. All three showed a large cold-pigiron addition about 15 min. before the tests

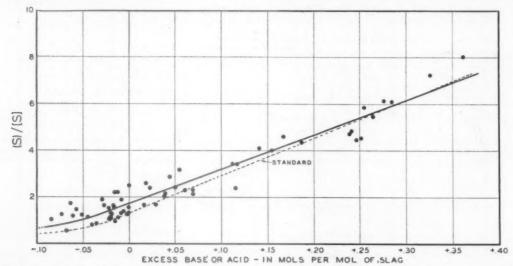


Fig. 7.—Sulphur distribution in simple slags containing lime, magnesium oxide, silica and iron oxide.

Data of heats E-5 through E-22.

have been discussed. It would be interesting to see how these same factors behave in the basic open hearth, where metalloids such as carbon contribute to the nonequilibrium conditions.

A search of the literature has shown that the maximum attainable sulphur ratio in the open hearth is about 10.8.4.17 Only one exception to this was noted, the values being 15.5 and 14.7, given by Darken and Larsen.26 These extreme figures might occur momentarily as a result of abnormal absorption from the furnace gases but seem more probably the results of errors in sampling and analysis. From our equilibrium study the best sulphur ratio is indicated to be only 8.

About 26 slag-metal groups were taken from open-hearth heats involved in studies by A. N. Diehl, Darken and Larsen, 26 and Tenenbaum and Brown. 27 These slags were calculated for excess base or acid by the

were made. In view of the fact that a vigorous boil always accompanies a pig addition, it would not be surprising to find that the slag picked up considerable sulphur from the producer gas flame, which showed very high sulphur content. This would explain the high sulphur ratios for these heats. Three tests were from heats refined under natural gas; these three values fit the equilibrium curve perfectly and are marked with an N in Fig. 8. With the exception of the three extra high sulphur-ratio points of Darken and Larsen, the others fit the curve well. All of Tenenbaum and Brown's points fall evenly on either side of the standard curve. The greater spread of values shown in Fig. 8 is undoubtedly due to errors in sampling and analysis. For example, in Diehl's heats,3 on four tests from doors 1, 2, 3 and the back of the furnace, as much as 0.000 per cent sulphur difference in the metal tests and 0.05 in the slag tests were noted. These differences can cause a deviation of 2.0 in the sulphur ratio from the average.

While higher temperatures and the use

An extremely wide range of slag compositions in both the simple and complex slag systems was investigated, wherein temperature was an additional variable.

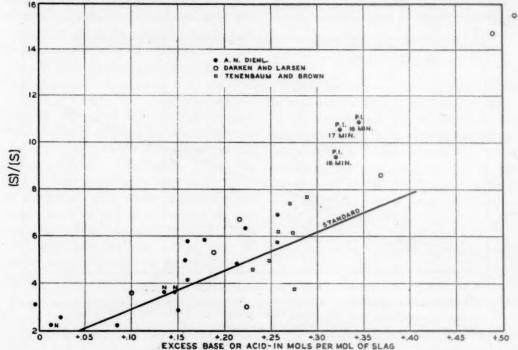


FIG. 8.—SULPHUR DISTRIBUTION IN THE BASIC OPEN HEARTH.

of fluorspar show no effect on the sulphur distribution from an equilibrium standpoint, nevertheless they are important in open-hearth operation. Both make it possible to dissolve lime more readily and make the slags more fluid. They therefore contribute greatly to the speed of open-hearth reactions without changing the end point. Fig. 8 indicates as a matter of fact that the sulphur reaction does generally approach equilibrium in the basic open hearth during the latter part of the refining period.

SUMMARY

A long series of experimental heats was made in an induction furnace for the purpose of studying the equilibrium distribution of sulphur between the metal and an assortment of basic slags ranging from strongly basic to slightly acidic. The constitution of the liquid slag was formulated on the basis of attraction between basic and acidic quantities according to the following rules. The basic oxides CaO, MgO and MnO were taken in all ranges to be equal on a mol per mol basis. The following molar ratios were taken as necessary for a neutral slag (the third one being deduced from the data presented):

2 Base: 1 SiO₂ 4 Base: 1 P₂O₅ 2 Base: 1 Al₂O₃ 1 Base: 1 Fe₂O₃

When insufficient base was available, Fe₂O₄ was considered neutral and added to the FeO. FeO was considered uncombined in all cases.

The remaining base or acids after these combinations were fulfilled were then added and designated as the "excess base or acid count," expressed in mols per mol of slag.

From plots of the sulphur ratio (S)/[S], where (S) is the slag sulphur and [S] is the metal sulphur in per cent values, against the excess base or acid count it was concluded that in slags of the type considered:

- 1. MnO and MgO on a mol per mol basis are as good desulphurizers as CaO.
- 2. Fluorspar is neutral and does not affect the sulphur ratio.
- 3. Alumina (Al₂O₅) requires the same number of mols of base to neutralize it as does SiO2.
- 4. Slag FeO (from 3 to 70 per cent) has only a dilution effect on the sulphur ratio. Therefore the equation

does not represent the controlling reaction in the open hearth; instead desulphurization is controlled by the distribution ratio of the metal sulphides between slag and metal.

5. Temperature in the range 1540° to 1660°C. shows no measurable effect on the sulphur ratio. Temperatures greater than 1670°C. appear to have a small harmful effect while temperatures below 1540°C. and/or FeO below 3 per cent appear to have a beneficial effect on desulphurization.

6. Sulphur distribution is controlled almost entirely by the excess base or acid count and the relationship is almost linear.

7. Basic open-hearth values of the sulphur ratio show reasonably good agreement with the equilibrium study values for the same basicity, regardless of carbon content. Sulphur equilibrium is closely approached during refining in the open hearth and the sulphur ratio in low-carbon heats reaches its maximum value at about 8.

ACKNOWLEDGMENT

The authors take this opportunity to express their appreciation to D. L. Guernsey, S. T. Yuan, T. B. Winkler and F. J. Radavich for assistance in both the analytical work and in the operation of the furnaces. Thanks are also due to J. R. Lane for drawing the curves and to Dr. K. L. Fetters for permission to use many of the data from heats made by him.

REFERENCES

- 1. Bettendorf and Wark: Stahl und Eisen
- (1932) **52,** 577-606. 2. Bardenheuer and Geller: *Mitt.* K. W. I. Eisenforschung (1934) 16, 77-91.
- 3. Diehl: Yearbook Amer. Iron and Steel Inst.
- (1926) **16**, 404-453. 4. Maurer and Bischoff: *Jnl*. Iron and Steel Inst. (1936) 133, 188-203.
- Schwerin: Metals and Alloys (1934) 5, 61.
 Joseph and Scott: Iron Age (Nov. 23, 1939) 34-37; (Nov. 30, 1939), 30-34; (Dec. 7,
- 1939) 49-53. 7. Laurie: *Jnl.* Iron and Steel Inst. (1939) **139**, 257.
- 8. Chipman and Li: Trans. Amer. Soc. for Metals (1937) 25, 435-465.
 9. Fetters and Chipman: Trans. A.I.M.E.
- (1941) 145, 95-112.

 10. Meyer and Görrissen: Archiv Eisenhütten-
- wesen (June 1934) 1, 665-672.
 11. Geiger: Bl. Fur. and Steel Plant (1931) 19,
- 12. Colclough: Trans. Amer. Faraday Soc.
- (1925-26) 21, 216-220. 13. Fetters and Chipman: Trans. A.I.M.E.
- (1940) 140, 170-203. 14. Trefarrow and Mirew: Archiv Eisenhüt-
- tenwesen (1933) 7, 337-341. 15. Köhler: Stahl und Eisen (1930) 50, 1257-
- 1266. 16. Bardenheuer: Stahl und Eisen (1933) 53,
- 488-496. 17. Manterfield: Metallurgia (1938) 19-20,
- 55-58.
 18. Schenck: Archiv Eisenhüttenwesen (1930) 3, 685-692.
- 19. Herasymenko: Archiv Eisenhüttenwesen (1940) 9, 369-374. 20. Schenck: Physikalische Chemie der Eisen-
- hüttenwesen, 2, Berlin, 1934, Julius Springer.
- 21. Schleicher: Stahl und Eisen (1921) 41, 357-364. 22. von Jonstorff: Jul. Iron and Steel Inst.
- (1902) 61, 304-329. 23. Williams: Bl. Fur. and Steel Plant (1932)
- 11, 51-54. 24. Görrissen: Archiv Eisenhüttenwesen (1942)
- 15, 347-350. 25. Schönwälder: Stahl und Eisen (1937) 57,
- 1381-1382. 26. Darken and Larsen: Trans. A.I.M.E.
- (1942) 150, 87-109. 27. Tenenbaum and Brown: Trans. A.I.M.E.
- (1945) 162, 685.
 28. Chipman: A.I.M.E. Open Hearth Proceedings (1937) 110.
 29. Winkler and Chipman: This volume, page
- III.
- 30. Kelley: U. S. Bur. Mines Bull. 406 (1937) 124

DISCUSSION

(John J. Golden presiding)

A. SKAPSKI.*-The work of Professor Chipman and his collaborators is well known and duly appreciated in Europe, from where I just came. All I can do is to congratulate the authors upon this new and excellent contribution to the study of sulphur equilibria in steel, which was executed in such a masterful way.

At the same time I should like to direct the attention of the authors to a paper referring to sulphur equilibria, which obviously could not have been known to them as it was presented to the Polish Academy of Technical Sciences by Goslawski, Kotlinski and myself³¹ and appeared in its Annales just before the war. To be clear I must give a brief résumé of this paper.

It has been generally accepted that sulphur in steel exists principally in two forms: FeS and MnS. We must make the point quite plain, however, by asking what experimental evidence supports this view. As a matter of fact, there are no standard methods for the determination of sulphides in steel separately. The first, and only method known so far, is that published by Fitterer.32 He uses electrolytic extraction of inclusions from steel under conditions that secure complete recovery of extracted sulphides. From the nonmetallic residue containing inclusions, Fitterer dissolves MnO in sodium-citrate solution; he also determines the total manganese content of the inclusions. By substracting Mn belonging to MnO from the total manganese content of the inclusions, MnS is calculated. The sulphur belonging to MnS is subtracted from the total amount of sulphur in the steel, and this difference is calculated as FeS. The figure thus obtained for FeS is only a speculative one, and is based on the correctness of the assumption that sulphur in steel is distributed between Fe and Mn.

Work on electrolytic methods for the determination of nonmetallic inclusions in steel done by myself and my collaborators, first in Stockholm, Metallografiska Institutet (1033-1934), and then in Krakow, Institute of Physical Chemistry, Mining Academy (1934-1030) has resulted in an improved electrolytic method of extracting nonmetallic inclusions in steel and their separation into the main constituents-oxides and silicates as well as sulphides. I wish to speak here only about the sulphidic inclusions, however. After our electrolytic and analytical methods had been perfected, we were very much surprised by their results, because no commercial plain carbon or low-alloy steel analyzed would show more than trace of FeS, while all would show manganese sulphide and, curiously enough, copper sulphide.

When we first obtained such results in 1036 I did not believe they were correct, and suspected that the presence of CuS was due to some error of method; i.e., that CuS was being produced from FeS + Cu (the latter being always present in steel) either during the electrolysis or through the subsequent chemical treatment of the extracted inclusions. But all the tests made and all precautions introduced in the analytical methods, particularly the direct extraction of copper sulphide with KCN solution from the electrolytic inclusions residue immediately after it had been washed with water have convinced us that copper sulphide could not be produced secondarily under the conditions of our procedure and that actually it must have existed in steel.

Consequently, we were obliged to accept that sulphur in steel is divided between manganese and copper and that FeS exists but in small amounts. We have since analyzed many samples of commercial plain carbon and low-alloy steels and in all we have found this sort of distribution of sulphur. It is to be emphasized that the sum of sulphur found in MnS and CuS agreed with the total sulphur content of the steel within the limits of experi-

I will quote here only one example of analysis for sulphides of a steel sample (obtained through the courtesy of Metallografiska Institutet, Stockholm) the copper content of which was the lowest of all commercial steels that have been under our investigation. The composition of the steel was: 0.97 per cent C, 0.43 Mn, 0.29 Si, 0.024 P, o.oo8 S, o.oo8 Cu.

^{*} University of Chicago, Chicago, Illinois, Goslawski, Kotlinski and Skapski: Ann.
 Acad. Sci. Tech. Varsone (1930) 6, 23.
 Fitterer: U.S. Bur. Mines R.I. 3205 (1933).

The composition of sulphides (two parallel electrolyses) was:

	Per Cent	Per Cent
MnS	0.013	0.014
CuS	0.009	0.010
FeS	trace	trace
S(MnS)S(FeS)	0.008	0.009

There is a considerable proportion of CuS and only trace of FeS in spite of the very small content of copper.

After the analytical results had been checked we made some direct measurements of affinities of sulphur for copper, iron and manganese at the temperatures approaching those of the steelmaking process, because it is clear that the analytical results obtained indicate that copper—at least at 1500° to 1600°C.—must have greater affinity for sulphur than iron and perhaps even manganese.

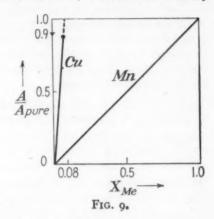
We calculated the affinities by measuring directly the equilibria

basing on the numerical data for $2H_1S \rightleftharpoons 2H_2$ + S_2 measured in a very exact and reliable way by Kelley in this country.

The results of our measurements confirmed our analytical results: the affinity of sulphur for copper at high temperatures was found greater than that for iron and at 1500° to 1600°C. very much greater, and indeed even considerably greater, than for manganese.

These affinities refer, of course, to the reactions between pure substances, and when they are dissolved in molten steel the problem becomes more complex. But even in the latter case, the affinity of sulphur for copper is favored by the circumstance that there is (at least in presence of small amounts of carbon) a miscibility gap between liquid iron and copper. To illustrate this, I assume, after Hansen, that at 1600°C. a layer containing 8 at. per cent Cu coexists with a layer containing 90 at. per cent Cu (both in iron solution). We then get the accompanying diagram (Fig. 9) for the activity of copper and manganese in liquid iron (schematically). The diagram shows that at 1600°C. the activity of copper is about 10 times greater than that of manganese at the same concentration.

Having in mind this favorable circumstance for copper and the very great difference in affinities of sulphur for copper and for iron (also in favor of copper sulphide formation) we may, even in the steel bath, accept that the affinity of sulphur is greatest for copper, smallest for iron, and that the affinity for



manganese lies between them. As the temperature decreases, however, the affinity of sulphur for copper decreases much faster than that for iron and manganese, consequently the affinity relations may reverse at lower temperatures.

We also made some attempts to show the presence of CuS in inclusions by direct etching. We got some encouraging results using warm, concentrated KCN solution, but our work was interrupted by war.

Although only Cu_2S , in the pure state, is stable at high temperatures, and although all the reactions at 1600° C. are consequently concerned only with Cu_2S , in inclusions in finished steel not Cu_2S but CuS is found. Whether this is due to the decomposition $Cu_2S \rightarrow CuS + Cu$ in steel during cooling, or to some other reason, no answer can be given at present.

I dare to suggest that the authors' results might gain in clarity by additional analyses of the bath samples for the form of the sulphides present. This would be especially useful in view of the fact that true equilibrium (partition) constants are concerned only with the same kind of dissolved component in both phases, and not with total sulphur.

I wish to stress the point that the problem of the presence of CuS in steel has been hardly more than started and needs much of further elaboration. So far only some of the corrosionists (U. R. Evans, Cambridge) accept the presence of CuS as an explanation of the corrosion-resistance influence of Cu and S in steel. Our paper concerning Copper Sulphide in Steel was published too late in 1939 to be circulated, and only a few copies, those sent to my friends in England and Sweden, were preserved. Then war broke out and, being put into prison for 26 months, I hardly had opportunity to take up further work. The problem has been taken up anew in the Institute for the Study of Metals, University of Chicago, and will be investigated in detail.

G. Soler.*-I want to raise a question with Dr. Grant, whom I know has had practical experience on the open hearth and the electric furnace. In considering the equilibria of the sulphur reaction, there are two conditions in the electric furnace. One is during the oxidizing period when the lime-silica ratio may be 2:1, the FeO high, and the temperature may be not quite as high as in the final stages. Then, comparing that condition with the reducing slag, we have higher basicity, very low FeO, and the temperature of the slag would be a little higher. Why are we able to reach low sulphurs with the final reducing slags and not able to do the same with the highly oxidizing slags?

G. DERGE †-This is an excellent paper and what I am going to say is in no way a criticism. However, the treatment is limited to oxidizing slags under open-hearth conditions and I think it might be well to point out the existence of other conditions in desulphurization, so that we do not lose track of them. Commonly we feel that sulphur removal is easiest under reducing conditions in basic slags. So the complete chemistry of the desulphurization picture should take that into account also. This is one case where it is especially true that our picture of these reactions is clarified considerably if we consider slags as ionic solutions instead of as dissociated oxides, as indicated by these reactions:

$$\begin{array}{ll} [S^-]_{M \in \text{ial}} \rightleftarrows (S^-)_{Slag} & [1] \\ (S^-) + (Ca^{++}) \rightleftarrows (CaS) & [2] \\ (2Ca^{++}) + (SiO_4^{\#}) \rightleftarrows (Ca_2SiO_4) & [3] \\ (Ca^{++}) + (Fe_2O_4^-) \rightleftarrows (CaFe_2O_4) & [4] \\ \end{array}$$

According to reaction 1, we are dealing with a distribution of sulphide ion between the slag and metal phases. In the slag this ion will react with calcium ions to form calcium sulphide, according to reaction 2. The extent to which this reaction goes to the right will be determined by the availability of calcium ions. This in turn will be determined by reactions of the types illustrated by 3 and 4, so that in acid or oxidizing slags the calcium ion concentration will be appreciably reduced and conditions will not be favorable for desulphurization. This is in qualitative agreement with observations that desulphurization of iron is easiest under the reducing slag of the basic electric furnace and impossible in acid open-hearth or bessemer processes, while it is subject to control in the blast furnace and basic open hearth.

We do not have quantitative data for such reactions, but it seems to me that this general sort of picture must be considered if we are going to analyze desulphurization in all of its aspects and not just in the basic open hearth.

A. Skapski.—I am referring to the suggestion made that we may be helped in the explanation and calculation of equilibria between the steel bath and the slag if we assume the electrolytical dissociation of the latter.

I am willing to admit that some qualitative hints can be gained by this assumption, but I am very sceptical as far as the derivation of any numerical data is concerned which might be useful in calculation of thermodynamic equilibria.

The reason is that numerical calculations connected with electrolytes are comparatively simple in two extreme cases only: that of very slight dissociation (weak electrolytes) and that of complete dissociation. In the first case we may apply the simple law of mass action, as expressed in concentrations; in the second we must use activities instead of concentrations. but we are able to calculate these activities, at least with some approximation, e.g., in the way shown by Debye, Hueckel, Bjerrum and others. As far as I know, we hardly can classify molten slags in either of these groups. The existing evidence seems rather to indicate that we have to deal with a very advanced but not complete dissociation. The introduction of dissociation in this particular case would therefore only cause further complications.

Timken Roller Bearing Co., Canton, Ohio.
 † Metals Research Laboratory, Carnegie Institute of Technology.

MEMBER.-I am particularly interested in desulphurization in the blast furnaces. I wonder if the authors of this paper have any comment to make on the mechanics of blast furnaces.

J. CHIPMAN AND N. J. GRANT (authors' reply).-The ionization of these slags is something that has given us considerable room for thought and study. It is quite feasible to take all of the sulphur distribution data and obtain a very satisfactory interpretation on the basis of complete ionization of the components of slag. Sulphur is a particularly simple case. When the same methods are applied to the distribution of oxygen between the slag and the metal the results have not yet made sense on the basis of any quantitative theory of ionization of the slags which we have studied. However, that need not discourage us from such studies in the future.

The recently published theory of Temkin, Samarin and Shvarzman,33 of the Moscow Institute of Steel, dealing with the concept of an ideal ionic solution, has not yet been applied to oxygen distribution, but if it will yield satisfactory results for oxygen, and there are now plenty of data available, it may prove to be a basis for a good theory of slag. Pending further development of ionic theory, we shall have to answer the questions on the basis of the well-worn theory of the formation of salts that are regarded as being little ionized.

With respect to desulphurization in the electric furnace in the oxidizing stage, there is probably no difference between the behavior of the electric slag and open-hearth slag. Our experiments are as applicable to oxidizing slags in electric furnaces as they are in the basic open hearth. In the case of reducing slag in the electric furnace and probably also in the case of blast-furnace slags, we shall return to the equation for the reaction we have discarded for open-hearth slags:

$$\overline{\text{FeS}} + \text{CaO(slag)} = \text{FeO(slag)} + \text{CaS(slag)}$$

At steelmaking temperatures this reaction can take place, but in the open hearth the reaction is forced very far to the left by the

FeO concentration of the slag. While we say the reaction is not the mechanism by which desulphurization is accomplished in the open hearth, we would not imply that it does not occur at all. It probably does occur at very low concentration of FeO. Now, put into the slag some carbon or ferrosilicon to remove the FeO, and the reaction is permitted to form more CaS. If there is something present to use up the FeO formed from the reaction. desulphurization can be achieved by the process, as is illustrated in the equation:

$$\frac{\text{FeS} + \text{CaO(slag)} + \text{C} = \underline{\text{Fe}} + \text{CaS(slag)}}{+ \text{CO(gas)}}$$

It is indeed regrettable that European data that appeared early in the war have not become available to American metallurgists. Dr. Skapski's conclusions that sulphur in molten steel is principally combined with copper, secondarily with manganese, and to a lesser degree with iron, is totally at variance with all results other than his own. His reasoning is perfectly sound, but we would question the dependability of the experimental results. Students of methods for determination of nonmetallic inclusions in steel have long recognized the limitations inherent in electrolytic methods, and conclusions based upon such methods alone should be regarded with caution until they can be confirmed by other means. In the present instance the other means that are applicable depend upon thermodynamic calculations that are outlined below and that definitely fail to support Dr. Skapski's conclusions.

The free energies of a number of metallic sulphides, among them FeS, MnS, Cu2S, were evaluated in a careful study of all existing data by K. K. Kelley.34 The data permitted mmor uncertainties in the numerical values but were sufficiently concordant to eliminate possibilities of gross errors. The free energy of dissolved sulphur in liquid iron, free from either copper or manganese, was determined by Chipman and Li35 by means of equilibrium measurements in the reaction of hydrogen

M. Temkin: Acta Physicochimica (U.S.-

S.R.) (1945) 20(4), 411. A. Samarin, M. Temkin and L. Shvarzman; Ibid, 421.

³⁴ K. K. Kelley: Contributions to the Data on Theoretical Metallurgy, VII—The Thermodynamic Properties of Sulfur, and its Inorganic

Compounds, U. S. Bur. Mines Bull. 406.

35 Chipman and Li; Trans Amer. Soc. for Metals (1937) 25, 435-465.

with iron-sulphur melts. These were the sources of the following equations, which are quoted from Basic Open Hearth Steelmaking.³⁶

Fe(liq.) +
$$\frac{1}{2}S_{3}(g) = \text{FeS(liq.)};$$

 $\Delta F^{\circ} = -28,000 + 10.2T$
Mn(liq.) + $\frac{1}{2}S_{3}(g) = \text{MnS(solid)};$
 $\Delta F^{\circ} = -65,000 + 19.0T$
2Cu(liq.) + $\frac{1}{2}S_{3}(g) = \text{Cu}_{3}S(\text{liq.});$
 $\Delta F^{\circ} = -27,920 + 5.6T$
 $\frac{1}{2}S_{3}(g) = S(\text{in Fe});$
 $\Delta F^{\circ} = -42,410 + 12.35T$

In addition, we require the free energy of fusion of MnS (obtainable with sufficient accuracy by analogy with FeS), and the free energies of solution in the melt for manganese (from BOHS) and for copper. This last is obtained from the method of approximation which Dr. Skapski suggested and the results are shown below. In accordance with the usual convention the standard free energies of the alloy elements refer to a 1 per cent solution in liquid iron.

$$MnS(solid) = MnS(liq.);$$

$$\Delta F^{\circ} = +6400 - 3.4T$$

$$Mn(liq.) = Mn(in Fe);$$

$$\Delta F^{\circ} = -9.11T$$

$$Cu(liq.) = Cu(in Fe);$$

$$\Delta F^{\circ} = -4.58T$$

We may reasonably claim to have answered the question of the form of sulphur in the liquid iron if we can show by calculation the ratio of iron to alloy element in the hypothetical phase which might form if its solubility in the melt were sufficiently low. For this purpose we combine several of the above equations to obtain:

FeS(liq.) +
$$\underline{Mn} = \underline{Fe} + \underline{MnS(liq.)};$$

 $\overline{\Delta F^{\circ}} = \underline{-30,600} + 14.5T$
FeS(liq.) + $\underline{2Cu} = \underline{Fe} + \underline{Cu_2S(liq.)};$
 $\overline{\Delta F^{\circ}} = \underline{+80 + 4.6T}$

The equilibrium constants obtained from these equations at approximately the melting point of iron are:

$$\frac{\text{(Cu}_{2}\text{S)}}{\text{(FeS) (\%Cu)}^{3}} = 0.1$$

$$\frac{\text{MnS}}{\text{(FeS) (\%Mn)}} = 3.5$$

This falls slightly short of confirming Dr. Skapski's statement that cuprous sulphide is more stable than manganese sulphide at high temperatures and that in liquid steel both are more stable than ferrous sulphide. Let us proceed, however, to calculate the ratio of alloy sulphide to iron sulphide as a function of metal composition, which gives the following results:

Metal Composition, Per Cent Mn or Cu	Sulphide MnS/FeS	Composition Cu ₂ S/FeS
0.50	1.75	0.025
0.20	0.70	0.004
0.10	0.35	0.001
0.05	0.17	0.00025
0.02	0.07	0.00004
0.01	0 035	7,0000

It is felt that these results confirm our assumption that the sulphur in the open-hearth bath of low manganese content exists principally as dissolved FeS.

^{**} Basic Open Hearth Steelmaking, A.I.M.E. New York, 1944.

Anelasticity of Metals

By Clarence Zener,* Member A.I.M.E. (Chicago Meeting, Pebruary 1946)

It is customary to regard the stressstrain relation as consisting of two parts, the elastic region and the plastic region. The essential attribute of the plastic region is the presence of a permanent set, which remains upon removal of all stresses. The essential attribute of the elastic region is the absence of such a permanent set. Absence of a permanent set does not imply a linear relation between stress and strain, nor even a single valued relation. In fact, in no real metal is stress a single valued function of strain in the elastic region. The property of a solid in virtue of which stress and strain are not uniquely related in the elastic range will be called "anelasticity." The purpose of the present article is to review and correlate the past work upon the anelasticity of metals. The following paper by W. A. West124 describes investigations upon anelastic properties of iron.

Many manifestations of anelasticity have been observed, the first as early as 1835 by Weber.^{1,2} In his experiments Weber subjected a specimen to a constant load (or deformation) for a given time, and then suddenly removed the load. He

observed that most of the deformation suddenly disappeared, but that there remained a residual deformation, which disappeared only gradually with time, as is illustrated in Fig. 1. The occurrence of a residual deformation which only gradually disappeared. Weber called the elastic after-effect (Elastische Nackwirkung). An extensive review of the early work upon elastic after-effects has been given by Auerbach.3 Another manifestation of anelasticity is the dependence of the elastic constants-e.g., Young's modulusupon the method of measurement. Thus, if dynamic methods are used, the measured value will depend upon the frequency of oscillation. Still another manifestation is dissipation of energy attending vibration, called damping or internal friction.

One objective of metallurgical science is the understanding of the plastic and fracture properties of metals in terms of their microstructure. Through such an understanding will come the ability to design microstructure to give the desired mechanical properties. A study of anelasticity will furnish an invaluable aid in the attainment of this objective. Such studies, when properly guided, yield information regarding the relation between stress and strain in the individual components of the microstructure. In order. however, that this type of information may be obtained, it is necessary that the experimental studies of anelasticity be interpreted by the appropriate mathematical analysis. This article, therefore, starts with the mathematical formulation of anelasticity.

The statements or opinions expressed in this article are to be considered those of the author, and do not necessarily express the views of the Ordnance Department. Manuscript received at the office of the Institute July 31, 1945. Issued as T.P. 1992 in METALS TECHNOLOGY, August 1946.

^{*}Principal Physicist, Watertown Arsenal, Watertown, Massachusetts (On leave, Professor of Physics, Washington State College); now Professor of Metallurgy, Institute for the Study of Metals, University of Chicago, Chicago, Illinois.

References are at the end of the paper.

MATHEMATICAL FORMULATION OF ANELASTICITY

BOLTZMANN'S THEORY

Extensive experiments were carried out by Kohlrausch^{4,5} in an attempt to forapproach, on the other hand, one first establishes, from very general considerations, the functional relation between stress and strain, and leaves for future developments the physical interpretation. Meyer⁶ and Voight⁷ adopted the first

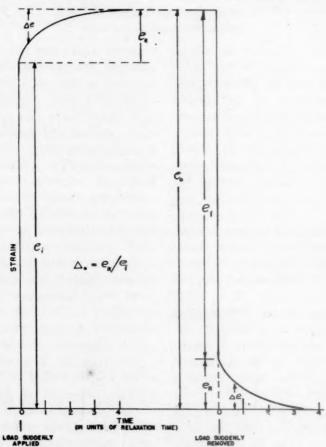


FIG. 1.—ILLUSTRATION OF ELASTIC AFTER-EFFECT.

mulate the general laws that govern the elastic after-effect. His only general conclusion was that residual deformation was proportional to the initial deformation.

Two theoretical approaches are available for the establishment of a theory of elasticity that embraces elastic aftereffects. In the first approach, one assumes a detailed physical mechanism and then incorporates this mechanism into the fundamental differential equations, the solution of which leads to the relation between stress and strain. In the second

approach; assuming that the stress at every point in the material was a linear function of both strain and strain rate. Boltzmann⁸ pointed out the inadequacy of such an assumption. He himself adopted the second approach. With all its simplicity, Boltzmann's method is based upon such general principles that it was able to fit into a precise mathematical formulation all previously observed elastic after-effects and also all later observed elastic after-effects and related phenomena. Progress since the time of Boltzmann has

been concerned solely with the physical interpretation of the elastic after-effect and related phenomena.

If the strain e were a unique function of the stress S within the elastic range, their relation could be expressed as follows:

$$Ee(t) = S(t)$$
 [1]

where E is the elastic modulus. This equation has two important properties: (1) it is linear, (2) it relates instantaneous values of strain to instantaneous values of stress. In Boltzmann's generalization of this equation, he retains the first property, that of linearity, but allows the strain to be a function also of the past history of the stress. The most general way of allowing for such an influence of the past history of the stress is to write the fundamental equation as follows:

$$E_{\infty}e(t) = S(t) + \int_{-\infty}^{t} \Phi(t - t')S(t') dt'$$
 [2]

Boltzmann has called Φ the remembrance function. In this equation E_{∞} is the limiting value the elastic modulus approaches as the frequency of measurement is increased. Once the remembrance function has been determined, Eq. 2 may be used to compute strain as a function of stress and of its past history.

From Eq. 2 it follows that the simple loading and simple unloading experiments are symmetrical. Upon defining the instantaneous strain by e_i ,

$$e_i = S/E_{\bullet}$$

it follows upon differentiation of Eq. 2 that

$$e(t) = e_i \Phi(t),$$
 if $S = \begin{cases} 0, & t < 0 \\ S_0, & t > 0 \end{cases}$ [3a]

$$\dot{e}(t) = -e_i \Phi(t), \quad \text{if} \quad S = \begin{cases} S_0, \ t < 0 \\ 0, \ t > 0 \end{cases} \quad [3b]$$

This symmetry has been reported by Chalmers⁴⁷ in his experiments upon tin. The remembrance function may therefore be determined experimentally by either the simple loading or unloading experiment.

Not only the elastic after-effect, but also all other anelastic phenomena, may be computed from the remembrance function by means of Eq. 2. Two anelastic effects deserve special consideration. One is the variation of the observed dynamic elastic modulus with the frequency of measurement. If E_f refers to the modulus measured dynamically using a frequency of vibration f, then a convenient measurement of the variation of elastic modulus with frequency is the modulus defect $\Delta(f)$ defined by

$$\Delta(f) = (E_{\infty} - E_f)/E_0$$
 [4]

The quasi-static modulus defect is then

$$\Delta_0 = (E_{\infty} - E_0)/E_0 = \int_0^{\infty} \Phi(\tau) d\tau$$
 [4a]

The other anelastic effect is the dissipation of vibrational energy. A convenient measure of this dissipation is the internal friction $Q^{-1}(f)$ defined by

$$Q^{-1}(f) = \ln n/(\pi t f)$$
 [5]

where t is the time required for the amplitude of vibration to be reduced to 1/nth of its initial value in free vibration, or defined by

$$Q^{-1}(f) = \Delta f/3^{\frac{1}{2}}f$$
 [6]

where Δf is the width of the resonance curve at half maximum in forced vibration. Boltzmann has shown that these two anelastic effects are related to the remembrance function by the following equations:

$$\Delta(w) = \int_0^\infty \Phi(t) \cos wt \, dt \qquad [7]$$

$$Q^{-1}(w) = \int_0^{\infty} \Phi(t) \sin wt \, dt \qquad [8]$$

where w is the angular frequency of vibration.

RELAXATION SPECTRUM

Shortly after Boltzmann proposed his general theory of anelasticity, J. J. Thomson⁹ and Wiechert^{10,11} arrived independently at the concept of representing

anelastic effects as the superposition of a set, either discrete or continuous, of relaxations with different relaxation times. Upon substituting this remembrance function into Eqs. 7 and 8, one sees that the modulus defect and the internal friction

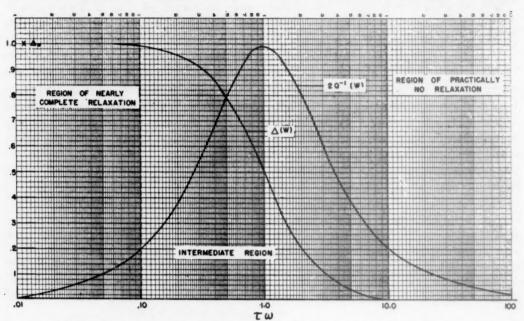


Fig. 2.—Modulus defect and internal friction for case of single-line relaxation spectrum.

This concept shifts the emphasis from the remembrance function, about which most scientists have little physical intuition, to a distribution function, which is capable of quite precise physical interpretation. The significance of the concept introduced by Thomson and Wiechert is therefore that it paves the way for a physical interpretation of anelasticity.

The elastic after-effect of a specimen with a single relaxation time is illustrated in Fig. 1. If τ is this time, and Δ_0 is the quasi-static modulus defect (see Eq. 4a), then, if the strain is held at the constant value e_0 for a very long time prior to t = 0, and the stress is removed at t = 0, the strain at later times is given by

$$e(t) = \Delta_0 e_i e^{-t/\tau}$$
 [9]

From Eq. 3b it may be seen that this system has the remembrance function

$$\Phi(t) = \Delta_0 \tau^{-1} e^{-t/\tau}$$
 [10]

are given by the following two equations:

$$\Delta(w) = \Delta_0/(1 + \tau^2 w^2)$$
 [11]

$$Q^{-1}(w) = \Delta_0 \tau w / (1 + \tau^2 w^2)$$
 [12]
we quantities are plotted in Fig. 2

These two quantities are plotted in Fig. 2 as a function of the product τw . For values of this product greater than 10, both the modulus defect and the internal friction are practically zero. In this region the frequency of vibration is so high that practically no relaxation occurs. For products of τw less than $\frac{1}{10}$, the modulus defect has practically its limiting value Δ_0 , and the internal friction is again very small. In this range the frequency of vibration is so low that the specimen may practically be regarded as relaxed at all times. Only in the intermediate frequency range does the modulus defect change appreciably and the internal friction have a value comparable to its maximum value. In this intermediate frequency range the specimen is partially but incompletely relaxed.

In representing the general case of anelasticity by a continuous distribution of relaxation constants, the question arises as to the most appropriate scale. Since the distribution frequently covers a very wide range, the logarithmic scale will be adopted. To this end the relaxation spectrum $\psi(\tau)$ will be so defined that the product $\psi(\tau)$ d $\ln \tau$ gives the contribution to Δ_0 of those relaxations whose relaxation times lie within the range d $\ln \tau$ at τ . Thus, from this definition and from Eq. 10, it follows that the remembrance function is related to ψ by

$$\Phi(t) = \int_{-\infty}^{\infty} \psi(\tau) \tau^{-1} e^{-t/\tau} d \ln \tau$$
 [13a]

and therefore by

$$\Phi(t) = \int_0^\infty \psi(\mu) e^{-t\mu} d\mu \qquad [13b]$$

where $\mu = 1/\tau$. Substituting Eq. 13a into Eq. 3a, shows that the area beneath the relaxation spectrum is equal to the quasistatic modulus defect; i.e.,

$$\Delta_0 = \int_{-\infty}^{\infty} \psi(\tau) \ d \ln \tau$$

While the remembrance function may be determined experimentally through Eqs. 3a or 3b, no simple analytical method exists for directly determining the relaxation spectrum from experiment. It is therefore expedient to make some simplifying assumption regarding the relaxation spectrum. One possible assumption, frequently found in the literature, is that ψ has a constant value ψ_0 within a certain range, and is zero outside this range. From Eq. 13b, it may be seen that this assumption leads to the following relations:

$$\Phi(t) = (\psi_0/t) \{ e^{-t/\tau_2} - e^{-t/\tau_1} \},$$

$$\psi = \begin{cases} \psi_0, \tau_1 < t < \tau_2 \\ 0, \text{ otherwise} \end{cases}$$

and therefore

$$\Phi(t) \simeq \psi_0/t, \quad \tau_1 < t < \tau_2 \quad [14]$$

Another possible assumption is to regard ψ as only a slowly varying function of its argument; i.e., to regard the relaxation spectrum as changing only slightly over a single cycle of 10 of τ . Under this assumption it is then possible to replace $\psi(\tau)$ in the integrand of Eq. 13a by its value at the maximum of the remaining portion of the integrand. This assumption leads to the following relation between the remembrance function and relaxation spectrum

$$\Phi(t) = \psi(t)/t \qquad [14a]$$

Upon using Eqs. 3a and 3b, it is seen that this assumption therefore leads to the following method of evaluating the relaxation spectrum directly from experiment:

$$\psi(t) = d\{e(t)/e_i\}/d \ln t$$
, simple loading experiment [15a] $\psi(t) = -d\{e(t)/e_i\}/d \ln t$, simple unloading experiment [15b]

In the case where ψ is only a slowly varying function of its argument, the relaxation spectrum is intimately related to the internal friction. In order to obtain this relation, Eq. 12, which is valid for a single relaxation time, is converted into an equation valid for a continuous relaxation spectrum by replacing Δ_0 by the operator

$$\int_{-\infty}^{\infty} d \ln \tau \cdot \psi(\tau)$$

Upon replacing ψ by its value at the maximum of the remaining portion of the integrand,

$$Q^{-1}(w) = (\pi/2)\psi(1/w)$$
 [(16a]

This equation, which was derived by Boltzmann in essentially this form, was verified by him for glass and later by Bennewitz^{12,13} for several metals.

In the case where ψ is only a slowly varying function of its argument, the relaxation spectrum is also intimately related to the modulus defect. In order to obtain this relation, we differentiate Eq.

11 with respect to w, and operate upon the resulting equation in the same manner used for Eq. 12. The following equation tic after-effects and related phenomena may be caused by the nonelastic response of isolated regions in the specimen, these

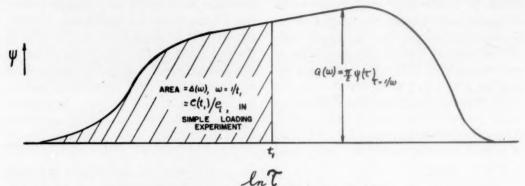


FIG. 3.—INTERPRETATION OF RELAXATION SPECTRUM.

is obtained:

$$d\Delta(w)/d \ln w = -\psi(\tau)$$
at $\tau = 1/w$ [16b]

An interpretation of Eq. 15a and 16b is presented in Fig. 3.

According to the above analysis, when & is a slowly varying function of its argument, it may be determined either through elastic after-effect experiments, by use of Eqs. 15a or 15b, or through internal friction measurements, by use of Eq. 16a. The first type of measurement is especially suitable for finding the relaxation spectrum at large values of relaxation times; e.g., greater than I sec. The second type of measurement is especially suitable for finding the relaxation spectrum at small values of relaxation times; e.g., smaller than I sec. The two methods combined can conveniently cover the range of relaxation times from 10-5 to 105 sec. In the intermediate range of relaxation times, in the neighborhood of 1 sec., the two methods overlap.

PHYSICAL ORIGINS OF ANELASTICITY

RELAXATION CENTERS

The idea appears to have first been advanced by Maxwell¹⁴ and later by several other investigators^{15,16,17} that elas-

regions being surrounded by a matrix that behaves in a perfectly elastic manner. The influence of such isolated regions may best be described with the aid of Fig. 4, where the boxed region is supposed to behave in a viscous manner. The instant a load is applied to the specimen, the deformation is essentially elastic, and constant throughout the specimen, as shown in Fig. 4b. As the stress within the localized region gradually relaxes, it suffers further deformation, thereby increasing the stress in the surrounding elastic region. The load originally carried by the localized region becomes transferred, so to speak, to the surrounding matrix. The situation after complete relaxation of stress is somewhat as depicted in Fig. 4c. When the load is removed, the localized region, as well as the surrounding elastic matrix, is left in a state of residual stress, as depicted in Fig. 4d. The original configuration is obtained only after the residual stresses in the localized region have become completely relaxed. Prandtl¹⁸ has shown that irregularities in the lattice structure may give rise to localized regions in which shear stress is gradually relaxed as here depicted.

The localized regions of Maxwell would lead to the linear relationship between macroscopic stress and strain postulated by Boltzmann, provided the microscopic relations between stress and strain were everywhere linear. Thus in the localized region the relation between shear stress S

regions. Since Becker's article, electrical methods of measuring internal friction have been developed^{20,21,22} which require only extremely low amplitudes of vibration.

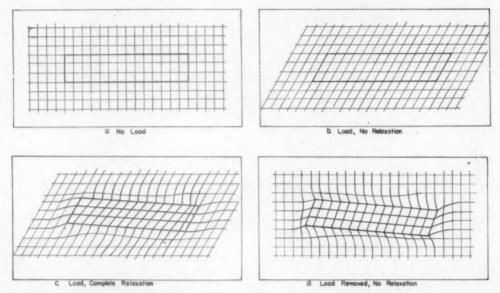


Fig. 4.—Illustration of stress concentration in elastic matrix introduced by stress relaxation in localized regions (c), and of residual stresses that remain after external load is removed (d).

and shear strain a could be of the form

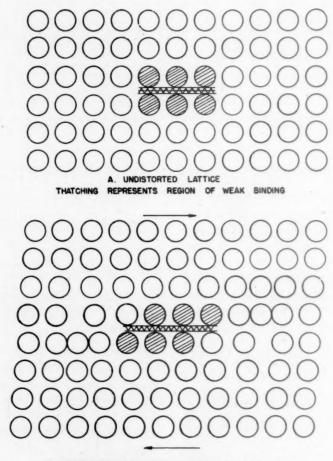
$$d(S - Ge)/dt = -S/\tau$$
 [17]

In this equation τ would be the relaxation time for the shear stress within the localized region.

An equation of the type 17 has been objected to by Becker19 on the ground that the observed rate of plastic deformation of metals increases with stress much faster than the first power. In corroboration of this viewpoint Becker points out that the internal friction of metals increases with increasing amplitude of vibration, in contradiction to the prediction of Boltzmann's theory. In answer to Becker's objections, it need only be pointed out that Boltzmann's analysis is applicable only to that low stress level in which powers of stress greater than the first can be neglected in the relationship between stress and strain for the localized All investigators using such methods have found that the internal friction does become independent of amplitude of vibration below a certain low stress level.

Slip Bands

Toward the end of the last century, it was observed that plastic deformation was confined to localized regions, called slip bands, and that plastic deformation introduced23,24,26 anelastic effects, effects, however, that rapidly disappeared upon low-temperature annealing (100°C). Upon combining these two observations, Rosenhain²⁶ concluded that freshly formed slip bands behaved in a viscous manner, and that the amorphous structure was gradually reabsorbed into the surrounding crystalline matrix upon a low-temperature anneal. Contrary to Beilby's viewpoint.27 Rosenhain regarded the material in freshly formed slip bands as essentially weaker than that in the surrounding crystalline matrix. The concept of amorphous slip bands is compatible with the atomistic concept of dislocations originally introregion is represented by thatching, the shaded atoms being foreign atoms with little binding with each other and with the other atoms. When a shearing stress is



B. DISTORTED LATTICE IN WHICH PAIR OF DIS-LOCATIONS HAVE BEEN FORMED. THE THATCHED REGION HAS INCREASED IN EXTENT

FIG. 5.—ILLUSTRATION OF INITIATION OF SLIP BAND.

duced by Orowan²⁸ and later extensively developed by Taylor,²⁹ and recently reviewed by Seitz and Read.³⁰

According to the concept of dislocations, the low resistance to plastic deformation of actual metals, as compared with that of ideal metals, is due to the presence of certain weak areas, which generate dislocations. This concept may best be explained by reference to Fig. 5. In illustration A of this figure, the weak

now applied, the weak region may be considered as offering no resistance to a shearing stress, thereby resulting in a stress concentration at its extremities. This stress concentration results in the rearrangement of atoms as depicted in Fig. 5B, which may be regarded as consisting of a pair of dislocations of opposite sign. If the shearing stress is sufficiently great, these dislocations will move away from the weak region in opposite directions.

If the weak region were unaltered by the formation and departure of a pair of dislocations, an indefinite number of pairs could be formed in a similar manner. Institut für Metallforschung, by Köster^{31,32,33} and his school, and later^{34–38,121} by several investigators in this country. Two observations are of special signifi-

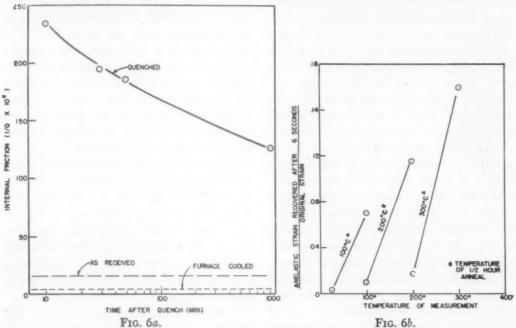


Fig. 6a.—Effect of heat-treatment on internal friction of a hardenable steel (after Ward).

Frequency of measurement \simeq 800 cycles per second.

FIG. 6b.—Effect of temperature of anneal and of measurement on elastic after-effects in quenched steel. (After Ward.)

However, it is very likely, as depicted in Fig. 5B, that the weak region is extended by the formation of a pair of dislocations, the formation and departure of one pair thereby lowering the stress necessary for the formation of successive pairs. The formation of dislocations therefore becomes a cataclysmic phenomenon. The resulting rapid slipping of one set of atomic planes over another will cause a general misalignment of atoms over the slip plane, thereby endowing the slip plane with an amorphous character.

The early studies of the anelastic effects introduced by plastic deformation, previously referred to, were made with comparatively large stress amplitudes. These anelastic effects were first studied at low stress amplitudes at the Kaiser Wilhelm

cance to the present discussion: (1) the room-temperature internal friction introduced by plastic deformation is partially removed by self-tempering at room temperature, and is completely removed by tempering at temperatures as low as 200° to 300°C.; (2) the internal friction introduced by plastic deformation is nearly constant over a wide frequency band, 38 thereby indicating that the relaxation spectrum associated with the localized amorphous regions is nearly constant over a wide range of relaxation times.

Prior studies upon the effect of plastic deformation on anelastic properties have been limited to cases where the deformation was introduced by mechanical means; e.g., by stretching or by rolling. B. C. Ward, of the Watertown Arsenal labora-

tory, has investigated the effect upon the anelasticity of steel of the plastic deformation attending the formation of martensite. His results are reproduced in Fig. 6a and 6b. The first figure illustrates the profound effect of heat-treatment upon anelasticity, the internal friction (Q^{-1}) of the freshly quenched specimen being 235×10^{-5} , that of the furnace-cooled specimen only 0.4 X 10-6. These results are in striking disagreement with the recent work of Frommer and Murray, 39 who reported that differences in heat-treatment of steel introduced at most differences of 50 per cent in the internal friction. Their specimens were not, however, hardenable, being low-alloy 0.40 per cent carbon steel in 3-in. rounds. This figure also illustrates the gradual decrease in the internal friction upon resting at room temperature, a decrease that has been frequently reported in the case of metals deformed by external forces. In Fig. 6b is shown the effect of annealing temperature, and of the temperature of measurement, upon the elastic after-effect of quenched steels. Upon comparing this figure with the work of West,124 it is seen that the anelasticity introduced by quenching responds to annealing and to the test temperature in precisely the same manner as that introduced by plastic deformation due to external forces.

Grain Boundaries

Since about 1912 the subject of amorphous grain boundaries has been a topic of almost continual controversy. On the one hand, the evidence, as reviewed by Rosenhain^{40,41} and by Jeffries and Archer,⁴² is very convincing that the grain boundaries behave as if they were amorphous. On the other hand, scientists have been reluctant to accept the concept of an amorphous phase. No controversy need arise once it is realized that it is not necessary for any portion of the metal to be

amorphous in order that the grain boundaries may behave in a viscous manner. It is necessary to assume only that the resistance to slipping of one grain over an adjacent grain obeys the laws commonly associated with amorphous materials rather than the laws associated with crystalline materials. The surface atoms of one grain cannot fit into the lattice positions of an adjacent grain, the binding across the interface of two grains may therefore reasonably be expected to have the characteristics associated with amorphous materials. Since shearing stresses gradually relax across any viscous boundary, and since relative movement is hindered at the edges and corners of the grains, viscous grain boundaries will behave as isolated relaxation centers. It is therefore pertinent to review here the various types of experimental evidence that point to the viscous behavior of such boundaries.

The primary difference between the behavior of amorphous and of crystalline materials lies in the rapid increase in the resistance to deformation of the former with respect to an increase in velocity of deformation and with respect to a decrease in temperature, compared with the relative insensitivity of the resistance to deformation of crystalline substances with respect to these variables. It is therefore to be expected that as the temperature is raised sufficiently, or as the rate of deformation is lowered sufficiently, the resistance to slipping across the grain boundaries will be so lowered with respect to the resistance to plastic deformation within the grains that effects will be observed that are attributable only to a slipping at the boundaries. Such effects were first observed by Rosenhain and Humfrey. 43 When specimens of copper are first polished and then slightly extended at an elevated temperature, they found that the grain boundaries become delineated by a relative displacement normal to the surface of

adjacent grains. Such delineation does not occur during extension at room temperature. Hanson and Wheeler107 made a thorough study of grain-boundary movement in aluminum. Here considerable movement is observed at the boundaries when specimens are extended slowly at temperatures of 250°C. and above, but not when the specimens are extended rapidly an equivalent amount. Andrade and Chalmers44 found that a slight extension of cadmium at room temperature results in a decrease in electrical resistivity, while a like extension at liquid-air temperature raises the resistivity. It looks as though at room temperature the grains rotate in such a manner as to bring the axis of low resistivity closer to the axis of tension, without appreciable plastic deformation within the grains. Such a rotation could occur only by a slipping along the grain boundaries. As a final example of the viscous behavior of grain boundaries, the experiments of Moore, Betty and Dollins⁴⁵ may be mentioned. They found that when specimens of lead are first polished, scratched with parallel straight lines, and then pulled several per cent at room temperature, the scratches remain straight and parallel within each grain, but assume different orientations in adjacent grains when the extension is slow. and maintain the same orientation when the extension is rapid.

Anelastic effects have been observed that can be interpreted only in terms of relaxation of shear stress across the grain boundaries. The room-temperature stress-strain curve of certain low-melting-point metals (for instance, tin and zinc) have no linear portion. Dalby¹²⁰ has shown that the initial curvature is associated with a marked delayed recovery following the instantaneous recovery upon release of load. The presence of such delayed recovery suggests that in these metals the initial curvature of the stress-strain curve was

due to a recoverable creep, which probably arises from stress relaxation across grain boundaries. In certain cases the initial portion of creep is completely recoverable. Such recovery, called by various authors creep recovery, delayed elasticity, or sub-permanent elasticity, is a special example of elastic after-effects. Johnson⁴⁶ quotes a case in 0.17 per cent carbon steel where the creep induced at 475°C. by a stress of 4 tons per sq. in. for 12 min. was completely recovered. According to Chalmers,47 the primary room-temperature creep is completely recoverable in tin specimens of small grain size but not in single crystals. In these cases it appears that primary creep was associated with stress relaxation at the grain boundaries. Jeffries and Archer⁴² quote the case of a very fine-grained ternary eutectic, which manifests elastic after-effects to a marked degree, an effect they attribute to the very large amount of grain-boundary area and to stress relaxation across such boundaries. Such stress relaxation may be the origin of the anomalous behavior of the Cu-Al and Cu-Sn eutectoids found by Guillet and Portevin.48 When these alloys are quenched their measured elastic moduli are only about 60 per cent of those when slowly cooled. Anelasticity as manifested by internal friction varies with temperature and with grain size in a manner that can be interpreted only in terms of viscous grain boundaries. 49,50

The quasi-static modulus defect Δ_0 associated with grain-boundary relaxation—i.e., the area beneath the relaxation spectrum associated with grain-boundary relaxation—cannot be evaluated exactly, but a fair estimate may be made. A computation has been made for the case of equiaxed grains of uniform size. The ratio of the completely relaxed Young's modulus to the unrelaxed modulus is here a slowly varying function of Poisson's ratio σ , increasing from 0.5 to 0.75

as σ covers its physically allowable range from 0 to 0.5. Corresponding to this range of Poisson's ratio, Δ_0 will lie within the range from 1.0 to 0.33, having a value of 0.55 for a Poisson's ratio of $\frac{1}{3}$ common to many metals. Any deviation from

RELAXATION BY DIFFUSION

Diffusion between Specimen and Surrounding Medium

A complete description of a specimen undergoing strain cannot be given without

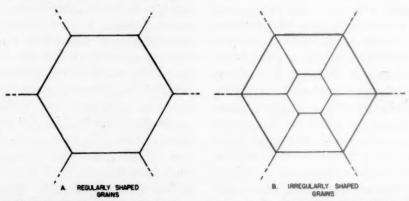


Fig. 7.—Illustration of effect of grain shape upon amount of stress relaxation. In example B stress relaxes across all the boundaries of case A, and in addition across new boundaries.

regularity of structure or from uniformity in grain size will increase the total amount of stress that may be relaxed; i.e., will increase Δ_0 , as may be seen in Fig. 7. Illustration A of this figure corresponds to a structure with regular grains of uniform grain size, while B corresponds to irregular grains. In the latter case, shearing stress is relaxed across the same boundaries as in the former, and also across new boundaries.

The above-mentioned value of 0.55 for Δ_0 should therefore be regarded only as the lower limiting value of Δ_0 , as the structure tends toward uniformity in grain size and regularity in grain shape.

No theoretical or experimental work has been given upon the shape of the relaxation spectrum associated with grain boundary relaxation. The position of the spectrum for a given material will depend upon both temperature and grain size, the relaxation time at the peak of the spectrum being proportional to the mean grain diameter.

reference to the surrounding medium. Thus a specimen that is undergoing elastic extension suffers a drop in temperature, and therefore absorbs heat from the surrounding medium. Elastic extension likewise produces a change in the partial pressure of the individual constituents, so that if equilibrium with the surrounding medium is maintained, an exchange of particles between the specimen and the medium will take place. If the surrounding medium has a magnetic field parallel to the specimen, an elastic extension of a ferromagnetic specimen will change the magnetic flux density therein, which flux diffuses into, or from, the surrounding medium. The response of a specimen to an applied load therefore depends, to some extent, upon the degree to which the specimen remains in equilibrium with its surroundings. The precise manner in which this response is affected may be most readily obtained by regarding the establishment of equilibrium as a relaxation, and then applying the concepts discussed

in the first part of this report. Here relaxation may be regarded as caused by diffusion currents. Thus thermal relaxation is caused by the flow of heat to or from the surrounding medium; magnetic relaxation is caused by the flow of magnetic flux; concentration relaxation is caused by the flow of particles.

A relaxation spectrum will be associated with each external parameter; i.e., with temperature, magnetic field strength and each partial pressure. The thermal relaxation spectrum lies within relaxation times comparable to the time usually taken in making a measurement of the elastic modulus by quasi-static methods. In making precise measurements of the modulus by quasi-static methods particular care is therefore taken 52,53 to attain complete thermal relaxation. Under such conditions the isothermal modulus is measured. On the other hand, the period of vibration used in making dynamic measurements of the modulus is very small compared with the position of the relaxation spectrum. The modulus so measured is therefore adiabatic. Thermal relaxation must also be taken into account in precise measurements on the initial part of creep curves. 126 The magnetic relaxation spectrum lies in a range of comparatively short times. The vibrations of iron in a magnetic field may therefore be attended by a considerable dissipation of energy54 associated with partial but incomplete magnetic relaxation. The concentration relaxation spectrum lies, under the usual experimental conditions, in such a high range of relaxation times that strain may be considered as taking place under conditions of constant composition.

The most important features of a relaxation spectrum are its position and its total strength; i.e., the quasi-static modulus defect Δ_0 . The relaxation spectrum is in the neighborhood of W^2/D , where W is the transverse dimension, D the appropriate diffusion coefficient. In the particular case of a specimen with circular cross section of radius r, the maximum of the relaxation spectrum occurs at 55

$$\tau = 2r^2/D$$

The total strength of the spectrum, Δ₀, is independent of the shape or dimensions of the cross section, and depends only on the material itself. It has previously been computed for the three cases of thermal, concentration⁵⁶ and magnetic relaxation⁵⁷ for specimens under uniaxial stresses. A method of computation applicable to all three cases is outlined in appendix A.

In the case of thermal relaxation,

$$\Delta_0 = T E_s \alpha^2 / \rho C_p \qquad [18]$$

Here T is the absolute temperature, E_{\bullet} is the adiabatic Young's modulus, α is the linear thermal expansion coefficient, ρ is the density, and C_{ρ} the specific heat at constant pressure. Table 1 gives the values of the thermal diffusion coefficient D and thermal relaxation strength Δ_0 for the common metals.

TABLE 1.—Thermal Relaxation Constants

Metal	D, Sq. Cm per Sec.	Δθ			
Cadmium	0.46	0.010			
Zinc	0.41	0.0088			
Magnesium	 0.60	0.0050			
Aluminum	0.88	0.0046			
Beryllium	0.53	0.0046			
Tin	 0.40	0.0040			
Brass (70-30)	0.38	0.0036			
Silver	1.74	0.0034			
Copper	1.2	0.0030			
Nickel	0.15	0.0029			
Lead	 0.24	0.0025			
Iron	0.20	0.0024			
Palladium	0.26	0.0020			
Antimony	0.12	0.0018			
Gold	 I.I	0.0017			
Platinum	 0.26	0.0015			
Bismuth	 0.065	0.0014			
Tungsten	0.61	0.00078			
Rhodium	0.29	0.00069			
Tantalum	 0.22	0.00030			

In the case of magnetic relaxation,

$$\Delta_0 = 4\pi E_B \mu_r \lambda^2 \qquad [10]$$

Here E_B is Young's modulus measured at constant magnetic flux density, μ_r is the

reversible permeability, λ is the magnetostriction coefficient defined by

$$\lambda = de/dB \qquad [20]$$

The magnetic relaxation strength of a ferromagnetic material depends greatly

equivalent to 30,000,000 lb. per sq. in.

$$\Delta_0 = 54c(c-1)$$

For a 0.20 weight per cent carbon austenite this ratio is 2.5. The relaxed modulus is

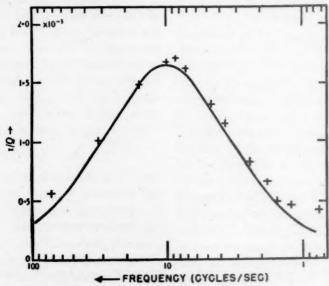


FIG. 8.—Example of internal friction due to transverse thermal currents. (After Bennewitz and Rotger. 64)

Curve, theory; crosses, experiment.

upon its magnetic hardness. The factors that influence it, as well as a summary of experimental work, have been discussed in detail by Becker and Doring.⁵⁸ Values as large as 0.4 have been observed in nickel specimens.

In the case of concentration relaxation,

$$\Delta_0 = (E_{\infty}W/\rho RT)(\delta e/\delta c)^2 c(1-c) \quad [21]$$

Here c is the atomic concentration of the solute, ρ and W are the density and the atomic weight of the solvent, respectively, and E_{∞} refers to the unrelaxed elastic modulus. As an illustration of the large values Δ_0 may attain, the example of carbon in austenite will be cited. From the known variation of the austenite lattice parameter with carbon concentration, be the value 0.30 is obtained for $\delta e/\delta c$. Substituting this value into Eq. 21, and taking E_{∞} as 800,000 cal. per cu. in., which is

therefore in this case only one third as large as the unrelaxed modulus.

Intra-specimen Diffusion

Thermal Diffusion.—The various types of diffusion, thermal, magnetic and concentration, need not necessarily take place between the specimen and the surrounding medium. The diffusion may be confined entirely within the specimen. The type of intra-specimen diffusion that has been most thoroughly investigated originates from thermoelastic coupling. The application of any stress system that is not homogeneous throughout the specimen will result in an inhomogeneous change in temperature, and therefore in thermal currents.

The stress inhomogeneity may be on either a macroscopic or a microscopic scale. The simplest case of a macroscopic stress inhomogeneity occurs in bending. Here the material on one side of the neutral plane is subjected to tension, the material on the other half is subjected to compression. If the specimen has either a circular or rectangular cross section, the thermal and concentration relaxation spectrum consists essentially of a single line at 60,61

$$\tau = \begin{cases} (\text{diameter})^2/(4.32\pi D) \\ (\text{trans. width})^2/(\pi^2 D) \end{cases}$$

respectively. The strength of the relaxation spectrum is the same as for diffusion from specimen to surrounding medium.

The experimental work 62,63,64 on thermal relaxation in bending has confirmed the theoretical predictions in every respect. An example of the agreement between theory and experiment is shown in Fig. 8. In this figure the theoretical curve contains no adjustable parameters.

Microscopic stress inhomogeneities arise from the elastic anisotropy and at least partial random orientation of the individual crystallites. As a stress is applied which is homogeneous on a macroscopic scale, the variation in stress from crystallite to crystallite will result in a like variation in temperature, magnetic field strength, and partial pressures of the individual constituents. The resulting thermal, magnetic flux or particle diffusion between adjacent grains endows a polycrystalline specimen with anelastic properties. The relaxation spectrum will be located at

$$\tau \sim d^2/D$$
 [22]

where d is the mean grain size. The relaxation strength for this intergrain diffusion, $\Delta_{\text{int-grain}}$, will be approximately equal to the relaxation strengths Δ_0 given by Eqs. 18 to 21 multiplied by a factor R equal to the mean square fluctuation of the elastic modulus. Thus

$$\Delta_{\text{int.grain}} = R\Delta_0$$
 [23]

Values of R, defined by the formula

$$R = \frac{(E^{-2})_{\text{ave.}} - (E^{-1})_{\text{ave.}}^2}{(E^{-2})_{\text{ave.}}}$$

have been computed for typical metals, and are given in Table 2.

A thorough experimental investigation has been made of the thermal anelasticity arising from the fluctuation of stress from crystallite to crystallite. This anelasticity may be thought of as arising from the intercrystalline thermal currents that accompany a change of macroscopic stress. The results 65 on 70-30 alpha brass are presented as Fig. o. Since dimensional considerations show that the internal friction can be a function of the frequency of measurement f, of the mean grain diameter d, and of the diffusion coefficient D only through the parameter fd^2/D , the observations are plotted in this figure as a function of this parameter. Through a variation of

TABLE 2.—Mean Square Fluctuation of Elastic Modulus

				N										R
Brass	(70)-	3	0)	 		*						0.094
Coppe	er													0.071
Gold.			*				*		*	0		*		0.067
														0.063
Iron (α).				×			*						0.040
														0.0060
Tungs	ster	1.	*		*	0	*		*				0	0.00004

both frequency and grain size, an effective variation of frequency over six cycles of 10 was thereby obtained. Not only is the position of the relaxation spectrum in agreement with Eq. 22, but also analysis of Fig. 9 shows that the relaxation strength is, within experimental error, given by Eq. 23 with the quantities Δ_0 and R taken from Tables 1 and 2, respectively.

Fig. 9 shows that the internal friction and therefore the relaxation spectrum, associated with intercrystalline diffusion is an asymmetrical function of the logarithm of τ (or of f). This asymmetry is in marked contrast to the symmetry of the relaxation spectrum associated with macroscopic diffusion in bending, and may be interpreted as follows. Under nearly adiabatic condi-

tions—e.g., high frequencies or large grain size—diffusion is limited to the immediate vicinity of the grain boundaries. The internal friction is therefore proportional

mean square fluctuation in the elastic modulus, and therefore the relaxation spectrum associated with intercrystalline diffusion, differs greatly between different

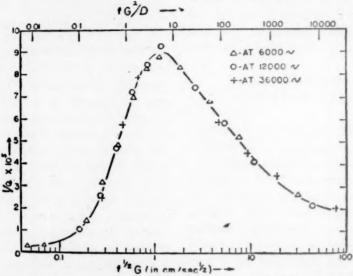


Fig. 9.—Example of internal friction due to intercrystalline thermal currents. (After Randall, Rose and Zener. 65)

to the grain-boundary area, which in turn is inversely proportional to the grain size as measured, for example, by the mean grain diameter. From dimensional considerations, therefore, it may be deduced that

$$\begin{cases} Q^{-1} \sim (D/fd^2)^{\frac{1}{2}} \\ \text{Intercrystalline diffusion currents} \end{cases} [24]$$

in contrast to

$$\begin{cases} Q^{-1} \sim (D/fd^2) \\ \text{Transverse diffusion currents for a single relaxation spectrum} \end{cases}$$

Eq. 24 has been verified by experiment. 66 It may be deduced, from general theoretical arguments, that the constant of proportionality in Eq. 24 is nearly $R\Delta_0$. Thus under nearly adiabatic conditions

$$Q^{-1} = \alpha R \Delta_0 (D/f d^2)^{\frac{1}{2}}$$
 [25]

where α is a numerical constant of the order of magnitude of unity.

From Table 2 it may be seen that the

metals; in particular, that the relaxation strength of aluminum is an order of magnitude less than for 70-30 alpha brass. Experiments ⁶⁷ have in fact verified that the relaxation strength for intercrystalline diffusion in aluminum is less than one tenth that in 70-30 alpha brass.

Concentration Diffusion.—The relaxation spectrum for concentration diffusion differs from that for thermal diffusion in two important respects. Firstly, the position of the relaxation spectrum associated with concentration diffusion is shifted with respect to that associated with the thermal diffusion many orders of magnitude toward longer times. Thus the diffusion coefficient of carbon in gamma iron near the eutectoid temperature is 10-7 times smaller than the thermal diffusion coefficient. A thermal relaxation that requires one second would therefore require one year for a corresponding relaxation of carbon concentration at this temperature. Secondly, the relaxation strength associated with concentration relaxation is several orders of magnitude higher than that associated with thermal relaxation. When therefore the period of observation extends over the appropriate range, the effects due to concentration relaxation would be more marked than those arising from thermal relaxation. The data necessary for the computation of the relaxation strengths and times in ferrous alloys are given in Table 3.

TABLE 3.—Data for Concentration Relaxation

			Diffusion Coefficient				
Solvent	Solute	õe/õc	Q, Cal. per Mol	A. Sq. Cm. per Sec.			
α Pe	Cr Ni W Mo Mn C	0.021 ⁶⁸ 0.022 ⁶⁰ 0.11 ⁷⁰ 0.0088 ⁷¹ 0.11 ⁷²					
γ Fe	C Mn N	0.30 ⁵⁰ 0.028 ⁷¹ 0.54 ⁷³	36,000 ⁷⁵ 34,000 ⁷⁶				
Cu (30 per cent Zn)	Zn	0.07174	41,70076	0.0020			

Since concentration and thermal diffusion both obey the same types of differential equations and the same boundary conditions, the internal friction due to intercrystalline diffusion currents will be the same function of the dimensionless parameter (fd^2/D) in the two cases, aside from a constant factor. The relaxation strength Δ_0 associated with concentration diffusion may be computed for 70-30 alpha brass from Eq. 20 as 0.50. Comparison of this value with the value 0.0036 for thermal diffusion from Table 1 shows that the internal friction associated with concentration diffusion is 140 times that due to thermal diffusion at the same values of fd2/D in alpha brass. However, the anelastic effects associated with the concentration relaxation between adjacent crystallites in 70-30 alpha brass cannot be conveniently observed because of the very large values of the relaxation time. Since the relaxation time is proportional to D/d^2 , it might be thought that it could be brought into a convenient range by working at high temperatures and with small grain sizes. However, the grain size increases so rapidly with increasing temperature that the relaxation time cannot be made smaller than 10^6 sec. at any temperature level.

Because of the very small values of the concentration diffusion coefficient, the anelastic effects due to concentration diffusion are the more readily observable the shorter the distances over which the diffusion must occur. The short-wavelength periodic concentration fluctuations, predicted by Hume-Rothery⁷⁷ and first observed by Daniel and Lipson,⁷⁸ are therefore of particular importance, and so will be discussed in some detail.

Hume-Rothery79 discovered that the lattice type of alloys is determined primarily by the number of valence electrons per atom. Jones 80,81 pointed out the significance of the number of free electrons per atom in terms of the modern theory of metals, and showed that the observations of Hume-Rothery are in accordance with this theory. Fundamental to Iones's theory is the function N(E), where N(E) dE is the number of electronic states per mol whose energies lie within the range dE at E. This function has irregularities of the type shown in Fig. 10a. The concentration of zinc in alpha brass that is just sufficient to fill all the electronic levels completely up to the peak of the N(E) curve is about 40 per cent. Hume-Rothery has argued77 that these irregularities in the N(E) curve may give rise to a slightly irregular curve for free energy vs. concentration, as in Fig. 10b. Phases with a concentration such that the free energy lies above a chord tangent at two points are unstable, and tend to separate into two phases having concentrations at the points of tangency; e.g., the concentrations C_1 and C_2 in Fig. 10. These two phases will have the same lattice type, and will differ only in concentration and, to some extent, in lattice parameter.

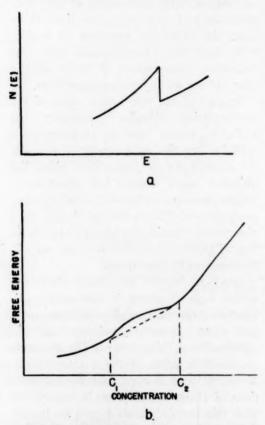


FIG. 10.—EXAMPLE OF HOW A SOLID SOLU-TION OF TWO ELEMENTS OF DIFFERENT VAL-ENCES MAY SEPARATE INTO TWO PHASES. (After Hume-Rothery.⁷⁷)

An essential separation into two phases, therefore, may occur without a disturbance of the lattice positions simply through a periodic fluctuation in concentration. This manner of separation into two phases avoids the formation of an interface and therefore the difficulties inherent in nucleation.

The detection through X-rays of a periodic fluctuation in concentration is more difficult than the detection of the presence of two distinct phases. It is possible that such fluctuations are of common occurrence but have remained

undetected. One example has been examined in detail by Daniel and Lipson. 78 Several years ago the author 82 found in a single crystal of alpha brass a characteristic type of anelasticity (Fig. 11), for which he could advance no explanation. This anelasticity could be represented by a single-line relaxation spectrum of strength 0.025, an order of magnitude higher than could be given by thermal diffusion. The relaxation time of this line had a heat of activation of 34,000 cal. per mol, thus

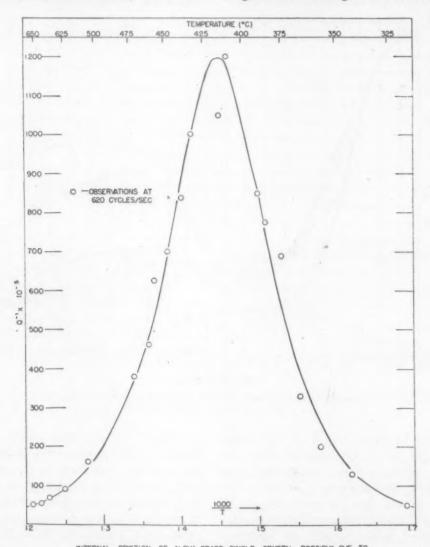
$\tau \sim e^{+34,000/RT}$

This value was sufficiently close to the heat of activation of the diffusion constant of zinc in copper (38,000 cal. per mol) to lead to the conclusion that the anelastic effects were due to the relaxation of zinc concentration, a relaxation that could occur only if the concentration had periodic fluctuations.

Magnetic Flux Diffusion.—As previously mentioned, the magnetoelastic coupling in ferromagnetic materials gives rise to anelasticity. At large stress amplitudes this coupling gives rise to an essentially plastic behavior in that a specimen retains a permanent set after the stress is removed.83 This essential plasticity is associated with the hysteresis loop in the B-H curve. As Lord Raleigh84 first pointed out, when the fluctuations in H approach zero, the hysteresis effects approach zero faster than the fluctuations in H. The essential plasticity caused by the magnetoelastic coupling, therefore, vanishes at sufficiently small stress amplitudes, leaving anelasticity as the only nonelastic effect.

One origin of the anelasticity arising from the magnetoelastic coupling lies in the diffusion of magnetic flux density, a diffusion that necessarily is accompanied by electrical eddy currents. Such diffusion occurs even in completely unmagnetized specimens, since such specimens remain magnetized in small domains. An externally

applied stress changes the boundaries of these domains, a change that involves diffusion of magnetic flux. Changes in the magnetic domain boundaries, and thererelaxation strength Δ_0 associated with the relaxation of the magnetic domain boundaries. The change in elastic modulus with magnetic field strength was observed first



INTERNAL FRICTION OF ALPHA-BRASS SINGLE CRYSTAL, POSSIBLY DUE TO FIG. 11.—INTERNAL FRICTION OF ALPHA-BRASS SINGLE CRYSTAL, POSSIBLY DUE TO CONCENTRATION RELAXATION. (After Zener. 32)

fore the anelasticity associated therewith, may be eliminated by applying a strong magnetic field. Such a magnetic field gives the domains a preferred orientation, and therefore effectively removes the domain boundaries. By comparing the quasistatic elastic modulus with and without a strong magnetic field, one obtains the

in 1901,85 and is known as the $\Delta E/E$ effect. The factors that control the magnitude of the $\Delta E/E$ effect have been thoroughly reviewed by Becker and Doring.86

Lattice Position

In many cases the solute atoms are not distributed at random, but, as pointed out by Tammann,⁸⁷ have a preferred distribution on certain sites. Such preferred distributions give rise to superlattices, first observed by Bain⁸⁸ and recently

by some average of these two atomic concentrations.

A strongly temperature-dependent type of anelasticity in steel was first observed

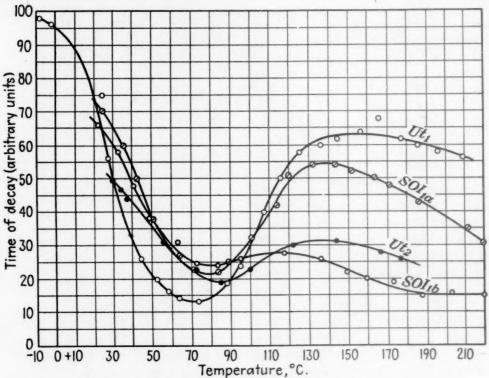


FIG. 12.—Damping characteristics of steel tuning forks. (After Woodruff. 91) $Ut_1, f = 128c/s$; $SOI_1, f = 192v/s$, $Ut_2, f = 256c/s$.

reviewed by Barrett.89 If all the solute atoms are not at the preferred sites-i.e., if the order is only partial—and if a change in this number is accompanied by lattice strains, then conversely an applied stress will change the equilibrium number of ordered solute atoms. As has been observed by Gorksy,90 the resulting diffusion of the solute atoms into or out of the preferred sites will give rise to the same type of relaxation as caused by the diffusion phenomena previously discussed. The strength of the relaxation spectrum will be given by a formula similar to Eq. 20, with $(\delta e/\delta c)$ replaced by $(\delta e/\delta c_1 - \delta e/\delta c_2)$, where c1 and c2 are the atomic concentrations on the preferred and nonpreferred sites, respectively, and with c replaced

by Woodruff⁹¹ in 1899. The internal friction of Woodruff's steel tuning forks had a sharp maximum in the neighborhood of 75°C., as illustrated in Fig. 12. The strongly temperature-dependent type of anelasticity was rediscovered several years later (1910) by Robin, 92-94 who gave the label "aphonia" to the phenomena. Robin performed many interesting types of experiments upon aphonia. He found that it disappeared with a slight amount of deformation, but returned slowly upon aging at room temperature, more rapidly upon annealing at slightly elevated temperatures. Typical examples of his results are shown in Fig. 13.

The strongly temperature-dependent type of anelasticity was again rediscovered by Richter^{95,96} in 1938. Richter worked with annealed carbonyl iron, and studied the anelasticity from the approach of elastic after-effects rather than internal

of the relaxation spectrum occurring at $\tau = 3 \times 10^{-15} e^{9800/T} \qquad [26]$

The second effect is a change in the

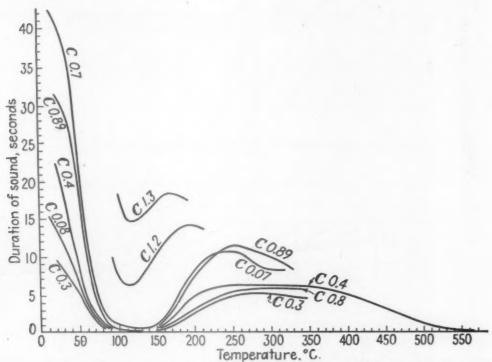


Fig. 13.—Duration of sound in annealed carbon steels. (After Robin. 94)

Frequency is 1800c/s.

friction. From a single elastic after-effect curve, he was able to obtain the complete relaxation spectrum. By observing the elastic after-effect at various temperatures, he was able to find how the relaxation spectrum varies with temperature. His data are reproduced as Fig. 14. The relaxation spectrum at -10°C. has been computed by applying Eq. 15b to these data, and is reproduced as Fig. 15. Also in this same figure is given the relaxation spectrum that Richter chose best to fit his data. From an analysis of his data at different temperatures Richter concluded that the temperature dependence of the relaxation spectrum could be represented as the superposition of two effects. The first effect is a horizontal shift of the spectrum, the peak magnitude of the relaxation spectrum, an increase of temperature being associated with a decrease in the magnitude of about 0.3 per cent per degree C. From Richter's formula for the relaxation time at the peak of the relaxation spectrum, may be obtained the relation between the frequency of vibration and the temperature at which the internal friction is a maximum. This relation is plotted in Fig. 16. Robin's data reproduced in Fig. 13 are seen to be consistent with this relation.

A key to an understanding of the strongly temperature-dependent type of anelasticity was given by Snoek⁹⁷ a year later. He found that by further purifying carbonyl iron through a high-temperature wet hydrogen treatment, all traces of

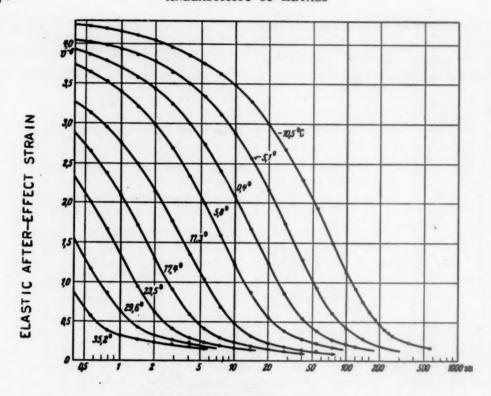


FIG. 14.—ELASTIC AFTER-EFFECT IN CARBONYÉ IRON WIRE. (After Richter. 96)
Initial strain: 5 × 10⁻⁴.

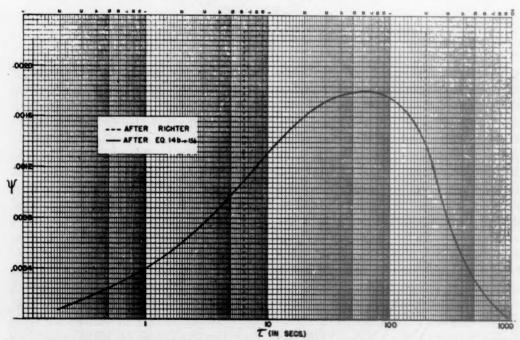


Fig. 15.—Relaxation spectrum of strongly temperature-dependent type of anelasticity in Carbonyl iron. (After experiments of Richter at -10° C. $\Delta_0 = 0.0083$.)

the strongly temperature-dependent type of anelasticity were removed. This anelasticity returned, however, to nearly its full strength through the reintroducThe strongly temperature-dependent type of anelasticity is closely related to the magnetic after-effects first reported by Ewing⁹⁸ in 1885. A thorough review of the

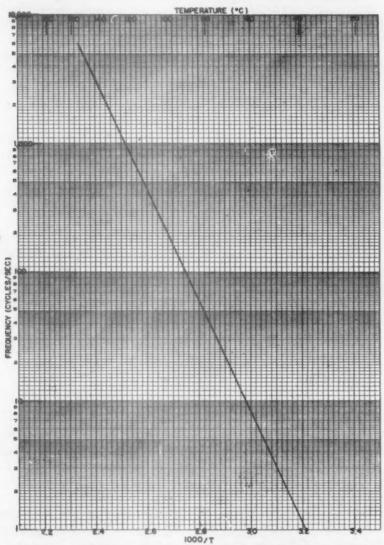


Fig. 16.—Relation between temperature at maximum internal friction and frequency of vibration. (After equation of Richter. 96)

tion of either 0.008 per cent of carbon or of 0.008 per cent of nitrogen. It must therefore be concluded that this anelasticity is in some way related to the presence of small traces of carbon and/or nitrogen. Snoek's experimental approach was through internal friction. His results are shown in Fig. 17.

investigations upon the magnetic aftereffect prior to 1939 has been given by Becker and Doring.⁹⁹ The close relation between the mechanical and the magnetic effects were shown by Richter.^{95,96} The relaxation spectra for the two effects not only have the same shape but are located at the same relaxation times, and have identically the same temperature dependence. Snoek¹⁰⁰ has shown that the magnetic elastic after-effect is removed by a high-temperature wet hydrogen treatment,

different type, such as the diffusion of carbon or of nitrogen. Richter⁹⁶ has outruled the first possibility by showing that the introduction of a strong magnetic field

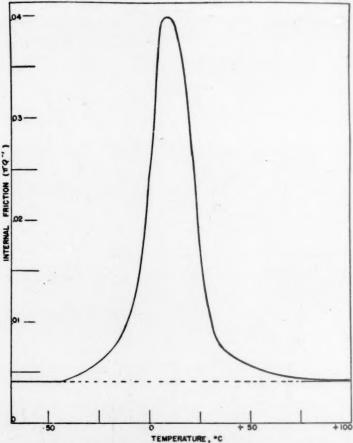


FIG. 17.—STRONGLY TEMPERATURE-DEPENDENT TYPE OF INTERNAL FRICTION IN CARBONYL IRON.

(After Snoek. 97)

—Before removal of carbon and nitrogen.

---After removal of carbon and nitrogen.

and is reintroduced by slight traces of carbon or of nitrogen. From the foregoing statements, it is apparent that the mechanical and the elastic effects have a common origin. From the results previously discussed it is not evident, however, whether this origin is of a purely magnetic nature, such as the irreversible movement of the magnetic domain boundaries caused by fixed restraints, or of a purely mechanical nature, such as the irreversible viscous flow in amorphous layers, or whether the origin of the irreversibility is of an entirely

removes the magnetic after-effect, and also the temperature-independent type of mechanical hysteresis discovered by Becker and Kornetzki, ⁸³ without altering the strongly temperature-dependent type of anelasticity. Snoek ¹⁰⁰ has advanced a theory, and has presented experimental evidence in support thereof, that is based upon the third possibility. According to this theory, the concentration of both carbon and nitrogen is greater at the boundaries of the magnetic domains than in the interior of the grains, and therefore

the motion of such boundaries is attended by a diffusion of the carbon and nitrogen. According to this theory the magnitude of the anelastic effects would be proportional to the area of the magnetic domain boundaries, and could therefore be influenced by the state of magnetization. As previously mentioned, such an influence does not exist.

Snoek 101,102,103 has recently advanced a new theory for the strongly temperaturedependent type of anelasticity, a theory that is consistent with all observations made to date, and that is fertile in suggestions for new experiments. According to this theory, the anelastic effects discussed are due to the tetragonality of the interstitial positions in the ferrite lattice, and to the consequent asymmetrical distortion suffered by the lattice surrounding each site when that site is occupied by a solute atom; e.g., by a carbon atom. Since each interstitial position may be one of three types, corresponding to the three lattice principal axes to which its tetragonal axis of symmetry may be parallel, the nature of the distortion varies from site to site. When the ferrite lattice is unstrained, the potential energy of a carbon atom does not depend upon which type of interstitial site it occupies. The equilibrium distribution in this case corresponds to complete randomness. When, on the other hand, the lattice is subjected to a tensile strain along one principal axis, the equilibrium distribution is no longer random. The resulting preferred distribution of the carbon atoms results in a relaxation of stress, and therefore in the observed anelastic effects.

It is shown in appendix B that these ideas lead to the following equation for the quasi-static modulus defect Δ_0 associated with the preferential distribution of carbon atoms, provided the interaction between carbon atoms is neglected:

$$\Delta_0 = \frac{590}{T} X_c \qquad [27]$$

where X_c is the concentration of carbon in weight per cent. The temperature variation given by this equation agrees with the previously mentioned observed variation of 0.3 per cent per degree C. in measurements made near room temperature. The Δ_0 observed by Richter in his experiments upon carbonyl wire, reproduced in Fig. 9, was 0.010. This value, when substituted into Eq. 27, gives for the carbon concentration the value 0.005 wt. per cent, a reasonable value. The heat of activation of 19,600 cal. per mol observed by Richter must be interpreted as the heat of activation of the carbon atoms in passing from one interstitial site to an adjacent site. This must then be the heat of activation for the diffusion of carbon in ferrite, a quantity that has not as yet been measured directly. The value 19,600 cal. per mol is not much more than one half the value of the heat of activation for the diffusion of carbon in austenite. Since there are three times as many interstitial positions in ferrite as in austenite, they must be closer together in the former type of lattice than in the latter, and it is therefore reasonable to expect that the heat of activation for diffusion of interstitial atoms should be considerably less in the former than in the latter type of lattice. A final check upon the theory may be made in the order of magnitude of the numerical coefficient in Eq. 26. The peak of the relaxation spectrum should occur at a \tau comparable to the mean lifetime of a carbon atom in an interstitial position. This lifetime in turn is given approximately by

$$\tau \simeq e^{Q/RT}/f$$
 [28]

where f is the frequency of vibration of the carbon atoms in the interstitial positions. Upon comparing Eqs. 26 and 28, one obtains

$$f = 1.0 \times 10^{14} \, \text{sec}^{-1}$$

which is a reasonable value.

In the derivation of Eq. 27 it was assumed that interaction between carbon

atoms could be neglected. The author 104 has recently shown that it is just this interaction that renders the tetragonal structure of martensite stable with respect

in reaching an understanding of the mechanical behavior of metals. A typical relaxation spectrum is reproduced in Fig. 18. Each change in a specimen,

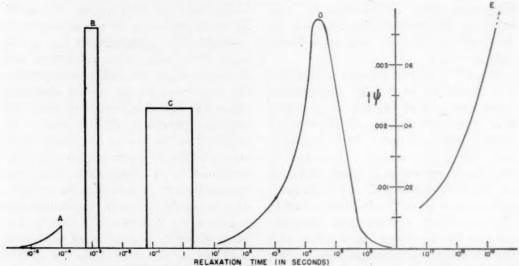


FIG. 18.—Typical relaxation spectrum of Iron (ROOM-TEMPERATURE, MAGNETIC EFFECTS NOT REPRESENTED)

A. Relaxation by intercrystalline thermal diffusion (After Randall, Rose and Zener⁶⁵).

B. Relaxation by transverse thermal diffusion in bending. 60.62,64

C. Relaxation by diffusion of carbon and nitrogen to and from preferred interstitial positions (After Richter⁹⁶).

D. Relaxation by viscous flow in amorphous regions introduced by plastic deformation, following 5-hour anneal at 300°C. (After West¹²⁴).

E. Relaxation by viscous flow along grain boundaries (After West¹²⁴).

to a cubic structure as long as the carbon concentration in solid solution remains above a certain critical value for every temperature, or as long as for every carbon concentration in solid solution the temperature remains below a critical value. When this interaction is taken into account, it is found that Eq. 27 is valid only when $T/T_c\gg 1$. Otherwise, Δ_0 is considerably larger than is given by this equation. The details are given in appendix B.

POTENTIAL IMPORTANCE OF ANELASTICITY

Just as X-ray diffraction spectra of metals have been of invaluable aid in determining the spatial relations of the constituent atoms, so it is anticipated that relaxation spectra will be of invaluable aid whether the change be in dimensions, in composition, in grain size, in plastic deformation, in annealing, or in temperature, is reflected by a characteristic change in the relaxation spectrum. Through an appropriate observation and interpretation of these changes, an insight may be gained into the mechanical properties of the individual elements of the microstructure, an insight that is obtainable in no other manner. Strangely enough, the first two peaks, which are due to thermal relaxation and which have little or no relation to the plastic or fracture behavior, have been exhaustively studied, while the last two peaks, which are much stronger, and which have an intimate relation to the plastic and fracture properties, have received scarcely any attention prior to that of West.¹²⁴ In the following pages, a review is given of the potential importance of the relaxations represented by these two peaks, in the hope that further research upon them will thereby be stimulated.

RELATION OF FRACTURE TO RELAXATION

The observed fracture stress of metals is from 10 to 100 times smaller than the calculated fracture stress. In order to reconcile this discrepancy, it is necessary to assume some sort of stress concentration. One is tempted to place the blame upon surface imperfections, which could act as stress raisers. Such in fact seems to be the case in rock salt, where by taking extreme care in avoiding surface imperfections (by continually dissolving away the surface) Joffe 105 has found that the fracture stress may be raised to near its theoretical value. The low fracture stress of metals cannot be attributed to surface defects, for, once necking has commenced, fracture starts at the center of the specimen. The microstructure of the metal itself, therefore, must be blamed for the low fracture stress.

It has been possible to interpret many fracture phenomena¹⁰⁶ in terms of small microcracks, which are assumed to be present. However, in order that such cracks may propagate under a given macroscopic stress, their radii must exceed a certain critical value.¹¹⁹ There has heretofore been no explanation as to how such cracks can grow to the critical size. There must exist some source of high stress concentration other than the cracks themselves.

Relaxation of shear stress across localized planes is able to provide all the stress concentration needed for the initiation of microcracks. A localized region that completely relaxes all shearing stresses will induce in the surrounding elastic matrix essentially the same stress pattern as would a cavity of the same shape. The factors that influence the stress

concentration of cavities were first investigated by Inglis.125 According to his work, if a disklike cavity of radius a has a radius of curvature r at its edge, and if it lies in the plane of maximum shear stress S, the maximum tensile stress at the edge is $2(a/r)^{\frac{1}{2}}S$. Since the relaxation regions in metals have a thickness comparable to atomic dimensions, the radius of curvature will also be of atomic dimensions. The length of the relaxation regions need therefore be only 10-4 cm. in order to induce stress-concentration factors of the order of magnitude of 100, factors that are sufficient to raise the observed macroscopic fracture stress to the theoretical fracture stress of the matrix.

One source of stress concentration that may initiate cracks lies in the relaxation of stress across grain boundaries. Such a source will be operative under conditions where the resistance to deformation at the grain boundaries is low with respect to resistance to deformation within the grains; that is, slow extensions at elevated temperatures. It is to be expected, therefore, that the initiation of cracks by grain-boundary relaxation will be prevalent under creep conditions. The role played by the viscosity of grain boundaries in the initiation of cracks under creep conditions was first recognized by Rosenhain and Humfrey122 in their work upon the deformation of gamma iron at high temperatures. When pulled under the usual test conditions, this iron manifested fair ductility and fractured in a fibrous manner. When extended very slowly at the same temperature, the iron fractured in an intercrystalline manner, with hardly any prior plastic deformation. The occurrence of this type of intercrystalline failure in a wide range of metals was later discussed by Rosenhain and Archbutt, 123 who demonstrated that such failure is facilitated by small plane grain boundaries, grain boundaries that could slip without mechanical hindrance. Season cracking in brass was ascribed by them to be associated with grain-boundary slip. More recently Hanson and Wheeler107 have made a detailed study of the role grain boundaries play in the fracture of aluminum under creep conditions. Hanson and Wheeler found that at elevated temperatures cracks invariably started at the grain boundaries under slow extension, and propagated into the grains only just before fracture, when the rate of extension was large. In single crystals failure occurred by shear along slip planes rather than by cracks. As spectacular evidence of crack formation at the grain boundaries, they showed that under creep conditions the density of polycrystalline specimens decreased appreciably, while that of single crystals remained constant. As pointed out by Carpenter and Robertson, 108 the elements that increase the resistance of metals to creep do not necessarily increase the resistance of the grain boundaries to slip by a like amount. In the development of high-temperature alloys, attention must therefore be directed toward resistance to fracture as well as to resistance to deformation at high temperatures.

Another source of stress concentration that may initiate cracks lies in the relaxation of stress across the amorphous regions introduced by plastic deformation. Since the stress concentration in the surrounding elastic matrix arises solely as the result of stress relaxation within the viscous regions, it is to be expected that conditions of stressing that hinder such relaxation will reduce the stress concentration and thereby raise the observed fracture stress. This is indeed the case. The stress relaxation that has occurred before a given macroscopic stress level has been reached may be reduced either by a lowering of the temperature or by an increase in the rate of strain. Both of these changes, a decrease of temperature and an increase in strain rate, have been found by Hollomon and Zener¹⁰⁹ to raise the fracture stress at a given strain. A similar effect of strain rate upon the fracture stress of glass has been reported by Haward. 110 Conversely, conditions that favor relaxation will increase the stress concentrations and thereby lower the observed fracture stress. Thus when a constant macroscopic stress is applied to a specimen, the increase in localized stress concentrations attending relaxation will result in a lowering of the fracture stress. If the asymptotic value of this fracture stress is lower than the applied macroscopic stress, fracture will eventually ensue. Familiar examples of such fracture occur in the cracking of quenched specimens some time after room temperature has been reached.111,112 According to Howe, 113 "In the early days of making armor-piercing shells, spontaneous and violent aging rupture was so common that shells, after hardening, used to be stored for a considerable time in a room to which nobody was admitted." This discussion suggests that this cracking following a quench would be delayed if the specimens were maintained at a low temperature, and would be accelerated by mild heating (to 100°C.). A spectacular example of the effect of temperature upon the acceleration of cracking at elevated temperature has been observed by the author in projectiles. Under appropriate conditions an uncapped projectile will pass through armor at normal incidence with a slight bulge. Though recovered intact, the tip of the projectile is apt to fly off (Fig. 19). Placing recovered projectiles in boiling water hastens the flying off of the tips; placing them in ice water seems to delay the flying off for an indefinite period. Presumably the plastic deformation of the projectile leaves the central portion of the ogive in tension, and the macroscopic fracture stress of the material gradually decreases below this tensile stress because of the stress relaxation in the localized amorphous centers previously introduced by the deformation.

In glass, likewise, local high stress concentrations appear to be generated, and regions. From the observation that the rise in bend strength occurs in the same temperature range as the disappearance of the internal friction introduced by plastic

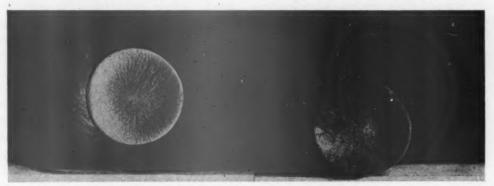


Fig. 19.—Example of tip of projectile that has been ejected after recovery of projectile.

hence the fracture stress to be lowered, by the application of stresses for a prolonged period. As an example, Griffith119 has shown that the fracture stress of freshly drawn glass fibers decreases with time. This decrease is more rapid the larger the wires, decreasing from 900,000 to 80,000 lb. per sq. in. for fibers of 0.02 in. diameter, to 500,000 lb. per sq. in. for fibers of 0.00013 in. diameter. Presumably the larger diameter fibers had the greatest residual stresses introduced by cooling. The well-known tendency of glass to crack spontaneously may be the result of the building up of local high stress concentrations by residual stresses.

Steels in the as-quenched hardness are usually brittle when this hardness lies above 60RC. In his work¹¹⁴ upon projectile steels at the Watertown Arsenal laboratory, Van Winkle has found one steel that in the as-quenched condition (61-62RC) is brittle, but that acquires considerable ductility without the loss of any hardness upon tempering for 5 min. at 250°C. This tempering in fact increases the bend strength by 100 per cent. It does not seem possible that such tempering could heal any microscopic cracks. Such tempering could however either relieve residual stresses or recrystallize the amorphous

deformation, it would appear that in this steel the rise in bend strength, and hence in fracture stress, was associated with the recrystallization of the amorphous regions.

Removal of the amorphous regions by low-temperature annealing should considerably raise the fracture stress. Recent experiments¹¹⁵ in this laboratory indicate that this is indeed the case.

STRESS RELAXATION

In some cases locked-in, or residual, stresses, are desirable features of a structure-always, for example, wherever members are held together by bolts. These structures cannot function properly for extended periods of time at elevated temperatures, for under such conditions the stresses relax to a small fraction of their original value. In other cases, residual stresses are undesirable-always when parts are to be machined, for when a portion of the material is removed the stresses become unbalanced, and the part warps. In these cases it is a usual practice partially to relax the residual stresses by extended holding at elevated temperatures.

The practical importance of stress relaxation has furnished the incentive for a great amount of work, which has been published in numerous articles during the past decade. In order to reduce the amount of work necessary to obtain the desired results, several attempts have been made to deduce stress relaxation properties from creep curves. However, as Davenport¹¹⁶ has stated emphatically, there is no method by logic alone by which available data on creep, obtained in constant stress tests, may be applied to a problem of varying stress; i.e., to stress relaxation.

It is commonly accepted that stress relaxation occurs by means of plastic deformation. As demonstrated by West, 124 the major part of locked-in stresses may be relaxed by viscous flow in localized relaxation centers. Such a relaxation cannot be thought of as plastic deformation, since it is completely reversible. It is apparent therefore that the only direct approach to the problem of the control of stress relaxation is through a study of relaxation centers, and of the factors that influence them.

CREEP

At elevated temperature, all metals suffer a continual change in shape under a constant applied stress. This continued deformation, known as creep, has been

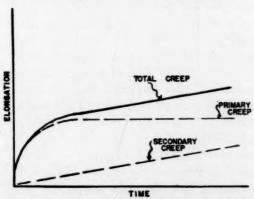


Fig. 20.—Schematic illustration of typical creep curve.

the subject of an immense amount of work during the past 20 years.

A property common to all creep curves (elongation vs. time) is an initial rapid rise followed by a gradually decreasing slope, as illustrated in Fig. 20. Such curves frequently are represented as the superposition of two curves-a primary creep curve, which approaches a horizontal asymptote, and a secondary creep curve, which has a constant slope. In structures in which considerable deformation is allowed in service, the secondary creep is of dominant importance; for example, in lead pipes. On the other hand, in structures where the allowable deformation is comparable to the elastic deformation, the primary creep is of dominant importance. Such is the case wherever tolerances are close, as in turbine blades.

As demonstrated by Johnson, 46 the major portion of the primary creep frequently is recoverable. This is true particularly at the lower stress levels. Recoverable creep must arise through stress relaxation within isolated relaxation centers. It is therefore apparent that the only direct approach to the problem of creep in structures with close tolerances is through a study of relaxation centers, and of the factors that influence them.

DIMENSIONAL CHANGES UNDER ZERO STRESS

In fine instruments difficulties frequently are encountered through slight changes in dimensions following fabrication. Sometimes expensive aging treatments are necessary in order to eliminate these changes; for example, with watch springs, 117,118 for which aging treatments of more than a year may be employed. In view of the work of West upon the relaxation centers introduced by plastic deformation, 124 there can be little doubt that such changes in dimensions as are mentioned above are due to stress relaxation within these centers. It is apparent therefore that the only direct approach to the problem of controlling such dimensional changes is through a study of the relaxation centers introduced by plastic deformation, and of the influence of annealing thereon.

APPENDIX A

In this appendix is outlined a method for the computation of the relaxation strengths applicable to thermal, concentration and magnetic relaxation.

According to whether thermal, concentration or magnetic relaxation is being considered, the symbol A will refer to temperature, partial pressure, or magnetic field strength, the symbol α will refer to entropy, the partial gaseous volume of the constituent in a unit volume of solid, or (magnetic flux density)/ 4π . The notation is summarized as follows:

Type of Re- laxation	Thermal	Concen- tration	- Magnetic
A	T	$\frac{P}{V}$	Η
a	S		B/4π

If only one type of relaxation is considered, the tensile stress X and the parameter A may be taken as the independent variables, the tensile strain e and α as the dependent variables. Thus

$$de = E_A^{-1} dX + \lambda dA \qquad [a_{-1}]$$

$$d\alpha = \lambda dX + \mu dA \qquad [a_{-2}]$$

The equality of the two cross coefficients is due to the fact that the definition of alpha was so chosen that the increment of internal energy density is

$$\delta U = X de + \Sigma A d\alpha$$

The equality therefore is derivable from the condition that $\delta(U - A\alpha)$ be a perfect differential.

From Eqs. a-1 and a-2, it follows that

$$(\delta e/\delta X)_A - (\delta e/\delta X)_\alpha = E_A^{-1} - E_\alpha^{-1} = \lambda^2/\mu$$

and therefore

$$\Delta_0 = \frac{E_\alpha - E_A}{E_A} = E_\alpha \lambda^2 / \mu \qquad [a-3]$$

Eqs. 18 to 21 are derivable directly from Eq. a-3.

APPENDIX B

In this appendix the computation is given of the quasi-static modulus defect Δ_0 associated with changes in the equilibrium distribution of carbon atoms among the interstitial positions in ferrite.

Suppose a stress $\delta \sigma$ is applied along a (100) axis of the ferrite lattice. The instantaneous strain will then be $E_{100}^{-1}\delta\sigma$. As time goes on, an additional strain will gradually take place, which arises from an increase in the number of carbon atoms occupying interstitial positions whose tetragonal axes are parallel to the tensile axis. Let δN_p denote the final increase in the number of such carbon atoms per unit volume, and let \(\lambda \) denote the tensile strain occasioned by the increase of one such carbon atom per unit volume. The strain introduced by this redistribution of carbon atoms, which will be denoted by δe_R , is therefore $\lambda \delta N_p$. The quasi-static modulus defect may be written as $\delta e_R/\delta e_i$, hence

$$\Delta_0 = E_{100} \lambda (\partial N_p / \partial \sigma) \qquad [b-1]$$

From appendix C of a recent article, ¹⁰⁴ the following equation may be derived in the case where δN_p is only a small fraction of the total number of dissolved carbon atoms:

$$\frac{\partial N_p/\partial \sigma}{(1-\text{o.g2}T_c/T)^{-1}} \quad [b\text{-}2]$$

Here T_c is the critical temperature below which most of the carbon atoms are in preferred interstitial positions, and is given in terms of the weight per cent X_c of carbon by the equation

$$T_c = 1330X_c$$
 °K

Eq. 27 of the text is obtained by substituting Eq. b-2 into Eq. b-1, averaging over all orientations (which introduces a factor of approximately ½), and utilizing the following equation from reference 104:

$$T_c = 0.243 N E_{100} \lambda^2 / k$$

SUMMARY

Anelasticity is defined as that property of solids in virtue of which stress and strain are not uniquely related in the elastic range. Examples of anelastic effects are: elastic after-effects, internal friction, and the frequency variation of the elastic moduli. A review is given of the mathematical formulation of anelasticity according to the fundamental ideas of Boltzmann as interpreted in terms of stress relaxation by Thomson and Wiechert.

A review is given of the various physical origins of anelasticity; i.e., of stress relaxation. One common source of anelasticity is diffusion: thermal diffusion, atomic diffusion, magnetic diffusion. Several heretofore unexplained types of anelasticity are herein interpreted in terms of atomic diffusion. As examples: the existence of a temperature band around 400°C. within which the internal friction of alpha brass is anomalously high implies that in alpha brass the zinc concentration suffers a periodic fluctuation; the existence of a temperature band around 100°C, within which the internal friction of mild steel is anomalously high implies that an applied stress causes a preferential distribution of dissolved carbon or nitrogen atoms among the various types of tetragonal interstitial positions. Through such anelastic studies information may be obtained regarding atomic distributions, which can be obtained in no other manner.

Another common source of anelasticity lies in the relaxation of shear stress across localized regions that behave in a viscous manner with respect to shear stresses, and that are surrounded by an elastic matrix. Grain boundaries and freshly formed slip bands are examples of such regions. The most direct approach to a study of shear stress relaxation along slip bands and along grain boundaries by viscous flow is through anelasticity. A discussion is given of the practical im-

portance of such stress relaxation. It is shown that such stress relaxation plays a dominant role in stress relief, in primary creep, and in small dimensional changes at room temperature. More important, such stress relaxation is intimately related to fracture. Stress relaxation within slip bands at room temperature leads to the initiation of microcracks, which ultimately lead to macroscopic fracture. Relaxation of shear stress across grain boundaries under creep conditions likewise leads to the initiation of microcracks, which ultimately cause macroscopic fracture.

BIBLIOGRAPHY

- I. W. Weber: Ueber die Elastizität der Seidenfaden. Poggendorff's Ann. (1834)
- 34, 247. 2. W. Weber: Ueber die Elastizität fester Korper. Poggendorff's Ann. (1841) 24
- (2), I. Auerbach: Winkelmann's Handbuch der Physik, I. Chapter on Elastische Nachwirkung, 796-831. Kohlrausch: Ueber die elastische
- Nachwirkung bei der Torsion. Ann. Phys. Chem. (1863) 29 (4), 335. 5. F. Kohlrausch: Experimental-Untersuch-
- ungen uber die elastische Nachwirkung bei der Torsion, Ausdehnung und Beigung. Ann. Phys. Chem. (1876) 8
- (6), 337. Meyer: Zur Theorie der inneren Rei-6. 0. bung. Inl. reine und angewandte Mathematik (1874) 78, 130.
 7. W. Voight: Ueber inneren Reibung fester
- Korper, insbesondere der Metalle.

 Ann. Phys. (1892) 47, 671.

 8. L. Boltzmann: Zur Theorie der elastische
- Boltzmann: Zur Theorie der elastische Nachwirkung. Ann. Phys. (1876) 7, 624; also Sitzungsber. Wien Akad. (1874) 70 (2), 275.
 J. J. Thomson: Applications of Dynamics to Physics and Chemistry, chap. VIII, on Residual Effects. London, 1888.
- E. Wiechert: Ueber elastische Nachwirkung. Inaugural Dissertation (Königsberg i, Pr., 1889).
 E. Wiechert: Gesetze der elastische Nach-
- wirkung fur konstant Temperature.
- Ann. Phys. (1893) 50, 335.

 12. K. Bennewitz: Uber die elastische Nachwirkung. Physikal. Ztsch. (1920) 21,
- 703. 13. K. Bennewitz: Elastische Nachwirkung und Hysteresis. Physikal. Ztsch. (1924)
- 25, 417. Maxwell: Scientific Papers 2, 623. 14. C.
- Cambridge, 1890.

 15. H. Wartenberg: Elastische Nachwirkung in Metallen. Deut. phys. Gesell. (1918)
- 20, 113. 16. H. Jeffries: On Plasticity and Creep in Solids. Proc. Roy. Soc. (1932) 138, 283.

17. M. Sayre: Elastic After-Effect in Metals.

Jnl. of Rheology (1932) 3.
Prandtl: Eine Gedankenmodell zur kinetischen Theorie der festen Korper. Zisch. angew. Math. Mech. (1928) 8,

R. Becker: Elastische Nachwirkung und Plastizität. Ztsch. Physik. (1925) 33,

20. R. Wegel and H. Walther: Internal Dissi-

pation in Solids for Small Cylic Strains.

Physics (1935) 6, 141.

21. F. Forster: Ein neues Messverfahren zur

Bestimmung des Elastizitätsmodul und Dampfung. Zisch. Metallkunde

(1937) 29, 109. 22. F. Forster and H. Breitfeld: Ein Gerat

zur unmittelbaren Dampfungsanzeige. Ztsch. Metallkunde (1938) 30, 343. Ewing: On Measurements of Small Strains in the Testing of Materials and Structures. Proc. Roy. Soc. (1895) 58,

J. Muir: The Recovery of Iron from Over-strain. Phil. Trans. Roy. Soc. (1900)

25. E. COKER: On the Effect of Low Temperature on the Recovery of Overstrained Iron and Steel. Phys. Rev. (1902) 15,

26. W. Rosenhain: Deformation and Fracture in Iron and Steel. Jnl. Iron and

Steel Inst. (1906) 70, 189.

27. G. Beilby: The Hard and Soft States in Metals. Phil. Mag. (1904) 8 (6), 258.

28. E. Orowan: Zur Kristallplastizitat III. Uber den Mechanismus des Gleitvorganges. Ztsch. Physik (1934) 89, 634; also diplomarbeit, 1929 (Technische

Hochschule, Berlin). 29. G. I. Taylor: Mechanisms of Plastic Deformation of Crystals-I. Theoretical.

Proc. Roy. Soc. (1934) 145, 362.
30. F. Seitz and T. Read: Theory of the Plastic Properties of Solids. Jnl. Applied

Physics (1941) 12, 100, 170, 470, 538.
31. F. Forster and W. Köster: Elastizitätsmodul und Dampfung in Abhangigkeit von Werkstoffzustand. Zisch. Metall-

kunde (1937) 29, 116. 32. W. Köster and K. Rosenthal: Die Anderung von Elastizitätsmodul und Dampfung bei der Verformung und Rekristallisation bon Messing. Ztsch. Metallkunde (1938) 30, 343. 33. W. Köster: Elastizitätsmodul und Damp-

fung von Alumininum und Aluminium-legierung. Ztsch. Metallkunde (1940) 32,

282.

34. J. Norton: Changes in Damping Capacity during Annealing of Alpha Brass. Trans.

A.I.M.E. (1940) 37, 49.
A. Read: The Internal Friction of Single Metal Crystals. Phys. Rev. (1940)

58, 371.

A. Read: Internal Friction of Single Crystals of Copper and Zinc. Trans.

A.I.M.E. (1941) 143, 30.
37. A. Lawson: The Effect of Stress on Internal Friction in Polycrystalline Copper.

Phys. Rev. (1941) 60, 330.
38. C. Zener, H. Clarke, C. S. Smith: Effect of Cold-work and Annealing upon Internal Friction of Alpha Brass. Trans. A.I.M.E. (1942) 147, 90.

39. L. Frommer and A. Murray: Damping Capacity at Low Stresses in Light Alloys and Carbon Steel, with Some Examples of Non-destructive Testing. Jnl. Inst. of Metals, (1944) 70, 11. 40. W. Rosenhain and D. Ewen: Intercrystal-

line Cohesion in Metals. Jul. Inst. of Metals (1912) 8, 149.

Nessenhain: Introduction to Physical

W. Kosenhain: Introduction to Physical Metallurgy, 255-264. Constable, 1915.
 Z. Jeffries and R. Archer: The Science of Metals (McGraw-Hill, 1924), chap. 4.
 W. Rosenhain and J. Humphrey: The Crystalline Structure of Iron at High Temperatures. Proc. Roy. Soc. (1909)

83, 200.
44. E. N. Da C. Andrade and B. Chalmers:
The Resistivity of Polycrystalline
Wires in Relation to Plastic Deforma-

tion, and the Mechanism of Plastic Flow. Proc. Roy. Soc. (1932) 138, 348. 45. H. Moore, B. Betty and C. Dollins: The Creep and Fracture of Lead and Lead Alloys. Univ. of Illinois Bulletin, No.

272 (1935).
46. A. Johnson: The Creep Recovery of a 0.17 per cent Carbon Steel Proc. Inst.

Mech. Engrs. (1941) 146, 187.
Chalmers: Precision Extensometer Measurements on Tin. Jnl. Inst. Metals

(1937) 61, 103. 48. L. Guillet and A. Portevin: Influence de la trempe sur le module elastique de certaines categories d'alliages. Compt.

rend. (1940) 210, 335.
49. A. Barnes and C. Zener: High-temperature Internal Friction, Phys. Rev.

(1940) 58, 87. 50. C. Zener, D. Van Winkle and H. Nielsen: High-temperature Internal Friction of Alpha Brass. Trans. A.I.M.E. (1942)

147, 98.
51. C. Zener: Theory of Elasticity of Polycrystals with Viscous Grain Boundaries. Phys. Rev. (1941) 60, 906.
52. M. Sayre: Elastic After-effect in Metals,

Jnl. of Rheology 3, (1932).
53. C. S. Smith: Proportional Limit Tests

C. S. Smith: Proportional Limit Tests on Copper Alloys. Proc. Amer. Soc. Test. Mat. (1940) 40, 864.
 Becker and Doring: Ferromagnetismus, 371-378, Berlin 1939.
 C. Zener: Internal Friction in Solids—V. General Theory of Macroscopic Eddy Currents. Phys. Rev. (1938) 53, 1010.
 W. Gorksi: Theorie der elastischen Nachwirkung in ungeordneten Mischkristen

wirkung in ungeordneten Mischkristallen (elastische Nachwirkung Zweiter Art). Phys. Ztsch. Sow. Union (1935) 8,

57. W. Brown: The Variation of the Internal Friction and Elastic Constants with Magnetization in Iron—II. Phys. Rev.

(1936) 50, 1165.
58. Becker and Doring: Ibid, 336-354.
59. S. Epstein: The Alloys of Iron and Steel—
I. Constitution, 212. McGraw-Hill Book Co.

60. C. Zener: Theory of Internal Friction in Reeds. Phys. Rev. (1937) 52, 230.
61. C. Zener: General Theory of Thermoelastic Internal Friction. Phys. Rev. (1938) 53, 90. 62. K. Bennewitz and H. Rotger: Ueber die

innere Reibung fester Korper; Absorp-

tionsfrequenzen von Metallen in akustischen Gebiet. Phys. Ztsch. (1936) 37,

63. C. Zener, W. Otis, and R. Nuckolls: Experimental Demonstration of Thermoelastic Internal Friction. Phys. Rev.

(1938) **53, 100**. 64. K. Bennewitz and H. Rotger: Ueber die innere Reibung fester Korper—II. Thermische Dampfung bei Biegeschwingungen. Ztsch. tech. Phys. (1938)

 F. C. Rose, and C. Zener: Intercrystalline Thermal Currents as a Source of Internal Friction. Phys. Rev.

(1939) 56, 343.
 C. Zener and R. H. Randall: Variation of Internal Friction with Grain Size.

67. R. H. Randall and C. Zener: Internal Friction of Aluminum. Phys. Rev. (1940)

58, 472.68. G. Preston: X-ray Examination of Chromium-iron Alloys. Jnl. Iron and Steel

Inst. (1931) 124, 99.
69. E. Jette and F. Foote: X-ray Studies of Iron-nickel Alloys. Trans. A.I.M.E.

(1936) 120, 259.
70. E. Chartkoff and W. Sykes: X-ray Notes on the Iron-molybdenum and Iron-tungsten Systems. Trans. A.I.M.E.

(1930) 89, 566. 71. A. Troiano and F. McGuire: A Study of the Iron-rich Iron-manganese Alloys. Trans. Amer. Soc. for Metals (1943) 31,

72. K. Honda and Z. Nishijama: On the Nature of the Cubic and Tetragonal Martensites. Sci. Repts. Sendai (1932)

73. O. Eisenhut and E.Kaupp: Das System Eisen-Stickstoff. Ztsch. Elektrochemie

(1930) 36, 392.
74. E. Owen and L. Pickup: Crystal Densities of Industrial Brasses from X-ray Data. Jnl. Inst. of Metals (1934) 55,

75. F. Seitz: The Physics of Metals, New York, 1943. McGraw-Hill Book

76. R. Mehl: Diffusion in Solid Metals. Trans.

A.I.M.E. (1938) 122, 11.

77. W. Hume-Rothery: Modern Views on Alloys and Their Possible Application.

Jul. Inst. of Metals (1944) 11, 229.

78. V. Daniel and H. Lipson: An X-ray Study of the Dissociation of an Alloy of Copper, Iron and Nickel. Proc. Roy. Soc. (1943) 181, 368.
79. W. Hume-Rothery: The Metallic State,

328. Oxford, 1931. 80. H. Jones: The Theory of Alloys in the Gamma Phase. Proc. Roy. Soc. (1934) A-144, 225.

 N. Mott and H. Jones: Properties of Metals and Alloys, chap. 5. Oxford, 1936.

 C. Zener: Internal Friction of an Alphabrass Crystal. Trans. A.I.M.E. (1943) 152, 122.

R. Becker and M. Kornetzki: Einige magneto-elastische Torsionsversuche. Ztsch Physik (1934) 88, 634.

84. Lord Raleigh: Phil. Mag. (1887) 23, 225.

85. K. Honda, S. Shimizu and S. Kusakabe: Veranderung des Elastizitatskoeffizienten ferromagnetischen Substanzen infolge von Magnetisierung. Phys. Ztsch. (1901-1902) 3, 380.

86. Becker and Doring: Ibid, 336-357. 87. G. Tammann: Die chemische und galvanische Eigenschaften von Misch-kristallen und ihre Atomverteilung.

Leipzig, 1919. 88. E. Bain: Crystal Structure of Solid Solutions. Trans. A.I.M.E. (1923) 68, 625.
89. C. Barrett: Structure of Metals, chap. 12.

New York, 1943. McGraw-Hill Book

90. W. Gorksy: On the Transitions in the Cu Au Alloy—III. On the Influence of Strain on the Equilibrium in the Ordered Lattice of Cu Au. Phys. Ztsch. Sowj. (1936) 6, 77.

 E. Woodruff: A Study of the Effects of Temperature upon a Tuning Fork. Phys. Rev. (1903) 16, 321.

92. F. Robin: Report on the Wear of Steels and on Their Resistance to Crushing. Iron and Steel Inst., Carnegie Schol. Mem. (1910) 2, 259.

93. F. Robin: Phenomène de l'extinction der son dans le fer. Compt. rend. (1910) 150, 780.

94. F. Robin: The Variation in the Acoustical Properties of Steel with Changes of Temperature. Iron and Steel Inst., Carnegie Schol. Mem. (1911) 3, 125.

95. G. Richter: Ueber die mechanische und magnetische Nachwirkung des Car-bonyleisens. Ann. Physik (1938) [5]

32, 683.
96. G. Richter: Chapter on Ueber magnetische und mechanische Nachwirkung in Probleme der Technischen Magnetisierungskurve, edited by R. Becker. Springer 1938; Edwards Bros, 1944. 97. J. Snoek: Mechanical After-Effect and

Chemical Constitution. Physica (1939)

6, 591. 98. J. Ewing: Phil. Trans. Roy. Soc. (1885) 176, 554.

99. R. Becker and W. Doring: Ferromagnetismus. Berlin, 1939.

J. Snoek: Time Effects in Magnetization Physica (1938) 5, 663.

101. J. Snoek: Physica (1941) 8, 711.

102. J. Snoek: Chemisch Weekblad (1942) 39 (2), 454.

103. J. Snoek: Tetragonal Martensite and Elastic After-Effect in Iron. Physica (1942) 9, 862.

104. C. Zener: Kinetics of Austenite Decomposition. This volume, page 550.

105. A. Joffe: Deformation und Pestigkeit der Kristallen. Zisch. Physik (1924) 22, 286; also The Physics of Crystals, 62. New York, 1928. McGraw-Hill Book Co.

106. C. Zener and J. Hollomon: Plastic Flow and Rupture of Metals. Trans. Amer.

Soc. for Metals (1944) 33, 163.

107. D. Hanson and M. A. Wheeler: The Deformation of Metals under Prolonged Loading—I. The Flow and Fracture of Aluminum. Jnl. Inst. of Metals (1931) 45, 229.

108. Carpenter and Robertson: Ibid, 184-194, 456-462.

109. J. Hollomon and C. Zener: Conditions of Fracture in Steel. Trans. A.I.M.E. (1944) 158, 283.

110. R. Haward: The Behavior of Glass under Impact and Static Loading. Jnl. Soc. Glass Technology (Feb. 1944) 28.

111. S. Epstein: Alloys of Iron and Carbon, II, 331. Nev Book Co. New York, 1936. McGraw-Hill

112. H. Carpenter and J. Robertson: Metals, 711. Oxford, 1939.

113. H. Howe and E. Groesbeck: A Volute Aging Break. Trans. A.I.M.E. (1920) 62, 522.

114. D. Van Winkle and C. Zener: Unpublished work at Watertown Arsenal.

115. J. H. Hollomon and C. Zener: Problems in Fracture. (Feb. 1946). Jnl. Applied Physics.

116. C. Davenport: Correlation of Creep and Relaxation Properties of Copper. Trans. Amer. Soc. Mech. Engrs. (1938) 60, 1-55.

117. Schlotzer: Ueber die elastische 'Nachwirkung. Zisch. Instrumen (1927) 57,

118. Schlotzer: Ueber elastische Nachwirkung, II. Zisch. Instrumen (1938) 58, 264.

119. A. A. Griffith: The Phenomena of Rupture and Flow in Solids. Phys. Trans. Roy. Soc. of London (1920) 221, 163; also Theory of Rupture. Proc. First Intl. Congress Applied Mechanics (Delft, 1924) 55.

120. W. E. Dalby: Researches on the Elastic Properties and the Plastic Extension of Metals. Phil. Trans. Roy. Soc. (1920-21)

A-221, 117

121. G. H. Found: Internal Friction of Single Crystals of Brass, Copper and Aluminum. Trans. A.I.M.E. (1945) 161, 120.

122. W. Rosenhain and J. C. W. Humfrey: The Tenacity, Deformation, and Fracture of Soft Steel at High Temperatures. Jnl. Iron and Steel Inst. (1913) 87, 219.

123. W. Rosenhain and S. L. Archbutt: On the Intercrystalline Fracture of Metals under Prolonged Application of Stress.

Proc. Roy. Soc. (1919-20) 95, 55.
124. W. A. West: This volume, page 192. 125. C. E. Inglis: Stresses in a Plate Due to the

Presence of Cracks and Sharp Corners. Trans. Inst. Naval Architects (1913) 55, 1, 219. 126. B. Chalmers: Microplasticity in Single

Crystals of Tin. Proc. Roy. Soc. (1936) 156, 427.

DISCUSSION

(C. S. Barrett presiding)

M. G. CORSON. *- I cannot call the presentation of the skeleton of a few generalized equations that cannot be converted into a live body (because of the lack of or even the possibility of producing the proper figures), a scientific contribution.

Zener's third paragraph on the first page appears to promise too much: "Through such an understanding will come the ability to design microstructure to give the desired mechanical properties." Some years ago an enthusiast of the X-ray methods exclaimed: "Nowadays the X-ray physicist can tell the metallurgist which elements to take, in which proportions, and how to treat them in order to get the desired physical and chemical properties." Both statements obviously have the same value.

The ideas of Boltzmann, J. J. Thomson, Wiechert, Meyer, Voigt, are not valid today. Those were the ideas of pure mathematicians who dealt with a continuum instead of dealing with matter formed of grains and atoms. For that very reason their formulas and equations are phantoms having no definite physical

meaning.

Far closer to the truth (as I see it) are the ideas of Maxwell et al., who thought that a strictly elastic matrix might enclose here and there regions devoid of perfect elasticity. The error of that idea lies in the hypothesis of isolated regions of an obviously accidental origin. I suggest that such regions are connected with every atom. So, the atom as conceived by Bohr might be much larger than a mere point in comparison with the interatomic distances, and the regions of the outer electrons might correspond to the "perfectly" elastic part of the total space, while the regions between the outer electrons of the adjacent atoms might correspond to the viscous, imperfectly elastic, part of that space. Or, in the theory which I am building now, and which assumes that the atoms are in true contact within the lattice of the grain, the "viscous part" is the heat shell surrounding each atom. In soft metals that heat shell is very large, therefore their elastic deformations are rather complicated. In the harder metals it is small and the elasticity nearly perfect (as in molybdenum and tungsten, for instance). I am restricting my remarks, because I expect to present a paper soon giving my concept of the elasticity and its complications. However, I shall say a few words regarding the subject of the "grain boundaries."

I am a thorough opponent of the very idea of the existence of amorphous substances. The

^{*}Consulting Chemical and Metallurgical Engineer, New York, N. Y.

"amorphism" is simply the result of large variations in atomic or molecular sizes causing the impossibility of the development of a geometrically uniform lattice. In the specific cases of metals where an individual grain of 0.002 mm. in diameter is close to the bottomnotch size attainable, the diameter of the grain carries some six to ten thousand atoms while the grain boundary is certainly far thinner. A very slight distortion of the lattice (or, in my concept, of the atoms) near the grain boundary, plus a slowly decreasing distortion of it toward the center of the grain, would be quite sufficient to bring the circumferential atoms of the adjacent grains into a complete proximity, so entirely eliminating the need for either an amorphous layer or a void between neighboring grains.

The stress at the boundaries might be either a tension or a pressure stress, and as a consequence the boundary might be either weaker or stronger than the grain. That is why some metals and alloys tend to break through the grain while in others the fracture follows preferentially the grain boundaries.

Finally, I wonder why Dr. Zener chose to present such a cramped and excessively abbreviated discussion of so many subjects. For instance, he presents Eq. 18 for the modular defect in a thermal relaxation. Shall we as metallurgists accept such formulas as a kind of gospel, or might we be permitted to ask for their logical derivation?

T. A. Read.*—Dr. Zener is to be congratulated for surveying in such a clear and comprehensive manner the field of the anelasticity of metals. This paper undoubtedly will be a stimulus to further work in this field.

One of the sources of anelasticity discussed by the author is the possible change, under stress, of the degree of order in substitutional solid solutions. An example of experimental data that might be interpreted in this way is furnished by the work of W. Köster, 127 who found anomalies in the internal friction of beta brass at temperatures near the critical temperature for ordering.

The periodic concentration fluctuations in

solid solutions predicted by Hume-Rothery are also discussed by the author as a source of anelasticity. The discussion, based on Fig. 10, of the way in which such fluctuations might arise, does not, however, appear to be valid. The existence of a chord tangent to the curve for free energy vs. concentration at two points, such as C1 and C2 shown in Fig. 10b, is possible only if the slope of this curve decreases with increasing concentration in part of the interval between C_1 and C_2 . Such a decrease in slope does not follow, however, from irregularities in the N(E) curve of the sort shown in Fig. 10a, since the slope of the free-energy curve is proportional to the energy of the added electrons and, as shown in Fig. 10a, this energy never decreases as more electrons are added. It appears, therefore, that a successful theoretical demonstration of the possibility of periodic concentration fluctuations must involve other considerations than those presented by the author.

A. Skapski.*—I should like to say a few words from the general standpoint of physical chemistry. What I am surprised by is the general line of Mr. Corson's criticism. From what he said, it may appear that the development of science went successively through three methods of theoretical approach: (1) the thermodynamical one, assuming the continuity of the system considered; (2) the kinetic one, visualizing the molecules and atoms and their movements; (3) the atomistic one, revealing the structure of the atoms themselves—each of them substituting and canceling some assumptions of the former ones. This is certainly a misapprehension of the development of science.

There are, indeed, three different lines of theoretical approach in treating a problem, but it is essential to emphasize that these three points of view do not exclude each other. On the contrary, they help each other. It is therefore unscientific to say that we cannot, at present, treat problems in the way Gibbs or Boltzmann did, because what they had assumed (e.g., the continuity of a system) is no longer true. I shall cite one single example only; namely, that of the relation between heat capacity of solid elements and temperature, as solved by Debye. He starts from the assumption that the solid is a continuum, substitutes

^{*} Frankford Arsenal, Philadelphia, Pennsyl-

vania.

127 W. Koster: Ztsch. Elektrochemie (1939)
45, 31-32.

^{*} University of Chicago, Chicago, Illinois.

a system of standing waves for that of oscillating atoms and, notwithstanding this strange assumption, he gives a very fine and precise solution of the problem in agreement with experimental facts.

Speaking from a general point of view, I do not think Mr. Corson's objections can be treated seriously.

C. S. BARRETT.*-Under the heading Slip Bands, Dr. Zener emphasizes the marked reduction in internal friction that accompanies stress-relief annealing at very low temperatures. It would be interesting to learn more about the structural changes associated with this process. One rather direct experimental approach to the problem is to study the slip bands by the X-ray diffraction micrograph technique¹²⁸ which records the distribution of X-ray reflecting power over the surface of a grain on a microscopic scale. Experiments thus far with this method have not disclosed any structural changes during annealing below recrystallization temperatures; the enhanced reflecting power of the slip lines seems to be retained throughout stress-relief annealing. This indicates that such annealing does not cause the strained metal at the slipped surfaces to be absorbed by the surrounding crystal in such a way as to produce a perfect crystal. Crystal imperfection remains, either in the form of elastic strains or of disoriented fragments along the slipped surfaces, regardless of changes in internal friction.

C. ZENER (author's reply).—Mr. Corson's first remarks arise from a difference in approach to the physical world from that of the author. Apparently he dislikes any formal description

of a phenomenon that is not derived from atomistic considerations, although the description may be derived from a few simple and reasonable assumptions. He even goes so far as to call those who formulate such descriptions pure mathematicians. Even Boltzmann, one of the world's greatest physicists, he has labeled a pure mathematician.

An atomistic description is always desirable. Frequently, however, such considerations do not lead to a quantitative description of the observed phenomena; then a more formal approach' is necessary. The mechanical behavior of grain boundaries is a case in point. Many phenomena receive a ready interpretation if we ascribe to these boundaries certain macroscopic concepts; to wit, viscosity. It is to be hoped, of course, that some day the coefficient of viscosity may be computed from purely atomistic considerations, but until that day we shall find it useful to continue to use the formal concept of viscous grain boundaries. As Mr. Corson says, no reference to derivation of Eq. 18 was given. This derivation is found in Voigt's Lehrbuch der Kristallphysik (1910) 788.

The author thanks Dr. Read for his reference to the work of Köster upon the influence of ordering on internal friction. Failure to mention this work was certainly an oversight. He also acknowledges the correctness of Dr. Read's criticism of Hume-Rothery's arguments, quoted in this paper, upon the basis for the occurrence of periodic fluctuations in concentration.

As Dr. Barrett has emphasized, much remains to be learned regarding the structural changes taking place during annealing below the recrystallization temperature. Complete knowledge will be obtained only by the combined attack of many methods, including the standard X-ray diffraction, Dr. Barrett's X-ray diffraction micrograph technique, and anelasticity.

^{*} Metals Research Laboratory, Carnegie Institute of Technology, Pittsburgh, Pennsylvania.

¹²⁸ C. S. Barrett: Trans. A.I.M.E. (1945) 161, 15.

Elastic After-effects in Iron Wires from 20° to 550°C.

BY WILLIAM A. WEST*

(Chicago Meeting, February 1946)

ONE manifestation of anelastic properties in solids is the mechanical elastic aftereffect, which may be described briefly as follows: If a stress is applied to a solid body, a deformation or strain is produced. On removal of the stress, this deformation disappears, at least in part. As a first approximation, this appearance or disappearance of deformation usually has been considered instantaneous. Actually, however, for a very wide variety of substances, on application of stress the instantaneous deformation is followed by a further slow yielding, which continues, although at a rapidly diminishing rate, for as long as the stress is applied. Similarly, on removal of the stress, the instantaneous recovery from deformation is followed by a further slow recovery, which continues, although at a rapidly diminishing rate, often for a long time. This latter phenomenon has been called the "elastic after-effect."

Experiments upon the elastic after-effect in metals, when properly designed and when properly interpreted, are capable of giving quite precise information regarding the relation between stress and strain in the various constituent parts of the metal. For example, if certain parts of the metal, such as grain boundaries or slip bands, behave in a viscous manner—that is, if

shear stress ~ rate of shear strain

therein—the relaxation spectrum will contain lines or bands associated with the relaxation of shear stress within these parts. No attempts have heretofore been made to utilize elastic after-effects for obtaining such detailed information. The purpose of the present paper is to explore the possibilities of properly designed and interpreted experiments on the elastic after-effect in metals. Since new procedures and principles are employed in this study, an attempt has been made to record each step taken.

Elastic after-effect observations are susceptible of simple interpretation only when the stress level employed is so low that all effects are linear with the stress. Just how low the stress level must be can be determined only by experiment. An advantage, other than simple interpretation, is associated with low stress levels. When all effects are linear, derived quantities, such as the relaxation spectrum, are independent of the stress distribution. It is, furthermore, possible to employ the type of deformation that is most convenient from the experimental standpoint; for example, torsion.

It appears that in experiments involving both loading and unloading the following would be observed:

- 1. Instantaneous deformation, recoverable instantaneously in whole, or in part.
- 2. Delayed deformation, recoverable slowly in whole, in part, or not at all.
- 3. Permanent deformation, the difference between total deformation and total recovery.

In the work here described, unloading experiments only were made. Wires were

Manuscript received at the office of the Institute July 31, 1945. Issued as T.P. 1993 in METALS TECHNOLOGY, August 1946.

* Physicist, Watertown Arsenal, Watertown 72, Mass. (On leave, Professor of Chemistry, The American University of Beirut, Beirut,

The statements or opinions in this article are those of the author and do not necessarily express the views of the Ordnance Department. Manuscript received at the office of the Institute July 31, 1945. Issued as T.P. 1993 in METALS TECHNOLOGY, August 1946

subjected to given constant torsional strains, under given conditions, and the recoveries after release were observed in more or less detail. Measurements were made of: (1) the instantaneous recovery; (2) the delayed recovery (or elastic aftereffect) beginning a given small time after release and continuing as long as desired; (3) the permanent deformation (or creep). These are the only observations to be made when constant strain is imposed.

A study was first made of the elastic after-effect manifested by a cold-worked wire.* It is known that in iron below room temperature this form of after-effect overlaps the range of a type of after-effect not introduced by plastic deformation. It is also known that annealing at successively higher temperatures diminishes, and finally eliminates, the after-effect introduced by cold-work. However, an attempt to find its upper temperature limit failed for a quite unexpected reason. At temperatures where this cold-work after-effect has not yet been eliminated by annealing, a marked increase in after-effect is observed. This high-temperature after-effect is very large (up to 50 per cent of the applied strain), and is not removed by annealing. It does not seem to have been previously studied, or, indeed, recognized as such, although the phenomenon of "recoverable creep" appears to be identical with it.

Two problems arise in the application of the method described: (1) How can instantaneous recovery be unmistakably distinguished from delayed recovery? (2) How can the observer know that delayed recovery is complete and that residual displacement is true plastic deformation? In most cases these problems may be solved by taking advantage of the interdependence of time and temperature in anelastic effects; i.e., the acceleration of recovery by a rise in temperature. The principles and procedures involved are described at some length below, since they are essential to the method employed, and apparently have not been so used before. Zener1 has discussed the interpretation of elastic aftereffect measurements in terms of relaxation centers, distributed in a "relaxation spectrum" according to their times of relaxation. Raising or lowering the temperature shortens or lengthens the relaxation times of all the centers (quantitative analyses of this interdependence are made later). If the relaxation spectrum has a lower limit it is only necessary to lower the temperature sufficiently before the stress is removed, and the most quickly acting relaxation centers will be delayed for as long as desired. The observed elastic recovery will then be the true instantaneous recovery. Similarly, if the strain has been applied at a given temperature, by heating to a sufficiently high temperature after release the relaxation of all operative centers may be hastened so that delayed recovery will be complete in a few minutes, instead of continuing for hours or days. Evidently the combination of these two procedures will give all the information referred to previously. This has been done successfully for the high-temperature after-effect, but the relaxation spectrum of the lower-temperature form overlaps that of a still lower type. It might be thought, when strain is applied at one temperature, and the specimen subsequently cooled before release, that the time of application of the strain during cooling, and at the lower temperature, would have to be taken into account. Actually, the factors are such that if the initial application of strain is for 5 min. or more, and if the rate of cooling is 10° to 15° in 30 sec., no appreciable addition to the delayed recovery ensues.

^{*} In the article just preceding this paper, 1 Zener has discussed the mathematical formulation of anelasticity, and has described the various forms which have been observed in metals in terms of the mechanisms that are thought to produce them. Throughout this paper it is assumed that Zener's article is available to the reader.

¹ References are at the end of the paper.

One way of determining the relaxation spectrum is from the rate of relaxation—i.e., the slope of the after-effect curve—at a given instant. If we plot residual delayed recovery against log time, and take the slope of the curve at, say, o.r min., this slope will be proportional to the average density of relaxation centers actually operative at that instant, provided the time of application of the strain is long compared with the time after release taken for the measurement, so that relaxation will be complete in the centers under observation.

In the method here described, constant applied strain was used. Properly speaking, all after-effect data should then be expressed in terms of instantaneous elastic recovery, since the latter represents effective stress at the time of release. In the sections dealing with the high-temperature after-effect this was done. Data on the lower-temperature type, are, however, given in terms of the applied strain, for the following reasons: As has been previously stated, the instantaneous recovery could not be precisely observed, and an estimated value would have to be taken in each case; applied strain and instantaneous recovery differed by 3 to 4 per cent at the most, which was about the uncertainty of measurement; data for different wires cannot be compared quantitatively, because of difficulty in controlling quantitatively the amount and nature of prior cold-work. For the high-temperature form, however, there appears to be a good prospect of making a quantitative correlation of aftereffect with microstructure.

Description of Apparatus and Material

APPARATUS

The wire was attached at each end by passing it through a longitudinal hole in a small steel plug shaped as a truncated quadrilateral pyramid, and then pressing in a tapered steel pin (see detail of Fig. 1).

These plugs were held in glass tubes whose tips had been constricted and molded to fit the plugs. The upper supporting tube was sealed into the top of a larger tube several inches longer than the wire. In the latter experiments this joint was not sealed, the wire holder being supported independently, and the opening being loosely packed with asbestos (Fig. 1). This larger tube, or jacket, was wound with resistance wire and insulation (not shown), and was provided with a side tube for a thermometer, and an opening near the top for blowing in cold air. Thus the temperature could be regulated and lowered without too great delay. The jacket was originally tested at various temperatures with the thermometer in different positions in the bore, to make sure that the temperature would be uniform throughout. The openings in the upper part of the tube were closed, of course, during heatings above room temperature.

The lower suspension tube had a mirror attached, and then passed through a graduated turntable (not shown) provided with a clamp. The tube could thus be turned, held in any desired position, and released, the wire thus being twisted a given amount. An enlargement at the lower end of the tube dipped into oil, the depth of immersion being regulated to give proper damping of the elastic recovery of the wire. By means of a lamp and scale, with a suitable timing device, it was possible to follow the elastic after-effect beginning 6 sec., or 15 sec., after release, for as long as desirable. The time to the first reading could have been reduced considerably, but it was thought that the uncertainty in the exact time of removal of the elastic strain, as well as the possible effect of the damping, would vitiate readings made after shorter intervals.

MATERIAL

The wire used was Baker's 0.012-in. diameter iron wire for analysis, given as 99.8 per cent Fe. Metallographic examination

showed that it had a very fine fibrous structure, the metallic grains having been highly distorted in the process of manufacture. This process had introduced considerable after-effect determinations. A method is described later by which a freshly strained, unannealed specimen free of torsional internal stresses was prepared. Wire No. 1

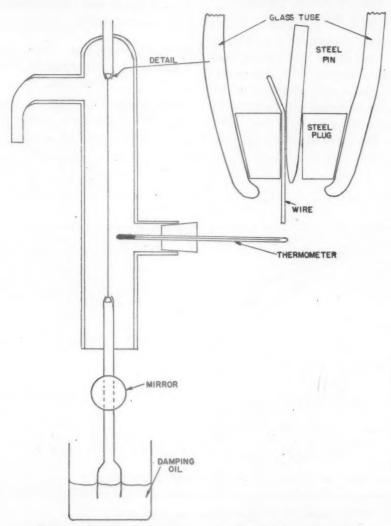


FIG. 1.—APPARATUS FOR OBSERVING ELASTIC AFTER-EFFECT.

internal torsional stress, which was released on heating. The lower end of a freely hung wire began to rotate when the temperature reached about 70°C., and this rotation proceeded as the temperature rose, amounting to about 10° in a 10-in. wire by the time 450°C. was reached. This made it necessary to anneal thoroughly, at some temperature above the highest to be used in the experiment, before a wire could be used for

was 15 in. long; all the others were 10 in. Wires used in the last two parts of the paper are identified by description rather than by number.

Elastic After-effect in Cold-worked Wire between 20°C. and 100°C.

The work described in the following four sections was done with wire No. 1 (15 in.

long). The only treatment given it was a thorough anneal at 105° to 110°C.

EFFECTS OF AMPLITUDE AND OF TIME OF APPLICATION OF PRIOR ELASTIC STRAIN, WIRE NO. 1

These relationships have been previously investigated,³ but a few experiments were made, which confirmed past experience. Fig. 2 shows elastic after-effect curves for wire No. 1 after straining 15 min. at 60°C. for amplitudes of 45°, 90°, and 180°, respectively. The residual strains are seen

amplitude and to log time of application of prior strain. In these experiments and in all those described in this part of the paper, permanent deformation is disregarded, since it was absent, or too small to be detected with certainty.

Interpretation of Time Effect in Terms of a Relaxation Spectrum, Wire No. 1

Boltzmann⁴ expressed the condition of strain of a specimen in terms of the past history of the stress by means of a so-called

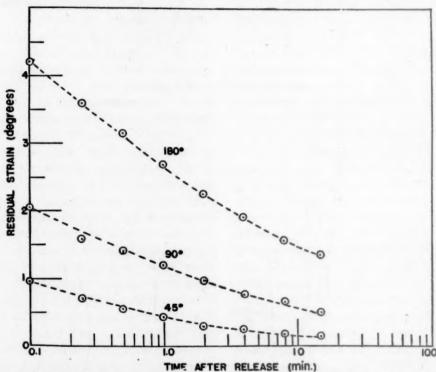


FIG. 2.—ELASTIC AFTER-EFFECT AT 60°C. AFTER STRAINING 15 MINUTES TO GIVEN AMPLITUDE WIRE NO. 1.

to be proportional to the amounts of prior strain applied.

In Fig. 3a are plotted curves for aftereffects produced at 80°C. by straining 90° for times varying from 10 sec. to 1150 min. Fig. 3b shows the initial readings of these curves plotted against log time of application of prior strain. These points lie quite close to a straight line. The results confirm that the elastic after-effect is proportional (at least within limits) to remembrance function. The following form of Boltzmann's equation applies to elastic after-effect:

$$e(t) = e_i \int_{-t_h}^{0} \Phi(t - t') dt'$$
 [1]

e(t) = residual strain at time t after removal of stress.

 e_i = instantaneous elastic recovery.

 $t_{\rm A}$ = time of application of strain.

 Φ = remembrance function.

If we postulate the existence of relaxation centers¹ as the mechanism underlying anelasticity, and further assume that these centers are uniformly distributed, on a logarithmic scale, from very short to quite the elastic after-effect for times long compared with the minimum relaxation time:

$$e(t) = e_i \psi \left\{ \ln \left(\frac{t + t_h}{t} \right) \right\}$$
 [3]

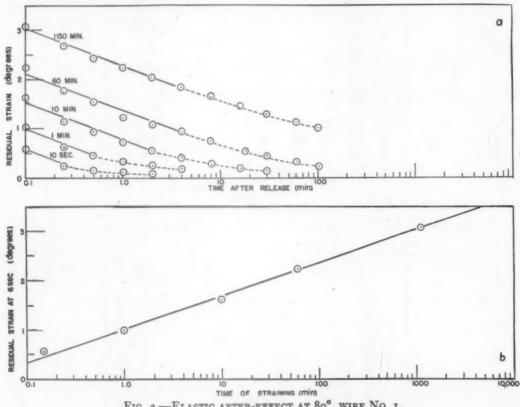


Fig. 3.—Elastic after-effect at 80° after straining 90° for given time. b. Initial (6 sec.) reading for given times of straining to 90°.

long relaxation times, the remembrance function Φ may be evaluated * as follows:

$$\Phi(t) = \psi\left(\frac{1 - e^{-\frac{t}{T_m}}}{t}\right)$$
 [2]

 T_{m} = minimum relaxation time, here assumed to be very small. ψ = amplitude of relaxation spectrum, here assumed constant. (This assumption of constancy of the relaxation spectrum implies that the internal friction would be independent of frequency of vibration.)

Under the conditions just described the two equations may be combined to give the symbols being as already defined. If t is small compared with t_h , ψ may be determined from the slope of the initial part of the after-effect curve, since then:

$$\psi = \frac{d\left(\frac{e}{e_i}\right)}{d\ln t_h} = -\frac{d\left(\frac{e}{e_i}\right)}{d\ln t}$$
 [4]

(As explained in the introduction, the true instantaneous elastic recovery cannot be measured in this case. The degree of approximation used, however, is within the experimental error if the applied strain is used instead.) If, now, we examine Fig. 3a, we find that the initial slopes of all the

^{*} From Eq. 13b of reference 1.

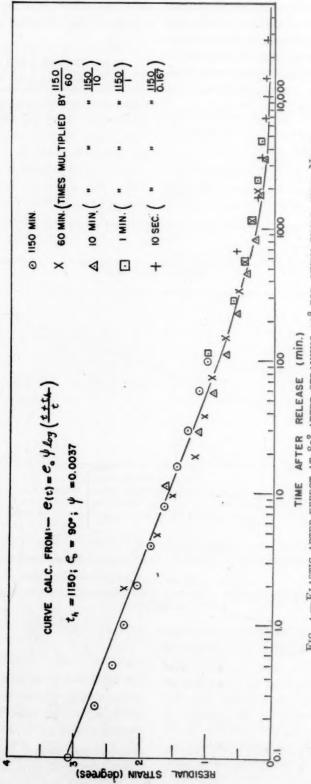


FIG. 4.—ELASTIC AFTER-EFFECT AT 80° AFTER STRAINING 90° FOR GIVEN TIMES, WIRE NO. 1.

curves are very nearly the same, which indicates that the above assumption of constancy of the relaxation spectrum is time of application of strain for that observation. The points lie very close to the curve.

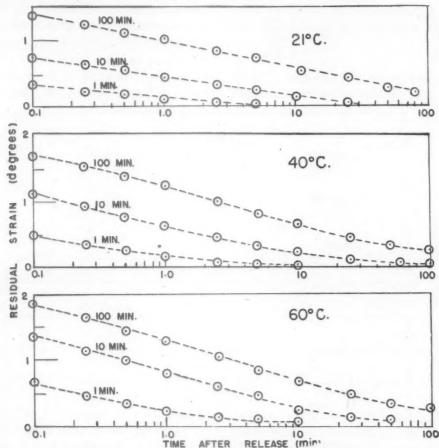


Fig. 5.—Elastic after-effect at given temperatures after straining 90° for given times wire No. 1.

justified for this wire, within the limits of the experiment. By taking lines that represent as well as possible the straight parts of the curves in Fig. 3a we obtain a slope of -0.73, which gives $\psi = 0.0037$. From the slope of Fig. 3b we obtain $\psi = 0.0034$, which is reasonably good agreement.

In Fig. 4 is drawn the curve for the aftereffect produced by a 90° strain applied at 80°C. for 1150 min. as calculated from Eq. 3, from 0.1 min. to 10,000 min., using $\psi = 0.0037$. The experimental points are plotted on the same diagram, each value of

t being multiplied by $\frac{1150}{t_h}$, t_h being the

Effect of Temperature Variation on the Relaxation Spectrum, Wire No. 1

It has been shown that the relaxation spectrum (approximately independent of relaxation time) may be determined from the slope of the after-effect curve as plotted against log time. To study the effect of temperature change, a series of observations were made, straining 90° for 1, 10, and 100 min., respectively, at temperatures of 22°, 40°, 60°, 80°, and 100°C. The results are shown in Figs. 5 and 6. The slopes of the curves in each set are reasonably consistent, and show a slow increase as the temperature

is raised, corresponding to values of ψ as follows:

										-	Γ	A	u	3	L	E		1	I				
	Г	E	3	•	21	3	R.	A	T	U	R	E			I)1	E	G		(3		V
22.																							0.0021
40.																							0.0027
60.																							0.0031
80.																							0.0035
																							0.0038

According to Eq. 3 increase of ψ should also be accompanied by increase in ampli-

effect is due to those regions whose times of relaxation are operative under the conditions of the experiment.

2. In respect to their times of relaxation, these centers are approximately uniformly distributed, at least over the observed range.

3. Changing the temperature changes the rates of relaxation of these centers so that a different part of the spectrum is

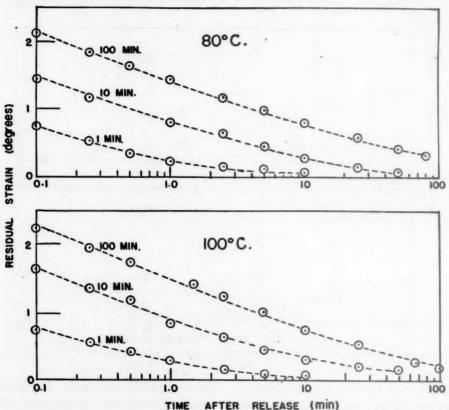


Fig. 6.—Elastic after-effect at given temperatures after straining 90° for given times, wire No. 1.

tude of after-effect, and Figs. 5 and 6 show that the initial amplitudes, for each time of strain, increase steadily as the temperature is raised.

From the results of this section and the last it appears that there is considerable justification for the following picture of the mechanism of anelasticity in material of the type used:

1. Relaxation is produced in localized regions or centers, and the observed after-

brought under observation for a given time range.

Whether or not the spectrum is also altered is considered in the next section.

4. Observation of different parts of the relaxation spectrum by changing the temperature shows a small but definite change in ψ .

Possible quantitative relations between temperature and relaxation time will be investigated in the next section. RELAXATION, HEAT OF ACTIVATION,
WIRE NO. 1

It is a general rule that material processes take place more rapidly at high temperature

are plotted in Fig. 7. In each case, after the plotted points were observed, the temperature was raised to 100°C. and maintained there overnight, by which time the wire had come to rest. The zero for each set of

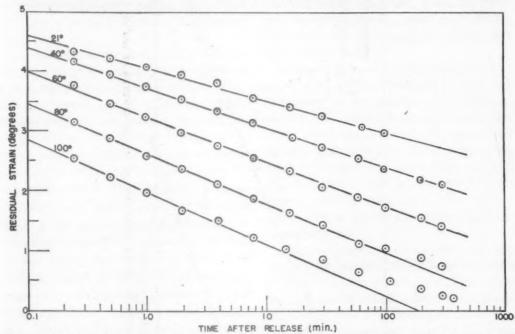


Fig. 7.—Elastic after-effect at given temperature after straining 90° for 60 min. at 100°C., wire No. 1.

than at low temperature. In the case of the elastic after-effect we may examine the influence of temperature on: (1) the rate at which after-effect disappears in a specimen released from a given elastic strain; (2) the amount of after-effect acquired from a given elastic strain.

Influence of Temperature on Rate of Disappearance of After-effect

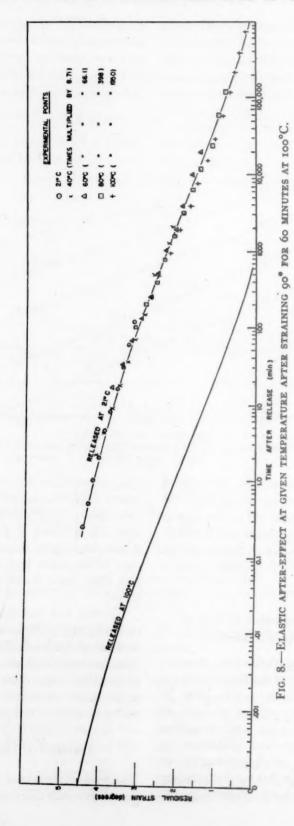
In order to investigate this case, observations of after-effect were made on wire No. 1 at 21°, 40°, 60°, 80°, and 100°C., after, in each case, straining 90° for 60 min. at 100°C. The applied prior strain was thus identical throughout, and differences in amount, and rate of disappearance, of after-effect would be due to temperature differences only. The experimental results

readings was obtained in this way. By this means amplitude as well as rate of loss of after-effect was determined in a reasonable time. As is shown in the following paragraphs, waiting for the after-effect to disappear at the lower temperatures would, in this case, have involved extremely long times.

We may first examine the slopes of the curves in Fig. 7. According to the previous analysis, ψ for each temperature may be obtained from the slope of the curve at that temperature, regardless of the conditions under which the strain was applied. The resultant values of ψ are:

TABLE 2
TEMPERATURE, DEG. C.

21.	•								×												0.0025
40.				×						×	15									•	0.0032
60.					*	*				*	*	8									0.0036
80.	٠		*	18		×		ě.						*		*	*	8	é		0.0040
100	١.									*			*							*	0.0043



The experiments on which these results are based were made several weeks before those used in calculating Table 1. It is seen that the two sets of values of ψ differ by an approximately constant factor, the ability to produce after-effect having diminished with the passage of time, as is discussed later.

If, as stated in the last section, we consider the effect of temperature change to be a shifting of the relaxation spectrum to bring a different part of it into our experimental range of observation, then all the curves of Fig. 7 are parts of a single curve, which could be determined if we could observe a sufficiently extended range of relaxation times. For example, a more complete 21°C, curve could be obtained by shifting the other curves horizontally so that they would fit into place as extensions of the actual observations at 21°C. This horizontal shift, on a logarithmic scale, corresponds to multiplying the observed times at a given temperature by a constant factor in order to transform them to equivalent times at 21°C. As is described more fully hereafter, a direct relationship between relaxation time and temperature requires that for a given residual strain log t plotted against $\frac{1}{T}$ should be a straight line, where t = relaxation time to reach the given relative residual strain at absolute temperature T. The data plotted in Fig. o give straight lines, of very nearly uniform slope. Taking

$$\frac{d \log t}{d \left(\frac{1}{T}\right)} = 4580$$

we find the time-temperature conversion factors given in Fig. 8, from which we may plot the points as shown there.

The resultant composite curve represents the elastic after-effect curve for this wire, at 21°C., following the given prior strain, from 15 sec. to more than one year after release. A parallel curve is also drawn, shifted horizontally to the position corresponding to 100°C. This latter curve may be confidently accepted as representing the relaxation at 100°C. for relaxation times down to about 0.001 min. A similar curve may be drawn for any other temperature for which the transformation factor has been determined.

Evidence that relaxation times of one or more years are not fantastic is given by Schlotzer,⁵ of the Institute fur Zeitmesskunde und Uhrentechnik, who states that newly manufactured watch springs are not reliable until they have stood a full year, after which they are stable. The curve in Fig. 8 indicates that holding for a single day at 100°C. might well have accomplished the same result as a year at room temperature.

The temperature dependence of any process can most conveniently be expressed in terms of a heat of activation. This means that, in mathematical terms, the state of the system may be defined in terms of time and of an exponential term of the form $e^{-\frac{Q}{RT}}$ where R = molar gas constant = 2 cal., T = absolute temperature, and Q = heat of activation in calories. For the elastic after-effect:

relative residual strain is a function of $u^{-\frac{Q}{RT}}$

If now we observe the relaxation times required, at various temperatures, to produce a given elastic after-effect, following release from a given strain, we may plot $\log t$ against $\frac{1}{T}$. From the equation above it is seen that the points so plotted should lie on a straight line, and that

slope =
$$\frac{d \log t}{d \frac{1}{T}} = \frac{Q}{2.3R}$$

Four such sets of points, taken from the data of Fig. 7, are plotted in Fig. 9. With a

single exception, the points of each set lie very close to a straight line, and the four lines agree reasonably well as to slope. We obtain:

$$\frac{d \log t}{d'\left(\frac{1}{T}\right)} = 4580; \quad \text{or} \quad Q = 21,\cos \text{ cal.}$$

tion spectrum is being observed in each case, although the total residual strains vary widely with temperature of straining.

If we apply the empirical time factors used in fitting together the parts of the composite curve in Fig. 8, we may calculate the times of strain at 21°, which would be

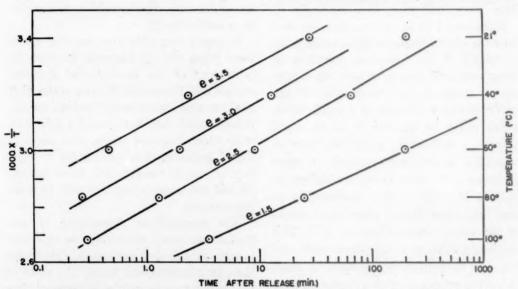


Fig. 9.—Time-temperature relations for given residual after-effects, wire No. 1, (taken from Fig. 7).

Since a single heat of activation appears to apply to the whole observed relaxation spectrum, the indication is that change of temperature shifts the whole spectrum but makes no relative changes in its different parts. The significance of the result lies in this, rather than in the numerical value of the constant.

Influence of Temperature on Rate of Acquiring After-effect

This was investigated by straining the wire 90° for 60 min. at 21°, 40°, 60°, 80°, and 100°C., respectively, then releasing at 21° and observing the after-effect for about 100 min. The point of rest was determined as before, by heating to 100° overnight, in order to save time. The experimental results are plotted in Fig. 10. The slopes of the lines are shown to be practically identical, indicating that the same part of the relaxa-

equivalent to 60 min. at, respectively, 40° , 60° , 80° , and 100° C. We may now plot the initial reading of each curve against the calculated time of straining at 21° , making use of the relationship in Eq. 4. The result, in Fig. 11, gives a line whose slope in its early part is very similar to that of the line in Fig. 3b. In its later part the slope increases, which indicates an increase of ψ at higher temperature, as found from Figs. 5, 6, and 7.

The results of this section are quite consistent with the interpretation of anelasticity given at the end of the previous section.

Cases of Marked Temperature Dependence of Relaxation Spectrum

In order to make a preliminary study of the influence of plastic deformation on the

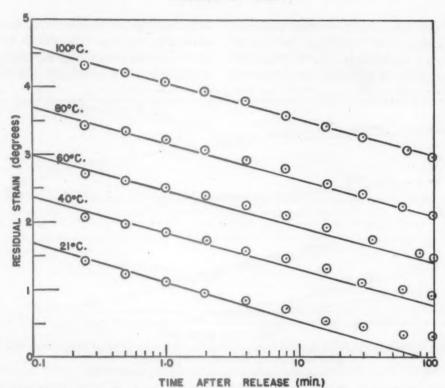


Fig. 10.—Elastic after-effect at 21°C. after straining 90° for 60 minutes at given temperature, wire No. 1.

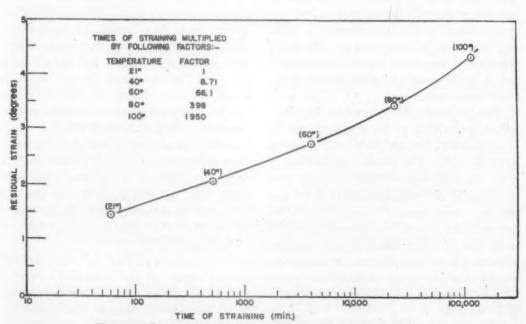


Fig. 11.—Initial readings of curves in Fig. 10. wire No. 1.

elastic after-effect characteristics, a number of specimens were annealed. As already mentioned, annealing at 700°C. makes the wire incapable of producing an after-effect effect was again observed, with the results shown in Fig. 12b. The values of ψ are now 0.0018 and 0.0022 at 60° and 100°C., respectively. The additional cold-work has

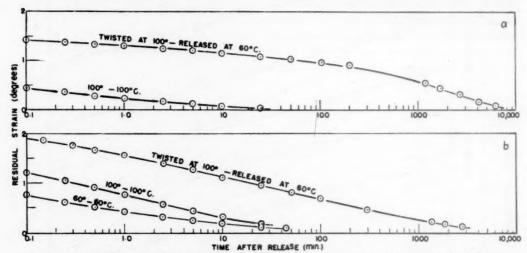


Fig. 12.—Released after twisting 90° for 10 minutes as indicated, wire No. 6.

a. Wire strained by twisting and pulling.

b. Wire additionally strained by rolling slightly flat.

below 100°C. It comes to a complete stop at the end of the instantaneous elastic recovery. Wire No. 6 was treated in this way and then was given plastic deformation by winding repeatedly around a ½-in rod and then pulling straight. The direction of winding was reversed each time. The lower yield phenomenon, of course, disappeared, and a small amount of work-hardening became noticeable.

The specimen was then tested for after-effect by straining 90° for 10 min. at 100°C., and releasing, first at 100°C and a second time at 60°C. The results are plotted in Fig. 12a. The slopes of these two lines give values of ψ of 0.0004 and 0.0011 at 60° and 100°C., respectively. These values are not only much less than those obtained for wire No. 1; they show a very marked dependence on temperature, ψ increasing nearly threefold over a temperature range that caused only a 23 per cent increase in ψ for wire No. 1.

Wire No. 6 was then further plastically deformed by rolling slightly flat. The afternot only increased the after-effect, but has diminished the temperature dependence to approximately that observed in wire No. 1.

Wire No. 8 was annealed at 400° C., strained by winding and pulling as described above, and then tested for after-effect. The results are plotted in Fig. 13, the conditions being indicated for each curve. From the slopes of the curves we find ψ to be 0.0005, 0.0009, 0.0022 at 25°, 60°, and 100°C., respectively, a result similar to that originally obtained for wire No. 6.

In Fig. 14a are plotted initial (at 0.1 min.) after-effects of wire No. 8 strained 90° at 60°C. for times of 1, 10, 100, 1000, and 4000 min., plotted against log time of straining. In contrast to Fig. 3b, the points do not lie on a straight line, but rather on an S-shaped curve.

In Fig. 14b is plotted the whole experimental curve for the after-effect of wire No. 8 after straining 90° for 4000 min. at 60°C. The general shape of this curve may be compared to the 100° to 60° curves in Figs. 12a and 13a and to the 60° to 25° curve

in Fig. 13b. It may also be contrasted with the 1150-min. curve in Fig. 3a, the composite curve in Fig. 8, and the 100° to 60° curve in Fig. 12b. It appears that a notice-

The general indication is that a wire that has undergone mild cold-work has a relaxation spectrum that is low for short relaxation times but increases steadily as the time

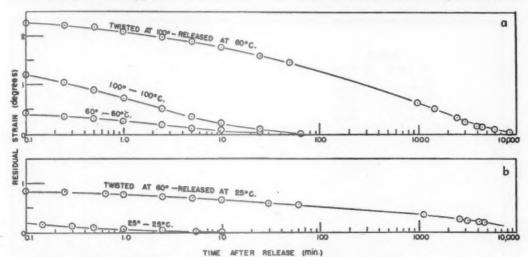


Fig. 13.—Released after twisting 90° for 10 minutes as indicated, wire No. 8.

able reverse S-shape results when the relaxation spectrum varies considerably with temperature and with time of relaxation, while an approximately constant relaxais increased, perhaps to a rather flat maximum. More severe plastic deformation, however, not only raises the whole spectrum, but flattens and spreads the maximum. For

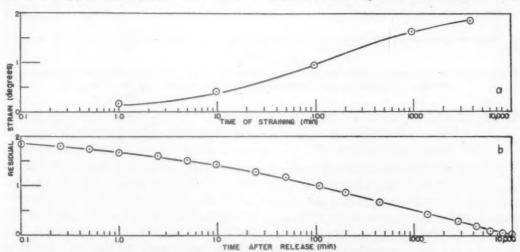


Fig. 14.—Released after twisting 90° at 60°C. as indicated, wire No. 8.

a. Readings o.1 minutes after release.

b. After twisting for 4000 minutes.

tion spectrum produces a curve that is very nearly straight in its earlier part. In a later section further evidence is given in support of this statement.

practical purposes, in the latter case, the relaxation spectrum may be considered nearly constant in the ordinary experimental range. It may be noted that the still lower temperature type of after-effect, referred to in the introduction, gives an after-effect curve with a very marked reverse S-shape.⁶

specimen after various treatments and also the after-effects for temperatures up to 250°C. following anneals of 5 hr. at 300° and 350°C. It is striking that the anelastic

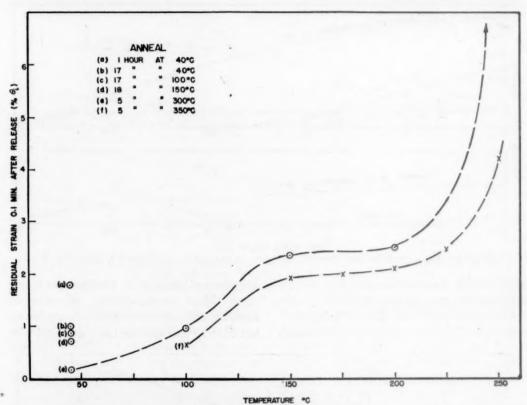


FIG. 15.—ELASTIC AFTER-EFFECTS AT GIVEN TEMPERATURES. EFFECTS OF LOW-TEMPERATURE ANNEALS ON FRESHLY COLD-WORKED WIRE (TWISTED 90° FOR 20 MINUTES).

Effects of Low-temperature Anneals on Elastic After-effect in Cold-worked Wires

In order to study the effects of low-temperature anneals, it was necessary to prepare freshly cold-worked specimens free from locked-in torsional stresses. This was done by first giving an anneal at 750° to 800°C., thus completely eliminating the effects of prior cold-work, then laying the wire on a smooth, flat surface and rolling longitudinally until the specimen was partly flattened. Elastic after-effects were then observed after holding for given times at various temperatures. In Fig. 15 are plotted the after-effects at 40°C. of one such

properties of the wire immediately following cold-work change rapidly even at 40°C. Curves e and f show that treatment at 300° to 350°C. practically eliminates anelasticity below 100°C., but that between 100° and 200°C. a considerable amount remains, while above 200°C. it increases very rapidly. This last phenomenon was wholly unexpected, and obviously was to be attributed to some other factor than prior cold-work.

The same experiments were also analyzed in terms of relaxation spectrum, the value of ψ for 0.1 min. relaxation at each temperature being calculated from the slope of the elastic after-effect curves, as previously

described. The values of ψ for curves e and f are plotted in Fig. 16, and the after-effect curves themselves for the points of curve e are plotted in Fig. 17. Referring to Fig. 16,

temperature annealing. The right-hand component, which rises steeply from zero, does not appear to have been observed before. Evidence is given later for the sug-

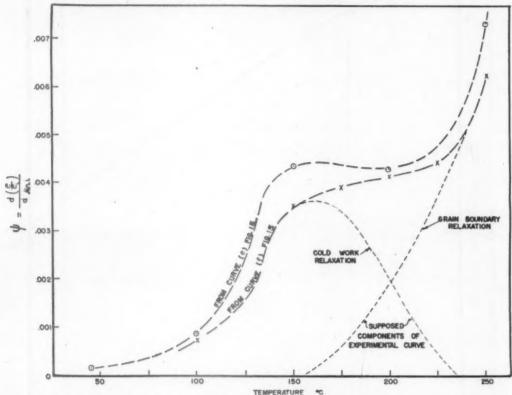


FIG. 16.—RELAXATION SPECTRUM. EFFECT OF LOW-TEMPERATURE ANNEALS ON FRESHLY COLD-WORKED WIRE (TWISTED 00° FOR 20 MINUTES).

we find once more a steady rise through 100° to 150°C., a "plateau" from 150° to 200°C., and finally a very rapid rise through 250°C. Later experiments show that still higher temperatures of anneal completely suppress the left-hand parts of the curve, leaving only a single branch, which rises steeply from zero, beginning at higher temperatures. It seems very probable, therefore, that the experimental curve actually consists of two components, as indicated by the lightly dotted lines. The left-hand component, which rises to a maximum and then falls, is considered to be due to the prior cold-work, whose effect has not been completely eliminated by lowgestion that it is due to relaxation at the grain boundaries.

Fig. 17 is of some interest in the theoretical interpretation of elastic after-effect. As pointed out previously, for a specimen with a constant relaxation spectrum the after-effect curve is practically a straight line in its earlier part, while in an increasing relaxation spectrum the curve is a reverse S-shape, being therefore concave downward in its earlier part. The shapes of the after-effect curves in Fig. 17 entirely confirm this relationship in a single specimen, whose relaxation spectrum is constant over one range, but increases over others.

Fig. 18 gives the results of a more de-

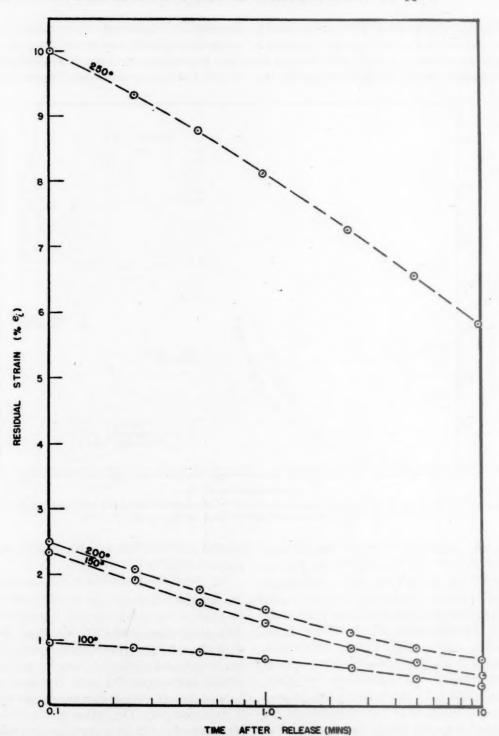


Fig. 17.—After-effect curves for different parts of relaxation spectrum (Curve ε of Fig. 15).

tailed study of low-temperature anneal. The specimen was prepared by the method rapid rise at higher temperatures is shown again.

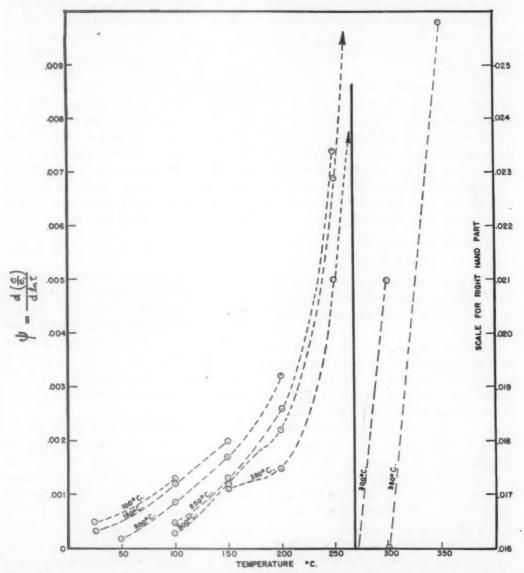


Fig. 18.—Relaxation spectrum of freshly cold-worked wire effect of low-temperature anneals. Held 100 minutes at each of indicated temperatures.

already described, but since there is no way of ensuring uniformity of cold-working, quantitative agreement between different specimens cannot be expected. The curves show the diminution of anelasticity caused by 100-min. anneals at successively higher temperatures, the development of a "plateau" in the curve is indicated, and the

Elastic After-effect in Fully Annealed (850°C.) Wires between 250° and 550°C.

It is well known that the ability of coldworked iron to manifest elastic after-effect at or near room temperature is completely removed by even low-temperature annealing. In the previous section it was shown that, while the above type of after-effect rapidly disappears as the temperature of annealing is raised, an apparently different type, of much greater amplitude, appears at higher temperatures. Wires were therefore annealed at 850°C., being heated slowly to that temperature, held 10 min., and cooled slowly. In these specimens recrystallization would be complete. Preliminary experiments showed that a 10° twist was safe, as far as danger of producing plastic deformation was concerned, while the magnitude of the effects to be observed made larger applied strains unnecessary. The wires showed a marked lower yield, an attempt to bend producing a series of angles rather than a smooth curve.

THE HIGH-TEMPERATURE ELASTIC AFTER-EFFECT

In Fig. 19 are plotted the results of measurements made from 250° to 550°C. At lower temperatures there was no aftereffect.

Total delayed recovery was determined by twisting the wire 10°, holding for 10 min. at the given temperature, cooling to below 200°C., and releasing. The instantaneous recovery immediately took place, and the light spot then became stationary. When the wire was heated to a temperature approaching that of twisting, the delayed recovery made itself felt, and the temperature was raised slowly until the light spot again became stationary. This usually took place in about 5 min. and at a temperature about 115°C. above that of twisting. This movement was taken as the elastic after-effect, or delayed recovery. The difference between the original position of the light spot before twisting and the final point of rest was taken as the permanent set, or creep.

The wire was then twisted in the same way at the given temperature, and released at that temperature, readings of the light spot being taken, beginning o. 1 min. after release. These readings were then plotted against log time, as in Fig. 17, and the slope

of the resultant curve at o.1 min. was determined graphically. The delayed recovery after o.1 min. was determined by raising the temperature, as described above, until the light spot came to rest.

In Fig. 18 all the data are expressed in terms of percentage of instantaneous recovery (e_i) , since the latter measures the effective elastic strain impressed on the specimen at the time of release. The values of the relaxation spectrum ψ are calculated from the slopes of the curves at 0.1 min., by means of the same formula used earlier. The following values, calculated from the observations at 550°C., could not be plotted with the scale used in Fig. 18:

Total delayed recovery...... 273 % at 550°C. ψ....... 0.147 at 550°C.

The observations used in Fig. 18 were all made on a single specimen, but experiments with other, similarly treated wires, showed that the results were quantitatively reproducible within a reasonably narrow range. A later section will discuss methods of varying these anelastic properties, and will suggest an hypothesis to explain them.

TIME-TEMPERATURE RELATIONS

Before taking up the subject matter of this section, it is necessary to show that, in the ranges employed, values of the relaxation spectrum, calculated by the formula already given, are nearly independent of amplitude and time of application of strain. Table 3 shows that for a twist of 10° applied for 10 min. these conditions apply sufficiently closely.

TABLE 3.—Time-temperature Relations
Time of Application of Strain, 10 Minutes,
400°C.

4
0.0281
0.0294
0.0320
0.0400
C.)
¥
0.0275
0.0295
0.0420

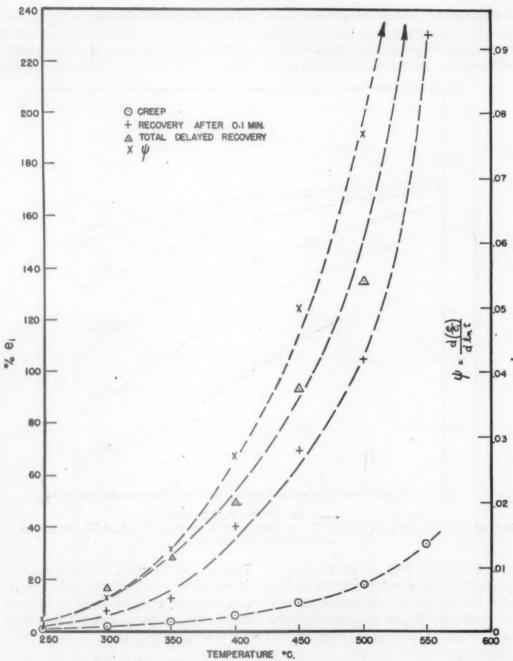


Fig. 19.—After-effect data at high temperatures. Wire annealed 10 minutes at 850°C. Twisted 10° for 10 minutes at given temperatures.

To investigate the relation of time to temperature the same method was used as in the previous study at lower temperatures. A wire was twisted 10°, held for 10 min. at a given temperature, then cooled to some lower temperature, and released.

Observations were made of the after-effect, at intervals, over 50 min. The delayed recovery was then brought to completion by raising the temperature as just described. This procedure was repeated at a series of temperatures, all lower than the chosen

temperature at which twisting took place. A series of curves was thus obtained, representing the after-effects at a series of temperatures produced by identical im-

is seen that where a series contains more than two points it closely approximates a straight line, and that all the lines agree closely as to slope, with two exceptions.

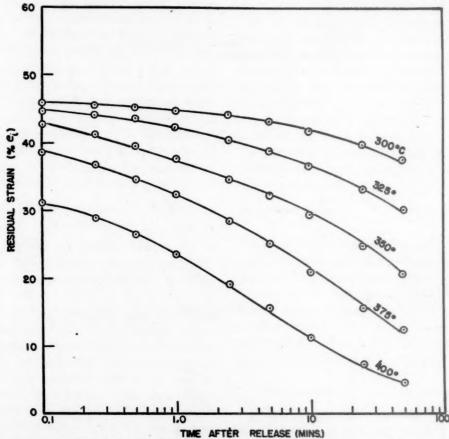


Fig. 20.—Wire annealed at 850°C., Twisted 10° for 10 minutes at 400°C., released at indicated temperature.

pressed strains. Fig. 20 shows such a series, the twisting being done at 400°C., while for Fig. 21 the twisting temperature was 450°. Still higher temperatures were not attempted because of the large amount of creep there encountered.

To test whether the time-temperature relation can be expressed in terms of a single heat of activation, the procedure was as previously described: For a given residual strain $\log t$ is plotted against 1/T for each curve of Fig. 20 that includes that strain. In Fig. 22 are plotted several series of such points for both Fig. 20 and Fig. 21. It

These two both involve the topmost curve of Fig. 21, which is nearly horizontal, so that a small constant error in residual strain would produce a large error in time. The average slope is taken as 11,000, or,

$$Q = 51,000$$
 cal. per mol

Using this heat of activation, and assuming the above relation of time to temperature, one may calculate factors for transforming any given relaxation time at one temperature to corresponding times at other temperatures. The factors that appear in Fig. 23 are designed to trans-

form times at the given temperatures to times at 300°C. The composite curves therefore represent the elastic after-effect curves at 300°C. resulting from a 10°

A SUGGESTED MECHANISM

The after-effect manifested by coldworked material at lower temperatures may be considered due to regions of at

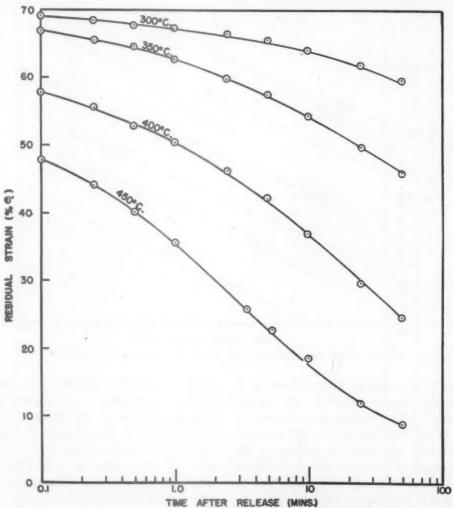


FIG. 21.—WIRE ANNEALED AT 850°C., TWISTED 10° FOR 10 MINUTES AT 450°C., RELEASED AT INDICATED TEMPERATURE.

twist applied for 10 min. at 400° and 450°C., respectively. The above interpretation, therefore, appears to be quite consistent with the experimental results, since nearly all the points fall along the continuous curves. As in the section on page 10 change of temperature appears to shift the relaxation spectrum as 11 whole.

least pseudo-amorphous nature, produced during the plastic deformation, and persisting thereafter for a shorter or longer time. Annealing at successively higher temperatures causes these regions to disappear, by recrystallization, beginning with those of shorter relaxation times, until the specimen is completely recrys-

stallized. The type of after-effect we are considering in this section seems to appear in the neighborhood of 200°C. (Fig. 18),

seems to support the suggestion that this anelasticity is due to relaxation along grain boundaries, since small grains correlate with

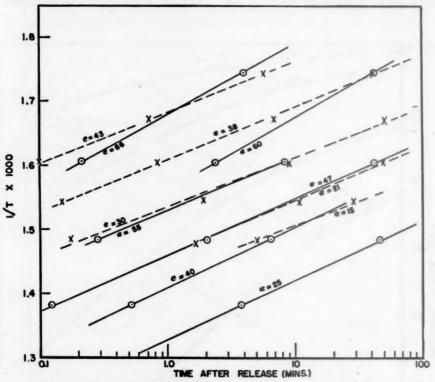


FIG. 22.—TIME-TEMPERATURE RELATIONS FOR GIVEN AFTER-EFFECTS.

at which temperature recrystallization is well under way, as shown by the marked lessening of low-temperature after-effect. Figs. 15, 16 and 18 indicate that the high-temperature after-effect diminishes as the temperature of anneal is raised. It seems legitimate to attribute this after-effect to the grain boundaries, which may be thought of as extremely thin films of a viscous nature, the viscosity decreasing with rise of temperature.

An obvious experiment is to apply treatments calculated to give different grain sizes, and then observe the difference, if any, of the after-effects manifested by the different specimens. Such an experiment was performed, and the after-effect was found to vary in an inverse manner to the grain size. This brief preliminary study greater after-effect. Obviously a more extended investigation is necessary before final conclusions can be drawn. Not only should effects of altered grain size be systematically examined, but also such subjects as grain-boundary precipitates or other heterogeneity, as well as gross chemical composition.

Summary

By means of a method employing given applied strains, torsional elastic aftereffects have been observed in iron wires of a considerable degree of purity.

In the after-effect manifested by coldworked wires, measured between 20° and 100°C., it is shown that relaxation time can be correlated with temperature by means of a heat of activation of 21,000

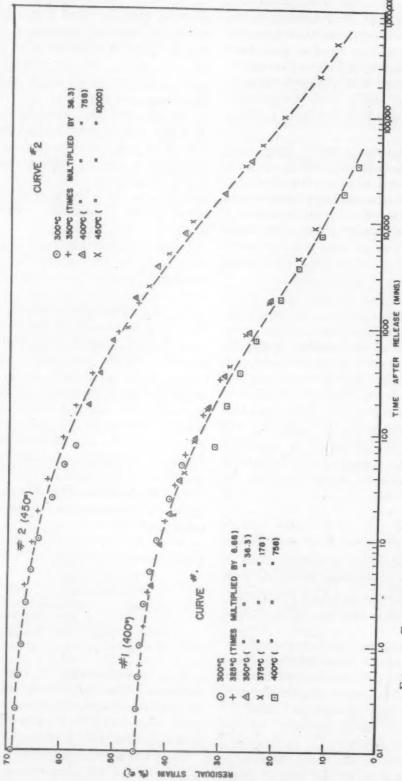


Fig. 23.—Elastic after-effect at 300°C. after straining 10° for 10 minutes at given temperature.

cal. per mol. This heat of activation is to be associated with the viscosity of slip bands. Values of the relaxation spectrum for this material over the range given have been calculated from observed relaxation rates, and have been shown to increase more or less slowly with temperature, and to be increased by increasing amounts of cold-work.

Low-temperature anneals have been shown to diminish the ability of coldworked material to show after-effect, the after-effect observed at lower temperatures being eliminated first. Wires annealed at 300° to 350°C., which still show this type of after-effect in the range 100° to 200°C. show at higher temperatures what seems to be a distinct type of after-effect.

This latter type of after-effect, which has not, apparently, been previously reported, shows very large effects, up to 50 per cent of the applied strain. Its relaxation spectrum increases rapidly up to 550°C., the highest temperature of measurement. The heat of activation of this type is found to be 51,000 cal. per mol. It is not eliminated by annealing, but appears to be diminished by increasing grain size The suggestion is made that it is due to shear-stress relaxation along the grain boundaries.

Appendix A.—An Anomalous After-EFFECT IN STRAINED RODS AND WIRES

The phenomenon described below is likely to be encountered in elastic aftereffect measurements at high temperature, and attention is therefore called to it at this time.

In an unpublished independent investigation in this laboratory, B. C. Ward observed that a 1/16-in. rod that has been plastically deformed in torsion and then released, at high temperature, shows: (1) instantaneous elastic recovery; (2) delayed elastic recovery; (3) twisting in a sense opposite to the above; namely, in the direction of the original twist for plastic

deformation. This last phenomenon was observed with the wires here employed, under the following conditions: (a) the wire had been annealed for some time at 450° to 500°C., but not higher; (b) a strain of 90° was applied at 350° to 400°C.; the temperature was raised (after release) to 450° to 500°C.; (c) a weight of about 50 grams was suspended from the wire. The effect was not observed at lower temperatures, nor in wires annealed at 850°C. Replacement of the 50 grams weight by a glass damping cylinder of about 10 grams markedly reduced the effect.

To test the hypothesis that the twisting was caused by the pull on the wire, a removable weight was devised, which could be attached or detached during a series of observations without unduly disturbing the setup. A wire, with 10gram weight attached, was twisted and released, and the temperature was then raised. After the delayed recovery was completed the reverse effect noted above appeared. Its rate of movement was recorded, the weight was increased to 75 grams and the rate once more was observed. The extra weight was removed, and then once more added. Table 4 gives the results as degrees per minute of reverse movement, in the direction, that is, of the original applied strain.

Table 4.—Reverse Twist in a Strained Wire

***	-																		4	n		. 30	
WBIGHT,	GR.	A.2	M:	8					W	1	0	V.	E	M	H	5]	A.	г,		DEG.	PER	MIM	
10																		-	0	.20			
75																			2	.0			
10						*			*								6	-	0	.15			
75						*				*	*				2		0		Ï	. 8			

These results seem to confirm the explanation that the twisting was caused by tension on the wire. Ward's experiments were made with a heavy steel chuck attached to the lower (free) end of the rod.

The following is suggested as a possible mechanism for this phenomenon: A wire

of fibrous structure held under torsional strain at these temperatures, or given torsional deformation, assumes a somewhat spiral internal structure. Under tension, creep takes place along the boundaries of the elongated grains that make up this structure, and a rotation of the end of the wire results, in the direction of twist of the spiral. The effect is found in wires such as No. 2 of the last section, which retains a fibrous structure, but has not been observed in a specimen such as No. 1, which is uniformly granular.

References

I. C. Zener: Anelasticity of Metals. This vol-

ume, page 155.
2. A. Johnson: The Creep Recovery of a 0.17
Per Cent Carbon Steel. Proc. Inst. of
Mech Engs (1041) 146, 187.

Mech. Engs. (1941) 146, 187.
3. F. Kohlrausch: Experimental-Untersuchungen uber die elastische Nachwirkung bei der Torsion, Ausdehnung und Beigung.

Ann. Physik Chem. (1876) 8, (6) 337.
4. L. Boltzmann: Zur Theorie der elastische

 L. Boltzmann: Zur Theorie der elastische Nachwirkung. Ann. Physik (1876) 7, 624.

 Schlotzer: Zisch. Instrument. (1937) \$7, 371.
 G. Richter: Chapter on Uber magnetische und mechanische Nachwirkung in Probleme der Technischen Magnetisierungskurve, edited by R. Becker. Berlin, 1938. Springer. (See Ref. 1, Fig. 9.)

DISCUSSION

(G. Edmunds presiding)

A. SKAPSKI.*—I should like to touch on one point in Dr. Zener's paper, i.e., Rosenhain's theory of the amorphous substance, which he assumes to exist in slip bands and grain boundaries (pp. 161 and 164).

If we consider all the problems that have to be explained by Rosenhain's "amorphous state theory," we must say that it has failed to furnish sufficient explanation and generally is not accepted any more. On the other hand, it seems certain, I believe, that nowadays we cannot look upon grain boundaries as mere geometrical lines forming some pattern that indicates where the crystals of the metal meet or where there is a discontinuity of the direction of crystal axes. I think, rather, we may take it for granted that in many cases consider-

able differences in concentration have been actually found in the composition of the grain boundaries and the bulk of the grains. In a recent book published by Taylor⁷ the microradiograms indicate clearly very distinct differences in composition of certain alloys in grain boundaries, and in the grains themselves.

Some investigations done recently in Stockholm by Benedicks and myself (using a special chemical technique of tracing the composition of thin sheets by volatilizing some components of the metal and leaving the others in situ) leave no doubt that we have to reckon with great differences in composition in the grain boundaries and in the bulk. This is not surprising, either, if we remember that the difference in surface tension (surface energy) between different planes (e.g., 1-0 and 1-1-1) of the same crystal may be estimated to be as high as 300 ergs per square centimeter. This is quite a high value for the interface free energy, which must, of course, have the tendency to decrease by concentrating (adsorbing) capillary-active substances in accordance with Gibb's law of adsorption.

Why do I say all this? Because if we take up again Rosenhain's theory and substitute for his term "amorphous substance" in the grain boundaries the words "substance of different composition," and, consequently, of different properties, we may well be successful in retaining all that is good in his theory without being forced to accept the rather difficult conception of amorphous state in grain boundaries.

What results from this point of view is that equilibria in solid metals must be considered with respect to the presence of interfaces possessing free energy. As has been shown by J. J. Thomson, the latter will influence these equilibria and the reactions will be shifted by the presence of grain boundaries in such direction as to produce predominantly the products that lower the surface tension.

On the other hand, systems usually are treated from the thermodynamic point of view with exclusion of presence of any external force. We are justified in expecting the influence of such forces (stresses and strains) on the equilibria, and the equilibria in the grain boundaries should be most sensitive to it.

If, instead of amorphous ones, we now assume

^{*} University of Chicago, Chicago, Illinois. London, 1945.

⁷ Taylor: X-Ray Metallography, 323-325 London, 1945.

grain boundaries having different composition (and different mechanical properties) caused by adsorption equilibria, and if we consider our system under stress, we should expect that the state of equilibrium corresponding to the stress conditions will be different from that in the metal without stress. The shifting of this equilibrium state will occur with a definite speed, involving some energy of activation similar to this assumed by Dr. Zener. If we come back from the state of stress to that of relaxation, similar shifting will occur in opposite directions.

I do not think that the assumption of any amorphous state is really necessary to explain the phenomena treated by Dr. Zener. The existence of the different compositions at the grain boundaries because of the adsorption equilibria should be sufficient and—although I cannot be more precise at present—should work in the same direction as Rosenhain's theory of amorphous state in the way that was pointed out by Dr. Zener.

C. ZENER. *- As I recall Rosenhain's work, he speaks of grain boundaries behaving in a viscous manner. In order that a shearing stress may be gradually relaxed in a viscous manner across a surface, it is not necessary that an amorphous region shall exist; it is merely necessary that the atomic arrangement across the boundaries be of a noncrystalline character. Obviously, at the boundary of two grains, unless the two grains are twins, the atoms on the two sides of the boundary are not arranged in a common geometrical pattern. So it is not at all necessary that there be an amorphous region for shear stress relaxation. As Dr. Skapski has said, the rate of such stress relaxation should be greatly influenced by the impurities that lower the surface tension; which, therefore, concentrate along the grain boundaries.

If the difference must occur from deep in the interior, then I can say that is not correct because the kinds of diffusion are too large. However, he would say the diffusion would occur from a short way off. He may of course be right. We are conducting experiments on mercurials, which if they give the same result, will I think, indicate that that viewpoint cannot be adopted.

J. C. McDonald.*—I would like to report an experimental observation which Dr. Zener might like to incorporate in his general theory of metals. We believe that magnesium is an exception to the statement that when stressed to rupture over long periods of time, their ductility decreases. Most of the alloys we have studied over a considerable range of temperature and up to times of a thousand hours have the same or higher ductilities at fracture as in a short-time test.

W. B. Brooks. †—The subject of anelasticity is one of intense practical importance, and it has not received enough attention. It seems to me that precise conformance to Hooke's law would detract greatly from the useful properties of our structural steels and cause them to behave in a very brittle manner. It has come as a shock and disappointment to some who practice as engineers to discover that structural steels do not exactly conform to Hooke's law, and that some of them possess distinctly curvelinear stress-strain relationships at stresses well below their yield strengths. Indeed, such steels have been avoided often in applications wherein a relatively high degree of anelasticity would have been most desirable. In massive and monolithic types of structures of a material having complete elasticity, stress-concentration effects would be disastrous, and severe dynamic loads would be transmitted undiminished to points of weakness. It is hoped that the authors will continue their work on this important subject.

C. Zener.‡—As has been pointed out by Dr. Skapski, a concentration of impurity atoms at grain boundaries will have a marked effect upon the rate of shear stress relaxation across these boundaries. It is believed, however, that his view is incorrect that the change of concentration of impurities at the boundaries due to stress application gives rise to the observed anelastic effects. The anelastic effects arising from such changes in concentration would be several orders of magnitude smaller than are observed. Dr. Skapski is right in saying that the

T Contributed for W. A. West, the author, who has returned to the University of Beirut, Svria.

^{*} Professor of Metallurgy, University of Chicago, Chicago, Illinois.

^{*} The Dow Chemical Co., Midland, Michigan.

[†] Metallurgist, Alloys Development Co., Pittsburgh, Pennsylvania. ‡ Contributed for W. A. West, the author,

presence of an amorphous layer at grain boundaries has never been demonstrated. An amorphous layer of finite width is not, however, necessary in order that shear stress be relaxed in a viscous-like manner. It is merely necessary that the atoms on one side of a grain boundary have no crystallographic relation to the atoms on the other side of the boundary. The laws that govern the resistance of the grain boundary to shear stress will then be different from the laws that govern the resistance to shear stress of a crystallographic plane in a single crystal. The laws will be more akin to those

that govern the resistance to shear of amorphous substances.

The absence of the loss of ductility of magnesium alloys under creep conditions, mentioned by Mr. McDonald, suggests that in these alloys relaxation of shear stress across grain boundaries is negligible under creep conditions. It would be anticipated that in these alloys the anelasticity associated with grain-boundary slip will be anomalously small.

Mr. Brooks can be assured that the further study of the anelasticity of metals is being vigorously pursued.

Vicalloy—a Workable Alloy for Permanent Magnets

By E. A. NESBITT*
(Chicago Meeting, February 1946)

ABSTRACT†

A NEW permanent-magnet material has been developed with unusual mechanical as well as magnetic properties. Specimens that have been cast or subjected to a small amount of hot reduction by rolling or swaging may be machined, punched, tapped or drilled.

The composition range of the alloys is 30 to 52 per cent iron, 36 to 62 per cent cobalt and 4 to 16 per cent vanadium. After being either quenched, annealed or given the usual cold finishing passes and

1.0 × 10⁶ gauss-oersteds. This product is equivalent to that of the well-known Honda steel (36 per cent Co, 4W, 2 Cr, 0.8 C, 0.3 Mn, balance Fe).

Material handled in the manner just described does not depend on cold-working for its magnetic properties, and is known as Vicalloy I. The preferred composition for Vicalloy I is 38.5 per cent iron, 52 per cent cobalt and 9.5 per cent vanadium. When the alloys are first hot-worked, then considerably reduced in area by cold-swaging, drawing or groove rolling and

Designation	Attempted Composition, Per Cent			Treatment	Magnetic Properties		
	Fe	Co	v		Br	H_{θ}	BH10-0
Vicalloy II	44	52	4	Hot-swaged, 87 per cent cold reduction, 600°C. aging	18,000	55	0.7
Vicalloy II	38.5	53.5	8	Hot-swaged, 94 per cent cold reduction, 600°C. aging	14,200	130	1.4
Vicalloy II	38	52	10	Hot-swaged, 75 per cent cold reduction, 600°C. aging	11,700	195	1.4
Vicalloy I	38	52	10	20 min. at 1200°C, quenched in oil, 600°C. aging	9,000	300	1.0
Vicalloy I	38	52	10	I hr. at 1100°C, furnace-cooled, 600°C.	8,630	399	1.0
Vicalloy II	38	52	11	Hot-swaged, 75 per cent cold reduction, 600°C. aging	11,000	270	1.9
Vicalloy II	35	53	12	Hot swaged, 92 per cent cold reduction, 600°C. aging	10,500	300	2.0
Vicalloy II	35	52	13	Hot swaged, 91 per cent cold reduction, 600°C. aging	10,000	375	2.4
Vicalloy II	34	52	14	Hot swaged, 98 per cent cold reduction, 600°C. aging	10,000	525	3.6

then heated for 2 hr. at 600°C., such materials have a magnetic energy product of

then heat-treated, the magnetic energy product measured in the direction of previous extension is increased to 2.0 to 3.5 × 10⁶ gauss-oersteds. These higher values have been obtained only after cold reductions in area of 75 to 95 per cent. Material handled in this manner is known as Vicalloy II and the preferred composi-

* Bell Telephone Laboratories, Murray Hill,

New Jersey.

† Manuscript received at the office of the Institute Sept. 4, 1945. Issued as T.P. 1973 in METALS TECHNOLOGY, February 1946. The entire paper appears in Trans. A.I.M.E. (1946) 166, 415.

tion is 35 per cent iron, 52 per cent cobalt, and 13 per cent vanadium.

These alloys differ from the usual type of age-hardening alloys in that the gamma phase, stable at high temperatures, is dispersed in the alpha phase stable at low temperatures, instead of vice versa. The cold-working transforms the gamma to the alpha phase and the subsequent aging at 600°C. transforms part of the alpha back to the gamma phase, so that the age-hardened alloy consists of the alpha phase

with a small amount of gamma phase dispersed in it.

The accompanying table gives the permanent-magnet properties on a series of alloys of varying vanadium content after different mechanical and thermal treatments. Outstanding values shown in the table are a residual induction of 18,000 gauss for the 4 per cent vanadium alloy, and a maximum energy product of 3.6 × 106 gauss-oersteds for the 14 per cent vanadium alloy.

Grain-growth Inhibitors in Steel

By James W. Halley, Member A.I.M.E. (Chicago Meeting, February 1946)

"FINE-GRAINED" steels have been standard products for many years. This paper describes an investigation of the effects of some of the more common grain-growth inhibitors used to produce these steels. The properties, response to heat-treatment, and the deoxidation practice necessary to produce "fine-grained" steels have been the subjects of numerous papers. It has been shown that a substantial quantity of aluminum is necessary to produce this type of steel, and it has been indicated that titanium and zirconium produce a similar result. For some time there was a lively argument between those who felt that aluminum refined the grain and those who felt that aluminum oxide was the effective agent. This argument subsided with an apparent victory for those promoting aluminum oxide. Most of the work on grain size has divided steels into two broad classifications based upon McQuaid and Ehn's original carburizing test at 1700°F. or some similar test at this temperature. If the steel coarsened at this temperature, it was coarse grained, while if it did not it was fine grained. Quantitative data concerning how much a certain amount of aluminum raised the coarsening temperature and affected the properties, all other factors being constant, are very meager. Similar information regarding titanium and zirconium is practically nonexistent.

The published information on aluminum yields some quantitative information. Epstein, Nead and Washburn1 gave the first

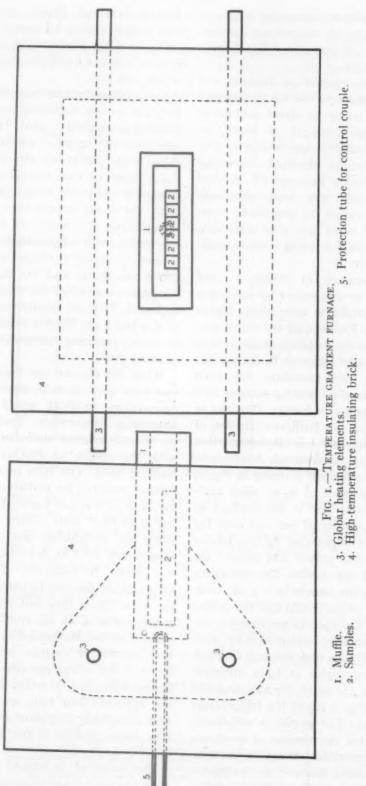
quantitative information on the amount of aluminum necessary to prevent grain growth at 1700°F. They showed that the addition of a pound to a pound and a half of aluminum per ton (0.05 to 0.075 per cent) would assure steel that would not coarsen during a McQuaid-Ehn test at 1700°F. Herty, McBride and Hough2 reported that a steel containing 0.020 per cent acid-soluble aluminum coarsened between 1742° and 1832°F., while steels containing 0.016 per cent and 0.017 per cent acid-soluble aluminum coarsened between 1652° and 1742°F. compared with similar aluminum-free steels that started to coarsen at 1580°F. Herty³ also showed a marked improvement in low-temperature notched impact resistance with increasing acid-soluble aluminum up to 0.030 per cent. McQuaid4 compared the coarsening of steels containing 0.011 to 0.204 per cent total aluminum and found a maximum coarsening temperature at 0.008 per cent aluminum. He had no samples between 0.015 and 0.098 per cent aluminum. Houdrement⁵ found a marked decrease in coarsening temperature with aluminum contents above 0.50 per cent. Kinzel, Crafts and Egan⁶ found that aluminum and zirconium improved the low-temperature impact resistance of a low-alloy steel, while titanium was detrimental. Sims7 shows that sulphur increases the coarsening temperature and that the maximum coarsening temperature is between 0.04 and 0.06 per cent added aluminum. The fact that the coarsening temperature passes through a maximum with increasing aluminum content appears to be well established. The aluminum content that

Manuscript received at the office of the Institute Dec. 26, 1945. Issued as T.P. 2030 in METALS TECHNOLOGY, June 1946; also in Open Hearth Proc., 1946.

* Metallurgist, Inland Steel Co. East

Chicago, Indiana.

¹ References are at the end of the paper.



gives the maximum coarsening temperature appears to be somewhere between 0.020 and 0.10 per cent of metallic or acidsoluble aluminum.

The only information on titanium and zirconium appears to be by Comstock.⁸ He added titanium to steels containing relatively large amounts of aluminum (0.05 to 0.15 per cent) and, with over 0.24 per cent titanium, obtained coarsening temperature higher than 1950°F. A steel containing 0.036 per cent zirconium showed no increase in coarsening temperature and 0.098 per cent zirconium produced a marked lowering of the coarsening temperature.

The temperature at which a steel coarsens can be determined by heating a number of samples to successively higher temperatures. The samples are cooled at a rate to outline the austenite grains so that coarsening can be followed. In the present investigation, this procedure has been greatly simplified by heating samples in a gradient temperature furnace. The use of such a furnace so facilitates studies of grain coarsening that a detailed description of the procedure is warranted. A schematic drawing of the furnace is shown in Fig. 1. The muffle is made of ½-in. thick heatresisting plate so that it will conduct an appreciable quantity of heat out from the hot end. Heat is provided by two Globar heating elements placed just beyond the back end of the muffle. The specimens consist of 1/2-in. square bars 5 in. long. The position of the muffle and the setting of the control couple to produce the desired gradient were determined by trial. A dummy specimen with 18-gauge chromelalumel thermocouples at 1/2-in. intervals was placed in the muffle for adjusting and calibrating. Fig. 2 shows the temperature gradient used. The muffle is sufficiently massive so that the number of specimens makes no appreciable change in the temperature gradient. About 2 hr. is required for the furnace to reach a stable condition. The gradient will change slowly over a long period of time because of decreasing thickness of the muffle at the hot end. The furnace is checked with the dummy sample before each run.

Low-carbon samples are oil-quenched from the furnace, sectioned longitudinally, polished and etched in nital. The temperature range during which coarsening occurs shows very clearly on the etched bars. Fig. 3 shows a series of samples containing increasing amount of aluminum. Since the grain coarsening occurs over a range of temperature, the results of the test are reported as two temperatures. The lower is the temperature at which the first coarse grains are found and the higher is the temperature at which fine grains have disappeared. Tests are usually run for periods of 2, 4 and 8 hr. There is a slight decrease in grain-coarsening temperature with increasing time.

When the furnace was first built there was some question as to whether or not a temperature gradient would affect the coarsening temperature. Tests were run on several hundred steels and compared with the results of McQuaid-Ehn carburizing tests. The tests in the gradient furnace were run for periods of 2, 4 and 8 hr., since it was not known how long the McQuaid-Ehn tests were at 1700°F. when the carburizing box was at this temperature for 8 hr. A perfect correlation was found between the McQuaid-Ehn tests and the gradient furnace tests heated for 4 hr. Steels that had not started to coarsen after 4 hr. at 1700°F. were fine grained in the McQuaid-Ehn tests; steels that started to coarsen below 1700°F., but were not completely coarsened at this temperature, had a mixed grain size in the McQuaid-Ehn test; and steels that were completely coarsened below 1700°F. were coarse grained in the McQuaid-Ehn test.

The effect of individual elements on grain coarsening was investigated by add-

ing increasing amounts of the elements to a series of ingots of an open-hearth heat. Additions of 1/4, 1/2, 1, 2 and 4 lb. per ton were made to successive ingots. Samples

per cent silicon were used for all of the series. Before grain-coarsening or physical tests were made, the samples were normalized from 1600°F. Results of an alumin-

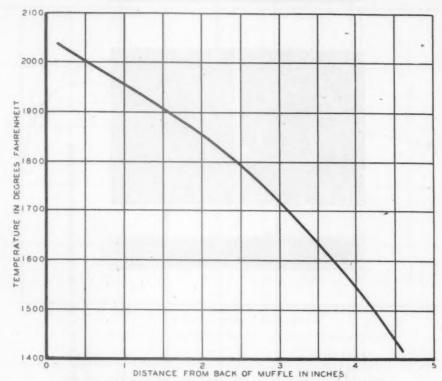


FIG. 2.—TEMPERATURE GRADIENT IN COARSENING FURNACE.

were taken from the middle cut of each ingot and forged to 1-in. rounds, which were used for grain coarsening and physical tests. Steels of about 0.30 per cent carbon, 0.80 per cent manganese and 0.25

TABLE 1.—Chemical Analyses of Aluminum Series

Alu- mi-		(Chemic	al Ana	lysis	, Per C	Cent	
num Addi- tion, Lb. per Ton	С	Mn	P	S	Si	Ti	Acid- solu- ble Al	Al ₂ O ₃
None	0.29 0.28 0.29 0.29	0.79 0.79 0.79 0.79	0.019 0.019 0.020 0.024	0.026 0.026 0.027 0.027	0.23 0.23 0.23 0.22	100.0 100.0 100.0 100.0 100.0	0.001 0.009 0.038 0.073	0.008

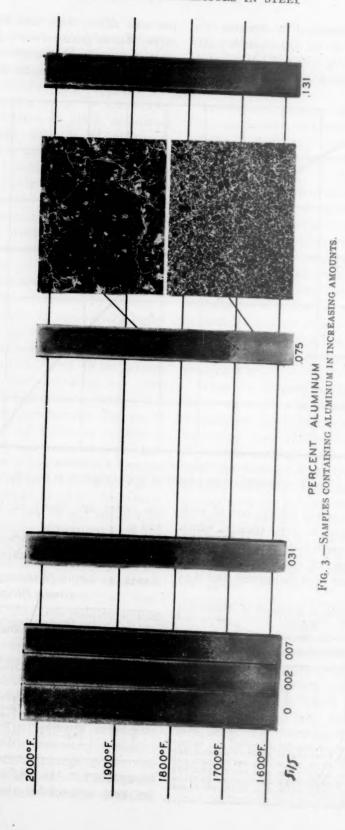
um series are shown in Tables 1, 2, 3 and 4.

The results of the coarsening test shown in Table 2 reveal a maximum coarsening

TABLE 2.—Grain-coarsening Tests of Aluminum Series

Acid-soluble	Grain-coa	Deg. F.	perature,
Per Cent	2 Hr. Heating	4 Hr. Heating	8 Hr. Heating
. 0	1530-1730	1510-1730	1500-1720
0.001	1540-1770	1540-1750	1540-1750
0.009	1730-1780	1710-1750	1700-1730
0.038	1790-1840	1730-1790	1740-1780
0.073	1640-1830	1640-1820	1640-1820
0.169	1540-1820	1540-1800	1540-1800

temperature in the neighborhood of 0.028 per cent acid-soluble aluminum. This is



shown graphically in Fig. 4, in which the mean of the grain-coarsening temperature after 4 hr. heating is plotted against the acid-soluble aluminum content. In addition

though there is a slight increase in strength and decrease in reduction of area with the larger additions. The notched impact resistance tabulated in Table 4 is greatly

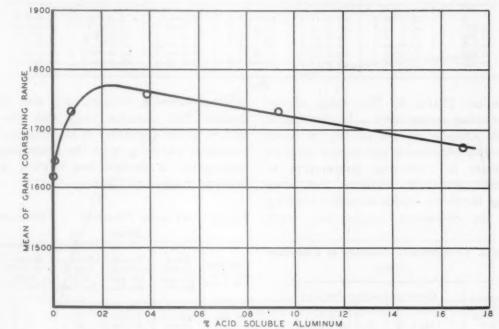


FIG. 4.—EFFECT OF ALUMINUM ON COARSENING TEMPERATURE.

to the lowering of the coarsening temperature by additions of over 0.028 per cent acid-soluble aluminum, the coarsening range is greatly widened by the higher aluminum additions. Larger quantities of aluminum lower the temperature at which coarsening starts, but cause little change in the temperature at which it is completed.

The tensile properties in Table 3 show little change with increasing aluminum,

TABLE 3.—Tensile Properties of Aluminum Series

Acid- soluble Alumi- num, Per Cent	Yield Point, Lb. per Sq. In.	Tensile Strength, Lb. per Sq. In.	Elonga- tion Per Cent in 2 In.	Reduc- tion of Area, Per Cent
0	52,000	76,000	32.5	60.0
0.001	51,000	76,000	31.2	47.5
0.009	51,000	77,000	31.0	52.5
0.038	52,000	76,000	32.5	58.0
0.073	55,000	78,000	30.0	53.6
0.169	55,000	79,000	31.0	53.6

improved by the addition of aluminum. The temperature at which brittle failure appears is reduced markedly and the amount of energy absorbed at room temperature is increased. This is not completely a grain-refining effect, because the largest aluminum addition reduces the temperature at which coarsening started to below the normalizing temperature of 1600°F. but does not raise the temperature of brittle failure.

The effects of titanium were investigated by adding metallic titanium to series of ingots from two heats. Low-carbon ferrotitanium could not be used because of its high aluminum content. The analyses and properties of these series are shown in Tables 5, 6, 7 and 8.

Titanium increases the coarsening temperature continuously up to 0.17 per cent

TABLE 4.—Notched Impact Resistance of Aluminum Series

Acid-soluble Aluminum,	1	С	harpy Impact,	Poot-pounds		
Per Cent	75°F.	o°F.	-25°F.	-50°F.	-75°F.	- 100°F.
0	35.0-36.0	22.5-22.5	18.0-18.0	16.0-3.5	3.0-2.0	2.0-2.0
0.001	37.0-35.0	26.5-25.0	24.5-21.0	20.0-20.0	15.0-2.5	6.0-2.0
0.009	39.0-38.0	30.0-30.0	28.0-28.5	28.5-25.5	20.5-19.5	17.5-3.0
0.038	41.0-40.0	35.5-33.5	28.5-28.0	25.0-21.5	21.0-20.0	19.0-17.0
0.073	37.0-39.0	29.0-30.0	20.5-24.0	22.0-26.5	23.0-20.0	22.0-20.0
0.169	37.0-38.0	30.0-32.0	29.0-27.5	25.0-25.5	26.0-24.5	21.0-17.0

titanium (Table 6). The mean of the coarsening ranges after 4 hr. heating of both series is plotted in Fig. 5. Small titanium additions do not cause as great an increase in coarsening temperature as similar aluminum additions, but since large aluminum additions cause a lowering of the coarsening temperature, much

TABLE 5.—Chemical Analyses of Titanium Series

Titanium Addition,		Chemical Analyses, Per Cent												
Lb. per Ton	С	Mn	P	s	Si	Al ₂ O ₈ a	Ti							
None	0.34	0.82	0.020	0.026 0.027 0.025 0.025	0.24	0.006 0.006 0.006	0.008							
None	0.3I 0.3I 0.3I	0.70 0.67 0.70	0.024 0.023 0.023	0.028 0.029 0.028 0.025 0.025	0.22 0.22 0.22	0.004 0.006 0.004 0.006 0.006	0.008							

a All the aluminum was found to be in the form of Al₂O₂.

TABLE 6.—Grain-coarsening Tests of Titanium Series

Titanium Content.	Grain-co	Grain-coarsening Temperature, Deg. F.								
Per Cent	2 Hr. Heating	4 Hr. Heating	8 Hr. Heating							
0.003	1400-1620	1400-1620	1400-1620							
0.008	1570-1700	1560-1680	1500-1660							
0.033	1760-1830	1710-1790	1710-1740							
0.003	1420-1640	1410-1640	1400-1600							
0.008	1480-1740	1460-1720	1420-1650							
0.040	1770-1850	1720-1820	1720-1800							
0.085	1830-1925	1830-1900	1770-1850							
0.170	1900-1940	1870-1940	1854-1910							

higher coarsening temperatures can be reached with titanium than with aluminum. If the logarithm of the titanium content is plotted against the coarsening temperature, a straight line relation is found as is shown in Fig. 6.

TABLE 7.—Tensile Properties of Titanium Series

Titanium Content, Per Cent	Yield Point, Lb. per Sq. In.	Tensile Strength, Lb. per Sq. In.	Elonga- tion in 2 In., Per Cent	Reduc- tion of Area, Per Cent
0.003 0.008 0.016	\$0,000 52,000 52,000	81,000 81,000 81,000	31.8 32.2 31.8	56.2 58.9 54.8
0.033	42,000	77,000	32.2	50.I 59.2
0.008	48,000	77,000	32.2	59.8 58.6
0.085	55,000	80,000	32.5	60.4

The results of tensile tests recorded in Table 7 make it clear that titanium additions result in an appreciable increase in yield point and tensile strength with little change in ductility.

The impact results of Table 8 demonstrate that titanium has much less effect than aluminum on the notched impact resistance. Small additions result in some decrease in the temperature of brittle failure and in a modest improvement in room-temperature resistance. This is probably a grain-refining effect, as there is little improvement until the coarsening temperature is raised above the normalizing temperature. Large additions are detrimental to the notched impact resistance

despite the extremely fine grain size resulting from these large additions.

The effect of titanium and aluminum together were indicated in an aluminum

first aluminum series. The higher titanium resulted in an appreciable increase in coarsening temperature. This shown in Fig. 6 in which the mean of the coarsening

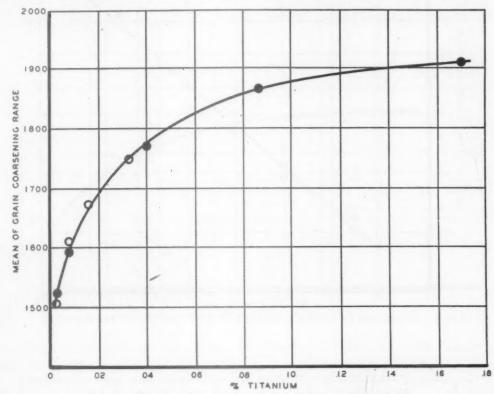


Fig. 5.—Effect of titanium on coarsening temperature.

series made from a heat in which enough ferrocarbon titanium was added to the ladle to give a residual titanium content of 0.005 per cent. This heat is practically identical in composition and physical properties with the heat described for the temperature after 4 hr. heating is plotted against the aluminum content.

A zirconium series was made by adding mixtures of ferrosilicon zirconium and ferrosilicon to a series of ingots of a lowsilicon heat. This involved the addition of

TABLE 8.—Notched Impact Resistance of Titanium Series

Titanium Content.	Charpy Impact, Foot-pounds											
Per Cent	75°P.	o°F.	-25°F.	-50°F.	-75°F.	-100°F.						
0.003	29.0-26.0	21.0-19.5	18.5-14.5	3.0-2.5	2.5-2.0	2.0-2.0						
0.008	32.0-30.0	25.0-17.5	21.0-15.5	3.0-3.0	7.0-2.5	2.0-2.0						
0.016	28.0-27.5	24.0-19.5	20.0-19.0	18.0-17.0	17.0-15.5	6.0-3.0						
0.033	30.0-27.5	25.0-21.5	21.0-19.5	17.5-16.0	17.0-16.0	15.0-4.0						
0.003	36.5-34.0	27.0-24.5	21.0-12.0	18.0-3.5	7.5-3.0	4.5-2.3						
0.008	36.0-34.0	25.5-25.0	18.5-4.0	21.5-19.0	2.5-2.5	3.5-2.3						
0.040	42.0-39.5	28.5-28.5	23.0-22.5	25.0-23.0	21.5-19.0	12.0-7.0						
0.085	41.5-40.5	28.0-25.5	23.5-23.5	24.0-20.5	20.0-19.0	12.5-3.0						
0.170	37.0-36.0	25.0-24.0	23.0-23.0	22.5	19.5-17.5	4.0-2.3						

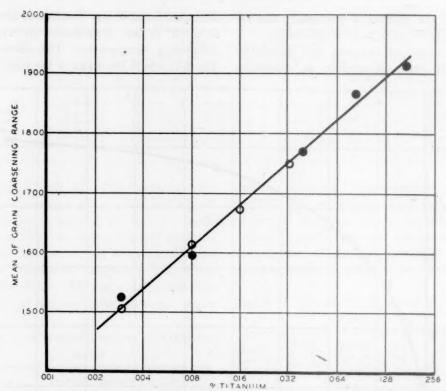


Fig. 6.—Logarithm of titanium content against coarsening temperature.

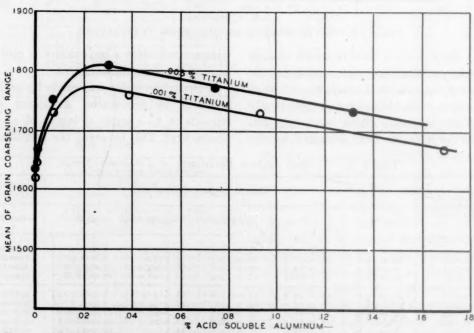


FIG. 7.—EFFECT OF ALUMINUM ON COARSENING TEMPERATURE WITH VARYING TITANIUM.

small amounts of aluminum and titanium, but much less than would have been added if low-silicon ferrozirconium had been used. The analyses and properties of the zirper cent. The mean of the coarsening temperature after 4 hr. heating is plotted against the zirconium content in Fig. 7.

Zirconium causes a slight increase in

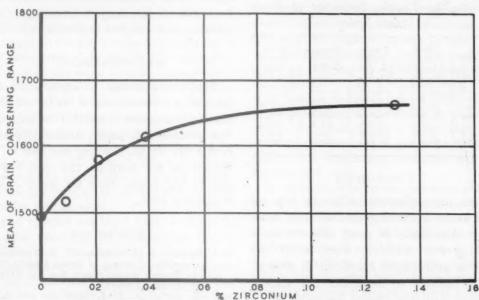


Fig. 8.—Effect of zirconium on coarsening temperature.

conium series are shown in Tables 9, 10, 11 and 12.

TABLE 9.—Chemical Analyses of Zirconium
Series

Zir- co- nium Addi-		С	hemic	al Ana	lysis,	Per C	ent	
tion, Lb. per Ton	0	Mn		co.		Al ₂ O ₈ °	Ti	Zr
None				0.028				
13				0.027				0.009
I				0.027			0.001	
4				0.019				

All the aluminum was found to be in the form of Al₂O₃.

The coarsening-temperature tests of Table 10 show that zirconium is less effective than either aluminum or titanium as a grain refiner. The increase in coarsening temperature caused by zirconium is not large, though continuous, up to 0.13

TABLE 10.—Grain-coarsening Tests of Zirconium Series

Zirconium Content,	Grain-coa	Deg. F.	perature,
Per Cent	2 Hr. Heating	4 Hr. Heating	8 Hr. Heating
None	1470-1570	1460-1530	1400-1500
0.009	1500-1650	1470-1560	1450-1540
0.038	1610-1790	1530-1700	1500-1660
0.134	1640-1810	1580-1750	1540-1700

yield point and decrease in ductility (Table 11).

Despite its modest effect on grain coarsening and tensile properites, the values in Table 12 demonstrate that zirconium has a profound effect on notched impact resistance. The temperature of brittle failure is reduced substantially by small additions, and the room-temperature resistance is increased. This is an alloying rather than a grain-

refining effect because the improvement in notched impact resistance is evident before the coarsening temperature is raised to the normalizing temperature.

TABLE 11.—Tensile Properties of Zirconium Series

Zir- conium Content, Per Cent	Yield Point, Lb. per Sq. In.	Tensile Strength, Lb. per Sq. In.	Elonga- tion, Per Cent in 2 In.	Reduc- tion of Area, Per Cent
None	46,500	77,000	32.5	62.0
0.009	47,000	76,000	31.2	61.3
0.021	47,000	77,000	32.2	61.4
0.038	48,000	76,000	30.0	59.1
0.134	48,000	75.500	32.0	58.7

Conclusions

The three elements differ in type as well as in degree of grain-inhibiting tendency. Aluminum is most effective as a grain-growth inhibitor when 0.028 per cent as acid-soluble aluminum is present. It is difficult to reconcile this critical amount with any theory involving graingrowth inhibiting by an aluminum oxide. The simple relation between titanium content and coarsening temperature indicates that the mechanism of grain-growth inhibiting by titanium is much less complex than that of aluminum. This relationship is perfectly compatible with, though not a proof of, grain-growth inhibiting by titanium carbide. Zirconium is less effective than either aluminum or titanium as a grain refiner.

The improvement in notched impact resistance at low temperatures by these elements is more of a direct alloying effect than the result of grain refinement. Grain refinement does improve the notched impact resistance and it is therefore difficult to distinguish alloy and grain-refining effects. Considering the alloying effects alone, aluminum and zirconium are beneficial to low-temperature impact resistance, and titanium is detrimental.

ACKNOWLEDGMENTS

The writer wishes to express his appreciation to the officials of the Inland Steel Co. for permission to publish the information given in this paper. Acknowledgment is due Mr. P. W. Nutting and Mr. C. C. Brown for the work on the open hearth and to Mr. Logan Mair for much of the laboratory work.

REFERENCES

- S. Epstein, J. H. Nead and T. S. Washburn: Grain-Size Control of Open Hearth Carbon Steels. Trans. Amer. Soc. for Metals (1034) 22, 042-072.
- C. H. Herty, Jr., D. L. McBride, and S. O. Hough: Effect of Deoxidation on Grain Size and Grain Growth in Plain Carbon Steel. Coop. Bull. 65, Min. and Met. Adv. Boards, Pittsburgh, Pa., 1024.
- Steel. Coop. Bull. 65, Min. and Met. Adv. Boards, Pittsburgh, Pa., 1934.
 3. C. H. Herty, Jr.: The Effect of Deoxidation on Some Properties of Steel. Trans. Amer. Soc. for Metals (1932) 23, 112-113.
- Soc. for Metals (1935) 23, 113-131.

 4. H. W. McQuaid: The Importance of Aluminum Additions in Modern Commercial Steels. Trans. Amer. Soc. for Metals (1935) 23, 797-838.
- 23, 797-838.
 5. E. Houdremont: Discussion. *Int.* Iron and Steel Inst. (1936) 134, 487p-493p.
- Steel Inst. (1936) 134, 487p-493p.
 6. A. B. Kinzel, W. Crafts and J. J. Egan:
 Fine-grained Structural Steel for Lowtemperature Pressure-vessel Service.
 Trans. A.I.M.E. (1937) 125, 560-583.
- 7. C. E. Sims: The Relation among Aluminum, Sulphur and Grain Size. Trans. A.I.M.E. (1045) 162. 734.
- (1945) 162, 734.

 8. G. F. Comstock: The Effect of Titanium on the Macrostructure and Grain-coarsening Temperature of Forged Steel. Trans. Amer. Soc. for Metals (1940) 28, 608-618.

TABLE 12.—Notched Impact Resistance of Zirconium Series

Zirconium Content, Per Cent	Charpy Impact, Foot-pounds						
	75°F.	o°F.	-25°F.	-50°F.	-75°₽.	-100°F.	
None 0.009 0.021 0.038	40.0-36.5 38.5-37.0 44.5-44.0 45.5-40.0	28.0-24.0 33.5-31.0 35.0-29.5 35.0-31.5	24.5-15.0 31.5-28.0 30.5-29.0 30.0-28.0	3.0-3.0 25.0-16.5 25.0-23.0 24.0-22.5	2.5-2.5 3.0-3.0 21.5-21.0 23.5-23.0	2.5-2.0 2.0-2.0 17.5-2.5 22.0-3.5	
0.134	41.5-38.0	34.0-32.5	27.0-26.5	27.0-24.0	21.0-20.5	17.0-8.0	

DISCUSSION

(R. L. Forrest presiding)

C. E. Sims. *- These are interesting data, which have been well presented. It was noted that there were differences in the effects of aluminum, titanium, and zirconium, notably in regard to notched-bar impact resistance at low temperatures. As Mr. Halley has pointed out, part of this seems to be an alloying effect, but there is also a coincidental change in inclusion types, which produces a superimposed effect. When small amounts of aluminum are added to steel, the silicates disappear, and the sulphides are changed from globular form to a eutectic type. Larger additions, sufficient to supply an appreciable unoxidized residue, reverse the form of the sulphides to a more massive, angular type.

The eutectic sulphides have a distinctly adverse effect on the notched-bar impact values, and the superior low-temperature properties are not obtained until the eutectic is destroyed with residual aluminum. This effect on notched-impact values is more pronounced in cast steel and is least apparent in rolled steel when the test is taken in the direction of rolling. Transverse tests may show the effect in an accentuated degree.

Zirconium produces the same eycle of changes in the sulphides as aluminum, but titanium acts differently. Small additions of titanium, but larger than required for aluminum, produce the eutectic type sulphides, but additional amounts do not reverse the trend. Instead, a more extreme eutectic type is produced, which turns light pink in color, indicating the formation of titanium sulphide.

Resistance to grain growth in aluminum-deoxidized steels has been attributed, in the past, to the presence of aluminum oxide. Considerable doubt has been cast on this belief of late, and it can be shown, for instance, that Al₂O₃ may be present when there is no inhibition to grain growth, that is, in a coarse-grained steel. A large number of careful analyses indicate that Al₂O₃ tends to reach a constant level of about 0.01 per cent in aluminum-deoxidized steels regardless of the aluminum addition. It is so constant, in fact, that the

best way to determine residual aluminum in steel seems to be to determine the total content spectrographically and subtract 0.005 per cent for the aluminum contained in the oxide. Residual aluminum, moreover, is necessary for fine grain. After the oxygen is satiated, the residual aluminum can form other compounds, such as nitride, sulphide, or even carbide.

It has been postulated that the causative factor in grain-growth inhibition must be a material that has an appreciable solid solubility in steel and that this solubility varies with temperature. This material is deposited in the boundaries of newly formed austenite and acts as a mechanical barrier to diffusion until such a temperature is reached that the barrier is dissolved.

In aluminum-killed steels, aluminum nitride seems to have all of the properties necessary to fulfill these requirements. It shows solid solubility that varies with temperature and does precipitate in grain boundaries. It seems a likely candidate for the honors. Titanium nitride, on the other hand, seems much too insoluble to function as a grain-growth inhibitor in titanium-treated steels, and in these, the evidence of high solubility for the sulphide (extreme eutectic) makes the latter a more likely material.

A. SKAPSKI.*—May I mention that a new technique developed in 1945 in Stockholm by Benedicks and myself offers a possibility of examining the distribution of various components in the grains and in their boundaries and may cast some new light on this problem?

In looking for the distribution of aluminum compounds in steel, thin sheets (0.02 to 0.1 mm.) reposing on quartz plate are treated with Cl₂ to get rid of Fe and then the remaining MnCl₂ is volatilized by the action of gaseous HCl at high temperature. All metallic substances are removed in this way; the distribution of remaining aluminum compounds is then examined under the microscope and the compounds themselves identified by microchemical reactions. In aluminum-regulated steels, Al₂O₃ residue seems to form a rather distinct network. Further investigations going on in the Institute for the Study of Metals at the University of Chicago should tell whether this network really

^{*} Battelle Memorial Institute, Columbus, Ohio.

^{*} University of Chicago, Chicago, Illinois,

corresponds to the austenite grain boundaries, and whether Al₂O₃, of which it mainly consists, did originally exist in steel or had been produced by the decomposition of aluminum nitride and subsequent reaction with the MnO and FeO oxygen.

J. W. HALLEY (author's reply).—The oxygen level in the steel before aluminum is added has been mentioned. Of course, this is important because it determines the amount of acid solid aluminum in the finished steel. The curves in the paper are based on acid-soluble aluminum. I am sorry I started the discussion of Al₂O₄ and aluminum as grain-

and the second second

growth inhibitors. There is not enough experimental evidence to support any theory, and theories were carefully avoided in the paper. As far as titanium is concerned, the facts are perfectly consistent with a theory of titanium carbide being the inhibiting agent. Such a theory is not necessarily true, but there is nothing to indicate that it is not true.

Mr. Sims' discussion of the relation between sulphide distribution and impact properties is a valuable addition to our information on this complex subject. There must be additional factors, however, because of the important influence of these elements on the longitudinal notched impact resistance of rolled material.

The Low-temperature Gaseous Reduction of Magnetite Ore to Sponge Iron

By O. George Specht, Jr.* and Carl A. Zapffe,† Member A.I.M.E. (Chicago Meeting, February 1946)

In recent print, some remarkably contradictory statements have appeared regarding the importance to be attached to sponge iron,1-6 a metallurgical commodity whose history goes back at least to the time of Diodorus Siculus in the fourth century B.C. This disagreement, however, expresses the lack of a satisfactory method for producing sponge iron rather than defection in the commodity. The blast furnace is admitted to have certain inherent disadvantages, such as a general unsuitability for magnetite and the heating and blowing of vast quantities of undesirable nitrogen, so that a workable sponge-iron process remains attractive.

In this respect, low-temperature gaseous reduction shows especial promise; but confusion persists regarding the factors involved.

The present paper, therefore, has three principal divisions: (1) an exhaustive examination of all previous work on low-temperature gaseous reduction, (2) experi-

mentation on the reduction of a magnetite with hydrogen, and (3) development of certain thermodynamic relationships in reduction, with a summarized depiction of the factors in the general process.

PREVIOUS INVESTIGATIONS

Gaseous media used in the reduction processes under discussion can be classified in three types: (1) H₂, (2) CO, and (3) other gases. In the second, the CO is often admixed with H₂. The third principally comprises hydrogeniferous gases, such as natural gas and producer gas, and in addition includes chlorine.

Because hydrogen therefore features in all three, a study of hydrogen reduction based on investigations using pure hydrogen alone may be incomplete. The present paper reviews the three groups of investigations in the listed order, paying particular attention to hydrogen reduction. For the benefit of future workers, an exhaustive bibliography has been prepared and similarly classified.

GROUP I: REDUCTION WITH HYDROGEN

Equilibria

Although the present problem is specifically one of kinetics, a first consideration is the equilibrium of the system, since the reactions to be studied comprise that equilibrium, and their direction and end points are defined by it. The historic development of these researches is interesting and informative.

The experimental work reported in this paper was performed by the senior author as undergraduate research under the direction of Prof. T. L. Joseph, Assistant Dean, Department of Mining and Metallurgy, Institute of Technology, University of Minnesota. The thesis by this title received the Andrews prize of the Minnesota Chapter of Sigma Xi, the Student Prize of the Northwest Chapter of A.I.M.E., and the 1943 Undergraduate Award of A.I.M.E.

Manuscript received at the office of the Institute July 20, 1944; revised Sept. 11, 1945. Issued as T.P. 1960 in METALS TECHNOLOGY, June 1946.

^{*} Lieutenant (jg), U. S. N. R.

[†] Consulting Metallurgist, Baltimore, Mary-land.

¹ References are at the end of the paper.

St. Claire Deville8 is often credited with being the first to study the Fe-O-H system. but Debray⁷ preceded him by 13 years. And Debray in turn undertook his investigation to check the statement made earlier by Bertholet that, in accordance with Bertholet's concept of mass action, steam should oxidize iron to iron oxide at the same temperature that hydrogen reduces the oxide to metallic iron, a startling statement at that time. Debray, working nearly a century ago, moistened H₂ at dew points providing ratios of $H_2O: H_2 = 1:1, 2, 3, \text{ and } 4, \text{ and found that}$ the first three formed oxide from iron, but that the 1:4 mixture reduced Fe₃O₄ to Fe. No temperatures were given.

St. Claire Deville,8 however, deserves credit for performing the first systematic investigation of the system Fe-Fe₃O₄-H₂-H₂O, in 1870, using controlled H₂-H₂O atmospheres in an apparatus serving as a model up to recent times. His technique was followed and refined by Preuner9 in 1904, Chaudron¹¹ in 1914, Wöhler and Prager12 in 1917, Schreiner and Grimnes¹³ in 1920, and Chaudron¹⁴ in 1921, and others up to the present time. 15,17,19-21,32,40,48,60 Chaudron 14 verified the existence of a quadruple point near 570°C. and developed the branched curve for Fe-FeO-Fe₃O₄ much as it stands today (Fig. 1). Other researches in this period might also be mentioned. 10,18,28,35, 37, 38, 41, 43, 44, 50, 54, 59, 62, 65, 68, 76

In 1920, Schreiner and Grimnes¹³ first directed attention to a great discrepancy among the results of these various investigators, whose values for the equilibrium constant, particularly at higher temperatures, differed widely and did not agree with that calculated by other means. Eastman, ¹⁶ writing a comprehensive paper in 1922, likewise discussed this discrepancy, as did Ferguson.²³ Neumann and Köhler²⁷ made an accurate determination of the water-gas equilibria, and then showed the unacceptable value provided by Fe-O-H

data. Krings and Kempkens, 29,33 with a rigorous research, established maximum values for K which lay below most of those obtained by others. The discrepancy prevented Ralston, in a masterful paper in 1929, 30 from smoothly combining calculations of ΔF based upon these data and upon the Third Law.

Finally, Emmett and Schultz, 32 in 1930, correlated all the data, grouping them along two separate curves, and two years later 40, 45 discovered that investigators using static atmospheres had provided the data for one curve and dynamic atmospheres the other, thermal diffusion in the static systems causing H₂O to accumulate preferentially in the cold parts of the apparatus. 51 For a measured H₂O-H₂ ratio, then, the effective ratio was hydrogen-rich in those experiments. The Fe-O-H system, similar to the Sn-O-H system, uses H₂O-H₂ ratios in a range making thermal diffusion especially important.

The equilibria culminating from these researches, depicted as one of the two sets of curves in Fig. 1, can now be regarded as securely established. They are represented on the thermodynamically useful coordinates $\log K$ and $1/T_{^{\circ}K}$ with the quadruple point at $565^{\circ}C$.

Temperature

Hydrogen begins to reduce Fe₃O₄ at 325°C., according to Olmer.⁷³ At 600°C. a rate maximum has been reported by Chufarov and his co-workers,^{52,53,57} Udy and Lorig,⁷¹ and Ramseyer.⁷⁷ Meyer²⁶ found sintering occurring at 650°C., which inhibited hydrogen infusion until 900°, where the rate of reduction again increased, presumably because of the greater solubility of hydrogen in gamma iron. Hofmann,^{24,25} attempting to imitate a blast furnace by using H₂, similarly reported a maximum rate for Fe₂O₃ at 550°C., with minima at 750° and 925°C. The minimum at 750°C. he suggested is

caused by the unreducible slags that form above 700°C.

Stålhane and Malmberg in a masterful series of papers^{31,36,43,55,56} showed reduc-

temperature range adds more confusion, for Hofmann's^{24,25} minimum at 925° is not necessarily in keeping with Barrett's^{48,49} selection of 950° as an operating tempera-

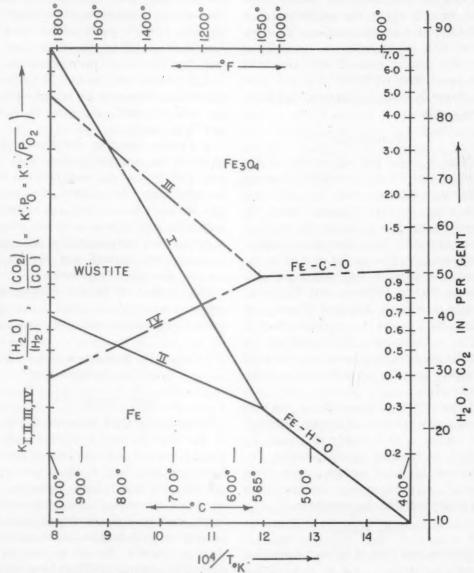


Fig. 1.—Depiction of the Fe-O-H and Fe-O-C equilibria in the range of low-temperature gaseous reduction.

tion at 910°C. to be much slower than at 890°, an observation having an obvious relationship to the alpha-to-gamma transformation, but in apparent contradiction to Meyer's ^{26,34} conclusion just noted.

Further examination of the higher

ture, although Hofmann reported a second maximum at 1000°C. Tenenbaum and Joseph's high rate at the intermediate temperature of 800°C. might seem confusing, but their tests were conducted under increased pressure; and pressure

will be shown to be an exceedingly effective variable.

Ramseyer⁷⁷ accounts for the 600°C. maximum on the basis of the Fe-O-H equilibrium diagram. He claims that FeO forming above the critical point is difficult to reduce and supports his argument with micrographs of semireduced ore. The present research will later treat this point directly, for it does not have the thermodynamic background that Ramseyer assumes.

Particle Size

There is some lack of clarity on the effect of particle size, principally because interfering factors, such as sintering, segregating, or pore clogging, affect the gas-solid contact and obscure the reaction. There has even been discussion whether metallization begins on the outside or the inside of a lump of ore, 47 although work such as that of Stålhane and Malmberg already mentioned, Klärding, 159 and Udy and Lorig 71 seems to establish that it begins on the outside. Oxide coatings on metallic particles that have been observed by others probably resulted from reoxidation by H₂O.

Hofmann^{24,25} recommends a particle size of 0.02 to 0.05 mm. diameter, although this matter is still widely discussed. In general, as particles become smaller, the advantage of larger surface-volume ratio is gained, but at the expense of permeability and other desirable characteristics.

Other Factors

Other factors that have been suggested as variables are:

- 1. Rate of gas flow. There is an optimum rate, which compromises between replenishment of the reacting gas and wastage, but must be determined separately for each type of unit.
- Permeability. An obvious factor in controlling gas-solid contact; not to be confused with porosity.

- 3. Impurities in the ore. By fluxing, for example, certain impurities may cause sintering and thereby seriously change the reducibility of the ore. Hofmann^{24,25} showed that both the 550° and 1000° maxima can be suppressed by adding MgO or SiO₂. Olmer⁶⁹ published an especially fine work detailing the formation and reduction of many of these impurities.
- 4. Impurities in the gas. Sedlatschek⁷⁰ effected an increase in the rate of reduction by adding small amounts of halides or CO₂ to the H₂.
- 5. Factors affecting diffusion and removal of the reaction product, H₂O. Udy and Lorig⁷¹ list six variables for that function alone. In addition, Sawamura⁶³ and Wiberg⁶⁷ have added the interesting suggestion that internal aerostatic pressure resulting from the products of the gaseous reaction may expand and disrupt the particle, thereby aiding effusion.

This listing of factors constitutes a general framework to which information from other processes will now be added.

GROUP II: REDUCTION WITH CO (AND CO-H₂ MIXTURES)

Early Investigations

Reduction by CO is rooted in the history of the blast furnace itself, but only researches that concern chemical and physical factors of importance to the present study will be considered here. Selection can be based somewhat upon temperature limits, and to a lesser degree upon the primary or secondary nature of the CO—that is, whether the ore is reduced by direct impingement of CO, or by admixture with a carboniferous material to produce CO in situ. For the most part, the latter is of but little interest to the present study.

Many of the investigations already discussed treated reduction both by CO and by H₂;⁷⁸ and Debray⁷ again stands first for studying Fe₃O₄ in CO-CO₂ atmospheres. Although he obtained no metallic

iron with the gas proportions he used, he did reduce the oxides of Ni, Co, and Zn completely, and the oxides of Mo and W to lower oxides.

Among subsequent investigators up to the turn of the present century,⁷⁹⁻⁸⁹ Sir J. Lowthian Bell^{80,81} was apparently the first to recognize the law of mass action in blast-furnace reactions; and his work, begun in 1868 with C. R. A. Wright, led to Åkerman's⁸³ establishing in 1883 rough measurements of the CO-CO₂ equilibrium over iron and iron oxide.

In 1903, Baur and Glaessner⁹⁰ published the Fe-O-C equilibria from 350° to 900°C. and calculated ΔH for Fe₃O₄ on the basis of data now known to be incorrect. In the same year, R. Schenck⁹¹ published a similar study, initiating his extensive work on this subject, which continued a few years 92,93,96 and then reappeared years later, in 1923,117,121 with the aim of applying chemical equilibria to blastfurnace reactions. His investigations led to a prodigious series of publications on Fe-C-O and associated equilibria, 129, 132-6, 142-4,147,148,164-7 finally winding up in prolonged polemics 138,141-4,154 and the admission that equilibrium was never attained in the blast furnace, time being the only important factor!

In between Schenck's two prolific periods, numerous papers and patents appeared,94-116 among which might be mentioned Mathesius'94,98,101,104 patents for producing sponge iron by CO reduction, Chaudron's14 and Matsubara's116 monumental papers on Fe-C-O equilibria, Eastman's thought-provoking critique of equilibrium determinations, and, most important, Wiberg's 115 first patent on his classic CO-reduction shaft furnace, built in 1920 at Woxna, Sweden-forerunner of the present Söderfors plant. In this furnace, Fe₃O₄ lumps up to 4-in. dia. were reduced at 1000°C., lumps 1.15 to 2.8-in. dia. requiring 20 to 50 hr. The CO2 reaction product was regenerated by passing the gas over hot charcoal.

In contrast to the rate maximum at 600°C. just discussed for H₂ reduction, Wiberg's CO process was 15 times faster at 1035° than at 600°C. The thermodynamic reason for this will be developed later.

R. Schenck's Studies

Many surprising things can be found among R. Schenck's wide writings in the 1920's, some since affirmed, others denied. Basing his conclusions upon the results of an elaborate and fundamental gas-metal study, Schenck discovered the solid solution of Fe₃O₄ and FeO, which he named "wüstite" in honor of a great German metallurgist. He showed that studies on the reduction of Fe₂O₄ must take into account the solution transition from Fe₃O₄ to FeO, and also the solubility of oxygen in metallic iron. In regard to the latter, he coined the terms "oxyferrite" and "oxyaustenite," and proceeded to overemphasize their importance on the basis of the monstrous deduction that from 2 to 5 per cent O can dissolve in Fe during carburizing. Because of this work, however, the intermediate field in Fig. 1 is more properly designated "wüstite," instead of the often used "FeO."

Again, Schenck claimed the existence of an iron suboxide, Fe₃O, probably stable below 720°C., and a percarbide of iron having a higher P_C than Fe₃C. The latter he named "bunsenite," in honor of another German scientist; but the honor has miscarried in the absence of subsequent confirmation. Bogitch, ²⁸ however, has reported an iron suboxide having less oxygen than FeO.

Next, Schenck pointed out the simultaneous solution of oxygen and carbon in austenite and showed that his data required solubility between oxides and carbides, an observation possibly corroborated by Becker's 150 and Winter and

Crocker's¹⁵⁶ work. The resultant solution he called "oxycarbide."¹⁵³ He also found a role for the evaporation of Fe as a carbonyl.

While these anomalies in the Fe-O system are of interest to the present research because they will influence removal of O from the ore by any process, especially pertinent are Schenck's studies showing the effect of MgO, SiO2, Al2O3, MnO, BeO, TiO2, P2O5, CaO, ZnO, CuO, and NiO on the rate of reduction of iron oxides. In brief, all these impurities affect reduction adversely whether they are reduced or not-a conclusion also reached by Fornander. 119 CuO and NiO are the only possible exceptions. Schenck discovered the importance of these impurities by finding completely different equilibrium values when an Al2O3 crucible was used instead of an MgO.

Schenck's Contemporaries

During this same period, noteworthy papers by other authors also appeared.21,23, 26,28,30,118-20,122-8,130,131,137-41,145,146 Royster, Joseph, and Kinney¹²⁰ measured CO₂ concentrations in an experimental blast furnace using ore of various sizes; and Furnas and Joseph 146,152 showed the necessity of gas-solid contact and uniformity of particle size. They recommended crushing lumps above 2-in. diameter, sintering minus 65-mesh material, dividing the ore into three sizes, and charging it separately to minimize pore clogging. Joseph¹⁴⁰ listed: (1) chemical nature of the ore, (2) fineness, and (3) uniformity as three principal factors in the rate of reduction. Iwasé127 included another factorthe expansive effect of occluded reaction products.

As for temperature, Kamura¹²⁴ found 900°C. an optimum for reduction of limonite and hematite, and temperatures above 900°C. for magnetite. Bogitch²⁸ recommended 1300°C. for iron silicate, which confirms Joseph's¹⁶⁹ conclusion that

iron silicate forms an undesirable reductionresistant film on magnetite.

Takahaski¹³⁰ and Johannsen and von Seth¹²⁸ pointed out that carbon dissolving in the iron strongly influences the CO-CO₂ ratio and therefore the optimum temperature of reduction.

Two monumental reviews appear in this period, one by Williams, Barrett, and Larsen¹³⁷ containing a bibliography of patents complete through 1925; the other, by Ralston,³⁰ presenting a comprehensive review of data extant in 1929. The CO-CO₂-Fe-FeO-Fe₃O₄ equilibria given by H. Schenck⁴² are believed to be the most accurate, and are depicted in Fig. 1.

Stålhane and Malmberg and Reduction with CO-H₂ Mixtures

One of the first important investigations on reduction by CO-H2 mixtures was that of Meyer²⁶ in 1928. He measured reduction rates with CO and H2 individually and mixed and found that H2 reduction was much more rapid than CO reduction under equal conditions, and that in mixtures the CO does not appear to be the active ore-reducing agent, but a regenerator of H2 from H2O instead. This is understandable, since H2 can penetrate Fe more readily than C or CO to reach unreduced ore, and the deoxidation of H₂O by CO is the well-known water-gas reaction. Meyer also observed a new factor—the breaking of lumps of ore from internal graphitization by CO; and he showed that hydrogen increases graphitization-although Bone, Reeve, and Saunders¹⁵¹ state the opposite.

Shortly thereafter, the two Swedish scientists, Stålhane and Malmberg, developed the theory and experimentation using CO, H₂, and CO-H₂ mixtures in an outstanding series of papers. 149, 155, 36, 43, 55, 56, 172, 173 By temporarily disregarding all physical factors influencing gas-solid contact, they developed for the reaction:

Iron Oxide + Reducing Gas = Iron + Gaseous Product the simple and general rate expression:

$$dm/dt = k \cdot s \cdot (P-P_e)$$

where:

m =mass of ore reduced,

t = time,

k = a constant,

s = surface of reaction,

 $P = \text{partial pressure of CO or H}_2$,

 P_e = partial pressure of CO or H_2 at equilibrium.

Consequently, they argued, the rate of reduction is simply proportional to the difference between the partial pressure of the reduced gas and its pressure at equilibrium. All other factors are important only in the extent to which they affect $P-P_e$.

Reduction from Fe₃O₄ to FeO they found rapid; from FeO to Fe slow. Like Meyer, 34,39 they were able to increase the rate of reduction from 4 to 7 times by adding 20 per cent H2 to the CO. An addition of 2 per cent H2 showed no effect. They suggested that the sixfold difference between the physical diffusion rates of H₂-H₂O and CO-CO₂ mixtures might account for this. Although Meyer had observed a drop in rate around 700°C. from metallization, Stålhane's tests were run for shorter periods and did not reveal that drop. Metallization, they found, begins on the surface and proceeds inward at an approximately linear rate except for the earliest and latest stages of reduction. A drop in rate around 906°C., similar to the one described for H2 reduction, was ascribed to the allotropic transformation of iron; and a break in the rate curve around 800°C. they ascribed to a lowering of the transformation temperature by dissolved carbon. Deposition of carbon they found to begin in late stages of reduction and to be completely inhibited by the presence of sufficient CO2. The latter, of course, can be predicted from the equation:

$$_2CO = C + CO_2$$

since the reaction goes to the right only

when the partial pressure of CO₂ is less than that required by the equilibrium.

Stålhane and Malmberg selected a temperature range of 900° to 1000°C. for their process. Particles of Kiruna magnetite from 0.2 to 4.0-mm. dia. were studied,36 though their patents172 recommend a maximum diameter of 0.2 mm. They also recommended 5 to 20 per cent additions of moist CaCO₃, or other alkaline earth substance, with a small quantity of soda or water glass to prevent caking and sticking of the finely divided ore. 178 When reduced, the sponge could be cooled in water and treated with CO2 to precipitate CaO and recover CaCO₃. The used gases, both H2O and CO2, were regenerated by passing over hot carbon.

Recent Work

Among the numerous publications appearing in the past 15 years, 35,38,42,44,46,49, 54,59,63,67,69,76,151,156-83 discussions of Wiberg's process are most interesting. 67,181 Wiberg 67 pointed out that reduction with CO is exothermic, causing a temperature increase of 100° to 150°C.; that H₂ reduction is endothermic, causing a temperature drop of approximately 350°; and that CH₄ or coke-oven gas requires so much heat that a retort furnace or special auxiliary heating is necessary, unless the CH₄ is first partly burned. A 64:36 mix of CO-H₂ causes no heat change.

Up to 75 per cent reduction, H₂ is faster than CO at 1000°C., but then loses efficiency rapidly, a CO-H₂ mix serving best. The high rate of CO reduction in late stages probably results from carburization of the iron, the dissolved C reacting with the enclosed wüstite to form rupturing pressures of trapped gas, a matter also discussed by Sawamura⁶³ and Baukloh and Jaeger.¹⁷⁴ Microscopic examination of partly reduced magnetite, similar to Udy and Lorig's⁷¹ and Klärding's¹⁵⁹ studies, showed an Fe shell, an intermediate layer of wüstite, and a magnetite core. No

porosity could be detected, but fissuring was evident. Wiberg remarks that with H₂ reduction similar entrapment is mitigated by the ability of H₂ to diffuse out through the Fe, leaving only H₂O. This reasoning is in error, as will be developed later.

Wetherill and Furnas¹⁷⁰ studied the effects of: (1) temperature, (2) ore type, (3) particle size, (4) gas velocity, and (5) gas composition, the last two factors remaining more or less indefinite. Reduction with CO they found slow at 500° to 600°C., becoming more rapid at higher temperatures, with nothing to be gained by temperatures above 1000°C. Slagforming constituents impeded reduction, but became less important at higher temperatures. As for particle size, they discerned no effect up to 1 cm. in diameter but the rate decreased with larger particles.

A distinction between porosity and permeability was pointed out by Joseph, Barrett, and Wood46 in a study of reduction of 13 commercial iron-ore sinters, porosity measurements indicating in no way the size, number, or distribution of the voids. Following Diepschlag's 171 excellent paper on reduction of iron ore under pressure, Tenenbaum and Joseph 176 found the rate to increase with CO pressure, with a temperature maximum occurring near 700°C. for higher pressures. Reduction with CO was slower than with H2, and still slower when admixed with bosh gas. These authors explained the pressure-rate relationship on the basis of surface adsorption in a convincing manner. Their discussion, and Körber's, 179 of carbon deposition is good, though thermodynamically incomplete.

An interesting and previously overlooked research by Scheepers, 180 in which magnetite was crushed, separated in three sizes, and treated in CO to study reduction and dissociation catalysis, deserves mention. The large particles were strongly magnetic, the medium particles weakly magnetic, and the fines nonmagnetic. No graphitization occurred over the fines; and a maximum occurred using the medium particles. Unsized material was strongly catalytic. These factors might be studied further in ore reduction. A slower rate of flowal so favored dissociation.

Similarly deserving mention is Gahl's patent⁵⁹ for regeneration by passing CO₂ and H₂O mixed with natural gas over Ni or Fe catalysts.

GROUP III: REDUCTION WITH OTHER GASES

Fuel gas, ^{188,190} coal gas, ^{192,198} water gas, ^{38,192} producer gas, ^{187,190,192,194} oil gas, ¹⁸⁵ ^{186,189,197} natural gas, ^{187,189,196,202-4} methane, ⁶⁷ illuminating gas, ¹⁹⁹ bosh gas, ^{49,195} and chlorine ²⁰⁰ are other media sometimes used for reduction. ^{184–204}

With natural gas or oil gas, Riveroll¹⁸⁹ recommended reduction in a high vertical retort furnace at 750° to 785°C. Maier and Thomas¹⁹⁶ state that magnetites are virtually unreducible below the sintering temperature in a natural gas having the following analysis: N₂, 42.7 per cent; H₂, 36.4; CO, 19.5; CH₄, 0.4; H₂O, 0.7; CO₂, 0.3.

Of greatest recent interest is the Madaras Steel Corporation's reduction plant operated at Longview, Texas, by the Bureau of Mines from November 1942 until February 1944.²⁰²⁻⁴ Reduction of lump ore by natural gas at 1000°C. yielded a product about 83 per cent metallized, which served successfully as a substitute for scrap in a steelmaking furnace.

Coal gas, according to Eastman, 192 reduces iron oxide at 600°. However, C deposition at that temperature is so severe that the CH₄ and unsaturated hydrocarbons are largely destroyed, and temperatures above 700°C. must be used. By raising the temperature from 700° to 1000°C., about 12 per cent is gained in maximum reducing power. Coal gas

requires more heat supplied to it per pound of iron produced than most other gases, but some of this heat can be obtained from combustion of the used gases.

At 600°C., water gas oxidizes Fe and deposits C;¹⁹² but about 700°C. the reverse is true. By raising the temperature from 700° to 1000°C., about 10 per cent is gained in maximum efficiency. The heat balance of water gas is favorable.

Producer gas likewise oxidizes Fe and deposits C at 600°, 192 reversing this action at temperatures above 700°C. At 1000°C., however, the maximum reduction is 30 per cent more efficient than at 700°; but the large proportion of N2 makes reduction slower, the thermal margin is inadequate, and from 3 to 15 times as much gas is required to reduce a pound of Fe as when using coal gas or water gas. The analysis of the producer gas used in Ekelund's process¹⁹⁴ for reducing Stripa ore and sinter is: CO, 33-36 per cent; H₂, 9.8; CH₄, 0.7; N₂, 55-59. Diepschlag, Zillgen, and Poetter, 195 discussing reduction up to 1050°C. with a blast-furnace gas of virtually this same composition, found reduction to increase directly with porosity, and graphitization to increase with decreasing particle size.

Reduction of Other Oxides

Information of some interest also lies in literature on the gaseous reduction of oxides other than iron oxide.²⁰⁵⁻²⁵

For example, Wright and Luff²⁰⁷ in 1878, and later Pease and Taylor,²¹² showed that the reduction of CuO by H₂ is an autocatalytic phenomenon requiring an incubation period before reduction begins, that the purity of the H₂ has much to do with the duration of this period, that the introduction of metallic Cu eliminates the incubation period, that reduction proceeds from the metal/metal-oxide interface, and that metallization does not begin, as commonly expected, at the surface of gas impingement, but within the ore

body and often along the tube wall. Similar observations with iron oxide do not appear in the literature; and the possibility of speeding reduction by admixing metallic iron holds some interest.

In the reduction of NiO, Pease and Cook²¹³ showed that equilibria determined for the massive state may not apply to reactions involving oxide films on metal and metal films on oxides because of the aggravated free energies of the films; and Fricke and Weitbrecht²²² made a similar observation for surface effects on very fine particle sizes. Both of these observations are pertinent to the present study.

Greenwood's research²⁰⁹ is interesting in showing the marked effect of impurities on reduction at higher temperatures, and in anticipating Olmer's⁷² temperature-interval technique for phase identification by about 40 years.

As for the stepwise reduction of $Fe_3O_4 \rightarrow FeO \rightarrow Fe$, which causes preliminary reduction to occur without metallization, this same type of phenomenon has been established for the reduction of Cr_2O_3 , 211,218 MnO₂, 209 PbO, 220 Ag₂O, 220 SiO₂, 223 and probably TiO₂²¹⁹ and other oxides. 226

EXPERIMENTAL PROCEDURE

Against this background, the following experimentation will be compared.

MATERIALS

A western New York magnetite concentrate, kindly supplied by the Republic Steel Corporation, served for all experiments reported in this paper. Its analysis was Fe, 65.92 per cent; SiO₂, 4.31; Al₂O₃, 3.93; Mn, 0.045. For the reduction of this magnetite, purified commercial tank hydrogen was used.

APPARATUS

The apparatus was of a type commonly used for such experiments, having the following gas train:

H₂(or N₂) → Catalytic Furnace → Absorption Towers → Reduction Furnace → Absorption Towers → Manometer → Exit

The catalytic furnace contained Cu turnings to remove free oxygen from the H₂ by catalyzing the H-O reaction; the absorption towers contained anhydrous magnesium perchlorate; the reduction furnace was an electric furnace containing a quartz combustion tube with the sample in a porcelain boat. The manometer was calibrated to measure the gas flow, which was kept constant at 1000 c.c. per min. throughout all experiments. Temperature measurement was effected by a thermocouple placed with the sample in the exact center of the furnace; and temperature control was maintained by manual adjustment of a resistance in the furnace circuit.

TECHNIQUE

The weighed sample of ore, contained in a carefully dried porcelain boat, was heated in an atmosphere of nitrogen, which was used to flush the system and to prevent either oxidation or reduction from occurring before the desired temperature was reached and the test was ready to begin. With the rate of gas flow adjusted to 1000 c.c. per min., alternate absorption towers were inserted at the exit of the reduction furnace, one being removed and weighed every 5 min. after the H₂ was admitted and reduction was begun. At the close of the experiment the boat was usually removed and weighed to serve as a further check.

Reduction was studied at the specific temperatures of 575°, 600°, 700°, and 800°C. (1067°, 1112°, 1292°, and 1472°F.) for the original ore, as crushed, and for three screened sizes. Thus, the effects of two important factors, temperature and particle size, could be examined.

Two complete sets of data are presented. For the first, percentage of reduction is represented on the arbitrary basis of the 600° asymptote being 100 per cent, since

in all cases reduction was most efficient at this temperature. The second set, a complete duplicate series, employs percentage of reduction based upon the calculated available oxygen as Fe₃O₄. Each of these methods is open to some minor criticism, which in no way affects the principal conclusions of the paper.

Since the curves are drawn through the experimental points in all figures, no tabulations are included.

EXPERIMENTAL RESULTS FIRST SERIES

Unsized Ore

The progress of reduction of unsized ore at the four selected temperatures is shown in Fig. 2. Screen analysis of this material showed 87.5 per cent passing 10 mesh, with fairly even distribution down to 85 per cent retention on 100 mesh.

Sized Ore

When sized particles were used, the data depicted in Figs. 3, 4, and 5 were obtained.

Effect of Temperature

Two characteristics of these curves immediately impress one: First, the initial reduction up to approximately 80 per cent is more rapid the higher the temperature; and, second, later stages of reduction decline in rate so greatly at 700° and 800°C. that these temperatures decidedly cannot be recommended when complete reduction of natural magnetite is sought.

In Fig. 6, the data from reduction of the sized ore in Fig. 4 are replotted to show this effect of temperature in another way. There the family of curves is surprisingly regular, in view of the experimental error to be expected from this type of experiment; and the curves show by their displacement against the time abscissa how a distinct rate maximum

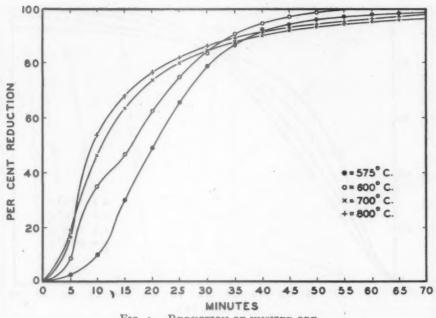


FIG. 2.—REDUCTION OF UNSIZED ORE.

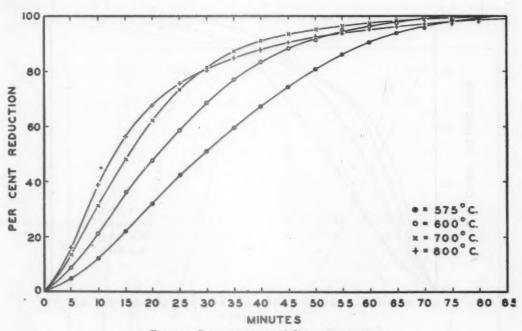


Fig. 3.—Reduction of +8-10-mesh ore.

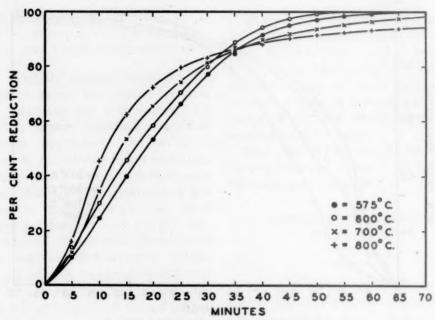


Fig. 4.—Reduction of +28-35-mesh ore.

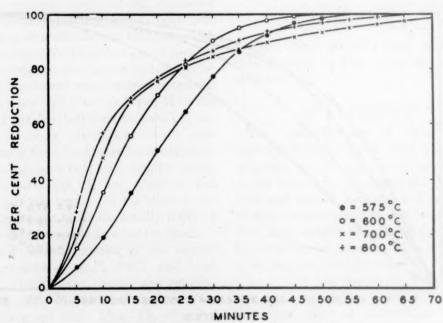


FIG. 5.—REDUCTION OF +65-100-MESH ORE.

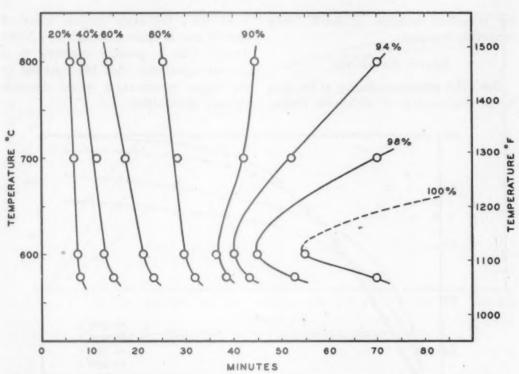


Fig. 6.—Data of Fig. 4 replotted to show development of a rate maximum at 600°C. As reduction proceeds to completion.

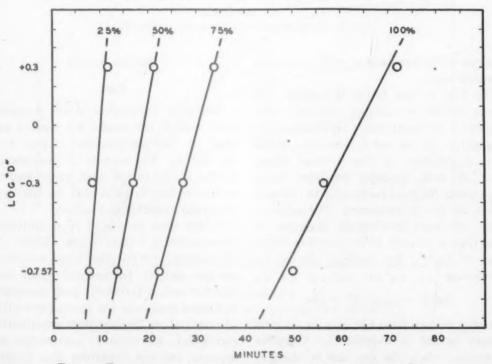


Fig. 7.—Effect of particle size on rate of reduction at 600°C

for reduction develops at 600°C. with increasing reduction.

Effect of Particle Size

One other prominent feature of the data is the displacement of all curves toward At 800°, the same general effect of particle size is evident, though to a lesser degree. This is possibly contrary to a general expectation that the sintering at the higher temperature would decrease the rate of reduction.

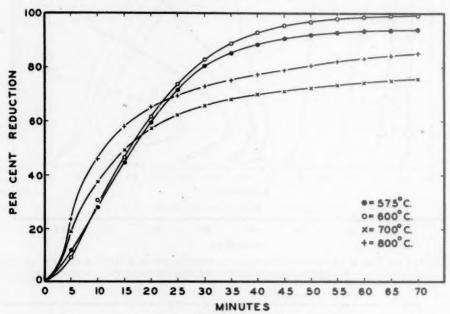


Fig. 8.—Reduction of unsized ore, series II.

shorter reduction periods with decreasing particle size.

In Fig. 7, this factor is brought out more clearly by plotting reduction time at 600° C. vs. particle size expressed as the logarithm of the mesh diameter. While the significance of the average diameter of such irregular particles might be argued, the good conformity to linearity on a log plot is reassuring. The relationship between screen-mesh diameter D and time in minutes M for complete reduction at 600° C., for example, can be expressed as:

$$\log D = 0.0475M - 3.04$$

As may be seen from Fig. 7, a 50 per cent longer period is required for complete reduction when the ore size is changed from -65 + 100 to -8 + 10.

SECOND SERIES

Data

Complete duplication of the foregoing tests yielded the results for unsized and sized ore that are presented in Figs. 8, 9, 10, and 11. The manner of presentation is the same, except that percentage of reduction here is calculated on the basis of oxygen available as Fe₃O₄.

If one were interested in quantitative reproducibility, these data might be discouraging. On the other hand, a rigorous position cannot be adopted when considering such a kinetically and chemically undefined system as the gaseous reduction of a natural ore. Studied from a qualitative standpoint, all essential information reappears; and the disparities then become a useful measurement of the safety factor

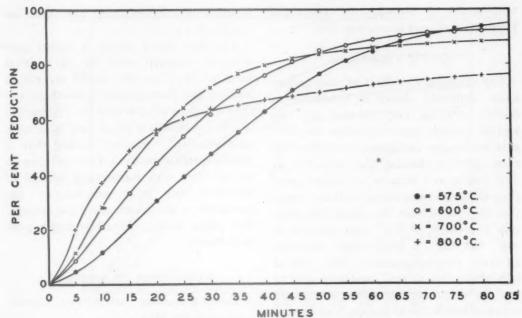


Fig. 9.—Reduction of -8+10-mesh ore, series II.

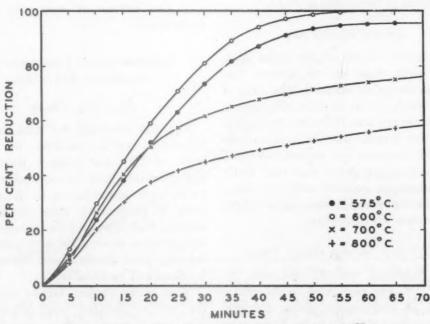


Fig. 10.—Reduction of -28+35-mesh ore, series II.

that would be necessary in commercial application of such laboratory tests.

Effect of Temperature

For example, the effect of temperature again definitely shows a maximum at 600°C., differing only in that the two smaller particle sizes now show the 600° rate maximum throughout reduction. All tests agree in showing that reduction at 575° begins and remains at slower speed than at 600°C.; and almost without exception they show that the initial reduction rate is greatest at 800°, next greatest at 700°, but that in later stages reduction at these two temperatures lags until it falls below that at 600°, and even that at 575°. In fact, reduction at the two elevated temperatures seems to approach an asymptote so obviously different from that of the 600° tests that the matter may have important bearing upon the nature and availability of the oxygen assumed in the calculations to be present as Fe₃O₄.

Effect of Particle Size

The results of the second series agree closely with those of the former. The principal exception occurs in the data of Fig. 9, which appear to show no complete reduction in any test. If the not implausible assumption is made that the sample in the 600° run contained less oxygen combined with Fe than calculated, and that Fe₃O₄ was completely reduced after 75 min., where the ore stopped showing a weight loss, the data are concordant.

TEST FOR A SECOND OXIDE PHASE

The technique recently discussed by Olmer^{69,72,78} was next used to determine whether an intermediate phase develops in the reduction of Fe₃O₄ to Fe. Three runs were made, each started at 400°C. and studied as the temperature was increased proportional to time up to final temperatures of 600°, 700°, and 800°C., attained

in each case in 85 min. The data are plotted in Fig. 12.

The 600° curve shows a rather pronounced upsweep close to the critical point at 565°; but the results are not in keeping with sharp phasial distinctions, and they therefore substantiate the designation of the intermediate phase in Fig. 1 as a solid solution, "wüstite," rather than a stoichiometric compound, FeO; and they do not conform with Ramseyer's concept of reduction rate being affected by the formation of an intermediate and singular FeO phase having characteristically poor reducibility.

DISCUSSION OF RESULTS

There are three outstanding characteristics of the data:

- 1. The 600°C, rate maximum for total reduction.
- 2. The high initial rate and subsequent lagging of the 700° and 800° curves.
- 3. The increase of rate with smaller particle size.

THERMODYNAMIC PRINCIPLES OF HYDROGEN REDUCTION

Free-energy Change

The rate maximum for total reduction found at 600°C. confirms the recent work of Udy and Lorig,⁷¹ Ramseyer,⁷⁷ and Chufarov and his co-workers.^{52,53,57} In fact, the conformation to the Russian work is particularly close in similarly showing high initial speeds of reduction at temperatures above 600° with subsequent lagging, which finally makes the elevated temperatures undesirable.

Most of the obvious factors in slowing the rate at elevated temperatures have been long discussed, such as crystallization or fusion of the metallized zone, sintering of the particles, formation of impervious nonmetallic surface coatings from fluxing silicates, and so forth. A generally held

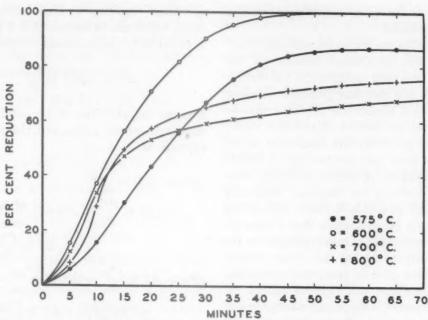


Fig. 11.—Reduction of -65+100-mesh ore, series II.

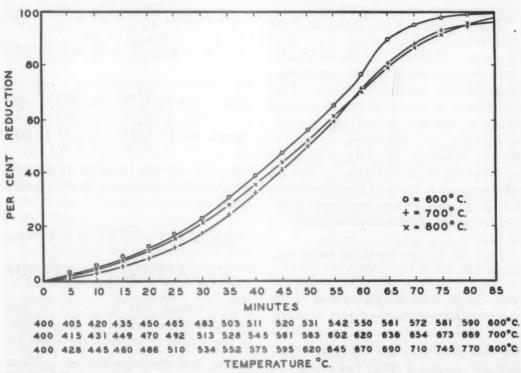


Fig. 12.—Progress of reduction over period of 85 minutes in which temperature was raised proportionately with time from 400°C. TO 600°, 700°, or 800°C., respectively.

conclusion, however, is that much remains to be explained.⁷¹

Reviewing the literature, one can understand that conclusion because of the absence of a clear treatment of the thermodynamic and chemical principles involved in reduction. Kinetic matters have received wide attention because reduction is visibly a kinetic problem; but insufficient attention has been paid the position of certain thermodynamic principles in kinetic matters in directing the reactions, measuring the energy available to them, and setting the bounds beyond which they cannot go.

The present paper calls into question the advisability of basing the entire process, as has been done to date, on conventional rate expressions, and explores instead the significance of the thermodynamic potential in regulating or affecting reduction by considering the passage of the reducing gas through the ore bed on the basis of a series of minute isolated systems.

Of first importance is clarification of the fundamental driving energy of the reaction—the free energy. This thermodynamic measurement depends upon the equilibrium concentrations, specifically activities, of the constituents as compared with their actual activities. It relates to the $(P-P_e)$ quantity of Stålhane and Malmberg, and to the feature described by Udy and Lorig as "distance from equilibrium;" but its relationship is in terms of energy available for the reaction, rather than simple linear measurements of concentration differences in $P_{\rm H_2O}$.

Thus, for the two equations under consideration:

$$Fe_3O_4 + H_2 = 3FeO + H_2O$$
 [I]
 $FeO + H_2 = Fe + H_2O$ [II]

the two gases H_2O and H_2 change from primary fugacities $P^*_{H_2O}$ and $P^*_{H_2}$ to equilibrium fugacities P_{H_2O} and P_{H_2} ; and, in so doing, the "distance from equilibrium" in an energetic sense is a logarithmic,

not linear, function of their partial pressures, which can be expressed as a thermodynamic potential, or change in free energy:

$$\Delta F = -aRT \ln \frac{P^*}{P}$$

Because the activities of the solid phases remain essentially unchanged, the complete expressions:

$$\Delta F_{\rm I} = 3RT \ln \frac{a^*_{\rm FeO}}{a_{\rm FeO}} + RT \ln \frac{P^*_{\rm H_2O}}{P_{\rm H_2O}} - RT \ln \frac{a^*_{\rm Fe_3O_4}}{a_{\rm Fe_3O_4}} - RT \ln \frac{P^*_{\rm H_2}}{P_{\rm H_2}} \quad [Ia]$$

$$\Delta F_{\rm II} = RT \ln \frac{a^*_{\rm Fe}}{a_{\rm Fe}} + RT \ln \frac{P^*_{\rm H_2O}}{P'_{\rm H_2O}} - RT \ln \frac{a^*_{\rm FeO}}{a_{\rm FeO}} - RT \ln \frac{P^*_{\rm H_2}}{P'_{\rm H_2}} \quad [IIa]$$

can be simplified to:

$$\Delta F_{\rm I} = RT \ln \frac{P^*_{\rm H_2O}}{P_{\rm H_2O}} - RT \ln \frac{P^*_{\rm H_2}}{P_{\rm H_2}}$$
 [Ib]

$$\Delta F_{\rm II} = RT \ln \frac{P_{\rm H_2O}^*}{P_{\rm H_2O}'} - RT \ln \frac{P_{\rm H_2}^*}{P_{\rm H_2}'}$$
 [IIb]

or

$$\Delta F_{\rm I} = RT \left(\ln \frac{P_{\rm H_2O}^*}{P_{\rm H_2}^*} - \ln \frac{P_{\rm H_2O}}{P_{\rm H_2}} \right)$$
 [Ic]

$$\Delta F_{\rm II} = RT \left(\ln \frac{P^*_{\rm H_2O}}{P^*_{\rm H_2}} - \ln \frac{P'_{\rm H_2O}}{P'_{\rm H_2}} \right)$$
 [IIc]

Because the last term in Ic and IIc is the equilibrium constant, these equations reduce to:

$$\Delta F_{\rm I} = RT \left(\ln \frac{P^*_{\rm H_2O}}{P^*_{\rm H_2}} - \ln K_{\rm I} \right) \quad [{\rm I}d]$$

$$\Delta F_{\rm II} = RT \left(\ln \frac{P^*_{\rm Hz0}}{P^*_{\rm Hz}} - \ln K_{\rm II} \right) \quad [{\rm II}d]$$

This measurement for "distance from equilibrium" is therefore proportional to the difference between the logarithm of $K_{I,II}$ and the logarithm of $\frac{P^*_{H_2O}}{P^*_{H_2}}$ at the moment of impingement. Regarding $\frac{P^*_{H_2O}}{P^*_{H_2}}$ as a temporary constant in any given

part of the system, one can compute the initial free-energy change for that part of the system at any of the temperatures in question by using the following general expression derived from I, IId:

$$\Delta F_{\rm I,II} = 4.575 T \; (\log K_{\rm P*} - \log K_{\rm I,II}) \ [{
m I, II}e]$$

$$\Delta F_{I,II} = -4.575T \log K_{I,II} + cT$$
 [I, IIf]

where $c = 4.575 \times \log K_{P*}$ and T is expressed in deg. K_{*}

Effect of Bed Depth

Immediately after impingement, $P^*_{H_2O}$ and $P^*_{H_2}$ are altered to $P^{*'}_{H_2O}$ and $P^{*'}_{H_2}$, so that subsequent layers of ore are swept by a gas having a progressively lowered thermodynamic potential. If the contamination of the incoming gas stream is arbitrarily assumed to be 0.01 per cent H_2O , the primary fugacities are:

$$P^*_{H_2} \approx \text{1.0 atm.}$$

 $P^*_{H_2O} = \text{10}^{-4} \text{ atm.}$

and $K_{P*} = 10^{-4}$. In such a system, the characteristics of the free-energy change over the temperature range in question are depicted by the uppermost curve family in Fig. 13. In that figure, the free-energy characteristics are also shown for arbitrary $P^*_{H,O}$ values of 10^{-2} and 10^{-1} atmospheres, representing the gas composition deeper in the ore bed.

The outstanding feature of the diagram is that the first few millimeters of H₂O picked up by the traversing gas depletes the thermodynamic potential of the reduction reaction by far greater proportions than subsequent equal additions. This is better shown in Fig. 14, which depicts thermodynamically this revised "distance from equilibrium" as a function of the H₂O content of the gas.

The marked departure from linearity exhibited by these curves suggests a new approach in explaining curve E in Fig. 18 of Udy and Lorig's paper,⁷¹ a curve classed as anomalous by those authors. The ordinates in their plot are thermodynamically meaningless; but when their data are translated from percentage of H_2O into thermodynamic potentials and plotted against the logarithm of the bed depth, curve E becomes virtually a straight line.

For example, adopting the values from the ordinate of their Fig. 18 into the thermodynamically applicable forms:

$$K^{a_{P*}} = \left\{ \frac{P^{*}_{\text{H}_{2}0}}{P^{*}_{\text{H}_{2}}} \right\}_{a}$$

$$K^{b_{P*}} = \left\{ \frac{P^{*}_{\text{H}_{2}0}}{P^{*}_{\text{H}_{2}}} \right\}_{b}$$

$$K^{n_{P*}} = \left\{ \frac{P^{*}_{\text{H}_{2}0}}{P^{*}_{\text{H}_{2}}} \right\}_{n}$$

where $a, b \dots n$ refer to the positions of increasing bed depth shown on the abscissa of their figure, and applying these to the general expression:

$$\Delta F_{\rm I,II} = 4.575 \ T \ (\log K_{\rm P*} - \log K_{\rm I,II})$$
[I, IIe]

one can obtain values for $\Delta F^a_{I,II}$ $\Delta F^b_{I,II}$... $\Delta F^a_{I,II}$ which give a measure of the "distance from equilibrium" in terms of free energy and provide the virtually straight line shown in Fig. 15 when plotted against the logarithm of the bed depth.

Minimum Effective Energy

From very close examination of Fig. 15 one might still claim a slight upbending of the curve with increasing bed depth. If that is true, however, the existence of a minimum effective energy should be given as early mention as the physical factors proposed by Udy and Lorig. Although pronounced roles of critical minimum energies are infrequent in metallurgical reactions at high temperatures, very few

chemical reactions proceed when ΔF is a small negative number, some critical minimum value being required to initiate the reaction.

of reduction, $\Delta F'$, on the basis of a minimum potential of 1000 cal. per mol:

$$\Delta F' = \Delta F_{1,11} - 1000 = -4.575T \text{ (log } K_{P*} - \log K_{11}) - 1000 = 0$$

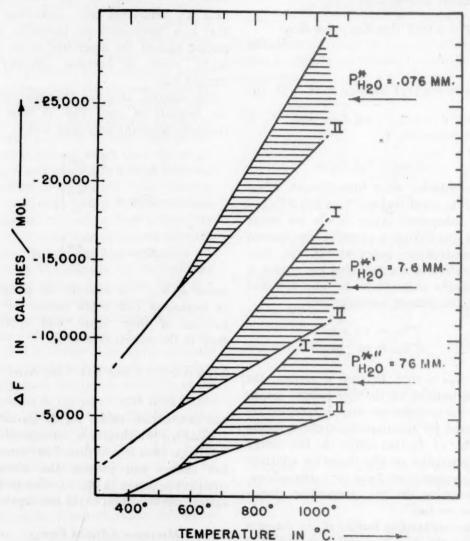


Fig. 13.—Plot of $\Delta F_{1,11}$ vs. T for reduction by hydrogen having moisture contents of 10^{-4} , 10^{-2} , and 10^{-1} atmospheres, respectively.

If the curvature in Fig. 15 is real, a critical or "threshold" energy of not more than 1000 cal. per mol is indicated. The effective abscissa in Fig. 13 would then be raised as indicated by the broken horizontal line, and all end-point $P_{\rm H_2O}$ values would be effectively decreased.

Calculating the effective driving energy

one obtains for reduction at 700°C.:

$$K_{P^*} = \frac{P^*_{\text{H}_2\text{O}}}{P^*_{\text{H}_2}} = 0.256$$

whereupon the quasi-equilibrium value becomes:

$$P_{\rm H_2O} = 0.204$$

Thus, reduction at 700°C. would stop with about 20 per cent H₂O in the atmosphere, in contrast to an equilibrium value of 29.5 per cent, which is in good agreement with Udy and Lorig's experimental curve.

of the temperatures shown, the thermodynamic potential of the system increasing markedly and continuously with temperature through and beyond the quadruple point. Consequently, a popular tendency,

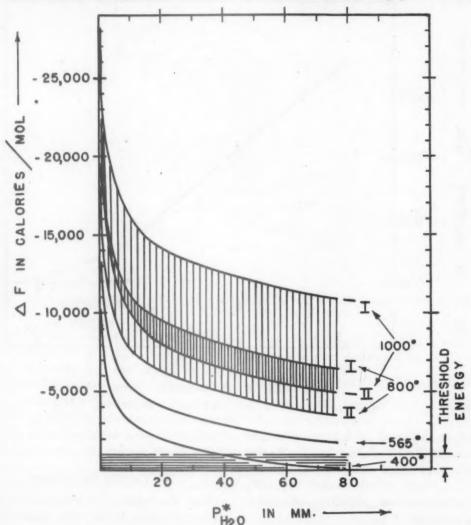


Fig. 14.—Plot of $\Delta F_{I,H}$ vs. H_2O content of hydrogen.

A second explanation for the possible deviation with advanced bed depths will appear later in discussion of the chemical principles of internal pressure.

The 600° Rate Maximum

As for the rate maximum at 600° , no indication of either a maximum or minimum appears on the ΔF curves at any

recently expressed by Ramseyer,⁷⁷ to relate the 600° maximum to stepwise reduction and the formation of an "interfering third phase" above the quadruple point temperature requires modification.

In the first place, the removal of oxygen is continuous, the solid solution, wüstite, not FeO, being formed from reduction of Fe₃O₄. Secondly, when the end member

FeO is finally produced, there is still no thermodynamic reason for expecting superior reduction to occur at 600°C., or for believing that FeO is especially difficult point, is a notably active flux. In magnetitic ores, the fluxing action with other constituents above 600° might produce a protective film like that described by

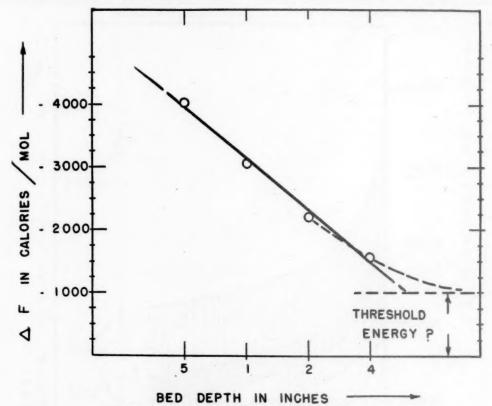


FIG. 15.—REPLOT OF UDY AND LORIG'S 71 FIGURE 18.

to reduce. Although ΔF for the metallizing reaction II (FeO \rightarrow Fe) lies on a line having slightly less slope than the line below 565°C. (Fe₃O₄ \rightarrow Fe), values of ΔF_{II} are always more negative at higher temperatures.

The reason, therefore, must lie in kinetic matters, such as the sintering found by Meyer²⁶ at 650°, or crystallization of the metallized zone. This latter is especially indicated by the fact in the present research that the rate increased with decreasing particle size at all temperatures. Consequently, interparticle sintering is less important than intraparticle sintering.

It might also be pointed out that wüstite, which forms only above the quadruple

Joseph. 169 In that case, reduction of pure Fe₃O₄ should not exhibit such a maximum.

The Lagging Phenomenon

Now the lagging phenomenon becomes understandable. Almost without exception the early stages of reduction showed rates increasing with temperature, as would be expected from studying the ΔF diagrams in Fig. 13. Furthermore, this lead at 700° and 800° was maintained up to stages of reduction as late as 80 and 90 per cent.

If the intermediate formation of FeO were responsible for the phenomenon of lagging, the curves would bend over at reductions of only 25 per cent and less,

since the reduction of Fe₃O₄ to FeO' involves removing only 25 per cent of the total oxygen. Once again the evidence stands contrary to the common supposition that FeO impedes reduction.

most interesting features of the system. Twenty-five per cent of the work of reduction can actually be dissipated in accomplishing nothing other than forming a second slag phase. Analogies in the reduc-

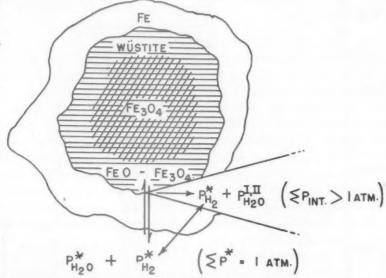


Fig. 16.—Illustration of chemical principles by which gas collects under pressure within a semireduced ore particle.

As further evidence, extrapolation of the single ΔF line from below 565° in Fig. 13 shows that the two-phase region changes the early energy characteristics by considerably *increasing* the thermodynamic potential of reaction I beyond the effect of temperature alone. That is, the slope of curve I in the two-phase region is greater than its slope below 565°, and Fe₃O₄ is therefore hyperactively dissociated at temperatures where wüstite is produced. This ready loss of a part of the oxygen again confirms the finding of early rate maxima at the higher temperatures.

One can observe in Fig. 13, by the approach of the lower curve family to the abscissa, that a point is reached at a certain bed depth where $P^*_{H_{\pi}0}$ is too great to allow the metallizing reaction II, and yet small enough to take further oxygen from Fe₃O₄. This ability to reduce magnetite in the two-phase region without producing a metallic phase is one of the

tion of Cr₂O₃,^{211,218} SiO₂,²²³ and other oxides²²⁶ were mentioned earlier.

Gas-solid Equilibria within the Particle

While the formation of H₂O in the furnace atmosphere simply depletes $P^*_{H_2}$ without an increase in the total pressure of the system, conditions within the particle are different. After surface metallization has occurred, the gas stream contacting that surface will be virtually H₂ at 1 atm. pressure. Diffusion of hydrogen into the metal layer will therefore occur on the basis of an external pressure of 1 atm. of H₂.

Within the particle, the reaction of the infusing H with encased FeO or Fe₃O₄ will produce H_2O , but without permanent depletion of P_{H_2} because of the continual infusion of H under an external pressure of 1 atm. of H_2 . That is, the metal shell furnishes a closed system having a diaphragm permeable virtually only to

hydrogen, as indicated in Fig. 16. Within the shell, H2 will collect at approximately the partial pressure P*H, maintained by H₂ outside the shell. For the equations:

critical point, a similar condition occurs when four phases coexist:

$$F_{565} = 3 - 4 + 2 = 1$$

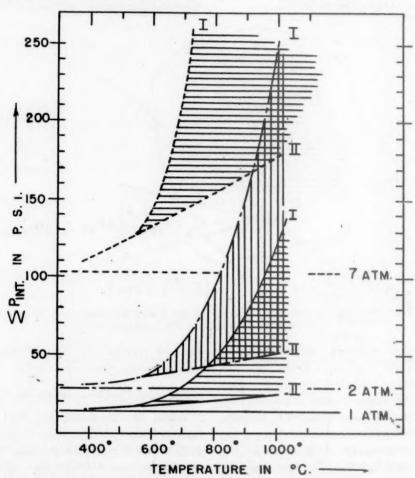


Fig. 17.—Plot of $\Sigma P_{\mathrm{int.}}$ vs. T for reactions I and II occurring inside an ore particle.

$$Fe_3O_4 + H_2 = 3FeO + H_2O$$
 [I]

 $FeO + H_2 = Fe + H_2O$ [II]

PH, is fixed at r atm. According to the phase rule:

$$F = C - P + 2$$

the internal system has three components and three phases. The degrees of freedom are therefore:

$$F = 3 - 3 + 2 = 2$$

and f(T, P) = 0. At any given temperature, only pressure remains a variable. At the Consequently, at any of the temperatures under consideration, fixing the partial pressure of either H2 or H2O immediately establishes the partial pressure of the other and the total pressure of the system. The problem is identical with that for gas reactions within the steel shell of a steam boiler as compared with reactions in the boiler itself.227

From the relationship:

$$\frac{P_{\rm H_2O}}{P_{\rm H_2}}=K_{\rm I,II}$$

the partial pressure of H₂O within the particle can be determined; and the total pressure becomes:

$$\Sigma P_{\text{int.}} = P^*_{\text{H}_2} + P_{\text{H}_2\text{O}} = P^*_{\text{H}_4} (\mathbf{1} + K_{\text{LH}})$$

In Fig. 17, the lower curve family depicts the variation of $\Sigma P_{\rm inx}$, with T for reduction at atmospheric pressure. The potential internal pressures are always greater than 1 atm., exceeding 120 lb. per sq. in. in the presence of Fe₃O₄ at 1000°C. and clearly indicating their role of counteraction to sealing surface films. Reaction with FeO causes but little pressure increase. Intermediate pressures, of course, occur at intermediate wüstite compositions, indicated in the figure as an area. Conversely, in the reduction of hematite, the Fe₂O₃ should cause exceptionally high pressures to obtain.

This phenomenon, therefore, belongs in a consideration of factors affecting reduction, for hydrogen is known to remove nonmetallic impurities even from solid steel by this pressure action leading to intergranular channeling and escape of the reaction product.227 However, mention should be made of a common fallacy, expressed by Wiberg, 67 for example, that hydrogen is able to escape, but not water vapor, and that the trapped gas must therefore be predominantly H₂O. While the conclusion may be partly true in fact, the premise is wrong because the chemical principles just discussed state that H2 cannot escape from an internal accumulation against an external atmosphere having the same partial pressure. If the trapped H₂ did effuse, which it could do only if the external $P_{\rm H_2}$ were diminished, the internal equilibrium ratio of H2O-H2 would be exceeded, and the H2O would promptly oxidize the surrounding Fe to reform H2 and deplete H2O. In that way, H2O is able to "escape" as readily as H2.

Also, it should be made clear that the

internal system is not truly isolated in the thermodynamic sense because of a measurable diffusion rate of H₂O, and that therefore these calculations yield only asymptotic values. The complete system is nonequilibrium, of course, for

$$(P_{\rm H_2O}/P_{\rm H_2})_{\rm ext.}$$

is less than the ratio demanded by the monovariant equilibrium at temperature T, and one phase, the oxide, must therefore disappear. This fact underwrites the reduction process. The calculations depend upon the much greater diffusion rate of H through Fe to equalize $(P_{\rm H_2})_{\rm int.}$ and $(P_{\rm H_2})_{\rm ext.}$ at the expense of the equalization of $(P_{\rm H_2})_{\rm int.}$ and $(P_{\rm H_2})_{\rm ext.}$

A second cause for the possible deviation in Udy and Lorig's curve E is now apparent; that is, a gas stream of composition A_{H2}-B_{H2O} actually approaches a quasi-equilibrium with a gas phase inside the semireduced particle whose composition is $A_{\rm H_2}$ - $B'_{\rm H_2O}$ where $B'_{\rm H_2O}$ is $> B_{\rm H_2O}$ because the diffusion of H2O through Fe is slower than the diffusion of H2, and the enclosure permits attaining the hyperatmospheric pressures required by $B'_{H_{2}O}$. Cessation of internal reduction is governed by the $A_{\rm H_2}$ - $B'_{\rm H_2O}$ ratio, of course; whereas an investigator measures only the A_{H_2} - B_{H_2} O ratio and includes this discrepancy among his data.

Reduction under Pressure

When reduction is performed under increased pressure, as in the investigation of Tenenbaum and Joseph⁶⁴ and Diepschlag,¹⁷¹ the potential internal pressures become those shown by the other curve families in Fig. 17. Using reduction under 2 atm. pressure, Tenenbaum and Joseph⁶⁴ found that with increasing T reduction under pressure had increasing efficiency, reduction at 800°64 and at 1000°176 being much more rapid than at 600°. This seeming contradiction of the 600° rate maximum in the present work is now readily

understood, for in Fig. 17 one may see that at 600° the potential disruptive pressures increase only from 20 to 40 lb. per sq. in. on changing P*H, from I to 2 atm. At 800°, however, the minimum pressure is greater than 40 lb. per sq. in., and may reach 100. At 1000°C., internal rupturing pressures greater than 200 lb. per sq. in. are indicated; and at $P_{\rm H_2}$ = 7 atm., as in Diepschlag's research, 171 disruptive pressures approaching 1000 lb. per sq. in. can be reached, which certainly can be effectively counteractant to formation of surface film.

This steep slope of ΣP_{int} with T therefore provides an alternative to Tenenbaum and Joseph's explanation for the lesser effect at 600°. Whereas they simply ascribe it to a slower diffusion rate at the lower temperature, the present discussion describes how the gas phase within ore particles at elevated temperatures may attain sufficient total pressure literally to blast open its diffusion path, destroying the protective skin causing the lagging phenomenon. The fundamental driving energies depicted in Fig. 13 are then allowed to proceed, making reduction at 800° faster than at 600°.

This ready explanation conversely makes it especially probable that the factor responsible for lagging has the nature of a protective envelope, either the metallic Fe itself or a nonmetallic film.

THERMODYNAMIC PRINCIPLES OF CO REDUCTION

Fundamental Reactions

As with H₂ reduction, certain thermodynamic principles of CO reduction submit to further clarification. The equations generally discussed are:

$$Fe_3O_4 + CO = CO_2 + 3FeO$$
 [III]
 $FeO + CO = CO_2 + Fe$ [IV]

If activity changes in FeO and Fe₃O₄ are again disregarded:

$$K_{\rm III} = \frac{P_{\rm CO_2}}{P_{\rm CO}} \qquad [IIIa]$$

$$K_{\rm IV} = \frac{P'_{\rm CO_2}}{P'_{\rm CO}} \qquad [{\rm IV}a]$$

Schenck⁴² gives probably the best evaluation for $K_{III,IV}$:

$$\log K_{\rm III} = -\frac{1373}{T} - 0.341 \log T + 0.00041T + 2.303 \text{ [IIIb]}$$

$$\log K_{IV} = \frac{381}{T} - 2.110 \log T + 0.000395T + 5.357 \text{ [IVb]}$$

and these are the equations that were used in plotting Fig. 1. The critical point is again assumed to lie between 560° and 570°C., in spite of a possibility that the C content of the Fe phase, and possibly the oxide phases, may drop the critical temperature to 540°C.31

Unlike H2 reduction, CO reduction suffers from two complications resulting from thermal dissociation of CO:

$$_{2}P_{\text{CO}} = P_{\text{CO}_{1}} + P_{\text{C}} \qquad [V]$$

$$_{2}P_{\text{CO}} = P_{\text{CO}_{2}} + P_{\text{C}}$$
 [V]
 $K_{\text{V}} = \frac{(P_{\text{CO}_{2}})(P_{\text{C}})}{(P_{\text{CO}})^{2}}$ [Va]

which shows the introduction of a possible new phase, carbon, into the system; and

$$_{2}P_{\text{CO}_{2}}^{\text{C}} = _{2}P_{\text{CO}} + P_{\text{O}_{2}}$$
 [VI]

$$2P_{\text{CO}_2}^{\text{C}} = 2P_{\text{CO}} + P_{\text{O}_2}$$
 [VI]
 $K_{\text{VI}} = \frac{(P_{\text{CO}})^2 (P_{\text{O}_2})}{(P_{\text{CO}_2})^2}$ [VIa]

which shows that this so-called "reducing" agent has oxidizing propensities.

For the variation of reactions V and VI with temperature, Schenck42 gives:

$$\log K_{\mathbf{v}} = \frac{40,800}{4.571T} - 4.864 \log T$$

$$+ 0.00301T - 0.627$$

$$\times 10^{-6}T^{2} + 0.479$$

$$\times 10^{-10}T^{3} + 2.926 \quad [Vb]$$

when $P_{\mathbf{C}}$ is the carbon saturation pressure of β graphite; and

$$\log K_{VI} = -\frac{29,500}{T} + 2.75 \log T$$

$$-1.215 \times 10^{-3}T + 1.35$$

$$\times 10^{-7}T^{2} + 2.20 \quad [VIb]$$

There are four principal forms in the gas phase: CO₂, CO, C, and O, which act in reduction, oxidation, and carburization of iron, forming both solid solutions and compounds of iron with oxygen and carbon. Consequently, the reduction equilibria expressed by Eqs. III and IV are incomplete and must include carburizing reactions:

$$P_{\mathbf{C}} = P_{[\mathbf{C}]} = \mathbf{m}.[\mathbf{C}] \qquad [VII]$$

$$K_{\text{VII}} = \frac{[C]}{P_{\text{C}}}$$
 [VIIa]

where $[C]_{aat.} = K_{VII} \cdot P_{\beta\text{-graphito}}$

$$_3$$
Fe + [C] = Fe $_3$ C [VIII]

$$K_{VIII} = \frac{Fe_3C}{[Fe]^3[C]}$$
 [VIIIa]

Also,

$$Fe + P_{CO} = FeO + [C]$$
 [IX]

$$K_{IX} = \frac{K_{V} \cdot K_{VII}}{K_{III}} = \frac{[C]}{[Fe](P_{CO})}$$
 [IXa]

which combines Eqs. III, V, and VII and expresses: (1) that CO simultaneously oxidizes and carburizes Fe, and (2) that carburization increases almost linearly with increasing $P_{\rm CO}$ until late stages when [Fe] becomes sufficiently less than unity to affect the ratio.

Combining Eqs. VIII and IX depicts the same reaction forming cementite:

$$4\text{Fe} + P_{\text{CO}} = \text{FeO} + \text{Fe}_{3}\text{C} \qquad [X]$$

$$K_{\mathbf{X}} = K_{\text{VIII}} \cdot K_{\text{IX}} = \frac{K_{\mathbf{V}} \cdot K_{\text{VII}} \cdot K_{\text{VIII}}}{K_{\text{III}}}$$

$$= \frac{[\text{Fe}_{3}\text{C}]}{[\text{Fe}]^{4}(P_{\text{CO}})} \quad [Xa]$$

Free-energy Characteristics of Reduction

Like the previous Fig. 13 for H_2 reduction, Fig. 18 contains ΔF families that express the driving energy of reactions III and IV, except that only one initial gas

composition is considered. In each case, calculations are based upon reduction by CO regenerated at 1000°C. over pure carbon and without further purification. That places the horizontal base line for the incoming gas system at:

$$P_{\rm CO_2} \approx 10^{-2}$$
 atm.

The ΔF families in Fig. 18 employ two extreme suppositions: (1) thermal dissociation is negligible before reduction (ΔF^*) , and (2) thermal dissociation is complete to the extent conforming to equilibrium (ΔF^D) .

In the first case, the gas stream at all temperatures impinges upon the ore with its primary composition of about 99.5 per cent CO and 0.5 per cent CO₂; and ΔF , for this case identified as ΔF^* , would at all temperatures under consideration be sizably negative and increasing along with temperature for both reactions III and IV.

In the second case, ΔF^D , the superscript designating reduction after thermal dissociation, proves to be zero for reaction III at 640°C. and for reaction IV at about 700°. At higher temperatures, ΔF^D then quickly becomes markedly negative, until at 1000° $\Delta F^D = \Delta F^*$.

Between these extremes lie the values involved in practice; and the lay of the two curve families show preference for reduction at temperatures considerably higher than the 600° selected for hydrogen reduction, which is in keeping with experience. 63,67,124,170,174 In fact, the dissociated gas will oxidize Fe to FeO at temperatures below 700°, and will oxidize it right back to magnetite below 640°.

The quintuple point at 565°C. should be noted, where FeO, Fe₃O₄, carboniferous Fe, graphite, and gas coexist, the gas phase obviously having subatmospheric pressure because the curve for one atmosphere lies to the right. Also, an infinite series of quadruple points lies along curve V between curves III and IV where carboni-

ferous Fe, gas, and graphite coexist with an oxide phase of fixed composition.

Principles of Graphitization

The solid curve sloping up toward the left in Fig. 18 represents the thermal dissociation over β -graphite of reaction V at 1 atm. total pressure, calculated from Eq. Vb. Therefore, the area included between that curve and the axes is a field of potential graphitization, the height of the area at any temperature being related to that potential by the expression:

$$\Delta F = RT \left(\ln K_{P^*} - \ln K_V \right)$$

= -2.303RT (log K_V + 2)

Also, the linear height of the area measures the proportion to which graphitization can occur.

Since P_{CO} and P_{CO_2} are fixed by the regenerating treatment over free carbon at 1000°C., P_{C} is greater than $P_{\beta\text{-graphite}}$ at all temperatures below 1000°C., becoming greater with decreasing temperature. When metallization begins, the Fe immediately absorbs C according to reaction VII or VIII, which counteracts the tendency toward forming free graphite in the early stages of reduction. Because P_{C} is so great with respect to $P_{\text{[C]}}$, however, Fe will tend to absorb C until saturation is reached and free carbon appears as a new phase.

This, then, accounts for the fact that graphitization is more pronounced in late stages of reduction. 43,56,56,176,179

Following similar reasoning, one can understand the temperature function of graphitization shown in Tenenbaum and Joseph's¹⁷⁶ Fig. 3 as representing the increasing graphitization potential as the temperature drops below the equilib rium, or regenerating, temperature, counteracted by a thermal barrier which likewise increases with decreasing temperature, becoming especially active below the temperatures known to be favorable to catalysis. The result is a reversed-rate

curve with maximum deposition at a temperature (500° to 600°C.) low enough to effect a large change in free energy and yet high enough to have the necessary thermal energy for expediting the reaction.

Also shown in Fig. 18 is an upsweeping dotted line lying below the dissociation curve for 1 atm. This second curve represents a total pressure of 0.1 atm. for CO₂ and CO and indicates that dilution with another gas, such as N₂ or H₂, should decrease graphitization even for equal quantities of CO-CO₂ passed. This substantiates Bone, Reeve, and Saunder's ¹⁵¹ conclusion and contradicts Meyer's. ²⁶ Decreasing pressure, of course, throws reaction V to the left.

Incidentally, increasing pressure, which throws reaction V toward proportionately higher $P_{\rm C}$ and lower $P_{\rm CO}$, does not "destroy the reducing power," as claimed by a recent writer," but on the contrary considerably increases it.^{171,176} The increased graphitization, of course, as a physical factor might seriously interfere with reduction.

If the rate of thermal dissociation were to exceed the rate of C absorption by the Fe, it would obviously be useless to attempt to "purify" CO as H2 may be purified. In fact, it would be harmful, for purification would increase the free energy driving graphitization and the quantity of graphite produced. Correspondingly, regeneration of the gas would then not be recommended at temperatures above the reduction temperature. Thus, reduction at 800° would be conducted with gas containing 10 per cent CO2 and having the thermodynamic potential indicated at 800° on the ΔF^D curve family. Conversely, this explains the fact that CO2 in sufficient quantity inhibits graphitization. 43,55,56,176

In fact, referring back to reaction V, one sees that halving P_{CO_2} doubles P_{C} at high P_{CO} values. The condensation of carbon therefore rapidly becomes more likely the purer the CO. For that reason, perhaps the further purification of CO by Ascarite,

for example, is inadvisable. Should carbon nuclei once form, primary P^* values would rapidly approach the dissociation values and the free-energy family ΔF^* would

the dissociation into CO₂ and carbon, and that dissociation therefore does not destroy the reducing power of the gas at higher temperatures.

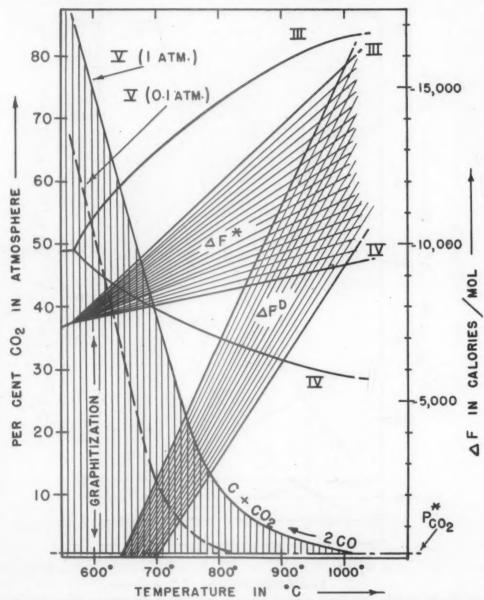


Fig. 18.—Plot of Fe-C-O equilibria and free-energy changes during reduction.

drop to a position approaching the ΔF^D family.

A significant feature of the system, however, is that ΔF^D for 1 atm. pressure remains negative above 700°, regardless of

Mechanism of CO Reduction

While it can readily be argued that CO is responsible for the initial surface reduction, the present writers believe that $P_{\rm C}$ is the active reducing agent in subsequent

stages. First, that assumption is eminently logical on the basis of the foregoing discussion of carbon activity; second, atomic carbon certainly diffuses through Fe more

reaction with the iron oxide must form CO according to reaction IX, which must therefore establish an over-all effusion of CO, rather than an infusion.

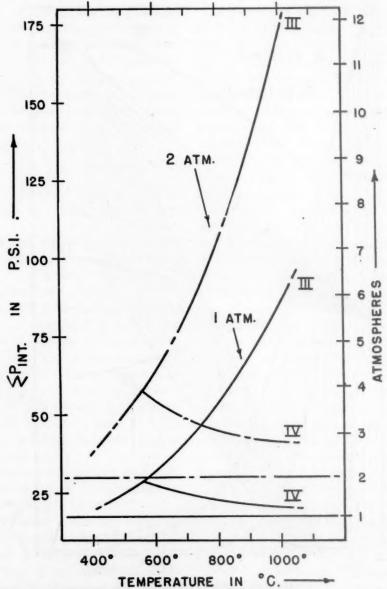


Fig. 19.—Plot of $\Sigma P_{\text{int.}}$ vs. T for internal reactions III and IV when diffusion rate of CO through Fe predominates as a factor.

rapidly than the diatomic CO and will therefore predominate as a factor in the quasi-equilibria of internal reactions just as H₂ predominates over H₂O; third, with C known to be dissolved in the Fe, its Considering the case, though presumed less likely, of P_{CO} controlling the internal reduction reactions through diaphragm activity as discussed for H_2 reduction, then:

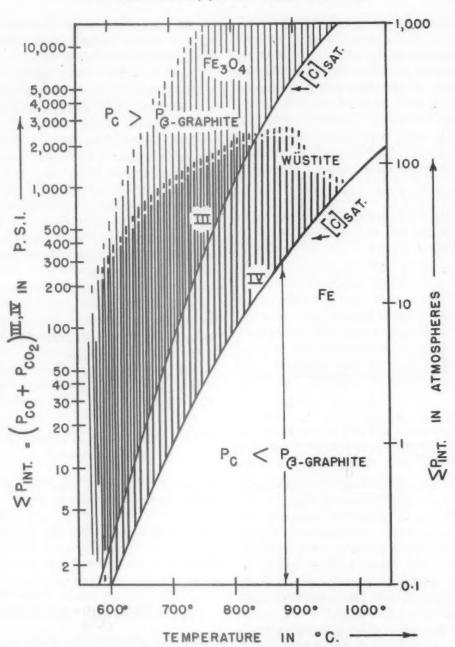


Fig. 20.—Potential ΣP vs. T for internal reactions III and IV when carbon activity predominates.

$$\Sigma P_{\text{int.}} = P_{\text{CO}}^{\text{V}} + P_{\text{III.IV}}^{\text{III.IV}} = P_{\text{CO}}^{\text{V}} (1 + K_{\text{III.IV}})$$

Here $(P_{CO})_{ext.}$ is fixed by the regenerating reaction V and approaches equalization

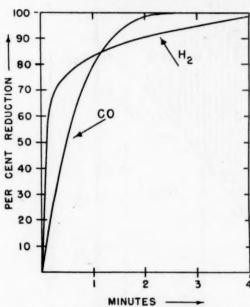


Fig. 21.—Reproduction of Wiberg's data for reduction of a Kiruna magnetite at 1000 $^{\circ}$ showing lagging phenomenon in the H_2 curve.

with $(P_{CO})_{int.}$ at the expense of equalization of the more slowly diffusing CO_2 .

Resulting ΣP curves for reduction at 1 atm. and at 2 atm. are presented in Fig. 19. As with H₂ reduction, $\Sigma P_{\rm III}$ increases sharply with T and with P. Unlike the curves in Fig. 17, however, the pressures obtainable in contact with FeO($\Sigma P_{\rm IV}$) decrease with increasing T.

On the other hand, calculations based upon carbon activity seem highly preferable, for reasons already mentioned. Too often overlooked in published work is the fact that CO not only reduces, but carburizes; and that the product of reduction is not Fe, but a carboniferous iron. In initial stages, the system comprises three components and three phases: oxide, carboniferous Fe, and gas. Since $P_{\rm C}$ is $> P_{\beta-{\rm exaphite}}$, the stage is likely

to be reached in which graphite nuclei appear. Indeed, *internal* graphitization is even commonly observed.

That condition would result in an outright irreversible reduction reaction if it were not for the LeChatelier principle active in Eq. V. Thus, the $P_{\rm CO_2}/P_{\rm CO}$ ratio required for reactions III and IV can be regained through the Boudouard reaction V at temperatures above the quadruple point at 700° by increasing ΣP to throw the reaction toward proportionately higher $P_{\rm CO_2}/P_{\rm CO}$ ratios. With pressures above atmospheric, curve V in Fig. 18 therefore moves to the right, raising the temperature of the four-phase zone.

The pressures necessary to effect this internal equilibrium are depicted in Fig. 20 by curves that refer to equilibria over free carbon. That is, from Eqs. III, IV, and V:

$$K_{\rm III} = \frac{P^{\rm III}_{\rm CO_2}}{P^{\rm III}_{\rm CO}} = \frac{1 - P^{\rm III}_{\rm CO}}{P^{\rm III}_{\rm CO}}$$
 [IIIa

$$K_{\text{IV}} = \frac{P^{\text{IV}}_{\text{CO}}}{P^{\text{IV}}_{\text{CO}}} = \frac{1 - P^{\text{IV}}_{\text{CO}}}{P^{\text{IV}}_{\text{CO}}}$$
[IVa]

$$K_{\mathbf{V}} = \frac{(P^{\mathbf{V}}_{CO_2})(P_{C})}{(P^{\mathbf{V}}_{CO})^2} = \frac{1}{P} \frac{(1 - P^{\mathbf{V}}_{CO})(P_{C})}{(P^{\mathbf{V}}_{CO})^2}$$
 [Va]

Equating $P^{\text{III}}_{\text{CO}} = P^{\text{IV}}_{\text{CO}} = P^{\text{V}}_{\text{CO}}$ and neglecting the small constant P_{C} :

$$\Sigma P_{\text{int.}} = P = P_{\text{CO}} + P_{\text{CO}_2} = \frac{(1 - P_{\text{CO}}^{\text{V}})}{K_{\text{V}}'(P_{\text{CO}}^{\text{V}})^2}$$

since:

$$\begin{split} P^{\text{III}}_{\text{CO}} &= P^{\text{IV}}_{\text{CO}} = P^{\text{V}}_{\text{CO}} = \frac{\text{I}}{K_{\text{III,IV}} + \text{I}} \\ \Sigma P_{\text{int.}} &= \frac{K_{\text{III,IV}}(K_{\text{III,IV}} + \text{I})}{(K'\text{v})} \end{split}$$

If free carbon does *not* form, the fact that $P_{\mathbf{C}}$ in applied reduction is invariably higher than $P_{\mathbf{\beta}\text{-graphite}}$ means that even higher total pressures are necessary to satisfy $K_{\mathbf{V}}$. These are indicated by the shaded areas.

Fig. 20 further clarifies the "lagging" phenomenon discussed earlier and accounts for Wiberg's data, reproduced in Fig. 21, which show lagging in H₂ reduction in contrast to the normal curve for CO

reduction. Thus, internal pressures of thousands of pounds per square inch are easily attained in CO reduction, which would readily counteract any tendency toward film formation and encasement of unreduced ore. Conversely, such pressures are necessary before the thermodynamic potential ΔF can be reduced to zero, stopping the reduction reaction. The progress of reduction is therefore quite normal. With H_2 reduction, however, only comparatively moderate pressures can be obtained even when supernormal furnace pressures are used.

The formation of Fe₃C might introduce another complication into this system, since it would represent a new phase in the sense of the phase rule. However, carboniferous Fe and graphite are the stable forms up to 1200°C., according to Seltz et al.,²²⁸ whose work corrects some earlier statements and allows confining the foregoing calculations to systems of graphite and carboniferous Fe.

REMARKS ON OTHER GASEOUS REDUCING MEDIA

Reduction with virtually all other commonly used gaseous media except chlorine utilizes H and CO as the active agents and therefore fundamentally involves the principles just discussed. Furthermore, when H₂ and CO are used together, as in H₂-CO mixtures and hydrocarbon gases, the system categorically becomes that of the well-known water-gas equilibrium:

$$H_2 + CO_2 = H_2O + CO$$
 [XI]
 $K_{XI} = \frac{K_I}{K_{III}} = \frac{K_{II}}{K_{IV}} = \frac{(H_2O)(CO)}{(H_2)(CO_2)}$ [XIa]

Chipman and Murphy⁴⁴ give a highly accurate expression for K_{XI} :

$$\log K_{XI} = -\frac{2190}{T} - 0.201 \log T$$

$$-0.000393T + 5.46 \times 10^{-8}T^{2}$$

$$+ 2.979 \text{ [XIb]}$$

The increase of K_{XI} with temperature indicates the greater relative reducing power of H_2 at elevated temperatures as compared with CO, caused by the thermal dissociation of CO producing O.

It should also be noted that the extra component in this combined system provides an extra degree of freedom, which complicates the analysis of reduction in a manner that will not be discussed here.

CONCLUSIONS

An exhaustive review of published work on low-temperature gaseous reduction of magnetite by H₂, CO, and other gases reveals confusion regarding certain thermodynamic and chemical factors fundamental to the process. On the basis of this review and an original research with H₂ reduction, these factors are discussed from the standpoint of thermodynamics, the phase rule, and chemical principles of gas-metal equilibria. The following conclusions have been reached:

GENERAL

1. The thermodynamic potential, or free-energy change, is the fundamental driving force for all reactions. A function of temperature, the composition of the ore, and the impinging gas, ΔF values can depict the general thermodynamic status of reduction at any period, the direction of the over-all reaction, the effect of temperature, the effect of the accumulating gaseous product H_2O or CO_2 on reduction deeper in the bed, the effect of preliminary gas purification, and the limit beyond which any given reaction cannot go.

REDUCTION WITH H2

1. With increasing temperature, the thermodynamic potential of reduction increases regularly and rapidly whether Fe₃O₄, FeO, or wüstite is considered; and initial reduction rates correspondingly increase regularly to indicate that the thermodynamic driving energy of the

reduction reaction is the principal factor in initial stages.

- 2. Above 600°C., these initial rates lag, causing a maximum for total reduction to occur at 600°. It is assumed that the accumulating reaction product, Fe, fuses or crystallizes above that temperature to form a physically impermeable diaphragm surrounding the semireduced particles. Nonmetallics fluxed by FeO may enhance this coating. Hydrogen, which is able to diffuse chemically through the Fe diaphragm, encounters enclosed iron oxide, forming entrapped H2O under quasiequilibrium pressures, which thereupon reduces the driving energy of the reaction to zero and reduction temporarily stops. This causes the "lagging" phenomenon at temperatures above 600°.
- 3. Calculations of these total internal gas pressures reveal an ability of the trapped gas to burst the enclosing film, depending upon the film's strength and thermodynamic conditions of temperature. partial pressure, and so forth. Especially with higher furnace pressures, the potential internal pressures rapidly increase to values of hundreds of pounds per square inch. Disruption of the metallic shell by these entrapped gases destroys the metastable equilibrium conditions and once again allows reduction to proceed. Thus, with reduction under pressure, maximum reduction rates occur at temperatures higher than 600°.
- 4. Confusion in published discussion on the effect of bed depth can be clarified on the basis of thermodynamic potentials and the principles of pressure in gas-metal equilibria, which are explored in the text.
- 5. Decreasing particle size from 10 to 100-mesh led regularly to increased reduction rates in the present work, indicating that intraparticle fusion is more important in slowing reduction than interparticle sintering.
 - 6. Miscellaneous kinetic factors reported

in the literature are also discussed in the text.

REDUCTION WITH CO

- r. With increasing temperature, the thermodynamic potential for CO reduction likewise regularly increases, whether thermal dissociation of the gas occurs or not.
- 2. Unlike H₂ reduction, CO reduction involves reducing, oxidizing, and carburizing propensities; an infinite series of quadruple points exists within a narrow region of the phase diagram where gas, graphite, and carboniferous iron coexist with oxide of a fixed composition; there is one quintuple point where gas, graphite, FeO, Fe₃O₄, and carboniferous Fe may coexist; and above a certain temperature and carbon pressure the reduction reaction becomes irreversible for any given furnace pressure.
- 3. Within a semireduced particle affording entrapment of gases, however, this irreversibility is counteracted by the pressure sensitivity of the Boudouard reaction, which allows reversible equilibrium conditions to obtain at high pressures because of the shift to higher $P_{\rm CO_2}/P_{\rm CO}$ ratios for a given $P_{\rm C}$.
- 4. This pressure phenomenon is of much greater degree than in H₂ reduction and accounts for the lack of a "lagging" phenomenon in CO reduction, and for the preference of temperatures as high as 1000°C., in contrast to the 600° recommended for H₂ reduction.
- 5. Carbon, rather than CO, is judged to be the active agent in reduction, at least after initial stages; and absorption of C by the Fe is therefore a principal factor. When [C] increases, a point is reached where graphite nuclei may appear, with consequent decomposition of the gas phase and deposition of carbon.
- 6. Graphitization becomes more likely the purer the incoming CO; is inhibited in initial stages of reduction by the absorp-

tion of C by Fe; decreases with decreasing total pressure of carbon oxides in the system even with equal total quantities of carbon oxides passed; and the thermodynamic potential of graphite formation increases so rapidly with further purging of CO2 from a CO atmosphere that overpurification should be avoided.

OTHER GASES

1. Except for such gases as chlorine, all other customary reducing gases are C-H compounds and therefore involve the fundamental principles of CO and H2 reduction.

ACKNOWLEDGMENT

Acknowledgment is made to Prof. T. L. Joseph, Assistant Dean, Department of Mining and Metallurgy, Institute of Technology, University of Minnesota, who suggested and directed the experimental work reported in this paper; and to the Republic Steel Corporation for supplying the magnetite ore used in the tests.

BIBLIOGRAPHY

- 1. R. S. Dean and C. E. Williams: Is Direct Iron (Sponge Iron) A Substitute for Melting Stock? Metal Progress (1942)
- 42, 1040-1047. 2. F. F. Foss: Exploding the "Sponge Iron"
- Myth for Modern Steelmaking Practice. Steel (1942) III (15), 100-103.

 3. C. E. Williams: Sponge Iron, An Unpromising Substitute for Scrap in Steel Production. Min. and Met. (1942) 23,
- 4. R. Durrer: Thoughts on the Production of Iron. Schweizer (1943) 9, 357-360; also, Bull. Iron and Steel Inst. (June,
- 1944) 36A. 5. W. A. Janssen: Sponge Iron Has Definite Place in Postwar Picture. Steel (1944)
- 6. Sponge Iron. Tech. Work Sheet for 1945. Status as of Jan. 1, 1945. Steel (Jan. 1, 1945) 116, 258.

REDUCTION WITH HYDROGEN

- 7. M. H. Debray: On the Action Caused by the Mixtures of an Oxidizing Body and a Reducing Body of Metals and Their Oxides. Compt. rend. (1857) 45, 1018-
- 8. St. Claire H. Deville: Action of Water upon Iron and of Hydrogen upon Iron Oxide. Compt. rend. (1870) 70, 1105-1111; 71, 30-34.

- 9. G. Preuner: Equilibria among Fe, Fe₂O₄, H₂, and H₂O. Zisch. physik. Chem. (1904)
- 47, 385-417. 10. H. N. Friend, T. E. Hull and J. H. Brown: The Action of Steam on Iron at High Temperatures. Trans. Chem.
- (1911) 99, 969. Chaudron: Reversible Reactions of Water Vapor upon Iron and upon the Oxide of Iron. Compt. rend. (1914) 159,
- 12. L. Wöhler and W. Prager: Determination of the Heterogeneous Equilibrium of Water Vapor, Particularly in the Case of Iron and Tungsten. Zisch. Elektrochem. (1917) 23, 199-206; also, Jnl. Chem. Soc. (1917) 112, 11, 455.

 13. E. Schreiner and F. B. Grimnes: The
- Reversible Reaction between Iron and Steam. Z. anorg. allgem. Chem. (1920)
- 110, 311-334.

 14. G. Chaudron: Reversible Reactions of Hydrogen and Carbon Monoxide on Metallic Oxides. Ann. chim. (1921) 16, 221-281.
- 15. L. Wöhler and O. Balz: Determination of the Valence of Scale of Iron, Cobalt, Nickel, Copper, Manganese, Tin and Tungsten by Means of Water Vapor Equilibrium and the Dissociation Pressure of the Oxides of These Metals.
- Z. Elektrochem. (1921) 27, 406-419.
 16. E. D. Eastman: Equilibria in the Systems: Fe-C-O and Fe-H-O, and the Free Energies of the Oxides of Iron. Jnl. Am. Chem. Soc. (1922) 44, 975-998.

 17. A. S. Richardson, V. C. Vibrans, and W. P. Bell: Equilibrium in the Reduc-
- tion of Iron Oxide and in the Oxidation of Iron by Steam. Science (1922) 56, 27.
- 18. H. S. Taylor: The Production of Nitrogen and Hydrogen for Synthetic Ammonia Manufacture. Chem. Met. Eng. (1922) 27, 1263-1266.
- J. B. Ferguson: The Oxides of Iron. Jnl. Wash. Acad. Sci. (1923) 13, 275-281.
 L. Wöhler and R. Günther: Steam Equi-
- librium over Iron, Tungsten, and Their Oxides. Z. Elektrochem. (1923) 29, 276-
- 21. E. D. Eastman and R. M. Evans: Equilibrium Involving Oxides of Iron. Jnl.
- Am. Chem. Soc. (1924) 46, 888-903.

 Wust and P. Rütten: Comparative Investigations of the Permeability to Gas, the Porosity, the Resistance to Compression and the Velocity of Reduction of Iron Ores. Mitt. Kaiser-Wilhelm Inst. Eisenforsch. (1929) Dusseldorf 5, 1-12.
- 23. J. B. Ferguson: Equilibrium in Systems Involving Ferrous Oxide. Trans. Far.
- Soc. (1924) 21, 240-242. 24. K. Hofmann: The Reduction Mechanism of Iron Oxides in a Gas Stream. II. Z. angew. Chem. (1925) 38, 715-721.
- 25. K. Hofmann: The Developments in Pigiron Production within the Last Decade with Respect to the Technical and Chemical-metallurgical Points of View. Z. angew Chem. (1925) 38, 1058 to 1064.
- 26. Hans H. Meyer: The Speed of Reduction of Iron Ores in Flowing Gases. Mitt.

Kaiser-Wilhelm Inst. Eisenforsch.

(1928) Düsseldorf 10, 107-116.

27. B. Neumann and G. Köhler: Equilibrium Relations in the Water-gas Reaction in the Temperature Range from 300° to 1000°. Z. Elektrochem. (1928) 34,

218-237.
28. B. Bogitch: The Oxidation and Reduc-

tion of Silicates of Iron by Gases.

Compt. rend. (1929) 189, 581-583.

29. W. Krings and J. Kempkens: On the
Solubility of Oxygen in Solid Iron.

Z. anorg. allgem. Chem. (1929) 183,

30. O. C. Ralston: Iron Oxide Reduction Equilibria—A Critic from the Stand-point of the Phase Rule and Thermodynamics. Bur. Mines. Bull. (1929)

296, 326 pp.
31. B. Stålhane and T. Malmberg: Investigation on the Mechanism of the Reduction of Iron Ore. Jernkontorets Ann.

(1929) 113, 95-127. 32. P. H. Emmett and J. F. Shultz: Equilibria in the Fe-H-O System. Indirect Calculation of the Water Gas Equilibrium Constant. Jnl. Am. Chem. Soc. (1930)

52, 4268-4285.
33. W. Krings and J. Kempkens: On the Solubility of Oxygen in Solid Iron.

Z. anorg. allgem. Chem. (1930) 190,

313-320. 34. H. H. Meyer: Investigation on the Mechanism of Reduction of Iron Ore. Stahl

und Eisen (1930) 50, 969-970. Ya. Rode: Iron Oxides and Their Reducibility with Hydrogen and Car-

bon. Jnl. Russ. Phys. Chem. Soc. (1930) 62, 1453-1466; C.A. 25, 2628.
36. B. Stalhane and T. Malmberg: Investigation on the Reduction Processes of Iron Ore. III. Jernkontorets Ann. (1930)

114, 609-722.
37. W. E. Jominy and D. W. Murphy:
Equilibrium in the Iron-oxygen-hydrogen System at Temperatures above
1000°C. Ind. Eng. Chem. (1931) 23,

38. S. L. Madorsky: Reduction of Iron Oxide Ores in Molten State by Means of Hydrogen and Other Gases. Ind. Eng.

Chem. (1931) 23, 99-103.

H. Meyer: Investigation on the Mechanism of Reduction of Iron Ore. Stahl und Eisen (Review) (1931) 51,

716-717. 40. P. H. Emmett and J. F. Shultz: Influence

P. H. Emmett and J. P. Shultz: Influence of Gaseous Thermal Diffusion on Equilibrium Measurements on the Fe-O-H System. Jnl. Chem. Soc. (1932) 54, 3780-3781.
 D. W. Murphy, W. P. Wood and W. E. Jominy: Scaling of Steel at Elevated Temperatures by Reaction with Gases and the Properties of the Resulting Oxides. Trans. Am. Soc. Steel Treating (1932) 19, 103-225.

(1932) 19, 193-225.

42. H. Schenck: Introduction to the Physical Chemistry of Steelmaking, I. Berlin,

1932. J. Springer. 306 pp.
43. O. Stålhane, and J. B. Stålhane, to
Allmänna Svenska Elektriska A.-B.
Reduction of Iron Ore. Swed. Pat. 75.804 (Nov. 15, 1932). 44. J. Chipman and D. W. Murphy: Free

Energy of Iron Oxides. Ind. Eng. Chem.

45. P. H. Emmett, and J. F. Shultz: Gaseous Thermal Diffusion—the Principal Cause of Discrepancies in Equilibrium Measurements on the Systems: Fe₃O₄-H₂-Fe-H₂O, Fe₃O₄-H₂-FeO-H₂O and FeO-H₂-Fe-H₂O. Jnl. Am. Chem. Soc.

46. T. L. Joseph, E. P. Barrett and C. E. Wood: Composition and Deoxidation of Iron Oxide Sinters. Blast Furnace and Steel Plant (1933) 21, 147-150, 207-

210, 260-263, 321-323, 336. 47. F. Weinert: The Reduction of Iron Ores with Hydrogen and Carbon Oxide.

48. E. P. Barrett: Shaft Furnace Reduction by the Glomerule Method. U. S. Bur.

Mines, R. I. 3229 (1934) 60 pp.
49. E. P. Barrett and C. E. Wood: Nitrogen
Content of Sponge Iron and of Metal
Obtained by Melting Sponge Iron.
U. S. Bur. Mines, R. I. 3229 (1934)

50. E. V. Britzke, A. F. Kapustinsky and T. I. Schaschkina: The Affinity of Metals for Oxygen. II. The Equilibrium between Iron and Steam. Z. anorg. allgem. chem. (1934) 287-295.

 J. Chipman and M. G. Fontana: Thermal Diffusion of Gases Near a Hot Metal Surface. Jnl. Am. Chem. Soc. (1934)

56, 2011.
52. G. I. Chufarov and B. D. Averbukh:
Reduction of Iron Oxides by Gaseous
Reducing Agents. II. The Rate of
Reduction of Magnetic Iron Oxide by Hydrogen. Jnl. Phys. Chem. (U.S.S.R.) (1934) 5, 1292-1298; cf. C.A. 29, 3901.

5336. 53. G. I. Chufarov and A. P. Lokhvitzkaya: Reduction of Iron Oxides by Gaseous Reducing Agents. I. Velocity of Reduction of Ferric Oxide by Hydrogen. Jnl. Phys. Chem. (U.S.S.R.) (1934) 5, 1103-1113; C.A. 29, 3901.

54. H. Schenck: Introduction to the Physical Chemistry of Steelmaking. Vol. II. Berlin, 1934. J. Springer. 274 pp.
55. O. Stålhane and J. B. Stålhane, to Allmänna Svenska Elektriska A.-B. Rotary Horizontal Drum Type Furnace for Treating Pulverized Ores with Gases as in Ore Reductions. II. S.

nace for Treating Pulverized Ores with Gases as in Ore Reductions. U. S. Pat. 1,959,772 (May 22, 1934).

56. Stålhane, O. and J. B. Staihane, to Allmänna Svenska Elektriska A.-B. Continuous Reduction of Iron Oxide Ores. U. S. Pat. 1,964,680 (June 26, 1934); C.A. 28, 5033.

57. G. Chufarov and B. Averbukh: Effect of Form of Intermediate Phases on the Velocity of the Reduction of Iron Oxide

Velocity of the Reduction of Iron Oxide by Hydrogen. Acta Physicochim. U.S.-S.R. (1936) 4, 617-635; cf. C.A. 30, 8115;

58. M. G. Fontana and J. Chipman: Equilibrium in the Reaction of Hydrogen with Ferrous Oxide in Liquid Iron at 1600°C. Trans. Amer. Soc. for Metals

59. R. Gahl: Apparatus for Reduction or Oxidation of Magnetic Metals and Metal

Compounds. U. S. Pat. 2,048,111

(July 21, 1936).

60. K. Iwasé and K. Sano: A Static Method of Investigation of the Oxidation and Reduction Equilibria of Iron with Water Vapor. Sci. Repts. Tohoku Imp. Univ., 1st. Ser., K. Honda Anniversary 1936, 465-475; C.A. 31, 3766.

61. T. L. Joseph: Porosity, Reducibility and Size Preparation of Iron Ores. Trans. A.I.M.E. (1936) 120, 72-90; disc.,

90-98.

62. E. V. Snopova and N. I. Rotkov: Treatment of Kusin Titanomagnetites Based on the Reduction of the Ore with Gaseous Reduction of the Ore with Gaseous Reducing Agents at Moderate Temperatures. Trudy Ural. Nauch.-Issledovatel. Inst. Geol. Razved. i Issled. Min. Syrya (1938), No. 3, 285–293; Khim. Referat. Zhur. 1, No. 11–12,

99-100 (1938); C.A. 33, 8151.
63. Hirosi Sawamura: The Volume Change of Iron Ore Due to Reduction by Hydrogen or Carbon Monoxide. Tetsu-to-Hagane (1939) 25, 548-559; C.A. 33,

8151.

 M. Tenenbaum and T. L. Joseph: Reduction of Iron Ores under Pressure by Hydrogen. Trans. A.I.M.E. (1939) 135,

59-72.65. J. Chipman and S. Marshall: The Equilibrium FeO + H₂O at Temperatures Up to the Melting Point of Iron. J. Am. Chem. Soc. (1940) 62, 299-305.

 T. L. Joseph, F. W. Scott and M. H. Kalina: Oxide Analysis in Iron Ore Reduction Problems. Blast Furnace and Steel Plant (1940) 28, 975-978, 1073-1077

67. M. Wiberg: The Reduction of Iron Ores with Carbon Monoxide, Hydrogen and Methane. Jernkoniorets Ann. (1940) 124, 179-212; Chem. Zenir. 1940, II.

68. V. O. Krenig and E. M. Zaretskii: The Removal of Scale from Steel by Pickling in Acids. Korrosion u. Metallschutz (1941) 17, 243-246; Chem. Zenir. 1941, II, 2864.

69. F. Olmer: Reduction of Iron Oxides in the Presence of Foreign Substances.

Rev. Met. (1941) 38, 129-134.

Sedlatschek: Reactions of Solids.
CXXIX. The Reducibility of Fe₂O₂ 70. K. by H under the Addition of Small Amounts of Extraneous Gases. Z.

Amounts of Extraneous Gases. Z. anorg. allgem. Chem. (1942) 250, 23-35.

71. M. C. Udy and C. H. Lorig: The Low-temperature Gaseous Reduction of a Magnetite. Metals Tech. (1942) 9, T.P. 1509, 19 pp.; also, Trans. A.I.M.E. (1943) 154, 162-180; disc., 180-181.

72. F. Olmer: A Method of Study of the Kinetics of Chemical Reactions. Int.

Kinetics of Chemical Reactions. Jnl.

Phys. Chem. (1943) 47, 313-317.
73. F. Olmer: Reduction of Fe₂O₃ by Hydrogen. Jnl. Phys. Chem. (1943) 47, 317-

74. R. L. Patterson, to Powder Metals and Alloys, Inc. Reduction of Finely Divided Metal Compounds Such as Fe Oxide. U. S. Pat. 2,334,434 (Nov. 16, 1943).

75. W. E. Brown: An Experiment in Making

Sponge Iron. Eng. and Min. Ind. J.

(Nov., 1944) 145, 83-86. 76. F. E. Harris: Reactions between Hot Steel and Furnace Atmospheres. Metal Prog-

ress (1944) 47, No. 1, 84-89.
77. C. F. Ramseyer: Sponge Iron—Its Possibilities and Limitations. Iron Steel Engr. (1944) 21, No. 7, pp. 35-44, 72.

REDUCTION WITH CARBON MONOXIDE

78. See Refs. 7, 14, 16, 21, 23, 26, 28, 30, 31, 34-36, 38, 39, 42-44, 46, 49, 54-56, 59, 63, 67, 69, 76.

M. Caron: On the Carburization of

79. H. Iron by Carbon Oxide. Compt. rend.

(1864) **59**, 333-336. 80. J. L. Bell: Chemical Phenomena of Iron Smelting: Section VIII—Action of Mixtures of CO and CO₂ on Fe₂O₃.

Jul. Iron Steel Inst. (1871) 1, 111-115.

81. J. L. Bell: On the Conditions Which Favour, and Those Which Limit the Economy of Fuel in the Blast Furnace for Smelting Iron. Proc. Inst. Civil Engrs.

(1872) 34, 111-155. 82. Gruner. Compt. rend. (1872) 74, 226. (See

Matsubara. 116)

. Åkerman: On the Reduction of Iron Oxide by Carbon Monoxide. Stahl und 83. R.

Eisen (1883) 3, 149-160.

84. J. G. Wiborgh: Investigations on the Reducibility of Iron Ores. Stahl und Eisen (1888) 8, 15-21.

85. B. Osann: On the Beneficiation of Iron

Ores. Stahl und Eisen (1893) 13, 986-

86. J. G. Wiborgh: Process for Determining the Reducibility of Iron Ores. Stahl und Eisen (1897) 17, 804-810.

87. J. G. Wiborgh: Ibid., (1897) 858-862.

88. B. Osann: The Beneficiation of Iron Ores and Other Smelting Materials. Stahl und Eisen (1902) 22, 1033-1038.

B. Osann: Ibid., (1902) 1101-1110.
 E. Baur and A. Glaessner: Equilibria of Iron Oxide with Carbon Monoxide and Carbon Dioxide. Z. phys. chem.

(1903) 43, 354-368.
91. R. Schenck and F. Zimmermann: On the Dissociation of Carbon Oxide and the Blast Furnace Equilibrium, Ber. Deut.

chem. Ges. (1903) 36, 1231-1251.
92. R. Schenck and W. Heller: Experimental Studies of the Conditions in the Reduction of Iron. Ber. deut. chem. Ges. (1905)

38, 2132-2139.
93. R. Schenck and W. Heller: Notes on the Varied Behavior of Different Forms of Carbon. Ber. deut. chem. Ges. (1905)

38, 2139-2143.
94. W. Mathesius: Reduction of Metallic Oxides. Ger. Pat. 203,086 (Jan. 29, 1907).

 T. Naske: Contribution to the Metallurgy of the Open-hearth Process. Stahl und Eisen (1907) 27, 157-161, 191-

194, 229-236, 265-269. 96. R. Schenck, H. Semiller and N. Falcke: Experimental Studies on Reduction and Carbide Formation in Iron. Ber.

Deut. chem. Ges. (1907) 40, 1704-1725.

97. G. Charpy: On the Carburization of Iron and Its Alloys by Carbon Monoxide.

Rev. Met. (1909) 6, 505-518.

98. W. Mathesius: Reduction of Metallic

Oxides. Br. Pat. 3,819 (Feb. 16, 1910).

99. A. Gautier and P. Clausmann: Action of Iron and Its Oxides at Red Heat on Carbon Monoxide—Application to Some Geologic Principles. Compt. rend.

100. A. Gautier and P. Clausmann: Action of Mixtures of Carbon Monoxide and Hydrogen, or of Carbon Dioxide and Hydrogen on the Oxides of Iron. Compt.

rend. (1910) 151, 355-359.

101. W. Mathesius: Process for the Reduction of Metallic Oxides. U. S. Pat. 1,003,627

(Sept. 19, 1911).
102. M. Levin: Reduction of Iron Oxides.
Nernst's Festschrift (Halle, 1912),

252-257. 103. V. Falcke: The Reaction between Ferrous Oxide and Carbon and between Carbon Monoxide and Iron. Ber. (1913) 46,

743-750.

104. W. Mathesius: Investigations on the Reducibility of Iron Ores in Flowing Gases. Stahl und Eisen (1914) 34, 866-873.

105. V. Falcke: The Reactions between FeO and C and between CO and Fe. Z.

and C and between CO and Fe. Z. Elektrochem. (1915) 21, 37-50.

106. S. Hilpert and T. Dieckmann: Iron Carbides and Their Catalytic Action on the Decomposition of Carbon Monoxide. Ber. (1915) 48, 1281-1286.

107. V. Falcke: Reaction between Ferrous Carbon and Carbon and Carbon and Carbon conductors.

Oxide and Carbon and between Carbon Monoxide and Iron. Z. Elektrochem.

(1016) 22, 121-133.
C. H. Carpenter and C. C. Smith:
Some Experiments on the Reaction
between Pure Carbon Monoxide and
Pure Electrolytic Iron below the A 108. H. Inversion. Inl. Iron Steel Inst. (1918)

98, 139-191; disc., 192-197.

109. R. Schenck and R. S. Dean: Physical Chemistry of the Metals, Ed. 1, 177.

New York, 1019.
110. E. Terres and A. Pongracz: Reactions in the Blast-furnace Equilibrium. Z. Elektrochem. (1919) 25, 386-407.

III. H. M. Ryder: The Relation between

Gases and Steel. Elec. Jnl. (1920) 17, 161-165.

112. G. Chaudron: Reversible Reaction. CO on the Oxides of Iron. Compt. rend.

113. V. Falcke: Reactions between Ferrous Oxide and Carbon and between Carbon Monoxide and Iron. IV. Z. Elektro-chem. (1921) 27, 268-278.

114. F. Giolitti: Case-hardening and Oxidation

of Steel. Chem. Met. Eng. (1921) 25,

312-313.
F. M. Wiberg: Method of and Furnace for Reducing Ores and Oxygen Compounds Utilized as Ores. U. S. Pat.

1,401,222 (Dec. 27, 1921).

Matsubara: Chemical Equilibrium between Iron, Carbon, and Oxygen.

Trans. A.I.M.E. (1922) 67, 3-54; disc.,

54-55.
117. R. Schenck: The Importance of Physical Chemistry in the Metallurgy of Iron. Stahl und Eisen (1923) 43, 65-69, 153-

118. A. Stansfield: The Electric Furnace for Iron and Steel, 3d ed., 151-157. New York, 1923.

119. E. Fornander: The Direct Production of Iron. Chem. Met. Eng. (1924) 30, 864-

868, 907-910.

120. P. H. Royster, T. L. Joseph and S. P. Kinney: Influence of Ore Size on Acquetion. Blast Furnace Steel Plant (1924) 12, 274-280.

121. R. Schenck: Use of Oxygen and Oxygen-enriched Air in Pig Iron Production.

Stahl und Eisen (1924) 44; 521-526.

122. C. E. Williams, E. P. Barrett and B. M. Larsen: A Process for the Production of Sponge Iron. U. S. Bur. Mines, R. I.,

Ser. 2578, Feb. 1924.

123. C. E. Williams, E. P. Barrett and B. M. Larsen: The Production of Sponge Iron. U. S. Bur. Mines, R. I., Ser. 2656,

(Nov. 1924) 14 pp.

Kamura: Reduction of Iron Ores by Carbon Monoxide. Trans. A.I.M.E. 124. H. (1925) 71, 549-564; disc., 564-567.
125. C. E. Williams: Recent Developments in

Sponge Iron. Min. and Met. (1925) 6,

126. V. Falcke and W. Fischer: Equilibria among Carbon Monoxide, Carbon, and Carbon Dioxide, and the Reactions between Ferric Oxide and Carbon and between Carbon Monoxide and Iron. Z. Elektrochem. (1926) 32, 194-201.

127. K. Iwasé: Equilibrium between Iron, Carbon and Oxygen: Reduction of Iron Ores, Cementation and Gas Occlusion of Iron and Steel. Science Repts. Tohoku

Imp. Univ. (1926) 15, 511-529.

128. A. Johansson and R. von Seth: The Carburization and Decarburization of Iron. The Surface Decarburization of Steel. Jnl. Iron Steel Inst. (London) (1926) 114, 295-353; disc., 353-357; also, Engineering (1926) 122, 460-464. Schenck: Equilibrium Relations

among Iron, Oxygen and Carbon. Stahl

und Eisen (1926) 46, 665-682.

130. Genske Takahashi: The Equilibrium between Austenite and the Carbon Oxides. Sci. Repts. Tohoku Imp. Univ.

(1926) 15, 157-175.

131. W. P. Fishel and J. F. Wooddell: Action of Pure Carbon Monoxide upon Iron at Elevated Temperatures. Trans. Am. Soc. Steel Treating (1927) 11, 730-740.

132. R. Schenck: Equilibrium Relations in the Reduction, Oxidation and Carburization of Iron. I. Z. anorg. allgem. Chem.

(1927) 164, 145-185.
133. R. Schenck: Investigations on the Equilibria of the Reduction, Oxidation, and Carburization Processes of Iron. II. Z. anorg. allgem. Chem. (1927) 164, 313-

325. 134. R. Schenck, et al: Equilibrium Relations in the Reduction, Oxidation and Carburization of Iron. III. 4. Systematic Investigations of the Oxidation-reduc-tion Relations Existing in the Systems of the Iron Oxides with Iron, Carbon Monoxide and Carbon Dioxide. Z. anorg. allgem. Chem. (1927) 166, 113-

135. R. Schenck, et al: Equilibrium Relations in the Reduction, Oxidation and Carbonization of Iron. IV. 5. Iron Carbide, Iron Oxides and Iron under an Atmosphere of Carbon Monoxide and Carbon

Dioxide, Z. anorg. allgem, Chem. (1027)

136. R. Schenck: Equilibrium in the Reduction, Oxidation and Carburization of Iron, V. Z. anorg. allgem. Chem. (1927)

137. C. E. Williams, E. P. Barrett and B. M. Larsen: Production of Sponge Iron.

U. S. Bur. Mines, Bull. 270 (1927).
Falcke: Reactions between Ferrous Oxide and Carbon and between Carbon Monoxide and Iron. Z. Elektrochem.

(1928) 34, 393-398.

139. R. R. Garran: Equilibria at High Temperatures in the System Iron-oxygencarbon. Trans. Faraday Soc. (1928) 24, 201-207.

L. Joseph: Importance of Gas-Solid Contact in the Blast Furnace. Fuels

and Furnaces (1928) 6, 635-640.

141. E. Maurer and W. Bischof: Equilibrium Investigations on the Reduction, Oxidation, and Carburization of Iron. Stahl und Eisen (Review) (1928) 48, 15-21, 271-274, 276; also, Concerning the Solubility of Oxygen in Iron. Ibid.

(1928) 1335-1337. Schenck: The First Stage in the Development of Our Conception of the Equilibria in the System Fe-C-O. Z.

Elektrochem. (1928) 34, 399-403.
143. R. Schenck: Equilibrium Investigations on the Reduction, Oxidation and Carburization Processes of Iron. Stahl und Eisen (Review) (1928) 48, 269-271.

274-276.

144. R. Schenck and T. Dingmann: Equilibrium Relations in the Reduction Oxidation and Carburization of Iron; Solubility of Oxygen in Iron. Z. anorg.

allgem. Chem. (1928) 171, 239-257.
145. R. Durrer: On the Reduction of Iron Ore.

Stahl und Eisen (1929) 49, 1835.

146. C. C. Furnas and T. L. Joseph: Blastfurnace Filling and Size Segregation.

Trans. A.I.M.E. (1929) 84, 98-124;

disc., 124-125.
147. R. Schenck, et al: Equilibrium Studies of the Reduction, Oxidation, and Car-burization Processes of Iron. VIII. 9. The System Iron-oxygen. Z. anorg.

allgem. Chem. (1929) 182, 97-117.
148. R. Schenck, H. Franz and H. Willeke: Equilibrium Relations in the Reduction, Oxidation and Carburization Processes of Iron. IX. 10. The Influence of Foreign Oxides upon the Equilibria. Z. anorg. allgem. Chem. (1929) 184,

149. B. Stalhane and T. Malmberg: Investi-gation on the Mechanism of the Reduction of Iron Ore. Jernkontorets Ann.

(1929) 113, 95-127. 150. M. L. Becker: Carburizing and Graphitizing Reactions between Iron-carbon Alloys, Carbon Monoxide and Carbon Dioxide. Jnl. Iron Steel Inst. (1930) 121, 337-361; disc., 362-365. 151. W. A. Bone, L. Reeve and H. L. Saunders:

An Experimental Inquiry into the An Experimental Inquiry into the Interactions of Gases and Ores in the Blast Furnace. I. At Temperatures up to 650°. II. Carbon Deposition at 450° and Its Influence upon the Ore Reduction: Equilibria between Gases and

Ore at 650° to 1000°. Jnl. Iron Steel Inst. (London) I, (1927) 115, 127-167; disc., 168-180; II, (1930) 121, 35-81;

disc., 82-95.

152. C. C. Furnas and T. L. Joseph: Stock
Distribution and Gas-solid Contact in the Blast Furnace. Bur. Mines Tech.

Pub. 476 (1930) 73 pp.
Sauerwald: Physical Chemistry of
Metallurgical Reactions. Berlin: 1930.

J. Springer. 142 pp.

154. E. Scheil and E. H. Schulz: Considerations Concerning the Ternary System Iron-carbon-oxygen on the Basis of Schenck's Measurements. Z. anorg.

allgem. Chem. (1930) 188, 290-308.

Stålhane and T. Malmberg: The Reduction of Iron Ore. Jernkontorets Ann. (1930) 114, 1-26; c. C.A. 25, 155. B.

2393. 3599. . Winter and P. B. Crocker: Effect of 156. M. Winter and P. B. Crocker. Carbon Gases on Steel. Heat Treating

Forging (1930) 16, 1450-1451.
157. H. Dünwald and C. Wagner: Thermodynamic Investigations on the System Iron-carbon-oxygen. Z. anorg. allgem.

Chem. (1931) 199, 321-346.
Esser: On the Question of Oxygen Solubility in Iron; Remarks on the Work of H. Dünwald and C. Wagner "Thermodynamic Investigation on the System: Iron-carbon-oxygen. Z. anorg. allgem. Chem. (1931) 202, 73-76.

159. J. Klärding: Reduction Characteristics of Some Iron Ores. Arch. Eisenhüttenw. (1931) 5, 129-138.

. Siegel: Reduction Experiments on Minette (Oölithic Iron) Ores and Sinter 160. H. Material. Arch. Eisenhüttenw. (1930/31) 4, 557-564.

Bramley and H. D. Lord: Equilibria 161. A. between Mixtures of Carbon Monoxide and Carbon Dioxide at Various Pressures in Contact with Steels of Different Carbon Concentrations at 750-1150°. Jnl. Chem. Soc. 1932, 1641-1669.
162. H. Kirscht: Influence of Small Amounts

of Copper, Nickel, and Cobalt on the Oxidation Reaction of Iron. Stahl und

Eisen (1932) 52, 71.

163. W. Ruff and E. Scheil: The Removal of Arsenic from Iron Ores. Stahl und

Eisen (1932) 52, 1193-1195.

164. R. Schenck, et al: Equilibrium Investigations of the Reduction, Oxidation and Carburization Process of Iron. X. 11. The System: Iron-oxygen: Abnormal Oxidation: Activation of Iron without Additions. Z. anorg. allgem. Chem.

(1932) 206, 73-95.

165. R. Schenck, H. Franz and A. Laymann: Equilibrium Investigations in the Reduction, Oxidation and Carburization Processes of Iron. XI. Z. anorg. allgem. Chem. (1932) 206, 129-151.

Schenck: Corrections in the Equilibrium Studies of Reduction and other Reactions of Iron. XI. Z. anorg. allgem. Chem. (1932) 208, 255-256.

167. R. Schenck and T. Dingman: Equilibrium Studies in the Reduction, Oxidation and Carburization Processes of Iron. XII. Z. anorg. allgem. Chem. (1932) 209, 1-10.

168. H. A. Bahr and V. Jessen: Dissociation of Carbon Monoxide on Iron Oxide and Iron. Ber. deut. chem. Ges. (1933) 66, 1238-1247.

169. T. L. Joseph: Progress Report—Metallurgical Division 6. Size Preparation of Iron Ores. Bur. Mines, R. I., 3240.

170. W. H. Wetherill and C. C. Furnas: The Rate of Reduction of Iron Ores with

Rate of Reduction of Iron Ores with Carbon Monoxide-effect of Particle Size, Gas Velocity, and Gas Composition. Ind. Eng. Chem. (1934) 26, 983-991.

171. E. Diepschlag: The Reduction of Iron Ore by Application of High Pressure. Arch. Eisenhüttenw. (1936) 9, 179-181.

172. O. Stålhane and J. B. Stålhane, to Allmänna Svenska Elektriska A.-B. Reduction of Iron Ores. Swed. Pat. 85,803 (March 17, 1936); C.A. 30, 5927.

5927.

173. Stålhane, O. and J. B. Stålhane, to Allmanna Svenska Elektriska A.-B. Reducing Iron Ore. Swed. Pat. 86,232

(May 5, 1936); C.A. 30, 8136.

Baukloh and F. Jaeger: Iron-ore Decomposition by Carbon Monoxide.

Arch. Eisenhültenw. (1939) 13, 65-67.

175. A. S. Timashev: The Reduction of Complex Chemical Compounds in Relation to Their Dissociation. Metallurg (1939, No. 3) 19-28.

176. M. Tenenbaum and T. L. Joseph: Reduction of Iron Ores under Pressure by Carbon Monoxide. Trans. A.I.M.E.

(1940) **140**, 106-125. K. Kozhina: Behavior of Fe₂C in a Stream of CO₂. Stal (N.S.), **1**, No. 7/8,

Stream of CO₂. Stal (N.S.), 1, No. 7/8, 78-79. (1941).

178. R. Durrer: Production of Iron from Ore.

Tek. Tid. 72, 69-71 (Sept. 12, 1942);
C.A. 38, 4549.

179. F. Körber, H. Wiemer and W. A. Fischer:

The Thermal Disintegration of CO on
Fe and Its Alloys and in Mixtures with
C. Arch. Eisenhüttenw. (1942) 17. C. Arch. Eisenhüttenw. (1943) 17,

180. L. Scheepers: The Catalytic Dissociation of CO. Rev. universelle mines (1943) 19, 121-131; Chem. Zentr. 1943, II, 1782-

1783.

181. E. Améen: Production of Iron Sponge at Söderfors by the Wiberg Method. Metallurgia (April, 1944) 29, 333-334; also, Bull. Iron and Steel Inst. No. 102, (June, 1944) 36A; also, Iron and Coal Trades Rev. (1944) 148, 211-213, 249-251; also, Iron Steel (1944) 17, 637-

642. 182. T. P. Colclough: Considerations on Blast-

Furnace Practice. Int. Iron and Steel
Inst. (advance copy) (Oct. 1944) 18 pp.
183. F. C. Wood Jr.: Low-carbon Iron and
Steel Produced Directly from Iron Ore. U. S. Pat. 2,349,688 (May 23, 1944).

REDUCTION WITH OTHER GASES

184. See Refs. 38, 46, 49, 67, 137.
185. J. A. Holmes: Second Annual Report of the Director of the Bureau of Mines.

pp. 69-79 (1912).

186. F. E. Agnew: Reducing Ores. U. S. Pat.
1,174,464 (March 7, 1916).

187. H. P. Tiemann: Iron and Steel Handbook,
2nd ed. New York, 1919.

188. A. E. Bourcoud: Reducing Metallic Oxides. U. S. Pat. 1,344,977 (June 29.

Riveroll: Method of and Apparatus for the Production of Iron and Steel. 180. E.

190. A. E. Bourcoud: Direct Process for Steel Manufacture. Proc. 20th Meeting Am. Iron and Steel Inst. No. 18, 1921; also,

Iron Age (1922) 109, 1349-1351.

191. W. E. F. Bradley: Metallurgical Process
Can. Pat. 230,928 (May 8, 1923).

192 E. D. Eastman: Reduction of Iron Oxides

by Fuel Gases. Bur. Mines, R. I. No. 2485 (1923) 14 pp.
193. J. E. Leonarz: Reduction of Ores. Can.

193. J. E. Leonarz: Reduction of Ores. Can.
Pat. 230,650 (May 1, 1923).

194. E. Ohmann: Sponge Iron Low in Impurities by Ekelund's Process. Metal
Progress (October 1931) 20, No. 4.

89-90.
195. E. Diepschlag, M. Zillgen and H. Poetter: Evaluation of Iron Ores for the Blast Furnace. Stahl und Eisen (1932) 52,

1154-1162.

196. C. G. Maier and S. B. Thomas: Reduction of Iron Ore by Natural Gas. U. S. Bur. Mines, R. I., 3229 (1934) 60 pp.

197. E. Bornhardt to G. Polysius A.-G. Reducing Metal Oxides. Ger. Pat. 629,540 (May 7, 1936).

198. J. D. Bradley: Reduction of Oxide Ores Such as Those of Iron, Etc. U. S. Pat.

2,057,554 (Oct. 13, 1936).

199. M. S. Novakovskii and L. I. Ponirovskaya: Reduction of Fe₂O₃ by Illuminating Gas. Trudy Inst. Khim. Khar'kov. Gosudarst. Univ. (1940) 5, 293-298; Khim. Referat. Zhur. (1941) 4, No. 9, 34; C.A. 38, 1711.

200. B. E. Carl: Apparatus for Recovering Metals Such as Iron. Chromium.

Metals Such as Iron, Chromium, Tungsten or Aluminum, from Their Oxides by Countercurrent-wise Chlorination and Fractional Condensation of Chlorides Formed. U. S. Pat. 2,296,422 (Sept. 22, 1942).

201. B. A. Jeffery, (50 per cent to Scott H. Lilly)
Reducing Ores Such as Those of Pe,
and Forming Sponge Metals and
Alloys. U. S. Pat. 2,351,765 (June 20,

1944). B. Whitman: An Experiment in 202. E. Making Sponge Iron. Eng. Mining Jul. (1944) 145, No. 11, 83-86.

203. R. S. Dean: Sponge Iron. A Progress Report. U. S. Bur. Mines, R. I., 3790 (1945) 29 pp.

204. Sponge Iron—A Progress Report. Steel (April 9, 1945) 116, 106—108, 148, 151, 152, 154, 156. (Prepared from a report by Dr. R. S. Dean.)

REDUCTION OF OTHER OXIDES

205. St. C. H. Deville: Note on the Obtaining of Very High Temperatures. Ann. chim. phys. (1856) 46, No. 3, 182-203.
206. St. C. H. Deville: The Dissociation of the Control of the Con

Spontaneous Decomposition of Substances under the Influence of Heat.

Compt. rend. (1857) 45, 857-861.

207. C. R. A. Wright and A. P. Luff: First Report to the Chemical Society on "Researches on Some Points in Chem-

ical Dynamics." Trans. Chem. Soc.

(1878) 33, 1-27.
208. W. A. Bone and R. V. Wheeler: Phil.

Trans. (1906) 206A, I.
209. H. C. Greenwood: The Reduction of

Refractory Oxides by Carbon. Inc. Chem. Soc. (1908) 93, 1483-1496.
210. H. C. Greenwood: The Production of Ferro-alloys. Inc. Chem. Soc. (1908)

93, 1496-1500.
211. R. E. Slade and G. I. Higson: Equilibria in the Reduction of Oxides by Carbon. Trans. Chem. Soc. (1919) 115, Part 1.

N. Pease and H. S. Taylor: The Reduction of Copper Oxide by Hydrogen. Jnl. Am. Chem. Soc. (1921) 43, 212. R.

2179-2188. 213. R. N. Pease and R. S. Cook: Equilibrium in the Reaction, NiO + H₂ = Ni + H₂O. The Free Energy of Nickelous Oxide. Jnl. Am. Chem. Soc. (1926) 48, 1199-1206

214. E. D. Eastman and P. Robinson: Equilibrium in the Reactions of Tin with Water Vapor and Carbon Dioxide. Inl. Am. Chem. Soc. (1928) 50, 1106-

215. P. H. Emmett and J. F. Shultz: Equilibrium in the System CO-H₂O-CoO-H₂. Jnl. Amer. Chem. Soc. (1929) 51,

3249-3262. 216. P. H. Emmett and J. F. Shultz: Equilibrium in the System Co-CO₂-CoO-CO. Indirect Calculation of the Water Gas Equilibrium Constant. Jnl. Am. Chem.

Soc. (1930) 52, 1782-1793. 217. E. Crepaz: Reduction of Stannic Oxide with Carbon Monoxide. Atti V. Congr. Nazl. Chim. Pura Applicata, Rome 1935, Pt. 1, 346-352 (1936); C.A. 31,

5659. 218. I. Ya. Granat: Reduction of Chromium Oxides. Metallurg (1936) 11, 35-41;
Metals and Alloys (1937) 8, MA340.
219. N. Nasu: Reduction Equilibria of TiO2
by H. Sc. Rept. Tohoku Imp. Univ. 1st

Ser. (1936) 25, 510-526. 220. J. M. Dunoyer: Reduction by H of Pb

and Ag Oxides. Compt. rend. (1942)

214, 556-557.
221. R. Fricke and G. Weitbrecht: Active Substances. II. The Equilibria of CO/CO₂ with Ni/NiO, and with (Ni + γ-Al₂O₃)/NiAl₂O₃, and Their Dependence on the Physical State of the Solid Reportants. The Elektrocket the Solid Reactants. Z. Elektrochem.

(1942) 48, 87-106.

Pricke and G. Weitbrecht: The Boudouard Reaction in the System Ni/NiO and (Ni + γ-Al₂O₃)/NiAl₂O₄.

Z. Elektrochem. (1942) 48, 106-110. A. Zapffe and C. E. Sims: Silicon Monoxide. Iron Age (1942) 149, No. 4.

29-31; No. 5, 34-39.
224. C. G. Maier to The Dow Chemical Co.:
Chlorination of Cr Ore. U. S. Pat. 2,349,801 (May 30, 1944); cf. U. S. Pat.

2,133,998.

225. I. E. Muskat to Pittsburgh Plate Glass
Co.: Chlorination of Chromite Ore.

U. S. Pat. 2,349,747 (May 23, 1944).

226. C. A. Zapffe: Conversion of Certain
Refractory Oxides to a Suboxide Form
at High Temperatures. Jnl. Am. Cer. Soc. (1944) 27, 293-298.

227. C. A. Zapffe: Boiler Bmbrittlement. Trans. A.S.M.E. (1944) 66, 81-117;

disc., 117-126. 228. H. Seltz, H. J. McDonald and C. Wells: Heat Capacity of Iron Carbide from 68° to 298° K. and the Thermodynamic Properties of Iron Carbide. Metals Tech. (1939) 6, 19 pp.

DISCUSSION

(C. H. Lorig presiding)

M. C. UDY.*-I wish to congratulate the authors on a very fine paper. The summary of previous work is particularly well done.

The more formal thermodynamic treatment of some of the data first presented by Dr. Lorig and me (author's reference 71) is well taken and seems to substantiate our conclusion that the diffusion rate of water vapor from the seat of reaction through the already reduced envelope of metal is the controlling factor in the over-all reduction process.

I am happy to see that the authors have been able to substantiate our disclosure of a lagging in the rate of reduction in the later stages of the reaction as the temperatures are increased. Our data, too, show an initially higher rate for the higher temperatures with the lagging coming at a later stage. This point was not emphasized in our paper.

Subsequent to our published work, tests were made on several other ores. The lagging phenomenon was noted with three different magnetites. The greatest degree of lagging in all cases seemed to come at about 700°C. The lowest temperature at which lagging became apparent, however, did not seem to be the same for the different materials. Mill scale, for example, showed lagging at 600°C. (as compared with 500°). Similar tests on a hematite ore showed no indication of lagging whatsoever, the rate of reduction increasing with temperature in a normal manner. This seems to be in agreement with the authors' statement that with Fe₂O₃ high internal pressures would be obtained (capable of disrupting the enclosing envelope of metal, and thus allowing the reduction to proceed).

M. B. Bever. †-The subject of this paper is of fundamental importance for an under-

Research Engineer, Battelle Memorial Institute, Columbus, Ohio.

[†] Assistant Professor, Massachusetts Institute of Technology, Cambridge, Massachusetts.

standing of the conventional blast-furnace process as well as of sponge-iron processes. Some of the reactions studied by the authors are also of interest to the physical metallurgist, as they are involved in scaling and carburizing of ferrous materials during heat-treating or in service at elevated temperatures. The detailed review of the literature contained in this paper will therefore be welcomed. The experimental results reported by the authors supplement the recent work of Joseph and Tenenbaum and of Udy and Lorig. The analysis of the factors affecting gaseous reduction is novel in several respects and raises a number of questions, some of which will be dealt with in this discussion.

The authors propose Eq. I, IIe as a measure of the driving force or distance from equilibrium, but there is little interest in such a function unless it can furnish information on the reaction rate. They have failed to show that their equation has more than qualitative significance in this respect. In particular, the authors have not demonstrated—either by theoretical deduction or by experiment—that their expression is superior from a kinetic standpoint to a linear expression in terms of concentrations.

It may be noted that the logarithmic nature of Eq. I,IIe results in a driving force of infinite magnitude for a pure reducing gas. If the reducing actions of two nearly pure gases such as hydrogen and carbon monoxide are to be compared, the ln KP* terms, which are independent of the nature of the reducing gas, are so large that they outweigh completely the ln K terms characteristic of the equilibria. These implications do not disprove the formal thermodynamic correctness of Eq. I,IIe but suggest that the rate of a reaction is not a simple function of the driving force defined by this or similar equations. This is universally accepted as a consequence of the essential difference between thermodynamics and kinetics.

It is well known that many reactions do not proceed at a measurable rate, although the resultant free-energy decrease would be large. Several facts can be quoted as evidence that the rate of a reaction depends also on other factors than the driving force. The occurrence of catalytic effects illustrates this point. The rate of a gas-solid reaction may be affected by the selective adsorption of a gas on the

solid. Diffusion and structural features may be important rate-determining factors. Finally, the effect of temperature on the driving force expressed by Eq. I,IIe is unquestionably not the only factor causing the reaction rate to change with temperature.

Throughout their discussion of the mechanism of reduction, the authors appear to assume the existence of a separate gas phase inside the semireduced particle. Rifts and defects existing in the particle and cracks caused by the reduotion process itself may admit gas to localized zones. The paper does not deal with the pertinent structural questions, but treats hydrogen and water vapor in simple terms of pressure. It is likely that at least part of the reduction takes place by reactions within the lattice of the solid particles. In applying equilibrium constants to these reactions, the change in activity of the reactants and products must be taken into account. For this reason, Eq. I,IIe unless suitably modified is not applicable to reactions in the solid state.

Even if the driving force calculated by Eq. I,IIe were related in a useful manner to the reaction rate, it would not be a convenient parameter in an equation describing the reduction of a large number of particles, since it could not apply to systems in which the gas composition varies with time or with position in space. The authors touch on this point when they suggest that the significance of the driving force can be appraised by "considering the passage of the reducing gas through the ore bed on the basis of a series of minute isolated systems." This would require a complicated experimental and mathematical technique. The present paper does not contain this type of analysis but gives only a few arbitrarily chosen illustrative examples.

The authors' interpretation of the data of Udy and Lorig concerning the effect of bed depth on reduction is not convincing. In Udy and Lorig's work the water vapor in the exit gas is the cumulative concentration that results from the action of the gas stream on the ore bed over a certain period. The composition of the exit gas cannot be assumed to be constant during this time. Further, this exit gas can affect only the last volume element traversed. The data of Udy and Lorig, therefore, are not suitable for a fundamental thermodynamic or kinetic analysis but merely describe

the over-all reduction of the bed. Incidentally, their paper contains a competent discussion of the significance of their results.

The tentative suggestion of a "minimum effective energy" or "threshold energy" must be rejected. As pointed out in the preceding paragraph, the data in Fig. 15 are not a suitable basis for any detailed analysis. Further, no a priori reason exists for plotting the logarithm of bed depth. Finally threshold energy as a concept is foreign to thermodynamics and will not be welcome in kinetics where activation energy is used.

This paper introduces the notion of "quasi-equilibrium" which, if sound, would revolutionize chemical thermodynamics. Obviously this quasi-equilibrium is not meant to be identical with metastable equilibrium. Assuming that such a quasi-equilibrium exists, two questions may be asked: How could the true equilibrium value be determined by experiment and what significance has it retained?

The authors state that large internal gas pressures may build up within the particles. This thesis calls for a far more thorough analysis of the structural features and diffusion phenomena involved than is contained in this paper. In particular, do the authors believe that the accumulation of gas occurs primarily in cavities or within the lattice itself? What are the factors that make diffusion into these high-pressure zones possible? Answers to these fundamental questions concerning the mechanism suggested by the authors will advance our knowledge of ore reduction.

In their discussion of internal pressures, the authors state that "intermediate pressures" (corresponding to the area between curves I and II in Fig. 17) "occur at intermediate wüstite compositions." This statement is in error. The area between curves I and II represents pressures that have not reached the possible maximum value for reaction I and the area below curve II represents pressures below the equilibrium value for reaction II. The authors' statement ignores the existence of the extensive two-phase field between magnetite and wüstite in the equilibrium diagram. A similar objection must be made to the statement " . . . the removal of oxygen is continuous, the solid solution, wüstite, not FeO, being formed from the reduction of Fe3O4."

It seems an underestimation of the impor-

tance of stepwise oxygen removal to characterize the reduction of magnetite to wüstite as a dissipation of 25 per cent of the work of reduction. Concerning the use of the phase rule in kinetic arguments, it should not be overlooked that this rule presupposes that equilibrium has been reached.

The authors assign the single ΔF line below 565°C. in their Fig. 13 to reaction I. This is surprising, as this reaction involves FeO, which is not stable in this temperature region. Above 565°C. Fe₃O₄ is "hyperactively dissociated," according to this paper. The thermodynamic or kinetic significance of this concept requires elucidation.

Much of the reasoning presented in this paper depends on the correct answer to questions involving diffusion; in particular, the diffusion of water vapor and of the oxides of carbon. While the authors seem to assume that these gases diffuse as such—that is, as molecules—it is generally held that polyatomic gases dissociate before diffusing through a solid. On this assumption, if water vapor diffuses outward simultaneously with the inward diffusion of hydrogen, the main effect is the outward movement of oxygen. The oxygen gradient is maintained by the removal of oxygen from the surface layer where it reacts with hydrogen and escapes as water vapor.

As Joseph and others have emphasized, diffusion must be recognized as one of the chief factors in the kinetics of reduction. If this is kept in mind, the effect of particle size on the rate of reduction becomes obvious and speculations about the relative importance of interparticle and intraparticle sintering lose their basis

Since the equilibrium data have been known for some time, the remaining basic problems of the gaseous reduction of iron oxides are those of kinetics. These problems should be studied quantitatively on carefully prepared individual particles in the manner already successfully used by Joseph and others. The main variables will be gas composition and pressure, temperature and the nature of the iron oxide. The results of such a study probably will establish that diffusion and the phencmena at the seat of reaction and at the solid-gas interface are the major rate-determining factors. On the basis of such fundamental kinetic data, composite systems made up of many particles may

be investigated with the promise of significant results.

O. G. SPECHT and C. A. ZAPFFE (authors' reply).—We wish to express our appreciation of the time and thought Dr. Bever obviously has given to examination of our paper. Some of his points are well taken; on others we must differ with him.

For example, the term "quasi-equilibrium" would be advisably replaced by Lewis and Randall's "partial equilibrium." If Dr. Bever is serious, however, in proposing that a revolution in chemical thermodynamics hinges on proving the concept denoted in the paper as "quasi-equilibrium," we can refer him to numerous experiments in which atomic hydrogen under pressures considerably less than atmospheric provides diffusion of H through solid steel from one side to form thousands of pounds per square inch of H₂ on the opposite side (see ref. 227). In such experiments, which are strictly analogous to the case under consideration, a steady state is reached between two portions of a chemical system whose junction is a membrane having differential permeabilities to H and to H2 in one case, and to H and H.O in the other.

Dr. Bever is again correct in pointing out the unlikelihood of our alternative explanation concerning a "minimum or threshold energy," although we similarly conclude in favor of the pressure theory. And, of course, on page 259 there is the obvious error of identifying reaction 1 with the Fe₂O₄ \rightarrow Fe reaction occurring below 565°C. Fortunately, this is nothing other than a loose statement having no effect on either calculations or conclusions, since the H₂O/H₂ ratio in unchanged form controls both the direct reduction of Fe₃O₄ and its component reactions, Eqs. I and II.

Some exceptions must be taken to Dr. Bever's remaining comments. This paper does not propose a new rate equation. It undertakes instead recognized abnormalities in existing rate determinations. By thermodynamics and the phase rule it first shows what reactions can proceed and to what limits they can go. Next it provides measurements for the energy available for those reactions, which is a worth-while factor to know regardless of the cliché which always revives in an argument over equilibrium and reaction rate. Lastly, it develops the concept of a double

(or partial) equilibrium system enabled by the existence of a diaphragm having an artificially supported atmosphere on one side and permeable only to one of the components.

This study does therefore "furnish information on the reaction rate." It informs us that the observed rate is a complicated function of at least two integral rates, for there are two differing chemical systems on either side of the diaphragm. The investigator makes his measurements only on the external side. As the gas enters the interior of the particle. the rate of deoxidation can be very high there, tapering off to zero under the conditions of trapping. Yet, neither the high nor the low rate is reflected in the recorded measurements because the gaseous product remains inside the particle. And if these occluded reaction products attain a pressure exceeding the particle's resistance to rupture, they suddenly effuse, modifying the measured rate for reasons that would not be recognized except for the type of discussion in this paper.

In regard to Dr. Bever's question on the location of the internal gas reaction, we assume that the principal deoxidation reaction occurs at surfaces inside the particle and that the principal mechanism for oxygen removal is channeling of the compressed reaction product. We believe that the particles are always sufficiently discontinuous in structure to afford these necessary latticular openings, and that the removal of oxygen by atomic diffusion is an unimportant process. Since these systems are pressure-sensitive, H2O does not precipitate within the lattice when H and O contact one another to develop potential H₂O pressures that are less than the rupturing strength of the lattice. Instead, the solubilities of H and O simply increase to regain the balance of the equilibrium system. At an internal surface, however, the fugacity of the reaction product can express itself through evaporation, and the pressure of this developed phase may then become mechanically effective in completing the chemical reaction.

Dr. Bever's criticism of the intermediate pressures assumed to exist over wüstite solutions of intermediate oxygen fugacity is acceptable in part for the reason that the area between curves I and II admittedly does not contain certain details relating to the Fe-O diagram which remain to be expressed in later refinements of this subject.

A Test for Hydrogen Embrittlement and Its Application to 17 Per Cent Chromium, 1 Per Cent Carbon Stainless-steel Wire

By Carl A. Zapffe,* Member A.I.M.E., and M. Eleanor Haslem†
(Cleveland Meeting, October 1944)

THE present investigation has three principal purposes:

r. To develop a method for measuring hydrogen embrittlement that avoids certain errors complicating previously used methods.

2. To explore in a preliminary way some of the fundamental factors controlling embrittlement.

 To apply the measurements specifically to stainless grades of steel, whose sensitivity or insensitivity to hydrogen embrittlement has never been clearly defined.

SELECTING A TEST METHOD

Hydrogen embrittlement is a condition of low ductility resulting from excessive absorption of hydrogen by the steel at some period in its history, and may be revealed by almost any test involving cold deformation. Tensile tests, impact tests, and bend tests are commonly used for detecting hydrogen embrittlement; although numerous other tests, such as cold-upsetting or extrusion, could be used. The simplicity of using a wire specimen for cathodic and acid pickling tests, and the especial adaptability of the bend test to wire specimens, led to selection of the bend test for the present research.

Bend tests usually have been of three general types: (1) fatigue, (2) reversed bend, and (3) single bend. The first two types, though widely used, are inaccurate because their measurements are counteracted by an aging effect; and the third type has not been developed to its fullest utility.

The effect of cold-working in removing hydrogen is well known. During a bend test hydrogen can be observed escaping from the convex side simply by coating the specimen with oil; and any technique employing flexing or reverse bending may therefore have its measurements masked because the mechanical action reduces the embrittlement during the test. This factor is so important that even elastic flexing of a hydrogen-charged wire specimen should be avoided before testing if accurate measurements are desired.

DEVELOPING A MACHINE FOR MEASURING HYDROGEN EMBRITTLEMENT

As for the single-bend test, its theory is good, and recovery caused by mechanical work is kept to a minimum. With a given degree of hydrogen embrittlement, a specimen will break at a given angle if the bending is applied unidirectionally and uniformly. The radius of the bend must be kept constant; and the rate of bending should be a constant, slow enough to allow reading of the breaking angle, and yet rapid enough to prevent significant recovery from the escape of hydrogen during bending.

A simple apparatus (Fig. 1) was constructed using a type H Foxboro drive unit A, which is a synchronous motor with a gear-reduction ratio of 600 to 1. A cord, fixed at one end to a wooden pulley B on the drive shaft of the motor, follows the pe-

Manuscript received at the office of the Institute Aug. 7, 1944; amended July 24, 1945. Issued as T.P. 1954 in METALS TECHNOLOGY, January 1946.

^{*} Consultant, Baltimore, Maryland.
† Research Metallurgist, Laboratory of the senior author, Baltimore, Maryland.

riphery of the horizontal semicircular base C upon which angular markings from o° to 180° are indicated. A hook is attached to the other end of this cord, which

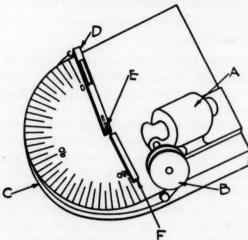


FIG. 1.—APPARATUS FOR MEASURING HYDRO-GEN EMBRITTLEMENT IN WIRE BY MEANS OF A STEADILY APPLIED SINGLE BEND.

catches a traveling arm D in the 0° position. This traveling arm is drilled longitudinally to receive one end of the wire specimen, the hole being drilled tangent to the axial pin E, which has a radius of 1_6 in. Thus, the wire is bent around the axis of the bending arm. A fixed arm F backs up the wire and stabilizes the specimen without allowing tensile or torsion stresses to develop, since the wire simply lies alongside the outside of this arm. The wooden pulley B is a in in diameter, allowing arm a to traverse the a 180° in 40 sec., a rate of a 1.5° per second.

Exactly 30 sec. after the specimen is removed from the test it is placed in this machine. As will be shown, no measurable recovery occurs in such a short period of time at ordinary temperatures. The temperature of the bend test also is kept fairly constant by washing the specimen in cold tap water previous to testing. The motor is then started with the traveling arm in the o° position; when the specimen breaks, its breaking angle is read through the slot in that arm.

PRELIMINARY EXPERIMENTS WITH STAINLESS GRADES OF STEEL

Nonhardenable Grades

First, a preliminary survey was made of some hardenable and some nonhardenable steels to get a rough indication of the sensitivity of the various grades to hydrogen embrittlement. Table 1 lists the results

TABLE 1.—Bend Tests with Austenitic

Stainless Grades

Angle of bend (average of three tests), = 180°

Type No.	Diameter of Wire, In.	Temperature		Charg- ing		
		Deg. C.	Deg. F.	Time,	Remarks	
302 303	0.065	50 50	122	4 4	Annealed Annealed	
302 302 302 302	0.065 0.065 0.065	50 80	122	0 1 3 4	Cold-drawn from 0.074 inch	
303 303 303 303	0.064 0.064 0.064 0.064	23 23 50 80	73 73 122 176	4 0 4 4	Cold-drawn from 0.0795 inch	

Electrolyte, 10 per cent NaOH; current density, 1.0 amp, per sq. inch.

obtained with two austenitic grades in the annealed and in the cold-drawn conditions. The specimens were charged cathodically in a 10 per cent NaOH electrolyte at a current density of 1.0 amp. per sq. in. for periods from 1 to 4 hr. and at temperatures from 23° to 80°C. (73° to 176°F.). There was no indication of embritlement.

These results do not mean that the ductility of types 302 and 303 steels cannot be lowered by hydrogen absorption. They do mean, however, that these grades are exceedingly resistant to hydrogen embrittlement, as shown by comparison with subsequent tests; and they show that after this relatively severe treatment the wire can still be bent 180° around a ½6-in. radius without breaking.

Hardenable Grades

Since carbon is a principal factor in determining the sensitivity of unalloyed steels to hydrogen, the straight-chromium stainless steels with high carbon contents naturally become of particular interest. Table 2 lists the results of bend tests using three of these grades in the annealed

TABLE 2.—Bend Tests with Hardenable Stainless Grades

Type No.	Diameter of Wire, In.	Angle of Bend, Deg.	Remarks
420	0.0554	180 180	Annealed
440-A	0.038	180 180 180	Annealed
440-C	0.062	180 50 50	Annealed
431	0.072	47 180 110 90	Cold-drawn

Electrolyte, 10 per cent NaOH; current density, 1.0 amp. per sq. in.; temperature, 50°C. (122°F.); charging period, 2 hours.

condition. Neither type 420 nor type 440-A, the latter containing 0.64 per cent carbon, showed embrittlement. Type 440-C, however, became badly embrittled. Colddrawn 16 Cr, 2 Ni wire, also tested, showed embrittlement, though to a lesser degree than the type 440-C material.

One further preliminary test might be

TABLE 3.—Impact Tests with Type 403
Steels

Charging Period, Min.	Time Elapsed between Charging and Testing, Min.	Izod Impact Value, Ft-lb,
0		100
1	4 7	94.5 100
2	7 3 7	100
4		98
8	5 2 6	99 104
16		100
32	3	94
64	4 7	99.5
128	2 5 3 7 4 7 5 7 3	97 100.5
256	3 4	103.5

^a Tempered and stress-relieved; Brinell hardness, 223-241.

reported in which turbine quality 12 per cent Cr steel was examined for hydrogen embrittlement by the Izod impact test (Table 3). Cathodic charging up to 4 hr. caused no change in impact values, which are good criteria of embrittlement.*

From the results of these preliminary tests, and particularly because type 440-C steel was already known to show sensitivity to hydrogen during processing, the 17 Cr, 1.00 C grade was selected as the test material. A 50-yd. coil of annealed 0.062-in. wire was obtained. The analysis of this steel is listed in Table 4, along with

Table 4.—Analysis of Specimens
Per Cent

Grade	Cr	Ni	C	Mn	Si	P	S
302	18.26	9.11	0.056	0.62	0.41	0.023	0.016
303	18.30		0.062	0.72		0.035	
403	11.85		0.090	0.43		0.015	
420	13.18		0.36	0.41		0.020	
440-A	17.60		0.636	0.39		0.016	
440-C	17.46		I.OI	0.34		0.021	
431	16.37	1.67	0.158	0.56	0.50	0.020	0.033

the analyses of the other specimens just discussed. Its hardness was Rockwell F 112/113, and its ultimate tensile strength was 115,000 lb. per sq. inch.

EXPERIMENTAL APPROACH USING TYPE 440-C STEEL

One of the principal difficulties in investigations of hydrogen embrittlement is the great number of variables influencing the system. A scientific approach requires the keeping of all factors constant except the one under observation, which is particularly difficult to do in this work. Consequently, inaccuracies in the measurements must be expected.

In the present study, 15 principal variables are recognized. They are listed in Table 5 in a self-explanatory manner. The first seven concern the steel and were kept

^{*}A seemingly consistent increase in Izod values with increasing lapses of time between charging and testing may be noted, but experimental inaccuracies probably do not allow making a point of it.

constant as indicated. Consequently, the present study throws no light on the effects of cold-working, heat-treatment, or size and shape of the specimen; nor does it allow comparison of grades of steel, either alloyed or unalloyed, except for the few incomplete tests that introduced the research. These factors remain for later exploration.

polished longitudinally with 120-grit emery paper and immersed 2 in. in the electrolyte. When several readings were desirable, two cells were run in series. Current was supplied by a 6-volt storage battery, and the amperage was controlled by a 9-ohm slidewire resistance. Bath temperatures, which were controlled by immersion in a water bath at 18°C. and by carefully insulated

TABLE 5.- Factors Influencing Hydrogen Embrittlement

Variable	Control	Designation Type 440-C None (annealed) Annealed 0.062-in. wire Hand-polished longitudinally with 120-grit emery	
Steel: 1. Composition (definitive analysis) 2. Inherent hydrogen content 3. Grain characteristics 4. Degree of cold-working 5. Heat-treatment 6. Size and shape 7. Surface	Constant as possible by using one roll of selected wire for all experiments Constant Constant Constant Constant		
Pickling bath: 8. Composition (solution type) 9. Presence of certain impurities 10. Temperature 11. Current density 12. Added reagents Aging: 13. Temperature 14. Chemical environment (such as oil, with HNO, etc.) 15. Mechanical factors (such as flexing)	permitting one factor to	le within experimental error be studied at a time	

Instead, the present study concerns only the last eight factors listed, which are the factors controlling the absorption of hydrogen during cathodic and acid pickling and the desorption of that gas during subsequent treatment; and it concerns only type 440-C wire.

MEASUREMENT OF HYDROGEN EMBRITTLEMENT RESULTING FROM CATHODIC CHARGING

Electrolyte: 10 Per Cent NaOH

Effect of Charging Time.—For these first controlled experiments, all factors except charging time were fixed in order to find the general course of embrittlement. Three series of tests were run, each at a different temperature. The wire specimens, which were cut approximately 4 in. long, were uniformly cleaned with ether, hand-

heating on a hot plate for higher temperatures, are believed to have an accuracy of $\pm 1^{\circ}$ C. for 18°C. and $\pm 2^{\circ}$ C. at the higher temperatures. The specimens were bent approximately one inch from the end after rinsing for 30 sec. in cold tap water.

The curves in Fig. 2 and the values in Table 6 give an idea of the general accuracy of the tests and the manner used in handling the data. Subsequent tests will be described in graph form only, without additional tabulation of the data.

Fig. 2 shows that for a certain initial period of charging no effect on the ductility is reflected in the bend values. Of course, it must be borne in mind that a 180° bend on this particular radius does not necessarily represent wholly unimpaired ductility.

After this initial period, a sudden impairment shows itself. On the steep portion

of the curve the values for several specimens may vary from 180° down to low angles of bend, and for that reason the individual values are usually represented.

geneous phenomenon involving compound formation or lattice distortion, the loss in ductility should correlate directly with the diffusion law and plot as a straight

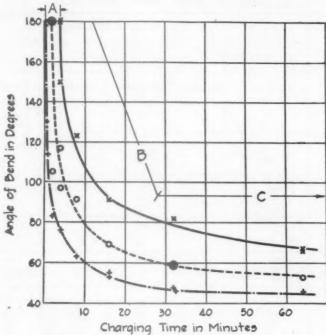


Fig. 2.—Embrittlement as a function of charging time. Electrolyte, 10 per cent NaOH.

Current density, 1.0 amp. per sq. inch.

X, T = 18°C. (64°F.).

0, T = 50°C. (122°F.).

+, T = 80°C. (176°F.).

Where the curve loses this steepness, each plotted point represents an average of three readings. The values in Table 6 may be taken to indicate an experimental error probably lying within $\pm 5^{\circ}$ of bend when all factors are carefully controlled and when the change in angle of bend with charging time is not too rapid.

There are two obvious features on each of these curves in Fig. 2 that warrant passing mention: (A) the "incubation period" required before embrittlement shows itself, and (B) the sharp drop in bend value once embrittlement begins. According to a widely accepted (but in the authors' opinion incorrect) concept of hydrogen embrittlement as a homo-

line on a logarithmic scale. On such a scale, however, the points still lie on a curve of the same general shape as those in the linear plot of Fig. 2, the deviation from a straight line indicating a retarded initiation of embrittlement followed by an excessively rapid deterioration.

Effect of Temperature.—From the relative positions of the three curves in Fig. 2, it is easy to recognize the anticipated effect of temperature. That is, with increasing temperature, cathodic charging becomes increasingly effective in causing embrittlement. In Fig. 3, the data from Fig. 2 are replotted to show specifically the effect of temperature when all other factors are constant. Over longer charging

periods, the distinction between hightemperature and low-temperature charging becomes less and less; but with decreasing periods a point is finally reached where controlling the many factors active in these tests. Fortunately, it was found that this change in bend value constituted a slow drift from one end of the coil to the

TABLE 6.—Bend Values for Figure 2

	Angle of Bend, Deg.						
Charging Time, Min.	18°C. (64°F.)		50°C. (122°F.)		80°C. (176°F.)		
	Reading	Average	Reading	Average	Reading	Average	
3/2					180 180 130		
1			180 180 180		137 110 95	114	
2	180 180 180		180 180 105		85 82 82	83	
4	180 180 150		100 97 95	97	77 77 75	76	
8	150 120 115	123	95 92 87	91	65 65 60	63	
16	95 92 87	91	77 67 65	69	55 55 55 55 52 52	55	
32	85 82 80	82	62 60 55 60 60 57	59	50 47 45 50 47 45	47	
64	67 65 65 70 67 65	66	55 52 52	53	47 47 45	46	

Electrolyte, 10 per cent NaOH; current density, 1.0 amp. per sq. inch.

charging at a lower temperature will not exceed the "incubation period," whereas the same test at a higher temperature produces embrittlement.

Effect of an Unknown Variable in the Steel.—Because wire is known to inherit some inhomogeneities from the original ingot, clippings from the two ends of the 50-yd. coil were tested with all factors constant except charging time. The results, shown in Fig. 4, make a good representation of the care that must be taken in

other and did not appreciably affect any set or several consecutive sets of tests.

Neither chemical nor microscopic analysis revealed any reason for this difference; but three specimens taken from each end of the coil and attached galvanically in all combinations in a 6 per cent NaCl electrolyte at room temperature showed the specimens of curve II uniformly anodic to the specimens of curve I, though the difference was slight. Only qualitative measurements were taken, using a high-

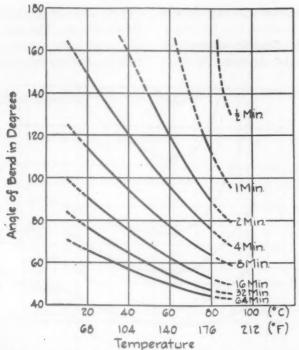


Fig. 3.—Embritlement as a function of temperature, for various charging periods. (Data from Fig. 2.)

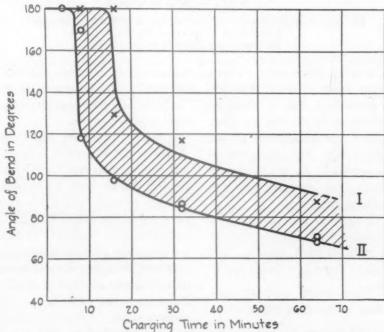


Fig. 4.—Embrittlement As a function of an unknown variable in the steel.

Electrolyte, 10 per cent NaOH.

Current density, 0.2 amp. per sq. inch.

Temperature, 18°C. (64°F.).

Curve I, Specimens from beginning of coil.

Curve II, Specimens from end of coil.

resistance galvanometer with an Ayrton shunt.

Effect of Current Density.—Since embrittlement would be expected to vary

Fig. 2, but using 10 per cent H₂SO₄ as the electrolyte. The results are compared in Fig. 6 with the results for the caustic electrolyte. The curves are identical. At higher

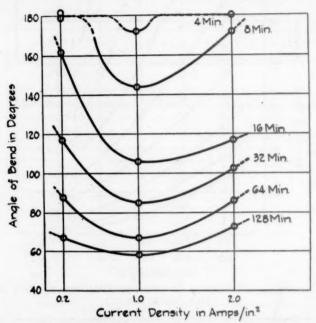


FIG. 5.—Embrittlement as a function of current density. Electrolyte, 10 per cent NaOH. Temperature, 18°C. (64°F.).

with current density, three series of tests were run using three current densities. The results, plotted in Fig. 5, show an interesting minimum at or near 1.0 amp. per sq. in. Note the consistency of the points, an unusually low experimental error being suggested. As with temperature, the distinction becomes less with increasing charging time.

This type of curve is inconsistent with the general concept of [H] varying directly and linearly with current density, and therefore points to some new factor operative in infusion.

Electrolyte: 10 Per Cent H2SO4

Comparison with Caustic Electrolyte.—To find whether the efficiency of cathodic charging is different for different electrolytes, a series of specimens was tested under the conditions of the 50° curve in temperatures, however, chemical attack by the acid finally obscures this comparison.

Chemically pure reagents were used in all tests reported so far.

Effect of Inhibitors and Other Reagents Added to the Electrolyte.—Since inhibitors and various reagents are frequently added to acid baths both in cathodic and in straight pickling of plain-carbon and lowalloy steels, the effects of some of them on embrittlement warrant attention, especially because they are often added with the understanding that they decrease or eliminate hydrogen absorption. While a study of plain steels lies outside the scope of the present study, it would be interesting to compare the efficiency of various inhibitors in respect to hydrogen embrittlement during cathodic pickling of 17 per cent chromium stainless steel.

For these tests, commercial carboy

H₂SO₄ was used. A standard charging time of 15 min. was selected, and all factors except the bath addition were kept constant. The results for additions of a

proprietary, or recommended, addition is indicated on the curve.

Another commercially advertised "inhibitor," reagent II, was tried with results

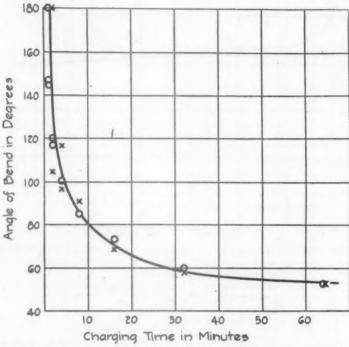


Fig. 6.—Comparison of embrittlement from cathodic charging in alkaline and in acid electrolytes.

Temperature, 50°C. (122°F.).

o, 10 per cent H₂SO₄.

×, 10 per cent NaOH.

commercial "inhibitor," reagent I (Table 7), are shown in Fig. 7.

These are surprising data, for the addition of this inhibitor increases embrittlement over that of the raw acid from the first addition up to saturation. The

TABLE 7.—Reagent Designations

Reagent No.	Trade Name	Manufacturer
. I	Rodine	American Chemical
II	Acitrol Liquid	E. F. Houghton & Co.
III	Nep No. 22 Acid Addition	William M. Parkin Co. The Enthone Co.
TA	Agent	The Enthone Co.
V	Inhibitor #3-A	E. I. du Pont de Ne- mours Co.
VI	Surfax T. R.	E. F. Houghton & Co.

shown in Fig. 8. This time the reagent neither inhibited nor promoted hydrogen embrittlement beyond the action in raw acid. Because the blank in this series was lower than in the previous one, it might possibly be argued that reagent II has a slightly deleterious effect, though the lay of the other points disputes that conclusion.

As for the peculiar action of reagent I, the possible presence of a "promoter" element suggests itself, isince this inhibitor is a chemically inhomogeneous powder. Arsenic is one of the most powerful in that series of promoters comprising groups V and VI of the elements in the Periodic

¹ References are at the end of the paper.



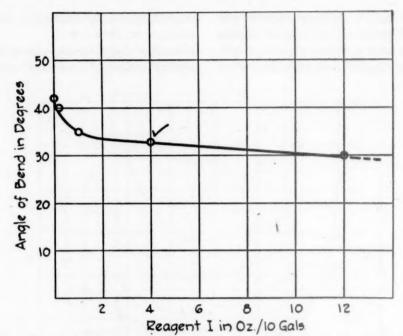


Fig. 7.—Effect of commercial inhibitor, reagent I, on embrittlement during cathodic PICKLING.

Electrolyte, 10 per cent H2SO4. Current density, 1.0 amp. per sq. inch. Temperature, 77°C. (170°F.). Charging period, 15 minutes. $\sqrt{}$, proprietary addition.

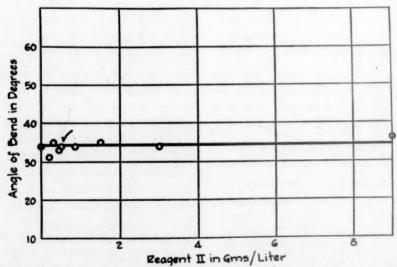


FIG. 8.—EFFECT OF COMMERCIAL INHIBITOR, REAGENT II, ON EMBRITTLEMENT DURING CATHODIC PICKLING. Conditions of Fig. 7.

Table. Consequently, the effect of arsenic added as As₂O₃* was studied, with the results shown in Fig. 9.

first they promote and then inhibit hydrogen absorption. Thus, we find a sharp minimum in the curve when all factors are

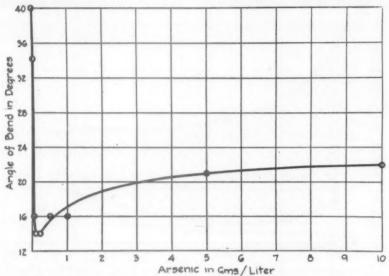


Fig. 9.—Effect of Arsenic on embrittlement during cathodic pickling. Conditions of Fig. 7.

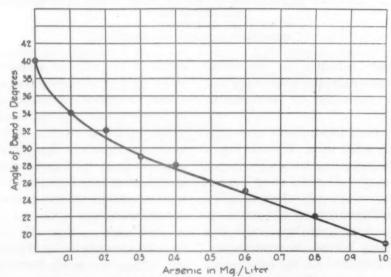


Fig. 10.—Detail of early portion of arsenic curve. Conditions of Fig. 7.

It is a peculiarity already known for many of these promoter elements that at held constant except arsenic content. On the other hand, the curve in Fig. 9 shows that arsenic never did act as an inhibitor in these tests, but simply became a weaker promoter as its content increased beyond a critical value.

^{*}Since As₂O₈ does not dissolve readily in an acid solution, water made slightly basic with NaOH was heated to boiling, the As₂O₈ dissolved in it, and the solution was then cooled, neutralized, and acidified to the desired concentration.

292

Two factors deserve attention in Fig. 9. First, the bend value of 15° effected by the critical arsenic content is an exceedingly low value. For these already low angles of

in the figure. The upper curve represents duplicate tests performed in the absence of H₂S. The upbending of the sulphide curve at higher temperatures is undoubtedly the

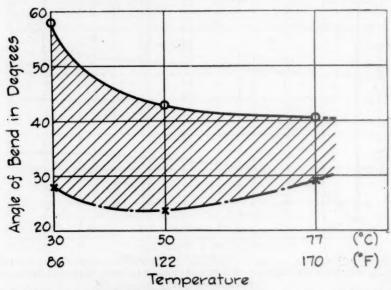


FIG. 11.—EFFECT OF SULPHIDE ION ON EMBRITTLEMENT DURING CATHODIC PICKLING.

Conditions of Fig. 7.

o, untreated electrolyte.

×, electrolyte saturated with H₂S.

bend, further reduction in the value becomes increasingly significant, since a o° fracture is obviously an unattainable asymptote.

Secondly, the critical arsenic content is an extremely small value. Whereas Fig. 9 expresses the arsenic content in grams per liter, Fig. 10 magnifies the steep portion of that curve using further tests with less than one milligram of arsenic per liter. With only 0.1 mg., the bend value has dropped plainly beyond the experimental error of the tests; and 1.0 mg. has lowered the bend value from 40° to only 20°.

Chemical analysis of reagent I revealed no arsenic; but there are other elements having a similar effect. In Fig. 11, for example, the effect of sulphur is shown. At three bath temperatures, H₂S was bubbled through the solution, presumably saturating it; and specimens tested under these conditions provided the low curve

result of the reduced solubility of H₂S occurring with increasing temperature.

Because sulphur is a common constituent in all steels and may therefore easily be picked up by a pickling solution, these results are especially significant. In many cases, various hydrogen-caused defects from pickling have been traced to old acid; and these special contaminations may contain the answer.

> MEASUREMENT OF HYDROGEN EMBRITTLEMENT RESULTING FROM ACID PICKLING

> > Effect of Reagent I

Batch I—Polished versus Unpolished Surfaces.—As for straight acid pickling, similar strong effects of bath reagents appear, and often to an even greater degree. This is especially surprising, since many of the reagents are advertised to inhibit or

prevent hydrogen embrittlement. In their favor, however, it might be pointed out that most of these inhibitors were developed for plain or low-alloy steels, and for I was added to 10 per cent H₂SO₄. Whereas in cathodic pickling the bend value was reduced about 10° below the blank, here it is reduced nearly 50° by addition of this

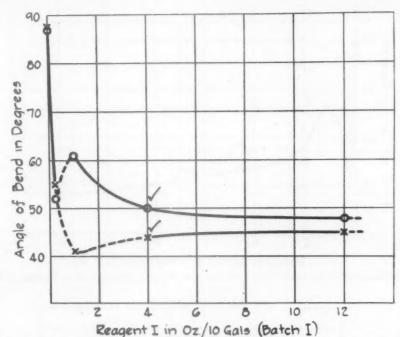


Fig. 12.—Effect of commercial inhibitor, reagent I, on embrittlement during acid

PICKLING, BATCH I.

Pickling bath, 10 per cent H₂SO₄.

Pickling period, 15 minutes.

Temperature, 77°C. (170°F.).

X, polished specimens.

o, unpolished specimens.

√, proprietary addition.

purposes generally transcending the prevention of hydrogen embrittlement; and that the present results may apply only to the one high-alloy steel investigated. The authors also wish to make clear at this point that the "proprietary addition" noted at various places throughout the work is simply a value lying within the generally recommended range, and may not be the specific addition that would have been recommended for these particular conditions if special advice had been sought in each case.

In the tests to be described, commercial carboy acid was used. In Fig. 12, two series of tests are depicted in which reagent

reagent. However, the blank for straight pickling is considerably higher than that for cathodic pickling under the conditions of these tests, the final values still lying above the final values for cathodic pickling.

A duplicate series of tests was run, except that the wire was used with its as-annealed surface. The upper curve in Fig. 12 shows, as was expected, that the principal action of the oxide layer here is simply to hinder the acid-metal contact, which probably is essential for hydrogen absorption.

Batch II—The "Well" Effect.—In both the foregoing runs, additions of this inhibitor up to 2 oz. per gal. showed what appeared at first to be erratic results. However, the variation exceeded the experimental error granted these tests by so The data, shown in Fig. 13, establish beyond reasonable doubt a curve having a double reversion. Early additions bring

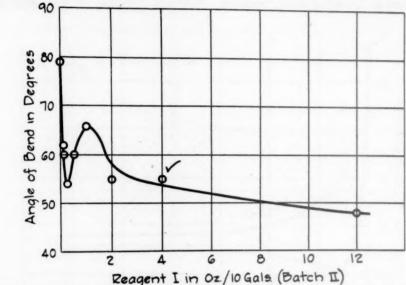


Fig. 13.—Tests of Fig. 12 repeated, using batch II of commercial inhibitor, reagent I.

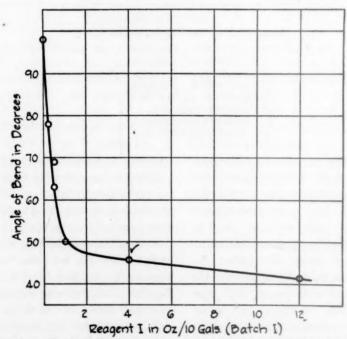


FIG. 14.—TESTS OF FIG. 12 REPEATED, USING 1:1 HYDROCHLORIC ACID.

much that the tests were repeated using a new batch of reagent I, with additional tests run in that uncertain region. the bend value to a minimum, further additions lose this effect until a maximum bend value is reached, and still further additions once more cause a progressive lowering of the ductility. No explanation is proposed for this action.

One might also note that the 1.0-oz.

Effect of Reagent II

Another unusual behavior was found for the inhibitor, reagent II. Neither small

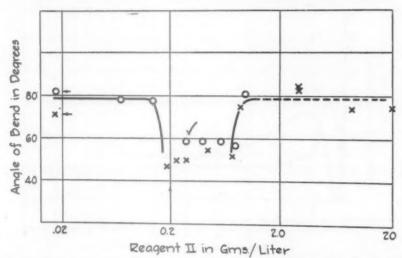


Fig. 15.—Effect of commercial inhibitor, reagent II, on embrittlement during acid pickling.

Conditions of Fig. 12.

o, run I.

X, run II.

√, proprietary addition.

addition of batch II lies on a markedly different part of the curve from the same addition of batch I (polished). This can be attributed to the chemical inhomogeneity of this inhibitor, making it differ from batch to batch; and to the fact that batch II was purchased for the experiment and batch I was taken from a 5-yr. old laboratory stock.

Hydrochloric Acid Pickling.—The same tests run in 1:1 HCl show a perfectly uniform curve with no indication of a reversion (Fig. 14). Here reagent I caused a drop of nearly 60° in the angle of bend, though the blank was even higher than with sulphuric acid pickling. In all these types of pickling this inhibitor brings the angle down to the same general value around 40° regardless of the blank. Why these two acids have different types of curves with reagent I is not clear.

additions nor large additions showed any effect on the bend values; but intermediate additions, including the proprietary, effected a noticeable decrease in ductility (Fig. 15). These data were more or less erratic at all additions, making it difficult to ascertain the real shape of the curve. A second series of tests was conducted, indicated in the figure as run II, which also indicated the presence of the same peculiar type of minimum, making its existence fairly certain. One will recall that this inhibitor caused no changes during cathodic pickling.

Effect of Reagent III

Once again, an interesting curve occurs containing a plainly marked double reversion (Fig. 16). Tests were run in both sulphuric and hydrochloric acid baths with this third commercial inhibitor; and

this time, in contrast to the action with reagent I, both acids display the double reversion, although the minima and maxima are at different concentrations.

second reversion, if it exists, lies within the experimental error. Also, the minimum occurs at a different bend angle and a different concentration in the two tests.

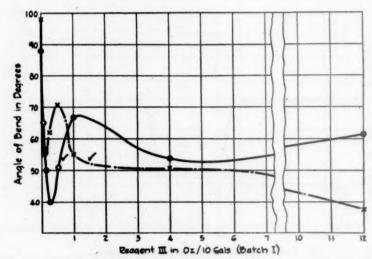


FIG. 16.—EFFECT OF COMMERCIAL INHIBITOR, REAGENT III, ON EMBRITTLEMENT DURING ACID PICKLING, BATCH I.

Conditions of Fig. 12.

o, 10 per cent H₂SO₄.

×, 1:1 HCl.

√, proprietary addition.

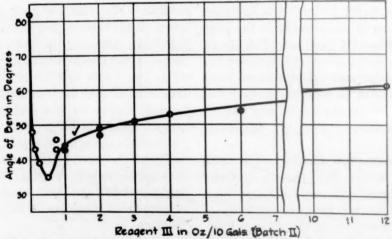


FIG. 17.—TESTS OF FIG. 16 REPEATED, USING BATCH II OF COMMERCIAL INHIBITOR, REAGENT III, AND SULPHURIC ACID.

Because this inhibitor was also from an old laboratory supply, a new batch was purchased, and the tests with sulphuric acid were repeated (Fig. 17). This time the

Since reagent III is a chemically impure liquid, these differences can be accounted for by an original difference in composition, or by some aging action, such as the evaporation of an active ingredient from the older solution. The curve for reagent III in both cases shows a late upswing with increasing concentration in sulphuric acid, evolution 50 per cent. No special claims are known to be made regarding hydrogen embrittlement; but it can be concluded from these tests that this reagent, while

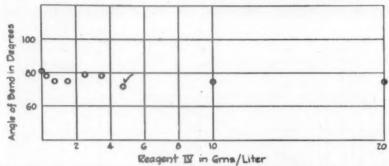


FIG. 18.—Effect of commercial acid addition agent, reagent IV, on embrittlement during acid pickling.

Conditions of Fig. 12.

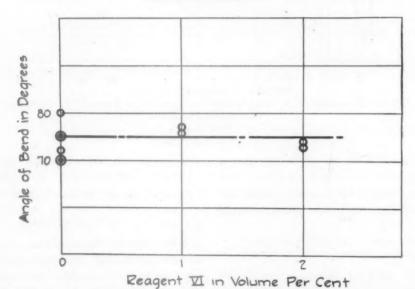


FIG. 19.—EFFECT OF COMMERCIAL WETTING AGENT, REAGENT VI, ON EMBRITTLEMENT DURING ACID
PICKLING.
Conditions of Fig. 12.

but the net effect at all concentrations is still a severe decrease in ductility.

Effect of Reagent IV

Although some small decrease in ductility may have occurred, Fig. 18 shows no appreciable effect of reagent IV, which is a commercial acid addition agent advertised, among other things, to decrease hydrogen

probably it does not augment embrittlement, certainly does not diminish it.

Effect of Reagent V

Another commercial inhibitor, reagent V, showed results that were similar and therefore were not plotted. An effervescent powder containing some other chemical, this reagent caused neither an increase nor

a decrease in embrittlement in concentrations up to saturation.

Effect of Reagent VI

A commercial wetting agent, though usually used in combination with the

by this test, seems entirely prohibited. It is interesting to note that Uhlig and Wallace report certain experiments using this inhibitor in that concentration.² Unfortunately, quinoline ethiodide, which is one of the only two true inhibitors

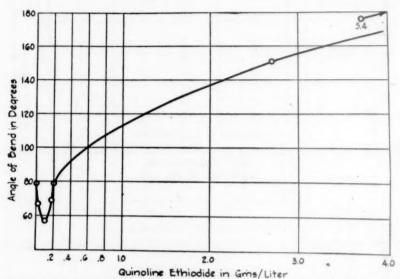


FIG. 20.—EFFECT OF CHEMICALLY PURE INHIBITOR, QUINOLINE ETHIODIDE, ON EMBRITTLEMENT DURING ACID PICKLING.

Conditions of Fig. 12.

inhibitor, reagent II, was investigated as a reagent in itself. No detectable change was found in bend value with additions throughout its proprietary range of 1 to 5 per cent (Fig. 19).

Effect of Quinoline Ethiodide

Because most of these extraordinary behaviorisms have been associated with chemically impure or complex reagents, considerable interest attaches to the behavior of a chemically pure inhibitor, such as quinoline ethiodide. The curve in Fig. 20 shows the customary "well," but there is no second reversion; and, more importantly, this inhibitor actually becomes an *inhibitor of hydrogen embrittle-ment*. Quantities greater than 0.2 gram per liter show improvement in the bend value over the blank; and, at about 5.4 grams, hydrogen embrittlement, as determined

discovered in this research as far as hydrogen embrittlement is concerned, is too expensive to warrant wide use.

Effect of Arsenic

Tests showed the customary early drop in bend value (Fig. 21) comparable to that in Figs. o and 10; but the curve from then on differed so greatly that with only 0.2 gram of arsenic the blank bend value was regained; and with 0.5 and more grams a complete return to a 180° bend was effected. Thus, as with the quinoline ethiodide, arsenic shows a preliminary embrittling, or "promoter," action followed swiftly by a protective, or inhibiting, action, until it becomes a true inhibitor in a class with quinoline ethiodide. In fact, by weight, arsenic is 10 times more effective than quinoline ethiodide. The difference between the effects of arsenic in cathodic

and in straight acid pickling is certainly striking (compare Figs. 9 and 21).

Effect of Sulphur

The test of Fig. 11 was repeated with the very similar results shown in Fig. 22.

FACTORS AFFECTING RECOVERY FROM EMBRITTLEMENT

Temperature

Presence of an Aging Minimum.—While the foregoing experiments demonstrate the

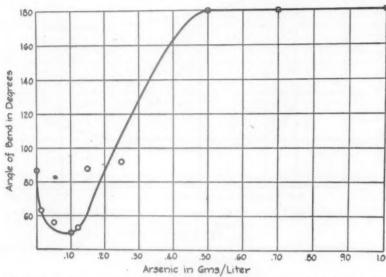


Fig. 21.—Effect of arsenic on embrittlement during acid pickling. Conditions of Fig. 12.

Consequently, the warning expressed in the discussion of cathodic pickling regarding sulphur pickup by the pickling solution is likewise applicable to straight pickling. Old pickling liquors should be watched with suspicion, particularly after handling sulphurous free-machining grades. Also, selenium-containing grades come in this category, for selenium is an avid "promoter."

Effect of Ferrous Ion

It is occasionally suggested that the concentration of Fe⁺⁺ ion is involved in pickling brittleness. Duplicate tests using 10 per cent H₂SO₄ were run with 5 grams of ferrous sulphate added to the ½-liter solution in one of the tests. No effect on the bend value was noted (see Table 8).

factors that control the absorption of hydrogen during aqueous pickling; it is obviously

TABLE 8 .- Effect of Ferrous Sulbhate

FeSO ₄ Content	Angle of Bend, Deg.				
resor content	Reading	Average			
None	72 70				
5 grams per 500 c.c	70 65 70	69			
	70 70 65	69			

10 per cent H₂SO₄. Pickling period = 30 minutes. T, 22°C. (72°F.).

as important to understand the factors regulating removal of the gas once it is absorbed.

Of these factors, temperature is fairly well understood, it being common knowledge that mild heating favors rapid removal of the gas. To demonstrate the role of time, of course, is represented by the lower curve in each case.

At least two features warrant special mention in regard to these curves: (1) that

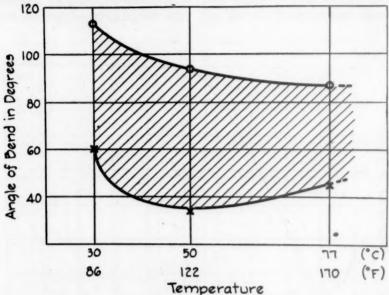


FIG. 22.—EFFECT OF SULPHIDE ION ON EMBRITTLEMENT DURING ACID PICKLING.

Conditions of Fig. 12.

o, untreated acid.

X, acid saturated with H₂S.

temperature and to obtain quantitative values for its effect, further tests were run using the following constant conditions for charging:

The specimens were charged, rinsed and dried immediately, and immersed in oil held at the desired temperature.

The results of runs at three temperatures are shown in Figs. 23, 24, and 25. All factors were kept constant in each series of tests except the aging temperature; and at each temperature two curves were obtained, one for a 16-min. and one for a 32-min. charging period. Each point represents an average of three runs, except on the 16-min. curve in Fig. 23 and on the 32-min. curve in Fig. 24, where they represent single tests. The longer charging

the curves for 30°C. are expressed in hours, the curves for 100°C. in minutes, and the curves for 180°C. in seconds; (2) that in every case there is a marked decrease in ductility during the early aging period.

This aging minimum is a phenomenon of great significance in revealing the condition of hydrogen dissolved in iron and will be discussed more fully later. If hydrogen embrittlement is a matter of compound formation or lattice distortion, one must conclude that the minimum ductility would conform with the maximum hydrogen content, which can occur only immediately at the conclusion of charging, and must thereafter become progressively less. This classical concept of lattice distortion and compound formation therefore fails completely to explain the "aging minimum."

To investigate this phenomenon further,

a series of specimens was aged in oil at 100°C. (212°F.) after charging for only 4 min. at 28°C. (82°F.) and a current

"range A" discussed earlier in the paper. That is, the pickling treatment itself appeared to cause no measurable embrittle-



FIG. 23.—RECOVERY CURVES FOR AGING AT 30°C. (86°F.).

*o, charged 16 minutes.

X, charged 32 minutes.

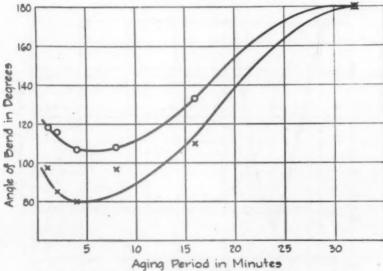


FIG. 24.—RECOVERY CURVES FOR AGING AT 100°C. (212°F.).

o, charged 16 minutes.

X, charged 32 minutes.

density of 1.0 amp. per sq. in. Immediately after this treatment, the specimens bent 180° without breaking, in conformity with

ment whatsoever. After aging for 30 sec. at 100°C., however, the specimens broke at an angle of 135°; and in 1 min. the angle

of bend had dropped to 95°. Then, after 2 min. at 100°C., all specimens showed complete recovery. The data are plotted in Fig. 26.

foregoing curves for 32-min. charging and plotted as temperature versus time for complete recovery. The result is a straight line on a logarithmic plot having the

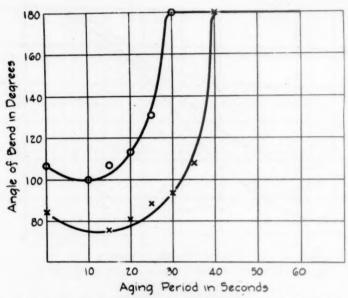


FIG. 25.—RECOVERY CURVES FOR AGING AT 180°C. (350°F.).

o, charged 16 minutes.

X, charged 32 minutes.

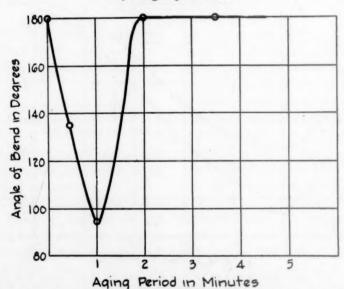


FIG. 26.—BEHAVIOR DURING AGING AT 100°C. (212°F.) OF A SPECIMEN CHARGED ONLY 4 MINUTES.

Calculating Recovery Period.—Especially interesting is the information in Fig. 27. For that plot the tangency points for the return to a 180° bend were taken from the

equation:

$$T_{(^{\circ}C.)} = -47 \log H + 87$$

where H is the aging time in hours.

recovery of commercial wire during ex- periods of time, with the results shown in posure to the weather, the period required Fig. 28. As closely as can be determined,

Since a practical aspect concerns the mixture in a thermos bottle for various

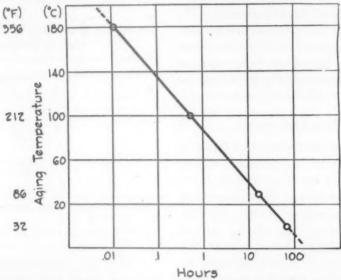


Fig. 27.—Plot showing aging period required for recovery of a 180° bend as a function of TEMPERATURE.

Electrolyte, 10 per cent NaOH. Current density, 1.0 amp. per sq. inch. Charging temp., 18°C. (64°F.). Charging period, 32 minutes.

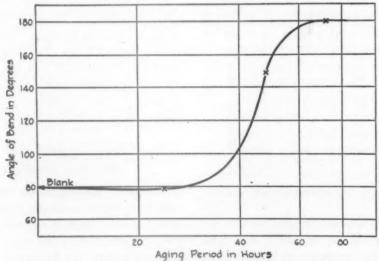


FIG. 28.—RECOVERY CURVE FOR AGING AT O°C. (32°F.). Conditions of Fig. 27.

for complete recovery at o°C. was calculated by using the equation just listed. The answer is 71 hr. Tests were then run in which the wires were aged in an ice-water complete recovery of a 180° bend was accomplished in the calculated period of time.

Consequently, with sufficient control of

the factors operative in hydrogen embrittlement, a valid equation can be obtained that expresses the time required for the complete recovery of bend value, which is highly accurate between o° and 180°C. (32° and 350°F.), and which can without doubt be extrapolated further with reasonable accuracy. The equation derived here, of course, is applicable only to the specific type of specimen used in this research.

Oxidizing Environment

If the removal of hydrogen is purely a process of diffusion, considerable benefit should be expected from a substantial reduction in the surface concentration of hydrogen atoms, or in any method expediting the removal of the effusing atoms. Miller, for example, has a patent for affording recovery from embrittlement by immersion of only a few seconds in dilute

TABLE 9.—Effects of Anodizing and Immersion in HNO3 on Recoverya

Period of	Angle of Bend, Deg.							
Treatment, Min.	Aged in Air ^b	Immersion in 20 Per Cent HNO ₂	Anodized at 0.45 Amps. per Sq. In.					
3/4	72	80						
34	75 80 78	95 80	78 70					
1	75 80 77	77 70	77					
5	77 75 77		85 75					
15	75	100	. /3					

T. 30°C. (86°F.).
Specimen in test tube immersed in bath at 30°C.
20 per cent HNO.

HNO3;3 and Sachtleben presumably degasses electrolytically deposited chromium by making the specimen an anode. Each process, of course, reduces the surface concentration of hydrogen to a minimum.

These factors were both investigated in the present research, with the results shown in Table 9. Up to 5 min., no noticeable improvement was effected either by immersion in 20 per cent HNO3 or by anodizing at 0.45 amp. per sq. in. After 15 min., some improvement was noticed in the HNO₂ treatment, but it was inappreciable.

TABLE 10.—Relation of Hydrogen Embrittlement to Hardness

Charging Period, Min.	Electrolyte	Rockwell C Hardness
0 I 8 64 240 I 8 64	10 % NaOH 10 % H ₂ SO ₄	54 54 53 53 55 55 55 55 54 55

Specimen, M₆-in, disk from 1-in, annealed type 440-C hexagonal bar.
T. 22°C.

Current density, 1.0 amp. per sq. inch.

MISCELLANEOUS OBSERVATIONS

Hydrogen Embrittlement and Hardness

To find whether hydrogen embrittlement is related to hardness, two sets of disks 3/16 in. thick, cut from an annealed 1-in. hexagonal bar, were cathodized for increasing periods of time with periodic measurements of hardness. The first set of tests appeared to show a slight increase in hardness (Table 10); but the second set did not reproduce that increase, and it is concluded that hydrogen embrittlement has no effect on hardness.

Hydrogen Embrittlement and Electrical Resistivity

Similarly, measurements of electrical resistivity after cathodic charging and after subsequent aging showed no measurable change in ρ (Table 11). This is an indication that the hydrogen is neither principally alloyed with the steel, which would cause an increase in resistivity, nor importantly ionized, which would decrease the resistivity. It might be possible, however, to detect some slight ionization by the method used by Moore on palladium.

TABLE 11.—Relation of Hydrogen Embrittlement to Electrical Resistivity

Condition of Wire	Temperature, Deg. C.	Resistivity, Micro-ohms-cm.
Untreated	28.0	65.6
Cathodizeds	29.5	65.6
Aged 1 hr. at 29°C. (85°F.)	29.5	65.6

* 10 per cent H₂SO₄.

Temperature, 50°C. (122°F.).
Charging period, 15 minutes.
Current density, 1.0 amp. per sq. inch.

b Corrected for temperature coefficient of 0.07 micro-ohms per deg. C.

DISCUSSION OF RESULTS

Planar-pressure Theory of Hydrogen Embrittlement

So many of the data in this research stand in marked disagreement with the prosaic concept of hydrogen embrittlement as compound formation or lattice distortion that the matter deserves special consideration. In discussing Fig. 2, for example, attention already has been drawn to the "incubation period" of zone A and the further behavior of embrittlement in zones B and C, which is inconsistent with this classical concept. The failure of hydrogen to affect hardness is difficult to reconcile with a theory of lattice distortion or compound formation; and the indifferent response of the specimens to recovery in oxidizing pickling baths deemphasizes chemical diffusion as a factor in removing hydrogen. Of principal significance, however, is the "aging minimum" occurring during recovery.

In several previous papers, 6-10 one of the present authors has described at length a theory for hydrogen embrittlement that is consistent with all these observations, which can be called the planar-pressure theory. According to this concept, hydrogen embrittlement is nothing other than the result of an aging action in which the precipitate is a gas.

Obviously, the mechanical properties of steel cannot be affected until an entrapped gaseous precipitate attains a pressure sufficient to deform the surrounding matrix. That pressure must have some value just as critical as a yield point or an elastic limit. It then immediately follows that after the hydrogen atoms enter the metal an incubation period will be necessary to allow them to precipitate from the lattice into the voids in that lattice where they must fulfill prescribed pressure relationships with a gaseous H2 phase.

On the basis of this concept, the behavior of the gas in the present research can be outlined as follows:

Infusion.

- 1. Nascent hydrogen atoms enter the metal lattice without measurably affecting the mechanical properties of the steel. This infusion begins with the current flow or the acid attack.
- 2. Diffusing hydrogen atoms encounter the internal planar disjunctions that constitute the imperfection structure of crystals. There they evaporate from the metal lattice in the direction of fulfilling their proscribed equilibrium with a gaseous H2 phase having terrific limiting pressures. This, along with step 1, is the incubation period shown as zone A in Fig. 2. It can also be the incubation period confirmed by Andrew et al. for the formation of flakes in steel,11 and by Hanson et al. for cracking in weld metal.12

Embrittlement.

3. When the pressure of this occluded gaseous precipitate exceeds a certain critical value, the intragranular structure of the steel is suddenly deformed, preventing subsequent slip movements. This stage is embrittlement; and its rapid spread throughout the grain is indicated by the sudden drop over zone B in Fig. 2.

4. After this sudden acceleration diminishes in zone B, a progressive lowering of ductility occurs, indicated in Fig. 2 as zone C, which probably relates more or less directly to the simple law of diffusion and plots logarithmically as a straight line.

Effusion.

- 5. When the source of hydrogen atoms is removed from the surface of the specimen, feeding of the lattice stops and the total hydrogen content of the specimen has reached a maximum. In the skin layer, the concentration gradient immediately becomes reversed, and the gas evaporates from the specimen. Below the skin layer, similar evaporation, or precipitation, within the planar voids not yet influenced by the change in external conditions may continue for a period to increase embrittlement further. This spontaneous embrittlement constitutes the aging minimum found in the present work and shown to a remarkable degree in Fig. 26.
- 6. Once the critical pressure is exceeded, the pockets of entrapped gas can force intercommunication with one another, allowing the gas ultimately to reach the surface and escape. This quantum-type activity accounts for the peculiar manner in which hydrogen bubbles of discrete size appear suddenly in oil films on steel;18 it accounts for the favorable effect of cold-working in removing hydrogen, since cold-work furthers the opening of these rifts; and the theory in general accounts for the evolution curve obtained by Andrew et al.,11 the first rapidly declining evolution relating to the preliminary skin evaporation just mentioned, and the sudden subsequent evolution relating to the attainment of critical internal precipitation pressures.

Recovery.

7. Ductility is recovered, not when all the gas has been removed, but when the planar pressure has been reduced below the critical value. Thus, the mildest heating of embrittled steel can effect recovery simply by increasing the pressure of the trapped gas beyond the balanced throttling force at the pocket boundaries. An increment of gas is thereby forced to the surface in a valvelike action; and, upon cooling, contraction of the residual gas phase may then result in pressures that are ineffective because they are less than the critical.

CONCLUSIONS

The foregoing work seems to establish that:

- r. The bend-testing apparatus developed in this research for measuring hydrogen embrittlement in wire is simple and effective. Using this apparatus, and keeping constant all factors concerning the nature of the specimen, such as grade, size, degree of cold-work, hardness, and so forth, the authors have studied certain remaining factors that regulate the absorption of hydrogen during cathodic and acid pickling and its desorption during aging.
- 2. With increasing pickling time, embrittlement increases along a curve having three stages:

Stage A is an incubation period in which atomic hydrogen is absorbed into the lattice without decreasing the bend value. The authors propose that during this initial period the hydrogen is simultaneously being precipitated from the lattice into crystallographic lattice voids where it gathers under constantly increasing pressure.

Stage B is a sudden decline in bend value, which is proposed to result from the precipitating gas suddenly attaining the critical pressure necessary to cause em-

brittlement according to the planarpressure theory described in the text.

Stage C is a gradual slope, which plots logarithmically as a straight line and is proposed to represent stabilized inward diffusion once the critical precipitation pressure is reached and maintained near the surface.

3. With increasing temperature during charging, embrittlement increases when all other factors are constant. Since this is also true for cathodic charging in an alkaline electrolyte at constant current density, the increase cannot be explained on the basis of an increased pickling action. The effect is especially prominent in short pickling periods, which lie within stage A at low temperatures and therefore cause no embrittlement, but which exceed stage A at higher temperatures and therefore lead to embrittlement.

4. Embrittlement is not directly proportional to current density, a maximum embrittling effect occurring close to 1.0 amp. per sq. inch.

5. Cathodic charging provides identical results whether the electrolyte is 10 per cent NaOH or 10 per cent H₂SO₄.

6. Numerous reagents, including commercial reagents added to pickling baths for various reasons and often advertised to inhibit or eliminate hydrogen embrittlement in the pickling of carbon and lowalloy steels, fall into three classes as far as 440-C stainless steel is concerned:

a. Additions in all proportions cause a marked *increase* in embrittlement over that caused by the raw acid;

b. Additions in all proportions neither decrease nor increase embrittlement;

c. Small additions increase embrittlement, but further additions decrease embrittlement, until at some critical content the reagent behaves as a true inhibitor of hydrogen embrittlement. The only reagents found in this research to have this property of inhibiting hydrogen embrittlement are quinoline ethiodide and arsenic, and only in acid pickling. All

commercial inhibitors studied fell in the first two classes.

7. Quinoline ethiodide and arsenic, although true inhibitors of hydrogen embrittlement when added in certain concentration in straight acid pickling, both have a range of concentration in which embrittlement is badly aggravated. Furthermore, arsenic shows no inhibiting effect at all in cathodic pickling.

8. Sulphide ion, supplied by dissolving H₂S in the solution, causes a marked lowering of the bend value. Consequently, contamination of the bath from pickling free-machining grades should be watched.

9. In aging, the bend value first decreases, which is ascribed to hydrogen atoms continuing to precipitate from the lattice into the lattice voids after charging has stopped. This phenomenon of an aging minimum is so marked that specimens charged within range A and showing a perfect bend may subsequently spontaneously embrittle themselves.

10. Recovery of a 180° bend occurs in a period of time (H, in hours) which is related to temperature (°C.) for these specimens by the equation:

$$T(^{\circ}_{C.}) = -47 \log H + 87$$

This equation has good accuracy between o° and 180°C. (32° and 350°F.).

11. Contrary to a widespread belief, recovery is but negligibly hastened by treatment in nitric acid. As for anodic treatment, even less of an effect is noted.

12. Hydrogen embrittlement confers no detected change on hardness or electrical resistivity.

13. In general, the results of the research stand as strong evidence in favor of the planar-pressure theory for hydrogen embrittlement and are definitely inconsistent with theories based upon lattice distortion or compound formation.

SUMMARY

An apparatus is devised for measuring hydrogen embrittlement in wire as a function of the angle at which breaking occurs during a single bend made at constant speed. Simple and effective, the instrument is used first to get an approximate indication of the sensitivity of various stainless grades of steel to hydrogen embrittlement, and then to study in detail certain factors controlling the absorption of hydrogen during cathodic and acid pickling and the desorption of that gas during subsequent recovery.

After establishing the fundamental relationships of charging time, temperature, and current density, the research reveals the fact that many of the bath reagents called "inhibitors," often advertised to inhibit or prevent hydrogen embrittlement, actually cause a marked increase in embrittlement over that of the raw acid for the conditions of these tests. Only two reagents, neither a commercially advertised inhibitor, are found to be true inhibitors at certain concentrations; and at other concentrations they, too, aggravate embrittlement. The peculiarities of a group of these reagents are studied in detail.

During recovery, the specimens first show a further decrease in ductility, or an aging minimum, a phenomenon of spontaneous embrittlement so marked that specimens showing unimpaired ductility after pickling may break at an angle of only 95° during subsequent aging. As for recovery, at 180°C. (350°F.) 40 sec. is equivalent to 71 hr. at o°C. (32°F.).

The significance of the tests in disclosing the nature of hydrogen in steel serves to prove the planar-pressure theory for hydrogen embrittlement and to void the concept of embrittlement as a function of compound formation or lattice distortion.

REFERENCES

1. C. A. Zapffe and C. L. Faust: Metallurgical Aspects of Hydrogen in Electroplating. Proc. Ed. Session Amer. Electroplaters' Soc. (1940) 28, 1-20; disc., 20-25. 2. H. H. Uhlig and E. M. Wallace: Effect of

Hydrochloric Acid plus Inhibitor on the Corrosion Resistance of 18/8 Stainless

Steel. Trans. Electrochem. Soc. (1942)

81, 511-520.
G. Miller: Cleaning Metals Such as Steel and Preventing Embrittlement and Corrosion. U.S. Patent 2109675 (March

1, 1938).
4. K. Sachtleben: Degassing of Chromium Deposits by the Intermitta Process. Korrosion und Metallschutz (1943) 19,

5. G. A. Moore: Comportment of the Palladium-hydrogen System Toward Alternating Current. Trans. Electrochem. Soc. (1939) 75, 237-269. 6. C. A. Zapffe and C. E. Sims: Hydrogen

Embrittlement, Internal Stress, and Defects in Steel. Trans. A.I.M.E. (1941)

145, 225-261; disc., 261-271.
7. C. A. Zapffe: Fisheyes in Steel Welds Caused by Hydrogen. Metal Progress

(1942) 42, 209-212. 8. C. A. Zapffe: Defects in Cast and Wrought Steel Caused by Hydrogen. Progress (1942) 42, 1051-1056.
9. C. A. Zapfie: Sources of Hydrogen in Steel

and Means for Its Elimination. Metal

Progress (1943) 43, 397-401.

10. C. A. Zapffe and G. A. Moore: A Micrographic Study of the Cleavage of Hydrogenized Ferrite. Trans. A.I.M.E.

(1943) 154, 335–352; disc., 352–359.

11. J. H. Andrew et al.: Formation of Hairline Cracks. Jnl. Iron Steel Inst. (1942) 146, 193P–202P; 203P–243P; disc., 244P– 282P.

12. D. Hanson et al.: Researches in Alloy Steel Welding. Welding Research Council (Nov. 1944) 9 (11), 573s-574s.
13. C. A. Zapffe: Neumann Bands and the Planar-Pressure Theory of Hydrogen Embrittlement. Not yet published.

DISCUSSION

S. I. ROSENBERG. *-It is with some diffidence that this discussion of the excellent paper by Dr. Zapffe and Miss Haslem is offered. The data presented by these authors give such apparently consistent results that it would appear that here, indeed, is a simple and effective method for evaluating the embrittling effects of hydrogen.

A few years ago we were asked to make a short study of the embrittling effects of zinc plating as compared with cadmium plating. Several different types of tests were tried as a means of evaluating changes in ductility, and among these was the machine described by Dr. Zapffe and Miss Haslem. The writer first became acquainted with this machine on a visit to Dr. Zapffe in the laboratory of the Rustless Iron and Steel Co. at Baltimore.

^{*} Metallurgist, National Bureau of Standards. Washington, D. C.

Following this visit, a similar machine was constructed in our laboratory.

Wire for study was supplied by the American Steel and Wire Co. and was of AISI-1065 analysis. The wires were furnished in three sizes (1/6, 1/8, and 81/2-in diameter) and in three different conditions (annealed, colddrawn, and oil-tempered). All wire was from the same heat of steel.

All wires were subjected to a cleaning procedure prior to plating.* Following this cleaning procedure the wires were plated in an acid zinc or a cyanide zinc bath (2 amp. per sq. dm. for 12 min.) or in a cyanide cadmium bath plating, were tested in four groups: immediately after treatment, 4 hr. after, 24 hr. after, and 24 hr. after with an intermediate anneal of 2 hr. at 300°F. In all cases the wires bent 180° without fracture.

It was thought that this method of test might be effective if the test conditions were made more severe. Additional bending arms were constructed, therefore, to bend the 1/8 and 3/6-in. diameter wires around a 1/6-in. radius. Tests were made on the 1/8 and 3/16-in. diameter wires as cold-drawn and as oil-tempered in the following conditions: (1) as received, (2) as cleaned (see footnote), (3) as

TABLE 12.—Bend Tests (Around 1/6-inch Radius) of Heat-treated Wires and Sheets

Treatment Original (as heat treated)		AISI-1065 Wire						SAE-X4130 Sheet			NE-8630 Sheet						
		1/2 In. Diameter			¾6 In. Diameter			0.096 In. Thick by				o.og6 In. Thick by					
		60°	55°	1800	50°	180°	180°	1100	180°	95°	88°	180°	1100	60°	48°	1400	1800
	10	180	180	180	180	180	95	180	180		no to	ests		135	130	IIO	110
Pickled only	b c d a	60 110 60 180	70	180	95 180	85 180	95 180	160	180	180	130	115			140 110 118 102	140 25 135 110	50
Pickled and cyanide sinc plated	600	180 180 90 180	180	85 95	95 180	110	110	85 50	105	110	90 110 140	105 112 115 140	95	95 30 120	35 110	45 110 105 115	100
Picked and acid zinc plated	b c d	55 120	70 70 180	58 180 80	58 180 70	180 120 120	90 158 110	100	100 100 98	130 120 180	180 125 180	180 180 150	128 125 180	135 145 120	120 125 112	120 130 115	125 126 125
Pickled and cyanide cadmium plated	a b c d	180 180 50 180	110	80 180	180 180	180	95	180	110	100	95 100	100 110 105 120	95 118	95 105 115 120	75 92 100 112	105	10

Tested immediately after treatment.

(2 amp. per sq. dm. for 8½ min.). The average thickness of the deposits was 0.0002 inch.

Preliminary bend tests around a 1/8-in. radius were made on the various wires in their original condition, as cleaned, and as cleaned and plated in a cyanide zinc bath. The wires that were plated after cleaning, or after cleaning and

cleaned and cyanide zinc plated, (4) as cleaned and acid zinc plated, (5) as cleaned and cyanide cadmium plated. All specimens bent 180° without fracture regardless of elapsed time after cleaning or plating.

Following these tests, it was decided to test the wires as heat-treated. Samples of the 1/8 and 3/16-in. diameter wires (original condition as annealed) were heat-treated by water quenching from 1475°F., followed by tempering at 750°F. The resultant Knoop hardness numbers were 517 and 531 for the 1/8 and 3/6-in. diameter wires, respectively. Tests were also made on heat-treated steel sheet (special bending arms were made to accommodate the

Tested 4 hr. after treatment.
Tested 24 hr. after treatment.
Tested 24 hr. after treatment with an intermediate anneal of 2 hr. at 390°F.

^{*} This cleaning consisted of the following steps:

^{1.} Degrease (20 sec.) in either hot or cold tri-chlor ethylene.

^{2.} Acid pickle (20 sec.) in 2:1 HCl.

Rinse

^{4.} Hot anodic alkaline cleaning (2 min.).

^{6.} Acid pickle (20 sec.) in 2:1 HCl.

^{7.} Rinse.

sheet). Two analyses were available, one corresponding to SAE-X4130 and the other to NE-8630. Both sheets were 0.096 in. thick (13 gauge). Test specimens were cut 3 in. long by 1/2 in. wide by gauge thickness, taken longitudinally; i.e., in the direction of rolling. Heattreatment consisted of oil quenching from 1550°F., followed by tempering at 750°F. The resultant Rockwell hardness numbers were C-41 and C-40 for the SAE-X4130 and NE-8630 steels, respectively. Plating procedures were the same as noted previously, but pickling was more severe because of the scale formed during heat-treatment. For the heat-treated wires, a hot 50 per cent HCl dip was used for several minutes instead of a short acid dip in 2:1 HCl. For the heat-treated sheet, a hot c. p. HCl dip was used for 30 to 60 min. with 0.5 per cent (by volume) of Rodine No. 50 added to inhibit the action of the acid on the steel. The results of the bend tests on the heattreated wire and sheet are given in Table 12. The results secured were quite erratic.

While no claim is made that the possibilities of this test were completely explored, it was disappointing to obtain such variable data when such high hopes had been entertained for rather consistent data. Perhaps the authors will express an opinion as to why such erratic results were secured.

D. J. MACK.*—This paper is interesting because it makes public experimental proof of a commonly observed fact; i.e., proprietary pickling inhibitors many times do not perform as advertised—or, putting it the other way, advertising claims are sometimes a trifle exuberant and not backed by sound engineering experience. This writer suspects that many such advertisements (he knows of a few actual cases) are written by the sales department or advertising agency and never checked by the engineering staff for technical correctness.

The effect of arsenic in preventing hydrogen embrittlement in acid pickling is not surprising because its inhibiting action on corrosion in acids has been known for many years. The inhibiting effect apparently arises from the high hydrogen overvoltage on the arsenic deposited by cementation on the cathodic areas on the metal surface. If this is true, it seems rather If the protective action of arsenic on hydrogen embrittlement during acid pickling is due to its high hydrogen overvoltage, it would be interesting to determine whether mercury and tin salts have a similar protective action. Both act as corrosion inhibitors for steel in acid pickling because of high hydrogen overvoltage.

Also, it would be interesting to know whether the authors have tried ordinary formaldehyde as an inhibitor for hydrogen embrittlement during pickling. Although it is not generally known, formaldehyde is an excellent corrosion inhibitor for steel in acid solutions.

One other question. Does hydrogen embrittlement occur in this type of stainless-steel wire if it is pickled in ferric sulphate (Ferrisul)?

L. P. Tarasov.*—By means of their bendtest method, the authors have found that certain commercial reagents, designed among other things to inhibit hydrogen embrittlement in the pickling of carbon and low-alloy steels, act instead as embrittlement promoters when the material investigated is a type 440-C stainless steel. Were the tests to be repeated upon a carbon or low-alloy steel, it is possible that these same reagents would inhibit embrittlement instead of promoting it, because the alloy content of the steel may have a marked effect on the behavior of the reagents with respect to embrittlement.

This is illustrated by the behavior of Fe⁺⁺ ions, which the authors have shown in Table 8 to have no measurable effect upon the embritlement of the stainless steel with which

surprising at first glance that a similar protection against hydrogen embrittlement does not occur during cathodic pickling. The reason is, undoubtedly, that in cathodic pickling the current density and voltage are high enough to deposit hydrogen simultaneously with the arsenic, thus preventing the building up of a coherent, protective film of arsenic over the normally cathodic areas on the metal surface. This could be proved in either of two ways: (1) by using a much reduced voltage and current density in the hope of selectively depositing the arsenic; (2) immersing the steel in the acid bath and waiting a few minutes before turning on the current, thus allowing time for the deposition of arsenic by cementation.

^{*} Engineer, U. S. Forest Products Laboratory, Madison, Wisconsin.

Research Laboratories, Norton Company, Worcester, Massachusetts.

they experimented. The writer, on the other hand, has found* that the same concentration of Fe++ ions in sulphuric acid can promote the embrittlement of a hardened tool steel of the manganese oil-hardening variety. This happens when the steel is ground too severely and is then etched in cold sulphuric acid, which causes etch cracks to appear. These etch cracks are simply another manifestation of hydrogen embrittlement, occurring when the surface of the steel is in a suitably stressed condition prior to etching. Under some experimental conditions, the addition of Fe++ ions to the etchant has been observed to double the amount of etch cracking. Thus we see that these ions may or may not have an effect on the embrittlement, depending on the steel.

It is to be hoped that the authors will find the opportunity to repeat some of their work with the addition agents, using a carbon or low-alloy steel in place of the stainless one. Such results would show definitely whether or not the embrittlement-promoting action of some of the commercial reagents is restricted to the stainless steel that happened to be used.

C. A. ZAPFFE and M. E. HASLEM .- (author's reply).-The data listed in Mr. Rosenberg's table, which certainly are erratic, do not surprise us. Testing for hydrogen embrittlement quantitatively is difficult, as indicated by Stuart and Evans, who found that zinc-plated steel broke during bending in the fingers, but survived a half-million cycles in a fatigue machine.

The secret of the present work first lies in the recognition and control of the many variables that affect hydrogen embrittlement, and then in the application of the described test. Fifteen variables are listed in this paper, at least one of which Mr. Rosenberg did not control, as will be explained later. To his credit, however, it should be pointed out that he was the first to apply this test to war problems; and that his difficulties mainly followed from using the machine before its controls were fully developed.

Second, this paper concerns only stainless steel; and it has now been found in an extension of the research to the effect of alloy content that SAE-1065 steel is virtually immune to embrittlement when in the patented or annealed and cold-drawn condition.

Third, this paper does not concern electroplating; and in an extension of the research into plating brittleness, new variables have been found. For example, one customary embrittlement curve drops to a low value and then recovers during further plating because the impermeability of the coating to hydrogen stops the infusion and permits effusion of the gas, with recovery often regained while the article is still being plated. Mr. Rosenberg's single-period tests may have missed the drop in the curve, lying either in front or back

Another type of curve has peculiarities from a double-aging effect in which a backwash of gas occurs as it precipitates from the coating into the metal, or vice versa, as originally identified by Zapffe and Faust.* Without the most careful appraisal of these effects, measurements can be meaningless.

If Mr. Rosenberg's question must be answered specifically, we will draw attention to the fact that we prepare our specimens by a uniform abrading treatment, and that he prepared his by pickling in an acid known to be highly hydrogenizing. In his first tests, the 20-sec. dip may or may not have become influential; but in the more extended cleaning for the tests in Table 12-specimens that finally did show hydrogen embrittlement-he not only exposed the steel to hydrogenizing previous to electroplating, but he exposed it to hydrogenizing that was as erratic as the data in the

That is, scale detaches itself nonuniformly during pickling, exposing local sections of the metal to widely differing periods of attack. Emphasizing this nonuniformity, the presence of the so-called "inhibitor" Rodine very likely behaved as described in the paper. The factor "inherent hydrogen content" was therefore not controlled, and the superimposed plating values lost their significance.

Iron and Steel Inst. (1943) 147, 131-144.

<sup>L. P. Tarasov: Detection, Causes and Prevention of Injury in Ground Surfaces. Preprint No. 26, Amer. Soc. for Metals (1945) Fig. 3.
† N. Stuart and U. R. Evans: The Effect of Zinc on the Corrosion-fatigue Life of Steel. Jnl.</sup>

^{*} C. A. Zapffe and C. L. Faust: Relation of Defects in Electroplate to the Gas Content of the Basis Metal. Proc. 32nd Tech. Session. Amer. Electroplaters' Soc. (1944) 93-108.

Mr. Mack's suggestions for investigating the effect of arsenic are good. Mercury and tin, on the basis of our present knowledge, do not behave in the same way as arsenic in respect to hydrogen embrittlement. We have not yet investigated either formaldehyde or Ferrisul.

Dr. Tarasov's excellent paper on cracking

came to our attention after the present paper was written. His results with ferrous sulphate warrant that the few tests reported here be extended.

As for extending the study in general to unalloyed steel, that has already been done and will be reported shortly.

A Precipitation-hardening Stainless Steel of the 18 Per Cent Chromium, 8 Per Cent Nickel Type

By R. Smith,* E. H. Wyche,† Member A.I.M.E., and W. W. Gorr*

(Chicago Meeting, February 1946)

THE combination of high strength and corrosion resistance of cold-worked 18 Cr. 8 Ni steel has been advantageously utilized for some time, particularly in aircraft and rail car structures. There are. however, certain limitations on the use of such materials because the high strengths can be obtained only by cold-working, limiting the available products to sheets, strip, wire and tubes.

The authors sought to overcome these limitations by resorting to precipitationhardening, which has been used so successfully in nonferrous metallurgy but only to a limited extent in iron-base alloys. Accomplishment of this objective not only overcame the limitations, but also effected certain improvements in mechanical and other properties.

This paper is an account of the development by Carnegie-Illinois Steel Corporation of a precipitation-hardening 18-8 stainless steel (called Stainless W1 and tentatively identified as type 322). A description is given of its composition and metallurgical characteristics, heat-treatment, physical and mechanical properties and corrosion resistance.

DEVELOPMENT OF THE NEW STEEL

For a considerable length of time the authors were unable to determine the mechanism of the precipitation-hardening process that had been noted by Ffield18,19 in 18-8 Ti or 18-8 Cb after cold-working and reheating to moderately elevated temperatures. All known variables were exhaustively studied, but with little success. However, results began to indicate that chemical composition was the most important variable, particularly the ratio of austenite-forming to ferrite-forming elements.

The investigators then focused their attention upon the composition, and, in particular, upon the element titanium and its mode of alloying in the presence of other elements. A heat was obtained that could not be brought to the softness level of annealed 18-8. The response to coldstraining and aging* was very marked by previous standards, and, more important, cold-straining was found to be entirely unnecessary to produce the precipitationhardening effect. The chemical composition of this heat was: C, 0.06 per cent; Mn, 0.54; P, 0.016; S, 0.016; Si, 0.58; Ni, 7.28; Cr, 17.60; Ti, 0.90; Al, 0.17.

For some time the development work, particularly on composition, was carried

Manuscript received at the office of the Institute Nov. 13, 1945. Issued as T.P. 2006 in METALS TECHNOLOGY, June 1946.

Carnegie-Illinois Steel Corporation, Pitts-

burgh, Pennsylvania.

[†] Formerly Carnegie-Illinois with Corporation; now with Titanium Alloy Manufacturing Co., Niagara Falls, New York.

Covered by U.S. Patents 2381416, 2374388 and others pending.

References are at the end of the paper.
The term "precipitation-hardening" * The term "precipitation-hardening in this paper refers to the broader concept of the term and "aging" refers to the hardening step following the solution treatment.

out on the product of 17 or 30-lb. induction heats, in both the as-cast and wrought states, but the bulk of the data reported in the following pages was obtained accounted for by such small amounts of delta ferrite (approximately 5 per cent), indicating that other magnetic phases were present. Quantitative X-ray diffraction

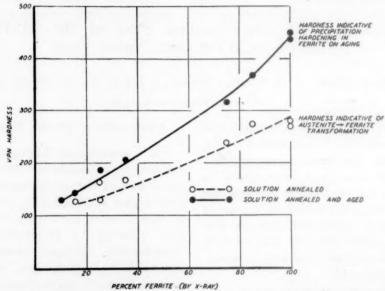


FIG. 1.—RELATIONSHIP BETWEEN VICKERS HARDNESS AND PERCENTAGE OF FERRITE.

on wrought material from commercial heats from arc furnaces of 7 and 35-tons capacities.

The microstructure of the wrought product from these and later heats showed data were then compiled, using, for comparison, standards of known amounts of austenite and ferrite mixtures. A correlation was found (Tables 1 and 2 and Fig. 1).

These data show the relationship be-

TABLE 1.—Analyses of Heats Used for X-ray Diffraction Tests

Heat	Composition, Per Cent										
No.	С	Mn	P	s	Si	Ni	Cr	Ti	A1	N ₂	Сь
223	0.06	0.45	0.020	0.006	0.60	9.56	17.40	0.66			
281	0.06	0.57	0.010	0.010	0.64	9.12	17.60	0.84	0.19	0.015	
280	0.05	0.55	0.020	0.005	0.70	8.24	18.68	0.88	0.22	0.018	
278	0.08	0.62	0.005	0.004	0.69	7.10	18.52	0.84	0.22	0.030	
265	0.06	0.62	0.025	0.006	0.57	7.60	17.04	0.85	0.21	0.033	
283	0.07	0.55	0.020	0.023	0.56	6.93	16.88		0.22	0.054	1.13
275	0.06	0.61	0.017	0.005	0.57	5.84	17.24	0.88	0.19	0.022	
244	0.06	0.54	0.016	0.016	0.58	7.28	17.60	0.90	0.17	0.013	

variable amounts of delta ferrite, ranging between 5 and 35 per cent, which appeared to have little correlation with aging response. The remaining constituents could not be identified at that time, but the ferromagnetism was too pronounced to be tween ferrite and aging response and indicate that aging, following the 2050°F. (1120°C.) solution anneal, produces no change in the amount of ferrite detectable within the limits of experimental error (about ±5 per cent). Thus, the previous

data, which for a time had been so discordant, began to take on an orderly arrangement.

Most of the data in this investigation relate to the titanium type of analysis,

TABLE 2.—Relationship between Amount of Ferrite^a and Vickers Hardness before and after Aging, for Heats Shown in Table 1

Heat No.	Solution at 20 (1120°(Water-q	50°F.	Annealed and Aged \$\frac{1}{2}\$ Hr. at 950°F. (510°C.) and Air-cooled			
-	Vickers Hardness	Ferrite,	Vickers Hardness	Ferrite, ⁵ Per Cent		
223 281 280 278 265 283 275 244	125 130 160 166 242 275 280 270	15 25 25 35 75 85 100	130 142 187 205 320 370 450 445	10 15 25 35 75 85 100		

Determined by X-ray diffraction.
 Ferrite includes both alpha and delta forms.

which had been selected for development, but the mode of action of columbium and other elements is thought to be very similar.

MECHANISM OF PRECIPITATION-HARDENING REACTION

In this precipitation-hardening 18-8 there is a change of phase involved in heating or cooling. Austenite is the stable phase at elevated temperatures while ferrite is the stable phase at atmospheric temperature. The reason for precipitationhardening in this material is that the hardening constituents are soluble in austenite and relatively insoluble in ferrite. Precipitation-hardening is brought about by reheating the supersaturated ferrite to a moderately elevated temperature, below that of transformation from ferrite to austenite. (Not all of the austenite may become transformed on cooling from the solution annealing temperature; indeed, some may even be purposely prevented

from transformation prior to aging.*) The simplest proof that the precipitation occurs in ferrite rather than in austenite is that the degree of precipitation-hardening that can occur on aging is approximately proportional to the attraction of a hand magnet prior to aging. More positive proof is provided by the X-ray diffraction data, which show that the increase in hardening is proportional to the amount of the bodycentered cubic lattice structure present (Tables 1 and 2 and Fig. 1). Additional evidence is provided by the fact that the slope of the dilatometric heating curve (Fig. 2), up to and beyond the aging range, is that of a ferritic steel, while above the transformation point it is the slope of an austenitic steel. Also, the density, which is unaffected by aging, is 7.65 grams per cubic centimeter, approximately that of ferritic stainless alloys (7.56 to 7.65 grams per c.c.).

Identification of the precipitate has not, to date, been possible because of its finely dispersed state. It is faintly discernible under the microscope but has not been agglomerated sufficiently by overaging to be analyzed chemically or identified by X-ray diffraction technique. The electron microscope reveals little more than the light microscope.

Direct evidence of the precipitationhardening is shown by certain changes in physical properties; a decrease of about 15 per cent in electrical resistivity and an increase of about 10 per cent in the thermal conductivity result from aging. Changes of this nature are indicative of a precipitation from supersaturated solid solution.

Composition and Effect of Various Elements

As stated previously, the composition of this material must be so balanced, chemically, that the austenite will transform to

^{*} U. S. Patent No. 2374388.

ferrite on cooling. This transformation, which is essential to precipitation-hardening, usually begins (Fig. 2) at approximately 250°F. (120°C.), and is practically complete

formation does not take place, then only limited precipitation-hardening is possible as shown in Fig. 1, unless means of forcing the transformation are resorted to, such as

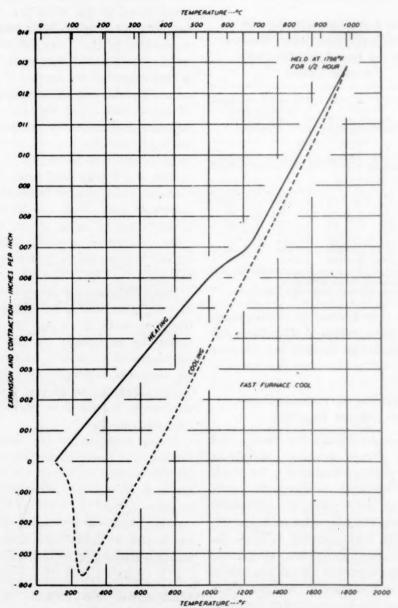


FIG. 2.—TEMPERATURE-DILATATION CURVE.

in from 2 to 4 hr. after the material has aircooled to room temperature (Fig. 3A). Should the amount of any of the elements be so varied that the austenite-ferrite trans-

cold-work or refrigeration. However, the fact that transformation does occur does not mean that the material will be amenable to controllable precipitation-hardening

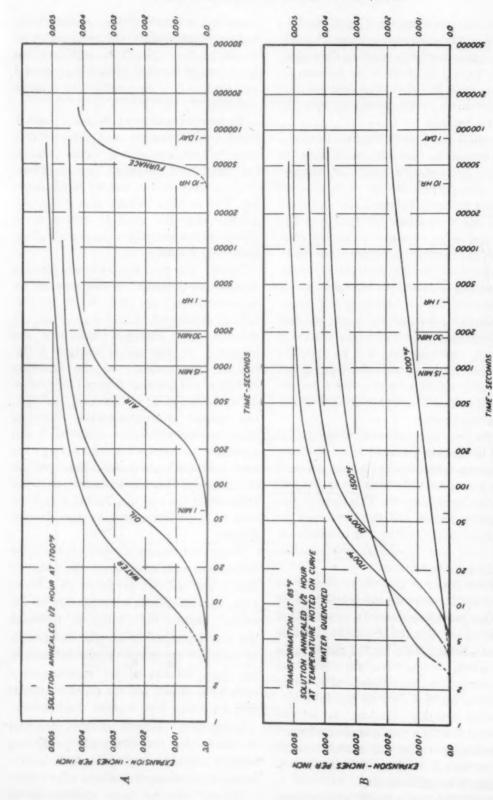


Fig. 3A.—Effect of cooling rate on rate of transformation. Fig. 3B.—Effect of solution annealing temperature on isothermal transformation.

because the elements relied upon must be present in the proper proportions. A workable composition range has been developed, and a typical analysis is as follows: C, 0.07 per cent; Mn, 0.50; P, 0.010; S, 0.010; Si, 0.50; Ni, 7.00; Cr, 17.00; Ti, 0.70; Al, 0.20; Fe, balance.

The most important element is titanium, which serves the dual purpose of being the primary precipitation-hardening element and a strong ferrite former. With all other elements properly balanced, the optimum percentage of titanium has been found to be in the range of 0.40 to 1.00 per cent. Should the titanium be appreciably lower, the matrix will remain partially austenitic after cooling to room temperature and only limited precipitation-hardening will be obtainable unless the material is cold-strained or refrigerated. If the titanium content is too high, the hardening will be excessive and there will be a corresponding decrease in ductility unless a lower solution annealing temperature or a higher aging temperature is employed.

In melting this material, aluminum is added to the bath primarily as a deoxidizer. The excess that remains in solid solution serves to augment the titanium in the precipitation-hardening role. This element also is a ferrite former and therefore must be considered in controlling the composition, and, thus, the resultant precipitation-hardening characteristics.

Carbon does not contribute directly to the precipitation-hardening reaction as do the other preceding elements, but it serves to control the amount of soluble titanium that will be available for the reaction. In other words, when the titanium is combined with carbon, it is immobilized and no longer capable of entering into the precipitation-hardening reaction. Carbon, as is well known, is directly a strong austenite former and indirectly a powerful austenite stabilizer, because it removes a ferrite former, titanium, from solid solution.

Nitrogen behaves in much the same man-

ner as carbon because it also combines with, and thus immobilizes, the titanium. Also, as shown by Uhlig,²⁸ it stabilizes the austenite and therefore should be controlled and held as low as possible (to residual amounts).

The remaining alloying elements—nickel, manganese, chromium and silicon—serve to control the austenite to ferrite balance; the first two elements are austenite formers while the two last are ferrite formers. The authors believe that these elements, with the possible exception of nickel, do not enter into the precipitation-hardening reactions.

Nickel, the primary austenite-forming element, is preferred in the amount of approximately 7 per cent. When the percentage is lowered to 5 or 6 per cent, the ductility and corrosion resistance are impaired. As the nickel content is increased, the stability of the austenite increases, and the time required for austenite transformation is increased. In fact, the amount of untransformed austenite may increase and, since austenite is not amenable to precipitation-hardening, the final hardness is decreased. The optimum percentage of nickel is dependent upon the demands of the end use. Nickel is replaceable to a certain extent by the element copper.

Manganese usually is present in the order of less than 2 per cent, about equivalent to that in the ordinary grades of 18-8. However, the manganese content can be increased beyond that indicated, provided the nickel content is lowered sufficiently to maintain the proper phase balance; it has been substituted for approximately half of the nickel, but the resultant corrosion resistance was lowered considerably.

Chromium is a ferrite former and aids in maintaining the proper phase balance, imparts corrosion resistance, and is preferred in the amount of about 17 per cent.

Silicon, over the range studied, up to

approximately 2 per cent, exerts no discernible effect upon the precipitation-hardening reaction. However, as a mild ferrite former, it has a bearing on the austenite

HEAT-TREATMENT

Like other precipitation-hardening materials, this material is heat-treated in two steps:

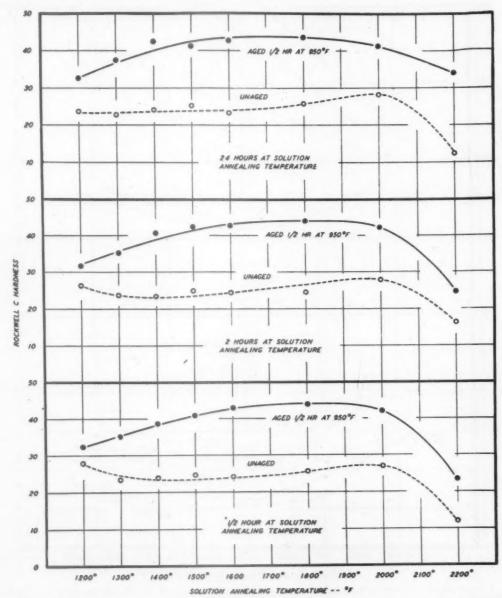


Fig. 4.—Effect of time and temperature of solution annealing on unaged and aged hardness.

to ferrite ratio. In addition, it serves as a preliminary deoxidizer.

Columbium has been substituted successfully for titanium to produce precipitation-hardening.

Solution Annealing.—Solution annealing consists of heating to put the precipitation-hardening constituents into solid solution in austenite; upon cooling to room temperature this transforms to ferrite, which

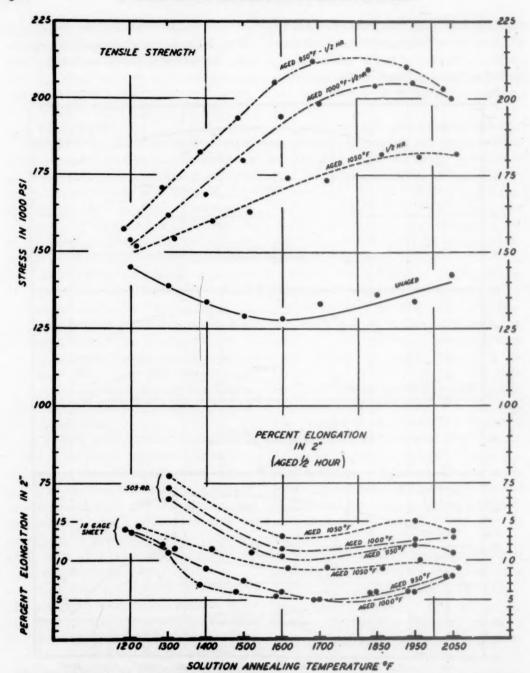
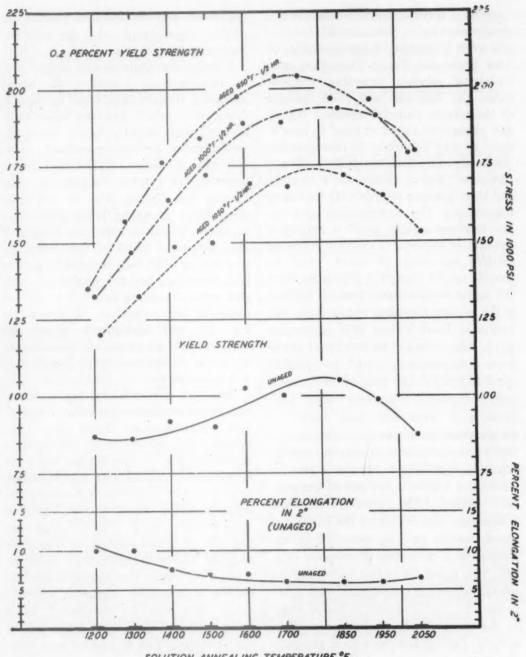


FIG. 5.—Effects of solution annealing and aging temperature on mechanical properties. Solution annealing treatments between 1200° and 1700°F. were preceded by a normalizing heat-treatment at 1850°F. All solution annealing treatments were for ½ hr. at temperature. Each point is an average of duplicate tests or five heats.

is then supersaturated with the precipitation-hardening constituent.

Aging (Precipitation-hardening).—Aging

consists of reheating, upon completion of austenite transformation, to a temperature at which precipitation-hardening con-



SOLUTION ANNEALING TEMPERATURE OF Fig. 5.—(CONTINUED).

stituents will precipitate out of the supersaturated ferrite and impart the desired change of properties.

SOLUTION ANNEALING

range for Stainless W begins at about 1200°F. (650°C.), which is 100° to 200°F above the temperature at which the material begins to transform to austenite, The solution annealing temperature and extends to approximately 2000°F. (1095°C.). Material solution-annealed at a temperature higher than 2000°F. (1095°C.) will show a decrease of hardness (Fig. 4). This figure and Fig. 5 show that, with increasing solution annealing temperatures, the hardness and yield strength of the unaged material increases slightly and passes over a peak at 1700° to 2000°F. (925° to 1095°C.), while the corresponding tensile strength simultaneously reaches a minimum value at about 1600°F (870°C.) and then increases slightly with increasing temperature. The corresponding aged values increase rapidly until a maximum strength or hardness is obtained following solution annealing at about 1700° to 2000°F. (925° to 1095°C.), depending upon the aging temperature. Further increase of the solution annealing temperature only results in lower values after subsequent aging. Also, it should be noted that at the lower temperatures, 1200° to 1600°F. (650° to 870°C.), the slope of the curve of aged mechanical properties versus temperature is steep and close control of temperature is necessary, while at the higher temperatures, 1600° to 2000°F. (870° to 1095°C.), a plateau is reached permitting a greater latitude of temperature control. The solution annealing temperature also influences the isothermal transformation rate as measured by expansion in a quenching dilatometer (Fig. 3B). This figure shows that increasing the solution annealing temperature from 1300° to 1900°F. (705° to 1040°C.) has no effect on the onset of isothermal transformation at 85°F. (30°C.) but the rate is generally slower, the lower the solution annealing temperature.

The holding time, over and above the minimum, at the solution annealing temperature has virtually no influence on the unaged, and aged, hardness, as is shown in Fig. 4. However, the minimum time should be sufficient to remove the effects of all

cold-work, and to take into solution the desired amounts of the precipitation-hardening constituents.

Usually, the minimum time is short, and on thin sections, 5 min. at the higher annealing temperatures 1850° to 1950°F. (1015° to 1070°C.), has been found satisfactory, while slightly longer times are recommended for heavier sections, where it is more difficult to determine when the material has reached temperature. The heating and cooling rates to and from the solution annealing temperature have no known effects on either the unaged or aged properties, provided that extremely slow cooling rates, such as are customary in box annealing, are not employed. Such slow rates of cooling retard the onset of austenite transformation, as shown by Fig. 3A, and reproducible results are difficult to obtain, because of the difficulty in readily determining when transformation is complete.

When this steel is heated and cooled to and from the solution annealing temperature, transformation takes place. On heating (at a rate of 5°F. per minute) as is shown by Fig. 2, the ferrite begins to transform to austenite at approximately 1050°F. (565°C.), and on fast cooling the austenite-ferrite transformation begins at approximately 250°F. (120°C.). However, the rate of transformation is inherently sluggish, therefore precautions must be taken to be certain that transformation on cooling is essentially complete prior to aging. This may be ascertained by a series of Rockwell readings taken over a period of time. Two to 4 hr. at room temperature following the 1700° to 2000°F. (925° to 1095°C.) solution anneal is usually considered satisfactory, but longer times are necessary following the lower (1200° to 1500°F. or 650° to 815°C.) solution annealing temperatures. (See Fig. 3B.) If transformation is not complete, reproducible results are difficult to obtain.

AGING (PRECIPITATION-HARDENING)

Precipitation-hardening takes place over the temperature range of 500°F. (260°C.) to approximately 1050°F. (565°C.). At temperature, 1050°F. (565°C.), approaches the transformation range, and actually results in some formation of austenite that improves the ductility and impact

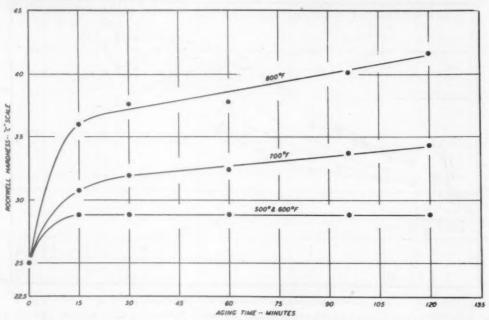


Fig. 6.—Characteristic curves for precipitation-hardening at lower temperatures.

the lower temperatures, 500° to 700°F. (260° to 370°C.), the precipitation-hardening begins and proceeds slowly as is shown in Fig. 6. At 800° to 900°F. (425° to 480°C.), the rate of hardening is greater (Fig. 7) and there is considerable latitude in time, but the resultant product is lacking in ductility and probably would be undesirable for most applications. At 950°F. (510°C.), 1000°F. (540°C.) and 1050°F. (565°C.), the three recommended temperatures, hardening takes place still more rapidly (Fig. 7), but the resultant properties are better balanced and considered to be of more commercial value. Of the three latter temperatures, 950°F. (510°C.) gives the maximum tensile and yield strength, but with the lowest impact strength and ductility, while 1000°F. (540°C.) gives a slightly lower tensile and yield strength with an improved impact strength and ductility. The highest aging strength, since it is retained at room temperature, but at some sacrifice of tensile and yield strengths (Figs. 5, 7 and 17). Temperature control of ±15°F. at the recommended aging temperatures is considered satisfactory for all practical purposes.

The time for beginning of precipitation-hardening is very short; in fact, after one minute at 950°F. (510°C.) the precipitation-hardening is approximately 60 per cent complete. In comparison with other precipitation-hardening systems, this reaction rate is very rapid, therefore it is possible to use short aging periods. However, more reproducible results have been obtained by using longer times, such as 15 or 30 min. at temperature (Fig. 7). As would be expected, the latitude of time is less when using the higher aging temperatures and this is particularly so when using 1050°F. (565°C.).

The heating rate to the aging temperature does not have an appreciable effect upon the resultant mechanical properties, but the cooling rate has a very pronounced by Fig. 10. The uniformity of hardness in the unaged condition is attributed to the fact that transformation on cooling from the solution annealing temperature, at

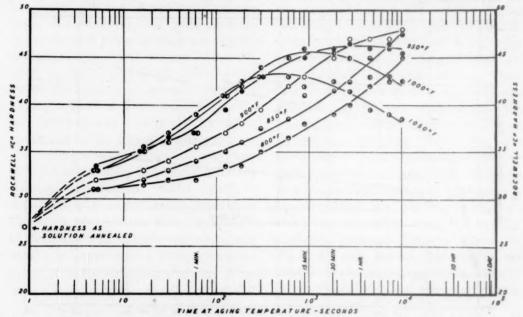


FIG. 7.—EFFECT OF AGING TEMPERATURE AND TIME UPON ROCKWELL C HARDNESS (LOG SCALE).

effect upon the impact strength. Water quenching improves impact values by as much as 40 to 50 per cent over those obtained by air cooling (Fig. 8). From this figure, it is also to be noted that the lower solution annealing temperature results in higher impact strengths in the aged material.

An illustration of the foregoing discussion on the steps of solution annealing and aging is given in Fig. 9, which shows schematically a recommended cycle.

This new 18-8 age-hardenable stainless steel will harden in either the as-cast, as hot-worked, or as cold-worked condition, but solution annealing prior to aging facilitates better control over the final results.

One of the most interesting characteristics of this material is the extreme uniformity of hardness, in both the unaged and aged conditions, obtainable over the cross section of bars of various sizes, as is shown

ordinary rates, takes place over a narrow range of temperature and well below the aging range, and therefore the material consists of only the unaged ferrite resulting from the austenite transformation. This product of transformation, therefore, is reasonably homogeneous and will ageharden uniformly. Also, the latitude of both temperature and time of the aging and solution annealing heat-treatment are believed to contribute to this characteristic.

MICROSTRUCTURE

The microstructure of the new agehardenable ferritic 18-8 stainless steel is

^{*} The etchant preferred by the authors is a 10 per cent aqueous solution of NaCN used electrolytically, as described by Arness; the photomicrographs shown in this paper were etched accordingly. Other electrolytic etchants, such as 10 per cent aqueous oxalic acid solution described by Ellinger, to per cent chromic acid developed by Baeyertz, '1' "lactal" (10 c.c. conc. HCl, 45 c.c. lactic acid and 45 c.c. alcohol) developed by one of the authors, and Marble's reagent, we should be used by immersion, have been found satisfactory but difficult to control.

material is solution annealed in the higher temperature range, 1600° to 2000°F. (870° to 1005°C.), or in the lower range

dependent primarily upon whether the low-carbon martensite, which has been termed "stress-laden ferrite," and is the product of transformed austenite (Fig. 11). Delta ferrite, which is discernible as

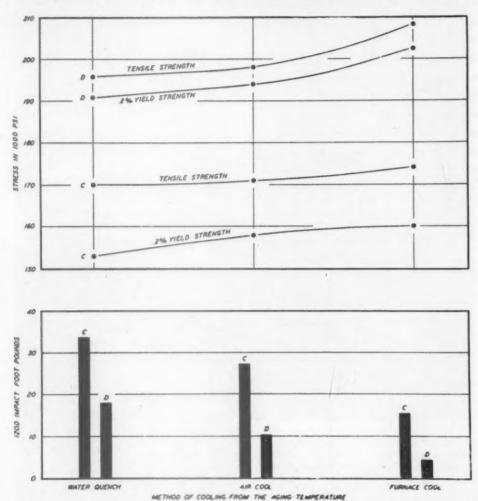


Fig. 8.—Effect of cooling rate from aging temperature on mechanical properties. C designates material solution-annealed ½ hr. at 1300°F. and aged ½ hr. at 1000°F.; D, material solution-annealed 1/2 hr. at 1600°F. and aged 1/2 hr. at 1000°F. Bar size constant.

1200° to 1600°F. (650° to 870°C.), and secondarily upon the aging temperature.

Following a solution anneal at the higher temperatures, 1600° to 2000°F. (870° to 1095°C.), and cooling to room temperature to permit transformation to take place, the microstructure is composed of four phases: alpha ferrite, delta ferrite, austenite and carbides. The supersaturated alpha ferrite, which constitutes the matrix, resembles

stringers or pools, is usually present in amounts varying from 5 to 25 per cent. At still higher temperatures, 2200°F. (1205°C.), the delta phase agglomerates, as is shown by Fig. 12. The carbides are randomly dispersed throughout the matrix. The austenite has never been discernible under the microscope, but X-ray determinations indicate it to be present in amounts up to approximately 5 per cent.

Following a solution anneal at the lower temperatures, 1200° to 1600°F. (650° to 870°C.) and subsequent transformation at

annealing temperature. At the lower temperatures, about 1300°F. (705°C.), the lamellar constituent covers the greater part

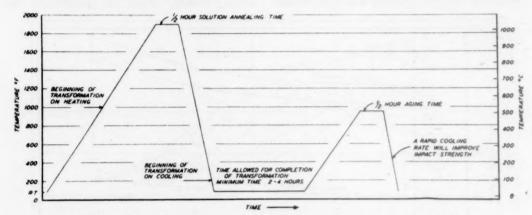


FIG. Q.—TYPICAL HEAT-TREATING CYCLE FOR THE AGE-HARDENABLE 18-8.

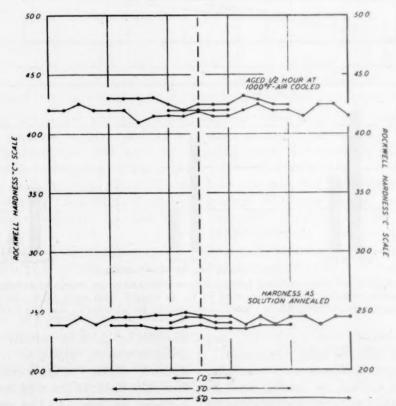
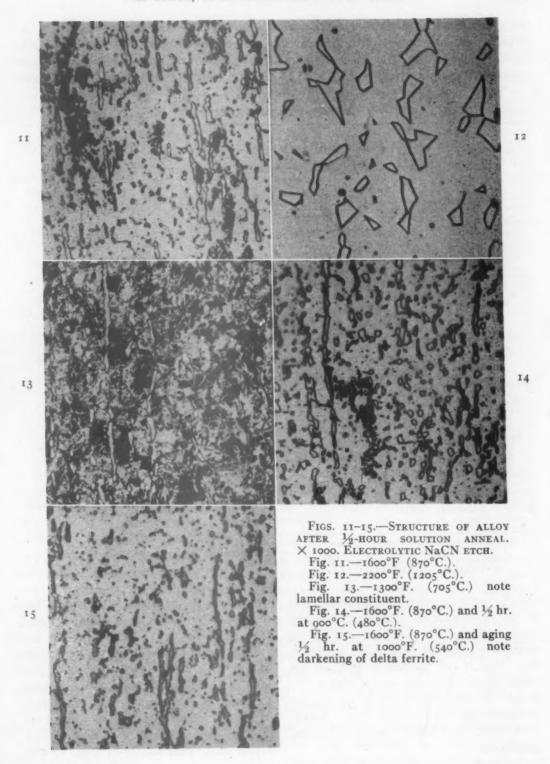


Fig. 10.—Hardness distribution across bars of three diameters, aged and unaged. All bars solution-annealed ½ hr. at 1600°F., a.c.

room temperature, the alpha phase takes on a lamellar appearance, the amount of which is dependent upon the solution of the matrix (Fig. 13). With increasing temperature, or longer times, the resolution of the lamellar constituent increases.



but the quantity decreases. This constituent is associated with improved ductility and impact strength, but the response to aging is less. Above 1400°F. a darkening of the alpha phase (Fig. 14); next a darkening of the delta phase (Fig. 15). This darkening is attributed to the submicroscopic hardening constituents,

TABLE 3.—Physical Constants

Constant	Stainless W		18-	8	18-8 (Fer- ritic) 28	17 Cr	
	Annealed	Aged	Annealed	Cold-rolled Full Hard	Annealed	Annealed	
Specific gravity:							
Lbs. per cu. in	0.28	0.28	0.29		0.283	0.2833	
Grams per c.c	7.65	7.65	7.933		7.74	7.788	
20°C	100	85	7233		93.5	6033	
Structure	Fd,b	Fb	Ad	A-F	F	F	
Thermal conductivity,							
Cal per sq. cm. per sec. per deg. C. per cm.:							
At 100°C	0.045	0.050	0.03938			0.06233	
200°C	0.0486	0.0530	0.042			0.063	
400°C	0.0560	0.059	0.048			0.063	
B.t.u. per sq. ft. per hr.							
per deg. F. per ft.: At 212°F	0		00				
392°F	10.8	12.1	9.4 ³³			15.138	
752°F	13.5	14.2	11.6			15.2	
Mean coefficient of thermal	13.3	14.2	22.0			.3	
expansion:							
Deg. C. × 10-8							
o to 100°C	9.9		17.3		1	10.4	
o to 400°C o to 500°C	11.2		17.8			11.0	
Deg. F. × 10-6	11.3		18.4			11.3	
32° to 212°F	5.5		9.633			5.833	
32° to 572°F	6.2		9.9			6.1	
32° to 932°F	6.3		10.2			6.3	
Magnetic permeability,							
H = 100	81	101	1.00388	1033	66.9	14728	
Modulus of elasticity (ten-	28,000,000	28,000,000	28.000.0000 83	26,000,0004		29,000,000	
sion), lb. per sq. in Modulus of elasticity (tor-	20,000,000	20,000,000	20,000,000	20,000,000		29,000,000	
sion), lb. per sq. in		11,300,00035	12,500,0000 88	11,000,00034			

As cold-worked these values decrease to 26,000,000 or less.
Ferritic approximately 3 hr. after cooling to room temperature from austenitizing temperature.
Estimated on basis of experience with other similar steels.

d F = ferritic; A = austenitic.

(760°C.), the lamellar constituent begins to go into solution and after one-half hour at 1600°F. (870°C.) solution is essentially complete (Fig. 11). Changes in the amount of austenite retained at room temperature also occur within this range of temperature, with the higher amounts (up to 35 per cent) associated with the lower solution heating temperatures.

Upon aging following solution annealing at 1600 to 2000°F. (870° to 1095°C.), the first visible change in the microstructure is

which first begin to precipitate when the temperature reaches approximately 500° to 600°F. (260° to 315°C.).

Upon aging following solution annealing at 1200 to 1600°F. (650° to 870°C.), the same submicroscopic precipitate darkens the matrix, but again the precipitate itself is not resolvable. The microstructure of such aged material is similar to, but darker than, that shown in Figs. 11 and 13, the amount of lamellar constituent depending on the solution annealing temperature.

PHYSICAL PROPERTIES

Physical properties of this steel are compared in Table 3 with those of annealed 18-8, cold-worked 18-8, Uhlig's²⁸ ferritic 18-8, and annealed 17 per cent Cr. As would be surmised from the discussion

MECHANICAL PROPERTIES

Properties at Room Temperature

The "soft" mechanical properties that make the conventional annealed 18-8 so easily adaptable to deep-drawing, forming

TABLE 4.—Typical Ranges of Tensile and Hardness Properties of the New Steel as Solution-annealed and as Aged at the Temperatures Indicated

Item No.		*** * *			Mini- ated				
	Treatment	Yield Strength, 0.2 Per Cent	Tensile Strength,	Shee	ts and S	Strips		tes Bars	Rockwell Hardness, C Scale
		Offset, 1000 Lb. per Sq. In.	per Sq. In.	0.030 In. and Less	Over 0.030 to 0.060 In.	Over 0.060 In.	1/2 In. and Less	Over	
I	Solution-annealed at 1850° to 1950°F. a.c.		*20 *50	2		5	8	10	22-28
2	No. 1 plus aged at 950°F., 1/2 hr.	75-115	120-150	3	4	3	0	10	22-20
-	a.c. No. 1 plus aged at 1000°F., ½ hr.	180-210	195-225	3	4	5	8	10	39-47
3	a.c.	170-210	190-220	3	4	5	8	10	38-46
4	No. 1 plus aged at 1050°F., ½ hr. a.c.	150-185	170-210	4	5	7	8	10	35-43
5	No. I plus solution anneal at								
6	1300°F. a.c. No. 5 plus aged at 950°F., ½ hr.	70-110	120-150	5	6	7	10	12	23-29
	a.c.	135-175	155-185	5	6	7	10	12	35-41
7	No. 5 plus aged at 1000°F., ½ hr.	125-165	145-175	5	6	7	10	12	34-40
8	No. 5 plus aged at 1050°F., ½ hr. a.c.	110-145	135-170	5	6	8	10	12	31-37

under Mechanism, and by the work of Uhlig²⁸ on 18-8 stainless steels with very low carbon and nitrogen, certain of the physical constants, which are more directly dependent upon metallographic structure than upon chemical composition, approach those of ferritic 17 per cent Cr and ferritic 18-8. Examples are: specific gravity, coefficient of thermal expansion, magnetic permeability and electrical resistivity. The difference in electrical resistance and thermal conductivity between the annealed and aged conditions is believed to be indicative of precipitation. The constant modulus of elasticity, as compared with the decreasing modulus of cold-worked 18-8, is significant, and will be discussed under Mechanical Properties.

and spinning operations are the characteristic properties of austenite. The high-strength properties of cold-rolled 18-8, which make this type of stainless a widely used structural material in the aircraft and transportation industries, are largely those of austenite strained by cold-work and in a certain stage of transformation into ferrite (martensite). The propensity for austenite -> ferrite (martensite) transformation is largely a function of the chemical composition. Some alloying elements-for instance, chromium, silicon, aluminum-tend to favor the transformation from austenite to ferrite, while others-nickel, manganese, carbon, nitrogen-tend to restrain it. Thus, by "balancing" the ratio of austenite formers to

ferrite formers, the austenite of conventional 18-8 can be made relatively stable, with a low rate of work-hardening for deep-drawing applications; or relatively unstable, with a high rate of work-harden-

As mentioned previously, however, the basic composition is so balanced as to ensure, without the necessity of cold-working, the approximate completion of the austenite → ferrite (martensite) transfor-

TABLE 5.—Mechanical Properties of Stainless W Wrought Products Plates, Sheets, Strip, Bars, Wire, Forgings

		Properties	Annealed 1850°-1950°F. (1010°-1065°C.)	Aged ½ hr. 950°F. (510°C.)
Tension	1 2 3 4 5	Ultimate stress, lb. per sq. in. Yield stress, lb. per sq. in. Proportional limit, lb. per sq. in. Initial modulus of elasticity, lb. per sq. in. Elongation in 2 in., per cent	120,000 75,000 40,000° 28,000,000 3-10	195,000 180,000 95,000 ⁶ 28,000,000 3-10
Compres- sion	6 7 8 9 10	Ultimate (block) stress, lb. per sq. in. Yield stress, lb. per sq. in. Proportional limit, lb. per sq. in. Column yield stress, lb. per sq. in. Initial modulus of elasticity, lb. per sq. in.	75,000 ⁴ 40,000 ⁴ 28,000,000	389,000 ^{b,b} 180,000 ^a 95,000 ^a 28,000,000
Shear	11 12 13	Ultimate stress, lb. per sq. in. Torsional modulus of rupture, lb. per sq. in. Proportional limit (torsion), lb. per sq. in. Modulus of rigidity (torsion), lb. per sq. in.		120,000 ^{5,6} 150,000 ^{6,6} 161,000 ^{5,6,6} 39,000 ^{5,6} 75,000 ^{5,6,6} 11,000,000 ^{6,8}
Bear- ing	15 16 17	Ultimate stress, lb. per sq. in. Rockwell No., C Brinell No., C	22 230	200,000 ^{b,j} 39 360
Fatigue	18	Bending endurance limit, lb. per sq. in. (20,000,000 cycles) Torsional endurance limit, lb. per sq. in. (20,000,000 cycles)		54,000°.6 70,000°.5 96,000 58,000°.6
	20	Specific weight, lb. per cu. in.	0.28	0.28

Based on relatively few tests.

Single test values. Wright Field data; 1600°F. solution-annealed and ½ hr. at 900° to 925°F. aging cycle.

Wright Field data; 1000 lb. per sq. inch.

4 Prestressed to 104,000 lb. per sq. inch.

Wright Field data. Unpolished sheets, longitudinal and transverse. Solution-annealed at 1950°F., aged 2 hr. at 925°F. (see p. 22).

Wright Field data. Polished sheets longitudinal. Solution-annealed at 1950°F.; aged 2 hr. at 925°F. (see

/ Wright Field data. Polished sheets longitudinal. Solution-annealed at 1950°F.; aged 2 nr. at 925°F. (see p. 21).

Wright Field data. Bars. Solution-annealed at 1950°F.; aged 2 hr. at 925°F. (see page 22).

Mupublished data from Fleetwings, Inc. Solution-annealed 1600°F.; aged ½ hr. at 900°F.

Unpublished data from Fleetwings, Inc. Interpolated to D/t ≤ 5.5.

Unpublished data from Fleetwings, Inc. Solution-annealed 1600°F.; aged 1 hr. at 920°F.

"Unpublished data from Fleetwings, Inc.: 150,000 lb. per sq. in. on material solution-annealed at 1600°F.; aged 1 hr. at 920°F.; and Wright Field: 156,000 lb. per sq. in. on material solution-annealed at 1600° and aged ½ hr. at 900° to 925°F.

"Unpublished data from Fleetwings, Inc.: 11,000,000 lb. per sq. in. on material solution-annealed at 1600°F.; aged ½ hr. at 900° to 925°F. and Wright Field: 11,300,000 on material solution-annealed at 1600°F.; aged ½ hr. at 900° to 925°F. and 11,500,000 on similar material prestressed to 104,000 lb. per sq. inch.

ing, wherein high strength can be obtained with a minimum of cold-work and a minimum sacrifice of ductility resulting from cold-work. The properties of cold-worked 18-8 have their advantages and disadvantages in the field of structural applications, particularly in the aircraft and rail-car industries, and have been discussed at great length in the literature. 34,36-49

mation, and the subsequent process of precipitation-hardening. This new agehardenable stainless steel is not intended for the applications for which the soft ductile austenitic 18-8 types are so well suited, but was developed to make the high-strength properties of cold-worked 18-8 available in all wrought and cast forms, irrespective of size and shape.

Since this steel in the annealed condition is essentially ferritic (martensitic), the normal mechanical properties (Table 4) are similar to those of 18-8 in the ½ hard

The mechanical properties, as discussed under Heat-treatment, are largely a function of the time and temperature of the solution annealing and the precipitation-

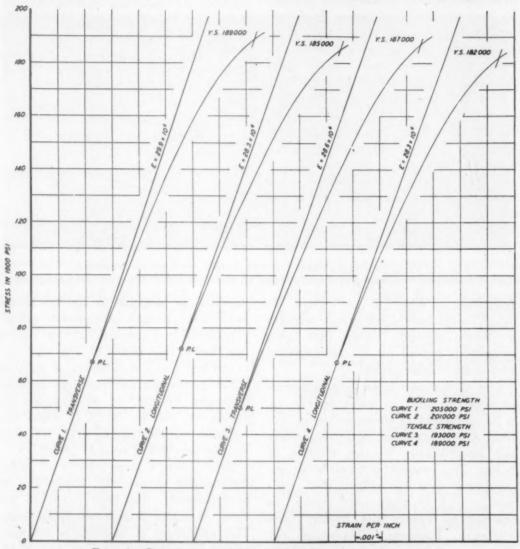


Fig. 16.—Stress-strain curves in tension and compression. Curves 1 and 2 show compression values; 3 and 4, tension values. All material solution-annealed at 1600°F., and aged ½ hr. at 950°F. 0.030-gauge material was used.

and ½ hard tempers (Table 5) and of Uhlig's²⁸ ferritic 18-8, which are as follows:

Yield Strength, o.2 Per Cent Offset, Lb. per Sq. In.	Tensile Strength, Lb. per Sq. In.	Elonga- tion, Per Cent in 2 In.	Reduc- tion of Area, Per Cent	Hardness, Brinell No.
84,000	113,000	17.5	65	246e

a Converts to Rockwell C-24.

hardening treatment and can be selectively varied over a considerable range. Typical conservative ranges of room-temperature tensile and hardness properties representative of several commercial heats, made in electric-arc furnaces of both 7 and 35 tons capacities, for certain selected heat-treatments are shown in Table 4.

In the aged condition, as shown by Table 4, the properties of this steel can be selected to match those of 18-8 in the ½, ¾ and full hard tempers; of Army-Navy Aeronautical

verse specimens. Design must be based upon the lowest value, of course. In this material, as shown in Fig. 16, little difference of offset yield strength is encountered

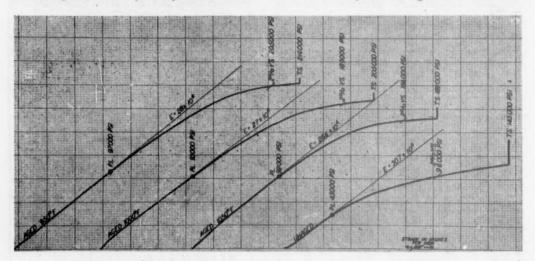


FIG. 17.—TYPICAL STRESS-STRAIN CURVES, AGED AND UNAGED CONDITIONS.

Tested transverse to direction of rolling. Actual stress-strain curves made on 0.065 gauge sheet.

Specification AN-QQ-S-772a (Sept. 8, 1943), on the basis of either yield strength or tensile strength, except that lower elongations prevail for the age-hardened 18-8 in the thinner gauges.

One of the most interesting characteristics of this steel, as shown by Fig. 16, is its uniformity of elastic values in tension* and compression, both transversely and longitudinally to the direction of rolling. This constitutes considerable improvement over the widely used coldworked 18-8 stainless steels, which, as reported by Franks and Binder, and Aitcheson, Ramberg, Tuckerman and Whittemore, have considerable spread in yield strength, particularly in compression, as determined on longitudinal and trans-

between the longitudinal and transverse tests made in either tension or compression.

A variation of proportional limit values is noticed in Figs. 16 and 17. This variation is attributed to the difference of solution annealing temperatures used. The material illustrated by Fig. 16 was solution-annealed at 1600°F. (870°C.), while the material represented by Fig. 17 was solution-annealed at 1950°F. (1065°C).

Based upon a large number of tests, the modulus of elasticity, irrespective of heat-treatment, has been found to be about 28 million pounds per square inch. This uniformity of modulus is not surprising, since the high strength is obtained by heat-treatment and not by cold-work. According to Franks and Binder, 36 the lowering of the modulus of the coldworked 18-8 is attributed to a state of internal stress.

Additional mechanical properties are shown in Table 7, for comparison with those of annealed and cold-worked 18-8 as given in the Government Bulletin ANC-5.34

^{*} Tensile tests were made on a Baldwin-Southwark hydraulic testing machine of 60,000 lb. capacity, using a Templin autographic stress-strain recorder and Templin grips. Tensile specimens were prepared in accordance with A.S.T.M. Standard E8-42. Compression tests were made using the cylinder test method described by Franks and Binder. 48 A photograph of a few actual autographic recordings is shown in Fig. 17.

Impact Strength

The Izod impact strength of the agehardenable 18-8 in the unaged condition is approximately 40 to 60 ft-lb., regardless of the solution annealing temperature. Upon aging, however, the solution anneal prior to aging will have a bearing upon the resultant impact strength (Fig. 8). The lower the solution annealing temperature used prior to aging, the higher the impact strength of the aged material. Also, as discussed under Heat-treatment, faster cooling rates from the aging temperature improve the impact strengths by as much as 40 to 50 per cent (Fig. 8).

Fatigue Tests

Fatigue tests were made on R. R. Moore rotating-beam testing machines at 1750 and 3500 r.p.m. on notched and unnotched specimens of Stainless W, as solution-annealed at 1600°F. (870°C.) and aged 1/2 hr. at 1000°F. (540°C.). Blanks from forged 34 by 34-in. bar stock were solution-annealed ½ hr. at 1600°F. (870°C.), air cooled. Unnotched specimens were machined oversize; notched specimens were machined to size except for taper ends. Heat-treatment was then completed by aging for ½ hr. at 1000°F. (540°C.) and air cooling. Specimens were then ground to final size. The circumferentially notched specimens had a straight cylindrical section 0.270 in. in diameter with a 60° (included angle) notch of 0.010 in. radius at its base and 0.220 in. in diameter. The unnotched specimens had a reduced diameter of 0.220 in. and were machine polished to obtain a surface satisfactorily free from pits and circumferential scratches when examined at a magnification of 30 diameters.

Tests on specimens that did not fail were stopped after 40×10^6 reversals. For the unnotched condition the data show some scatter, as indicated by the band in Fig. 18, the upper limit of which

is drawn to approach 95,000 lb. per sq. in., while the lower limit approaches 85,000 lb. per sq. in. For the notched condition, the endurance limit is shown as 37,000 lb. per sq. in., which is in agreement with values of 40,000 to 50,000 obtained by U. S. Army Air Forces, Materiel Center, Wright Field, Dayton, Ohio,35 on specimens variously heat-treated. The endurance ratio for the unnotched condition is therefore approximately 0.46, based on a tensile strength of 195,000 lb. per sq. in., and approximately 0.20 for the notched condition. Results of other tests, some of which were made at Wright Field,36 indicate the unnotched value to be, conservatively, about 96,000 lb. per sq. in. The approximate 60 per cent reduction in endurance limit resulting from notching indicates a higher degree of notch sensitivity than is characteristic of austenitic 18-8, but one that is not unexpected for a hard ferritic material. Moore and Kommers⁵⁰ have found that the endurance limit (49,000 lb. per sq. in.) of a 0.50 per cent carbon steel heat-treated to a "sorbitic" condition was reduced about 60 per cent by a 90° V-notch.

Sheet fatigue tests were conducted at Wright Field35 on Krouse sheet fatiguetesting machines rated at 1750 r.p.m. Specimens were tested with principal axis parallel to, and transverse to, the direction of rolling, with the surface finish as received from the mill, which was somewhat inferior to the commercial No. 1 sheet finish. The surfaces of three of the specimens cut longitudinally from a 0.050-in. sheet were ground and polished with Nos. 1, o and ooo emery paper, to determine the effect of surface condition upon the fatigue strength. Results are given in Table 6, and show that the fatigue strength of thin sheets is influenced to a considerable degree by surface finish. Brick and Phillips 1 have previously reported similar findings relative to influence of surface condition on sheet fatigue strength of various 18-8 steels.

Fatigue tests in torsional shear were also made at Wright Field³⁵ on an H. F. Moore fatigue-testing machine operating at a speed of 1500 r.p.m. using a specimen

zero stress as a reference. The specimens were machined from a forged bar 1-in. square [which had been previously solution-annealed at 1950°F. (1065°C.) and

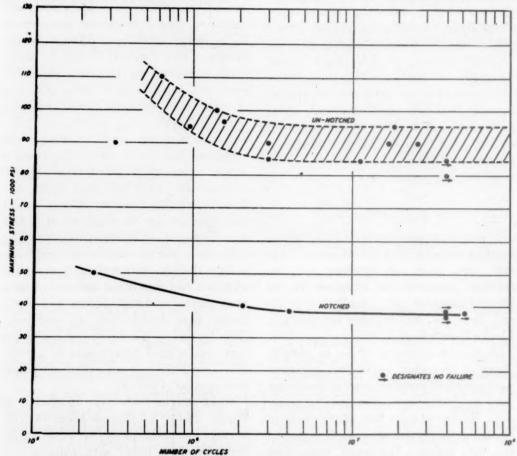


FIG. 18.—NOTCHED AND UNNOTCHED FATIGUE STRENGTH OF AGED MATERIAL. Solution-annealed at 1600°F. (870°C.) and aged ½ hr. at 1000°F. (540°C.)

with a 0.30-in. gauge diameter. The stress was alternated between maximum values of equal magnitude and opposite sign, with

aged at 925° F. $(495^{\circ}$ C.) for 2 hr.] and polished. Fatigue limit at 20×10^{6} cycles was found to be 58,000 lb. per sq. inch.

TABLE 6.—Fatigue Tests on Sheet Material

Thick-		Solution Annealing	Agi	ng	Tensile		nit, Lb. per In.	Ratio
ness of Sheet, In.	Direction to Rolling	Tempera- ture, Deg. F.	Tempera- ture, Deg. F.	Time, Hr.	Strength, Lb. per Sq. In.	As Received	Ground and Polished	Fatigue Limit Tensile Strength
0.018	Long.	1950	925	2	183,500	56,000		0.306
0.018	Trans.	1950	925	2	168,600	54,000		0.320
0.018	Long.	1600	925	2	168,400	50,000		0.297
0.050	Long.	1950	925	2	196,500	54,000		0.275
0.050	Trans.	1950	925	2	201,000	54,000		0.269
0.050	Long.	1950	925	2			70,000	0.348

PROPERTIES AT ELEVATED TEMPERATURE

At elevated temperature (above 800°F., or 425°C.), the strength of the age-hardenable 18-8 is about the same as that of

hardening process is maintained and may be utilized.

Some comparative properties at elevated temperatures are shown in Fig. 10. The

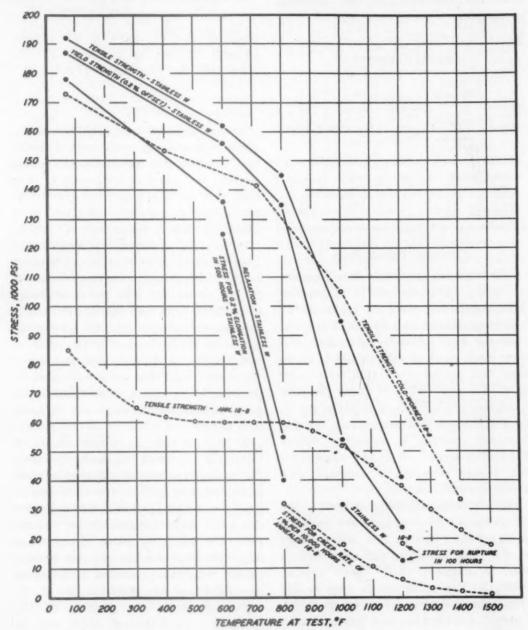


Fig. 19.—Effect of temperature on tensile, yield, relaxation, rupture, and creep strength.

annealed ordinary 18-8. However, at moderate temperatures, the strength imparted to Stainless W by the precipitation-

specimens of this material were solutionannealed at 1650°F. (895°C.) for 40 min. in the form of forged bars 1 in. in diameter. The specimens were then machined and the heat-treatment was completed by aging for one hour at 1000°F. (540°C.), followed by air cooling. The results of the tests are described in the following paragraphs.

TABLE 7.—Results of Tensile Tests at Elevated Temperature

Temperature, Deg. F.	Yield Strength (Stress for 0.2 Per Cent Offset), 1000 Lb. per Sq. In.	Tensile Strength, 100 Lb. per Sq. In.	Elonga- tion, Per Cent	Reduc- tion of Area, Per Cent
80 600	187	192	13.5	53.5 51.5
800	135	145.5	13.5	53
1000	54	94.1	22.5	
1200	24	41	40	75 88

Short-time Tensile Tests

The results of the tensile tests are given in Table 7, and plotted in Fig. 19, together with comparable data on cold-worked⁵² and on annealed⁵³ 18-8. It should be noted that the tests of the cold-worked 18-8 were made on sheet material. It is shown that this age-hardened 18-8 is stronger than 18-8 cold-worked to about the same hardness (390 V.P.N.) up to about 800°F. (425°C.). Above this temperature, the age-hardened material is somewhat weaker than cold-worked 18-8, and approaches the tensile strength of annealed 18-8 at about 1200°F. (650°C.).

At all temperatures investigated, the elongation of the age-hardened material is higher than that of 18-8 cold-worked⁵² to the same hardness, and even exceeds that of annealed 18-8⁵³ above 1150°F. (620°C.). The reduction of area is less than that of annealed 18-8 up to 950°F. (510°C.), but then becomes greater.

Stress-rupture Tests at 1000° and 1200°F. (540° and 650°C.)

The results of the stress-rupture tests are tabulated in Table 8, which shows

TABLE 8.—Stress for Rupture in 100 Hours at 1000° and 1200°F. (540° and 650°C.)

Temperature, Deg. F.	STRESS FOR RUPTURE IN 100 Hr., 1000 LB. PER SQ. IN.
1000	31.5
1200	12.5
1200	18.0 (Annealed 18-8) 84

that, at 1200°F. (650°C.), the rupture strength of the age-hardened material is less than that of annealed 18-8.54

"Relaxation" Tests

In order to determine, quickly and simply, whether or not creep would occur at 600°F. (315°C.), modified relaxation tests were carried out at this temperature. The tests were made in a modified gear-driven tensile-testing machine, described in a paper by Miller, Smith and Kehl.55 In this test, the specimen was loaded at a head speed of about 0.21 in. per hour up to the yield strength (the stress indicated by the short-time tensile test as necessary to produce 0.2 per cent offset). The loading mechanism was then shut off, leaving the specimen firmly locked in the strained position, but free to creep and thus reduce the stress (relax). The stress was measured periodically by means of an Olsen strain gauge attached to a weigh bar in series with the specimen.

At room temperature, a slight amount of relaxation occurred immediately after the loading mechanism was shut off (the stress decreased from 187,000 to 180,000 lb. per sq. in., about 4 per cent), but no further change of shape occurred during the ensuing 120 hr., after which the test was discontinued. It was thought that the apparent relaxation at room temperature may have been due to lost motion in the apparatus before the position of the specimen became locked; there was no progressive change of shape of the specimen, indicating the absence of creep at room temperature.

At 600°F. (315°C.), however, definite indications of creep were evident. The

specimen was stressed to 156,000 lb. per sq. in., and sufficient creep occurred in 200 hr. to reduce the stress to 136,000 lb. per sq. in. (about 13 per cent). No further extension was found to occur, although the test was continued to 330 hours.

At 800°F. (425°C.), considerable creep occurred, resulting in a decrease of the applied stress from 135,000 to 54,000 lb. per sq. in. (about 60 per cent) in 280 hr. No further decrease of stress occurred in the ensuing 70 hr., and the test was discontinued. The "relaxation" values are shown in Fig. 19 for comparison with the results of the short-time tensile tests.

Creep Tests at 600° and 800°F. (315° and 405°C.)

Since the "relaxation" test indicated that there is no appreciable creep at room temperature, the short-time tensile properties are adequate for design purposes at this temperature. At 600° and 800°F. (315° and 425°C.), however, creep does occur, and it was felt desirable to determine the effect of stress on the time to reach 0.2 per cent permanent deformation. This was done by running a series of creep tests at each temperature.

In 500 hr., 0.2 per cent permanent deformation is produced by 125,000 lb. per sq. in. at 600°F. (315°C.) and by 40,000 ft. per sq. in. at 800°F. (425°C.). These values are plotted in Fig. 10 for comparison with the other high-temperature properties. At 800°F. (425°C.), the stress for 0.2 per cent permanent deformation in 500 hr. is slightly higher than the stress for a creep rate of 1 per cent per 10,000 hr. in annealed 18-8.56 The curve for the creep strength of annealed 18-8 probably gives a fair idea of the creep behavior of the new age-hardenable 18-8, since at 800°F. (425°C.), the stress for a creep rate of 1 per cent for 10,000 hr. was found to be about 35,000 lb. per sq. in., and about 32,000 lb. per sq. in. for annealed 18-8.56

The results of the short-time and long-time tests are given in Table 9.

TABLE 9.—Summation of Short-time and Long-time Strengths at Elevated Temperatures

Temperature, Deg. F.	Stress for o.2 Per Cent Offset (from Tensile Test), 1000 Lb. per Sq. In.	Relaxation Value, 1000 Lb. per Sq. In.	Stress for o.2 Per Cent Permanent Deforma- tion in 500 Hr., 1000 Lb. per Sq. In.
80	187	180	125
600	156	136	
800	135	54	

It should be noted that Table 9 relates to 0.2 per cent permanent deformation and, therefore, does not represent the total deformation obtained on loading. The total deformation would include the elastic extension as well as the plastic or permanent deformation, and the elastic extension itself may exceed 0.2 per cent. The amount of elastic extension depends on the stress, and on the modulus of elasticity at the temperature in question; the moduli were determined to be approximately as shown in Table 10.

TABLE 10.—Tensile Modulus of Elasticity

at Eleva	ted Temperature
TEMPERATURE, DEG. F.	MODULUS OF ELASTICITY, 1,000,000 LB. PER SQ. IN.
80	29
400	29
800	27
1000	20
1200	14

No creep tests were made at 1000°F. (540°C.), or at higher temperatures, since overaging occurs in 16 hr. at 1000°F. (540°C.).

CORROSION RESISTANCE

The new age-hardenable 18-8 was developed primarily as a high-strength stainless steel for structural purposes. Early tests for evaluating its corrosion resistance were conducted with that field of application in mind. They consisted of intergranular embrittlement, accelerated salt-spray tests, and also some field tests;

immersion in the sea, exposure to atmospheres selected and classified as industrial, semirural and sea-coast.

Intergranular Embrittlement Tests

A number of tests were made on specimens in the solution-annealed and in the aged conditions, with and without the addition of a heat-treatment of 2 hr. at a temperature of 1200° to 1250°F. (650° to 680°C.) for inducing sensitization. The specimens were then immersed for a period of 100 hr. in a boiling solution of copper sulphate and sulphuric acid (modified Strauss solution containing 13 grams CuSO_{4.5}H₂O, 47 ml. H₂SO₄ of 1.83 sp. gr., balance H₂O to make 1 liter). The Results, evaluated by bend tests and microscopic examination, showed that the steel was not susceptible to intergranular corrosion.

Salt-spray Tests

Stainless W, in both the solutionannealed and in the aged and acid-pickled conditions, the material resists the saltspray test about as well as standard 18-8. The 100-hr. salt-spray test conducted in accordance with the Army-Navy Aeronautical Specification AN-QQ-S-91 was satisfactory; and in fact, tests conducted by the Army Air Corps⁴⁰ at Wright Field, Dayton, Ohio, on aged and acid-pickled material showed no pitting after more than 1000 hours.

Sea-water Immersion Tests

Over the span of three years, several series of specimens in various conditions of heat-treatment, along with control specimens of full hard 18-8 with cold-rolled finish, annealed 18-8 and 18-8 Ti in No. 2-D finish, were totally immersed for a period of one year each in sea water at the cooperative test site* at Kure Beach, Wilmington, N. C. LaQue⁵⁸ has described

in detail the test conditions at the site, while Larrabee⁵⁹ cites corrosion losses and pitting characteristics obtained on 1/4-in. thick specimens of stainless steels of types similar to some of those mentioned above. No appreciable difference in corrosive attack was observable between the annealed 18-8 and 18-8 Ti controls, and the age-hardenable 18-8 in either the solutionannealed or aged condition. Aged specimens that were exposed without removal of the aging-temperature heat tint, developed a greater number of pits, which were shallower as compared with duplicate specimens from which the heat tint had been removed by acid pickling. It is interesting to note in Fig. 20 that the corrosion attack is generally dispersed, whereas 18-8 is attached preferentially with respect to rolling direction. The specimens shown in Fig. 20 were approximately 0.050 in. thick.

Atmospheric Corrosion Tests

A number of corrosion panels representative of various heat-treatments have been exposed to the atmosphere at the following test sites:

ATMOSPHERE TEST SITE

Marine Kure Beach, Wilmington, N. C.

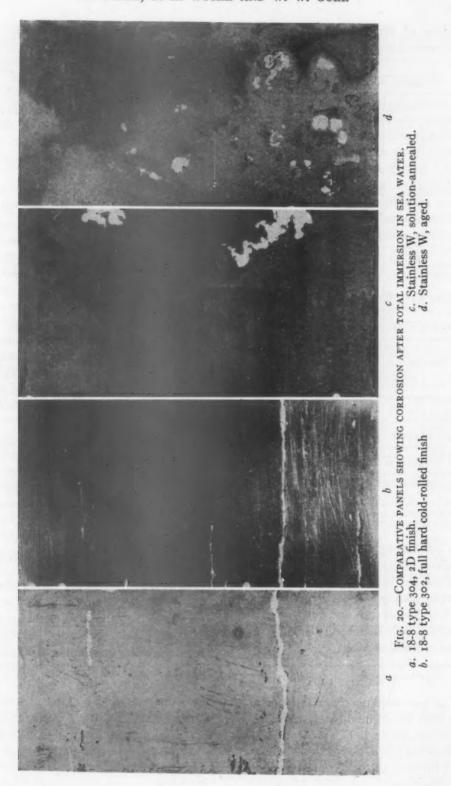
Semi-rural South Bend, Pennsylvania

Industrial Kearny, New Jersey

Periods of exposure extend to 3½ years and the tests are being continued. Results based upon visual examination show that the corrosion resistance of the new agehardenable material is approximately that of 18-8. Precipitation-hardening of this new material does not impair its corrosion resistance.

However, in view of the increasing number of applications requiring materials possessing high strength and hardness, together with high corrosion resistance, and because of the favorable results of the early tests, additional laboratory and service tests are contemplated. Results

Carnegie-Illinois Steel Corporation, International Nickel Company, and Dow Chemical Company.



of some of the more recent laboratory tests are as follows:

Standard Boiling Nitric Acid Test

Results obtained by this test 60 are shown in Table 11. Maximum corrosion rates of various grades of 18 per cent Cr, 8 per cent Ni and 17 Cr, allowable by some specifications, are given for comparison. It is evident that in this severe test the corrosion resistance in the solution-annealed condition is inferior to that of the other types of stainless steels and is considerably inferior after precipitation-hardening at 950°F.

TABLE 11.—Results of Standard Boiling
Nitric Acid Test
Rates in Inches Penetration per Month

Material	Period of 48 Hr.	2nd Period of 48 Hr.	Period of 48 Hr.
Stainless W type			
322: Solution-an-	-		1
nealed	0.0038	0.0067	0.0086
Aged at 950°F	0.0182	0.0305	Discontinued
18-8 type 304 an-			
nealed	0.00154	0.00154	0.0015
18-8 Ti type 321			- 11
annealed	0.00154	0.00154	0.00154
17 Cr type 430 an- nealed	0.00608	0.00608	0.00608

Maximum allowable rate for any one period.
 Maximum mean value for five periods.

A limited amount of preliminary data obtained thus far from service tests, particularly those associated with valve parts operating in hydrogen sulphide gas, sulphur dioxide gas, and hot milk, indicate corrosion resistance equivalent to the 18-8 types of stainless steels.

WELDABILITY

The spot-welding characteristics of the new steel are approximately those of 18-8, which are known to be excellent.

Since the properties of this new material are a function of the chemical composition and heat-treatment, the properties of welded joints will also depend upon these variables. The problem of depositing weld metal of chemical composition similar to that of parent metal, particularly with respect to titanium, was solved by the development of a suitable flux coating for core wire of the age-hardenable parentmetal composition. The special electrodes were subjected to a number of welding tests, results of which are given in Fig. 21, and show that:

- r. The as-welded strength of joints in solution-annealed sheets and plates is about the same as that of the unwelded material; i.e., 100 per cent efficiency.
- 2. The as-welded strength of the joints in aged sheets and plates is about 70 to 80 per cent of that of the unwelded material.
- 3. The strength of joints given post heat-treatment of aging only, was erratic, particularly on specimens on which the weld beads were not ground flush, and varied from the strength value of solution-annealed material to that of fully aged material.
- 4. Solution annealing and aging after welding produced strengths across the welded joints exceeding 90 per cent of the strength of fully aged parent metal. The hardness values shown in columns 8 and 10 of Fig. 21 show that the heat resulting from the deposition of the second bead has an effect on the aging response of the first bead.

In general, the results are very favorable and show that Stainless W can be readily joined by the process of metal arc welding and high joint efficiencies obtained, particularly when solution annealing followed by aging is employed as a post-welding heat-treatment. The need for further investigation of the aging characteristics of single and multipass welds is indicated, and work in this direction is in progress.

Welding by means of the atomic hydrogen and heli-arc methods is now being investigated, and preliminary results have been successful. The new material lends

_		JAN N	-			2	3	4	5	6	7	8	9	10			
PLATE THICKNESS									1	A	60°	_					
	JO	IOLAIT THE						2				1					
			-		1/8" - 3/32"					1/4		71	1/8"				
TEMPER BEFORE WELDING			BEFORE			BEFORE			A 0°F - 1/2 R COOL		950°F-1		160	A 0°F-1/2 IR COOL		950°E-1	
		ST HE			NONE	ANN. &	AGED (950°F. 1/2-HR. AIR- COOLED)	NONE	AGED (950°F. 1/2-HR. AIR- COOLED)	NONE	SOLU- TION ANN. & AGED®	AGED (1025°F, 1/2-HR. AIR- COOLED)	NONE	AGED (1025°) 1/2-HR AIR- COOLES			
	SPECS.	BEAL AS DEPOSI		PSI	131400P 128300P	_		148000B		126500P		162400B 196800B	147700 Z	178500 E			
LE TESTS	TRANS.	GROU FLUS	ND S								158000B 155600W		153800V				
TENSILE	SPECS	BEADS GROUND FLUSH	GROUND -		PSI		191600		159000		129600		173500	156000	173100		
	SPE		EL.2	15%	10%	11.5%	12%	=	21%	=	15%	19%	16%				
	UNWELDED &		0	124200	197000	197000	197000	197000		197800		194400	19780				
			E	11.5	12.0	12.0	12.0	12.0	18 5	13.0	13.0	13.0	13.0				
RDNESS(RC)	8	OND	NO.	1	_		_	_		28	41	43-44	26-27	46-47			
DNES		WELD BE AD		-	-	_	_	-	26-29	41-43	36-43	21-28	42-46				
HAR			NO.		_	_	-	-	_	25-27	38-40	25-33	21-23	22-36			
	8	ASE M	ETAI	L	_	_	-	-	_	29-34	41-43	41-44	27-44	41-4			
	SPECS	W GROU			160B 180B		180W	180B 180N	180W 150W	180B 150B	-	30W	120B	45B 30W-			
ND TESTS	SPECS.	AS	S		BEADS W		180W	_	180P 180W-P	180P	180W-P	180W	-	180W-P	150P	150W-	
BEND	LONG. S	BEA GROU	DNL		180N 180N	-	180P	180P	180P 180P	ISOW	_	ISOW-F	160P	150W			

Fig. 21.—Results of tests of arc-welded new age-hardenable 18-8 steel.

itself more readily to atomic hydrogen welding than does 18-8 Ti, type 321.

SUMMARY

The new age-hardenable 18-8 is a precipitation-hardening ferritic stainless steel of the 18 Cr, 8 Ni type, which can be heattreated in all wrought and cast forms to give a range of mechanical properties similar to that of the cold-worked austenitic 18-8 steels. The variation of mechanical properties is brought about by varying either the solution annealing temperature or the aging temperature and time, or both,

The mechanism of the precipitationhardening reaction involves heating the material to dissolve the hardening constituents in austenite and air cooling to effect a transformation to ferrite, in which the hardening constituents are less soluble than in the austenite. The ferrite is then supersaturated and, on reheating to a moderately elevated temperature, the conventional process of precipitating-hardening occurs. Titanium is the primary element involved in the precipitationhardening reaction.

Since this material is ferritic (magnetic) some of its physical properties correspond more closely to those of 17 Cr. than to those of austenitic 18-8.

The strength of the new material at elevated temperatures (above 600° to 800°F. or 315° to 430°C.) is about the same as that of annealed 18-8. Below this temperature range, the strength is equivalent to that of 18-8 cold-worked to the fullhard condition.

The corrosion resistance of Stainless W is equivalent to that of the 18-8 grades of stainless steel in mild corrosive media.

Stainless W is readily weldable by any of the methods customarily used for stainless steels.

ACKNOWLEDGMENT

The authors wish to acknowledge their appreciation of the assistance and information contributed by Carnegie-Illinois Steel Corporation and its Wood Works, and by United States Steel Corporation Research Laboratory, Wright Field, Fleetwings, Inc., Arcos Corporation, Titanium Alloy Manufacturing Co., as well as that of Messrs. W. D. Brown, R. H. Aborn, J. B. Austin, G. V. Smith, R. F. Miller, J. T. MacKenzie, Jr., C. O. Tarr and C. P. Larrabee.

REFERENCES

1-5. Pilling and Merica: U. S. Patents 2048163 to 2048167.
6. J. A. Duma: Effect of Titanium on Some

Cast Ferrous and Non-ferrous Metals. Trans. Amer. Soc. for Metals (1937) 25,

J. Kroll: Heat Treatable Nickel Alloys. Metals and Alloys (Dec. 1944) 1604-1606.

Talbot: U. S. Patent 2266481.
 C. R. Austin and C. H. Samans: Study of the Metallography and Certain Physical Properties of Alloys of Cobalt, Iron and Titanium. Trans. A.I.M.E.

(1941) 143, 216-227. Wasmuht: Iron-Boron Alloys and 18-8 10. R. Steels with Boron-Their Hardening and Precipitation Hardening. Metals and

Alloys (1932) 105-110.

11. R. Wasmuht: The Precipitation-hardening of Iron by Titanium. Archiv Eisenhuttenwesen (1931) 5, 45-56, 261-266.

12. D. W. Rudorff: Niobium as an Alloying Element in Heat-resisting Steels. Metal-

lurgia (Oct. 1942) 26, 193-196, 224.

13. E. R. Parker: The Development of Alloys for Use at Temperatures above 1000°F.

Trans. Amer. Soc. for Metals (1940)

28, 797-810.

Wever and W. Peter: Precipitation-hardening and Creep Limit of Iron-columbium Alloys and Columbium Alloyed Steels. Archiv Eisenhuttenwesen

(1942) 15, 357-361.
 A Borzdika: Dispersion-hardening of High alloy Gr-Mn-Ti Steel. Metallurg (1940)

15 (10), 31-35.

16. F. R. Hensel: Age-hardening of Austenite.

Trans. A.I.M.E. (1931) 95, 255-283.

17. Titanium and Its Use in Steel. Niagara
Falls, N. Y., 1940. Titanium Alloy
Mfg. Co.

18-19. P. D. Ffield: U. S. Patents 2080367 to 2080368.

20. H. Cornelius: Hardening of Boron Containing Austenitic Chromium-nickel taining Austenitic Chromium-nickel Steels by Tempering after Quenching. Archiv Eisenhuttenwesen (1939) 12, 499

505. 21. H. Bennek and P. Schafmeister: Precipitation-hardening of 18 Cr, 8 Ni Steels by Means of Additions of Be, B or Ti and Effect of These Additions on the Corrosion Resistance. (Brutcher Translation) Archiv Eisenhuttenwesen (1932)

5, 615-620 . Vyáznikov and E. Andreyeva: 18-8 Steel with Increased Carbon Content 22. N. and Ti or Be Additions. Metallurg (1938)

13 (7-8), 40-44.

23. L. B. Pfeil and D. G. Jones: A Contribution to the Study of the Properties of Austenitic Steels. Jnl. Iron and Steel Inst.

(1933) 127, 337-390. 24. R. H. Harrington: The Present Status of Age Hardening. Trans. Amer. Soc. for

Metals (1934) 22, 505-524.

 N. B. Pilling and A. M. Talbot: Dispersion Hardening Alloys of Nickel and Iron-Nickel-Titanium. Amer. Soc. for Metals Preprint (Oct. 1939). 26. H. Witte and H. J. Wallbaum: Thermische

und Roentgenographische Untersuchung in System Eisen-Titan. Zisch. Metall-

kunde (1938) 30, 100.
27. C. R. Austin and G. P. Halliwell: Some Developments in High-temperature Al-

loys in the Nickel-cobalt-iron System.

A.I.M.E. Tech. Pub. 430 (1931). 28. H. H. Uhlig: The Role of Nitrogen in 18-8 Stainless Steel. Trans. Amer. Soc. for

Metals (1942) 30, 947-980.

B. Arness: The Sodium Cyanide Metallographic Etch Test for Revealing 20. W. Precipitated Carbides in the 18-8 Type Stainless Steels. Trans. Amer. Soc. for

Metals (1936) 24, 701-720. 30. G. A. Ellinger: Oxalic Acid as an Electrolytic Etching Reagent for Stainless Steels. Trans. Amer. Soc. for Metals

(1936) 24, 26-45.

Baeyertz: The Use of Chromic Acid in Electrolytic Etching of Iron and Steel. Trans. Amer. Soc. for Metals (1937) 1185-1197.

32. Metals Handbook, 193 Amer. Soc. for Metals. 1939 Edition, 723.

33. Tables of Data on Chemical Compositions,
Physical and Mechanical Properties of Wrought Corrosion Resisting and Heat-Resisting Chromium and Chromiumnickel Steels, Amer. Soc. Test. Mat. 1042).

34. Bulletin ANC-5, Strength of Aircraft Elements; Amendment 1, Oct. 22, 1943 issued by Army-Navy-Civil Committee

on Aircraft Design Criteria. 35. Data from U. S. Army Air Forces, Material Center, Wright Field, Dayton, Ohio. 36. R. Franks and W. O. Binder: Effects of

Low-temperature Heat-treatment on Elastic Properties of Cold-rolled Austenitic Stainless Steels. Trans. A.I.M.E.

37. R F. Miller, W. G. Benz and M. J. Day: Creep Strength, Stability of Micro-structure and Oxidation Resistance of Cr-Mo and 18 Cr - 8 Ni Steels. Trans. Amer. Soc. for Metals (1944) 32, 381-

38. L. C. Bibber and J. Heuschkel: The Spot Weldability of Low Carbon and Other Aircraft Steels. The Welding Jnl. (1943)

22, 616s-632s. J. W. Ragsdal: Railway Rolling Stock. The Book of Stainless Steels, by E. E. 39. E.

Thum, Ed. 2. 694-700. 1935. D. Ffield: Airship Construction. The 40. P. Book of Stainless Steels, by E. E. Thum,

Ed. 2, 679-686, 1935.

41. W. L. Sutton: Stainless for Aircraft Design and Fabrication. Metal Progress (1936)

31, 40-44. Campbell: Building Budd Stainless Steel Railway Cars. Modern Machine 42 H. Shop (1936) 10, 39-48.

43. W. L. Sutton: Aluminum Alloys vs. Stainless Steels for Aircraft. Metal Progress (Jan. 1937) 36-42. N. Krivobok and R. A. Lincoln:

44. V. Austenitic Stainless Alloys. Trans. Amer.

Austentic Stainless Alloys. 17ans. Amer.
Soc. for Metals (1937) 25, 637-689.
45. H. C. Knerr: Heat Treated Alloy Steel,
the Lightest Material of Construction.
Metal Progress (1937) 31, 37-41.
46. H. V. Thaden: Stainless Steel in Aircraft.
Jul. Aeronautical Sciences (1938) 5, 447-

47. C. S. Aitchison, W. Ramberg, L. B. Tuckerman, and H. L. Whittemore: Tensile and Compressive Properties of Some Stainless Steel Sheets. Jnl. of Res., Nat. Bur. Stds., R. P. 1467 (April 1942) 28. 48. R. Franks and W. O. Binder: The Stress Characteristics of Cold-Rolled Strain Austenitic Stainless Steels in Compression as Determined by the Cylinder Test Method. Proc. Amer. Soc. Test.

Mat. (1941) 41, 629-645.
49. T. H. Huff: The Place of Plywood, Plastics and Corrosion Resistant Steel in Aircraft Construction. The Iron Age (1941) 149 (No. 16), 35-40.

50. Moore and Kommers: Univ. Ill. Eng. Expt.

Sta. Bull. (1921) 124, 20.

51. R. M. Brick and A. Phillips: Trans. Amer.
Soc. Metals (1941) 29, 435-469.

52. Unpublished Data of United States Steel

Corporation Research Laboratory, Report No. 360 Jan. 9, 1939.

53. Timken Digest of Steels for High-temperature Service.

54. R. H. Thielemann: Some Effects of Composition and Heat Treatment on the High Temperature Rupture Properties Ferrous Alloys. Proc. Amer. Soc. Test.

Mat. (1940) 40, 788-810. 55. R. F. Miller, G. V. Smith and G. L. Kehl: Influence of Strain Rate on Strength and Type of Failure of Carbon Molybdenum Steel at 850°, 1000° and 1100°F. Trans. Amer. Soc. for Metals (1943) 31 (4), 817-848.

56. Bull. 26, National Tube Co., 1942 Revision. 57. E. C. Bain, R. H. Aborn and J. J. B. Rutherford: The Nature and Prevention of Intergranular Corrosion in Austenitic Stainless Steels. Trans. Amer. Soc. Steel Treat. (June 1933) 21, 481.

58. F. L. LaQue: Proving Ground of Marine

Corrosion. Inco Magazine 19, 1.
P. Larrabee: Corrosion of Steels in

Marine Atmospheres and in Sea Water. Trans. Electrochem. Soc. (1945) 87.
60. Tentative Standard A-262-43T: Recommended Practice for Boiling Nitric Acid Corrosion Test for Corrosion-resist-ing Steels. A.S.T.M. Standards, 1943

DISCUSSION

Supplement.

(J. H. Hollomon presiding)

F. M. WALTERS, JR. *- The authors are to be congratulated on carrying through to a successful conclusion this rather difficult work.

I should like to ask them, first, their opinion as to the precipitating phase and, second, do they have observations on the low-temperature impact of the precipitation-hardening material as quenched and as slowly cooled after the precipitation treatment?

R. SMITH, E. H. WYCHE and W. W. GORR (authors' reply).-With regard to the impact strength at subzero temperatures, the impact resistance is relatively unchanged (on tests

Metallurgist, Naval Research Laboratory, Washington, D. C.

TABLE 12.—Tests on All-weld-metal Specimens

			ength, Lb.	Tensile	Elonga-	Reduc-
Heat Treatments	Test	o.1 Per Cent Offset	o.2 Per Cent Offset	Strength Lb. per Sq. In.	in 2 In., Per Cent	in Area Per Cent
Aged	Transverse All-weld-metal ^b Transverse	60,000	66,750	133,400° 120,500 157,000°	24.0	46.0
Solution-annealed and aged	All-weld-metal ^b Transverse All-weld-metal ^b	69,250	77,500	130,900 182,000 163,000	17.3	23.0

• Heat-treatments for all-weld-metal specimens:
Aged at 1000°F. I hour, air cooled.
Solution anneal, 1600°F. I hour, air cooled, and aged.
1000°F. I hour, air cooled.

• Average of two "505" specimens.
• Average of eight specimens in columns 1, 4, 6, and 9, Fig. 21.
• Average of eight specimens in columns 3, 5, 8, and 10, Fig. 21.
• Average of four specimens in columns 2 and 7, Fig. 21.

made at -110°F. after holding for 100 hr. at temperature), when the aging treatment follows solution annealing at 1300°F.; but when the aging treatment follows a high temperature 1600° to 1950°F. solution anneal the impact strength is reduced to about 40 per cent. These observations were made on quenched material. No low-temperature tests have been made on material slow-cooled from the precipitation treatment. However, the effect of cooling rate from the aging temperature (aged in molten salt) on impact resistance at room temperature is illustrated by Fig. 8 in the paper.

F. M. WALTERS, JR .- I should like to reinforce what the speaker said about the importance of the lack of effect of the rate of cooling on the material from the solution temperature. This is an extremely important factor.

R. D. THOMAS, JR. *- The technical literature is filled with newly proposed alloys, but it is rare that the initial presentation covers so many of the important engineering considerations as this paper does. It is even rarer that the property of weldability is even considered when the new alloy is in the research stage. Usually the welding problems are left to the poor welding engineer after the steel has been shipped to the plant for fabrication. This paper is gratifying evidence that steel metallurgists are awakening to the fact that steel and other alloys are sometimes welded.

We are especially pleased that the authors approached us several years ago to assist in the welding problems connected with this new steel. The development of arc-welding electrodes that would deposit weld metal of the same composition as the Stainless W plates and sheet relied entirely on a method for introducing titanium and aluminum into the weld metal. This was a major problem, which required considerably more research than would be required by the more common stainless electrodes.

Among welding metallurgists it has been generally conceded that titanium and aluminum, whether in the core wire or in the flux covering, are almost completely oxidized in the welding arc; recoveries of these elements have never exceeded 10 per cent. However, by a special deoxidizing practice* making use of a powdered titanium-aluminum alloy in the electrode covering, recoveries as high as 60 per cent of the titanium added have been obtained.

In the course of our investigation to produce a weld metal that will precipitation-harden to give high-strength stainless welds, several allweld-metal tensile specimens were produced, using the same lot of electrodes the authors used for their transverse specimens. Somewhat lower strengths were obtained in the all-weldmetal tests, as shown in Table 12.

Vice President and Director of Research and Engineering, Arcos Corporation, Philadelphia, Pennsylvania.

[·] Patent applied for.

The all-weld-metal tests indicate the strength that may be obtained in heavy multipass welds. The authors quite justifiably point out the need for further investigation of the aging characteristics of weld metal. Some of the problems requiring additional work are the investigation of: (1) the composition balance for weld metal. particularly with respect to titanium content; (2) the uniformity of microstructure and of composition of the weld metal within each bead; (3) the heat-treatment required to achieve the best properties in the weld metal.

R. SMITH, E. H. WYCHE and W. W. GORR.— Early in the work on this new steel the authors realized that weldability would be a pertinent problem in many applications and therefore proceeded to investigate the weldability. Mr. Thomas' comments dealing with future work are well taken and work is proceeding along these lines. The authors are grateful for the cooperation given by Mr. Thomas and wish to congratulate him on his work of improving the titanium recovery of the arcwelding electrode.

Constitution of Commercial Low-carbon Iron-silicon Alloys

BY R. L. RICKETT,* MEMBER AND N. C. FICK,* JUNIOR MEMBER A.I.M.E. (Chicago Meeting, February 1946)

DESPITE the large volume of literature on alloys of iron and silicon,1 there is little published information dealing specifically with the constitution, at various temperatures, of the alloys containing less than o.10 per cent carbon and from 0.5 to 4.5 per cent silicon that are used extensively in the electrical industry. Because such information was needed by those engaged in the production of these alloys in sheet and strip form, the constitution was determined of a series of commercial silicon steels containing 0.05 to 0.08 per cent carbon and 0.20 to 4.1 per cent silicon. over the temperature range 1300° to 2500°F. These alloys were all from regular production heats and of commercial quality. The results of the tests are given in Fig. 1 and for comparison the constitution diagram of iron-silicon alloys with o.o1 to o.o2 per cent carbon, taken from the literature, is also presented.

MATERIAL AND PROCEDURE

All steels were hot-rolled to a thickness of 0.060 to 0.080 in. and used in this condition. Their chemical compositions, including over-all check analysis, and "center" analysis for carbon and silicon. are given in Table 1. The so-called center analysis was determined on samples pickled to remove the outer surface and leave only the center third of the gauge thickness-the portion of the sample on which metallographic ratings were based. In most, but not all, of the alloys, slightly higher carbon was found at the center than when the whole strip was sampled; the two methods of sampling show relatively little difference in silicon. Two of the steels, A and E, contain relatively high phosphorus, while I and K are somewhat higher in manganese than the others.

TABLE 1.—Composition of Materials Used

Desig-	Cente		Over-all Check Analysis, Per Cent						
nation	С	Si	С	Mn	P	S	Si		
A	0.071	0.20	0.064	0.26	0.052	0.023	0.20		
ABCDEFG			0.073		0.020	0.022	0.58		
C			0.048		<0.010	0.018	1.19		
D			0.074			0.015			
E			0.065			0.012			
F			0.052	0.28	<0.010	0.026	1.60		
	0.072								
H			0.052		<0.010				
I			0.051			0.013			
J_			0.067		0.008	0.011	3.50		
K	0.064	4.13	0.062	0.35	0.013	0.010	4.0		

Portion of sheet used in determination of constitution diagram.

The procedure consisted essentially of heating specimens (about 1/16 by 3/8 by 34 in.), protected from oxidation or change in carbon content, at a temperature in the desired range and for a selected period, after which they were quenched in iced brine; the degree of transformation that had then occurred was determined by metallographic examination. The soaking periods were selected after preliminary investigation had shown that a con-

Manuscript received at the office of the Institute Aug. 24, 1945. Issued as T.P. 1966 in Metals Technology, February 1946.

* Research Laboratory, United States Steel Corporation, Kearny, N. J.; N. C. Fick is now with Battelle Memorial Institute, Columbus, Ohio.

¹ References are at the end of the paper.

siderably longer period resulted in no observable further change in microstructure. The soaking period used and the means employed to minimize oxidation or change in carbon content are listed in Table 2.

TABLE 2.-Procedure

Tempera- ture, Range, Deg. F.	Time at Tem- pera- ture, Hr.	Protection of Samples
1300-1550	2	Immersed in deoxidized lead bath Samples copper plated and em-
1850-2500	1/2	bedded in coke dust Sealed in evacuated fused silica bombs

Since the diagram is intended to show the constituents present during mill processing, and heat-treatment of commercial silicon steels, no attempt was made to ensure the attainment of true equilibrium.

RESULTS

Diagram for Iron-silicon Alloys Containing 0.05 to 0.08 Per Cent Carbon

The constitution diagram derived as a result of this investigation (Fig. 1) shows the constituents present when iron-silicon alloys of commercial purity containing 0.05 to 0.08 per cent carbon and up to approximately 4.25 per cent silicon are held at a temperature in the range 1300° to 2700°F. for a substantial period of time, as in annealing. The diagram also indicates the direction in which changes in the constituents may occur on heating or cooling, but gives no information as to the rate at which such changes proceed. The principal features of the diagram will now be considered briefly.

The Ferrite + Carbide + Austenite Field. Ferrite, carbide and austenite may exist simultaneously within a narrow temperature range. In Fig. 1 circles are used to

indicate temperatures at which only carbide and ferrite were found, half-shaded circles those at which the three phases were found to exist, and solid circles those found to be above the three-phase region. The width of the three-phase band was not determined precisely, but appears to be of the order of 10° to 15°F. The effect of increasing silicon is to raise the temperatures bounding this field.

The Ferrite + Austenite Field.—Above this three-phase field is a region in which ferrite and austenite coexist. Dotted lines denoting approximately 10, 25 and 50 per cent austenite are shown in this field; the significance of these lines is obvious. The part of this two-phase field to the right of the vertical line corresponding to approximately 4.25 per cent silicon was not determined because higher silicon alloys containing 0.05 to 0.08 per cent carbon were not available.

The Delta Field .- As temperature increases, austenite eventually disappears, leaving the single delta phase or "hightemperature ferrite." Because of the high temperatures involved, the experimental determination of the lower boundary of this field is the least satisfactory part of the diagram. In Fig. 1, a heavy dashed curve is drawn from a value for fairly pure ironcarbon alloys, taken from the literature,2 through the experimentally determined points (solid triangles). No carbides were found in this region, indicating that delta ferrite at these temperatures is capable of dissolving at least 0.05 to 0.08 per cent carbon.

The Austenite Field.—For all alloys within the carbon range under consideration and containing less than about 2.3 per cent silicon, there is a temperature range within which the structure is entirely austenitic. The experimentally determined points corresponding to the boundary of this field are shown as crosses in Fig. 1; the upper limiting value at zero silicon, taken from published work on the iron-

carbon diagram² corresponds to 0.06 to 0.07 per cent carbon; the lower value was obtained by extrapolation. This extrapolated value is slightly lower than that for

vertical line corresponding to the silicon content of the alloy. Fig. 2 illustrates the constituents that occur in three representative alloys, containing respectively 1.2,

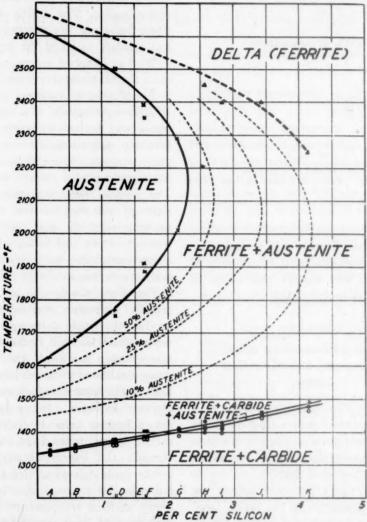


FIG. 1.—CONSTITUTION DIAGRAM OF IRON-SILICON ALLOYS WITH 0.05 TO 0.08 PER CENT CARBON.

very pure iron-carbon alloys,³ as might be expected in commercial plain carbon steels containing manganese and small amounts of other elements that tend to lower the Ae₃ temperature.

Effect of Temperature on Microstructure. The structural constituents of any 0.05 to 0.08 per cent carbon, iron-silicon alloy at temperatures within the range covered may be found from Fig. 1 by following a

2.1 and 2.8 per cent silicon, in the temperature range 1300° to 2400°F. In the 1.2 per cent silicon alloy, austenite first forms at about 1370°F., then increases in amount as temperature increases up to 1770°F.; from 1770° to 2400°F., the structure is entirely austenitic. Austenite begins to appear in the 2.1 per cent silicon alloy at a slightly higher temperature, 1400°F., and the structure is completely austenitic

in the range 2000° to 2300°F. Above 2300°F., ferrite ("delta") again appears and the amount of austenite decreases as temperature increases. Figs. 3 and 4

carbide particles, as illustrated in Figs. 3b, 3c and 3d. Fig. 5 shows the distribution of austenite in several representative alloys when heated to a temperature at which a

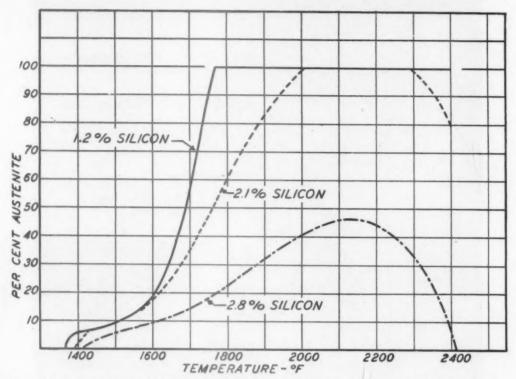


FIG. 2.—PERCENTAGE OF AUSTENITE VS. TEMPERATURE FOR STEELS OF THREE SILICON CONTENTS.

show the structures observed in this 2.1 per cent silicon alloy after quenching from various temperatures. In the 2.8 per cent silicon alloy (Fig. 2), austenite first forms at about 1420°F. and increases in amount in the range 1420° to 2150°F.; in this alloy the maximum amount of austenite that may exist is some 45 per cent, and as temperature increases above 2150°F. the amount of austenite decreases until the alloy is again entirely ferritic (delta), at approximately 2400°F.

Distribution of Constituents.—In the hotrolled condition, nearly all the alloys exhibit a nonuniform distribution of carbide particles, or of pearlite in some instances, as shown in Fig. 3a. The first areas of austenite to form on heating occur in the bands that originally contained relatively small amount of austenite exists. Heating to still higher temperature tends to bring about a more uniform distribution of constituents but may not completely eliminate "banding." This banding may be a factor of considerable practical importance, since the presence of strings or bands of carbide particles or of austenite retards recrystallization and grain growth of ferrite during annealing. It should be emphasized, however, that banding is not present to nearly the same extent in cold-reduced or in annealed sheet or strip as in the hot-rolled condition as illustrated here.

Diagram for Iron-silicon Alloys with Lower Carbon.—Fig. 6 shows our experimental diagram for alloys with 0.05 to 0.08 per cent carbon, and a diagram for

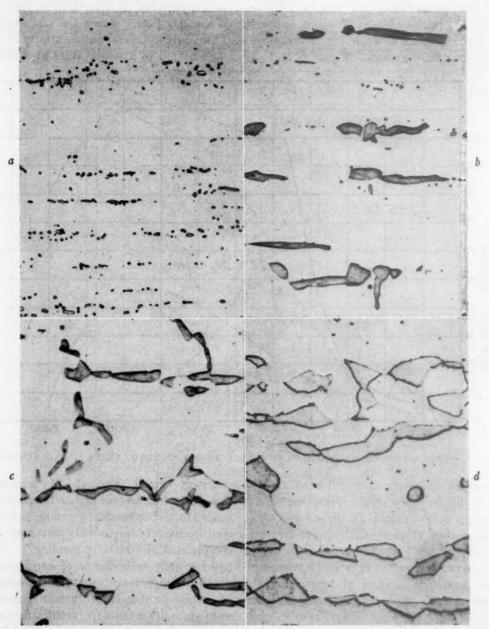


Fig. 3.—Effect of temperature (1390° to 1700°F.) on microstructure of a 2.1 per cent silicon steel (steel G). × 1000.

Any austenite present at the indicated temperature has transformed to martensite on

quenching.

a. 1390°F. Ferrite + carbide.
b. 1400°F. Ferrite + carbide + austenite.
c. 1410°F. Ferrite + austenite.
d. 1700°F. Ferrite + austenite.

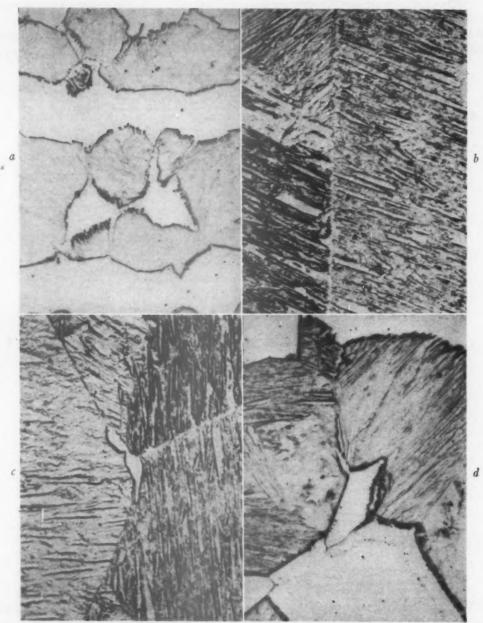


Fig. 4.—Effect of temperature (1900° to 2400°F.) on microstructure of a 2.1 per cent silicon steel (steel G). × 1000.

Austenite present at the indicated temperature has transformed to martensite on quenching.

a. 1900°F. Ferrite + austenite.
b. 2010°-2290°F. Austenite.
c. 2300°F. Austenite + ferrite (delta).
d. 2400°F. Austenite + ferrite (delta).

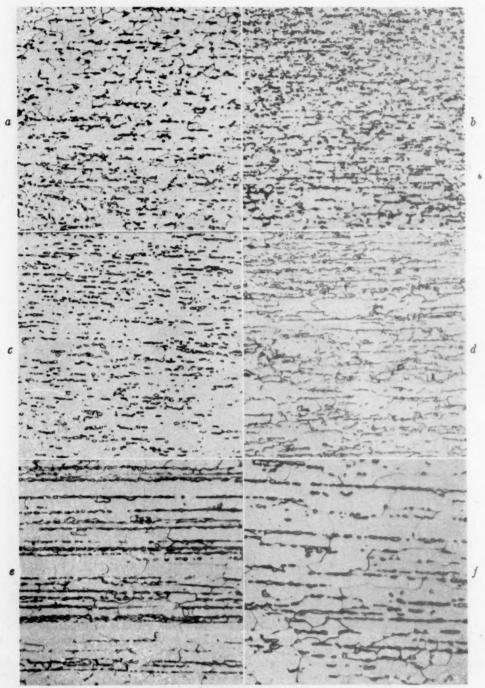


FIG. 5.—BANDING IN REPRESENTATIVE COMMERCIAL IRON-SILICON ALLOYS IN HOT-ROLLED CONDI-

TION. X 100.

Specimens heated to a suitable temperature to form a small amount of austenite then quenched.

- a. Steel A, 0.20 per cent Si.
 b. Steel B, 0.58 per cent Si.
 c. Steel D, 1.2 per cent Si.

- d. Steel G, 2.1 per cent Si.
 e. Steel I, 2.8 per cent Si.
 f. Steel K. 4.1 per cent Si.

alloys with 0.01 to 0.02 per cent carbon taken from the literature. Comparison indicates that this increase in carbon enlarges the austenite field to only a

difficult to estimate. In the present investigation, two alloys containing 44 and 4.8 per cent silicon with 0.02 to 0.03 per cent carbon were found to be entirely

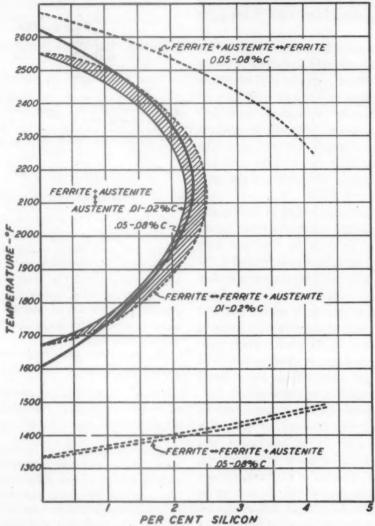


Fig. 6.—Constitution diagram of iron-silicon alloys with 0.01 to 0.02 per cent and 0.05 to 0.08 per cent carbon.

moderate extent, but very markedly extends the limits of the two-phase, austenite + ferrite, region. For alloys containing carbon in amount intermediate between those to which these diagrams apply, a fairly close approximation of the austenite-field boundary may be made. The other boundary of the two-phase region (austenite + ferrite), however, is

ferritic at all temperatures up to 2400°F.; these silicon contents are, therefore, to the right of the ferrite + austenite field for alloys with 0.02 to 0.03 per cent carbon.

SUMMARY

The results on commercial silicon steels presented in the foregoing pages may be summarized as follows:

- 1. The A₁ temperature, or lowest temperature at which any austenite can form, increases as silicon increases and as carbon decreases. In 0.05 to 0.08 per cent carbon alloys, it is approximately 1335°F. for o per cent silicon and 1480°F. for 4 per cent silicon.
- 2. The temperature range within which the structure is entirely austenitic becomes narrower as silicon increases and as carbon decreases; alloys containing 0.05 to 0.08 per cent carbon are not entirely austenitic at any temperature if the silicon content is over approximately 2.3 per cent; the corresponding limit for o.o1 to o.o2 per cent carbon alloys is about 2.2 per cent
- 3. Alloys sufficiently high in silicon and low in carbon are entirely ferritic at all temperatures. In o.o1 to o.o2 per cent carbon alloys, no austenite is formed if the silicon content is more than approximately 2.5 per cent; the corresponding limit in 0.05 to 0.08 per cent alloys was not determined, but is considerably over 4 per cent silicon. Commercial alloys containing 0.02 to 0.03 per cent carbon and 4.4 to 4.8 per cent silicon were found to be ferritic at all temperatures.
- 4. In alloys that are not ferritic at all temperatures, the amount of austenite present increases to a maximum and then decreases as temperature increases. The maximum amount of austenite formed may be 100 per cent or less, depending on the composition. In general, this maximum decreases as silicon content increases or as carbon content decreases.

ACKNOWLEDGMENTS

The authors wish to express their indebtedness to Mr. E. S. Davenport, under whose direction this investigation was carried on, and to Mr. S. C. Snyder, and others in Carnegie-Illinois Steel Corporation, who supplied the steels and offered helpful comments and suggestions during the course of the work. They also appreciate

the aid of Mr. M. H. Pakkala, now of Carnegie-Illinois Steel Corporation, who conducted some of the preliminary work while at the United States Steel Corporation Research Laboratory.

REFERENCES

- I Greiner, Marsh and Stoughton: Alloys of Iron and Silicon. New McGraw-Hill Book Co. York, 1933.
- 2. Ruer and Klesper, as reported by Epstein in Alloys of Iron and Carbon, I, 53. New York, 1936 McGraw-Hill Book Co. 3. Mehl and Wells: Trans. A.I.M.E. (1937)
- 125, 429 469. 4. Oberhoffer and Kreutzer: Archiv Eisenhuttenwesen (1928-1929) 2, 449, 456.

DISCUSSION

(Howard Scott presiding)

- C. ZENER.*—The writer has recently outlined a method for computing the constitution of ternary and higher order medium alloy steels from the empirical data contained in the constitution of the binary systems, and W. A. West⁶ has successfully applied this method to a number of systems. The present paper provides an opportunity for testing this method once again.
- The equations that determine the alphagamma equilibrium in the Fe-Si-C system are

$$C_c^{\alpha}/C_c^{\gamma} = 3e^{\Delta Gc/RT}$$
 [1]

$$C_{\rm Si}^{\alpha}/C_{\rm Si}^{\gamma} = e^{\Delta G_{\rm Si}/RT}$$
 [2]

$$(C_e^{\gamma} - C_e^{\alpha}) - (C_{8i}^{\alpha} - C_{8i}^{\gamma}) = \Delta G_{Fe}/RT \quad [3]$$

In these equations C refers to atomic concentrations, ΔG to standard free-energy changes;* suffixes refer to phases; subscripts to elements. The standard free-energy change ΔG_{F_0} is given as a function of temperature in Table A-1 of reference 5, while ΔG_e and ΔG_{8i} , determined from the iron-carbon and iron-silicon systems, respectively, are given in Tables 2 and 1 of this reference as -8100 and 475 cal. per mol.

The solution of Eqs. 1 to 3 for the alpha and

^{*} Professor of Metallurgy, Institute for the Study of Metals, The University of Chicago.

6 C. Zener: Equilibrium Relations in Medium-

alloy Steels. This volume, page 513.

W. A. West: Phase Boundaries in Medium-Steels. This volume, page 535.

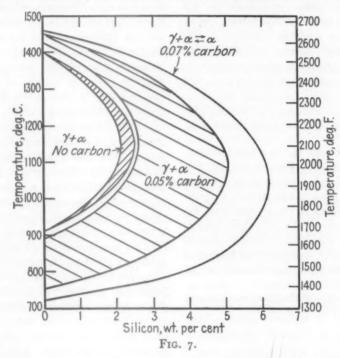
This definition is slightly modified for AGc.

gamma boundaries in the Fe-Si plane may be written in the form

$$X_{8i}^{\alpha} = \{X_{8i}^{\alpha}\}_0 + a_c X_c$$
 [4]

$$X_{\mathbf{S}\mathbf{i}}^{\gamma} = \{X_{\mathbf{S}\mathbf{i}}^{\gamma}\}_{0} + b_{c}X_{c}$$
 [5]

where X refers to concentrations in weight per cent, and the first term in the right member of was chosen so as to obtain agreement for the binary Fe-Si system. Boundaries are also given for a carbon concentration of 0.05 per cent, since this is the approximate carbon concentration in the lower silicon steels investigated by Rickett and Fick, and the alpha boundary is given for a carbon concentration of 0.07 per



each equation refers to the corresponding boundary in the pure Fe-Si system. From the free-energy changes given in reference 5, the quantities $\{X_{\mathbf{S}\mathbf{i}}^{\alpha}\}_{0}$, $\{X_{\mathbf{S}\mathbf{i}}^{\gamma}\}_{0}$, a_{c} and b_{c} have been computed as a function of temperature, and are given in Table 3.

Several examples are given in Fig. 7 of the

cent, corresponding to the carbon concentration of their higher silicon steels. The gamma boundary for the 0.05 per cent carbon steel, and the alpha boundary for the 0.07 per cent steel, are seen to coincide almost exactly with those determined experimentally by Rickett and Fick.

TABLE 3.—Quantities for Computation of Boundaries in Fe-Si-C System

T. (Deg. C.)	700	800	910	1000	1100	1200	1300	1400	1500
$\{X \mathrm{Si}^{\alpha}\}_{0}$. $\{X \mathrm{Si}^{\lambda}\}_{0}$. b_{ϵ} .	-11.35 - 9.1 143 8.1	-3.38 -2.71 105 8.7	0 0 79.0 9.6	1.59 1.35 64.2 10.3	2.44 2.02 53.0 10.5	2.38 2.02 44.0 10.7	1.57 1.33 36.2 10.8	0 0 32.7 10.9	-3.57 -3.1 28.2 11.0

boundaries according to Eqs. 4 and 5, and to Table 3. The boundaries are given for zero carbon concentration. These should agree, of course with the corresponding empirical boundaries, since the free-energy change $\Delta G_{\rm Bi}$

The lower portion of the theoretical alpha boundary cannot strictly be compared with experiment, for below this boundary cementite is present. However, the equilibrium relation between ferrite and cementite is such (Fig. 11 of ref. 7) that with carbon concentrations between 0.05 and 0.07 all the cementite would go into solution between 700° and 800°C. It is to be anticipated therefore that the alpha boundary will be essentially unaltered by the existence of the cementite phase.

The close agreement between the computed and experimental phase boundaries in the Fe-Si-C system is evidence that in this system the laws of dilute solution, assumed in the theory, are essentially correct. It is anticipated that in further determinations of constitutions in medium alloy steels experimental work will be greatly shortened by appropriate use of the method outlined in reference 5 of utilizing past experimental observations upon binary systems.

R. L. RICKETT and N. C. FICK (authors' reply).—We share Dr. Zener's gratification that it is possible to predict, even approximately, some portions of the ternary diagram from binary diagrams of the components. We cannot agree, however, that the agreement is sufficiently good to indicate that the amount of experimental work necessary to determine a diagram would be materially lessened by use

of his method or that much reliance could be placed on a predicted diagram in the absence of experimental confirmation.

In his iron-carbon-silicon diagram, a marked difference in the alpha-alpha + gamma (Ae₁) boundary for 0.05 per cent and for 0.07 per cent carbon Fe-Si alloys is shown; whereas we found no such difference experimentally. These boundaries are drawn by Zener to indicate a marked difference in Ae, for zero silicon with change in carbon from 0.05 to 0.07 per cent, although the usually accepted iron-carbon diagram shows no change in Ae, within this carbon range. In view of this marked variation in the calculated alpha-alpha +- gamma boundary with change in carbon content, it may be something of a coincidence that one of them agrees with the experimentally determined boundary. Dr. Zener states that at carbon concentrations between 0.05 and 0.07 per cent all the cementite would go into solution between 700° and 800°C. (1200° to 1470°F.); this is contrary to our observations on the 0.05 to 0.08 per cent carbon alloys used in our investigation, in all of which cementite was observed up to the beginning of the alpha-gamma transformation, yet this may in some instances be due to failure to reach equilibrium.

⁷ C. Zener: Kinetics of the Decomposition of Austenite. This volume, page 550.

Effect of Original Orientation on Orientation Changes during Recrystallization in Silicon Ferrite

By C. G. DUNN,* MEMBER A.I.M.E.

(Chicago Meeting, February 1946)

NUCLEI that are formed during the recrystallization of a grain following plastic deformation generally have orientations that differ from the original. This aspect of recrystallization may be described in terms of orientation changes. It was shown previously, in an investigation on recrystallization in silicon ferrite, that the observed orientation changes were highly improbable on a chance basis, and that some mechanism must be involved. Analysis showed that the data could be satisfactorily classified into the smaller of two subclasses of the 36 third-order twin transformations.

No attempt was made at that time to classify the data within the special class of 12 third-order twin transformations, although results did indicate a greater probability for some of them to occur. A classification of this type would be more valuable, of course, with more data on orientation changes per old deformed grain. The present work fulfills this condition to some degree and also extends the scope of the investigation to include the effects of original orientation and the amount of plastic deformation.

The effect of original orientation is of

considerable interest because of the known effects of orientation on plastic deformation, particularly with regard to degree of fragmentation and the formation of deformation bands, and because the orientations produced by deformation should influence the orientations obtained through recrystallization. Barrett and Levenson² reported that single crystals of iron deformed in the range 82 to 07 per cent could be put into three general classes; namely, crystals in class 1 maintained a reasonably sharp single orientation, those in class 2 transformed into two distinct orientations, and those in class 3 changed into a large number of major and minor orientations. Something similar would be expected for silicon ferrite crystals, and verification of this for a few cases of types class I and class 2 deformation has been reported elsewhere3 for single crystals of silicon ferrite cold-rolled in the range 10 to 20 per cent. As an example of class 2 deformation, it was shown that a crystal of silicon ferrite cold-rolled in a [110] plane in a <100> direction developed two layers, or deformation bands differing in orientation. When this happens it is possible to etch away one band and leave a single structure for use in studying the orientation changes that occur during recrystallization.

When preferred crystal orientations are obtained in recrystallization, it is not particularly necessary to evaluate groups of common orientation, as was done previously (ref. 1, Table 6); but an

Manuscript received at the office of the Institute Nov. 21, 1945. Issued as T.P. 1990 in METALS TECHNOLOGY. August 1946.

METALS TECHNOLOGY, August 1946.

* Research Physicist, General Electric Co.,
Pittsfield, Massachusetts.

Pittsfield, Massachusetts.

† All third-order twin transformations (36) comprise a C class. The two subclasses are C₃ with 12 members and C₄ with 24 members. 1.4

¹ References are at the end of the paper.

evaluation along the lines indicated in the Appendix of this paper is very helpful in showing how far the results depart from those expected with orientation changes occurring in a haphazard manner. left by the wheel, the narrow surfaces of each crystal were first surface-ground with grit No. 180, then etched for 3 min. in a 4 to 1 aqueous solution of nitric acid, while the large flat surfaces were protected

TABLE 1.—Chemical Compositions

Specimens	Composition, Per Cent								
Specimens	Si	С	P	S	Mn	Al	Cu	Sn	
E and F series. G sample. H sample.	3.45 3.55 3.65	0.003 0.004 0.002	0.008 0.011 0.010	0.009 0.008 0.007	0.075 0.045 0.036	0.03I trace trace	0.072 0.080 0.028	trace 0.014 0.009	

The present investigation, a sequel to that described in the former paper, is a continuation of the work on recrystallization in silicon ferrite extended to include five original orientations and higher percentages of cold reduction—351 recrystallization nuclei are involved. It is the purpose of this paper to present the data on changes of orientation due to recrystallization and to discuss them from an analytical viewpoint.

PREPARATION OF SPECIMENS AND EXPERIMENTAL PROCEDURE

Materials used in the present investigation were obtained from heats of steel made by the Allegheny-Ludlum Steel Corporation. Final processing and heattreating were done at the Pittsfield Works' Laboratory of the General Electric Co., to give fairly large grains of various orientations. Designation of specimens and chemical compositions are given in Table 1.

All crystals were as thick as the sheets, which were 0.007 in. for the E series, 0.012 in. for the F series, and 0.014 in. for the G and H samples. Sheet specimens were deformed on a mill with 8-in. diameter rolls. Single-crystal samples were then obtained for annealing by either of two methods. In one method, an abrasive cutoff wheel was used. To remove strains

with acid-resistant lacquer. In the other method, nitric acid alone made the cut, acid-resisting lacquer protecting the large flat surfaces.

To designate the original orientations and to aid in the analysis of results, it will be convenient to employ the term "state" as follows: If all cube poles of orientations A1, A2, A3, etc. lie within alpha radians of the cube poles of an orientation A, the orientations A₁, A₂, A₂, and so on fall into a state A of size alpha. An orientation is represented in a hemisphere or in a stereographic projection plot by three points mutually 90° apart; a state is represented by three circular areas each of radius alpha with centers mutually 90° apart. The location of these centers may be used to designate the position or orientation of the state.

Data on the original orientations, on the amount of cold-rolling, on lattice rotation, and on crystal distortion are given in Table 2. The orientation of the state into which the original orientation of each crystal falls is given in terms of two directions; namely, the pole of a specified plane (designated by N) normal to the plane of rolling and a crystallographic direction, which is parallel to the rolling direction (R.D.). Departure of the corresponding crystallographic directions of each crystal from these two directions

is given in separate columns in the table. The size of each state is also given. Axes of rotation and of bending are given in the last two columns (C.D. is a direction 90°

Of the 10 crystals listed in Table 2, only crystal F₅C developed a few observable Neumann bands. In general, the formation of visible Neumann bands

TABLE 2.—Orientations Prior to Cold-rolling and the Amount of Plastic Deformation

Specimen	State			Angle of	Angle of	Reduc-	Lattice	Laue Spot
	N	R.D.	Size, Deg.	Plane from N. Deg.	Direction from R.D., Deg.	tion, Per Cent	Rotation and Axis	Distortion and Axes
E4A	(111)	[112]	3	23/2	3	19		
E4C	(111)	[112]	141/2	13	13	19	6°:C.D.	6°:C.D. and others
E4B1	(100)	[011]	II	II	8	19	3-4°: C.D.	12°: C.D.
E4B ₂ G4D	(110)	1001	11	II	5	19	3-4°: (N-C.D.)	100:3
G4D	(110)	[IIIO]	0	31/2	5	10	2": [8°: R.D. and others
H ₄ A	(110)	[110]	3	21/2	I	10	6°: R.D.	8°: R.D. and others
F5A	(110)	[001]	12	10	63/2	20)	
F5A F5B F5C F5D	(110)	100	7 7	5 0	03/2	20	7-10°: C.D.	12-14°: C.D.
F5D	(110)	001	,	0		20		

to both N and R.D.). These axes pertain to the major changes only.

During the cold-rolling operation, it was noted that E4B1 and E4C reduced in thickness with about equal ease, that E4B2 (part of the same crystal from which E₄B₁ was obtained) required more passes through the mill, and that E4A was relatively difficult to cold-reduce. Although direct comparison of these crystals with the G, H and F crystals was not made, it seemed that crystals of the F5 type were easiest to cold-reduce and that those of the G4 or H4 type were the most difficult. Crystals with (110) [110] orientations have a tendency to deform laterally (for example, a single crystal in the form of a rectangle ½ in. wide—not represented by any of the samples described hereindeformed more sideways than it did in the direction of rolling under a cold reduction of 10 per cent). This tendency for lateral extension was held in check as much as possible for samples G4D and H4A by leaving the crystals in the polycrystalline sheet during the deformation process; however, some extension sideward was unavoidable.

is accompanied by a noticeable crying or tearing sound (this is a well-known occurrence for twin formation in metals); but all samples except F₅ of the present group deformed quietly.

Following the plastic deformation, singlecrystal samples were prepared as described previously. Crystals forming the F5 series, however, were left in the polycrystalline sheet. Laue diffraction patterns were taken with tungsten radiation prior to annealing. X-ray patterns indicated that crystal F5A was composed of a single part, whereas crystal F5C was composed of two parts, presumably platelike, as described elsewhere.3 The polycrystalline sample was then etched to a thickness of 0.004 to 0.005 in. from one side only. An X-ray re-examination indicated that the etching treatment had removed one of the doublets in F5C. Laue photographs of crystals F5A, F5B, and F5D likewise showed single lattice structures, each highly strained. Crystals E4C, E4A, E4B₁, E4B₂, and G4D were annealed 4 hr. at 1175°C. in pure, dry hydrogen. Complete recrystallization occurred in all. The grains in E₄A were too small to X-ray conveniently; so this sample was discarded. The other samples were satisfactory. Crystal H₄A was divided into several parts and these samples were

enough nuclei for the present investigation. Seventy-eight nuclei were selected from grains A, B, C, and D as follows: 34 from grain A, 15 from grain B, 17 from grain C, and 12 from grain D.

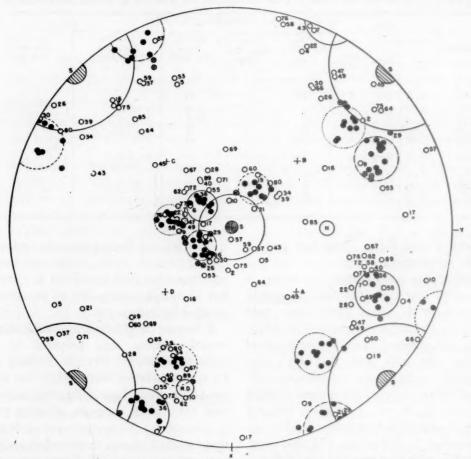


Fig. 1.—Stereographic projection plot of cube poles of grain E4C (at position S) and the 90 new grains obtained by recrystallization. The four highly populated states are each $7\frac{1}{2}^{\circ}$ in size.

annealed for various periods of time at 750°C. Two parts annealed for 30 and 90 min., respectively, produced a total of 41 nuclei in a matrix that had recrystallized to the extent of 30 to 70 per cent. Grains Nos. 29 and 30 (two parts) formed a combination with serrated boundaries that suggested a twinned structure. The F5 sample was annealed for 15 min. at 800°C., a time sufficient to produce only a small amount of recrystallization but

Orientations of old and new grains were determined from transmission Laue diffraction patterns. Because of distortion, the orientation of an unrecrystallized grain has a range of values, and this range is represented in the stereographic projection plots by shaded areas. All orientations are given in terms of three {100} poles mutually 90° apart, the accuracy in general being to within one degree for the recrystallized grains.

ANALYSES AND RESULTS

After the orientations of old and new grains were plotted in stereographic projection form, each group was rotated with the aid of a Wulff net until the old grain tion of the four old grains has not been included in Fig. 6; otherwise these orientations coincide at position S. The directions N and R.D. are different for each grain and appear unidentified in the figure.

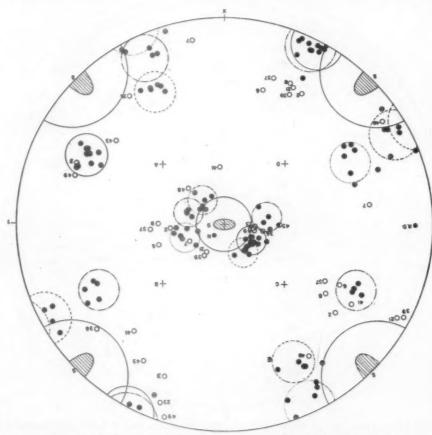


FIG. 2.—Stereographic projection plot of cube poles of grain E4B₁ (at position S) and the 52 new grains obtained by recrystallization.

Six orientation states are indicated.

coincided with the fourfold symmetry position marked S in the diagrams. Plots for E4C, E4B₁, E4B₂, G4D, H4A, and all the F5 samples appear in Figs. 1, 2, 3, 4, 5, and 6, respectively. The direction normal to the plane of rolling N and the rolling direction R.D. are indicated in the diagrams. In Fig. 6 the orientations of the recrystallized grains of F5A have numbers 1 to 34; those of F5B, 35 to 49; F5D, 50 to 61; and F5C, 62 to 78. Because of some differences, the spread in orienta-

Certain orientations occur more often than others in each plot and these form preferred crystal orientations. Most of these common orientations (excluding any that are present in Fig. 6) have been associated with orientation states, each $7\frac{1}{2}$ ° in size, as indicated in the figures. Orientations that fall within such states are indicated in general by black dots without numbers. Orientations falling near a state are also left unnumbered but have a small circled cross. In connection

with analyses that involve comparison with third-order twins, these unnumbered orientations all belong to a C₃ classification, of which more will be said later.

given value of alpha gives the total number of orientations that fall into the C class. A similar statement applies to the D class. The A, B, C, and D classes, however, are

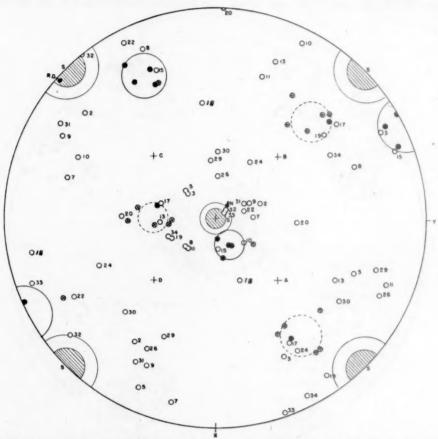


Fig. 3.— Stereographic projection plot of cube poles of grain E_4B_2 (at position S) and the 34 New grains obtained by recrystallization.

The data of orientations were then analyzed, using nets of first, second, third. and fourth-order twin orientations. To obtain data independent of the method of plotting orientations in pole figures, such results must be reclassified according to nine general classes composed of one first-order, one second-order, two third-order and five fourth-order twin relationships. 1.4 Results so classified are listed in Table 3 using four values of alpha. An orientation is placed within the C class according to best fit. Therefore, the sum of the numbers in the columns headed C₃ and C₄ for a

independent. Consequently, some orientations listed under C₃ may also be listed under B, because these orientations are near each other. If an orientation does not belong to an A, B, C, or D class, it is put into a miscellaneous class called M. The number of orientations listed under M naturally increases as alpha decreases.

Values for Δ_n^q , the difference in orientation between old and new grains, were also obtained. Averaged values will be given later. Minimum values, however, appear in Figs. 1, 2, 3, 4 and 5 in the form of large circles concentric with S. These

have radii of 17°, 15°, 9°, 20½° and 19° for E4C, E4B₁, E4B₂, G4D and H4A, respectively. No new orientation can be found with all three cube poles within these circles.

shown in Fig. 6 with alpha equal to 10°) and also among the 12 members of a special γ_3 class. It is important to note that each member of the C_3 class may be obtained from the orientation called S by a rotation

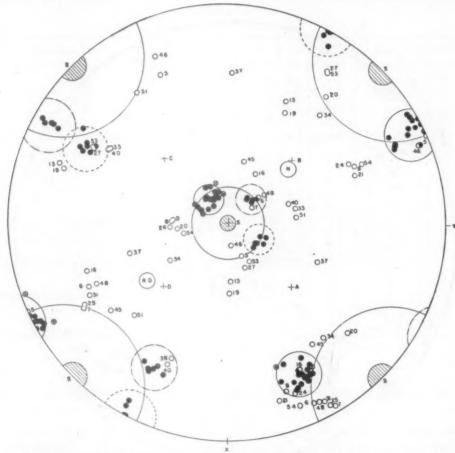


Fig. 4.—Stereographic projection plot of cube poles of grain G_4D (at position S) and the 56 new grains obtained by recrystallization.

The results obtained for alpha equal to 10°, given in Table 3, were converted into percentages and the corresponding distribution assembled into Table 4. At the bottom of this table appear the results of all samples. These results and corresponding ones obtained from the data in the previous report¹ are shown in the bar graph in Fig. 7.

It was decided to obtain the distribution of orientations among the 12 members of the C₃ class (these 12 members are

of $31^{\circ}36'$ about the proper face diagonal direction (<110> directions are marked by X, Y, A, B, C, and D in the figures). Because of clockwise and counterclockwise rotations, each axis gives rise to two third-order twin orientations. Each member of the γ_3 class may be formed similarly, the amount of rotation, however, being set at 25° for a reason that will appear later. Results are given in Table 5, with each state correlated with the axis it has in common with orientation S.

Grains 29 and 30 in specimen H₄A (see Fig. 5) were found to be twins and therefore not examples of independent nuclei. In general dependent nuclei should be eliminated from the present types of

ANALYSIS AND DISCUSSION

In the section on analyses and results, preferred crystal orientations were associated with orientation states of size 7½°. The form of the distribution of

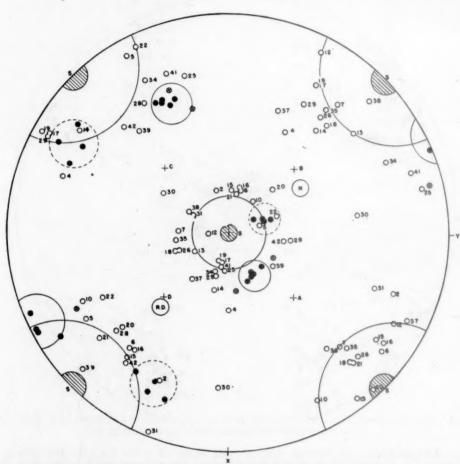


Fig. 5.—Stereographic projection plot of cube poles of grain H_4A (at position S) and the 41 recrystallization nuclei.

analyses. With regard to the twins, grain No. 29 could be classified best as a C₃ within 10° but grain No. 30 did not fall near any C classification. It did fall within 15° of the A (i.e., first-order twin) classification. Because orientation No. 30 applies to two separate parts or grains associated with grain No. 29, it would be reasonable to say that it and not No. 29 was the dependent one.

orientations indicates, according to probability, that the changes in orientation did not occur in a haphazard manner (see Appendix for a detailed discussion). This confirms the results reported previously. Tables 3 and 4 and Fig. 7 indicate that classifications made according to first, second, third, and fourth-order twin orientation relationships also confirm the results reported previously; namely, that

the data correlate best with a subclass of the third-order twin transformations. Fig. 7 brings this into striking relief. In evaluating the bar graph, it must be was not taken independently of the others in that class. Table 4 also shows that the results for each specimen (i.e., E4C, E4B₁, etc.) are classified best under C₃.

TABLE 3.—Distribution of Orientations Among the Nine General Classes Using Four Values of Alpha

Number of Orientations

Specimen	Deg.	Me	A	В	Cs	C4	D24	Dn	D:1	D ₁₅	D ₁	Мв
E4C	15	90	0	60	76	9	7	1	29	32	0	I
	10	90	0	26	53	8	3	0	16	17	0	18
	7.5	90	0	12	31	3	3	0	5	6	.0	44
	5	90	0	5	13	I	2	0	0	I	0	71
E4B1	15	52	0	30	42	3	0	I	18	15	0	6
	10	52	0	4	28	2	0	0	5	2	0	20
	7.5	52	0	2	15	2	0	0	I	1	0	35
	5	52	0	0	3	0	0	0	0	0	0	49
E4B2	15	34	0	18	21	4	I	I	9	13	I	5
	10	34	0	7	15	1	0	I	3	6	0	II
	7.5	34	0	I	7	0	0	0	2	2	0	24
	5	34	0	0	4	0	0	0	0	0	0	30
G4D	15	56	I	23	46	I	I	0	15	II	I	5
	IO	56	I	3	28	0	0	0	3	I	1	25
	7.5	56	1	0	15	0	0	0	I	0	1	41
	5	56	I	0	3	0	0	0	1	0	I	52
H4A	15	41	I	17	27	9	2	2	14	10	0	3
	IO	41	0	5	14	2	0	2	5	4	0	20
	7.5	41	0	2	IO	0	0	I	3	1	0	28
	5	41	0	0	3	0	0	0	0	0	0	38
F5	15	78	0	43	44	23	5	I	27	26	0	3
	10	78	0	13	18	9	I	0	13	7	0	42
	7.5	78	0	8	7	3	0	0	9	3	0	55
	5	78	0	1	4	0	0	0	I	I	0	72
Results for all samples		351	2	191	256	49	16	6	II2	107	2	23
	IO	351	I	59	156	22	6	3	45	37	I	136
	7.5	351	I	25	85	8	3	I	21	13	I	227
	5	351	I	6	30	I	2	0	2	2	I	302

<sup>Number of new grains.
Number of orientations not classified.</sup>

TABLE 4.—Distribution of Orientations Among the Nine General Classes for Alpha

Equal to 10°

PER CENT

Specimen	Ma	A	В	Ca	Ca	D24	D22	D21	D ₁₅	Dı	M ^b
B4C	90	0.0	28.9	58.9	8.9	5.6	0.0	17.8	18.9	0.0	20.0
E4B1	52	0.0	7.7	53.8	3.8	0.0	0.0	9.6	3.8	0.0	38.5
E4B ₈	34	0.0	20.6	44.I	2.9	0.0	2.9	8.8	17.6	0.0	32.4
G4D	56	1.8	5.4	50.0	0.0	0.0	0.0	5.4	1.8	1.8	44.
H4A	41	0.0	12.2	34.2	4.9	0.0	4.9	12.2	9.8	0.0	44.
5	78	0.0	16.7	23.I	11.5	1.3	0.0	16.7	9.0	0.0	53.5
All samples	351	0.3	16.8	44.5	6.3	1.7	0.9	12.8	10.5	0.3	38.

Number of new grains.
 Percentage not classified.

remembered that there are 24 members in the C₄ class and only 12 in the C₃ class and that there are 108 members in all the D classes. It would not be easy to replot the results according to relative weights because each subclass of a class (C or D)

Consequently, the C₃ classification is independent of the original orientation, at least for the orientations reported in the present work. Incidentally, Table 3 shows in the case of specimen G₄D, the only example to date of a good first-

order twin classification. This applies to grain No. 37 (see Fig. 4 for the orientation).

Fig. 6 shows a plot not only of the new orientations of the F5 series but also

considered less than one state). This accounts for the fact that 18 orientations are listed in Table 3 under C₃ for alpha equal to 10°, whereas 22 are found in Fig. 6.

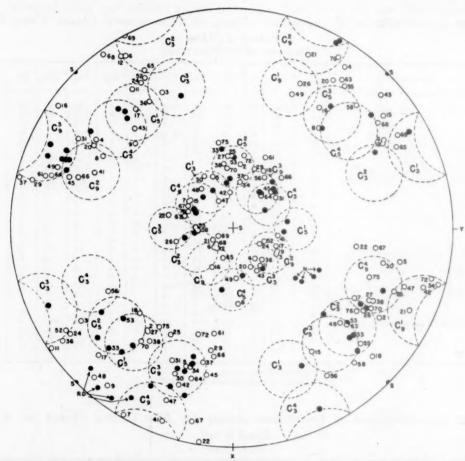


Fig. 6.—Stereographic projection plot of cube poles of grains F5A, F5B, F5C, and F5D (all at position S) and of the 78 recrystallization nuclei.

Also shown are the 12 members, each 10° in size, of the C2 class of third-order twins.

of the 12 C₃ states previously mentioned each of size 10°. (Each C₃ state has a superscript and a subscript to identify it; and its orientation—accurate to the nearest minute—may be found in the standards previously published.⁴) Fig. 6 shows that it is not possible for any single orientation to fall into two of these 12 states. If C₄ states of the same size were also present, some orientations could fall into two states (overlapping states, however, are degenerate and each must be

Incidentally the percentage falling into C₂ would be raised from 23.1 (Table 4) to 28.2 for specimen F₅ by an independent classification of C₃ and C₄. Table 4 shows that the F₅ series does not classify as well as the other groups. It is interesting to note from Fig. 6 that most of the orientations, although falling somewhat near to the members of the C₂ class, actually do fall on the outside of these classifications. The situation is made clearer by reference to Table 3, keeping

in mind that orientation states nearest C₃ are B, C₄, D₁₅, and D₂₁, and observing the distribution for alpha equal to 15° as well as 10°.

tions obtained as Δ_{n}^{q} is increased from the lower to the higher value in each zone. The solid-line curve indicates the form of the distribution and shows that the most prob-

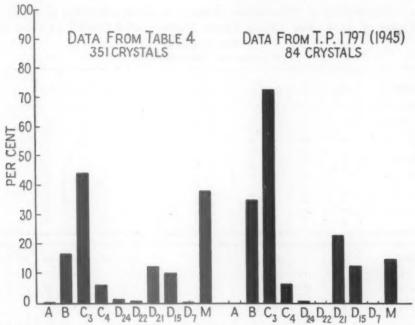


Fig. 7.—Bar graph of percentage of orientations classed as A, B, C (C_2 or C_4) and D (D_{24} , D_{22} , D_{21} , D_{16} , and D_7) for alpha equal to 10°; and the percentage of miscellaneous orientations M with no A, B, etc., classification.

When the other pole-figure plots are superimposed on a C3 net, each preferred crystal orientation (or highly populated state) is generally displaced a certain amount from C3, more often toward the orientation designated by S. This may be indicated in another way. Plot the number of orientations for all the examples against equal increments of solid angle taken in conical shells about the cube poles of S. Such a plot appears in Fig. 8 with linear angle Δ_{n}^{e} for abscissa. For example, the first solid angle is a cone circumscribed about S with Δ_{n^0} equal to 15°. The next increment of solid angle is a conical shell with Δ_{sq} varying from 15° to 21°20'. The other succeeding angles are indicated by the lengths of horizontal lines in the plot, which, from their positions on the axis of ordinates, also give the number of orientaable value of Δ_{n^q} obtained during recrystallization is slightly under 25° . This value is less than that expected for a C_2 classification; so the γ_3 group, previously described, was introduced into the analyses. In obtaining the results listed in Table 3, C_3 and γ_3 were treated independently. There are 128 orientations under γ_3 and 86 under C_4 . It is interesting to compare some γ_2 and C_3 classifications (marked with asterisks in Table 5) that are associated with preferred crystal orientations. In E4C, C_3 and C_4 are about the same, but in E4B₁ and G4D, C_4 is definitely better.

On the other hand, there is some evidence in the pole-figure plots that some groups are further away and therefore nearer a second-order twin, or a B orientation.

Displacements of orientations from C₃

toward γ_i or toward B may be explained in terms of the spread in orientation of the old grain; i.e., as the old grain becomes more distorted the departure from C3 inassurance about mechanisms that would enable one to predict not only a Ca-classification but also the correct distribution within the C2 class. On the other hand,

TABLE 5.—Distribution of Orientations Among the Twelve Members of the C3 Class for Two Values of Alpha and Among Twelve Members of a Special 78 Class for One Value of Alpha NUMBER OF ORIENTATIONS

Specimen	Deg.	C ₁	Cs1	Cs3	Cs4	C ₅ ²	Cas	C ₉ 1	Co2	C ₂ 1	C98	C ₃ ²	Ca ⁸	C
E4C	10	54	1	9	I	I	1	I	I	0	11 8*	14	I	13
	7.5	32	1 1	4*	0	0	0	0	I	0	8*	14	I	10*
E4B1	10	29		0	I	0	4	0	4 2*	4 2*	2 2	2	3	9
	7.5	15	0	0	0	0	1*	0	2*	2*		0*	2*	6*
E4B ₁	10	16	0	4	0	I	1	1	I	I	0	2	4	I
	7.5	7		0*	0	I	0	I	I	I	0	I	1*	
G4D	10	27	1	I		0	4	0	5	10	o 5 3*	0	I	0
	7.5	15	1	0		0	3	0	5 3*	4*	3*	0	I	0 0 1
H4A	10	14	2	2	-	0	2	2		0	0	0	5	I
n-	7.5	10	2	2	0	0	I	0	0	0	0	0	5 4* I	I
P5	10	22	2	I	2	4	0	0	. 0	I	7 2	I	I	3
	7.5	7	2	0	0	1	0	0	0	I	2	0	1	0
Specimen	α	γι	751	753	γs4	752	γ2 ⁴	γv^1	γ ₉ ²	γ ₃ 1	798	γ2 ²	γ3 ⁸	γ94
E4C	7.5	36	0	4*	1	0	1	2	1	0	5*	9*	3	10*
E4B1	7.5	27	0	0	0	0	2*	0	4*	5*	2	9*	4*	9*
E4B2	7.5	7		2		0	I	0	I	I	0	0		0
G4D	. 7.5	32	0	2	0	0	4	0	6*	14*	5*	0	1	0 0 2
H4A	7.5	11	1 2	4	0	1		0	0	0		0	3	0
	7.5	15		3	I	I	0	0	T		I	2	I	

creases (measured with respect to the principal orientation of the old grain). This seems to be the case for the F5 group (having orientations of the type formerly used).1 Not only are there displacements, but there are dispersions that require larger orientation states for the same percentage of orientations occurring in a C3 classification. Some increase in dispersion should be expected with increasing distortion of the deformed grain.

When the data on distribution of orientations according to axes X, Y, A, etc., in Table 5 are analyzed with respect to the data on deformation given in Table 2—these data correlating with directions N., R.D. and C.D., no simple connection between the two sets of directions or sets of axes appears to result. Until more correlated data on deformation and recrystallization are made available, little can be said with Burgers, in support of the theory of local curvature on slip planes, has obtained results from the recrystallization of aluminum that indicate a good correlation between slip planes and axes of rotation involved in recrystallization.

There seems to be evidence from the present silicon-steel samples and others3 that {112} slip planes are active in the range of deformation studied. According to published results,8 {110} slip planes should also be active because of temperature of rolling (room temperature) and because of composition. [110] slip planes alone remain active when the silicon content exceeds 4 per cent.8 Therefore, data on recrystallization for samples with more than 4 per cent silicon should be valuable in a study involving the origin of recrystallization nuclei.

To eliminate the effect of small varia-

F5A and F5C and by grains G4D and H4A, it would be desirable to use very large single crystals and subdivide them

3. The distribution of orientations among the 12 members of the C₃ class shows that some members are more highly populated than others. The data

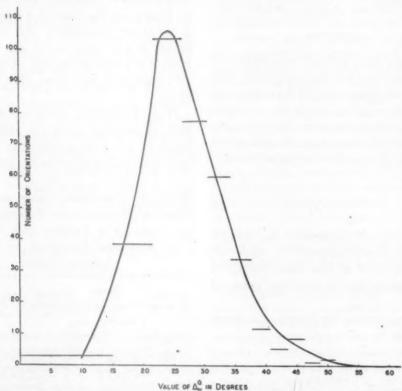


Fig. 8.—Curve of distribution of orientations according to amount of orientation change for recrystallization in samples E4C, E4B₁, E4B₂, G4D, H4A, and F5.

for studies involving the effect of amount of cold-rolling on the distribution of orientations obtained through recrystallization.

SUMMARY

1. Analyses of 351 examples of recrystallization give a high probability for obtaining a third-order twin relationship between new and old structures.

2. The distribution of orientations between the C₃ and the C₄ classes, comprising 12 and 24 orientations, respectively, of all third-order twins, indicates that the C₃ class is largely involved in recrystallization. This relationship is clearly shown in tables of data and in pole-figure plots.

appear insufficient, however, to indicate a satisfactory reason for the form of the distribution.

4. Orientation changes due to recrystallization classified best as C₃ regardless of original orientation. The form of the distribution among the members of the C₃ class, however, appeared to be influenced by the original orientation and the way in which each crystal deformed.

5. With greater amounts of cold reduction, or with increasing spread in orientation of the deformed grain, there was an increase in the spread of orientations away from the C₃ classification.

6. Every case of recrystallization involved a change in orientation; and very few occurred with a change in orientation of less than 15°. The most probable value of the change in orientation (given by the number Δ_{n^q}) was slightly less than 25° for the 351 nuclei.

APPENDIX

Equations have already been developed6 for determining: (1) the probability that a single orientation will fall into a specified state of size alpha, nucleation occurring in a haphazard manner, and, (2) the probability of occurrence of orientations in various groups. The equation for the first case is

$$P = 1.43\alpha^3$$
 [1]

where alpha is expressed in radians. Writing N for the reciprocal of 1.43 α^3 , we may think of N as the total number of possible states for a specified value of alpha.

The equation for the groups of common orientations is

$$P^{k}_{m_{1}}, m_{2}, \dots m_{k} = [2]$$

$$N!n!$$

$$m_{1}!m_{2}! \dots m_{k}!(N-l)!(l-k)!N^{n}r_{1}!r_{2}!\dots$$

where n is the number of recrystallization nuclei $(n \leq N)$ that are distributed among l states of equal size in such a way that m_1 orientations fall into one state, m2 in another, and so on up to mk in a kth state. and one each in the remaining l - k states. The number of states, among those with two or more orientations, that contain the same number of orientations are given by the numbers r_1 , r_2 , and so forth.

In the present analysis; we are interested in a value of alpha of 71/2° and this, using Eq. 1, gives a value of N of 300. Now consider the case of n equal to 50 for various types of groups. Application of Eq. 2 gives the probabilities listed in Table 6 in the order of diminishing values. Three or four groups of two's are the most probable, and a situation where no groups are formed (one or no orientations in each state) is far down on the list.

Some idea of the probabilities involved over a range of values of n may be obtained by computing the value of n that produces a maximum probability for a specified group. A few such values appear in the table. For example, the highest probability for obtaining a pair occurs when n is equal to 25.

If the probability of obtaining a group with 16 orientations in one state (n still equal to 50) were considered, we would find that the most probable group is m_1

TABLE 6.—Probability Values for Various Groups of Common Orientations with n = 50, and Value of n Together with Probability for Maximum Probability for Certain Specified Groups

Number	Group	Prob-	Maximum	
of States,	m ₁ , m ₂ ,	ability, n = 50	Prob- ability	22
- 3	2,2,2		0.2233869	44
4 2	2,2,2,2		0.1836560	51
	2,2		0.2811002	36
5	2,2,2,2,2		0.1531755	57
	2		0.3886760	25
6	2,2,2,2,2,2		0.1286577	63
4	2,2,2,3		0.0434777	55
4 3 5 7	2,2,3	0.0340261		
5	2,2,2,2,3	0.0321627		
7	2,2,2,2,2,2,2	0.0245082		
6	2,2,2,2,2,3	0.0185467		
2	2,3	0.0174599	0.0240473	40
8		0.0131872		
8	2,2,2,2,2,2,2,2	0.0074807		

equal to 16 and m2 equal to 2, the probability being about 10-25. The probability of obtaining a 16,6,6,2 group, however (which corresponds more nearly to the case involved in sample G4D) would be 10-13 times the value for the 16,2 groupi.e., about 10-38. What is needed actually is the probability of obtaining at least 16 orientations in one state. But this is hard to obtain. It does not seem possible that the sum of probabilities $(m_1 \ge 16)$ would become large, because each probability decreases rapidly (m1 equal to 16 and m2 equal to 2) as more states or populated states are added, or as m1 is made greater than 16. This may be indicated in another way. Take the sum for those groups that have no m1 greater than 15. The value for the first 14 (Table 6) is 0.06, and this is scarcely a start as far as the number of groups is concerned. Consequently, there cannot be much left for the groups that have an m_1 equal to or greater than 16 (the sum for all possible groups is one).

In addition to this, there are fairly simple groups that would be likely to occur; so the probability of obtaining a 16,6,6,2 group, for example, is not only small but is small compared with a 2.2.2 group, or with any of the groups listed in Table 6.

The foregoing type of analysis, therefore, enables us to estimate what to expect when nucleation occurs in a haphazard manner.

ACKNOWLEDGMENT

It is a pleasure for the writer to acknowledge aid given by Mr. Fabian Lionetti in the X-ray diffraction work and in the determination of crystal orientations, by Miss Margaret E. Smith in the analysis of data and in the careful construction of diagrams, and by the Calculating Section in the determination of numerical values used in the Appendix.

REFERENCES

- 1. C. G. Dunn: Orientation Changes during Recrystallization in Silicon Ferrite.

 Trans. A.I.M.E. (1945) 161, 98.

 2. C. S. Barrett and L. H. Levenson: Trans.

 A.I.M.E. (1941) 145, 281.

 3. C. G. Dunn: Some Aspects of Crystal Recovery in Silicon Farrite Following Plastic
- covery in Silicon Ferrite Following Plastic
- Strains. This volume, page 373.
 4. C. G. Dunn: Standards for Identifying Complex Twin Relationships in Cubic Crystals. Trans. A.I.M.E. (1945) 161, 90.
- C. G. Dunn: Recrystallization and Twin Relationships in Silicon Ferrite. Trans. A.I.M.E. (1944) 158, 372.
 C. G. Dunn: Phys. Rev (1944) 66, 215.
 W. G. Burgers: Papers Int. Confer. Physics,
- London (1934) 2, 139. 8. C. S. Barrett, G. Ansel, and R. F. Mehl: Trans. A.I.M.E. (1937) 125, 516.

DISCUSSION

(A. R. Troiano presiding)

C. S. BARRETT. *- Dr. Dunn's theory of highorder twinning provides one very interesting way of analyzing the data. Another theory that has received much discussion is that certain rotated portions of the grains are the nuclei of recrystallization that govern the orientation of recrystallized grains. It would add much to the value of Dr. Dunn's studies, I think, if the data could be analyzed in some way that would show which of these theories is able to account for the facts. It might be necessary to calculate probabilities on the basis of degrees of rotation that are chosen purely arbitrarily, but in the present analysis there is also some arbitrariness in the choice of the orders of twins, for there are no a priori reasons for singling out any particular order or orders of twins that should be important (except, perhaps, the first order, which according to the data, is not found).

C. G. DUNN (author's reply).-In order to follow the changes in orientation that occur during recrystallization it seems to me that one should start either with a single-crystal specimen or with a polycrystalline sheet having a strong single texture. It is not clear to me what we can expect to find if the polycrystalline material lacks this property. The spread in orientation in any polycrystalline sheet is certain to add some confusion to the relationship between recrystallized textures and coldrolled textures. Consequently, I prefer to use single-crystal specimens.

Dr. Barrett expresses the belief that the data could have been analyzed in another way and that we then could see what theory accounts for the facts. I prefer to speak of the high-order twin relationship as a form of classification rather than as a theory. In this connection, I have thought for some time that an arbitrary set of standards, sufficient in number to include any orientation-a set of 300 might do well enough-would have been better than the first, second, third, and fourth-order twin standards. Such a set, however, has not been prepared yet. Never-

^{*} Physicist, Metals Research Laboratory, Carnegie Institute of Technology. Pittsburgh, Pennsylvania.

theless if such a set had been used in the analysis, the data would still have shown a most probable relationship very near that of the C₁ type of third-order twin—a relationship that becomes almost self-evident in con-

sidering the groups of common orientation

(i.e., highly populated states).

Now the C₂ type of third-order twin orientation can be obtained from the original (orientation S) by a rotation of 31°36' about the proper face diagonal direction, as was pointed out in the paper. Therefore rotated portions of grains could act as nuclei of recrystallization but the larger portion of them would have to be near 30° and have a <110> type axis to account for the facts. In other words, the C₂ type of third-order twin expresses the nature of the results obtained on silicon ferrite with cold-rolling reductions in the low percentage range. One probably could build a theory on this, but such a theory

might be only a special case of the theory that nuclei of recrystallization are rotated portions of the parent grain. As a matter of fact, a speculation was made in a prior paper (ref. 1 of the paper) that second or third-order twin relationships might have had their origin in repeated mechanical twinning during the deformation. In the present work, however, there was little evidence that mechanical twinning occurred during the cold-rolling operations. Obviously more detailed information on the nature of recrystallization is needed to account for the facts obtained on orientation changes. On the other hand, when more data of the type presented are obtained, it may be possible to predict accurately, without knowledge of the exact mechanism involved, what changes in orientation will occur during recrystallization given the initial orientation and the nature of the plastic deformation.

Some Aspects of Crystal Recovery in Silicon Ferrite Following Plastic Strains

By C. G. DUNN, MEMBER A.I.M.E.

(Chicago Meeting, February 1946)

It is well known that plastic deformation alters many of the properties of a metal and subsequent heat-treatment partially or completely restores these properties. In the deformed or strained state, the metal is unstable and tends to change toward a condition called a "strain-free state." The transformation occurs through recovery, recrystallization, and grain growth—processes that may take place singly or in combination.

The distortion of the lattice of an individual grain of a metal in a state of strain may be rather complex in nature, because plastic deformation produces: (1) dislocations within mosaic blocks: (2) elastic variations of the lattice spacings; and (3) gross alterations throughout the lattice, especially along slip planes, along composition planes between a grain and its mechanical twins, and along boundaries of deformation bands. These gross alterations are of the nature of bent planes or rotated regions of the crystal lattice and are revealed by a spread in the orientation of the grain. Although we cannot describe these strains and their formation accurately because of insufficient knowledge, we can, nevertheless, use the information as well as possible to obtain a better understanding of recovery processes.

In recovery, the lattice of a grain is

not made anew as it is in recrystallization, but is improved or mended in such a way that the basic structure remains unaltered. Until recently observations were that recovery produced no marked changes in the shapes of spots in Laue diffraction patterns, whereas recrystallization did, but now it is known for silicon ferrite2 that Laue spots may become quite sharp entirely through recovery. Consequently, the shape of Laue spots alone would not be a suitable test to distinguish between recovery and recrystallization. There is considerable evidence that the microstructure usually does not change visibly during recovery. Absence of a visible change in the microstructure, therefore. provides a sufficient test of recovery in many cases. However, including this observation in a definition of recovery as a necessary condition (this is usually done) is unfortunate, because recovery may, as will become evident later, produce new grain boundaries that are visible not only in the microstructure but also in the macrostructure. For the present, therefore, let us say that a necessary condition for a process to be one of recovery is that the principal orientation or orientations of a deformed grain be essentially unchanged throughout the transformation toward the strain-free state. Several transformations may occur that fulfill this condition, and the nature of the distortion in a grain indicates what these must be if the lattice is to be mended in part or fully. Consequently, it will be convenient as well as

Manuscript received at the office of the Institute Nov. 21, 1945. Issued as T.P. 1991 in METALS TECHNOLOGY, August 1946.
*Research Physicist, General Electric Co.,

Pittsfield, Massachusetts.

References are at the end of the paper.

logical to divide recovery into three classes corresponding to those previously listed for distortions existing in the metal in the strained state:

1. Class-1 recovery: the removal of dislocations within mosaic blocks. Dislocations* are not easily detected by means of X-rays; however, line widths and line intensities may be involved.

2. Class-2 recovery: the removal of elastic strains. This recovery process alters the lattice parameters and either restores sharpness to X-ray diffraction lines or produces a shift in their positions.

3. Class-3 recovery: The removal of distortions that produce a spread in orientation over regions that are larger than 10⁻⁴ cm., i.e., larger than mosaic blocks. This type of recovery produces a very marked alteration in the spots of Laue diffraction patterns.

These classifications probably do not introduce any new concepts about recovery, but they do help to determine the scope of the subject. On the other hand, the statement that recovery may produce visible changes in a metal is new. It means for one thing that grain refinement† is possible through deformation and recovery; and experimental proof of this will be given later.

With regard to present knowledge concerning recovery, only some of the main points that pertain to our investigations will be reviewed. First, in connection with class-1 recovery, it has been reported on theoretical grounds that dislocations tend to diffuse to the surface of a metal.^{3,4} Barrett^{5a} suggested that such diffusion may constitute recovery. Koehler⁴ also pointed out that positive and negative dislocations might come together within a metal and annihilate each other. Therefore, as a working definition, we would

say that the removal of dislocations (under the previously mentioned necessary condition for recovery) is a recovery process and the diffusion and annihilation features represent possible mechanisms.

Secondly, in connection with class-2 recovery, it has long been established that elastic strains and their attendant internal stresses can be removed, at least partially, by a recovery process. Because of this fact, recovery is frequently associated with the removal of stresses that affect. among other things, the stability of shape of an object and the ability of the metal to withstand corrosion. On the other hand, we must remember that any strain that produces a strained state will also produce stresses, even though they be highly localized in character and have little effect on diffraction lines. Further, an elastically bent lattice can produce a spread in orientation6 of the type associated with asterism; and along with the spread in orientation there are, of course, compression and tension stresses with corresponding elastic changes in the lattice spacings. However, asterism without internal stresses 56,7 may be present in an annealed sample of metal; so, in spite of some apparent overlapping of terms; the expression "elastic strains" will serve to describe the well-known changes in lattice spacings and the expression "class-2 recovery" will deal with their removal:

Finally, with regard to recovery of the type now called class 3, Elam^{8a} reported, while summarizing numerous data on the effect of structure on X-ray diffraction patterns, that the elongation of Laue spots remains until recrystallization takes place. Collins and Mathewson⁹ reported for aluminum crystals that small intensity maxima develop in the Laue diffraction spots during recovery. This effect has been interpreted generally as due to changes in internal stress, although Collins and Mathewson offered another possible

sufficient proof of recrystallization,

^{*} It is believed that most of the energy in the lattice produced by plastic deformation is due to dislocations. † Grain refinement has often been used as

interpretation that involved partial coalescence of crystal fragments. They believed, however, that such a recovery process should have continued until the crystal lattice was perfect, and offered no explanation why this did not occur, except to note that such recovery was reported by Yoshida and Nagata on material deformed 2 per cent or less. Complete removal of the elongation of Laue spots was reported recently for the case of deformed silicon ferrite crystals.2 In the same work, it was noted that Neumann bands were removed during recovery of an old grain and that growth of new grains became negligible after recovery had proceeded far enough.

far recovery can go in removing strains, to what extent recovery can stop grain growth or stop nucleation of new grains, and what active role, if any, recovery may have in a nucleation process.

The present paper is chiefly concerned experimentally with the process termed class-3 recovery or with those changes that reduce the spread in orientation of a grain over relatively large regions, not through the development of a new lattice but rather through adjustments that put the old one into a more perfect condition. The separate subjects and experiments that appear under Experimental Results were arranged whenever possible to form a logical sequence; but in general each sub-

TABLE 1.—Composition of Materials Investigated
PER CENT

Specimens	Si '	С	Р.	S	Mn	A1	Cu	Sn
E and T series G series H sample	3.45 3.55 3.65 3.65	0.003 0.004 0.003 0.002	0.008 0.011 0.011 0.010	0.009 0.008 0.014 0.007	0.075 0.045 0.16	0.031 tr. tr. tr.	0.072 0.080 0.028 0.028	tr. 0.014 0.014 0.009

Although no formal attempt to define recovery has been made by the writer, the commonly accepted meaning of the term has been retained as closely as possible. No restrictions were made with regard to its place relative to recrystallization because strains may also be present in a recrystallized structure. The idea that a recrystallized structure is often not free of strain86,10 has been maintained for a long time to explain certain observations on grain growth. Others have maintained that grain-boundary areas provide the sole source of energy necessary for grain growth. There is, therefore, a need for a better understanding of the effects of strain and recovery on recrystallization and grain-growth processes. This need may require experimental results to determine how much energy is present in a strained state and how it is distributed among the various types of strains, how

ject represents an independent and different aspect of crystal recovery.

PREPARATION OF SPECIMENS AND EXPERIMENTAL PROCEDURE

Materials used in the present investigation were obtained from some heats of steel made by the Allegheny-Ludlum Steel Corporation. Final processing and heat treating were done at the Pittsfield Works' Laboratory of the General Electric Co., to give fairly large grains of suitable orientations for work on recrystallization. Designation of specimens and chemical composition are given in Table 1.

During the course of work on recrystallization over a period of two years, a number of interesting types of recovery processes were discovered. These have been assembled together either according to degree of complexity of the structure or according to some effect associated with recovery. In general, the complexity of the structure of a deformed crystal depends upon the original orientation, the influence of surrounding grains, the type the narrow surfaces of each crystal were first surface-ground with grit No. 180, then etched for 3 min. in a 4 to 1 aqueous solution of nitric acid, while the large

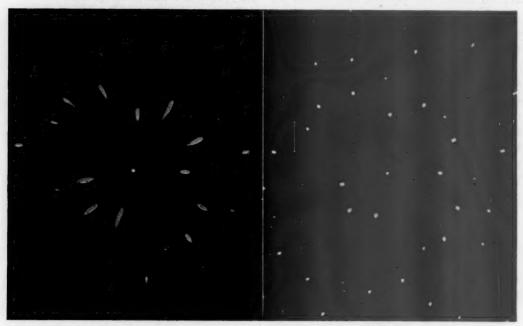


Fig. 1. Figs. 1 and 2.—Laue photographs of grain E₂B.

Fig. 1. After cold reduction of 21 per cent.

Fig. 2. After cold reduction of 21 per cent and anneal of 3 days at 980°C

of deformation, and the amount of the deformation. Because it is not possible at this time to cover these factors adequately as they may relate to recovery, only a brief description of the deformed structure will be given.

All crystals were as thick as the sheets, which were 0.007 in. for the E series, 0.012 in. for the T series, 0.014 in. for the G series and 0.014 in. for the A and H samples. A cold mill with 8-in. dia. rolls was used to deform all specimens except those in the T series, which were pulled on a tensile machine. After the proper amount of deformation, single-crystal samples were obtained from the sheet specimens by either of two methods. In one an abrasive cut-off wheel was used. To remove strains left by the cut-off wheel,

flat surfaces were protected with acidresisting lacquer. In the other method, nitric acid alone made the cut, acidresisting lacquer again protecting the large flat surfaces.

All samples were annealed in an atmosphere of pure, dry hydrogen.

EXPERIMENTAL RESULTS Single-lattice Type

In this example the structure of a coldrolled crystal consists of a single orientation with some spread.

Experimentally, a polycrystalline sample 0.007 in. thick was cold-rolled 21 per cent. After the sample was lightly etched to reveal grain boundaries, large crystals were removed and annealed for 3 days at 980°C. Laue photographs of the crystals

before and after the anneal, except one photograph that had some residual distortion of the Laue spots, were similar to those shown in Figs. 1 and 2 for crystal E2B. Three Laue patterns taken at

Double-lattice Type

The structure of the deformed crystal prior to recovery consists of two orientations, each with some spread.



Fig. 3.—Laue photograph of grain G5A before plastic deformation.

positions 34 in. apart in E2B checked identically with that of Fig. 2; so it is reasonable to say that the annealed sample consists of a single lattice. Comparison of the Laue patterns discloses that the orientation of E2B did not change during the anneal; only the spread in orientation changed. Therefore, the necessary condition for recovery, previously imposed, has been satisfied. However, this condition alone is not sufficient to distinguish between recovery and a special case of recrystallization that theoretically might occur; namely, recrystallization without change in orientation. The latter would require a nucleation and growth process; the former would not require any growth. More will be said later about this after the effect of time at temperature on recovery has been considered.

A single-crystal specimen G5A 0.014 in. thick with a (011) plane within one degree of the surface was cut into a rectangle of size ½ by 1½ in., the long dimension coinciding with a [100] direction. After the crystal had been cold-rolled 10 per cent in the [100] direction, it was trimmed to a width of ¼ in. and then divided into two pieces. One piece was annealed for 4 hr. at 1175°C.; the other was retained as cold-rolled. No new grains were seen in either surface of the annealed crystal. Laue photographs of this piece before rolling, after rolling, and after annealing are shown in Figs. 3, 4 and 5, respectively.

From the Laue photographs in Figs. 4 and 5, it is apparent that the cold-rolled specimen is composed of two lattice structures and that the annealed sample is also a doublet of the same orientations,

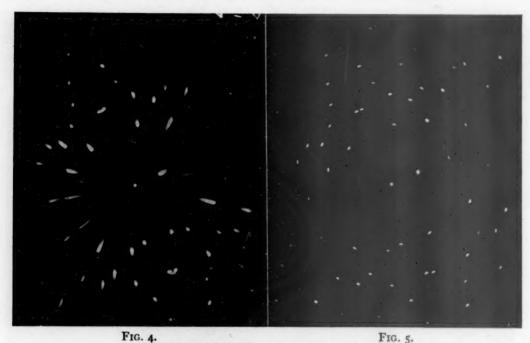


FIG. 4. FIGS. 4 AND 5.—LAUE PHOTOGRAPHS OF GRAIN G5A.

Fig. 4. After cold reduction of 10 per cent in a <100> direction.

Fig. 5. After cold reduction of 10 per cent and an anneal of 4 hr. at 1175°C.

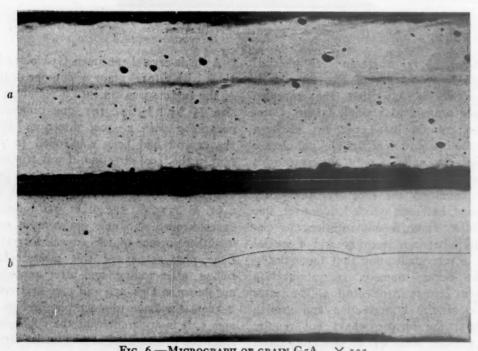


FIG. 6.—MICROGRAPH OF GRAIN G5A. × 125.

a. As cold-rolled. Etched 4 min. in 4 per cent Nital.

b. Cold-rolled and annealed. Etched 7 sec. in 4 per cent Nital.

the difference in the patterns being one of spread in orientation. Cross-section microstructures were prepared from the annealed and unannealed pieces in order to find separately, producing, through the difference in orientation, a very sharp boundary between the bands. Fig. 7 is a stereographic projection plot showing the

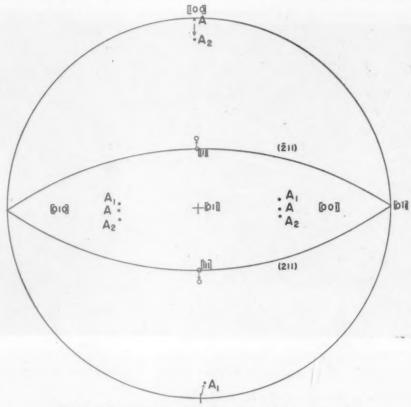


Fig. 7.—Stereographic projection plot of grain G5A.

A. Cube poles of original orientation.

 A_1 . Cube poles of one part of doublet structure after recovery.

A2. Cube poles of other part of doublet structure after recovery.

the reason for the doublets. Micrographs that are representative of the entire cross section are shown in Figs. 6a and 6b. The two layers shown in Fig. 6a were not observed until the cold-rolled specimen was heavily etched, but the doublets present in the annealed specimen (Fig. 6b) were readily disclosed.

It may be concluded from the foregoing results that the original crystal divided roughly through the middle to form a sample of two layers, each a region of one crystal orientation, and that each layer or deformation band recovered original and final orientations, A being the orientation prior to the deformation and A_1 and A_2 the orientation of each layer after the anneal. A simple explanation of the change in orientation is that one band A_1 deformed through slip on a (211) plane; the other, A_2 , through slip on a (211) plane, with both lattice rotations occurring about a common [011] direction.

Complex-lattice Type

In these examples the deformed crystal may be composed of two or more preferred crystal orientations or deformation bands, but the recovered sample is definitely quite complex. Two examples will be illustrated, one with a visible change in the microstructure, the other with a visible change in the macrostructure. the well-known pattern called pseudo asterism. A Laue pattern from a region originally free of Neumann bands disclosed a structure very much like that of G5A (Fig. 5) except that one of the

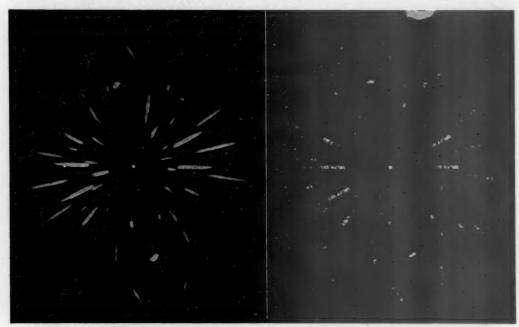


FIG. 8. FIG. 9. FIGS. 8 AND Q.—LAUE PHOTOGRAPHS OF GRAIN GAC.

Fig. 8. After cold reduction of 10 per cent in a <100> direction. Area containing Neumann bands.

Fig. 9. Same area after anneal of 4 hr. at 1175°C.

In the first example, a large single crystal, G4C, part of a polycrystalline sample 0.014 in. thick, was cold-rolled 10 per cent approximately in a <100> direction, then cut from the sample in the manner previously described. During the deformation, Neumann bands formed across one section of the crystal. Laue photographs of this area before and after a 4-hr. anneal at 1175°C. are shown in Figs. 8 and 9. Inspection of the crystal after the anneal disclosed no recrystallization, only the removal of the Neumann bands. Although the Laue patterns are much alike, the one in Fig. 9 appears to represent an aggregate of small crystals of nearly common orientation, producing

doublets contained a fine structure of two or three very close orientations. A longitudinal specimen was prepared to show the microstructure of an entire section of the crystal. A micrograph of the sample, heavily etched, is shown in Fig. 10 for the area originally containing Neumann bands. As with G5A, a grain boundary (heavy black lines in the micrograph) appeared early in the etching treatment, roughly through the middle of the specimen, dividing the crystal into two layers. One of these layers, however, was divided into two or three parts (these do not show in the micrograph), and they, no doubt, produced the fine structure mentioned for the area originally free of Neumann

bands. Etching of the sample was continued until a large number of crystallites became visible. Boundaries were hard to see because of the near common mann bands in other areas could be seen. The sample was then annealed slowly; i.e., 20 hr. in the range of 500° to 900°C. A small amount of recrystallization oc-

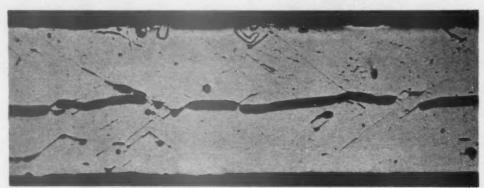


Fig. 10.—Micrograph of grain G4C after annealing. X 125. Area originally containing Neumann bands. Etched 90 sec. in 4 per cent Nital.

orientations, but they are discernible in Fig. 10.

Reasons for the development of crystallites in a Neumann band area and not in other areas of the deformed crystal will be discussed later, after the effect of curred, but only in the region containing Neumann bands. One old grain had grown a small amount. The sample was annealed for 4 hr. at 1175°C. Further growth was observed; but recrystallization, generally, appeared little advanced. As a final



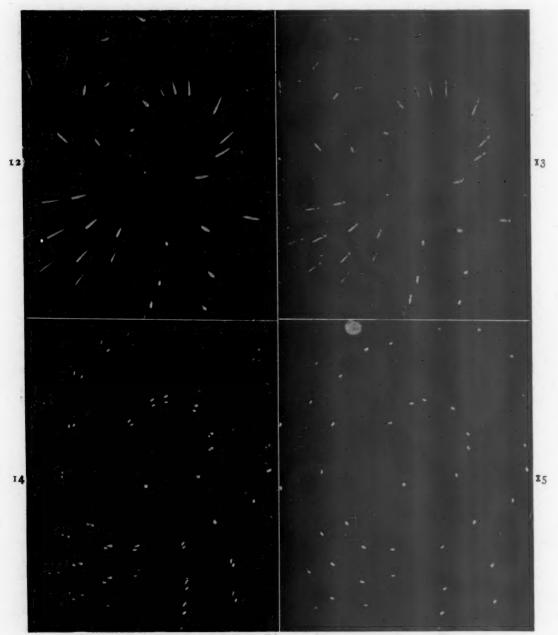
Fig. 11.—Macrograph of grain E in specimen TW12. Sample etched with dilute acid. × 3 a. After 900°C. anneal. b. After 1450°C. anneal.

Neumann bands on the distortion of a lattice has been considered.

In the second example a polycrystalline sample, TW12, was prepared in the form of a tensile specimen and pulled 8 per cent. Following the deformation, highly distorted grains in some areas and Neu-

treatment the sample was annealed to a temperature of 1450°C. and held about one hour. Little additional recrystallization was observed, but other changes could be seen.

Photographs in Figs. 11a and 11b show the appearance of a distorted grain after



Figs. 12-15.—Laue Photographs of Grain E.

Fig. 12. At position L (Fig. 11a) after 1175°C. anneal.

Fig. 13. At position L (Fig. 11b) after 1450°C. anneal.

Fig. 14. At boundary position M (Fig. 11b) after 1450°C. anneal.

Fig. 15. At position N in area having boundary at position M.

the anneals at 900° and 1450°C., the illumination of the grain for Fig. 11b being adjusted to bring out points of similarity (in general grain E reflected light almost like a single crystal). Inspection of these photographs discloses that the boundaries of the distorted areas within grain E are indistinct in Fig. 11a and sharp (except for one boundary that passes through position L) in Fig. 11b. The high-temperature anneal, therefore, transformed indistinct boundaries into sharp ones.

The Laue photographs shown in Figs. 12 through 15 illustrate some of the structural changes that occurred during the anneals; for example, a Laue photograph for position L after the anneal at 900°C. was practically identical with the one shown in Fig. 12 for the same position after the 1175°C. anneal. The diffraction pattern in Fig. 13, however, shows that some change occurred during the 1450°C. anneal. Another example is the change that occurred for positions of the type marked M and N in the photograph. A Laue photograph for position M after the 900°C. anneal consisted of overlapping patterns for two orientations. Another picture, Fig. 14, for the same position after the anneal at 1450°C. shows these two orientations with the distortion removed. The single Laue pattern in Fig. 15 is identical with one of those in Fig. 14, even though position N is 3 mm. from position M. In general, Laue patterns for other boundaries and areas were composed of double and single orientations.

The aggregate of crystals within the area of old grain E have a spread of 7° in orientation in such a way that plotted in stereographic projection ther fall into an orientation state of size $3\frac{1}{2}^{\circ}$. The orientation at position L together with its spread of about 3° falls also within this state.

The microstructure at position L was investigated for fine structure. Little was disclosed until the surface was etched

for 5 min. with 4 per cent Nital; then five parallel lines became visible. These were spaced roughly 20 microns apart and at an angle of 60° with the surface. From this angle, and the one made in the surface, it appeared that the narrow bands were separated on (211) planes. The structure of Laue spots for large Bragg angle (Fig. 13) also indicates the possible presence of at least six different orientations.

It is to be noted from the photograph in Fig. 11b that there are other lines that are roughly parallel to the diagonal one passing through position L. Consequently, slip on (211) planes and other [112] planes may have occurred during the formation of the various bands or distorted areas; and recovery may have removed the spread in orientation, not only within a distorted area, but also at a boundary produced by two regions undergoing different amounts of lattice rotation about the same axis through different amounts of slip in the same slip direction. The appearance of Laue spots in Fig. 12 confirms this for the case of the five parallel bands described previously, because the [OII] direction that would be required for the axis of rotation of the lattice undergoing slip in a [111] direction on (211) planes lies near the best single axis for Fig. 12. This fact also checks with the analysis of the microstructure.

Effect of Neumann Bands on Distortion of a Grain and on Class-3 Recovery

One specimen will be used to illustrate the distortion of a grain and two others will be used to show some transformations produced in the initial stages of an anneal.

Specimen TW14 developed a small group of Neumann bands in one large grain during a tensile extension of 0.6 per cent. Laue photographs for the position of the bands and 2 mm. from them appear in Figs. 16 and 17, respectively. A 4-hr.

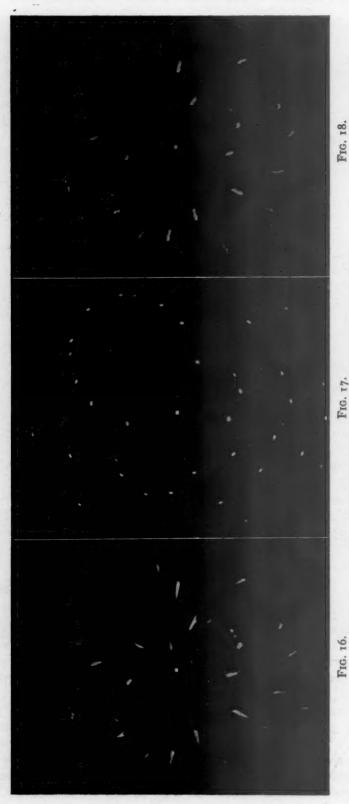


Fig. 16. At position of Neumann bands.
Fig. 17. At 2 mm. away from position of Neumann bands.
Fig. 17. At 2 mm. away from position of Neumann bands.
Fig. 18. After 4 hr. anneal at 1175°C. and at position of original Neumann bands.

anneal at 1175°C. removed the Neumann bands but no recrystallization occurred. Fig. 18 shows a Laue photograph for the Neumann band region after the 1175°C.

samples were selected from these two specimens. Each single crystal was then divided into two parts and one part of each was annealed for 2 hr. in the range

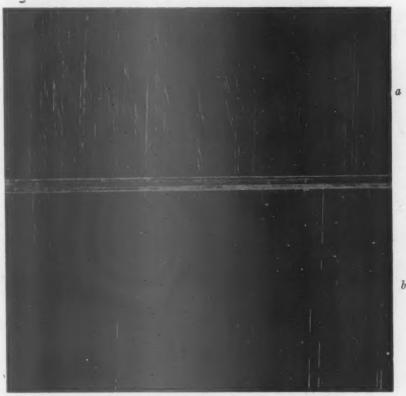


Fig. 19.—Micrograph of sample A3, showing appearance of Neumann bands. Etched 10 seconds in 4 per cent Nital. X 10.

a, before annealing; b, after annealing.

anneal. An analysis of these Laue patterns shows that the Neumann bands produced a spread of 3½° to 4° in the main lattice, and that the anneal reduced this spread a small amount. Some reflection spots for Neumann-band structure are plainly visible in the Laue pattern in Fig. 16, but these reflection spots are not present in Fig. 18 for the annealed sample. This, incidentally, confirms the visual observation that the bands were removed.

Another specimen, TW22, contained many Neumann bands after a tensile extension of 0.6 per cent. Specimen A3 also contained many bands after a cold-rolling reduction of 4 per cent. Single-crystal

500° to 900°C.; the other was left as deformed. Comparison of the annealed and unannealed parts of the same crystal disclosed that Neumann bands grew a small amount in some regions (were enlarged) and were removed in other regions by the old grain (Laue patterns indicated no change in the orientation of the old grain). Fig. 19, which shows the microstructure of a crystal before and after annealing. clearly indicates these two transformations. Fig. 20, at 100 diameters magnification, however, not only shows growth of Neumann bands in some areas and their removal in other areas, but also shows where Neumann bands were before the old grain absorbed them. (One such region is marked by an arrow.)

Lattice Structures in Recovery and Growth of a Deformed Grain

In this example, a deformed grain grows at the expense of a neighboring Figs. 11a and 11b is only a fair illustration). Both of these grains originally contained Neumann bands; those in grain F were in one corner, whereas those in grain B were distributed rather uniformly throughout the grain. Macrographs and Laue photographs were obtained after anneals

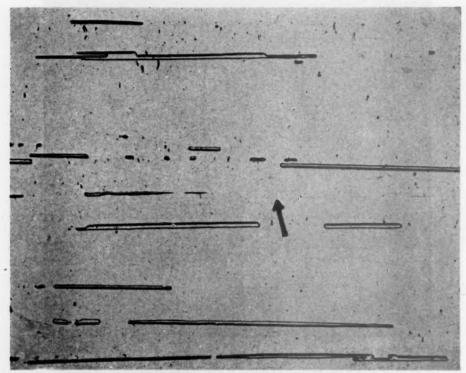


Fig. 20.—Micrograph of sample TW22 after annealing. Etched 2 minutes in 4 per cent Nital. × 100.

grain. Two grains, B and F (Fig. 21) of specimen TW12 are taken for illustration (boundary changes in grain E shown in



FIG. 21.—POSITION OF GRAINS B AND F IN SPECIMEN TW12 AFTER ANNEAL AT 1450°C. ETCHED WITH DILUTE NITRIC ACID. X 3.

of 900°, 1175° and 1450°C. Comparison of the photographs showed that grain F did not grow until the 1175°C, anneal, but the area of grain B increased about 10 per cent during the 900°C. anneal in one boundary region where Neumann bands were present in the adjacent grain. During the final anneal the new part of grain F (this part is about one third the size of the original grain) became a neighbor of grain B and grew a small amount at the expense of grain B. Figs. 22, 23 and 24 show Laue photographs for positions 1, 2 and 3 of grain F as marked on the photo-

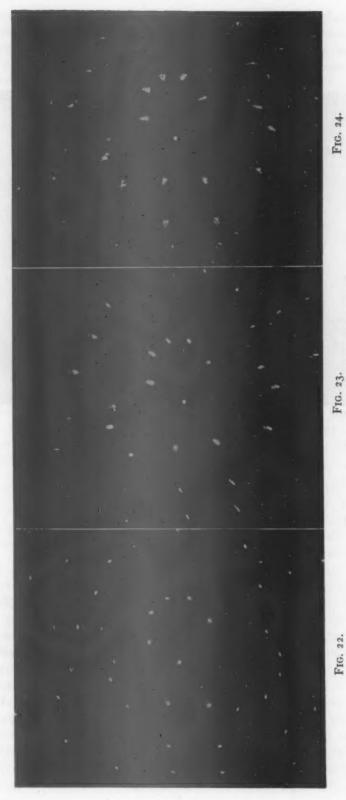


Fig. 22. New area formed by growth, at position 1 in Fig. 21. Fig. 23. Old area, at position 2 in Fig. 21. Fig. 24. At position 3 in Fig. 21.

graph in Fig. 21. Position 1 is in the area of the new grain; position 2, in the area of the old grain; and position 3, once a grain boundary, is now a point where new

were present in the area represented. This, however, is not quite the picture of the entire grain, because some areas gave very close doublet structures either partially

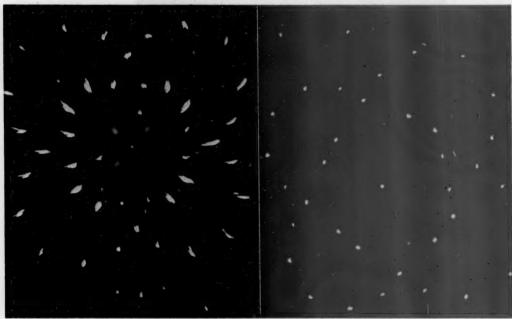


Fig. 25.

Figs. 25 and 26.—Laue photographs of grain B.

Fig. 25. After 900°C. anneal.

Fig. 26. After 1450°C. anneal.

and old join together. On both sides of position 3 there is a distinct boundary between the new grain and parts of the old one, as would be expected from the fact that the old grain did not recover to a single lattice structure. Comparison of Figs. 22 and 23 shows that new and old orientations fall within about one degree of each other. At position 3, however, they fall together. A finer beam would have been used to eliminate some of the structure variation except for the fact that it was not possible to locate the proper boundary position accurately enough.

The effect of the annealing on the lattice of grain B can be seen by comparing Figs. 25 and 26. Recovery occurred to a high degree. The transformation is remarkable because originally Neumann bands

or just completely separated in the Laue patterns.

Effect of Time and Temperature on Class-3 Recovery

In any heat-treatment the factors of time and temperature are involved. From the previous results, one could say that the average rate of recovery increases with temperature. If class-3 recovery were simply the removal of asterism and the production of single sharp Laue spots, the rate of change of size of a Laue spot could be measured and used to get the rate of recovery. Fortunately, this can be done if there is available a case of single-lattice type of class-3 recovery and a single crystal large enough to be divided according to the number of heat-treat-

ments needed. These conditions are not easy to meet simultaneously.

An attempt was made, nevertheless, to select a fairly large crystal suitably oriented for a study of amount of orientation spread for certain Laue reflection spots versus time at 1000°C. Results for a sample originally cold-rolled 12.7 per cent were as follows:

Since the final structure, which varied some from sample to sample, was a close doublet, it is necessary to view these results as essentially qualitative. They do confirm the previous results, however, which showed that class-3 recovery is a slow process. They also point to a rather rapid recovery at the beginning of the heat-treatment (if the temperature is high enough) and a rather slow change, as would be expected, toward the end of a long heat-treatment.

Large single crystals seem to be needed to obtain quantitative data for various temperatures as well as for various times at temperature. They are also needed to study the effect of recovery on rate of growth (see next section). Consequently, we are now making an effort to prepare large single crystals for use in these investigations.

Effect of Recovery on Rate of Growth

If a deformed single crystal is in a condition only to recover at some temperature (for example, 1100°C.), it provides an ideal sample for studying the effect of recovery on the rate of growth of one or more nuclei introduced after a recovery heat-treatment. Nuclei may be introduced into such a crystal through a Rockwell indentation in one corner of the sample. (Experience has shown that a Rockwell indentation is sufficient to cause recrystallization to occur in the area of the

indentation of an otherwise undeformed single crystal during an anneal of 5 min. at 000°C.)

Results for two crystals, E₅A and E₅B, each subdivided into three parts, following a cold reduction of 10 per cent, appear in Table 2. Anneal No. 1 was given prior to the Rockwell indentation, anneal No. 2 after it.

TABLE 2.—Effect of Recovery on Growth

Crystals	Anneal No. 1	Recovery
A ₁ , B ₁	4 hr. at 1100°C. 15 min. at 1100°C. None	Some class-3 Some class-3
Crystals	Anneal No. 2	Growth, Per Cent
A ₁ , B ₁ , A ₂ , B ₂ A ₈ , B ₈	30 min. at 1100°C. 5 min. at 1100°C.	O Ba, 100; Aa, 50

All single-crystal samples contained nuclei after the second anneal; so whatever the transformation was during the preliminary heat-treatments, it must be admitted that it modified the ability of these new grains to grow; and unless a small amount of class-3 recovery could do this, it must be assumed that recovery in the other two classes was also involved.

It is hoped that quantitative data on rate of growth may be presented at a later date for recovery temperatures taken above and below the growth temperature, and with orientation differences between new and old grains taken into consideration.

Crystal Distortion in a Recrystallized Matrix and Class-3 Recovery after Recrystallization

If Laue reflection spots show asterism or other forms of departure from good reflection spots for a new grain, the grain is said to be distorted or strained in a way to produce a spread in orientation.

Although many samples could be cited



FIG. 29.

FIGS. 27-29.—LAUE PHOTOGRAPHS OF GRAIN H4A. Fig. 27. After cold reduction of 10 per cent. Fig. 28. New grain No. 19 after 750°C. anneal. Fig. 29. Grain No. 19 after reanneal of 8 hr. at 1175°C.

FIG. 27.

that show distortion in nuclei early in their growth and in recrystallized grains heat-treated well beyond the temperature and time required for complete recrystallization, only one case will be given for illustration, a case where the distortion produced marked asterism in Laue reflection spots. A single crystal, H4A, 0.014 in. thick and cold-rolled 10 per cent in a <110> direction in a {110} plane, was divided into five parts for annealing various lengths of time at 750°C., to obtain the early appearance of recrystallization nuclei. One piece, annealed for 90 min., was about 70 per cent transformed according to surface area on one side. The other side appeared to be transformed only about 10 or 15 per cent.

Nucleus No. 19 was about 2.5 mm. long, and largely surrounded by other nuclei, but it did not extend through the thickness of the old single grain. Directly behind it was the unrecrystallized grain. Some of this old grain structure was etched away to leave a specimen approximately 0.006 in. thick. Asterism was present in Laue photographs of grain No. 19 before the etching treatment and also after it. Two other nuclei out of a total of 21 showed distorted Laue spots, but to a lesser degree.

The sample was then reannealed for 8 hr. at 1175°C. Recrystallization was complete. Figs. 27, 28 and 20 show, respectively, Laue photographs of the old grain, grain No. 10 and the old grain, and grain No. 10 after 1175°C. anneal. Although the condition of Laue spots in Fig. 29 indicates some distortion in grain No. 19 even after the 1175°C. anneal, the spread in orientation-roughly 1/4°-is considerably less than the original 2° spread that was present after the 750°C. anneal. Consequently, it is evident that crystal distortion existed in grain No. 10, a recrystallization nucleus, and that most of this distortion was removed by recovery of reannealing at a higher temperature.

DISCUSSION OF RESULTS

There are two reasons why the experimental results have been listed under recovery and not under a special case of recrystallization—namely, one without change in orientation through growth of a fragment of the deformed crystal.

First, specimens G₅A and G₄C had microstructure doublets after annealing that were closely related to the structures before annealing; and grain E of specimen TW₁₂ appeared to change visibly only through a sharpening of indistinct boundaries. If a fragment of a crystal were to grow for each of the final orientations, it would be expected that these boundaries would be modified to a noticeable degree, because a difference in orientation is known to be no barrier to grain growth.

Second, crystals that were heat-treated for various periods of time at temperature (some, in fact, heat-treated several times in succession) changed in such a way that the elongations of Laue spots diminished slowly with time. Growth of a small fragment would require a sudden change from full asterism to sharp Laue spots as the boundary advanced; but the observed changes were always of a continuous type.

In addition to the continuous change of the spread in orientation with time and temperature, as was clearly illustrated in a prior report (see Fig. 12 of ref. 2), there is for some cases of recovery in a polycrystalline sample almost complete retention of the old grain boundaries.

The present work confirms some observations on silicon ferrite that were reported earlier: namely, high-temperature anneals can produce sharp Laue spots through recovery; an old grain during recovery can remove Neumann bands; the spread in orientation near Neumann bands may be 1½° greater than in adjacent regions free of bands, and recovery can inhibit grain growth. In the present work, how-

ever, the spread in orientation due to Neumann bands was found to be as high as 4°. In the case having 1½° spread, the sample was cold-rolled 3 per cent; but in that having 4° spread the sample was elongated 0.6 per cent in tension. Consequently, there may have been a greater differential of cold-work in the latter case, with most of the distortion occurring near the Neumann bands. (This statement is in agreement with the Laue photographs, which show very little distortion except in the Neumann-band area.) Barrett¹¹ recently reported a value of 1° for the extra distortion near Neumann bands.

Knowing that the lattice adjacent to Neumann bands is more distorted than in other areas, and that the lattice is also interrupted by a number of jagged parallel Neumann bands, it is reasonable to expect a complex recovered structure of the type reported for sample G4C. This is not to say that the structure after recovery must be more complex in a Neumann-band area. Neumann bands may grow at the expense of the highly distorted region adjacent to them, as indicated in the micrographs of Figs. 19 and 20, and this may remove orientations otherwise capable of recovery. When the old grain absorbs these enlarged Neumann bands, it may do so according to the less distorted matrix structure. Such a process may have occurred in grain B of specimen TW12, for example, because grain B recovered remarkably well from distortion produced by many Neumann bands as well as by an 8 per cent elongation.

It is known that a deformed crystal is an extremely imperfect one, and that small adjustments of a few atoms are able to remove an imperfection such as a dislocation (class-1 recovery). Larger adjustments or the accumulation of many small adjustments could produce local orientation changes capable of sharpening Laue spots. Except for the element of size involved it is possible that class-3 recovery and class-1 recovery have similar

mechanisms. This is no argument, however, against the separate classifications, which were purposely made according to size of sample involved in a test and according to experimental methods employed.

Qualitatively it would appear that recovery has a pronounced effect on the growth process in recrystallization. Furthermore, when recovery has proceeded far enough to stop growth in a deformed grain (as it did in four crystals of E5A and E5B), it assuredly has recovered enough to prevent recrystallization. Laue photographs for crystals E5A and E5B indicated that class-3 recovery was not at all complete when growth was stopped; so a more complete recovery treatment-as, for example, that in grain E2B or grain TW12B -would produce a sample even less likely to recrystallize. Consequently, the ideas expressed recently11 that a grain will recrystallize if it has a fragmented structure, and that no recovery will remove the fragmented character of images in X-ray micrographs, must be held in doubt.

It is theoretically possible that the rate of growth of a recrystallization nucleus may become negative during recovery of the parent grain. In such a case the new grain would be absorbed by the old crystal in a manner similar to that reported for the removal of Neumann bands.

Results obtained on specimen H4A indicate that recrystallized grains can exist in strained states of varying degrees of strain. Although further heat-treatment of this sample completed the recrystallization process, it also changed the strained nuclei that were present into grains that appeared to be almost free of strain. Recovery need not be the only transformation following recrystallization—grain growth or even recrystallization may occur.

Because of the results on strain (sample H4A), on growth (specimen TW12, grains B and F) and on recovery (sample H4A and others), and because of existing differences in the meaning attached to the

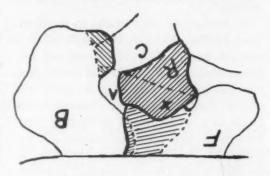
terms "grain growth" and "recrystallization," a discussion of them seems to be in order.

We note that there is little to differentiate between a recrystallized sample and one plastically deformed a small amount because both have strains. On being heat-treated, both may either undergo recovery or develop large grains through growth of favored grains (grain F of strained specimen TW12 grew, for example) or possibly through nucleation and growth. Both samples, therefore, appear to be cases of either grain growth or recrystallization, depending upon what it is that grows. The first transformation that occurs following cold-work excluding recovery, however, is usually considered to be recrystallization, and it may be in most cases. Nevertheless, unless nucleation can be established for the strained sample and lack of nucleation established for the recrystallized one, can we say that the one recrystallizes and the other merely undergoes grain growth?

This is a dilemma. As a suggestion, which would involve some change in the meaning of the terms "recrystallization" and "grain growth," more emphasis might be given to the similar and well-known features of these two processes and less emphasis to the different and, in some cases, unknown features. For illustration, consider what happened in sample TW12 with the aid of the following diagram. The dotted lines represent original grain boundaries, the heavy solid lines* final and new grain boundaries, and the light solid lines, boundaries that remained essentially unchanged.

Grain R resulted from the growth of a nucleus formed among Neumann bands (not shown) at the position of the cross in grain A. Omitting an infinitesimal amount of material for the nucleus, we can say that the rest of the metal of grain R (shaded area) recrystallized during the anneals. This recrystallization occurred

through growth of the nucleus at the expense of grains A and C. The shaded areas of grains B and F also represent metal similarly transformed; so it would be



logical to say that these shaded areas represent recrystallized metal. Note that part of grain B recrystallized through growth of grain F. Otherwise these old grains themselves did not recrystallize. The quantitative measure of the amount of recrystallization would correspond to the shaded areas.

Although sample TW12 was plastically deformed prior to annealing, we might similarly consider such transformations if they should occur without prior deformation—transformations more likely to occur for fine-grained samples. This would give two features of recrystallization: namely, (1) formation of new grains (nucleation) or the start of growth of old (or parts of old) grains, and (2) the growth of these grains. The quantitative measure of the amount of recrystallization would be the metal transformed through growth.

Recrystallization in this sense might be subdivided into primary recrystallization, secondary recrystallization, and so on, according to order of occurrence following plastic deformation. Primary recrystallization could occur by nucleation and growth or by growth of grains already present; secondary recrystallization could occur theoretically by nucleation and growth as well as by grain growth, the usual expression for the second transformation.

The writer believes that the use of the term "recrystallization" in this sense

^{*} Taken from photograph shown in Fig. 21.

rather than the usual one would eliminate controversial viewpoints of the type recently expressed on results involving nucleation, recrystallization, and grain growth.12

In connection with strains in recrystallized grains, we know that it is easy to convert an elastic strain (produced mechanically) into a plastic one by heating the elastically deformed grain until the elastic limit is exceeded. Moreover, we know that a cold-rolled grain may have both macroscopic and microscopic stresses within it. Should a nucleus, therefore, be formed before the stresses are removed, it might similarly undergo plastic deformation as the stresses near it become relieved. If this explanation is approximately correct (further experimental work is needed) it might be that the effect would be more pronounced for silicon ferrite when recrystallization occurs below 750°C., the temperature used in sample H4A.

CONCLUSIONS

Recovery of the type called class 3 can occur to the extent of almost 100 per cent and thus produce sharp Laue spots in X-ray diffraction patterns.

When a deformed grain consists of two structures or deformation bands, class-3 recovery can produce a sharp grain boundary between them as well as form two separate undistorted lattices. When a distorted grain consist of several regions differing in orientation, class-3 recovery can produce grain boundaries and thus complete the final step in a grain-refinement process.

The distortion of the lattice of a grain adjacent to Neumann bands is of the nature of a spread in orientation of the order of one to four degrees additional to the spread in orientation of the lattice free of Neumann bands.

A Neumann band within a deformed grain can be absorbed by the old grain during recovery or can grow a small amount and then be absorbed.

Although class-3 recovery may be rapid in the early part of a high-temperature anneal, usually it is far from complete after a few hours (temperature approximately 1100°C.) and nears completion only in a time measured in days.

The amount of recovery that occurs in a time of about 15 min. at 1100°C seems to be sufficient to reduce the rate of growth of a new grain to practically zero. More complete recovery of the type reported, therefore, should not only stop grain growth but should stop all recrystallization.

A recrystallization nucleus formed in an anneal may be distorted sufficiently to show a spread of as much as two degrees in the orientation of its lattice. Consequently, all nuclei formed in an anneal are not free of plastic strains.

ACKNOWLEDGMENTS

The writer wishes to thank Mr. Weston Morrill and Mr. Raymond Ward for valuable discussions on grain growth, recrystallization and recovery, and Miss Margaret E. Smith for her aid in the preparation of diagrams and figures

RFFERENCES

- I. R. F. Mehl: Metals Handbook (1939) 207.
- Amer. Soc. for Metals.
 2. C. G. Dunn: Trans. A.I.M.E. (1944) 158,
- 372.
 3. F. Seitz and T. A. Read: Inl. Applied Physics (1941) 12, 100.
 4. J. S. Koehler: Phys. Rev. (1941) 60, 397.
 5. C. S. Barrett: Structure of Metals, (a) 339, (b) 354, New York, 1943. McGraw-Hill Book Co.
- Hill Book Co.
 6. G. L. Clark and W. M. Shafer: Trans.
 Amer. Soc. for Metals (1940) 28, 853.
 7. F. S. Goucher: Phil. Mag. (1926) 2, 289.
 8. C. F. Elam: Distortion of Metal Crystals,
 (a) 159, (b) 158 Oxford, New York, 1935.
 9. J. A. Collins and C. H. Mathewson: Trans.
 A I M. E. (1940) 127, 150.

- A.I.M.E. (1940) 137, 150.

 10. U. Dehlinger: Metallw. (1933) 12, 48.

 11. C. S. Barrett: Trans. A.I.M.E. (1945) 161,
- 12. J. K. Stanley: Trans. A.I.M.E. (1945) 161, 169.

The Solubility of Hydrogen in Molten Iron-silicon Alloys

By Hung Liang,* Student Associate, Michael B. Bever,† Junior Member and Carl F. Floe,‡ Member A.I.M.E.

(Chicago Meeting, February 1946)

DATA on the solubility of hydrogen in iron-silicon alloys are of practical interest, as hydrogen causes gas unsoundness and embrittlement in iron and steel and is also a factor in the metallurgy of cast iron. Zapffe and Sims1 have recently demonstrated that in deoxidized iron and steel castings gassiness and bleeding are primarily functions of the hydrogen content of the liquid metal. These authors also suggested convincingly that ordinary melting and casting practice provides several sources of hydrogen for absorption by the metal. Norbury and Morgan,2 and Boyles3 have shown that dissolved hydrogen affects the graphitization of cast iron. Schneble and Chipman4 included in a study of the effects of superheating on the properties of cast iron an investigation of the part played by hydrogen. Schwartz. Guiler and Barnett⁵ investigated the significance of hydrogen in the metallurgy of malleable cast iron. A complete interpretation of investigations of this kind calls for equilibrium values of the solubility of hydrogen in the liquid and solid phases.

From the theoretical standpoint, the solubility of gases, especially hydrogen, may reveal some aspects of the nature of liquid metallic solutions. This was implied in the early work of Sieverts6 on the effect of alloying additions on the solubility of hydrogen in copper. Recent work by Bever and Floe⁷ has shown that in liquid copper-tin alloys the solubility of hydrogen changes abruptly at the composition of the intermetallic compound Cu₃Sn. It is of considerable interest to determine whether liquid alloys of iron also have compositions at which the solubility of hydrogen exhibits a discontinuous or otherwise unique behavior.

Among the various alloys of iron the iron-silicon system is important because of the presence of silicon in various structural alloy steels, transformer sheets, cast irons and special acid-resisting castings. The various grades of ferrosilicon, finally, cover almost the entire remainder of the composition range.

Published information on the solubility of hydrogen in iron-silicon alloys is meager. The first values for pure liquid iron were reported in 1910–1911 by Sieverts and Krumbhaar⁸ and by Sieverts.⁹ They found that 100 grams of iron absorbs 28 c.c. of hydrogen at 1550°C. and one atmosphere pressure, and 31 c.c. at 1650°C. In 1938 Sieverts, Zapf and Moritz¹⁰ published a value of 26.3 c.c. at 1550°C. Data on the solubility of hydrogen in liquid iron-silicon alloys and in liquid silicon are not available. Martin¹¹ investigated

* Graduate Student, Department of Metallurgy, Massachusetts Institute of Technology, Cambridge, Massachusetts.

This work represents a portion of a thesis submitted by H. Liang in partial fulfillment of the requirements for the degree of Master of Science from the Massachusetts Institute of Technology, Manuscript received at the office of the Institute Oct. 26, 1945. Issued as T.P. 1975 in Metals Technology, February 1946.

[†] Assistant Professor of Process Metallurgy, Massachusetts Institute of Technology. ‡ Associate Professor of Physical Metallurgy,

Massachusetts Institute of Technology.

References are at the end of the paper.

the solubility for solid alloys up to about 5 per cent silicon in the temperature range from 400° to 1200°C. and found that silicon had only a small effect. The solubility of

at a certain temperature and pressure and the so-called hot volume, which is the volume of an insoluble gas necessary to fill the furnace under the same conditions.

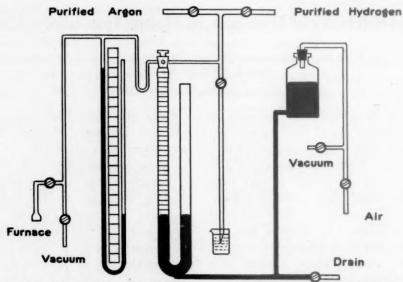


FIG. 1.—DIAGRAM OF APPARATUS USED FOR SOLUBILITY DETERMINATIONS.

hydrogen in solid iron-silicon alloys has also been studied by Iwasé and Fukusima.¹² Vaughan and Chipman¹³ investigated the solubility of nitrogen in molten iron-silicon alloys.

This paper presents the results of an investigation of the solubility of hydrogen in representative compositions of the ironsilicon system up to 65 per cent silicon at temperatures ranging from above the liquidus to 1650°C. and at one atmosphere pressure.

EXPERIMENTAL METHODS

In choosing between the two methods for the determination of gas solubility in liquid metals, the extraction method was rejected because of anticipated difficulties in quenching and analyzing the samples. The hot-volume method was therefore used. In this method, originally developed by Sieverts, the solubility is determined by finding the difference between the volume of the soluble gas admitted to the furnace

Fig. 1 shows the layout of the apparatus, which consisted of the furnace proper, the gas-measuring system and the gas-purification equipment.

The furnace, shown in detail in Fig. 2, was a modification of the furnace of Vaughan and Chipman.13 Its chief parts were a silica tube and a brass head joined together permanently by a picein seal. The brass head consisted of three sections. For charging and cleaning, the top and center sections could be removed in one piece. These sections could be separated in order to insert a glass shutter in a horizontal slot between them. The shutter was used to protect the glass window in the top section from fogging during the highsilicon runs. The glass fitted into an iron ring and could be moved out of the way by a magnet before temperature measurements were taken.

In the preliminary experimental work, the metal was melted in alundum thimbles but the runs reported here were all made in beryllia crucibles backed by beryllia sand. The crucibles were 30 mm. o.d. by 80 mm. high, with a wall thickness of 1 to 2 millimeters.

In order to decrease the hot volume, the open space inside the furnace was reduced

about 0.5 per cent of impurities, chiefly nitrogen. The gas was passed through a furnace containing metallic calcium turnings at about 500°C. and then through a phosphorus pentoxide absorption tube. The

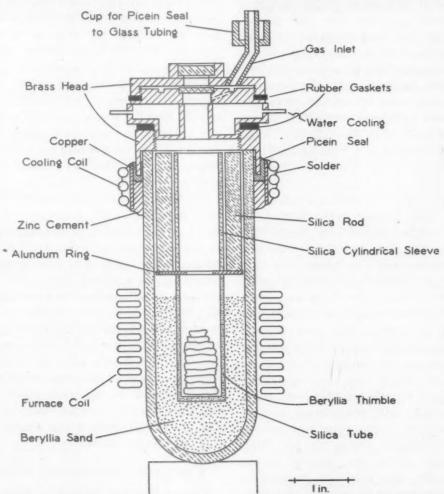


Fig. 2.—Cross section of furnace used for solubility determinations.

by a cylindrical sleeve of silica surrounded by silica rods. The sleeve and rods rested on an alundum disk, which was supported by the crucible as shown in Fig. 2. This arrangement allowed unhindered inspection of the metal surface through the glass window along the central axis of the furnace. A Leeds and Northrup "Pyro" optical pyrometer was used for temperature measurements.

The tank argon was reported to analyze

tank hydrogen was treated in a furnace packed with platinized asbestos and heated to about 600°C. This unit was followed by an absorption tower containing silica gel and a U-tube containing phosphorus pentoxide.

The purified gases were admitted to the measuring system by a two-way stopcock at the top of the burette. The burette had a capacity of 100 c.c. and could be read to 0.1 c.c. Mercury was used to

displace the gas. The two-way stopcock at the top connected the burette to the furnace.

Two kinds of iron were used, electrolytic analyzing 99.9 per cent and iron made from electrolytic sheet under hydrogen and containing 0.08 per cent silicon. The latter had been prepared for some previous experiments. The metallic silicon analyzed higher than 98 per cent with iron the chief impurity. A silicon-bearing master alloy made by melting electrolytic iron under hydrogen and adding silicon was also used. With the induction equipment available, alloys containing more than about 70 per cent silicon could not be melted.

The procedure for making a run was as follows: The furnace was charged by placing weighed amounts of charge constituents into the crucible and setting the fillers in place. The furnace was then closed, sealed to the system and evacuated for an hour or more. The charge was melted and held under vacuum for at least half an hour to extract any gases present. Hydrogen was then passed in for approximately one hour to deoxidize the metal.

The hot volume was next determined with argon. Burette readings were taken simultaneously with temperature readings until both the temperature and volume became constant. Owing to the large amount of refractory material inside the furnace, the time for reaching a steady state ran up to one hour. Readings at four to five different temperatures were sufficient to determine the hot volume, which is a straight-line function of temperature within the experimental error. The hot volume in the various runs amounted to 70 to 90 c.c. and its temperature coefficient averaged minus 2.5 c.c. per 100°C.

After determination of the hot volumes, the argon was evacuated and hydrogen was measured into the system. In the runs with alloy compositions dissolving large amounts of hydrogen, it was necessary to refill the burette before the metal became saturated, as the sum of the hot volume and the volume of absorbed gas exceeded the capacity of the burette. The general procedure for obtaining readings with hydrogen was the same as that used with argon. The sequence of temperatures for observation was so chosen that some equilibrium values were established by raising the temperature while others were reached by cooling. This assured that the observed solubility readings represented equilibrium values. In a number of runs the hot volumes were again measured after the determinations of hydrogen solubility.

The equipment and experimental procedure described in the foregoing was the result of considerable preliminary work. In particular, an end point could not be reached in the initial runs, since hydrogen disappeared at a rate of from 5 to 10 c.c. per hour. After considerable experimentation, it was found that condensed water could exist inside the hot furnace along the water-cooled surfaces and it was suspected that near to the iron bath the alundum refractories used at that time might react with hydrogen. It was then decided to substitute beryllia crucibles and beryllia sand, and as a result of this change the drift of hydrogen ceased.

RESULTS OF EXPERIMENTAL WORK

Table I lists the volumes of hydrogen soluble in iron at one atmosphere pressure as a function of temperature. The values of Sieverts and collaborators^{8,10} are given for comparison. The iron used analyzed 0.08 per cent silicon, but such a small amount has no appreciable effect on gas solubility. A plot of the solubility of hydrogen in iron as a function of temperature gives a slightly curved line, but the accuracy of the values is not sufficient to establish this curvature definitely. The best straight line was therefore drawn

through the points, which resulted in a solubility value of 29.2 c.c. (S.T.P.) of hydrogen per 100 grams of iron at 1550°C. and one atmosphere pressure and a temperature coefficient of 3.3 c.c. per 100°C.

TABLE 1.—Solubility of Hydrogen in Iron at One Atmosphere Pressure as a Function of Temperature

Investigation	Deg. C.	H: (S.T.P.) in 100 Grams Fe, C.C.	Temperature Coefficient $\Delta H_2/\Delta T$ C.C. in 100 Grams per 100°C.
This investigation	1556 1590 1654	28.9 30.8 32.9	3.3
Sieverts and Krumb-	1696 1744	34.4	
haar (1910)	1550	28.0	3.0
Sieverts, Zapf and	1650	31.0	
Moritz (1938)	1550	26.3	

Table 2.—Solubility of Hydrogen in Ironsilicon Alloys at One Atmosphere Pressure—Observed Values

Run	Deg. C.	H ₂ (S.T.P.) in 100 Grams Metal, C.C.	Run	Deg. C.	H ₂ (S.T.P.) in 100 Grams Metal, C.C.
16	1696	34.4	17	1593	7.5
	1654	32.9		1475	6.3
	1744	34.9 28.9		1519	6.1
	-		25	1411	7.6
22	1599	29.9		1569	9.4
	1688	32.5		1470	8.1
	1519	26.3		1592	9.7
	1545	31.4	24	1452	10.9
	1343	27.4	24	1507	11.4
20	1411	12.7		1362	9.5
	1641	17.2		1572	11.9
	1470	13.9		1651	13.1
	1556	15.8		1403	9.2
	1342	11.3			
			21	1411	12.9
18	1511	9.0		1597	14.7
	1290	6.5		1300	11.7
	1611	10.0		1507	14.5
	1250	7.5		1230	12.7
	1428	7.9	27	1310	20.4
	1556	9.7		1549	22.6
	20-	1		1611	23.5
				1385	21.5

Table 2 gives the measured hydrogen solubilities for the various alloy compositions in the temperature sequence in which they were made. In Table 3 and Fig. 3

these solubilities are presented for even temperatures; these values were found graphically on the assumption that the solubility is a straight-line function of the temperature. The solubilities may be read in two different units from Fig. 3.

Table 3.—Solubility of Hydrogen (C.C. H₂ in 100 Grams of Metal) in Ironsilicon Alloys at One Atmosphere Pressure and Various Temperatures

	Compo	sition	Temperature, Deg. C.											
Run No.	Wt. Per Cent Si	At. Per Cent Si	1350	1400	1500	1550	1650							
16	0.08	0.28				29.2	32.5							
22	1.78	3.48			25.5	27.5	31.6							
20	11.0	19.7	11.5	12.5	14.4	15.4	17.4							
18	21.7	35.6	7.0	7.6	8.9	9.5	10.7							
17	31.5	47.8		6.0	6.5	6.8	7.3							
25	39.I	56.1			8.5	9.1	10.3							
24	45.7	62.7	9.3	9.9	II.I	11.8	13.1							
21	51.5	67.8	12.7	13.1	14.0	14.4	15.3							
27	63.7	77.7	20.9	21.4	22.4	22.9	23.8							

DISCUSSION OF RESULTS

The hydrogen solubility values for pure iron of Sieverts and collaborators and of this investigation show satisfactory agreement. No attempt will be made to evaluate the comparative accuracy of these results, but the possible sources of error occurring in this investigation will be discussed. These were changes in weight and composition of the metal bath, side reactions and adsorption, impurities in the gases used, inaccuracy of pressure and temperature measurements and experimental difficulties inherent in the hot-volume method.

The weight of metal charged in most of the runs ranged from 90 to 115 grams. After each run the metal that solidified in the crucible weighed less by 2.5 to 11 grams. These losses were due to splashing caused by too rapid evacuation of hydrogen and to evaporation. The evaporation loss was mainly a function of time. Under the conditions of the experiments an

appreciable change in the composition of the alloys by fractional distillation was not likely to occur, which was confirmed by a comparison of the amounts of conThe possibility that hydrogen was adsorbed on various parts of the furnace, and especially on the beryllia sand, should be considered. Since induction heating

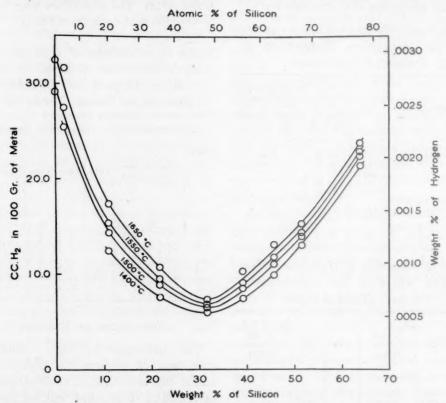


FIG. 3.—Solubility of hydrogen in iron-silicon alloys at one atmosphere pressure and various temperatures as a function of composition.

stituents charged and the chemical analyses after each run. While there were no difficulties due to composition changes, weight changes had to be allowed for by finding the average loss of metal per hour and thus determining the probable true weight of the metal at the time each measurement of hydrogen solubility was made. This correction ignores the solubility of hydrogen in the lost metal. The error thus introduced is small, since much of the metal was probably at relatively low temperatures and dissolved little hydrogen.

In the preliminary work a side reaction occurred between hydrogen and alundum, but was suppressed when beryllia was substituted for alundum. was used, the magnitude of the effect could not be determined in an empty furnace, but because of the high temperatures of most of the surfaces it was probably not large.

The tank gases used were purified as described. However, the possibility of gas contamination through a leak in the purification system remained. Positive pressure was relied on to minimize this danger. If the hydrogen used had been contaminated with air, unduly high apparent solubility values would have been found, while contaminated argon would result in too large apparent hot volumes and consequently in too small hydrogen solubility values.

The solubility values were measured at the existing barometric pressures. Owing to the square-root relation between the pressure and the solubility in metals of a diatomic gas (Sieverts' law), the corrections for the difference between the observed barometric pressure and the standard pressure of one atmosphere were less than 0.1 cubic centimeter.

The temperature measurements were made with an optical pyrometer. Since the bath was not under black-body conditions, and radiation was absorbed by the glass window, the temperatures read were not the true temperatures. The following correction formula was used:

$$\frac{\mathbf{I}}{S} - \frac{\mathbf{I}}{T} = K$$

where S is the true temperature and T the observed temperature in degrees absolute. K was determined repeatedly at the freezing point of electrolytic iron, which was taken as 1535° C. Actually, the emissivity of the metal surface of the various alloys differed from that of pure iron but the use of the K value thus determined caused only a negligible error.

Since the solubility of hydrogen was found by subtracting from the total hydrogen the hot volume determined with argon at the same temperature and pressure, any difference in the thermal behavior of the two gases affected the accuracy. It was found that with hydrogen in the furnace more power was required to maintain the metal at any one temperature than with argon and that the furnace walls glowed with brighter colors, which indicated that the thermal conditions above the bath were different. Consequently, the temperature distributions and hot volumes were also different. However, the accumulated experience of investigators in this field suggests that the difference in terms of gas volumes is not significant. Sieverts and Bergner¹⁴ have shown this specifically for nitrogen, argon and helium. Moreover, any error in hot volumes due to different thermal behaviors of hydrogen and argon was the same in all runs. For the solubility of hydrogen as a function of alloy composition, it would therefore only mean that all curves in Fig. 3 would be displaced in a vertical direction, but their shapes would not be affected.

The hot-volume determinations were repeated in a number of runs after the hydrogen-solubility determinations. In several instances the later hot volumes were smaller than the earlier values. This can be explained by the fact that vaporized metal condensed along the upper crucible walls and also stuck there if splashing had occurred. Such deposits acted as additional heating elements and raised the temperature in the furnace, which reduced the hot volume. In some cases the later hot volumes were found to be larger. This was probably caused by a change in the effect of the cooling water, since more severe cooling increased the hot volume. The differences between the earlier and later values normally did not exceed one cubic centimeter. Since in these cases the average hot volume was used for calculation of solubility, the probable error on this account amounted to about 0.5 c.c. or less.

The results of this investigation show that the solubility of hydrogen in liquid iron-silicon alloys as a function of composition decreases rapidly up to about 33 wt. per cent of silicon. Above this composition the solubility increases again at a fairly fast rate. It is thus a minimum at 33 wt. per cent. This composition is equivalent to 50 atomic per cent and corresponds to the intermetallic compound FeSi.

The existence of FeSi in liquid ironsilicon alloys has been postulated in the literature. In a comprehensive review of liquid alloys, Sauerwald¹⁵ lists the ironsilicon system as one that forms compounds in the liquid phase with FeSi as the compound. Herasymenko and Poboril 16 applied a thermodynamic analysis to the iron-silicon system and concluded that iron silicide exists in the liquid alloys. They based this conclusion on the fact that solid FeSi melts congruently, on the shape of the liquidus-solidus curves near the melting point of iron containing some silicon, and on the equilibrium

$$_{2}$$
FeO (in Fe) + Si (in Fe) = $_{2}$ Fe + SiO $_{2}$

Körber and Oelsen¹⁷ determined the heats of formation of molten iron-silicon alloys and found a maximum at the composition of FeSi. They interpreted this as an indication that FeSi exists in the melt. They further concluded from their experimental results that FeSi is dissociated to some extent and suggested that the primary dissociation products are probably Fe₃Si₂ and FeSi₂ rather than iron and silicon atoms.

The minimum in hydrogen solubility at the composition of FeSi can also be explained by the existence of FeSi in the liquid. No conclusion can be drawn from the curves in Fig. 3 as to the degree of dissociation or the composition of the dissociation products.

From a practical standpoint, small or moderate additions of silicon have only a minor direct effect on the solubility of hydrogen. However, with silicon contents of 15 per cent, as in acid-resisting castings, the hydrogen solubility is reduced to an extent that may be of practical significance.

Attention should be called to the fact that in accordance with Sieverts' law the solubility of hydrogen is proportional to the square root of the pressure. Consequently, appreciable fractions of the solubility values at one atmosphere are associated with relatively small partial pressures of hydrogen.

SUMMARY AND CONCLUSIONS

The solubility of hydrogen in representative compositions of the iron-silicon system up to about 65 weight per cent silicon has been studied as a function of temperature and composition. The following results were obtained:

1. The solubility of hydrogen in pure iron between the melting point and about 1750°C. is nearly directly proportional to the temperature. The results agree satisfactorily with two previous determinations by other investigators.

2. The solubility of hydrogen in molten iron-silicon alloys is a regular function of composition. It decreases rapidly from the value for pure iron with additions of silicon up to approximately 33 per cent by weight, or 50 atomic per cent, and increases again with a further increase in silicon.

3. The minimum of hydrogen solubility at about 50 atomic per cent is interpreted as an indication that undissociated iron silicide FeSi exists in the liquid phase and that the undissociated compound has a smaller ability for the solution of hydrogen than either of the constituent elements.

ACKNOWLEDGMENTS

The authors wish to acknowledge gratefully the advice and encouragement received from Professor John Chipman. They also thank Professors G. Dietrichson and N. J. Grant and Dr. Shadburn Marshall for advice.

Thanks are due to Mr. D. L. Guernsey for the chemical analyses and to Mr. R. N. Palmer for helpful suggestions.

The authors are indebted to the late J. C. Vaughan, Jr., who in 1938-1939 built the modified furnace and prepared some of the metals used in this investigation.

REFERENCES

- 1. C. A. Zapffe and C. E. Sims: Trans. Amer.
- Foundrymen's Assn. (1944) 51, 517.

 2. A. L. Norbury and E. Morgan: Inl. Iron and Steel Inst. (1926) 124, 227.
- and Steel Inst. (1936) 134, 327.
 3. A. Boyles: Trans. A.I.M.E. (1937) 125,

A. W. Schneble, Jr. and J. Chipman: Trans. Amer. Foundrymen's Assn. (1944) 52,

5. H. A. Schwartz, G. M. Guiler and M. K. Barnett: Trans. Amer. Soc. for Metals (1940) 28, 811.

6. A. Sieverts: Zisch. Elektrochem. (1910) 16,

707. B. 7. M. Bever and C. F. Floe: Trans. A.I.M.E. (1944) **156**, 149. 8. A. Sieverts and W. Krumbhaar: *Ber.* deut.

Chem. Ges. (1910) 43 (I), 893. 9. A. Sieverts: Ztsch. physik. Chem. (1911)

77, 591.
10. A. Sieverts, G. Zapf and H. Moritz: Zisch.

physik. Chem. (1938) 183, 19. 11. E. Martin: Archiv Eisenhuellenw. (1929)

3, 407. 12. K. Iwasé and M. Fukusima: Jnl. Jap.

Inst. of Met. (1937) 1, 202.

13. J. C. Vaughan, Jr. and J. Chipman: Trans.

A.I.M.E. (1940) 140, 224.

14. A. Sieverts and E. Bergner: Ber. deut.
Chem. Ges. (1912) 45 (II), 2576.

15. F. Sauerwald: Ztsch. Metallkunde (1943)

35, 105.
16. P. Herasymenko and F. Poboril: Collection Czechoslovak Chem. Commun.

(1933) 5, 331. 17. F. Körber and W. Oelsen: Mitt. Kaiser-Wilhelm Inst. Eisenforsch., Düsseldorf (1936) 18, 109.

DISCUSSION

(Howard Scott presiding)

C. A. ZAPFFE. *-Investigations such as this on the behavior of hydrogen in liquid metals are certainly much needed.

Since a great deal of confusion persists regarding the nature of hydrogen in iron and steel, attention should be called here to certain fundamental features of the research, which need be understood if misinterpretation of both its practical and its theoretical aspects is to be avoided; that is, hydrogen dissolves in metals as the atom H, not as the molecule H2. According to Henry's law, [H] is therefore a direct function of (H), not of H2; and this function explains the square-root relationship with H2, since H2 dissociates thermally to produce H according to a quadratic expression.

Consequently, the partial pressure of (H) deserves first attention, rather than the partial pressure of H₂; and it must not be forgotten that the principal significance of the entity PH2 is its convenience of measurement in controlled experiments such as the present one.

In most practical operations, hydrogen is

supplied not by H2, but by the reaction of the metal with H2O:

$$H_2O + M = MO + 2H$$

For different metals, this equation lies more or less to the right, the stronger deoxidizers requiring, and developing, higher balancing pressures of (H).

Consequently, silicon in iron by this massaction factor alone can effect a greater absorption of [H] than iron without silicon present, in contradiction to a hasty conclusion that one might draw from this paper. The pronounced liability of aluminum to pinholding from traces of H₂O even at its comparatively low melting temperatures is an example of this fact; and Fig. 3 therefore may fail entirely to have practical significance regarding H absorption during ordinary melting of iron-silicon alloys. Under one atmosphere of He, aluminum scarcely absorbs measurable [H], simply because the atmospheric pressure of (H) is so low.

Lastly, Fig. 3 would be improved from a theoretical standpoint by expressing the [H] also in atomic per cent, or at least in relative volumes, since 100 grams of high-silicon iron differs considerably from the same weight of pure iron, both with respect to volume and to the number of mols involved.

H. A. SCHWARTZ.*-The writer is particularly interested in the use the authors have made of their solubility curves to demonstrate what they believe to be the existence of molecules in the liquid metal. This view, which has now become quite orthodox, was rejected a quarter of a century ago by most physical chemists. Its acceptance should greatly improve the understanding of constitutional diagrams, and more especially that of the equilibrium compositions.

The authors have pointed to the fact that the solubility of hydrogen should vary at a given temperature with the square root of the partial pressure of that gas. This is a point not to be overlooked by the casual reader, for, although nothing very accurate is known about the partial pressure of hydrogen in a commercial melting furnace, that partial pressure is certainly small compared with the pressure of the atmosphere. Most steel melters believe

[·] Consulting Metallurgist, Baltimore, Maryland.

^{*} Manager of Research, National Malleable and Steel Castings Co., Cleveland, Ohio.

it to be good practice to add silicon as late in the heat as possible, and ascribe this preference to a desire to minimize a resorption of hydrogen. Indeed, it is quite easy to demonstrate the hydrogen pickup after the silicon addition. Since the present authors demonstrate a decrease in solubility in the low ranges of the silicon concentrations with that concentration, the steel melters' practice must be otherwise explained, perhaps by an assumption concerning the incomplete removal of ferrous oxide by the time the heat is tapped. The hydrogen contents reported by the authors for low-silicon materials are of the order of 10 times as great as those commonly observed in the practice of the National Malleable and Steel Castings Co. in steel that has stood in air for a considerable time-several months, for example. It is usual in those steels to find a hydrogen content of the order of 0.0002 per cent.

YUAN H. CHOU* and G. DERGE.*—A doctorate thesis in the course of preparation provides additional confirmation for the conclusion drawn in this paper, that FeSi exists in liquid iron as a very stable compound. Molten iron and silver form two immiscible liquid layers. The distribution of various alloying elements in iron between these two liquids has been studied and the data for silicon are of interest in connection with the title paper. Liquid silicon and silver are miscible in all proportions, but when iron and silver layers are brought together almost all of the silicon is found in the iron layer. This is interpreted as indicating some compound of iron and silicon that is only very slightly dissociated, resulting in a very low silicon activity in the iron. The distribution has a definite temperature coefficient, which indicates that the transference of silicon from the silver layer to the iron layer is accompanied by an evolution of heat, which amounts to 4600 cal. at a concentration of 30 per cent Si in

Another interesting experimental observation is that more power is required to maintain a given metal temperature with a hydrogen atmosphere than with argon. We have observed the same difference between nitrogen and helium and have explained it by the higher thermal conductivity of helium. H. LIANG, M. B. BEVER and C. F. FLOE (authors' reply).—Chou and Derge's findings on the distribution of silicon between molten silver and iron are novel and of genuine importance. The publication of their work is awaited with interest.

The authors do not agree with Dr. Zapffe on the predominant role ascribed by him to the partial pressure of monatomic hydrogen. It is true that a small concentration of monatomic hydrogen exists in the gas phase, owing to the dissociation of molecular hydrogen, and that hydrogen dissolves in iron in the atomic state. However, from the standpoint of equilibrium the partial pressure of monatomic hydrogen in the gas phase may be disregarded. The dissolved hydrogen is in equilibrium with the monatomic gaseous hydrogen, which in turn is in equilibrium with the diatomic gaseous hydrogen. The dissolved hydrogen is thus also in equilibrium with the diatomic hydrogen. Thermodynamically it does not matter which view one takes. In either case the square-root relation (Sieverts' law) holds. However, from the standpoint of the rate and mechanism of solution it is very likely that hydrogen molecules are decomposed at the surface of the metal. In its kinetic effect this latter process at the gas-metal interface probably far outweighs the homogeneous thermal dissociation of molecular hydrogen.

The type of reaction investigated in the present paper is not the only way in which a metal may absorb hydrogen. The role of water vapor as a source of hydrogen is well recognized. Dr. Zapffe's comments on this point are especially helpful from a practical standpoint. In his equation, the metal M may be iron itself. It is understood that experiments have been made that show that molten iron may absorb a great deal of hydrogen if water is allowed to drip on to the surface of the bath.

The remarks made by Dr. Schwartz on industrial experience are of interest. His observations as well as those of others show that the process of hydrogen absorption in melting practice is complex. The fundamental reactions are the reduction of water vapor and direct absorption of hydrogen, but they are complicated by the state of oxidation of the metal, the effect of alloy elements and other factors.

^{*} Metals Research Laboratory Carnegie Institute of Technology, Pittsburgh, Pennsylvania.

Some Factors Affecting Edgewise Growth of Pearlite

By W. H. BRANDT*

(New York Meeting, October 1945)

THERE has been much progress in the last two decades in understanding the hardenability of steel. Roughly, the progress has been along two lines, which may be designated as empirical and fundamental. This empirical work has progressed to the point where steels may be manufactured to the desired characteristics quite closely and heat-treatment and application problems can be approached with considerable confidence. Particularly noteworthy among the empirical work is that of Grossmann, 12 who has given formulas for calculating hardenability as a function of composition, and the establishment of the isothermal transformation curve by Davenport and Bain.13 The latter does not fall entirely in the class of an empirical study, for while it provides a means of presenting a tremendous amount of empirical data in the form of a single curve, it also outlines clearly the problems that face the fundamental investigator.

The isothermal transformation curve shows clearly that the phenomena occurring in the neighborhood of the knee of the curve are those that limit the hardenability of steel. Above the knee of the curve, the product of decomposition of austenite is lamellar pearlite and fundamental progress has consisted chiefly of a detailed study of structure and formation of pearlite, largely

at the hands of Mehl and his collaborators. 1-5 They have shown that formation of pearlite proceeds by a process of nucleation and growth and they measured both the nucleation and growth rate. However, there is still a wide gap between our empirical knowledge and fundamental knowledge, owing largely to the fact that there is no satisfactory theory of nucleation rate or of growth rate. This paper is being written in an attempt to fill in a small part of the gap.

A method was presented recently14 for calculating the velocity of edgewise growth of pearlite using an expression for the carbon concentration that satisfies the diffusion equation. The edgewise velocity of pearlite growth in a plain carbon eutectoid steel was calculated, using linear extrapolations of the ferrite and cementite solubilities. While the results are in fairly good agreement with the experimental facts, the calculated velocity of edgewise growth is smaller at 600°C. than G, the radial growth velocity of pearlite nodules, whereas one would expect it to be larger. In this paper the calculation will be repeated using a new extrapolation for the ferrite solubility, which gives better agreement between G and V, the calculated velocity of edgewise growth. A calculation will also be made of the effect of carbon content on velocity of edgewise growth, and the problems of calculating the effects of other alloving elements on growth rates will be discussed.

It will be assumed that the mechanism of pearlite growth, established by Mehl and

References are at the end of the paper,

Manuscript received at the office of the Institute Dec. 1, 1944. Issued as T.P. 1857 in METALS TECHNOLOGY, December 1945.

* Westinghouse Electric Corporation, East Pittsburgh, Pennsylvania.

others, $^{1-5}$ is substantially correct; i.e., that the rate of transformation of austenite to pearlite is determined by two factors, N_v and G, where N_v is the nucleation rate. In the discussion it will be assumed that G

so the first three terms only are used and the following is obtained:

$$C - C_a = K_0 e^{a_0 x} + K_1 e^{a_1 x} \cos b_1 y$$
 [1]

where C is the carbon concentration, C. is

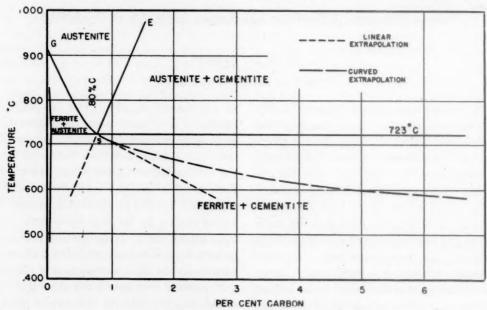


FIG. 1.—IRON-CARBON CONSTITUTION DIAGRAM.

Showing extrapolations of the ferrite and cementite solubilities. New extrapolation of the ferrite solubility is to the right. (Metals Handbook, Amer. Soc. for Metals, 1939, 355.)

is substantially equal to V, an assumption that is justified within present limits of experimental accuracy by the agreement between calculated values of V and experimentally determined values of G. Except where otherwise stated, all calculations will be made for a plain carbon eutectoid steel.

THE THEORY

Since the discussion will require certain equations, these will be presented by a brief recapitulation of the theory.

If the diffusion equation is transformed to a set of coordinates moving with the pearlite-austenite interface, which is assumed to grow with constant velocity, a solution for the carbon concentration may be derived in the form of an infinite series of terms. One does not have enough knowledge of boundary conditions to determine an infinite number of arbitrary constants

the original carbon concentration in austenite, K_0 and K_1 are arbitrary constants,

$$b_1 = \frac{2\pi}{S_0} \tag{2}$$

$$a_0 = -\frac{V}{D}^{\dagger} \tag{3}$$

and

$$a_1 = \frac{-\frac{V}{D} - \left\{ \left(\frac{V}{D}\right)^2 + \left(\frac{4\pi}{S_0}\right)^2 \right\}^{\frac{1}{2}}}{2}$$
 [4]

 S_0 being the pearlite spacing, V the velocity of edgewise growth and D the diffusion coefficient. Defining C_{af} as the carbon concentration in austenite at the center of the ferrite-austenite interface, C_{ac} as the carbon concentration in austenite at the center of the cementite-austenite interface C_c as the carbon concentration in cementite and C_f as the carbon concentration in

ferrite (equals the solubility of carbon in ferrite), one obtains the equation,

$$P = I + N \frac{L^{\frac{2}{1+P}} + L}{M + L^{\frac{2}{1+P}}}$$
 [5]

where

$$N = 2 \frac{C_{\epsilon} - C_{a}}{C_{a} - C_{ac}}$$
 [6]

$$L = \frac{C_a - C_f}{C_c - C_a} \tag{7}$$

$$M = \frac{C_{af} - C_a}{C_a - C_{ac}}$$
 [8]

and

$$P = \left\{ 1 + \left(\frac{4\pi}{S_0} / \frac{V}{D} \right)^2 \right\}^{\frac{1}{2}}$$
 [9]

When N, M, and L are known, Eq. 5 can be solved for P by successive approximations and V calculated by use of Eq. 9, which can be more conveniently written

$$V = \frac{4\pi D}{S_0} (P^2 - 1)^{-\frac{1}{2}} = \frac{4\pi D}{S_0} V_o \quad [10]$$

where

$$V_a = (P^2 - 1)^{-1/2}$$
 [11]

The shapes of the cementite-austenite and

ferrite-austenite interfaces are given by the equations,

$$e_1^{ax_0} = \frac{b_1 y_0}{\sin b_1 y_0}$$
 [12]

and

$$e^{a_1 x_0} = \frac{(C_a - C_f) b_1 (S_0 / 2 - y_o)}{(C_c - C_a) \sin b_1 (S_0 / 2 - y_0)}$$
[13]

where x_0 and y_0 are the interface coordinates. At the center of the ferrite-austenite interface Eq. 13 becomes

$$e^{a_1 x_f} = \frac{C_a - C_f}{C_c - C_a}$$

where x_f is the x-coordinate of the center of the ferrite-austenite interface.

N, M, and L are determined by identifying C_{ac} and C_{af} with the extrapolations of the ferrite and cementite solubilities below the eutectoid temperature and calculating the corresponding values from Eqs. 6, 7 and 8. When these extrapolations are linear, as shown dotted in Fig. 1, the corresponding velocity of edgewise growth for a plain carbon eutectoid steel is that given by the dotted curve in Fig. 2. In this calculation, the values of the diffusion coefficient were extrapolated from the data of Wells

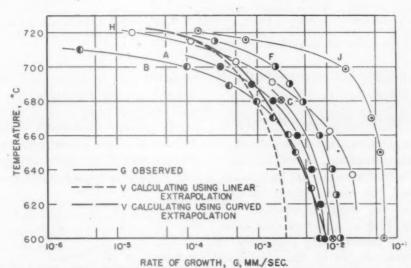


Fig. 2.—Calculation values of V superimposed on G curves of Hull, Colton, and Merl. V-curve to the right corresponds to the curved extrapolation of Fig. 1. Curve J was obtained on a high-purity plain carbon steel; all other curves were obtained on "commercial" steels containing various impurities.

and Mehl⁷ and the interlamellar spacing data were obtained from a curve given by Pelissier, Johnston, Hawkes and Mehl.⁸ A model showing the interface shape and and unfortunately one's knowledge of boundary conditions is not sufficiently good in this case to permit rigorous proof. However, the lamellar structure and its

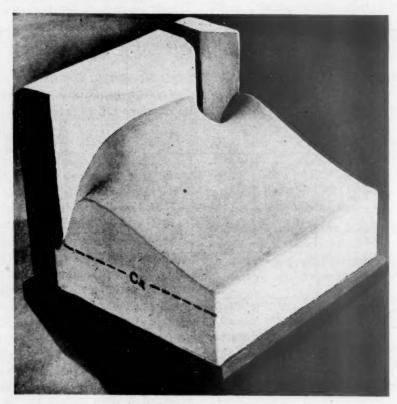


FIG. 3.—Model of the carbon concentration near the pearlite interface. Surface of cementite lamellae is black, surface of ferrite lamellae is white and surface representing the carbon concentration is gray. The original carbon concentration in austenite, C_a , is shown by the dotted line at the side of the figure.

the corresponding carbon concentration is shown in Fig. 3.

EXISTENCE OF LAMELLAR STRUCTURE

Eq I requires regular lamellar structure as a boundary condition. It does not rigorously prove that growth must be lamellar, and, in fact, one cannot expect that the solution to the diffusion equation will prove that lamellar structure does exist. It can only indicate the possibility of lamellar structure, as by the occurrence of a periodic term in Eq. 1. The proof of actual existence can result only from application of the boundary conditions,

regularity may be shown to follow qualitatively from the assumption of a constant velocity of growth.*

The growth of pearlite involves the diffusion of carbon in austenite from a high concentration at the ferrite-austenite interface to a low concentration at the cement-

^{*} This is an assumption rather well justified by the experimental proof of Hull and Mehl* that G is a constant in a given steel at a given temperature.

After nucleation, lamellar structure must be established before G and V can achieve a constant velocity. The same authors have given a mechanism whereby this can happen and have shown that the time required is very small compared with the period of growth of a nodule.

ite-austenite interface. Both ferrite and cementite must be present at the boundary, and it is clear that the growth of each must be continuous if the velocity is to remain The regularity of the lamellae follows from the fact that the rate of growth is inversely proportional to the spacing as given in Eq. 10. Any lamella that is larger than the



Fig. 4.—Electron micrograph (\times 11,000) of pearlite showing bridges between cementite lamellae (courtesy of R. F. Mehl).

Occasional bridges may be seen in the area at the center of the picture. Region of more frequent bridging is at lower right. Reaction temperature was probably 640°C.

constant, as has been assumed. In two dimensions, this means that the growth of ferrite and cementite will be in lamellae.*

* Growth could conceivably be in the form of cementite rods in a ferrite matrix and the solution of the diffusion equation in three dimensions allows for this possibility. Because of lack of detailed knowledge of the boundary conditions, it is not clear why pearlite does not grow in this form.

average will lag behind its thinner neighbors and immediately the neighbors will encroach upon it and grow wider at its expense, thereby making it narrower. It will then grow at a more rapid rate until it overtakes its neighbors. A lamella smaller than average will grow in advance of the interface, become wider by the reverse

process, and slow up. The net result is a substantially uniform spacing. Some fluctuations in spacing are to be expected as a result of this mechanism, and for other reasons. Such fluctuations are found experimentally.8

The same process should enable pearlite to engulf a discontinuity in the austenite, such as a small inclusion that has not caused nucleation, without a permanent disruption of its regular structure.

These remarks clearly are valid only when two phases are growing simultaneously at the expense of a third. When only a single phase is growing, or when two phases grow alternately, as in sidewise growth of pearlite, the assumption of a constant velocity of growth and of a carbon concentration independent of time can no longer be made. Obviously it is also possible to have two phases growing simultaneously in nonlamellar form when the velocity of growth is not a constant.

EXTRAPOLATIONS OF FERRITE AND CEMENTITE SOLUBILITIES

The agreement of V with G, using the linear extrapolations of C_{af} and C_{ac} (Fig. 2), is rather good for the commercial steels A and B, considering that precise agreement is not to be expected and considering the accuracy with which the spacings, the diffusion constant and the ferrite and cementite solubilities are known. The disagreement at the higher temperature is not perturbing since the impurities in the "commercial" steels probably affect the upper temperature limit of pearlite growth. Spacing data are not known for steel J, which is of high purity, so the disagreement in this case is not surprising. However, at the lower temperatures, one would prefer that V be somewhat greater⁴ than G. This desideratum, plus the fact that the ferrite and cementite solubilities are at least a part of the key to the effect of alloying elements on growth rates, is

sufficient inducement to reexamine the extrapolations of these solubilities.

The cementite solubility is the least important of the two, as it has little effect on the velocity of growth in the region near the knee of the S-curve (Fig. 7), although the effect percentagewise is appreciable near the Ae1 temperature. Furthermore, the linear extrapolation can be made with some confidence in this case, since the curve is linear above Ae₁. In the case of the ferrite solubility, however there is curvature above Ae₁, and it is obvious that continuing this curvature below Ae1 will give better agreement with the experimental G values. However, there is an upper limit to the value that may be assigned to the ferrite solubility, and it is the determination of this limit that suggests an interesting mechanism that may control the lower temperature limit of pearlite growth.

In the following discussion, the symbol T_p will be used to refer to the temperature below which lamellar pearlite ceases to form. It is not a sharply defined temperature, but probably corresponds, or nearly so, with the temperature of the "knee" of the isothermal transformation curve.

It is clear that the carbon concentration ahead of a ferrite lamella cannot be higher (or only very little higher) than the carbon concentration in cementite, since this would cause the nucleation rate of cementite to be infinite ahead of the ferriteaustenite interface and stop lamellar growth in an edgewise direction. If this is in fact the phenomenon that limits the lower temperature of pearlite growth, it enables one to determine approximately the last point of the ferrite solubility curve and to draw the curve reasonably accurately. Such a curve has been drawn and shown in Fig. 1 (dashed) using 580°C. as T_p and 6.68 per cent as C_c . The corresponding value of V is shown dashed in Fig. 2, the numerical data being given in Table 1. The values of S_0 and D are the same as those used in the earlier calculation. The agreement with the G values is improved over those resulting from the linear extrapolation.

Furthermore, there is an independent

experimental fact, which may be cited in support of this theory of the limitation of pearlite growth. If the theory is correct, the disruption of lamellar structure should occur gradually as the temperature is



Fig. 5.—Electron micrograph (shown by Mehl²) of a sample of pearlite reacted isothermally at 580° C. \times 30,000.

decreased and there should be visual evidence of this on photomicrographs. Fine pearlite, since it is formed near the knee of the curve, should show evidence

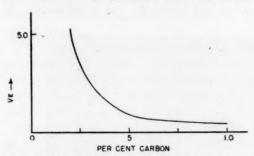


FIG. 6. CALCULATED CHANGE IN V₆ WITH CHANGING CARBON CONTENT (600°C.)

of occasional nucleation ahead of the ferrite lamellae, and as the temperature is gradually lowered this nucleation should become more and more frequent until finally the regular lamellar structure ceases to appear altogether. Fortunately, within the past few years, the electron microscope has made it possible to resolve these fine structures satisfactorily, and one of the earliest papers describing the use of the electron microscope in metallurgy² mentions the occurrence of "bridges" in fine pearlite. Quoting from that lecture:

Figure 20 at 30,000 diameters of pearlite formed at 1075°F. (580°C.) shows an effect which has frequently been noted in very fine pearlites, an effect which appears to become more pronounced as the temperature of formation is decreased namely, that the cementite occasionally seems to bridge the lamellae, i.e., occasionally to cross-connect one cementite layer with the next.

The writer has obtained from Dr. Mehl another excellent electron micrograph (Fig. 4), which shows an area in the center of very regular lamellar structure with just occasional "bridges" and another area, lower right, in which the "bridging" is so frequent that the structure is almost cellular. Mehl's Fig. 20 (reproduced here as Fig. 5) shows a rather more advanced disruption of lamellar growth than Fig.

4; in fact, the regularity of lamellar structure has almost entirely disappeared.*

These "bridges" are almost precisely what one would expect from occasional

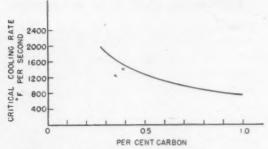


FIG. 7.—CRITICAL COOLING RATE AS A FUNCTION OF CARBON ACCORDING TO DIGGES. nucleation ahead of ferrite lamellae; and as the nucleation rate is further increased, one would expect further disruption of lamellar structure as shown in Fig. 5.

The evidence (Fig. 4) is quite convincing of a nonlamellar ferrite-cementite aggregate occurring near the knee of the S-curve. This should probably not be identified with bainite, since bainite does not appear to be closely related to pearlite, at least in its mode of formation. It seems reasonable, in the light of this theory, to think of it tentatively as a form of pearlite.

It is to be expected on the basis of this theory that changing carbon content in a plain carbon steel would not affect T_p , and if T_p coincides with the temperature of the "knee" of the isothermal transformation curve, this should also be unaffected. Data so far seen by the writer do not permit the checking of this point. The presence of other alloying elements may change T_p and the temperature of the "knee," and this is clearly the case.† It is, furthermore, to be expected that proeutectoid ferrite would never form below T_p , at least in plain carbon and low alloy

^{*} The discontinuity of cementite in Fig. 5 may be due to imperfections in the replica. However, there is little doubt that the structure is quite different from regular lamellae.

[†] This point may be checked by a study of the Atlas of Isothermal Transformation Diagrams, published by the United States Steel Corporation.

steels, since any formation of ferrite would nucleate cementite.

Effect of Carbon Content on Pearlite Growth

A change in the carbon content of a steel affects only the directly observable quantity Ca in Eq. 5, and therefore it is possible to calculate the effect on V. quite simply. The resultant curve at 600°C. is shown in Fig. 6. There are no experimental data against which Fig. 6 may be checked directly, but Fig. 7, from Digges, 10 is given for comparison of V, with the critical cooling rate. The calculated variation in Ve with carbon content is somewhat greater proportionally than the variation in critical cooling rate. Possible changes in spacing with carbon content and the appearance of proeutectoid ferrite at lower carbon content are reasons for expecting some difference in the proportionality of the curves,* but the change in V. is in the right direction and of the right order of magnitude to explain the change in hardenability with changing carbon content.

The data from which Fig. 6 is plotted are given in Table 2. As the carbon content decreases, K_0 and K_1 increase, and at the

* The exact relationship between V_a and critical cooling rate is not known. According to Hull, Colton, and Mehl^s

$$f(t) = 1 - e^{-\frac{\pi}{3}N_vGs_tA}$$

where f(t) is the fraction of austenite transformed (isothermally) to pearlite, t is the time, N_{\bullet} is the nucleation rate (assumed constant) and G the radial growth rate of pearlite nodules.

When f(i) is held constant, as was done in Digges' experiments,

$$\frac{x}{t} = KG^{3/4}N_{*}^{1/4}$$

where K is a constant. The reciprocal of the time required for a constant percentage of transformation is proportional to the three-fourths power of G. One would expect that the reciprocal of the reaction time would be approximately proportional to the three-fourths power of V_{θ} provided that the pearlite spacing does not change with carbon content.

Since Digges' experiments were not carried out isothermally, one cannot carry the analysis further, but it is clear that a plot of V_a^{34} would be more nearly of the shape of the critical cooling-rate curve.

same time the pearlite-austenite interface becomes flatter; that is, the ferrite leads the cementite by a smaller distance. The rate of growth is faster when the amount of carbon to be moved is smaller, but is not proportional to the reciprocal of the carbon content.

The predictions of the theory with regard to changing carbon content offer the most attractive possibilities of being directly checked by experiment. The variation in G with carbon content can be measured. This can be compared with V if S_0 and D are known. The appearance of proeutectoid ferrite, however, may be a serious complication in such an experimental study.

The variations of the shape of the pearlite-austenite interface with carbon content may or may not be observable. A survey of dozens of unpublished micrographs of steels partially reacted to pearlite, taken by F. C. Hull, has failed to show any preference for the shape indicated in Fig. 3, although it does appear occasionally. It seems probable that enough growth of ferrite or cementite or both will occur during quenching to change the shape that existed during isothermal growth.

EFFECTS OF ALLOYING ELEMENTS ON PEARLITE GROWTH AND HARDENABILITY

While the effect of carbon content on V_a permits direct calculation, the effects of other alloying elements are very complex since they may involve changes in C_a , C_f , C_c , C_{af} , and C_{ac} . Since the effect of C_a was calculated in the preceding section, it will not be necessary to consider it further except to point out the obvious fact that Fig. 4 may be used to explain effects due to the presence of a third element on C_a , such as the effect of incomplete solution of carbides on hardenability. It is well known experimentally that this effect is similar to the effect of decreasing carbon content.

The simplifying assumption that C_f , C_e , C_{af} , and C_{ae} have the same value during growth as in static equilibrium, although it worked reasonably well with plain carbon

In discussion of hardenability, one must consider a fifth factor, T_p . If an alloying element changes T_p upward, it should have the effect of improving hardenability,

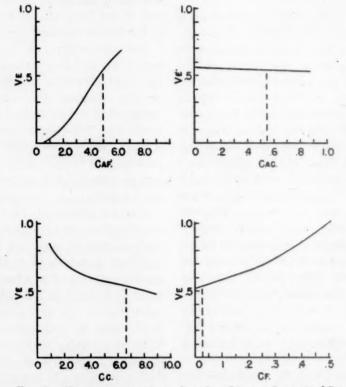


Fig. 8.— V_e As a function of C_{af} , C_{ac} , C_c , and C_f At 600°C. Dotted lines show values used in calculation shown in Fig. 2 for a plain carbon eutectoid steel (curved extrapolation).

steel, becomes dangerous in connection with an alloy steel. There is the additional difficulty that nearly all experimental data concern hardenability. It would be much easier to study the effects of alloying elements if the effects on G were known. In spite of these difficulties, it is instructive to analyze certain simple hypothetical cases.

As pointed out earlier, the rate of transformation of austenite to pearlite is determined by two quantities: N, the nucleation rate, and G, the radial growth rate of pearlite nodules. The agreement between V and G (Fig. 2) indicates that they are proportional, so that it is substantially correct to say that G is determined by D, S_0 and V_{\bullet} (Eq. 10).

provided that T_p corresponds to the knee of the S-curve, since the rate of transformation decreases as the temperature is raised. This discussion will be limited to V_a and T_p , as nothing further can be learned about N, S_0 and D by this type of treatment. V_a will be considered first.

Although we do not know how C_{af} , C_{ac} , C_{c} , and C_{f} change when an alloying element is added to a steel, it is possible to calculate V_{c} , for any value of each of these variables. This has been done for each variable over a range of values, including the one (dotted line) used in making the improved calculation of V at 600° C., holding all other variables constant (Fig. 8). The dotted lines may be thought of as representing

the most probable values of the variables for a plain carbon eutectoid steel. The range of values given in Fig. 8 for each variable probably represents the maximum change that one would expect to find with the addition of a small percentage of an alloying element.

TABLE 1.—Values of P, V₀, and V Calculated from New Extrapolation of Figure 1

T	P	V.	$\log_{10} V \left(\frac{\text{cm.}}{\text{sec.}}\right)$
580	1.69	0.736	7.11-10
600	2.10	0.544	6.97-10
650	5.39	0.188	6.52-10
700	32.4	3.18 × 10-2	5.73-10
720	320.	3.13 X 10-8	4.71-10

 V_{\bullet} is almost unaffected by changes in C_{ae} . C_{e} has somewhat more effect but only decreases V_{\bullet} (and improves hardenability) when it is increased above 6.68 per cent, and then the effect is small. V_{\bullet} increases with increasing C_{f} , and since C_{f} is already very small (0.029 per cent) in a plain carbon steel, the effect is in the wrong direction. Only C_{af} can decrease V_{\bullet} by the orders of magnitude required to explain the several fold changes in hardenability found with the addition of a single per cent of alloying element.

The only clue to the behavior of C_{af} when alloying elements are added is the behavior of the ferrite solubility above the eutectoid temperature. It is instructive to calculate the corresponding change in V_{\bullet} for the case of manganese. According to curves given by Bain,11 the addition of one per cent manganese to steel shifts the eutectoid temperature downward by about 3°C. and the eutectoid carbon concentration to 0.74 per cent. This is equivalent to a change in the ferrite solubility of about 0.3 per cent. If Cas shifts correspondingly from 5.0 to 4.7 per cent, it will be seen that the effect on V_e is only about 5 per cent, in contrast to the several fold changes in hardenability due to the addition of one per cent manganese.

Bain's curves also indicate that the shift in ferrite solubility, caused by the addition of alloying elements, is approximately linearly proportional to the amount of element added. This being the case, one would expect that the shift in C_{af} with the addition of alloying elements would not be far different and, therefore, one would expect from the curve shown in Fig. 8 that the first added increments of the alloy addition would have less effect than further increments, since a much lower change in C_{af} is required to reduce V_a by any given factor as C_{af} becomes smaller.*

Table 2.—Variation in P, V_e , K_1 , K_0 , and x_f/S_0 with carbon content at 600° C.

	PER (LENT		
P	V.	K ₁	K_0	$\frac{x_f}{S_0}$
1.17	5.26	-77.8 -42.6	78.I	0.05
1.75	0.70	-16.2 -10.7 - 7.8	16.1	0.19
	I.17 I.29 I.75	P V. 1.17 5.26 1.29 1.48 1.75 0.70	P V _e K ₁ 1.17 5.26 -77.8 1.29 1.48 -42.6 1.75 0.70 -16.2	1.17 5.26 -77.8 78.1 1.29 1.48 -42.6 42.7 1.75 0.70 -16.2 16.1

According to Grossmann, 12 the opposite is true; that is, the first added increments of an alloying element have a relatively more important effect than further increments. It appears, therefore, that changes in $V_{\mathfrak{e}}$ due to changes in $C_{\mathfrak{a}f}$ with the addition of an alloying element are unlikely to constitute an important part of the effect of

* This is particularly true if the changes in C_{af} are large enough to affect V_{\bullet} appreciably. For example, suppose C_{af} changes sufficiently with the addition of one per cent of an alloying element to reduce V_{\bullet} by one-half. From Fig. 8, it will be seen that C_{af} will then be equal to approximately 2.75 per cent C, the reduction being 2.25 per cent C. The addition of one more per cent of the alloying element would then be expected to reduce V_{\bullet} nearly to zero, which clearly does not happen.

With this in mind, the arguments first given appear to be somewhat mutually supporting and can be restated as follows: The change in V_e with C_{af} is either numerically negligible or it is not. If it were not, the first added increments of an alloying element would be less effective in hardenability than further increments, which would be contrary to Grossmann's studies. Therefore, one concludes that changes in V_e , due to changes in C_{af} by addition of an alloying element, are not important in hardenability.

that element on hardenability, and therefore, since changes in V_{\bullet} with C_{ϵ} , C_{f} , and C_{ac} are small or in the wrong direction, it appears unlikely that changes in V. are numerically very important in hardenability effects of alloying elements.

By contrast it appears that changes in T_p with the addition of an alloying element are likely to be much more important numerically. The S-curve shows that any factor that turns the knee of the curve at 20°C. higher temperature will decrease the critical cooling rate by a factor of from 2 to 4. It seems, furthermore, quite possible that a single per cent of an alloying element could have this effect, although it will be impossible to estimate such effects until the mechanism is better understood. Since T_p may be determined by nucleation, it is not safe to conclude that hardenability is not influenced by Ce, Cf, Cae, and Caf, even though it does appear that V, is not greatly affected by these variables. They may also have an effect on the pearlite spacing, S_0 , and therefore on V and G.

These rather complex considerations make it seem somewhat less surprising that practically no correlation has been found to date between the effects of alloying elements on the ferrite and cementite solubilities and the effects of alloying elements on hardenability.

CONCLUSIONS

r. The assumption that the lower temperature limit of pearlite growth is reached when the carbon concentration in austenite ahead of the ferrite-austenite interface reaches the carbon concentration of cementite leads to improved agreement between the calculated velocity of edgewise growth and experimentally observed G values.

2. The same assumption leads to an explanation for the "bridges" and for the breakdown of lamellar structure found on electron micrographs of fine pearlite.

3. The effect of carbon content on V.

has been calculated. The effect is greater proportionally than the effect on critical cooling rate determined experimentally by Digges, but is in the right direction and of the right order of magnitude.

4. The theory indicates that the effects of alloying elements on V. are probably not of great importance in hardenability except as the alloying elements change the effective carbon content of austenite.

5. Effects of alloying elements on T_p , the lower temperature limit of pearlite growth, may be of such a magnitude as to be of importance in hardenability.

ACKNOWLEDGMENT

The author wishes to thank Dr. R. F. Mehl and Dr. C. S. Barrett for providing an electron micrograph, and for much constructive criticism offered in the course of preparation of this paper.

REFERENCES

- R. F. Mehl: Physics of Hardenability. Hardenability of Alloy Steels, Amer. Soc. for Metals Symposium, 1939.
- 2. R. F. Mehl: Structure and the Rate of Formation of Pearlite. 16th Campbell Memorial Lecture, Amer. Soc. for Metals (Oct. 1941).
- W. A. Johnson and R. F. Mehl: Reaction Kinetics in Processes of Nucleation and Growth. Trans. A.I.M.E. (1939) 135,
- F. C. Hull and R. F. Mehl: Structure of Pearlite. Trans. Amer. Soc. for Metals
- 5. F. C. Hull, R. A. Colton, and R. F. Mehl: Rate of Nucleation and Rate of Growth of Pearlite. Trans. A.I.M.E. (1942) 150, 185
- 6. Metals Handbook, 1939. Amer. Soc. for Metals.
- 7. C. Wells and R. F. Mehl: Rate of Diffusion of Carbon in Austenite, in Plain Carbon,
- in Nickel, and in Manganese Steels.

 Trans. A.I.M.E. (1940) 140, 279.

 8. G. E. Pellissier, M. F. Hawkes, W. A.

 Johnston and R. F. Mehl: Interlamellar Spacing of Pearlite, Trans. Amer. Soc.
- for Metals (1942) 30, 1049. V. Smith and R. F. Mehl: Lattice Relationships in Decomposition of Austenite to Pearlite, Bainite and Martensite. Trans. A.I.M.E. (1942) 150, 211.

 10. T. G. Digges: Effect of Carbon on the
- Hardenability of High-Purity Iron Car-bon Alloys. Trans. Amer. Soc. for Metals (1938) 26, 408.

 II. E. C. Bain: Functions of Alloying Elements
- in Steel. Amer. Soc. for Metals, 1939.

M. A. Grossmann: Hardenability Calculated from Chemical Composition. Trans.
 A. I. M. E. (1942) 150, 227.

A.I.M.E. (1942) 150, 227.

13. E. S. Davenport and E. C. Bain: Transformation of Austenite at Constant Subcritical Temperature. Trans. A.I. M.E. (1930) 90, 117.

14. W. H. Brandt: Solution of the Diffusion

14. W. H. Brandt: Solution of the Diffusion Equation Applicable to the Edgewise Growth of Pearlite. Jnl. Applied Physics (1945) 18, 139.

DISCUSSION

(J. B. Austin presiding)

J. B. Austin. *- I have one question, if the chairman may put in his question first. I have a little difficulty, I must confess, in adjusting my mental processes to changes in nomenclature. I think I have gotten fairly accustomed to Dr. Zener's ΔG instead of the ΔF that I was raised on, and now I find that the G and N values that I had been accustomed to are appearing in new guises. I should like to ask Dr. Brandt to explain a little more the relation between his V and the quantity G, which Dr. Mehl and his associates used, particularly because he made the statement that, as I recall it, G represents the linear growth of a colony and V is the rate of growth of a nodule, which seems just a little different from the way I have thought of it.

W. H. Brandt (author's reply).—The answer to Dr. Austin's question is that V and G are in the same quantities and therefore must be distinguished by different symbols. G is the average rate of increase in diameter of a pearlite nodule whereas V is the growth velocity of a pearlite colony in edgewise direction. It is clear that G is related to V, and it seems likely that G will be either approximately equal to V or somewhat smaller.

C. ZENER.*—I should like to ask whether Dr. Brandt took the carbon concentration in the austenite ahead of the ferrite to be given by the equilibrium diagram, or considered the effect of the curvature of the interface on the equilibrium concentration? The two will not, of course, be the same.

W. B. Brandt.—The question raised by Dr. Zener is an interesting one and was touched on briefly in a previous paper.¹⁴

The value assigned to the carbon concentration at the center of the ferrite-austenite interface was equal to the value indicated by the extrapolation of the conventional equilibrium diagram; that is, no account was taken of the curvature at the interface. Originally this was done because it was thought that the interface calculated from Eq. 13 was flat at the center; however, actual calculation has shown that this is not true, and that the radius of curvature at this point is about one half of the pearlite spacing. The situation was not corrected because the author knows of no way in which it can be done, lacking knowledge of the interface energy. If the ferrite-austenite interface energy is small, the correction will be small; if it is very large, the correction will be large. The effect of the correction would be to make Caf smaller (and possibly make Cac larger), which would decrease the values of V correspondingly.

The carbon concentration must change in austenite along the ferrite-austenite interface and this change probably is due to changing curvature of the interface. Qualitatively it seems reasonable that this would lead one to pearlite spacing decreasing with temperature, but it appears that quantitative work will be very difficult.

C. Zener.—It is indeed fortunate that this society now has before it two computations of the velocity of growth of pearlite; Brandt's computation based upon the solution of the appropriate differential equation, and the writer's computation (see pp. 561 and 572), based upon only general dimensional arguments. Few of us have the ability to find solutions of differential equations, but most of us can learn to proceed a long way by dimensional reasoning. In order further to encourage the use of dimensional reasoning by members of this society, a detailed comparison will be made between the results of Brandt's and those of the writer.

From the solution of a differential equation, Brandt has obtained for the velocity of edgewise growth of a pearlite nodule

$$V = \frac{4\eta D}{S_a} V_a$$

* Physical Chemist, Assistant Director, Research Laboratory, U. S. Steel Corporation, Kearny, N. J.

* Professor of Metallurgy, University of Chicago, Chicago, Illinois. where D is the atomic diffusion coefficient for carbon in austenite, S_o is the interlamellar spacing, and V_e is a numerical coefficient determinable from Brandt's equations 5 to 8. From dimensional arguments the writer obtained for the same velocity

$$V = \frac{\Delta C}{(C_2 - C_1)_B} \cdot \frac{D}{\alpha S_o}$$

where ΔC is the difference in carbon concentration in the austenite just ahead of the ferrite and just ahead of the cementite plates, and $(C_2 - C_1)_B$ is the change in carbon concentration across the cementite-austenite interface. The precise value of the numerical coefficient alpha was unknown, but was estimated to be comparable to the ratio of (width of cementite plate)/ S_0 ; namely 0.12. Assuming Brandt's computation as correct, we may now evaluate alpha precisely from the equation

$$\alpha = \frac{\Delta C}{(C_2 - C_1)_B} \cdot \frac{V_e}{4\eta}$$

If his linear extrapolation of the GS boundary is used, one finds that alpha deviates by not more than 10 per cent from the value 0.20. On the other hand, if his curved extrapolation is used, alpha varies from 0.20 to 0.11 as the temperature is lowered from 723° to 580°C. The agreement between formulas 1 and 2 is therefore much closer than is the agreement between different sets of experimental data, which differ among themselves by more than a factor of 10.

At the time of the writing of his paper, Brandt had no guide as to the proper extrapolation of the GS boundary below the eutectoid temperature. In a current paper (This volume, p. 531.) the writer has computed this extrapolation from thermodynamical data. It is found to be essentially linear, having the value 2.58 at 600°C. (from Table A-1).

W. H. Brandt.—The agreement between Zener's alpha as estimated by him and as

computed from the equations in this paper is interesting. However, the writer is not completely convinced that the agreement is not fortuitous. It will be seen that the change in carbon concentration across the ferrite-austenite interface, as well as the change in concentration across the ferrite-austenite interface, influences the velocity of growth. Since this does not enter into Zener's estimate, it would not be surprising if his estimated alpha were considerably more in error than actually turns out to be true.

Zener's preference for the linear extrapolation of the ferrite solubility may well be correct. Since this paper was submitted for publication, the writer has also calculated the position of the GOS boundary below the eutectoid temperature by the method of Körber and Oelsen¹⁵ and this calculation also agrees more nearly with the linear extrapolation.

It does appear, however, that the two extrapolations given in Fig. 1 probably bracket the ferrite solubility, and one may think of the calculated curves of Fig. 2 as representing the probable limits on V based on data now available.

It should be pointed out that the curved extrapolation of the ferrite solubility is not demanded by the theory that formation of pearlite is stopped by growth of cementite ahead of ferrite lamellae. To stop regular lamellar growth, it is only necessary that the rate of nucleation ahead of a ferrite lamella be high enough that the average time of formation of a cementite nucleus ahead of a ferrite lamella is about equal to the time required for a lamella to grow a distance equal to the pearlite spacing. In the present state of nucleation theory, one cannot make any quantitative predictions of nucleation rate, but can say that the rate will become infinite when the carbon concentration is equal to the carbon concentration in cementite, and therefore the curved extrapolation in Fig. 1 is certainly an upper limit to the ferrite solubility.

¹⁵ Körber and Oelsen: Archiv Eisenhuttenwesen (1932) 5, 569.

Anisothermal Decomposition of Austenite

By J. H. Hollomon,* L. D. Jaffe,† Junior Members, and M. R. Norton,† Member A.I.M.E. (Chicago Meeting, February 1946)

In the practical heat-treatment of steel the decomposition of austenite usually occurs during cooling rather than at constant temperature. Nevertheless, the course of this decomposition has generally been studied only isothermally. Isothermal studies are not only simpler experimentally, but have the great theoretical advantage that one of the variables, temperature, is constant.

It is the purpose of this paper to outline the principles that govern the relations between isothermal and anisothermal‡ decomposition of austenite, to present and systematize the available experimental information, and to indicate the gaps in the existing knowledge. Some of the experimental information is the result of new work.§ Most of it is derived from scattered data in the literature. Many of these data were obtained incidentally in the course of research on other subjects and their significance has not been pointed out and perhaps not understood. It is hoped that this paper will aid future planning of

more extensive research on anisothermal decomposition.

METHOD

In order to study the relations between isothermal and anisothermal decomposition, it appears fruitful to view anisothermal decomposition as taking place at a series of constant temperatures1 (except for the martensite reaction, which does not occur isothermally to an appreciable extent). When the time the steel is at each temperature is finite, the over-all amount of the reaction is considered to be the sum of the amounts occurring at each of the successive temperatures. During continuous cooling or heating, the time the steel is at each temperature and the difference between successive temperatures can be considered to approach zero. The over-all amount of transformation will then be given by integration over the range of temperatures involved. This point of view is advantageous in that it considers anisothermal transformation to be a series of isothermal transformations. The problem thus becomes one of determining the effect of partial decomposition at any given temperature upon subsequent decomposition at another temperature.

Single Anisothermal Reaction

Consider a phase brought to a temperature at which it is unstable, held there until it has partially transformed, and then brought to another temperature at

The statements or opinions in this article are those of the authors and do not necessarily express the views of the Ordnance Department. Manuscript received at the office of the Institute Dec. 11, 1945. Issued as T.P. 2008 in METALS TECHNOLOGY, August 1946.

^{*} Captain, Ordnance Department, Watertown Arsenal Laboratory, Watertown, Massachusetts.

[†] Metallurgist, Watertown Arsenal Labora-

[‡] By anisothermal decomposition of austenite is meant decomposition occurring not at a single constant temperature.

Other new work is described in a paper by G. K. Manning and C. H. Lorig: Relationship between Transformation at Constant Temperature and Transformation during Cooling. This volume, page 442.

¹ References are at the end of the paper.

which it tends to transform further by the same reaction. In general, the reaction at the second temperature will not proceed as though no holding at the first temperature has occurred. Probably the simplest case would be one in which the transformation at the second temperature proceeds just as though the prior partial transformation had occurred at the second temperature. Such a reaction will be termed "additive." As an example, suppose the time necessary for 5 per cent isothermal transformation, in a specimen quenched directly to the second temperature and left there, is 30 min. and for 15 per cent transformation is 40 min. A specimen previously held at the first temperature long enough to transform 5 per cent would, if brought to the second temperature and held there, transform a total of 15 per cent in 10 more minutes, provided the reaction is additive.

A reaction involving nucleation and growth will be additive, over a range of temperature, if the rate of nucleation is proportional to the rate of growth over that temperature range.* Such a reaction has been termed "isokinetic."2,3 The course of an isokinetic reaction is the same at any two temperatures except for a time factor; the rate at the first temperature is, for example, 10 times as great as the rate at the second temperature for the same percentage transformation. A reaction that is isokinetic must be additive.2,3 Nevertheless, even if a reaction is not isokinetic, it may be, at least approximately, additive.

Many investigators of the isothermal decomposition of austenite have presented data for the time for "initiation of reaction." There is no reason to believe that any finite time is required for decomposition to begin. In most cases of nucleation and growth, however, the reaction begins

As is indicated below, many of the available data bearing on the anisothermal decomposition of austenite cover the times for initiation of transformation rather than the times for fixed percentages of transformation. The minimum detectable amount of transformation is presumably about the same for all temperatures of reaction. For an isokinetic reaction it may be assumed that the amounts of transformation at times prior to the nominal initiation are the same when the fractional times are the same.3 If the products of an anisothermal reaction become detectable when and only when the fractional time (added or integrated over the various temperatures) is equal to one, then it may be assumed that the reaction is additive, at least for small amounts of transformation.

Proeutectoid Ferrite and Carbide.—Grange and Kiefer⁴ measured the time for initiation of the proeutectoid ferrite reaction in an SAE 4340 steel during cooling at a constant rate. The time for initiation of isothermal transformation to ferrite had been determined experimentally for the same heat of steel and after the same austenitizing treatment. These data can be used for testing the hypothesis of additivity. A curve for the initiation of ferrite formation during cooling at a constant rate has been

very slowly, but after some time the rate of reaction increases markedly.3 The reported "initiation time" is, then, the time necessary for some small amount (presumably the minimum detectable amount) of transformation to occur, but it must not be assumed that no transformation takes place before this time has elapsed. The phrase "time for initiation" will be used in this sense in the subsequent discussion. In dealing with data concerning the initiation of reaction it is convenient to use the term "fractional time." The fractional time is defined as the actual time that a steel is held at a constant temperature divided by the time for initiation of reaction at that temperature.

^{*} If the rate of nucleation or growth changes as the reaction proceeds, rates at the same percentage transformation should be compared.

computed* from the isothermal data given by Grange and Kiefer and is presented in Fig. 1, together with their experimental measurements for transformation during ferrite reaction is approximately additive, at least for small percentages of ferrite.*

No pertinent experimental data for the anisothermal formation of proeutectoid

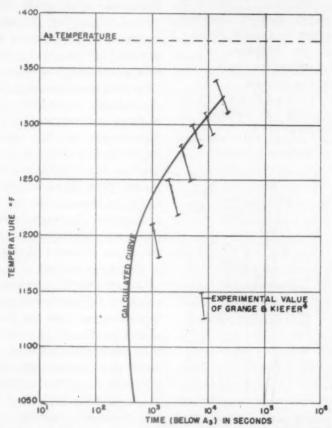


FIG. 1.—INITIATION OF FERRITE REACTION ON COOLING AT CONSTANT RATE.

SAE 4340 austenitized 15 minutes at 1550°F. Curve calculated on assumption of additivity.

cooling. The agreement is fairly good. Appreciable deviation does occur, the calculated times being shorter than the experimental by a factor of 2 at the lowest temperature. However, the isothermal curve upon which the calculations were based may not have been determined to times closer than a factor of 2. Thus, the agreement between the calculated and measured values for continuous cooling appears sufficiently satisfactory to indicate that the progress of the proeutectoid

carbide seem to be available.† It might be anticipated that the carbide reaction would behave similarly to the ferrite.

Pearlite Reaction.—Krainer⁶ measured the time for initiation of transformation in specimens of approximately SAE 4150

† The carbide formed may be cementite or a carbide of different crystal structure. For simplicity, no distinction will be drawn in this paper between the reactions leading to different varieties of carbide.

^{*} Details of the derivation for constant cooling rate have been given by Scheil. Details of derivations for any type of cooling or heating have been given by Steinberg. 5

^{*}It may be noted that Grange and Kiefer developed an empirical relation between the isothermal diagram and the diagram for cooling at a constant rate. They found this relation to agree closely with experiment for the part of the SAE 4340 diagram that they investigated. It seems unlikely, however, that their relation is generally applicable.

composition (0.5 per cent C, 1.1 per cent Cr, 0.25 per cent Mo), held at single temperatures within the range 500° to 680°C. and at two successive temperatures

TABLE 1.º-Effect of Holding Austenite at One Temperature in Pearlite Range Upon Times for Initiation of Pearlite Transformation at a Second Temperature Steel Containing 0.5 Per Cent C, 1.1 Per Cent Cr, 0.25 Per Cent Mo. Austenitized 30 Minutes at 850°C.

	rature	d Tempe	Secon	ature	Tempera	First '
Sum of Frac- tional Times	Frac- tional Time	Min- utes to Initiate Trans- forma- tion	Deg. C.	Frac- tional Time	Min- utes Held	Deg. C.
1.00	1.00	8	640	0.00	0	
1.02	0.77	6.15	640	0.25	9.0	680
10.1	0.51	4.10	640	0.50	18.0	680
0.99	0.24	1.95	640	0.75	27.0	680
1.00	0.00			1.00	36.0	680
1.00	1.00	28	590	0.00	0	
0.97	0.72	20.15	590	0.25	2.0	640
0.98	0.48	13.50	590	0.50	4.0	640
1.03	0.28	7.70	590	0.75	6.0	640
1.00	0.00	-0		1.00	8.0	640
1.00	1.00	28	590	0.00	0	
1.02	0.77	21.50	590	0.25	9.0	680
10.1	0.51	14.30	590	0.50	18.0	680
0.99	0.24	6.70	590	0.75	27.0	680
1.00	0.00			1.00	36.	680

a Data of Krainer.

within this range. As Table 1 shows, Krainer found that the initiation of transformation is additive throughout the range investigated. Since a magnetic method was used to detect the transformation, it is difficult to be certain that the reaction involved was to pearlite and not to proeutectoid ferrite; Krainer states that it was to pearlite.*

Lange and Hansel⁷ compared the progress of transformation during cooling with the isothermal transformation in a 1.16 per cent C, 0.14 per cent Mn plain carbon steel. The amount of transforma-

tion, determined isothermally, was integrated step by step over the measured cooling curves. Lange and Hansel reported that the integrated amounts of transformation agree with those measured during the cooling, throughout the entire course of the reaction at 610° to 660°C., and for the first 15 per cent of transformation at temperatures down to 450°C. This statement would indicate that the reaction (presumably to pearlite) is approximately additive over the range studied. However, examination of the curves themselves raises some question as to the agreement between the calculations and the experimental data. The calculated times appear to be significantly shorter than the measured times, the more so, the greater the percentage transformed. The divergencies are within one order of magnitude, a factor of 5 in the worst case.

Lange8 has also pointed out that the shape of the curve for percentage transformed versus time for isothermal formation of pearlite in plain carbon steels varies little with temperature of transformation; a change of temperature simply multiplies all times by a factor. This similarity of shape would indicate that the reaction is approximately isokinetic and so, necessarily, approximately additive. Direct measurements of the rates of nucleation and growth at various temperatures for the isothermal formation of pearlite have been made^{9,10} and indicate that the reaction is far from isokinetic.

The information available concerning pearlite formation is thus seen to be somewhat contradictory. The reaction can evidently be considered additive to a first approximation, but the approximation may not be very good.

Bainite.—By studying the effect of holding an 8.7 per cent Ni, 0.77 per cent C steel at one temperature in the bainite range upon its subsequent transformation at another temperature in the bainite range, Lange and Mathieu11 found that

Times are averages for many specimens.
Transformation was initiated.

^{*} Jolivet and Portevin34 state that they too have found the pearlite reaction to be additive, but do not present their experimental data.

the bainite transformation is not additive. Rather, a specimen transformed a few per cent at 425°C. subsequently transformed more slowly at 400°C. than did a specimen in which the initial transformation had taken place at the lower temperature. Similarly, several per cent of transformation at 400°C. somewhat delayed subsequent reaction at 350°C. On the other hand, a moderate amount of transformation at 350°C. hastened subsequent transformation at the higher temperature of 400°C., and a moderate amount of transformation at 400°C. hastened the transformation at 425°C. In this last case the degree of completion attained by the reaction was also found to increase. It may be noted that in the steel studied no bainite was found to form at temperatures above 450°C.

These findings of Lange and Mathieu are readily clarified by a review of the nature of the isothermal bainite reaction. as described by Zener.12 At temperatures not far below the maximum at which bainite forms, the bainite reaction is accompanied by diffusion of carbon from the growing bainite to the remaining austenite.12,13 The carbon enrichment of the austenite slows the progress of the isothermal bainite reaction. It also decreases the maximum temperature at which the austenite can transform to bainite. If the carbon enrichment is sufficient, this maximum temperature is reduced below the temperature at which the steel is held, and the reaction ceases. Lowering the steel temperature below the maximum for bainite formation in the enriched austenite will, however, permit the reaction to resume. The carbon diffusion into the austenite and the resulting enrichment are greater the higher the temperature within the bainite range. At low temperatures they are probably negligible.

For the upper portion of the bainite range, then, the carbon content of the remaining austenite for a given percentage of transformation is greater, the higher the transformation temperature. Transformation at a higher temperature thus slows subsequent transformation at a lower temperature by providing austenite of a higher carbon content. It may also decrease the extent to which the transformation can proceed. Transformation at a lower temperature, on the contrary, hastens subsequent transformation at a higher temperature, and increases the extent to which the transformation can proceed, by reducing the carbon content of the residual austenite.

Besides the 8.7 per cent Ni, 0.77 per cent C steel, for which the experimental results agree very well with the hypothesis just given, Lange and Mathieu also studied anisothermal transformation in a steel containing 5.1 per cent Ni and 1.1 per cent C. Their results for this steel cannot be safely interpreted, however, because no distinction between pearlite and bainite formation was made in the measurements, which were carried out magnetically.

Martensite Reaction.—Even though the martensite reaction does not occur isothermally, there is still the problem of determining how the initial martensite formation affects further martensite formation. Since martensite forms by a shear reaction rather than by diffusion, the problem is not complicated by changes of the composition of the residual austenite. The martensite formed initially does not nucleate the formation of additional martensite; rather, the contrary seems to occur. In fact, Steinberg and Zyuzin14 view the failure of the martensite reaction to proceed isothermally as due to the formation of martensite inhibiting further martensite formation (until the temperature is lowered).

Two Reactions

The problem now to be examined is whether one decomposition reaction has-

tens or delays a subsequent second reaction, and by what amount.

There are two ways in which the progress of the first reaction may influence the progress of the second: by affecting its nucleation, and by changing the composition of the remaining austenite. The composition change of most importance is change in carbon content arising from diffusion of carbon between the growing first-reaction product and the remaining austenite. A moderate percentage of the austenite would have to transform by the first reaction in order to change the composition of the bulk of the remaining austenite, and, hence, the rate of the second reaction, by a moderate amount.

The products of the first reaction may nucleate the second reaction or facilitate its nucleation, thus accelerating the second reaction. On the other hand, it is possible that the first and second reactions may tend to nucleate preferentially at the same sites. Products of the first reaction, by using these nucleation sites, may make them unavailable for the second reaction. If the products of the first reaction do not themselves nucleate the second reaction or provide sites at which it nucleates readily, this elimination of sites for preferential nucleation may delay the second reaction. Nucleation effects may greatly change the rate of the second reaction even though the first one has progressed to a small extent only.

One decomposition reaction may affect another even during isothermal decomposition, for austenite may decompose by several reactions, simultaneous or successive, at a single temperature.

Effect on Bainite Reaction.—Especial interest in the influence of prior ferrite formation upon the bainite reaction was aroused through a study of the effect of austenitic grain size upon the hardenability of SAE 4140 steel. Details of this study are given in the Appendix. It was found that decreasing the austenitic grain size

considerably decreased the time (increased the cooling rate) necessary to obtain I to 70 per cent bainite on continuous cooling. The effect of grain size upon the isothermal initiation of the bainite reaction had been previously studied in SAE 4140 and found to be negligible.15 It was concluded that the change in the rate of formation of bainite occurring during continuous cooling is associated with the change in fractional time at the higher decomposition temperatures. The actual time at these temperatures is not changed, but the time necessary for the appearance of detectable amounts of proeutectoid ferrite and pearlite is considerably decreased by decrease in grain size.15 For a fixed cooling rate, therefore, the extent of the ferrite and pearlite reaction is increased by decreasing the grain size, and this must be so even if the extent is too small to be detected microscopically. Inasmuch as the iso thermal diagram indicates that proeutectoid ferrite forms at considerably shorter times than pearlite, it appears that the increased progress of the proeutectoid ferrite reaction is responsible for the more rapid appearance of bainite when the grain size is small. Both the isothermal diagram and examination of the hardenability specimens indicate that the amount of proeutectoid ferrite, formed at times as short as those associated with the first appearance of bainite, is too small to be noticed under the microscope. Apparently this small amount of ferrite nucleates and so hastens the bainite reaction. That nucleation rather than growth is accelerated is indicated also by the fact that the time necessary for the formation of large percentages of bainite in the SAE 4140 steel was much less affected by grain size than the time necessary for the formation of small percentages.

Because of the importance of bainitic hardenability¹⁶ in hypocutectoid steels, it seemed advisable to make a more direct investigation of the effect of holding austenite in the range of proeutectoid ferrite formation upon its subsequent transformation to bainite. Slivers approximately ½ by ¼ by ½ 6 in. were cut from a forging of a modified SAE 4330 steel, having the following composition:

C, 0.30 per cent; Mn, 0.69; Si, 0.22; Ni, 2.83; Cr, 0.85; Mo, 0.30; V, nil.

for various times, and water-quenched. Determination of the times required to form a visible amount of ferrite at 1200°F. and bainite at 800°F. was next made by a metallographic study of the quenched samples.

Following this determination, groups of specimens, austenitized at 1700°F.,

TABLE 2.—Effect of Holding Austenite in Procutectoid Ferrite Range upon Time for Formation of Bainite

Modified SAE 4330 Steel Austenitized 1 hour at 1700°F. Grain Size ASTM 5

Time, min	32	52	56	61	64	68	
Ferrite, per cent	*	*	*	*	<1	<1	

Time, sec	8	II	12	13	14	15	16	17	18	32
Bainite, per cent	*	*		<1	<1	<1	<1	<1	1	<10

Transformation at 800°F. After Indicated Times at 1200°F.

Time, Sec. at 800°F.	Direct Quench	1	2	3	4	5	6	7	8	9	10	11	12	13	14	15
Percentage of bainite:							*	*	*	*		*	<1	*	I to IO	<1
After 1 min After 16 min After 32 min After 48 min	*	* * I	* * <i< td=""><td><1 <1 I</td><td></td><td><1 1 1</td><td><i 1 10</i </td><td>10 1 1 to 10</td><td>* I</td><td>1 2</td><td>I <i I to IO</i </td><td></td><td><1 1 to 10 10</td><td><1 10 >10</td><td>>10 >10</td><td><1 1 1 to 1</td></i<>	<1 <1 I		<1 1 1	<i 1 10</i 	10 1 1 to 10	* I	1 2	I <i I to IO</i 		<1 1 to 10 10	<1 10 >10	>10 >10	<1 1 1 to 1

^{*} None visible at 500 diameters.

The slivers were nickel-plated to reduce decarburization and austenitized in a nitrogen atmosphere. This atmosphere was obtained by passing commercial cylinder nitrogen through an alkaline pyrogallol solution to reduce its oxygen content and then over silica gel to dry it.

Two series of specimens, austenitized at different temperatures, were investigated. In the first series the specimens were austenitized one hour at 1700°F., and had an austenite grain size of ASTM 5. One group from this series was quenched directly into a metal bath at 1200°F., held for various periods of time, and water-quenched. A second group from the first series was quenched directly from 1700°F. into a metal bath at 800°F., held

were quenched directly into a metal bath at 1200°F. and held for one minute as well as for times approximately ¼, ½, and ¾ the time required for the formation of visible ferrite. These specimens were then transferred from the bath at 1200°F. directly to another metal bath at 800°F. held for various periods at 800°F., and water-quenched. Metallographic study of the quenched samples indicated the time at 800°F. required for the formation of visible amounts of bainite.

The second series of specimens was austenitized one hour at 2000°F., and had a grain size of ASTM oo to o. Again, the times required for the formation of a detectable amount of ferrite at 1200°F. and bainite at 800°F. were determined.

Groups of specimens austenitized at 2000°F. were next quenched directly to 1200°F. and held for one minute and for a time equal to one of the times for which specimens of the first series had been held at that temperature. The specimens were

Table 2 indicates that holding at 1200°F., without detectable formation of ferrite, definitely decreases the time necessary for visible bainite formation. With no hold at 1200°F. bainite was first visible after approximately 13 sec. at 800°F.

TABLE 3.—Effect of Holding Austenite in Proeutectoid Ferrite Range upon Time for Formation of Bainite

Modified SAE 4330 Steel Austenitized 1 hour at 2000°F. Grain Size ASTM 00 to 0
Transformation at 1200°F. (Direct Quench)

			1		1					1	1		_		
	Time, min	85	5	90	5	05	100		110	120	0	130			
	Ferrite, per cent	*		*		1	1		I	I		to 1	01		
	Transformat	tion	at	800°	F. (Dir	ect (Quer	nch)				_		
	Time, sec	9		10	1	I	12		13	14		15			
	Bainite, per cent	*		*		*	*		*	<		1			
	Transformation at 800°F. After Indicated Times at 1200°F.														
Tim	ne, Sec., at 800°F.	5	6	7	8	9	10	11	12	13	14	15	16	17	18
Percentage of	bainite:						-								

^{*} None visible at 500 diameters.

then transferred from the bath at 1200°F. to a bath at 800°F., held for various times, and water-quenched. The time at 800°F. required for the formation of a detectable amount of bainite was then determined in these specimens.

For the metallographic studies, the specimens were cut in half after quenching, polished, etched with I per cent nital, and studied at 500 diameters. No undissolved carbides were noted after either austenitizing treatment.

The one minute holds at 1200°F. were used because of the possibility that the difference between cooling from the austenitizing temperature and cooling from 1200°F. would affect the subsequent transformation at 800°F. The results, presented in Tables 2 and 3, show that the effect was negligible.

Holding for ½ the time for detectable ferrite formation definitely decreased the time for bainite to become visible. Holding for ½ the time at which ferrite was first observed decreased the time at 800°F. to less than 3 sec., much less than ½ the time without the 1200°F. treatment. Holding for ¾ the time at 1200°F. caused visible bainite formation to occur in the small specimens upon water-quenching from 1200°F.

That the effect is related to the fractional time in the ferrite range is illustrated by the data of Table 3. These data are for specimens austenitized at 2000°F. and having an ASTM grain size of 00 to 0. The grain size of the specimens covered by Table 2 and austenitized at 1700°F. was only ASTM 5. The increase of grain size fncreased the time for the formation of



Figs. 2 and 3.—Bainite nucleated at grain boundary in modified SAE 4330.

Fig. 2. Heat-treatment: 1700°F., 1 hour; cooled to 800°F., held 32 seconds, water-quenched.

Fig. 3. Heat-treatment: 1700°F., 1 hour; cooled to 1200°F., held one minute; transferred to 800°F., held 14 seconds; water-quenched.

× 2500. Etchant: 1 per cent nital. Objective used: Apochromat, 1.4. N.A.

visible ferrite from 61-64 min. to 120-130 min. The time for visible bainite formation after quenching directly from the austenitizing temperature was hardly observed that in specimens not held in the ferrite range there is a noticeable but apparently slight tendency for bainite to form at austenite grain boundaries

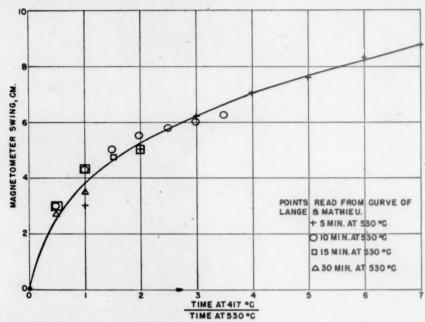


FIG. 4.—Effect of holding austenite in proeutectoid carbide range upon its subsequent transformation to bainite.

7.0 per cent Ni, 0.7 per cent C. Austenitized 5 to 7 minutes at 850°C.; temperature of carbide formation, 530°C.; temperature of bainite formation, 417°C. Data of Lange and Mathieu. 11

affected, possibly increasing from 13 to 15 sec. However, with the large grain size, holding for 32 min. at 1200°F only decreased the time for formation of detectable bainite to 11 sec., a decrease of less than 30 per cent. Holding for the same time with the small-grained specimens decreased the time for visible bainite formation about 85 per cent. Thus, the longer the time required for ferrite formation, the less is the effect (on the bainite transformation) of holding in the ferrite range for a constant time. The data are not sufficiently complete, however, to establish whether or not the time for detectable bainite formation depends directly upon the fractional time in the ferrite range.

These experimental results indicate that ferrite nucleates the formation of bainite, as had been stated by Mehl.¹⁷ It was

(Fig. 2). In specimens previously held in the ferrite range the tendency for bainite to form at grain boundaries is much more marked (Fig. 3).

That proeutectoid ferrite would nucleate the bainite reaction is certainly to be expected. Freshly formed bainite differs from proeutectoid ferrite only in its carbon content. The lattice structures and the crystallographic orientations with respect to the parent austenite¹⁸ are the same.

Information on the effect of the small quantities of proeutectoid carbide upon subsequent transformation to bainite is contained in a paper by Lange and Mathieu. They used steels having 8.7 per cent Ni with 0.77 per cent C and 7.04 per cent Ni with 0.7 per cent C. Holding in the temperature range at which carbide formed greatly decreased the speed of

subsequent reaction to bainite at a lower temperature. No pearlite formed in these experiments. The longer the time and the lower the temperature of holding in the carbide range, the slower was the subsequent transformation to bainite. Since no determinations were made of the times necessary for carbide formation, it is difficult to evaluate the data quantitatively. One comparison of interest is made in Fig. 4. Here a measure of the amount of transformation to bainite at 417°C. is plotted against the ratio of the time at 417°C. to the time of prior holding in the carbide range at 530°C. For times of 5 to 30 min. at 530°C. the progress of the reaction can be approximated by a single curve when plotted in this fashion. Over this time range, therefore, the time necessary for formation of a given percentage of bainite is approximately proportional to the time of holding in the carbide range. For times of 30 to 270 min. at 530°C. no further slowing of the bainite reaction occurred. This might be due to the carbide reaction having had its full effect upon the nucleation of bainite within 30 minutes.

The experiments discussed above involve the formation of only small amounts of proeutectoid ferrite and carbides, which influence the bainite reaction through nucleation. Larger amounts would be expected to influence the bainite reaction primarily through their effect upon the composition of the austenite, especially upon its carbon content. Ferrite formation, by enriching the austenite in carbon, would retard the bainite reaction, lower the maximum temperature at which it occurs, and decrease its degree of completion at any fixed temperature. Carbide formation would have the opposite effects.

Liedholm and Coons¹⁹ have experimentally confirmed, in SAE 4330 steel, the prediction that precipitation of large amounts of ferrite retards the bainite reaction. Gorden, Cohen, and Rose²⁰ found that, in high-speed steel, formation of large

amounts of mixed pearlite and proeutectoid carbide at 1200°F. accelerates the bainite reaction. These authors noted further that holding high-speed steel for several minutes at 1100°F. or hours at 1000°F. after austenitizing also hastens subsequent bainite formation. At 1000° and 1100°F. no transformation was observed in 24 hr. either dilatometrically or, presumably, metallographically. It seems likely that the acceleration of the bainite reaction again resulted from precipitation of proeutectoid carbide. Such carbide precipitation would be difficult to detect dilatometrically. If the precipitation occurred around undisolved carbide particles, it would also be difficult to detect metallographically.

Evidence that the degree of completion of the bainite reaction is increased by precipitation of proeutectoid carbide has been noted by Jaffe and Hollomon.21 Evidence that the maximum temperature of bainite formation is raised may be found in the papers of Lyman and Troiano.22,23 These authors reported that, in 2.9 per cent Cr steels with 1.02 and 1.28 per cent C, bainite forms at high temperatures following such carbide precipitation. The shape of the isothermal diagram at lower temperatures, as well as other data, indicate that bainite would not be expected to form at these high temperatures without prior carbide precipitation. The example just cited is complicated by the formation of appreciable amounts of pearlite (as well as proeutectoid carbide) prior to the appearance of bainite. However, the occurrence of pearlite could hardly affect the maximum temperature at which bainite can form, for pearlite formation does not change the gross composition of the remaining austenite.

It is possible that pearlite formation might tend to delay the transformation to bainite by eliminating sites of ready nucleation. On the other hand, the ferrite lamellae of the pearlite might tend themselves to nucleate bainite formation. Nucleation by lamellae is made less probable by the fact that the crystallographic orientation of the ferrite in these lamellae, with respect to the parent austenite, differs from that of bainite. Is Jolivet and Portevin²⁴ found that partial transformation to pearlite does not change the rate of subsequent reaction to low-temperature bainite. The two reactions (occurring in that order) are approximately additive.

A number of investigations 11,20,25-27 have definitely established that martensite hastens the subsequent transformation of austenite to bainite. Lange and Mathieu¹¹ reported that the effect is more marked the greater the percentage of martensite. Both these authors and Gorden, Cohen, and Rose²⁰ found that acceleration of the bainite reaction could more precisely be described as the rapid formation of a small amount of bainite, followed later by formation of larger quantities of bainite. Gorden, Cohen, and Rose noted, moreover. that the initial rapid formation of bainite was localized near the martensite plates, while the later formation of large quantities of bainite was general throughout the microstructure. Such local bainite formation prior to the general bainite formation is probably responsible for the reports of the martensite reaction continuing isothermally to a small extent after cooling had ceased: the local bainite formation may have been erroneously interpreted as martensite formation.*

Since martensite formation does not change the composition of the austenite, martensite must nucleate or accelerate the nucleation of bainite. The martensite itself may act as a nucleus for bainite, for their crystallographic orientations differ but little. The additional discontinuities along the martensite-austenite interfaces

Effect on Pearlite Reaction .- As pointed out and discussed by Scheil,1 the data of Sato²⁸ give some indication of the effect of prior proeutectoid reaction upon the transformation of austenite to pearlite. Sato measured dilatometrically the temperatures at which the pearlite and proeutectoid reactions initiate during cooling at various rates in iron-carbon alloys, ranging from 0.008 to 1.55 per cent carbon. Similar dilatometric and thermal arrest measurements were later made by Wever, Rose, and Lange.29 Pertinent data are also available in the isothermal transformation diagrams for 3 per cent Cr steels containing 0.08 to 1.28 per cent C, determined metallographically by Lyman and Trioano.22 The grain size of the austenite was unfortunately not controlled or reported in these studies, but it does not seem likely that the results could be attributed to variations in grain size.

In all these investigations it was found that the time necessary for the formation of small amounts of pearlite decreases smoothly as the carbon content of the steel increased over the entire range.* No discontinuties were found even though proeutectoid ferrite was observed prior to the pearlite at low carbon contents, proeutectoid carbide prior to the pearlite at high carbon contents and neither at intermediate carbon contents. Scheil concluded that proeutectoid ferrite and carbide (in small quantities) have little effect upon the subsequent formation of pearlite.

It might be expected that either the ferrite or the carbide would nucleate

may provide more area for ready nucleation. The stresses set up by martensite formation may, as Gorden, Cohen, and Rose point out, lower the additional energy required.

^{*} In some cases, too, a small amount of cooling undoubtedly took place after the investigators thought cooling had ceased. During this cooling martensite would continue to form.

^{*} This, it should be noted, is in direct contradiction to the widespread belief that increase of carbon content increases the time necessary for pearlite formation.

the pearlite. However, the crystallographic orientation of proeutectoid ferrite with respect to the austenite is known to differ from that of the ferrite lamellae in pearlite.18 The orientation of cementite lamellae in pearlite has not vet been determined; it may differ from that of proeutectoid cementite. Such differences in orientation may well be responsible for the apparent failure of proeutectoid constituents to nucleate pearlite. Scheil has suggested another explanation: that adjacent nuclei of ferrite and carbide form more readily than single nuclei of either phase. If Scheil's hypothesis is correct, the rate of growth of cementite would have to be greater than the rate of growth of pearlite under all conditions where first cementite and then pearlite form isothermally. This conclusion has not been checked experimentally.

It is well known that the presence of even small amounts of carbides undissolved by the austenitizing treatment considerably hastens the transformation of the austenite to pearlite, and that pearlite nucleates preferentially around such carbides. In this case the carbides are distributed throughout the structure and provide additional areas of discontinuity where pearlite nucleation may readily take place. Proeutectoid carbides, however, tend to form at grain boundaries, where discontinuities already exist, and so add little if any to the area of discontinuity available for the pearlite.

Large amounts of proeutectoid carbide undoubtedly will affect pearlite formation by changing the composition of the austenite. The decrease in carbon content will tend to delay pearlite formation. In some alloy steels, this may possibly be counteracted by the depletion of the austenite in carbide-forming alloying elements, which tends to accelerate pearlite formation.

Large amounts of proeutectoid ferrite may also affect the pearlite formation by changing the austenite composition. The carbon enrichment resulting from ferrite reaction would tend to hasten the transformation to pearlite.

That moderate amounts of bainite (at least when formed at high temperatures) accelerate the transformation of austenite to pearlite is evident from the isothermal transformation diagrams of Klier and Lyman¹³ and of Lyman and Troiano,²² in 3 per cent Cr steels containing 0.08 to 0.38 per cent C. At temperatures where first bainite and later pearlite forms, they found that the pearlite reaction is detected much earlier than the timetemperature plot for its detection at higher temperatures (where no bainite forms) would lead one to expect. The effect may arise from the carbon enrichment of the austenite or from nucleation. By the time pearlite formation was detected, carbides had precipitated from the bainite, and both carbide and ferrite were available to provide nuclei. However, the ferrite would not be of the orientation found in pearlite;18 whether the orientation of the carbide would be the same as that in the pearlite is not known. The formation of bainite may simply increase the area for preferential pearlite nucleation. An experimental check of whether the pearlite reaction is hastened by low-temperature bainite or by a very small amount of hightemperature bainite would indicate whether the effect is due to nucleation or to carbon enrichment of the austenite.

The only data concerning the effect of martensite upon subsequent formation of pearlite seem to be those of Steinberg, Zyuzin, and Goldin.²⁵ In a steel containing 0.35 per cent C, 8.92 per cent Cr, and 3.13 per cent Si, they found that the presence of a moderate amount of martensite considerably hastens the initiation of the pearlite reaction at 600°C. Since the martensite undoubtedly tempered considerably during reheating to this temperature and holding at it, the products of

the tempering of martensite—ferrite and carbide—were evidently responsible for the more rapid nucleation of the pearlite reaction. The ferrite in tempered martensite would not have the same orientation as the ferrite lamellae in pearlite, and it seems unlikely that the carbide in tempered martensite would have the same orientation as carbide lamellae in pearlite. Perhaps the carbide and ferrite of the tempered martensite act merely to provide additional discontinuities where nucleation of pearlite can take place readily.

Effect on Martensite Reaction.—Since the martensite reaction does not proceed isothermally, it is hardly feasible to talk of delaying or hastening it. However, the effect of other reactions upon the temperature range of the martensite transformation may be examined. Lowering the martensite temperature range corresponds to delaying the bainite reaction, and raising the martensite range to accelerating the bainite reaction.¹²

Since martensite does not form by nucleation and growth, and the temperature at which it appears is thermodynamically fixed by the composition of the austenite, 12 other reactions can presumably affect the formation of martensite only by changing the composition of the austenite, and not by nucleating martensite or hindering its nucleation.

The effect of proeutectoid ferrite formation upon the martensite reaction has not been studied. Since an increase in carbon content greatly lowers the martensite temperature range, it would be anticipated that the formation of moderate quantities of proeutectoid ferrite would lower the martensite range by enriching the remaining austenite in carbon.

It seems unlikely that the pearlite reaction would have any significant effect on subsequent martensite formation. Lange and Mathieu¹¹ found that formation of moderate amounts of, presumably, pearlite

does not influence the martensite-start temperature.

Formation of moderate amounts of proeutectoid carbide would be expected to raise the martensite range by depleting the austenite in carbon. This is confirmed by the results of Steinberg and his coworkers14,31 and of Lange and Mathieu.11 In each case the martensite-start temperature was raised by the formation of carbide. The results of Steinberg are somewhat clouded by the possibility of pearlite formation, though this would not be expected to have any effect. Lange and Mathieu definitely established that carbides formed at the austenite grain boundaries during the hold in the carbide range, and that no microscopically or magnetically detectable pearlite was present. Steinberg and his co-workers²⁵ also found that the martensite-start temperature in 0.35 per cent C, 8.92 per cent Cr, 3.13 per cent Si steel was raised by holding at 600°C. It is not evident that proeutectoid carbide would precipitate in a steel of this composition, and its presence was deduced only from the effect on the temperature of martensite formation.

It is generally accepted that the precipitation of carbides from austenite retained during quenching and then reheated raises the maximum temperature of martensite formation in high-speed steel. This has been reported to occur also in the 0.35 per cent C chromium-silicon steel²⁵ just mentioned, and in a 0.30 per cent C steel³² containing 1.47 per cent Cr and 3.6 per cent Ni.

Many investigations have shown that the formation of bainite (at temperatures not too far below the upper limit of bainite formation) lowers the range at which martensite forms from the remaining austenite. 13,14,20,22,23,31-33 There is no reason to doubt that this is due to carbon enrichment of the austenite by the bainite reaction. Klier and Lyman 13 found that

bainite formation at low temperatures (at which it would cause little carbon enrichment of the austenite¹²) has little if any effect on the extent of the martensite reaction at room temperature. These authors noted that bainite formation at higher temperatures produced a significant decrease in the extent of the martensite reaction at room temperature.

Effect on Proeutectoid Reactions.—There seems to be almost no experimental evidence as to the effect of other reactions upon subsequent transformation of austenite to proeutectoid ferrite and to proeutectoid carbide. The prior formation of pearlite does not change the austenite composition. The ferrite lamellae presumably would not nucleate proeutectoid ferrite because of their differing orientation.18 If the orientation of the carbide lamellae is the same as that of proeutectoid carbide, the lamellae will nucleate proeutectoid carbide and so hasten its formation. If the orientation of the carbides differ, pearlite might have little effect on formation of proeutectoid carbide, or might delay it by eliminating nucleation sites. Pearlite may perhaps delay proeutectoid ferrite formation by similar elimination of nucleation sites.

Bainite in small amounts would generally be expected to nucleate and so hasten the proeutectoid ferrite reaction. (The two structures have approximately the same crystallographic orientation. 18) Larger quantities of bainite, formed at temperatures high in the bainite range, would tend to have less effect and might even slow ferrite formation, by increasing the carbon content of the austenite. Jolivet and Portevin²⁴ did find that large quantities of high-temperature bainite slow reaction at 600°C. in a steel containing 0.65 per cent C, 2.75 per cent Ni, 0.75 per cent Cr, o.6 per cent Mo. The austenitizing treatment may have been insufficient to dissolve all carbide particles, and it is not clear whether the reaction observed dilatometrically at 600°C, was to ferrite or to pearlite.

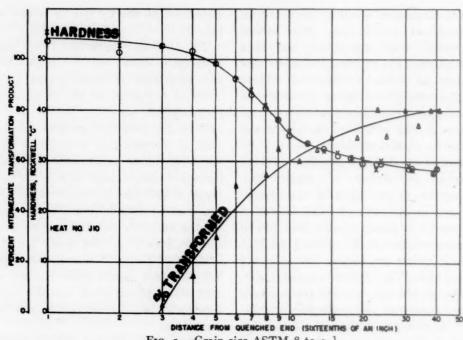
The carbide particles that rapidly precipitate from bainite might hasten the nucleation of proeutectoid carbide. Nothing is known of the orientation of these carbide particles, but in any case the bainite probaby provides additional areas of discontinuity to facilitate nucleation. Moderate quantities of bainite formed at temperatures high in the bainite range would also be expected to hasten proeutectoid carbide formation by enriching the austenite in carbon. Proeutectoid carbide formation has been found by Lyman and Troiano²² to occur isothermally following such bainite formation, where no isothermal proeutectoid carbide formation could be observed under any other conditions.

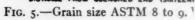
Martensite does not change the austenite composition, but does increase the area of discontinuity available for nucleation of proeutectoid products. The orientation of the martensite is not much different from that of proeutectoid ferrite, so martensite may directly nucleate this constituent. Since martensite tempers rapidly at any temperature where proeutectoid carbide forms, carbides resulting from this tempering would be available for nucleation. Whether these carbides do act as nuclei for proeutectoid carbide seems doubtful, as it is hardly likely that the orientations are the same.

The effect of the proeutectoid ferrite and proeutectoid carbide reactions upon each other seems to be of no interest, since the two reactions have never been noted in the same steel.

SUMMARY

Although the bulk of the experimental and theoretical studies of austenite decomposition have dealt with the simpler isothermal decomposition, anisothermal decomposition is of far greater practical importance. In this paper the available





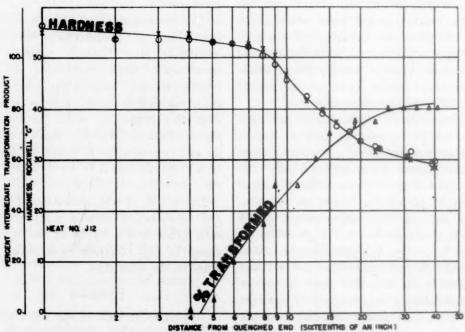
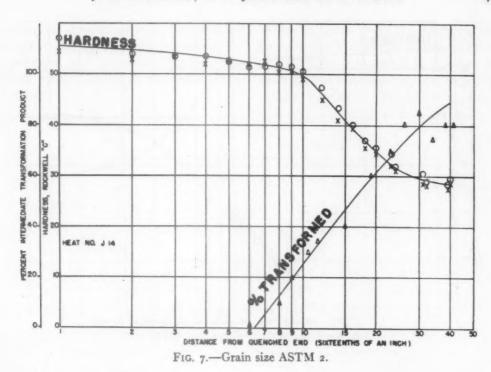


Fig. 6.—Grain size ASTM 4 to 5. FIGS. 5 AND 6.—SURVEYS OF SAE 4140 JOMINY BARS.



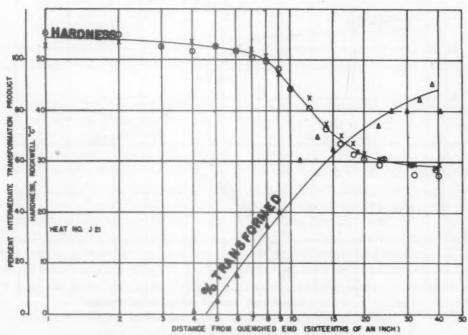


Fig. 8.—Grain size ASTM 000.
Figs. 7 and 8.—Surveys of SAE 4140 Jominy bars.

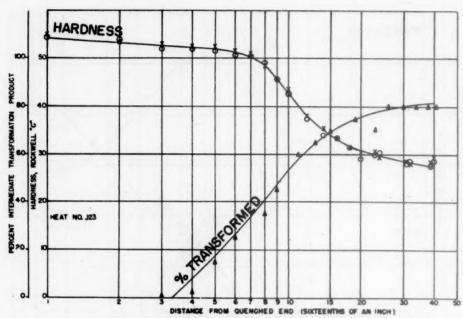


Fig. 9.—Homogenized. Grain size ASTM 7.

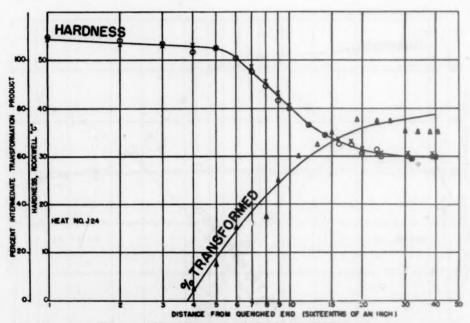


Fig. 10.—Not homogenized. Grain size ASTM 7-8. Figs. 9 and 10.—Surveys of SAE 4140 Jominy bars.

information concerning relations between isothermal and anisothermal decomposition is presented and correlated. New experimental work on some of the relations is described. ferrite in small quantities nucleates and so markedly hastens the bainite reaction, but in large quantities it changes the austenite composition so as to hinder bainite formation. Proeutectoid carbide

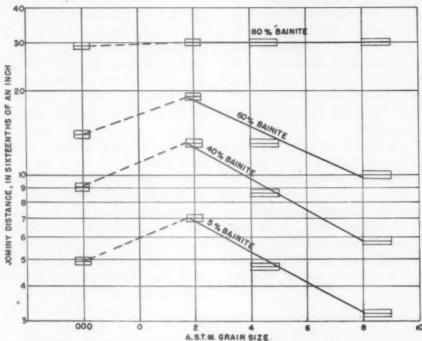


Fig. 11.—Relation between austenitic grain size and bainitic hardenability of SAE 4140 STEEL.

For anisothermal decomposition involving a single reaction, the concept of "additivity" is discussed. There is some evidence that the proeutectoid ferrite reaction is approximately additive. No data are available on the proeutectoid carbide reaction; it may well be additive. The pearlite reaction appears to be at least roughly additive. The bainite reaction deviates from additivity because, for a given per cent transformation, the carbon content of the remaining austenite varies with the transformation temperature. The additivity concept does not apply to the martensite reaction.

One reaction may influence a second by changing the composition of the austenite and by affecting the nucleation of the second reaction. Proeutectoid has the opposite effect. Martensite facilitates the nucleation of bainite. No influence of the pearlite reaction upon bainite formation has been found.

Small amounts of the proeutectoid products have little influence upon the pearlite reaction. The effect of larger quantities has not been tested, but they probably affect pearlite formation by changing the austenite composition. Moderate amounts of high-temperature bainite hasten transformation to pearlite. Martensite does likewise, apparently by facilitating pearlite nucleation.

Formation of moderate amounts of proeutectoid carbide raises the temperature at which martensite forms by decreasing the carbon content of the austenite. High-temperature bainite has the opposite

result. The effect of proeutectoid ferrite has not been studied but is undoubtedly similar to that of the bainite. Pearlite seems to have no influence on the martensite reaction.

The effects of prior reactions on the formation of proeutectoid ferrite and carbide have hardly been studied. Pearlite, bainite, and tempered martensite may hasten the nucleation of ferrite and carbide. High-temperature bainite in moderate quantities apparently facilitates proeutectoid carbide formation by enriching the austenite in carbon.

A great deal of work remains to be done upon the interactions of the various transformations by which austenite decomposes and upon the general question of the relations between isothermal and anisothermal decomposition. It is only through these relations that the results of isothermal studies can be applied quantitatively to most problems of practical heat-treatment.

APPENDIX.—Effect of Grain Size on the Bainite Transformation

Jominy specimens were machined from SAE 4140 bar stock of the following composition:

C, 0.37 per cent; Mn, 0.71; Si, 0.28; S, 0.028; P, 0.016; Ni, 0.26; Cr, 1.05; Mo, 0.18; V, nil.

The specimens were heat-treated in carbonaceous muffles, as follows:

HEAT-TREATMENT*
1500°F., 2 hr., end-quenched
{1850°F., 1 hr., furnace-cooled to 1500°F., 1 hr., end-quenched
∫2200°F., 1 hr., furnace-cooled to
1500°F., 1 hr., end-quenched
{2450°F., 1 hr., furnace-cooled to 1500°F., 1 hr., end-quenched
Heated to 1500°F., 2 hr., end- quenched

J24...... 1500°F., 2 hr., end-quenched

* Temperatures may have varied as much
as 35°F. from the nominal.

After heat-treatment, flats 1/10 in. deep were ground on opposite sides of each specimen, and hardness surveys made. One flat was then polished, etched with I per cent nital and examined microscopically.

Results of microstructural and hardness surveys on specimens J10, J12, J14, J21, J23, and J24 are given in Figs. 5 to 10. The hardnesses found on J11, J13, and J15 duplicated those of the companion bars, so no metallographic examination was made on these specimens. The percentages of intermediate transformation product (bainite) given in the figures are the averages of three surveys, made at 500 diameters.

The distances from the quenched end at which several percentages of bainite were found in bars J10, J12, J14, and J21 are plotted against the austenitic grain size in Fig. 11. These distances were read from Figs. 5 to 8. The cause of the decrease from J14 (ASTM grain size 2) to J21 (grain size 000) has not been ascertained.

No undissolved carbides were observed in any of the specimens. To check the possibility that the increase in Jominy distance noted in the series J10, J12, J14 could be due to increased homogenization at the higher autenitizing temperatures, bars J23 and J24 were run. Both were austenitized at 1500°F., but J23 received a preliminary homogenization treatment while J24 did not. As Figs. 9 and 10 indicate, no significant difference was found.

REFERENCES

 E. Scheil: Initiation Time of the Austenite Transformation. (In German.) Archiv Eisenhuttenwesen (1935) 8, 565-567.
 M. Avrami: Kinetics of Phase Change—I.

 M. Avrami: Kinetics of Phase Change—I. General Theory, Jnl. Chem. Phys. (1939)
 7, 1103-1112.
 M. Avrami: Kinetics of Phase Change—II.

 M. Avrami: Kinetics of Phase Change—II. Transformation-Time Relations for Random Distribution of Nuclei. Jnl. Chem. Phys. (1040) 8, 212-224.

Phys. (1940) 8, 212-224.

4. R. A. Grange and J. M. Kiefer: Transformation of Austenite on Continuous Cooling and Its Relation to Transformation at Constant Temperature. Trans.

Amer. Soc. for Metals (1941) 29, 85-116.

5. S. Steinberg: Relationship between Rate of Cooling, Rate of Transformation, Undercooling of Austenite, and Critical Rate of Quenching. (In Russian.) Metal-

lurg (1938) 13 (1), 7-12.
6. H. Krainer: The Conditions for Throughhardening of Steel. (In German) Archiv

Eisenhultenwesen (1936) 9, 619-622.
7. H. Lange and H. Hansel: The Course of the Austenite Transformation in the Undercooled State According to Investigations on Pure Plain Carbon Steels, (In German.) Mitt. K-W-I.

Eisenforschung (1937) 19, 199-208.

Lange: Austenite Decomposition in Plain Carbon Steels. (In German.) Mitt. K-W-I. Eisenforschung (1940) 22, 229-

J. E. Dorn, E. P. De Garmo, and A. E. Planigan: Nucleation and Growth Rates of Pearlite. Trans. Amer. Soc. for Metals

(1941) 29, 1022-1036.
10. F. C. Hull, R. A. Colton, and R. F. Mehl:
Rate of Nucleation and Rate of Growth of Pearlite. Trans. A.I.M.E. (1942) 150, 185-210.

11. H. Lange and K. Mathieu: The Course of the Austenite Transformation in the Supercooled State for Iron-nickel-carbon Alloys. (In German.) Mitt. K-W-I. Eisenforschung, Düsseldorf (1938) 20,

125-134.

12. C. Zener: Kinetics of the Decomposition of Austenite. This volume, page 550.

13. E. P. Klier and T. Lyman: The Bainite

Reaction in Hypoeutectoid Steels. Trans.

A.I.M.E. (1944) 158, 394-422.

14. S. Steinberg and V. Zyuzin: Transformations of Austenite in a Chromium Steel. (In French.) Rev. Metal. (1934) 31,

554-559. 15. E. S. Davenport, R. A. Grange, and R. J. Hafsten: Influence of Austenite Grain upon Isothermal Transformation Behavior of SAE 4140 Steel. Trans.

A.I.M.E. (1941) 145, 301-314.

16. J. H. Hollomon and L. D. Jaffe: The Hardenability Concept. This volume,

17. R. F. Mehl: The Physics of Hardenability; in Hardenability of Alloy Steels, 1-65. Amer. Soc. for Metals, Cleveland, 1939. 18. G. V. Smith and R. F. Mehl: Lattice Relationships in Decomposition of Aus-

tenite to Pearlite, Bainite, and Martensite. Trans. A.I.M.E. (1942) 150, 211-226.

 C. A. Liedholm and W. C. Coons: Effect of Cooling Transformation upon Subsequent Isothermal Reactions. Metal

sequent Isothermal Reactions. Metal Progress (1946) 46, 104-107.

20. P. Gorden, M. Cohen, and R. S. Rose: Kinetics of Austenite Decomposition in High-speed Steel. Trans. Amer. Soc for Metals (1943) 31, 161-217.

21. L. D. Jaffe and J. H. Hollomon: Discussion to Reference 22.

22. T. Lyman and A. R. Troiano: Influence of Carbon Content upon the Transformations in 3 Per Cent Chromium Steel. Preprint 16, Amer. Soc. for Metals (1945).

Metals (1945).

23. T. Lyman and A. R. Troiano: Isothermal Transformation of Austenite in One Per Cent Carbon, High-chromium Steels. Trans. A.I.M.E. (1945) 162, 196.

24. H. Jolivet and A. Portevin: Kinetics of Austenite Decomposition. (In French.)

Compt. rend. (1939) 209, 379-381, 556-558; also Genie Civil (1939) 115, 464-465. Steinberg, V. Zyuzin, and I. Goldin: Transformations of Austenite in a Chromium-silicon Steel. (In French.)

Rev. Met. (1937) 34, 190-194. 26. S. Steinberg and V. I. Zyuzin: Transformations of Austenite in Plain Carbon Steels and Some Special Steels at Low Temperature. (In Russian.) Metallurg (1939)

27. H. J. Elmendorf: The Effect of Varying Amounts of Martensite upon the Isothermal Transformation of Austenite Remaining after Controlled Quenching. Trans. Amer. Soc. for Metals (1944) 33, 236-260.

T. Sato: On the Critical Points of Pure Carbon Steels. Tech. Repts. Tohoku

Imp. Univ. (1929) 8, 27-52.
Wever, A. Rose, and H. Lange: The Influence of Cooling Velocity on the Transformations of Steels. (In German.)

Mitt. K-W-I. Eisenforschung, Düsseldorf (1937) 19, 289-298; (1938) 20,

30. G. A. Roberts and R. F. Mehl: Effect of Inhomogeneity in Austenite on the Rate of the Austenite-pearlite Reaction in Plain Carbon Steels. Trans. A.I.M.E.

(1943) 154, 318-334.
31. Steinberg and V. Zyuzin: Transformation of Austenite in High-speed Steels. (In German.) Archiv Eisenhuttenwesen

(1934) 7, 537-538.
32. V. Sadovski and N. Chuprakova: Effect of Mode of Quenching on Quantity of Retained Austenite in Chrome-nickel Constructional Steel. (In Russian.)

Metallurg (1939) 14 (10-11), 80-89.

33. A. Gulyaev: Decomposition of Austenite in High-speed Steel at Constant Temperature. (In Russian.) Metallurg (1940)

15 (9), 43-50.
34. H. Jolivet and A. Portevin: The Inhibition
Time at the Beginning of Austenite
(In French.) Compt. Decomposition. (In French.) Compt. rend. (1941) 213, 687-689.

DISCUSSION

(F. M. Walters, Jr., presiding)

G. K. Manning.*-It seems to me that Table 2 deserves considerably more attention than has been given it in the paper. In the lower part of this table, it may be noted that increased time at 800°F. produced no consistent trend in increasing the amount of transformation that occurred. For example, with an initial treatment of 16 min. at 1200°F., 7 sec. at 800°F. caused the formation of 10 per cent bainite, but after 8 sec. at 800°F. (using the same initial treatment) none was visible at 500 diameters.

^{*} Assistant Supervisor of Process Metal-lurgy, Battelle Memorial Institute, Columbus, Ohio.

Furthermore, the lower part of Table 2 indicates that specimens held for 32 and 48 min. at 1200°F. and then quenched to room temperature, though containing no ferrite, did contain some bainite that formed during cooling from 1200°F. The implication is that all isothermal studies conducted over the past 15 years are open to question. If time spent at 1200°F. is capable of so nucleating bainite that even a severe quench to room temperature permits the formation of bainite, one wonders how it was possible to construct the early isothermal diagrams, especially if one recalls that many of the early diagrams were for steel of far lower hardenability than that studied by the authors.

To me, the results suggest that the authors did not have proper control of all the variables that might affect the isothermal results, such as decarburization of their thin specimens during austenitizing at rather high temperatures, failure to obtain a reasonable degree of homogeneity within the steel prior to making the tests, or any one of a number of other things.

R. A. GRANGE.*—The authors have nicely summarized the little that has been published relative to the effect of holding austenite for a time too short for its complete transformation at a given temperature level upon subsequent transformation at another temperature level. It is evident that a large amount of new data will be necessary to permit theoretically sound and accurate estimation from isothermal data of the beginning, progress, and ending of transformation as it occurs during continuous cooling. There are, however, difficulties in acquiring the necessary experimental data, since probably the ordinary methods of measuring isothermal transformation are not sufficiently precise for this purpose. We have found, in particular, that segregation (banding), present to some degree in most steels, makes accurate and reproducible measurement of "nucleation effects" extremely difficult, and suggest that this may account for the erratic results presented in Tables 2 and 3.

We have studied the effect of holding for a "fractional time" at a temperature level where proeutectoid ferrite forms upon subsequent transformation to bainite, and such data as

we have confirm those of the authors, which show that the "nucleating effect" of proeutectoid ferrite is approximately additive with respect to transformation to bainite. We are inclined to believe, however, that its importance with respect to hardenability may have been somewhat overemphasized in the paper. Fig. 11, which summarizes the authors' data on the effect of austenite grain size upon the endquench hardenability of SAE-4140 steel, is interpreted by them as evidence that the longer "initiation time" for ferrite in coarse-grained austenite decidedly increases hardenability. While in agreement with the authors that this effect would contribute to greater hardenability, we doubt that all the difference in hardenability shown in Fig. 11 can be attributed entirely to this source. It would seem to us that some other factor that influenced hardenability had not been eliminated, since, on the basis of the effect of nucleation, one would expect the hardenability for an austenite grain size of No. 000 ASTM to be greater than for a grain size of only No. 2; in Fig. 11, however, the reverse is shown. We happened to have results of end-quench hardenability tests for SAE-4140 steel austenitized at 1550°F. (grain size 7-8) and at 2000°F. (grain size 2-3). Unlike the authors' tests, these were quenched directly from the austenitizing temperature, but, according to Jackson and Christenson, 35 this difference should have no very great effect in a steel with as much hardenability as SAE-4140. In our tests, we observed that the measurable beginning of transformation to bainite in the coarse-grained bar occurred slightly nearer the quenched end than it did in the fine-grained bar. Since the "nucleating effect" would be expected to have its greatest influence on the location of the first trace of bainite, it is evident that in these particular tests, which were quenched directly from the austenitizing temperature, as would usually be done in practice, the difference in "fractional time" spent in the proeutectoid-ferrite temperature range had no observed effect upon hardenability; presumably the effect was there, but masked by other factors. Therefore, it would seem that in practice the increase in hardenability due to

^{*} U. S. Steel Corporation, Research Laboratory, Kearny, N. J.

³⁵ C. E. Jackson and A. L. Christenson: The Effect of Quenching Temperature on the Results of the End-quench Hardenability Test. Trans. A.I.M.E. (1944) 158, 125.

"nucleation effects" may sometimes be obscured by other factors.

MEMBER.—I would like to ask Capt. Holloman if he would tell us the exact procedure in his method of quenching in determining his point. I noticed that the specimen size is exceedingly thin, $\frac{1}{40}$ of an inch. This thin specimen might have a great deal of effect on the results on temperature, especially with the very short quenching times he used.

J. H. HOLLOMON, J. D. JAFFE, M. R. NORTON (authors' reply).—The scatter in our results, pointed out by Mr. Manning, has been well explained in Mr. Grange's discussion. It is true that our data raise some doubt as to the validity of previously determined isothermal diagrams. However, in most isothermal studies, little attention has been paid to formation of less than 1 per cent transformation product. We found that after holding SAE-4330 for 32 to 48 min. at 1200°F. only traces of bainite formed during quenching to room temperature. Subsequent work, not yet published, indicates that

the time for formation of r per cent bainite may be less sensitive to incubation in the ferrite range than is the time for the appearance of traces of bainite.

Through error, the thickness of our SAE-4330 specimens was given in the Preprint as 1/40 in., instead of the correct 1/6 in. Most of the details of the quenching procedure used for these specimens are given in the paper. An iron wire inserted in a small hole drilled near one end of the specimen was used for handling. A small horizontal tube furnace was employed for austenitizing, a 3-in. diameter solder pot for the 1200°F. treatments, and a 3-in. diameter pot containing Wood's metal for the 800°F. treatments. To minimize transfer times, the furnaces were placed only a few inches from each other and from the beaker of quenching water. The time for each transfer probably never exceeded 1/2 sec. Handling and timing were done manually; timing errors of perhaps 1 sec. at 800°F. probably contributed to the scatter of the data. Temperatures used for treatment of the SAE-4330 were controlled automatically and were reproducible to ±2°C.

The Relationship between Transformation at Constant Temperature and Transformation during Cooling

By G. K. Manning* and C. H. Lorig,† Members A.I.M.E.

(Chicago Meeting, February 1946)

Two metallurgical tools have acquired wide use within the past several years as a means of studying the transformation characteristics of steel. One is a technique used first by Bain and Davenport for determining the transformation characteristics of a steel at constant temperature; the second is the end-quench hardenability test.

Constant-temperature transformation curves like those of Bain and Davenport have done much to rationalize the metallography of steel; however, in commercial practices, constant-temperature transformation is seldom encountered, therefore only rarely can such curves be directly applied. The real reason for the determination of such curves lies in the fact that they provide a way of thinking about transformation that is both convenient and productive.

The end-quench hardenability test is a more practical means of studying transformation, for, by correlating positions on the hardenability bar with shapes of different masses, an almost direct application of the results can be made. Unfortunately, the end-quench test, though practical, can do very little toward improving the metallurgists' way of thinking about transformation.

These two metallurgical tools, dealing

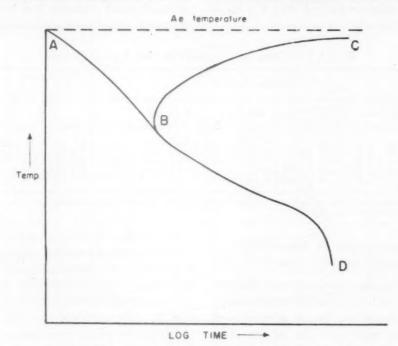
with precisely the same phenomenon, should be very closely associated in metallurgists' minds. Actually, they are frequently pushed into separate mental corners and considered as being more or less distinct and unrelated. The reason for this is that no strong connecting link between them has been developed. An attempt is sometimes made to relate these two tools by projecting the critical cooling rate on the isothermal transformation plot as illustrated in Fig. 1. The critical cooling rate is considered as a constant ratethough in practical applications, cooling rates are never constant-and this constant cooling rate is given uniform significance from the Ae temperature down to the temperature of initial transformation. A little thought indicates the errors of such a procedure. Certainly the time interval spent just below point A of Fig. 1 cannot be as effective in promoting nucleation as is the time interval spent just above point B. Yet the procedure represented in Fig. 1 considers all the time spent between temperatures A and B to be just as effective in promoting nucleation as though all the time were spent at temperature B. Furthermore, change the shape of the isothermal curve between points B and C in any way desired, and the required critical cooling rate is not changed one iota. This cannot possibly be true. Such a way of thinking about critical cooling rates not only is incapable of giving any results that are quantitatively satisfactory but is likely to give very misleading qualitative results.

Manuscript received at the office of the Institute Nov. 5, 1945. Issued as T.P. 2014 in METALS TECHNOLOGY, June 1946.

^{*} Assistant Supervisor, Battelle Memorial Institute, Columbus, Ohio.

[†] Supervisor, Battelle Memorial Institute.

Another method of relating cooling rates to isothermal transformations has been developed by Grange and Kiefer.¹ The proposed formulas are empirical and are as N.D.R.C. Research Project NRC-14. Grateful acknowledgment is made to the Office of Scientific Research and Development* for its support and for its permission



Line CBD represents the initial transformation curve of a given steel.

Line AB represents the cooling curve sometimes visualized as the

Fig. 1.—One commonly used method of relating transformation during cooling and transformation at constant temperature.

of no assistance in improving one's way of thinking about the relationship between transformation during cooling and transformation at constant temperature. Such empirical formulas cannot be used with confidence, because even though they may have been satisfactory for a number of tested steels, one cannot be confident that they will apply to a new steel.

An investigation of the relationship between the transformation at constant temperature and transformation during cooling constituted part of a research program sponsored by the National Defense Research Committee of the Office of Scientific Research and Development, to publish this work, to the War Metallurgy Division of N.D.R.C. and the War Metallurgy Committee for supervising and directing the research, and to various members of the Battelle staff, particularly P. C. Rosenthal and A. R. Elsea, for their helpful contributions.

EXPERIMENTAL WORK

Five steels that varied in chromium content from 0.5 to 2.5 per cent were used in the experimental work. These steels were made as induction-furnace heats, and

References are at the end of the paper.

^{*} This work was done in whole under Contract No. OEMsr-450 between Battelle Memorial Institute and the Office of Scientific Research and Development, which assumes no responsibility for the accuracy of the statements contained herein.

cast as 50 lb., big-end-up, hot-topped ingots. The chemical analysis of each steel and the sizes to which the ingots were forged and rolled are given in Table 1. All five steels were deoxidized with 1½ lb. of aluminum per ton.

to represent "the beginning and the end of transformation." An average of two nuclei per field at 500 diameters was chosen as the beginning, and an average of two untransformed particles per field at 500 diameters was chosen as the end.

TABLE 1.—Chemical Composition and Size of Product

Steel				Ci Dd I						
	С	Mn	Si	Cr	Мо	Cu	Ni	S	P	Size Product, In.ª
A B C D E	0.30 0.28 0.29 0.30 0.29	0.49 0.49 0.49 0.60 0.50	0.41 0.41 0.40 0.36 0.34	0.51 1.00 1.49 2.04 2.40	0.4I 0.4I 0.4I 0.33 0.34	0.05 0.05 0.05 0.04 0.05	0.04 0.04 0.04 0.03 0.03	0.03 0.03 0.03 0.027 0.026	0.011 0.011 0.011 0.008 0.008	% plate, % round % plate, % round % plate, % round, 11/4 round % plate, 11/4 round % plate, 11/4 round

^a After forging and rolling, both the round and flat stock of all heats were heated for 2 hr. at 1700°F., aircooled, and drawn for 1 hr. at 1200°F.

DETERMINATION OF ISOTHERMAL TRANSFORMATION CURVES

The 3/16-in. plate stock was used throughout for the isothermal transformation specimens. Approximately 1/16 in. was removed by grinding from each side of the plate and the resultant 1/6-in. sheet was sawed into strips about 1/2 in. wide, after discarding 1/4 in. from all edges of the original sheet. The ½- by ½6-in. strips were then sheared to specimens approximately 1/6 by 1/6 by 1/2 in. The specimens were attached to wire of 0.080-in. diameter, and were austenitized by heating for 10 min. (total time) at 1700°F. in a small electric muffle furnace. Isothermal treatments above 800°F. were done in a small lead pot, and those at 800°F. or below in a small Wood's metal pot. After treatment, the specimens were cut midway their length, mounted in Bakelite with the freshly cut face exposed, polished, and examined at a magnification of 500 diameters. The method of sectioning resulted in the examined plane being always parallel to the direction of rolling. Since transformation follows an asymptotic curve, it became necessary to choose two arbitrary points on the transformation-time curve

In an effort to determine the beginning and end of transformation (particularly the beginning) as accurately as possible, specimens were isothermally treated at 50°F. intervals between 1500° and 700°F. and at 25°F. intervals in the positions of the curves where the slopes were changing rapidly. About 250 specimens of each steel were isothermally treated and examined.

Isothermal transformation curves for the five steels are shown in Figs. 2 through 4. The nature of the first transformation product to appear at any temperature attracted particular attention. From the Ae₃ temperature down to approximately 1200°F., the first product to appear in all five steels was equiaxed ferrite, as illustrated in Fig. 5. For the purpose of this paper, such transformation particles have been termed "blocky ferrite." Below 1200°F., the shape of many of the first ferrite particles to appear changed from equiaxed to acicular. At 1100°F., all of the blocky ferrite disappeared and the beginning transformation product was found to consist entirely of acicular ferrite, herein termed "spear ferrite," as illustrated in Fig. 6. The first transformation product appeared to be 50 per cent

blocky ferrite and 50 per cent spear ferrite at 1130°F. The temperatures given for the transition from blocky to spear ferrite seemed to be common to all five bainite was 930°F., but the whole transition range covered not more than 50°F. (900° to 950°F.). Again, the temperature of transition appeared to be common to

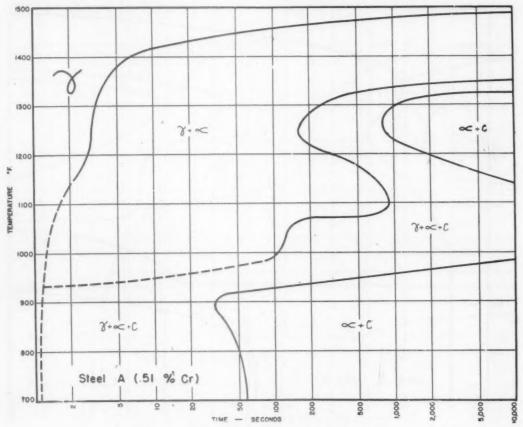


FIG. 20.—ISOTHERMAL TRANSFORMATION CURVE.

steels, though, of course, the time required to start transformation differed greatly for the different steels. Spear ferrite was observed to be the initial transformation product from 1100 to about 930°F. Below 930°F. the general shape of the first product was still acicular but became an agglomerate of ferrite and carbide rather than simply ferrite. This agglomerate is termed bainite (see Fig. 7) in this report. The transition from spear ferrite to bainite was somewhat sharper than the transition from blocky ferrite to spear ferrite. The temperature at which the first product was 50 per cent spear ferrite and 50 per cent

all five steels. As isothermal treatments were carried out at still lower temperatures, the bainite became gradually finer in appearance. Below 825°F., it was difficult to resolve the transformation product at 500 diameters, and at 750°F. and below, it was impossible to resolve the product even with the use of oil-immersion objectives.

This series of steels, differing principally in chromium content, permits some observation about the effect of chromium on the isothermal transformation curves. The most conspicuous change is the split that occurs between the pearlite and bainite portions of the curves, previously recorded by several investigators. Beginning transformation at the nose of the blocky ferrite range is progressively

end of transformation, on the other hand, was not uniformly retarded by increasing chromium contents. Note from Fig. 2a that the minimum time for complete

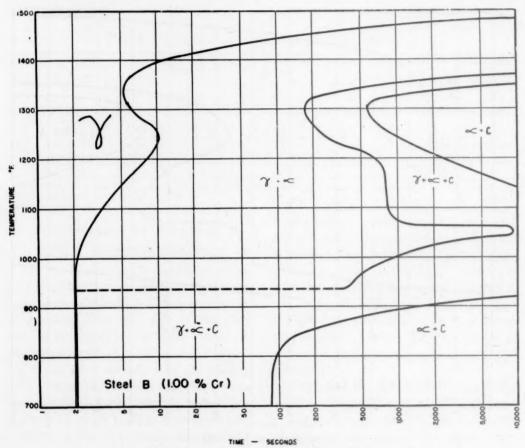


FIG. 2b.—ISOTHERMAL TRANSFORMATION CURVE.

retarded by increasing the chromium. A change in the chromium content from 0.5 to 2.5 per cent causes an increase of somewhat more than 1000 per cent in the time required for initial transformation at 1350°F. The beginning bainite transformation line is similarly shifted, but at 800°F. the shift occasioned by varying the chromium from 0.5 to 2.5 per cent is less than 600 per cent. Chromium, then, appears to have a very material effect on both the upper and lower portion of the isothermal curves, though the effect is somewhat less in the lower portion. The

transformation of the 0.5 per cent chromium steel was 800 sec. at about 1260°F., but in the 1 per cent chromium steel it was 550 sec. at about 1300°F. Thus, it is not inevitable that annealability will decrease with each increase in hardenability.

STEP-COOLING TESTS

In attempting to relate beginning transformation during cooling with beginning transformation at some constant temperature, it became important to know the effect of time spent at, say, 1300°F. upon subsequent nucleation at, say

1200°F. Consequently, a series of step tests was made on steels C and E. Specimens of the same size used for determination of the isothermal transformation curves, temperature. This temperature range corresponds with the blocky ferrite range previously noted. From about 1100°F. down to 700°F., the results indicate the presence

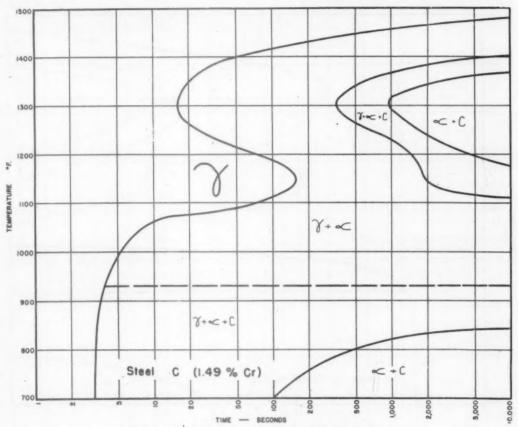


FIG. 3a.—ISOTHERMAL TRANSFORMATION CURVE.

and the same austenitizing time and temperature, were employed. Two lead pots were used instead of one. The specimens were quenched for a prearranged time, first in the lead pot operating at the higher prearranged temperature, then in the lead pot operating at the lower prearranged temperature, and finally, quenched to room temperature in water. The results of these tests are given in Table 2.

The results indicate that, from the Ae₃ temperature down to 1200°F., the fraction of nucleation time spent at a given temperature is additive with the fraction of nucleation time spent at another lower

of a second additive range, and the temperature range is composed of both the spear ferrite and bainite ranges previously noted. Thus, nucleation intervals in the spear ferrite and bainite ranges appear to be additive to themselves and also to each other. However, the tests started in the blocky ferrite range and completed in either the spear ferrite or bainite range do not indicate an additive effect. For the steels examined, time spent in the blocky ferrite temperature range did not materially reduce the time subsequently required for nucleation at any temperature below 1100°F.

Such a situation suggests two prime

modes of nucleation that are distinct from one another. The first is the blocky ferrite type of nucleation occurring from Ae₃ down to about 1200°F. The second is

tion curves between 1150° and 1250°F. of the steels containing 2 and 2.5 per cent chromium may be associated with this change in mode of nucleation.

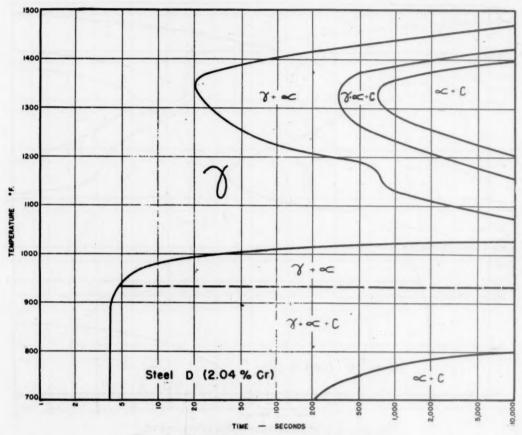


FIG. 3b.—ISOTHERMAL TRANSFORMATION CURVE.

the spear-ferrite, bainite type of nucleation occurring from about 1100°F. down to 700°F. and perhaps even somewhat lower. The fact that carbides precipitate "in place" at temperatures below 930°F. appears to be only incidental and not significant of a real change in the mechanism by which transformation proceeds. Recognition of these different modes of nucleation suggests that beginning transformation between 1200° and 1100°F. should be represented by two separate lines, as illustrated in Fig. 8, rather than by the customary continuous line. The unusual bulge in the beginning transforma-

Mathematical Relationship between Initial Transformation during Cooling and Initial Transformation at Constant Temperature

The results of the step tests described may be made the basis of a rational relationship between initial transformation during cooling and initial transformation at constant temperature. The time spent at a particular temperature divided by the time required for beginning transformation at that temperature is considered to represent a fraction of the total nucleation time required. When the sum of a number of such fractions equals one, beginning

TABLE 2.—Time for Beginning Transformation, Using Two Isothermal Steps.

	F	irst Ste	р		Second Step	,	
Steel	Tempera- ture, Deg. F.	Time Used, Sec.	Fraction of Beginning Transfor- mation	Tempera- ture, Deg. F.	Time Required for Beginning Transfor- mation, Sec.	Fraction of Beginning Transfor- mation Time Required	Comments
E E E	1400 1400 1400 1400	150 150 150 150	0.75 0.75 0.75 0.75	1300 950 900 850	30 15 8 6	0.25 I.0 I.0 0.86	Nucleation additive Nucleation not additive Nucleation not additive Nucleation substantially Nucleation
EEEEEEECCCCC	1400 1150 1150	150 2000 2000	0.75 0.5 0.5	750 950 850	5½ 8	1.0 0.53 0.43	additive Nucleation not additive Nucleation additive Nucleation additive
E	950 950 950	8 8	0.53 0.53 0.53	900 800 700	5 3 3 3	0.62 0.50 0.60	Nucleation substantially additive Nucleation substantially additive Nucleation substantially additive
CC	900 1450 1450	4 400 400	0.50 0.50 0.50	800 1300 1200	3 7 35	0.50 0.44 0.50	Nucleation additive Nucleation substantially additive Nucleation additive
000	1300 1300 1300	10	0.62 0.62 0.62	1200 1100 800	25 75 3	0.36 1.0 0.94	Nucleation additive Nucleation not additive Nucleation substantially non-
CC	1100	60	0.80	900	<2b		additive Nucleation substantially additive Nucleation substantially additive

Each line of the table represents for the most part the average of several duplicate tests.
 Times were too short for accurate determination.

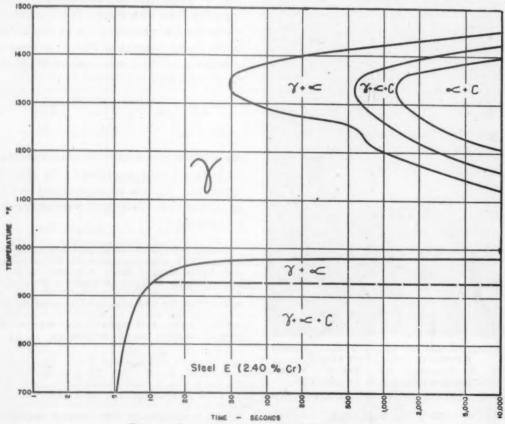


Fig. 4.—Isothermal transformation curve.

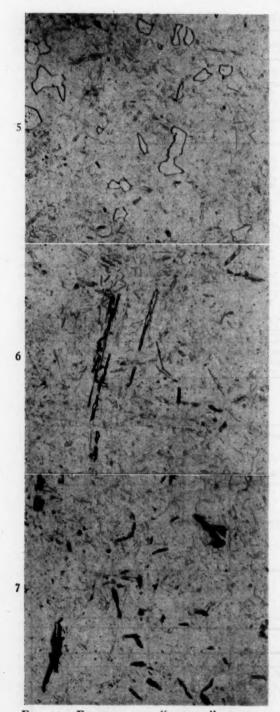


Fig. 5.—Example of "blocky" ferrite formed in steel D at 1350°F.

Fig. 6.—Example of "spear" ferrite formed in steel D at 1000°F.

Fig. 7.—Example of bainite formed in steel D at 900°F.

All × 500. Picral etch.

transformation as herein defined (two nuclei per field at 500 diameters) occurs. Such a line of reasoning leads to the following mathematical expression:

$$\sum_{\substack{X=0\\(T=\text{Ae}_3)}}^{X\pi} \frac{\Delta X_{(T)}}{Z_{(T)}} = 1 \qquad [1]^*$$

where $Z_{(T)}$ equals the time in seconds for beginning transformation at temperature T, X equals the elapsed time on the cooling curve, $(\Delta X_{(T)})$ then equals a small increment in cooling time at temperature T), and Xn equals the time for nucleation during cooling.

The derivation of the expression may be illustrated by imagining the cooling curve as a succession of small instantaneous temperature steps rather than a continuous change as shown in the upper diagram of Fig. 9. Then, ΔX divided by the corresponding time with respect to temperature for isothermal nucleation (Z as illustrated in the lower diagram of Fig. 9) represents a fraction of the total nucleation period. If the fractions

$$\frac{\Delta X_1}{Z_1} + \frac{\Delta X_2}{Z_2} + \frac{\Delta X_3}{Z_3} \cdot \cdot \cdot \frac{\Delta X_n}{Z_n}$$

are added together until the total equals 1, nucleation begins according to the original hypothesis. Eq. 1 is an abbreviated way of indicating that these small fractions are to be summed.†

on a single test using a 0.9 per cent carbon steel.

† Eq. 1, by the fundamental theorem of integral calculus, may be written as:

$$\int_{X=0}^{Xn} \frac{dX}{Z} = 1$$

$$X = 0$$

$$(T = Aea)$$

However, solution of this integral makes it

^{*}Substantially the same mathematical representation has been suggested by S. Steinberg² and Erich Scheil.³ Both, however, consider nucleation as additive throughout the entire Ae to Ms range. Scheil presents no data to substantiate his equation, and Steinberg reports on a single test using a 0.9 per cent carbon steel.

The lower limit $(X = 0, T = Ae_a)$ imposed on Eq. 1 follows from the observation that as Z becomes large the fraction $\frac{\Delta X}{Z}$ becomes small. At $T = Ae_a$ and above,

applies:

$$\sum_{\substack{X=0\\(T=1130^{\circ}\text{F.})}}^{Xn} \frac{\Delta X_{(T)}}{Z_{(T)}} = 1 \qquad [2]$$

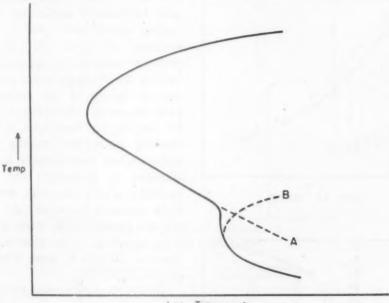


Fig. 8.

Solid line represents usual method of representing beginning of transformation. Broken line A represents the beginning of blocky ferrite transformation and broken line B represents the beginning of spear-ferrite transformation. Use of two separate lines seems more reasonable than the single line commonly used.

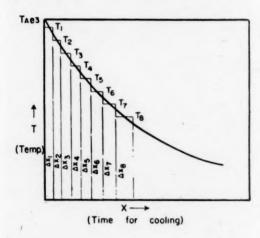
Z becomes infinite and since ΔX must still be finite, the values for $\frac{\Delta X}{Z}$ become zero, hence time X is measured from the instant when $T=\mathrm{Ae_1}$. The upper limit $(Xn,T>1130^\circ\mathrm{F.})$ means that the instant when the sum reaches one is called X=Xn. However, if the temperature falls to 1130°F. before the sum reaches one, the sum can never reach one (since $\frac{\Delta X}{Z}$ becomes zero) and the summation should be abandoned.

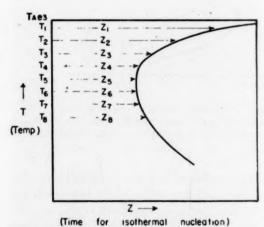
Below 1130°F. a new nucleation process begins, and to it a different equation The results of the step tests indicate that Eqs. 1 and 2 are not additive or related. For lack of better experimental data, 1130°F. has been used as a sharp division point between the two summations. Actually, if separate Z values for blocky ferrite and for spear ferrite could be determined within their overlapping range, there would be no justification for arbitrarily restricting the lower limit of Eq. 1 or the upper limit of Eq. 2. Practically, however, such overlapping Z values for the steels tested are sufficiently large that no significant error results from dividing the two summations at 1130°F.

The accuracy of the graphical solution for Eqs. 1 and 2 is determined by the difference in the T values for which corresponding ΔX

necessary that Z be expressed in terms of X. Although both X and Z have the dimension of time, and although both X and Z are some function of temperature, the expression of one in terms of the other is awkward and a graphical solution is more easily accomplished.

and Z values are computed. As the difference T_1 minus T_2 , T_2 minus T_4 , . . . becomes smaller the accuracy is improved.





(Time for isothermal nucleation)
Fig. 9.—Chart illustrating symbols used
in deriving equation i.

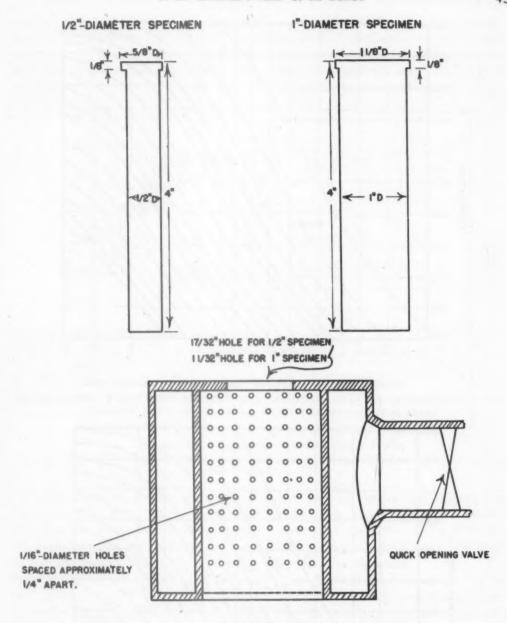
Eqs. 1 and 2 are not dependent for solution upon a constant cooling rate. The only requirement is that the cooling rate throughout the significant range be known. Furthermore, no undue importance is attached to the Ae₁ temperature. As the Ae₂ temperature is approached, values for Z become very large and individual values for $\frac{\Delta X}{Z}$ become insignificantly small. Actually, the Ae₁ temperature need not even be known.

INTERRUPTED END-OUENCH TESTS

It was desirable to check the validity of Eqs. 1 and 2 when applied to continuously cooled specimens. The very commonly used end-quench hardenability test seemed well suited for such a purpose. Liedholm's4 publication of complete cooling curves from 1500° to 200°F. for specimen of 1/2-in. diameter, together with the method he described of interrupting the standard quench by a drastic over-all quench of the end-quench bar. gave the needed information and a method for carrying out such tests. A little later. carefully determined cooling curves for end-quenched hardenability bars of 1-in. diameter, by Boegehold and Weinman,5 became available. However, work with the ½-in.-diameter bars already had been started. Consequently, steels A, B, and C were tested as 1/2-in.-diameter bars and steels C, D, and E, were tested as 1-in.

Details of each hardenability specimen and of the quenching apparatus employed are given in Fig. 10.

The hardenability bars (both sizes) were austenitized by heating for 20 min. (total time) at 1700°F. Twenty minutes heating for these specimens gave roughly the same time at temperature as heating the small isothermal specimens for 10 min. Specimens of each steel were then placed in the quenching jig and end-quenched in the usual way for some prearranged time, and then quenched all over by use of a spray attachment. Periods of 5, 10, 15, 20, 25, 30, 40, 50, 60, 80, 90, 100, 110, 120, 130, 140, 150, 160, 170, 180, 190, and 200 sec. before complete quenching were used for all the steels. Time was counted from the instant the standard water column touched the end of the specimen, the 2 to 3 sec. required to transfer the specimen from the furnace to the jig being disregarded. After quenching, flats o.o15-in. deep were wet-ground 180° apart on the specimens and the usual hardness determinations



QUENCHING JIG

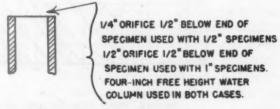


Fig. 10.—Type of specimens and quenching jig used.

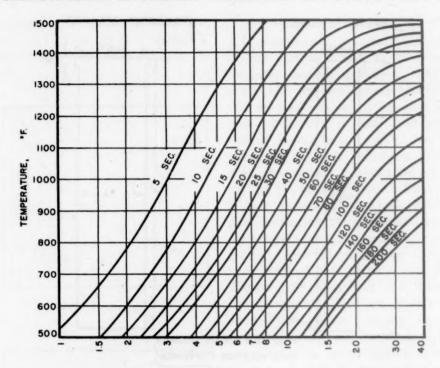
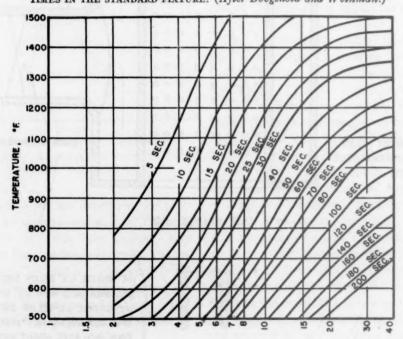


FIG. 11.—TEMPERATURE OF ½-IN. SPECIMEN (END-QUENCHED FROM 1700°F.) AFTER VARIOUS TIMES IN THE STANDARD FIXTURE. (After Boegehold and Weinman.)



DISTANCE FROM QUENCHED END OF 1/2° - DIAMETER 86R
FIG. 12.—TEMPERATURE OF INCH SPECIMEN (END QUENCHED FROM 1650°F.) AFTER VARIOUS TIMES
IN THE STANDARD FIXTURE. (After Liedholm.)

were made.* An additional 0.015 in. was then removed from one side of each specimen, to give a band sufficiently wide for metallographic polishing and examination. the bands described in any one of the interrupted specimens was dependent on the time that elapsed before the specimen was quenched all over. The martensite formed at the slow-cooled end of the bar by

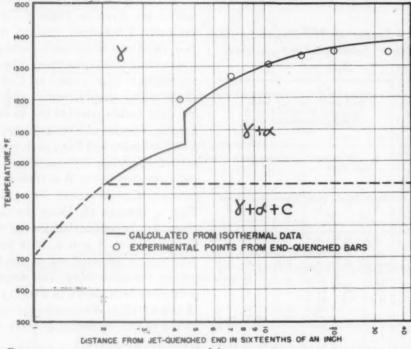


Fig. 13.—Beginning transformation using ½-in. diameter end-quenched bar. Steel A (0.51 per cent Cr).

Various microconstituents were apparent along the side of the hardenability bars quenched for 10 min. with the standard jet. Starting at the fast cooled end, a band of 100 per cent martensite was first encountered; following this, a band of bainite and martensite in which the bainite gradually became coarser was apparent; further back, spear ferrite, bainite, and martensite were found; and finally, in all the steels except D and E, blocky ferrite, spear ferrite, bainite, and martensite were evident. The hardenability of all five steels was sufficient to prevent pearlite from being formed. The presence of all

the over-all quench was always slightly lighter in color than the martensite present at the fast-cooled end, indicating that a drastic quench was being obtained by the over-all quench.

A clear-cut separation of the bands described was not possible because the various structures gradually shaded into one another. Transformation was occurring during cooling rather than at constant temperature, as with isothermal specimens. Therefore, a variety of microconstituents was present in a single field under the microscope, and an accurate classification of each constituent could not be made.

However, the presence of the last trace of transformation product (other than the white martensite formed by the over-all quench) as the slow-cooled end of the bar

^{*} These hardness determinations have not been included in the report because nothing unusual developed from the surveys. The hardness curves had the general shape illustrated by Liedholm.

was approached could be determined accurately. The specimens were rated by measuring with a micrometer stage the distance from the jet-quenched end to the location at which an average of two nuclei per field at 500 diameters was

TABLE 3.—Results of Metallographic Examination of Interrupted end-quenched Bars

Time in End	Distance from Jet-quenched End to "Two per Field" Location of Transformed Product, Sixteenths of an Inch										
Fixture Prior to Quenching All Over, Sec.		nch-di er Bar		1-inch-diam- eter Bars							
	Steel A	Steel B	Steel C	Steel C	Steel D	Steel E					
5	4.3	3.6	2.1	1.7	1.9	1.9					
15	7.1	7.9	5.9	3.9 5.3	3.1	3.7					
20	14.5	9.7	7.4		5.8	4.2					
25	20.0	11.4	8.8		6.6	5.0					
30 40	34.5 off	17.4 off	10.6	9.0	7.8	5.6					
40	bar	bar	15.9	****	9.4						
50			19.0	15.1	11.2	7.7					
60		-	off		12.6	10.1					
70			-bar		14.0	10.9					
80					15.4	11.9					
90					16.6	14.2					
100					18.5	14.6					
110					21.9	15.9					
130			*		24.2	18.2					
140			41		26.5	19.8					
150					28.9	21.1					
160					31.3	22.7					
170					33.5 36.5	24.1					
190		-			39.4	26.6					
200					off bar	29.6					

apparent. Two nuclei per field at 500 diameters was taken as the point of beginning transformation, to be consistent with the method used in determining the isothermal diagrams. Usually the nature of this constituent was apparent (i.e., whether it was bainite, spear ferrite, or blocky ferrite), but it was not necessary to classify it. It must have just started to form at the time the bar was quenched all over. By determining its distance from the jet-quenched end, by knowing the elapsed time before quenching

all over, and by use of the available cooling data, the temperature of formation of the constituent could be determined, and its nature, therefore, known by reference to the isothermal diagram.

The results of the metallographic examination are given in Table 3. To use conveniently Liedholm's cooling data and Boegehold and Weinman's cooling data, it was necessary to replot them. These replots are shown in Figs. 11 and 12. Combination of the metallographic results and the cooling data makes possible the location of a number of points on a temperature-distance plot (end-quenched bar), each point representing beginning transformation along an end-quenched bar as it is cooled. Such experimental points have been plotted in Figs. 13 through 18. Using the isothermal diagrams, the cooling data for end-quenched bars, and Eqs. 1 and 2, it is possible to determine a different set of points representing the same thing. This second set of points has been shown in Figs. 13 through 18 as a solid line. The mechanics of arriving at the points constituting these lines are given in the Appendix.

The significance of plots such as those shown in Figs. 13 through 18 is to indicate the temperature at which beginning transformation occurs along an end-quench bar. Once transformation begins, additional transformation occurs on continued cooling. Such diagrams would be more complete if they contained an "end of transformation" line. However, because of the laboratory work involved, and because the "beginning transformation" line appears to be the more important from a practical standpoint, the "end of transformation" line was not considered.

It should be noted that while endquenched bars have been used to test the validity of the mathematical expression presented, the application of the expression is by no means limited to end-quenched bars. Similar plots can be made for any shape or any sized part, provided the cool-

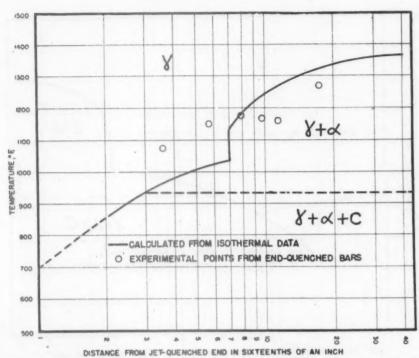


Fig. 14.—Beginning transformation using ½-diameter end-quenched bar. Steel B (1 00 per cent Cr).

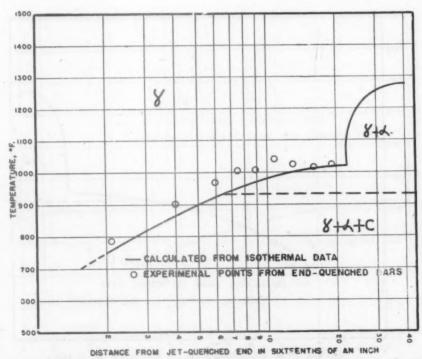


Fig. 15.—Beginning transformation using ½-diameter end-quenched bar. Steel C (1.49 per cent Cr).

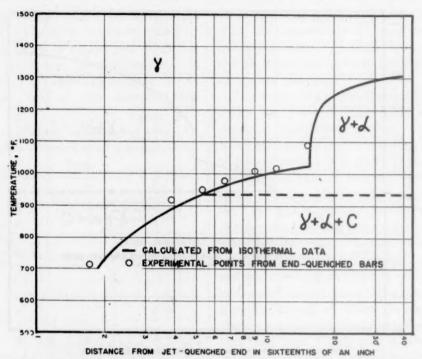


FIG. 16.—BEGINNING TRANSFORMATION USING 1-INCH DIAMETER END-QUENCHED BAR. STEEL C (1.49 PER CENT Cr).

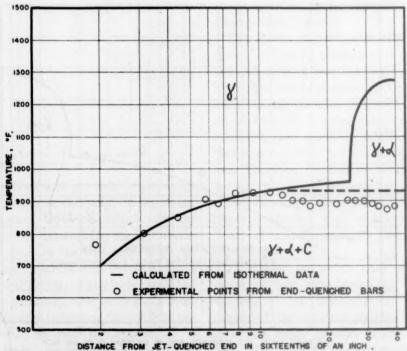


Fig. 17.—Beginning transformation using 1-in. diameter end-quenched bar. Steel D (2.04 per cent Cr).

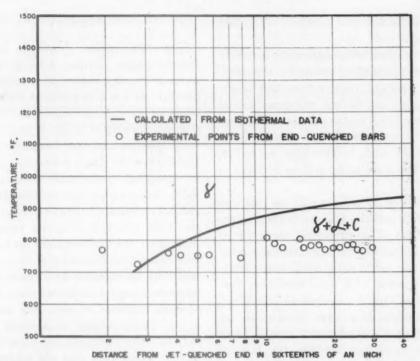


Fig. 18.—Beginning transformation using 1-in.-diameter end-quenched bar. Steel E (2.40 per cent Cr).

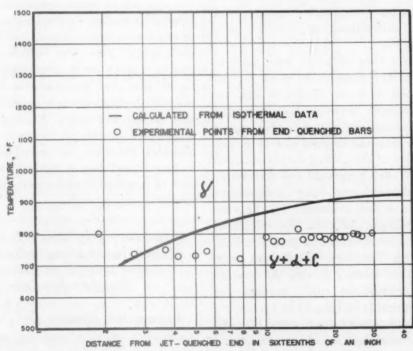


Fig. 19.—Beginning transformation using 1-inch-diameter end-quenched bar. Steel E (2.40 per cent Cr).

ing curves for different locations in the part are known.

If the mathematical expression correctly represents the relation between transformation at constant temperature and transformation during cooling, the experimental points should fall on the calculated line, but while the calculated and experimental values check quite well for Figs. 13, 15, 16, and 17, the correlation is poor in Figs. 14 and 18.

One source of error might be that the cooling rate actually realized in the hardenability bars of a particular steel varied materially from the cooling rates used in the calculation. Liedholm's data were determined by using SAE 6130 specimens austenitized at 1700°F.; Boegehold and Weinman's cooling data were determined by using NE 9445 austentized at 1650°F. In an effort to determine whether the lack of agreement between the calculated and experimental data could be assigned to use of improper cooling rates in the calculations, the cooling rates at various positions of 1-in.-diameter end-quenched specimens of steel E austenitized at 1700°F. were measured.

The data thus obtained were used to recalculate the diagram for steel E. The recalculated data are shown in Fig. 10. The agreement between the calculated line and experimental points (Fig. 19) is no better than the original plot (Fig. 18). Comparison of the cooling curves obtained for steel E with Boegehold and Weinman's curves showed only very insignificant variations, a fact evidenced by the very close agreement between the calculated lines and the experimental points in Figs. 18 and 19. Therefore, it does not seem possible that errors involving the coolingrate determinations could account for the disagreement in Figs. 18 or 10.

The discrepancies that occur between the experimental points and the calculated lines on two of the plots cannot be properly explained at present.

SUMMARY

The relationship between beginning transformation during cooling and beginning transformation at constant temperature of five 0.30 per cent carbon alloy steels of various chromium contents was studied. Specimens of two of the five steels were quenched in two temperature steps rather than the single step commonly used in studying isothermal transformation. With this procedure, it was found that from the Ae3 temperature down to about 1130°F. the time spent at a given temperature divided by the time required for beginning isothermal transformation at that temperature may be regarded as a fraction of the nucleation period, and that when the sum of such fractions equaled one nucleation began. Temperatures from about 1130°F. to the M, temperature constituted a distinct range that was not additive with the higher range mentioned. This concept may be used as the basis of a mathematical expression that permits calculation of the temperature at which transformation begins during cooling. In checking the validity of the mathematical expression by use of end-quench bars (for which accurate cooling curves were available), it was found that the experimental data and calculated data differed appreciably for two of the five steels. Evidently, some further refinements in the procedure are desirable. However, the procedure appears to be a logical way of linking transformation at constant temperature with transformation during cooling.

APPENDIX.—Calculating of Beginning Transformation during Cooling, from Cooling Data and the Isothermal Transformation Curve

To use the equation $\sum \frac{\Delta X}{Z} = \mathbf{1}$ for calculation of beginning transformation during cooling, it is convenient to first plot the cooling curve on linear coordinates

using temperature as the ordinate. The finite range to be represented by individual ΔX values must next be selected. Choice of this range affects the preciseness of the

each 20°F. interval. The reciprocal of the slope multiplied by the chosen interval (in this case 20°F.) give the ΔX values.* These ΔX values are interpreted as apply-

TABLE 4.- ΔX (20°F.) Values from Boegehold and Weinman's Cooling Data

Hean Temp.			Dist	ance Pr	om Jat-	Quenche	t End o	f laInd	h Harde	na h4 7 4 4		. 61=1	onths of a	a Tach		
• 7.	1	2	3	14	5	6	7	8	10	12	14	16	20	n Inch	32	40
1460 1440 1420 1400	0.046 0.044 0.043 0.041 0.039	0.06 0.06 0.06 0.06 0.06	0.09 0.10 0.11 0.11 0.11	0.12 0.14 0.15 0.16 0.17	0.18 0.19 0.23 0.27 0.27	0.27 0.28 0.29 0.33 0.35	0,38 0.40 0.42 0.43 0.45	0.54 0.55 0.58 0.60 0.61	0.75 0.8 0.82 0.83 0.86	1.0 1.05 1.06 1.13 1.15	1.33 1.35 1.38 1.40 1.47	1.60 1.62 1.65 1.70 1.80	2.41 2.42 2.43 2.44 2.45	2.60 2.62 2.70 2.80 2.90	3.80 3.85 3.90 3.95 4.00	3.8 3.9 4.1 4.1
360 340 320 320	0.038 0.037 0.035 0.034 0.032	0.06 0.06 0.06 0.07 0.07	0.11 0.11 0.11 0.12 0.13	0.18 0.19 0.20 0.22 0.23	0, 32 0, 32 0, 32 0, 34 0, 34	0.36 0.38 0.41 0.43 0.44	0.47 0.50 0.53 0.58 0.62	0.62 0.63 0.65 0.70 0.74	0.88 0.93 0.97 1.00 1.02	1.18 1.20 1.23 1.29 1.30	1.49 1.50 1.52 1.55 1.60	1.82 1.85 1.92 1.95 2.00	2.46 2.47 2.48 2.50 2.52	2.93 3.00 3.20 3.28 3.30	4.01 4.02 4.05 4.10 4.20	4.2 4.3 4.6
.260 .260 .240 .220	0.031 0.031 0.030 0.030 0.030	0.08 0.09 0.09 0.10 0.10	0.14 0.14 0.15 0.16 0.17	0.24 0.25 0.26 0.27 0.28	0.38 0.40 0.40 0.42 0.43	0.45 0.47 0.50 0.51 0.52	0.64 0.66 0.70 0.72 0.74	0.78 0.80 0.83 0.85 0.92	1.05 1.11 1.14 1.22 1.25	1.35 1.40 1.43 1.45 1.53	1.67 1.73 1.75 1.80 1.90	2.10 2.13 2.15 2.21 2.30	2.55 2.58 2.61 2.63 2.70	3.35 3.40 3.45 3.60 3.65	4.40 4.45 4.50 4.70 4.90	4.7 4.8 4.8 4.9
160 140 120 100	0.030 0.030 0.030 0.030 0.030	0.10 0.11 0.11 0.12 0.12	0.18 0.19 0.19 0.20 0.21	0.29 0.30 0.31 0.33 0.35	0,45 0,48 0,50 0,50 0,53	0.57 0.63 0.65 0.66 0.72	0.80 0.84 0.87 0.90 0.95	0.95 0.98 1.0 1.09 1.15	1.30 1.32 1.40 1.42 1.55	1.62 1.65 1.69 1.75 1.86	2.00 2.05 2.10 2.23 2.26	2.33 2.40 2.50 2.60 2.70	2.82 2.85 2.95 3.05 3.25	3.85 3.85 3.95 4.00 4.30	4.95 5.00 5.05 5.10 5.30	5.5 5.5 5.5
080 040 040 020	0.030 0.031 0.031 0.031 0.032	0.13 0.14 0.15 0.15	0.23 0.26 0.28 0.29 0.31	0.37 0.40 0.43 0.46 0.50	0.54 0.56 0.62 0.65 0.70	0.76 0.80 0.83 0.86 0.92	1.01 1.06 1.1 1.14 1.15	1.25 1.35 1.40 1.53 1.57	1.62 1.66 1.72 1.85 1.93	1.96 2.00 2.14 2.26 2.33	2.35 2.40 2.55 2.63 2.72	2.75 2.84 2.92 3.20 3.30	3.52 3.63 3.73 4.05 4.10	4.50 4.60 4.75 4.90 5.20	5.40 5.60 5.70 5.85 6.20	6.1
980 960 940 920 900	0.034 0.035 0.036 0.038 0.043	0.16 0.17 0.18 0.19 0.20	0.33 0.35 0.37 0.40 0.45	0.54 0.58 0.61 0.64 0.67	0.72 0.77 0.80 0.82 0.88	1.0 1.09 1.15 1.29 1.33	1.23 1.35 1.4 1.52 1.53	1.66 1.75 1.92 1.94 2.1	1.97 2.06 2.20 2.28 2.32	2.45 2.51 2.70 2.81 3.00	2,80 3,00 3,02 3,22 3,50	3.50 3.60 3.70 3.80 3.90	4.2 4.42 4.80 5.00 5.30	5.25 5.50 5.60 5.90 6.10	6.65 6.85 7.05 7.50 7.80	7.1 7.8 8.1 8.1
880 860 840 820 800	0.047 0.051 0.056 0.058 0.064	0.22 0.24 0:27 0.29 0.32	0.50 0.55 0.58 0.62 0.65	0.71 0.76 0.80 0.86 0.91	0.96 1.06 1.13 1.23 1.36	1.44 1.52 1.54 1.64 1.76	1.69 1.84 1.9 1.97 2.16	2.23 2.32 2.40 2.44	2.48 2.60 2.74 2.90 3.18	3.18 3.30 3.40 3.65 3.87	3.80 4.00 4.18 4.30 4.62	4.10 4.40 4.55 4.85 5.15	5.45 5.80 6.00 6.15 6.50	6.40 6.70 6.90 7.10 7.80	8.30 8.90 9.40 9.60 9.90	9.10.11.11.11.11.11.11.11.11.11.11.11.11.
780 760 740 720 700	0.074 0.080 0.096 0.105 0.118	0.35 0.40 0.46 0.50 0.56	0.70 0.80 0.92 1.00 1.06	0.96 1.02 1.11 1.20 1.32	1.5 1.6 1.65 1.83 2.0	1.87 1.94 2.1 2.28 2.43	2.29 2.37 2.4 2.54 2.7	2.55 2.62 2.68 2.89 3.15	3.30 3.52 3.85 4.10 4.30	4.00 4.37 4.60 4.89 5.43	4.71 5.00 5.30 5.60 6.00	5.45 5.70 6.00 6.50 7.00	6.80 7.15 7.40 7.80 8.20	8.00 8.40 9.00 9.20 10.00	10.20 10.60 11.00 11.30 11.80	12.0
680 660 640 620 600	0.138 0.162 0.193 0.210 0.300	0.59 0.65 0.69 0.76 0.84	1,16 1,27 1,35 1,50 1,58	1.54 1.78 2.00 2.20 2.40	2.1 2.3 2.5 2.67 2.98	2.65 2.82 3.16 3.43 3.63	2.8 3.15 3.4 3.78 4.1	3.49 3.75 4.01 4.37 4.84	4.72 4.90 5.25 5.71 6.10	5.70 5.96 6.43 7.00 7.56	6.25 6.80 7.43 8.00 8.40	7.40 8.00 8.50 9.15 9.80	9.00 9.50 10.25 11.00 11.25	10,20 11,00 12,00 12,90 13,20	12.3 13.0 13.4 13.7 14.5	13.0 13.1 13.6 14.0
580 560 540 520 500	0.422 0.588 0.664 0.784	0.88 1.00 1.40 1.8h	1.66 1.74 1.87 2.00	2.60 2.80 3.00 3.20	3.25 3.35 3.7 4.1	3.85 4.1 4.32 4.77	4.3 4.9 5.8 7.4	5.2 5.82 6.28 6.70	6.70 7.18 8.05 8.64	7.98 8.6 9.4 9.9	9.20 10.2 10.7 10.8	10.9 11.8 13.2 14.2	12.7 13.85 14.00 14.10	14.00 14.90 15.95 17.00	14.95 15.1 15.8 16.0	14.1 14.2 14.2

results. A very large range reduces the number of values entering into the summation, but it also reduces the accuracy of the values that are obtained. For the purpose of this paper, 20°F, has been chosen as the temperature range to be represented by each ΔX value. Having made this choice, the slope of the cooling curve is determined at the mid-point of

ing to an interval 10°F. above and 10°F. below the temperature at which the slope was determined. ΔX values calculated

^{*} Theoretically, more accurate ΔX values might be obtained by reading directly from the cooling-curve plot time values that correspond to the upper and lower temperature of each ΔX interval and taking the difference as the ΔX value. Practically, such a method is less accurate and much more tedious.

from both Liedholm's data and Boegehold and Weinman's data for 20°F. intervals have been tabulated in Tables 4 and 5.

transformation plot values for beginning transformation at temperatures of 1300°F., 1280°F., 1260°F., and so on. Having

TABLE 5.— ΔX (20°F.) Values from Liedholm's Cooling Data

Mean Temp.,		Distance	From Jet	-Quenched	End of 1	/2-Inch H	ardenabil	ity Bar	in Sixtee	nths of a	n Inch	
•7.	2	4	6	g	10	12	14	16	20	24	32	40
1480	0.03*	0.15	0.34*	0.52	0.70*	0.91*	0.99*	1.24	1.27*	1.59*	2.34*	2.46
1460	0.03*	0.15	0.34*	0.53*	0.72	0.92	1,000	1.25	1.310	1.640	2.390	2.52
PHO	0.030	0.16	0.35	0.530	0.73*	0.93	1,02*	1,26	1.350	1.700	2.450	2,58
1420	0.03	0.17	0.36*	0.530	0.75	0. 5	1.040	1.27	1 70	1.760	2.51*	2.64
1400	0.03	0.17	0.36	0.55*	0.76	0.97	1.06	1.29	1.39	1,82*	2.57*	2.71
380	0.04	0.18*	0.37*	0.56	0.78	1.00	1.08*	1.31	1.49	1.88*	2.63*	2.78
1360	0.04	0.18*	0.38*	0.56	0.80	1.01	1.100	1.33	1.54	1.940	-2.69*	2.85
340	0.040	0.19*	0.39*	0.57	0.81	1.03	1.130	1.35	1.59	2.00*	2.75	2.92
1320	0.040	0.20*	0.39	0.58	0.83	1.05	1,160	1.38	1,65	2.060	2.81	2.99
1300	0.05	0.20	0.40	0.59	0.85	1.07	1.19*	1.38	1.72	2.120	2.87	3.06
1280	0.05	0.21*	0.41.	0.60	0.88	1.09	1.22*	1.44	1.80	2.18*	2,94	3.13
1260	0.05*	0.22*	0,420	0.62	0.90	1,11	1,260	1,48	1.88	2.25	3.01	3.21
1240	0.05	0.23*	0. 440	0.63	0.93	1.13	1.300	1.52	1.96	2.32	3.09	3.29
1220	0.06*	0.23*	0.450	0.65	0.95	1.15	1.34*	1.56	2.02	2.39	3, 18	3 27
1500	0.06	0.24.	0.46	0.66	0.98	1.18	1.38°	1.60	2.08	2.47	3.28	3.37
1180	0.07*	0,25*	0,48	0,68	1.02	1,21	1,420	1,65	2.15	2.55	3.38	7 5h
1160	0.07*	0.26	0.49	0.71	1.05	1.24	1.460	1.71	2,25	2.63	3.38	3.54
1140	0.08*	0.28*	0.51	0.73	1.09	1.27	1.51	1.78	2.35	2.70	3.58	3.74
1120	0.08*	0.29*	0.52	0.75	1.13	1.31	1.56	1.85	2.45	2.78	3.68	3.84
1100	0.09	0.30	0.54	0.78	1.17	1.35	1.62	1.92	2.55	2.86	3.78	3.94
1080	0.10	0.32	0.56	0.81	1.22	1.41	1,68	2,00	2.65	2.96	3.92	4.04
1060	0.110	0.33*	0.58	0.85	1.27	1.47	1.75	2.08	2.75	3.08	4.04	4.16
1040	0,120	0.35	0.61	0.69	1.32	1.53	1.82	2,16	2,85	3,20	4.16	4.29
1020	0.13*	0.37	0.63	0.93		1,60	1.89	2.25	2.95		4,28	4,43
1000	0.14	0.39	0.66	0.97	1.37	1.67	1.98	2.35	3.02	3.32	4.40	4.57
980	0.16	0.41*	0.69	1.02	1.49	1.75	2.06	2.47	3.12	3.56	4 53	4.71
960	0.17	0.430	0.73	1.07	1.55	1.85	2.15	2.59	3.23	3.56 3.69	4.53	4.86
940	0.19	0.46.	0.77	1,12	1.62	1.95	2.25	2.71	3.35	3.82	4.79	5.01
920	0.20	0.48*	0.82	1.18	1.69	2.05	2.38	2.83	3.49	3.95	4.94	5.17
900	0.22	0.51	0.87	1.25	1.79	2.15	2.51	2.95	3.64	4.08	5.10	5.37
880	0.24	0.54	0.93	1.32	1.89	2,27	2,64	3,10	3.84	4,21	5,26	5.72
860	0.270	0.57	1.00	1.32	1,99	2.40	2.78	3.28	4.00	4.35	5.43	5.87
840	0.30	0.61	1.08	1.50	2,10	2.56	2.92	3.45	4.17	4.50	5.60	6.03
820	0.33	0.65	1,16	1.59	2,22	2.70	3.08	3.64	4.35	4.67	5.77	6.18
800	0.36	0.69	1.25	1.69	2,36	2.86	3.24	3.84	4.55	4.85	5.94	6.33
780	0.40	0.75	1.35	1,81	2.52	3.08	3,40	4.07	4,65	5,04	6.11	6,48
760	0.440	0.82	1.35	1.95	2.70	3.30	3.57	4.34	4.88	5.25	6,28	6.68
740	0.50*	0.90	1.60	2.12	2.90	3.50	3.84	4.61	5.13	5.47	6.46	6.90
720	0.56	0.99	1.74	2.30	3.13	3.72	4.08	4.78	5.40	5.71	6.67	7.14
700	0.63	1,08	1.90	2.50	3.39	4.00	4.34	5.10	5.72	5.97	6.90	7.42

*Extrapolated

It is next necessary to tabulate the Z values for the particular steel being considered. These Z values, representing the time in seconds for isothermal transformation to begin, must represent temperature intervals that are consistent with the intervals chosen for the ΔX values. If ΔX values are used for the intervals 1310° to 1290°F., 1290° to 1270°F., 1270° to 1250°F., and so on, mean Z values for the same intervals must be determined. Practically, mid-values of Z may be used without significant error, and it is only necessary to read from the isothermal

obtained the ΔX and Z values, a table is made up as illustrated:

	Position in the Cooling Specimen													
Mean Tempera- ture,		1			2		3							
Deg. F.	ΔX	Z	$\frac{\Delta X}{Z}$	ΔX	Z	$\frac{\Delta X}{Z}$	ΔΧ	Z	$\frac{\Delta X}{Z}$					
1480 1460 1440 1420 1400 1380 1360 etc.									,					

Individual $\frac{\Delta X}{Z}$ values are calculated and these individual values added downward in each $\frac{\Delta X}{Z}$ column until the sum equals one. The equation indicates that, when the sum of $\frac{\Delta X}{Z}$ values equals one, transformation begins. If the sum does not equal one by the time 1130°F. is reached, the fraction obtained is discarded and the addition started anew for intervals below 1130°F. If the sum does not equal one by the time the M, temperature is reached, it merely means that martensite will be the first product to form.

From such calculations a plot for temperature vs. position beginning transformation may be constructed. The method described was used in determining the solid lines of Figs. 13 through 18.

Though it is possible to construct a temperature-position plot if given the isothermal diagram and the cooling curves. it is quite awkward to construct an isothermal diagram if given the temperature-position plot and the cooling curves.

REFERENCES

I. R. A. Grange and J. M. Keifer: Transformation of Austenite on Continuous Cooling and Its Relation to Transformation at Constant Temperature, Trans. Amer. Soc.

for Metals (March 1941) 29, 85-114.
2. S. Steinberg: Relationship between Rate of Cooling, Rate of Transformation, Undercooling of Austenite, and Critical Rate of Quenching, Metallurgy (1938) 13 (1). Translation available from Henry Brut-

cher, 3185 North Marengo Avenue, Altadena, California.

3. E. Scheil: "Nucleation Period" of the Austenite Transformation. Archiv Eisen-

huttenwesen (June 1935) 12, 565-567. 4. C. A. Liedholm: Continuous Cooling Transformation Diagrams from Modified Endquench Method. Metal Progress (January

1944) 04-99. L. Boegehold and E. W. Weinman: 5. A. L. Boegehold and E. W. Progress Report on Heat Treatment of National Emergency Steels for Use in Tanks, Combat Cars, Gun Mounts and Other Ordnance Material (OD115) O.S.-R.D. 3743, Ser. No. M277 (June 1, 1944).

DISCUSSION

(F. M. Walters, Jr., presiding)

R. A. GRANGE.*-Considering the importance of correlating isothermal and cooling transformation, surprisingly little attention has been devoted to it in the past; this interesting paper by Messrs. Manning and Lorig is therefore timely and valuable.

The authors comment that the Grange and Kiefer method for estimating transformation as it occurs during continuous cooling, from the isothermal transformation diagram, is empirical and cannot be used with confidence for steels in general. As we see it, the Grange and Kiefer method for predicting the beginning of cooling transformation is based on the same principles as the method described by the authors, being merely a somewhat rougher approximation. Its nature is more empirical in respect to the progress and ending of transformation on cooling, which are not discussed by Manning and Lorig but cannot be ignored in any complete and practically useful method of correlating isothermal and cooling transformation. Moreover, we have applied it to many types of steel, and, although admittedly not highly accurate, this method has proved to be practically useful and helpful in understanding the transformation behavior of steel during cooling.

As the authors point out, their method of calculating the beginning of transformation on cooling from the isothermal transformation diagram is essentially that previously proposed by Scheil⁸ and Steinberg.² In developing our method, these older methods were investigated, whereupon it became evident that there was no justification from the practical standpoint for such involved and tedious calculation, since the cooling curve and the isothermal data seldom, if ever, are known with the requisite accuracy. For this reason, a simple approximation, which we found gave a result agreeing well enough with that resulting from the tedious calculations proposed by Steinberg, was adopted. The Manning and Lorig method is also a justifiable simplification of the Steinberg method; in fact, this same simplification was proposed by Hoyt in 1939.6

* U. S. Steel Corporation, Research Laboratory, Kearny, N. J.

S. L. Hoyt: The Weldability of Casing
Steel. Presented before the American Petroleum

Institute, New Orleans, La., May 18, 1939.

Manning and Lorig find that holding hypoeutectoid steels for a time period too short to permit any measurable transformation at a temperature above about 1130°F. did not affect

ture is lowered, and we have not observed such a limited temperature range within which the type of ferrite suddenly changes. Furthermore, we have always found that holding above

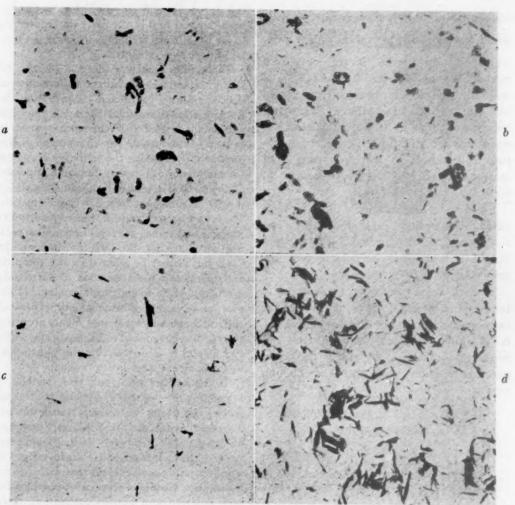


Fig. 20.—Effect of holding for a time just short of the measurable beginning of transformation at 1200°f. On subsequent isothermal transformation at 800°f. and at 600°f. SAE-4340 steel. × 500. Picral etch.

a.
$$1550^{\circ}F$$
. $\rightarrow 1200^{\circ}F$., $3 \text{ min.} \rightarrow 800^{\circ}F$., $1 \text{ min.} \rightarrow \text{quench.}$
b. $1550^{\circ}F$. $\rightarrow 1200^{\circ}F$., $3 \text{ min.} \rightarrow 800^{\circ}F$., $1 \text{ min.} \rightarrow \text{quench.}$
c. $1550^{\circ}F$. $\rightarrow 1200^{\circ}F$., $3 \text{ min.} \rightarrow 600^{\circ}F$., $3 \text{ min.} \rightarrow \text{quench.}$
d. $1550^{\circ}F$. $\rightarrow 1200^{\circ}F$., $3 \text{ min.} \rightarrow 600^{\circ}F$., $3 \text{ min.} \rightarrow \text{quench.}$

the beginning time for transformation at any temperature below 1130°F.; they associate this with the observation that "blocky" ferrite formed above 1130°F. and "spear" ferrite or bainite below. In our experience, the character of proeutectoid ferrite changes gradually from the "blocky" type at high temperature to the "spear" type as the transformation tempera-

1130°F. for a time too short to produce microscopically visible transformation reduces the time required for transformation of austenite at a temperature below 1130°F.; in this we are in agreement with the results of Hollomon, Jaffe and Norton. It is difficult to be certain

⁷ J. H. Hollomon, L. D. Jaffe and M. R. Norton: This volume, page 419.

that the nucleating effect is additive to the extent, for example, that holding for one half the beginning time at the higher temperature reduces the beginning time at the subsequent lower temperature level by exactly one half, but it is easily demonstrated that there is a decided influence in this direction. Previous experience had always indicated that this was so, but, as a check, we have again recently investigated this nucleating effect. Pairs of small samples of SAE-4340 steel, which previously had been heated for two days at 2350°F. to ensure freedom from banding (segregation),8 were austenitized at 1550°F. One of each pair was quenched into lead at 1200°F. for 3 min. (just short of the measurable beginning of isothermal transformation at 1200°F.) and then quenched into a second lead-alloy bath at 800°F, or at 600°F. The other sample of each pair was quenched from 1550°F. directly to 800°F. or to 600°F. A number of such pairs of samples were treated, each being held for one of a series of times at 600°F, or at 800°F, and then brinequenched. Comparison of the microstructure of two such pairs of samples is shown in Fig. 20, one pair held for 1 min. at 800°F. (top) and the other pair at 600°F. for 3 min. (bottom). The "100 per cent nucleated" sample is at the right in each row. It is evident that, contrary to Manning and Lorig's results, the "nucleation" at 1200°F. decreased the time required for transformation at both 800°F, and 600°F. The examples shown in Fig. 20 represent only one pair in each time series, but in the others there was also a correspondingly greater proportion of bainite in the nucleated sample; in particular, a nucleated sample contained a detectable amount of bainite when held for a time too short for a measurable beginning of transformation in the corresponding direct-quenched sample. This same trend has been observed in several other types of low-alloy steel, and we see no logical reason why certain compositions should show such "additive nucleation" below 1130°F. after a prequench above 1130°F. while others do not.

We searched in vain for the austenite grain size for each of the isothermal transformation diagrams in the paper; since this information is necessary in making full use of these valuable diagrams, we ask the authors if they would care to mention it in their reply to this discussion.

G. K. Manning and C. H. Lorig (authors' reply).—The A.S.T.M. grain size of all five steels for the austenitizing conditions employed was 7-8. Mr. Grange has pointed out that the temperature ranges in which blocky and spear ferrite form overlap somewhat. That subject was discussed to a considerable extent in the paper. The authors did not intend to imply that either the degree of overlapping or the mean temperature at which the overlapping occurred would be common for all steels, as Mr. Grange apparently has assumed. The five steels tested varied appreciably only in chromium and, although chromium apparently had no effect on the ranges, it would indeed be surprising if other elements, particularly carbon, did not affect these temperature ranges. Since the paper was written, some information has been obtained that suggests that austenitizing temperature (grain size possibly) has an important influence on the respective temperature ranges for "spear" and "blocky" ferrite. In view of the uncertainty as to the extent to which various factors may affect these temperature ranges, we find nothing particularly contradictory about the micrographs Mr. Grange presents; although we would, at the same time, hesitate to interpret them.

Described in the paper are two methods that may be used to some advantage in studying the rather complex subjects of austenite decomposition, during cooling. Many factors affecting this decomposition, such as composition, austenitizing conditions, stress, and the presence of numerous minute oxides or carbides, have not been considered thus far. It is hoped that other investigators may be able to make use of these two methods in quantitatively studying this important subject.

C. ZENER.*—I should like to know whether there are any differences in the upper range of

^{*}Such homogenizing treatments greatly facilitate microscopic comparison of pairs of samples that differ only slightly in the percentage of transformation product, since each field of view contains essentially the same proportion of constituents as any other.

^{*} Professor of Metallurgy, University of Chicago, Chicago, Illinois.

the blocky kind—whether that is imitated at the grain boundary.

G. K. Manning.—In studying the steels reported in this paper, blocky ferrite nucleation was not found to occur preferentially at the grain boundaries. This is illustrated by the distribution of the blocky ferrite in Fig. 5.

Later, in observing another steel that has not been reported in this paper, it was found that there was a rather strong tendency for blocky ferrite to appear predominantly at the grain boundaries. Perhaps it is too early to offer any definite opinion concerning the nucleation characteristics of blocky ferrite.

The Temperature Range of Martensite Formation

By R. A. GRANGE* AND H. M. STEWART*
(Chicago Meeting, February 1946)

Many steel parts may crack if quenched directly into a bath near room temperature, but not if quenched at a temperature just above the range where martensite forms and then allowed to cool slowly to room temperature. This latter procedure, which is the basis for such modern hardening techniques as "martempering" and "isothermal quenching," may entail some sacrifice in depth of hardening but very little, if any, in intensity of hardening. In planning such treatments, it is necessary to know the upper limit of the martensite range, and often desirable to know the proportion of martensite that would form on cooling to any lower temperature; furthermore, the tendency of a particular steel to crack when quenched is unquestionably associated with the temperature range of martensite formation, and consequently knowledge of this range aids in selecting the optimum composition for a given application. Certain puzzling phenomena associated with the properties of quenched and tempered steel may be at least partly clarified as the manner in which martensite forms is more fully understood. Information on the temperature range of martensite formation, particularly with respect to how much martensite results from quenching to a given temperature, is lacking for most commercial types of carbon and low-alloy steel.

These considerations led us to study martensite formation in 14 carbon and low-alloy steels. The resultant data may be directly used in the following ways: (1) for selecting the lowest quenching temperature at which no martensite will form; (2) for selecting the highest quenching temperature at which virtually all marten. site will form, thereby avoiding quenching to an unnecessarily lower temperature with attendant danger of cracking; and (3) in producing a mixture of tempered martensite and bainite, which in high-carbon steels has been found to possess somewhat better ductility than tempered martensite. vet does not require the full transformation time necessary for a completely bainitic (austempered) structure.

PART I. OBSERVATIONS OF MARTEN-SITE FORMATION IN FOURTEEN CARBON AND LOW-ALLOY STEELS

Transformation of austenite to pearlite or bainite can be conveniently studied by observing the change that occurs over a period of time at constant temperature; such studies are the basis of the isothermal transformation diagram (S-curve). This isothermal technique is not applicable to martensite formation, which occurs within a time interval too small to measure, at least by any ordinary means. For all practical purposes, therefore, martensite may be regarded as forming only during cooling and not during a period of time at constant temperature. As austenite is cooled below

*Research Laboratory, United States Steel Corporation, Kearny, New Jersey.

Manuscript received at the office of the Institute Nov. 21, 1945. Issued as T.P. 1996 in METALS TECHNOLOGY, June 1946.

a certain temperature, designated M_S , a definite proportion of it transforms to martensite, this proportion being dependent upon the temperature finally reached in cooling rather than upon the time required to cool (cooling rate); holding for a prolonged time at this temperature is considered to result in the transformation of the remaining austenite to bainite and not in any increase in amount of martensite. Thus, in martensite formation, time is significant only insofar as it determines the temperature finally attained during cooling at any particular rate, and the formation of martensite can be represented on a quantitative basis by plotting the proportion of martensite against temperature, but not time. This concept of martensite formation has been generally accepted in recent years, largely as a result of the work of Greninger and Troiano.1

EXPERIMENTAL TECHNIQUES

The temperature range of martensite formation can be determined by thermal analysis, in which case it has long been known as Ar"; but with this method it is difficult, if not impossible, to estimate the proportion of martensite formed on cooling to an intermediate temperature within the range. Measurement of change of volume or length during continuous cooling is a somewhat better method, but again a quantitative estimate is difficult. These considerations led us to select the metallographic technique first described by Greninger and Troiano¹ in 1939, and since used by others.

Since the principles involved in measuring martensite formation by the metallographic technique may be unfamiliar to some, and since intelligent interpretation and application of the results require knowledge of how they were obtained, a discussion of technique seems warranted. The series of schematic charts in Fig. 1

will serve as a basis for discussion. A small specimen that has been heated to form austenite (T_A in Fig. 1) is quenched into a liquid bath (low-melting lead alloy) maintained at a previously selected temperature (T_1) and held for a time just sufficient to ensure that it has cooled throughout to this temperature. After this timed quench, a certain proportion of martensite will have formed provided T_1 is low enough, but if the specimen is removed from the bath and allowed to cool to room temperature this initial martensite will ordinarily not be microscopically distinguishable from that formed subsequently during cooling to room temperature. Therefore further heat-treatment is required in order to permit estimation of the proportion of this initial martensite. as follows. From the first bath, the specimen is quickly transferred, without cooling below T_1 , to a second metal bath maintained at a higher temperature (T_2) and held there for a short time, after which it is quenched in brine. In this second bath any martensite that had formed on quenching to T_1 is tempered, while the austenite remains unaltered but subsequently transforms to martensite during the final quench to room temperature; consequently, the final structure is, as illustrated in Fig. 1, entirely light-etching martensite if no martensite had formed on quenching to T₁ (top diagram), entirely dark-etching tempered martensite if T_1 was so low that all the austenite had transformed to martensite in the initial quench (middle diagram), or a mixture of the two if T_1 was in the range where only part of the austenite transformed to martensite in the first quench (bottom diagram). Liquid baths, preferably of metal, are essential in order to cool and heat the specimen rapidly enough to avoid transformation to products other than martensite.

For each steel, T_1 was varied at intervals of 10° to 20°F, throughout the martensite-formation range. The quenching time in

¹ References are at the end of the paper.

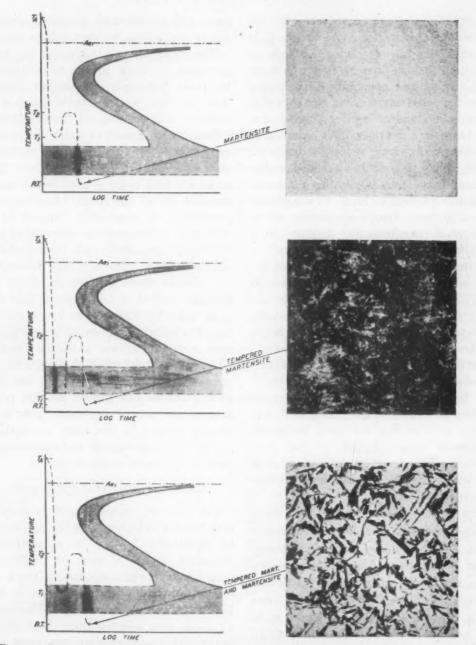


Fig. 1.—Schematic charts and micrographs illustrating heat-treating technique. Micrographs, originally × 500; reduced one fourth in reproduction. Picral etch. Example shown is eutectoid carbon steel.

the bath at T_1 was 3 sec.,* this being little longer than necessary to cool the whole specimen consistently to T_1 ; it was selected

as a reasonable compromise between a shorter time, which might not always suffice for thorough cooling, and a longer time, which, in some of the steels, might permit some transformation to bainite. The temperature of the second bath (T_2) was constant for any one steel, but varied

^{*}In two special cases, specimens were austenitized at 1950° F. or 2000° F., and the quenching time at T_1 was increased to 5 sec. to allow for the longer time required to cool from these high temperatures.

for different steels in accordance with the isothermal transformation behavior. It is essential that no significant amounts of pearlite or bainite form at T_2 , for both are dark-etching and not easily distinguished from tempered martensite; consequently, choice of T_2 and of holding time thereat was based on a treatment that would, after polishing and etching, reveal the tempered martensite as thoroughly blackened needles without permitting any isothermal transformation product to form. T2 was chosen for each steel, after examination of its isothermal transformation diagram, at a level where there is a decided "bay" in the beginning line. In steels with 0.6 per cent or more of carbon, such a bay occurs above the martensite-formation range and below the knee (Fig. 1); in those containing less carbon, the bay is too shallow below the knee, and it was necessary to select T_2 above the knee, where, as Ae₁ is approached. transformation proceeds relatively slowly. The holding period at T_2 to temper the martensite formed on quenching to T_1 was 3 to 5 sec.—a time too short to permit isothermal transformation at the temperature selected and yet almost as good as a longer time for "blackening" martensite needles.

This technique is least satisfactory when dealing with steels of low hardenability where T_2 is necessarily above the "knee" of the isothermal transformation diagram. In such a case, it is necessary: (1) to cool through the "knee" region (quench down to T_1), (2) to heat through it (quench up to T2), and (3) finally cool through it again (brine quench to room temperature). During this multiple passing through the knee region, some ferrite, pearlite and upper bainite sometimes formed; these products were found by experimental observation to form only after the significant martensite formation at T_1 , and their presence, therefore, does not invalidate the results provided they are distinguished

from, and not rated as, tempered martensite (as we believe we were able to do).

The experimental technique has been discussed at some length to emphasize the point that study of martensite formation by this metallographic method is indirect, since additional heat-treatment follows the treatment in which the change occurs that it is desired to measure: unquestionably it involves factors that prevent a high order of precision in measurement for all the steels. Moreover, the proportion of martensite formed at a particular temperature as measured in this way applies specifically only to steel treated like our small specimens; it may reasonably be inferred that the results apply to samples treated in other ways, but this is an inference and not, as yet, a proved fact. For instance, our results may indicate that austenite in one particular steel is og per cent transformed to martensite on quenching for 3 sec. at 300°F., but this should not be interpreted as final proof that 99 per cent of martensite must have already formed in this steel on reaching 300°F. when it is rapidly and continuously quenched to room temperature.

MATERIAL AND HEAT-TREATMENT

Our primary purpose was to acquire quantitative data regarding the proportion of martensite formed in commercially important grades of steel on cooling to successively lower temperatures, such information being a useful adjunct to isothermal transformation data. Therefore, 13 steels were selected from those whose isothermal transformation diagrams appeared in an Atlas2; these, and an NE-8630 steel, comprise the 14 steels discussed in the first part of the paper. Samples were all taken from the same bar that had previously provided samples for the isothermal diagram in the Atlas, or from a companion bar. From each, small specimens were prepared by cutting transverse slices 0.04 to 0.05 in. thick; these thin slices were then cut into segments (wedge shaped when slices were round), each having a transverse face of approximately 0.3 sq. in. Pertinent data regarding the steels used are listed in Table 1.

important, since, for reasons already mentioned, the specific quenching time in the first metal bath and the temperature and time of the subsequent "blackening" treatment may have influenced the result.

TABLE 1.—Composition and Nature of Material

Type			Compos	ition, P	er Cent			Stock Used for of Specia	
., p.	С	Mn	Si	Ni	Cr	Мо	v	Size	Condition
0.9 per cent C SAE-1065 T1335 2340 3140 4130 4140 4340 4040 5140 52100 6140 NE-8630 NE-9442	0.89 0.63 0.35 0.37 0.38 0.29 0.37 0.42 0.36 0.42 1.02 0.43 0.30	0.29 0.87 1.85 0.68 0.72 0.77 0.78 0.63 0.68 0.36 0.74 0.91	0.15 0.22 0.19 0.21 0.21 0.30 0.15 0.24 0.19 0.16 0.33 0.23 0.31	3.4I 1.32 1.79 1.84 0.20 0.6I 0.34	0.49 0.68 0.98 0.80 0.93 1.41 0.92 0.52 0.40	0.20 0.21 0.33 0.23	0.16	y" square " diam. 1%" diam. 1%" diam. 1" diam. 1" diam. 14" diam.	annealed normalized normalized normalized hot-rolled normalized normalized normalized annealed normalized cold-drawn hot-rolled

TABLE 2.—Details of Heat-treatment Prior to Metallographic Examination

	Austenitized	Austenite	First Que	ench T ₁	Second Qu	ench T2	
Type	at Tas Deg. F.	Grain Size, A.S.T.M. No.	Range ^b Deg. F.	Time, Sec.	Tempera- ture, Deg. F.	Time, Sec.	Final Quench
0.9 per cent C	1625	4-5	200-450	3	700	5	Brine
SAE-1065	1500	6	250-550	3 3 5	650	5	Brine
1065	2000	2	250-550	5	650	5	Brine
T1335	1550	2-7	400-700	3	1250	3	Brine
2340	1450	7-8	400-650	3	1200	3	Brine
3140	1550	7-8	400-650	3	1250	3	Brine
4130	1600	8-9	500-750	3	1300	5	Brine
4140	1550	7-8 7-8	450-700	3	1300	5	Brine
4340	1550	7-8	300-600	3	1275°	5	Brine
4640	1550	6-7	450-700	3	1250	5	Brine Brine
5140	1550	0-7	450-700	3	1300	5	Brine
52100	1950	2	32-300	3	700	5	Brine
52100 6140	1550	8	400-700	3	1300	5	Brine
NE-8630	1600	9-10	500-725	3	1300	5	Brine
NE-9442	1575	10-11	400-650	3	1270	3	Brine

Small specimens from each steel were treated according to the technique previously discussed; specifically, the heattreatment varied with composition (Table 2). These temperatures and times are

RESULTS

After heat-treatment, the percentage of dark-etching tempered martensite in each specimen was estimated. A series of typical

<sup>Carbides were essentially in solution except in SAE-52100 austenitized at 1550°F. and in SAE-6140, which contained only a very few small carbides.
At intervals of 10° to 20°F. throughout the indicated range.
Another series of SAE-4340 specimens was heat-treated similarly except that the quench at T₂ was I min. at 1050°F. instead of 5 sec. at 1275°F.; this difference in "blackening" treatment did not affect the result.</sup>

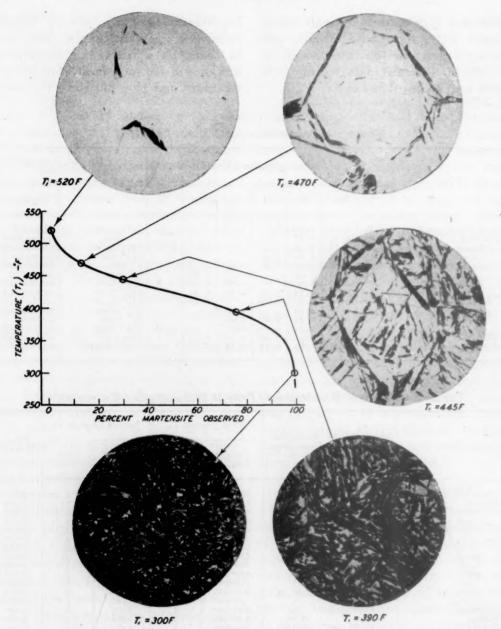


FIG. 2.—Transformation of austenite to martensite. SAE-1065 steel austenitized at 2000°F., quenched for 3 seconds at temperature T_1 , then tempered 5 seconds at 650°F. and brine quenched. Micrographs originally \times 500; reduced one fourth in reproduction. Picral etch.

microstructures is illustrated in Fig. 2, which includes a graph (based upon examination of a larger number of specimens) in which the percentage of martensite observed in SAE-1065 steel is plotted against T_1 , the temperature of the first

metal bath.* The first micrograph in the series contains about enough martensite for a measurable beginning; the last, what we

^{*} Temperature is plotted vertically to convey the impression of cooling down and because temperature is plotted vertically on isothermal transformation diagrams.

estimated to be 99 per cent tempered martensite.

In Fig. 2, the first tempered martensite needles to appear are relatively large and

together with the fact that the last traces of austenite were found to disappear so gradually in specimens quenched to successively lower temperatures, led us to

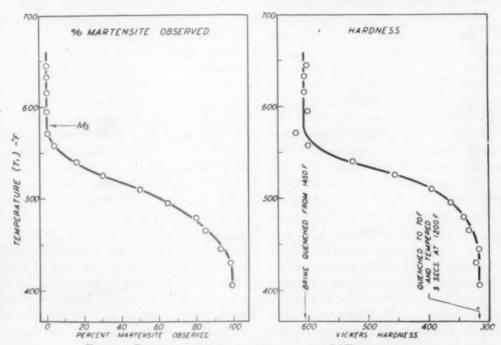


FIG. 3.—PLOT OF EXPERIMENTAL DATA FOR SAE-2340 STEEL.

Steel treated as follows: (1) austenitized at 1450°F.; (2) quenched in liquid lead alloy at T₁ for 3 seconds; (3) tempered, without cooling below T₁, for 5 seconds at 1200°F.; (4) brine quenched.

seem to show a preference for austenite grain boundaries. Since the needles appear not to grow appreciably once they have formed, nor to cross one another, it is impossible to completely fill space with such needles, therefore later ones must necessarily become ever shorter as smaller and smaller interstitial volumes of austenite are trapped between previously formed larger needles of martensite. The last austenite to transform appears to exist in small angular areas, which disappear entirely only after cooling to a temperature disproportionately far below that where 90-odd per cent had transformed. It is quite apparent that an accurate estimate of the percentage of tempered martensite in a structure like that represented in the lower left micrograph is difficult. This, stop our curves at the 99 per cent point rather than attempt to decide at just what particular temperature the last visible trace of austenite had disappeared. Moreover, in some steels, minute light-etching areas suggestive of retained austenite could be observed at high magnification in specimens tempered after quenching to room temperature.

Data for one steel (SAE-2340) are plotted in Fig. 3 to illustrate in a typical case the number of temperatures investigated and the consistency of the measurements. Each point represents the average of three specimens that were heat-treated simultaneously. The percentage of tempered martensite in each specimen is essentially one observer's opinion and subject to some error, even though con-

firmed approximately by one or more other observers. There is little doubt, however, as to the temperature (to the nearest 5° or 10° F.) at which tempered martensite needles first definitely appear (M_8) . M_8

microscopic observations, although it is considerably less precise in indicating the temperature where martensite begins to form or where martensite formation is virtually complete.

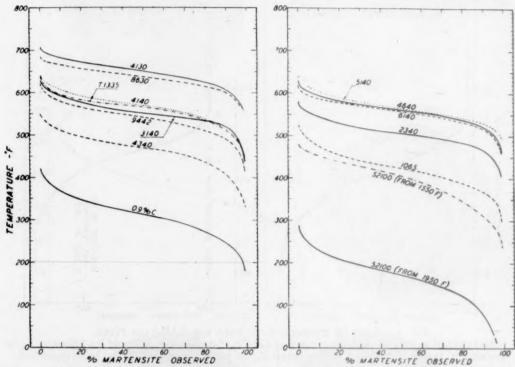


FIG. 4.—RELATION OF PERCENTAGE OF MARTENSITE TO TEMPERATURE IN FOURTEEN COMMERCIAL GRADES OF STEEL.

frequently seems to lie between two experimentally determined points, in which case, as in Fig. 3, it was estimated by interpolation.

Hardness measurements proved useful as a check on the microscopic observations and were especially helpful in the lower carbon steels, which were tempered at 1200°F. or higher. Hardness ranged from that of quenched martensite down to that of a sample quenched to room temperature and then tempered at the temperature, and for the time, used in the "blackening" treatment for that particular steel. The measurements for the SAE-2340 steel are plotted in Fig. 3, wherein it is evident that hardness correlates satisfactorily with the

Data for each of the steels listed in Table 2 are summarized in Fig. 4; two charts, each of which includes nominally half of the steels, have been drawn to avoid overlapping of the individual curves drawn through experimental points, the points themselves having been subsequently deleted. Values of "per cent martensite observed" plotted along the abscissa represent the observed proportion of tempered martensite in specimens treated as previously described. The results are also summarized in Table 3, in which the percentage of martensite, taken from the curves of Fig. 4, is listed for each 25°F. change in temperature; this scheme has been employed in preference to tabulating the much larger number of actual measurements, which, in themselves, are of no special significance.

In general, these curves are all similar in shape and differ principally in position on the temperature scale. They indicate that equal increments of martensite are not formed on cooling through successively lower equal temperature intervals; on the contrary, a greater temperature change is required to form the first 10 per cent of martensite than to form the second 10 per cent. As the proportion of martensite approaches 100 per cent, the curves appear to become asymptotic; it is doubtful therefore whether a particular temperature can properly be designated as representing the precise end of martensite formation. Consequently, the curves of Fig. 4 have not been continued below the temperature where about 99 per cent martensite was present, although data were obtained at lower temperatures in some tests. No great accuracy is implied in this portion of the curve nor is any special implication attached to this 99 per cent point. In SAE 52100 austenitized at 1950°F., only 95 per cent martensite was estimated to have formed on quenching to 32°F.; no data were obtained at a lower temperature.

The shape of these curves, particularly in the higher temperature region where the proportion of martensite is small, may be somewhat influenced by segregation in the steel. Certainly all of these steels were segregated (banded) to some extent, as was very evident in their microstructure. Martensite needles first appeared in bands and, in most specimens, a corresponding proportion formed at a slightly higher temperature in the half of the specimen adjacent to the surface of the original bar sample; the latter observation is interpreted as evidence of "positive" segregation in the central area of the cross section of the bar.

In spite of small individual differences in shape, it seemed possible that some method of plotting (as, for example, the logistic method described by Austin and Rickett³) might be found that would convert all these curves into straight lines-a step that would, if successful, considerably facilitate measurement of martensite formation. Such attempts, however, were unsuccessful for the reason that the curve was never symmetrical about its midpoint, the lower portion approaching 100 per cent martensite much more gradually than the upper portion approaches o per cent martensite; nevertheless, it was possible, by plotting the percentage of martensite on the logistic scale, to straighten the lower three fourths of the curve, and such a plot, even though not a straight line throughout, was helpful in anticipating the remainder of the curve after the portion from o to about 25 per cent had been measured experimentally.

The conventional isothermal transformation diagram aids greatly in understanding and planning heat-treatment; it would be even more valuable if it included information on martensite formation. It is therefore of interest to see how martensiteformation data might be fitted into the isothermal transformation diagram. Since no one has ever measured a rate of formation of martensite at a particular temperature level, the time scale of the isothermal diagram is without significance in martensite formation. In Fig. 5, the lower portion of the isothermal diagram for SAE-2340 steel has been modified to include our measurements of martensite formation by indicating at the proper temperature several arbitrary percentages of martensite; the arrows point to the temperature at which the indicated proportion of martensite will have formed on quenching. Obviously, the diagram does not, strictly speaking, represent completely isothermal transformation below Ms, and a dash line has been drawn horizontally to indicate this. The continuation of the ending line of isothermal transformation below M_S indicates the time required for

SAE 2340

C-0.37 Mn-0.68 Ni-3.41

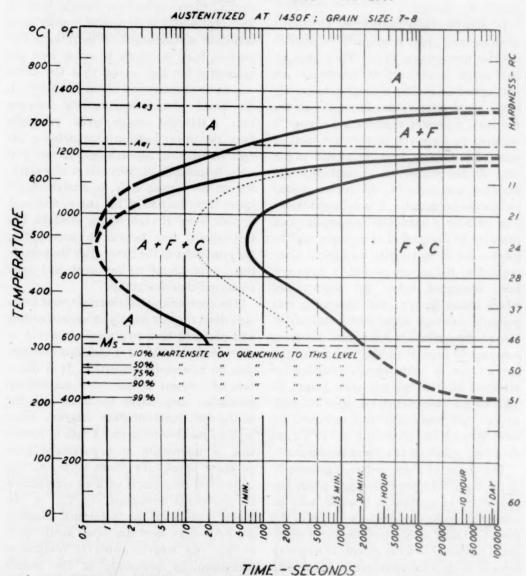


Fig. 5.—Isothermal transformation diagram, with data on martensite formation added. Transformation occurs at constant temperature only above M_S .

the portion of austenite that did not transform to martensite to transform isothermally to what is probably best regarded as bainite, even though this low-temperature bainite is microscopically indistinguishable from martensite, which on holding at such elevated temperature

becomes slightly tempered (darkened after etching). In the Atlas,² there is an isothermal diagram for each steel (except NE-8630) whose martensite formation is given in Fig. 4 or Table 3; consequently, a diagram similar to Fig. 5 can be constructed for each.

INFLUENCE OF AUSTENITE GRAIN SIZE

In any steel, quench cracking is likely to be worse when austenite grains are large than when they are small; from this size), the carbides being completely dissolved in austenite in either case. The resulting data, summarized in Fig. 6, show that this difference in austenite grain size

TABLE 3.—M. and Estimated Percentage Martensite at Different Quenching Temperatures
Arranged in order of decreasing Ms temperature

	SAE	NE	SAE	SAE	SAE	SAE	SAE	SAE	NE	SAE	SAE	SAE	0.9 Per	SAE-	521000
				T1335				6140			4340	1065	Cent	1950°F.	1550°F
Ms, deg. F 99 per cent mar- tensite, deg.	710	690	640	640	640	630	630	620	620	580	550	525	420	290	480
	550	540	490	450	425	460	440	460	410	400	330	300	175	below	235
Range M./99 per cent mar-														32	
tensite, deg.	160	150	150	190	215	170	190	160	210	180	220	225	245	more than 260	245
Quenching Temperature, Deg. F. Ti 725	0 1 1 15 50 80 92 97 99	0 1 30 65 90 96 98 99	0 2 12 35 70 92 98 98 99	0 1 7 30 70 85 93 93 97 99	9 2 15 40 70 85 94 97 98 99	0 1 - 7 30 70 96 98 99	0 — 1 — 6 6 6 7 6 7 6 7 6 7 6 7 6 7 6 7 6 7 6	0 2 25 60 85 98 99 99	0 2 12 40 70 85 94 97 98 98 99	0 1 – 7 30 60 85 98 98 99	0 + 5 15 40 70 85 92 95 98 99	0 0 10 25 50 72 87 95 98 99	0 2 8 18 37 62 78 88 95 98	0 1 4 10 25 45 65 80 85 90	0 1 10 33 555 68 73 86 92 97 98 99

All carbides were not in solution in SAE-52100 austenitized at 1550°F.; in other steels, including SAE-52100 austenitized at 1950°F., essentially all carbides were dissolved in austenite.

it might be inferred that large austenite grains, all other things being equal, transform to martensite over a lower temperature range than small austenite grains. Therefore, martensite formation in the SAE-1065 steel was studied after austenitizing at 1500°F. (No. 6 austenite grain size) and at 2000°F. (No. 2 austenite grain

had no effect on the proportion of martensite formed on quenching for 3 sec. at any corresponding temperature. The microstructure for large and small austenite grains, both at a common temperature, is shown respectively by the left and right micrographs of Fig. 6; obviously, the martensite needles in the former are larger and fewer, but the total proportion (appearing as dark-etching tempered martensite needles) is about the same in both.

same, at any corresponding temperature, as previously measured for the same steel with small austenite grains. Greninger⁵ and

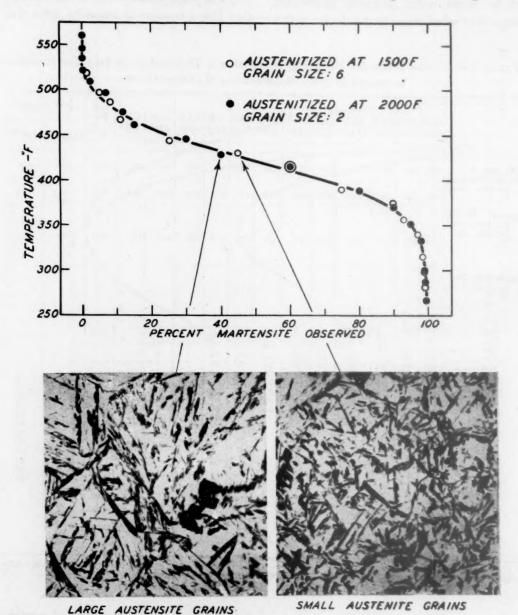


Fig. 6.—Comparison of martensite formation in fine-grained and coarse-grained austenite (SAE-1065).

Micrographs originally × 500; reduced one fourth in reproduction. Picral etch.

A few specimens from several other steels were austenitized at a high temperature to coarsen their austenite grains; the estimated proportion of martensite was the Payson and Savage⁴ likewise imply that they observed no change in the temperature range of martensite formation due to difference in austenite grain size. EFFECT OF UNDISSOLVED CARBIDES

In practice a hypereutectoid steel such as SAE-52100 would rarely, if ever, be

present in austenite, subsequent martensite formation is shown by Fig. 7 to be entirely unlike that in the same steel after heating

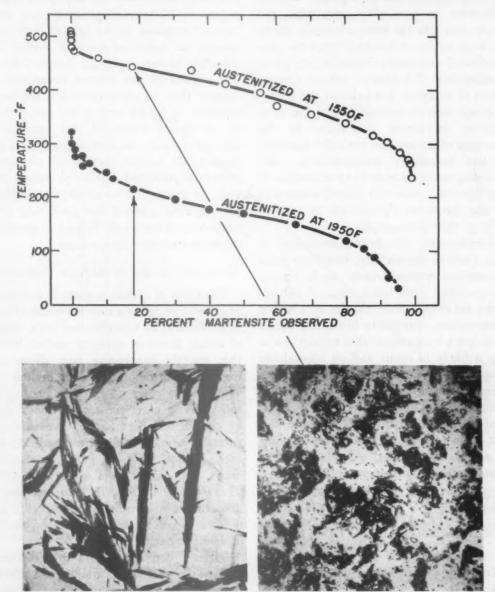


Fig. 7.—Influence of undissolved carbides upon martensite formation in SAE-52100 STEEL.

Difference in austenite grain size is not a factor, as shown by Fig. 6. Micrographs originally X 500; reduced one fourth in reproduction. Picral etch.

quenched from a temperature high enough to dissolve all the carbides (in our sample, 1950°F. was required for complete solution). When undissolved carbides are to dissolve all carbides. In SAE-52100 steel austenitized at 1550°F. (many undissolved carbides, as shown by the right micrograph), martensite formation is virtually

complete at the temperature at which it has just begun in the same steel austenitized at 1950°F. (no undissolved carbides. as shown by the left micrograph). A large difference in austenite grain size also exists, but this has been previously shown to have no direct influence upon the proportion of martensite formed at any given temperature. Obviously, actual composition of austenite just prior to quenching. and not over-all composition of the steel, governs martensite formation. In the presence of undissolved carbides, austenite is also necessarily inhomogeneous; this inhomogeneity appears to have resulted in the "patchy" areas of tempered martensite in the specimens austenitized at 1500°F. (Fig. 7, right micrograph).

Incidentally, the data summarized in Fig. 7 help to explain why, aside from grain coarsening, hypereutectoid steels should be quenched from below Ac_{em}; if all carbides are dissolved by heating to a higher temperature, martensite formation occurs at so low a temperature that quench cracking is likely to occur and an appreciable proportion of austenite remains untransformed (retained) on quenching to room temperature. Our SAE-52100 specimens austenitized at 1950°F., for example, did not begin to form martensite until cooled to 290°F. and retained about 10 per cent austenite at room temperature.

PART II. ESTIMATION OF TEMPERATURE RANGE OF MARTENSITE FORMATION FROM STEEL COMPOSITION

In 1939, Zyuzin et al.⁶ determined the effect of individual alloying elements upon the upper temperature limit of martensite formation (M_S) ; we have used these data to estimate M_S in any carbon or lowalloy steel by means of an empirical formula, which for the past several years has been applied to many steels whose M_S has been experimentally determined. While the predicted M_S was often in considerable

error, the usefulness of such a formula and the general dependence of M_8 upon composition has repeatedly been demonstrated. Recently, more data on this point have appeared;4,5,7 in particular, Payson and Savage proposed, on the basis of their own results, an empirical formula similar in principle to ours based on Zyuzin's data. The results of the present investigation suggest that, in addition to M_s , the temperature at which any given proportion of martensite forms is also essentially dependent upon composition and therefore predictable. In this section all available data from published sources, as well as our own, are analyzed in an attempt to develop an empirical method for predicting the proportion of martensite formed on quenching to any selected temperature.

Relation of M_S to Carbon Content

The effect of carbon content in lowering $M_{\mathcal{S}}$ is well recognized and established by a large amount of experimental data, most of which, however, apply to carbon steels that contain manganese and silicon as well as impurities. Since it is desired to evaluate the effect of carbon alone, only substantially pure iron-carbon alloys can be considered. Fortunately, two investigators 5.8 have carefully measured M_S in each of two series of pure iron-carbon alloys, and their results agree very well. The effect of carbon, therefore, is based upon these two investigations, disregarding data on carbon steels or iron-carbon alloys of doubtful purity.

Digges⁸ determined M_s by thermal analysis for each of six iron-carbon alloys ranging from 0.23 to 0.80 per cent carbon, and Greninger,⁵ by using both thermal analysis and the metallographic method, for four iron-carbon alloys ranging from 0.19 to 0.85 per cent carbon. Their data are plotted in Fig. 8 and a straight line is drawn through the points, which shows that within the limits 0.2 to 0.85 per cent carbon each additional 0.1 per cent incre-

ment in carbon lowers M_8 by 65°F. The straight line extrapolates to 1025°F. at o per cent carbon, and M_8 for pure iron-carbon alloys may therefore be computed

contain more carbon, the carbides will not ordinarily be completely dissolved in austenite in commercial hardening, and hence over-all carbon content could not be

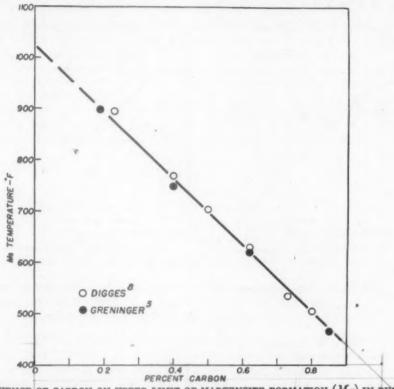


Fig. 8.—Influence of carbon on upper limit of martensite formation (M_S) in pure-iron-carbon alloys.

by the formula

 $M_8(^{\circ}\text{F.}) = 1025 - 650 \times \% \text{ carbon [1]}$

This formula is probably valid for carbon content up to 0.85 per cent; that is, for hypocutectoid alloys. Greninger's data for two hypercutectoid carbon steels (not represented in Fig. 8) would lie well above the extrapolated straight line, which suggests that application of formula 1 to alloys containing more than 0.85 per cent carbon would give a calculated $M_{\mathcal{B}}$ lower than the measured $M_{\mathcal{B}}$, and that the discrepancy would be greater the higher the carbon. This limitation does not interfere with the practical usefulness of the formula, since most commercial steels contain less than 0.85 per cent carbon; when they

substituted in the formula in any case.

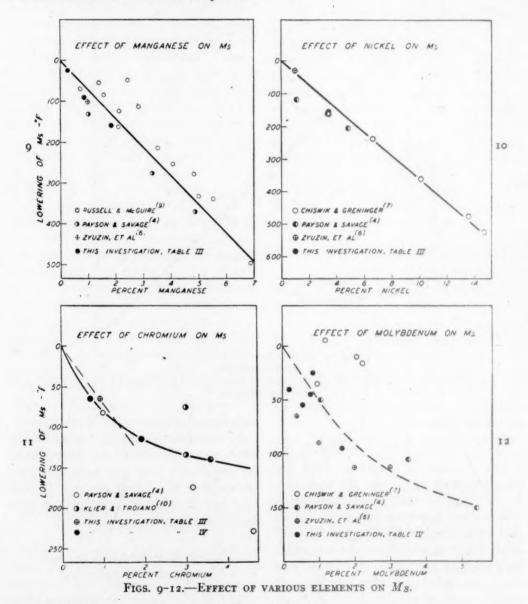
Since carbon apparently has an orderly effect upon M_s , which may be expressed by means of a simple formula, this gives the promise that other elements likewise may have a simple and orderly effect upon martensite formation.

Effect of Individual Alloying Elements upon $M_{\mathcal{S}}$

The effect of each of the common alloying elements upon M_B is now to be considered. The most desirable data for this purpose are those for alloys containing only iron, carbon and the particular alloying element under consideration; but scarcity of data makes it necessary to consider

also steels that contain some manganese, silicon and impurities in addition to iron, carbon and the particular alloying element.

Silicon.—Chiswik and Greninger⁷ studied a series of iron-carbon-silicon alloys conPayson and Savage,⁴ however, interpreted their measurement of M_s for a 0.5 per cent carbon, 1 per cent silicon steel as indicating that 1 per cent silicon lowers M_s by 20°F.



taining 0.8 per cent carbon and 1.6 to 3.6 per cent silicon, and concluded that silicon (at least up to 3.6 per cent) neither raises nor lowers M_s . Zyuzin⁶ also reported that silicon has no effect upon M_s in nominally 1 per cent carbon steel.

On the basis of these results it is concluded that silicon, in the amount present in commercial grades of hardenable steel, has no effect upon M_S . For iron-carbon-silicon alloys, therefore, M_S may be computed by the empirical formula:

$$M_s(^{\circ}\text{F.}) = 1025 - 650 \times \% \text{ carbon}$$

 $- 0 \times \% \text{ silicon}$ [2]

Manganese.—No data are available for pure iron-carbon-manganese alloys, but M_8 has been measured in many plain carbon steels (which, of course, contain a

lated according to formula 3, are shown on the chart, principal reliance is placed upon the former. It is concluded from this chart that each τ per cent nickel lowers M_8 by $_{3}6^{\circ}\mathrm{F}$.

Chromium and Molybdenum.—Published data that reveal the effect of chromium or

Table 4.—Composition and M. of a Series of Chromium and of Molybdenum Steels

		Compositi	on, Per Ce	int		Measured	Calculated M.	Lowering of
Cr	С	Mn	P	S	Si	M. Deg. F.	without Cr or Mo, Deg. F.	M. by Cr or Mo, Deg. F.
0.55 1.91 3.59	0.38 0.27 0.36	0.37 0.45 0.48	0.022 0.007 0.007	0.022 0.011 0.024	0.24 0.25 0.26	685 700 620	750 815 760	65 115 140
Mo 0.20 0.56 0.78 0.84 1.65	0.63 0.39 0.37 0.68 0.80	0.18 0.43 0.16 0.19 0.31	o.oii	0.007 b	0.13 0.19 0.14 0.16 0.18	560 685 730 545 390	600 740 775 570 485	40 55 45 25 95

According to formula 3.
Not determined; reportedly low.

significant percentage of manganese) and in a few manganese steels. Neglecting the possible effect of small amounts of impurities, the lowering of Ms due to manganese may be calculated in each case by subtracting the measured M_S from the M_S calculated by formula 2 for the same composition without manganese. On this basis, data from the literature 4,6,9 and from our investigation have been plotted in Fig. 9. Although somewhat scattered, the points, in confirmation of this method of analysis, define a straight line, which passes through zero. It is concluded that each I per cent manganese lowers M_S by 70°F.; therefore, for plain carbon and carbon-manganese steels Ms may be calculated by the formula

$$M_s(^{\circ}\text{F.}) = 1025 - 650 \times \% \text{ carbon} - 70 \times \% \text{ manganese}$$
 [3]

Nickel.—The effect of nickel is shown in Fig. 10. The points from Chiswik and Greninger⁷ were determined for iron-carbon-nickel alloys, and although several points for nickel steels, calculated by subtracting the measured M_S from that calcu-

molybdenum upon M, are few and, particularly for molybdenum, are in disagreement. Consequently, we measured $M_{\mathcal{S}}$ for each of a series of chromium steels and of molybdenum steels. Since banding (segregation) was found to have an important effect upon M_8 and is likely to vary in severity from steel to steel, our steels were heated for 2 days at 2350°F. (homogenized) to eliminate banding. The Ms was determined by the metallographic technique in accordance with the principles discussed previously. All steels were austenitized at 2000°F. to ensure complete solution of chromium or molybdenum in austenite. The composition of each steel, determined after homogenization, and the measured M_S , is listed in Table 4. In each steel, the effect of chromium, or molybdenum, was estimated by subtracting the measured M_S from an M_S for that particular steel composition, without chromium or molybdenum, calculated according to formula 3 (Table 4).

The data for chromium steels are plotted in Fig. 11. Unlike corresponding data for manganese or nickel, they do not lie on a straight line that extrapolates to zero. As compared with elements previously considered, these data are very scattered; however, since our data for the homogenized series of chromium steels are centrally located with respect to other data, a smooth curve has been drawn through them and extrapolated to zero. This curve, as drawn, indicates that small percentages of chromium are proportionally more effective in lowering Ms than larger percentages; consequently, the effect of chromium cannot be expressed by a simple factor in an empirical formula. Within the range of chromium content in most commercial lowalloy steels, however, it suffices to approximate the effect of chromium by the dashed line shown in Fig. 11. For present purposes, we shall tentatively conclude that, in the range o to about 1.5 per cent, each 1 per cent chromium lowers M_8 by 70°F.

The data for molybdenum steel are even more difficult to analyze than those for chromium steel, as is apparent in the scattered points of Fig. 12. Our own homogenized series of molybdenum steels fails to define any particular curve and published data are equally inconsistent. Before selecting our steels for determining the effect of molybdenum upon Ms, it was thought that perhaps the effect of molybdenum might vary with carbon content, and, for this reason, two steels containing nominally 0.3 per cent carbon and three containing nominally 0.7 per cent carbon were selected; however, it is apparent that the effect of molybdenum is about equally erratic in either carbon range. Obviously, additional experimental measurements are needed; however, it is possible that the effect of molybdenum will always be found to be consistently erratic, as in the present data. For the present, a compromise and tentative curve has been drawn in Fig. 12 and, just as for chromium, it is indicated that small percentages of molybdenum are proportionally more effective than larger ones in lowering M_S . The curve, as drawn,

is a straight line in the range o to 1 per cent molybdenum (the range that includes commercial low-alloy steels), and 1 per cent molybdenum lowers M_S by 50° F.

Other Alloying Elements.—The elements thus far considered include the principal ones present in hardenable low-alloy steels, and it is not essential for most practical purposes to estimate the quantitative effect of the minor elements. Qualitatively, Zyuzin⁶ reported that M_S is raised by aluminum and cobalt (this effect of cobalt is confirmed by Chiswik and Greninger⁷) and lowered by copper, vanadium and tungsten, the latter two being about like molybdenum in quantitative effect when dissolved in austenite.

Estimation of $M_{\mathcal{S}}$ from Chemical Composition

Assuming that the individual effect of each alloying element is additive when two or more are present and that the effect of impurities and small amounts of elements not to be considered have no significant effect on M_s , it is possible to write a single empirical formula, as follows:

$$M_8$$
(°F.) = 1025 - 650 × % C
- 70 × % Mn - 36 × % Ni
- [70 × % Cr] - [50 × % Mo]* [4]

This formula should make it possible to calculate the approximate M_B in any carbon or low-alloy steel whose composition is known, subject to the following limitations:

- 1. The carbon content must be within the range 0.20 to 0.85 per cent (the formula may be found to apply to lower carbon, but only steels containing carbon within the specified range were considered in its development).
 - 2. The chromium content must be less

^{*} The factors for chromium and molybdenum are enclosed in brackets to indicate that more uncertainty exists in the correct value, and also because these factors apply only to a limited range of chromium or molybdenum content.

than about 1.5 per cent and the molybdenum content less than about 1 per cent; for a steel containing a higher percentage mation of M_B in commercial carbon and low-alloy steels such as those considered in the first part of this paper, we feel justified

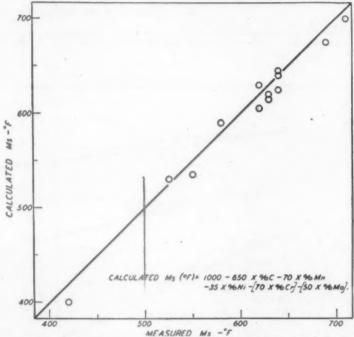


Fig. 13.—Correlation between calculated M_o and measured M_o for steels listed in table 1.

of either of these two elements, the curves of Figs. 11 and 12 for chromium and molybdenum, respectively, may be used for substituting a value in the formula.

3. All carbides (therefore carbon and alloying elements) must be dissolved in austenite.

When formula 4 was applied to the 14 steels whose M_8 we measured (Table 3), the calculated M_8 was usually higher than the measured M_8 by about 25° F. This difference may be due to error in some of the factors in the formula, or it may be that impurities such as phosphorus and the small amounts of other alloying elements present in commercial steel, while having as individuals a small effect, may combine to cause this relatively constant error. Inasmuch as this analysis is empirical, and designed to permit esti-

in modifying formula 4 to read:

$$M_s(^{\circ}\text{F.}) = 1000 - 650 \times \% \text{ C}$$

- $70 \times \% \text{ Mn} - 35 \times \% \text{ Ni}$
- $[70 \times \% \text{ Cr}] - [50 \times \% \text{ Mo}]$ [5]

The $M_{\mathcal{S}}$ of each steel measured in part I has been calculated by this revised formula (formula 5) and plotted in Fig. 13 against the corresponding measured M_8 . The correlation is quite acceptable for this typical group of carbon and low-alloy steels, the calculated Ms being in all within 20°F. of the measured value. For SAE-52100 (not plotted in Fig. 13), the calculated Ms was 70°F. low, because the carbon content of this steel is above the range in which the formula applies; it confirms the earlier statement that the lowering of M_S is no longer directly proportional to carbon content above 0.85 per cent. Within the limitations of the formula, as stated above, it would appear that M_S may be calculated with sufficient accuracy for many purposes, and, if M_S is to be actually measured, will serve as a useful guide in planning such measurements.

general type, although their precise shape and temperature range vary considerably. This is evident in comparing the curves for SAE-52100, SAE-1065 and SAE-2340; apparently, the higher the carbon content,

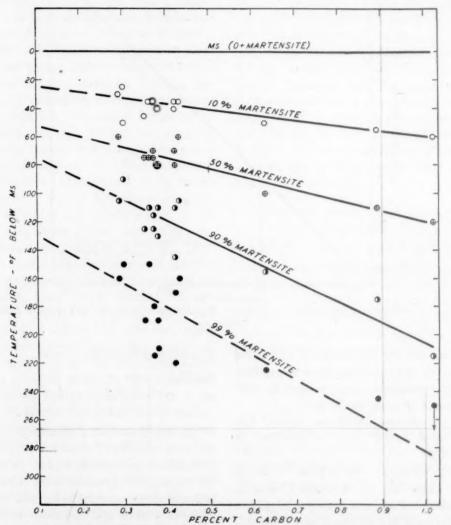


Fig. 14.—Chart for estimating proportion of martensite at any given temperature when M_{ullet} and carbon content are known.

ESTIMATION OF PERCENTAGE OF MAR-TENSITE FORMED AT ANY GIVEN TEMPERATURE

The curves summarizing our measurement of the proportion of martensite formed on quenching for 3 sec. at each of a series of temperatures (Fig. 4) are of the same

the greater the temperature difference between beginning and ending of the curve. Other alloying elements also widen the temperature range of martensite formation according to Payson and Savage,⁴ and this is confirmed in a qualitative way by our data; however, their effect seems to be small compared with that of carbon, at least in most commercial types of lowalloy steel. Based upon the observation that carbon widens the temperature range of ing that they define the straight lines drawn. However, the dependence of the extent of martensite formation range upon carbon content is demonstrated, and, in view of

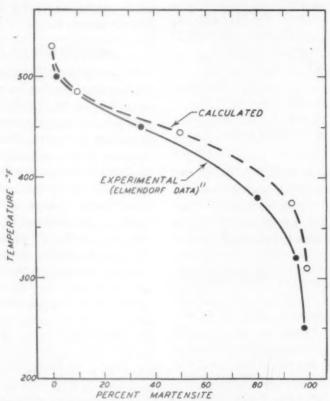


Fig. 15.—Comparison of martensite-formation curve, calculated from formula 5 and Figure 14, with measured data for an AISI A-4063 steel.

martensite formation, and neglecting for the present, because of lack of adequate data, the effect of other elements, it seems worth while to utilize present data to predict the proportion of martensite formed at any given temperature, even though it is admittedly only a rough approximation.

If for each of the steels in part I the temperature interval below M_S (to the nearest 5°F.) in which 10, 50, 90 and 99 per cent martensite has formed is determined from Fig. 4, the chart shown in Fig. 14 results. The points are scattered, particularly those for the higher percentage of martensite, and considerable liberty is taken in assum-

the several factors that are not considered, it is not surprising that the points are scattered.

Fig. 14, in conjunction with formula 5, may be used to predict the approximate temperature at which any given percentage of martensite will have formed, subject to the limitations discussed above with reference to the formula. For example, suppose it is desired to roughly estimate martensite formation in a steel of the following composition: C, 0.64 per cent; Mn, 0.61; P, 0.014; S, 0.017; Si, 0.20; Mo, 0.25. Selection of this particular steel was influenced by the fact that Elmendorf¹¹ has experimen-

tally measured its martensite formation in some detail. For this steel, M_s may be computed as follows:

$$M_8(^{\circ}\text{F.}) = 1000 - 650 \times \% \text{ C} - 70$$

 $\times \% \text{ Mn} - 35 \times \% \text{ Ni}$
 $- [70 \times \% \text{ Cr}] - [50$
 $\times \% \text{ Mo}] \text{ (formula 5)}$
 $= 1000 - 650 \times 0.64 - 70$
 $\times 0.61 - 35 \times 0 - 70$
 $\times 0 - 50 \times 0.25$
 $= 1000 - 416 - 43 - 0 - 0 - 12$
 $= 1000 - 471$
 $= 529 \text{ (or to the nearest 5°F.,}$
 $= 530^{\circ}\text{F.})$

The temperature at which 10, 50, 90 and 99 per cent martensite forms is then estimated from Fig. 14 by noting the intersection of a vertical coordinate line at 0.64 per cent carbon with the slanting lines on the chart; thus,

10% martensite forms at 45° F. below M_s , or $530^{\circ} - 45^{\circ} = 485^{\circ}$ F. 50% martensite forms at 90° F. below M_s , or $530^{\circ} - 90^{\circ} = 445^{\circ}$ F. 90% martensite forms at 155° F. below M_s , or $530^{\circ} - 155^{\circ} = 375^{\circ}$ F. 99% martensite forms at 220° F. below M_s , or $530^{\circ} - 220^{\circ} = 310^{\circ}$ F.

These values, plotted in Fig. 15, are sufficient to define a smooth curve from which the temperature for any intermediate percentage of martensite can be estimated. For comparison, Elmendorf's experimental data are also plotted in Fig. 15. When it is recalled that experimental measurement of martensite formation by the metallographic technique is not highly accurate, and is so influenced by the quenching time and tempering treatment, as well as by segregation in different steels of the same over-all composition, that different investigators rarely agree exactly when working with steel of comparable composition, the agreement in this case between the calculated and the experimental curve seems surprisingly good—perhaps better than can be generally expected. It appears that estimation of martensite formation by this empirical method may be sufficiently accurate for many practical purposes and if actual measurements are to be made would be useful in planning the measurements.

DISCUSSION OF RESULTS

In part I, in which the determination of martensite formation by a metallographic technique was discussed at some length, it was pointed out that the results apply specifically to very small samples quenched for about 3 sec. in liquid media. It is not known for certain whether such results apply exactly to the more general cases where larger masses of steel are timequenched or cooled continuously to room temperature. In all probability, thermal and transformation stresses, which were relatively insignificant in our very small specimens, may play an important role in martensite formation. For example, it has been claimed that compressive stress lowers the temperature range of martensite formation and tensile stress raises it. The observation sometimes made, that in a steel such as SAE-3140 an appreciable proportion of austenite is retained, particularly in the center, on quenching larger masses to room temperature is not entirely consistent with our data unless we assume that in the larger mass stress has influenced the transformation of austenite to martensite. There are also puzzling observations associated with the breakdown of retained austenite by refrigeration in relatively highcarbon steels, wherein, for example, it appears that the proportion of austenite to transform during refrigeration is decidedly affected by prior "aging" at room temperature before refrigeration; again, an important effect of stress, or possibly some other factor, is indicated. Obviously, the subject of martensite formation is one that, at present, is not well understood, and a great deal of investigation must be done before the limitations of present data are clear.

Subject to limitations imposed by lack of knowledge concerning all the factors that influence martensite formation, the present data should prove helpful in planning heattreatment, for they suggest an orderly and predictable behavior for transformation of austenite to martensite and provide information of a sort that has been almost entirely lacking. As more information develops, the empirical method proposed for estimating martensite formation as a function of austenite composition may be extended and improved or perhaps abandoned as an oversimplification. It is evident that unavoidable segregation in commercial steels introduces a variable and seemingly not measurable factor, which will always preclude really precise estimation of martensite formation based on overall steel composition.

SUMMARY

This paper is divided into two parts, the first being a presentation of experimental results; the second, an analysis of these and of pertinent published data* for the purpose of developing an empirical relationship between chemical composition and the proportion of martensite formed on quenching to any given temperature.

In agreement with the published results of others, it was found that in a given composition martensite does not form above a certain temperature now commonly designated M_S ; on quenching to a lower and lower temperature, more and more martensite forms, until finally virtually all of the austenite has transformed to martensite. Thus, martensite appears to form over a

The results of our observations, based on the metallographic technique of Greninger and Troiano (Figs. 1, 2), of each of 14 popular steel compositions, are summarized in a curve, which shows the proportion of martensite formed on quenching at each of a series of temperatures (Fig. 4); the curves for all the steels are generally similar, but are displaced with respect to one another on the temperature scale. The temperature range in which martensite forms is decidedly influenced by composition, especially carbon content; but in a steel containing undissolved carbides after austenitizing, it depends upon the actual composition of the austenite rather than upon the over-all composition of the steel (Fig. 7).

Neither M_s nor the proportion of martensite at any lower temperature was affected by difference in austenite grain size (Fig. 6)

Carbon and individual alloying elements appear to have an orderly effect upon the temperature of martensite formation, particularly upon M_S , the upper limit of the range (Figs. 8 to 12). On this basis, assuming that when several alloying elements are present the individual effects are additive, the following empirical formula is proposed for estimating M_S in degrees Fahrenheit for any hypocutectoid steel of known composition:

$$M_8$$
(°F.) = 1000 - 650 × % C
- 70 × % Mn - 35 × % Ni - [70
× % Cr] - [50 × % Mo].*

Those alloying elements not represented in

range of temperature rather than progressively at any constant temperature during a measurable time period; nevertheless, the lower portion of the conventional isothermal transformation diagram may be modified to depict martensite formation (Fig. 5).

^{*}A considerable number of published papers dealing with martensite formation are not specifically mentioned for the reason that their data on Ar", though pertinent, were obtained by thermal or dilatometric analysis, neither of which, unless special care is taken, yields the M₀ temperature with sufficient precision for our purposes.

^{*}Brackets enclose the chromium and the molybdenum factor because more uncertainty exists as to the correct value and because the factor given seems to apply, in either case, only up to a certain percentage.

the formula are believed not to appreciably affect martensite formation when present in the amount usually encountered in commercial carbon and low-alloy steels.

The extent of the temperature range of martensite formation seems to depend principally upon carbon content, and a chart (Fig. 14) based upon our measurements makes it possible to approximate the proportion of martensite formed at any particular temperature in any steel whose Ms has been previously calculated or otherwise determined. A curve representing the relationship between percentage of martensite and temperature derived in this way agrees sufficiently well for many practical purposes with experimental data from a published source (Fig. 15). It is thought that this empirical approximation may prove useful in planning heat-treatment of steel whose martensite formation has not been experimentally studied, although failure to take into account the probable effect of certain alloying elements in extending the temperature range of martensite formation (because of insufficient data at present) precludes accurate derived results, particularly in steels containing an appreciable percentage of alloying elements.

ACKNOWLEDGMENT

We take this opportunity to gratefully acknowledge helpful suggestions and comments from Messrs. E. C. Bain, J. R. Vilella, R. E. Brien, and other associates.

REFERENCES

I. A. B. Greninger and A. R. Troiano: Kinetics of the Austenite to Martensite Transformation in Steel. Trans. Amer.

Soc. for Metals (1940) 28, 537-574.

2. Atlas of Isothermal Transformation Diagrams. United States Steel Corporation (1943). Most of these diagrams also appeared on a smaller scale in the publication by E. S. Davenport: Isothermal Transformation in Steels (Campbell Memorial Lecture). Trans. Amer. Soc. for Metals (1939) 27, 837-886.
3. J. B. Austin and R. L. Rickett: Kinetics

of the Decomposition of Austenite at Constant Temperature. Trans. A.I.M.E.

(1939) 135, 396-415.

4. P. Payson and C. H. Savage: Martensite Reactions in Alloy Steels. Trans. Amer. Soc. for Metals (1944) 33, 261-280. 5. A. B. Greninger: The Martensite Thermal

Arrest in Iron-Carbon Alloys and Plain

Carbon Steels. Trans. Amer. Soc. for Metals (1942) 30, 1-26.

6. V. Zyuzin, V. Sadovski and S. Baranchuk: Influence of Alloy Elements on Position of Martensite Point. Metallurg (1939)

 H. H. Chiswik and A. B. Greninger: Influence of Nickel, Molybdenum, Cobalt and Silicon on the Kinetics and Ar" Temperatures of the Austenite to Martensite Transformation in Steels. Trans. Amer. Soc. for Metals (1044) 32.

483-520.

8. T. G. Digges: Transformation of Austenite on Quenching High Purity Iron-Carbon Alloys. Trans. Amer. Soc. for Metals

9. J. V. Russell and F. T. McGuire: A Metallographic Study of the Decomposition of Austenite in Manganese Steels. Trans. Amer. Soc. for Metals (1944) 33, 103-125.

10. E. P. Klier and A. R. Troiano: Ar" in Chromium Steels. Trans. A.I.M.E.

(1945) 162, 175.

Elmendorf: Effect of Varying 11. H. Amounts of Martensite upon the Iso-thermal Transformation of Austenite thermal Transformation of Austenite Remaining after Controlled Quenching. Trans. Amer. Soc. for Metals (1944) 33, 236-260.

DISCUSSION

(Walter Crafts presiding)

M. F. HAWKES.*-I should like to mention some unpublished work done recently at Carnegie Institute of Technology. We found that cobalt increases the Ms temperature when it is in solution in homogeneous austenite. This behavior, which is opposite to that of the elements discussed in this paper, is not so surprising when one remembers that cobalt also acts anomalously to decrease hardenability; that is, to increase the rates of transformation of austenite to ferrite and/or pearlite.

C. ZENER. †-I am pleased to learn from Dr. Hawkes that cobalt actually raises the Ms temperature. In two papers recently presented

† Professor of Metallurgy. University of Chicago, Chicago, Illinois.

C. Zener: Equilibrium Relations in Mediumalloy Steels. This volume, page 513.

C. Zener: Kinetics of the Decomposition of

Austenite. This volume, page 550.

Metals Research Laboratory, Institute of Technology, Pittsburgh, Pennsyl-

before this society,12 the Ms temperature has been regarded as the temperature at which the free energy of the gamma phase is equal to the free energy of the alpha phase of the same composition but containing strains that inevitably arise from its mode of formation. According to this viewpoint, the influence of alloying elements upon the Ms temperature is determined uniquely by their standard free energy difference in the alpha and gamma phases. Anomalies in the influence of alloying elements upon the M_S temperature must therefore be a reflection of anomalies in the difference of their standard free energies in the two phases. Now the alpha-gamma phase boundaries of the binary iron-alloy system are uniquely determined by these standard free-energy differences; hence anomalies in the influence of any alloying element upon the Ms temperature should be interpretable in terms of anomalies in the appropriate iron-alloy constitution diagram.

In the iron-chromium constitution diagram the closed gamma loop has a minimum, indicating that at temperatures below 900°C. the difference in standard free energy of chromium between the alpha and gamma phases changes sign as the concentration is increased. This dependence of standard free energy difference of chromium upon concentration must result in a nonlinear influence upon the Ms temperature.

In the iron-cobalt constitution diagram an increase of cobalt concentration raises the gamma-delta boundary, but leaves the alphagamma boundary essentially unaltered. Such an effect is evidence that the standard free energy of cobalt in alpha iron is lowered with respect to its value in gamma iron as the temperature is lowered from 1400° to 900°C., the two free energies being identical at the latter temperature. By extrapolation, therefore, it can be surmised that the standard free energy of cobalt is lower in alpha than in gamma iron below 900°C. If such an extrapolation is correct, it must follow that cobalt will raise the Ms temperature.

J. H. HOLLOMON.*—I should like to ask the authors if the method of presenting the martensite start and finish data that they used in constructing their S-curves means to imply that the temperature of the completion of the

martensite reaction is independent of cooling rate. Furthermore, does this means of presentation of the data imply that the temperature for 20 per cent martensite formation, for example. would also be independent of cooling rate? There is definite evidence that the amount of martensite formed upon cooling to any temperature below the M_S varies with cooling rate. These data would indicate that the temperatures at which fixed amount of martensite formed other than the first few per cent would depend upon the rate of cooling. I agree that the Ms temperature is independent of cooling rate but that the temperatures at which finite amounts of martensite form do depend on cooling rate.

W. WILSON.*—The implication has been made that the dilatometric method might give erroneous results on the first martensite formation or M_S point. We have correlated some of our work on the contraction of austenite on quenching from a fixed austenitizing temperature to various subcritical temperatures. These results are best fitted by two straight lines; for temperatures below the M_S point, the contraction observed is independent of the temperature. The experimental points follow the horizontal line quite closely. This, I believe, would indicate that martensite formation can readily be detected by the dilatometer (Fig. 16) and further that the results are reproducible.

A. Skapski.†—Dr. Zener just gave us a very good example of how metallurgical phenomena can be treated from the thermodynamical point of view using characteristic functions such as free energy and avoiding any special assumptions.

It seems to me that the difficulty he had in dealing with the Fe-Cr-C case may be perhaps connected with the capillary activity of chromium carbide; i.e., with its tendency to concentrate in the grain boundaries. In trying to base our calculations of heterogeneous thermodynamic equilibria upon the familiar composition-temperature diagrams, we may come across deviations of facts from theory unless we take under consideration these phenomena of adsorption in grain boundaries for two reasons.

^{*} Watertown Arsenal, Watertown, Mass.

^{*} Assistant Metallurgist, Armour Research Foundation, Chicago, Illinois.
† University of Chicago, Chicago, Illinois.

First, the diagrams refer always to average bulk composition of the respective phase, while the reaction itself occurs in the grain boundaries whose composition may be different from that

in the grain boundaries must be shifted, as shown already by J. J. Thomson, by the influence of interface free energy and in such a way as to increase the equilibrium concentrations of

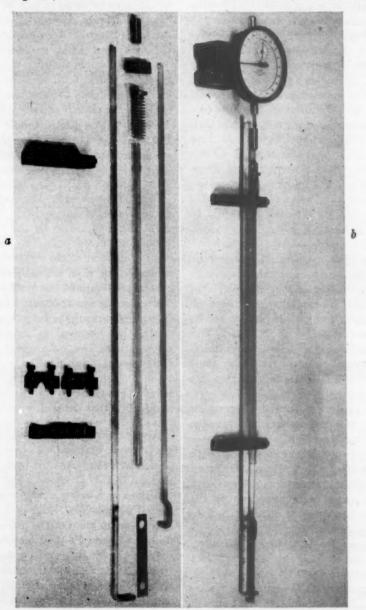
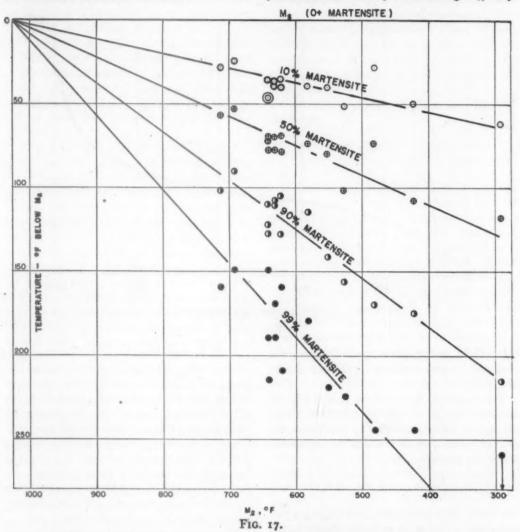


FIG. 16.—DILATOMETER IN USE: (a) "EXPLODED"; (b) "ASSEMBLED".

of the bulk of the grains owing to mere adsorption. This difference will increase with the difference between the respective surface energies of the phases and with increasing capillary activity of the other components. Second, the equilibrium constant of the reactions occurring capillary active products of the reaction and to suppress the concentration of others.

I sincerely believe that a wider application of the laws of physical chemistry of heterogeneous reactions and especially those of surface chemistry to the domain of metallurgical phenomena would help considerably in clearing up many apparently obscure facts, and I wish to welcome most heartily Dr. Zener's excellent and fruitful work in this direction. average lines are for the SAE-52100 austenitized at 1550° F. ($M_S = 480^{\circ}$ F.), in which the carbides were undissolved. The corresponding points had not been plotted in Fig. 14; they



L. D. JAFFE.*—Messrs. Grange and Stewart have presented in their fine paper information that has been long and badly needed.

The percentage of martensite formed at various temperatures below the M_S might well be expected to depend upon the M_S itself, rather than directly upon composition. Data taken from Fig. 4 have been plotted in Fig. 17. The scatter is perhaps somewhat less than in Fig. 14, and the trend perhaps somewhat more clearly defined. The greatest deviations from

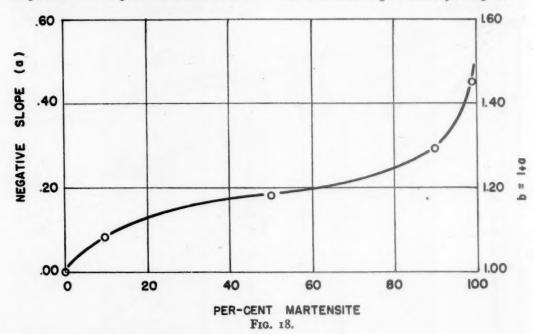
would deviate greatly, of course, from lines shown in that figure.

It is of particular interest that all the lines of Fig. 17, including the M_S , converge to a single point. This point is shown as 1025°F., though the scatter permits drawing lines converging at any temperature between 1000° and 1100°F. This suggests that a steel with an M_S of about 1025°F would transform wholly (and instantly) to martensite at this single temperature. Simple thermodynamic theory would suggest that austenite should always transform wholly to martensite at a single temperature; the phenomerous

^{*} Metallurgist, Watertown Arsenal, Watertown, Massachusetts.

enon responsible for the failure of the austenite to do so evidently is less important the higher the temperature, and becomes negligible in the neighborhood of 1025°F. It is of added interest $M_p(^{\circ}F) = 1000 - b[650 \times \%C + 70 \times \%Mn + 35 \times \%Ni + (70 \times \%Cr) + (50 \times \%Mo)]$

The coefficient b is given directly in Fig. 18.



that 1025°F. is approximately the temperature obtained, by extrapolation, for the M_S of pure iron.

The (negative) slope a of the lines of Fig. 17, has been plotted in Fig. 18 against the percentage of martensite. The degrees below the M_S at which any percentage of martensite forms are then given by

$$^{\circ}$$
F below $M_S = a(1025 - M_S)$

the coefficient a being read from Fig. 18. Upon substitution in Eq. 4 and simplification, the temperature at which any percentage of martensite is formed is found to be

$$M_p(^{\circ}F) = 1025 - (1 + a)[650 \times \%C + 70 \times \%Mn + 35 \times \%Ni + (70 \times \%Cr) = (50 \times \%Mo)]$$

The 1025°F. may be changed to 1000°F., as suggested in the paper. Then substituting

$$b = r + a$$

there is obtained, for the temperature at which any percentage of martensite is found.

A. E. Nehrenberg.*—As the authors have pointed out, isothermal transformation diagrams are of greater practical value when they include data on the martensite reaction. Many of the published diagrams do not contain this information, so Grange and Stewart have performed a real service in developing a method whereby the temperature range of martensite formation in a steel of a given chemical composition, and the proportion of martensite formed during cooling to a given temperature within this range, can be calculated.

The formula they have developed for calculating the M_S point of low-alloy steels is somewhat different from that of Payson and Savage, 12 who concluded that the following relationship exists between chemical composition and M_S temperature:

$$M_S(^{\circ}F) = 930 - 570C - 60Mn - 50Cr - 30Ni - 20Si - 20Mo$$

for Metals (1944) 33, 261-280.

^{*} Assistant Supervisor of Research, Crucible Steel Company of America, Harrison, N. J. ¹² P. Payson and C. H. Savage: Martensite Reactions in Alloy Steels. *Trans.* Amer. Soc.

The Grange-Stewart formula is based upon the data of Digges¹³ and Greninger,¹⁴ both of whom evaluated the effect of carbon on the M_S point of high-purity iron-carbon alloys. These investigators found that 1 per cent carbon lowers the M_S of these alloys 650° F.

Greninger¹⁴ also determined the effect of carbon on the M_S temperature of plain carbon steels containing low manganese and silicon and found that 1 per cent carbon in such steels lowers their M_S point 570°F. Payson and Savage used these data as a basis for their formula.

It has been quite definitely established that τ per cent Mn lowers the M_S temperature about 60° to 70°F. and that τ per cent Si does not lower it by more than 20°F. Consequently, Greninger's curve for plain carbon steels can be corrected to 0 per cent Mn and 0 per cent Si by using factors of 70 and 20, respectively. It makes no appreciable difference whether a factor of 60 or 70 for manganese and 0 or 20 for silicon is used. The corrected curve is shown in Fig. 19 along with Greninger's curves showing the effect of carbon on the M_S point of both high-purity iron-carbon alloys and on plain carbon steels containing low manganese and silicon.

The corrected curve has a slightly different slope from that of the plain carbon steels because the manganese content of the steels used by Greninger increased somewhat with increasing carbon content. Consequently, the effect of carbon alone in plain carbon steels is not as great as indicated by the uncorrected curve. The corrected curve indicates that τ per cent carbon lowers the M_S temperature of plain carbon steels containing o per cent Mn and o per cent Si 540°F. This curve extrapolates to a temperature of 930°F. at o per cent carbon.

It has been found that by reducing the factor for carbon from 570 to 540 in the original Payson-Savage formula, as is justified by the preceding discussion, closer agreement results between calculated and measured M_S points. Also, it has been found desirable to lower the

factor for chromium, because when the original data that Payson and Savage used for evaluating the effect of chromium is corrected for differences in carbon content the factor becomes 40, instead of 50 as originally reported. Klier and Troiano¹⁵ investigated the effect of chromium on the M_S point of iron-carbon-chromium alloys at four different levels of carbon content and concluded that 1 per cent Cr lowers the M_S point 40° F.

The revised Payson-Savage formula then becomes:

$$M_S(^{\circ}F) = 930 - 540C - 60Mn - 40Cr - 30Ni - 20Si - 20Mo$$

This factor for molybdenum is considerably less than that in the Grange-Stewart formula. These authors recognize that their factor is not necessarily accurate, but the discrepancy between the two formulas was thought to be great enough to warrant some additional investigation. Consequently, another individual determined the M_S points of the highmolybdenum steels used by Payson and Savage¹² in their investigation. He also found that 1 per cent Mo lowers the M_S about 20°F. Since Chiswick and Greninger¹⁶ concluded that molybdenum has no effect on M_S , the use of such a low factor for it cannot be very greatly in error.

In Table 5 a comparison is made between the M_S points calculated by using each of the three formulas mentioned above and the values determined by Grange and Stewart for the 14 steels used for this investigation. Additional data taken from other investigations are also included.

Consider first only the data taken from this paper. Best agreement with measured values was obtained by using the revised Payson-Savage formula for calculating M_S points. When this formula is used, calculated values for 11 of the 14 steels are no more than 10°F. off from the measured values, one is off by 15°F., one by 20°F. and one by 25°F. When the

¹³ T. G. Digges: Transformation of Austenite on Quenching High-purity Iron-Carbon Alloys. Trans. Amer. Soc. for Metals (1940) 28, 575-

<sup>607.

14</sup> A. B. Greninger: The Martensite Thermal Arrest in Iron-carbon Alloys and Plain Carbon Steels. *Trans.* Amer. Soc. for Metals (1942) 30, 1-26.

¹⁵ E. P. Klier and A. R. Troiano: Ar" in Chromium Steels. Trans. A.I.M.E. (1945) 162,

<sup>175-185.

18</sup> H. H. Chiswick and A. B. Greninger: Influence of Nickel, Molybdenum, Cobalt and Silicon on the Kinetics and Ar" Temperatures of the Austenite to Martensite Transformation in Steels. Trans. Amer. Soc. for Metals (1944) 32, 483-520.

Grange-Stewart formula is used, calculated values for 7 of the 14 steels are no more than 10°F. off from the measured values. 5 are off 15°F., one is off 20°F. but one is off 85°F. This

carbon and 3 per cent Cr are included in Table 5. When the M_S points are calculated using the revised Payson-Savage formula, they all agree very well with the measured values.

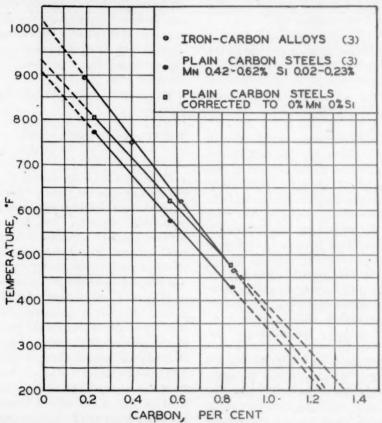


Fig. 19.—Effect of carbon on the M_S point of high-purity iron-carbon alloys and plain carbon steels. ¹⁴

I per cent carbon lowers the M_S point of high-purity iron-carbon alloys 650°F.; of plain carbon steels containing low manganese and silicon 570°F.; and of plain carbon steels corrected to 0 per cent Mn and 0 per cent Si. 540°F.

discrepancy occurred in the SAE-52100 steel austenitized at 1950°F. in order to dissolve all the carbides. Grange and Stewart limit the use of their formula to the range of carbon between 0.20 and 0.85 per cent, since only that range of carbon was considered in its development. It is interesting to note that when the revised Payson-Savage formula is used, the calculating result for SAE-52100 exactly agrees with the measured value.

Klier and Troiano¹⁶ have determined the M_S point for a number of iron-carbon-chromium alloys containing up to 1.3 per cent carbon. Their data for steels containing 1 per cent carbon with varying chromium up to 9 per cent, and for a steel containing 1.3 per cent

Evidently, then, a linear relation does exist between carbon content and M_S temperature in commercial alloys up to at least 1 per cent carbon. For the 1.3 per cent carbon, 3 per cent Cr alloy, there is an indication that there may be some departure from this linear relationship, although it is not very great. This departure may have been due to incomplete solution of the carbides.

Because of the rapidity of the bainite reaction in the low-carbon, low-alloy steels, it is not ordinarily possible to determine M_S points using the Greninger-Troiano¹⁷ technique, so

¹⁷ A. B. Greninger and A. R. Troiano: Kinetics of the Austenite to Martensite Transformation in Steel. *Trans.* Amer. Soc. for Metals (1940) 28, 537-574.

TABLE 5.—Comparison of Measured and Calculated Ms Points

	Austenia		A	Analysis, Per Cent	s, Per	Cent	-				Calcul	Calculated Ms Points, Deg. F.	Points,	D	Deviation of	
Steel	tizing Temper- ature, Deg. F.	O	MN	IS .	IN	CR	MO	>	Meas-	Source of Data	Grange- Stewart For- mula*	Payson- Savage For- mula ^b	Revised Payson- Savage For- mula	Grange- Stewart For- mula	Payson- Savage For- mula	Revised Payson- Savage For- mula
0.9 % Carbon SAE-1065	1625 2000 1550	0.89	0.20						420F 525 640	Grange-Stewart	400 530 640	405	430 535 625	+ 20	- 15 - 10 - 25	+10 +10 -15
SAE-2340	1550	0.38	000	00.21	3.41	0.0	000		580		625	570	585	1 1 1 1 2 2	130	+5
SAE-4140.	1550	0.37	0.77	0.15	1.79	0.08	0.33		550		535	540	560	1 1 1 1 1 2 2	1 25	+10
SAE-4640	1550	0.36	0.63	0.19	1.84	0.93	0.23		640		645	625	635	+15	-15	- 5
SAE-52100	1950	1.02	0.36	0.33	0.20	I.41		0.16			205	245	290	1 1	1 45	0 - 10
NE-8630	1500	0.30			0.61	0.52	0.17				675	650	665	+10	-40	0 0
I % silicon	1800	0.47	0.40	I.00 I.89	0.30	0.11			610	Payson-Savage 18 Crucible Steel Co.4	565	615	630	++	+5	+20
1%C-1%C	2190	I.04	0.34			2.80			310	Klier-Troiano16	110	265	305	-75	1 - 65	11
\$ \$ \$ \$ \$ \$ \$ \$ \$ \$ \$ \$ \$ \$ \$ \$ \$ \$ \$	2190 2190 2190	I.05 I.28	0.31	0.35		2 8 6 9			120 23 to 5 130		- 100 - 300 - 40	12004	100	- 220 - 315 - 170	1 1 1 1 1 1 1 1 1 1 1 1 1 1 1 1 1 1 1 1	1110
Steel 386	1600	0.17	1.21	0.27	0.13	0.05	0.04		720	Christenson-Nelson-	795	750	755	+75	+30	+35
Steel 384	1600	0.17	1.19	0.24	0. IO	0.05	0.03		750	Jackson	795	750	755	+45	0	+5

* Ms (°F.) = 1000 - 650 × %C - 70 × %Mn - 35 × %Ni - (70 × %Cr) - (50 × %Mo). * b Ms (°F.) = 900 - 570 × %C - 60 × %Mn - 30 × %Ni - 50 × %Cr - 20 × %Mo - 20 × * Ms (°F.) = 930 - 540 × %C - 60 × %Mn - 30 × %Ni - 40 × %Cr - 20 × %Mo - 20 × 4 Eastern Research Laboratory, Crucible Steel Company of America: Unpublished data.

there are few published data for steels containing less than about 0.30 per cent carbon that can be used for checking the revised formula for calculating M_S points. Christenson, Nelson and Jackson 18 have determined the Ms points of two similar steels containing 0.17 per cent carbon by employing a gas-quenching technique in a high-speed dilatometer. While their technique admittedly is not yet entirely perfected, it is interesting to note that the calculated Ms points for these steels obtained by using the revised formula agree reasonably well with their experimentally determined values. Here again there is a greater discrepancy when the Grange-Stewart formula is used, the deviation in this case being in the opposite direction from that in the high-carbon steels.

Data on two additional steels containing 1.0 and 1.0 Si are also included in Table 5. It is shown that the calculated M_S points agree reasonably well with the measured values when the revised formula, which contains a factor of 20 for silicon, is used. A discrepancy exists between the measured and calculated M_S points when the Grange-Stewart formula is used. If a factor of 20 for silicon is used in this formula also closer agreement with the experimental values results, and this would seem to justify the use of this factor.

As Grange and Stewart have stated, in practice the carbides are seldom completely dissolved in the higher carbon, low-alloy steels, and it may at first seem that it is irrelevant to demonstrate that one formula has a greater degree of accuracy than another for such materials. However, since it has been found that the revised Payson-Savage formula for calculating M_S points in low-alloy steels is more accurate over a range of carbon from about 0.2 to 1.3 per cent than any other formula yet proposed, it follows that it can be used with a greater degree of confidence over the more limited range of carbon of most commercial low-alloy steels.

The present authors have imposed certain limitations on their formula. It is not to be used for carbon contents outside the range 0.20 to 0.85 per cent, for chromium over 1.5 per cent or

for molybdenum over r per cent. No such limitations appear to be necessary when the revised Payson-Savage formula is used, the only requirement being that there shall be complete solution in the austenite of all the carbides present.

R. A. Grange and H. M. Stewart (authors' reply).—The anomalous effect of cobalt in raising M_S , reported by Dr. Hawkes, confirms the results of Zyuzin et al., it is interesting to note that the latter investigators found that aluminum also raised M_S , which suggests that possibly aluminum, like cobalt, may also increase the rates of transformation of austenite to ferrite and pearlite.

Dr. Zener and Dr. Skapski rationalize, from thermodynamic considerations, on the significance of the M_S temperature with respect to equilibrium conditions in iron-base alloys. We are pleased to have this additional evidence that chromium may lower M_S in a nonlinear manner.

Captain Hollomon has raised a question that had previously caused us some concern, and to which we do not know the answer. Our method of including data on martensite formation in the isothermal transformation diagram (Fig. 5) was designed to minimize such implications as that about which he inquires. The arrows on this diagram, as drawn, simply point to the temperature at which, under the conditions of our measurements, the indicated percentage of martensite was observed; just how well such data may apply to quenched steel in general is admittedly open to question. We have made a few measurements of martensite formation by the metallographic technique in which specimens comprised several thicknesses in the range 1/32 to 1/5 in., thus, in effect, varying the cooling rate when all were quenched alike; in these, no difference was observed in the proportion of martensite formed on quenching to a temperature about midway in the martensite-formation range. On the other hand, there are several statements in the literature to the effect that, in a particular steel and identical size of specimen, more austenite is retained after oil quenching (slower cooling) than after water quenching (faster cooling). As pointed out in the paper, thermal and transformation stresses,

¹⁸ A. L. Christenson, E. C. Nelson and C. E. Jackson: A High-speed Dilatometer and the Transformational Behavior of Six Steels in Cooling. *Trans.* A.I.M.E. (1945) 162, 606-626.

⁶ Unless otherwise indicated by a footnote, this and other such numbers refer to the list of references given in the paper.

which are relatively insignificant in small specimens, may play an important role in martensite formation when larger masses of steel are quenched, and thus account for

in a lead-alloy or salt bath that interference from bainite formation resulted.

Mr. Jaffe has contributed an ingenious and valuable analysis of our data, based on the

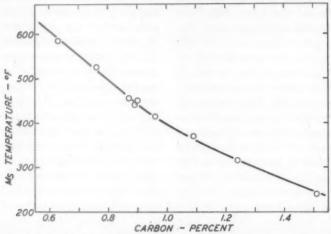


Fig. 20.—Influence of carbon on M_S temperature of a series of commercial carbon steels.

such seeming discrepancies in experimental observations.

With reference to Mr. Wilson's discussion, we did not intend to imply that it is impossible to measure Ms accurately by dilatometric methods, but rather that it is more difficult than by the metallographic technique; furthermore, the percentage of martensite formed at a temperature below Ms, which was an important consideration in our work, probably could not have been measured accurately with the dilatometer because a partly martensitic specimen is likely to be in such a strained condition that change in length is not a reliable measure of change in volume. Apparently, the dilatometric method used by Mr. Wilson is similar to that described in greater detail by Flinn, Cook and Fellows.19 We have had experience with this method, using a dilatometer similar to that illustrated by him except that ours comprised two concentric quartz tubes instead of two parallel rods. It was found that this method worked satisfactorily for high-carbon steels (although tedious and time consuming), but was not satisfactory for medium and low-carbon steels, for which so much time was required to establish thermal equilibrium after quenching

assumption that the temperature at which any given percentage of martensite forms on quenching is directly related to the M_S temperature. As demonstrated very nicely by Mr. Jaffe, our data indicate this to be true, but these data may not comprise a sufficient variety of compositions, particularly with respect to alloying elements, to generalize to this extent. Nevertheless, it will be most interesting to apply Mr. Jaffe's formula as more data become available.

Mr. Nehrenberg has made what appears to be a desirable revision of the empirical formula proposed by Payson and Savage; certainly, the revised formula applies to our data with greater accuracy than the original version.

In comparing empirical formulas for calculating M_S from chemical composition, there is little point in considering or trying to evaluate factors for other elements until that for carbon has been established, because carbon is at least nine times as effective in lowering M_S as any other single element. The discrepancy between the effect of carbon on Ms, as measured for pure iron-carbon alloys by both Greninger⁵ and Digges,8 and as measured for commercial carbon steels by Greninger,5 is consequently a matter of some concern; Nehrenberg, in Fig. 19 and discussion relating thereto, has emphasized this discrepancy. In developing our empirical formula, we chose to use the data for pure ironcarbon alloys, since it comprised measurements

¹⁹ R. A. Flinn, E. Cook and J. A. Fellows: A Quantitative Study of Austenite Transformation. *Trans.* Amer. Soc. for Metals (1943) 31, 41-66.

by independent investigators and, accordingly, would likely be the more reliable; Payson and Savage (and subsequently Nehrenberg) used the data for commercial carbon steels as a basis for their formulas. Much of the difference between their formulas and ours arises from this source, for not only the constant of the formulas and the carbon factor but also the factors for all other elements are affected. At present, there would seem to be no way of determining which of these two sets of data more accurately portrays the effect of carbon on $M_{\mathcal{S}}$ in steel in general; it is possible that the experimental measurements are equally accurate in either case, but indicate a slightly different effect of carbon because the carbon steels (but not the pure iron-carbon alloys) contained some minor element whose effect on Ms may account for the difference.

designed. In order that an empirical formula such as either of these may apply with accuracy to all steel compositions, two conditions must be met: (1) over the entire composition range there must be a linear relationship between Ms and the percentage by weight of each element, and (2) the effect of individual elements on Ms must likewise be additive. It would indeed be a fortuitous circumstance if condition I were universally true, since there is nothing fundamental about weight per cent, as there might be, for example, if this relationship were claimed for atomic per cent. Condition 2 seems to apply, at least approximately, but thus far only enough measurements of M_8 have been made to test its validity over a limited range of composition. On the other hand, there is evidence that condition I does not apply to carbon, the most important of the elements in

TABLE 6.—Composition and Ms Temperatures for a Series of Carbon Steels

		Composi	tion, Per	Cent			Measured	Manganese ^b Correction	Measured Ms Corrected to
С	Mn	P	S	Si	Ni	Cr	Ms °F.	(70 × % Mn), Deg. F.	o% Mn, Deg. F
0.63*	0.87	0.023	0.018	0.22	0.02	0.04	525	60	585
0.76	0.42	0.018	0.031	0.21			495	30	525
0.87	0.25	0.022	0.013	0.22	0.00	0.04	435	30	455
0.894	0.29			0.15		0.11	420	20	440
0.90	0.29	0.013	0.013	0.16		0.08	430	20	450
0.96	0.29	0.017	0.012	0.14	0.04	0.03	395	20	415
1.09	0.23	0.012	0.010	0.08	0.03	0.12	355	15	370
1.24	0.33	0.029	0.030	0.26	0.06	0.06	290	25	315
1.51	0.34	0.009	0.035	0.19			215 /	25	240

• Data taken from Table 3 of the paper. • To nearest 5°F.

In his comprehensive discussion, Nehrenberg cites data (Table 5) as evidence that the revised Payson and Savage formula affords greater accuracy than the formula presented in the paper; the latter, however, was specifically designed for a specified range in carbon, chromium and molybdenum, and if we exclude from Table 5 the steels that lie outside this range of composition our formula is fully as accurate as the revised Payson and Savage formula. We do not agree with Nehrenberg's contention that the greater accuracy of M_S for the high-carbon, high-chromium steels calculated by the revised Payson and Savage formula constitutes evidence that this formula must also be more accurate than ours when applied to steels of composition in the limited range for which our formula was specifically steel with respect to effect on M_S . Greningers found that in pure iron-carbon alloys the relationship between M_S and the percentage by weight of carbon was not linear for alloys containing more than about 0.85 per cent carbon; this was the principal reason for limiting application of our empirical formula to steel containing less than 0.85 per cent carbon.

Recently, we have measured $M_{\mathcal{S}}$ for a series of commercial steels, using the metallographic technique. Pertinent data are listed in Table 6 and the results, after correcting all steels in the series to 0 per cent manganese, are presented graphically in Fig. 20. These measurements indicate that Nehrenberg was not justified in extrapolating the straight lines in his Fig. 20 beyond about 0.9 per cent carbon, and consequently that the revised Payson and

Savage formula probably will not always apply with accuracy to steel containing more than this percentage of carbon. The fact that this formula applied so well to the steels in Nehrenberg's Table 5, which contained 1 to 1.3 per cent carbon, is possibly due to a compensating effect of incorrect factors for other elements.

With lower carbon, measurement of M_S becomes increasingly difficult; consequently, there are very few measured M_S temperatures for steels containing less than 0.2 per cent carbon. The effect of carbon in the range 0 to 0.2 per cent must therefore remain in question for the present; in view of the nonlinear effect of carbon in high-carbon steels, the line showing relationship of M_S to carbon content probably cannot be safely extrapolated to 0 per cent carbon. While the revised Payson and Savage formula applied with greater accuracy than ours to the two low-carbon steels in Nehrenberg's Table 6, the measurement of M_S in these cases is not claimed to be accurate. 20

for computing M_S is also a matter of some doubt at present, particularly the factor for chromium and for molybdenum. There is little to be gained by discussion of these factors on

other than carbon in the empirical formulas

The correct factors for each of the elements

the basis of the existing data; more measurements are needed.

For each steel whose Ms has been measured, either by ourselves or by others, we have compared Ms as computed by the revised Payson and Savage formula with that computed by the formula presented in the paper; for commercial carbon or low-alloy steels containing 0.3 to 0.85 per cent carbon, the agreement between computed and measured value is generally satisfactory; so much so, in fact, that one might logically question the measurement when a measured value disagrees with either formula by more than 25°F. Furthermore, despite considerable difference in the factors in the two empirical formulas, the agreement in computed Ms is surprisingly good. Consequently, we believe that either or both formulas can be used to good advantage. There is, however, reason to believe that when more data become available a new improved formula can be developed, but even if the factors in such a formula are precisely evaluated, some error must be expected because of segregation in most commercial steels. For reasons discussed, any single empirical formula based on a linear relationship between M_8 and percentage by weight of each element will necessarily be limited to a certain range of steel composition, we believe.

²⁰ Discussion of ref. 18. Trans. A.I.M.E. (1945) 162, 622-626.

Hardenability Effects in Relation to the Percentage of Martensite

By J. M. Hodge, * Member A.I.M.E. and M. A. Orehoskit (Chicago Meeting, February 1946)

THE relationship between hardenability based on a 50 per cent martensite criterion, and that based on higher percentages of martensite in a number of low-alloy steels was discussed in a previous paper by the authors.1 It was found that the differences between the hardenability values based on the 50 per cent martensite and full martensite criterions increased as the hardenability increased and that, in the steels of higher hardenability, these differ-

1 References are at the end of the paper.

TABLE 1.—Chemical Analysis of Specimens

Heat No.	Specimen			C	omposition	, Per Cen	t		
neat No.	No.	С	Mn	P	S	Si	Ni	Cr	Мо
			M	anganese S	eries				
920	E196	0.40	0.22	0.006	0.033	0.21	0.04	1.03	0.0
017	E107	0.40	0.35	0.008	0.032	0.21	0.04	1.03	0.0
917 876	E65	0.39	0.65	0.011	0.030	0.24	0.03	0.98	0.0
928	E198	0.42	0.81	0.015	0.027	0.23	0.02	0.98	0.0
929	E199	0.43	1.02	0.018	0.028	0.19	0.03	1.00	0.0
924	E200	0.42	1.32	0.018	0.031	0.25	0.02	1.01	0.0
925	E201	0.42	1.57	0.018	0.028	0.25	0.02	1.03	0.0
			5	Silicon Serie	es				
959	E810	0.37	0.58	0.007	0.030	0.06	0.02	1.01	0.0
950	E804	0.41	0.65	0.016	0.030	0.12	0.01	1.01	0.0
876	E65	0.39	0.65	0.011	0.030	0.24	0.03	0.98	0.0
952	E805	0.40	0.65	0.017	0.026	0.41	0.03	0.99	0.0
		1		Nickel Ser	ies	+			
938	E308	0.39	0.65	0.017	0.028	0.21	0.03	0.04	0.1
939	E309	0.40	0.62	0.016	0.027	0.24	0.54	0.02	0.1
940	E310	0.38	0.59	0.017	0.029	0.17	1.03	0.04	0.1
941	E311	0.41	0.62	0.016	0.028	0.21	2.04	0.04	0.1
942	E312	0.40	0.65	0.016	0.027	0.22	3.01	0.04	0.1
932	E302	0.39	0.62	0.016	Q.027	0.22	3.99	0.03	0.1
			Mo	olybdenum	Series				
901	E50	0.40	0.57	0.016	0.026	0.19	3.49	0.05	0.0
902	E51	0.41	0.60	0.016	0.027	0.22	3.51	0.04	0.2
903	E52	0.42	0.64	0.015	0.027	0.22	3.50	0.04	0.5
904	E53	0.39	0.56	0.015	0.029	0.20	3.53	0.03	0.7
				Carbon Ser	ries				
887	E81	0.09	0.60	0.014	0.034	0.21	3.46	0.03	0.2
906	E82	0.22	0.61	0.018	0.025	0.21	3.45	0.04	0.2
907	E83	0.33	0.67	0.015	0.025	0.23	3.49	0.04	0.2
902	E51 E85	0.41	0.60	0.016	0.027	0.22	3.51	0.04	0.2
909	E85	0.51	0.60	0.016	0.028	0.21	3.47	0.05	0.2

Manuscript received at the office of the Institute Dec. 1, 1945. Issued as T.P. 1994 in METALS TECHNOLOGY, April 1946.

* Development Engineer, Steel Heat Treatment, Carnegie Illinois Steel Corporation, Pittsburgh, Pennsylvania.

† Metallurgist, Duquesne Works, Carnegie-Illinois Steel Corporation, Pennsylvania.

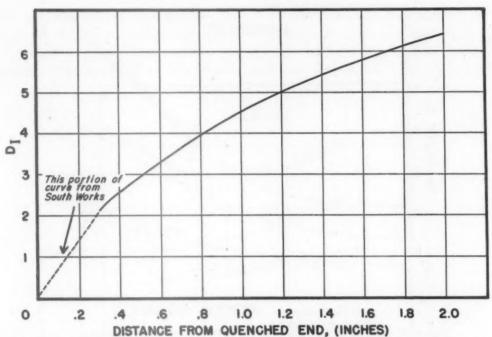


Fig. 1.—Revised curve for conversion of Jominy distance to ideal diameter.

TABLE 2.—Distances from Quenched End and Corresponding DI Values

Specimen No.	Percentage of	99.9 Pe Marte		95 Per Marter		50 Per Marte	
Specimen No.	Alloy	Distance	D_I	Distance	D_I	Distance	D_{I}
E106	0.22 Mn	0.110	0.80	0.200	1.45	0.325	2.25
E197	0.35 Mn	0.13	0.95	0.215	1.55	0.330	2.30
E65	0.65 Mn	0.135	1.00	0.250	1.80	0.410	2.60
E198	0.81 Mn	0.145	1.05	0.280	2.00	0.485	2.95
E199	1.02 Mn	0.190	1.40	0.440	2.75	0.9	4.25
E200	1.32 Mn	0.23	1.65	0.630	3.45	1.53	5.70
E201	1.57 Mn	0.255	1.85	0.780	3.95	1.95	6.45
E810	0.06 Si	0.115	0.85	0.180	1.3	0.285	2.05
E804	0.12 Si	0.12	0.90	0.18	1.3	0.300	2.15
E65	0.24 Si	0.135	1.00	0.250	1.7	0.410	2.60
E805	0.41 Si	0.150	1.10	0.260	1.90	0.490	2.95
E308	0.03 Ni	0.080	0.60	0.145	1.05	0.210	1.50
E309	0.54 Ni	0.085	0.65	0.170	1.25	0.245	I.75
E310	1.03 Ni	0.085	0.65	0.155	1.15	0.230	1.65
E311	2.04 Ni	0.115	0.85	0.240	1.70	0.360	2.40
E312	3.01 Ni	0.155	1.15	0.340	2.35	0.650	3.50
E51	3.50 Ni	0.185	1.35	0.570	3.25	1.09	4.75
E302	3.99 Ni	0.220	1.60	0.62	3.40	1.60	5.8
E50	0.01 Mo 0.21 Mo	0.100	0.75	0.570	1.6	0.390	2.55
E51	0.50 Mo	0.600	3.35	0.570	3.25	1.09	4.75
E52 E53	0.74 Mo	1.165	4.95	-			
E81	0.09 C	1,103	4.93	0.125	0.90	0.25	1.70
E82	0.22 C	0.135	1.00	0.275	2.00	0.49	2.95
E83	0.33 C	0.155	1.15	0.400	2.60	0.815	4.0
E51	0.41 C	0.185	1.35	0.570	3.25	1.00	4.7
E85	0.51 C	0.280	2.00	0,700	3.70	1.46	5.5

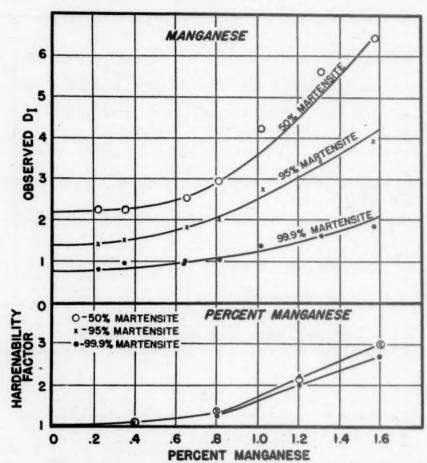


Fig. 2.—Hardenability values and factors for the manganese series.

TABLE 3 .- Average Values for Base Carbon Hardenability and Alloy Factors

				Consti	tuents			
Percentage of Alloy	Mn	Si	Ni	Mo	С		Martensite	
		0.		-		99.9 %	95 %	50 %
0.1	1.02	1.05		1.5	0.1	0.05	0.135	0.23
0.2	1.05	1.15		1.95	0.12	0.06	0.15	0.26
0.3	1.08	1.25		2.8	0.14	0.07	0.17	0.20
0.4	1.1	1.5		3.8	0.16	0.085	0.19	0.31
0.5	1.13		1.05	4.8	0.18	0.095	0.21	0.33
0.6	1.15				0.20	0.105	0.23	0.36
0.7	1.22				0.22	0.115	0.25	0.39
0.8	1.3		1.1		0.24	0.13	0.27	0.42
0.9	1.5				0.26	0.14	0.29	0.44
1.0	1.7		1.15		0.28	0.15	0.31	0.47
1.1	1.92			i	0.30	0.16	0.325	0.49
1.2	2.15				0.32	0.17	0.34	0.51
1.3	2.35		1.2		0.34	0.175	0.36	0.53
1.4	2.6		* 25		0.36	0.185	0.38	0.56
2.00	4.0		1.35		0.40	0.19	0.40	0.58
2.5			1.85		0.42	0.21	0.42	0.63
3.0			2.25		0.44	0.215	0.455	0.65
3.5			2.0		0.46	0.22	0.433	0.68
4.0			3.85		0.48	0.23	0.49	0.71
1			0.00		0.50	0.24	0.50	0.73

ences were fairly large. Furthermore, it was found that these relationships could be expressed with reasonable accuracy as a function of the hardenability. The impor-

EXPERIMENTAL PROCEDURE

Induction-furnace heats weighing 17-lb., of the compositions given in Table 1, were cast and forged into 114-in. round

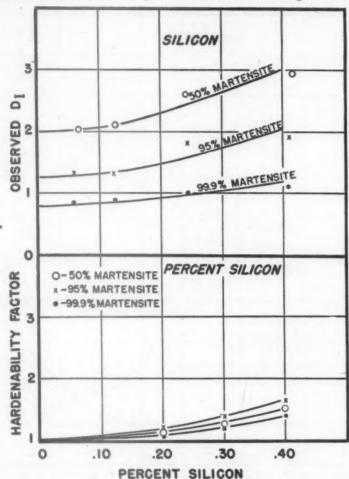


FIG. 3.—HARDENABILITY VALUES AND FACTORS FOR THE SILICON SERIES.

tance of the full martensite criterion of hardenability in relation to the attainment of the optimum mechanical properties of tempered martensite was emphasized in the earlier paper.

The purpose of the present work is to study the effects of some of the individual alloying elements on hardenability, using three different percentages of martensite as criteria, and thereby to evaluate the role of these individual elements in the general hardenability relationships previously reported.

bars. All heats were killed with aluminum additions corresponding to I lb. per ton. The compositions were chosen to represent several series of steels, in which only one alloying element would vary and in which the nonmartensitic constituents on quenching would be predominantly bainitic.

All bars were normalized from 1650°F. and tempered one hour at 1150°F. prior to the hardenability determinations.

Hardenability values are based on metallographic examination of standard Jominy bars, quenched from 1600°F. (1 hr.

and 20 min. heating time). The general procedure was the same as outlined in detail in the previous paper; (1) that is, the distance from the quenched end of the

ideal diameter is based on a revised correlation curve (Fig. 1). This curve is based on work carried out at the Research Department of the South Chicago

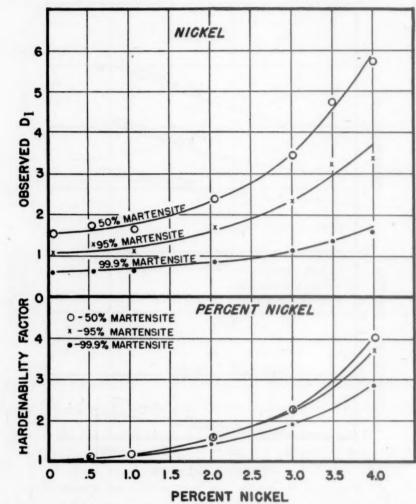


FIG. 4.—HARDENABILITY VALUES AND FACTORS FOR THE NICKEL SERIES.

bar to the point of 0.1 per cent transformation was first measured on the microscope and then the percentage of martensite was estimated at every 0.05 in. from the quenched end, and these percentage values plotted against the distance along the bar. In this case, samples 2 in. long were cut from the quenched end of the Jominy bars and 10 fields were examined and averaged at each distance.

The conversion of Jominy distance to

Works, Carnegie-Illinois Steel Corporation, and represents a direct correlation between hardenability values as determined on cylinder series and end-quench tests from the same material. At a distance beyond 0.3 in. from the quenched end, the conversion is the same as previously published but D_I values corresponding to distances closer to the quenched end were found to be lower than the previously published curve would indicate.

EXPERIMENTAL RESULTS

The Jominy distances and the corresponding hardenability values for the steels studied, on the basis of 99.9, 95 and

were observed in the martensitic portion near the quenched ends of most of the samples. The grain size was 8 to 9 for all samples.

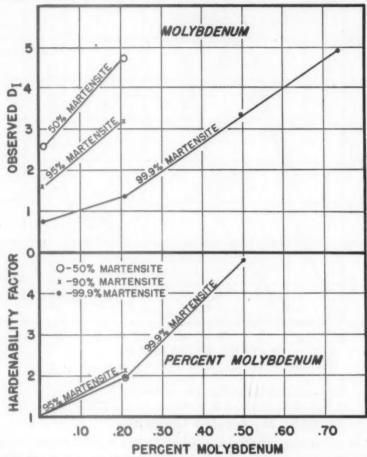


FIG. 5.—HARDENABILITY VALUES AND FACTORS FOR THE MOLYBDENUM SERIES.

50 per cent martensite, are tabulated in Table 2. These values are shown plotted against alloy or carbon content in the upper portions of Figs. 2, 3, 4, 5 and 7.

MICROSTRUCTURES

The nonmartensitic constituent was bainitic in every case at the 99.9 and 95 per cent martensite points. However, in some of the steels of lower alloy content, small amounts of pearlite were noted in the 50 per cent martensite structures.

Small amounts of undissolved carbides

DISCUSSION OF RESULTS

The hardenability factors for Mn, Si, Ni and Mo are plotted in the lower parts of Figs. 2, 3, 4 and 5. These were derived by extrapolating the hardenability curves to zero alloy and dividing the hardenability values by the intercept value.

The curves for the hardenability factor, which express the manner in which hardenability changes with alloy content, are all very nearly coincidental for the 50 and 95 per cent martensite criteria, while there is some tendency for the curves for 99.9

per cent martensite to indicate somewhat lower hardenability effects. It is felt that this latter observation is largely a reflection of the fact that the 99.9 per cent

plotted in Fig. 6, and these average values have been listed in Table 3.

It should be noted that, since undissolved carbides were present in these steels as

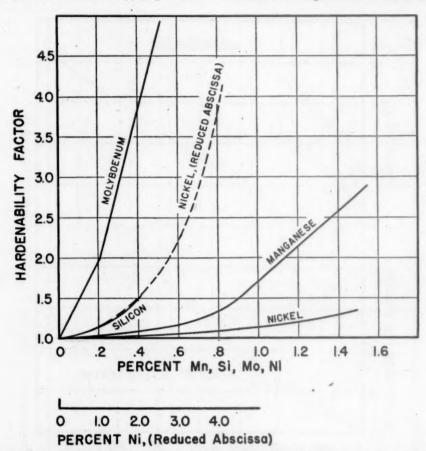


FIG. 6.—AVERAGE HARDENABILITY FACTORS FOR MANGANESE, SILICON, NICKEL AND MOYLBDENUM.

martensite values represent the lowest hardenability point on the sample examined, and not average values, as do the 95 and 50 per cent martensite points. Therefore, this deviation of the 99.9 per cent martensite values may well represent only the increased microsegregation associated with the higher alloy contents. However, even this discrepancy is not large and the results indicate strongly that the hardenability effects of these alloying elements are the same whether the criterion is 50 per cent martensite or higher percentages of martensite. Therefore, average lines representing these effects have been

quenched, the curves for the hardenability factor presented here do not represent the full hardenability effects of these alloys. They will, however, represent the effects associated with commercial austenitization of similar steels at 1600°F.

If we accept the multiplying factor hypothesis of Grossmann, this means that the relationship between the hardenability values on the basis of the different criteria in respect to the percentage of martensite becomes a function of the base hardenability of the pure iron-carbon alloys in terms of these criteria. Such hardenability values for iron-carbon alloys on the basis

of 50, 95 and 99.9 per cent martensite are shown plotted in the lower part of Fig. 7. These were derived by dividing the actual These carbon values are also tabulated in Table 3. It might be noted that these carbon values on the 50 per cent martensite

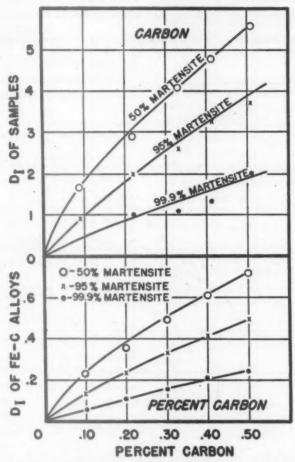


Fig. 7.—Hardenability values for the carbon series and derived values for iron-carbon alloys.

hardenability values by the product of the average factors for Mn, Si, Ni and Mo for the base composition as follows:

BASE COMPOSITION Ms Si Ni Me PRODUCT 0.60 0.20 3.50 20

Factor... 1.15 1.15 2.9 1.95 7.5

These curves, therefore, represent the hardenability of iron-carbon alloys, for the grain size of 8 to 9, which was characteristic of the steels studied, on the basis of essentially full martensite, 95 per cent martensite and 50 per cent martensite.

basis are very similar to those recently reported by Kramer, Siegel and Brooks.³

This hypothesis, that the hardenability effects of the alloys may be represented by a single factor curve for 50, 95 or 99.9 per cent martensite, can be further checked and illustrated by a comparison of the measured hardenability values of the steels in this paper with values calculated by multiplying the base carbon values by the alloy factors.

However, in order to do this for the steels studied, it will be necessary to evaluate the hardenability effect of I per cent chromium. This can be done by dividing the hardenability of steel E65 by the product of the factors for carbon, manganese and silicon. This indicates a factor of 3.1 for 1 per cent chromium in these steels.

assumption may be applied to chromium as well as to the other elements studied.

However, it should be pointed out that, since these calculations have been applied only to the steels that have been used to

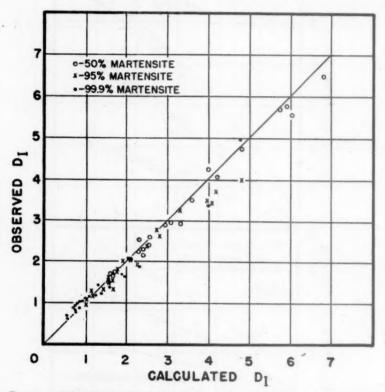


FIG. 8.—CORRELATION BETWEEN CALCULATED AND OBSERVED HARDENABILITY VALUES.

The comparison of these calculated and actual hardenability values is shown in Fig. 8. The correlation is in general very good. The maximum deviation is less than 10 per cent, and this occurs in the steels of the highest alloy content, in which it is probable that carbide solution was less complete and in which segregation would be most pronounced.

This correlation indicates that no significant error will be introduced by the assumption of identical hardenability effects, regardless of whether the criterion is full martensite or 50 per cent martensite. Furthermore, since a single value for chromium was used in these calculations, it furnishes a strong indication that this

develop the factors, this correlation does not necessarily imply that these factors themselves are correct for other alloy combinations.

SUMMARY

The effects of manganese, silicon, nickel and molybdenum on hardenability, in terms of 99.9, 95 and 50 per cent martensite, have been studied by means of metallographic examination of end-quench tests from several series of steels with only one alloy variable. It has been found that the hardenability effects of the alloying elements are essentially the same on the basis of the three criteria studied, 99.9, 95 and 50 per cent martensite.

A set of curves depicting the hardenabilities of iron-carbon alloys on the basis of the 99.9, 95 and 50 per cent martensite criteria has been derived from a study of a series of nickel-molybdenum steels in which carbon was the only variable.

It is proposed that the relationship between full martensite hardenability and 50 per cent martensite hardenability is a function only of the base hardenability of the iron-carbon alloy.

REFERENCES

 J. M. Hodge and M. A. Orehoski: Relationship between Hardenability and Percentage of Martensite in some Low-alloy Steels. This volume, page 627.

 Asimow, Craig and Grossmann: Correlation between Jominy Test and Quenched Round Bars. Jnl. Soc. Auto. Engrs. (1941)

 (1941).
 I. R. Kramer, S. Siegel and J. Brooks: Factors for the Calculation of Hardenability. This volume, page 670.

DISCUSSION

(Walter Crafts presiding)

M. A. GROSSMANN.*—One of the great services rendered by this paper is the demonstration that the hardenability factors for full hardening are substantially the same as those for half hardening employed hitherto. In view of the nature of their findings, would the authors agree that probably this will hold for other alloying elements as well, in addition to those actually investigated here?

These findings emphasize the importance of their data on the base hardenability due to carbon alone, at different percentages of martensite (different extents of hardening), as given in their Table 3. Incidentally, it should not be overlooked that they show higher values for the carbon effect, and correspondingly lower for the manganese effect, than those that have been in use for some time, although the product carbon times manganese is about the same as the product in use up to now. (As they state, these new data are of an order of magnitude similar to recent data of Kramer, Siegel and Brooks.) Would the authors agree that a word of caution is in order here; namely, that their

new high values for carbon must not be used in connection with the former high values for manganese? Such a step would be misleading, the proper procedure being the use of their new factors throughout.

Would the authors care to comment on the fact that their molybdenum factors are somewhat higher than commonly reported?

J. A. Hodge and M. A. Orehoski (authors' reply).—In reply to Dr. Grossmann's discussion, we feel that the assumption we have made on the basis of our findings, that the effects of the alloying elements on hardenability are essentially independent of the percentage of martensite used as a criterion, is indeed a generalization, and that it will apply to other alloying elements as well as those studied. In this connection, we might mention that further studies on a series of steels containing chromium in which molybdenum was varied have likewise indicated essential coincidence among the hardenability factors based on these three criteria.

We have no particular comment on the fact that the molybdenum factors seem high except to mention that they correspond roughly to the probable maximum factor mentioned in the paper by Kramer, Siegel and Brooks.

As Dr. Grossmann points out, it is of course extremely important that these higher carbon values be used only with the corresponding alloy factors, and this will apply particularly to the manganese factors, which are much lower than those previously reported.

W. R. TAYLOR.*—In considering hardenability as a function of the percentage of martensite, no satisfactory method other than microexamination is normally available to the metallurgist. Direct hardness values such as those obtained by Rockwell or Vickers tests are not always true criteria that a desired percentage of martensite has been obtained in the hardening cycle. In applications where a maximum percentage of martensite is required, it should be brought forth that the metallurgist should depend on microinspection rather than on hardness tests for evaluation of the degree of martensitic transformation that has occurred in hardening.

^{*} Director of Research, Carnegie-Illinois Steel Corporation, Chicago, Illinois.

^{*} Armour Research Foundation, Chicago, Illinois.

I. R. KRAMER. *- Messrs. Hodge and Orehoski have brought forth some very interesting information on the effect of alloying elements on the hardenability of steel. They have pointed out that the hardenability factor curve for carbon is very similar to that obtained by Kramer, Siegel, and Brooks, for steels in which pearlite tends to limit the hardenability. The similarity in the factor curves does not stop there, for it may be noted that the manganese curves are also very similar. In fact, when the hardenability of the steels presented here are calculated with the factors we had derived, agreement within ±15 per cent is obtained between the observed and calculated values. From this it appears, for the purpose of calculating the hardenability, that it makes little difference whether pearlite or bainite tends to limit the hardenability.

J. M. Honge (author's reply).—In reply to Mr. Taylor, we feel very strongly that hardenability criteria should be in terms of a specific microstructure and that hardness criteria, if they have any advantages, have only the advantage of convenience.

In reply to Mr. Kramer, I might say that these results as presented are in a way a byproduct of what we started to study. We began to study hardenability effects in steels in which the nonmartensitic products would be predominantly bainitic, and thereby to evaluate the hardenability effects of the alloying elements in such steels. The findings we have reported in regard to the relative effects of the elements in relation to the hardenability criterion used seemed important enough to report

The uncertainties involved in measuring hardenability leave a great deal of the work on the hardenability factor that has been done to date, including that reported in this paper, decidedly open to question. The published work includes hardenability values based on 50 per cent martensite measured metallographically, measured by a critical hardness value, or measured by an inflection point, and the correlation between these methods is far from precise and certainly leaves many of the evaluations open to question. Furthermore, if a cylinder series method is used for this evaluation, the results are completely dependent upon an accurate evaluation of the H-value of the quench, which may be very difficult; or, if end-quench methods are used, the evaluation is dependent upon the correlation between end-quench distance and ideal diameter, which has not been definitely and accurately established, although we feel that the correlation curve we have used in this paper is closer to the truth than the previously published correlation. Therefore, in general, I feel very strongly that a great deal more work must be carried out before we can say with any confidence that hardenability-factor values are accurate and actually represent quantitatively the effects of the elements of hardenability.

as a paper, but we are finding indications, as Mr. Kramer points out, that, as far as the experimental evidence goes, the differences between the hardenability effects of the elements in these cases in which the nonmartensitic products are bainitic and those reported by other experimenters in which the nonmartensitic products would be expected to be pearlitic are not nearly as large as might be predicted from isothermal transformation studies.

^{*} Metallurgist, Office of Research and Inventions, Washington, D. C.

Equilibrium Relations in Medium-alloy Steels*

BY CLARENCE ZENER, † JUNIOR MEMBER A.I.M.E. (New York Meeting, October 1945)

THE heat-treatment of steels will not pass from the stage of an art into that of a science until the mechanism of the phase transformations associated therewith is thoroughly understood. Such an understanding will involve two distinct types of inquiry: (1) the direction of the transformation, (2) the speed of the transformation. The first type of inquiry, which involves only the equilibrium relations between the various phases in steel, is the subject of the present and of a succeeding article; the second type, which involves the kinetics of transformations, will be the subject of a later article.

In order that a theory of equilibrium relations may give useful information, certain experimental data must be put into the theory. It is customary for these data to be of a thermal nature. In the system discussed herein-steel-such thermal data are very scarce. In medium-alloy steels another type of data might possibly be used. In these steels the concentration of solute is so low that it may be possible to use the approximation of dilute solutions, an approximation that leads to linear relationships. The unknown functions, or constants, may then be determined in some cases from the binary ironalloy system and in other cases from the ternary iron-carbon-alloy system. From the functions, or constants, so determined may then be computed the equilibrium relations in more complex medium-alloy steels. In the present article this second approach is used, the necessary experimental data being obtained from the simple binary and ternary equilibrium diagrams.

FUNDAMENTAL EQUATIONS

In this article are derived the equilibrium relations between the gamma, alpha and cementite phases. In these three phases all important alloying elements except carbon form substitutional solutions, each alloying atom occupying a potential site for an iron atom. Carbon, on the other hand, forms an interstitial solution. In the face-centered cubic gamma phase, the interstitial positions are at the center of the unit cube and at the centers of the cube edges. There are therefore four interstitial positions per unit cell, or one per iron atom. In the bodycentered cubic alpha phase, the interstitial positions are probably at the face centers, and also at the centers of the edges, which are crystallographically equivalent to the face centers. There are therefore six interstitial positions per unit cube, or three per iron atom. In cementite, (Fe, Alloy) 2C, the carbon atoms may be regarded as filling all the lattice positions of a given type.

The introduction of the fundamental equations of equilibrium has presented the author with a quandary. These equations are formally so similar to other equations that have been derived1,2 for related systems that they may appear to some readers

^{*} The statements or opinions expressed in this article are to be considered those of the author, and do not necessarily express those Ordnance Department. Manuscript of the Ordnance Department. Manuscript received at the office of the Institute Nov. 24, 1944. Listed for New York Meeting, February 1945, which was canceled. Issued as T.P. 1856 in Metals Technology, January 1946.
† Senior Physicist, Watertown Arsenal, Watertown, Mass. (On leave, Professor of Physics, Washington State College.)

¹ References are at the end of the paper.

to require no proof. In deference to such readers, the equations are introduced in the text without proof. On the other hand, since the equilibrium equations have not

iron and substitutional alloys. It is equal to 3 for alloying elements occupying interstitial positions, such as carbon. The quantity ΔG_i is associated with the transfer of

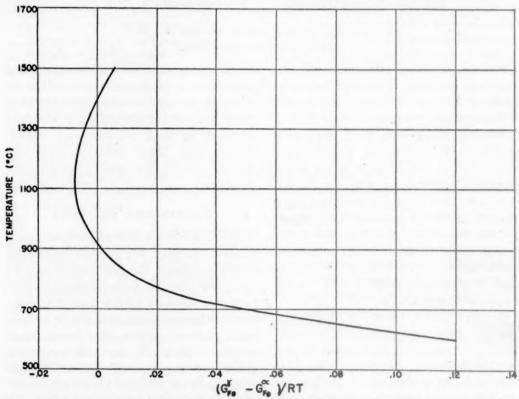


FIG. 1.—CHANGE IN FREE ENERGY ASSOCIATED WITH ISOTHERMAL TRANSFER OF ONE MOL OF IRON FROM ALPHA TO GAMMA PHASE—COMPLETE TEMPERATURE RANGE.

previously been deduced for this system, their derivation is presented in an appendix.

Alpha-gamma Equilibrium

The following equations describe completely the equilibrium relations between the alpha and gamma phases in mediumalloy steels when the concentration of alloys is sufficiently small to permit the assumption of a dilute solution:

$$(C_i^{\alpha}/C_i^{\gamma}) = \beta_i e^{\Delta G i/RT}$$

$$j = 1, 2 \cdot \cdot \cdot \qquad [1]$$

In these equations subscripts refer to a particular constituent. C_i refers to mol fractions. The weight factor β_i is unity for atoms occupying lattice sites; i.e., for

one mol of the indicated element from the alpha to the gamma phase, but has a quite different significance for the solvent iron than for the solute elements. For iron, this quantity refers to the change in free energy accompanying the transfer of one mol of iron from the alpha to the gamma phase in the absence of all alloying elements. This change in free energy is computed from thermal data in appendix A, and is given in Table A-1 of that appendix. For the alloying elements, the quantity ΔG_i , when independent of temperature, represents the heat absorbed when one mol of the indicated element is transferred from the alpha to the gamma phase. In the general case, where ΔG_i varies with temperature,

it can be assigned no simple physical interpretation. Such an interpretation, however, would not add to the usefulness of the equilibrium equations.

Alpha and Gamma-cementite Equilibria

In the system at present under consideration two different types of phase are in equilibrium. In both, the iron and substitutional alloy atoms are randomly distributed on the iron lattice positions. The carbon atoms, however, are distributed at random in interstitial positions in one phase (alpha or gamma), while they occupy fixed positions in the other phase (cementite).

The fundamental equations of the system under consideration are

$$\beta(C_i)^3/C_c(C_i)^3 = e^{\Delta G_i \circ / RT}$$

$$j = 1, 2 \cdot \cdot \cdot$$
[2]

Here j refers to iron or to a substitutional alloying element. C indicates mol fractions of the indicated elements in the alpha or gamma phase. C' represents the mol fractions in the cementite computed without considering the carbon. Thus if half the iron of cementite has been replaced by chromium, $C_{cr}' = \frac{1}{2}$. The weight factor β is unity in the gamma-cementite system, 3 in the alpha-cementite system. The derivative of $(\Delta G_i^c/T)$ with respect to I/Tgives the heat absorbed when one mol of the complex (3 atoms of type j, 1 carbon atom) is transferred from cementite to the second phase. Therefore ΔG_i^{\bullet} , when independent of temperature, represents a heat of solution.

ALPHA-GAMMA EQUILIBRIUM

In the analysis of the equilibrium relations between the alpha and gamma phases, it is convenient to rewrite in another form the equation in the set Eq. 1 that corresponds to iron. In medium-alloy steels both $C_{F_0}{}^{\alpha}$ and $C_{F_0}{}^{\beta}$ are very nearly unity. One is justified therefore in neglecting the squares of $(\mathbf{I} - C_{F_0}{}^{\alpha})$ and of $(\mathbf{I} - C_{F_0}{}^{\beta})$

compared with unity. The use of this approximation gives

$$\ln \left(C_{\text{Fe}}^{\alpha} / C_{\text{Fe}}^{\gamma} \right) = \sum_{i}' \left(C_{i}^{\gamma} - C_{i}^{\alpha} \right)$$

where the primed summation sign denotes a summation over all elements except iron.

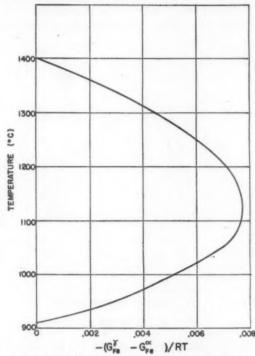


FIG. 2.—CHANGE IN FREE ENERGY ASSOCIATED WITH ISOTHERMAL TRANSFER OF ONE MOL OF IRON FROM ALPHA TO GAMMA PHASE—TEMPERATURE INTERVAL BETWEEN CRITICAL TEMPERATURES.

Taking the logarithm of Eq. 1 with j = Fe, gives

$$\Sigma_i'(C_i^{\gamma} - C_i^{\alpha}) = \Delta G_{F_0}/RT$$
 [3]

The right member of this equation is evaluated in Appendix A and is plotted as Figs. 1 and 2.

Binary Systems

In the binary iron-alloy system, Eqs. 1 and 3 give two equations for the two unknown concentrations of the alloying element in the alpha and gamma phase, $C_A{}^{\alpha}$ and $C_A{}^{\beta}$, respectively. These equations are

$$C_{\mathbf{A}}^{\gamma} - C_{\mathbf{A}}^{\alpha} = \Delta G_{\mathbf{F}_{\mathbf{0}}}/RT$$
 [4]

and

$$C_{\mathbf{A}^{\alpha}}/C_{\mathbf{A}^{\gamma}} = e^{\Delta g_{\mathbf{A}}/RT}$$
 (substitutional alloys)
[5]
$$C_{\mathbf{A}^{\alpha}}/C_{\mathbf{A}^{\gamma}} = 3e^{\Delta g_{\mathbf{A}}/RT}$$
 (interstitial alloys—carbon) [6]

Fig. 1 shows that ΔG_{F_0} is positive only below the lower transformation temper-

iron-alloy phases. In all of the binary alloy systems of iron with Ti, Sn, P, V, W, Mo, Al, Si and Cr except the last the general form of the gamma phase boundary is as shown in illustration a of Fig. 3. The anomalous shape of the closed gamma phase in the iron-chromium system indicates that in this system the assumption of a dilute solu-

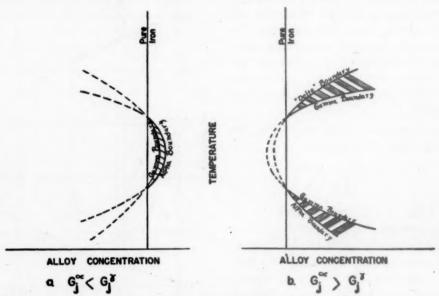


Fig. 3.—Schematic solution of equations 4 and 5 for binary iron-alloy systems. Two-Phase regions are shaded.

ature 910°C. and above the upper transformation temperature 1400°C. Eqs. 4 and 5 show that the mol fractions C_A^{α} and C_A^{γ} are positive in these temperature regions only if ΔG_A is negative. Conversely, these equations show that these mol fractions are positive in the temperature interval 910° to 1400°C. only when ΔG_A is positive. This effect of the sign of ΔG_A in determining the type of equilibrium diagram is illustrated in Fig. 3, in which are presented schematic solutions of Eqs. 4 and 5. The case of a positive ΔG_A , shown as illustration a of this figure, corresponds to a closed gamma phase. The case of a negative ΔG_A , shown as illustration b, corresponds to an open gamma phase.

Closed Gamma Phase.—Many examples of closed gamma phases occur in binary

tion is invalid beyond several per cent of chromium.

From Fig. 2 it may be seen that the maximum extent of the gamma phase is in the vicinity of 1150°C. From the value of this maximum extent, the value of ΔG_A may be computed at 1150°C. from Eqs. 4 and 5. Thus from these equations can be obtained

$$C_{\mathbf{A}^{\alpha}} = \frac{-\Delta G_{Fe}/RT}{1 - \beta^{-1} e^{-\Delta G_{\mathbf{A}}/RT}}$$
 [7]

with

$$\beta = \begin{cases} 1, \text{ substitutional alloys} \\ 3, \text{ interstitial alloys} \end{cases}$$

an equation that relates the values of C_{A}^{α} and of ΔG_{A} at any one temperature. This relation is given in Fig. 4 for 1150°C. The values of ΔG_{A} obtained from the observed

values of C_A^{α} at 1150°C. and from this figure are given in Table 1.

In only a few cases are the experimental data sufficiently complete to allow a detailed comparison with the theoretical equations 4 and 5. Examples are given in Figs. 5 and 6. In drawing the theoretical curves ΔG_A was taken to be independent of temperature.

Open Gamma Phase.—The best known

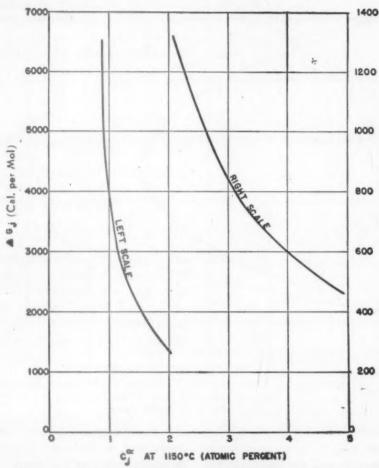


Fig. 4.—Method of computing ΔG from observed gamma loop.

Table 1.—Values of ∆G_A for Elements That Give a Closed Gamma Phase

Alloy	Ti	Sn	P	v	W
C _A ^α at 1150°C. (at. per cent) ΔG _A (cal per mol)	0.80 ³ 9,000	0.90 ⁴ 5,500	1.0 ⁵ 4,180	1.2 ⁴ 2,830	2.0 ⁶ 1,360
Alloy	,	Мо	A1	Ве	Si
Cam at 1150°C. (at cent)		2.0 ⁷ 1,360	2.1 ⁶ 1,300	3.1 ⁶ 810	4.9 ⁸ 475

example of the open gamma phase is that in the iron-carbon system. Other examples are the binary alloys of iron with Cu, Zn, Mn, Ni and N. The general form of the relationship between the alpha and gamma phases in typical open gamma-phase systems is represented as illustration b of Fig. 3. The alpha phase is separated by the gamma phase into a low-temperature and a high-temperature region. The upper temperature region is frequently referred to as the delta phase.

The value of ΔG_A at any one temperature may be obtained through Eqs. 5 or 6 from a knowledge of C_A^{α} and C_A^{γ} at that temperature. In this manner the values of ΔG_A

mined boundaries with experiment is given in Figs. 7 and 8. While perfect agreement between theory and experiment exists in the iron-carbon system, the agreement in

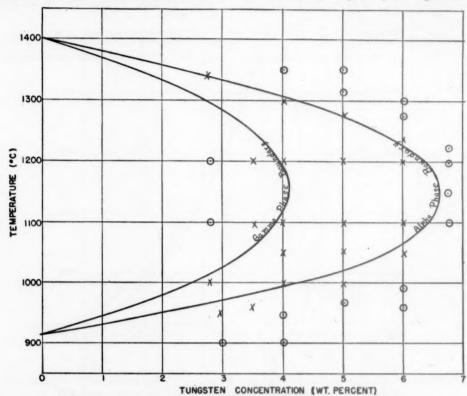


Fig. 5.—Comparison of theoretical Fe-W diagram with experimental data. (Experimental data after Sykes. 6)

o, single phase; ×, double phase.

of Table 2 have been computed. Having obtained these quantities, an approximation to the boundary of the gamma phase in equilibrium with the alpha phase may be made through the solution of Eqs. 4 and 5 or 6 for C_4 ; namely,

$$C_i^{\gamma} = \frac{\Delta G_{Fe}/RT}{1 - \beta e^{\Delta G_{A}/RT}}$$
 [8]

with

$$\beta = \begin{cases} 1, \text{ substitutional alloys} \\ 3, \text{ interstitial alloys} \end{cases}$$

and by regarding ΔG_{\perp} as independent of temperature. Conversely, the theoretical boundary of the alpha phase in equilibrium with the gamma phase is given by Eq. 7. A comparison of these theoretically deter-

the iron-manganese system is comparatively poor. At present it is not possible to determine whether the cause of this disagreement is the experimental data, through the lack of equilibrium conditions, or the theory, through the assumption that ΔG_{Fe} is independent of manganese concentration, or that ΔG_{Mn} is independent of temperature.

Ternary and Higher Order Systems

In this section the general case will be considered of a medium-alloy steel with n types of alloying elements, including carbon. One is generally interested in the iron-carbon diagram when the alloy content, other than carbon, is known for one phase,

usually the gamma phase. Under these conditions the determination of the alphagamma equilibrium will involve finding the concentration of n alloying elements on the boundary of the alpha phase, and of the carbon concentration on the boundary of the gamma phase. For the determination of these n + 1 unknowns the n + 1 equations of Eq. 1 are just sufficient.

The solution of Eq. 1, with Eq. 3 substituted for that equation in which j refers to carbon, gives for the mol fraction of carbon on the boundary of the alpha phase

$$C_e^{\alpha} = \{C_e^{\alpha}\}_0 + \Delta C^{\alpha}$$
 [9]

and for the mol fraction of carbon on the boundary of the gamma phase in equilibrium with the alpha phase

$$C_a{}^{\gamma} = \{C_a{}^{\gamma}\}_0 + \Delta C^{\gamma} \qquad [10]$$

In these equations the first term in the right member refers to the mol fraction of carbon on the boundary when no other alloying elements are present; e.g., for the pure iron-carbon system. The second terms in the right members are defined by the following equations:

$$\Delta C^{\alpha} = \sum_{i} \left\{ \frac{\mathbf{I} - e^{-\Delta G_{i}/RT}}{\frac{1}{3}e^{-\Delta G_{a}/RT} - \mathbf{I}} \right\} C_{i}^{\alpha} \quad [\mathbf{II}]$$

$$\Delta C^{\gamma} = \sum_{i''} \left\{ \frac{e^{\Delta G_{i}/RT} - 1}{1 - 3e^{\Delta G_{e}/RT}} \right\} C_{i}^{\gamma}$$
 [12]

The double primed summation sign denotes a summation over all constituents other than carbon and iron.

According to Eqs. 9 and 10, the effect of the alloying elements upon the boundaries of the alpha and of the gamma phases is to produce a horizontal shift of the boundaries. The amount of this shift is a linear function of the concentration of the alloying elements, and the effects of the alloy-

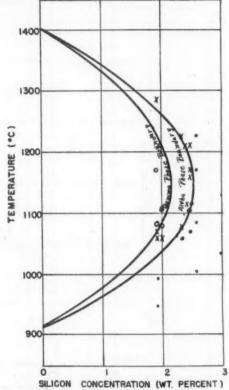


Fig. 6.—Comparison of theoretical Fe-Si Diagram with experimental data. (Experimental data after Kruetzer. 13)

•, alpha phase; X, alpha and gamma phase; O, gamma phase.

ing elements are therefore additive. The elements whose ΔG_i is positive—i.e., whose binary iron-alloy system has a closed gamma loop—cause a horizontal shift to the right. Conversely, the elements whose ΔG_i is negative—i.e., whose binary iron-

TABLE 2.—Values of ΔG_A for Elements That Give an Open Gamma Phase

Alloy	Zn4	Cu ⁴	Ni 10	Mn*	N4.a	С
Temperature, deg. C	623	833	600	600	591	910
Ci7	25	2.3	15	13	2.35	0.83
C_i^{α} . ΔG_i , cal. per mol	- 590	-1,280	-1,600	3.25 -2,440	0.42 -5.360	0.045 -8,100

[·] Interstitial solution in gamma phase, substitutional solution in alpha phase.

alloy has an open gamma phase—cause a horizontal shift to the left.

The coefficients of the alloy concentrations in ΔC^{α} and in ΔC^{γ} are only weak func-

Examples of the comparison of the theoretical alpha-gamma equilibrium relation for ternary systems with experimental data are given in Fig. 10.

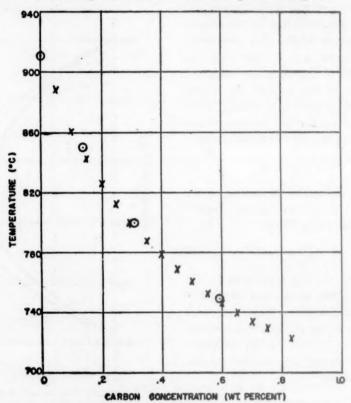


FIG. 7.—COMPARISON OF COMPUTED AND OBSERVED BOUNDARY OF GAMMA PHASE IN EQUILIBRIUM WITH ALPHA PHASE.

(Observed boundary after Epstein. 14)

O, computed; ×, observed.

tions of the temperature. To a first approximation, the horizontal shifts ΔC^{α} and ΔC^{γ} may therefore be regarded as independent of temperature. To this approximation the alpha and gamma boundaries may be regarded as being shifted horizontally without a change in shape.

The general effects of a horizontal shift to the right are illustrated in Fig. 9. A small shift reduces the extent of the gamma phase, as in Fig. 9b. A larger alloy concentration shifts the boundary of the gamma phase past the axis of zero carbon content, as in Fig. 9c. Still larger alloy contents also shift the boundary of the alpha phase past the axis of zero carbon content, as in Fig. 9d.

GAMMA-CEMENTITE EQUILIBRIUM

Cementite refers to an orthorhombic phase that contains three lattice-type atoms for each carbon atom. This is the only carbide phase that exists in the pure iron-carbon system. Steels containing alloying elements in addition to carbon usually also form other types of carbides in addition to cementite. If these alloying elements form a substitutional solution in the gamma phase, they may also be regarded as forming a substitutional solution in cementite and in the other carbides. Thus, in the iron-carbon-chromium system the composition of the cementite phase is written as (Fe, Cr). C. indicating that

chromium atoms may substitute for iron atoms.

When the concentration of the alloying elements, other than carbon, is sufficiently

 C_i . The carbon concentration C_e in the alpha or gamma phase may be obtained in terms of the concentration of the other alloying elements in that phase as follows:

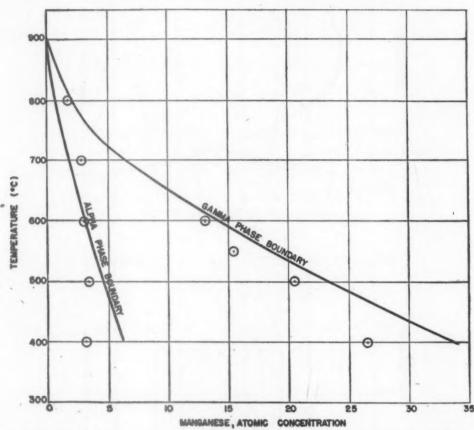


Fig. 8.—Comparison of computed and observed boundaries of alpha and gamma phases in Fe-Nn system.

(Experimental boundaries after Troiano and McGuire.8)

Solid lines; computed. ©, experimental.

low, the cementite phase is the only carbide that forms. The lowest value of the alloy concentration at which a new carbide phase is formed varies with different alloying elements and with the temperature. In the present report it will be assumed that the alloy concentration is sufficiently low and the temperature sufficiently high so that cementite is the only carbide phase formed from the austenite phase.

The equilibrium relations given by Eq. 2 contain the unknown concentrations in the cemeratie; namely, those represented by

Eq. 2 is rewritten as

$$C_{i}' = \left(\frac{C_c}{\beta}\right)^{\frac{1}{2}\delta} C_i e^{\Delta G_i e/3BT}$$

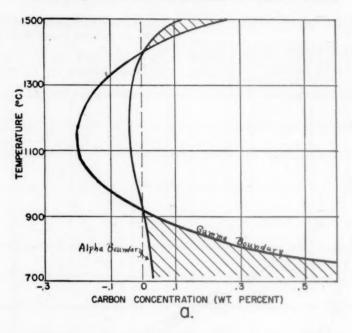
Now sum this equation over all values of j. Upon utilizing the fact that the sum of all the mol fractions C_i is unity, i.e.,

$$\Sigma C_i' = 1$$

we obtain

$$C_c = \beta [\Sigma_j C_j e^{\Delta G^c j/3RT}]^{-3}$$
 [13]

In line with a notation previously adopted, $\{C_e\}_1$ will be used to denote the



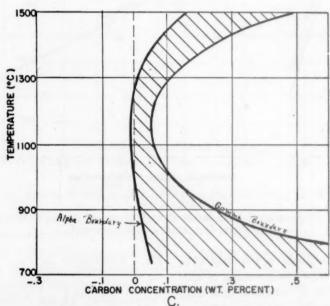
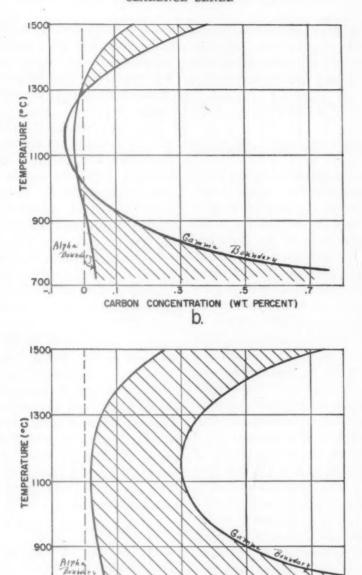


FIG. 9.—ILLUSTRATION OF EFFECT UPON ALPHA-GAMMA EQUILIBRIUM IN a. Pure iron-carbon system.
c. Gamma boundary lies entirely to right of axis of zero carbon concentration.



IRON-CARBON DIAGRAM OF ADDING INCREASING AMOUNTS OF ALLOY WITH $\Delta G_i > 0$. b Axis of zero carbon content passes through two two-phase regions. d. Both alpha and gamma boundary lie to right of axis of zero carbon concentration

CARBON

700

d.

CONCENTRATION (WT. PERCENT)

mol fraction of carbon on the boundary of the alpha or gamma phase in equilibrium with cementite in the pure iron-carbon system. Eq. 13 may then be rewritten as

$$C_e = \{C_e\}_1/D \qquad [14]$$

where

$$D = [1 + \Sigma' \{ e^{(\Delta G_i^{\bullet} - \Delta G_{p,\bullet}^{\bullet})/3RT} - 1 \} C_i]^3 [15]$$

Here the primed summation denotes a sum over all elements other than iron or carbon.

According to Eq. 14, the effect of alloying elements upon the mol fraction of carbon at the boundaries of the alpha and gamma phases in equilibrium with cementite is to introduce a dividing factor D rather than a horizontal shift as in the case where these two phases are in equilibrium with one another. An example is given in Fig. 11.

In using Eq. 14, the experimental value of $\{C_c\}_1$ may be taken. The boundary of the gamma phase in equilibrium with cementite is known with considerable accuracy for the pure iron-carbon system. Unfortunately this is not true for the alpha phase in equilibrium with cementite. It is to be expected that the heat of solution of cementite into alpha iron will be relatively independent of temperature below 700°C. This expectation requires that the carbon concentration on the boundary of the alpha phase lie upon a straight line when plotted against temperature as in Fig. 12. The deviation of the experimental points from such a straight line below 500°C. suggests that the experimental values are too high at the lower temperatures, too high by a factor of about 105 at room temperature.

GAMMA-MARTENSITE EQUILIBRIUM

The gamma-martensite transformation is reputedly not of the standard type of transformation between two phases in equilibrium. Two distinct characteristics distinguish it from the standard type: (1) the transformation does not occur isothermally, but occurs only during a lower-

ing of temperature; (2) the transformation is not reversible. These unusual characteristics should not discourage one from thinking about the thermodynamics of the transformation, and from gaining valuable insight therefrom.

Two types of gamma-alpha equilibrium may be envisaged in iron containing carbon in solution. One is of the usual type in which during the growth of the alpha phase carbon diffuses in the gamma phase away from the advancing boundary. Another type of equilibrium is one in which the carbon atoms are immobile, and in which therefore the carbon concentrations of the alpha and gamma phases are identical. It is with this second type that the gamma-martensite transformation will be compared.

If the carbon atoms are to be considered as fixed in their equilibrium positions, a transition of the second type will not involve a change in positional entropy.* At the equilibrium temperature the atomic free energy* of a given number of iron atoms and their associated carbon atoms must therefore, according to Eq. 8 of appendix B, be identical in the two phases. This equivalence may be expressed in the following equation:

$$G_{Fe}^{\gamma} + G_c^{\gamma}C_c = G_{Fe}^{\alpha} + G_c^{\alpha}C_c$$

where C_e is the mol fraction of carbon. From Table 2 is obtained:

$$G_{\epsilon}^{\alpha} - G_{\epsilon}^{\gamma} = 8$$
, roo cal. per mol

therefore

$$G_{\mathbf{Fe}}^{\gamma} - G_{\mathbf{Fe}}^{\alpha} = 8, \text{roo} \times C_{\alpha}$$
 cal. per mol [16]

The quantity $G_{Fe}^{\gamma} - G_{Fe}^{\alpha}$ is given in Table A-1 of Appendix A as a function of temperature. From this table and from Eq. 16, may be obtained the equilibrium temperature as a function of carbon concentration. This relationship is given in Fig. 13 as curve A.

^{*} See Appendix B for definitions.

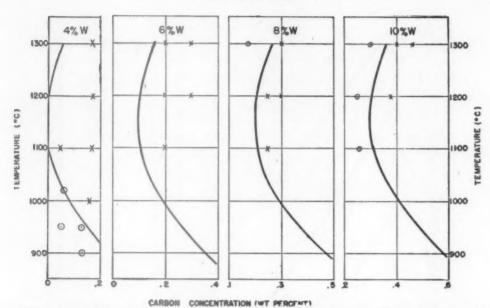


FIG. 10a.—Comparison of theoretical Fe-C-W system with experimental data. 16 Full line, theoretical boundary of gamma phase in equilibrium with alpha phase; X, gamma phase; O, alpha plus gamma phase.

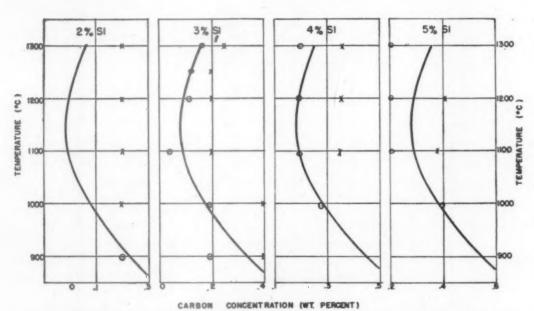


Fig. 10b.—Comparison of theoretical Fe-C-Si system with experimental data. 16 Full line, theoretical boundary of gamma phase in equilibrium with alpha phase; X, gamma phase; O, alpha plus gamma phase.

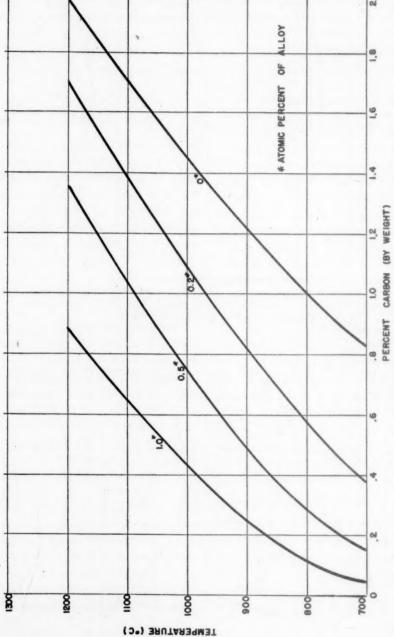
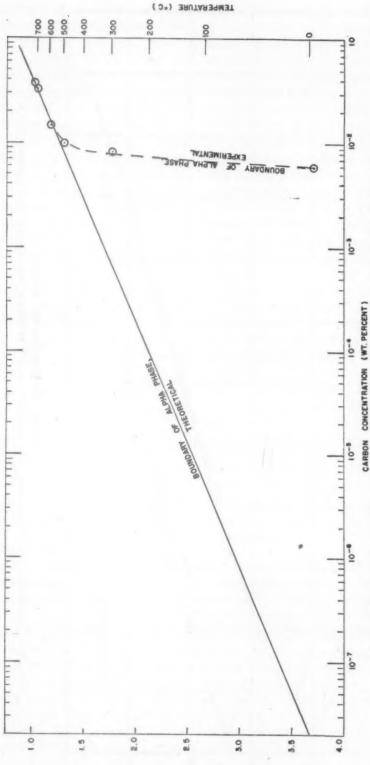


FIG. 11.—ILLUSTRATION OF EFFECT OF ALLOYS UPON BOUNDARY OF GAMMA PHASE IN EQUILIBRIUM WITH CEMENTITE. HEAT OF SOLUTION OF CARBIDE M₃C TAKEN AS 35,000 CALORIES PER GRAM MOL.

0



1 / 0001

Fig. 12.—Boundary of alpha phase in equilibrium with cementite in pure iron-carbon system. O, experimental data after Epstein. 12

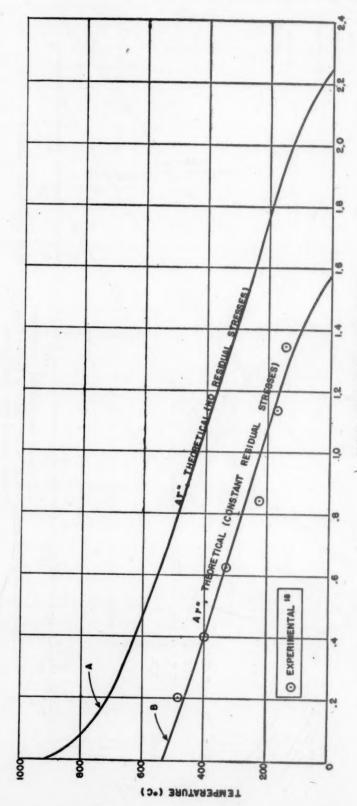


Fig. 13.—Comparison of experimental and theoretical Al" temperature in pure iron-carbon system. CARBON CONCENTRATION (WT. PERCENT)

The observed start of the gamma-martensite transformation temperature, called the Ar" temperature, lies about 200°C. below the computed values. This discrepancy finds a ready interpretation in the manner in which martensite is formed. As is well known, martensite does not form by the usual method of nucleation and growth, but by some sort of lattice strain. These permanent lattice strains introduce large residual stresses. The transformation must therefore occur at a temperature sufficiently below the equilibrium transformation temperature so that enough free energy is evolved from the reaction to provide for the elastic energy associated therewith. Thus, suppose that the elastic strain energy is ΔE for every mol of martensite initially formed. Then Eq. 16 becomes modified as follows:

$$G_{\text{Fe}}^{\gamma} - G_{\text{Fe}}^{\alpha} = 8,100 C_{\alpha} + \Delta E$$
 [17]

If ΔE is now considered to be independent of carbon concentration, the effect of its introduction in Eq. 17 is to displace the theoretical curve of C_{α} to the left by the amount $\Delta E/8$,100. Upon choosing

$$\Delta E$$
 = 290 cal. per mol

the horizontal shift is such as to bring the theoretical Ar'' curve into precise agreement with the experimental values, as shown by curve B of Fig. 13.

Consideration of the residual stresses not only brings the theoretical Ar" temperature into agreement with the experimental values, it also affords a ready interpretation of the nonisothermal nature of the reaction. 20 The stress system introduced by each succeeding amount of transformed iron is superimposed upon the original stress system. The elastic energy associated with each additional amount of transformed iron thus increases as the transformation proceeds; therefore the transformation temperature drops.

The irreversibility of the gamma-marten-

site transformation is associated with the comparatively rapid diffusion rate of carbon in the martensite, resulting in the separation of carbides. No direct measurements of the diffusion coefficient of carbon in alpha iron have been made, but, as may be seen from a comparison of the nature of the interstices in alpha and in gamma iron, diffusion must be much more rapid in alpha than in gamma iron. The alpha iron contains three times as many interstices as gamma iron for the same number of iron atoms. The interstices are thus considerably closer together in the alpha than in the gamma iron, therefore the potential hump between neighboring interstices is lower.

Nearly all alloying elements lower the Ar" temperature. Some of these elements, such as tungsten and molybdenum, have a lower free energy in the alpha than in the gamma phase, therefore they would be expected to raise the Ar" temperature. The reason these elements appear to behave in a manner contrary to that which is expected may be sought in their strong carbide-forming tendency. During the quench the carbon may become concentrated to some extent about these alloying elements. Such segregations would hinder the formation of the martensite structures and therefore would lower the Ar" temperature.

SUMMARY

The general theory of the equilibrium between two solid phases is developed from thermodynamical and statistical mechanical concepts. The general theory is applied to the equilibrium relations in the ironcarbon system between the alpha, gamma and cementite phases, and to the effects of alloying elements thereon. Not only is it possible to bring observed equilibrium data into a consistent picture, but a method has been developed for rapidly computing the equilibrium relations in any mediumalloy steel.

The influence of alloys upon the boundary of the gamma phase in equilibrium with the alpha phase may best be visualized in terms of a master boundary curve. In the pure iron-carbon system the lower branch of this curve forms the boundary in equilibrium with the alpha phase, the upper branch the boundary in equilibrium with the delta phase. Alloys simply shift this master curve horizontally. Certain elements, such as Ti, Sn, P, V, W, Mo, Al, Si, shift the curve to the right, thereby raising the temperature for the α - γ transformation, lowering the temperature for the δ-γ transformation. After these two transformation temperatures coincide, the left-hand boundary of the gamma phase leaves the ordinate axis. In the binary ironalloy systems with these elements, the gamma phase forms a closed loop.

Other elements, such as Cu, Zn, Mn, Ni, N, shift the master curve to the left, thereby lowering the temperature of the α - γ transformation, raising the temperature of the δ - γ transformation. The shift associated with each element is proportional to its concentration, and is independent of the concentrations of the other elements. In other words, the shift is a linear function of the alloy concentrations, the coefficients of some concentrations being positive, others being negative.

The influence of alloying elements upon the boundary of the gamma phase in equilibrium with the carbide phase may best be visualized in terms of a dividing function. The carbon concentration at this boundary is equal to the concentration for the pure iron-carbon system divided by this function, which is different for each temperature. The cube root of this dividing function is a linear function of the concentration of the alloying elements. This problem of the right-hand boundary of the gamma phase is solved through use of the concept of the complex carbide (Fe, Alloy). C.

It is found that the austenite → mar-

tensite transformation is demanded by thermodynamical considerations. This transformation is regarded essentially as the transformation from the face-centered to the body-centered lattice with the concentration of carbon unchanged. Agreement is obtained between the observed and the computed variation of the Ar" temperature with carbon concentration.

APPENDIX A

In this appendix a computation is given of the increase in free energy ΔG_{F_0} , associated with the transformation of one mol of alpha iron into gamma iron.

Tables have been published for the free energy of the alpha and gamma phases as a function of temperature. It might be thought that these tables could be used to find the difference in free energy ΔG_{Fe} of one mol of iron in the two phases, but they are not sufficiently accurate for our present purpose. Above 700°C. the difference in free energy of the two phases is less than 1 per cent of the free energy of either phase. Thus an error in computation of only 1 per cent would lead to an error of the order of 100 per cent in the difference. It is necessary, therefore, to compute the difference ΔG_{Fe} directly from the thermal data.

From the definition of G, it may be seen that for changes in temperature occurring at constant pressure,

$$\frac{d}{dT}\Delta G_{Fe} = -\Delta S_{Fe}$$

therefore

$$\Delta G_{\rm Fe} = -\int_{T_e}^{T} \Delta S_{\rm Fe} dT$$

where T_o is the transformation temperature from the alpha phase to the gamma phase. Denoting by L the latent heat of transition from the alpha to the gamma phase per mol gives:

$$\Delta G_{\mathbb{F}_{\bullet}} = L \times (T_{\bullet} - T)/T_{\bullet}$$
$$- \int_{T}^{T_{\bullet}} \int_{T'}^{T_{\bullet}} (\Delta C_{\mathbb{F}_{\bullet}}/T'') dT'' dT' \quad [a-1]$$

where ΔC_{Fe} is the difference in specific heats of the two phases, in calories per mol per degree.

TABLE A-1.—Summary of Computations

re, deg. C. (∆C _{Fe} /T'')dT'' dT''		(ACFe/T'')dT" dT'		Computed Boundary of Gamma Phase in Equi- librium with Alpha Phase		
Temperature, deg.	$\int_T^{T_o} \int_T^{T'}$	$G_{ m Fe}^{\gamma} - G_{ m F}$	$(G_{\rm Fe}^{\gamma} - G_{\rm Fe}^{\gamma})$	Atomic Per Cent, Carbon	Weight Per Cent, Carbon	
0 100 200 300 400 500	872 770 649 520 371 264	1045 924 784 622 487 342	1.91 1.24 0.830 0.543 0.362 0.222			
600 650 700 750 800 850	150 98 58 24 8.5 2.4	209 147 98 54 29 14	0.120 0.080 0.050 0.0264 0.0135 0.0061	12.3 8.0 5.2 2.78 1.46 0.67	2.58 1.76 1.11 0.59 0.31 0.14	
910 950 1000 1050 1100 1150	0	-6.85 -13.7 -18.5 -21.1 -21.9	0 -0.0028 -0.0054 -0.0070 -0.0077	0 -0.316 -0.615 -0.836 -0.935 -0.960	0 -0.068 -0.132 -0.180 -0.201 -0.207	
1200 1250 1300 1350 1400 1500		-20.9 -18.3 -13.8 -7.5 0 31.5	-0.0071 -0.0060 -0.0044 -0.0023 0	-0.920 -0.810 -0.610 -0.335 0	-0.198 -0.174 -0.131 -0.072 0	

Below the transformation temperature 910°C., the double integral in Eq. a-1 has been evaluated from the specific heat data of Austin. The heat of transformation L was so chosen as to give the observed value of the carbon concentration at the eutectoid temperature. This value was 225 cal. per mol, which lies within the measured range. The details and the results of the computation are given in Table A-1. Above the transformation temperature 910°C., the difference in specific heats of the alpha and gamma phases, ΔC_{F0} , was taken as a constant. The analytical evaluation of the integral in Eq. a-1 then gives

$$\Delta G_{\text{Fe}} = -L(T - T_{\text{o}})/T_{\text{o}} + \Delta C_{\text{Fe}} \{T \ln (T/T_{\text{o}}) - (T - T_{\text{o}})\} \quad [a-2]$$

where T_o is the lower transformation temperature, 910°C., in degrees absolute. The condition that ΔG_{Fo} be zero at the upper transformation temperature, 1400°C., imposes a relation between the heat of transformation L and the difference in specific heats ΔC_{Fo} . This relation is

$$\Delta C_{Fo} = 5.84L/T_{o}$$

Upon taking the value of 225 cal. per mol for L, one obtains

$$\Delta C_{Fo} = 1.11$$
 cal. per mol per deg. C.

The values of ΔG_{Fe} above 910°C. were computed from Eq. a-2, using 225 cal. per mol and 1.11 cal. for mol per deg. C. for L and ΔC_{Fe} , respectively. These values are given in Table A-1 also.

APPENDIX B

The condition for the equilibrium of a system may be most succinctly stated in terms of its free energy G. This free energy is defined in terms of the heat function H, absolute temperature T, and entropy S by the equation

$$G = H - TS \qquad [b-1]$$

The heat function is defined, in turn, by the equation

$$H = U + PV . [b-2]$$

where U is the total energy, P the pressure and V the volume. The nomenclature heat content arises from the circumstance that whenever a reversible change occurs under the condition of constant pressure, the usual experimental condition, the increment of H is equal to the heat that flows into the system during the change. The absolute value of the total energy, and hence also of H, is unknown. All equilibrium equations involve, however, only differences of heat functions, therefore the equilibrium equations themselves contain no ambiguity.

From the thermodynamical viewpoint, entropy is defined only in terms of its differential:

$$dS = dQ/T [b-3]$$

where dQ represents the heat absorbed. From the statistical mechanical viewpoint, entropy has rich physical significance. It is, in fact, a measure of the uncertainty in the specification of the internal coordinates of a system. According to this viewpoint, the precise definition of entropy is

$$S = k \ln W \qquad [b-4]$$

where k is Boltzmann's constant and W is the total number of ways in which the coordinates of the system may be specified while the system still maintains the same macroscopic properties. The two definitions for entropy contained in Eqs. b-3 and b-4 are, of course, compatible.

In the study of the equilibrium relations between solid phases, the statistical mechanical concept of entropy has a decided advantage over the thermodynamical concept. In solids the atoms have two independent types of coordinates. The first type specifies the equilibrium positions of the atoms. The second type specifies the position and motion of the atoms with respect to the equilibrium positions. If W_1 and W_2 are the total number of ways of specifying these coordinates, then

$$W = W_1 \times W_2$$

and, according to the definition, (b-4)

$$S = k \ln W_1 + k \ln W_2$$

Therefore, according to the statistical mechanical concept, the entropy of a solid may be represented as the sum of two parts, one part being the uncertainty in the equilibrium positions of the atoms and the second part being the measure of the uncertainty of the positions and motions of the atoms about their equilibrium positions and of the uncertainty in the elec-

tronic configurations of the atoms. The first part will be called positional entropy and will be denoted by S_p . The second part will be called atomic entropy, and will be denoted by S_a . This separation of the entropy into two parts is expressed formally by the following equation:

$$S = S_p + S_o \qquad [b-5]$$

The fundamental principle of equilibrium is that at equilibrium the free energy is a minimum with respect to any variation that leaves the pressure and temperature unchanged. Thus if δ refers to an arbitrary variation, which leaves the pressure and temperature unchanged, at equilibrium

$$\delta G = 0$$
 [b-6]

In order that this equation may be thrown into a more usable form, the atomic free energy G_{\bullet} is introduced. This quantity is defined by the equation

$$G_a = H - TS_a [b-7]$$

The atomic free energy G_a may be related to experimental quantities by the following consideration. The free energy G obeys the equation:

$$d(G/T)/d(I/T) = H$$

Upon observing that S_p is not an explicit function of temperature, we obtain

$$d(G_a/T)/dT = d(G/T)/dT$$

and therefore

$$d(G_a/T)/d(I/T) = H$$

By combining Eqs. b-1, b-5, b-6 and b-7, we obtain

$$\delta S_p = T^{-1} \delta G_a \qquad [b-8]$$

The change in positional entropy δS_p in Eq. b-8 refers to the positional entropy of the complete system when a transfer of atoms takes place between two or more phases. This change in positional entropy is equal to the sum of the changes in positional entropy of the individual phases when such a transfer occurs. For the cal-

culation of δS_p it is therefore sufficient to know the changes in positional entropy of the individual phases. These changes are computed below.

A solid phase contains two types of atoms, lattice atoms and interstitial atoms. The uncertainties in the distribution of the two types of atoms are independent of one another. The positional entropy of a phase may therefore be separated into two parts. one associated with the uncertainty in distribution of the lattice atoms, the other associated with the uncertainty in distribution of the interstitial atoms. Thus in alpha iron containing iron, manganese and carbon atoms, the first type of entropy refers to the uncertainty as to which lattice positions are occupied by the manganese atoms, the second type of entropy refers to the uncertainty as to which interstitial positions are occupied by the carbon atoms.

In the computation of the positional entropy the following symbols will be employed:

M, total number of lattice atoms. Ni, number of lattice atoms of type j.

 $X_i, N_i/M$

m, total number of interstitial atoms. ni, number of interstitial atoms of type j.

8, ratio of number of possible interstitial positions to number of lattice atoms. s_i , $n_i/\beta M$.

The positional entropy associated with the uncertainty in distribution of the lattice atoms is obtained by finding the number of ways W_L in which the lattice atoms may be arranged in the M lattice positions, the atoms of each type being regarded as identical, as follows:

$$W_L = \frac{M!}{\pi_i N_i!}$$

From Eq. 4 it therefore follows that

$$S_{p. \text{ lattice}} = k \ln \left(\frac{M!}{\pi_i N_i!} \right)$$

The entropy associated with the uncertainty in the positions of the interstitial atoms is obtained by considering the num-

ber of ways, Wi, in which the interstitial atoms may be arranged on βM positions, the interstitial atoms of each type being regarded as identical. The result is:

$$W_i = \frac{(\beta M)!}{(\beta M - m)! \pi_i n_i!}$$

It therefore follows from Eq. 4 that

$$S_{p, \text{ interetitial}} = k \ln \left(\frac{(\beta M)!}{(\beta M - m)! \pi_i n_i!} \right)$$

The change in total positional entropy, δS_{p} , associated with changes in the number of atoms of the various types, is obtained by taking the differential of the sum of the two entropies given above. Thus, upon forming the sum

$$S_p = S_{p, \text{ lattice}} + S_{p, \text{ interestitial}}$$

and upon observing that when N is a large number.

$$\delta \ln N! = (\ln N) \delta N$$

one obtains

$$\delta S_{p} = -k \left[\Sigma \ln X_{i} \times \delta N_{i} + \ln \left(\mathbf{I} - m/\beta M \right) \times \beta \Sigma \delta N_{i} + \Sigma \ln \left(\frac{\dot{S}_{i}}{\mathbf{I} - m/\beta M} \right) \times \delta n_{i} \right] \cdot [b-9]$$

The first line comes from the change in the positional entropy of the lattice atoms caused by changes in their number; the last line comes from the change in positional entropy of the interstitial atoms caused by changes in their number, while the middle line represents an interaction term. It represents the change in the positional entropy of the interstitial atoms due to changes in the number of the lattice atoms; i.e., changes in the number of possible interstitial positions. When the number of interstitial atoms is very small compared with the number of interstitial positions, as always is true for mediumalloy steels, Eq. b-9 may be written as

$$\delta S_p = -k\Sigma \ln (\beta_i C_i) \delta N_i$$
 [b-10]

In this equation the summation extends

over all types of atoms, both lattice and interstitial, C, refers to mol fractions, and β_i is equal to unity for lattice atoms, to 3 for interstitial atoms.

All the equilibrium equations in the text are derivable directly from Eqs. b-8 and b-10.

REFERENCES

- J. Slater: Introduction to Chemical Physics, chapters I and II. New York 1939. McGraw-Hill Book Co.
- Fowler and Guggenheim: Statistical Mechanics. Cambridge, 1939.
 E. Bain: The Alloying Elements in Steel.
 Trans. Amer. Soc. Metals (1939) 122.

 M. Hansen: Der Aufbau der Zweistofflegie-

- rungen. Berlin, 1936.

 5. R. Vogel and H. Gontermann: Archiv Eisenhuttenwesen (1929) 3, 369.

 6. W. P. Sykes: Trans. A.I.M.E. (1931) 95,
- 7. A. Kriz and F. Poborie: Jnl. Iron and Steel Inst. (1930) 191.

- 8. A Troiano and F. McGuire: Trans. Amer.
- Soc. Metals (1943) 31, 340.

 9. J. S. Marsh: Alloys of Iron and Nickel.
 New York, 1938. McGraw-Hill Book Co.
 10. J. B. Austin: Int. Ind. and Eng. Chem.
- (1932) 24, 1225.

 11. H. E. Cleaves and J. G. Thompson: The Metal Iron, 148. New York, 1935. McGraw-Hill Book Co.
- S. Epstein: Alloys of Iron and Carbon, 1,
 New York, 1936. McGraw-Hill Book
 Co.
- C. Kreutzer: Ztsch. Physik (1928) 48, 559.
 S. Epstein: Ibid, 81.
 S. Takeda: Tech. Repts. Tohoku Imp. Univ.
- (1929-31) 9, 627.

 16. T. Sato: Tech. Repts. Tohoku Imp. Univ.
- (1929-31) 9, 515.

 17. A. Greninger: Trans. Amer. Soc. Metals
- (1942) 30, I.

 18. S. Epstein: *Ibid*, 107.

 19. P. Oberhoffer and H. Esser: *Stahl und*
- Eisen (1927) 47, 2021.
 20. H. Carpenter and J. M. Robertson: Metals, 885. Oxford, 1939.

DISCUSSION

See page 546.

Phase Boundaries in Medium-alloy Steels

By W. A. West*

(New York Meeting, October 1945)

One who attempts to collect and classify equilibrium data from various iron-alloy systems is soon struck with the absence of any quantitative theory that can serve as a general background against which to compare and contrast results from different systems, at different temperatures, and with different concentrations. It is not necessary to wait for a perfect theory; investigation of divergences of theory from observation may prove of great value in acquiring understanding of the subject. For example, one has only to think of Raoult's law as applied to aqueous solutions.

The equations developed by Zener¹ represent an effort to provide such a quantitative theoretical background, and it is therefore desirable to subject this theory to such tests as can be applied. The present article is intended to be an application of available tests, and may thus be considered as a supplement to Zener's paper. It is assumed that this paper is available to the reader.

The equations make it possible to calculate the effect on the equilibrium concentration of one alloying element due to the presence of one or more other elements. In particular, they are intended to give, for alloy steels, the carbon concentrations in alpha and gamma phases in equilibrium with each other, and in gamma in equilibrium with cementite. They may, however, be modified for use for carbon-free alloys. A summary is given later of the equations used in analyzing the data in this paper, and the symbols are there defined.

About 125 papers have been examined for experimental data suitable for this investigation. An effort was made to look up all available reports of ternary systems including iron and carbon, as well as similar systems of higher order. Supplementary material was also obtained from a number of binary systems. A few noncarbon ternary systems were also found to which these methods could be applied.

A comparatively small proportion of the papers read provided usable material. In many systems the number of quantitative observations made in the iron-rich region is extremely small, and the smoothed curves to be found in most published phase diagrams are entirely useless for quantitative treatment. This opinion is confirmed by the authors of the series on Alloys of Iron Research, whose remarks show clearly that they have no illusions as to the accuracy of many diagrams that they present. A further difficulty arises from the fact that these equations apply only to rather low percentages of alloying elements. The result is that at the lowest concentrations. where the best agreement might be hoped for, the errors of observation become relatively very large. The experimental difficulties in measurements of this kind of equilibrium are, of course, an old story.

The statements or opinions in this article are those of the author and do not necessarily express the views of the Ordnance Department. Manuscript received at the office of the Institute Feb. 23, 1945. Issued as T.P. 1924 in METALS TECHNOLOGY, January 1946.

^{*} Physicist, Watertown Arsenal, Watertown, Mass., on leave. Professor of Chemistry, The American University of Beirut, Beirut, Lebanon.

¹ References are at the end of the paper.

In view of these facts, it is gratifying to find a fairly substantial agreement of theory with experiment, only two cases having come to light of clear-cut disagreement. Referring to Table 2, the $\alpha \rightarrow \gamma$ column, ternary systems, it may be said that for three metals, Mo, W, V, the calculated constant seems reliably established. As described later, the value for Si is so small that its relative uncertainty is rather great. For the important alloving elements Mn and Ni, considerable uncertainty exists, no doubt largely because of the difficulty of attaining equilibrium at the lowered temperatures. Cu suffers from the same disability, and in addition has only a few points from but a single observer. Cr is discussed in detail later. In the cementite $\rightarrow \gamma$ column, Cr and Mn seem fairly reliable, and Cu very doubtful. because of insufficient and inconsistent data. For other elements, data are either lacking or refer to carbides other than cementite. Of special interest are the cases that clearly disagree with the theory, Fe-Cr-C and Fe-Ni-P. It might be worth while to investigate other cases of the latter type, with and without carbon, since experimental and theoretical study of these may well be illuminating to the whole theory. As is shown later, it is possible to get at Ni indirectly through the system Fe-Ni-W. Study of this combination with carbon, and of Fe-Ni-V with or without carbon, might throw light on the important but hitherto inscrutable question of Ni. The same method might succeed for Mn.

SUMMARY OF EQUATIONS AND SYMBOLS

The following equations and constants are taken from Zener's paper, the numbers used there being retained.

Note that in the equations temperatures refer to the absolute scale and compositions to atomic concentrations. All numerical data in this paper employ centigrade temperatures and weight percentages.

Superscripts refer to phases, and subscripts to components.

R = molecular gas constant = 1.99 cal.

T = absolute temperature.

 C_i = atomic concentration of element j.

 $\Delta G = \text{constant characteristic of element } j$.

 Σ = a summation covering all elements present except iron and carbon.

Alpha-gamma Equilibrium.-

$$C_{c} \gamma = (C_{c} \gamma)_{0} + \sum \left\{ \frac{e^{\Delta G_{i}RT} - 1}{1 - 3e^{\Delta G_{e}RT}} \right\} C \gamma_{i}$$
[10, 12]

The suffix Δ refers to the constant for the transfer of one gram atom of the indicated element from the alpha to the gamma phase. $\Delta G_o = -8100$. For $(C_o \gamma)_0$ see Table 1.

 $(C_c \gamma)_0$ = carbon concentration in absence of other alloying elements

Cementite-gamma Equilibrium.-

$$C_c^{\gamma} = (C_c^{\gamma})_1 \left[1 + \sum C_i^{\gamma} \left\{ e^{(\Delta G_i - \Delta G_{F_{\bullet}})/3RT} - 1 \right\} \right]^3$$
[14, 15]

 Δ here refers to a transfer of one mol of carbide, (metal)₂C, from the cementite to the gamma phase. $\Delta G_{Fo} = 5300$. For $(C_c \gamma)_1$ see Table 1.

 $(C_c \gamma)_1$ = carbon concentration in absence of other alloying elements

 ΔG for iron (in the alpha-gamma equilibrium) is the free energy of transfer per gram atom, from the alpha to the gamma phase in pure iron. For the other elements it may be considered an empirically determined quantity. If it is desired to interpret it in terms of thermodynamic conventions, it may be thought of as the standard free energy of transfer; that is, between alpha and gamma phases of the pure element. This corresponds to reality in the case of iron (see above), but represents hypothetical reference states for the other elements. The number of positions available for carbon are not the same in the two phases;

instead, however, of expressing the carbon concentrations differently, we make use of the factor β . For substitutional elements this situation does not arise, and β is

calculated curves agreeing as closely as possible with the experimental results, and the degree of correlation is observed over the available temperature and concentra-

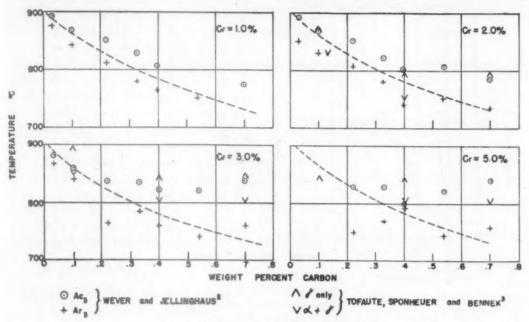


Fig. 1.—System Fe-Cr-C ($\gamma \rightleftharpoons \gamma + \alpha$).

therefore unity. Similar considerations may be applied to the gamma-cementite equilibrium.

TABLE 1.—Constants for Use in Equationsa

Temperature, Deg. C.	$(C_{e\gamma})_o$ $(\gamma \leftrightarrows \alpha)_c$ Wt. Per Cent	(Cγ ₀) ₁ (γ ≒ cementite), Wt. Per Cent
700	1.11	0.83
800	0.31	1.00
910	0	1.24
1000	-0.13	1.45
1100	-0.20	1.71
1200	-0.20	
1300	-0.13	
1400	0	
1500	0.25	

When used in the equations these values are, of course, transformed to atomic concentrations.

Examination of Individual Alloying Elements

In the following pages analyses are made of the experimental data on the carbon content of the gamma phase in equilibrium with, respectively, alpha phase and cementite. Constants have been chosen to give tion ranges. Two noncarbon systems have also been included.

In Table 2 are given the constants as determined. In the first column ($\Delta G(\alpha \rightleftharpoons \gamma)$), binary systems), are given the values as determined by Zener. In the second column are corresponding values as determined from the data analyzed in this paper. In the third column are constants for the cementite-gamma equilibrium as determined in this paper.

Chromium

Alpha-gamma Equilibrium.—In Fig. 1 are plotted a large number of observations of Ac_3 and Ar_3 obtained dilatometrically by Wever and Jellinghaus² and also some points based on observations of microstructures by Tofaute, Sponheuer and Bennek.³ A few cooling-curve results by the former, and dilatometric points by the latter authors, have not been plotted, but show no divergence from the results given.

The dotted curves represent $(C_{\iota})_{\circ}$ for the iron-carbon system. Near the axis the transformation curve is lowered slightly (as must necessarily occur for small per-

that have stable ranges in contact with the gamma phase, orthorhombic (Fe, Cr)₃C, (cementite), and trigonal (Cr, Fe)₇C₃. As is indicated, iron and chromium are found

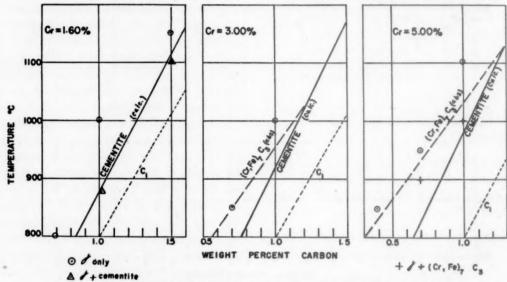


FIG. 2.—System Fe-Cr-C ($\gamma \rightleftharpoons \gamma + \text{CARBIDE}$). (Tofaute, Sponheuer and Bennek.*)

centages of chromium), and as carbon is increased the Ar₃ points maintain this slight lowering, while the Aca points rise markedly above the iron-carbon curve. The possibility exists that this rise is only apparent, and is due to slow rate of dissolving of carbide present before heating began. This hypothesis is supported by the increasing carbon. On the other hand, Ac points are generally considered more reliable than Ar. Further, there has been acceptance of an A2 curve crossing the C. curve for low chromium content.4 The latter situation would require that a small amount of chromium should appreciably change the heat of transfer of carbon from gamma to alpha phase, a possibility that cannot be ruled out, in view of the anomalous effect of chromium on pure iron. This case is in definite disagreement with the theory, at least for more than very small concentrations.

Gamma-carbide Equilibrium.—For low chromium contents there are two carbides

in both forms, at least within limits. In Fig. 2 are plotted observations on microstructure by Tofaute, Sponheuer and

TABLE 2.—Constants

	ΔG(a		
Alloying Element	Binary Systems (Zener ¹)	Ternary Systems	$\Delta G(\text{cem.} \leftrightarrows \gamma)$
C N Mn Ni Cu Zn Si Be Al W Mo V P Sn Ti	-8100 -5360 -2440 -1700 -1285 -590 475 810 1300 1360 2830 4180 5500 9000	- 1000(?) - 1050a - 500(?) 450 1250 1500 2000	11,000
Cr	see dis	cussion	13,000*

[•] Above 1000°. • For Cr < 2.5 per cent only.

Bennek,³ corrected for the given contents of manganese and silicon. Making use of the cementite points under Cr = 1.60 per cent, we obtain $\Delta G = 13,000$, giving the calculated curve as drawn. For higher chromium contents the points observed are of trigonal carbide, and, in fact, the calculated curves fall increasingly to the right of the observations, as is required by theory. The heavy dotted lines represent approximate positions for the y-trigonal carbide boundary, increasingly encroaching on the \gamma-cementite boundary as the chromium content increases. Wever and Jellinghaus,2 using X-ray analysis, found cementite at Cr = 1.6 per cent and C = 1.3per cent. At Cr = 3.0 per cent they found cementite and trigonal carbide at C = 0.5 per cent, and cementite alone at 0.02 per cent C. These fit fairly well with the diagrams of Fig. 2.

It appears that $\Delta G = 13,000$ is applicable up to 2 to 2.5 per cent chromium.

Copper

Alpha-gamma Equilibrium.—Copper is known to lower the temperature of this transformation in its alloys with iron, but the few experimental data on the iron-copper-carbon system⁵ indicate a marked rise of Ac₃ temperature with copper content.

TABLE 3.—Calculated Values, Gammacarbide Equilibrium

T	Cu, Per	C, Per Cent		T	Cu, Per		Per
	Cent	Obs.	Calc.		Cent	Obs.	Calc.
850	2.08	0.48	0.72	980	2.08	1.27	0.99
990 1020	4.10	0.49	0.72	990	3.11	1.14	0.84
1050	5.80	0.54	0.68	1100	4.85	I.II	0.90

Gamma-carbide Equilibrium.—Ishiwara, Yonekura and Ishigaki published three series of experimental data. Four points, with Cu = 1 per cent, are plotted in Fig. 3, with a line calculated for $\Delta G = 20,000$. The agreement appears fairly good. This promise, however, is not fulfilled with the other

two series. In Table 3 the calculated value of carbon assumes $\Delta G_{\text{Cu}} = 20,000$. In one series the calculated values fall consistently well above the observations, and in the

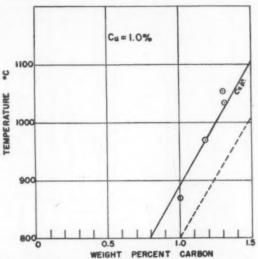


Fig. 3.—System Fe-Cu-C ($\gamma \rightleftharpoons \gamma + \text{CARBIDE}$). (Ishiwara, Yonekura and Ishigaki.⁵)

other equally far below. In the absence of further data, the constant cannot be determined with any certainty.

Manganese

Gamma-alpha Equilibrium.—Inspection of results on the iron-manganese system⁶ indicate a value for ΔG of minus 1400 cal. The only observed points for the iron-manganese-carbon system, at low concentrations, are those of Gensamer,⁷ which are

TABLE 4.—Points in Iron-manganese-carbon
System

Mn,	C,	Temperature, Deg. C.		Δ	С
Per Cent	Per Cent	a Present	No α Present	Calc.	Obs.
2.5	0.16	770	795 775	-0.21 -0.41	-0.24 -0.32
4.5	0.45	710	730	-0.41	-0.4

listed in Table 4. ΔC gives the calculated and observed distances from the iron-carbon curve of points midway in the

observed temperature range of dilatometric change. ΔG was taken as minus 1000 cal., which roughly fits the points. One approximate point is given for Mn = 7 per cent⁷

Molybdenum

Gamma-alpha Equilibrium.—The ironmolybdenum system forms a gamma loop, but estimates of the value of maximum

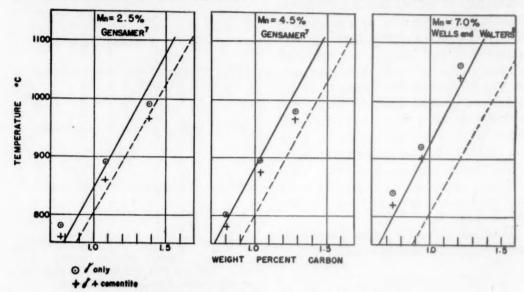


Fig. 4.—System Fe-Mn-C ($\gamma \rightleftharpoons \gamma + \text{carbide}$).

and two for Mn = 10 per cent, all of which indicate ΔG as approximately minus 2500. Recent observations by Troiano and McGuire on the iron-manganese system indicate a very similar ΔG with a similar increase at higher manganese concentrations and lower temperatures. The limited vidence, then, points to a constant of minus 1000 cal. for low percentages of manganese and temperatures of 800° to 000°.

Gamma-carbide Equilibrium.—Three series of experimental results exist for this boundary, two by Gensamer⁷ for 2.5 per cent and 4.5 per cent Mn, and one by Wells Walters for 7 per cent Mn.⁸ These are plotted in Fig. 4, together with the C_1 line for the iron-carbon system, and a calculated line using $\Delta G = 11,000$. This value gives the best fit that can be obtained, although the observational lines, especially those of Gensamer, show appreciably less slope than the calculated. The agreement is better at 7 per cent Mn, where the equation might not be expected to apply so well.

molybdenum on the alpha boundary vary from less than 3 per cent to more than 4 per cent. To corresponding to values of ΔG from 1500 to 1000. The only available data from the iron-molybdenum-carbon system is from a set of curves by Svetchnikoff and Alferova. Reading from these curves for Mo = 1 per cent, we obtain the points plotted in Fig. 5. A calculated curve with $\Delta G = 1750$ fits the points fairly well. No information is available as to the methods employed by these authors.

Gamma-carbide Equilibrium.—The gamma phase is in equilibrium with complex carbides other than cementite in concentration ranges for which observations are available, so that the boundary cannot be studied.

Nickel

Gamma-alpha Equilibrium.—Attempts to calculate ΔG from the Fe-Ni diagram fail, because of the wide divergence of experimental results obtained on heating and on cooling, the interpretation of this being

uncertain.¹⁸ The diagram widely accepted as of practical use is that showing two wide bands, representing gamma-alpha transformation ranges on cooling and heating, respectively.

Marsh¹³ quotes three investigators whose results indicate that the true upper and lower boundaries of the alpha-gamma two-phase region lie, respectively, in the heating and cooling transformation bands. There is, however, disagreement as to the exact position of these lines.

Few experimental results exist for the iron-nickel-carbon system. Kasé14 gives a few values of Ars, which correspond to $\Delta G = -2500$ or more, with considerable divergences. Bain (p. 74 of ref. 13) reported points on the $\gamma \rightleftharpoons \alpha + \gamma$ boundary, which give fairly consistent results of $\Delta G =$ -2000 or less. Jones 15 reported a long series of Ac2 and Ar2 points for nickel steels containing up to I per cent Mn. When corrected for the effect of the manganese, which is somewhat uncertain, the Ac₃ points indicate $\Delta G \cong -1000$. No mention was made of Si, which was almost certainly present, and which may have been in fact responsible for this low result. It may be noted that his Ara points fell 60° to 140° below the Ac3, indicating that the previously mentioned effect of nickel on this transformation persists in the presence of at least some other alloying elements.

A series of observations on the ternary system iron-nickel-tungsten¹⁶ provides an opportunity to determine ΔG at temperatures where the delayed transformation may be less troublesome. As will be shown later, ΔG_W for tungsten appears to be known with sufficient accuracy. Using $\Delta G_W = 1250$, and applying Eq. 10 modified for a substitutional alloying element (nickel) in place of an interstitial element (carbon), we obtain the calculated curve as shown, with $\Delta G = -1050$ (Fig. 6). Agreement is good with the experimental data. This would indicate that the true

two phase region for the iron-nickel system lies inside the heating range of transformation as the latter is shown on current diagrams.

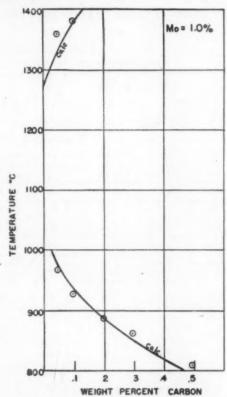


Fig. 5.—System Fe-Mo-C ($\gamma \rightleftharpoons \alpha + \gamma$). (Svetchnikoff and Alferova. 13)

Gamma-carbide Equilibrium.—No experimental data exist on this transformation.

Silicon

Gamma-alpha Equilibrium.—The gamma loop for iron-silicon alloys is known fairly accurately, 17 and from it we find the maximum silicon on the alpha boundary = 2.5 per cent, giving $\Delta G = 485$. As is indicated by the magnitude of ΔG , silicon has a rather small effect on the boundary of the gamma phase. It takes nearly 0.5 per cent Si to change the amount of carbon by 0.05 per cent, an effect produced by a 10° change in temperature over most of the temperature range involved, which means that the uncertainty

to be expected in thermal analysis will be at least a considerable fraction of the effects to be observed.

In Table 5 are given the results of three observers^{18,19,20} for Ac₃ for this system. ΔC , the distance of the point to the right of the

highly probable that manganese was present.

On inspecting the columns showing divergences, we find that the results of Kříž and Pobořil are nearly all high, but irregular, those of Wilhelm and Reschka

Table 5.— ΔC for Ac_3 for Silicon Alloys Calculated ($\Delta G = 450$ cal.). Observed (Corrected; See Text)

Kříž and Pobořil				D:-	. Sato				
Т	Si Per Cent	Calc.	Obs.	Div.	Т	Si Per Cent	Calc.	Obs.	Div.
910	0.74	0.08	0.31	+0.23	890	0.26	0.02	0.04	+0.02
800	1.25	0.13	0.22	+0.09	828	0.54	0.06	0.02	-,0.04
965	1,25	0.12	0.20	+0.08	814	0.50	0.06	0.00	-0.06
935	1.70	0.17	0.50	+0.33	804	0.51	0.06	0.04	-0.02
900	2.33	0.23	0.40	+0.17	790	0.71	0.08	0.02	-0.06
950	3.65	0.36	0.51	+0.15	762	0.54	0.06	0.08	+0.02
1090	3.93	0.36	0.34	-0.02	751	0.53	0.06	0.11	+0.05
	Wilhelm and Reschka				900	0.97	0.10	0.11	+0.01
840	0.30	0.04	0.12	+0.08	831	0.99	0.11	0.08	-0.03
825	0.43	0.05	0.07	+0.02	823	0.98	0.11	0.09	-0.02
832	0.64	0.07	0.15	+0.08	780	1.05	0.11	0.08	€0.03
860	0.88	0.10	0.20	+0.10	768	1,26	0.14	0.02	-0.12
847	0.99	0.11	0.13	+0.02	965	1.34	0.13	0.17	+0.04
852	1.08	0.12	0.14	+0.02	924	1.63	0.17	0.15	-0.02
850	1.17	0.13	0.16	+0.03	830	1.58	0.18	0.11	-0.07
775	1.13	0.13	0.21	+0.08	800	1.45	0.17	0.11	-0.06
					782	1.60	0.18	0.11	-0.07
					923	2.25	0.22	0.22	0
					810	1.80	0.20	0.15	-0.05
	1				790	2.16	0.24	0.13	-0.11

curve for the iron-carbon diagram, was calculated from Eq. 10, using $\Delta G = 450$. The results of Kříž and Pobořil and of Wilhelm and Reschka, were corrected for manganese content; that is, the carbon contents were increased to compensate for the effects of the given percentages of manganese. Other elements present had small effects and practically canceled each other. Sato did not give the complete analysis of his specimens, although it seems

also high, but not by large amounts, while those of Sato average low but show no great divergence. In view of the fact that the manganese probably present in Sato's specimens would make his results too low, the results mentioned above seem to show good concordance with theory.

Gamma-carbide Equilibrium.—A few observations are given by Hanson²¹ and also some by Kříž and Pobořil, ¹⁸ but in view of the small amount of information and

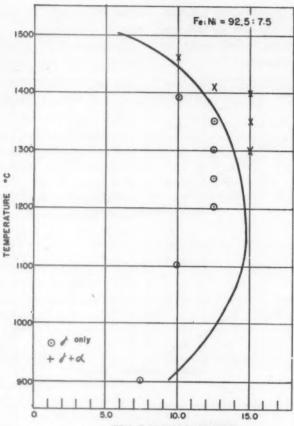
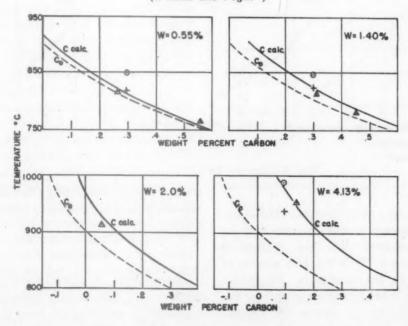


Fig. 6.—System Fe-Ni-W $(\gamma \rightleftharpoons \gamma + \alpha)$. (Winkler and Vogel.16)



As (DILATOMETRIC) \odot gamma phase only + alpha and gamma phases Fig. 7.—System Fe-W-C ($\gamma \rightleftarrows \alpha + \gamma$). (Takeda. 33)

of the uncertainty regarding the relationship of carbides and graphite in this system, it does not seem worth while to attempt a theoretical analysis. from $\Delta G = 1250$ fit the points as well as can be expected.

Gamma-carbide Equilibrium.—Complex carbides only are present at the concen-

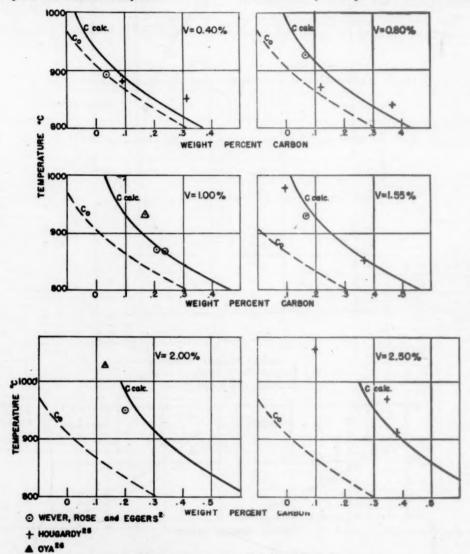


Fig. 8.—System Fe-V-C $(\gamma \rightleftharpoons \gamma + \alpha)$.

Tungsten

Gamma-alpha Equilibrium.—The irontungsten diagram shows a gamma loop for which convincing data are available, 22 with maximum $C_e^{\alpha} = 6.5$ and maximum $C_e^{\gamma} = 3.2$ at the maximum. We obtain $\Delta G = 1250$. When observed points 23 for the iron-tungsten-carbon system are plotted Fig. 7), it is found that curves calculated

tration ranges available, so that the gamma-cementite boundary cannot be studied.

Vanadium

Gamma-alpha Equilibrium.—Since this element, with iron, forms a gamma loop, it is possible to calculate ΔG from the maximum C_c^{α} in equilibrium with the gamma

phase. There is some uncertainty regarding this value, estimates by different observers varying from 1.2 per cent V to about 2.0 per cent, giving corresponding ΔG 's of 2300 and 1200, respectively, with the probability favoring the former. Experimental data 4.26,26 on the boundary of the gamma phase in the Fe-V-C system was plotted in Fig. 8, and it was found that $\Delta G = 2000$, from which the theoretical curves were calculated, gave as good a fit as could be obtained. Although the number of points is not large, it represents three different observers, and no set shows systematic divergence.

Gamma-carbide Equilibrium.—In this system the gamma phase is considered to be in equilibrium with V₄C₃ even at quite low vanadium concentrations.

Iron-nickel-phosphorus

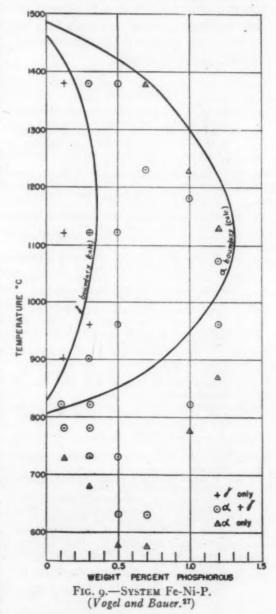
Gamma-alpha- Equilibrium.—As was mentioned previously, the iron-chromium system is an exception to the theory, in that the A_3 point is first lowered and then raised as increasing (but small) amounts of chromium are added. The iron-nickel-phosphorus system is of interest, since it does much the same thing with increasing addition of phosphorus, although phosphorus alone produces a normal type of gamma loop with iron.

In Fig. 9 are plotted the results of Vogel and Bauer²⁷ for this system, with Ni = 2 per cent. The calculated curves are based on $\Delta G_{\rm Ni} = -1050$ (as used in Fig. 6), and $\Delta G_P = 3100$, as determined from the gamma loop of the iron-phosphorus system, and the curves were calculated by Eq. 10 modified for a substitutional solute, and by the corresponding equation for the alpha boundary. The latter gives fairly good agreement, but the gamma boundary shows great distortion as compared with the theoretical curve. Apparently there is a marked interaction of nickel and phosphorus of such nature as to affect the

solubility relationships in the gamma phase.

SUMMARY

Equations have been developed by Zener¹ to permit calculation of phase



boundaries in medium alloy steels in terms of certain constants. The literature has been searched for experimental data from which the constants have been determined for a number of alloying elements. A discussion is given of the degree of consistency with which these empirical constants represent the data. Two systems have been found in clear-cut disagreement with the theory; in certain others the data are insufficient or inconclusive; in a considerable number, however, constants may be chosen that represent the experimental results reasonably closely.

REFERENCES

1. C. Zener: Equilibrium Relations in Medium

C. Zener: Equilibrium Relations in Medium Alloy Steels. This volume, page 513.
 F. Wever and W. Jellinghaus: Mitt K-W-I. Eisenforschung (1932) 14, 105.
 W. Tofaute, A. Sponheuer and H. Bennek: Tech. Mitt. Krupp (1936) 6, 172.
 E. C. Bain: Alloying Elements in Steel, 119.
 T. Ishiwara, T. Yonekura and T. Ishigaki: Sci. Repts. Tohôku Imp. Univ. (1926) 15, 81.

6. M. Hansen: Aufbau der Zweistofflegier-

ungen. Berlin, 1936. 7. M. Gensamer: Amer. Soc. Steel Treat.

(1933) 21, 1028. Wells and F. M. Walters: Trans.

Amer. Soc. for Metals (1935) 23, 751.
9. J. F. Eckel and V. N. Krivobok: Trans. Amer. Soc. for Metals (1933) 21, 846.

10. A. R. Troiano and F. McGuire: Trans.

A. R. Iroland and F. McGuire: 1743.
Amer. Soc. for Metals (1943) 31, 340.

II. J. L. Gregg: The Alloys of Iron and Molybdenum, Chap. II. New York 1932, McGraw-Hill Book Co.

12. V. N. Svetchnikoff and N. S. Alferova:
Theory and Practice of Metallurgy
(Russia) (1936) 4, 72, as quoted by
Herzig: Trans. Amer. Soc. for Metals

(1941) 29, 131.

13. J. S. Marsh: Alloys of Iron and Nickel, 1, chap. II. New York, 1938. McGraw-Hill Book Co.

14. T. Kasé: Sci. Repts. Tohôku Imp. Univ.

(1925) 14, 173. 15. J. A. Jones: Jnl. Iron and Steel Inst. (1928)

117, 295. 16. K. Winkler and R. Vogel: Archiv Eisen-

huttenwesen (1932) 6, 165. 17. E. S. Greiner, J. S. Marsh and B. Stoughton: The Alloys of Iron and Silicon, 38. New York, 1933. McGraw-Hill Book Co. 18. A. Kříž and Pobořil: Jnl. Iron and Steel

Inst. (1930) 122, 191. 19. T. Sato: Tech. Repts. Tohôku Imp. Univ.

(1931) 9, 515. 20. H. Wilhelm and J. Reschka: Archiv Eisen-

huttenwesen, (1939) 12, 607.
21. D. Hanson: Jnl. Iron and Steel Inst.
(1927) 116, 129.
22. W. P. Sykes: Trans. A.I.M.E. (1931) 95,

23. S. Takeda: Tech. Repts. Tohôku Imp.
Univ. (1931) 9, 627.
24. F. Wever, A. Rose, and H. Eggers: Mitt.
K-W-I. Eisenforschung (1936) 18, 239.
25. H. Hougardy: Archiv Eisenhuttenwesen

(1931) 4, 497.

26. M. Oya: Sci. Repts. Tohôku Imp. Univ. (1930) 19, 331. Vogel and H. Bauer: Archiv Eisen-

27. R. huttenwesen (1931) 5, 275.

DISCUSSION

(R. F. Mehl presiding)

(This discussion refers also to the paper by Clarence Zener that begins on page 513.)

L. S. DARKEN.*-Dr. Zener presents a very interesting schematic picture, particularly in Fig. 9, of the influence of alloying elements on equilibria involving iron. The quantitative development presented, however, is a bit confusing. This development is primarily an application of well-known laws of dilute solutions, but involves also an additional assumption which seems unwarranted.

The derivation in appendix B, which leads to the equations used, is in a sense independent of the statistics. Combination of Eqs. B-8 and B-10 leads to the following equation for the change in "atomic free energy" accompanying the transfer of N, atoms of type i from one phase to another

$$\partial G_a = -kT\Sigma \ln C_i \partial N_i$$

(for the sake of simplicity interstitial solid solutions other than in the face-centered cubic or γ phase are omitted and B = 0). Considering now the transfer corresponding to as many gram atoms as are represented by the chemical equation representing the equilibrium, the above reduces to

$$\Delta G_{\alpha} = -RT \ln K_{\infty}$$

in which K_m is the familiar mass law constant; the concentrations used therein are to be expressed as usual in terms of atom fraction for substitutional solid solutions and in nearly identical units for small amounts of interstitial elements in the γ phase.

The meaning of ΔG_a may be made clear by consideration of the relation between the thermodynamic equilibrium constant and the free energy change when all substances involved are in the standard state

$$\Delta G^0 = -RT \ln K$$

This thermodynamic equilibrium constant is written in terms of activities and may be expressed in terms of the mass law constant

Research Chemist, U. S. Steel Research Laboratory, Kearny, New Jersey.

by introducing activity coefficients thus

$$\Delta G^0 + RT \ln \frac{\gamma_1 \gamma_2 \dots}{\gamma_1 \gamma_2 \gamma_2 \dots} = -RT \ln K_m$$

By comparison of this strictly thermodynamic relation with that first written it is seen that ΔG_a is equal to the standard free energy change plus a term involving the activity coefficients that measure the departure from ideal solution behavior.

If the treatment is restricted to very dilute solutions, this second term may be regarded as constant at constant temperature, and may, by proper choice of standard state, be included in the first.

Thus ΔG_a is identical with the standard free energy change providing the standard state is properly chosen. West makes essentially this same statement. Zener claims this quantity has this significance only for iron and regards it usually as a heat change (ΔH) for other elements dissolved therein, and gives it no physical meaning in the general case; this is very puzzling.

The manner in which the standard free energy change of a reaction varies with temperature is one of the primary problems in a large number of thermodynamic investigations. In fact, the bulk of the application of thermodynamics to metallurgy has consisted of the formulation of this free energy change as a function of temperature.

In general, as is well known, the relation is complex—an example being the free energy change accompanying the transition from α to γ iron as shown by Zener in Figs. 1 and 2.

In other cases it is approximated over short ranges of temperature by an expression of the form $\Delta G^0 = a + bT$ where a and b are constants; in such cases $a = \Delta H^0$ and $b = \Delta S^0$. The variation with temperature is frequently very great—several thousand calories per 100°C.

In the present papers the surprising assumption is made that for the equilibria considered ΔG^0 is a constant.

Nearly all the calculations are based thereon. From the second law of thermodynamics it follows directly that the first derivative of the standard free energy change with respect to temperature is the standard entropy change.

Hence if the standard free energy change is a constant, the standard entropy change is zero. Thus Zener's postulate is equivalent to the statement that the entropy change is zero at all temperatures for all reactions involving crystalline substances in their standard states.

The third law of thermodynamics states that this is so at the absolute zero of temperature but reference to any table of entropies of formation will immediately convince one that it is by no means true at other temperatures. Hence it is clear that Zener's fundamental postulate is theoretically unsound.

In the cases considered, the variation of ΔG with temperature may be reasonably small and the experimental error is regrettably quite large, so that the error involved may be partially concealed.

In the iron-carbon system, where the experimental data are probably the best of the systems considered, it might be thought that Fig. 7 of Zener's paper constitutes an excellent corroboration of the assumption. However, it is to be noted that in this case the amount of carbon in the alpha phase is very small, hence ΔG_{α} is a large negative quantity and the effect of this term on the calculated composition of the gamma phase in equilibrium with the alpha phase is negligible, since it occurs exponentially in Eq. 8.

Moreover, as mentioned in appendix A, the carbon content at the eutectoid was used to establish ΔG_{F_0} so that the agreement shown in Fig. 7 is forced, at least at this point.

In the other cases considered (e.g., those depicted in Figs. 5, 6 and 8) the agreement is also to some extent forced.

In view of this and the lack of precision of the experimental data, it can hardly be said that there is experimental verification of the startling postulate of the constancy of ΔG . The Fe-Cr system considered by West is admittedly in marked disagreement with the theory and it seems only reasonable to conclude that a theory that is fundamentally open to such serious question, and that may lead to such a wide discrepancy, leaves much to be desired.

Thus it is seen that the theoretical treatment is based on well-known laws of dilute solutions plus an assumption that appears to be unjustified.

In addition to the objections already made to this hypothesis, it seems appropriate also to question the adequacy of the laws of dilute solution as applied to the cases considered in medium alloy steels.

Recent precise measurements in our laboratory by Dr. R. P. Smith show that in the iron-carbon system at 1000°C. the activity coefficient of carbon changes about 60 per cent between zero and 1.5 per cent C. This is a rather marked departure from ideal behavior.

Measurements of this sort are far from numerous in the metallurgical field. A few binary liquid alloys have been investigated.

Measurements of Schneider and Schmidt²¹ indicate that the activity coefficient of gold in zinc-gold alloys changes by a factor of two between zero and 7 atom per cent gold.

In the ternary systems the indications are that the departure from ideal solution laws is even greater. The measurements of Marshall and Chipman²² indicate that in liquid steel the activity coefficient of oxygen (in small amounts) is depressed to one third its original value by the presence of 2 per cent carbon. Preliminary measurements in our laboratory indicate that in austenite the presence of 4 per cent silicon increases the activity of carbon by a factor of two.

Thus the indications are that departures from the simple solution laws play a large role in the physical chemistry of steel and it would seem more fitting at this time to emphasize and, if possible, interpret, these departures rather than to oversimplify the picture.

For example, in the austenitic iron-siliconcarbon alloys it is possible to shed a little light on the marked ability of silicon to depress the solubility of carbon. Let it be supposed that it requires very high energy for a carbon atom to occupy an interstitial position immediately adjacent to a silicon atom. Then there will be a negligibly small number of carbon atoms in such positions; but there are six such positions for every silicon atom.

In a 4 per cent Si-Fe alloy, the atom per cent of silicon is about 8, hence six times this, or 48 per cent, of the interstitial positions are barred to carbon atoms.

On this basis, then, it would be expected that the solubility of carbon would be only about half as great in the alloy as in iron—a fact verified by experiment. This example is given merely to illustrate the type and magnitude of the effect that has been ignored in the present papers, but which seems of considerable importance and awaits a competent treatment perhaps by the methods of statistical mechanics.

C. ZENER (author's reply).-Mr. Darken has added considerably to the discussion of these papers by emphasizing the assumptions made therein. For this, the authors are deeply indebted. A real difference of opinion exists. however, regarding the value of the results obtained using these assumptions, a difference that no doubt stems from a divergence in their approach to scientific problems. In obtaining an understanding of a problem the writer prefers first to see under what simplifying assumptions the broad features of the problem may be explained, and then to relax these simplifying assumptions only as deviation of the theoretical deductions with experiment demand. In the particular problem under consideration, the equilibrium relations of medium alloy steels, the published experimental data require a modification of the assumptions only for the alloying elements of chromium and cobalt, and for the ternary system Fe-Ni-P, as was explicitly stated in the papers. The science of the metallurgy of steel will indeed be enriched through publication of data of the type Mr. Darken indicates has been obtained in his laboratory, data that may require a relaxation of the simplifying assumptions herein made. However, the data* that have come from his laboratory since the meeting, describing the influence of carbon upon the Fe-Si system, is in striking agreement with the results of this paper, an agreement that is discussed elsewhere.† Perhaps the other data likewise are not in such disagreement as Mr. Darken believes.

Of the two assumptions introduced, that of dilute solutions is fundamental to the analysis. Only through this assumption is one

²¹ Schneider and Schmidt: Ztsch. Elektrochemie (1942) 48, 627. ²² Marshall and Chipman: Trans. Amer.

Soc. for Metals (1942) 30, 695.

^{*} R. L. Rickett and N. C. Fick: Constitution of Commercial Low-carbon Iron-silicon Alloys. This volume, page 346.

[†] This volume, page 354.

able to deduce the equilibrium of ternary and higher order systems directly from the equilibrium of the binary systems. The real question of dispute is not whether this assumption is correct, for of course it is only an approximation. The question is rather whether the assumption of a dilute solution corresponds sufficiently close to reality in medium alloy steels so that the conclusions deduced therefrom are of aid in understanding equilibrium relations.

The second assumption, constancy of ΔG_a for the alloying elements, is not essential to

the analysis, and was made only because the published data do not give any clue as to how it varies with temperature. The regarding of ΔG_a as constant over a limited temperature range is not equivalent to regarding ΔS_a as zero; rather, it amounts to neglecting the variation of $T\Delta S_a$ with temperature over that temperature range. The writer adheres to his original statement that ΔG_a has physical significance only for the solvent iron. We cannot impart physical meaning to it simply by assigning to it the label "standard free energy."

Kinetics of the Decomposition of Austenite

By Clarence Zener,* Junior Member A.I.M.E.

(New York Meeting, October 1945)

CONTENTS

	PAGE
General Principles	 551
Equilibrium Diagrams	 551
Nucleation	
Kinetics of Phase-boundary Propagation	 555
Kinetics of Growth of New Phase	
Spheroidization	 560
Pure Iron-carbon System	 561
Formation of Pearlite	 561
Interlamellar Spacing	 562
· Pearlite C-curve	 563
Bainite Formation	 565
Formation of Martensite	 570
Loss of Tetragonality of Martensite	 570
Effect of Alloys upon Decomposition of Austenite	 572
Pearlite	 572
Bainite and Martensite	 574
Time-temperature-transformation Curves	 576
Appendix A	
Appendix B	 580
Annendix C	-80

INTRODUCTION

THE present investigation started in an attempt to understand certain details of the decomposition of austenite, and of the effect of alloying elements thereon. As the investigation proceeded it became apparent that not only these details, but all the general features of austenite decomposition, could be understood in terms of

fundamental physical principles. Since the direct applicability of these physical principles has not been previously recognized, it was decided to incorporate the original results of the investigation into a review of the general subject of the kinetics of austenite decomposition. This review constitutes the present article. An extended summary of the results is given on pages 576 to 579.

This article, which deals with the kinetics of phase transformations, may appropriately be considered as a sequel to two recent articles^{1,2} from this laboratory on the equilibrium relations in medium alloy steels.

NoLogy, January 1946.

Principal Physicist, Watertown Arsenal (on leave, Professor of Physics, Washington State College). Now Professor of Metallurgy in the Institute for the Study of Metals, University of Chicago.

The statements or opinions expressed in this article are to be considered those of the author, and do not necessarily express those of the Ordnance Department. Manuscript received at the office of the Institute March 3, 1945. Issued as T.P. 1925 in METALS TECHNOLOGY. January 1946.

¹ References are at the end of the paper.

GENERAL PRINCIPLES EQUILIBRIUM DIAGRAMS

As is well known, many conventional equilibrium diagrams do not represent true equilibrium conditions. This is true

is not taken explicitly into account. When the interface is curved, as it always is if one phase is dispersed and the other phase is continuous, the equilibrium concentrations are not those given by the equilibrium diagrams. As was first pointed out by

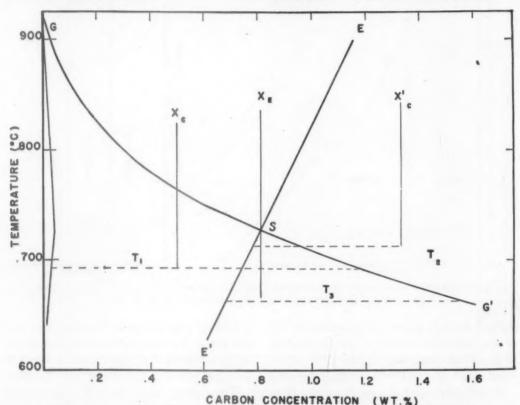


Fig. 1.—Method of determining carbon concentration in austenite just ahead of an advancing ferrite or cementite grain.

of the iron-carbon diagram as usually drawn, since cementite may decompose with the formation of graphite. Such a lack of true equilibrium in no way detracts from the usefulness of the conventional diagrams, since, when properly used, they do represent the actual equilibrium concentrations in the absence of nuclei of the more stable phase.

Caution must be used in the interpretation of equilibrium diagrams, even those representing true equilibrium. In such diagrams the implicit assumption is usually made that the interface between two phases is a plane. In other words, surface tension Gibbs, the equilibrium relations must then be computed from first principles, using the condition that any transfer of atoms must be accompanied by no change in free energy.

Equilibrium relations have physical significance even when the system as a whole is not in equilibrium, as when a new dispersed phase is growing in an undercooled continuous phase. As an example, the case of the growth of ferrite grains from a hypoeutectoid austenite will be considered. The advance of the phase boundary is accompanied by two distinct phenomena: (1) a shift in the position of

each lattice atom so as to produce a bodycentered structure from a face-centered structure; (2) a diffusion of carbon atoms away from the advancing interface. The According to the viewpoint herein adopted, the growth of one phase in another is therefore completely specified by the partial differential equations that govern

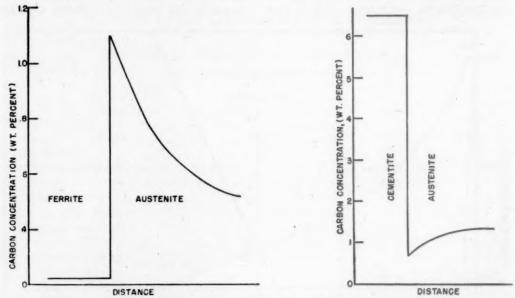


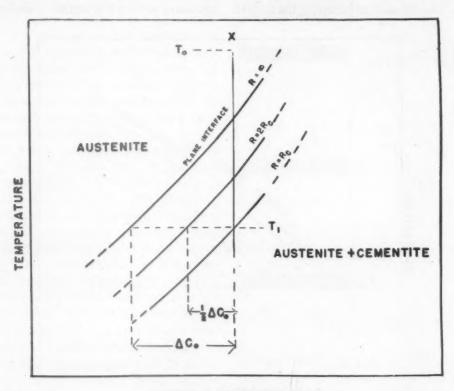
Fig. 2.—Variation of Carbon concentration on two sides of advancing phase boundaries. Examples of hypoeutectoid and hypereutectoid steels of Fig. 1.

shift of an iron atom on the austenite side of the phase boundary to the ferrite side of the phase boundary represents a movement that is relatively small compared with the movement of a carbon atom from one interstitial position to another. One therefore anticipates that the rate at which the ferrite grain grows will be determined solely by the diffusion of the carbon atoms and not by the transfer of the iron atoms from the austenite to the ferrite lattice positions, except of course in the case of very small carbon concentrations. According to this viewpoint, the position of the phase boundary will be determined solely by the condition that the free energy be a minimum. The rate of advance is just such as to maintain the equilibrium concentration of carbon on the austenite side of the interface. How fast this rate of advance must be in order to maintain this equilibrium concentration depends in turn upon the rate at which the carbon diffuses away.

diffusion, together with the condition that the phase boundaries move at such a rate as to maintain the equilibrium concentration just ahead of the advancing boundary.

The extensions of the phase boundaries into the so-called metastable regions have just as much physical meaning as have the phase boundaries themselves. Such extensions are illustrated in Fig. 1 for the iron-carbon system. Thus, suppose a hypoeutectoid steel of carbon concentration X_e is quenched to the temperature T_1 . Free ferrite will then begin to grow. The composition of the austenite just ahead of an advancing ferrite grain with a plane boundary is then given by the value of the extension SG' at T_1 . Similarly, if a hypereutectoid steel of composition X_c' is quenched to the temperature T_2 , free cementite will begin to grow. The carbon concentration in the austenite just ahead of an advancing cementite grain with a plane boundary will be given by the value of the extension SE' at T_2 . Finally, if a nearly eutectoid steel is quenched to the temperature T_3 , both ferrite and cementite will begin to form. If the phase boundaries

the system, including the interface energy. This condition acts as a severe hindrance to the initiation of grains of the new phase. The mechanism of this restraint may best



CARBON CONCENTRATION

Fig. 3.—Schematic illustration of variation of equilibrium relations with curvature of interface surface.

could be regarded as plane, the austenite just ahead of the advancing ferrite and of the advancing cementite grains would have the compositions given by the extensions SG' and SE', respectively, at T_3 . The modification of the concentrations due to the finite curvature of the phase boundaries is of precisely the same nature as when the ferrite and cementite form above the eutectoid temperature where the conventional equilibrium diagrams are applicable.

NUCLEATION

As has been mentioned, the condition for growth of a new phase is that such growth decrease the total free energy of

be illustrated for the case of a spherical grain. If the radius of a spherical grain increases from R to $R + \Delta R$, the ratio of the increase in volume to the increase in surface area is (1/2) R. Therefore the ratio of the free energy liberated by the volume transformation to the free energy needed to increase the interface varies as R. At any given temperature below the equilibrium temperature a critical radius will therefore exist such that all the free energy liberated by the transformation is used up in increasing the area of the interface. If the radius is smaller than this critical value. the total free energy would be increased rather than decreased by growth. Grains having radii smaller than the critical value will therefore become smaller and finally completely disappear.

This thermodynamical argument explains the difficulty of initiating the growth size in contradiction to the laws of thermodynamics. This probability may, in principle, be computed. It is proportional to $exp \{-G_e/kT\}$, where G_e is the free energy necessary to form the particle of critical size

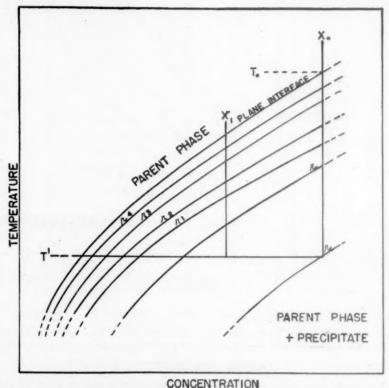


FIG. 4.—ILLUSTRATION OF MECHANISM OF SPHEROIDIZATION OF PLATE AT THE INITIAL TEMPERATURE OF FORMATION.

of a thermodynamically stable phase, a difficulty that is illustrated by the numerous well-known examples of undercooling. A serious problem arises in understanding how a grain can ever attain its critical size, since, according to thermodynamics, smaller grains can only grow still smaller. The standard method of resolving this problem is by means of the theory of nucleation.^{3,4,34}

According to the science of statistical mechanics, thermodynamics tells only what is most likely to happen, not what must happen. It is therefore possible, but perhaps very unlikely, that a grain may grow from atomic dimensions to the critical

and k is Boltzman's constant, 3.3×10^{-24} cal. per degree centigrade. Grains of the critical size are called nuclei, and their formation is called nucleation.

Two properties of the nucleation factor $exp \{-G_e/kT\}$ are of particular pertinence to the present discussion. The free energy G_e becomes infinite as the amount of undercooling becomes zero. The explicit expression for G_e may readily be shown (Appendix B) to be

$$G_{\bullet} = (16\pi/3) \times G_{\bullet}^{3}/(\Delta G_{\bullet})^{2}$$
 [1]

where G_s is the energy of the interface per unit area, and ΔG_s is the free energy liberated per unit volume by the transfor-

mation. The interface free energy is nearly independent of temperature, while the volume free energy is proportional to the amount of undercooling ΔT . Therefore

$$G_a \sim 1/\Delta T^2$$
 [2]

so the nucleation factor rapidly approaches zero as the amount of undercooling itself approaches zero. As a consequence, the rate of formation of a new phase is always zero at the critical temperature, and increases to a maximum value at some finite amount of undercooling.

The second important property of the nucleation factor $exp \{-G_c/kT\}$ is its extreme smallness. As a consequence of this smallness, nucleation will proceed in the manner in which the critical free energy is a minimum, however improbable such nucleation may seem. The condensation of water vapor may be cited as a familiar example of this deduction. The critical free energy of a water droplet is much smaller when the droplet contains an electric charge than when it contains none. The path of a single high-speed electron in a supersaturated vapor may therefore be detected by the droplets that condense about molecules ionized by the electron. Similarly, the critical free energy of a precipitate from a solid solution is much smaller when the precipitate is adjacent to some imperfection than when it occurs in a perfect lattice. Grain boundaries constitute a common type of imperfection. As an example of the influence of grain boundaries in aiding nucleation, the case of cementite precipitating from eutectoid austenite will be considered. At 100°C. below the eutectoid temperature, the critical free energy for a nucleus is 1.0 × 10⁻¹⁴ cal., provided the nucleus is completely surrounded by an austenite matrix (Appendix B). For this case the nucleation factor is 10-1,300,000. If, on the other hand, the nucleus is a hemisphere bounded on its plane side by a grain boundary, and if the interface energy is the same between the new and old phase as between two grains of the same phase, the nucleation energy is only one half of its previous value. The grain-boundary nucleation factor is there-

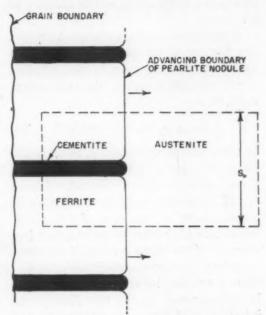


Fig. 5.—Illustration of advancing pearlite nodule.

fore 10^{-650,000}, which is 10^{650,000} times as large as for nucleation within the grain. The factor 10^{650,000} is so large as to ensure that nucleation will occur at the grain boundary rather than in the interior of a grain, in spite of the fact that there are many more potential nucleation positions within the grain than on the grain boundaries.

KINETICS OF PHASE-BOUNDARY PROPAGATION

The advance of an interface boundary may involve only a change in lattice type, as in an allotropic transformation of a pure metal. The advance may also involve only a change in composition, as may occur when two elements of the same lattice types are completely soluble in one another at a high temperature but not at a lower temperature. Finally, the advance of an interface boundary may involve both a change in lattice type and a change in composition. This last case is the most common of the three, and is the only one that will be discussed here. In this discussion only a single solute will be assumed to be present.

If the phase boundary remained stationary, the ratio of the concentration of solute atoms on the two sides of the interface would rapidly approach the equilibrium ratio; i.e.,¹

$$C_2/C_1 = (\beta_2/\beta_1)e^{-(g_2-g_1)/RT}$$
 [3]

In this equation the subscript refers to the phase, β is unity in the case of substitutional solutes, is equal to the ratio of number of interstitial positions to number of lattice atoms in the case of interstitial solutions, and G refers to the standard free energy^{1,2} of the solute per mol. If the phase boundary advances sufficiently rapidly, there is not time for an appreciable change in concentration on the two sides of the interface, and the concentration of the solute remains unchanged.

The equilibrium ratio is essentially maintained whenever the rate at which the phase boundary advances is limited primarily by the rate of diffusion of the solute atoms away from or toward the advancing phase boundary. This situation appears to arise in the high-temperature decomposition of austenite into free ferrite, free cementite, or pearlite. The phase boundary can advance without any change in composition only when the temperature is sufficiently low so that the free energy of the system is decreased by such advance. As is discussed later, this situation arises in the formation of low-temperature bainite. It is also possible that the phase boundary advances at such a rate that the equilibrium ratio of solute concentration on its two sides is partially but incompletely attained. It will be shown later that this is the situation in the formation

of high-temperature bainite. In such

an intermediate case, the kinetics of

the phase-boundary advance is especially complex. The simpler case of complete equilibrium on the two sides of the phase boundary is discussed in detail in the following paragraphs.

The variation of the solute concentration on the two sides of an advancing phase boundary is shown schematically in Fig. 2. In computing the velocity of the phase boundary V_B , the assumption will be made that the density of the solvent atoms is essentially the same in the two phases, thereby avoiding an irrelevant complication. We shall let the concentrations C_1 and C_2 refer to the number of solute atoms per unit volume of the two phases. The current density of atoms in the old phase away from the phase boundary is then given by

Current density =
$$(C_2 - C_1)_B V_B$$

where current density refers to the net number of solute atoms that cross a unit area in unit time. The current density may also be expressed in terms of the atomic diffusion coefficient D by the following equation

Current density =
$$-D(\delta C_2/\delta X)_B$$

where X refers to the coordinate normal to the phase boundary and whose positive axis extends into the old phase. Combining these two equations for the current density gives:

$$V_{B} = \frac{-D}{(C_{2} - C_{1})_{B}} \cdot (\delta C_{2} / \delta X)_{B}$$
 [4]

In certain cases, such as the growth of cementite, the concentration C_1 is fixed. In others, as in the growth of ferrite, this concentration is to some extent indeterminate. The only unavoidable restriction upon C_1 is that it be such that in no element of volume can the free energy be increasing. Upon applying this restriction to an element containing the interface, it is found in Appendix A that

$$(C_2 - C_1)_B \le \Delta G/kT$$
 [5]

where k is Boltzman's constant and ΔG is the free energy liberated by the transfer of a unit volume of solvent from pure phase No. 2 to pure phase No. 1. When the equality sign is valid in Eq. 5, no free energy is dissipated at the interface boundary itself as the boundary advances; all the

sign in Eq. 5 is valid. This equality sign in Eq. 5 will therefore be assumed to be valid unless special consideration demands otherwise; i.e.,

$$(C_2 - C_1)_B = \Delta G/kT$$
 [6]

It is to be noted that Eqs. 3 and 6 are just

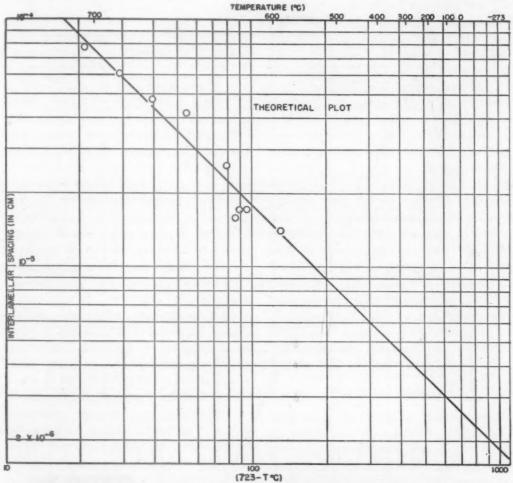


Fig. 6.—Variation of interlamellar spacing with temperature, plotted according to theoretical equation 13.

Straight line has slope of -1. Data for eutectoid steel A of reference 11.

free energy is dissipated by the diffusion of the solute atoms ahead of the advancing boundary. Eq. 4 and Fig. 2 show that the gradient of C_2 at the boundary increases in magnitude with $(C_2 - C_1)_B$ faster than $(C_2 - C_1)_B$ itself. The velocity of the phase boundary may hence be seen from Eq. 4 to have a maximum value when the equality

the equations that determine the concentration of the solute in two phases when they are in absolute equilibrium.

KINETICS OF GROWTH OF NEW PHASE

The general principles that govern the growth of a new phase into an old phase have been discussed by Carpenter and Robertson.⁶ In the present section the principles that they clearly enunciated are presented in a more quantitative form than heretofore.

The velocity with which every part of the phase boundary propagates is given by Eq. 4. In this equation the concentration gradient $(\delta C_2/\delta X)_B$ may be represented as the ratio

$$-(\delta C_2/\delta X)_B = \Delta C/L$$
 [7]

Here ΔC is the difference in carbon concentration in the parent phase just at the advancing boundary and far away from

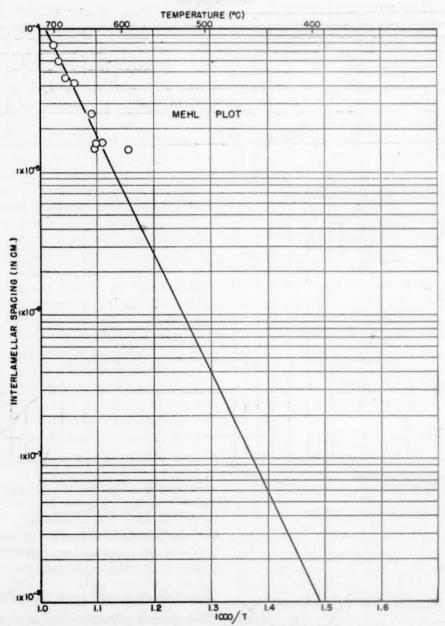


FIG 7.—VARIATION OF INTERLAMELLAR SPACING WITH TEMPERATURE, PLOTTED ACCORDING TO METHOD OF MEHL.

Same data as plotted in Fig. 6.

the boundary. It is this concentration difference that gives rise to diffusion. The quantity L has dimensions of length, and will in every case be related to some linear dimension of the advancing phase.

Combining Eqs. 4 and 7 gives

$$V_B = \frac{\Delta C}{(C_2 - C_1)_B} (D/L)$$
 [8]

Since in this equation the concentrations occur only as a ratio, they may be expressed in any desired units.

From Eq. 8, one may reach certain conclusions regarding the shape of a growing grain, conclusions that may also be reached from general considerations upon diffusion.6 If the phase boundary were a plane of such large extent that diffusion was everywhere normal to the plane, the effective diffusion distance L would gradually increase, thereby lowering the velocity of growth. On the other hand, if the phase boundary is convex toward the parent phase, as it usually is, the effective diffusion distance L will be comparable to the radius of curvature of the surface. From this fact, one therefore deduces that the smaller the radius of curvature the more rapid the rate of growth. If a grain grew as a spheroid, its linear rate of growth would gradually decrease as its size, and hence the radius of curvature of its surface, increased. On the other hand, a plate may grow edgewise and maintain a constant radius of curvature at the growing surface, and therefore also a constant rate of growth. The rate at which the thickness of such a plate increases will gradually decrease with time, as previously explained. An initially platelike grain will therefore remain platelike. On the other hand, a growing spheroidal grain will not remain spheroidal, for the slightest fluctuation from a spherical form will grow, resulting finally in a plate. This facility with which plates grow edgewise compared with the radial growth of spheroids explains the nearly universal occurrence⁷ of platelike structures in the initial stage of precipitation in solid solutions.

One might surmise from the preceding discussion that the radius of curvature of the edge of a plate would continually decrease as it advanced. A lower limit to this radius of curvature is imposed however by the change in equilibrium relation with change in curvature of the interface. The example of a free cementite plate growing in austenite is shown in Fig. 3. It is supposed that when the steel is at a high temperature To it has a homogeneous austenite structure of carbon concentration X. When the temperature is now lowered to T_1 , the concentration of carbon in the austenite, which is in equilibrium with the cementite, is $X - \Delta C_0$, provided the interface is plane. The maximum concentration difference in the austenite just at the interface and further away is therefore ΔC_0 . On the other hand, if the interface is convex toward the austenite, as it must be for continued rapid growth of cementite, the boundary of the gamma phase is lower than for a plane interface; therefore the concentration difference is less than ΔC_0 . Since for small curvatures of interface the shift in boundary is proportional to the curvature, the concentration difference is given by

$$\Delta C = (\mathbf{1} - r_c/r)\Delta C_0 \qquad [9]$$

where r_e is the critical radius of curvature at which the concentration difference is zero. Upon combining Eqs. 8 and 9, one may now determine what curvature the edge of an advancing plate approaches. This limiting curvature will be such as to make the velocity of advance V_B a maximum. Since the effective diffusion distance L is proportional to the radius of curvature r, the radius of curvature will approach the value that maximizes the ratio $(\mathbf{1} - r_e/r)/r$. This value is $2r_e$.

Fig. 3 shows that when the radius of curvature of the interface is $2r_c$, the amount of undercooling is exactly half its value for

a plane interface. Since the change in free energy is proportional to the amount of under-cooling, we conclude that as the plate advances, only one half the available free energy is irreversibly dissipated in diffusion, the other half remaining as interface energy.

We are now in a position to determine how the velocity varies with temperature. The concentration difference ΔC that causes diffusion in the parent phase is proportional to the amount of undercooling ΔT . The effective diffusion distance L is proportional to r_c , which in turn is inversely proportional to ΔT . Finally, the diffusion coefficient varies with temperature as

$$D \sim e^{-Q/RT}$$
 [10]

Upon combining these three factors, we obtain from Eq. 8,

$$V_B \sim (\Delta T)^2 e^{-Q/RT}$$
 [II]

This velocity is very small at small amounts of undercooling due to the small concentration difference ΔC , which drives the diffusion, and to the large distances over which diffusion must occur. It is also very small for larger amounts of undercooling, because of the slow rate of diffusion at low temperatures. An intermediate amount of undercooling exists at which V_B is a maximum.

SPHEROIDIZATION

If only a single grain were growing in a matrix, it would continue to extend indefinitely. That portion which was extending the most rapidly would maintain a constant radius of curvature; namely, twice the critical radius r_e . The growing grain would therefore maintain a platelike shape. In all actual cases, neighboring growing grains eventually impede growth. Such an impediment may be taken account of phenomenologically by considering the concentration of the parent matrix to be gradually changing. If the growing phase can be regarded as a precipitate, such as

cementite, the concentration of the parent phase may be regarded as gradually decreasing. Such a decrease in concentration will eventually lead to the spheroidization of the original plates, even though the temperature be maintained constant. The mechanism of such spheroidization is discussed in the following paragraphs.

The process of spheroidization may best be described by reference to Fig. 4. In this figure are drawn the boundaries of the parent phase for a series of values of the radius of curvature of the interface, the curvature being taken as convex toward the parent phase. The uppermost boundary corresponds to a plane interface, the lowermost boundary to an interface with the critical radius of curvature for the concentration X_0 and temperature T^1 . If now the temperature of the parent phase with concentration X₀ is suddenly lowered to and maintained at T^1 , the radius of curvature of the advancing phase will be $r_0 = 2r_e$, as previously explained. This radius of curvature is that for which the rate of growth is a maximum. As growth proceeds, the concentration of the surrounding parent phase is gradually reduced by the growth of neighboring grains. The critical radius of curvature, as well as the actual radius of curvature, will therefore increase. Thus when the concentration has been reduced to X_1 , the actual radius of curvature is increased to r1, etc. As growth proceeds, and the concentration of the parent phase becomes reduced, the critical radius of curvature will increase so fast that the actual radius of curvature will begin to lag behind the radius for maximum rate of growth; namely, twice the critical value. Finally the critical radius of curvature will become equal to the actual radius. At this time growth ceases at the edges. Further growth can then proceed only upon the faces. As the critical radius of curvature further increases, the edges begin to dissolve. Spheroidization has then commenced.

PURE IRON-CARBON SYSTEM FORMATION OF PEARLITE

The manner in which a single ferrite or a single cementite grain grows isothermally depends markedly upon whether the temcementite nuclei. Similarly, a cementite grain growing above the eutectoid temperature can continue to extend indefinitely until impeded by neighboring grains, while below the eutectoid temperature it will eventually become surrounded by ferrite.

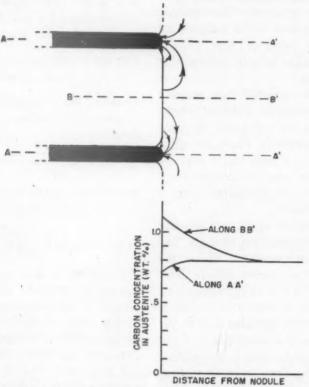


Fig. 8.—Carbon concentration in austenite ahead of advancing pearlite nodule, drawn for 700°C. After concept of Hultgren. 15

perature of growth is above or below the eutectoid temperature. If a ferrite grain grows above the eutectoid temperature, the carbon concentration of the austenite immediately surrounding the growing grain is along the boundary GS in Fig. 1, and is therefore not sufficiently high for cementite nuclei to form and grow. The grains therefore will grow indefinitely, given time, until impeded by neighboring grains. On the other hand, if the temperature is below the eutectoid, the carbon concentration in the austenite immediately surrounding the grain lies upon SG', and is therefore sufficiently high for the formation of stable

The growth of either a ferrite or a cementite grain below the eutectoid temperature cannot at present be adequately described, since the theory for nucleation in the surrounding austenite has not been developed.

If the temperature is below the eutectoid, and the carbon concentration lies between SE' and SG', ferrite and cementite nuclei may form and grow simultaneously. In such cases the cementite and ferrite grow as parallel plates, and form what is known as pearlite. The laws of formation of pearlite are described in the following sections.

Interlamellar Spacing

The temperature variation of interlamellar spacing in pearlite of eutectoid composition has been the subject of careful experimental study by Mehl and his collaborators.⁸⁻¹² The pearlite that forms just below the eutectoid temperature has comparatively large spacing. This spacing decreases continuously as the temperature of formation is lowered. The pearlite finally becomes so fine as to be unresolvable by the microscope.

The minimum possible interlamellar spacing S_0 in eutectoid pearlite formed isothermally may be computed by pure thermodynamic methods. From the arguments presented on page 10, it may be deduced that the pearlite in which the spacing is twice this minimum spacing grows the most rapidly.

In the computation of S_0 , one inquires as to what is the condition that the free energy of the complete system be lowered by the growth of a pearlite nodule. This condition is that the free energy released by the transformation be more than sufficient to supply the energy associated with the interface between the cementite and the ferrite plates. In order that this condition may be expressed in a precise mathematical form, a pearlite nodule of interlamellar spacing S_0 is considered to be advancing into the parent austenite, as illustrated in Fig. 5. An equation will be set up which says that as the nodule grows the free energy remains unchanged in a region that includes one cementite and one ferrite plate. This volume is indicated by dotted lines in Fig. 5, and will be considered to have the depth W. When the nodule advances a distance dX, the volume of austenite transformed in the region under consideration is $S_0 \cdot W \cdot dX$, and therefore the mass of the austenite transformed is $\rho S_0 \cdot W \cdot dX$, where ρ is the density. The free energy that is available at temperature T for the formation of new interfaces is therefore

Available free energy

$$= Q \cdot \frac{T_{\bullet} - T}{T_{\bullet}} \cdot \rho S_{0} \cdot W \cdot dX \quad [\text{II}a]$$

where Q is the heat of transformation per unit mass and T_s is the eutectoid temperature. The increase in the total interface area is $W \cdot 2dX$. Upon taking S as the surface energy per unit area, the increase in interface energy is given by

Increase in interface energy

$$= 2S \cdot W \cdot dX$$
 [11b]

Equating the available free energy to the increase in interface energy, therefore, gives

$$Q \cdot \frac{T_0 - T}{T_0} \rho S_0 = 2S \qquad [12]$$

The solution of this equation for the interlamellar spacing gives

$$S_0 = \frac{2T_o S}{\rho Q(T_o - T)}$$
 [13]

According to Eq. 13, the interlamellar spacing is inversely proportional to the amount of undercooling. Therefore a plot on log paper of the interlamellar spacing vs. the amount of undercooling should give a straight line with a slope of -1. Such a plot is given as Fig. 6, of the data from reference 11 for a eutectoid steel. The data are seen to be consistent with Eq. 13.

By extrapolation, one surmises from Fig. 6 that if pearlite could form at the absolute zero its interlamellar spacing would be of the order of magnitude of 200A. This conclusion is in violent contradiction to the view of Mehl8 that the interlamellar spacing has a heat of activation, and approaches atomic dimensions at temperatures not far below the nose of the S-curve. The same data that were plotted in Fig. 6 have also been plotted in Fig. 7 according to Mehl's viewpoint; i.e., the log of S_0 vs. 1/T. The experimental points fall upon a straight line in this graph, just as in Fig. 6. The extrapolation of this plot to lower temperatures however gives radically different results from the extrapolation in Fig. 6. Thus at 400°C. the interlamellar spacing is given as one Angstrom. A comparison of Figs. 6 and 7 illustrates the danger of

This interfacial tension of cementite in alpha iron is nearly twice the reported¹⁴ macroscopic surface tension of steel in air; namely, 1500 dynes per centimeter.

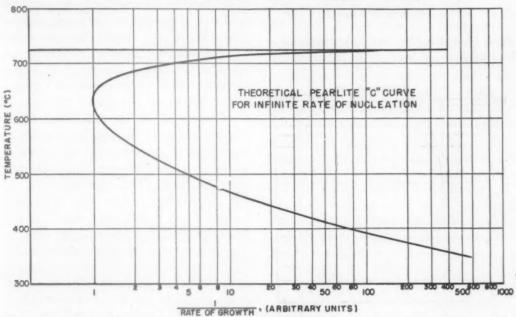


Fig. 9.—Pearlite C-curve for infinite rate of boundary nucleation, drawn according to theoretical equation 18.

extrapolating a formula that fits experimental data over a limited range but that has no sound theoretical basis.

Eq. 13 may now be used to compute the interface energy density S. In this equation S_0 refers to the minimum interlamellar spacing that allows growth. As has been mentioned, those nodules grow most rapidly whose interlamellar spacings are twice the minimum. Therefore the spacings given in Fig. 6 may be considered as twice the minimum spacing. The equation of the straight line in this figure is then

$$2S_0 \cdot (T_e - T) = 0.0017 \text{ cm.}^{\circ}\text{C.}$$
 [14]

The experimental value for the heat of decomposition of a eutectoid austenite is¹⁸

$$Q = 20.5$$
 cal. per gram [15]

Substitution of Eqs. 14 and 15 into Eq. 13 leads to

$$S = 6.8 \times 10^{-5}$$
 cal. per sq. cm.
= 2,800 dynes per cm. [16]

Pearlite C-curve

A clear picture of the kinetics of the edgewise growth of a pearlite nodule was first presented by Hultgren, ¹⁵ and is shown in Fig. 8. The concentration of carbon in the austenite is greater just ahead of the ferrite than just ahead of the cementite. This difference in concentration results in a diffusion current of carbon in the austenite from the ferrite interface to the cementite interface, as indicated in this figure.

Since a growing pearlite nodule does not appreciably change the carbon concentration of the surrounding austenite at distances greater than one interlamellar spacing, neighboring pearlite nodules do not influence each other's growth until they impinge upon one another. Their rate of growth therefore is constant. In the particular case where nucleation at the grain boundary is infinite—i.e., when the boundary upon undercooling instantly becomes

covered with pearlite growing inwards—the time for completion of the reaction in an austenite grain is given by

$$\tau = \frac{\text{Radius of Grain}}{\text{Velocity of Growth}} \quad [17]$$

Upon observing that the heat of activation for diffusion of carbon in austenite is⁸

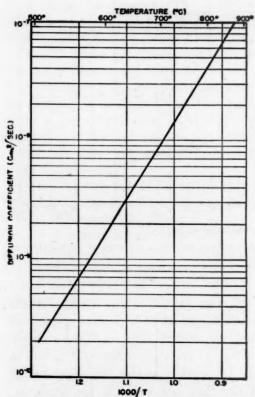


FIG. 10.—DIFFUSION COEFFICIENT OF CARBON IN AUSTENITE, AFTER DATA OF WELLS AND MEHL. 16

36,000 cal. per mol, one therefore obtains from Eq. 10 for the velocity of growth at a phase boundary in a eutectoid steel,

$$V_B \sim e^{-18.000/T}(T_e - T)^2$$
 [18]

where T_{\bullet} is the eutectoid temperature. A plot of this equation is presented as Fig. 9. This theoretical C-curve for infinite nucleation rate is precisely of the same shape as observed. The nose of this theoretical curve occurs slightly above the temperature

of the nose of the observed C-curve for eutectoid plain carbon steels. If due account were taken of the fact that the rate of nucleation is not infinite, the upper portion of the pearlite C-curve would be displaced to the right relative to the lower portion. This relative shift would lower somewhat the temperature of the nose, thereby bringing the theoretical C-curve into better agreement with the experimental C-curve.

The horizontal position of the nose of the C-curve may be computed from Eq. 8. The numerator of the first factor refers to the excess in concentration of carbon in the austenite just ahead of the ferrite over that just ahead of the cementite plates. At the temperature where the theoretical C-curve is at a minimum (630°C.), this concentration difference is 1.4 per cent. At this temperature the denominator of the first factor—namely, the excess of carbon concentration in the cementite over that in the austenite just ahead of cementiteis 6 per cent. The first factor is therefore 0.23. The diffusion coefficient of carbon in austenite at 630°C. may be estimated by an extrapolation of the data of Wells and Mehl. 16 From Fig. 10 this extrapolation is seen to give the value 2.5 × 10-9 sq. cm. per sec. The effective diffusion distance L will be related to the interlamellar spacing So. We shall set

$$L = \alpha S_0$$
 [10]

where α is a numerical coefficient. Although the velocities of the ferrite and of the cementite plates must be equal, the individual factors in Eq. 8 depend upon which type of plate is under consideration. When, as in the present case, the cementite plate is considered, the effective diffusion length L will be comparable to the thickness of a cementite plate, so that the coefficient α will be comparable to 0.12. Finally, upon taking from Fig. 6 the interlamellar spacing at 630°C. as 1.8×10^{-5} cm., we obtain

$$V_B = (3.2 \times 10^{-8}/\alpha)$$
 cm. per sec. [20]

as the velocity at which a pearlite nodule advances at 630°C.

The time for the completion of the reaction may now be obtained by substituting Eq. 20 into Eq. 17. For an A.S.T.M. grain size of 4 to 5, the radius of the average grain¹⁷ may be taken as 0.004 cm. For such a grain size the time for completion of the pearlite reaction is, according to Eqs. 17 and 20,

$\tau = 120 \alpha \text{ sec.}$

The experimental value18 for the completion time at the nose of the C-curve for a plain carbon steel (0.3 per cent Mn) of this grain size is 5 sec. In order to bring the theoretical and experimental times for completion into agreement, it is necessary that the numerical constant α be 0.04, one third the value obtained by identifying the effective diffusion distance with the cementite plate thickness. This value of α is sufficiently close to that predicted from general considerations so that one can be confident that the picture of growth herewith persented is essentially correct. A precise computation of the time of completion would involve a precise computation of the time of completion would involve a precise computation of the velocity of growth V_B , which in turn would require the precise determination of the shape of the cementite-austenite and of the ferrite-austenite interfaces, and the solution of the differential equations for carbon diffusion from the advancing ferrite plates to the advancing cementite plates.*

BAINITE FORMATION

As previously mentioned, the only condition that must be satisfied for the growth of a new phase is that such growth be attended by a decrease in the total free energy of the system. It is not at all necessary that the old or new phases be in equilibrium

As mentioned above, the only condition necessary to enable a transformation to proceed is that the free energy be decreased thereby. If one mol of iron, in which is dissolved C mol of carbon, transforms from austenite to ferrite of the same composition, the change in free energy of the system is

$$\Delta G = -\Delta G_{F_0}^{\alpha \to \gamma} + C\Delta G_C^{\gamma \to \alpha} - CT\Delta S_C^{\gamma \to \alpha} \quad [21]$$

In this equation $\Delta G_{F_0}^{\bullet \to \gamma}$ is the excess of free energy of one mol of pure iron in the austenite phase over that in the ferrite phase, and is given in Table A-1 of reference 1; $\Delta G_c^{\gamma \to \alpha}$ is the excess in standard free energy as defined in ref. 2, of one mol of carbon in the alpha phase over that in the gamma phase, and is approximately 8100 cal. per mol; and $\Delta S_c^{\gamma \to \alpha}$ is the excess of entropy of one mol of carbon when dissolved in austenite, which, from considerations given in reference 1, may be seen to be R ln 3. Upon setting $\Delta G = 0$, one obtains an equation for the critical temperature below which the austenite may transform into ferrite of the same carbon concentration. This

with one another, or that the end product be in a condition of stable equilibrium. Any type of phase change whatsoever may occur provided such a change be accompanied by a decrease of free energy. In other words, the phase change that does occur is not necessarily the phase change that decreases the free energy the most, but rather that which proceeds at the greatest rate. As one example of this statement, the formation of pearlite may be cited. Here the end product has a much higher free energy in the form of interface energy than it need have. However, the end product that forms is the product that forms the most rapidly. Another example occurs when a solid solution suffers a change in phase without a change in composition. The transformation of austenite without a change in composition, first suggested by Wever and Lauge, 35 is discussed in detail in the following paragraphs.

^{*}Such a computation has first appeared by W. H. Brandt: Jnl. Applied Physics (1945) 16, 139.

equation may be most conveniently solved for the atomic carbon concentration C in terms of the critical temperature. This equation is

$$C = \frac{\Delta G_{Fe}^{\alpha}}{\Delta G_{c}^{\gamma \to \alpha} - T \Delta S_{c}^{\gamma \to \alpha}}$$
 [22]

A plot of Eq. 22 is given in Fig. 11 as the upper boundary of the shaded band. The

lower boundary of the shaded region represents the same equation in which $\Delta S_c^{\gamma \to \alpha}$ has been set equal to zero. The shaded region itself represents the uncertainty that exists as to whether the change in entropy of the carbon atoms should or should not be considered. There can be no doubt that this entropy change should be considered if the transformation proceeds sufficiently slowly,

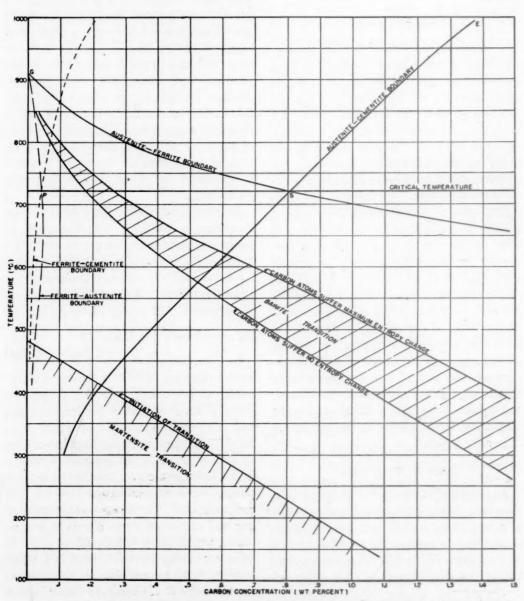


Fig. 11.—Equilibrium relations in iron-carbon system.

Equilibrium relations between ferrite, austenite and cementite are as derived in reference 1.

as certainly it does when the new phase arises through grain growth. When, however, comparatively large regions transform, by some sort of lattice distortion, in more properly as bainite before any carbon diffusion has occurred. For a check upon the manner in which the critical temperature for bainite formation changes with

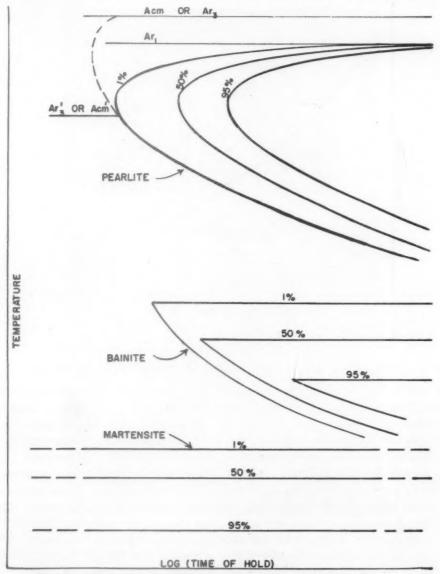


FIG. 12.—IDEALIZED TIME-TEMPERATURE-TRANSFORMATION DIAGRAM.

a time short compared with the time required for the carbon atoms to jump from one interstitial position to another, the entropy term should not be considered.

The ferrite that forms from austenite without a change in carbon concentration is to be identified as bainite, or perhaps carbon concentration, one must go to alloy steels where the pearlite and bainite reactions may be clearly separated. A comparison of the highest temperatures at which bainite forms in 3 per cent chromium steels of two different carbon concentrations, ^{28, 29} shows that the bainite curve in Fig. 11

agrees very well with experiment (100°C. lowering of temperature for an increase of carbon concentration from 0.6 to 1.0 per cent). The diffusion of carbon within

temperature is lowered to the temperature at which the steel is being held, the transformation stops, as indeed it does under isothermal conditions at the highest tem-

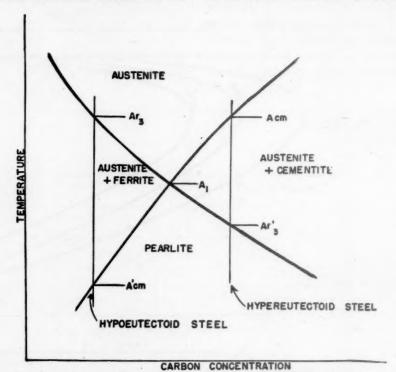


FIG. 13.—Interpretation of critical temperatures in figure 12.

bainite during its formation leads to a diversity of structures, which are described in the following paragraphs.

At the highest temperature at which the bainite reaction can proceed, the diffusion rate of carbon is still fairly high in the austenite. It is expected to be much higher in the ferrite because in the body-centered lattice the interstitial positions are fairly close to one another, therefore the potential-energy hill separating adjacent positions should be comparatively low. This diffusibility of the carbon will cause the carbon to diffuse out of a growing ferrite grain into the surrounding austenite matrix, where the free energy for carbon is lower. This increase of carbon concentration in the surrounding austenite, however, will lower the critical temperature for the formation of bainite. As this critical

peratures of bainite formation.¹⁹ Further transformation may then be obtained only by a lowering of the temperature. Such increase in amount of transformation with a lowering of the temperature has been frequently reported in the literature.²⁰

The enhancement of carbon concentration in the austenite immediately surrounding the bainite grain may likewise lead to the precipitation of a cementite film surrounding the banite, thereby preventing further growth even at lower temperatures.²¹ An example of a bainite grain whose growth was so impeded is shown in Fig. 14a.

Suppose, on the other hand, that the bainite is formed at such a low temperature that the carbon cannot diffuse out of a growing bainite grain. If the steel is then maintained at the transformation tempera-

ture for a sufficiently long time, or if it is elevated for a shorter time, the carbon will precipitate as cementite. The initial distribution of the cementite will be in the spheroids will be grouped on planes corresponding to the original plates. Such a grouping of cementite spheroids may be seen in the illustrations of Davenport.22

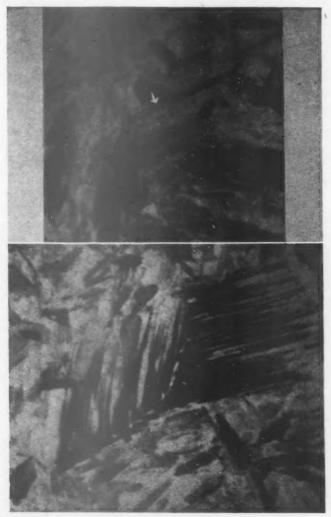


Fig. 14.—Examples of ways in which cementite may precipitate out of bainite grains. × 2500. (Courtesy of Miss Mary R. Norton.) S.A.E. steel 4140 water quenched in 34-inch rounds.

a. Bainite plate prevented from further growth by surrounding film of cementite.

b. Precipitation of cementite as plates within bainite area.

form of plates (see p. 560). An example of such a platelike distribution is shown in Fig. 14b. If the steel is held at the transformation or at a higher temperature for a sufficiently long time, the individual plates will spheroidize, as explained in the section on spheroidization. These

In the section upon rate of pearlite formation (p. 14), the difficulties inherent in the computation of nucleation rates were circumvented by the assumption of infinite nucleation rate at the boundaries. For bainite, where to a large extent the nucleation presumably takes place in the interior of the grains, no such simplifying assumption can be made. In order to obtain even a rough estimate of the rate of bainite formation, some estimate would have to be made of the rate of nucleation. The theory has not yet been developed from which such an estimate could be made. The extensive experimental work of Wever and his school (Kaiser-Wilhelm-Institut fur Eisenforschung) upon the rate of formation of bainite cannot therefore at present be compared with theory.

FORMATION OF MARTENSITE

It is well recognized that martensite forms from austenite by some sort of shear mechanism. Whatever the mechanism, the free energy of the end product must certainly be smaller than the free energy of the initial austenite. In computing this change in free energy, the slight distortion of the martensite from the cubic lattice will be neglected, aside from possible elastic strains. Since the individual martensite needles form so very rapidly, the carbon atoms cannot be considered as undergoing a change in entropy during the transformation. The last term in Eq. 21 must therefore be omitted. However, by the very mechanism by which the martensite forms, the lattice must be left in a stressed condition. An additional term must therefore be added to Eq. 21 to take account of this strain energy. If ΔU denotes this strain energy per mol of transformed iron, Eq. 21 becomes

$$\Delta G = -\Delta G_{F_0}^{\alpha \to \gamma} + C\Delta G_0^{\gamma \to \alpha} + \Delta U \quad [23]$$

As for bainite, the critical temperature for the formation of martensite is obtained by equating ΔG to zero. The resulting equation may be most readily solved for the atomic carbon concentration C. This equation is

$$C = (\Delta G_{Fe}^{\alpha \to \gamma} - \Delta U) / \Delta G_c^{\gamma \to \alpha}$$
 [24]

Complete agreement with experiment is obtained for the critical temperature

for martensite formation, the Ar" temperature, by taking the strain energy as a constant independent of carbon concentration. The energy is found in ref. 1 to be

$$\Delta U = 290$$
 cal. per mol [25]

If the strain energy were to be concentrated in the martensite itself, and if no plastic deformation relieved the stress, the stress corresponding to this value of ΔU would be 1,500,000 lb. per sq. in. The assumption of constant strain energy may seem contradictory to experience, since it is known that the higher the carbon content the higher are the residual stresses. This observation is not, however, contradictory to the assumption of constant strain energy, for the martensite of low carbon concentrations forms at a comparatively high temperature where high stresses are quickly relieved through plastic deformation.

The continual lowering of the martensite transformation temperature by the transformation itself finds a ready interpretation in the hypothesis that the interference of martensite needles already formed with the needles being formed raises the strain energy ΔU needed for further transformation.^{1,5}

LOSS OF TETRAGONALITY OF MARTENSITE

In the previous section, martensite was considered simply as supersaturated ferrite. As was first pointed out by Fink and Campbell, 23 the lattice of freshly formed martensite differs from the body-centered cubic structure of ferrite in that one principal axis is elongated slightly with respect to the other two principal axes. Bain 24 has pointed out that the tetragonality of freshly formed martensite is due to the restraints imposed by the carbon atoms upon the transformation of a face-centered to a body-centered cubic lattice.

Fink and Campbell likewise found that the tetragonality of martensite is removed by tempering at temperatures as low as 100°C. Two mechanisms have been proposed whereby this tetragonality is lost. According to one mechanism, introduced by Honda and Nishiyama,25 the tetragonality is lost as soon as the carbon atoms diffuse out of their original interstitial positions into neighboring interstitial positions. According to the second mechanism, introduced by Hagg26 and adopted by Cohen²⁷ and his co-workers, the loss of tetragonality is merely a reflection of the decrease of the carbon in solid solution occurring through some sort of precipitation. These two mechanisms would lead to quite different types of cubic ferrite. In the first case the freshly formed cubic ferrite would have the same quantity of carbon in solid solution as the parent martensite; in the second, a cubic structure would necessarily imply a very low carbon content. A satisfactory decision as to which of the two mechanisms is correct cannot be arrived at merely by more precise experiments, for convincing arguments can be advanced against either mechanism. Rather, a satisfactory solution is to be found through a theoretical analysis of the stability of the tetragonal structure. Before this analysis is presented, the arguments against the two mechanisms discussed above will be given.

It is generally accepted that the interstitial positions in a body-centered lattice are at the centers of the edges and face of the unit cells. These interstitial positions do not have cubic symmetry. Of the six neighboring iron atoms, two are closer than the other four. The line passing through the interstitial position and through the two nearest iron atoms is called the tetragonal axis of the interstitial position. This axis may be parallel to any one of the three principal axes of the cubic lattice. Only one third of these interstitial positions correspond to interstitial positions of the original face-centered cubic lattice; namely, those interstitial positions whose tetragonal axes are parallel to the axis of compression in the f.c. -> b.c. transi-

tion. Therefore, although the carbon atoms are randomly distributed among the interstitial positions of austenite, they will have a preferred distribution in the derived body-centered lattice. It is this preferred distribution among the interstitial positions whose tetragonal axes are all parallel that gives rise to an over-all tetragonality. If the carbon atoms became randomly distributed among all types of interstitial positions, the tetragonality would disappear. Considerable diffusion of the carbon atoms must precede any kind of precipitation, and the conclusion appears unavoidable that such diffusion would cause a random distribution, and therefore a loss of tetragonality prior to precipitation.

An equally convincing argument may be advanced against the first proposed mechanism. The tetragonality of martensite persists at room temperature for several months. On the other hand, the author²⁸ points out in a current paper that the anelastic properties of steel indicate that at room temperature the carbon atoms require only about a second to jump from one interstitial position to another.

All these difficulties would be resolved if the preferred distribution of carbon atoms were the equilibrium distribution. Diffusion would not then disturb the preferred distribution. The carbon atoms would simply spend a much longer time in the interstitial positions whose tetragonal axes were parallel to the lattice tetragonal axes than in the other interstitial positions. An analysis is given in Appendix C of the stability of the preferred distribution, and therefore of the orthogonality of the lattice. It is found that a critical temperature Te exists above which the random distribution is in equilibrium, below which a preferred distribution is in equilibrium. This critical temperature is related to the carbon content by the equation

$$T_e = 1330 X_e \deg. K$$

where X_{ϵ} is the weight per cent of carbon.

It must therefore be concluded that in a stress-free martensite lattice the initial loss of tetragonality occurs by the second proposed mechanism; namely, the lowering, by precipitation, of the quantity of carbon in solid solution. Once the concentration of the carbon has been lowered to several tenths of one per cent by weight, further loss of tetragonality occurs by the first mechanism; namely, the transition of the carbon atoms from a preferred to a random distribution.

EFFECT OF ALLOYS UPON DECOMPOSITION OF AUSTENITE

According to the way in which alloying elements affect austenite decomposition, they may be divided into two classes. The elements of one class have qualitatively the same effect upon the S-curve as has carbon itself. These elements retard the formation of both pearlite and bainite by about the same amount, and also lower the temperature for the initiation of martensite. Mn and Ni are the commonest elements of this class. The elements of a second class retard the formation of pearlite much more than the formation of bainite. Molybdenum is the most outstanding example of this class. It thus appears that each alloying element has two characteristic properties, one of which has a moderate effect upon retarding all types of austenite decomposition, the other of which has a specific influence upon pearlite formation.

PEARLITE

The specific effect of alloying elements of the second class in retarding pearlite formation appears to be associated with their carbide-forming tendency.²⁹ The greater this tendency, the more potent is the element in retarding pearlite. As an example of the magnitude of this retardation, the effect of molybdenum will be cited: I per cent of this element retards by more than a factor of 1000 the time re-

quired for a perceptible amount of pearlite to be formed.¹⁸

A current explanation of this retarding effect to be found in the literature runs as follows. 30 The concentration of the alloying element is observed to be greater in the cementite phase than in the ferrite phase. The formation of pearlite is therefore associated with a segregation of the alloying element. Since the diffusion coefficient of all alloying elements is considerably less than that of carbon, such segregation must necessarily retard the rate at which the pearlite nodule grows.

As previously stated, all the elements that are very effective in retarding the formation of pearlite, molybdenum, titanium, etc., have a considerably stronger affinity for cementite than for austenite, and also have at most only a slight preference for austenite over ferrite. Therefore the free energy liberated by the propagation of a pearlite nodule would be increased by the presence of these alloying elements even if they remained uniformly distributed. The circumstance that the free energy would be still further lowered if the alloying elements became segregated in no way necessitates that the propagation of pearlite be attended by such segregation. As discussed in the section on bainite, the reaction that takes place is not necessarily associated with the greatest liberation of free energy, but proceeds at the fastest

This explanation of the retarding effect of certain alloying elements leaves unanswered the fundamental question as to why the propagation of pearlite should have to wait for the segregation of the alloying elements. It is in fact doubtful whether any segregation of alloying elements takes place in the immediate vicinity of the expanding surface of a ferrite-cementite nodule. Such segregation as is observed could well take place within the nodule during the completion of the pearlite formation.

Under certain conditions the pearlite consists of alternate lamellae of ferrite and of a special alloy carbide, which has a different structure from cementite. 30,31

nucleus must exceed a certain critical value before it becomes stable and is able to grow. As has been pointed out, this critical free energy is less when the nucleus

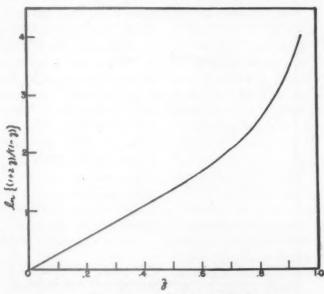


FIG. 15.—GRAPH FOR SOLUTION OF EQUATION 6-0.

The growth of such a pearlite nodule must necessarily be accompanied by a segregation of the alloying element, and so proceeds very slowly. The question still remains unanswered, however, as to why in such cases ferrite-cementite nodules do not grow at their customary rate.

Any phase transformation involves both nucleation and growth. From the foregoing discussion, the fruitlessness is apparent of attempting to seek in growth an interpretation of the retarding effect of strong carbideforming elements upon pearlite formation. One is therefore led to seek for this interpretation in the phenomenon of nucleation.

Nucleation of pearlite always takes place at the grain boundaries unless the parent austenite has been imperfectly homogenized. This preference of nuclei for surfaces finds a ready interpretation in the fact that, as already explained in the section on nucleation, the formation of a nucleus entails the formation of an interface, and as a consequence the free energy of the

forms at a boundary than when it forms in the interior of a grain.

The same argument that has been used to show why nucleation is more prevalent at the boundary between two grains than in the interior of a grain may be extended to demonstrate that nucleation is still more frequent along an edge common to these grains, most frequent at corners common to four grains, and that the more acute the corner of any one grain, the more quickly will a nucleus be generated therein.

In any solid solution, when the binding between a solute and a solvent atom is less than between two solvent atoms, the solute atoms tend to congregate wherever the lattice is most disorganized. The situation is analogous to that of liquid solutions, in which the concentration of certain solute atoms is greater near the surfaces than in the interior. One therefore anticipates that the concentration of alloying elements in austenite will be greatest at places that are potential nucleation sites—and the

more effective are the sites for nucleation, the greater will be the concentration of alloying elements. If now the concentration of a strong carbide-forming element tion of bainite and lower the initial temperature, Ar", for the formation of martensite, and also have at least a normal influence in retarding pearlite formation.

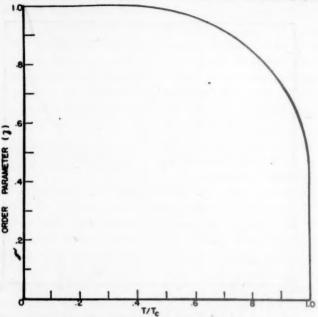


FIG. 16.—DEPENDENCE OF PREFERENTIAL DISTRIBUTION UPON TEMPERATURE, CASE OF ZERO STRESS.

is sufficiently large, the carbide nucleus that forms will not be cementite but will be a special carbide with a lattice structure different from that of cementite. The growth of the carbide grain resulting from such a nucleus will be slow, since it will be dependent upon diffusion of the alloving element. The growth will be sufficient, however, completely to eliminate the original site as a potential nucleation site for cementite. The first additions of strong carbide-forming elements, therefore, eliminate the sites that are most effective in nucleating cementite, and therefore retard slightly the initiation of pearlite growth. Further additions will lead to the elimination of the next most effective nucleation sites, retarding still more the initiation of pearlite growth.

BAINITE AND MARTENSITE

All alloying elements, save for the single exception of cobalt, both hinder the forma-

The observation that the order 36 of alloying elements arranged according to effectiveness in retarding the bainite reaction is the same order37 with respect to the lowering of the martensite transformation temperature,* indicates that these two effects are closely related. In the martensite reaction nucleation apparently is nearly instantaneous,32 the initial transformation temperature not changing, within experimental error, in the range of cooling rates from 100° to 4000°C. per sec. It therefore appears that the influence of alloying elements upon both the bainite and martensite reaction is not connected in any way with nucleation, as in pearlite, but rather with a change in the equilibrium temperature of the two reactions.

As previously pointed out, the transformation from austenite to bainite and to martensite in pure iron-carbon steel is

^{*} Private communication, J. H. Hollomon.

accompanied by no change in carbon distribution. Since the diffusion of alloying elements is even slower than that of carbon, it may safely be assumed that they also suffer no diffusion during these two transformations. This assumption allows a ready calculation of the change in transformation temperature induced by these elements.

Let C_i be the ratio of the number of lattice atoms of type j to the total number of lattice atoms, $\Delta G_i^{\gamma \to \alpha}$ the change in atomic free energy when one mol of atoms of type j are transferred from the gamma to the alpha phase. The ratio of carbon to total number of lattice atoms will be denoted by C_c . Then the change in free energy associated with a transformation of one mol of lattice atoms and C mols of carbon from the austenite to the ferrite phase is given by the following equation,

$$\Delta G = \Delta G_{Fe}^{\gamma \to \alpha} + \Sigma' (\Delta G_i^{\gamma \to \alpha} - \Delta G_{Fe}^{\gamma \to \alpha})$$

$$C_i + \Delta G_e^{\gamma \to \alpha} C_e + \phi \quad [26]$$

where the primed summation refers to all lattice-type atoms other than iron. In the bainite reaction, ϕ has a value lying between zero and $-(RT \ln 3)C_e$, in the martensite reaction it has the value of 357 cal. per mol.

The influence of the alloying elements may most conveniently be expressed in terms of a horizontal shift of the curve for transformation temperature vs. carbon content. From Eq. 26, it may be seen that this shift is a linear function of the concentrations of the alloying elements, and therefore that the shifts are additive. This additive effect of different alloying elements has recently been suggested by Payson and Savage³³ from their empirical data. The effect of a particular alloying element of type j with the atomic concentrations C; is to shift to the left the curve for transformation temperature vs. carbon concentration, by the amount

$$\Delta C_c = \{ (\Delta G_i^{\gamma \to \alpha} - \Delta G_{Fe}^{\gamma \to \alpha}) / \Delta G_c^{\gamma \to \alpha} \} C_i \quad [27]$$

In the derivation of this equation, the last term in Eq. 26 has been assumed to be a constant. This assumption introduces a slight approximation in the case of bainite.

It may be seen from Eq. 27 that the larger the quantity $\Delta G_i^{\gamma \to \alpha}$, the greater the influence of the alloying element upon the banite and the martensite transformation. At present the only method of evaluating ΔG_i is through its influence^{1,2} upon the iron-alloy equilibrium diagram. In such diagrams the equilibrium relations are usually between austenite and nonmagnetic ferrite. It is to be expected that the standard free-energy change $\Delta G_i^{\gamma \to \alpha}$ will be greater below the Curie temperature than above, with the possible exception of cobalt, which increases the Curie temperature at small concentrations. It is to be expected, nevertheless, that the order of the alloying elements should be the same when arranged according to the magnitude of their influence upon the bainite and the martensite transformation as when arranged according to their $\Delta G_i^{\gamma \to \alpha}$ as measured at higher temperatures. Table 1 shows that this is true.

TABLE 1.—Correlation of Effectiveness of Elements in Suppressing Bainite Reaction with Thermodynamical Quantities

Order of Effective- ness ³⁶ in Suppres- sing Bainite	С	N(?)	Mn	Ni	Cu
$\Delta G^{\gamma \to \alpha}$, cal. per mol	8,100	3,000	2,400	1,600	1,280

As previously mentioned, cobalt behaves in an anomalous manner. It actually hastens the bainite reaction, and raises the Ar" temperature. An interpretation of this anomaly may be found from an inspection of the iron-cobalt equilibrium diagram. In this the gamma-delta boundary rises with increasing cobalt content, while the gamma-alpha boundary is nearly horizontal. Such behavior is evidence that from 1400° to 900°C. $\Delta G_{\text{Co}}^{\gamma \to \alpha}$ changes from a positive quantity to zero. By extrapolation,

one surmises that at the lower temperatures at which bainite and martensite form, $\Delta G_{Co}^{\gamma \to \alpha}$ is a negative quantity.

TIME-TEMPERATURE-TRANSFORMATION CURVES

In this country the standard method of studying the decomposition of austenite idealized in that each set of curves is completely separated from the other two sets. The uppermost two sets are completely separated only in high-alloy steel, as in high-speed tool steels. In plain carbon steels they are interpenetrating, the noses of the two sets nearly coinciding. In most steels the lower two sets of curves are

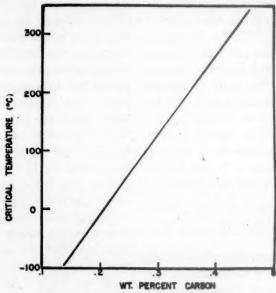


FIG. 17.—CRITICAL TEMPERATURE.

is to quench the specimens from the austenitizing temperature to a lower temperature T, to hold at that temperature for a time t, and then to quench to room temperature. From an examination of the final specimens, certain information may be gained as to the nature of the transformation at the temperature T during the time t. The data so obtained are usually utilized to construct a diagram of the type represented in Fig. 12, called the time-temperature-transformation (T-T-T) diagram. This diagram will be discussed in the light of the preceding pages. The present discussion serves in part as a review of the salient features of this report.

The T-T-T diagram of Fig. 12 consists of three sets of curves, each set corresponding to a distinct transformation product. Two sets consist of C-curves, the other set of nearly horizontal lines. This figure is

separated to some extent, but never completely so. Wherever two sets of curves interpenetrate, it is not possible simply to superimpose the two sets. In such cases not only does one reaction affect the growth of the second reaction product, either retarding or accelerating, but the two reaction products may become indistinguishable.

None of the reaction products represent complete equilibrium at the temperature of formation. In the first reaction product, pearlite, complete equilibrium is attained only with respect to carbon. Here the carbide phase and ferrite occur as alternate lamella growing edgewise into the parent austenite. The second reaction product, bainite, forms by grain growth from nuclei of ferrite of the same composition as the parent austenite. During the grain growth some carbon diffuses out of the ferrite grains into the surrounding austenite

matrix. The higher the temperature of formation, the freer the ferrite is of super-saturated carbon. The third reaction product, martensite, forms by some sort of

perature range the time required for growth is limited not only by the rate of growth of the pearlite nodules but also by their nucleation rate.

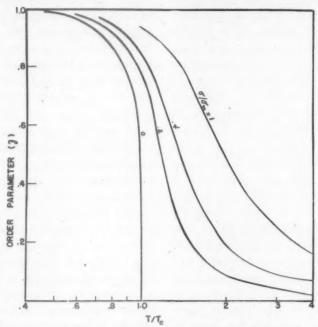


Fig. 18.—Dependence of preferential distribution upon temperature, case of nonzero stress.

lattice shear, which is homogeneous over macroscopic regions of the parent grains. This shear occurs so rapidly that there is no time for a change in composition. The only segregation of constituents that can occur in the martensite is that which may occur during self-tempering after it has been formed.

In pearlite, and only in pearlite, may successive C-curves be obtained essentially by a horizontal shift to the right of prior C-curves. This essential parallelism of the pearlite curves means that the ratio of the times required to come to two different completions is independent of temperature. Thus 10 times as long may be required to come to 90 per cent completion as to come to 10 per cent completion. Only slightly below the eutectoid temperature are the curves no longer essentially parallel. Such nonparallelism occurs because in this tem-

The velocity with which a pearlite nodule advances is proportional to the diffusion coefficient of the carbon atoms, to the difference in the carbon concentration in the austenite just ahead of the advancing pearlite and cementite nodules, and is inversely proportional to the interlamellar spacing. This difference in carbon concentration is directly proportional, the interlamellar spacing is inversely proportional, to the amount of undercooling. When these various factors are properly considered, theoretical curves are obtained for the pearlite transformation, which are nearly identical with the observed, except for a slight horizontal shift.

Only in the case of a eutectoid steel is pearlite the initial decomposition product of austenite. If the carbon concentration is greater than the eutectoid, a carbide first precipitates. If the carbon concentration is less than the eutectoid, free ferrite first forms. The critical temperatures that limit the range in which these products form are interpreted by Fig. 13.

In contrast to pearlite formation, bainite formation requires no diffusion of carbon. While the rate of growth of a pearlite nodule is proportional to the square of the amount of undercooling for temperatures just under the critical, the rate of growth of a bainite grain is independent of amount of undercooling for temperatures close to the critical temperature for bainite formation. The upper portion of the initial C-curve for bainite is therefore essentially horizontal. Although the growth of a bainite grain does not require carbon diffusion, nevertheless at the higher temperatures of formation carbon diffusion does occur—diffusion out of the growing bainite grain into the surrounding austenite matrix. Such diffusion finally stops the growth of a bainite grain, by one of two methods. The enrichment of the austenite in carbon tends to lower the transformation temperature of austenite to bainite, a tendency that eventually would stop the growth of all grains. On the other hand, the enrichment of the austenite in carbon immediately surrounding the bainite grain may give rise to a cementite film, which would prevent further growth. However the cessation of growth of bainite grains occurs, it results in all the upper halves of the bainite isotransformation curves being horizontal. While, as previously mentioned, bainite grain growth is not dependent upon carbon diffusion, it does require the transfer of iron atoms from equilibrium positions on the austenite side of an interface to new equilibrium positions on the bainite side of the interface. The rate of such transfer will decrease with decreasing temperatures in the same manner, but less slowly, than does the rate of carbon diffusion. This decrease of rate of transfer of iron atoms with decreasing temperature causes the lower parts of the bainite isotransformation curves to take the same shape as for pearlite.

Freshly formed untempered martensite and bainite have essentially the same structure; namely, ferrite supersaturated with carbon. The tetragonality of the martensite, in contrast with the cubic structure of bainite and of ferrite, is due to the circumstance that in the formation of martensite from austenite the carbon atoms are left in certain preferred interstitial positions. These preferred positions produce a strain with tetragonal symmetry, all the axes of the preferred positions being parallel. The essential difference, from the thermodynamical standpoint, of freshly formed martensite and freshly formed bainite lies in the elastic strains introduced during the formation of the former phase. These elastic strains require additional free energy for their formation, which can be obtained only by a lowering of the transformation temperature for the austenite -- martensite reaction below that for the austenite -> bainite reaction. The residual strains introduced by the first martensite that forms renders it still more difficult; i.e., requires more free energy and therefore a lower temperature for the formation of further martensite. The martensite reaction does not therefore proceed isothermally, a continual lowering of the temperatures being required for a continuance of the transformation. This circumstance leads to the isotransformation curves for martensite being nearly horizontal lines. The vertical positions of the three sets of curves are determined primarily by the equilibrium relations. These relations are given in Fig. 11 for plain carbon steels. Thus the upper boundary of the pearlite C-curves is the eutectoid temperature. This temperature is raised by strong carbide-forming elements such as molybdenum, tungsten or chromium, and is lowered most strongly by manganese and nickel. According to the theory developed in this paper, the upper temperature of the bainite C-curves should be within the shaded region of Fig. 11 for plain carbon steels, while the temperature for the initiation of martensite is given by the lowermost of the curves in this figure. Theory and experiment are in complete agreement for the case of martensite, while in the case of bainite the experimental data are inconclusive.

The horizontal positions of the two sets of C-curves are sensitive to slight additions of alloying elements. The pearlite C-curves are especially sensitive to strong carbideforming elements. These elements retard the formation of pearlite by covering up, with their own carbides, the sites that are effective in the nucleation of cementite. Other elements, such as manganese and nickel, move all the C-curves to the right through their effect in lowering the critical temperature for the formation of pearlite and of bainite. A lowering of the upper halves of the C-curves must necessarily result in a shift of their noses to the right

SUMMARY

An extended review of the results of this report is given on pages 576 to 579, where the results are applied to an interpretation of the time-temperature-transformation diagram. A brief review of the results is as follows:

1. A review is given of the general principles that govern the phenomena accompanying the decomposition of austenite. These phenomena include nucleation, propagation of interfaces, grain growth and spheroidization.

2. The main features of pearlite formation are found to be derivable directly from fundamental principles. These features include: the variation of interlamellar spacing with temperature, the shape and the position of the pearlite C-curve, the mechanism whereby strong carbide-forming alloys retard the formation of pearlite.

3. The formation of bainite is interpreted as a transformation of the facecentered austenite lattice to the bodycentered ferrite lattice without a change in carbon distribution.

4. Many of the characteristics of bainite and of bainite formation are readily derivable from this interpretation. These characteristics include: the formation of only a limited amount of bainite at the highest transformation temperatures, the improvement in physical properties of low-temperature bainite over high-temperature bainite, the order of alloying elements arranged according to their effectiveness in retarding the formation of bainite.

5. Martensite is interpreted as having essentially the same structure as untempered bainite, except that, owing to its mode of formation, residual stresses are present.

6. The manner in which alloying elements affect the formation of martensite is found to be such that, when arranged in the order in which they lower the Ar" temperature, the order is the same as when arranged according to effectiveness in retarding the bainite transformation.

7. The transition of martensite from a tetragonal lattice to a cubic lattice is interpreted as a change from an ordered distribution of carbon to a random distribution.

APPENDIX A

In this appendix is computed the free energy that is liberated within the interface itself as it advances. For the purposes of this computation, we shall assume the solute concentration to be constant on both sides of the boundary.

As a unit area of the boundary advances a distance δX , the change in free energy δG may be written as¹

$$\delta G = \delta G_a - T \delta S_p \qquad [a-1]$$

when δG_{\bullet} is the change in atomic free energy (or in standard free energy²), δS_{p} the change in positional entropy. Upon

using the notation of the section on page 565, we obtain

$$\delta G_a = \{ -\Delta G + (C_2 - C_1)(G_1 - G_2) \} \delta X \quad [a-2]$$

Further, upon using the methods in reference I, we obtain

$$\delta S_p = \{ k(C_1 - C_2) - k(C_2 - C_1) \ln (\beta_2 C_1 / \beta_1 C_2) \} \delta X \quad [a-3]$$

Upon combining Eqs. a-1 to a-3 and using Eq. 3:

$$\delta G = -\Delta G - kT(C_1 - C_2) \quad [a-4]$$

In order that δG may be less than or equal to zero, it is necessary that

$$(C_2 - C_1) \leq \Delta G/kT$$

a relation that was used in the text.

APPENDIX B

In this appendix an analysis is made of the critical size and of the critical free energy of a nucleus.

The free energy liberated by the formation of a unit volume of the new phase will be denoted by G_{\bullet} , the energy required to form a unit area of interface between the new and old phase will be denoted by G_{\bullet} . The increase in free energy associated with the formation of a nucleus of the new phase is therefore

$$\Delta G = -VG_{\bullet} + SG_{\bullet} \qquad [b-1]$$

where V and S represent the volume and surface area of the nucleus, respectively. When the nucleus is completely surrounded by the old phase, its surface area, and therefore its free energy, is a minimum for a given volume when it is spherical. Such a nucleus, therefore, may be regarded as spherical. Its critical radius is such as will make its free energy a maximum. From Eq. b-1, this critical radius is found to be

$$R_{\bullet} = 2G_{\bullet}/G_{\bullet} \qquad [b-2]$$

Substitution of Eq. b-2 into Eq. b-1 gives for the critical free energy:

$$\Delta G_o = (16\pi/3)G_{\bullet}^3/G_{\bullet}^2$$
 [b-3]

As an example of these equations, the case of a cementite nucleus will be considered. Upon taking the energy per unit area of interface between cementite and austenite to be the same as between cementite and ferrite, one obtains, from Eq. 16, that G_{\bullet} is equal to 6.8×10^{-5} cal. per sq. cm. Further, upon taking the heat of solution of cementite in austenite as 5300 cal. per mol,1 we find that for a eutectoid steel 100°C. below the eutectoid temperature the free energy G, is 23 cal. per c.c. Substitution of these quantities into Eq. b-3 gives, for the critical radius and the critical free energy of a cementite nucleus of a eutectoid steel at 623°C.,

$$R_e = 0.6 \times 10^{-5} \text{ cm}.$$

and

$$G_e = 1.0 \times 10^{-14} \text{ cal.}$$

respectively.

APPENDIX C

In this appendix the conditions will be found under which a ferrite lattice with carbon dissolved interstitially will spontaneously acquire a tetragonal structure. The ferrite lattice will automatically acquire the structure that renders its free energy a minimum. The conditions, therefore, are to be found under which the free energy is less in the tetragonal than in the cubic structure; that is, less with a preferred than with a random distribution of carbon atoms. The free energy of a unit volume is

$$G = U - TS - e\sigma$$
 [c-1]

where U is the internal energy and S the entropy per unit volume, and e and σ are the tensile strain and stress, respectively. In the computation of the strain e, the reference configuration will be taken as that in which σ is zero and in which the

distribution of carbon atoms is random. The condition that the free energy be a minimum may be expressed by the following equation

$$\delta G = 0$$
 [c-2]

where the variation δ refers to any small change of internal parameters that leaves the stress σ unchanged. This variation will be taken as the transfer of a carbon atom from an interstitial position whose tetragonal axis is normal to the preferred axis (n position) to an interstitial position whose tetragonal axis is parallel to this axis (p position). If N_n and N_p represent the number per unit volume of carbon atoms in these two types of positions, respectively, the variation δ may be defined as

$$\delta N_p = 1, \, \delta N_n = -1 \quad [c-3]$$

The corresponding variation in energy U is given by

$$\delta U = u_p - u_n + \sigma \delta e$$

where u_p and u_n refer to the energy of a carbon atom in a p and an n position, respectively. The equilibrium equation c-2 therefore becomes

$$u_p - u_n = T\delta S$$
 [c-4]

An estimation of the left-hand member of Eq. c-4 may be made if it is assumed that it is a function of the tensile strain e irrespective of how this strain is obtained; e.g. by a tensile stress or by a preferred distribution. We start with a random distribution and with no stress. The material is then subjected to such a tensile stress along a lattice principal axis as will produce the strain e, the distribution of carbon remaining random. The internal energy is thereby raised by the amount $(\frac{1}{2})E_{100}e^2$. Next, keeping the strain constant, all the carbon atoms are moved to p positions. The change in internal energy associated therewith is $(\frac{2}{3})N(u_p - u_n)$, where N is the total number of carbon atoms per unit

volume. The total change in energy is therefore

$$(\frac{1}{2})E_{100}e^2 + (\frac{2}{3})N(u_p - u_n)$$

The final stress necessary to maintain the strain e will be zero if the derivative of this energy with respect to e is zero; i.e., when

$$E_{100e} + (3/3)N\delta(u_p - u_n)/\delta e = 0$$

Since, for small strains, $u_p - u_n$ may be taken as a linear function of the strain, this equation reduces to

$$u_p - u_n = -E_{100}\lambda e \qquad [c-5]$$

where

$$\lambda = e/(\frac{2}{3})N$$
, $N_p = N$

The quantity λ may be interpreted as the strain introduced by the transfer of one carbon atom per unit volume from an n to a p position. Eq. 5 was derived for the case of complete order $(N_p = N)$. Since $u_p - u_n$ is a linear function of e, it must be of general validity.

The right-hand side of Eq. c-4, the change in entropy associated with the transfer of a carbon atom from an n to a p position, may be shown by the standard methods of statistical mechanics to be given by the equation

$$\delta S = -k \ln \left(2N_p/N_p \right)$$

It will be found more suitable to express the entropy change in terms of a parameter that changes from zero, in the case of random distribution, to unity, in the case where all carbon atoms are in p positions. Such a parameter is given by

$$z = (\frac{3}{2}) (N_p/N - \frac{1}{3})$$

In terms of this order parameter

$$\delta S = -k \ln \left(\frac{1 + 2z}{1 - z} \right) \qquad [c-6]$$

Combining Eqs. c-4 to c-6 gives:

$$E_{100} \lambda e = kT \ln \left(\frac{1 + 2z}{1 - z} \right) \quad [c-7]$$

Case of Zero Tensile Stress

When no tensile stress is present, the strain is proportional to the order parameter.

$$e = (\frac{2}{3})N\lambda z \qquad [c-8]$$

In this case the order parameter itself may be interpreted as the ratio of the actual tetragonality over the maximum tetragonality, which occurs in the case of complete order. Substitution of Eq. 8 into Eq. 7 leads to

$$(2E_{100}N\lambda^2/3kT)z = \ln\frac{1+2z}{1-z}$$
 [c-9]

The qualitative nature of this solution may be obtained from an examination of the graph of the right-hand side of this equation, presented as Fig. 15. The abscissa of the intercept of this curve with the straight line $(2NE_{100}\lambda^2/3kT)z$ gives the value of the order parameter z at the temperature T. When T is above a certain critical value Te, the only intercept is at z = 0, corresponding to a random distribution of the carbon atom in the p and n positions. At this critical temperature the straight line is tangent to the curve at z = 0.33. Therefore, as the temperature is slowly lowered, the order parameter z suddenly changes from o to 0.33 when the critical temperature is reached. The gradual increase of z as the temperature is further lowered is shown in Fig. 16, obtained by graphically solving Eq. c-9.

At the critical temperature the product $z^{-1} \ln \{(1+2z)/(1-z)\}$ may be computed as 2.75. Therefore the critical temperature is given by

$$T_e = 0.243 NE_{100} \lambda^2/k$$
 [c-10]

In order that T_e may be expressed in terms of the weight per cent of carbon X_e , the following substitutions are made:

$$N = 3.92 \times 10^{21} X_e$$

 $E_{100} = 1.3 \times 10^{12}$ dyne per sq. cm.

$$\lambda = 1.2 \times 10^{-23}$$

$$k = 1.39 \times 10^{-16}$$

The result is:

$$T_e = 1330X_e \text{ deg. K}$$

This equation is given graphically in Fig. 17.

CASE OF NONVANISHING STRESS

A tensile stress parallel to a lattice principal axis will lower the potential energy of carbon atoms in p positions with respect to n positions, and therefore will result in a preferred distribution of carbon atoms at all temperatures. The presence of microscopic residual stresses will therefore result in a smoothing out of the abrupt transition shown in Fig. 16. The analysis of the preferred distribution in the presence of a tensile stress may be carried out by a slight modification of the analysis of the preceding section. Eq. c-8 must be replaced by the equation

$$e = (\frac{2}{3})N\lambda z + E_{100}^{-1}\sigma$$

and therefore Eq. c-9 by

$$(2E_{100}N\lambda^2/3kT)z + \sigma\lambda/kT = \ln\left(\frac{x + 2z}{x - z}\right)$$

This equation has been solved graphically for several values of the ratio σ/σ_m , where $\sigma_{\mathbf{n}}$ is the tensile stress that would have to be applied to produce the same strain as that produced by a transition of the order parameter from zero to unity. Thus

$$\sigma_{\rm m} = E_{100}(2N/3)\lambda$$

The solutions are presented as Fig. 18.

REFERENCES

- 1. C. Zener: Equilibrium Relations in Medium
- Alloy Steels. This volume, page 513.

 2. W. A. West: Phase Boundaries in Medium Alloy Steels. This volume, page 535.

 3. M. Volmer and A. Weber: Keimbildung in
- übersättigten Gebilden, Ztsch. phys. Chem.
- (1926) 119, 277. 4. R. Becker: Die Keimbildung bei der
- Ausscheidung in Metallischen Mischkristallen. Ann. der Physik (1938) 32, 128.
 5. H. Carpenter and J. M. Robertson: Metals,
 chapters V. VI and VII. Oxford, 1939.
 6. L. W. McKeehan: Discussion of Mehl and
- Barrett: Studies upon the Widmanstatten Structure. Trans. A.I.M.E. (1931) 93, 78.

- 7. C. S. Barrett: Structure of Metals, 470-474.
- New York, 1943. McGraw-Hill Book Co. R. Mehl: Hardenability of Alloy Steels. Trans. Amer. Soc. for Metals (1939) 1-54.
 R. Mehl: The Structure and Rate of
- Formation of Pearlite. Trans. Amer. Soc.
- for Metals (1942) 29, 813.

 10. F. Hull and R. Mehl: The Structure of Pearlite. Trans. Amer. Soc. for Metals
- (1942) 30. 381.

 11. G. Pellissier, M. Hawkes, W. Johnson and R. Mehl: The Interlamellar Spacing of Pearlite. Trans. Amer. Soc. for Metals (1942) 30, 1049.
- 12. G. Roberts and R. Mehl: Effect of In-homogeneity in Austenite on the Rate of the Austenite-Pearlite Reaction in Plain Carbon Steels. Trans. A.I.M.E. (1943) 154,
- 318.
 13. S. Epstein: The Alloys of Iron and Carbon,
 1, 88. New York, 1936. McGraw-Hill Book
- Metals Handbook, 1939, 99. Amer. Soc. for Metals.
- 15. A. Hultgren: Hardenability of Alloy Steels.
- 55. Amer. Soc. for Metals, 1939. C. Wells and R. Mehl: Rate of Diffusion of Carbon in Austenite. Trans. A.I.M.E.
- (1940) 140, 294. Metals Handbook, 1939, 760. Amer. Soc. for Metals.
- Atlas of Isothermal Transformations, 24.
 U. S. Steel, 1943.
 F. Wever and H. Lange: Zur Umwand-
- lungskinetik des Austenite I, Mitt. K-W-I.
- Eisenforchung (1932) 14, 71. 20. S. Steinberg and V. Zyuzin: Transformations of Austenite in a Chromium Steel.
- Rev. Metall. (1934) 31, 554.
 21. H. Jolivet: Transformation of Austenite on Cooling; Morphology and Genesis of the Aggregates Formed. Jnl. Iron and Steel
- Inst. (1939) 140, 95. 22. E. Davenport: Isothermal Transformations in Steels. Trans. Amer. Soc. for
- Metals (1939) 27, 837.
 23. W. L. Fink and E. D. Campbell: Influence of Heat Treatment and Carbon Content on the Structure of Pure Iron-Carbon Alloys. Trans. Amer. Soc. Steel Treat.
- (1926) 9, 717. E. C. Bain: Discussion of reference 23. Ibid., 752.
- K. Honda and Z. Nishiyama: On the Nature of Cubic and Tetragonal Martens-
- ite. Sci. Repts. Sendai (1932) [1] 21, 299.
 26. G. Hagg: The Decomposition of Austenite.

 Jul. Iron and Steel Inst. (1934) 130,
- 439. M. Cohen et al: Trans. Amer. Soc. for
- Metals (1944) 32, 290, 333, 363. 28. C. Zener: Anelasticity of Metals. This
- volume, page 155. 29. Bain: Functions of Alloying Elements in
- Steel, 33. Amer. Soc. for Metals, 1939.
 30. F. Bowman: The Partition of Molybdenum in Steel and its Relation to Hardenability.
- Amer. Soc. for Metals (1945) 35, 112.
 31. F. Bowman and R. Parke: The Partition of Molybdenum in Iron-Carbon-Molybdenum Alloys at 1300°F, and the Nature of the Carbides Formed. Trans. Amer. Soc.
- for Metals (1944) 33, 481.
 32. A. Greninger: The Martensite Thermal Arrest in Iron-Carbon Alloys and Plain

- Carbon Steels. Trans. Amer. Soc. for
- Metals (1942) 30, 1. P. Payson and C. Savage: Martensite Reactions in Alloy Steels. Trans. Amer.
- Soc. for Metals (1944) 33, 261.
 34. M. Volmer: Kinetic der Phasenbildung.
 1939. Reproduced by Edwards Brothers,
- P. Wever and H. Lange: Magnetic Investigation of Austenite Decomposition.
- Mitt. K-W-I. Eisenforschung (1932) 14, 71. J. H. Hollomon and L. D. Jaffe: The Hardenability Concept. This volume, page
- L. D. Jaffe and J. H. Hollomon: Harden-ability and Quench Cracking. This volume,
- page 617.
 E. P. Klier and T. Lyman: The Bainite Reaction in Hypocutectoid Steels. Trans.
- A.I.M.E. (1944) 158, 394.
 T. Lyman and A. Trojano: Isothermal T. Lyman and A. Trojano: Isothermal Transformation of Austenite in One Per High-chromium Cent Carbon Trans. A.I.M.E. (1945) 162, 196.

DISCUSSION

(J. B. Austin presiding)

A. R. TROIANO. *- Dr. Zener has presented an interesting and ambitious treatment of a most difficult problem. I shall limit my remarks to pointing out some of the more important inconsistencies between the theory as stated and the experimental facts with reference to the decomposition of austenite in the bainite and martensite temperature ranges.

Dr. Zener has adopted the shear type (martensite-like) mechanism of bainite formation, suggested in various modifications by a number of investigators. There is no direct experimental evidence to indicate that this mechanism is more probable than say a conventional nucleation and growth. It is well recognized that bainite does grow, although admittedly not nearly to the same extent as pearlite. In addition, the bainite reaction has a definite period of induction and a reaction rate curve that in many respects is similar to that of pearlite. In other words, the bainite reaction is time-dependent and in this respect completely dissimilar to the martensite reaction. My view is that the present status of either theory or experiment will not allow a definite choice. However, for purposes of the present discussion it is not necessary that any choice be made.

From theoretical considerations the author obtains a curve (Fig. 11) that gives the rate

^{*} Professor of Metallurgy, University of Notre Dame, Notre Dame, Indiana.

of lowering of the critical temperature for bainite formation as a function of carbon content. Then he purportedly shows that good agreement exists with experiment. To accomplish this he makes reference to two 3 per cent Cr steels of 0.60 and 1.0 per cent C. Unfortunately, no 3 per cent Cr, 0.60 per cent C steel exists in either of the references given. It is obvious from the text that reference is being made to a 3 per cent Cr, 0.38 per cent C steel. When the proper value of 0.38 per cent C is applied to the curve of Fig. 11, no agreement exists. In fact, Lyman and Troiano23 have recently shown experimentally the actual amount of lowering of bainite that will occur in a series of seven 3 per cent Cr steels with carbon contents ranging from 0.08 to 1.28 per cent. For the case mentioned by Zener (0.60 to 1.0 per cent C) the lowering is 50°C., not 100°C.

The author explains the incomplete nature of the bainite reaction by proposing a carbon enrichment of austenite following the austenite to bainite reaction, which results in lowering the critical temperature and the cessation of the reaction. An alternative mechanism proposed by the author is that the increase of carbon concentration in the austenite immediately surrounding the bainite will produce a cementite film around the bainite preventing further growth. With regard to the first mechanism proposed, no carbon enrichment of the austenite (measured by the axial ratio of the martensite) has ever been detected in any case where the structure is definitely bainite alone. From a consideration of the experimentally determined rate of lowering of the critical temperature with increasing carbon content,23 it is obvious that such a change would be experimentally detectable. For example, see reply to discussion.24 The second proposed mechanism is equally incapable of explaining the incomplete nature of the bainite reaction. The absence of a thin carbide film is difficult to prove experimentally. For purposes of this discussion this is not

necessary. For the sake of argument, let us allow (only temporarily) the thesis of a carbide film. This means that large volumes of unreacted and not enriched (see above) austenite will remain after partial reaction. The reaction has ceased but the major portion of this austenite is no different in carbon content than the original. How then does this remaining austenite "know" that it is no longer permitted to react? From the above it is obvious that any successful theory of bainite formation must consider both the nature and rate of nucleation* of bainite. Dr. Zener has clearly stated that bainite nucleation theory is not sufficiently well developed to handle at present.

The sentence containing Eq. 25, and the one immediately preceding are apt to be misleading if one does not refer to Zener's previous paper. 25 A theoretically derived curve for Ar" as a function of carbon content was obtained and compared with the experimental curve. Agreement was obtained after assuming a constant strain energy of 290 cal. per mol. As Zener points out, the difference was one of temperature, and the introduction of the concept of a constant strain energy produced agreement.

This leads us to a consideration of the interesting case of bainite formation at temperatures below Ar" (Ms). Upon quenching to some temperature below Ar" martensite forms during the quench upon cooling below Ar". As is now well recognized, the amount of martensite is characteristic of the temperature and independent of the time. It follows that at least several units of austenite volume must have transformed to martensite at essentially the bath temperature. Upon continued holding at the same bath temperature the bainite reaction will start and proceed in its characteristic manner. Thus one observes martensite and bainite both formed at essentially the same temperature and each in its own characteristic manner. According to the theory, there is no difference in the conditions for

²³ T. Lyman and A. R. Troiano: The Influence of Carbon Content upon the Transformations in 3 per cent Chromium Steels. Manuscript submitted to A.S.M., June 1945.

²⁴ T. Lyman and A. R. Troiano: Isothermal

²⁴ T. Lyman and A. R. Troiano: Isothermal Transformation of Austenite in One Per Cent Carbon, High-chromium Steels. *Trans.* A.I.M.E. (1945) 162, 196.

^{*}With certain alloy steel compositions, especially in the lower temperature range of formation of bainite, the growth of bainite is almost negligible. Thus, as an excellent first approximation, the reaction rate curve is a direct reflection of the rate of nucleation.

²⁶ C. Zener: Equilibrium Relations in Medium Alloy Steels. This volume, page 513.

the formation of lower bainite (carbon atoms suffer no entropy change) and martensite, except that of the assumed constant strain energy. The author makes this quite clear in discussing the application of Eqs. 21 and 23. It is not clear how the theory when applied to the above case (same bath temperature) can make any differentiation between the austenite → martensite and the austenite → bainite reaction. All volumes of austenite are cooled to the same temperature; how then, according to theory, does a given volume of austenite "know" that it must form martensite while others must wait awhile and form bainite? In fact, it is difficult to conceive of how any thermodynamic treatment could make this differentiation.

Let us return momentarily to the assumption of a constant strain energy. From this assumption and the rest of the theory, it necessarily follows that the rate of lowering of bainite must be equal to the rate of lowering of Ar". This is not true for 3 per cent Cr steels;25,26 the only case for which sufficient experimental data exists for a careful check of this type.

As a matter of general principle, I strongly object to the statement regarding the two mechanism of martensite decomposition, which reads in effect that further experimental work on this problem is useless and that the answer can be found only in a theoretical analysis. A theoretical analysis is welcome but further experimental work should not be discouraged. The value of any theory can be judged only in so far as it either explains existing experimental facts or predicts future ones; and thus can be both a guide and a stimulus for planning future experimental work.

It is not precisely clear what the author means by a random interstitial solid solution of carbon in austenite. It is generally accepted that the carbon atoms occupy the octahedral (largest) interstices in austenite.27 It is logical to presume that, although there is never sufficient carbon to fill all these interstices, the carbon atoms will arrange themselves in as orderly a fashion as possible, attempting to get as far from each other as possible. The selective nature of the carbon interstitial positions necessary to produce tetragonality is well known and has been recently considered by Petch.28 In an interesting discussion to Petch's paper Lyman29 applied the experimentally determined shear mechanism of Greninger and Troiano³⁰ for the formation of martensite. It was shown that the carbon atoms are "carried along" (no diffusion) with the shear, from the accepted positions in austenite to those for martensite. Thus, with carbon atoms orderly arranged in the accepted austenite interstices, it is quite logical to expect a selective distribution of carbon in the accepted martensite interstices.

Any successful theory of austenite decomposition must explain the phenomenon of stabilization. This is true especially because many of the phenomena attributed to carbon enrichment are actually cases of austenite stabilization. For example, Lyman and Troiano23 have recently shown that it is possible to retain gamma (austenite) in an alloy of 3 per cent Cr plus Fe after partial reaction. This alloy does not retain gamma after a direct quench. Obviously, carbon enrichment cannot account for this phenomenon.

Finally, I should like to call attention to an investigation by Johansson, 31 which, to the best of my knowledge, represents the first recognized direct applicability of fundamental physical principles (thermodynamic) to the problem of austenite decomposition. Dr. Zener would make a distinct contribution if he would comment on this work, especially since Johansson's approach to the problem was the same (thermodynamic) as Zener's.

W. H. Brandt. *- The author is to be commended for his courage in attacking the theory of austenite decomposition in such a vigorous and catholic manner. The formation of pearlite, the formation of bainite, the formation of martensite, time-temperature

²⁸ N. J. Petch: The Structure of Martensite.

Inl. Iron and Steel Inst. (1943) 147, 221.

Inl. Iron and Steel Inst. (1943) 147, 221.

Inl. Iron and Steel Inst. (1943) 147, 221.

A. B. Greninger and A. R. Troiano: Mechanism of Martensite Formation. Trans.

A.I.M.E. (1941) 145, 291.

31 C. H. Johansson: Basic Thermodynamic Interpretation of the Process of Austenite-Martensite Transformation. Archiv Eisen-

hüttenwesen (1937-38) II, 241.

* Assistant Manager, Materials Engineering Department, Westinghouse Electric Corporation, East Pittsburgh, Pennsylvania.

²⁶ E. P. Klier and A. R. Troiano: Ar" in Chromium Steels. Trans. A.I.M.E. (1945) 162,

^{175.} N. J. Petch: The Positions of the Carbon Atoms in Austenite. *Jnl.* Iron and Steel Inst. (1942) 145, 111.

transformation curves and nucleation are all covered in this paper. Each of these topics is a complex and puzzling field for theoretical investigation and to cover all of them in a single paper is an ambitious undertaking, to say the least.

It is probably only natural that in covering so many subjects, many of the derivations are so brief as to be quite difficult to follow, so that the reader gathers the impression that not all of these derivations have been worked out with sufficient rigor.

In this discussion, attention will be called to a number of points that should be developed with more precision or else require somewhat more detailed clarification. Incidentally, these remarks will refer chiefly to that portion of the paper dealing with the formation of pearlite. On page 556, the author's Eq. 4 is: $V_B = \frac{-D}{(C_1 - C_1)} \cdot (SC/SX)_B.$ This equation is merely the mathematical statement of the fact that precipitation occurs at a growing interface at the rate at which the precipitating element arrives at that interface.

The equation as written is precisely true only when the interface is at right angles to and is growing in the opposite direction to the gradient.

When the interface is not at right angles to the gradient, a more general equation applies, which may be found in a paper published in March 1945.32 Furthermore, the author does not seem to recognize the fact that an equation of the type of Eq. 4 should apply to each point of the growing interface between cementite and austenite and between ferrite and austenite. In other words, the carbon gradient and carbon concentration vary from point to point along the interface and at each point an equation the type of Eq. 4 is obeyed, and it would seem, therefore, a questionable procedure to write a single equation and treat the gradient or the carbon concentration, as constant.

In connection with Eq. 4, the author makes the following statement: "In certain cases, such as the growth of cementite, the concentration C1 is fixed. G1 in the case of cementite would correspond to the concentration of carbon in cementite. In others, as in the

growth of ferrite, this concentration is to some extent indeterminate."

It would appear that C_1 can be interpreted as the solubility of carbon in ferrite and it is not clear why this was not done directly. In other words, there seems to be little reason for writing equations such as Eq. 5 and Eq. 6, derived on the basis of thermodynamic arguments unless one can show that there is reason to doubt that the values for C_2 and C_1 as derived from the equilibrium diagram are correct when one is dealing with a process of growth. Thermodynamic expressions, such as Eq. 5 and Eq. 6, would be more properly used in evaluating or determining equilibrium diagrams, to substitute them for numerical data appears to be a misuse of such relations.

On page 557, the following statement is made: "Eq. 4 and Fig. 2 show that the gradient of C2 at the boundary increases in magnitude with $(C_2 - C_1)_B$ faster than $(C_2 - C_1)_B$ itself. Eq. 4 contains the unknown VB which, in fact, is the quantity that is to be determined by the theory and therefore must be treated as an unknown. Fig. 2 is entirely schematic with respect to the carbon concentration near the ferrite and cementite interfaces and therefore with respect to the carbon gradients in the same neighborhood, and it appears injudicious to derive a semiquantitative relation between carbon gradients and carbon concentrations on the basis of this equation and this figure.

In Eq. 7, the author sets the concentration gradient of Eq. 4 equal to C/L. This gradient is treated as a sort of average gradient governing the whole growth process. If such a concept of an average gradient is to be used at all, it would be better to define the concentration difference as that existing in the austenite between the centers of the ferrite-austenite and cementite-austenite interfaces. Correspondingly, it would be better to define L as one half the interlamellar spacing rather than as one half the thickness of the cementite lamella.

The author is quite correct in calling attention to the fact that the carbon concentration ahead of a growing interface will depend on the curvature of that interface. As mentioned earlier, if Eq. 4 is correct, the interface is everywhere at right angles to the gradient and the direction of growth, and it is therefore plane.

³² W. H. Brandt: Jnl. Applied Physics (1945) 16, 139.

In other words, in writing such an equation, one has implictly made the assumption that one is dealing with plane interfaces. Nevertheless, this equation is combined with results derived from the assumption of a uniform radius of curvature r at the interface.

Actually, either of these assumptions involves an inherent mathematical difficulty, since, if either one is true, the carbon concentration will be constant over both the cementite-austenite interface and the ferrite-austenite interface, therefore there will be a discontinuity in the carbon concentration at the point where austenite, cementite, and ferrite join.

The question should also be raised whether it is justified to extrapolate a curve developed on the basis of a mechanism of pearlite growth into the region where lamellar pearlite clearly does not form. This was done in Fig. 9. It is commonly agreed among metallurgists that bainite formed below the knee of the curve involved some quite different mechanism than formation of pearlite and, as a matter of fact, this is quite conclusively shown by the work of Smith and Mehl.³⁸

Some reason should be given by the author for not comparing the results of his calculation with the directly measured growth rates that are available in the literature. To compare results with the upper section of the time-temperature transformation curve is a rather dubious way of confirming the correctness of a theoretical equation since these curves are affected by nucleation rates.

The disagreement of the author with the theory that alloying elements retard formation of pearlite because they must diffuse to the cementite while the pearlite is growing, thus requiring a longer time, appears to be sound. His picture of the effect of alloying elements on nucleation rates is not convincing, since precipitation of a complex carbide at a point of potential nucleation would be likely to aid rather than retard the nucleation process.

These are a few of the specific points upon which it is felt that improvement in this paper would be possible. The paper also has the general weakness that in calculating the velocity of growth, which certainly in the case of pearlite involves diffusion, the diffusion equation is completely ignored and little attention is given to the boundary conditions that must apply.

R. F. Mehl.—The theoretical problems involved in the decomposition of austenite are many, and in some respects of extraordinary difficulty. Certainly this paper deserves and requires much attention. We need the point of view that Dr. Zener can with facility bring to such problems. The paper invites an almost interminable discussion.

I think many readers would be pleased if references were handled somewhat differently. Many of the ideas are old, but the paper is not documented to show this. To take a few examples: The extrapolation of equilibrium lines into fields of instability is old, going back at least to Miers and Isaacs in 1907. The variation of carbon concentration as shown in Figs. 2 and 8 is likewise old; the assumption of an initial formation of ferrite in bainite of a carbon concentration unchanged from the original austenite is old. These are but a few examples. I am inclined to think that a proper regard in this sense for the history of a subject is essential, especially when theories are proposed, not in order to assign credit but so that the record may show the origins, and so that the interested worker may then be able to inspect the original evidence and weigh it, and finally so that the reader may be able clearly to distinguish between accepted theory and fact and that which the author newly proposes.

After having lectured my own students for some years on the dangers inherent in extrapolation, I am somewhat shocked to be taken to task by the author (pp. 562 and 563). He observes that Eq. 13 for the dependence of the interlamellar spacing on temperature is "in violent contradiction to the view of Mehl that the interlamellar spacing has a heat of activation," by which is meant that the logarithm of the spacing was plotted against 1/T. And on page 14 he states that extrapolating this curve on an exponential plot "illustrates the danger of extrapolating a formula over a limited range but that has no sound theoretical basis." And then, sur-

(1942) 150, 185.

²² C. V. Smith and R. F. Mehl: Lattice Relationships in Decomposition of Austenite to Pearlite, Bainite, and Martensite, *Trans.* A.I.M.E. (1942) 150, 211. ²⁴ Hull, Colton, and Mehl: *Trans.* A.I.M.E.

prisingly, where I had in the early history of this subject, when only approximations of the spacing were available—not the data plotted in Fig. 7—suggested this extrapolation of the spacing curve some 65°C., the author proceeds to extrapolate his curve some 870° to the absolute zero!

In 1938 it was not foolish to suggest an exponential plot, for several features of the process of the formation of pearlite were recognized as exponential in nature; indeed, that early paper stated that the plot "will probably be found to be not wholly correct when better data are available (page 34);" in subsequent papers, particularly the one by Pellisier, Hawkes, Johnson and myself in 1942, the data from which the author employs, where the interlamellar spacing was measured with as much care and precision as possible, it was shown that the logarithm of the interlamellar spacing could be plotted against I/T (the exponential plot), or against T, or against the degree of undercooling (which the author selects), and it was shown that the data are not precise enough to allow a choice among these, thus rendering all extrapolation foolish.

The author should have quoted this. Spacing data thus cannot be said uniquely to support the plot in Fig. 6, and thus do not lend appreciable support to the author's presumably "sound theoretical" basis. Fig. 7, the so-called Mehl plot, is, I fear, a straw man. I would not be willing myself to argue for one type of plot. I might observe, however, that results on pearlite spacing in fine pearlite as seen under the electron microscope, first published in 1941 and since in 1944, have disclosed minimum spacings of 300° to 500°A. This pearlite, definitely recognizable as pearlite, could not have formed in plain carbon eutectoid steels much below 570°C. If these values are introduced into Fig. 6, they are clearly not on the author's extrapolated curve. Perhaps the author should have considered these data, for they have been available. It is interesting to note that they do fall upon the exponential plot in Fig. 7.

Fig. 9 plots a "theoretical pearlite C-curve for infinite rate of nucleation." Let the unwary beware, for what is in fact plotted is a calculated rate-of-growth curve, not a curve of the rate of formation of pearlite. It is well recognized that the pearlite C-curve or S-curve is determined by the rate of growth and the rate of nucleation. An assumption of an infinite rate of nucleation is, as the author states, purely a circumvention. It is a device to avoid nucleation as a factor: the rate of nucleation is much the more important factor. On growth alone there would be no effect of austenite grain size on the rate of formation of pearlite, nor of austenite heterogeneity. Nor is there any basis to believe that growth alone would give even correct values of relative hardenability in these two steels.

I know that the author is aware of this, but being so, it would have been better to call that curve simply "a calculated rate of growth." Incidentally, it is strange that no comparison was made between these calculated values of the rate of growth and the measured values reported some time ago. Instead, the author uses (pp. 564-565) the time of completion of reaction at the nose of the S-curve for a steel with 0.30 per cent manganese, from which a very rough approximation of the rate of growth is taken. Manganese is very powerful in small amounts in changing the value of the rate of growth, as might be expected, and as the measurements quoted show. Inasmuch as the author's method does not provide a calculation for the effect of alloy, it would have been better to use data on the time of completion at the nose for a pure steel, for which the time is in the neighborhood of 2 sec. instead of 5. This would reduce his value for alpha still further to 0.02. But it would be even better to compare the results of Eq. 20 with measured values. Taking the measured rate of growth at 630° in a pure steel as 6 × 10-2, and accepting alpha as 0.12, the calculated rate of growth is only 1/10 the observed.

Evidently alpha is of uncertain significance. It should be said, however, that Eq. 18, which gives the temperature variation of the rate of growth, will, if the constant introduced to provide an equation is calculated from one measured value, furnish a very nice check with the observed variation of the rate with temperature. This is true for measured values on a pure steel; the check is poor for commercial steels, as would be expected from their impurity.

As I understand it, there is no apparent way in which the effect of alloy upon the rate of growth of pearlite may be calculated. At this point, the author changes his argument to nucleation, proposing that alloy elements concentrate at grain boundaries and corners, inhibiting nucleation in some way. The possibilities of such a concentration were pointed out originally by Gibbs, who showed that the effect should occur when such a concentration would lead to decreases in surface energy. Is there any evidence for this in austenite?

Finally, as to the calculation of the energy of the cementite-ferrite interface on page 14. The statement at the top of the second column does not have the candor it should: the experimental value to which the calculated value is compared is, as reference to the A.S.M. handbook will show, to cast iron (not steel), and to *liquid* cast iron at 1400°C. What bearing such a value may have upon the solid-solid ferrite-cementite interface energy, I cannot say, but I would like the author to try to do so.

The statement that the interface energy is nearly independent of temperature is wholly an assumption. Both Volmer and Becker assume a variation; but without knowledge of interface energies we are, of course, also without knowledge of their variation with temperature. The whole theory of nucleation and growth, especially nucleation, has been stultified by lack of any information on solid-solid interface energies—to my knowledge they have never been measured.

I am inclined to think that real progress in this field will continue to depend upon careful experimental work; in the case of nucleation it would be very useful to so many problems in physical metallurgy if the physicist would devise a method to measure these surface energies. If this could be done, the problem could be taken out of the realm of pace hypothesis, and this much to be desired.

The problem of bainite is attacked in a new and highly interesting way. We have needed an explanation of why bainite forms only within a certain temperature range. The author now provides a method of calculating the upper temperature limit. Is there some way by which this may be tested further? What would constitute a rigorous check against experimental values? Apart from the thermodynamics, the method involves

an assumption that the first bainite nucleus contains the same carbon in solid solution as the austenite from which it formed, an old idea, due originally, I believe, to Davenport, for which we still have no experimental proof.

The calculation of the upper temperature limit for martensite, the M_S point is new also. The fundamental equation in the latter case is identical to that for bainite, except that a strain energy term is added. If this is done in the latter case, why not in the former, for it would appear that the mechanism is assumed to be the same in the two cases? Apart from strain energy, what difference can there be between the nucleus of bainite—assumed as ferrite supersaturated in carbon—and martensite, which is also ferrite supersaturated in the carbon?

It should be observed that the treatment given for bainite is not truly kinetics, for there is no quantitative treatment of isothermal rates; indeed the only true kinetics in this paper is that relating to the rate of growth of pearlite in pure steels; the paper as a whole should probably be entitled differently.

As we might view today's session, our position would seem to be as follows: We have two methods by which the rate of growth of pearlite may be calculated. These methods seem different, and an effort should be made to reconcile them.

We have no way, unless Dr. Brandt's methods suffice, of calculating the effect of alloy content upon the rate of growth of pearlite: we have no method whatsoever for explaining and calculating the isothermal rate of formation of bainite; we have no theoretical method of treating the basically important factor of the rate of nucleation in pearlite; and we are not sure that the formation of bainite should be considered as a nucleation and growth process.

Indeed, our progress in theoretical kinetics of the decomposition of austenite is small, apart from the success in calculating the rate of growth in pure steels. But the problem is in fact extremely difficult. As against these deficiencies in kinetics, we have a new point of view on the factors that limit the temperature ranges in which bainite and martensite can form. These points of view should certainly be explored.

Having written this discussion, and having thought of all of the years I have sat at meetings and listened to discussions, most of which start with compliments to the authors, it occurred to me you might be interested in hearing a brief quotation from a famous American scientist, Benjamin Franklin:

"Nothing certainly can be more improving to a Searcher into Nature, than Objections judiciously made to his Opinions, taken up perhaps too hastily: for such Objections oblige him to restudy the Point, consider every Circumstance carefully, compare Facts, Make Experiments, weight Arguments, and be slow in drawing Conclusions. And hence a sure Advantage results; for he either confirms a Truth, before too lightly supported; or discovers an Error, and receives Instruction from the Objector. In this View I consider the Objections and Remarks you sent me, and thank you for them sincerely."

C. CRUSSARD.*—Among all the very important and interesting things Dr. Zener has told us, I would like to emphasize the role of internal stresses that he has invoked to explain the laws of martensite's formation, and also that of plastic glide.

Thermodynamics tells us whether a transformation is possible, but does not explain its submicroscopic mechanism. When martensite transformation occurs, the atoms swing from a position of relative minimum free energy, corresponding to the gamma lattice, or another relative minimum corresponding to the martensite. This requires an additional energy (activation energy) to jump over the relative maximum between those two states; this extra energy can proceed from two causes: thermal motion, as in many transformations, or high local stresses (as in slip dislocation).

As Dr. Zener has told us, we are obliged to assume that the very high stresses due to the martensite formation are released by plastic deformation.

I think that the role played by plastic glide is even more important, being not only consequence but often cause of the martensite formation. It is well known that martensite can be formed by plastic deformation of Hadfield or 18-8 steels. Mr. Idivet and myself have studied the matter. As the general laws

The martensite produced in these experiments was in form of needles, along (III) planes (slip-plane, in austenite) which, for small strains, could be resolved in separate points. [This had already been observed by Farlew and McCreery, Metals and Alloys (1941) 692.]

Let us now consider the relations between orientation of martensite platelets and atomic movements during the transformation.

Many authors have found that martensite forms in (111) planes, but some others have found (133) planes, or approximate (124) planes (Greninger and Troiano). If we assume the generally accepted Kurdjumow-Sachs shear theory of martensite formation, we can find a rather good explanation of those complex orientations: calculating in the case the plane of maximum shear strength (related to austenite lattice), I found a plane having the generalized Miller's indices (1-2.35-2.67). This gives rise to a trend for shear-glide along such planes. As there are no crystal lattice planes, the glide will occur either on the nearest (111) plane, or on still nearer planes as (133)(123) or (124), where the glide is much more difficult. The glide so initiated at one point will extend a little further and facilitate (or cause) the martensite formation, either on (111) plane, or more complex. The fact that the martensite platelets are often formed in the (111) slip planes seems to move the role played by slip in the propagation of the martensite transformation. We must rather think we observe a complex glidemartensite process.

If we now consider the magnitude of the shear strain, we see that the martensite formation corresponds to a unit shear of 0.35, and the glide 0.6, so that the martensite formation is likely to initiate before the glide, if no external tresses (or internal stresses due to

are not yet very certain, nothing has been published of those experiments at the present time. I can tell you, nevertheless, that we found the amount of martensite increasing more rapidly than proportional to the strain (elongation) showing not only that the glide produces martensite but that the martensite formed has a stimulating effect on the phenomenon, so that the connection between martensite formation and g ide must be very close.

The martensite produced in these experi-

^{*} School of Mines, Paris, France.

quenching) is applied. The glide would play its role afterward.

This unit-shear of 0.35 gives rise to a stress of about 4,000,000 lb. per sq. m., a higher value than the one given by Dr. Zener in his paper on Kinetics of the Decomposition of Austenite, page 570. The discrepancy between the two values probably occurs because the martensite initiates in place where the lattice structure is imperfect. This is quite probable if one thinks of the relation between glide and martensite and the fact that slip-dislocations also initiate in points of lattice imperfection (see Orowan's theory).

Most of the things I have said are rather hints than certainty, but I think it important to know there is surely a relation between martensite formation and glide, and that martensite is very probably formed in places of imperfect lattice structure, sometimes by thermal motion, sometimes by stresses (internal or external) or by both.

E. P. KLIER.*—The discussion developed under Equilibrium Diagrams is based on the acceptance of the theory of nucleation and grain growth, as explained in a subsequent section. However, if pearlite formation were considered as based on the operation of some other transformation mechanism, it might well be that the compositions determined by the extension of phase boundaries into the unstable regions have little or no significance.

In the development of the notion of nucleation an inherent contradiction, which has been of concern to several investigators, is involved. In its fundamental aspects the problem thus arising is very important, but need not be considered here; the assumption being allowed that nucleation as described may take place. To allow the formation of pearlite, then, carbon concentration gradients ahead of the ferrite and carbide plates must conform essentially to the conditions shown in Fig. 2. From the discussion, two important conclusions are immediately obtained:

1. Pearlite formation progresses at the maximum possible rate when no alloying element is present, unless that alloying element accelerates the rate of diffusion of carbon

while remaining uniformly distributed through the transformation products.

2. Composition adjustments (carbon) take place because of the concentration gradients existing ahead of the ferrite and carbide plates, so must be confined to a zone ahead of the advancing interface of width comparable to the interlamellar spacing.

Experimental data whereby both of these conclusions may be tested are available.

It is recognized that cobalt accelerates the rate of austenite decomposition throughout the subcritical range.35,36 Thus the presence of cobalt in a steel brings about the formation of pearlite at a higher rate than obtains for a plain carbon steel. The effect of cobalt content on the diffusion characteristics of carbon in the low-alloy range is debatable; however, it appears safe to assume that small additions of cobalt retard diffusion of carbon-thus lower the diffusion coefficient. Since cobalt steels transform to pearlite in a manner not logically to be anticipated, it may well be that the postulated mechanism of transformation is inadequate.

The recent work of Lyman and Troiano³⁷ on a steel containing 9 per cent chromium and 1 per cent carbon is of importance in the consideration of the second point. These investigators were led to the conclusion that in the steel studied carbon diffusion from the austenite to the pearlite-austenite interface was required to allow the continued growth of the pearlite. The region encompassed by the diffusion process is very great as compared with interlamellar distances and is readily distinguishable even when the lamellar pearlite is undissolved. These data conclusively show that the diffusion process is not governed other than in a subordinate sense by the carbon concentrations ahead of the ferrite and carbide lamellae in the steel concerned.

The validity of two of the most important deductions from the theory of nucleation and grain growth may be seriously contested. The theory cannot be expected to account for certain experimental data until fundamental changes are made in its structure.

The mechanism of bainite formation at-

^{*} Research Metallurgist, School of Mineral Industries, Pennsylvania State College, State College, Pennsylvania.

⁷⁵ H. H. Chiswik and A. B. Greninger: Trans. Amer. Soc. for Metals (1944) 32, 483.
88 E. C. Bain: Ref. 29 in Zener's paper.
87 T. Lyman and A. R. Troiano: Ref. 39 of

Zener's paper.

tributed to Wever and Lange was first proposed by Davenport and Bain.38 The tacit assumption that this mechanism is essentially correct seemingly results from a misunderstanding of the data Klier and Lyman³⁹ have obtained for this reaction; as it is seemingly impossible to mistake the conclusions these investigators have arrived at.

The earlier work on this reaction was not in the nature of a rigorous proof, as the methods employed were not free of ambiguities. The results of Klier and Lyman, on the other hand, are rigorous if the validity of X-ray analysis is to be allowed. Metallographic evidence presented by Klier⁴⁰ agrees completely with the results of X-ray investigation.

The mechanism of bainite formation proposed by Klier and Lyman is contrary to the basic concepts involved in consideration of the bainite reaction in the above. The experimental data are believed to be incontrovertible; necessarily, then, invalidating the author's treatment of this reaction.

In addition to problems arising from experimental data that conflict with the theory of austenite decomposition developed by Dr. Zener, there appear to be logical inconsistencies in the theory itself as applied to the bainite and martensite reactions.

If bainite is to be considered as structurally identical with martensite except for the magnitude of the stress system involved, it seems proper that Ar" be very sensitive to cooling velocity, when specimen size is held constant. Greninger⁴¹ has shown that no such sensitivity is found in iron-carbon alloys and in plain carbon steels.

By the analysis that has been offered, a steel cooled partially through the martensite range and then held should transform to martensite as the stress built up by transformation relaxes. Actually the reverse is true; a steel so treated is more difficult to transform completely to martensite than one continuously cooled.

By considering carbon diffusion from the bainite structure to the surrounding austenite as ultimately causing a cessation of the reaction, it is indicated as adequate that carbon diffusion in the ferrite be greater than in the austenite. This condition has no bearing on the problem. It is necessary that carbon diffusion in the austenite be greater than the propagation of the austenite-bainite interface. If this were not true the carbon atoms, even if conceivably projected through the interface would be repeatedly engulfed by the expanding bainite structure. The conditions specified by the author are inadequate, then, to give rise to an enriched austenite and cannot account for the cessation of the bainite reaction.

It is stated that "all the general features of austenite decomposition" can "be understood in terms of fundamental physical principles." It is contended here that no such statement holds. None of the three reactions by which austenite decomposes is accounted for either by fundamental principles or by assumptions that the author has required at various stages in the development of the theory.

C. ZENER (author's reply).-Mr. Brandt is particularly able to comment upon the mathematical rigor of the treatment on pearlite growth, since he himself has so ably attacked this problem from the standpoint of the solution of the pertinent differential equations. The most appropriate reply to his general criticisms is that no pretense was made at mathematical rigor; rather, an attempt was made to find, from general physical arguments, the manner in which the velocity of growth varied with temperature.

Certain questions, however, require specific answers. The question was raised as to whether the length L should not be associated with the interlamellar spacing rather than with the cementite plate thickness. The interpretation of L must depend upon the interpretation of the quantity $(C_2 - C_1)_B$, which also occurs in the denominator of the expression for the velocity of growth, and which refers to the difference in carbon concentration on the two sides of an advancing interface. If we analyze the conditions in front of the advancing ferrite phase, both L and $(C_2 - C_1)_B$ must refer to the ferrite lamella. On the other hand, both these quantities may be regarded as referring to the advancing cementite phase. The final answer is essentially independent of the viewpoint

³⁸ E. S. Davenport and E. C. Bain: Trans.

A.I.M.E. (1930) 90, 117. 39 E. P. Klier and T. Lyman: Ref. 38 of

Zener's paper.

6 E. P. Klier: Discussion of paper by J. L. Ham. Trans. Amer. Soc. for Metals (1945) 35, 355. A. B. Greninger: Ref. 32 of Zener's paper.

adopted. Objection was raised to the extension of the pearlite time-temperature transformation curve below its nose, since in plain carbon steels bainite rather than pearlite forms in this

range from 600° to 721°C., over which the velocity varies by a factor of 400. The value of the constant alpha necessary to obtain this agreement is 0.005. The computed velocity of

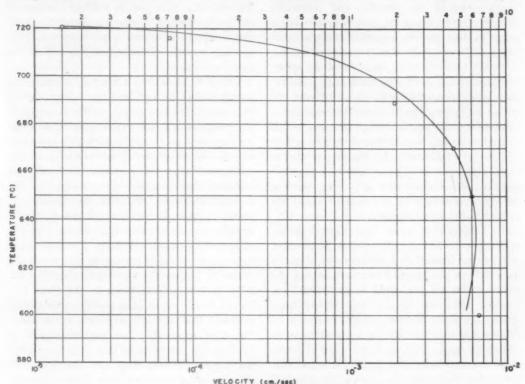


FIG. 19.—PEARLITE GROWTH.

Full curve: velocity of pearlite growth according to equation 18, with constant alpha adjusted to agree with experiment at 650°C.

Circles: experimental data for a high-purity eutectoid steel, after Hull, Colton and Mehl. 42

temperature region. It was not intended that the analysis in this paper be restricted to plain carbon steels. Fig. 19 gives the general features of the *TTT* relation when the only mechanism of transformation is by pearlite growth.

Both Messrs. Brandt and Mehl have suggested that a more appropriate test of the theory of pearlite growth would be a comparison with the observed velocity of growth rather than with a C-curve. This comparison is given in the accompanying figure (Fig. 10), the experimental data being that of Hull, Colton and Mehl⁴² upon a high-purity iron-carbon steel (steel J). The unknown parameter alpha was adjusted to give agreement at the temperature 650°C. Essential agreement is obtained throughout the entire temperature

growth, taking the parameter L as one half the width of the cementite lamellae, therefore varies with temperature in essentially the observed manner, but has a magnitude only one tenth the observed value. This discrepancy -which, incidentally, is just as large in the contemporary computations of Brandt-the author is inclined to attribute to certain simplifications that have been made in the calculation of the rate of diffusion. Thus the diffusion coefficient for carbon has been assumed to be that for a steel of eutectoid composition. Actually the carbon concentration just in front of an advancing pearlite nodule varies considerably, by a factor of 5 at 600°C. The concentration is, on the average, considerably greater than the eutectic concentration. If the computations could be carried out taking into account the observed variation of diffusion

⁴² Trans. A.I.M.E. (1942) 150, 185.

coefficient with carbon concentration, an increase in computed velocity would be obtained. Again, in estimating the diffusion, a strain-free lattice was assumed. The difference in densities of the pearlite and cementite lamellae must result in considerable elastic strain in the austenite just ahead of the advancing interfaces. Such strains must affect the diffusion rate. However, in view of the many places in which approximations must be introduced in a computation of this type, some of which were discussed by Brandt, it would give an incorrect impression of an attempt at an exact calculation to eliminate only one or two of the approximations by lengthy computations. Rather, it is believed that more physical insight into the factors governing pearlite growth is obtained by not being waylaid by such detailed considerations.

Dr. Mehl's remarks upon interlamellar spacing invite a lengthy discussion. The author will confine himself to a few remarks. Even in 1938 it was not justified to consider that the interlamellar spacing could be governed by a heat of activation type of law. It had been known for many decades that the limitation of free energy available during a transformation places an upper limit upon the area of interfaces that can be formed. In fact, it is just this limitation that forms the basis of the classical theories of nucleation quoted by Mehl in his 1938 paper. The disagreement of the interlamellar spacing obtained by the electron microscope with the author's plot in Fig. 6 illustrates the urgent need for further experimental work with high-purity plain carbon steels. The steel to which Fig. 6 pertainsin fact, as are all steels for which interlamellar spacing data are available—is commercial plain carbon steel. The small amounts of manganese these steels contain will have an appreciable influence upon the interlamellar spacing at all temperatures; a very large effect at temperatures only slightly below the eutectoid. The experimental verification of the temperature dependence of interlamellar spacing formulated in this paper must await further experiments with high-purity plain carbon steels. The method developed in this paper provides a very direct method for an evaluation of the influence of alloying elements upon the interlamellar spacing, and hence upon the velocity of growth. Thus the velocity is inversely proportional to the spacing, which in turn is inversely proportional to the free energy available, which in turn is a linear function of the concentration of alloying elements present. The velocity, therefore, is a linear function of the concentration of alloying elements. Additional effects of alloys upon velocity occur through a slight alteration of the carbon diffusion coefficient.

Cobalt is anomalous among all alloying elements in that its standard free-energy change in passing from austenite to ferrite decreases as the temperature is lowered, passing through zero at about 900°C. and presumably becoming negative below this temperature. One therefore anticipates that the presence of cobalt will increase the available free energy in the decomposition of austenite to ferrite and cementite, and will therefore decrease the interlamellar spacing, thereby increasing the velocity of growth of pearlite nodules. The anomalous behavior of cobalt in increasing the rate of the austenite to pearlite transition, cited by Dr. Klier as a stumbling block to the ideas presented in this paper, is in reality experimental evidence that actually supports these ideas. Dr. Klier supposedly has another stumbling block in the observations that in certain steels the carbon diffuses from the austenite into the advancing pearlite nodule from a distance great compared with the interlamellar spacing. In these steels (9 per cent chromium) the carbide is thought to be Cr7C2 rather than cementite. If that is indeed true, the primary factor that limits the velocity of advance of a pearlite nodule is the diffusion of chromium, just as in plain carbon steel the primary limiting factor is the diffusion of carbon. Information is not at present available to determine whether the diffusion of chromium into the carbide plates would be hastened or retarded by the transformation of the austenite between the carbide plates into ferrite. It is possible, therefore, that in 9 per cent chromium steels the advancing pearlite nodules consist of alternate plates of Cr7C2 and austenite. If that is true, carbon will diffuse into the Cr7C3 plates from a long way in front of the advancing plates. The relatively slow rate of growth of these plates would enable such long-distance carbon diffusion to take place, a diffusion that Klier observes does take place in high-chromium steels. The difficulty any theory of austenite decomposition has in satisfying all the "experimental" data is seen by a comparison of the discussions of Klier and of Troiano upon bainite formation. According to the former, the experimental evidence is incontrovertible that a fluctuation of carbon concentration precedes the formation of bainite, the bainite forming in the carbon-impoverished regions, the untransformed austenite thereby being enriched in carbon. According to the latter, no experimental evidence exists for the opinion that the untransformed austenite is enriched in carbon.

The author acknowledges the error pointed out by Troiano in the interpretation of his paper, and agrees with Troiano that an understanding of many of the features of bainite formation must await the development of a theory of nucleation. In fact, nearly all the questions raised by Troiano relate to problems in nucleation. He further acknowledges the

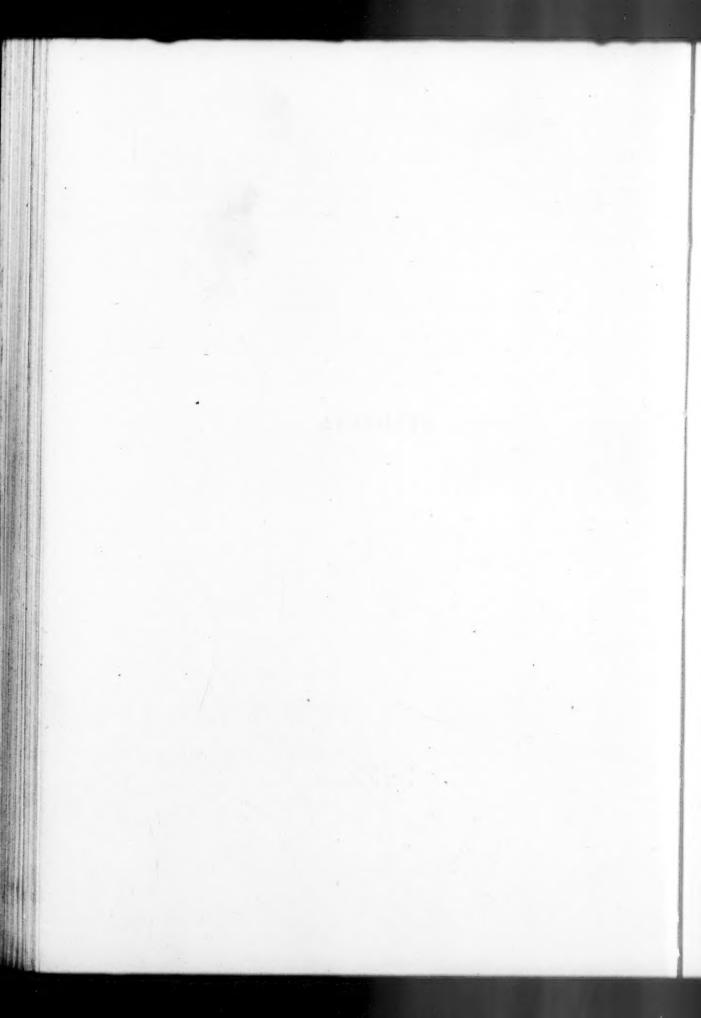
error in not referring to Johansson's prior work. Johansson had indeed the concept that the Ar" temperature for austenite to martensite transition may be computed from considerations of thermodynamic stability. His method of analysis did not, however, allow him to compute how this temperature varies with carbon concentration.

The author was very interested to hear of Crussard's experiments, and hopes that their publication will be not long delayed.

The author wishes to thank all the discussers for their comments. It is inevitable that in such a complex subject as austenite decomposition differences of opinion will arise over the interpretation of observations, and over the value of a theory that leaves many data unexplained. The uninhibited discussions at this meeting, however, will lead to a lessening of these differences.

.

SYMPOSIA



Symposium on Hardenability

(New York Meeting, October 1945)

CONTENTS

Introduction. By M. A. GROSSMANN
The Hardenability Concept. By J. H. HOLLOMON and L. D. JAFFE. With discussion 601
Hardenability and Quench Cracking. By L. D. JAFFE and J. H. HOLLEMON. With discussion . 617
Relationship between Hardenability and Percentage of Martensite in Some Low-alloy Steels.
By J. M. Hodge and M. A. Orehoski. With discussion 627
Determination of Most Efficient Alloy Combinations for Hardenability. By H. E. HOSTETTER.
With discussion
An Appraisal of the Factor Method for Calculating the Hardenability of Steel from Composi-
tion. By G. R. Brophy and A. J. Miller. With discussion 654
Factors for the Calculation of Hardenability. By IRVIN R. KRAMER, SIDNEY SIEGEL and J.
GARDNER BROOKS. With discussion
Addition Method for Calculating Rockwell C Hardness of the Jominy Hardenability Test. By
WALTER CRAFTS and J. L. LAMONT. With discussion
Influence of Titanium on the Hardenability of Steel. By G. F. Comstock. With discussion 719

Introduction

By M. A. GROSSMANN

THE science of hardenability, when it arrives at a state of perfection, will tell us quantitatively the effect of all variables on hardenability, and will also tell us the effect of variable hardenability on the properties and behavior of a piece during and after hardening.

That our science has not yet arrived at such a beatific state is attested by the differences of opinion so often encountered. This need not alarm us unduly, though it may perhaps remind us that we are no cleverer than the physicians or the physicists, the engineers or the entomologists, who likewise have a small residuum of unsolved problems.

From the philosophic standpoint, we may remind ourselves that differences of opinion show only that our data are inadequate. If we had enough good data, there could be no differences of opinion. The lack of data in the field of hardenability is thus recognized. but it is being remedied today to an agreeable extent by contributions from some of the most active and expert workers in the field. In some cases, as you have seen from the program, we shall hear about the relation of hardenability to other features, such as cracking during quenching, and also the cost of obtaining a desired hardenability. We shall also hear a good deal about that other question: How quantitative is our knowledge of the calculation of hardenability from composition? We shall also hear about calculation of hardness of the hardened product.

In regard to calculation of hardenability from composition, we should perhaps ask ourselves some questions:

- 1. Do we always bear in mind the fact that we cannot measure hardenability directly? That is to say, in laboratory measurements we always have the influence of the quenching medium. A true measure of hardenability alone would be obtained if we could quench in an idealized medium, in which the surface of the piece would be cooled instantly to the temperature of the quenching medium, and kept there. In that case only the hardening propensity of the steel and the heat flow (i.e., diffusivity) would be involved and we should have a true measure of hardenability. Such a unit is the "ideal diameter, D_I," which is a real measure of hardenability, but which requires an estimate (mind you, an estimate) for translation from actual quench to the idealized quench.
- 2. When we attempt to calculate hardenability from chemical composition and grain size, we thus assume that no other influences need be considered. Is this justified? It seems that it is justified, inasmuch as calculations of hardenability, based on composition and grain size alone seem in simple steels at least to agree pretty well

with reality, and in view further of the fact that there is little evidence of other influences at work.

3. In basing studies on chemical composition, are we always sure that we are considering the actual composition of austenite? The item that plagues us here is undissolved carbides. The factor scheme for calculating hardenability seems to be fairly reliable in simple steels if all carbides are dissolved, but unfortunately, in the SAE steels, NE steels, and the other common low-alloy steels, the usual heat-treatment often leaves undissolved carbides. These may confuse the issue both by reason of the carbon and alloy which are held in the carbides and are therefore ineffective, and by reason of the action of precipitated carbides in acting as nuclei to defeat a hardening tendency. These several interfering influences of precipitated carbides have not yet been evaluated adequately.

By way of summary, then, one may perhaps say that the era of first approximations is past, and that in any proposed closer approximations we have a right to expect a refinement of techniques. The contributions we shall hear today constitute a long step forward.

The Hardenability Concept

By John H. Hollomon* and L. D. Jaffe,† Junior Members A.I.M.E.

(New York Meeting, October 1945)

THE hardenability concept has become widely used during the last few years for the choice and substitution of steels. Before the work of Grossmann,1 the systems for predicting hardenability from chemical composition could be used only over a narrow range of composition. Grossmann introduced a comprehensive system, which has been effective in calculating the hardenability of most types of moderate or low-alloy steels. However, occasions often arise that require the calculation of the hardenability of high-alloy steels from their chemical compositions. Experimental determinations of the hardenabilities of such steels indicate that the Grossmann system predicts much greater hardenabilities than are realized. The fact that cases do arise in which the Grossmann method does not apply indicates that the fundamental hypothesis of the system may not be generally applicable. It seems advisable to re-examine not only Grossmann's system but also the concept of hardenability itself.

HARDENABILITY

If steel parts are to possess a martensitic structure after quenching, they must first be austenitized and then cooled through the pearlite and bainite transformation ranges sufficiently rapidly to avoid the formation of pearlite, bainite, and proeutectoid products.* If, on cooling, these transformations are avoided, the resulting structure can consist only of martensite (and retained austenite). The hardenability of a steel is measured in terms of the severity of the cooling conditions necessary to avoid the pearlite and bainite transformations. The less rapid is the cooling necessary to prevent the formation of bainite and pearlite, the higher is the hardenability.

The pearlite and bainite reactions appear to be differently affected by the alloying elements. Not only is this indicated by the published isothermal transformation data, but recent work by Zener² affords a rational interpretation of the differing effects of the alloying elements. Manganese,³ for example, appears to decrease the rates of the pearlite and bainite transformations by equal percentages, while molybdenum^{4,5} is approximately 10,000 times more effective in retarding the pearlite than in retarding the bainite transformation, on the basis of isothermal measurements.

In some steels, the formation of bainite restricts the formation of martensite while

The statements or opinions in this article are those of the authors and do not necessarily express the views of the Ordnance Department. Manuscript received at the office of the Institute April 18, 1945. Issued as T.P. 1926 in METALS TECHNOLOGY, January 1946.

[•] Captain, Ordnance Department, Watertown Arsenal Laboratory, Watertown, Massachusetts.

[†] Metallurgist, Watertown Arsenal Labora-

References are at the end of the paper.

^{*}Proeutectoid ferrite or carbide may form within or above the pearlite temperature range. For the purposes of this discussion, the distinction between the formation of pearlite and the formation of proeutectoid products need not be considered. Further references in this paper to pearlite formation will be understood to apply also to formation of proeutectoid products.

in others pearlite is the limiting factor. Consider an element (like molybdenum) that greatly retards the pearlite reaction but has little effect upon the bainite reaction. If this element is added to a steel in which the formation of pearlite restricts the formation of martensite, the hardenability of the steel may be increased greatly. If the same element is added to a steel for which the formation of bainite limits the formation of martenstte, the hardenability of the steel will not be appreciably increased. It is not sufficient, therefore, in considering the effect of alloying elements upon hardenability to speak simply of their relative ability to facilitate the formation of martensite. Rather, it is necessary to consider separately the relative tendencies of the alloying elements to retard the bainite transformation and to retard the pearlite transformation. Thus, there are two hardenabilities, the pearlitic and the bainitic.

An important conclusion from the considerations mentioned above is that, since the previous experiments did not separate the pearlitic and bainitic hardenabilities, there may be some doubt as to the applicability of the multiplicative system introduced by Grossmann. If one element affects primarily the pearlitic hardenability and another has the same effect on pearlitic and bainitic hardenabilities, additions of the two elements simultaneously may be more effective than additions of either separately. This difference in the effects of the alloying elements possibly may be responsible for the apparently multiplicative effects of the elements. The data presented by Grossmann in evidence of the applicability of his system, as well as subsequent experience, do indicate, however, that the effects of the alloying elements on the pearlitic hardenability are approximately multiplicative. Until further knowledge of the nature of the transformations' is available the justification for the multiplicative method of combining the effects

of the alloying elements must remain purely empirical.

MEASUREMENTS OF EFFECT OF COMPOSITION ON HARDENABILITY

Among the considerations that complicate the evaluation of experimental data on hardenability is the fact that investigators have generally not used the appearance of the first trace of nonmartensitic product as their criterion of hardenability, because of the additional experimental work involved. Instead, criteria intended to represent 50 per cent nonmartensitic product have been utilized. In some cases this product might be partly pearlite and partly bainite. Moreover, various criteria based upon hardness measurements have been commonly used to indicate the percentage of nonmartensitic product, and there is some question as to the general applicability, as well as the accuracy, of these criteria.

If a plain carbon steel of moderate or small grain size has been cooled at such a rate that it consists of 50 per cent martensite, and 50 per cent nonmartensitic product, the nonmartensitic product is generally believed to be pearlite. Grossmann, Asimow, and Urban, among others. have reported it as pearlite. Therefore, if alloying elements that retard equally the pearlite and bainite reactions (or which retard the bainite reaction more than the pearlite) are added to plain carbon steels, the measured hardenability of the resulting steels, on the basis of 50 per cent martensite, will be the pearlitic hardenability. If, on the other hand, alloying elements are added that have a greater retarding effect on the pearlite transformation than on the bainite, a composition will be reached in which bainite will restrict the formation of martensite, and measurements of the effects of further additions of the alloying elements will then apply to bainitic hardenability.

It is not possible from the papers of Grossmann or of the other investigators

who measured the effects of alloying elements on hardenability to determine whether for each measurement pearlite or bainite restricted the formation of martensite. Grossmann^{1,6} and Kramer. Hafner, and Toleman,7 as well as Crafts and Lamont in their early study,8 used hardness measurements as criteria of hardening. In a later study,9 Crafts and Lamont used the direct microscopic technique for determining the degree of hardening but reported that the nonmartensitic product was bainite in some cases and pearlite in others. They did not specify the nonmartensitic structure that was found in each case. Thus, it can only be deduced whether for each alloying element the pearlitic or bainitic hardenability was measured. In the investigation of Grossmann and Stephenson10 on the effect of grain size, essentially plain carbon steels were studied and direct microscopic measurements were employed to determine the extent of the hardening. The nonmartensitic structure was reported to be pearlite; hence the effect of grain size determined by these investigators refers to the pearlitic hardenability.

PEARLITIC HARDENABILITY

The isothermal transformation data indicate that the elements that have the same or less of a carbide-forming tendency than iron retard the pearlite and the bainite transformations by approximately equal percentages. Thus, the elements carbon, manganese, nickel, and silicon do not appear to affect the nonmartensitic transformations selectively for small or moderate additions. (An element such as manganese, which has a slightly greater tendency than iron to form carbides in steel, may have a greater effect on the pearlite than on the bainite transformation when added in large percentages.) Since Grossmann and those who subsequently performed such experiments added single alloying elements to essentially plain carbon steels, it can be assumed that their data for carbon, manganese, nickel, silicon, copper, phosphorus, and sulphur, as well as for grain size, apply to the pearlitic hardenability.

It has been reported7 that as chromium is added to hypoeutectoid plain carbon steels the hardenability first increases very rapidly, but after about 0.50 per cent of this element is added the effect becomes less pronounced and is not reproducible Similarly, after 0.20 per cent molybdenum has been added to a plain carbon steel, the effect of molybdenum becomes less pronounced and is not reproducible. It was suggested by Grossmann¹ that since chromium and molybdenum have strong tendencies to form carbides, the smaller and less reproducible effect at higher percentages is due to the decrease in alloy and carbon content of the austenite before quenching caused by the presence of undissolved carbides. Undoubtedly such an effect exists, but it is also reasonable to assume that, as these elements are added, the pearlitic hardenability increases more rapidly than does the bainitic, so that the formation of bainite begins to limit the formation of martensite. This assumption is substantiated by the published S-curves. 3,4,5,11,12 It seems likely that the effect of chromium and molybdenum on the pearlitic hardenability will be given by the data for the addition of small amounts of these elements to plain carbon steels. The effect of large percentages upon the pearlitic hardenability has not been studied. Until these data are available, it can be assumed that, since the ideal round size for almost all the alloving elements has been found to vary linearly with the percentage of alloving element, the effects of large percentages of chromium and molybdenum upon the pearlitic hardenability may be obtained by extrapolating the data for small percentages of these elements.

Information available on the elements boron, 1,9 titanium, 7,9,18 and vanadium 1,9 is contradictory, and may indicate that

the effects of these elements upon hardenability depend to some extent upon factors other than the amount of the element contained in the austenite. Therefore, it does not appear possible at present to delineate the quantitative effects of these elements on the hardenability or to conclude whether they affect primarily the pearlitic or bainitic hardenability.

(which tentatively can be extrapolated to larger percentages). These values are based upon those selected from the literature by Grossmann¹⁴ (except the value for copper, which is based upon the data of Kramer, Hafner, and Toleman7).

These values are intended to give the diameter in inches of the ideal round that will be 50 per cent pearlite at its center.

TABLE 1.—Effect of Carbon and Alloying Elements upon Hardenability (Ideal Round)

Elements	Grossmann Pearlitic Hardenability Factors	Assumed Bainitic Hardenability Factor			
50 per cent martensite	$\begin{array}{c} 0.338 \times \sqrt{\% \text{ C in.}^b} \\ 0.254 \times \sqrt{\% \text{ C in.}^b} \\ 1+4.10 \times (\% \text{ Mn}) \\ 1+2.83 \times (\% \text{ P}) \\ 1-0.62 \times (\% \text{ S}) \\ 1+0.64 \times (\% \text{ Si}) \\ 1+2.33 \times (\% \text{ Cr}) \\ 1+0.52 \times (\% \text{ Ni}) \\ 1+3.14 \times (\% \text{ Mo}) \\ 1+0.27 \times (\% \text{ Cu})^a \end{array}$	$\begin{array}{c} 0.494 \times \sqrt{\% \text{ C in.}} \\ 0.272 \times \sqrt{\% \text{ C in.}} \\ 1 + 4.10 \times \sqrt{\% \text{ Mn.}} \\ 1 + 2.83 \times (\% \text{ P)} \\ 1 - 0.62 \times (\% \text{ S)} \\ 1 + 0.64 \times (\% \text{ Si)} \\ 1 + 1.16 \times (\% \text{ Cr)} \\ 1 + 0.52 \times (\% \text{ Ni)} \\ 1 \\ 1 + 0.27 \times (\% \text{ Cu)} \end{array}$			

Calculated from data selected by Grossmann, it except copper factor.
 For grain size A.S.T.M. 7. For other grain sizes see Table 2.
 Calculated from data of Kramer, Hafner, and Toleman.

Tables 1 and 2 present in tabular form values for the pearlitic hardenability (ideal round size) of iron-carbon alloys with various carbon contents and for the effects upon pearlitic hardenability of grain size, manganese, nickel, silicon, copper, phosphorus, and sulphur, and of small percentages of chromium and molybdenum

TABLE 2.—Effect of Austenitic Grain Size upon Pearlitic Hardenability (Ideal Round)

Austenitic Grain Size	Carbon Factor for Pearlitic Harden- ability, In.								
(A.S.T.M. No.)	50 Per Cent Martensite	Essentially All Martensite							
I 2	0.546	0.410							
3	0.465	0.350							
. 5	0.429 0.397 × √9								
	0.366	0.275							
8	0.338	0.254							
	0.312	0.234							
9	0.288	0.217							
10	0.266/	0.200/							

a Calculated from data of Grossmann.1

Very little information is available as to the relation between the size that will be 50 per cent pearlite and the largest size that will contain no pearlite. Nevertheless, it is often desirable to obtain an estimate of the size that will fully harden. A few measurements15,16 indicate that the ideal round size for a few per cent of pearlite is of the order of 0.75 times the size for 50 per cent pearlite. A value for the effect of carbon including this factor is given in Tables 1 and 2 and can be used in calculating the ideal round size that will fully harden as far as pearlite is concerned.

BAINITIC HARDENABILITY

As yet there have been no comprehensive experiments designed to determine the effects of alloying elements upon the bainitic hardenability. A method of making these measurements, at least approximately, can be suggested. Instead of adding the various elements to plain carbon steels, they can be added to a steel for

which bainite limits the hardenability. The hardenability can then be measured as a function of the alloy additions, probably using direct microstructural examinations to determine the extent of the hardening. In a steel containing about 0.25 per cent molybdenum, bainite rather than pearlite will limit the hardenability, and such a steel would form a suitable base for an investigation of this sort. Another approach would be to study the effects of the alloying elements after austenitizing at temperatures that produce a large (and constant) austenitic grain size. Since increasing the grain size of a steel increases the pearlitic hardenability more than the bainitic, at sufficiently large grain sizes bainite rather than pearlite should restrict the formation of martensite. One difficulty in the interpretation of such measurements is that the addition of an alloying element, such as molybdenum, which retards the pearlitic formation and does not modify the rate of bainite formation as measured isothermally, may induce indirectly a decrease of the bainitic hardenability, as will be discussed later.

Since no direct measurements of the bainitic hardenability have been made and it is frequently desired to design steels for parts that are not to contain bainite on quenching, an approximate determination of the effects of alloying elements on the bainitic hardenability of hypocutectoid steels has been attempted.

It was noted that additions of carbon, manganese, and nickel cause little change in the shape of the isothermal S-curves, their principal effect being to shift the entire curve toward longer times.^{3,12,23} Similar assumptions appear justifiable for copper, sulphur, and phosphorus. A recent investigation¹⁷ indicates that silicon, too, affects the bainitic hardenability to about the extent it affects the pearlitic. Molybdenum, on the other hand, increases markedly the times for transformation in the pearlite range, but has very little effect upon the

S-curve in the bainite region. 4.5.23 Previous work also indicates that increases in austenitic grain size act similarly, increasing the transformation times in the pearlite range, but having little effect in the bainite. 3.18 A scheme for rough calculation of the bainitic hardenability from composition was set up on the basis of the following assumptions:

1. A change in the percentage of carbon or of an alloying element produces a corresponding percentage change in bainitic hardenability (expressed as ideal round diameter), regardless of the original hardenability. This assumption is the equivalent of that made by Grossmann¹ for pearlitic hardenability.

2. Changes in the percentages of carbon, manganese, nickel, copper, sulphur, phosphorus, and silicon produce the same percentage changes in bainitic hardenability that they do in pearlitic hardenability.

3. Changes in molybdenum content and in austenitic grain size have negligible effects upon bainitic hardenability.

It remained, however, to set up the base value that is to be multiplied by the factors for the various elements. In Grossmann's work on pearlitic hardenability, this base value was included in the graphs for effect of carbon and grain size.1 (Grossmann assumed in accordance with previous work¹⁹ that the hardenability was proportional to the square root of the carbon content.) Such a bainitic base value was obtained by calculation from available Jominy hardness data. It was necessary to consider steels containing sufficient amounts of carbide-forming elements to ensure that bainite rather than pearlite limited the formation of martensite. Moreover, since the effect of chromium on bainitic hardenability was not known even approximately, it was necessary to obtain Jominy curves of steels having a constant chromium content. A survey of available Jominy data revealed a number of apparently trustworthy Jominy curves for

hypoeutectoid heats containing approximately 0.50 per cent chromium plus enough molybdenum (at least 0.25 per cent) to ensure that the bainite reaction limited the martensite formation. Since, in the absence of more complete data, the point of inflection of the hardness curve on logarithmic Jominy paper was taken as the criterion of half-hardening, only heats giving a satisfactory inflection point could be used. Heats quenched from so low vanadium and aluminum were neglected. The resulting values are given in Table 3 as "base values including chromium factor."

The effect of chromium remained to be determined. The S-curves indicate that chromium retards the pearlite reaction in hypoeutectoid steels to a greater extent than it does the bainite, 3,11,12 so that its effect on bainitic hardenability should be less than on pearlitic. Preliminary results

TABLE 3.—Steels Used in Determining Base Value for Bainitic Hardenability

Identifi- cation												Aus-			Base Value	
	Composition, Per Cent								ten- itizing Tem- pera- ture, Deg.	Jom- iny Dis- tance in 1/16 Inche	Equivalent D _I , Inches	In- clud- ing Cr Fac-	Not In- clud- ing Cr Fac-			
	С	Mn	P	S	Si	Ni	Cr	Мо	v	Cu	A1	F.			tor, In.	tor, In.
Q90 3 2627	0.25 0.29 0.20	1.26	0.033	0.027 0.026 0.019	0.36	0.54	0.51	0.43		0.04 ^b 0.04 ^b 0.11		1600 1625 1700	8 13 8½	2.95 3.90 3.05	0.841 0.687 0.646	0.537
NE8739 NE8744 2N1388	0.40	0.83	0.015	0.016 0.031 0.022	0.30	0.48	0.48	0.25		0.046		1575 1550 1550	9	3.16 3.55 3.16	0.732 0.766 0.834	0.470
2N1436	0.23	1.48	0.0084	0.0184	0.25	0.02	0.50	0.27	0.05	0.04 ^b 0.04 ^b 0.04 ^b		1600 1600	9	3.16 3.55 3.16	0.779 0.772 0.752	0.493
AI A4		1.01	0.014	0.016	0.22	0.32	0.48	0.35		0.04		1650 1650	11 16 Average	3.55	0.888 0.840 0.776	

a temperature that carbide solution appeared doubtful were discarded. Moreover, it was decided to use only curves in which the experimental points were available, since different workers may tend to smooth data differently. After these eliminations the curves on the 11 steels indicated in Table 3 remained. The inflection points were read by two observers independently, their Jominy readings averaged, and the results converted to ideal round sizes by the use of a conversion chart derived from that of Asimow, Craig, and Grossmann.20 The ideal round diameters were then divided by the factors for manganese, nickel, copper, silicon, sulphur, and phosphorus (Table 1) and by the square root of the carbon percentage. The effects of indicate, however, that chromium does increase the bainitic hardenability. Since it is necessary to make some assumption in the absence of data, it has been assumed that the effect of chromium upon bainitic hardenability is one-half its effect upon pearlitic. On this basis the values listed in Table 3 as "base values not including chromium factor" were obtained. Their average has been tentatively adopted as the bainitic base value for iron-carbon alloys.

The tentative factors for the effects of carbon (including the base value), manganese, nickel, chromium, molybdenum, copper, silicon, phosphorus, and sulphur upon bainitic hardenability are given in Table 1. (The carbon values are also pre-

<sup>Ladle analysis.
Estimated analysis.
To point of inflection on logarithmic hardness plot.</sup>

value, it must be remembered, is based

sented graphically in Fig. 1.) The base is reduced will be bainite. On the other hand, when the cooling rate is such that upon the point of inflection of Rockwell C the structure is half nonmartensitic, this hardness plotted against Jominy distance half is primarily pearlite. The view that

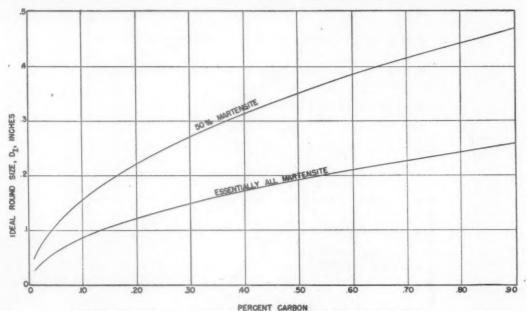


FIG. 1.—ASSUMED BAINITIC HARDENABILITY OF IRON-CARBON ALLOYS.

on a logarithmic scale. Available evidence indicates that this corresponds to 50 per cent bainite or slightly more. On the basis of a recent publication by Hodge and Orehoski16 and some other evidence,15 the ideal round size for a trace of bainite is of the order of 0.5-0.6 that for 50 per cent bainite. A value for the effect of carbon based upon a factor of 0.55 is given in Table 1 and Fig. 1 for use in calculating the ideal round size that will fully harden with respect to bainite.

It is of interest to note that the ratio of the ideal round size for full hardening to that for half hardening is considerably smaller (about 0.55 as compared with approximately 0.75) when the nonmartensitic product is bainite than when it is pearlite. As is indicated by Tables 1 and 2, it appears that for plain carbon steels with medium austenitic grain size, the first trace of nonmartensitic product obtained as the cooling rate on continuous cooling

the first nonmartensitic product is bainite in plain carbon steels with medium or coarse grain is in contradiction to the report of Digges¹⁹ and to common belief, but there is some experimental evidence to support it.15,21 The validity of the statement that most of the published work on the effect of alloying elements upon hardenability deals with pearlitic hardenability is not in question, since half hardening rather than full hardening was used for these measurements.

No measurements of the effects of alloying elements upon the hardenability of hypereutectoid steels seem to have been published and there is some reason²² to believe that these effects may differ from those in hypoeutectoid steels. The values in Table 1 are therefore proposed, at present, for hypoeutectoid steels only.

It must be emphasized that the scheme suggested above for computing bainitic hardenability from composition is tentative and that the numerical values included in it are based upon scant data. The system may serve, however, as the best approxi-

ing constant the time the steel is held in that range, may similarly change the rate of subsequent transformation in the bainite

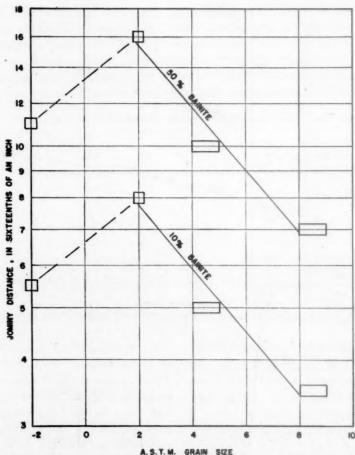


FIG. 2.—RELATION BETWEEN AUSTENITIC GRAIN SIZE AND BAINITIC HARDENABILITY OF S.A.E. 4140 STEEL.

mation possible until further experimental data are available.

RELATIONS BETWEEN PEARLITIC AND BAINITIC HARDENABILITIES

In the foregoing discussion, the pearlitic and bainitic hardenabilities have been treated independently. However, the time spent in the pearlite transformation range may affect the rate of the bainite transformation. Changing the fractional time spent in the pearlite range, by changing the time necessary for pearlite formation while holdrange. Thus, changes in pearlitic hardenability may induce changes in the bainitic hardenability even though the rate of bainite formation as measured isothermally (without holding in the pearlite range) is not altered.

Certain data do exist that indicate that increasing the pearlitic hardenability results in an increase in the bainitic hardenability, although the exact nature of this effect is by no means thoroughly understood. For example, as already mentioned, consideration of the isothermal data leads

to the conclusion that austenitic grain size has a negligible influence on the rate of bainite formation. However, when continuous cooling experiments were perThe resultant hardenability was consistent with the grain size and was not affected by the prior solution treatment.

At present, the only interpretation of

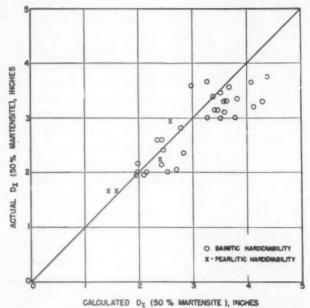


Fig. 3.—Comparison of measured hardenability with hardenability calculated by proposed system (for steels studied by Hodge and Orehoski 16).

formed, it was found that changes in grain size do affect the rate of bainite formation. These tests were made on an S.A.E. 4140 steel by austenitizing Jominy bars at 1500°, 1850°, 2200°, and 2450°F., cooling to 1500°F. and end-quenching. In Fig. 2, the Jominy distances at which to per cent bainite and 50 per cent bainite were found are plotted as a function of grain size. The bainitic hardenability increases with grain size up to a grain size of A.S.T.M. 2 (austenitizing temperature 2200°F.).* It was at first believed that this considerable increase in hardenability was associated with the increased solution of the carbides at the elevated austenitizing temperatures. Therefore a specimen was austenitized at 2200°F., quenched with water on all surfaces, and then reheated rapidly to 1500°F.

Because of the effect of fractional time spent in the pearlite range upon bainitic hardenability, molybdenum would be expected to have an indirect effect upon bainitic hardenability. Thus, the bainitic hardenability is probably not wholly independent of molybdenum content or grain size. Quantitative evaluation of the indirect effect awaits establishment of the dependence of rate of formation of bainite upon time of prior holding in the pearlite range.

this effect of grain size is that incubation in the temperature range at which the pearlite transformation occurs increases the rate of the bainite transformation. The smaller the fractional time spent in the pearlite range, the greater is the bainitic hardenability. Insufficient data are available to establish the interdependence quantitatively. This question will be the subject of a future paper.

^{*} The reason for the decrease of hardenability when the temperature is raised from 2200° to 2450°F. is not known.

APPLICATIONS

To apply the concept outlined in the foregoing pages to the calculation of hardenability from chemical composition, the pearlitic and bainitic hardenabilities are calculated separately. The lower of the two hardenabilities is then the hardenability that limits the formation of martensite, and is the significant value when martensitic structures are sought.

In designing steels that are to be directly quenched to martensite, there is no advantage in having a high pearlitic hardenability if bainite restricts the formation of martensite. Similarly, there is no advantage in having a high bainitic hardenability when pearlite is the limiting transformation.*

If it is desired to predict the structure obtained under conditions of continuous cooling that do not permit complete hardening, both the lower and the higher of the calculated hardenabilities are of interest. When the bainitic hardenability for full hardening is greater than the pearlitic, bainite will not appear to an appreciable extent. When the pearlitic hardenability for full hardening is greater than the bainitic, bainite will form under cooling conditions just insufficiently severe to produce only martensite, and pearlite will form under certain less severe conditions. The conditions for the transition from bainite to pearlite are then given by the pearlitic hardenability.

Example

As an example of the application of the concept of the dual nature of hardenability and of the system tentatively suggested

*With special types of quenches, the bainitic hardenability necessary for hardening may differ from the pearlitic hardenability necessary for hardening. Thus, when a delayed quench is used, in which a steel part is to be air-cooled through the pearlite range and water-quenched through the bainite, sufficient pearlitic hardenability may be required to permit hardening in air and only enough bainitic to permit hardening in water.

for calculating hardenability, data recently published by Hodge and Orehoski¹⁶ may be utilized. These authors measured the hardenabilities (50 per cent martensite) of 35 steels having various compositions and compared them with the hardenabilities calculated from composition by Grossmann's original method; that is, with the calculated pearlitic hardenabilities. They found that almost all of the measured hardenabilities were considerably lower than the calculated. The bainitic hardenabilities of the 35 steels have been computed from the compositions given by Hodge and Orehoski using the tentative values for the effects of the various elements given in Table 1. The carbon factor for nominally 50 per cent bainite was used. The bainitic hardenability so computed for each steel was compared with the pearlitic hardenability calculated by Hodge and Orehoski. The measured hardenability is plotted against the lower of these two in Fig. 3. Comparison of this figure with Fig. 8 of the paper by Hodge and Orehoski shows that when computed in the way suggested above the points fall much closer to the expected theoretical values than when computed on the basis of pearlitic hardenability alone.

Hodge and Orehoski state that complete solution of the carbides was generally not attained with the austenitizing treatments used. The carbon and alloy percentages in the austenite were, therefore, in most cases lower than the over-all percentages in the steel. This decrease in alloy and carbon contents may account for the tendency of the measured hardenabilities in Fig. 3 to fall slightly lower than the calculated hardenabilities.

It will be noted that most of the steels have lower computed bainitic than pearlitic hardenabilities. This is in accord with Hodge and Orehoski's finding that in most cases the nonmartensitic products were predominantly bainite. Considering the approximate nature of the numerical values

available for use in calculating bainitic hardenability and the reported lack of complete solution of carbides, the results of this example give a good illustration of the validity of the dual-hardenability concept and of the usefulness of the scheme proposed for calculating hardenability from composition.

CONCLUSIONS

An analysis of the nature of the decomposition of austenite and of the effects of the alloying elements on the rates of bainite and pearlite transformation indicates that in some cases pearlite and in others bainite will limit the formation of martensite on continuous cooling. Since alloying elements may have different effects upon the bainite reaction than upon the pearlite reaction, it is necessary to consider two hardenabilities: the pearlitic and the bainitic. If pearlite restricts the formation of martensite on continuous cooling, the pearlitic hardenability is less than the bainitic, and vice versa.

In determining the effects of the alloying elements on the hardenability, both the cooling conditions at which some specified amount of the nonmartensitic product is formed and the identity of this product should be established. In none of the previous investigations of the effect of alloying elements on the hardenability was the nonmartensitic product identified. It can, therefore, only be deduced whether the data refer to pearlitic or bainitic hardenability. As the alloying elements were added to essentially plain carbon steels and measurements of half hardening were made, it may be concluded that in most cases the data apply to pearlitic hardenability.

In order to determine the effects of the alloying elements on the bainitic hardenability, the alloying elements should be added to steels for which bainite limits the formation of martensite. In steels containing about 0.25 per cent molybdenum, this

occurs. Since no carefully designed experiments of this type have been performed. a tentative system is suggested as an interim measure to permit very rough estimates of the bainitic hardenability. Hardenabilities calculated by this system for a number of steels have been found to check well with the measured hardenabilities

One of the conclusions based on isothermal data that has been incorporated into the system is that molybdenum and austenitic grain size have little, if any, effect on the rate of bainite formation. Continuous cooling experiments indicate that grain size does have an effect on the bainitic hardenability. This effect appears to arise from an indirect influence of changes in pearlitic hardenability upon the bainitic hardenability, through inoculation or incubation in the pearlite transformationtemperature range. Changes that induce increases in the pearlitic hardenability without affecting the isothermal rate of bainite formation appear to increase the bainitic hardenability. Increases in grain size and in molybdenum content do, therefore, appear to increase the bainitic hardenability somewhat, but the extent of this effect is not known.

ACKNOWLEDGMENT

The authors wish to acknowledge the assistance of Miss Mary Norton, who was responsible for the experimental work on the effect of grain size upon the bainitic hardenability, and who criticized the manuscript. They also wish to thank Mr. M. A. Grossmann for reviewing the manuscript and for his constructive suggestions.

REFERENCES

 M. A. Grossmann: Hardenability Calculated from Chemical Composition. lated from Chemical Composition.

Trans. A.I.M.E. (1942) 150, 226-259.

2. C. Zener: Kinetics of the Decomposition of

Austenite. This volume, page 550.
3. E. S. Davenport: Isothermal Transformation in Steels. Trans. Amer. Soc. for Metals (1939) 27, 837-886.

 J. R. Blanchard, R. M. Parke, and A. J. Herzig: Effect of Molybdenum on the Isothermal Subcritical Transformation of Austenite in Low and Medium Carbon Steels. Trans. Amer. Soc. for Metals

(1941) 29, 317-338.
5. J. R. Blanchard, R. M. Parke, and A. J. Herzig: Effect of Molybdenum on the Isothermal Subcritical Transformation of Austenite in Eutectoid and Hyper-eutectoid Steels. Trans. Amer. Soc. for

Metals (1943) 31, 849-876.

6. M. A. Grossmann, M. Asimow, and S. F. Urban: Hardenability, Its Relation to Quenching, and Some Quantitative Data. In Hardenability of Alloy Steels, Amer.

Soc. for Metals, 124-196. 1939.
7. I. R. Kramer, R. H. Hafner, and S. L. Toleman: Effect of Sixteen Alloying Elements on the Hardenability of Steels. Trans. A.I.M.E. (1944) 158, 138-156.

W. Crafts and J. L. Lamont: The Effect of Silicon on Hardenability. Trans.

of Silicon on Hardenability. Trans.
A.I.M.E. (1943) 154, 386-394.

9. W. Crafts and J. L. Lamont: Effect of Some Alloying Elements on Hardenability. Trans. A.I.M.E. (1944) 158, 157-167.

10. M. A. Grossmann and R. L. Stephenson: The Effect of Grain Size upon Hardenability. Trans. Amer. Soc. for Metals (1941) 29, 1-19.

11. E. P. Klier and T. Lyman: The Bainite Reaction in Hypocutectoid Steels. Trans.

Reaction in Hypoeutectoid Steels. Trans.

A.I.M.E. (1944) 158, 394-422. 12. United States Steel Corp. Research Laboratory: Atlas of Isothermal Transformation Diagrams, 1943.

13. G. F. Comstock: Discussion to Reference 7.

 M. A. Grossmann: Unpublished Work.
 Unpublished Work, Watertown Arsenal.
 J. M. Hodge and M. A. Orehoski: Relationship between Hardenability and Percentage of Martensite in Some Lowalloy Steels. This volume, page 627.

17. A. Hurlich: Watertown Arsenal, Unpub-

lished Work.

lished Work.

18. E. S. Davenport, R. A. Grange, and R. J. Hafsten: Influence of Austenite Grain Size Upon Isothermal Transformation Behavior of S.A.E. 4140 Steel. Trans. A.I.M.E. (1941) 145, 301-314.

19. T. G. Digges: Effect of Carbon on the Hardenability of High Purity Iron-Carbon Alloys. Trans. Amer. Soc. for Metals (1938) 26, 408-424.

20. M. Asimow, W. F. Craig, and M. A. Grossmann: Correlation Between Iominy Test

mann: Correlation Between Jominy Test and Quenched Round Bars. Jnl. Soc.

Auto. Engrs. (1941) 49, 283-292. 21. M. Hill: Discussion of R. F. Thomson and

C. A. Siebert: Trans. Amer. Soc. for Metals (1942) 30, 43-44.

22. T. Lyman and A. R. Troiano: Isothermal Transformation of Austenite in One Per

Cent Carbon, High-chromium Steels.

Trans. A.I.M.E. (1945) 162, 196.

T. Griffiths, L. B. Pfeil and N. P. Allen: The Intermediate Transformation in Alloy Steels. Second Rept., Alloy Steels Research Committee, Iron and Steel Inst. (1939) 343-367.

DISCUSSION

(C. M. Loeb, Jr., presiding)

W. CRAFTS.*-The authors have made a commendable effort to improve the accuracy of the calculation of hardenability of the chromium-molybdenum steels. However, rationalizing a purely empirical formula requires assumptions that are hard to justify without considerable data, regardless of how reasonable they seem. In the calculation of bainitic 50 per cent martensite hardenability, it has been assumed that more than a certain amount of molybdenum has no effect and that this critical amount of molybdenum is lowered to nothing in the presence of about I per cent chromium. It should be noted that the use of one half of the pearlitic factor for chromium is balanced by a correspondingly higher carbon base, so that the ideal critical diameter of any plain chromium steel is calculated to virtually the same value whether pearlitic or bainitic factors are used. In the case of "bainitic" plain molybdenum and chromium-molybdenum steels, increase of molybdenum is considered to add nothing to the calculated hardenability. This assumption is not in accord with our observed results. We have not found fading in steels containing up to I per cent molybdenum without chromium, but have noted that significant chromium residuals tend to produce less than calculated hardenability. Similar results have been found in chromium steels with significant residual molybdenum contents. In chromium-molybdenum steels we have found fractional proportions of the "pearlitic" calculated hardenability, but within that range have found that increase of either chromium or molybdenum increases actual hardenability. We have seen no reason to blame molybdenum any more than chromium for the lowered hardenability and have seen indications that low carbon, high silicon, nickel, and possibly manganese, tend to aggravate the condition. Therefore, although the correlation appears to be somewhat better than with the "pearlitic" calculation, the proposed method of correcting the hardenability calculation does not agree with our observations and appears to be a

Research Metallurgist, Union Carbide and Carbon Research Laboratories, Inc., Niagara Falls, N. Y.

mathematical expedient rather than a rational solution of the problem.

The 50 per cent martensite criterion of hardenability has no special significance, and difficulty of measuring it has led to a great deal of confusion. Further, the ferrite and bainite reactions are so complex as to make a rational interpretation improbable in the present state of our knowledge. It would seem that any correlation of hardenability with austenite transformation must be based on 100 per cent martensite in order to simplify the problem and to evaluate hardenability in terms of real physical significance. The authors start in this direction is encouraging.

I. R. KRAMER.*-The authors are to be complimented for their explanation of the problems confronting the investigators of bainitic hardenability. Several items, however, are worthy of more consideration. Messrs. Hollomon and Jaffe have pointed out that the rate of bainite transformation is affected by the fractional time spent in the pearlite region. They have applied this consideration to explain the effect of grain size on steels in which bainite limits the hardenability; but, in the derivation of the hardenability factors, the authors have assigned a value of unity to the factor for molybdenum because it has very little effect on the bainite region in an isothermal transformation. Since molybdenum (like grain size) has a marked influence on the pearlite region, it logically follows that it will affect the bainite hardenability and that the value of one for the molybdenum factor is erroneous. The fact that the factors obtained by Hollomon and Jaffe were applicable for the calculation of the hardenability data of Hodge and Orehoski³⁴ does not constitute proof of the accuracy of the individual factor curves. In the paper by Kramer, Siegel, and Brooks25 it was shown that it is possible to derive a system of multiplying factors in which the individual factors are incorrect but, owing to compensating effect, can be used to calculate the hardenability. To

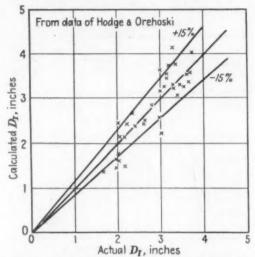


FIG. 4.—CORRELATION BETWEEN OBSERVED IDEAL CRITICAL DIAMETER AND THOSE CALCU-LATED BY THE HARDENABILITY FACTORS OF KRAMER, SIEGEL AND BROOKS. 25

emphasize this point further we wish to present Fig. 4, in which is shown, for the data of Hodge and Orehoski, a correlation between the observed ideal critical diameter and those calculated by the hardenability factors of Kramer, Siegel, and Brooks, indicating that these factors can also be used to calculate the hardenability of steels containing bainite, despite the fact that they are entirely different from those of Hollomon and Jaffe.

Hollomon and Jaffe have attempted to explain the "fading" effect and the scatter of the hardenability data for molybdenum and chromium by assuming that hardenability is limited by the formation of bainite. No doubt this assumption may explain some of the vagaries, but the effect of undissolved carbides should not be underestimated. The effect of undissolved carbides on the hardenability of several steels containing stable carbide-forming elements may be seen in Table 4. These data were obtained from Jominy bars that were austenitized for 2 hr. at 2100°F. and rapidly transferred to a furnace at 1550°F. where they were held for 15 min. or 4 hr. To facilitate comparisons, and to correct for variations in grain size of steels GPN and GPK, the factors25

This volume, page 670.

Metallurgist, Naval Research Laboratory, Washington, D. C.

hardenability data of Hodge and Orehoski²⁴ ²⁴ J. M. Hodge and M. A. Orehoski: Relationship between Hardenability and Percentage of Martensite in Some Low-alloy Steels. This volume, page 627.

²⁵ I. R. Kramer, S. Siegel and J. G. Brooks: Factors for the Calculation of Hardenability.

Table 4.—Effect of Undissolved Carbides on Hardenability

Heat Treatment: 2100°F., 2 hours. Transferred to furnace at 1550°F., held for indicated time.

Steel	Time, Min.	Dī	Grain Size	Factor	Devi- ation, Per Cent
GPO	15 240	3.23	51/2 51/2	2.44 2.12	13
GPN	15 240	2.18	514	1.92	6
GPK	15 240	2.50 2.33	5 234	I.59 I.26	21
GPL	15 240	2.60 2.30	4.5	I.50 I.39	9.3
GPM	15 240	2.77 2.57	4 3	I.63 I.42	13

Composition, Per Cent

Steel	С	Mn	Si	Various
GPO	0.42	0.83	0.23	Cr 0.66
GPK	0.39	1.06	0.18	Ti 0.072
GPN	0.34	0.81	0.11	Mo 0.34
GPL	0.38	1.04	0.20	V 0.11
GPM	0.36	1.06	0.33	Zr 0.078

for the carbide-forming elements are given. That the precipitation of carbides caused a marked decrease in the hardenability is evidenced by a comparison of the ideal critical diameter or the hardenability factors of the steel held for 15 min. or 4 hr. at 1550°F. For steel GPO, the chromium factor decreased 13 per cent; for the other steels the hardenability factors decreased from 6 to 21 per cent on long holding at 1550°F. after high-temperature austenitizing. In addition, it can be shown, by the data for acid-soluble as opposed to total titanium, that the amount of insoluble carbides is sufficient to explain the scatter of the hardenability factors for titanium (Figs. 21 and 22 of reference 25).

It would be of interest to know the length of time the bars were held at the various temperatures in the grain-size experiments performed by Hollomon and Jaffe. Since our experience has shown that undissolved carbides influence the hardenability, it is difficult to explain the authors' results; however, it may be that if the steels were held at 1500°F. for a time long enough to establish a condition of equilibrium

for the solution of the carbides, the grain-size effect could be found; provided that the coalesence of carbides do not interfere.

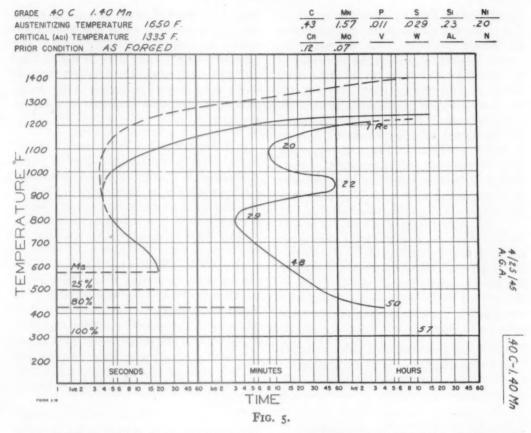
R. A. Schmucker, Jr.*—The validity of applying the original Grossmann hardenability calculations to steels containing substantial percentages of chromium and molybdenum, and having TTT curves of the types showing two distinct "noses" or points of maximum transformation has always appeared somewhat questionable to us. We therefore feel that the authors are to be particularly commended for their clarification of this problem by their proposal of separate factors for pearlitic and bainitic hardenabilities.

It is believed that the presentation of some of our own hardenability data, representing a number of heats of modified SAE-1340, together with hardenability calculations made according to the authors' proposed methods, would be of interest.

As part of an investigation carried out by M. Metzger, of the Atha Works Metallurgical Laboratory, some time prior to the presentation of the authors' paper, Jominy specimens were cut from rather large cylindrical forgings representing 13 heats of the modified SAE-1340 steel, and then end-quenched from an austenitizing temperature of 1750°F. Not only were the Jominy hardenability data obtained from these specimens, but also the distances from the quenched end at which a 50 per cent pearlitic structure occurred were measured metallographically. Because of the particular requirements of this investigation, only the 50 per cent pearlite distance and not the 50 per cent martensite distance was measured. Later, when it was decided to use these data for checking hardenability calculated by the authors' proposed methods, the specimens themselves were not available. Therefore, the 50 per cent martensite distances were measured by the inflection point method, and these distances were converted to equivalent D_I values. The bainitic and pearlitic hardenabilities were then calculated from the analyses of the forgings, using the factors proposed by the authors.

Some difficulty was encountered in the choice of a carbon factor for pearlitic hardenability calculations because heats of this steel showed

^{*} Metallurgist, Crucible Steel Company of America, Atha Works, Harrison, N. J.



a mixed though fairly similar grain size at 1750°F. Since a grain size of 4 seemed a satisfactory average, the corresponding carbon factor was used for all heats.

The chemical compositions, measured D_I values and calculated bainitic and pearlitic

hardenabilities are shown in Table 5. For ease of inspection, the data have been arranged in order of increasing actual D_I value. In all heats the bainitic hardenability was less than the pearlitic, indicating that bainite should restrict the formation of martensite on con-

TABLE. 5.—Comparison of Actual D_I Values with Calculated Values

Heat		Analyses, Per Cent 50 Per Cent Martensite											
Code	С	Mn	P	S	Si	Ni	Cr	Мо	Cu	Jominy Dis- tance, In.	Equivalent in D _I	Bainitic Harden- ability	
5268 5244 5198 5224 5202 5237 X 5186 5133 5177 5179 5074 4353	0.37 0.44 0.42 0.43 0.45 0.45 0.45 0.45 0.45	1.47 1.48 1.49 1.56 1.58 1.56 1.55 1.61 1.55 1.61	0.020 0.010 0.020 0.010 0.015 0.016 0.026 0.024 0.021 0.018	0.035 0.033 0.035 0.035 0.027 0.033 0.035 0.030 0.037	0.27 0.28 0.32 0.26 0.28 0.32 0.33	0.16 0.22 0.18 0.24 0.18 0.23 0.10 0.14 0.10 0.22 0.20	0.13 0.10 0.13 0.14 0.21 0.18 0.10 0.19 0.12 0.16 0.23 0.14	0.03 0.04 0.05 0.05 0.05 0.04 0.02 0.04 0.03 0.04 0.05	0.04 0.03 0.04 0.05 0.06 0.07 0.05 0.06 0.09 0.08 0.05	0.313 0.406 0.468 0.468 0.562 0.594 0.625 0.625 0.625 0.688 0.888	2.30 2.62 2.85 2.85 3.15 3.45 3.45 3.60 3.60	3.14 3.48 3.51 3.74 3.98 4.12 3.46 3.58 3.71 4.13 4.12 4.16	3.32 3.78 4.00 4.28 4.83 4.72 3.53 4.10 3.96 4.67 5.12 4.63 5.47

tinuous cooling. This conclusion is substantiated by our previous metallographic examination of the Jominy specimens, which disclosed in all a zone of bainite separating the martensite at the quenched end from the pearlitic areas farther back on the specimen. However, the calculated bainitic hardenabilities are all somewhat greater than the actual D_I values, the discrepancy being more apparent in heats of lower hardenability. No explanation for these discrepancies will be attempted. Nevertheless, the calculated bainitic hardenabilities are always closer to the actual D_I values than are the calculated pearlitic hardenabilities.

A TTT curve representing a typical heat of this analysis austenitized at 1650°F. shows only a single point of maximum initial transformation rather than distinctly separate regions of pearlitic and bainitic transformation. However, the products of transformation above 1000°F. were found to be distinctly pearlitic and those below 950°F. to be bainitic.

TABLE 6.—Correlation of Jominy Distance for 50 Per Cent Pearlite with Calculated Pearlitic Hardenability

Heat Code	50 Per Cent Pearlite Jominy Distance, In.	Calculated D _I Pearlitic Harden ability
5268	1.38	3.32
5198 5244	1.56	4.00
X	1.75	3.76
5133	1.75	3.96
5186	1.75	4.10
5224	2.38	4.28
5074	2.44	4.63
5177	2.50	4.67
5237	2.75	4.72
5202	3.13	4.83
5179	30 per cent pearlite @ 31/8	5.12
4353	No pearlite @ 3%	5.47

As a point of interest, the heats shown in Table 5 have been arranged in Table 6 in order of increasing pearlitic hardenability with the corresponding measured Jominy distances for a 50 per cent pearlitic, 50 per cent bainitic structure. The data show a general increase in calculated pearlitic hardenability with increasing Jominy distances for 50 per cent pearlite. (Reversals of the data occur in two heats.)

As the authors have mentioned in their paper, the nonmartensitic products have rarely been identified in the literature of hardenability calculations. The data just given suggest that the identification of structures beyond the point of 50 per cent martensite on the Jominy specimen would give added information in future hardenability studies. Our experience with Jominy tests on the modified SAE-1340 analysis was that hardness measurements alone gave no indication of the change from a bainitic to a pearlitic zone on the specimen.

J. H. HOLLOMON and L. D. JAFFE (authors' reply).—It is to be emphasized that the object of the paper is to point out that hardenability is not a single concept, but a dual or multiple one, and that in measurement and calculation of hardenability it is important to determine whether the limiting factor is the formation of pearlite or of bainite (or perhaps, of ferrite or of cementite). This is true regardless of the validity of the Grossmann or any other empirical system of computing hardenability. The suggested modification of the Grossmann scheme and the numerical values suggested for use in it are recognized to be tentative and with little foundation and are proposed for use only until better information is available. They are not pertinent to the basic hardenability concept.

The existence of an incubation effect through which holding in the pearlite range increases the rate of formation of bainite has now been verified experimentally for a hypocutectoid steel.26 The importance of distinguishing incubation effects from direct effects upon the bainite reaction may be brought out by an example: Consider two steels, in one of which the pearlite and bainite noses involve times of the same order, while in the other the pearlite nose involves times very much longer than the bainite. In the first steel, a change (as in grain size) that produces a moderate shift in the pearlite nose is likely, through incubation, to produce also a moderate shift in the bainite nose. In the second steel, a moderate shift in the pearlite nose will have no significant effect upon the bainite nose.

In the experimental grain-size study mentioned in the paper, the minimum austenitizing treatment was 2 hr. at 1500°F.; no undissolved carbides could be detected in any of the specimens. Details are given in a forthcoming paper.²⁶

²⁶ J. H. Hollomon, L. D. Jaffe, and M. R. Norton: Anisothermal Decomposition of Austenite This volume, page 419.

Hardenability and Quench Cracking

By L. D. Jaffe* and John H. Hollomon,† Junior Members A.I.M.E.

(New York Meeting, October 1945)

For many steel parts it is desired to obtain the maximum toughness consistent with the strength required by the mechanical design. It is generally recognized that the greatest toughness at any given strength is found in steels having a tempered martensitic structure, and is virtually independent of the composition of the steel (except for carbon). The choice of the composition of a steel for the parts in question should be based, therefore, on hardenability considerations and on manufacturing facility and economy.

In a recent paper³ the concept of hardenability was discussed and a somewhat new approach to the problem was suggested. The hardenability was defined in terms of the cooling conditions (speed of cooling) required to avoid the pearlite and the bainite reactions. Since all the alloying elements do not have the same effects on the two reactions, the bainitic and pearlitic hardenabilities must be considered separately.

In order to design a steel for a given part, it is necessary to design a composition that has both sufficient pearlitic and sufficient bainitic hardenability. However, this requirement does not fix the combination of alloying elements to be used; an infinite

number of steels would have the required hardenabilities. Other considerations limit the choice. For example, decreasing the carbon content increases the toughness at a given hardness, and for this reason lowcarbon steels are often desired. Limitations or requirements of refining, casting, or forming practices often affect the level of some of the alloying elements. Price considerations enter. Frequently, however, it is very desirable to minimize the tendency toward quench-cracking while maintaining the necessary hardenability. This paper is concerned with suggesting a method for choosing compositions that will have the required hardenability together with minimum tendency toward quench-cracking.

QUENCH CRACKING

Since only the case in which the entire part will transform to martensite in the particular quench employed is being considered, the analysis of the quench-cracking problem is somewhat simplified. Quench-cracking arises from the temperature gradients existing throughout the piece during cooling. Because of these temperature gradients, the contraction arising from the decreasing temperature and the expansion arising from the austenite-martensite reaction do not occur uniformly over the parts, and stresses are set up that tend to cause cracking.

The temperature gradients can be reduced by decreasing the severity of quench. This, however, requires that the hardenability be correspondingly increased by increasing the carbon or alloy content. An

The statements and opinions expressed in this article are those of the authors and do not necessarily express the views of the Ordnance Department. Manuscript received at the office of the Institute May 15, 1945. Issued as T.P. 1927 in METALS TECHNOLOGY, January 1946.

* Metallurgist, Watertown Arsenal Labora-

tory, Watertown, Massachusetts.
† Captain, Ordnance Department, Watertown Arsenal.

References are at the end of the paper.

increase in carbon content is often undesirable because it decreases the toughness of the steel both as quenched and after tempering to the required hardness, in-

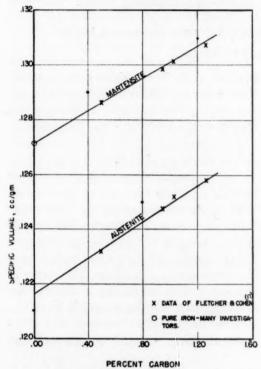


FIG. 1.—Specific volumes of austenite and martensite vs. carbon content, plain carbon steels, room temperature.

creases the amount of austenite retained after the quench, with its associated difficulties, and may introduce some processing difficulties. Increasing the alloy content is often undesirable because it increases, generally, the susceptibility to temper brittleness, increases the amount of retained austenite, increases the cost of the steel, and may introduce processing difficulties. Quench-cracking could, in principle, be eliminated by increasing the hardenability until the steel would harden on furnace cooling, but in practice the factors just mentioned will set a minimum limit to the quenching severity that can be used.

The shape of the part, as quenched, has, of course, a great effect upon its tendency to quench-crack. Nevertheless, even though

the shape is properly designed for quenching and the quenching severity reduced as far as is desirable, many parts are likely to crack upon quenching unless the composition is properly selected. Little can be done to minimize the thermal contraction. However, the volume expansion that occurs during the austenite-martensite reaction (and is primarily responsible for quench-cracking) can be decreased.

TABLE 1.— Effect of Carbon and Alloying Elements on M. Temperature

Element	Effect for Each Per Cen of Element				
	Deg. C.s	Deg. F.			
C (0.20-0.90 per cent)	-350	-630			
Mn	- 40	- 72			
<u>V</u>	- 35	- 63			
Cr	- 20	- 36			
Ni	- 17	- 31			
Cu	- 10	- 18			
Mo	- 10	- 18			
W	- 5	- 9			
Si	. 0	. 0			
Co	+ 15	+ 27			
Al	+ 30	+ 54			

Selected from the literature(5,11-15)
 Converted from deg. C.

Changes in carbon content (Fig. 1) and in alloy content* affect the specific volume of austenite to about the same extent that they affect the specific volume of martensite, at a given temperature. Thus, for constant temperatures of transformation, the volume change from austenite to martensite is practically independent of composition. However, because of the difference between the coefficients of thermal expansion for austenite and for martensite, the change in volume is markedly dependent upon the temperature at which the expansion takes place. The lower the temperature at which the martensite forms, the greater will be the expansion accompanying the transformation. Furthermore, the lower

^{*} This conclusion is based upon analyses of a considerable quantity of dilatometric data obtained at the Watertown Arsenal Laboratory on steels of many compositions.

the temperature at which the martensite forms, the less is the stress relief that can occur during the quench, and the harder and less ductile is the martensite. Values than only the M_{\bullet} temperature, but reliable data for the effect of composition upon the entire range are not available.

Carbon affects the susceptibility to

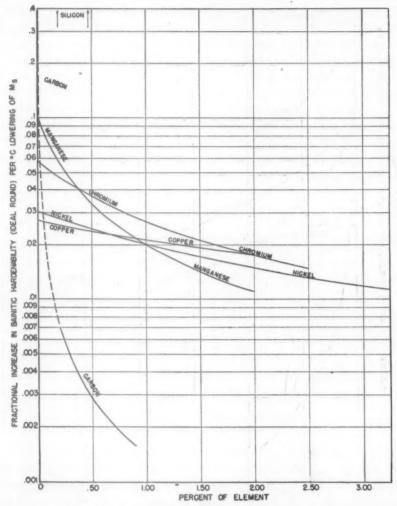


Fig. 2.—Ratio of effect of alloying elements upon bainitic hardenability to their effect upon the M_{σ} temperature.

for the effects of various elements upon the temperature at which the austenite to martensite reaction begins (M_{\circ} temperature) are given in Table 1. Zener's interpretation of the martensite reaction⁴ as well as the experimental data⁵ indicate that the effects of alloying elements upon the M_{\circ} temperature are additive. It may be more pertinent to quench-cracking to consider the entire martensite range rather

quench-cracking, not only by lowering the M_s temperature, but also in another way. The hardness of martensite increases and the ductility decreases with increasing carbon content. Thus, the possibility of marked plastic flow with concurrent decrease of stress becomes less as the carbon content increases.

In addition to increasing the tendency toward quench-cracking, a low M. tem-

perature has another undesirable effect; it increases the amount of austenite retained after the quench. This austenite may decompose during the tempering cycle fully hardened in a given medium, the problem of designing a steel that will have the minimum tendency toward quenchcracking and austenite retention reduces

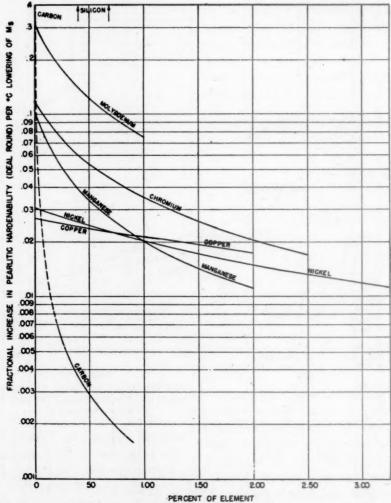


Fig. 3.—Ratio of effect of alloying elements upon pearlitic hardenability to their effect upon the $M_{\mathfrak{g}}$ temperature.

to products that lower the toughness of the steel, while if the austenite is not decomposed it may have other detrimental effects.*

Thus, for a part of a given shape to be

* It may be noted that while decreasing the severity of quench decreases the tendency toward quench-cracking, if the composition is unchanged and the steel transforms only to martensite, the resultant decrease in speed of cooling increases the amount of austenite retained.

to a more specific problem. It is necessary simply to design the steel to have the required hardenability with the maximum martensite start temperature.

HARDENABILITY AND MARTENSITE-START TEMPERATURE

It may be assumed that, to a first approximation, the pearlitic hardenability of hypoeutectoid steels may be calculated from composition on the basis of the multiplicative system introduced by Grossmann,6 using the data given in Table 2. It is, as yet, possible only to suggest a tentative system for calculating bainitic hardenability; assumed values for use in this system are also given in Table 2.

Since it is desired to compare the relative effects of the alloying elements upon hardenability and on lowering the martensite transformation temperature, it is necessary to determine the effect of each element on the fractional increase in hardenability per degree lowering of the martensite transformation.

such as vanadium, 6,7 boron, 6,7 and titanium, 7,8,9 have not been considered, since even the data on their effect upon pearlitic hardenability are contradictory, and may indicate that this effect depends to some extent upon factors other than the amount of element contained in the austenite.) Since little is known concerning the effect of alloying elements on hypereutectoid steels, Figs. 2 and 3 are intended to apply to hypoeutectoid steels only.

The higher a point on a curve for anelement of the figures, the greater the increase in hardenability per degree lowering of the M, temperature for further

TABLE 2.—Effect of Carbon and Alloying Elements upon Hardenability (Ideal Round)

Elements	Grossmann Pearlitic Hardenability Factors	Assumed Bainitic Hardenability Factors
{ 50 per cent martensite. Essentially all martensite. Mn. P. S. Si. Cr. Ni. Mo. Cu.	$\begin{array}{c} 0.338 \times \sqrt{\% \text{ C in.}^{b}} \\ 0.254 \times \sqrt{\% \text{ C in.}^{b}} \\ 1+4.10 \times (\% \text{ Mn}) \\ 1+2.83 \times (\% \text{ P}) \\ 1-0.62 \times (\% \text{ S}) \\ 1+0.64 \times (\% \text{ Si}) \\ 1+2.33 \times (\% \text{ Cr}) \\ 1+0.52 \times (\% \text{ Ni}) \\ 1+3.34 \times (\% \text{ Mo}) \\ 1+0.27 \times (\% \text{ Cu})^{d}. \end{array}$	0.494 \times $\sqrt{\%}$ C in. 0.272 \times $\sqrt{\%}$ C in. 1 + 4.10 \times (% Mn) 1 + 2.83 \times (% P) 1 - 0.62 \times (% S) 1 + 0.64 \times (% Si) 1 + 1.16 \times (% Cr) 1 + 0.52 \times (% Ni) 1 + 0.27 \times (% Cu)

Calculated from data selected by Grossmann, 16 except copper factor,
 For grain size A.S.T.M. 7. For other grain sizes the constant differs. 6
 From Hollomon and Jaffe. 6

d Calculated from data of Kramer, Hafner, and Toleman.

In Fig. 2 the fractional increase in bainitic hardenability (ideal round, D_I) per degree centigrade lowering of the martensite start temperature (M_s) ,

$$-\frac{\frac{d(D_I)}{D_I}}{\frac{d(M_s)}{d(M_s)}}$$

is plotted for various amounts of the different alloying elements. Fig. 3 is the corresponding plot for pearlitic hardenability. These figures are based upon the data presented in Tables 1 and 2. When more complete and accurate information becomes available, the new data may be used but the general principles should remain unchanged. (The special addition elements, additions of that element. Moderate additions of molybdenum increase the pearlitic hardenability with less lowering of the M. temperature than do additions of manganese, chromium, nickel, copper, or carbon. However, 0.30 per cent molybdenum increases the pearlitic hardenability greatly, and is sufficient to ensure that the pearlitic hardenability is greater than the bainitic. Thus, it is only necessary to select the composition giving the desired bainitic hardenability with the maximum M, temperature and then add enough molybdenum to increase the pearlitic hardenability as far as may be needed. The choice of the combination of alloying elements other than molybdenum can, therefore, be based

upon bainitic hardenability versus M_s . (molybdenum itself has very little direct effect upon bainitic hardenability.)

Fig. 2 indicates that the minimum in-

However, in adding this element to cast steels, at least, it has been found that additions much in excess of 0.50 per cent lower the impact properties.¹⁰ Possibly this de-

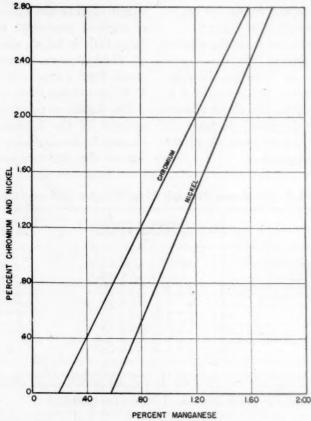


Fig. 4.—Optimum proportions for manganese, nickel and chromium based upon maximum bainitic hardenability with minimum lowering of M_s temperature.

crease in bainitic hardenability for a given lowering of the martensite-start temperature is obtained with the addition of carbon (after the first 0.05 per cent). Thus, the carbon content should be kept to a minimum not only to permit the maximum toughness of the tempered steel and the minimum hardness of the quenched steel, but also to maximize the martensite transformation temperature.

Since the addition of silicon does not affect the martensite transformation temperature (Table 1), yet increases the bainitic hardenability (Table 2), as much of this element should be added as possible.

crease is due to the formation of certain silica-base inclusions. At least at present, the percentage of silicon that can be used is limited to about 0.50.

Fig. 2 indicates that, of the three elements manganese, nickel, and chromium, manganese should, theoretically at least, be added first until about 0.20 per cent is present. Then, since the next addition of manganese would lower the martensite-start temperature more than would an initial addition of chromium (for a given increase in hardenability), chromium should be added. But if chromium were added alone, the martensite-start temperature

would again be unnecessarily lowered, for the chromium curve will drop to a lower value than that for 0.20 per cent manganese. Therefore, after a steel contains available information as to the effect of the alloying elements on the bainitic hardenability and on the martensite-start temperature, manganese, nickel, and chro-

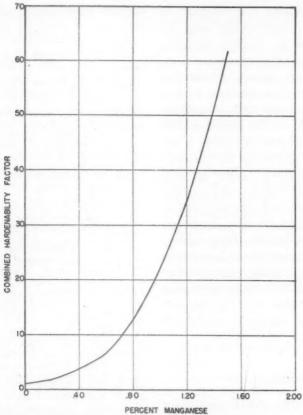


Fig. 5.—Combined hardenability factor for manganese, nickel and chromium in optimum proportions (as given in Figure 4).

about 0.20 per cent manganese, chromium and manganese should be added together, and in such quantities that the points corresponding to their concentrations are on the same horizontal line in Fig. 2. These concentrations are indicated in Fig. 4. The same situation arises with regard to nickel; after the steel contains about 0.60 per cent manganese and 0.80 per cent chromium, nickel, chromium, and manganese should be added together, and in such quantities that the points corresponding to their concentrations are on the same horizontal line in Fig. 2. These concentrations are also indicated in Fig. 4. Thus, based on the

mium should be added simultaneously and in concentrations bearing a definite relationship to each other. Instead, then, of considering individual hardenability factors for each element, it is possible to determine a combined factor for the three elements in the relative amounts given by Fig. 4 This factor, plotted in Fig. 5 as a function of the manganese content, is a product of the individual factors for the three elements manganese, nickel, and chromium

Fig. 2 indicates that for manganese contents above about 0.70 per cent, copper should be added simultaneously with manganese, chromium, and nickel. How-

ever, because copper has limited solubility in ferrite and causes age-hardening, it is not ordinarily considered as an alloying element for obtaining hardenability.

Besides hardenability and tendency toward quench-cracking and retention of austenite, other considerations may influence the choice of alloying elements. High-manganese and high-chromium heats cannot be made by certain steelmaking practices, certain alloying elements may be unavailable or too costly, and so on. However, the composition of the steel should be adjusted as suggested in this paper if the required hardenability is to be obtained with minimum tendency toward quenchcracking and toward retention of austenite.

It must be emphasized that the numerical values mentioned in this paper are tentative, since they are based upon incomplete data, and are used simply because no better values are available. When better data are obtained, the numerical values can be changed. However, it is believed that the principles described herein will nevertheless apply.

SUMMARY

In order to attain the hardenability required for a steel part to be fully hardened by a given treatment with a minimum susceptibility to quench-cracking and to retention of austenite, the composition should be such that further slight additions of each element give as great a fractional increase of hardenability per degree lowering of the martensite temperature range as possible. On the basis of the data now available, this means that for hypoeutectoid steels:

- 1. The carbon should be as low as possible.
- 2. Silicon should be as high as is consistent with good steel quality and toughness.
- 3. Manganese, chromium, and nickel concentrations should bear a definite relationship to each other (indicated in

Fig. 4) and should be as high as is necessary to give the required bainitic hardenability.

4. Molybdenum should be added in the quantity necessary to give the required pearlitic hardenability once the required bainitic hardenability has been obtained.

REFERENCES

- 1. J. H. Hollomon: The Notched-bar Impact Test. Trans. A.I.M.E. (1944) 158, 298-
- W. G. Patton: Mechanical Properties of N.E. S.A.E. and Other Hardened Steels. Metal Progress (1943) 43, 726-733 and Equivalence of Hardened Steels When Tested in Tension and Impact. Metal
- Progress (1944) 45, 1094-1096.
 3. J. H. Hollomon and L. D. Jaffe: The Hardenability Concept. This volume,
- page 601. 4. C. Zener: Kinetics of the Decomposition of
- Austenite. This volume, page 550.

 5. P. Payson and C. H. Savage: Martensite Reactions in Alloy Steels. Trans. Amer.
- Soc. for Metals (1944) 33, 261-280.
 6. M. A. Grossmann: Hardenability Calcu-
- lated from Chemical Composition.

 Trans. A.I.M.E. (1942) 150, 226-259.

 Crafts and J. L. Lamont: Effect of
 Some Alloying Elements on Hardenability. Trans. A.I.M.E. (1944) 158,
- 157-167. 8. I. R. Kramer, R. H. Hafner, and S. L. Toleman: Effect of Sixteen Alloying Elements on the Hardenability of Steel.
- Trans. A.I.M.E. (1944) 158, 138-156.
 9. G. F. Comstock: Discussion to Reference 8.
- A. Hurlich: Unpublished work.
 V. I. Zyuzin, V. Sadovski, and S. Baranchuk: Influence of Alloying Elements on Position of Martensite Point, Quantity of Retained Austenite, and Stability of Retained Austenite During Tempering. (In Russian.) Metallurg (1939) 14, (8-11)
- 75-80. B. Greninger: Martensite Thermal 12. A. Arrest in Iron-Carbon Alloys and Plain Carbon Steels. Trans. Amer. Soc. for
- Metals (1942) 30, 1-26.

 13. H. H. Chiswik, and A. B. Greninger: Influence of Nickel, Molybdenum, Cobalt, and Silicon on the Kinetics and Ar" Temperatures of the Austenite to Martensite Transformation in Steels. Trans. Amer.
- Soc. for Metals (1944) 32, 483-520.

 14. J. V. Russell and F. F. McGuire: Metallographic Study of the Decomposition of Austenite in Manganese Steels. Trans. Amer. Soc. for Metals (1944) 33, 103-
- E. P. Klier and A. R. Troiano: Ar" in Chromium Steels. Trans. A.I.M.E.
- (1945) 162, 175. 16. M. A. Grossmann: Unpublished work. 17. S. G. Fletcher and M. Cohen: The Effect of Carbon on the Tempering of Steel. Trans. Amer. Soc. for Metals (1944) 32, 333-362.

DISCUSSION

(I. R. Kramer presiding)

C. Wells. *- The general approach of the authors to the problem of designing compositions for quenched and tempered steels is highly commendable. One expects that, other things being equal, the danger of cracking is on the average likely to be less in a steel with a high M_S than in one with a low M_S , especially if the M_f , too, is higher in the steel with the higher Ms point. However, to date, efforts made at the Carnegie Institute of Technology to correlate (1) cracking susceptibility with M_S , and (2) cracking susceptibility with D_I , have completely failed. Several hundred D1 and Ms values were calculated from SAE-4335 composition data. The range of D_I values among several heats varies between the limits of 7.03 and 11.04 in., and the range of Ms values between the limits of 274°C. (525°F.) and 326°C. (620°F.). A plot of Ms values versus the percentages of cracked tubes per heat showed: (1) considerable scatter, and (2) the correlation coefficient to be close to zero. A similar plot in which D_I values were substituted for Ms also showed no correlation between D_I and cracking susceptibility.

Despite the general soundness of the authors' logic, at least for the commercial tubes studied at C.I.T., the major losses imposed on industry by quench cracks have resulted from causes other than the choice of unsuitable compositions. Of these causes may be mentioned: (1) stress raisers (flakes, forging cracks, seams, segregation, nonmetallic inclusions), (2) lack of uniformity of the ingot primary structure.

It has been observed among heats of essentially the same composition (SAE-4335) that cracking susceptibility varies considerably; occasionally quench cracks have been observed in every tube from a given heat, while no quenching cracks have been observed in any tube from several other heats having a composition similar to that of the heat containing the cracked tube. The percentage of tubes lost from one heat because of quench cracks was zero

According to the authors, reducing the severity of quench results in a lessened tendency of a part to quench-crack when quenched completely to martensite. The experiences of a number of investigators may have raised doubts in their minds as to whether this is always true. It is understood, for example, that A. J. Herzig18 has presented data that show that in the quenching of 37-mm. and 3-in. shot made of 4150 grade steel, where longitudinal cracks were observed an increased rate of quenching resulted in less cracking. Mr. Herzig has conveyed the thought that when the rate of cooling varies, the distribution and magnitude of residual stresses vary also; these residual stresses may be favorable or unfavorable. In his experience with shot of 37-mm. and 3-in. sizes, a more drastic quench apparently resulted in a more favorable distribution of stress, therefore he recommended that the shot should be more drastically (not less drastically) quenched.

The authors have suggested a procedure for designing compositions that seems to offer considerable promise. However, the extent to which it may be used commercially to practical advantage has still to be demonstrated. An investigation at C.I.T. is now being made of the influence of composition on the cracking susceptibility of tubes, and it is hoped that as a result of this the practical significance of the author's approach for designing compositions to give the required physical properties and the minimum susceptibility can be evaluated.

L. D. JAFFE and J. H. HOLLOMON (authors' reply).—There is no doubt that factors other than composition, such as steel shape and quenching procedure, seams and flakes, have marked effects upon the likelihood of quench-cracking. In the experimental work cited by Dr.

despite the fact that the average cracking susceptibility according to a test developed at C.I.T. was relatively high while the percentage of tubes lost from another heat was quite high, despite the fact that the determined average cracking susceptibility of this heat was quite low. As far as is known, the heat-treatment was essentially the same for both heats.

^{*} Metals Research Laboratory, Carnegie Institute of Technology, Pittsburgh, Pennsylvania. This discussion is based on contributions made by J. W. Spretnak, I. Broverman, and C. F. Sawyer in a study of the causes of and remedies for cracking in tubes.

¹⁸ A. J. Herzig: The Metallurgical Laboratory in War Production. Presented before the Washington, D. C., chapter of the American Society for Metals, November 9, 1942.

Wells, the M_S temperatures varied by only 50°C. The effect upon quench cracking of this comparatively small change in M_S was evidently hidden by the effects of changes in the other variables. On the other hand, there is no doubt that the effect of composition upon quench cracking may sometimes be very large: surely 0.90 per cent carbon steels are more likely to crack than 0.30 per cent steels.

When quench cracking is encountered, efforts to improve the mechanical design, the quenching procedure, and the steel quality are indicated, of course. Cases of cracking have been noted, however, even though design, quenching procedure, and steel quality were apparently as good as possible. Adjustments in composition that would decrease the tendency to quench cracking would clearly be desirable in such cases.

It appears to be true that increasing the severity of quench occasionally decreases the tendency toward quench cracking in fully hardened steel. This was observed and explained by Scott¹⁹ some time ago.

¹⁹ H. Scott: Origin of Quenching Cracks. Sci. Papers, Nat. Bur. of Stds. (1925) 20, 399-444.

Relationship between Hardenability and Percentage of Martensite in Some Low-alloy Steels

By J. M. Hodge* and M. A. Orehoski†

(New York Meeting, October 1945)

It is now generally conceded that if a steel is to develop optimum physical properties in the conventionally quenched and tempered condition, the microstrucunder the heating and quenching conditions to which it will be subjected, and this premise is probably the most important reason for hardenability control.

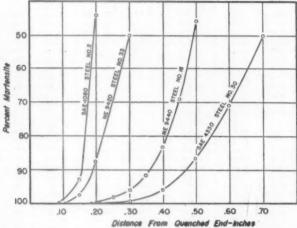


FIG. 1.—TYPICAL CURVES FOR PERCENTAGE OF MARTENSITE VERSUS DISTANCE FROM QUENCHED END.

ture after quenching should consist wholly of martensite; and that transformation of austenite to intermediate-temperature products during quenching will have a deleterious effect upon the physical properties, particularly the toughness, of the tempered material. This implies that, in order to obtain the optimum physical properties from a given steel, its "hardenability" should be high enough to suppress all transformation except that to martensite

However, the criterion of hardenability that at present is most widely accepted and used is based on a microstructure of 50 per cent martensite. This criterion, which was suggested by Grossmann, does have considerable justification. It may be readily measured by a fracture or etch test and, since it represents the point at which the hardness is changing most rapidly with variations in cooling rate, it may be determined empirically from a hardness-depth curve by determining the point of steepest slope (the inflection point). Furthermore, in plain carbon steels or in steels of low hardenability, the difference in hardenability expressed in

Manuscript received at the office of the Institute Dec. 1, 1944. Listed for New York Meeting, February 1945, which was canceled. Issued as T.P. 1800 in METALS TECHNOLOGY, September 1945.

^{*} Development Engineer, Carnegie-Illinois Steel Corporation, Pittsburgh, Pennsylvania. † Metallurgist, Duquesne Works, Carnegie-Illinois Steel Corporation.

¹ References are at the end of the paper.

terms of a 50 per cent martensite microstructure and one of full martensite will not be large, and a hardenability only slightly in excess of that indicated by the 50 per cent martensite criterion will suffice to ensure full hardening to martensite.

However, with steels of higher hardenability, the difference between hardenability on the basis of 50 per cent marquench tests to determine the relationship between the percentage of martensite and the distance from the quenched end. These distances were then converted to hardenability values in terms of ideal diameter, using the relationship as determined by Grossmann,² and the hardenability value for the microstructure of 50 per cent martensite plotted against that for 99.9,

TABLE 1.—Chemical Analyses of Specimens

Specin	nen No.	Grade		4		Analyses,	Per Cent	Analyses, Per Cent									
орест		orace	С	Mn	P	S	Si	Ni	Cr	Mo							
1	A-813	C-1050	0.48	0.88	0.022	0.028	0.26	0.05	0.05	0.0							
2	A-81	C-1080	0.79	0.81	0.020	0.031	0.21	0.02	0.05	0.0							
3	A-858	NE-1340	0.38	1.75	0.027	0.026	0.31	0.02	0.05	0.0							
	A-734	NE-8615	0.15	0.85	0.010	0.013	0.20	0.48	0.50	0.2							
5	AA-233	NE-8620	0.19	0.76	0.022	0.021	0.26	0.56	0.46	0.2							
4 5 6 7 8	A-752	NE-8622	0.23	0.77	0.016	0.031	0.26	0.28	0.40	0.1							
7	A-835	NE-8625	0.25	0.75	0.011	0.011	0.22	0.60	0.49	0.1							
8	AA-239	NE-8627	0.28	0.74	0.016	0.013	0.25	0.53	0.49	0.1							
9	A-857	NE-8630	0.32	0.81	0.013	0.010	0.26	0.47	0.50	0.2							
10	A-861	NE-8640	0.39	0.87	0.011	0.009	0.30	0.50	0.50	0.2							
II	AA-73	NE-8645	0.44.	0.85	0.015	0.023	0.29	0.51	0.45	0.2							
12	A-853	NE-8650	0.48	0.88	0.013	0.012	0.20	0.55	0.47	0.2							
13	A-860	NE-9420	0.21	0.97	0.010	0.011	0.27	0.50	0.50	0.2							
14	A-744	NE-9420	0.22	0.01	0.016	0.030	0.27	0.30	0.32	0.2							
15	AA-411	NE-0440	0.39	1.21	0.016	0.026	0.24	0.56	0.45	0.1							
16	AA-320	NE-9440	0.40	1.18	0.028	0.027	0.28	0.54	0.43	0.1							
17	AA-129	NE-9440	0.41	1.12	0.027	0.025	0.29	0.44	0.44	0.1							
18	AA-387	NE-9440	0.42	I.II	0.020	0.030	0.14	0.49	0.43	0.1							
19	A-583	A-4130	0.30	0.53	0.017	0.014	0.25	0.13	0.97	0.2							
20	A-805	A-4130	0.31	0.58	0.015	0.012	0.25	0.12	0.91	0.2							
21	A-781	A-4134	0.34	0.58	0.014	0.015	0.25	0.04	0.92	0.1							
22	AA-393	E-4135	0.35	0.84	0.020	0.022	0.24	0.07	0.95	0.2							
23	A-802	A-4134	0.36	0.62	0.010	0.010	0.27	0.13	0.91	0.1							
24	AA-298	A-4137	0.36	0.80	0.017	0.015	0.27	0.11	1.00	0.2							
25	A-621	A-4137	0.37	0.88	0.016	0.017	0.24	0.09	0.96	0.1							
26	A-616	A-4137	0.37	0.87	0.010	0.017	0.27	0.12	0.92	0.2							
27	A-615	A-4137	0.38	0.87	0.009	0.015	0.28	0.09	0.93	0.1							
28	AA-430	A-4137	0.38	0.88	0.016	0.072	0.26	0.08	0.96	0.2							
29	AA-170	A-4137	0.38	0.80	0.016	0.021	0.28	0.08	0.97	0.2							
30	AA-417	A-4330	0.26	0.47	0.010	0.017	0.21	1.73	0.73	0.3							
31	AA-185	A-4330	0.28	0.51	0.010	0.018	0.32	1.73	0.63	0.3							
32	AA-343	A-4330	0.30	0.72	0.013	0.013	0 30	1.73	0.52	0.2							
33	A-881	SAE-4620	0.19	0.56	0.010	0.014	0.29	1.77	0.18	0.2							
34	A-819	SAE-4820	0.19	0.64	110.0	0.007	0.23	3.51	0.22	0.2							
35	AA-204		0.51	1.02	0.031	0.036	0.19	0.03	0.35	0.0							

tensitic structures and full hardenability to martensite may prove to be considerable and this difference is a function of the hardenability. The purpose of the present work is to study this relationship in steels of medium hardenability as exemplified by the NE 8600 or the SAE 4100 types of composition.

EXPERIMENTAL PROCEDURE

The general procedure consisted of a metallographic study of a series of end95, 90 and 80 per cent martensite. In addition, the hardenabilities on a 50 per cent martensite basis were calculated from the chemical composition using the method developed by Grossmann³ and the calculated values compare with the results of the metallographic determination. Rockwell hardness values corresponding to these microstructures were also determined on each sample and the results were plotted against carbon content. The samples were cut from routine Jominy hardenability tests

made at the laboratory of the Duquesne Works of the Carnegie-Illinois Steel Corporation. The details of the procedure were as follows:

A sample, 11/4 in. long, was cut from the quenched end of each Jominy bar. The surface, which had been ground for hardness determination, was polished and

fields averaged to obtain the average percentage at each depth. The shortest distance at which o.r per cent high-temperature transformation occurred was also noted and recorded as the distance to 99.9 per cent martensite. These values were then plotted as percentage of martensite versus distance, yielding a family

TABLE 2.—Distances from Quenched End and Corresponding DI Values

Speci	imen No.	99.9 Pe Marte		95 Per Marte		90 Per Marte		80 Per Marte		50 Per Marte		Calcu
		Dist.	DI	Dist.	D_{I}	Dist.	D_I	Dist.	D_I	Dist.	D_I	DI
I	A-813	0.096	1.20	0.120	1.30	0.140	1.40	0.160	1.50	0.185	1.65	1.45
2	18-A	0.000	1.15	0.140	1.40	0.160	1.50	0.170	1.55	0.190	1.65	1.60
3	A-858	0.138	1.40	0.250	1.95	0.325	2.25	0.400	2.60	0.490	2.95	2.60
4	A-734	0.000	1.15	0.130	1.35	0.155	1.50	0.195	1.70	0.250	1.95	3.35
5	AA-233	0,000	1.15	0.175	1.60	0.195	1.70	0.215	1.75	0.260	3.00	3.80
0	A-752	0.110	1.25	0.170	1.55	0.190	1.65	0.215	1.75	0.260	2.00	2.54
7	A-835	0.112	1.25	0.195	1.70	0.220	1.80	0.250	1.95	0.205	2.15	4.00
7 8	AA-239	0.110	1.25	0.170	1.55	0.190	1.65	0.210	1.75	0.260	2.00	3.90
9	A-857	0.128	1.35	0.210	1.75	0.250	1.95	0.290	2.15	0.345	2.35	4.45
10	A-861	0.160	1.50	0.300	2.15	0.365	2.45	0.435	2.70	0.550	3.15	5.50
-11	AA-73	0.149	1.45	0.310	2.20	0.360	2.40	0.420	2.65	0.545	3.15	5.60
12	A-853	0.198	1.70	0.330	2.30	0.410	2.65	0.500	3.00	0.605	3.35	6.10
13	A-860	0.117	1.30	0.150	1.45	0.170	1.55	0.205	1.75	0.270	2.05	4.30
14	A-744	0.005	1.20	0.145	1.45	0.170	1.55	0.200	1.70	0.250	1.95	3.10
15	AA-411	0.170	1.55	0.335	2.35	0.400	2.60	0.470	2.85	0.585	3.30	6.40
16	AA-320	0.235	1.90	0.425	2.70	0.500	3.00	0.590	3.30	0.720	3.75	5.90
17	AA-129	0.186	1.65	0.340	2.35	0.410	2.65	0.470	2.85	0.570	3.20	5.50
18	AA-387	0.185	1.65	0.315	2.25	0.360	2.40	0.415	2.65	0.495	3.00	5.40
10	A-583	0.160	1.50	0.250	1.95	0.285	2.10	0.345	2.35	0.400	2.60	4.00
20	A-805	0.133	1.35	0.210	1.75	0.260	2.00	0.330	2.30	0.400	2.60	4.20
21	A-781	0.139	1.40	0.210	1.75	0.250	1.95	0.310	2.20	0.360	2.40	4.30
22	AA-393	0.195	1.70	0.340	2.35	0.410	2.65	0.480	2.90	0.610	3.40	6.50
23	A-802	0.168	1.55	0.240	1.90	0.300	2.15	0.370	2.45	0.450	2.80	4.70
24	AA-208	0.210	1.75	0.365	2.45	0.425	2.70	0.490	2.95	0.625	3.45	5.90
25	A-621	0.182	1.60	0.340	2.35	0.425	2.70	0.520	3.05	0.660	3.55	6.40
26	A-616	0.154	1.50	0.320	2.25	0.390	2.55	0.490	2.95	0.590	3.30	6.20
27	A-615	0.150	1.45	0.340	2.35	0.410	2.65	0.490	2.95	0.590	3.30	6.30
28	AA-430	0.180	1.60	0.310	2.20	0.360	2.40	0.425	2.70	0.530	3.10	6.10
29	AA-170	0.164	1.50	0.300	2.15	0.355	2.40	0.405	2.60	0.500	3.00	6.19
30	AA-417	0.210	1.75	0.415	2.65	0.475	2.90	0.550	3.15	0.700	3.60	7.00
31	AA-185	0.220	1.80	0.400	2.60	0.465	2.85	0.545	3.15	0.690	3.65	7.50
32	AA-343	0.175	1.60	0.380	2.50	0.450	2.80	0.550	3.15	0.690	3.65	7.50
33	A-881	0.106	1.25	0.165	1.55	0.195	1.70	0.235	1.90	0.300	2 15	2.9
34	A-819	0.191	1.65	0.285	2.10	0.335	2.35	0.390	2.55	0.500	3.00	6.6
35	AA-204	0.100	1.20	0.200	1.70	0.225	1.85	0.260	2.00	0.305	2.20	2.40

etched in picral. It was generally necessary to grind somewhat deeper than for hardness determination in order to get a wide enough surface for metallographic determination. The specimens were then examined at a magnification of 1000 diameters at every 0.1 in., or in some cases every 0.05 in. from the quenched end. At least six, and when banding was most pronounced, as many as 15 fields were examined at each distance, the percentage of martensite in each field being estimated by comparison with a standard chart and the values of the several

of curves as shown in Fig. 1. The distances corresponding to 99.9, 95, 90, 80 and 50 per cent martensite were then read from these curves for each sample. These distances were then converted to hardenability values in terms of ideal diameter, using the relationship as developed by Grossmann, and the 50 per cent value plotted against the 99.9, 95, 90 and 80 per cent values.

Rockwell hardness measurements were made every 1/16 in. on the surfaces as polished for microexamination, these results were plotted and the hardnesses at

the distances corresponding to 99.9, 95, 90, 80 and 50 per cent martensite were read from these curves. These hardness values were then plotted against carbon content for each of the microstructures.

COMPOSITIONS

Check analyses of the materials studied are tabulated in Table 1. The compositions

cent martensite structures as well as the calculated 50 per cent martensite values are tabulated in Table 2. The results of the Rockwell hardness surveys are tabulated in Table 3, and the hardness values at the 99.9, 95, 90, 80 and 50 per cent martensite levels in Table 4.

The D_I values for 99.9, 95, 90, and 80 per cent martensite, respectively, are

TABLE 3.—Rockwell C Hardness Surveys of End-quenched Hardenability Tests

			Di	stance fr	om Quer	nched En	d, in Six	teenths o	of an Incl	b -		
i-	1	2	3	4	5	6	7	8	9	10	II	12
					Ro	ockwell F	Iardness,	C				
	60.5	58	41.5	32	31	31	30					
	65	63	49	41	40	39.5	39					
	57.5	57	53	52	49.5	45	41	37.5	34	31	30	
	41	57 36	29.5	26	22.5	20	10	18.5	04	9-	0-	
	44.5	43	37.5	31	27	24			-			
	45.5	45	39.5	31.5	27	23.5	22			1		
- 1	48.5	45 48	42.5	36	33	29.5	30	29.5				
- 1	48	46	41.5	37	32	28	27	25				
	51.5	49.5	47.5	44	39	34.5	31	29				
- 1	57.5	57.5	56	54.5	53.5	51	49	46.5	43	40	39	36
_	57.5	57	56	55	53.5	51	49	44.5	40.5	37	35	34
-1	60	60	57.5	57	57	55.5	52.5	50	47	45.5	43	40
- 1	. 44	44	39	32.5	57 28	27	25	24	4,	40.0	40	-4-
- 1	44	43	37.5	32	26	24	22.5	21				
- 1	55.5	54.5	54	54	52	51	49	48	46.5	45.5	43	40
	58	58	56	56	54.5	54.5	52	51	48.5	45	42	40
- 1	58	57.5	55.5	54	50	30	46	42	40	38	35.5	34
- 1	56.5	56.5	54.5	54.5	52	52.5	44	40	36	34	32	31
	52.5	52	49.5	49	41	39.5	38.5	38	36.5	35	7-	
	50.5	50.5	47	43	38	35	34.5	33	30	28.5		
- 1	53	52.5	50	43 46	41	35.5	34	31	30	29.5	28.5	27
1	54	54	53	53	51	47.5	43.5	42.5	39.5	38.5	37	35
1	54.5	54	52.5	52	48.5	45	40	39	35	32.5	33	25
- 1	53	52	52	51	50	48.5	47	44	42	38.5	38	37
1	56.5	56	55.5	54	52	50.5	49.5	48.5	46.5	43	42	40
1	56.5	56	56	55.5	52	50.5	49.5	45	44	40	39	37
	57.5	56	56	56.5	55	52.5	49	48.5	45	45	40	37
-1	55	55	55	54	51	47.5	45	44	41	39	38	-
	54.5	54.5	53	51	49	47	44.5	42.5	40	38	36	35
	49.5	49	53 48	48	47.5	47	44	42.5	40	38	36.5	35
2	50	49.5	50	49	48.5	47	46.5	42.5	42.5	39.5	39	36
	50	50	50	49.5	47.5	47.5	44.5	43	40	38.5	35	36
	46	44	39	32	27		23	1-00				
	44.5	43.5	44	42	41	41	36	36	33.5		31	30
	60	. 59	55.5	50	45	36.5	32	30				

include the following types over a range of 0.15 to 0.79 per cent carbon: (1) plain carbon, (2) NE 1300 series, (3) NE 8600 series, (4) NE 9400 series, (5) SAE 4100 series, (6) SAE 4300 series, (7) SAE 4800 series, (8) SAE 4600 series.

EXPERIMENTAL RESULTS Hardenability Relationships

The distances and corresponding D_I values for the 99.9, 95, 90, 80 and 50 per

shown plotted singly against the 50 per cent martensite D_I values in Figs. 2, 3, 4 and 5. The plot for 99.9 per cent martensite shows the widest scatter, and it is felt that this is largely the result of microsegregation, as the 99.9 per cent value represents the lowest hardenability point on the sample examined and not an average value, as do the other measurements. The average lines of these curves are shown plotted together in Fig. 6.

The significance of these relationships will perhaps be more apparent if plotted as in Fig. 7, which illustrates the manner in which the hardenability on the basis of the higher percentages of martensite varies

TABLE 4.—Rockwell C Hardness at Different Percentages of Martensite

Specimen	No.	99.9 % Mar- ten- site	Mar- ten- site	90 % Mar- ten- site	80 % Mar- ten- site	Mar- ten- site
2 3 4 4 5 6 6 7 7 8 A A 10 11 12 13 114 15 A 117 18 A 117 18 A 117 18 A 119 19 19 19 19 19 19 19 19 19 19 19 19	A-813 A-813 A-858 A-734 A-233 A-853 A-853 A-861 A-853 A-860 A-411 A-320 A-441 A-320 A-129 A-129 A-298 A-616 A-615 A-430 A-417 A-129 A-430 A-417 A-129 A-430 A-417 A-129 A-430 A-417 A-129 A-430 A-417 A-129 A-430 A-417 A-129 A-430 A-417 A-129 A-430 A-417 A-129 A-430 A-417 A-129 A-430 A-417 A-129 A-430 A-417 A-129 A-430 A-417 A-129 A-430 A-417 A-129 A-430 A-417 A-129 A-430 A-4417 A-129 A-430 A-4417 A-129 A-4417 A-129 A-4417 A-129 A-4417 A-129 A-4417 A-129 A-4417 A-129 A-4417 A-129 A-4417 A-129 A-4417 A-129 A-4417 A-129 A-4417 A-129 A-4417 A-129 A-4417 A-129 A-4417 A-129 A-4417 A-129 A-4417 A-129 A-4417 A-129 A-4417 A-129 A-4417	59 - 5 - 5 - 5 - 5 - 5 - 5 - 5 - 5 - 5 -	58 63 53 55 55 55 55 55 55 55 55 5	55 5 60 8 5 5 5 6 6 8 5 5 6 6 8 6 7 6 7 6 7 6 7 6 7 6 7 6 7 6 7 6	50 57 43.5 29 36.5 40 49 48 50 37 36 48 47.5 40 37.5 44.5 47.5 42 45.5 45.5 47.5 48.5 47.5 48.5 48.5 47.5 48.5 48.5 48.5 48.5 48.5 48.5 48.5 48	43 54 38 55 30 33 35 35 35 35 35 35 35 35 35 35 35 35

with the 50 per cent martensite hardenability in terms of percentage of this hardenability value.

Calculated versus Actual Hardenability

The hardenability values as calculated from the chemical composition by the method of Grossmann are shown plotted against the actual hardenability as determined metallographically in Fig. 8. Although the actual values are in most cases lower than the calculated values, and although the discrepancy increases as the hardenability increases, there seems nevertheless to be a fairly good straight-line

relationship between the calculated and actual hardenabilities. Since the laboratory practice in making these hardenability determinations is to use a quenching temperature and holding time similar to that which will be employed in the commercial heat-treatment of the steel, it is felt that the relationship as shown in Fig. 8 is a reflection of the lack of complete carbide solubility and of the heterogeneity of the austenite accompanying commercial heattreatment of steels of this type. This, therefore, implies that while the correlation of Fig. 8 would represent the probable relationship in commercial practice, this relationship will vary with the austenitizing temperatures and times used in the hardenability determination.

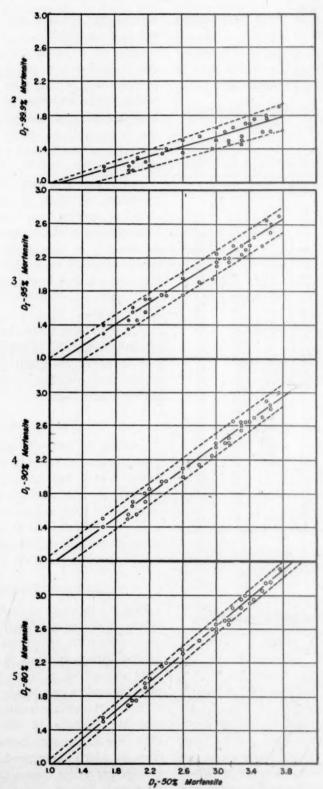
The results of Figs. 6 and 8 are combined in Fig. 9, to form a basis for the prediction of the hardenability in terms of the desired percentage of martensite from the calculated hardenability on the basis of 50 per cent martensite.

Microstructures

Typical microstructures of the 99.9, 95, 90, 80 and 50 per cent martensite levels in a NE 8640 steel are shown in Figs. 10 through 14. The nonmartensitic products seem to be predominantly upper bainite. This was characteristic of most of the lowalloy steels studied, although fine pearlite was observed in the plain carbon steels.

Hardness Relationships

Figs. 15 through 19 show the hardness values of the 99.9, 95, 90, 80 and 50 per cent martensitic structures plotted singly against carbon content, in order to illustrate the spread of these results. In this case, the scatter increases as the percentage of nonmartensitic constituents increases, probably because of the rather wide variations in the transformation temperatures at which these products form. The average curves for these values are plotted together in Fig. 20.



Figs. 2–5.—Relationship between hardenability based on percentage of martensite and 50 per cent martensite hardenability.

DISCUSSION OF RESULTS

Because of the relatively small number of steels studied, this work is not intended to represent a final quantitative answer to the relationships between hardenability tions having only one variable; that is, in compositions that are held constant except for variations in carbon content or a single alloying element. This would permit an analysis of the effects of carbon or the

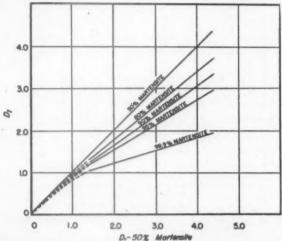


Fig. 6.—Average relationship between hardenability based on higher percentages of martensite and 50 per cent martensite hardenability.

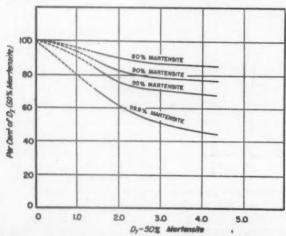


Fig. 7.—Relationship between high martensite hardenability, 50 per cent martensite hardenability ratio and 50 per cent martensite hardenability.

on the 50 per cent martensite basis and full hardenability, but rather as a preliminary survey to indicate the general direction of these relationships. As a matter of fact, it is felt that a more logical approach to a quantitative analysis of this problem would involve a study of these relationships in a series of composi-

individual alloying elements on full hardenability, and inasmuch as carbon and the alloying elements exhibit differences in their effect on transformation rates in the pearlite and bainite regions, it is probable that the relationships between hardenability on the 50 per cent martensite basis and full martensitic hardenability would be a function of the carbon and alloy combinations rather than of the hardenability itself. However, lack of time, manpower and facilities have made this hardness values of a hardenability test such as an end-quench test the point corresponding to a desired percentage of martensite. The first of these may be

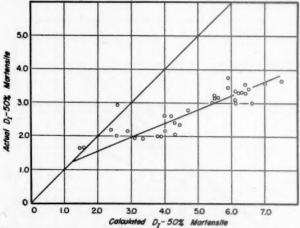


FIG. 8.—RELATIONSHIP BETWEEN CALCULATED AND ACTUAL HARDENABILITY OF STEELS STUDIED

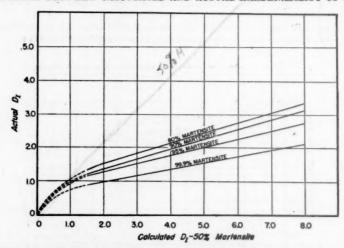
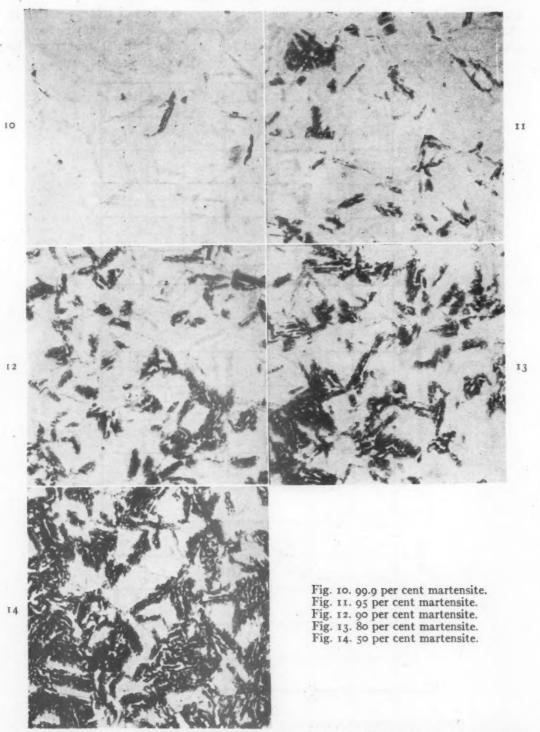


Fig. 9.—Average relationships between hardenability based on higher percentages of martensite and calculated hardenability.

more comprehensive study impracticable at present and it is felt that the trends as indicated by the present study would be helpful in making an intelligent application of hardenability data.

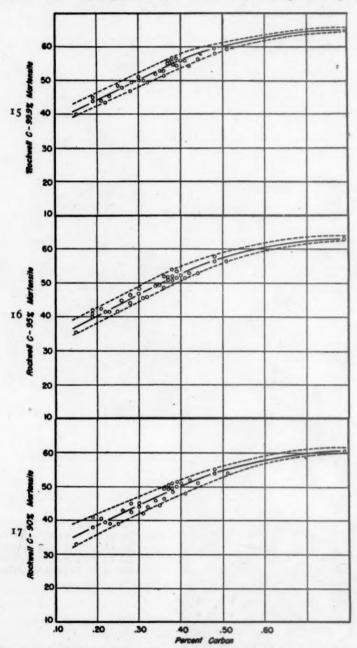
This study was initiated with two primary aims: (1) to enable workers to predict the full martensitic hardenability from a calculation of the hardenability on a 50 per cent martensite criterion and (2) to enable them to determine from the

accomplished by calculating the hardenability on the 50 per cent martensite basis by the method of Grossmann, predicting the actual hardenability from Fig. 8 and then predicting the hardenability in terms of the desired percentage of martensite from Fig. 7, or this may be read directly from Fig. 9. This work indicates that this prediction would be accurate within approximately plus or minus 0.3 in. in ideal diameter for low-alloy steels of the



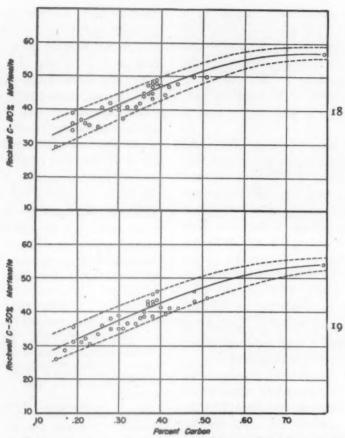
Figs. 10-14.—Typical microstructures of martensite in an NE-8640 steel. \times 1000. 4 per cent picral etch.

types studied here, but further studies of this nature may indicate wider discrepancies. Furthermore, it is felt that an attempt to extend these results to higher alloy relationships as shown will be useful in choosing compositions or applying hardenability data for material that must be heat-treated to optimum properties.



FIGS. 15-17.—HARDNESS OF MARTENSITE PRODUCTS AS FUNCTION OF CARBON CO.

steels would result in large discrepancies from the individual effects of the alloying elements. However, it is felt that the The carbon-hardness curve for 99.9 per cent martensite seems to be accurate within about 3 points Rockwell C, so that



Figs. 18-19.—HARDNESS OF MARTENSITE PRODUCTS AS FUNCTION OF CARBON CONTENT.

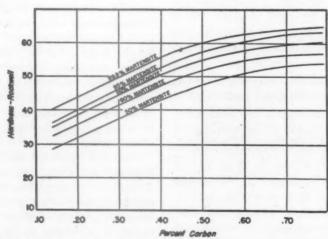


Fig. 20.—Average relationships between carbon content, hardness and percentage of martensite.

it does furnish a reasonable indication of the point of full martensite. However, with increasing amounts of transformation products the scatter becomes larger, and the carbon-hardness curve would seem to be quite unsatisfactory as a means of estimating the corresponding microstructure in such cases.

The magnitude of these differences between hardenability on the 50 per cent martensite basis and that based on full martensite or martensite plus small amounts of higher-temperature transformation products may be quite large in these low alloy steels (Fig. 7). For example, a steel having an ideal diameter of 3 in. on the 50 per cent martensite basis, such as steels of the 8640 or 4140 series, will actually have only half that hardenability on the full martensite basis, or about 70 per cent of that value when 5 per cent of upper transformation products is present.

In terms of commercial practice, this means that if 50 per cent of upper transformation products can be tolerated at the center of the section, this steel can be hardened in oil in about 11/2-in. diameter sections, but if full martensite is desired thorough hardening cannot be attained in sections more than approximately ½ in. in diameter. If 5 per cent of upper transformation products can be tolerated, the section size is still limited to about 0.8 inches.

The full significance of these results cannot be realized until our knowledge of the effects if these upper transformation products upon physical properties is more complete, but it would seem that differences of this magnitude should be given careful consideration in the choice of compositions for critical parts, or in applying hardenability data in cases where optimum properties are necessary.

SUMMARY

The relationships between hardenability based on a 50 per cent martensitic microstructure and hardenability on the basis of higher percentages of martensite have been studied in some plain carbon and lowalloy steels by means of a metallographic survey of a series of end-quenched hardenability tests. The results are presented graphically as follows: (1) A series of curves correlating hardenability on the 50 per cent martensite basis with hardenability on the basis of 99.9, 95, 90 and 80 per cent martensitic structures, (2) curves correlating calculated and actual hardenability on the basis of 99.9, 95, 90 and 80 per cent martensite structures, and (3) curves correlating carbon content and the hardness of 99.9, 95, 90, 80 and 50 per cent martensitic structures.

REFERENCES

- M. A. Grossmann, M. Asimow and S. F. Urban: Hardenability, Its Relation to Quenching, and Some Quantitative Data. Amer. Soc. Metals Preprint 26, 1938.
 Asimow, Craig and Grossmann: Correlation between Jominy Test and Quenched
- between Jominy Test and Quenched Round Bars. Inl. Soc. Automotive Engrs (1941)
- 1. A. Grossmann: Hardenability Calculated from Chemical Composition. Trans 3. M. A.I.M.E. (1942) 150, 227.

DISCUSSION

(C. M. Loeb, Jr., presiding)

I. H. HOLLOMON* and L. D. JAFFE. +-The authors are to be congratulated on obtaining information that has long been needed for the design of steels that are to be completely martensitic upon quenching. The relationships presented by the authors for converting the ideal round size for one percentage of nonmartensitic product to that for another percentage are extremely helpful in this regard.

The data presented in Fig. 8 appear to illustrate a fundamental difficulty with the Grossmann system. The authors attribute the discrepancy between the calculated and measured hardenabilities to lack of complete carbide solution and to the heterogeniety of

^{*} Captain, Ordnance Department, Water-town Arsenal Laboratory, Watertown, Massachusetts.

[†] Metallurgist, Watertown Arsenal Labora-

the austenite before quenching. The discrepancy is, however, too large to be accounted for in this manner. Many steels of types similar to those investigated by the authors have been tested at the Watertown Arsenal Laboratory and special care has been taken to obtain as nearly complete carbide solution as possible. A large discrepancy has still been observed between the calculated and the measured hardenabilities, which is the subject of a paper by the present writers.⁴

In this paper it is pointed out that the hardenability should be defined in terms of the cooling conditions (speeds of cooling) necessary to avoid the pearlite transformation and to avoid the bainite transformation. Since the alloying elements do not in general have the same effects upon the bainite and upon the pearlite transformations, two hardenabilities must be considered: the bainitic and the pearlitic. Grossmann and those who have subsequently measured the effects of alloying elements upon the hardenability were in general determining their effects on the pearlitic hardenability. Since for most of the steels studied by Hodge and Orehoski, bainite restricted the formation of martensite, the Grossmann system cannot be expected to apply. For alloy steels containing more than about 0.25 per cent molybdenum or about 0.60 per cent chromium, bainite probably restricts the formation of martensite and a new system of calculating hardenability is required. A tentative system for this purpose is included in the paper just mentioned.4

W. Crafts* and J. L. Lamont.*—This paper emphasizes an important phase of the study of hardenability that has been neglected unduly in the recent preoccupation with measurement of hardenability in terms of 50 per cent martensite, and the authors are to be complimented on an effective presentation of the subject. Although the depth of 50 per cent martensite hardening is very useful for calculating hardenability according to Grossmann's method, it has little real significance except in high-carbon steels. Several studies of the effect of as-quenched

microstructure on the mechanical properties, however, have shown that 100 per cent martensite is essential to development of the maximum combinations of strength with

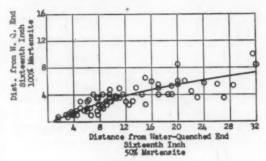


FIG. 21.

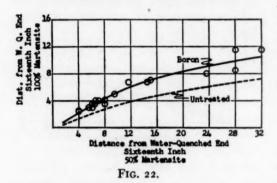
ductility and toughness. It is furthermore indicated by the data shown in Fig. 2 that very great 50 per cent martensite hardenability is required in order to harden moderately small sections to fully martensitic structures. This implies that heat-treating steels for engineering purposes must be hardened to almost maximum hardness at the center to obtain 100 per cent martensite, and therefore maximum properties, at the surface.

Observations of end-quenched Jominy specimens that were examined at the Union Carbide and Carbon Research Laboratories are shown in Fig. 21 to be very similar to the data presented in Fig. 2. These results were obtained from commercial American NE types of steel and from a fairly complete series of British Standard Engineering Steels made in Great Britain. These points extend over a somewhat greater range of hardenability and the spread of the points is greater than is shown in Fig. 2. The average is about the same and supports the relation shown in the paper. Deviation from the average did not appear to be related to alloy composition. The first appearance of nonmartensitic constituents is noticed in the segregated bands, and it is presumed that deoxidation and solidification factors have a strong influence on the relation between 50 and 100 per cent martensite.

All the steels represented in Fig. 21 were either coarse grained or appeared to have been treated with aluminum. It is considered very probable that the type of deoxidizing agent has a considerable effect and, although

⁴ J. H. Hollomon and L. D. Jaffe: The Hardenability Concept. Page 601, this volume. * Union Carbide and Carbon Research Laboratories, Inc., Niagara Falls, N. Y.

treatment with boron may be considered not a normal deoxidation treatment, it has a strong effect on the relation between 50 per cent martensite and 100 per cent martensite



hardenability. This is illustrated in Fig. 22 which is based on commercial steels of various alloy compositions that were treated with several different simple and complex boron addition agents.

For a given depth of 50 per cent martensite, the depth of 100 per cent martensite is increased by about 50 per cent. The apparent spread of points is also reduced. In view of these results, it is apparent that the boron treatment has the specific property of increasing the depth of 100 per cent martensite in addition to its capacity to increase the depth of 50 per cent martensite hardening. The boron treatment, therefore, should be of specific value in steels that require 100 per cent martensite after quenching in order to develop maximum combinations of strength, ductility, and toughness. It should be noted that even in sections as small as one inch a fairly substantial alloy content is required to give enough hardenability, so that it is possible to derive full benefit from the boron treatment.

H. W. GILLETT.*—The most futile discussion is that which only says that an author did a fine job. In spite of this, I can't keep from saying just that. Many papers have been written and many mathematical calculations made using the assumption that a 50 per cent hardened steel is hardened, in spite of Bain's comment in "Effects of Alloying Elements in Steel" that a much higher martensite content in the quenched steel would have been a more

practical basis, and in spite of our general appreciation, when we stop to think, that it makes a pile of difference whether the other 50 per cent is ferrite, bainite, or some conglomeration. The "ideal diameter," too, though a logical base line, is not a very practical measuring stick.

The poor engineer, reading the earlier articles, is subconsciously led to the idea that 50 per cent martensite is enough, and that sections the size of the calculated ideal diameter actually will harden. If he happens to deal with heavy armor, where the properties of the middle of the plate are as important as at the face, he soon wakes up to the fact that slack quenching is different from full quenching.

This paper, showing that a steel rated by paper after paper as having a 50 per cent hardenable ideal diameter of 4 in., in an actual quench has one of some $2\frac{1}{2}\pm$ in., and then that that $2\frac{1}{2}\pm$ in. of 50 per cent martensite corresponds to some $1\frac{1}{2}\pm$ in. of all martensite, brings the real facts of life to light and should wake up a lot of people to thinking in terms of $1\frac{1}{2}\pm$ instead of 4.

The evidence that calculated hardenability is a weak reed is very valuable. Fig. 8, with its scatter, and Fig. 9, with its relationships, ought to be duplicated in quantity and pasted into the library copies of a myriad of earlier articles. Anything that leads the heat-treater to make an actual Jominy test instead of relying on pencil and paper methods, alleged to be accurate to some ±15 per cent, on the 50 per cent martensite, ideal-diameter criteria, but misleading in respect to cold facts by some 265 per cent, or more, deserves high commendation.

It is true that not all uses demand thorough hardening, but if we are to talk about hardenability, let's talk in terms of honest-to-God hardenability and let the engineer be the one to decide whether his use can stand a slack-quenched core, not allow him to think that we metallurgists are indifferent to slack quenching, hence he can be indifferent, too.

P. R. CASSIDY.*—There is a considerable interest in hardenability from a viewpoint entirely different from the one from which you are approaching it; that is, the interest of

^{*} Chief Technical Adviser, Battelle Memorial Institute, Columbus, Ohio.

^{*} Babcock and Wilcox Co., Barberton, Ohio.

those concerned in the subject of weldability. The viewpoints are almost diammetrically opposite.

In weldability, we are interested in reducing the hardenability as far as possible to prevent quench-cracking or martensite cracking in the heat-affected zone of the weld. Our interest in that is inapplicable sometimes to the methods that are developed purely from the standpoint of desirable hardenability. For example, if you plot a cooling curve for a given Iominy position on a log time against temperature, and start at the zero point at the upper critical, you get a curve that comes asymtotic to the water temperature.

are less than those for the maximum hardness of martensite as determined by Burns, Moore and Archer.5 This variation of the hardness of martensite might be explained by the variation in quenching speed.

The values for the hardness of martensite in steels with 0.23, 0.30 and 0.40 per cent carbon as reported by different investigators (1, 2, 3, 4, 5) are given in Table 5. All of this work was carried out under carefully controlled conditions. Digges⁵ determined the hardness of high-purity iron-carbon alloys varying only in carbon content by quenching in gas specimens 0.04 in. thick, at rates just sufficiently fast to produce all martensite. Since

TABLE 5.—Comparison of Martensitic Hardness of Steels of Three Different Carbon Contents

						Ro	ockwell	С
Refer- ence No.*	Type Composition	Size of Specimen	Place of Hardness Measure- ment	Quenching Tempera- ture	Quenching Medium	Carbo	on, Per	Cent
				,		0.23	0.30	0.40
I	Iron-carbon al-	0.04" thick	Surface	1800°F.	Gas	42	46	53
2	Low-alloy steels	1" × 1½" × 5"	Surface	Near melting temp.	Water at 50°F.	44.5	49	54.5
3	Plain carbon and low-alloy steels	1/4" round	Midway be- tween cen- ter and sur- face	Near melting temp.		45	50	56.5
4	Plain carbon steels	I" round	Surface	1425 to 1650°F.	5 % NaOH at 65 to 75°F.	48	53 - 5	59
5	Plain carbon and alloy steels	1/4" thick or 1/4" round	Surface	Varying	Iced NaOH and others	51	56	60.5

Data from: (1) T. G. Digges, (2) R. O. Kern, (3) K. L. Clark and N. Kowall, (4) C. A. Rowe and R. A. Ragatz, (5) Burns, Moore and Archer, (8)

In welding, we deal with pre-heat if the steel is at all hardenable; therefore, if we have a pre-heat from 300° to 500°F., the cooling curve in the heat-affected zone tends to become asymtotic to the pre-heat. The higher the pre-heat, the less applicable is the Jominy test to the conditions that actually will exist in the heat-affected zone of the weld.

G. DE VRIES. *- The hardness shown on the curve in Fig. 20 for 99.9 per cent martensite of varying carbon contents is less than the hardness 1/16 in. from the water-cooled end of the Jominy bars of the authors' steels, and the latter values for a given carbon content these were high-purity alloys, relatively high cooling rates were required to produce fully martensitic structures. It is believed that the hardness values reported by Digges for alloys ranging up to about 0.60 per cent carbon are the minimum for untempered martensite. Kern⁶ quenched a 1 by 1½ by 5-in. bar in water at 50°F. and measured the hardness at the surface. Clark and Kowall7 quenched a

⁵ T. G. Digges: Influence of Austenitic Grain Size on the Critical Cooling Rate of Highpurity Iron-carbon Alloys. Trans. Amer. Soc.

for Metals, 29 311 (1941).

R. O. Kern: Rapid Carbon Determination at the Furnace of Remelted Alloy Steels.

Amer. Foundryman (Sept. 1942) 4 (9), 8.

K. L. Clark and N. Kowall: Hardness Measurements as a Rapid Means for Determining Carbon Content of Carbon and Lowalloy Steels.

Trans. A.I.M.E. (1944) 158,

^{*} National Bureau of Standards, Washington, D. C.

¼-in. round in ice water and measured the hardness at the center. Rowe and Ragatz³ quenched a r-in. round in 5 per cent sodium hydroxide at 70°F. and measured the hardness at the surface. Burns, Moore, and Archer³ determined the hardness of small samples ¼ in. round, quenched in iced sodium hydroxide. A comparison of the hardness values obtained by the different investigators indicates that the hardness of martensite of hypoeutectoid steels increases with increase in rate of cooling from the quenching temperature or severity of quench.

Table 6.—Effect of Variation in Cooling Medium on the Rockwell C Hardness of 3 Steels

	Roc	Rockwell C Hardness as Quenched							
C, Per Cent	Quenching Medium								
Cent	Oil	Water	5 Per Cent Iced Sodium Hydroxide						
0.18 0.30 0.44	37·5 47·5 54·5	43.I 50.5 57.0	44.8 53.5 60.5						

The results obtained by the writer on quenching specimens prepared from steels with 1.6 per cent manganese, a hardenability intensifier containing boron and 0.18, 0.30 and 0.44 per cent carbon, respectively, are summarized in Table 6. The specimens were quenched from 1600°F. in oil, water or iced 5 per cent sodium hydroxide. The specimens quenched in oil and water were 1.0 by 0.4 by 0.4 in., while the specimens quenched in iced sodium hydroxide were 0.2 by 0.2 by 0.4 in. The quenched specimens were cut in half without tempering and Rockwell C measurements were made on the cut surface. The average of the two highest values of six or more Rockwell impressions is given in Table 6 because nearly all errors in Rockwell measurements are likely to cause low readings. The specimens with 0.18 and 0.30 per cent carbon

quenched in oil, water and iced sodium hydroxide were polished, etched in 4 per cent picral and given a microscopic examination. The specimens quenched in iced 5 per cent sodium hydroxide etched the lightest and the oil-quenched specimens etched the darkest. The 0.30 per cent carbon steel etched darker than the 0.18 per cent carbon steel. All of the specimens had a martensitic structure, the oil-quenched specimens having the coarsest structure. These results also indicate that increasing the cooling rate increases the martensitic hardness of hypoeutectoid steels. This might mean that martensite does not form instantly on cooling but takes a little time to form, or the strains set up by the fast quenching increase the hardness. If martensite does not form instantly on cooling, a faster quench will cause more martensite to form at a lower temperature.

J. M. Hodge (author's reply).—The data in this discussion on the hardness of martensite as a function of cooling rate and carbon content is extremely interesting, and decidedly pertinent to the choice of a hardness value to be used as a criterion of hardenability in terms of full martensite in a steel of a given carbon content. The variations in hardness with cooling rate as shown in this discussion means, of course, that the choice of a hardness value for full martensite will be a function of the hardenability itself, and would be lower for steels of high hardenability. Thus, if in a high-alloy steel the point of first transformation to upper transformation products was found to be 11/2 in. from the end of an end-quench test, the hardness of the martensite at this relatively slow cooling rate would be expected to be lower than in a steel of the same carbon content for which the first transformation occurred at 1/2 in. from the quenched end with a correspondingly more rapid cooling rate. This is undoubtedly true, and furnishes another illustration of the dangers involved in the use of hardness rather than microstructural criteria of hardenability. Over a rather limited hardenability range, such as was covered by the steels in this paper, however, it is felt (and is so indicated by the data) that hardness values may furnish a reasonably accurate indication of the location of the full martensite or 95 per cent martensite values.

[•] C. A. Rowe and R. A. Ragatz: Hardness Gradients in Tempered Steel Cylinders. Trans. Amer. Soc. for Metals (1939) 27, 739.

Amer. Soc. for Metals (1939) 27, 730.

Burns, Moore, and Archer: Quantitative Hardenability. Trans. Amer. Soc. for Metals (1938) 26, 1.

Determination of Most Efficient Alloy Combinations for Hardenability

BY H. E. HOSTETTER,* MEMBER A.I.M.E.

(New York Meeting, October 1045)

GROSSMANN'S method1 for calculating the hardenability of steel from the composition and grain size has gained wide acceptance, and when properly used, has been well proved in practical application, both for estimating the hardenability of known compositions and for selecting compositions to meet known hardenability requirements.

The Grossmann method uses as the criterion of hardenability the "ideal critical diameter," DI, which is the size round that will just harden to a structure of 50 per cent martensite at the center when given the theoretically fastest quench, or "ideal quench." The DI can be related to actual quenching practice if the severity of quench is known; or the D_1 can be correlated with hardenability as determined by the Jominy end-quench method.2

The effect on hardenability of each element present in a steel can be represented by a multiplying factor, the value of which depends on the amount of the element present and the degree of effectiveness of the particular element. (The value of the factor for a given carbon content varies with the grain size.) When the factors for all elements present in a steel have been determined from charts, they are multiplied, and the resultant product is the D_I of the steel. The validity of Grossmann's scheme of multiplying factors has been confirmed in a number of other investigations.3-6

It can be appreciated that a certain

desired level of hardenability can be obtained by adding chromium, molybdenum, nickel and vanadium to a base composition containing carbon, manganese, silicon and the usual impurities. Many of the ranges of hardenability used commercially can be obtained by any of the foregoing alloying elements used singly in the base composition. The same hardenability levels also can be obtained through use of any of a great number of multiple element combinations of these alloying elements. In this report a method will be presented for determining what one combination is the most efficient (based on hardenability and cost of added alloy) for a given level of hardenability.

It should not be assumed from the emphasis given to hardenability, that hardenability is the only criterion for the selection of an alloy composition. Such properties as the hot-working characteristics, machinability, carburizing characteristics, amount of distortion during quenching and the retention of austenite may be considerations of importance in many applications. However, hardenability is one of the most important properties of an alloy steel and one that must be considered in almost all cases involving heattreatment by quenching. Therefore, a method for determining the lowest-cost alloy combination should be of considerable value.

DETERMINATION OF MOST EFFICIENT COMBINATIONS

For comparing the alloying elements on standards of cost and hardenability, it

Manuscript received at the office of the Institute Jan. 22, 1945. Issued as T.P. 1905 in METALS TECHNOLOGY, September 1945.

* Climax Molybdenum Company of Michigan, Detroit, Michigan.

References are at the end of the paper.

is first necessary to select increments of alloy content of equal cost. The increments of alloy content listed in Table 1, for which average recoveries of added alloy

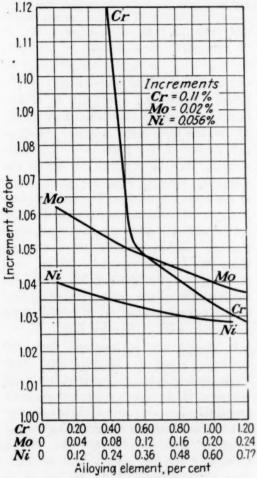


FIG. 1.—CALCULATED INCREMENT FACTORS.

are considered, are convenient for later calculations. Thus, with these prices and

TABLE 1.—Increments of Alloy Content

Alloying Element	Price per Lb.	Recovery, Per Cent	Cost per Lb. Re- covered	Increments of Alloy Content of Equal Cost, Per Cent
Chromium	\$0.13	80	\$0.162	0.11
Molybdenum	0.80	90	0.889	0.02
Nickel	0.30	95	0.316	0.056

recoveries, o.11 per cent chromium in the steel costs the same as 0.02 per cent molybdenum or 0.056 per cent nickel. The figures on alloy recoveries are for illustrative purposes for the method to be described, but they are fairly representative of basic open-hearth practice for production of 0.30 to 0.50 per cent carbon-alloy steels. When more applicable recovery figures are known, they should be used, but they will in no way change the fundamentals of the method.

In determining the most efficient alloy combinations, use is made of what are termed "increment factors." Considering the case of chromium, the multiplying factor for 0.11 per cent chromium is 1.26 and for 0.22 per cent chromium is 1.52. The increment factor for the increase from 0.11 to 0.22 per cent chromium is X in the following computations:

$$(X)(1.26) = 1.52$$

 $X = 1.21$

Thus, the increment factor, 1.21 in this example, is the factor by which the D_I of a composition containing o.11 per cent chromium is increased by an additional o.11 per cent of chromium. It will be noted that the D_I of a composition free of chromium is increased by a factor of 1.26 by the addition of the first o.11 per cent of chromium, while the D_I of a composition with o.11 per cent chromium is increased by a factor of only 1.21 by the addition of another o.11 per cent chromium. The increment factors are a quantitative means of expressing the general qualitative principle that, in terms of multiplying factors, each added increment of alloying element gives decreasing returns in hardenability.

The calculated increment factors for chromium, molybdenum and nickel are given in Table 2 and plotted in Fig. 1. The multiplying factors used for chromium are taken from the lower curve shown by Grossmann¹ for chromium contents greater

than 0.35 per cent. The reasons for using the lower curve will be discussed later. The molybdenum multiplying factors employed are those reported by Grossmann, which have been checked at slightly higher and lower values in the work of the Naval Research Laboratory and of Crafts and Lamont. For nickel, the multiplying factors used are in substantial agreement with those reported by Edson and Crafts and Lamont. It should be emphasized that a point on an increment-factor curve in Fig. 1 gives the increment factor (not the multiplying factor) for only the last added increment of alloy content.

increments of molybdenum. With a higher molybdenum, lower chromium composition the last increments of molybdenum would be less effective than the increments of chromium.

In Table 3 are given the most efficient combinations of chromium, molybdenum and nickel for various levels of hardenability. These are simply values of chromium, molybdenum and nickel found at intersections made by horizontal lines with the increment-factor curves of Fig. 1. After the alloy contents at the intersections have been determined, the multiplying factors are obtained from the

TABLE 2.—Calculated Increment Factors

Chromium		Molybdenum			Nickel			
Cr. Per Cent	Multiply- ing Factor	Increment Factor	Mo, Per Cent	Multiply- ing Factor	Increment Factor	Ni, Per Cent	Multiply- ing Factor	Increment Factor
0.00	1.00		0.00	1.00		0.00	1.00	
O.II	1.26	1.26	0.02	1.062	1.062	0.056	1.04	1.040
0.22	1.52	1.21	0.04	1.125	1.050	0.112	1.08	1.038
0.33	F. 78	1.17	0.06	1.187	1.056	0.168	1.12	1.037
0.44	1.96	I.IOI	0.08	1.25	1.053	0.224	1.16	1.036
0.55	2.06	1.051	0.10	1.312	1.050	0.28	1.20	1.034
0.66	2.155	1.046	0.12	1.375	1.048	0.336	1.24	1.033
0.77	2.245	1.042	0.14	1.437	1.046	0.392	1.28	1.032
0.88	2.33	1.038	0.16	1.50	1.044	0.448	1.32	1.031
0.99	2.41	1.034	0.18	1.562	1.042	0.504	1.36	1.030
1.10	2.485	1.031	0.20	1.625	1.040	0.56	1.40	1.029
1.21	2.555	1.028	0.22	1.687	1.038	0.616	1.44	1.029
1.32	2.63	1.025	0.24	1.75	1.037	0.672	1.48	1.028

It can be realized from the foregoing that the most efficient combination of alloying elements for a given hardenability level is found at the intersections with curves of Fig. 1 made by some particular horizontal line. For example, the values 0.57 per cent chromium, 0.10 per cent molybdenum are found at intersections made by a horizontal line with the chromium curve and the molybdenum curve. The last added increment of chromium is equally effective as to hardenability, and equal in cost, to the last added increment of molybdenum. If the same hardenability were obtained with a higher chromium, lower molybdenum composition, the last increments of chromium would be less effective as to hardenability than the appropriate charts and the combined multiplying factor of the combination is calculated and entered as column 7 in Table 3.

MOST EFFICIENT COMBINATIONS

Those familiar with the multiplyingfactor system for calculation of hardenability will find it a simple matter to use the data derived by the method that has been described. The following examples will serve to illustrate.

Example I

Assume that a composition having an average D_I of 4.80 is desired. Based on various considerations, the average alloy-free composition selected might be No. 7

grain size, 0.40 per cent carbon, 0.85 per cent manganese, 0.25 per cent silicon. The D_I of the alloy-free composition is then calculated:

-		Multiplying Factor
Grain size	7	
Carbon	0.40%	0.213
Manganese	0.85	4.50
Silicon	0.25	1.17
Product		1.12

The combined multiplying factor for chromium, molybdenum and nickel to provide the desired D_I , 4.80, is the term (Cr \times Mo \times Ni), where Cr is the multiplying factor for chromium, Mo for molybdenum, and Ni for nickel.

$$(Cr \times Mo \times Ni)(1.12) = 4.80$$

 $(Cr \times Mo \times Ni) = 4.28$

TABLE 3.—Most Efficient Alloy Combinations

Element, Per Cent				ltiply Factor	Cr Factor X Mo Factor X	
Cr	Mo	Ni	Cr	Мо	Ni	Ni Factor
0.10	0.00	0.00	1.24	1.00	1.00	1.24
0.20	0.00	0.00	1.47	1.00	1.00	1.47
0.30	0.00	0.00	1.71	1.00	1.00	1.71
0.40	0.00	0.00	1.92	1.00	1.00	1.92
0.51	0.02	0.00	2.03	1.06	1.00	2.15
0.53	0.06	0.00	2.04	1.19	1.00	2.43
0.57	0.10	0.00	2.08	1.31	1.00	2.72
0.66	0.14	0.00	2.16	1.44	1.00	3.11
0.77	0.18	0.00	2.25	1.56	1.00	3.51
0.82	0.20	0.06	2.29	1.63	1.04	3.88
0.88	0.22	0.13	2.33	1.69	1.09	4.30
0.91	0.24	0.17	2.36	1.75	1.12	4.62

Table 3 shows that 0.88 per cent chromium, 0.22 per cent molybdenum, 0.13 per cent nickel is the most efficient alloy combination with a combined multiplying factor of 4.30. This is sufficiently close to the desired combined factor of 4.28.

If known quantities of residual alloying elements other than chromium, molybdenum and nickel are present in the steel, their multiplying factors can be determined from charts and multiplied with the carbon, manganese and silicon factors of the base composition, thus reducing the hardenability required of the chromiummolybdenum-nickel combination.

Example II

The average chromium content of the former S.A.E. 5140 is 0.95 per cent. Assuming an average residual of 0.05 per cent molybdenum, the combined multiplying factor for chromium and molybdenum is as follows:

Element, Per Cent		Multi Fac	plying	Cr Factor X Mo Factor
Cr	Mo	Cr	Мо	Mo ractor
0.95	0.05	2.38	1.15	2.74

From Table 3, the data indicate that 0.57 per cent chromium, 0.10 per cent molybdenum is the most efficient combination with a combined multiplying factor of 2.72; this is sufficiently close to the desired 2.74. In this instance the other residual alloying elements in 5140 need not be considered because they should be present in approximately the same amounts and contribute equally to the hardenability of the 0.57 per cent chromium, 0.10 per cent molybdenum composition.

The determination of a most efficient alloy combination can be performed graphically by adding to Fig. 1 another curve representing the combined multiplying factors for chromium, molybdenum and nickel in the most efficient combinations. The added curve for the combined multiplying factors is shown in Fig. 2. The following will serve to illustrate the graphical solution to the hardenability problem previously presented as Example I:

On the upper scale find the value 4.28, the combined multiplying factor required of the alloy combination. From this point draw a vertical line to the $Cr \times Mo \times Ni$ multiplying-factor curve, intersecting at

point A. From point A draw a horizontal line to intersections with the Mo curve at point B, 0.22 per cent Mo; with the Cr curve at point C, 0.88 per cent Cr; with

reported in only two researches, 1.6 and the two sets of factors are in considerable variance. Calculation of the increment factors from the multiplying factors

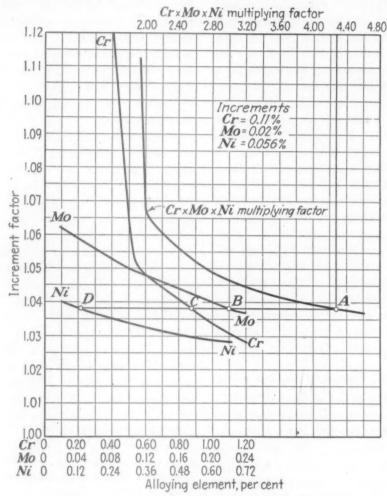


FIG. 2.—CALCULATED COMBINED MULTIPLYING FACTORS.

the Ni curve at point D, 0.13 per cent Ni. These values of alloy content give the desired combined multiplying factor.

OTHER ELEMENTS

The increment factors for vanadium are not presented in the report because of a number of considerations that prevent even the preliminary approach that has been made with chromium, molybdenum and nickel. In the first place, the multiplying factors for vanadium have been

reported by Crafts and Lamont⁶ results in no change in the most efficient alloy combinations given in Table 3. Using Grossmann's data¹ on vanadium multiplying factors, it is indicated that vanadium could be considered in the range 0.00 to 0.03 per cent for the hardenability levels given in Table 3. However, because of the difficulty of commercial control in this range and the variation in multiplying factors reported by Crafts and Lamont⁶ in the same range, it is felt advisable to

obtain further data before submitting increment factors for vanadium.

It is appreciated that carbon, manganese and silicon, while not usually classed as alloying elements, do contribute to hardenability and are relatively inexpensive. It is common knowledge that the highmanganese steels in the medium and high-carbon ranges are compositions of high hardenability for the cost of added alloy. However, practical experience has shown that the amounts of carbon, manganese and silicon should be limited in steels for most hardenability applications by other considerations involved in making, fabricating and heat-treating the steel. Among these considerations are control of the composition, cleanliness of the steel, segregation during solidification, hot-working characteristics, banding, machinability, cracking tendencies during quenching, amount of retained austenite, and temper brittleness. For these reasons this report has been limited to determining the role of the conventional alloying elements.

MULTIPLYING FACTORS FOR CHROMIUM

The multiplying factors used in Table 2 for calculation of the increment factors for chromium are taken from the lower curve shown by Grossmann¹ for the higher chromium contents. It is believed that these values for chromium represent the effect of chromium in normal heat-treating practice more closely than do the higher values. The chromium multiplying factors determined by the Naval Research Laboratory and Crafts and Lamont are for steels given a prior normalizing treatment. Since results of these researches are in fair agreement with Grossmann's straightline portion of the chromium curve, it is presumed that Grossmann also used a prior normalizing treatment for most of his work.

It is known that normalized steels containing appreciable quantities of chro-

mium, molybdenum and vanadium usually have higher hardenability than annealed steels.^{8,9} Most alloy steel is given an annealing treatment to make it suitable for machining operations, and is then heated for hardening without an intervening heat-treatment. For this reason it would be of considerable value to have the multiplying factors for chromium, molybdenum and vanadium applicable to steels given an annealing treatment before hardening.

A method is available for approximating the effective multiplying factors for chromium from data on the composition, grain size and Jominy end-quench test. From the Jominy hardenability curve the actual D_I of the steel can be determined for the particular prior structure and austenitizing treatment involved.2 The multiplying factors for all elements present in the steel, with the exception of chromium, are found on the charts and then multiplied. The resultant product is the D_I of the chromium-free composition; this divided into the actual D_I obtained from the Jominy curve gives an approximation of the effective multiplying factor for chromium. The following example for S.A.E. 4140 is taken from hardenability data previously reported.10

Prior structure—annealed
Treatment of Jominy specimen, 60 min. in
1550°F. furnace

		Multi- plying Factor
Coolo eles	61/ (at ====°E)	
Grain size	. 072 (at 1550 F.)	
Carbon	. 0.40%	0.223
Manganese	. 0.68	3.80
Silicon	. 0.20	1.13
Chromium	. 1.00	
Molybdenum		1.66
Nickel	0.22	1.16
D _I (Cr-free)		1.85
Actual DI (from Jon		
iny curve)		2 60
		3.60
Cr multiplying facto	r	1.95

In this instance the effective multiplying factor for chromium, 1.95, is considerably less than even the lowest values previously reported for 1.00 per cent chromium. It is agreed that this calculation assigns the full multiplying factor to molybdenum, and that the low multiplying factor calculated for chromium represents the summation of various causes tending to reduce hardenability. On the other hand, this calculation also assigns to chromium any hardenability effect produced by elements not reported in the foregoing analysis. Similar calculations carried out for carbon-chromium and chromium-nickel steels (containing only residual molybdenum) have shown effective multiplying factors for chromium quite comparable with those obtained for the chromiummolybdenum steels.

Because of lack of complete information on a sufficient number of compositions, it has been impossible to assign values for the effective multiplying factors for chromium in steels annealed prior to hardening. As previously indicated, it would be of considerable practical value to determine for prior-annealed structures, the multiplying factors for chromium, molybdenum and vanadium. Recent work of Bowman and Parke11 on carbon-molybdenum steels has shown that the molybdenum content of the carbide in a given composition of steel varies with the heat-treatment. Presumably a similar situation should hold for steels containing chromium and vanadium. The alloy content of the carbide should influence hardenability because the alloy carbides are slow to dissolve in austenite and because the alloying elements diffuse slowly in the austenite after being taken into solution. Since the alloy content of the carbide varies with the treatment prior to heating for hardening, the importance of determining multiplying factors for annealed prior structures is apparent. Obviously, the more directly applicable the multiplying factors are, the more precise will be the determinations made from the derived increment factors.

APPENDIX.—Recovery of Alloy from Scrap

In the method that has been presented in the body of this report for determination of the most efficient alloy combinations, consideration has been given only to costs of new alloy additions. In the production of most alloy steel it is standard practice to employ alloy-containing scrap as a portion of the furnace charge. This alloy-containing scrap may be produced within the steel plant or it may be obtained from outside sources. Although it is somewhat of a problem to segregate alloycontaining scrap, it is true nevertheless that the alloy recovered upon remelting such scrap makes possible a commensurate reduction in the addition of new alloy. This holds true if the alloy-containing scrap is used in the making of any alloysteel heat of a composition containing the same alloying elements present in the scrap. It is not necessary, of course, that the percentages of alloying elements in the scrap and in the desired composition of the heat melted be the same.

If desired, it is possible to calculate increments of alloy content of equal cost taking into consideration the percentage of return scrap, the recovery of alloy on remelting of return scrap and the recovery of the new alloy addition. A complete case for alloy costs, as determined by the composition being melted, is made possible by such calculations without the necessity of considering the alloy recovery from other scrap:

Let A = percentage of alloying element recovered from new added alloy,

Let B = percentage of alloying element in final composition,

Let C = percentage of alloying element recovered from return scrap of same type composition, Let D = percentage of alloying element recovered from other scrap

Then
$$A = B - C - D$$

Obviously, the cost of making an addition from which the alloying element will tion for alloy-containing return scrap. The following case covers the cost of an increment of 0.02 per cent molybdenum under the conditions given below.

Mo in the steel, 0.02 per cent Return scrap remelted in alloy steel heats, 25 per cent

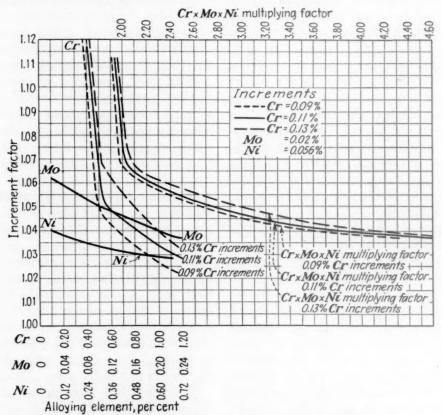


FIG. 3.—MULTIPLYING FACTORS FOR EFFICIENT COMBINATIONS.

be recovered in an amount equal to term A represents the alloy cost of that alloying element for the heat. Likewise, in comparing the alloy costs of two different types of compositions, as determined by the compositions being melted, it is necessary to consider only terms A, B and C. If the return scrap produced from the composition under consideration is used in the making of any heat in which the specific alloying element is desired, term C can be regarded as a credit to the alloy cost of the original type composition.

The cost of an increment of alloy content can now be calculated with due consideraRecovery of Mo on remelting of scrap, 90 per cent Cost per pound of new Mo, \$0.80 Recovery of new Mo addition, 90 per cent

Alloy cost (per 100 lb. of steel) $= \frac{[(0.02) - (0.02)(0.25)(0.90)][0.80]}{(0.90)}$ Alloy cost = \$0.01378

Calculation of the increment of chromium content of equal cost with the same percentage of return scrap under the following conditions is shown below.

Alloy cost, \$0.01378

Equal cost Cr increment, Cr

Return scrap remelted in alloy steel heats, 25

per cent

Recovery of Cr on remelting of scrap, 30 per cent Cost per pound of new Cr, \$0.13

Recovery of new Cr addition, 80 per cent

 $0.01378 = \frac{[(Cr) - (Cr)(0.25)(0.30)][0.13]}{(0.80)_{1}}$ Cr = 0.092 per cent

Similarly, the increment of nickel content of equal cost, with 25 per cent return scrap, 95 per cent recovery on remelting, 95 per cent recovery of a new addition and \$0.30 per pound of nickel, is 0.057 per cent nickel.

Using 0.02 per cent Mo as the base increment from which the equal-cost increments for the other alloying elements are calculated, it will be found that in most cases covering commercial practice the nickel increment is quite close to the value 0.056 per cent nickel used in the body of this report.

The recovery of chromium from an addition of ferrochromium and the recovery of chromium on remelting of scrap vary to a greater extent than the recoveries of molybdenum and nickel. Accordingly, increment factors for o.oo per cent and 0.13 per cent chromium increments have been calculated and plotted to supplement the data on o.11 per cent chromium increments. These data are presented in Table 4 and Figure 3. It will be found that the range 0.09 to 0.13 per cent chromium increments will cover most of the cases of percentages of return scrap, recovery of chromium from scrap and recovery of new chromium additions with chromium at \$0.13 per pound, that are encountered in commercial production of rolled alloy steels.

The most efficient combinations of chromium, molybdenum and nickel for increments of 0.02 per cent molybdenum and 0.056 per cent nickel equal in cost to increments of 0.09 and 0.13 per cent chromium are given in Table 5. The multiplying-factor curves applicable to chromium increments of 0.09 per cent, 0.11 per cent and 0.13 per cent chromium

in most efficient combinations with increments of 0.02 per cent molybdenum

TABLE 4.—Increment Factors for 0.09 and 0.13 Per Cent Chromium Increments

Cr, Per Cent	Multi- plying Factor	Incre- ment Factor	Cr. Per Cent	Multi- plying Factor	Incre- ment Factor
0.00	1.00		0.00	1.00	
0.09	1.21	1.21	0.13	1.31	1.31
0.18	1.42	1.173	0.26	1.62	1.24
0.27	1.63	1.148	0.39	I.OI	1.179
0.36	1.84	1.129	0.52	2.04	1.068
0.45	1.97	1.071	0.65	2.16	1.059
0.54	2.059	1.045	0.78	2.27	1.051
0.63	2.143	1.041	0.91	2.37	1.044
0.72	2.222	1.037	1.04	2.46	1.038
0.81	2.296	1.033	1.17	2.54	1.033
0.90	2.365	1.030	1.30	2.61	1.028
0.99	2.429	1.027			
1.08	2.488	1.024			
1.17	2.542	1.022			

TABLE 5.—Most Efficient Alloy Combinations

Cr Factor	ng	ltiplyi actor	Mu		ement, er Cent	
Ni Factor	fo Ni Ni		Cr	Ni	Mo	Cr
02; Ni 0.056	Mo o.	Cent;	9 Per	Cr o.o	ments:	Incre
1.24	1.00	1.00	1.24	0.00	0.00	0.10
1.47	1.00	1.00	1.47	0.00	0.00	0.20
1.71	I.00	1.00	1.71	0.00	0.00	0.30
1.92	1.00	1.00	1.92	0.00	0.00	0.40
2.10	1.00	1.06	1.98	0.00	0.02	0.46
2.36	1.00	1.19	1.98	0.00	0.06	0.47
2.65	1.00	1.31	2.02	0.00	0.10	0.50
2.94	1.00	1.44	2.04	0.00	0.14	0.53
3.31	1.00	1.56	2.12	0.00	0.18	0.61
3.64	1.04	1.63	2.15	0.06	0.20	0.65
4.03	1.09	1.69	2.19	0.13	0.22	0.70
4.33	1.12	1.75	2.21	0.17	0.24	0.72
.02; Ni 0.05	Моо	Cent;	13 Per	Cr o.	ments	Incre
1.24	1.00	1.00	1.24	0.00	0.00	0.10
	1.00	1.00	1.47	0.00	0.00	0.20
1.71	1.00	1.00	1.71	0.00	0.00	0.30
	1.00	1.00	1.92	0.00	0.00	0.40
	1.00	I.00	2.02	0.00	0.00	0.50
	1.00	1.06	2.12	0.00	0.02	0.61
	1.00	1.19	2.19	0.00	0.06	0.70
	1.00	1.31	2.27	0.00	0.10	0.80
	1.00	1.44	2.33	0.00	0.14	0.87
	1.00	1.56	2.38	0.00	0.18	0.95
	1.04	1.63	2.41	0.06	0.20	0.99
	1.09	1.69	2.45	0.13	0.22	1.04
4.85	1.12	1.75	2.47	0.17	0.24	1.07

and 0.056 per cent nickel are plotted in Fig. 3. In using the multiplying-factor curves in the manner described on page 4, it must be remembered that the intersections drawn from a multiplying-factor

curve of Fig. 3 must be made with the chromium-increment-factor curve of the same chromium increment for which the multiplying factor curve is applicable.

For a specific set of conditions covering percentage of return scrap, recoveries of alloy on remelting of scrap and recoveries of new added alloy, it is first necessary to calculate the cost of an increment of 0.02 per cent molybdenum in the manner that has been shown on page 650. Increments of chromium and nickel of equal cost are then determined, and the curves for increment factor and multiplying factor of Fig. 3 that are most applicable are used. As previously inferred, the curve for 0.056 per cent nickel increments will be found satisfactory for most cases covering commercial practice. Interpolations of sufficient accuracy can be made between the curves for the various increments of chromium.

REFERENCES

- M. A. Grossmann: Hardenability Calculated from Chemical Composition. Trans. A.I.M.E. (1942) 150, 227.
- Asimow, Craig and Grossmann: Correlation between Jominy Test and Quenched Round Bars. Jnl. Soc. Automotive Engrs. (1941) 283.
- 3. C. R. Austin, W. G. VanNote and T. A. Prater: Third Element Effects on Hardenability of a Pure Hypereutectoid Iron-Carbon Alloy. *Trans.* Amer. Soc. Metals (1943) 31, 517.
- W. Crafts and J. L. Lamont: The Effect of Silicon on Hardenability. Trans. A.I.M.E. (1943) 154, 386.
- I. R. Kramer, R. H. Hafner and S. L. Toleman: Effect of Sixteen Alloying Elements on Hardenability of Steel. Trans. A.I.M.E. (1944) 158, 138.
- 6. W. Crafts and J. L. Lamont: Effect of Some Elements on Hardenability. Trans.
- A.I.M.E. (1944) 158, 157. 7. Edson: Discussion of reference 1.
- G. T. Williams: Hardenability Variations in Alloy Steels. Trans. Amer. Soc. Metals (1940) 28, 157.
- J. Welchner, E. S. Rowland and J. E. Ubben: Effect of Time, Temperature and Prior Structure on the Hardenability of Several Alloy Steels. Trans. Amer. Soc. Metals (1944) 32, 521.
- R. M. Parke and A. J. Herzig: Hardenability of Molybdenum S.A.E. Steels. Metals and Alloys (1940) 11, 6.

11. F. E. Bowman and R. M. Parke: Partition of Molybdenum in Iron-Carbon-Molybdenum Alloys at 1300°F. and Nature of Carbides Formed. Trans. Amer. Soc. Metals (1944) 33, 481.

DISCUSSION

(I. R. Kramer presiding)

W. CRAFTS.*-Mr. Hostetter has offered a very attractive method for determining the most economical combination of alloys on the basis of the Grossmann principle. It does, however, appear to be prone to some difficulties in application because errors in the multiplying factors are magnified in the derived increment factors. For example, according to the selection made by Mr. Hostetter, it becomes economical to use molybdenum in a chromium steel when the chromium is greater than 0.5 per cent, whereas with our published factors molybdenum does not become economical until the chromium exceeds 1.5 per cent. In this case differences of the order of 10 to 25 per cent in the multiplying factors result in a threefold difference in the economical maximum for chromium in plain chromium steel. Calculations of relative cost of alloys in common heat-treating steels by this method apparently will require much more accurate factors than are now available.

The basis for selection of the chromium factor seems questionable. In our work on normalized plain chromium steels and plain molybdenum steels we have not found significantly less hardenability than that calculated using multiplying factors that do not allow for fading. However, in nominally simple chromium steels and molybdenum steels that contain significant residuals of molybdenum or chromium, respectively, we have found fading, and consider that these steels represent borderline examples of the less than calculated hardenability typical of chromium-molybdenum steels. Hollomon and Jaffe have laid the blame on molybdenum; in this paper chromium is the culprit, and Steven demonstrated that the combination of chromium and molybdenum is responsible. We should like to add our observation that carbon, silicon, nickel and possibly manganese also have some influence on less than cal-

^{*} Research Metallurgist, Union Carbide and Carbon Research Laboratories, Inc., Niagara Falls, N. Y.

culated hardenability. Steels that do not contain chromium are also sensitive to prior condition. It is evident therefore that the deficiencies in the hardening of alloy steels that have been charged to the chromium factor could, with equal unfairness, be applied to the molybdenum factor. The fictitious loading of one multiplying factor with a correction for all the unknowns is doubtless helpful in making the calculated ideal diameter approach the actual value, but seems illogical. It is even more unreasonable to use such a loaded factor to determine the relative cost of alloys.

In spite of the apparent difficulties of determining the cost of alloys in terms of hardenability, there is a real need for such a formula. At the risk of increasing the confusion, it is proposed that the addition method for predicting Jominy hardness be considered for evaluating the relative cost of alloys. It has been found that the effects of alloys on Rockwell C hardness are additive and independent of the balance of the composition. As the alloy addition units are linear with respect to the amount of alloy, the relative effects on hardness are the same in all combinations and amounts of alloys commonly used. In the addition method the alloys show the following relative costs of the Rockwell C addition unit when figured on the same recoveries as those used by Mr. Hostetter:

Alloying Element	Percentage per R. Unit	Cost per Ton per Re Unit
Chromium	0.067 0.027 0.182	\$0.22 0.47 1.15

It must be emphasized that these figures are based on costs and recoveries that may vary, but within reasonable expectation the relative position of the alloys will not be changed. In the range of martensitic hardness the cost of all will be somewhat lower than indicated but the same relative ratios will be maintained. This method of calculation appears to be free from the difficulties connected with chromium-molybdenum steels in using the multiplying method and the simple addition does not multiply errors. It is considered therefore to be a more reliable method of evaluating the relative cost of alloys for heattreating steels.

H. E. HOSTETTER (author's reply).—It is interesting to have Mr. Crafts' method of comparing alloy costs on the basis of the addition system of Crafts and Lamont.

The purpose of the present paper was primarily to offer a method of calculation rather than to propose precise factors or arrive at final conclusions.

It is evident that the selection of hardenability factors for the various alloying elements on the basis of either the multiplication or the addition method must involve considerations of prior structure and of the criterion of hardenability most applicable to the case in hand.

The selected hardenability factors for chromium were taken from the lower of Grossmann's curves, recognizing that in many cases the hardenability effect of chromium is greater.

It should be pointed out that the assumed recovery of chromium added to the bath probably is unusually high except for highcarbon steels.

It might also be mentioned that Mr. Crafts' calculations are based on the assumption that all of the alloying element in the steel is obtained from an addition. When scrap is considered in basic open-hearth practice, alloy costs for elements like nickel and molybdenum, which have high recoveries on remelting of scrap, are reduced to a greater extent than for elements like chromium, which have lower recoveries.

In low-carbon steels such as the carburizing grades, it is also to be considered that the recoveries of oxidizable elements such as manganese and chromium are relatively low, and that special low-carbon grades of higher cost might have to be used.

It is agreed that calculations of relative cost of alloys in common constructional steels will require more accurate hardenability factors than are now available. These factors will have to be considered with specific reference to the prior structure of the steel, and perhaps certain variables in steelmaking practice.

It is also recognized that the cost of alloy additions is only one of many factors that affect the final cost of finished alloy-steel products.

An Appraisal of the Factor Method for Calculating the Hardenability of Steel from Composition*

BY G. R. BROPHYT AND A. J. MILLERT

(New York Meeting, October 1945)

THE Grossmann principle1 for the calculation of hardenability of steel from composition is attractive because of its simplicity. It postulates that the hardenability of a steel for any particular grain size may be expressed in terms of an ideal critical diameter, which is the product of an ideal critical diameter for a "pure" iron-carbon base multiplied by a succession of factors for each element of composition contained, including the incidentals. It infers that the multiplying factor for a given quantity of an element is constant for all combinations of composition. Grossmann has stated that in the great majority of cases the experimental values of hardenability are found to be well within 10 per cent of the calculated values.

The validity of the scheme has been confirmed in principle by Crafts and Lamont^{2,3} and by Kramer et al.⁴ Their results differ from the original in the magnitude of the effect of some elements but, since they accepted the product concept and followed its direction, it is to be expected that similar results would be obtained. Crafts and Lamont, in their second paper, recognized that the factor relations for manganese and nickel were not continuously linear, but beyond certain critical amounts increase sharply.

Austin, Van Note and Prater⁵ demonstrated nonlinear relations between hardenability and alloy contents. Their curves for chromium, silicon, manganese and nickel were all convex upward to show decreasing incremental effects. They concluded that Grossmann's factors underevaluate the hardening effect of low percentage additions of these elements, and overevaluate the larger additions.

Table 1.—Calculated Ideal Critical Diameter of N.E. 8739 Steel

Element	Per Cent	Multi- plying Factor	Calcu- lated D _I , In.	Ob- served D _I , In.
Carbon, grain size 7 Manganese. Silicon. Nickel. Chromium. Molybdenum. Phosphorus Sulphur. Boron.	0.40 0.83 0.30 0.48 0.48 0.25 0.015 0.016	3.75 1.25 1.18 2.13 1.78 1.04 0.99 1.12	0.213 0.8 1.0 1.18 2.52 4.47 4.65 4.60 6.53	3.23

More recently W. Steven⁶ has found that the factor method fails when applied to complex steels containing two or three principal alloying elements other than carbon. Multiplying factors derived from his results bear a complex relation to composition and are not constant for a given amount of an element as the base composition varies.

C. A. Liedholm⁷ found that, using either the Grossmann or the Crafts-Lamont multiplying factor values, not only were the relative hardenabilities of two heats of S.A.E. 6130 chromium-vanadium steel

^{*} Manuscript received at the office of the Institute Jan. 24, 1945; revised July 6, 1945. Issued as T.P. 1933 in Metals Technology, October 1945.

[†] Metallurgist, The International Nickel Co. Inc. Research Laboratory, Bayonne, N. J.

References are at the end of the paper.

incorrectly predicted but that each was underestimated.

Finally, in the authors' experience, the application of the principle badly over-

The situation suggests either that the concept of predicting hardenability from steel composition is incorrect in its entirety, or that the quantity multiplying

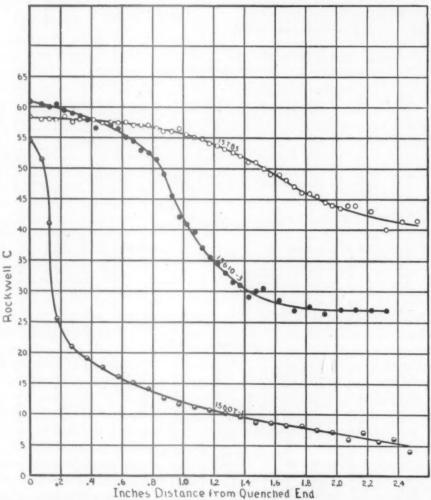


Fig. 1.—Typical Jominy hardenability curves of shallow, intermediate and deep-hardening steels.

estimated the hardenability of an N.E. 8739 steel of No. 7 as-quenched grain size. The measured Jominy distance for this steel was 0.58 in., which converts, according to the basic relations, to an ideal critical diameter of 3.23 in. The calculated ideal critical diameter, on the other hand, was 6.8 in. when the original published factors were used. The calculation is given in Table 1.

factors for the several elements as determined to date are not constant with changes in base composition and are not simply related to the element content as originally proposed. These facts led to a critical examination of the application of the principle to steels containing nickel, manganese, chromium and molybdenum, both singly and in dual combinations of nickel with the other three elements. The

result of this study leads to the conclusion that a further elaboration of the principle will be necessary before it can be safely added the required alloys and finally 0.05 per cent aluminum, for deoxidation. The melts were cast into 4-in. square ingots and

TABLE 2.—Compositions of Steels Tested

Heat	Austenitiz- ing Tem- perature	A.Q.						Ana	lyses,	Per Ce	ent				
No.	Deg. F.	Grain Size	С	Mn	Si	Ni	Cr	Мо	P	S	Cu	Va	В	Co	Al
					N	ICKEL-	CARBO	N SER	IBS						
01682	1550	8	0.15	0.51	0.20	4.06			0 014	0.010			None		
15607-1	1575	8 8 7 5 7 7 8 8				0.05	0.016	0.003				0.003		0.006	0.024
-2	1550	7				0.98	0.009	0.002	0.011	0.013	0.071	0.003	None	0.013	0.01
3	1525	5	0.36	0.69	0.12	2.90						0.003		0.037	
15608-1	1575	7	0.30	0.73	0.10	0.49						0.004		0.007	
-2 -3	1525	7				1.99						0.005		0.017	
15609-1	1475	8	0.35	0.59	0.00	5.06						0.003		0.044	
-2	1525	7	0.50	0.71	0.15	0.04						0.007		0.006	
-3	1475	1 '2	0.51	0.62	0.13	3.08	0.010	0.003	0.010	0.017	0.003	0.007	None	0.029	
15610-1	1550	6.5				0.52	0.000	0.002	0.007	0.017	0.065	0.007	None	0.010	
-2	1500	7.0	0.40	0.66	0.12	2.03	0.000	0.002	0.014	0.017	0.065	0.007	None	0.019	
-3	1450	7.0 6.5	0.47	0.56	0.07	5.04						0.006		0.042	
			'		Nic	KEL-M	ANGAN	ESE SE	RIES	1		1			
		1.	1	1	1 .	1	1	1	1		1			1	
16163	1575	6.5			0.16				0.008	0.021	1				
15809	1550	7.5				0.027	0.01								
15834 15780	1525	7.5	0.40	1.41	0.14		-								0.01
15781	1525 1525	7.0			0.19	0.95			0.008						0,010
15782	1500	7.5	0.45	T 50	0.17	0.98			0.000	0.016				1	
15783	1500	7.5	0.48	0 32	0.20	2.86	1		0.006						
15784	1475	7.5 8.6	0.47	1.04	0.16	2.81	1		0.000	0.02					
15785	1450	8.3	0.48	1.45	0.15	2.90				1	-				0.01
		1		1	Nic	KEL-C	HROMI	UM SE	RIES				1	1	
15835	1575	7.3	0 45	10 70	0.14		0.50		1	1	1			1	
16165	1550	7.3				0.50	0.97			1					
15836	1575	7.5	0.48	0.67	0.15		10.1	1	-						1
15786	1550	7.0	0.48	30.76	0.18	0.97	0.52						1		1
16164	1525	8	0.48	0.51	0.12	2.76	0.23								
15787	1550	7.8				0.97	1.04								
15837	1550	8.2	0.48	0.67	0.14	1.46	1.00		1			1			
15789	1525	6.8	0.40	0.72	0.14	2.89	0.52								
				1	Nick	EL-MO	LYBDE	NUM S	ERIES	•	1	,		•	-
15838	1550		10 .0	10	0.12		1	0.071				1		1	
15839	1575	7.3			0.14			0.071					-		
15840	1575	7.0			0.11			0.40							
16166	1550	7.0 8.0				0.45	0.008								
15792	1525	8.0				0.97	10.000	0.08							
15793	1550	0				0.95		0.37	1						
15794	1550	9.8	0.43	0.74	Q. 14	0.96		0.38							
15841	1550		0.47	0.54	0.07	1.68		0.41							
15795	1500	7.5				2.88		0.08							
		8.3				2.89		0.23		1					1
15796	1525	8.3	0.48	0.70	0.12	2.89	1	0.23		1				1	

applied to steels of ordinary commercial complexity.

MATERIALS AND PROCEDURE

The steels studied were the products of laboratory high-frequency furnaces, made from an Armco iron base to which were then forged to 1¼-in. bars. These were double normalized, first from 1800°F. and then from 1600°F. Compositions and heattreated grain sizes are given in Table 2.

Standard and quenched hardenability bars were hardened in a General Motors quenching rig after having been heated one hour at the temperatures shown in Table 2. The hardness distribution was determined over their lengths at two flats 180° apart and the readings were averaged. Typical hardenability curves are shown in Fig. 1.

Based upon the observation⁸ that the rate of change of hardness is greatest at the 50 per cent martensite point, and the recommendation by Grossmann that this point may be judged readily from the point

per cent unless one of these elements was the variant being studied. The adjustment for each element in turn was accomplished by multiplying the observed critical diameter by the ratio:

Factor for base quantity of Element Factor for contained quantity of Element

The factors used were Grossmann's, which serve as a first approximation for correction within a limited range.

TABLE 3 .- Distance Determined by Three Methods

Element	in Steel	J	ominy Distanc	ees	Ideal	Critical Diamete	ers, In.
Per C		Metallo- graphic Average	50 Per Cent Martensite Hardness	Point of Inflection,	Metallo- graphic	50 Per Cent Martensite	Inflection
С	Ni	of Three Estimates	for Carbon Steel, In.	In.	grapme	Martensite	
0.38	0.05	0.138	0.13 0.155	0.13	I.42 I.5	I.4 I.52	1.4
0.36 0.35 0.36 0.35	0.98 1.99 2.90 5.06	0.16 0.188 0.40 0.69	0.16 0.195 0.43 0.72	0.16 0.18 0.38 0.70	1.53 1.65 2.53 3.55	1.53 1.68 2.65 3.66	1.53 1.62 2.48 3.60

of inflection in the hardness-distribution curve, the Jominy distance was taken as the distance from the quenched end to the point of inflection. This procedure is more convenient than the metallographic determination and should be more accurate for alloy steels than the practice of taking the distance to the hardness corresponding to 50 per cent martensite in carbon steel. A comparison of the distance determined by the three methods on the 0.35 to 0.38 per cent carbon nickel steel series is shown in Table 3, along with the converted ideal critical diameters.

Conversion to ideal critical diameters was accomplished by the use of the Grossmann relation. Because variations occurred in the base composition sufficient to cause a considerable scatter within each series, the ideal critical diameters thus determined were corrected to a common grain size of No. 7 and a base composition of carbon 0.48 per cent, manganese 0.70, silicon 0.16, aluminum 0.016 and nickel of 0, 1, or 3

As an example, steel 15608-3 of Table 2 has a No. 8 grain size and contains 0.35 per cent carbon, 0.59 manganese, 0.09 silicon, 5.06 nickel, 0.011 chromium, and has an observed critical diameter of 3.6 in. From Grossmann's chart No. 18, the grain size is adjusted from No. 8 to No. 7 by multiplying

$$3.6 \times \frac{0.2}{0.183} = 3.94$$

For carbon multiply by 1, since 0.35 per cent carbon was desired. For adjusting manganese from 0.59 to 0.70 per cent, multiply

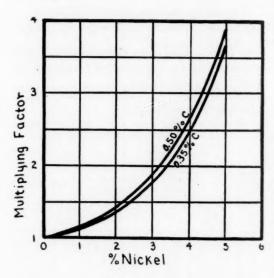
$$3.94 \times \frac{3.3^2}{2.97} = 4.4$$

For silicon from 0.09 to 0.16 per cent, multiply

$$4.44 \times \frac{1.13}{1.07} = 4.65$$
, etc.

In this case, no adjustment is made for nickel, since it is the variant element.

Corrections were made for the incidental elements contained in the nickel-carbon series of Table 2 but were of such small magnitude that they were omitted in the other series.



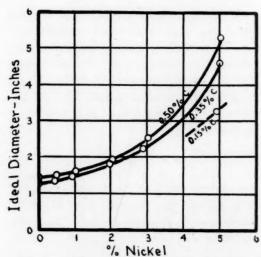


FIG. 2.—INFLUENCE OF NICKEL AND CARBON ON HARDENABILITY OF 0.70 PER CENT MANGANESE STEEL.

The corrected ideal critical diameters thus derived were then plotted against the content of the variant element, and, finally, the multiplying factors calculated by dividing the critical diameters by the intercept on the critical diameter axis at zero per cent of the element.

Grain sizes usually were determined on small specimens, which accompanied the hardenability bars. A few of these were checked against the grain sizes exhibited in the transition zone at the hardenability bars.

RESULTS

Nickel and Carbon Effects

The hardenability data for the nickelcarbon series of steels of 0.70 per cent manganese and 0.16 per cent silicon are arranged in Table 4 in groups according to carbon content and in each group according to increasing nickel. They are shown graphically in Fig. 2. A separate hardenability curve is constructed for each group, since it is quite evident that carbon has an appreciable influence but one that decreases as the carbon increases—a trend that is in accord with that shown by Grossmann for carbon. The data on calculated multiplying factor can be represented accurately only by two separate curves, although for practical purposes a single curve for these and higher carbon contents might be used.

Manganese Effect-Variable Nickel

The hardenability data for the manganese-nickel series are shown in Table 4 and graphically in Fig. 3A. As nickel is increased, the specific manganese effect is progressively increased and well beyond the extent indicated by the multiplication of the factors for the manganese and the nickel addition. The curves for manganese contribution are also smoothly concave upward, indicating that manganese is self-reinforcing, as was nickel, and that this self-reinforcement is greatly augmented by the presence of nickel.

The multiplying factors for manganese can be represented only by a family of curves that are concave upward, one for each level of nickel content.

Chromium Effect-Variable Nickel

Families of rising curves represent the data for the contribution of chromium to the hardenability of steel, Table 4 and Fig. 3B. The absence of any decrease in

appeared on the hardenability curve at this distance, the hardness exceeds the probable maximum hardness for a 50 per cent martensite of a 0.46 per cent carbon steel. As a matter of fact, the hardness over

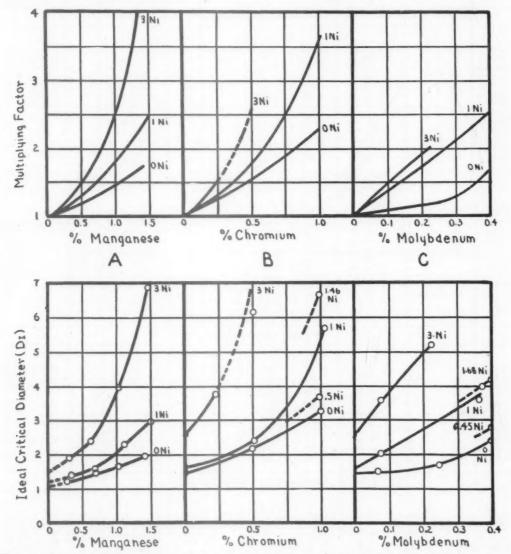


Fig. 3.—Influence of second element additions on hardenability of nickel steel

hardenability at the higher chromium levels may be the result of double normalizing previous to hardening.

Steel 15789 of this series requires special comment. In Table 4 the Jominy distance is given as 1.73 in. and the hardness at this point is Rc 52. While a point of inflection

the full length of the bar exceeded Rc 50, so it is believed that the true half-hardness point was not attained. Therefore the indicated hardenability and factor for this steel containing 2.9 per cent nickel and 0.5 per cent chromium is probably much too low.

TABLE 4.—Hardenability Data

Steel No.	Maxi- mum Hard- ness Rc. Quench- ed End	Hard- ness of Inflec- tion Point, Rc	Jominy Dis- tance, In.	Derived DI, In.	Corrected DI, In.	Inter- cept	Multi- plying Factor	Vari- ant	Corrected to
				Nici	EL-CARBO	N SERI	ES		
01682 15607-1 15608-1 15607-2 15608-2 15608-3 15609-1 15610-1 15609-2 15610-2 15609-3 15610-3	44 52.5 52 51 54 55 54 59 60 60 60.5 60.5	30 37 41 37 43 42 39 41 41 42 45 45	0.40 0.13 0.14 0.16 0.18 0.38 0.70 0.12 0.16 0.16 0.21 0.34	2.54 1.39 1.43 1.53 1.62 2.48 3.60 1.35 1.52 1.52 1.75 2.30 4.21	3.29 1.27 1.35 1.48 1.81 2.22 4.60 1.44 1.57 1.90 2.58 5.36	1.27	1.0+ 1.06 1.16+ 1.42 1.75 3.66 1.06 1.06 1.15 1.40 1.95 3.94	Ni 4.96 0.05 0.49 0.98 1.99 2.9 5.06 0.04 0.52 1.02 2.03 3.08 5.04	0.15 C, 0.70 Mn, 0.16 Si 0.35 C, 0.70 Mn, 0.16 Si 0.50 C 0.50 C 0.50 C
	ı		!	Nicke	L-MANGAN	VESE SE	RIES		
16163 15609-1 15809 15834 15780 15609-2 15781 15782 15783 15609-3 15784 15785	62 59 57 60 58.5 60 60 61.5 60 60.5 59 58.5	42 41 46 45 42 46 45 45 45 45 47	0.11 0.12 0.16 0.23 0.13 0.16 0.29 0.42 0.22 0.34 0.61	1.25 1.35 1.53 1.84 1.40 1.53 2.10 2.60 1.80 2.30 3.30 5.92	1.21 1.43 1.63 1.91 1.39 1.53 2.28 2.90 1.88 2.36 3.96 6.82	1.11	1.09 1.29 1.47 1.72 1.18 1.30 1.93 2.46 1.29 1.61 2.72 4.67	Mn 0.27 0.70 1.03 1.41 0.33 0.68 1.12 1.5 0.32 0.63 1.04 1.45	0 Ni 0 Ni, 0.16 Si 0 Ni, 0.16 Si 0 Ni, 0.16 Si 1 Ni, 0.16 Si 1 Ni, 0.16 Si 1 Ni, 0.16 Si 1 Ni, 0.16 Si 3 Ni, 0.16 Si 3 Ni, 0.16 Si 3 Ni, 0.16 Si 3 Ni, 0.16 Si
				Nicke	L-CHROMI	UM SER	IES		
15609-1 15835 15836 16165 15609-2 15786 15787 15837 15609-3 16164 15789	59 58 57 63 60 60 61 60.0 60.5 62	41 45 44 43 42 45 46 46 45 43 52°	0.12 0.28 0.53 0.57 0.16 0.40 1.30 1.58 0.34 0.60 1.73°	1.35 2.07 3.00 3.18 1.53 2.53 5.23 5.77 2.30 3.27 6.024	1.42 2.13 3.24 3.66 1.56 2.38 5.67 6.67 2.54 3.72 6.16°	1.41	1.01 1.51 2.30 1.01 1.54 3.66 1.00 1.47 2.44 ^a	Cr 0 0.5 1.01 1.00 0.01 0.52 1.04 1.0 0.007 0.23 0.52	0 Ni, 0.70 Mn, 0.16 S 0 Ni, 0.70 Mn, 0.16 S 0 Ni, 0.70 Mn, 0.16 S 0.50 Ni 1.0 Ni, 0.70 Mn, 0.16 S 1.0 Ni, 0.70 Mn, 0.16 S 1.0 Ni, 0.70 Mn, 0.16 S 1.46 Ni, 0.70 Mn, 0.16 S 3.0 Ni, 0.70 Mn, 0.16 S 3.00 Ni, 0.70 Mn, 0.16 S
		1		NICKEL	-MOLYBDI	ENUM SI	BRIES		
15609-1 15838 15839 15840 16166 15609-2 15792 15793 15794 15841 15609-3 15795	59 56 57 57.5 61 60 60 60 60 58.5 60.5 61	41 45 45 45 43 42 45 45 45 45 42 45 46	0.12 0.14 0.20 0.30 0.30 0.16 0.23 0.57 0.57 0.55 0.34 0.54	1.35 1.43 1.72 2.13 2.13 1.53 1.84 3.15 3.15 3.10 2.30 3.05 4.50	1.42 1.49 1.66 2.39 2.75 1.56 1.99 3.58 3.96 4.15 2.54 3.54 5.22	1.42	1.00 1.05 1.17 1.68 1.01 1.28 2.31 2.56 1.01 1.41 2.04	Mo 0 0.07 0.25 0.40 0.40 0 0.08 0.37 0.38 0.41 0.02 0.08 0.23	0 Ni, 0.70 Mn, 0.16 S 0 Ni, 0.70 Mn, 0.16 S 0 Ni, 0.70 Mn, 0.16 S 0 Ni, 0.70 Mn, 0.16 S 0.45 Ni 1 Ni, 0.70 Mn, 0.16 S 1 Ni, 0.70 Mn, 0.16 S 3.0 Ni, 0.70 Mn, 0.16 S

[•] Hardness exceeds 50 Rc over length of Jominy bar. Therefore DI and MP probably are much higher.

Molybdenum Effect-Variable Nickel

The curve representing the contribution of molybdenum, Fig. 3C, is, in the absence of nickel, concave upward as for the other

Nickel Effect—Manganese, Chromium or Molybdenum Variable

By cross-plotting the graphs of Fig. 3 (or by making suitable composition correc-

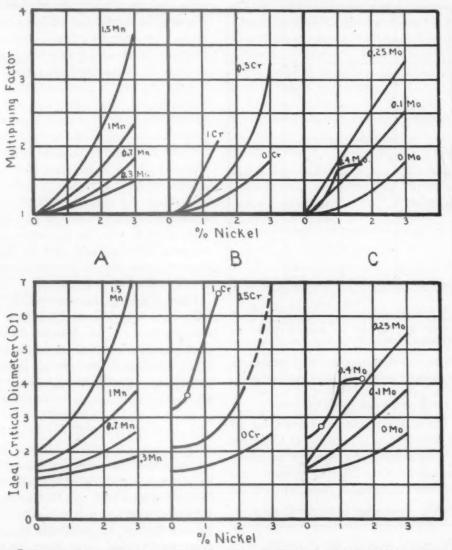


Fig. 4.—Influence of nickel as a second element addition on the hardenability of steel.

elements studied. As nickel increases beyond I per cent, the curves change to convex, passing through a linear relation. This suggests that molybdenum carbide, perhaps, becomes more insoluble with increasing nickel content and that these steels require higher hardening temperatures to obtain the full molybdenum effect.

tion to the data of Table 4) the nickel curves shown in Fig. 4 are obtained. These demonstrate that the nickel contribution to hardenability is quite as variable and dependent upon the base composition as is the contribution of the other elements. Certainly no single line, linear or curved, can truly represent its contribution under all circumstances. From the point of view

of hardenability alone, the self-reinforcing effect seems amply to justify the larger nickel addition, but its real value even in the smaller amounts lies in its combination

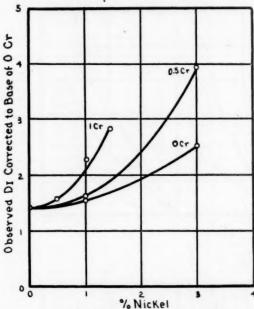


FIG. 5.—CALCULATED HARDENABILITY CONTRIBUTION OF NICKEL IN NICKEL CHROMIUM STEELS AFTER CORRECTION FOR ALL CHROMIUM. with a second element, such as chromium or molybdenum, as experience has taught.

DISCUSSION OF RESULTS

If the factor concept is correct for all steels, it should be possible to multiply the base hardenability of a steel by the quantity factor for each alloying element contained, even in complex steels, and obtain

TABLE 5.—Failure of Factor Concept

	ent in	Bases	Cr or Mo	Ni Fac-		DI
	eel, Cent	DI	Fac- torb	tor	Calcu- lated	Ob- served
Ni	Cr					
3	0.5	1.41	1.51	1.82	3.88	6.16 min.
3 1 3	I	1.41	2.36	1.14	3.79	5.63
3	Mo	1.41	2.36	1.82	6.05	7.0 min.
3	0.2	1.41	1.16	1.92	3.14	5.22
I	0.4	1.41	1.62	1.14	2.60	3.96

^a Base = o Ni, o Cr, o.70 Mn, o.48 C, o.16 Si; No. 7 grain size. ^b Revised factors,

the hardenability D_I of that steel. The failure of the application is illustrated by data taken from Table 4 and shown in Table 5.

In each case where the actions of two elements in substantial amounts are combined, the observed critical diameters are greater than those calculated by the multiplication of the determined single element quantity factors. A similar situation can be shown for the other series and probably is further exaggerated when three or more principal alloying elements are combined.

Again, it should be possible to divide the observed D_I of a complex steel by the product of all multiplying factors but one and obtain the multiplying factor for the remaining element as a single addition. This actually was the procedure used in previous investigations and is found to lead to erroneously high values, as illustrated in the following example:

From Table 5, the observed D_I of the base o per cent chromium, o nickel, 0.70 manganese is 1.41 in. A factor for 0.5 per cent chromium had been determined as 1.51. Therefore if Grossmann's principle is correct the 3 per cent nickel factor should be

$$\frac{6.1}{1.41 \times 1.51}$$
 or 2.9

Instead, the single element quantity factor for 3 per cent nickel was determined from the simple steel as 1.82 (Fig.2).

By the application of determined single element factors, as previously illustrated, small corrections have been made for variation in composition. If the concept is correct, this should be a valid procedure, and likewise it should be valid for correcting large variations, even to correcting completely for the presence of a substantial amount of one element in a complex steel. It should be possible, therefore, to correct any one of the D_I curve families of Figs. 3 and 4 for the second element and obtain a single curve representing the influence

of the first element. Obviously, this is incorrect, but to follow through take, for instance, the nickel-chromium family and correct for all chromium present by using the revised chromium single element factor. The data are shown in Table 6 and in Fig. 5.

TABLE 6.—Correction for Chromium

in S	nents teel, Cent	Ob- served Di ⁶	Single Element Cr Factor	Dr Corrected to Bases Ni + O	Observed DI, Base + Ni Only
Ni	Cr	1.41	I	1.41	1.41
0	0.5	2.13	1.51	1.41	1.41
0	1.01	3.34	2.37	1.41	1.41
0.5 I	0.97	3.66	1.01	1.59 1.54	1.48
Î	0.52	2.38	1.54	1.54	1.56
I	1.04	5.67	2.43	2.33	1.56
3	0	2.54	1.0	3.54	2.54
3	0.52	6.16	1.54	3.990	2.54
1.46	1	6.67	2.35	2.84	1.75

[·] Corrected to base 0.70 Mn, 0.16 Si. Data from Table 4.

b From Fig. 3.
 Values low. Hardness exceeds 50 Rc over full ength of Jominy bar.

Instead of a single curve to represent the effect of nickel on the base composition, as demanded by the simple factor concept, three curves result. These demonstrate and emphasize the dependence of the nickel contribution to hardenability when a second principal element is present in substantial amounts. Corrections for all of the manganese or all of the molybdenum produce similar families of curves but in each case a particular quantity factor for nickel is different. Likewise, it can be demonstrated that the quantity factors for manganese, chromium or molybdenum vary with the amount of nickel present in the steel.

Thus, the idealized concept of constant quantity multiplying factors is found to be misleading and incorrect for all but the simplest steels.

SUMMARY

A test of the factor principle of calculating hardenability of steels from their compositions encounters difficulty when applied to steels that contain substantial amounts of a single element or to complex alloy steels. In such steels, it either overestimates or underestimates hardenability. The relation of the hardenability contribution to composition for manganese, chromium, molybdenum or nickel is a sharply rising curve showing that the power of each increases with the content.

The hardenability contribution of nickel in the presence of chromium, manganese, or molybdenum, after making due allowance for their presence, is much greater than for nickel as a single element. Likewise, the contributions of manganese, chromium or molybdenum are similarly increased in the presence of nickel.

REFERENCES

I. M. A. Grossmann: Trans. A.I.M.E. (1942) 150, 227.

W. Crafts and J. L. Lamont: Trans. A.I .-M.E. (1943) 154, 386. 3. W. Crafts and J. L. Lamont: Trans. A.I.-

M.E. (1944) 158, 157. 4. I. R. Kramer, R. H. Hafner and S. L. Toleman: Trans. A.I.M.E. (1944) 158, 138.

 Austin, Van Note and Prater: Trans. Amer. Soc. for Metals (1943) 31.
 W. Steven: Effects on Hardenability of Small Additions of Chromium and Molybdenum to a Grain Size Controlled 0.9 Per Cent Nickel Steel. Iron and Steel Inst., Advance Copy, Dec. 1943.
A. Liedholm: Metal Progress (Jan. 1944).

8. Queneau and Mayo: Hardenability and Its Designation. Amer. Soc. for Metals Symposium (1938).

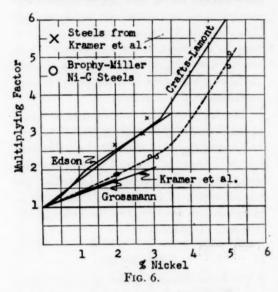
DISCUSSION

(C. M. Loeb, Jr., presiding)

W. CRAFTS. *-In this paper Messrs. Brophy and Miller have concluded that the Grossmann principle for calculating ideal critical diameter is inapplicable to nickel steels containing chromium, molybdenum, or high manganese. This conclusion appears to have been inferred as a result of two errors in interpretation of the Jominy test data. One was the use of the Grossmann relation between ideal critical

^{*} Research Metallurgist, Union Carbide and Carbon Research Laboratories, Inc., Niagara Falis, N Y.

diameter and Jominy depth for distances of less than $\frac{1}{4}$ in. from the quenched end (see Brophy's discussion of Kramer, Hafner, and Toleman. The other error was in the use of the



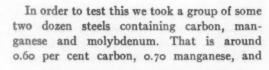
inflection point of the Jominy hardness curve instead of an actual observation of the 50 per cent martensite point.

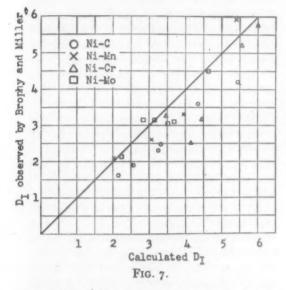
It is true that Grossmann suggested that the point of inflection or an arbitrary hardness be used to estimate the location of 50 per cent martensite structures, but in our work at the Union Carbide and Carbon Research Laboratories these criteria have been found misleading in alloy steels. Except for comparison between steels of similar composition, such as those studied by Steven, it appears to be essential to determine 50 per cent martensite by direct microscopic observation, as emphasized in our 1944 paper.9 The order of the difference in the apparent nickel factor that may result from use of hardness as opposed to the metallographic method as a criterion of the 50 per cent martensite point is illustrated in Fig. 6. In an effort to reconcile the differences between the nickel factors derived by Kramer, Hafner, and Toleman¹⁰ from critical hardness, and by Crafts and Lamont from metallographic examination, Jominy specimens of nickel steels were exchanged. Each laboratory confirmed its own nickel factor on the other laboratory's steels; that is, the discrepancies were not in the steels but in the interpretation of the test data. Our interpretation of the Kramer steels is indicated by the crosses in Fig. 6. The evidence indicates that both nickel factors are correct, but each is correct only for the criterion by which it was established.

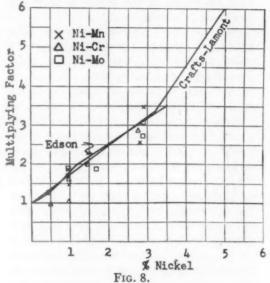
In order to visualize the data in a more conventional form, the ideal critical diameters of Brophy and Miller's nickel-bearing steels were calculated using Grossmann's factors for carbon grain size, phosphorus and sulphur; Kramer, Hafner, and Toleman's for copper and cobalt, and Crafts' and Lamont's for manganese, silicon, nickel, chromium, molybdenum, vanadium and aluminum. Steels with a critical Jominy depth of less than 1/4 in., and the very deep-hardening heat 15789, were discarded. The ideal critical diameters calculated on the basis of 50 per cent martensite and those determined from the inflection point by Brophy and Miller are compared in Fig. 7. The nickel-carbon steels, the I per cent manganese-nickel steels, and two of the chromium-nickel steels form a trend that is offset from the line of 100 per cent correlation, while the balance of the manganesenickel, chromium-nickel, and molybdenumnickel steels show fairly good agreement. The calculated ideal critical diameter without nickel was then divided into the reported ideal critical diameter to obtain the nickel factor. The nickel-carbon steels shown in Fig. 6 gave a factor comparable with the lower group of multiplying factors for nickel. The alloy steels, shown in Fig. 8, with the exception of the steels noted above, agree on the other hand with the upper group of nickel-multiplying factors. It is evident that the inflection-point criterion of critical diameter differs appreciably from the 50 per cent martensite criterion in simple nickel steels, but that the two criteria are in agreement in the binary nickel steels. It is inferred from this that the percentage of martensite at the point of inflection of the hardness curve shifts with the alloy content. For this reason, it is believed that the discrepancies found by the authors resulted from misinterpretation of the hardenability of the steels rather than from a major deficiency of the Grossmann principle.

⁹ Trans. A.I.M.E. (1944) 158, 150. ¹⁰ Kramer, Hafner and Toleman: Trans. A.I.M.E. (1944) 158, 138.

The accuracy of the multiplying factors used in Grossmann's method could be improved and the validity of the original formula is certainly open to question in the case of







chromium-molybdenum steels, but this latter problem was not investigated by the authors. Within the recognized limits of accuracy of the multiplying factors, however, it is believed that the data in this paper not only do not discredit, but, indeed, substantiate the validity of the Grossmann principle. In addition, the success during the last three years with which the hardenability of alloy steels of "ordinary commercial complexity" has been predicted and controlled by the Grossmann principle confirms its validity and utility more strongly than any academic discussion of technicalities.

M. A. GROSSMANN.*—I cannot refrain from offering a few words of discussion about Fig. 3 of the paper by Brophy and Miller. In the upper part of that diagram, the multiplying factors for three elements are shown in the presence of certain amounts of nickel, and in the absence of nickel.

If the lower curve, in the absence of nickel, were to turn out to be much higher—for example, as high as in the presence of nickel—their general thesis regarding the increase of the multiplying factor because of the presence of nickel would have to be reexamined.

around 0.20 molybdenum with only incidental amounts of chromium and nickel; namely, below about 0.20, meaning that they should come in the general classification of zero nickel. Using the currently accepted values for carbon, manganese and molybdenum, the predictions checked very well with the determinations of hardenability from a Jominy test, and using the conversions to D_1 . The low value for molybdenum, as shown in Fig. 3, thus departed markedly from the values found in these commercial steels.

E. H. BUCKNALL.*—This paper is on a subject in which I am much interested. It is felt, however, that it would be easy to exaggerate the importance of the calculation of hardenability, as available data make one unprepared to admit that the optimum combination of mechanical properties to be secured from an alloy steel is controlled only by its hardenability. Moreover, the assessment of the merits of an alloy steel solely on the basis of hardenability tends to belittle some alloying elements, since attention is drawn to the fact that they do not increase the

^{*} Director of Research, Carnegie-Illinois Steel Corporation, Chicago, Illinois.

^{*}Research and Development Department, The Mond Nickel Co., Ltd., Birmingham, England.

depth of hardening of a steel as markedly as do other additions, while sight is lost of the usual freedom of steels that owe their hardenability to gently acting elements from sharp local differences in the extent of hardening as a result of microsegregation.

Grossmann's insistence on a linear connection between composition and hardenability for a single element but a multiplying principle for several elements together favors the use of small, simultaneous additions of the different alloying elements as a means of securing hardenability. I wonder to what extent the acceptance in America of this line of argument (which seems to have played an important part in the development of the NE triple-alloy steels) may have been altered by the later work of Kramer, Hafner and Toleman¹⁰ and of Crafts and Lamont, especially the latter, who have shown nonlinear multiplying factor versus composition relations for manganese, nickel, vanadium, titanium and boron, while Kramer and his co-workers have shown the relations to be nonlinear also for antimony and arsenic additions. My view is that, as a result of such work and that included in the present paper, it will be difficult in future to maintain a hardenability argument in favor of triple-alloy steels unless large disagreements between the values ascribed to individual elements by different workers cause the recent work to be dismissed and Grossmann's original results still to be accepted. One point where this danger seems to be serious is in regard to the factors ascribed to manganese, where, for a 1 per cent addition, Grossmann gave a factor of 4.3, Crafts and Lamont of 5.0 and Kramer of 5.2, but Brophy and Miller in the present paper give a factor of only 1.45 in the absence of nickel. Another point arises from the diversity of opinions as to the role of molybdenum at the higher levels.

Recently there has been much interest over here in the subject of hardenability, and the view is commonly held that a given amount of a given element does not make a fixed contribution to hardenability independent of other factors in the composition. There is little in the present paper that could give rise to misinterpretation, but it seems possible that more conviction might have been secured if a different example had been chosen from that given on page 657 to indicate the

divergence between the observed ideal critical diameter and that calculated by Grossmann's method, where most of the recorded divergence could possibly be attributed to failure of the boron addition to have its expected effect at the points where the hardness was measured. Billets of boron-treated steels of the NE types often show pronounced variation of hardenability across the section, which gives rise to etching patterns on transverse sections similar to those caused by segregation. The contrast in such cases can be heightened by partial isothermal transformation in the bainite range and can be demonstrated by dilatometric measurements to correspond with local variations in transformation characteristics. In such steels the boron effect has been found often to be practically confined either to the outside material or to that within the central "segregate," and it is believed, therefore, to be to some extent a matter of chance whether the hardness flats on Jominy test pieces taken without special reference to the "hardenability pattern" include material enhanced in hardenability by the boron addition, although the effect of boron at some parts of the section can readily be shown by tests along the lines employed by Walker, Eckel, Hino and Mueller.11

The inclusion in Brophy and Miller's paper of typical Jominy curves makes it clear that in the steels of lower hardenability the interpretation of the Jominy curves does not depend to any appreciable extent on the precise criterion of hardness employed, so that no significance is attached to the fact that the hardness values that I associate with a 50 per cent martensite structure are rather higher than those referred to in Tables 2 and 3 as corresponding to points of inflection of the Jominy curves; and, in fact, range from Rc 40 at 0.22 per cent carbon to Rc 50 at 0.56 per cent carbon in an average low-alloy steel. Although the point of inflection, therefore, seems quite a suitable index with the steels of lower hardenability, it does not seem fair to put the same interpretation on the point of inflection with the more hardenable steels where the softest part of the bar has a hardness of 25 to 30 Rc.

¹¹ Walker et al.: Metals and Alloys (1944) 19, 346.

The opinion has been formed that a 50 per cent martensite criterion of hardenability is satisfactory for steels used at relatively low tensile levels, but that this criterion is inadequate for steels used at tensile levels in excess of 175,000 lb. per sq. in. In such cases a close approach to full hardening is required in steels with the carbon contents of around 0.3 per cent customary in this country, and any estimate of suitability must be based on a criterion involving a considerably higher hardness level than corresponds to 50 per cent martensite. Even with such a criterion there seems to be no certainty that the Izod impact value will be up to specification requirements, so that the Jominy test can then only be regarded as a preliminary means of sorting steels.

In the course of measurements of transformation characteristics of alloy steels made in this laboratory in 1938-1939, it was found that the relationship between maximum transformation velocity12 and percentage of alloying element, for steels made by the same melting technique, could be stated to a fair approximation by a multiplying rule, so that equal increments in alloy content were regarded as reducing the maximum transformation velocity by a factor that was constant for a given alloying element; for example, between o.1 and 0.6 per cent carbon in a nickel-chromium steel, each addition of o.1 per cent carbon was found to reduce the transformation velocity to X o.4 its former value, the corresponding factors for o.1 per cent additions of other alloying elements being:

ALLOYING ELEMENT OF WHICH
O.1 PER CENT IS ADDED

Carbon (with molybdenum and nickel)... 0.40 × original value

Nickel (with chromium) 0.90

Chromium (with molybdenum)... 0.88

Chromium (with nickel) 0.84

Manganese... 0.76

Molybdenum (with nickel) 0.68

As the maximum transformation velocitycomposition relationship is of this type, a straight line in each case can be drawn through the experimental points for these series, when presented as a plot of log (maximum transformation velocity) versus percentage of alloying element, from which the effect of each alloying addition can be read directly, and by multiplying the individual element factors together the total factor can be obtained. Since the reciprocal of the maximum transformation velocity has been found to be approximately proportional to the section in which a steel can be fully hardened by oil quenching, it would be anticipated that a similar trend would apply to Brophy and Miller's results if these were converted by means of Grossmann's curve to H = 0.4, corresponding to normal oil-quenching conditions. With this in view, the critical diameters for oil quenching derived from the experimental Jominy results in this way for the various series of steels in Brophy and Miller's paper have been plotted on logarithmic paper against the percentage of alloying element. In practically every series the results fell closely on a straight line except that the initial addition of an alloying element had occasionally a smaller effect than expected. The extent of the conformity with expectation from the transformation studies was felt to be sufficient to indicate that curves of the type presented by Brophy and Miller have a much greater probability than the linear relations put forward by Grossmann, though the disagreement over the apparent roles of manganese and molybdenum as hardening additions on the basis of Jominy tests and transformation data is disconcerting.

Consideration has been given to the possibility of developing an alternative method of calculation of hardenability on this basis. The slopes of the straight lines on the log plots should indicate multiplying factors for each 1 per cent of the individual alloying elements. The values for each element obtained in this way varied widely according to the percentage of accompanying elements; e.g., the factor for chromium appeared to be raised from \times 3.4 to \times 13.0 by the presence of 3 per cent nickel and that for molybdenum from \times 6 to \times 20 by 1 per cent nickel. This degree of variation in the factors makes it

¹² See Allen, Pfeil and Griffiths: Second Report Alloy Steels Research Committee, 1939, Iron and Steel Inst. Special Report No. 24, Sec. 13, 369. This term is employed in the sense of the velocity constant of the equivalent first-order reaction, which fits the dilatometric observations of the times for 30 and 70 per cent completion of transformation.

very difficult or impossible to choose appropriate values for complex steels, and much further thought, therefore, seems to be necessary before any alternative method of calculation can be put forward. Attempts to carry the matter further by attributing a fixed effectiveness to a given alloying element whenever it is added to a steel possessing in its absence a given hardenability have been unsuccessful, whether made on the basis of the multiplying factors derived as above for oil hardening or by direct inference from Figs. 1, 2 and 3 of Brophy and Miller's paper.

G. R. Brophy and A. J. Miller (authors' reply).—The differences of opinion brought out in the discussion emphasize the need for more experimental study and less reliance on paper work. We hope that others will be led to test our conclusions in carefully planned and rigorously executed laboratory investigations.

first, the uncertainties of the initial branch of the Grossmann curve for translating Jominy distances to ideal critical diameters is recognized and has been discussed elsewhere. Since our purpose was not to introduce new elements of controversy, it seemed only fair to follow the same practice as preceding investigators, including Mr. Crafts, in adhering to the Grossmann conversion. As a matter of fact, this uncertainty at low hardenabilities does not affect the conclusion, for the same qualitative result comes out if the conversion is omitted and Jominy distances are analyzed directly, provided that none of the data are left out.

As to his second criticism, he takes the position that if Jominy distances had been measured to the point of 50 per cent martensite by direct microscopic observation of the Jominy bar, instead of the inflection point on the hardness curve, a totally different

Table 7.—Hardenability Data

			P	oint of	Inflection	Method	1	50 H	Per Cent	Marten	site Met	hod
Steel	Mn, Per Cent	Ni, Per Cent	Jominy Dis- tance	De- rived D1	Corrected D _I	Inter- cept	Multi- plying Factor	Jominy Dis- tance	De- rived D1	Corrected D1	Inter- cept	Multi- plying Factor
16163 15609-1	0.27	0	0.11	1.25	1.21	1.11	1.09	0.11	1.25	1.21	1.11	1.09
15809 15834	1.03		0.16	1.53	1.63		1.47	0.16	2.08	2.16		1.44
15780 15609-2	0.33	I	0.13	1.40	I.39 I.53	1.18	1.18	0.15	1.48	I.37 I.55	1.15	1.19
15781	1.12		0.29	2.10	2.28		1.93	0.30	2.14	3.00		2.02
15783 15609-3	0.32	3	0.22	1.80	1.88	1.46	1.29	0.25	1.88	1.97	1.52	1.72
15784	1.04		0.61	3.30	3.96		4.67	0.69 X	3.57	4.28 X		2.9I

Mr. Crafts' opening remark misstates our principal conclusion; for the sake of emphasis and clarity we would like to repeat it: "The factor principle . . . encounters difficulty when applied to steels that contain substantial amounts of a single element or to complex alloy steels." It was our intent, based on facts as we know them, to apply this broadly to steels containing relatively large amounts of hardening alloy, and particularly to those in which more than one major alloying element was present.

Mr. Crafts has raised two important points, regarding the conversion curve and the measurement of Jominy distance. As to the

relation would have been revealed, which would have destroyed our principal conclusion. Perhaps Table 3 in the paper had been overlooked. This compared, with only minor discrepancies, the measurement of this distance for a simple nickel-steel series using three different methods, including the 50 per cent martensite method. As a further check on our conclusions, we have remeasured the Jominy distance for the entire set of nickel-manganese steels, using the 50 per cent martensite method recommended by Mr. Crafts. The data are given in Table 7. Because of segregation banding and the low hardness gradient, it was practically impossible to

measure this distance microscopically in No. 15785. For a steel of this type, the point of inflection is at least definite. Fig. 9 analyzes these data graphically. The dashed curves, representing "point of inflection method,"

fall as a family of curves. From the lowest silicon group a multiplying factor of 2.0 may be calculated for 1 per cent manganese.

With regard to the NE-8739 steel used in Table 1 as an example of the divergence of

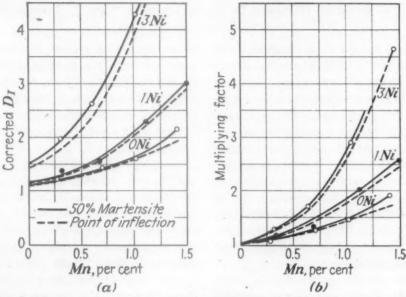


Fig. 9.—Hardenability and factor curves for nickel-manganese steels developed by different criteria.

are reproduced from Fig. 3a of the paper; the plotted points and full-line curves represent the "50 per cent martensite method." It is evident at a glance that no significant difference exists and that our original conclusion is unimpaired.

Dr. Grossmann's comments, which are interesting, do not test the question he raises. It should be obvious that in such a complicated subject it is scientifically unsound to reject the base line established in a carefully controlled experimental sequence and substitute, as a basis for comparison, data derived from miscellaneous sources.

Answering Mr. Bucknall's question regarding the discrepancies in the manganese factors, the differences in base compositions and in interpretations, already explained, can account for them. For instance, Crafts and Lamont's data may be broken down into groups according to silicon content and, when thus plotted, observed and calculated critical diameters, we cannot agree with Mr. Bucknall that the interesting boron effect he mentions is responsible for all the divergence: first, because when boron is neglected entirely the calculated hardenability of 4.6 in. is still about 42 per cent in excess of the observed; and second, the divergence agrees with that shown by Hodge and Orehoski for steels of different composition but equal hardenability.

No strong defense is offered for the method of determining the end-quench distance we used. As Mr. Bucknall says, the error involved at low hardenabilities for this method, or any of the others, is not large, but as hardenability increases all methods are subject to increasing uncertainty. The inflection point method evidently errs on the conservative side at high hardenabilities, which tends, therefore, to decrease the upward curvature of the hardenability and factor curves.

Factors for the Calculation of Hardenability

BY IRVIN R. KRAMER, * MEMBER A.I.M.E., SIDNEY SIEGEL * AND J. GARDNER BROOKS * (New York Meeting, October 1945)

In 1942 Grossmann¹ proposed that the hardenability of a steel may be calculated from its chemical composition by considering the base hardenability associated with its carbon content and grain size and multiplying this base by factors for each element present. Since Grossmann's original publication, several investigators²⁻⁵ have reexamined the multiplying factors for the individual elements and in general have found that the multiplying principle is valid. However, some of the individual factor curves developed have been in poor agreement.

Inasmuch as the carbon-factor curve obtained by Grossmann was dependent upon the factors for all the other alloying other alloying elements. Furthermore, in order to avoid the possibility that errors in the manganese, silicon, or other curves might influence the carbon-factor curve, investigation of iron-carbon alloys containing little or no manganese and silicon was necessary.

That the effect of carbon on hardenability was greater than indicated by Grossmann is shown by a comparison of the diameters of completely hardened rounds of iron-carbon alloys with the ideal critical diameter calculated from Grossmann's factors. These alloys have a greater hardenability in a finite quench than predicted by Grossmann's factors for an infinite quench (Table 1).

TABLE 1.—Comparison of Calculated D, with Actual Ouenched Bars

A11			C	ompositio	n, Per Cer	nt			Calc.	Diameter of Fully Har-	
C Mn Si	Si P S Ni Cr		Cr Cu		dened Bars						
GSM	0.34	0.07	0.02	0.003	0.014	0.10	0.01	0.01	0.238	0.35	
GSM GSO	0.40	0.07	0.02	0.004	0.010	0.11	0.01	0.01	0.260	0.40	

· Grossmann's factors.

elements present in the steel, it logically followed that his results were in need of correction in the light of the new data available for manganese, silicon, and the

Among the other important variables that were in need of further investigation were the effect of deoxidation practice on the grain-size correction curves and the effect of stable carbide-forming elements on the depth of hardening.

Most of the work by Kramer, Hafner, and Toleman4 was done on silicon-killed steels. It was not known whether Grossmann's grain-size correction curves, determined on aluminum-killed steels, was valid when applied to steels with different deoxidation practice. More data on the

Published by permission of the Navy Department. This paper represents only the personal opinions of the authors and in no way reflects the official attitude of the United States Navy. Manuscript received at the office of the Institute Oct. 15, 1945. Issued as T.P. 2029 in METALS TECHNOLOGY, June 1946.

* Division of Physical Metallurgy, Naval

Research Laboratory, Office of Research and Inventions, Anacostia Station, Washington, D. C.
References are at the end of the paper.

effect of deoxidation on grain-size correction were necessary.

The effect on hardenability of the elements that form stable carbides quite naturally depends on the austenitizing treatment, since that determines the amount of the element that goes into solution. The effect of elements like molybdenum and chromium would be greater if steels containing these elements were austenitized at a temperature high enough and for a time long enough for the carbides to dissolve. When such steels are quenched from too low a temperature, the hardenability may be lower than expected, either because the alloying element has combined with the carbon and prevented it from contributing its full share to hardenability, or because the undissolved carbides act as nuclei to start the upper transformation reaction sooner than expected from the alloy content. The effect of incomplete solution of carbides on hardenability has been indicated by the work of Comstock¹⁰ on low-alloy titanium steels. The tensile and yield strength of these steels were markedly increased by normalizing at temperatures above 1800°F. as compared with normalizing at 1650°F.

Steven,⁵ investigating the effect of chromium and molybdenum on the hardenability of steel, found that when both elements were present the hardenability was lower than that predicted by the product of the hardenability factors for the individual elements. Such interactions make it likely that the problem of determining hardenability factors becomes more complex as the number of stable carbideforming elements in a steel is increased.

METHODS

The steels used in this investigation were melted in a 100-lb. basic high-frequency induction furnace. They were generally split into four parts and appropriate alloying additions were made in the furnace before the steels were poured

into cast-iron ingot molds. Two pounds of aluminum per ton was added to the steels that were aluminum killed. The ingots were homogenized for approximately 12 hr. at 2300°F. and forged into 1½-in. rounds. These bars were normalized as indicated in Tables 11B-23B* before machining into Jominy-Boegehold test bars.

The composition was determined by standard methods of chemical analysis. Most of the samples for analysis were taken from the Jominy bars. The quenching apparatus and quenching method were standard. The specimens were held at the austenitizing temperature for 2 hr. in graphite blocks. After quenching, the specimens were wet-ground to a depth sufficient to avoid surface effects.

Hardness impressions were made at first with a diamond pyramid hardnesstesting machine; later it was found that Rockwell C hardness readings were sufficiently accurate. The Vickers impressions were spaced 0.050 in. apart starting 0.025 in. from the quenched end, while the Rockwell C impressions were spaced 1/6 in. apart. The "half-hardness" was determined from the curve of half-hardness position versus carbon content, presented by Grossmann.1 Many bars were examined under the microscope for determination of the 50 per cent martensite area until it was found that the two methods gave the same results within ± 10 per cent for most steels (Fig. 1).

Most of the grain-size determinations were made by a count on photographs taken at appropriate positions on the Jominy specimens after electrolytic polishing and suitable etching. When it was

^{*} Tables IIA to 23B have been deposited with the American Documentation Institute. To obtain them, write to American Documentation Institute, Bibliofilm Service, 1719 N St., N. W., Washington 6, D. C., asking for Document No. 2223 and enclosing 50 cents for microfilm (images I in. high on standard 35mm. motion-picture film) or \$3.10 for photostat (6 by 8 in.).

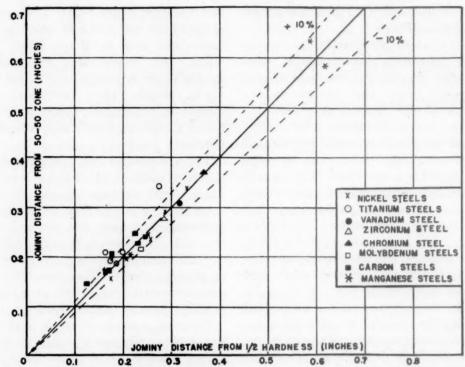


FIG. 1.—COMPARISON OF HALF HARDNESS AND 50 PER CENT MARTENSITE MEASUREMENTS.

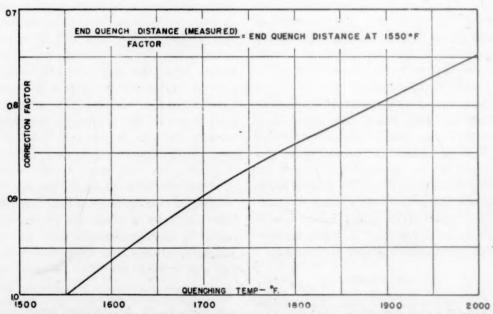


Fig. 2.—Correction of Jominy distance as a function of quenching temperature (Jackson and Christenson, Revised⁹).

found that two independent observers could estimate the grain size with sufficient accuracy by comparison with charts, this method was used. distance less than 0.15 in. were not used in the calculations.

The steels used in the determination of the grain-size correction curves (Fig. 3),

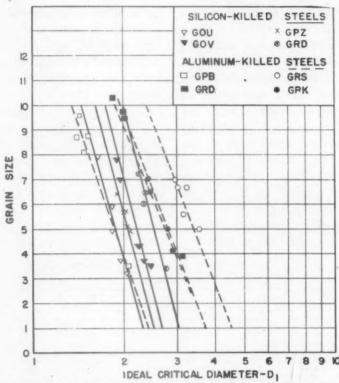


FIG. 3.—EFFECT OF DEOXIDIZING PRACTICE ON GRAIN-SIZE CORRECTION CURVES.

The Jominy distance determined from the location of half hardness or 50 per cent martensite point was corrected for quenching temperature by the use of Fig. 2. This curve, derived by Jackson and Christenson,9 gives the correction at 0.4 in. from the quenched end. The quenching-temperature correction varies somewhat with the distance along the Iominy bar, but this curve is sufficiently accurate for distances from 0.20 to 0.50 in. Each Jominy distance was corrected to a 1550°F. quench, which was used as a standard, and then converted to ideal critical diameter by the use of Grossmann's conversion curve.1 Because of the uncertainty in the lower portion of this curve, the data for steels having a Jominy were given special austenitizing treatments in order to develop a range of grain sizes. These bars were held at temperatures ranging from 1650° to 2200°F. (Table 11B) for 2 hr., then rapidly transferred to a furnace at 1550° or 1600°F. and quenched after 15 min. at the lower temperature. Steels free from stable carbide-forming elements were used in the grain-size experiments in order to avoid the possibility of indeterminate results because of changes in the solubility of the carbides.

DETERMINATION OF THE FACTOR CURVES FOR CARBON

There are essentially two methods that may be used for the determination of hardenability factors. Grossmann¹ in his paper on calculated hardenability was able to obtain the factors for manganese, silicon, nickel, and other elements by determining the increase in hardenability with an increase in a given alloying element in a series whose base composition was kept constant. To find the factor curve for a given element it was only necessary to plot the ideal critical diameter against the percentage of alloving element under consideration, and divide each point on the curve by the intercept at zero per cent alloying element. As it is extremely difficult to prepare a series with all the elements in the steel remaining constant except the one being studied, other investigators determined the factors by the equation $D_I = f_C \times f_{Mn} \times f_{Si} \times \dots$, a method that makes it possible to include data that could not otherwise be used.

To establish the level of the carbon curve it was necessary to determine the ideal critical diameters of iron-carbon alloys very low in residual elements. The hardenability-factor curves were then derived by a series of successive approximations in which the previously determined curves were used at first. For example, Crafts and Lamont's manganese and silicon curves were used to develop a carbon curve, which was then corrected to the level established by the low-alloy Fe-C steels.

This new carbon curve was then employed to develop new manganese and silicon curves, and the procedure was repeated until further cycling caused no change. This process of cycling establishes the general shape of the carbon curve, whose level was determined from low-alloy steels. The balanced carbon, man-

Table 2.—Chemical Composition of Low-alloy Steels
Per Cent

Alloy	С	Mn	Si	P	S	Ni	Cr	Cu	A1	Mo
GSB	0.41	0.018	0.08	0.015	0.016	0.02	0.01	0.074	0.045	0.01
GSC	0.43	0.022	0.40	0.015	0.016	0.02	0.01	0.074		0.01
GSD	0.39	0.021	1.13	0.015	0.016	0.02	10.0	0.074		0.01
GSM	0.34	0.07	0.02	0.003	0.014	0.10	<0.01	<0.01	0.07	
GSN	0.46	0.07	0.02	0.004	0.016	O.II	<0.01	<0.01	0.06	
GSO	0.55	0.08	0.02	0.004	0.017	0.11	<0.01	<0.0I	0.07	

During the determination of the factor curves for carbon, manganese, and silicon, it became evident that their effect on hardenability was not a linear function of the alloy content. This made extrapolation dangerous, particularly near zero per cent alloving element, since these intercepts for the manganese and silicon curves were important in establishing the level of the carbon curve. In the absence of data for iron-carbon alloys low in residual elements, it would be possible to derive a system of hardenability-factor curves in which errors in the manganese and carbon curve levels would compensate each other over a wide range of compositions, resulting in a set of curves that would appear to yield fairly accurate calculations but that actually would be incorrect.

ganese, and silicon curves were then used to redetermine the effect of the other alloying elements on hardenability, and these factor curves were again cycled through a process of successive corrections until a completely balanced system was obtained.

Details of Determination of Ideal Critical Diameter for Low-hardenability Șteels

The steels selected for establishing the level of the carbon curve were of the compositions given in Table 2. Since iron-carbon base alloys with only residual amounts of alloying elements are very shallow hardening, the determination of ideal critical diameters for these steels required very careful quenching of small rounds. To make it possible to work with

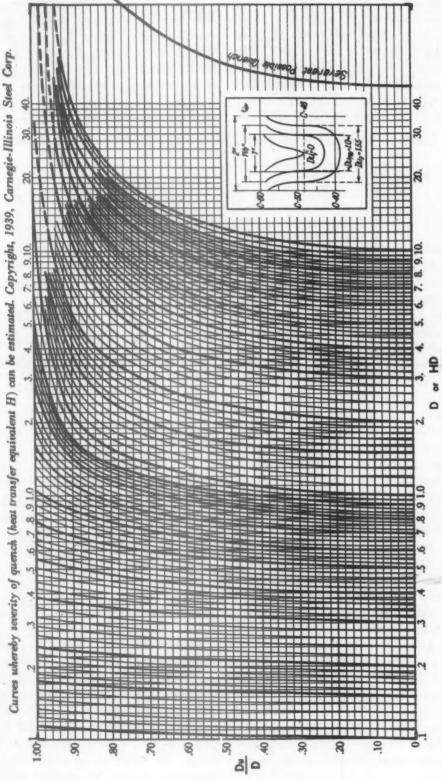


Fig. 4.—D"/D vs. HD or D. Cooling power of Quenching baths.

larger rounds or with Jominy bars, four iron-carbon-base alloys containing nickel were made up (Table 3). Steels PLJ and PLK were quenched as Jominy bars, while GSS and GST were quenched as rounds.

For each of these alloys, except PLJ and PLK, a series of rounds, each having a length at least five times its diameter,

After the bars were quenched, they were carefully sectioned by a water-cooled cutoff wheel. Vickers hardness surveys were made on two diameters and the results were averaged for the determination of the hardness-distribution curve.

Eight bars of steel GSD formed an excellent series for the determination of

TABLE 3.—Chemical Composition of the Low-alloy Steels Containing Nickel
PER CENT

Alloy	С	Mn	Si	P	S	Ni	Cr	Cu	A1
PLJ	0.55	0.016	0.03	0.004	0.015	1.27	<0.01	0.046	0.05
PLK	0.66	0.016	0.07	0.005	0.016	1.24	<0.01	0.040	
GSS	0.40	0.09	0.02	0.002	0.016	1.50	<0.01	0.01	
GST	0.50	0.09	0.02	0.003	0.015	1.51	<0.01	0.01	

was machined. These bars were heated to 1550°F. in a reducing gas atmosphere and held in the furnace for at least 15 min. after the center of the bar had reached temperature. The bars of series GSB, GSC and GSD were quenched in a 4-in. diameter vertical flush pipe, in which the flow of water was adjusted by means of a Pitot tube in the inlet pipe. Series GSM, GSN, GSO, GSS, and GST were quenched in a similar flush pipe 8 in. in diameter. Two brass plates with 1/16-in. holes were placed at the bottom of the flush pipes, approximately i in. apart, to ensure lamellar flow and uniform conditions over the cross section.

A chromel-alumel thermocouple was inserted radially into the center of each bar and flash-welded so that the cooling rate at the center during quenching could be measured. In order to follow the rapid cooling rates encountered when small rounds are quenched, special equipment was developed,16 which increased the range of cooling rates that could be measured by the Leeds and Northrup Speedomax. In addition, step bars of series GSM, GSN, GSO, GSS, and GST were quenched without thermocouples under the same experimental conditions as the individual rounds of the same alloys.

the severity of the quench in the 4-in. flush pipe (Table 4). In accordance with

TABLE 4.—Determination of D_u/D for Series GSD

Run No.	Diameter (D), In.	Unhardened Diameter (Du) at 320 VPN., In.	D_u/D
35	0.502	0	0
34 38	0.506	0.150	0.296
38	0.549	0.220	0.401
37	0.552	0.220	0.366
40B	0.601	0.340	0.566
4I 42	0.601	0.290	0.483
42	0.653	0.460	0.704
43	0.653	0.450	0.689

the method of Grossmann and Asimow,⁷ the critical diameter (D_o) and the severity of quench (H) were determined by matching the D_u/D vs. D curve (Fig. 4) with the proper HD curve. For the bars of series GSD,

$$HD = 0.90$$
 from which $H = \frac{0.90}{0.50} = 1.8$

The bars of GSB and GSC were quenched under exactly the same experimental conditions as GSD. Fig. 5, in which the experimentally measured half-temperature time is plotted against bar size, indicates that the cooling conditions for the bars of GSB and GSC were the same as for GSD within the limit of experimental error. Therefore, it can be assumed that the

H value for quenching these two series of rounds was the same (H = 1.8).

It is now possible to find the ideal critical diameter for GSB and GSC by the following method:

1. Multiply the value D for any bar by the H value of the quench.

2. Next plot the Du/D value of this bar against HD on Fig. 4.

3. Follow the curve on which this point falls down to $D_u/D = 0$ to find HD_o .

4. Divide HDo by H to find Do.

5. Now use Fig. 3 to plot D_o at H = 1.8to find D_I. The data for all the bars of

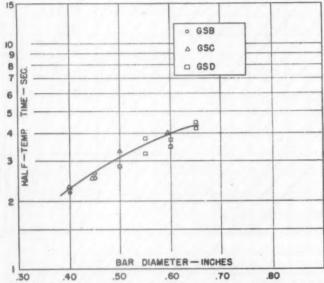


FIG. 5.—HALF-TEMPERATURE TIME VS. BAR SIZE FOR GSB, GSC, GSD.

TABLE 5.—Determination of D_I for GSB, GSC, and GSD

Run	D	D_uD	Sec. 3/21	HD	HD.	D ₀	D_I	G.S.	Dr at G.S.7
GSB 21 20C 31 27	0.397 0.393 0.451 0.450	0.792 0.865	2.19 2.30 2.53 2.65	0.715	0.56	0.311	0.65	1034	0.82
		1	Ave	rage D _I at	G.S. 7 =	0.81			1
GSC 29 32 33 39	0.394 0.445 0.499 0.595	<0.0 0.669	2.30 2.52 3.35 4.00	0,801	0.675	>0.394 0.375	>0.78	934 934 935	0.92
		1	Ave	rage D _I at	G.S. 7 =	0.91	1		1
GSD 35 38 37 40B 41 42 43	0.502 0.549 0.552 0.601 0.603 0.653	0.478 0.575 0.515 0.665 0.615	2.85 3.25 3.80 3.48 3.75 4.50	0.904 0.988 0.994 1.082 1.082 1.176	0.81 0.825 0.87 0.83 0.86	0.445 0.458 0.584 0.461 0.478	0.83 0.85 0.88 0.85 0.88	9½ 9½ 9½ 9¾ 10½	0.96 0.97 1.05 1.08

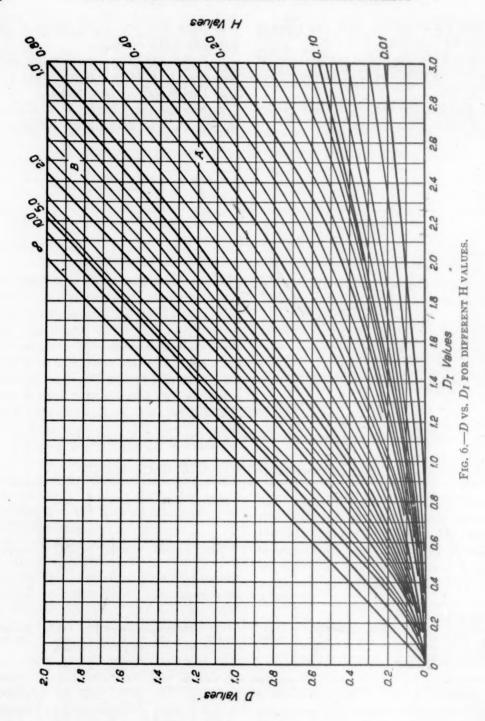


TABLE 6.—Determination of D_l for GSM, GSN, GSO, GSS, and GST

Bar	D, In.	Du, In.	Du/D	Half-tem- perature Time, Sec
GSM 88B	0.35 0.65 0.70 0.30 0.40	<0 0.50 0.55 <0 <0	<0 0.77 0.79 <0 <0	1.75 3.70 4.35
Stepbar	0.55	0.20	0.51	

From	ma	ıt	ch	1	0	£	I),	M,	1	D		v	S		Ŀ	Ī.	D	curves:
HD	0							*			*	×							2.00
																			0.47
H.						*											×		4.26
D_I .							*	*				×			,				0.67
G.S							С												81/4

GSN				
89B	0.35	<0	<0	1.60
84A	0.50	0.15	0.30	2.40
94C	0.55	0.28	0.51	2.90
82A	0.60	0.26	0.43	3.45
81A	0.70	0.405	0.58	4.15
58	0.80	0.54	0.68	5.85
63	0.90	0.66	0.73	6.60
Stepbar	0.30	<0	<0	
Stepbar	0.40	<0	<0	
Stepbar	0.55	0.12	0.22	
Stepbar	0.70	0.42	0.60	

Bar	D, In.	Du, In.	D_u/D	Half-tem- perature Time, Sec.
GSO				
85A	0.40	<0	<0	1.85
83A	0.60	0.12	0.20	3.20
93A	0.60	0.22	0.37	3.25
80A	0.70	0.36	0.515	5.05
72B	0.90	0.62	0.685	7.10
66	0.95	0.77	0.81	8.75
73B	1.00	0.78	0.78	9.25
Stepbar	0.30	<0	<0	
Stepbar	0.40	<0	<0	
Stepbar	0.55	<0	<0	
Stepbar	0.70	0.33	0.47	

D_{\bullet} H D_{I}	******		3.6	7
GSS 71C 64 Stepbar Stepbar Stepbar	0.80 0.90 0.80 1.00	0.57 0.59 0.43 0.69 1.02	0.71 0.65 0.53 0.69 0.82	6.90

From match of Du/D vs. HD curves:

TABLE	6-	(Continued)

HD ₀ D ₀ H D _I			s. HD curv 2.0 0.6 2.9 0.95	75
GST 60 62 Stepbar Stepbar Stepbar	0.80 0.90 0.80 0.90 1.05	0.51 0.54 0.28 0.47 0.68	0.63 0.60 0.35 0.52 0.65	6.70 6.65
HD. D H DI			0.7 3.4	0 5 7

GSB, GSC, and GSD are given in Table 5.

The results of the quenching experiments for GSM, GSN, GSO, GSS, and GST (quenched in the 8-in. flush pipe) are shown in Table 6. These data have been matched with the curves of Fig. 4 according to the method of Asimow and Grossmann and the resulting critical diameters and H values are listed in the same table. Fig. 6 was then used to convert the values of critical diameter to ideal critical diameter. The average H value determined from the five sets of steels by this method was 4.0.

In order to determine whether the severity of quench H in the 8-in. flush pipe varied as a function of bar diameter, a theoretical curve of half-temperature time versus bar size was derived by the use of Russell's tables,13 assuming a severity of quench of 4.0 and a diffusivity of 0.009 sq. in. per sec. This curve, together with the experimental points, is shown in Fig. 7. The excellent correlation indicates that under these experimental conditions the severity of quench H for bars ranging in diameter from 0.35 to 1.00 in. did not change as a function of bar size within the experimental error of the half-temperature time determinations.

After the ideal critical diameters of the low-alloy steels were found as described above, the level of the factor curve for

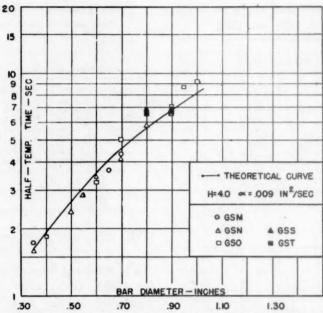
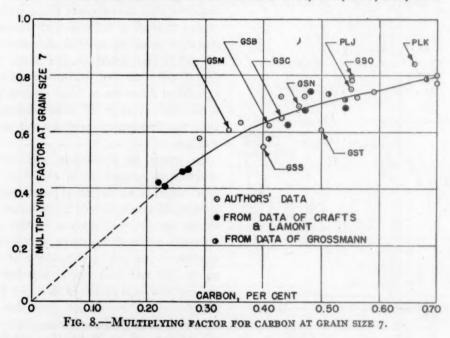


Fig. 7.—Half-temperature time vs. bar size for GSM, GSN, GSO, GSS, GST.



carbon was determined by correcting for grain size by means of the curves of Fig. 9 and dividing the corrected ideal critical diameter by the product of the factors for the small amount of alloy present. These data are shown in Table 7 and are plotted in Fig. 8.

DISCUSSION OF RESULTS*

Preliminary work on the effect of silicon on hardenability revealed that the data for silicon-killed steels resulted in a factor curve entirely different from that derived

^{*} See footnote on page 671 regarding Tables 11 to 23.

from the data for aluminum-killed steels. An investigation of the effect of austenitic grain size on the ideal critical diameter of both silicon and aluminum-killed steels

effect of grain size on hardenability is less for silicon-killed steels than for aluminum-killed steels. When the appropriate family of grain-size correction

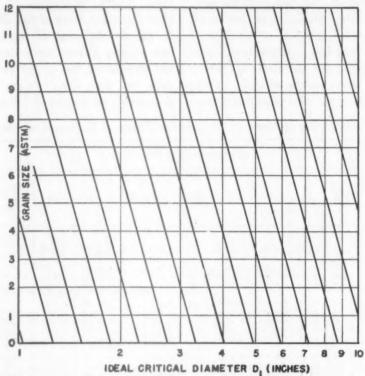


Fig. q.—Grain-size correction curves for silicon-killed steels.

showed two distinct families of correction curves (Fig. 3 and Table 11). The relation-

TABLE 7.—Carbon Factors for the Low-alloy Steels

0			0.0	Dr at	Prod- uct of	Facto	
Steel	JD	D _I	G.S.	G.S.7	Fac- tors	Car- bon	Per
GSB GSC GSM' GSN GSO PLJ PLK GSS GST	0.113		1034 934 834 9 934 10 9 8	0.81 0.91 0.73 0.82 0.95 1.45 1.60 1.02	I.29 I.39 I.19 I.19 I.19 I.91 I.88 I.86 I.86	0.627 0.654 0.614 0.688 0.798 0.760 0.850 0.550 0.610	0.41 0.43 0.34 0.46 0.55 0.55 0.66 0.40

[·] Product of factors for residual elements.

ship for aluminum-killed steels is the same as reported by Grossmann, but the

curves was used for the data for silicon steels, the silicon-factor curves coincided. The effect of deoxidation on the grain-size correction curves was investigated only for silicon-killed and aluminum-killed steels. If this effect is associated with the oxygen or nitrogen content of the steel, the grainsize correction curves presented here might represent only two classes of deoxidized steels, with the possibility that other correction curves might be expected for steels deoxidized in a different manner. Idealized grain-size correction curves, Figs. 9 and 10, were used to correct the data for carbon, manganese, silicon, and other elements.

Determinations of the 50 per cent martensite zone or of the "half-hardness" position have both been used as criteria for the measurement of hardenability. A comparison of the two methods of measuring the depth of hardening for the steels of Table 8 is shown graphically in Fig. 1. In general, the two systems gave the same results within ±10 per cent, with no apparent trend as a function of changes in chemical composition. This is to be expected for the steels for which the Jominy curve drops sharply in the vicinity of the 50 per cent martensite area.

In general, "50 per cent martensite" and "half-hardness" results are used interchangeably in this paper. This may explain some of the scatter of the nickelsteel points (explained in more detail later), but for most of the alloys involved in the development of the factor curves, the Jominy curves were steep enough in the vicinity of the 50 per cent martensite zone so that the two methods might reasonably be employed indiscriminately.

TABLE 8.—Steels Used in Comparison of 50-50 Zone and Half-hardness Measurements

					Compos	ition,	Per Cent	;					
Alloy	C Mn Si P	P	S	Ni	Cr	Мо	Cu	A1	Other Ele- ments	Half Hard- ness	50-50		
GOV-1 GOV-3 GPB-1 GPB-4 GPC	0.38 0.38 0.45 0.45 0.45	0.43 0.43 0.46 0.46 0.45	0.28 0.28 0.34 0.34	0.003 0.003 <0.001 <0.001 <0.001	0.02I 0.02I 0.020 0.020 0.020	2.03 2.03 1.05 1.05 2.09	0.005 0.005 0.01 0.01 0.01		0.06 0.06 0.07 0.07 0.07	Si Killed Killed 0.087 0.087		0.250 0.331 0.175 0.288 0.188	0.243 0.338 0.155 0.290 0.188
GPD GPE GPG GHP-2 GPJ	0.43 0.41 0.38 0.38 0.40	0.45 1.14 1.12 1.12 1.14	0.35 0.22 0.25 0.28 0.31	100.00 100.00 100.00 100.00	0.020 0.017 0.017 0.017 0.017	3.07	0.01 0.03 0.03 0.03 0.03		0.07 0.09 0.09 0.09 0.09	0.038 0.088 0.081 0.061 0.070	0.036Ti 0.090Ti 0.173Ti 0.362Ti	0.256 0.273 0.175 0.200 0.169	0.236 0.344 0.190 0.208 0.208
GPK-1 GPL-3 GPM-2 GPO-1 GPN-1	0.39 0.38 0.36 0.42 0.34	1.06 1.04 1.06 0.83 0.81	0.18 0.20 0.33 0.23 0.11	<0.001 <0.001 <0.001 <0.001 <0.001	0.022 0.021 0.020 0.023 0.020		0.01 0.01 0.01 0.66 0.01	0.35	0.07 0.07 0.06 0.07 0.07	0.066 0.051 0.051 0.065 0.073	0.072Ti 0.11V 0.078Zr	0.188 0.314 0.281 0.363 0.237	0.187 0.310 0.278 0.370 0.215
GPR GPS GPT PCB PCC	0.44 0.40 0.38 0.33 0.50	1.06 1.06 1.07 0.47 0.45	0.14 0.33 0.83 0.30 0.30	0.005 0.005 0.005	0.025 0.025 0.025		10.0>		0.09	0.060 0.060 0.042		0.169 0.244 0.231 0.125 0.163	0.171 0.242 0.227 0.145 0.167
GAA GBM GBL GPX GPY GPZ	0.43 0.59 0.47 0.22 0.32 0.43	0.64 1.39 1.47 0.74 0.70 0.65	0.34 0.30 0.30 0.66 0.67 0.75	0.016 0.015 0.015 0.002 0.002 0.002	0.026 0.033 0.033 0.026 0.026 0.026	4111	0.10 0.079 0.079 0.010 0.010 0.010		0.10 0.24 0.22 0.06 0.06 0.06	0.00		0.202 0.584 0.615 0.213 0.175 0.225	0.197 0.631 0.581 0.202 0.205

It has been considered³ that "half-hardness" measurements for bainitic steels may be a source of error in the determination of the depth of hardening. For these steels, the position of the half-hardness and the 50 per cent martensite zone are not necessarily coincident, and since the slope of the Jominy curve in the transition region is not steep, large errors are apt to occur in the determination of the ideal critical diameter.

Fig. 8 (Table 12) shows the hardenability factor curve for carbon at grain size 7. The level of the carbon curve is approximately three times higher than that reported by Grossmann. As stated previously, this was established by five ironcarbon alloys, GSB, GSC, GSM, GSN, GSO, whose manganese content was so low that there was little likelihood of compensating errors in the carbon and manganese-factor curves. The points GSS,

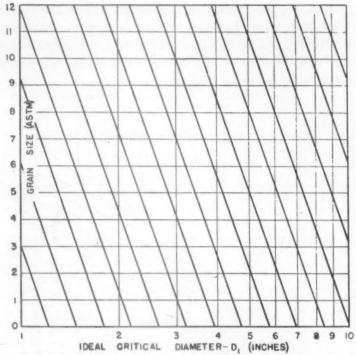


FIG. 10.—GRAIN-SIZE CORRECTION CURVES FOR ALUMINUM-KILLED STEELS.

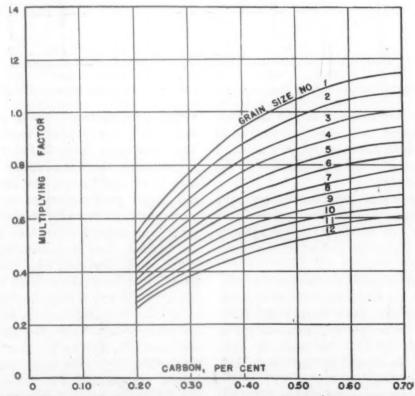


Fig. 11.—Multiplying factor for carbon at indicated grain size (aluminum-killed steels).

GST, PLJ, and PLK are for steels that also had very low manganese, but that contained approximately 1.25 to 1.50 per cent nickel to increase the hardenability.

Table 14) is also lower than reported by previous workers. In general, silicon has relatively a small effect on hardenability.

Because of the lack of agreement among

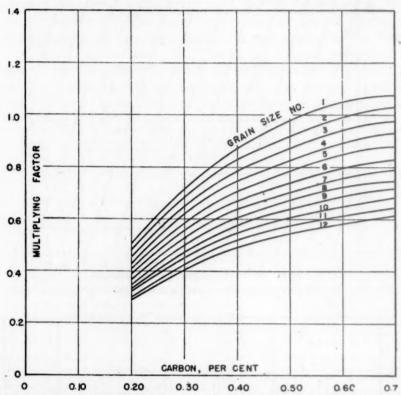


FIG. 12.—MULTIPLYING FACTOR FOR CARBON AT INDICATED GRAIN SIZE (SILICON-KILLED STEELS).

Since the hardenability of PLJ and PLK was measured by Jominy bars instead of rounds, these points constitute a check of the accuracy of the determination of the effect of carbon.

The grain-size correction curves have been combined with the carbon curve (Figs. 11 and 12) to make it possible to find the factor for carbon at any grain size.

The factor curve for manganese (Fig. 13, Table 13) differs markedly as to shape and magnitude from those reported by previous investigators. Manganese up to about 1.00 per cent has relatively little effect on hardenability, but above this level a very large effect.

The factor curve for silicon (Fig. 14,

various investigators, 1,3,4,8 the curve for nickel has been a subject of much interest. The factor curve shown in Fig. 15 (Table 15) contains the hardenability data of both Crafts and Lamont and the authors and shows good agreement up to approximately 3 per cent nickel. Above 3 per cent nickel for the data of Crafts and Lamont, there is considerable scatter in the points. However, since the Jominy distances for these points varied from 0.66 to 1.45 in., the scatter might be attributable to difficulty in determining the 50 per cent martensite zone or to the fact that 50 per cent martensite may not be a good criterion for hardenability when large amounts of bainite are present. The shape of the nickel-factor curve indicates that nickel up to 0.50 per cent has a very large effect on hardenability, after which the curve flattens out until at approximately 2.5 per cent further amounts of nickel again have a large effect. As generally recognized, however, it does influence hardenability by decreasing the austenitic grain size.

The determination of hardenability factors for alloying elements that form

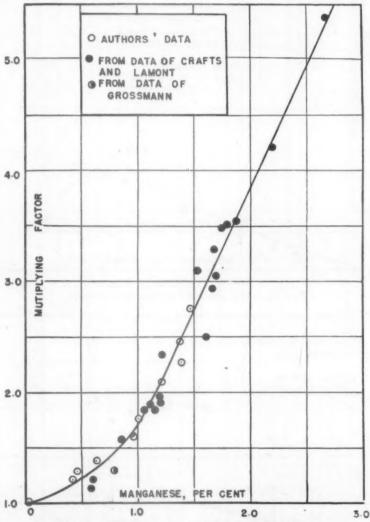


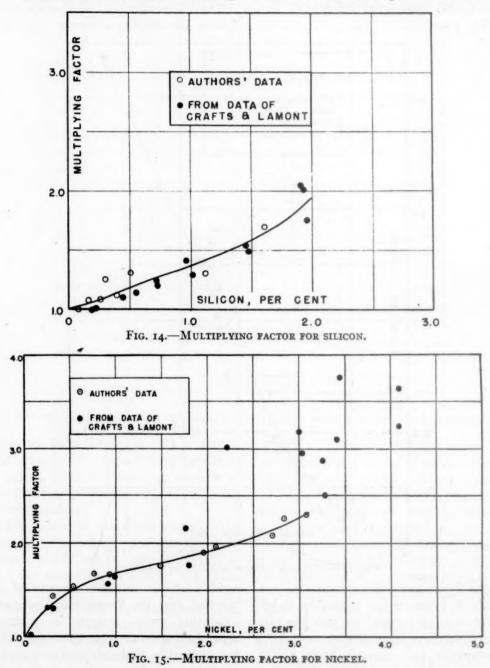
FIG. 13.-MULTIPLYING FACTOR FOR MANGANESE.

The factor curve for copper (Fig. 16, Table 16) is very similar to that for nickel. Percentages of copper that hitherto have been considered unimportant, and as a consequence not reported, exert a considerable influence on the hardenability. As little as 0.10 per cent copper raises the hardenability 17 per cent.

Aluminum, per se, has a very small effect on hardenability (Fig. 17, Table 17).

stable carbides has been complicated by the fact that the hardenability of steels containing such elements is strongly dependent upon the heat-treatment. This has resulted in hardenability-factor curves that were at variance with one another and showed a large scattering of points at the higher percentages of alloying elements. To determine the effect of heat-treatment, steels containing chromium, molybdenum, titanium, vanadium and zirconium (Table 9A) were heat-treated to find the effect of prior normalizing treatment, austenitizing

hardenability factors; but, as expected, the austenitizing treatment had a marked influence. Austenitizing at 2100°F. fol-

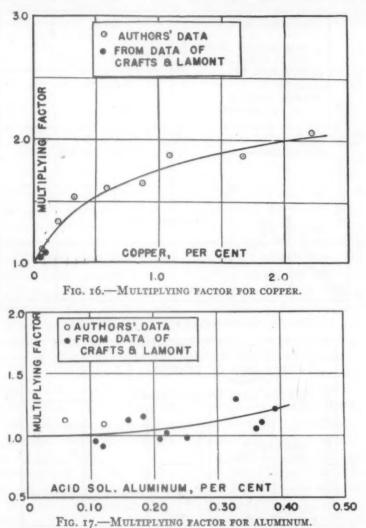


temperature, and precipitation of carbides at 1550°F. after a complete solution treatment (Table 9B). In general, the normalizing temperature had little effect on the

lowed by holding at 1550°F. for 4 hr. before quenching showed that the carbides were less soluble in the austenite at the latter temperature than at 2100°F. That

the carbides dissolved at 2100°F. were precipitated by holding at 1550°F. was evidenced by the fact that the hardenability on quenching from 1550°F. was

perature high enough to dissolve all of the carbides, the factors obtained by quenching these steels from 2100° or 1800°F. may give some indication of the maximum



lower than on quenching from 2100°F. As expected, the amount of carbide that precipitated from the austenite depended on time as well as on temperature. For most steels, the factors obtained upon holding for 15 min. at 1550°F. after austenitizing at higher temperatures were the same as those obtained after direct quenching from those temperatures. Since it is expected that the highest hardenability is obtained after austenitizing at a tem-

factors that can be obtained in steels containing alloying elements that form stable carbides.

In Fig. 18 (Table 16), the curve that seems best to represent all the available data on chromium steels has been designated "average factor." In order to indicate the "probable maximum factor," a straight line has been drawn between the origin and the maximum factor obtained by quenching from 2100° or

1800°F. The same method of designating the curves was used for molybdenum. Considerable scatter was encountered in the molybdenum factors (Fig. 18, Table combinations, found that when both elements were present the hardenability was lower than that expected from a consideration of the factors of the indi-

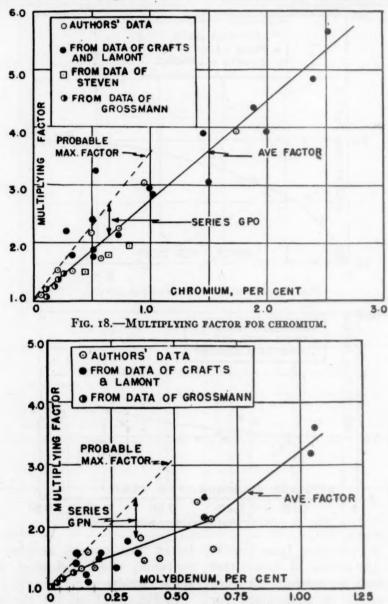


FIG. 19.-MULTIPLYING FACTOR FOR MOLYBDENUM.

19), indicating that steels containing molybdenum may have widely varying hardenability, depending upon their thermal history.

Steven,⁵ studying the effect on hardenability of chromium and molybdenum vidual elements. This appears to be a significant violation of the multiplying principle, but, as suggested by Grossmann, one that is not unexpected where stable carbide-forming elements are concerned. It is possible that interactions may occur

wherever two or more stable carbideforming elements are present in the same alloy.

ability data for titanium, provided undissolved carbides do not greatly affect the upper transformation by acting as

TABLE 9A.—Chemical Composition of Steels Used in Study of Effect of Heat-treatment on Hardenability of Steels Containing Stable Carbide-forming Elements

	Composition, Per Cent										
Alloy	С	Mn	Si	P	s	Cu	Cr	Acid- soluble Al	Other Elements		
GPO GPN GPK GPL GPM	0.42 0.34 0.39 0.38 0.36	0.83 0.81 1.06 1.04 1.06	0.23 0.11 0.18 0.20 0.33	10.0 10.0 10.0 10.0 10.0	0.023 0.020 0.022 0.021 0.020	0.07 0.07 0.07 0.07 0.06	0.66 0.01 0.01 0.01	0.065 0.073 0.066 0.051 0.051	0.34 Mo 0.072 total Ti 0.11 total V 0.078 acid-soluble 2		

Steven's data have been plotted in (Fig. 20, Table 20) to show the combined chromium-molybdenum factor as a function of molybdenum at different levels of chromium. Of course, variations in the heat-treatment of steels containing chromium and molybdenum may result in hardenability factors that are different from those shown, but Fig. 20 represents the best available data for chromiummolvodenum steels. The curve has been replotted in Fig. 27 to simplify interpolation. Ideal critical diameters for chromium-molybdenum steels quenched in the usual way calculated by the use of this chart usually check experimental values within ± 15 per cent.

It has been suggested that the hardenability-factor curve for titanium should be expressed in terms of acid-soluble rather than total titanium,* since it was felt that this method of chemical analysis determined the part of the titanium that had been in solution in the austenite and contributed to hardenability. It is conceivable that such a system of analysis might explain the vagaries of the hardennuclei. Data on the hardenability and analysis of acid-soluble titanium for steels that were heat-treated in various manners were obtained from Comstock.1 The chemical analyses showed that, in general, the percentage of acid-soluble titanium increased with austenitizing temperature. When the factors were calculated (Fig. 20, Table 21), the results showed a good correlation between hardenability and the percentage of acid-soluble titanium. In these calculations the acid-insoluble titanium was assumed to be present in the steel as TiC and the total carbon content was corrected accordingly. Steels having Jominy distances less than 0.15 in. were not used. Considerable scatter of points was found when the titanium factors were derived on the basis of total titanium (Fig. 22, Table 21).

The factors for vanadium (Fig. 23, Table 22) and zirconium (Fig. 24, Table 23) revealed the same susceptibility to variations in thermal history as did the factors for titanium. On each of these curves the range of hardenability factors obtained from the data of Table 9 has been designated by an arrow. For some unexplained reason the hardenability factors of steels GPL were very much higher than those obtained from other sources. This seems to imply that the hardenability factors for vanadium can vary between wide limits.

^{*} The words "acid-soluble titanium," as used here, refer to the portion of the titanium that has gone into solution in the ferrite. "Total titanium" includes both the titanium in the ferrite and the titanium carbides and nitrides, which are present in the steel and do not dissolve in the weak acid used in the analysis.

TABLE 9B.—Effect of Heat-treatment on the Hardenability of Steels Containing Stable Carbide-forming Elements

Alloy	Normalizing Tempera- ture, Deg. F.	Quenching Tempera- ture, Deg. F.	Time, at 1550°F. Min.	Grain Size, A.S.T.M.	J.D. Half Hardness	Ideal Critical Diameter Corrected to 1550°F.	Factor
			Снгом	HUM STEEL			
GPO-1	1550	1550	90	932	0.363	2.35	2.37
-6	1550 1650	1550	90	9 934 8.8	0.331	2.23	2.12
-2	1050	1550	90	934	0.388	2.45	2.45
-7 -3	1650 1800	1550	90	934	0.331	2.23	2.11
	1	1330	90	974	0.375	2.40	2.41
-8	1800	1550	90	8.5	0.363	2.37	2.11
-4 -9	2000	1550	90	81/2	0.388	2.45	2.32
-5	2200	1550 1550	90	9	0.350	2.30	2.11
-10	2200	1550	90	7.8	0.432	2.65	2.32
			Transfer an	d Quench Seri	es	1	
-11	1550	1650-1550Q	**	1 - 0	1	1 1	
-13	1550	2100-1550Q	15	7.8	0.375	3.23	2.12
-14	1550	2100-1550Q	240	51/2 51/2	0.475	2.80	2.12
-15	1550	1800-1550Q	240	8.4	0.419	2.60	2.38
			Direct-q	uench Series			
-16	1550	1650		9.2	0.344	2.39	2 21
-17	1550	1800		91/2	0.375	2.70	2.31
			Morven	ENUM SERIES			
			Norma	lizing Series			
GPN-1 -6	1550	1550	90	934	0.237	1.84	2.25
-2	1550 1650	1550	90	10	0.225	1.80	2.14
-7	1650	1550	90	9.3	0.247	1.90	2.19
-3	1800	1500	90	9.3	0.237	1.83	2.25
-8	1800	1550	90	01/	0.029	- 0-	
-4	2000	1550	90	914	0.238	1.83	2.11
-9	2000	1550	90	8.8	0.288	2.05	2.29
-5	2200	1550	90	8.3	0.225	1.80	2.04
-10	2200	1550	90	8.3	0.250	1.90	2.06
			Transfer an	d Quench Seri	es	,	
-11	1550	1650-1550Q	15	10	0.263	1.95	2.34
-12	1550	1800-1550Q	15	8.8	0.269	1.98	2.10
-13 -14	1550 1550	2100-1550Q 2100-1550Q	15 240	5.3	0.319	2.18	1.92
-15	1550	1800-1550Q	240	4	0.431	2.30	1.88
			Direct-q	uench Series		1	
-16	1550	1650		10	0.263	2.04	2.45
-17	1550	1800		9.6	0.188	1.80	2.22
			TITAN	IUM SERIES	,		
			Norma	lizing Series			
GPK-1	1550	1550	90	101/2	0.188	1.64	1.48
-6	1550	1550	90	8.8	0.181	1.61	1.32
-2 -7	1650 1650	1550	90	91/2	0.194	1.65	1.32
-3	1800	1550 1550	90	9.3	0.200	1.70	1.64
-8	1800	1550	90	81/2	0.238	1.84	
	2000	1550	90	8.5	0.238	1.76	1.47
-4 -9	2000	1550	90	8.5 8.8	0.219	1.76	1.41
-5 -10	2200	1550	90	8.3	0.188	1.64	1.29
-10	2200	1550	90	7.8	0.212	1.73	1.32

All the factor curves have been assembled in Figs. 25, 26, 27 to facilitate a comparison of the effect of alloying elements on factor curves for phosphorus and sulphur

turned out to be the same as reported by Grossmann.

It has been shown that the hardenability hardenability. It will be noted that the factors for carbon and manganese are markedly different from those formerly

TABLE 9B.—(Continued)

Alloy	Normalizing Tempera- ture, Deg. F.	Quenching Tempera- ture, Deg. F.	Time, at 1550°F. Min.	Grain Size A.S.T.M.	J.D. Half Hardness	Ideal Critical Diameter Corrected to 1550°F.	Factor
	4		Transfer an	d Quench Seri	es		
-12 -13 -14	*	1800-1550Q 2100-1550Q 2100-1550Q	15 15 240	9.6 5 2.3	0.188 0.402 0.356	1.64 2.50 2.33	I.40 I.59 I.26
	1	1	Direct-o	uench Series			
-17		1800	1	73/4	0.206	1.90	1.44
	1		VANAD	IUM SERIES		,	
			Norma	lizing Series			
GPL-1 -6 -2 -7	1550 1550 1650 1650	1550 1550 1550 1550	90 90 90	9.8 91/2 91/2 81/2	0.318 0.325 0.325 0.302	2.17 2.21 2.21 2.11	1.90 1.92 1.92 1.71
-3 -8 -4 -9	1800 1800 2000 2000	1550 1550 1550 1550	90 90 90 90	93/4 8.8 9 8.3	0.314 0.269 0.325 0.288	2.16 1.98 2.21 2.05	1.88 1.61 1.85 1.63
			Transfer ar	d Quench Ser	ies		
-12 -13 -14 -15		1800-1550Q 2100-1550Q 2100-1550Q 1800-1550Q	15 15 240 240	7½ 4.5 4 8¾	0.487 0.418 0.350 0.381	2.85 2.60 2.30 2.42	2.15 1.50 1.39 1.99
	1	1	Direct-	quench Series		1	
-16		1650		634	0.469	2.91	2.06
			. Zircoi	NIUM SERIES			,
			Norma	lizing Series			
GPM-I -6 -2 -7 -3	1550 1550 1650 1650 1800	1550 1550 1550 1550 1550	90 90 90 90	9 8½ 8.8 7¾ 9½	0.270 0.263 0.281 0.275 0.275	2.00 1.96 2.03 2.00 2.00	1.63 1.56 1.65 1.52 1.70
-8 -4 -9 -5 -10	1800 2000 2000 2200 2200	1550 1550 1550 1550	90 90 90 90	8.3 9 814 834 714	0.269 0.300 0.275 0.295 0.281	2.00 2.10 2.00 2.09 2.03	1.57 1.70 1.59 1.68 1.48
			Transfer as	nd Quench Ser	ies		
-11 -12 -13 -14	1550 1550 1550 1550 1550	1650-1550Q 1800-1550Q 2100-1550Q 2100-1550Q 1800-1550Q	15 15 15 240 240	734 9 4 3 714	0.275 0.269 0.462 0.412 0.300	2.00 2.00 2.77 2.57 2.10	1.52 1.64 1.63 1.42 1.55

reported. It is believed that a statement is in order to explain why the previously determined factors appear to have worked so well in spite of the fact that the in-

factor found by Grossmann, the new manganese factor is approximately 28 per cent as high as reported by Crafts and Lamont, while the new silicon curve is

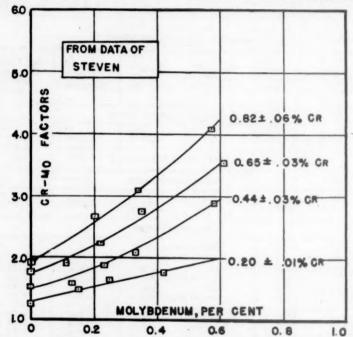
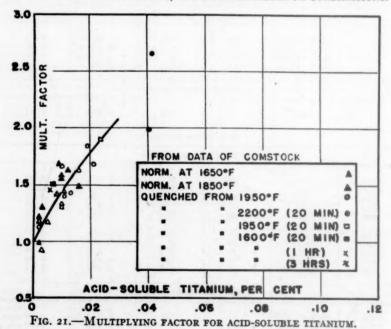


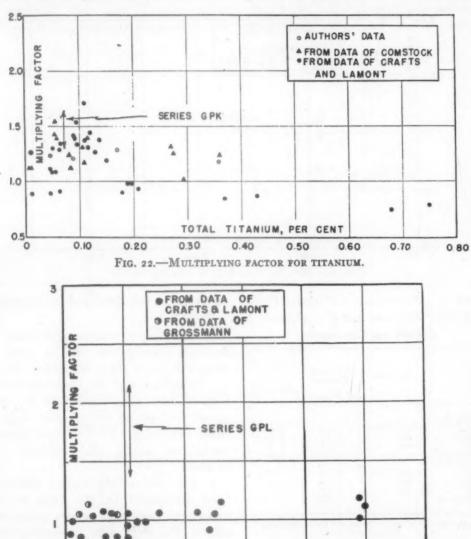
FIG. 20.—MULTIPLYING FACTOR, CHROMIUM-MOLYBDENUM COMBINATIONS.



dividual curves were inaccurate. The newly determined carbon factor is approximately three times higher than the carbon

85 per cent as high. Therefore, in certain ranges of composition, the product of the factors for carbon, manganese, and silicon are the same for both systems of factors. This area of "compensating error," found by plotting the ratio of the new factors to the old, lies approximately within the

is the same whether the new factors or the old are used; example B, however, shows a steel in which the products calculated by the two systems of factors are considerably



TOTAL VANADIUM, PER CENT

030

FIG. 23.—MULTIPLYING FACTOR FOR VANADIUM.

0.40

0.20

following percentages: C, 0.30 to 0.60 per cent; Mn, 0.50 to 1.50 per cent; and Si 0.50 to 2.00 per cent. Some examples may serve to clarify this point. The steel represented by example A (Table 10) has a composition such that the product of the factors for carbon, manganese, and silicon

0.10

0

different. Perhaps this will explain why the previously determined factors worked in some cases and not in others. For the proper use of the factor curves developed in this paper the reader is cautioned to use the complete set of curves and not to substitute curves derived elsewhere.

0.50

0.60

The factor curves herein developed have been tested on the hardenability data for many steels, ranging in composition from the plain carbon type to those containing 2. Half-hardness or 50 per cent martensite measurements may be used interchangeably as a criterion for hardenability for Jominy-bar curves that fall

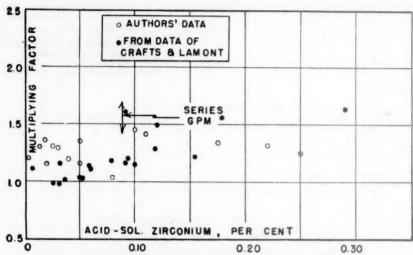


FIG. 24.—MULTIPLYING FACTOR FOR ZIRCONIUM.

TABLE 10.—Examples of Calculation Using Authors' Data and that of Crafts and Lamont and Grossmann

	Per Cent	Authors' Factors	Previously Deter- mined Factors
Example A	0.40 (GS-7)	. 6.	
Mn	1.50	0.64	6.95
Si	0.75	2.75 1.28	
Product	0.75		1.50
Example B		2.25	2.22
C	0.40 (GS-7)	0.64	0.213
Mn	0.20	1.08	1.17
Si	0.25	1.08	1.17
Product		. 748	.450

Manganese and silicon, Crafts and Lamont; Carbon, Grossmann.

many alloying elements. In general, the over-all accuracy is approximately ± 15 per cent; greater error occurring in the calculation of steels containing stable carbides.

CONCLUSIONS

r. Grain-size correction is dependent on deoxidation practice, aluminum-deoxidized steels involving a greater correction than silicon-deoxidized steels. off steeply in the vicinity of the 50 per cent martensite zone.

- 3. The factor curves developed by previous investigators were in error because the factor curve for carbon derived by Grossmann was not corrected to correspond with subsequent data for manganese and silicon and because data on steels containing very low percentages of manganese, silicon, and residuals were lacking.
- 4. The level of the carbon curve has been determined on the basis of low-manganese iron-carbon alloys whose ideal critical diameters were determined from quenched rounds. The results of this work have been checked by data obtained from quenched rounds and Jominy bars of steels containing iron, carbon, nickel, and low residuals.
- 5. Based on all the data available, the factor curves for carbon, manganese, and silicon have been derived so that they form a balanced system.
- 6. The multiplying factor principle proposed by Grossmann for the calculation

of hardenability from the chemical composition is valid. However, as indicated by Steven's data,⁵ the principle that alloying elements act independently must be modified when two or more stable carbide-forming elements are present. For

steels containing both chromium and molybdenum it has been found that their over-all effect on hardenability is less than would be predicted by the product of their individual factors. These statements may apply only when the austenitizing

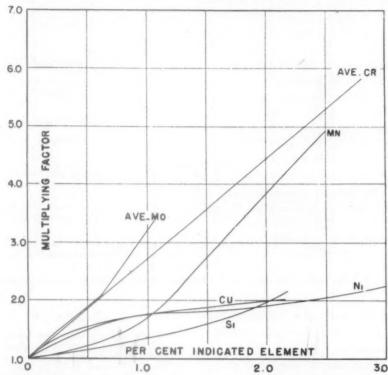


Fig. 25.—Composite chart of multiplying factors for various alloying elements.

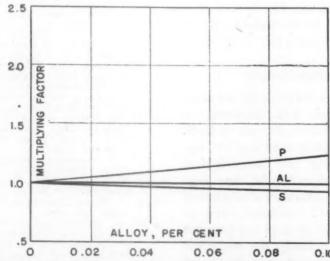


FIG. 26.—MULTIPLYING FACTORS FOR VARIOUS ALLOYING ELEMENTS.

treatment does not effect a complete solution of carbides.

7. Austenitizing temperature and time

Research Laboratory for their work of analyzing and preparing the specimens used in this paper.

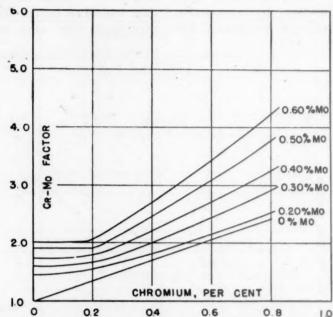


FIG. 27.—MULTIPLYING FACTOR FOR CHROMIUM-MOLYBDENUM COMBINATIONS.

at temperature markedly influence the effect of stable carbide-forming elements upon hardenability.

8. It is not necessarily true that many small additions of alloying elements are more effective in increasing hardenability than one large addition. The most effective combinations can be determined only by examining the individual factor curves.

ACKNOWLEDGMENTS

It is a pleasure to acknowledge the many helpful suggestions and criticisms of Dr. Francis M. Walters, Jr., and to thank Dr. Marcus A. Grossmann for his suggestions concerning the determination of ideal critical diameter for very lowalloy steels. The authors are also indebted to Mr. George F. Comstock, who so graciously supplied his data for titanium steels. Thanks are due to the Analytical and Metallography sections of the Naval

REFERENCES

- M. A. Grossmann: Hardenability Calculated from Chemical Composition Trans.
- A.I.M.E. (1942) 150, 227-257.

 2. W. Crafts and J. L. Lamont: The Effect of Silicon on Hardenability: Trans.
- A.I.M.E. (1943) 154, 386.

 Crafts and J. L. Lamont: The Effect of Some Elements on Hardenability Trans.
- A.I.M.E. (1944) 158, 157-167.

 4. I. R. Kramer, R. H. Hafner and S. L. Toleman: The Effect of Sixteen Alloying
- Elements on the Hardenability of Steel.

 Trans. A.I.M.E. (1944) 158, 138-156.

 5. W. Steven: The Effect on the Hardenability of Small Additions of Chromium and Molybdenum to a Grain Size Con-
- and Molybuenum to a Grain Size Controlled 0.9 Per Cent Nickel Steel. Inl. Iron and Steel Inst. (1944) 149, 230 P. E. Jominy and A. L. Boegehold: A Hardenability Test for Carburizing Steel. Trans. Amer. Soc. for Metals (1938) 26, 574.
- 7. M. A. Grossmann, M. Asimow and S. F. Urban: Hardenability, Its Relation to Quenching and Some Quantitative Data. Amer. Soc. for Metals, (1939) 125. 8. A. P. Edson: Discussion. Trans. A.I.M.E.
- 9. C. E. Jackson and A. L. Christenson:
 The Effect of Quenching Temperature
 on the Results of the End-quench Hardenablity Test. Trans. A.I.M.E. (1944) 158, 125-137.

- G. F. Comstock: Some Effects of Heattreatment on Low-alloy Titanium Steels. Trans. Amer. Soc. for Metals (1944)
- 11. T. F. Russell: First Report Alloy Steel Research Committee, Iron and Steel Inst. Special Report, (1936) 14, 149.
- M. Asimow and M. A. Grossmann: Hardening Characteristics of Various Shapes. Trans. Amer. Soc. for Metals (1940) 28,
- 949-978.

 13. M. Asimow and M. A. Grossmann: Correlation between Jominy Test and Quenched Round Bars. Jnl. Soc. Automotive Engrs. (1941) 40, 282-202
- motive Engrs. (1941) 49, 283-292.

 14. G. F. Comstock. Private Communication.

 15. W. T. Haswell. Naval Research Laboratory.
 Private Communications.

DISCUSSION

(C. M. Loeb, Jr., presiding)

M. A. GROSSMANN.*—The authors have been kind enough to let me see this work all during the course of its preparation, for which I want to express my thanks.

Their work points out one difficulty; namely, that the effects of the alloying elements cannot be determined by themselves apart from the effect of carbon. So that we must know first the effect of carbon on hardenability, and then by using carbon-manganese alloys or carbon-nickel alloys or carbon-molybdenum, or whatever, find the effect of the alloying element as it is superimposed on the effect of the carbon.

We believe that their carbon results, in being stated to be substantially higher than the former carbon factors, are in the right direction. We believe now that the earlier carbon values were too low; also, as a result, the former manganese factors were too high.

Our results did not happen to indicate values for carbon quite as large as those found by the present authors, but I should like to compliment the authors on their careful techniques.

^{*} Director of Research, Carnegie Illinois Steel Corporation, Chicago, Illinois.

Addition Method for Calculating Rockwell C Hardness of the Jominy Hardenability Test

BY WALTER CRAFTS,* MEMBER A.I.M.E., AND JOHN L. LAMONT*

(New York Meeting, October 1945)

ADEQUATE hardenability has long been recognized as one of the first requirements for producing desired mechanical properties in a heat-treated steel. Since the introduction of the Jominy end-quench test1 and the development of correlative information to expand its use, industry has had an effective measure of hardenability. Prediction and control of the hardenability have been made possible by Grossmann's principle² for calculating hardenability from chemical composition; and Field's conversion³ from depth of half-martensite hardening to Rockwell C hardness has made the relation more quantitative. These developments have facilitated the design of new steels and the control of standard grades to the extent that it has been possible to establish tentative hardenability bands for some of the more commonly used alloy steels.4

As the depth of hardening of the Jominy test specimen is usually measured by Rockwell C hardness, it was considered that it should be possible to predict the hardness by a more direct calculation. It has been found that this can be accomplished by the addition of Rockwell C units proportional to the carbon and alloy content, grain size, and position in the Jominy test specimen. The calculation has been found to be fairly accurate, and because of its additive character is relatively simple to use.

In principle the method of calculation is somewhat similar to the expressions developed by Herty, McBride, and Hollenback, Burns, Moore, and Archer, and Burns and Riegel.7 The calculation is started from a base that includes the effects of carbon content and position in the Jominy test speimen. Rockwell C units are added to the base in proportion to the alloy content and grain size. This sum represents the Rockwell C hardness up to the level at which a disproportionate increase of hardness is caused by the formation of martensite, and above this level an increment for martensite hardening is added. The effects of alloys are directly proportional to the amounts present and are independent of each other, the carbon content, and the position in the specimen. Furthermore, the factors for determining the martensite increment are dependent only on carbon content and are independent of cooling rate and alloy content. It is this absence of interrelation between the different factors that makes it possible to calculate the hardness and makes the method of calculation consistent with the principle that the character of the hardening reaction is governed primarily by carbon and that alloys exert their effect chiefly through control of the critical cooling rate.

The principle of the calculation, and the effects of alloys on the critical cooling rate,

Manuscript received at the office of the Institute March 20, 1945. Issued as T.P. 1928 in METALS TECHNOLOGY, October 1945.

* Research Metallurgist, Union Carbide and

Carbon Research Laboratories, Inc., Niagara

¹ References are at the end of the paper.

may be visualized by reference to the pattern of transformation indicated by the isothermal S-curve. The nonmartensitic hardness levels correspond to structures the total alloy and carbon content, estimation of the amount of martensite is indirect and, therefore, of doubtful value. On the other hand, Grossmann's multiplying

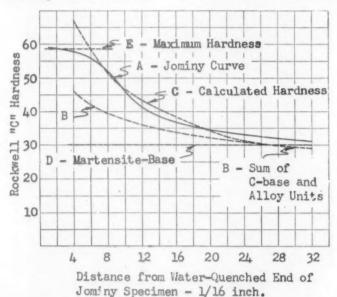


FIG. 1.—CALCULATED ROCKWELL C HARDNESS OF JOMINY CURVE FOR N.E. 8645 STEEL.

formed in time-temperature ranges beyond the end of transformation at the nose of the S-curve in which all of the austenite is transformed at elevated temperatures. The first appearance of martensite hardening corresponds to the end of transformation at the nose of the S-curve and attainment of full hardening corresponds to the beginning of transformation. The analogy is modified by the differences between continuous cooling and isothermal transformation, but even with this restriction a sufficiently quantitative relation has been established to justify the qualitative soundness of the concept. The hardness calculation reflects the effect of alloys on hardness over the range from submartensitic to wholly martensitic structures directly rather than by inference from some one critical point or structure.

Since the additive method is based on the effect of alloys on the hardness of nonmartensitic structures, and martensite hardening is calculated as a function of

method for determining the ideal critical diameter is based on the effect of composition on the half-martensite structure and for similar reasons is a relatively inaccurate guide to hardness. The main reason for the discrepancy appears to be the differences in the hardness of nonmartensitic structures that result from specific alloys and combinations of alloys. The difference in half-martensite hardness between steels of the same carbon content and different alloy compositions may be more than 15 Rockwell C and is difficult to predict on account of interrelated effects of carbon and alloys. The two methods of calculation, therefore, measure different properties and are considered to be complementary rather than substitutional.

OUTLINE OF METHOD

The method used for calculating Rockwell C hardness of the Jominy test specimen may be visualized in Fig. 1, which shows the Jominy curve determined by test on an N.E. 8645 steel as the solid line A. The calculated hardness is indicated by the dashed lines B, C, and E. In proceeding from the air-cooled end toward the

line C exceeds the maximum hardness (line E) that can be obtained in a steel of this carbon content. The maximum hardness shown by line E is considered to repre-

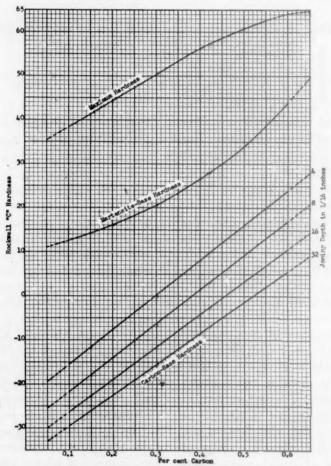


FIG. 2.—CARBON-BASE HARDNESS, MARTENSITE-BASE HARDNESS, AND MAXIMUM HARDNESS WITH RESPECT TO CARBON CONTENT.

water-quenched end of the specimen, the calculated hardness is represented by the simple sum of the effects of carbon and alloy content (line B) from $^32_{16}$ to $^27_{16}$ in. from the water-cooled end. Above the hardness level shown by line D, the hardness becomes higher than is indicated by line B, and an increment for martensite hardening is added to obtain the calculated hardness. This calculated hardness is represented by line C from $^27_{16}$ to $^47_{16}$ in. from the water-quenched end. At the $^47_{16}$ -in. point the hardness indicated by

sent the calculated hardness between the % 6-in. point and the water-quenched end of the specimen. The discrepancies between the actual and calculated hardness are fairly typical and result primarily from the characteristic shape of the Jominy curve for this specific type of steel, from the rounded shoulder of the Jominy curve, and from accidental errors. The degrees of divergence will be discussed in connection with the determination of the factors used for the calculation.

The different factors used in the calculation are shown in Figs. 2 to 6. In Figs. 2 and 3 is shown the "carbon-base hardness," which represents the hardness of "pure"

grain-size number represents the Rockwell C units to be added for the effect of grain size in the calculation. The Rockwell C addition units for alloys and grain size

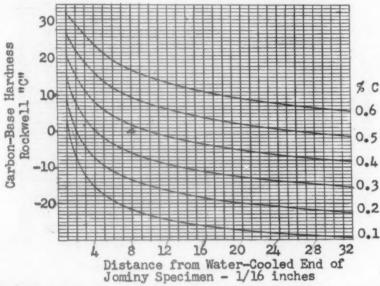


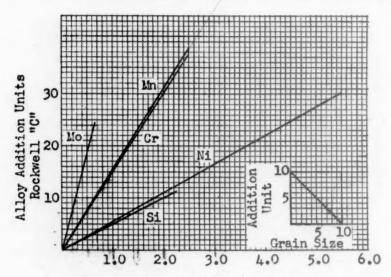
FIG. 3.—CARBON-BASE HARDNESS WITH RESPECT TO POSITION ON THE JOMINY TEST SPECIMEN.

iron-carbon alloys quenched at rates corresponding to different positions in the Jominy specimen. The carbon-base hardness number, which is expressed by an extrapolated Rockwell C scale, includes the effects of both carbon content and position in the specimen. As shown in Fig. 2, the carbon-base hardness is directly proportional to the carbon content; and, as shown in Fig. 3, it increases at an accelerated rate in approaching the water-quenched end of the specimen. The carbon-base hardness was determined for a No. 10 actual grain size.

The effects of manganese, silicon, nickel, chromium, and molybdenum on the Rockwell C hardness are shown as "alloy addition units" in Fig. 4. The effects of alloys differ with each alloying element, but in all cases the effect on hardness is directly proportional to the amount in the steel. Grain size has a similar effect, and the difference between No. 10 and the actual

are added to the carbon-base hardness, and their sum is the calculated Rockwell C hardness, if it is below the level at which martensite hardening becomes apparent.

When the observed hardness exceeds a certain level, it tends to become somewhat higher than is indicated by the sum of the carbon-base hardness and alloy addition units. The hardness level at which the disproportionate increase of hardness begins is designated as the "martensite-base hardness." The martensite-base hardness is not affected by alloy content or position in the specimen, but is dependent solely on carbon content, as indicated in Fig. 2. Above the martensite-base hardness level, the degree of the disproportionate increase is determined by the "martensite factor" shown in Fig. 5. This factor is multiplied by the number of Rockwell C units by which the sum of the carbon-base hardness and alloy addition units exceeds the martensite-base hardness. The product is then added to the martensite-base hardness to obtain the calculated hardness. The martensite factor increases progressively with the carbon content and is independent are added to the carbon-base hardness. This sum is indicated by line B in Fig. 1. The martensite-base hardness for the carbon content is taken from Fig. 2 or Fig. 6



Per cent Alloying Element

FIG. 4.—ALLOY ADDITION UNITS FOR INDICATED ELEMENTS, AND ACTUAL GRAIN SIZE.

of the effects of alloys and position. For convenience, the martensite increment has been computed and is included in the nomographic chart shown in Fig. 6.

The "maximum hardness," Fig. 2, represents the highest average hardness that is found in Jominy specimens of steel with the indicated carbon contents. As it is assumed that a higher hardness cannot be produced, the maximum hardness imposes a ceiling on the calculation. When the sum of the carbon-base hardness and alloy addition units plus the martensite increment is greater than the maximum hardness, the maximum hardness is considered to be the calculated hardness.

The method of calculation for steel of a given composition, such as the N.E. 8645 steel shown in Fig. 1, is to determine the carbon-base hardness for the carbon content of the steel at the desired point on the Jominy specimen from Fig. 2 or Fig. 3. The alloy addition units, from Fig. 4, for each element and for the actual grain size

and is illustrated as line D in Fig. 1. Lines B and D cross at the 21/16-in. point, so that the martensite increment must be added for points nearer to the waterquenched end. The calculated hardness including the martensite increment shown by line C may be obtained by multiplying the difference between lines B and D by the martensite factor (Fig. 5) and adding the sum to the martensite-base hardness, or the calculated hardness may be determined directly from Fig. 6. The maximum hardness is taken from Fig. 2 or Fig. 6 and is indicated by line E in Fig. 1. Lines C and E intersect at the 6/16-in. point, so that the calculated hardness is the same as the maximum hardness at points nearer to the water-quenched end of the specimen. The Jominy hardness of the N.E. 8645 steel illustrated in Fig. 1 is calculated as shown in Table 1.

The hardness calculated for the ³%₁₆-in. position is below the martensite-base hardness of 30.0 Rockwell C indicated for

o.45 per cent carbon steel in Fig. 2, so that 29 Rockwell-C represents the calculated hardness at this position and compares with the hardness of 31 Rockwell C deter-

In using Fig. 6, the sum of carbon-base and alloy units is found on the right-hand side and is followed toward the left along the curved lines until the carbon content

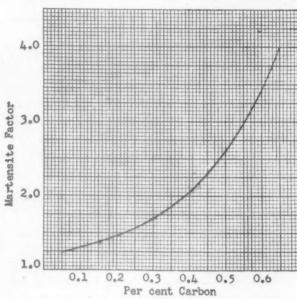


FIG. 5.—FACTOR FOR DETERMINING MARTENSITE INCREMENT.

mined by test. The other locations are higher than the martensite-base hardness,

Table 1.—Jominy Hardness of N.E. 8645

Steel	
COMPOSITION, PER CENT A	DDITION UNITS
0.45 carbon	
0.85 manganese	13.2
0.22 Silicon	I.I
0.50 nickel	2.7
0.50 chromium	7.5
0.20 molybdenum	7.5
No. 8 grain size	2.0
Alloy addition units	

ence	1/16	%16	1916	83/16
				710
Pig. 2	+12.1	+ 5.4	- 0.3	- 5.0
Pig. 4	34.0 46.1	34.0 39.4	34.0 33.7	34.0
Pig. 6	58.6	51.6	38.5	29.0
	Pig. 4	Fig. 4 34.0 46.1 Fig. 6 58.6	Fig. 4 34.0 34.0 39.4 Fig. 6 58.6 51.6	Fig. 4 34.0 34.0 34.0 34.0 34.0 35.7 Fig. 6 58.6 51.6 38.5

and the calculated hardness may be obtained from the nomographic chart, Fig. 6.

of the steel is reached. The hardness calculated to include the martensite increment is then read by the horizontal lines from the scale at the left. If the indicated hardness is above and to the left of the maximum hardness line, as it is at the ½ 6-in. point, the maximum hardness for the carbon content is considered to be the calculated hardness.

DETERMINATION OF ADDITION INCREMENTS

The carbon-base hardness, alloy addition units, and martensite increment factors shown in Figs. 2 to 6 were developed by the reverse of the method outlined for the calculation of hardness. A carbon-base hardness was estimated for one location on the Jominy specimen and subtracted from the actual hardness determined at that point on Jominy test specimens of a series of shallow-hardening plain manganese steels. The line representing the approximate increment of hardness due to man-

ganese was fairly straight and indicated that the addition method might be suitable. The manganese increment was then subtracted from the actual hardness values to develop a more accurate carbon-base factors accurately. The data from 448 steels were used for determining the factors, but this number probably represents only a bare minimum for indicating the feasibility of the method.

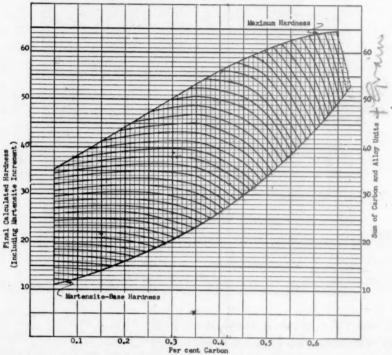
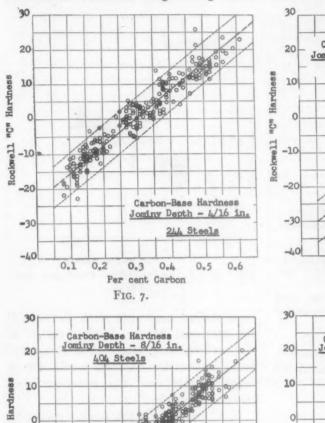
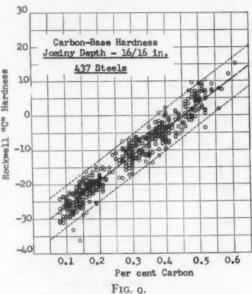


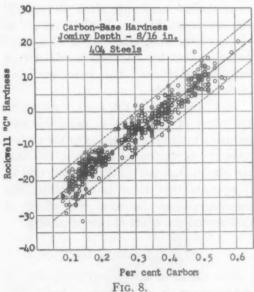
FIG. 6.—DIAGRAM FOR OBTAINING CALCULATED HARDNESS INCLUDING MARTENSITE INCREMENT FROM SUM OF CARBON-BASE HARDNESS AND ALLOY UNITS.

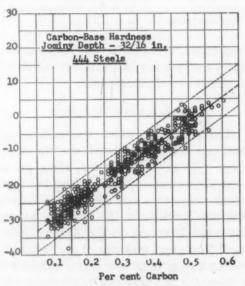
hardness and to adjust it to a No. 10 grain size. Subsequently the Jominy test data of steels containing the other alloys were studied to determine their respective effects. The alloy increments were used to determine the carbon-base hardness at other positions nearer to the waterquenched end of the specimen. By using steels that were relatively soft at the aircooled end, and noting the divergence at points nearer the water-cooled end, it was possible to determine the martensite factor. The carbon-base, position, alloy, and martensite factors were successively redetermined until no significant changes were indicated. It was found that a great number of steels covering a wide range of composition are necessary to establish the

The data used for the determination of the factors were restricted as much as possible to simple types in which only one alloying element was predominant. The steels covered a range of composition from 0.08 to 0.61 per cent carbon, and up to 2.68 per cent manganese, 2.18 per cent silicon, 5.32 per cent nickel, 2.53 per cent chromium, 0.62 per cent molybdenum, 0.047 per cent phosphorus, 0.058 per cent sulphur and 0.97 per cent aluminum. The actual grain sizes ranged from No. 3 to 9½ and, as far as is known, the fine-grained steels were treated with aluminum. The effects of other grain-refining elements were not included in this investigation. Of the 448 steels used in determining the factors, 137 were experimental high-frequency or arc-furnace steels made and tested at the Union Carbide and Carbon Research Laboratories; 69 were commercial steels of the British Standard Engineering Steel 242 were taken from data on commercial S.A.E. and N.E. steels produced and tested by several companies. Actual grain-size data were lacking for the last group of









Figs. 7 and 8.—Effect of carbon on base hardness on Jominy test specimens.

Figs. 9 and 10.—Effect of carbon on base hardness on Jominy test specimens.

types supplied by the Technical Advisory Committee of the Special and Alloy Steels Committee (Steel Control of the Ministry of Supply) and tested at the Union Carbide and Carbon Research Laboratories, and steels, which were assumed to be No. 8 grain size. The samples tested at the Union Carbide and Carbon Research Laboratories were prenormalized and quenched from conventional heat-treating temperatures,

and it is presumed that the commercially tested steels were treated in an equivalent manner. The amount and confidential character of some of the data make it the 1/6-in. position accurately, but the available data have been shown in Fig. 11, in order to permit an estimate of whether

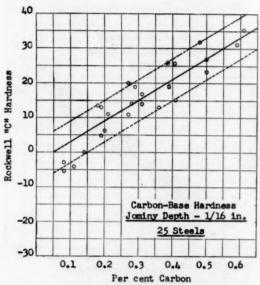


FIG. 11.—EFFECT OF CARBON ON BASE HARDNESS AT A DEPTH OF 1/16 INCH ON JOMINY TEST SPECIMEN.

impossible to tabulate the composition, grain size, Jominy hardness and calculated hardness of individual steels.

CARBON-BASE HARDNESS

The points on which the carbon-base hardness were established are shown in Figs. 7 to 11. As indicated, these points were determined by subtracting the martensite increment and alloy and grain-size addition units from the hardness at the indicated locations on the Jominy specimen. The great majority of the points lie within a band of plus or minus 6 Rockwell C from the line drawn through the middle of the range. As the data were insufficient to provide a statistical basis for establishing a mean, it was necessary to draw the trend lines by inspection. More emphasis was given to the extreme edges of the consistent band than to the averages of the points. Too few points were available to establish the carbon-base hardness of the maximum hardness can be obtained Manganese 50 134 Steels 40

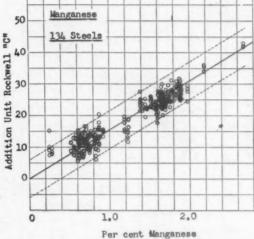


FIG. 12.—ALLOY ADDITION UNIT FOR MAN-GANESE.

in a shallow-hardening steel. Because of the steepness of the Jominy curves of shallow-hardening steels, it is considered probable that the hardness would not be very accurate near the water-quenched end of such steels.

At all positions in the Jominy specimen, the effect of carbon is to raise the base hardness in direct proportion to the carbon content. As illustrated in Fig. 2, the lines are almost, but not quite, parallel; that is, it appears that there is relatively little interdependence between the effect of carbon and the effect of rate of cooling.

ALLOY ADDITION UNITS

The effects of alloys and grain size on hardness are shown in Figs. 12 to 20. The points shown on the diagrams represent the \$16, \$16, 1616 and 3216-in. positions except when the actual hardness approached the maximum hardness. The effects of copper and other secondary elements were neglected. The increments of hardness due to all of the alloys may be

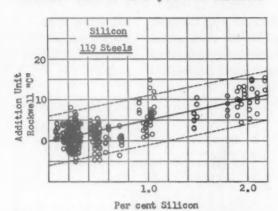


FIG. 13.—ALLOY ADDITION UNIT FOR SILICON.

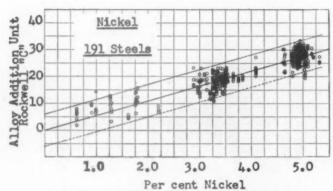
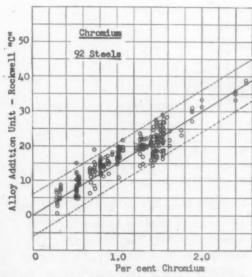


Fig. 14.—Alloy addition unit for nickel.



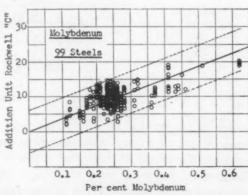


FIG. 15.—ALLOY ADDITION UNIT FOR CHROMIUM. FIG. 16.—ALLOY ADDITION UNIT FOR MOLYB-DENUM.

represented by straight lines with the same degree of accuracy as for the carbon-base hardness. Thus, the effect of each alloy increases in direct proportion to the amount hardening than is indicated by the nonmartensitic addition unit, but the relative effects of different alloys are in the same proportion.

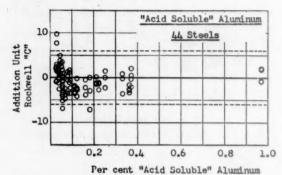


Fig. 17.—Alloy addition unit for aluminum.

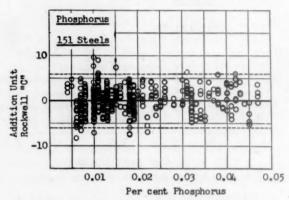


FIG. 18.—ALLOY ADDITION UNIT FOR PHOSPHORUS.

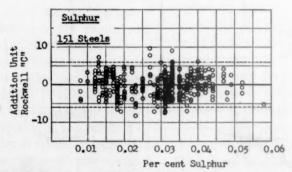


FIG. 19.—ALLOY ADDITION UNIT FOR SULPHUR.

and is independent of position in the specimen. It is, therefore, relatively easy to evaluate the effects of individual alloys on Rockwell-C hardness over the whole of the Jominy specimen. In the martensitic range alloys produce a greater degree of The increment of hardness for each 1 per cent of alloy is shown in Table 2 in comparison with the Grossmann multiplying factors determined previously by the authors. Since the multiplying factors measure the effect on the half-martensite

structure, and the hardness addition units measure the effect on nonmartensitic structures, the comparison is not qualitatively sound, and is justified only because the mium and molybdenum, however, add much more to hardness than might be anticipated from the relative size of their multiplying factors in comparison with

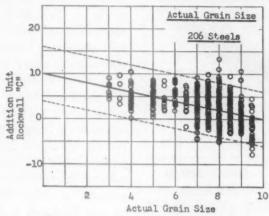


FIG. 20.—ADDITION UNIT FOR GRAIN SIZE.

two methods of calculation may be used for the same purpose.

Table 2.—Comparison of Multiplying
Hardness

Element	Rc Units per I Per Cent of Alloy	Multiplying Factor	Ratio of Addition Units to Multiplying Factor for I Per Cent of Alloy
Manganese	15.5	1 + (4.08) (% Mn)	3.1
Silicon Nickel	5.0 5.5	up to 1.7 % Mn 1 + (0.67)(% Si) 1 + (0.74)(% Ni)	3.0
Chromium Molybdenum	15.0 37.5	up to 3.2 % Ni 1 + (2.16)(% Cr) 1 + (2.53)(% Mo)	4.7

Phosphorus, sulphur, and aluminum, which have significant effects on ideal critical diameter, were found to have no appreciable effect on hardness within the ranges covered in this investigation. The relative effects of manganese, silicon, and nickel are similar in that their hardness increments are in about the same relative ratio as their multiplying factors. Chro-

manganese, silicon, and nickel. It is evident that the evaluation of the effects of alloys on hardenability is dependent on the criterion used for measuring hardenability.

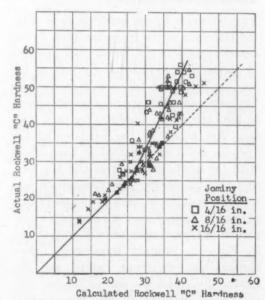


FIG. 21.—METHOD OF DETERMINING MARTEN-SITE BASE HARDNESS AND MARTENSITE FACTOR FOR 0.38 TO 0.42 PER CENT CARBON STEELS.

MARTENSITE INCREMENT

The martensite increment was determined by divergence of hardness above that calculated as the sum of the carbonbase hardness and alloy addition units. Although this extra increment of hardness is considered to be due to martensite, it

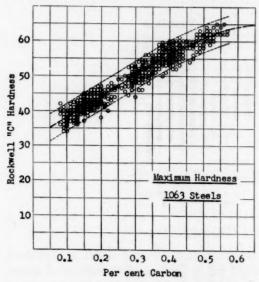


FIG. 22.—RELATION BETWEEN MAXIMUM HARDNESS OBTAINED ON JOMINY TEST SPECIMENS AND CARBON CONTENT.

was determined from hardness alone without reference to the microstructure. In the determination of the factor, the hardness of steels that were relatively soft at the 32/16-in. point was assumed to be the true hardness, and the appropriate increment in the carbon-base hardness for each position was added to the hardness at the 33/16-in. point and plotted in comparison with the actual hardness at the 1/16, 8/16, and 16/16-in. points. This comparison was made with suitable steels in ranges of 0.05 per cent carbon at intervals of 0.05 per cent carbon. A typical correlation chart is shown in Fig. 21. Straight lines were drawn through the divergent points, and the intersections with the line of 100 per cent correlation resulted in the "martensitebase hardness" line shown in Fig. 2. The slopes of the divergent lines permitted the development of the martensite factor shown in Fig. 5. Thus, if the amount by which the sum of the carbon-base hardness and alloy addition units exceeds the martensite-base hardness is multiplied by the martensite factor, and the product is added to the martensite-base hardness, the resultant calculated hardness follows a divergent line corresponding to that shown in Fig. 21. In order to facilitate its use, the martensite increment has been computed over the whole range and included in the nomographic chart of Fig. 6.

Both the martensite-base hardness and the martensite factor become higher as the carbon content is increased. The martensite increment is independent of position in the Jominy specimen and of the alloy composition, and is dependent only on the carbon content. It is evident that the same amounts of alloys that raise the hardness by one Rockwell C addition unit in the nonmartensitic range are sufficient to raise the hardness in the martensitic range by 1.25 to 4 Rockwell C, depending on carbon content.

MAXIMUM HARDNESS

Maximum hardness was presumed to be dependent only on carbon content. The line shown in Fig. 22 was derived from data on 1063 commercially produced and tested steels. Relatively shallow-hardening steels that might not have attained full hardness were not used for this purpose. The line was constructed by averaging the maximum hardness values at each carbon content and then averaging the averages of five adjacent carbon contents to determine the hardness of the middle carbon content. Below 0.45 per cent carbon, this line agrees quite well with that given by Parker.³

At carbon contents where a considerable number of points were available, the maximum deviation from the average was slightly greater than plus or minus 4 Rockwell C. This illustrates what has appeared to be the greatest difficulty in attempting to calculate hardness. A large part of the differences shown in the diagrams for carbon-base hardness and alloy

addition units seemed to be derived from errors in analysis, segregation, heat-treatment and hardness testing. These errors appeared to account for about half of the divergence from the calculated hardness. In view of the current effort to supply steel within narrow hardenability bands, it appears that some study of hardness testing would be desirable. The Rockwell tester itself is guaranteed to have an accuracy of only plus or minus 2 Rockwell C, and careful maintenance is required to stay within this range. The degree of microsegregation in the steel also seems to be a prominent source of error, especially in the parts of the specimens that are not completely hardened.

Discussion of the Method of Calculation

In summarizing the development of a method for calculating the Rockwell C hardness of the Jominy test specimen, it appears that the addition principle is a reasonable approach to the problem. The increments of Rockwell C hardness due to carbon and alloys are directly proportional to the amounts present. These increments are additive, so that their sum, including that for grain size and with the appropriate martensite increment, represents the hardness of the steel within an error of about plus or minus 6 Rockwell C. Although the calculation has been developed with respect to position in the Jominy specimen, the calculation may also be used with reference to rate of cooling9 or to diameter of the quenched bar.10

It is notable that of the different types of factor used in the calculation, only the carbon-base hardness is dependent on cooling rate or position in the specimen, and even this relation is of a secondary order. The alloy and grain-size increments are entirely independent of the other factors, whereas the carbon-base hardness, martensite-base hardness, martensite factor and maximum hardness are dependent on

carbon. Therefore it appears that the alloy factors and the cooling-rate factor are qualitatively quite similar. The character of the factors, therefore, confirms the long recognized principle that hardening is essentially a reaction of the iron-carbon alloy and that the hardening effect of alloys is almost entirely exerted through control of the rate of the reaction. This concept is an obvious oversimplification, but it serves to indicate that the method of calculation is rational.

JOMINY HARDNESS OF S.A.E. AND N.E. STEELS

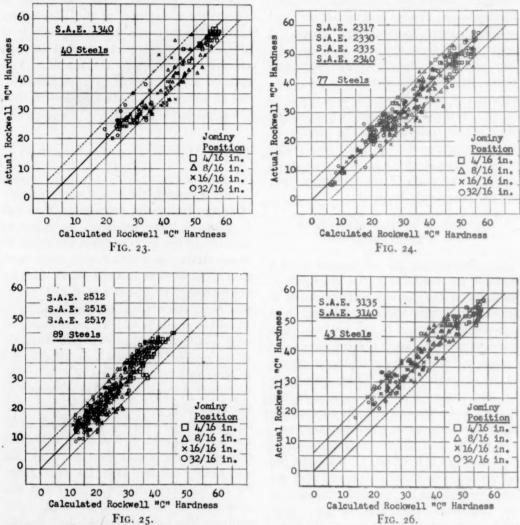
As mentioned, the steels used to determine the factors for calculating Rockwell C hardness were restricted as much as possible to the simpler types. In order to demonstrate the correlation in more complex types of heat-treating steels, data on commercially produced and tested S.A.E. and N.E. steels are shown in Figs. 21 to 36 for the grades in which enough examples were available to illustrate the character of the results. The steels were all assumed to have an actual grain size of 8. With the exception of three heats, all of the available examples were included unless the chemical analysis was incomplete or a coarse grain size was indicated. Of the three heats discarded, one had a maximum hardness that was greatly different from the usual range for the indicated carbon content and was presumed to have been of some other analysis. The other two steels had Jominy curves typical of an effective boron treatment.

The comparison of actual and calculated hardness of plain manganese S.A.E. 1340 steel is shown in Fig. 23. The correlation was fairly good at the ½16 and ½16-in. points, but the calculation tended to give high results at the ¾16 and ½16-in. points. This reflects the tendency of this steel to have a more abrupt change from non-martensitic to martensitic hardness levels

than the average Jominy curve on which the calculation is based.

The 3.5 per cent nickel steels (S.A.E. 2317, 2330, 2335 and 2340), shown in Fig.

The chromium-nickel steels, S.A.E. 3135 and 3140 (Fig. 26), show a slight tendency for the actual hardness to be slightly greater than the calculated hardness. The



Figs. 23 TO 26.—Comparison between actual and calculated hardness determined on S.A.E. steels.

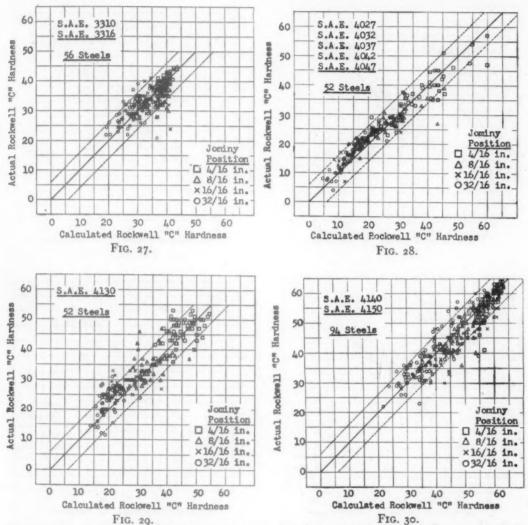
24, show fairly good correlation over the whole range, with a slight tendency for the actual hardness to be slightly lower than the calculated hardness. The 5 per cent nickel carburizing steels, S.A.E. 2512, 2515, and 2517 (Fig. 25), show a good fit, with some tendency for the actual hardness to be slightly higher than the calculated hardness near the water-quenched end of the specimen.

high-chromium-nickel carburizing steels, S.A.E. 3310 and 3316 (Fig. 27) have a good fit except for one widely divergent value. Such examples, which are well beyond the limit of reasonable error, are encountered more or less infrequently and appear to be due primarily to some unaccountable error, such as mixed steel, clerical mistakes, or faulty testing. Usually these heats show no abnormality in com-

position that would explain the reported hardness.

The lower carbon steels of the plain molybdenum group, S.A.E. 4027, 4032,

greater than the normal degree of error. A similar proportion of points with more than the usual error was found in the higher carbon S.A.E. 4140 and 4150 steels shown



Figs. 27 to 30.—Comparison between actual and calculated hardness determined on S.A.E. steels.

4037, 4042 and 4047 (Fig. 28), tend to have a higher than calculated hardness through the middle part of the specimen.

The lower carbon chromium-molybdenum steels, S.A.E. 4130 (Fig. 29), show a tendency for the calculated hardness to be slightly low near the air-cooled end of the specimen. There also appears to be a relatively high proportion of steels with in Fig. 30. The steels containing combinations of chromium and molybdenum have been reported² to develop less than the calculated ideal critical diameter, but no evidence of such a tendency has been observed in the calculation of hardness.

The nickel-chromium-molybdenum steels, S.A.E. 4320 and 4340 (Fig. 3i), have good correlation between actual and

calculated hardness. This is also true of the nickel-molybdenum steels, S.A.E. 4615, 4620, and 4640 (Fig. 32), and of S.A.E. 4815 and 4820 (Fig. 33).

range of error, although the average of calculated hardness is slightly lower than the actual hardness. The medium-carbon group, N.E. 8630, 8635, 8730, and 8735

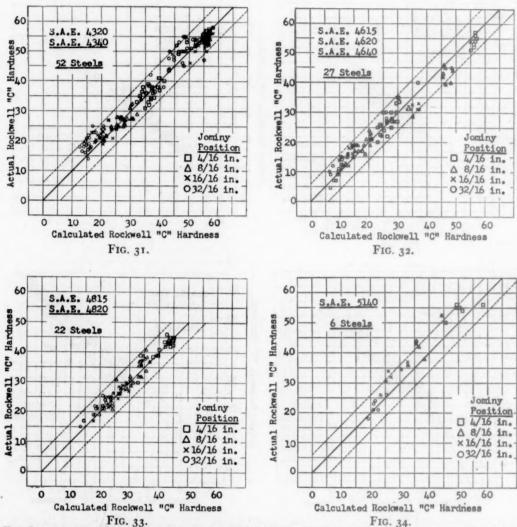


Fig. 33. Fig. 34.—Comparison between actual and calculated hardness determined on S.A.E. steels.

The number of plain chromium steels, S.A.E. 5140 (Fig. 34), is insufficient to represent the type of steel. The examples shown, however, are quite consistent and have slightly higher than calculated hardness through the whole range.

The low-carbon nickel-chromium-molybdenum carburizing steels, N.E. 8615, 8620, and 8720 (Fig. 35), are within the normal (Fig. 36), tend to have slightly lower than, calculated hardness at the $^3\frac{2}{16}$ -in. point but are generally within the usual range of error. In the higher carbon groups, N.E. 8640 and 8740 (Fig. 37), and N.E. 8645, 8650, 8745 and 8750 (Fig. 38), there is a tendency for the calculated hardness to be slightly high through the middle of the specimen. This appears to be due to an

incomplete correction for the abrupt change in the slope of the Jominy curve similar to that noted in the plain manganese steels. With the exception of a few scattered ening and testing procedures, but a part is due to consistent divergence from the typical shape of the average Jominy curve that is inherent to the calculation. The

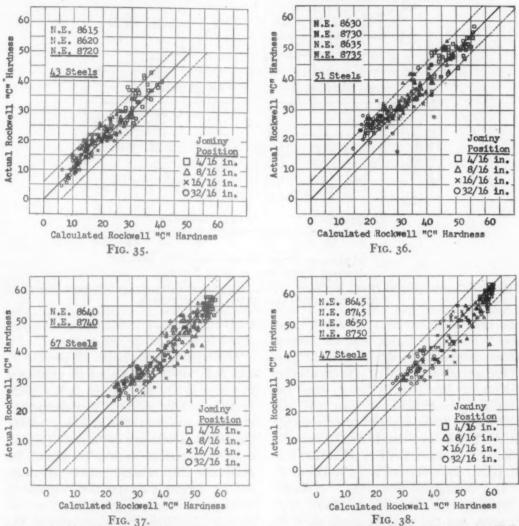


Fig. 37.

Fig. 38.

Figs 35 to 38.—Comparison between actual and calculated hardness determined on N.E.

points and the tendency toward lower than calculated hardness in the middle range of the plain manganese and the higher-carbon N.E. 8600 and 8700 steels, the calculated hardness of the S.A.E. and N.E. steels is accurate within the same degree of error that was indicated in the determination of the factors. A part of the error results from deficiencies in the hard-

character and degree of this divergence were difficult to estimate with the data available, as a large number of examples of one grade representing a number of sources is required for demonstrating the typical shape of the Jominy curve. Among the grades of steel that were suitable for this purpose there were a sufficient number only of S.A.E. 1340, 2340, 4130, and N.E.

8640. The average Jominy curves of actual and calculated hardness of these steels are shown in Fig. 39. As was found in the comparison of individual points, the aver-

different types of steel. The error from this source is probably of the same order as that involved in hardness testing, and under controlled conditions it is probable

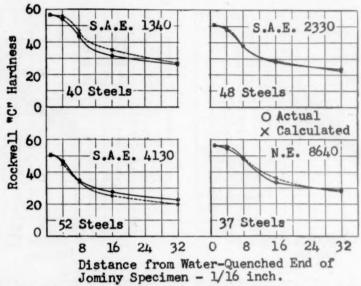


Fig. 39.—Comparison between average actual and average calculated Jominy curves of S.A.E. 1340, 2330, 4130 and N.E. 8640 steels.

age calculated hardness of S.A.E. 1340 and N.E. 8640 is higher than the average actual hardness through the middle part of the specimen. In S.A.E. 4130 the average calculated hardness is lower than the average actual hardness near the aircooled end. There is very little divergence in the S.A.E. 2330 steel. At the point of poorest agreement, S.A.E. 1340 at the ¹⁶16-in. point, the difference is 3.5 Rockwell C.

The divergence from the "average" Jominy curve is characteristic of each type of steel, but the complex steels show no consistent tendency resulting from the combination of alloys. In the intermediate, partially martensitic part of the Jominy curve, the chromium-molybdenum steel S.A.E. 4130 has slightly higher than the calculated hardness, whereas the nickel-chromium-molybdenum steel, N.E. 8640, has less than the calculated hardness. The divergences are smaller than might have been expected from the different types of microstructure that may be produced in

that much closer estimates of hardness might be made on specific grades.

Although this discussion of the S.A.E. and N.E. steels has tended to emphasize the error in the calculation, it is evident that the general suitability of the method of calculation and the accuracy of the individual factors are confirmed. The calculation therefore should be useful for evaluating the relative effects of alloys and for designing compositions capable of developing a desired hardness. One use may be illustrated by comparison of the actual and calculated Jominy hardness with the tentative hardenability band4 of N.E. 8640 in Fig. 40. The degree of agreement is sufficiently good to suggest that the calculation has a degree of accuracy that may be useful for controlling hardenability.

CONCLUSIONS

It may be concluded from this study of the Rockwell C hardness of the Jominy test that: 1. The Jominy hardness of steel may be calculated in terms of Rockwell C units by addition of empirically determined increments for alloys, grain size, and mar-

Rockwell C, or, depending on carbon content, these amounts of alloy raise the hardness by 1.25 to 4 Rockwell C.

In comparison with the multiplying

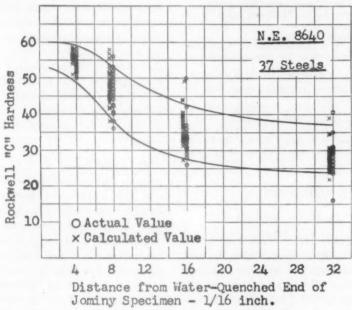


Fig. 40.—Comparison of actual and calculated hardness with the tentative hardenability band for N.E. 8640 steel.

tensite to the base hardness corresponding to that of a "pure" iron-carbon alloy cooled at a certain rate. The calculation usually is accurate within a range of about plus or minus 6 Rockwell C, of which approximately one half results from errors in testing and the other half is caused by real differences between steels of different compositions.

2. The increments of hardness added by alloys are directly proportional to the amount present and are independent of position in the Jominy specimen, so that their relative effects may be evaluated simply. The amounts of alloying elements required for one Rockwell C addition unit are as follows: manganese, 0.065 per cent; silicon, 0.200; nickel, 0.182; chromium, 0.067; molybdenum, 0.027. In the martensitic range the effects of the alloying elements are in the same proportion but

smaller amounts raise the hardness by one

factors used for calculating ideal critical diameter, the alloy addition increments maintain a similar ratio for manganese, silicon, and nickel, whereas chromium and molybdenum have a relatively greater effect on Rockwell C hardness. Steels with combinations of alloys, such as chromium and molybdenum, have been found to develop the full hardness estimated from the individual effects of their component alloys.

3. The validity of the calculation of the hardness of the Jominy test specimen has been confirmed on data from standard grades of steel, and the degree of accuracy indicates that the calculation may be useful in facilitating the prediction and control of hardenability.

REFERENCES

 W. E. Jominy and A. L. Boegehold: Trans. Amer. Soc. for Metals (1938) 26, 574-599.

- 2. M. A. Grossmann: Trans. A.I.M.E. (1942)
- 150, pp. 227-255. 3. J. Field: Metal Progress (March 1943)
- 402-405.
 4. Tentative Hardenability Bands. Contributions to the Metallurgy of Steel, No. 11.
 Soc. Auto. Engineers Inc., and American
 Iron and Steel Institute, July 1944.
 5. C. H. Herty, D. L. McBride, and E. N.
 Hollenback: Trans. Amer. Soc. for
- Metals (1937) 25, 297-314.
 6. J. L. Burns, T. L. Moore, and R. S. Archer:
 Trans. Amer. Soc. for Metals (1938) 26,
- 7. J. L. Burns and G. C. Riegel: Hardenability of Alloy Steels, 262-291. Amer. Soc. for Metals, 1939.
- W. Crafts and J. L. Lamont: Trans. A.I.M.E. (1944) 158, 157-167.
 W. E. Jominy: Amer. Soc. for Metals, 1939.
- Hardenability of Alloy Steels, 66-87.
- 10. J. L. Lamont: Iron Age (Oct. 14, 1943), 152, 16, 64-70.

DISCUSSION

(C. M. Loeb, Jr., presiding)

F. M. WALTERS, JR. *-When I read this paper, I was a little disappointed because we had a phenomenon in which the combined effect of alloying elements was gotten by adding the effect of individual elements when we have so many phenomena in steel where the effect multiplies; that is, a given amount of an alloying element increases the tensile strength of a 50,000-lb. steel by 10,000 lb. per sq. in. The same amount of alloying element will increase a 100,000-lb. steel by 20,000 lb., that is, by 20 per cent. Gensamer

found that the effect of alloying elements on the strength of ferrite followed the same sort of law. However, if you look into the method of measuring hardness, the Rockwell C is a perfectly arbitrary scale, and if we compare a Rockwell C with tensile strength or Brinell hardness, you will find that as we go to the higher Rockwell numbers we get a greater increase in tensile strength, and apparently that comes in so that roughly we do have here multiplication; that is, increment of Rockwell C for an alloying element gives a greater increase in tensile strength or Brinell hardness at the higher hardness levels than at the

W. CRAFTS and J. L. LAMONT (author's reply).—The authors agree with Dr. Walters that the addition of Rockwell C hardness units is essentially a multiplying operation, since the Rockwell C hardness scale is roughly proportional to the logarithm of the tensile strength or the Brinell hardness. Since Jominy specimens are readily tested by Rockwell hardness, the use of Rockwell C units for measuring the effects of the alloys is direct and additive, so that comparative evaluation is relatively simple. Although the addition of Rockwell C units is essentially multiplicative and therefore similar in character to other methods of estimating the effects of alloys on tensile strength, it is specifically advantageous in estimating hardenability, as the errors involved in estimating ideal critical diameter are avoided.

^{*} Naval Research Laboratory, Anacostia Station, Washington, D. C.

The Influence of Titanium on the Hardenability of Steel

By G. F. Comstock,* Member A.I.M.E.

(New York Meeting, October 1945)

A SERIOUS disagreement as to the effect of titanium on the hardenability of steel exists in published references to this subject. Kramer, Hafner and Toleman reported that acid-soluble titanium decreased the hardenability, with multiplying factors less than unity according to

tion for the carbon that was combined with titanium and therefore occurred in a similarly ineffective form.

It is suggested by the literature referred to that titanium may have different effects on hardenability, depending on the mode of its occurrence in the steel. The different

TABLE 1.—Chemical Analyses of Steels

Steel No.		Acid- soluble	Total							
No.	С	Mn	Si	Cu	Ni	Cr	Мо	v	Al	Ti
1 2 3 4 5	0.360 0.368 0.367 0.364 0.404	0.68 0.62 0.63 0.66 0.66	0.22 0.28 0.33 0.38 0.19	0.040 0.042 0.038	0.038 0.052 0.046	0.07I 0.072 0.076	0.003	0.00I 0.00I 0.10	0.163 0.183 0.077	0.055 0.360 0.777

Grossmann's system for calculating hardenability from the composition. Crafts and Lamont, on the other hand, showed2 how titanium increased the hardenability, with multiplying factors up to nearly 1.7 for about o.1 per cent titanium, though reducing the hardenability with higher titanium. Their data, however, were obtained almost exclusively from steels containing more than 1.4 per cent manganese, and thus should be considered as applying mainly to manganese steels. Likewise, the results of Kramer, Hafner and Toleman regarding titanium are subject to the limitation that although they eliminated the effect of the insoluble titanium compounds from their calculations, they did not make a similar correceffects on strength, ductility, etc., have already been discussed by the author.³ In the present discussion some comparisons, on the basis of hardenability as revealed by the Jominy end-quench test, are given between three titanium and two non-titanium steels heat-treated in the same ways, and between other titanium steels heat-treated in several different ways.

COMPARISON OF PLAIN-CARBON, VANADIUM AND TITANIUM STEELS

The five steels used for these experiments were commercially melted and rolled products received in the form of 1.5-in. rounds from three different mills. Their analyses are given in Table 1.

Steels 2, 3, and 4 are from the same basic electric heat, containing 0.009 per cent of phosphorus and the same amount of sulphur. They were made by adding aluminum and low-carbon ferrotitanium to different ingots. No. 1 is a plain carbon

Manuscript received at the office of the Institute Jan. 24, 1945. Listed for New York Meeting, February, 1945 which was canceled. Issued as T.P. 1904 in METALS TECHNOLOGY, September 1945.

September 1945.

* Metallurgist, Titanium Alloy Manufacturing Co., Niagara Falls, New York.

1 References are at the end of the paper.

coarse-grained S.A.E. 1040 steel made by the basic open-hearth process. No. 5 is a vanadium steel made in a basic electricarc furnace. This is the same steel desdiameter were machined from the samples. and after heating in various ways were end-quenched by the standard Jominy procedure. In heating, the bottom ends of

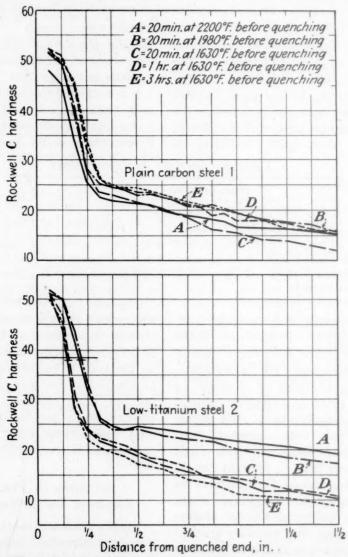


FIG. 1.—HARDNESS DISTRIBUTION ALONG SIDES OF END-QUENCHED SPECIMENS.

ignated as V in the author's paper referred to above;³ No. 1 is the steel designated as O in that paper, and No. 3 the same steel as T.

Samples of 1.5-in. rounds of these five steels, 6 in. to about one foot long, were heated for 4 hr. at 2200°F. and air cooled. Hardenability test specimens of 1-in.

the specimens were protected from scaling by insertion in close-fitting holders or cups of high-chromium steel. By preliminary heating of a dummy specimen having a central hole in which a thermocouple was placed, it was determined that, with the cup already at the furnace temperature, about 20 min. was required for the inserted specimen to come up to the same temperature. The heating times for the specimens to be quenched were measured from the expiration of that period. These heating without heating, along the sides of the specimens, and the Rockwell-C hardness was determined at various distances from the quenched end. The average results are

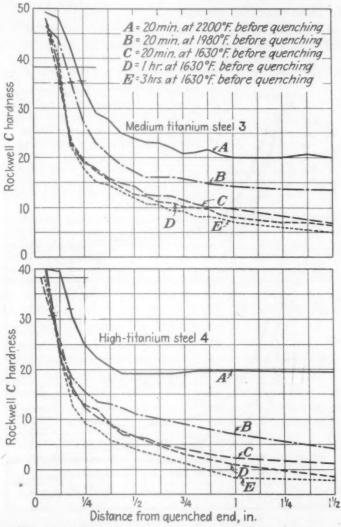


Fig. 2.—HARDNESS DISTRIBUTION ALONG SIDES OF END-QUENCHED SPECIMENS.

times, and the temperatures, were as follows for the different specimens of each steel:

A, 20 min. at 2200°F. B, 20 min. at 1980°F. C, 20 min. at 1630°F. D, 1 hr. at 1630°F. E, 3 hr. at 1630°F.

After end-quenching from these temperatures, two flat strips were ground carefully, plotted on Figs. 1, 2, and 3. Subsequently the microstructure of one flat strip of each specimen was examined near the quenched end to determine the grain size and the distance from that end to the point where there was only 50 per cent martensite; and the softer end of each specimen of the titanium steels was sampled for chemical determination of the soluble and insoluble titanium.

For the determination of soluble titanium, the samples were dissolved in 10 per cent sulphuric acid, heated without boiling until the reaction ceased. Special care was found to be necessary in filtering to separate the finest insoluble particles from the solution. Filtering through packed paper pulp about ½ in. thick seemed to be

29 of Grossmann's paper on hardenability calculated from cehmical composition,⁴ or the formula

Rockwell C (for 50 per cent martensite) = 24.6+ per cent carbon × 37.4.

The longer horizontal lines cutting the hardenability curves of Figs. 1, 2, and 3

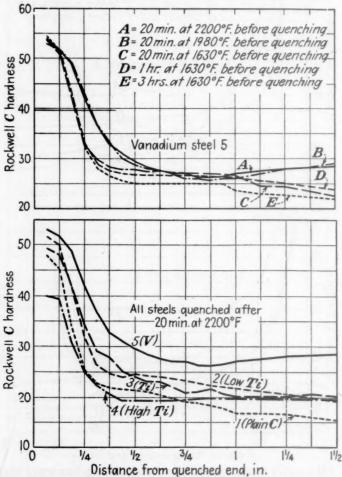


FIG. 3.—HARDNESS DISTRIBUTION ALONG SIDES OF END-QUENCHED SPECIMENS.

satisfactory. Many puzzling results reported previously were explainable on the basis of imperfect filtering.

The depth of hardening, or so-called Jominy distance, was estimated not only from the microstructure of each specimen but also from the hardenability curves. These were used in two ways for the titanium steels, both involving the use of Fig.

show these "half-hardness" values derived in this way by using the total carbon contents of each steel. The shorter broken horizontal lines give similar values derived from the effective carbon contents of the titanium steels, or the carbon not tied up with insoluble titanium, and, therefore, available for hardening. The latter method is preferable, provided it is kept in mind that one of the effects of titanium on steel is to reduce the amount of carbon available for hardening. There is an appreciable difference in the results arby Jackson and Christenson⁵ in 1943. Since this curve was not published with the paper, it is presented here as Fig. 4, with Mr. Jackson's permission. The correcting

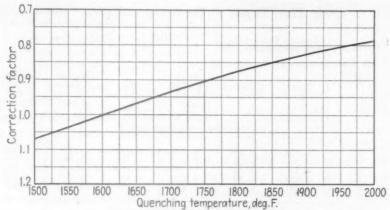


Fig. 4.—Correction for quenching temperature of distance along end-quenched hardenability bar (C. E. Jackson).

 $\frac{\text{End-quench distance (measured)}}{\text{Factor}} = \text{End quench distance at } 1600^{\circ}\text{F.}$

rived at by the two methods in the higher titanium steels, especially after quenching from the higher temperatures.

The metallographic estimation of the depth of hardening was also done in two ways. The ordinary method of noting the distance from the quenched end where the structure consisted of equal parts of martensite and troostite was difficult and uncertain with the fine-grained hightitanium steel, where there was considerable ferrite and very little dark-etching troostite. In such specimens, however, a fairly definite change of color could be noted with the naked eye after a deeper etch, at about the boundary between the martensitic and sorbitic structures. The distance of this line from the quenched end was taken as a measure of the hardening depth by macroetching. These data are given in Table 2.

After the three measurements of depth of hardening had been averaged, as noted in Table 2, the results were corrected to eliminate the influence of the quenching temperature, by use of the curve shown by C. E. Jackson in presenting the paper

factors used were 0.75 for 2200°F. and 0.81 for 1980°F., to convert to values comparable to those obtained by quenching from 1630°F.

The "ideal critical diameters," indicating relative hardenabilities, as given in the last column of Table 2, were computed from the corrected depth of hardening by means of Grossmann's Fig. 28.4

Several interesting comparisons can be found in Table 2. The vanadium steel 5 has a greater ideal critical diameter—in other words, is more deeply hardenable—than either the plain steel 1 or the titanium steels, when quenched from 1980° or 2200°F., but when quenched from 1630°F. it is less deeply hardenable than the coarse-grained plain steel, though more so than the titanium steels. The plain steel increases in grain size and in depth of hardening as the time at 1630°F. increases, but the other steels do not change much at 1630°F.

The low-titanium steel 2 and mediumtitanium steel 3 are intermediate in depth of hardening between the plain steel and the vanadium steel when quenched from 724

2200°F., a temperature that may be taken as fairly representative of welding conditions. This is illustrated graphically by the curves on the lower part of Fig. 3.

of the titanium steels decreases as the titanium content increases, the high titanium steel being always the shallowest hardening.

TABLE 2.—Grain Sizes, Depths of Hardening and Ideal Critical Diameters

			Distance at less, In., for		Depth of Ha	rđening, In		
Steel No.	A.S.T.M. Grain Size	Total Carbon			of Three Columns	Corrected for 1630°F. Quench	Ideal Diameter In.	
		A	. Samples Q	uenched fro	m 2200°F.			1
1 2	1 2.5	0.165 0.21 0.22	0.165 0.21 0.24	0.254 0.237 0.228	0.227 0.235 0.212	0.215 0.227 0.227	0,286 0,303 0,303	2.07
3 4 5	5 6 1.5	0.135	0.18	0.185	0.17	0.178	0.238	2.15 1.85 2.47
			B. Samples (Quenched fr	om 1980°F.	•	1	
1	1.5	0.195	0.195	0.252	0.21	0.210	0.270	3.00
2		0.22	0.22	0.256	0.24	0.239	0.295	2.11
3	3.5	0.165	0.185	0.203	0.20	0.196	0.242	1.87
4	8	0.07	0.095	0.118	0.095	0.103	0.127	1.33
5	2.5	0.285	0.285	0.332	0.275	0.297	0.366	2.41
		C. Sam	ples Quenche	ed after 20	Minutes at 10	530°F.		
I	4	0.205	0.205	0.205	0.185	0.198	0.198	1.67
2	4 8 8.5	0.145	0.15	0.151	0.15	0.150	0.150	1.44
3	8.5	0.125	0.135	0.134	0.13	0.133	0.133	1.36
3 4	9	0.035	0.085	0.130	0.097	0.104	0.104	1.22
5	8	0.20	0.20	0.171	0.18	0.184	0.184	1.60
		D. San	nples Quench	ed after On	e Hour at 16	30°F.		
I	2.5	0.22	0.22	0.224	0.22	0.221	0.221	1.77
2	7.5	0.155	0.16	0.181	0.155	0.165	0.165	1.51
3	7.5 8.5	0.115	0.13	0.140	0.13	0.133	0.133	1.36
3 4	8.5	0.07	0.095	0.106	0.09	0.097	0.097	1.19
5	8	0.205	0.205	0.185	0.18	0.190	0.190	1.62
	-	E. Samp	ples Quenche	d after Thr	ee Hours at	630°F.		
1	1.5	0.23	0.23	0.276	0.262	0.256	0.256	1.93
2	7 8	0.15	0.15	0.173	0.162	0.162	0.162	1.50
3 4	8	0.13	0.14	0.155	0.14	0.145	0.145	1.42
4	8.5	0.055	0.09	0.102	0.095	0.096	0.096	1.19
5	7	0.205	0.205	0.195	0.19	0.197	0.197	1.66

In this condition, however, the titanium steels are finer grained than the others, even the vanadium steel being much coarser. When quenched from 1980°F., only the lowest titanium steel is more deeply hardenable than the plain steel, and when quenched from 1630°F. the titanium steels are much less deeply hardenable than the others. In all conditions of these experiments the hardenability

The lower portions of the hardenability curves of Figs. 1, 2, and 3, representing the air-cooled parts of the test specimens, are of interest as well as the upper parts that show the depth of hardening. The plain carbon steel 1 has the right-hand ends of the curves sloping down with reasonable uniformity in the normal manner. With the titanium steels 2, 3 and 4, however, the higher position of the curves

derived from the quenches at higher temperatures is maintained through the air-cooled ends. This illustrates the fact that the hardening and strengthening effect of soluble titanium is not dependent on quenching from the solution temperature, but is found also after air cooling. In this respect the hardening effect of titanium is quite different from that of boron, which is found only after very rapid rates of cooling.

Reheating for only 20 min. at 1630°F. produces a very marked reduction in hardenability of a titanium steel previously air cooled from 2200°F. All of the hardening effect of the soluble titanium is not lost, however, by the 20-min. treatment at 1630°F., inasmuch as the hardenability is lowered still further by 1-hr. and 3-hr. treatments.

In the vanadium steel 5, the middle portions of the curves are closer together than in the titanium steels, indicating that with the intermediate rates of cooling occurring between 0.5 and 1 in. from the quenched end of the Jominy test specimen, it makes no difference in the hardening effect whether vanadium carbide was first dissolved at a high temperature or allowed to precipitate at 1630°F. This is quite different from the results with the titanium steels under the same conditions. However, the curves for the vanadium steel quenched from 2200° and 1980°F., where greater hardenability was shown at the higher hardness levels, have an abnormal upward direction at the righthand or air-cooled end. The reason for this is not entirely clear; perhaps there is some precipitation-hardening from the vanadium carbide in solid solution, at the particular rate of cooling occurring about 1.25 or 1.5 in from the quenched end of the Jominy test specimen. It seems significant that this hardness increase at the air-cooled end is found only in the two specimens quenched from the higher temperatures required for increased hardenability. A similar occurrence is shown to a barely perceptible degree in the high-titanium steel 4.

HARDENABILITY FACTORS FOR TOTAL TITANIUM

The hardenability factors for total titanium were computed with the ideal diameters given in Table 2, using the grain sizes also given there and the analytical data of Table 1, by the methods explained by other investigators in the papers cited. The procedure, briefly, is to multiply together the hardenability factors for grain size, carbon, and all other components of the steel (except titanium) and then determine the factor that will make the product equal to the experimentally determined "ideal critical diameter." This factor is the one corresponding to the titanium content.

The factors used for grain size and carbon were those proposed by Grossmann in Fig. 18.4 The factors used for the other elements were those used by Crafts and Lamont.2 Those for phosphorus and sulphur are the original factors proposed by Grossman4 and used also by Kramer, Hafner and Toleman.1 The copper factor is also due to Grossmann, but was checked very closely by Kramer, Hafner and Toleman. The complete list of the factors used in the present work is as follows:

Manganese	1 + 4.08 × per cent Mn
Phosphorus	$1 + 2.60 \times per cent P$
Sulphur	$1 - 0.65 \times per cent S$
Silicon	
	$1 + 0.36 \times per cent Cu$
	$1 + 0.74 \times per cent Ni$
	$1 + 2.16 \times per cent Cr$
Molybdenum	$1 + 2.53 \times \text{per cent Mo}$
	$1 + 1.73 \times per cent V$
Aluminum	$1 + 0.93 \times per cent acid-$
	soluble Al

The results of the calculations of the multiplying factors for titanium are given in Table 3, and the factors arrived at are plotted against total titanium on the upper part of Fig. 5.

The multiplying factors for total titanium given in Table 3 and plotted on the upper part of Fig. 5 are in fair agreement with those given by Crafts and Lamont,² but there are insufficient points on this chart to show the true form of the curve

Table 3.—Hardenability Factors for Total
Titanium

				Multip	olying F	actors
Steel No.	Total Tita- nium Con- tent	A.S.T.M. Grain Size	Crit- ical Ideal Diam- eter, Inches	For Car- bon and Grain Size	Product of all Except Titanium	For Total Tita- nium
	A. S	amples Qu	enched	from 2	200°F.	
2	0.055	2.5	2.15	0.294	1.750	1.23
3	0.360	5	2.15	0.241	1.537	1.40
4	0.777	6	1.85	0.221	1.393	1.33
	B. S	amples Qu	enched	from 1	980°F.	
2	0.055	3.5	2.11	0.274	1.632	1.29
3	0.360	6	1.87	0.222	1.416	1.32
4	0.777	8	1.33	0.188	1.219	1.09
Avera	ge of (C, D, and	E San 1630°F.	nples C	uenche	d from
2	0.055	7.5	1.48	0.198	1.180	1.25
3	0.360	8.3	1.38	0.184	1.174	1.18
4	0.777	8.7	1.20	0.177	1.116	1.07

for the hardenability factor for total titanium below 0.3 per cent. Additional data to amplify it will be presented later. The lines drawn on the present chart could of course be extended to the origin, at a factor of unity for zero titanium. The correct factor to use for total titanium is shown by the upper part of Fig. 5 to depend, at least in the higher titanium steels, on the quenching temperature. Quenching from 2200°F. gives more titanium in solution in the steel and a higher hardenability factor then quenching from 1630°F., except in steel containing as little as 0.05 per cent titanium. With titanium contents above about 0.35 per cent, the hardenability factors for total titanium decrease, because the formation of titanium carbide reduces the effective carbon content.

HARDENABILIY FACTORS FOR SOLUBLE TITANIUM

In these calculations both the insoluble titanium and the carbon combined with it were eliminated. The soluble and insoluble titanium were determined by

Table 4.—Hardenability Factors for Soluble Titanium

	Titan		Con	bon tent		ltiplyi Pactors	
Steel No.	Acid- Sol- uble	In- Sol- uble	Com- bined as TiC	Effec- tive Bal- ance	For Effec- tive Car- bon and Grain Size	Prod- uct of All Ex- cept Tita- nium	For Sol- uble Tita- nium
	A. San	nples (Quench	ned fro	m 220	o°F.	
2	0.010	0.045	0.011	0.357	0.289	1.720	1.25
3					0.214		1.58
4	0.041	0.733	0.183	0.181	0.159	1.003	1.84
	B. Sar	nples (Quench	ned fro	m 198	o°F.	
2	0.010	0.047	0.012	0.356	0.269	1.602	1.32
3	0.023	0.333	0.083	0.284	0.197	1.255	1.49
4	0.017	0.772	0.193	0.171	0.129	0.835	1.59
C. Sam	ples Qu	enche	d after	20 N	dinute	s at 16	30°F.
2	0.004	0.051	0.013	0.355	0.186	1.108	1.30
3					0.157		1.36
4	0.020	0.766	0.192	0.172	0.114	0.746	1.63
D. Sa	mples C	uench	ed aft	er One	Hour	at 163	o°F.
2	0.007	0.048	0.012	0.356	0.194	1.155	1.31
3					0.156		1.37
4	0.007	0.763	0.191	0.173	0.121	0.792	1.50
E. Samı	ples Qu	enched	i after	Three	e Hour	s at I	30°F.
2	0.006	0.040	0.012	0.356	0.202	1,202	1.25
3	0.012	0.351	0.088	0.279	0.163	1.040	1.36
4					0.123		1.48

chemical analysis of the hardenability test specimens, and the combined carbon was assumed to be one fourth of the insoluble titanium, neglecting the probably small contents of titanium nitride and oxide. The results of the calculations are set forth in Table 4 and the factors arrived at are plotted against the soluble titanium on the lower part of Fig. 5.

The line drawn on the lower chart of Fig. 5 indicates the effect of titanium in solution on the depth of hardening, and must be understood to be entirely distinct

from the hardenability curves of Figs. 1, 2, and 3 in connection with the soluble titanium contents reported in Table 4. In the low-titanium steel 2 and the vanadium

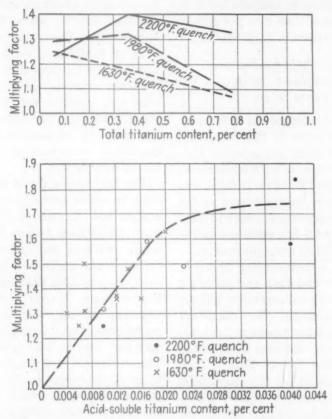


FIG. 5.—HARDENABILITY FACTORS FOR TOTAL AND ACID-SOLUBLE TITANIUM.

from the simultaneous action of titanium in forming a stable carbide and thus eliminating the hardening effect of part of the carbon in the steel. The fact that Kramer, Hafner and Toleman¹ did not separate these two effects probably accounts for their widely different conclusion regarding the effect of soluble titanium on hardenability. The amount of carbon removed by titanium from effective action in hardening the steel is roughly proportional to the amount of titanium present, but is not generally of much practical importance with less than about 0.2 per cent titanium.

Some interesting indications of the effect of soluble titanium can be derived

steel 5, the curves for the 2200°F. and 1080°F. quenches are practically coincident, showing distinctly greater hardenability than with quenching from 1630°F. In the higher titanium steels 3 and 4, the 2200°F. quench gave the greatest hardenability. This is directly in line with the soluble titanium contents, for in the low-titanium steel 2 the soluble titanium is higher in the A and B samples than in the others, while in the other titanium steels 3 and 4 it is only the A samples that are highest in soluble titanium. In steel 2, with insufficient insoluble titanium to reduce the effective carbon content appreciably, only o.o. per cent soluble titanium is required to produce a noticeably

greater hardenability when the quenching temperature is high; but in steels 3 and 4 there is enough insoluble titanium to make a difference in the effective carbon content, and the soluble titanium has to be considerably higher than o.or per cent to give a notable increase in hardenability.

EFFECT OF GRAIN-COARSENING HEAT-TREATMENT ON ONE TITANIUM STEEL

An important feature of the tests so far reported in this paper is that the steels were cooled to room temperature after the soaking treatment at high temperature designed to dissolve titanium carbide, and the specimens were then reheated to the end-quenching temperature, which in most instances produced a fine grain size in the titanium steels. When titanium steel No. 3 was soaked at a temperature giving a coarse grain size, and then end-quenched from various lower temperatures without cooling and reheating, the calculated results for the soluble titanium hardenability factors were different from those reported in Table 4 and Fig. 5. Ten samples were treated in this way, with quenching from 2200° to 1500°F., and the ideal critical diameters were determined carefully by the methods described above and in Table 2. The grain sizes of all these specimens were either 31/2 or 3, and the soluble titanium contents varied from 0.027 to 0.057 per cent. The factors for total titanium were all around unity, instead of what would be expected from Fig. 5 and the factors for soluble titanium came out mostly between 0.97 and 1.14. Thus the values given in Tables 3 and 4 and in Fig. 5 must be taken to apply only to steels that have received some grainrefining treatment from the high soaking temperature, and not to overheated and coarse-grained steel.

The reason for this discrepancy is believed to lie in the factors for carbon and grain size, which were originally proposed by Grossmann, and apparently have been accepted by subsequent workers on this subject without checking. Possibly the factors for coarse grain sizes also include some allowance for other elements dissolved in the coarse grains at high temperatures. The accuracy of the present work on titanium is wholly dependent on whether the hardenability factors for all the other elements, taken from the literature, are correct or not. A comparatively slight change in the curves used to get the grain-size factors would make very important differences in the calculated factors for titanium.

The low factors found for soluble titanium in coarse-grained steel may help to explain how Kramer, Hafner, and Toleman¹ found these factors to be less than unity. Without any allowance for the carbon made ineffective by combination with the insoluble titanium, most of the factors found in our work for soluble titanium between 0.027 and 0.057 in the coarse-grained specimens would be between 0.87 and one, as was reported by them. The correction for insoluble carbon is believed, however, to be an important one, so that undoubtedly there is some increase in hardenability produced by titanium in solution, although in coarsegrained samples it may be hidden, as far as the multiplying factors are concerned, in the factors now generally accepted for coarse grain size.

Additional Data on Total Titanium in Other Steels

End-quench hardenability tests were made in the way described in the foregoing pages, on two series of laboratory-melted titanium steels, in order to determine the factors for total titanium contents between the values of 0.055 and 0.36 per cent as given on Fig. 5. The steels in one of these series contained over 1.6 per cent manganese with 0.24 per cent carbon, while the other series included steels with 0.40 per

cent carbon and 0.93 per cent manganese. The hardened specimens were examined microscopically to determine their grain sizes and "ideal critical diameters," and

Fig. 6 is given a composite plot of all the factors for total titanium, including those for the 1630° and 1980°F. quenches from Fig. 5.

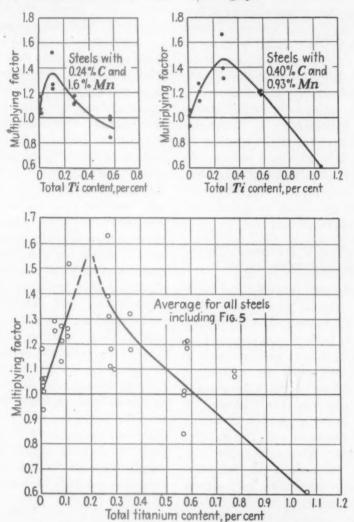


Fig. 6.—HARDENABILITY FACTORS FOR TOTAL TITANIUM.

complete chemical analyses were made so that the hardenability factors for titanium could be calculated. The quenching temperatures were between 1550° and 1950°F., and most of the samples were fine-grained. Jackson's correction for the effect of the quenching temperature was made as before.

The results are reported graphically on the upper part of Fig. 6, where the steels with different manganese contents are separated and on the lower part of The curve for the higher manganese steels on Fig. 6 is in fair agreement with the data presented by Crafts and Lamont,² which were also obtained with high-manganese steels. The difference between these data and those for the lower manganese steels support the view derived from experience with steel castings that titanium has a different effect on steels with higher manganese than on those with lower manganese. Or the difference may be

due merely to incorrectness of the factors used for elements other than titanium in the calculations. The curve in the lower part of Fig. 6 is believed to represent a fair average for the titanium hardenability factors in most forging grades of steel when reasonably fine-grained. With up to about 0.1 or 0.2 per cent titanium, there is a marked increase in hardenability with increasing titanium, but above about 0.4 to 0.6 per cent titanium in forging grades of steel the hardenability is drastically decreased because of the formation of titanium carbide to an extent sufficient to isolate an appreciable portion of the carbon content in a form that does not contribute to hardness on quenching from the usual heat-treating temperatures.

METALLOGRAPHIC DETECTION OF INSOLUBLE TITANIUM

Since the strength, hardness, and hardenability of titanium steels have been found to depend on the form of occurrence of the titanium carbide as determined by the heat-treatment, and titanium carbide can be recognized with the microscope in polished sections, it might be thought possible to correlate the changes in properties, or in the proportion of soluble and insoluble titanium, with the metallographic appearance of the carbide particles. Houdremont, Naumann and Schrader⁶ have exhibited micrographs to illustrate how the finer particles of titanium carbide disappear from microsections at increasing hardening temperatures. Numerous attempts to check this in our laboratory have been unsuccessful, however, and it has been our experience that the prominence of the fine carbide particles in a section of titanium steel depends primarily on the character of the polished surface of the specimen. The situation here seems to be rather similar to that so well illustrated recently by Harrington for an aluminumbase alloy.7

The four micrographs presented as Fig. 7

show how the carbides appear in some of our No. 3 titanium-steel specimens, polished carefully and thoroughly without pitting. These specimens were all lightly etched with picral and magnified 1000 diameters. The large angular crystals are believed to have separated from the steel before complete solidification, and possibly contain nitrogen as well as ticanium carbide. The fine specks may have separated later, and may be more nearly pure carbide. They are less prominent in the water-quenched specimen, possibly because of the different polishing quality of the martensite matrix. It is evident from the analyses of these specimens for soluble and insoluble titanium that there is no correlation of these chemically determined values with the number of carbide specks visible in the micrographs. It seems necessary to conclude, therefore, either (1) that the titanium that causes strengthening and hardening in steels heat-treated at temperatures above about 1900°F. must occur in a submicroscopic form, even after the strengthening and hardening are lost by treatment at lower temperatures and the titanium is reported as insoluble by chemical analysis; or (2) that the proportion of the total titanium that dissolves at 2200°F, is so small that it cannot be appreciated metallographically in comparison with the large amount always remaining insoluble at that temperature.

SUMMARY AND CONCLUSIONS

The effect of titanium on the hardenability of steel evidently depends on the heat-treatment of the steel, on whether total titanium or acid-soluble titanium is used as the basis of calculations, and on the amount of titanium present relative to the carbon. Thus a single definite value for the hardenability factor cannot be given for titanium as has been done for other common alloying elements in steel, without careful qualification as to the correct conditions under which it may be applied. In

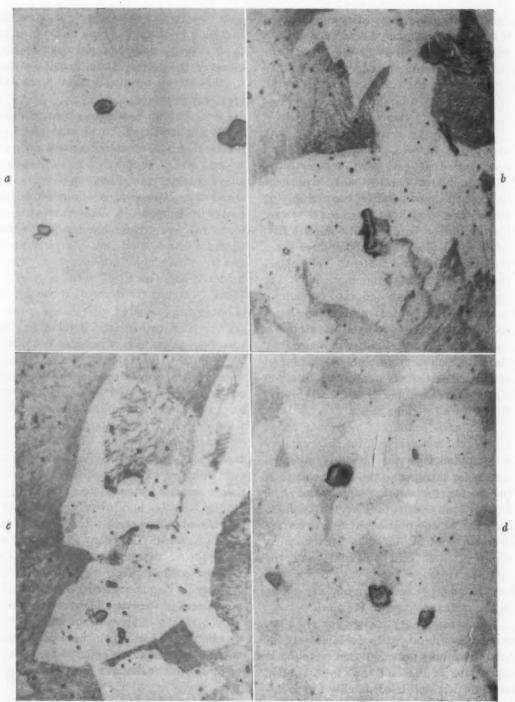


FIG. 7.—CARBIDES IN No. 3 TITANIUM STEEL:

a. Quenched end of hardenability test specimen of steel No. 3 heated 20 min. at 2200°F., containing 0.042 per cent soluble and 0.315 per cent insoluble titanium.

c. Steel No. 3 heated 4 hr. at 2200°F. in form of 1.5-in. round bar, and air cooled, containing 0.021 per cent soluble and 0.340 per cent insoluble titanium.

d. Air-cooled end of hardenability test specimen of steel No. 3 heated 3 hr. at 1630°F., containing 0.012 per cent soluble and 0.351 per cent insoluble titanium.

ble titanium.

d. Air-cooled end of hardenability test specimen of steel No. 3 heated 3 hr. at 1630°F., containing 0.012 per cent soluble and 0.351 per cent insoluble titanium.

All etched with 4 per cent picral and magnified 1000 diameters.

general, small amounts of titanium below o.1 per cent increase the hardenability of steel quite effectively, while above o.2 per cent titanium the effect is reduced in proportion to the titanium content, until, with sufficient titanium, steel may lose its hardenability completely.

In steels of the usual forging grade, with about 0.20 to 0.50 per cent carbon and heat-treated at customary temperatures, titanium contents up to about 0.2 per cent increase the hardenability; the multiplying factor, according to Grossmann's system for computing hardenability numerically, being equal to one plus about three times the total titanium content. This places small amounts of titanium in about the same class with phosphorus, chromium, or molybdenum for promoting hardenability. Larger amounts of titanium decrease the hardenability, however, by the formation of an insoluble carbide, and above about 0.6 per cent total titanium the factors become less than unity, indicating a softening effect.

With steels containing more than about 1.4 per cent manganese, if the hardenability is computed with the presently accepted factors for manganese and other elements, the factor for total titanium may be higher than with ordinary manganese contents, or one plus about five times the titanium content, up to a maximum at about 0.1 per cent titanium; and the decrease to below unity may occur with less than 0.6 per cent titanium, depending on the carbon content of the seel.

The hardenability factors for titanium can be based on acid-soluble instead of total titanium, provided that account is taken also of the fact that the insoluble titanium decreases hardenability by rendering ineffective a proportional amount of carbon. With reasonably fine-grained steels of forging grade, the hardenability factor for soluble titanium, at least up to about 0.02 per cent, is equal to one plus about 33 times the soluble titanium percentage.

This represents a stronger influence on hardenability than has been found for any other element except boron. In most steels, however, the decrease in hardenability due to the carbide-forming action is of far greater importance.

Comparing the hardening characteristics of forging steels of about 0.37 to 0.40 per cent carbon, moderate manganese and silicon, and negligible contents of other alloys except vanadium and titanium, shows some interesting relations according to the tests reported. Vanadium steel is found to have greater hardenability than titanium steel, and low-titanium steel greater than high-titanium steel, when hardened either at 1630°, 1980° or 2200°F. When quenched from 2200°F., the depth of hardening compared with that of coarsegrained plain carbon steel is increased by vanadium or up to 0.36 per cent titanium, but decreased by 0.78 per cent titanium; when quenched from 1980°F. the depth of hardening is increased by vanadium or 0.055 per cent titanium, but decreased by 0.36 per cent or more titanium, and when quenched from 1630°F, the depth of hardening is decreased by both vanadium and titanium. The vanadium steel was always coarser grained than the higher titanium steels, and even coarser than the low-titanium steel after heating to 1680° or 2200°F. The increased hardening effect due to titanium is found after air cooling as well as quenching, but is mostly lost after only 20 min. at 1630°F., although some traces of it persist for more than an hour at 1630°F. This was not true of the vanadium steel, in which, however, some evidence of slight secondary hardening appeared with the slower rates of cooling.

ACKNOWLEDGMENTS

The thanks of the author are due to numerous associates on the staff of the Titanium Alloy Manufacturing Co., and to the Company itself, without whose help this investigation could not have been carried out. Special acknowledgment is made to J. R. Lewis, who made most of the hardenability tests and prepared the microsections and photomicrographs; to A. S. Yocco, who melted and forged the experimental steels and also helped with the hardenability testing; and to K. W. Traub, who determined the soluble and insoluble titanium contents.

Thanks are due also to Dr. R. H. Aborn, of the Research Laboratory, United States Steel Corporation, for supplying the 1.5-in. rounds of the three titanium steels listed in Table 1.

REFERENCES

I. I. R. Kramer, R. H. Hafner and S. L. Toleman: Effect of Sixteen Alloying Toleman: Effect Sixteen Alloying Elements on the Hardenability of Steel.

Trans, A.I.M.E. (1944) 158, 138.
2. W. Crafts and J. L. Lamont: Effect of Some Elements on Hardenability. Trans.

A.I.M.E. (1944) 158, 157.
3. G. F. Comstock: Some Effects of Heat-treatment on Low-alloy Titanium Steels. Trans. Amer. Soc. Metals (1944) 33, 324. 4. M. A. Grossmann: Hardenability Calcu-

A.I.M.E. (1942) 150, 227.

5. C. E. Jackson and A. L. Christenson: Effect of Quenching Temperature and the control of the cont of Quenching Temperature on the Results of the End-quench Hardenability Test. Trans. A.I.M.E. (1944) 158, 125.
6. E. Houdremont, F. K. Naumann, and H.

Schrader: Solubility of Titanium Carbide and its Effect in the Hardening and Toughening of Steels. Archiv Eisenhuttenwesen (1942) 16, 57. Brutcher translation No. 1440.

7. R. H. Harrington: Interrupted Quench and Isothermal Treatments of Precipitation Hardening Alloys-Introductory Trans. Amer. Soc. Metals (1944) 33, 494, Figs. 2 and 3.

DISCUSSION

(I. R. Kramer presiding)

L. D. JAFFE. *-I should like to comment on only one point in Mr. Comstock's paper; that is, to suggest a possible explanation for the phenomenon he found, that the effect of titanium upon the hardenability of finegrained steels is much greater than in coarsegrained steels.

If we go back to the isothermal transformation diagrams, the temperature against the log time for fairly fine-grained plain carbon

* Watertown Arsenal, Watertown, Massachusetts.

steels, the diagram is probably something like Fig. 8a. There is a pearlite nose and a bainite nose, and ordinarily on continuously cooling the pearlite nose is what is encountered. It seems probable, from what we know of the other carbide-forming elements, that titanium has a much greater effect upon the pearlite nose than upon the bainite. So in a fine-grained steel additions of titanium would move this curve back considerably. If we move the pearlite curve back as in Fig. 8b, by additions of titanium, there would be a marked effect in the measured hardenability.

However, in a coarse-grained steel the pearlite curve is farther to the right to start with, whereas the bainite curve is about in the same position (Fig. 9a). In such a steel, additions of titanium that presumably would move the pearlite curve over to the right (Fig. ob) would have little effect upon the measured hardenability, because in continuous cooling what would be hit would not be the pearlite curve but the bainite curve. Therefore, in such steels the apparent effect of titanium would be much less than in fine-grained steels, presuming they are basically plain carbon steels.

In other words, the phenomenon can be explained simply as a case of pearlitic hardenability or bainitic hardenability being measured in the two separate experiments.

G. DEVRIES. *- The author made use of the curve shown by Jackson and Christenson in correcting the results to eliminate the influence of the quenching temperature in Jominy bars. In the discussion of the paper by Jackson and Christenson, it was pointed out that these correction factors become less with increase in distance from the quenched end of the bar.

In a test of the effect of quenching temperature, Jominy specimens were prepared by the writer from initially normalized bars of a steel containing 0.45 per cent carbon and 1.6 per cent manganese. Two specimens were heated at 1900°F. preparatory to quenching in a Jominy fixture in accordance with the recommended practice of the American Society for Testing Materials. One specimen was quenched directly from 1900°F. whereas the other specimen was transferred to a furnace at 1425°F., held for 30 min., and then quenched

^{*} National Bureau of Standards, Washington, D. C.

in the fixture. The hardenability curves of the two specimens were alike, thus indicating that this variation in quenching temperature had no effect on the hardenability of the steel. titanium steels. According to most of these diagrams that have been reported—as, for instance, in the Atlas of Isothermal Transformation Diagrams published in 1943 by the

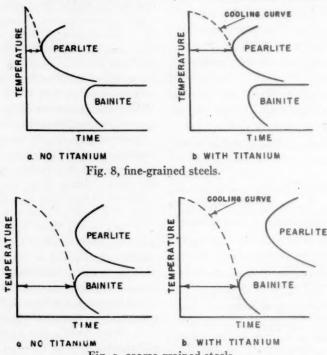


Fig. 9, coarse-grained steels.
Figs. 8 and 9.—Schematic transformation diagrams.

The point on the Jominy bars corresponding to a hardness of Rockwell C-40 (half-hard) was located approximately $\frac{1}{2}$ in. from the quenched end, signifying that the correction factor was unity at $\frac{1}{2}$ in. from the quenched end for this particular steel.

The hardenability of this steel was somewhat greater than that of the steels used by the author. Since the latter steels are relatively shallow hardening, the correction factors as used should be correct. However, the writer wishes to point out that in the use of such correction factors, consideration should be given to the distance from the quenched end.

G. F. Comstock (author's reply).—Mr. Jaffe has offered an interesting explanation for some of the results reported in the paper, which seems reasonable except for the assumption that there is a so-called "bainite nose" in the transformation diagrams of these

U.S. Steel Corporation Research Laboratory—this form of curve is found only in the alloy steels, especially molybdenum. Unfortunately, we do not have definite data as to whether it was actually bainite that limited the hardenability of the coarse-grained titanium steels. Although this seems quite unlikely to the author, it must be admitted that Mr. Jaffe's hypothesis is an interesting one and may be at least partially correct.

Mr. DeVries has presented a valuable record of a test indicating that under certain conditions the correction for quenching temperature worked out by Jackson and Christenson, largely by theoretical reasoning, does not actually apply in practice. The author also has encountered instances where this correction did not seem to be needed, and evidently it should be applied only with considerable caution. A more complete study of the subject would seem to be desirable.

Symposium on Hot-working

(New York Meeting, October 1945)

CONTENTS

A Laboratory Evaluation of the Hot-working Characteristics of Metals. By C. L. Clark	and	
J. J. Russ		736
Effect of Various Elements on the Hot-workability of Steel. By Harry K. IHRIG		749
Discussion		777

The Symposium on Hot-working was held on Friday, October 26, 1945, at the Hotel Pennsylvania, New York, as part of the fall meeting of the Iron and Steel Division.

F. B. Foley and K. L. Fetters presided. Mr. Foley presented the first paper, as neither Mr. Clark nor Mr. Russ could be present. Mr. Ihrig presented his own paper. The two papers were discussed together.

A Laboratory Evaluation of the Hot-working Characteristics of Metals

By C. L. CLARK, MEMBER A.I.M.E., AND J. J. RUSS*
(New York Meeting, October 1945)

For many years attempts have been made to develop a laboratory test that would serve to indicate the proper temperatures to be used in the various hot-working applications to which metals may be subjected as they are being processed from the cast ingot to the desired finished products. That these attempts have not been very successful is indicated by the fact that most of the temperatures in use today in these operations have been developed over a period of years by trial and error. In other words, the selection of the proper temperatures for the hot-working of metals is generally an art rather than a science.

Our knowledge with respect to the behavior of metals at elevated temperatures has been greatly extended during the past several years. While most of the work in this field has been done at proposed operating temperatures of equipment, rather than at processing or fabricating temperatures, one outstanding fact has been developed, which is applicable to the entire high-temperature range; that is, that the rate of deformation to which the metal is subjected is of the same order of importance as the temperature. The failure to properly recognize this fact has greatly retarded the development of a suitable laboratory test for determining hot-working temperatures.

Manuscript received at the office of the Institute Nov. 16, 1944. Listed for New York Meeting, February 1945, which was canceled. Issued as T.P. 1839 in METALS TECHNOLOGY, December 1945.

* Metallurgical Department, Steel and Tube Division, Timken Roller Bearing Co., Canton, Ohio. INFLUENCE OF RATE OF DEFORMATION ON HIGH-TEMPERATURE PROPERTIES

It is not the intent of this paper to survey all the work that has been done on the effect of deformation rate on the properties of metals. The importance of this factor, however, was shown by Zay Jeffries¹ as early as 1919, when he called attention to the existence of the so-called equicohesive temperature and to the effect of certain factors on the location of this temperature.

Fig. 1 is a diagrammatic sketch showing the effect of temperature on the relative strength of the crystals and grain boundaries and the type of fracture that will result, depending on the location of the test, or working temperature with respect to the equicohesive temperature. Since the type fracture varies, it also follows that at temperatures below the equicohesive temperature the major deformation occurs in the grains; while at temperatures above, the deformation results either from the movement of the grains with respect to each other or recrystallization of the strained material occurs almost instantaneously, producing new crystals at the fracture.

As previously indicated, it is an established fact that the position of this equicohesive temperature for any given metal is dependent on the deformation rate. For example, in 0.15 per cent plain carbon steel the location of this temperature under

References are at the end of the paper.

the rates of deformation encountered in creep tests (of the order of 1 per cent per 10,000 or 100,000 hr.) is less than 800°F., while in the rupture tests and for fracture

THE HOT TWIST TEST

The hot twist test²⁻⁵ is an ideal procedure for determining proper temperatures for hot processing and fabrication

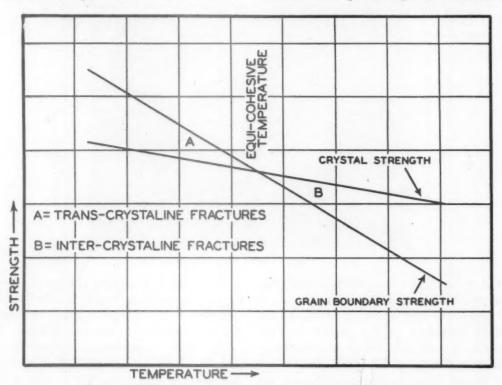


FIG. 1.—EFFECT OF TEMPERATURE ON FRACTURE OF METALS.

times of 1000 hr. or greater, it is about 900°F. On the other hand, under the rates of deformation usually employed in tensile tests, this temperature is of the order of 1500°F.

Since the rates of deformation usually encountered in hot processing operations are greater than those of the tensile test, it follows that the equicohesive temperature for this carbon steel under these conditions would be considerably in excess of 1500°F. Likewise, because the characteristics vary, depending on whether the processing temperature is above or below this equicohesive temperature, it also follows that any test for evaluating processing temperatures will have to be capable of employing rates of deformation at least comparable to those to be encountered commercially.

because: (1) the equipment involved is simple and inexpensive, (2) the test requires very little time, (3) the rate of deformation during the test can be readily varied over a very wide range, and (4) it is a torsion test and thus the predominating stresses are in shear.

A photograph of the equipment in use in our laboratories for this test is shown in Fig. 2. It consists essentially of a furnace for heating and maintaining the specimen at the given temperature, a variable-speed motor for turning the specimen at the desired rate, a chuck mounted in a bearing to which the torque arm is attached and a platform scales for measuring the force produced during the twisting of the specimen.

and fastened in the chuck of the variablespeed motor. The specimen is rotated at slow speed while it is being heated to and

The specimen is placed in the apparatus in: (1) the number of twists required for fracture at a given temperature, (2) the rate at which the number of required twists increases with temperature, (3) the

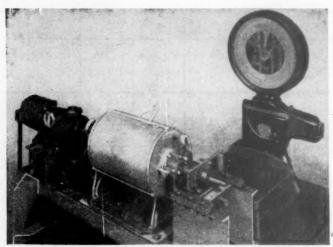


FIG. 2.—HOT-TWIST TESTING APPARATUS.

held at the desired temperature and after 15 min. at temperature the motor is stopped, the other chuck tightened and the motor restarted at the desired rate of speed. A counter, which automatically starts and stops at the beginning and end of the test, gives the number of revolutions required for fracture while the force exerted on the scale is read and recorded. The scale reading, multiplied by the length of the lever arm, gives the torque, expressed in inch-pounds.

Work has been done on different sizes of specimens and with the steel in various conditions of initial heat-treatment. For convenience, however, the specimen size has been standardized at % in. round with the material in the hot-rolled condition since, at temperatures of 1800° to 2500°F. the initial heat-treatment has little, if any, influence on the results obtained.

In each case the number of twists required for fracture increases as the temperature is raised, until a critical temperature is reached after which the number of twists decreases. There are, however, as shown in Fig. 3, differences between steels temperature at which the number of twists reaches a maximum, and (4) the rate of decrease in the number of required twists after the critical temperature is passed.

The steel represented by curve A in Fig. 3 would be the most foolproof in hot-working operations, for it requires a large number of twists for fracture at each temperature and the required number of twists decreases slowly as the temperature of maximum twist is exceeded. On the other hand, the material represented by curve E would be the most difficult to work, and that represented by curve C would be very sensitive to overheating.

RESULTS OF HOT TWIST TESTS ON TYPICAL STEELS

Representative results obtained from the hot twist tests on various steels are given in Figs. 4 to 8, inclusive, while the composition of these steels is given in Table 1. In addition to the torque and twist characteristics, the ratio of the twist to the torque is also included. While this ratio may have no definite physical significance, other than the average force required per

unit twist, it does appear, as will be discussed later, to offer a convenient means for evaluating the hot-workability of a steel. In other words, this ratio

temperature at which the maximum number of twists occurs. In torque characteristics, the lowest carbon steel possesses the maximum values and the highest carbon

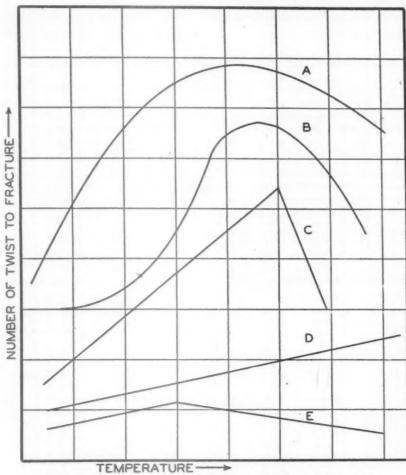


FIG. 3.—TYPICAL CURVES OBTAINED FROM HOT TWIST TESTS.

involves both strength (torque) and ductility (number of twists to fracture), both of which are important in certain processes.

Fig. 4, presenting the results on four carbon steels with the carbon content varying 0.065 to 1.02 per cent, indicates all of these steels to possess satisfactory hotworkability, although, as would be expected, differences exist between them. With the exception of the lowest carbon steel, the number of twists for fracture decreases at each temperature with increasing carbon content, as does the

steel the minimum. However, the differences are not as pronounced as with the twist curves.

Similar results for a series of constructional alloy steels containing 0.10 to 0.20 per cent carbon are given in Fig. 5 and for the same type of steels with about 0.40 per cent carbon in Fig. 6. In both cases a rather wide spread exists in the torque and twist characteristics, thus indicating that the alloy content of a given steel, as well as its carbon content, influences the apparent hot-working characteristics. For example,

with neither series of steels is the temperature of maximum twist solely a function of carbon content, for with the 0.10 to 0.20 per cent carbon-bearing steels the range in this temperature is from 2300° to 2400°F. and with the 0.40 per cent carbon steels from 2250° to 2450°F. plus.

about 30 to 300. Likewise, appreciable differences exist in the torque characteristics with the plain carbon steel having the lowest strength and the graphitic steels the highest values.

The hot-twist characteristics of various grades of the austenitic stainless steels

Table 1.—Chemical Composition of Steels Subjected to Hot Twist Test
Per Cent

Steel Designation	С	Mn	P	S	Si	Cr	Ni	Мо	Others
			Plain	Carbon Ste	els (Figur	re 4)			
0.065 C	0.065	0.17	0.013	0.014	0.14	0.00	0.19	0.04	
0.16 C	0.16	0.46	0.013	0.017	0.27	0.07	0.09	0.03	
0.39 C	0.39	0.86	0.019	0.023	0.22	0.00	0.17	0.03	
1.02 C	1.02	0.31	0.015	0.018	0.35	0.30	0.09	0.03	
		1	0.10 to 0.	20 C Alloy	Steels (F	igure 5)			
		1	1						1
1015	0.16	0.46	0.013	0.017	0.27	0.07	0.09	0.03	1
2512	0.10	0.56	0.018	0.020	0.28	0.15	5.01	0.05	
3312	0.08	0.35	0.015	0.016	0.29	1.28	3.60	0.06	
4320	0.19	0.56	0.017	0.018	0.31	0.58	1.84	0.27	
4615	0.14	0.62	0.022	0.021	0.30	0.15	1.72	0.25	
5120	0.19	0.88	0.017	0.019	0.26	0.83	0.19	0.03	
6120	0.19	0.81	0.023	0.026	0.26	0.84	0.26	0.07	(0.11 V)
			0.40 (C Alloy Ste	els (Figur	e 6)			1
1040	0.39	0.86	0.019	0.023	0.22	0.09	0.17	0.02	
2340	0.42	0.78	0.019	0.020	0.31	0.15	3.41	0.04	
3240	0.43	0.62	0.017	0.022	0.28	1.20	1.67	0.05	
4140	0.39	0.86	0.017	0.016	0.26	1.00	0.14	0.15	
4340	0.39	0.71	0.019	0.021	0.31	0.68	1.75	0.34	
4640	0.39	0.69	0.017	0.016	0.28	0.25	1.74	0.24	1
5140	0.38	0.77	0.018	0.022	0.23	1.04	0.27	0.06	1
8740	0.41	0.79	0.018	0.022	0.26	0.56	0.60	0.24	
Nitralloy	0.39	0.58	0.016	0.016	0.31	1.56	0.24	0.35	(1.01 Al)
			High-	carbon Ste	els (Figur	e 7)		1	
10105	1.02	0.31	0.015	0.018	0.35	0.30	0.00	0.03	
52100	1.03	0.44	0.014	0.012	0.32	1.37	0.12	0.03	
62125	1.21	0.61	0.016	0.015	0.30	1.81	0.13	0.03	(0.15 V)
Mo	1.49	0.40	0.014	0.017	0.72	0.12	0.17	0.25	(0.13 1)
Sil.	1.49	0.45	0.019	0.016	0.95	0.16	0.18	0.03	
		0.45	0.023	0.015	0.66				(3.03 W)
Tung MNS	1.45	1.30	0.011	0.017	1.54	0.09	1.76	0.54	(3.03 11)
			Austeniti	ic Stainless	Steels (Fi	gure 8)		1	1
		1							1
18-8(304)	0.05	0.52	0.006	0.012	0.52	17.78	9.60		
18-8(303)	0.12	0.94	0.022	0.239	0.35	18.08	8.85	0.24	
18-12 + Ti 18-12 + Cb	0.06	1.33	0.021	0.013	0.28	17.41	10.03	0.06	(0.43 Ti)
18-12 + Cb	0.07	1.75	0.010	0.017	0.68	18.85	12.87		(0.82 Cb)
25-12	0.06	1.55	0.011	0.017	0.42	24.96	13.40	0.01	
25-20	0.11	0.58	0.013	0.017	0.75	23.60	20.65	0.03	1

Alloy content is of even greater importance on the apparent hot-workability of steels containing 1.0 per cent or more carbon, as shown in Fig. 7. With these steels the temperature of maximum twist ranges from 1875° to 2200°F. while the maximum number of twists varies from

are given in Fig. 8, and again marked differences exist in the apparent hot-workability. The temperature of maximum twist varies from 2250° to 2450°F. plus while the maximum number of twists ranges from 25 to 142. It is worthy of note that the addition of stabilizing elements, such as

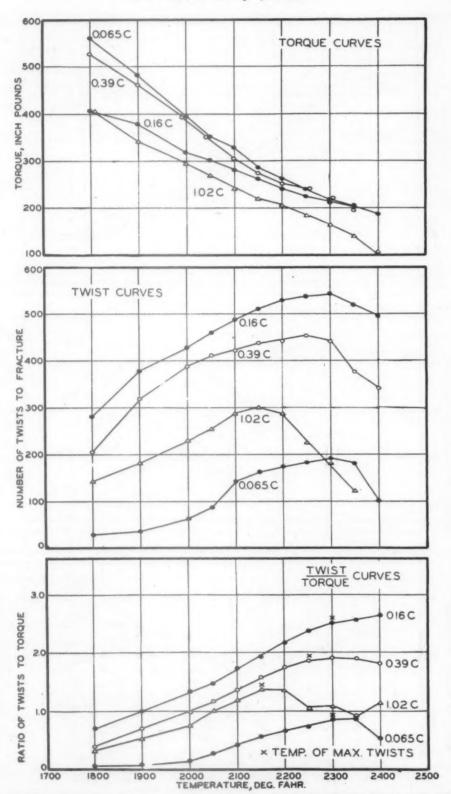


Fig. 4.—Effect of carbon content on hot-twist characteristics of carbon steel.

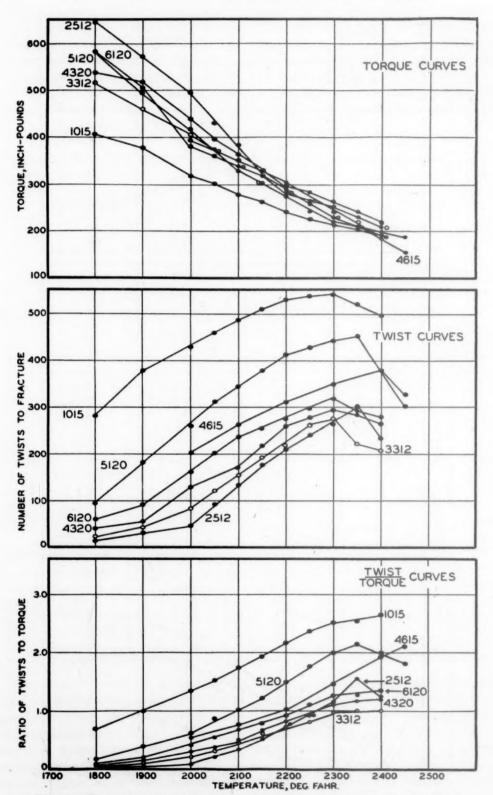


FIG. 5-HOT-TWIST CHARACTERISTICS OF 0.10 TO 0.20 CARBON ALLOY STEELS.

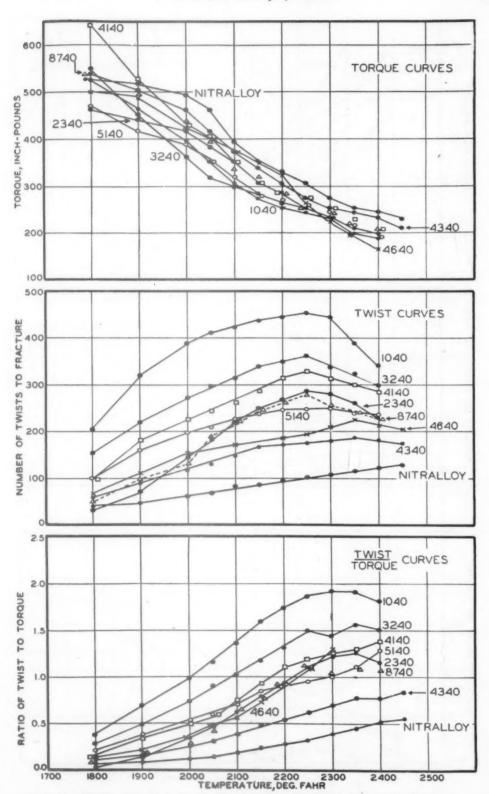


Fig. 6.—Hot-twist characteristics of 0.40 per cent carbon alloy steel.

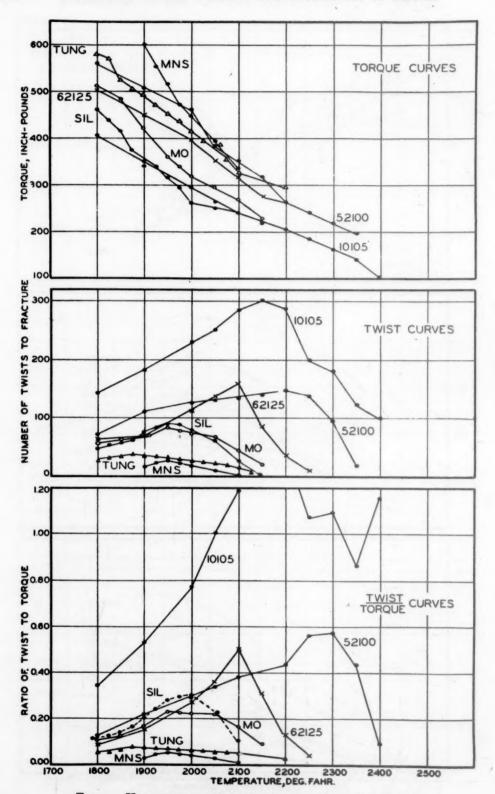


FIG. 7.—HOT-TWIST CHARACTERISTICS OF HIGH-CARBON STEELS.

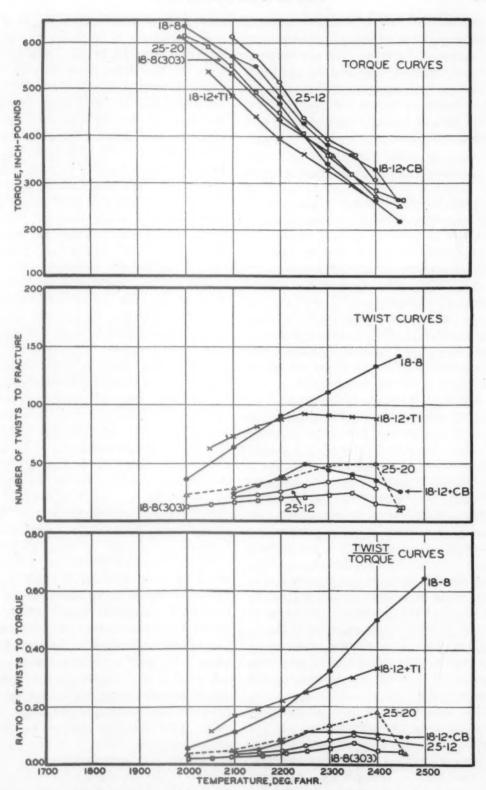


Fig. 8.—Hot-twist characteristics of austenitic stainless steels.

columbium or titanium, and free-machining additions, such as sulphur, selenium, or phosphorus, decreases both the temperature of maximum twist and the number of twists at this temperature. Likewise, increasing the chromium and nickel content, as in 25-20 and 25-12, lowers the number of twists to fracture.

INTERPRETATION OF TWIST TEST RESULTS

From the preceding figures it is apparent that for each steel the number of twists for fracture increases with temperature up to a certain point and then decreases as the temperature is further raised. In other words, each steel possesses a critical temperature as far as its ductility (as measured by the twists to fracture) is concerned. The question then arises as to the cause of this critical temperature and its possible relationship, if any, to proper maximum processing temperatures.

Twists to Fracture.—Metallographic examination of the fractured twist specimens reveals the cause of this decrease in the required number of twists after a certain temperature is reached as well as for a correlation existing between this temperature and the hot-working characteristics. As this temperature is exceeded, the nature of failure changes in that intergranular cracking appears, even in sections removed from the actual fracture. The degree of this intergranular cracking increases the higher the testing temperature, and this accounts for the resultant decrease in the number of twists. In other words, referring to Fig. 1. for the rate of deformation involved in the twist test, the temperature of maximum twists is the equicohesive temperature for the particular steel.

The appearance of this intergranular cracking at temperatures in excess of the critical temperature also explains the cause of certain defects in metals when processed at too high a temperature. At these temperatures, and for the given rate of

application of stress, the strength of the grain boundaries is decreased to such an extent that intergranular cracking will occur if the deformation exceeds that which the metal is capable of withstanding. Burning of steel has often been considered the cause of this cracking even though oxides are not present in the grain boundaries. While burning of steel is possible and the path of fracture in such cases is intergranular, distinction should be made between steel that has been burned and that which has been processed at too high a temperature. In the first case, the damage occurs during the heating cycle and the steel is permanently damaged, while the defects due to processing at too high a temperature occur during the processing operation, although of course the heating has established the conditions for making those defects possible.

Summarizing, it is believed that the temperature of maximum twist represents the maximum temperature that can safely be used in all hot processing operations. This does not necessarily imply, however, that higher temperatures cannot be used with certain steels if the processing is such that little deformation results. For example, from Fig. 3, a steel represented by curve A could be worked at very high temperatures provided the amount of deformation in the working operation could be controlled within the necessary limits. On the other hand, steels represented by curves B, C and E would be much more susceptible to overheating.

Torque.—While, as previously indicated, the number of twists to fracture is a measure of the hot ductility, and also an indication of the temperature that should not be exceeded in processing, the torque represents the strength of the metal. For many hot processing operations these torque values are believed to be of great importance for, comparatively at least, they are a measure of the force required to displace the metal at the various tempera-

tures and also an indication of possible temperature build-up.

For example, in the piercing of seamless tubes the major part of the work is done at the center of the billet and a large part of this work is transformed to heat. As is well known, a temperature rise occurs in the interior of the billet during the piercing operation and the torque value is believed to be a good indication of the temperature rise to be expected in the different steels. In general, austenitic stainless steels possess a greater torque at their respective piercing temperatures than do the constructional alloys; also the temperature rise during piercing is greater in these austenitic steels. When it is definitely shown by the twist results that the torque value is high, the temperature rise can, and has been, controlled by variations in the rate of piercing.

Twist-torque Ratio.—While the number of twists required for fracture divided by the torque may have no greater meaning or significance than the ratio of the ductility as determined in the tensile test to the tensile strength, it has been found in certain of our own work to serve as a good indication of the material's ability to be processed by certain operations.

Our correlation would indicate the hotworkability to be improved as this ratio is increased, and when it falls below a certain minimum value the material can not meet severe hot-working requirements, such as are encountered in the piercing of seamless tubes. Furthermore, the magnitude of this ratio may also serve as a convenient guide in the selection of the proper piercing speeds. As more data are accumulated, it is hoped that this ratio may also be useful in determining the minimum temperature of working that can be employed in the different hot-working processes. If this hope is fulfilled, laboratory tests can serve as a guide for the complete temperature range of hot-workability.

APPLICATION OF HOT-TWIST DATA

In the application of the results from the hot twist test, consideration must, of course, be given to the particular type of hot-working process involved. If the metal is to be forged and the section size is such that the heat losses are small, it is believed that the maximum temperature of forging should be about 50°F. below the temperature of maximum twist, especially if considerable deformation is involved. Of course, if the deformation is small and can be controlled, and if the steel possesses a hot-twist curve similar to curve A of Fig. 3, temperatures in excess of the temperature of maximum twist can be employed.

If an appreciable heat loss occurs from the time of heating until the forging operation, the steel can be heated to higher temperatures than those indicated by the twist curves, for these temperatures do apply to the metal at the time of processing. The extent to which this overheating can be done safely is, however, again a function of the shape of the twist curve, especially after the temperature of maximum twist has been passed.

In certain operations, such as the piercing of seamless tubes, the temperature rises during processing and in such cases the temperature should be adjusted so that after the temperature rise the maximum temperature does not exceed the temperature of maximum twist. As previously indicated the torque values are of importance in estimating the temperature rise to be expected and if these appear to be excessive then alteration can be made in the piercing mill to decrease the magnitude of this temperature rise. If the twist to torque ratio is high at temperatures in excess of the temperature of maximum twist there are indications that this critical temperature may be exceeded without harmful effects but it is believed safer practice to keep the maximum temperature below this value.

LIMITATIONS OF THE HOT TWIST TESTS

While the hot twist test is believed to be a very suitable laboratory means for evaluating the hot-workability of metals, it does, as is true of all test procedures, have certain limitations. In reality, however, certain of these limitations are a function of the material being tested rather than of the test itself.

For example, while excellent agreement has always been obtained in the results for multiple tests on specimens taken from bars of a given heat, variation in results may occur with different heats of the same analysis, and these differences appear to be more pronounced the higher the total alloy content of the steel. The magnitude of these differences depends on the shape of the twist curve for a given steel, tending to be greater the more rapidly the curve approaches and departs from the temperature of maximum twist. These possible variations from heat to heat are certainly caused by the steel and not by the test.

Another limitation of this procedure of evaluation results from the fact that most of the tests to date have been conducted on rolled or forged bars. There is still a question as to whether or not the hot-twist characteristics of a steel when in this condition will be similar to those of the same steel when in the cast ingot form. Since, in steel processing at least, all hot-working originally starts on the ingot, it would be advantageous to have the twist test results applicable to the ingot. This matter of the comparative twist characteristics of rolled versus cast structures is worthy of investigation.

CONCLUSIONS

Even admitting that under present-day melting-practice procedures it is impossible always to obtain exact agreement on the hot-twist characteristics from different heats of the same analysis, it is still believed that the twist test is of great value in providing rapid and inexpensive means for the selection of the most suitable temperatures for the various hot-processing operations. In time, it is hoped the results from this test will serve to place the selection of these temperatures on a scientific. rather than trial and error, basis.

Most of the variations from heat to heat observed to date have been of a low order of magnitude and in most cases this variable can be eliminated by using, as a maximum hot-working temperature, one 50°F. below the temperature of maximum twist.

REFERENCES

- I. Z. Jeffries: Effect of Temperature, Deformation and Grain Size on the Mechanical Properties of Metals. Trans. A.I.M.E.
- (1919) 60, 474. 2. A Sauveur: Metals at Elevated Temperatures. Trans. Amer. Soc. Steel Treat. (1930) 17, 410-448.
 3. C. L. Clark: Evaluating Steel Forgeability.
- Jron Age (March 1944).

 4. H. K. Ihrig: Quantitative Hot Work Tests for Metals. Iron Age (Apr. 20, 1944).

 5. C. L. Clark: Evaluating the Forgeability of Company of the Co
- Steels. Timken Roller Bearing Company Booklet, 1944.

DISCUSSION

See pag 777.

The Effect of Various Elements on the Hot-workability of Steel

By HARRY K. IRRIG,* MEMBER A.I.M.E.

(New York Meeting, October 1945)

THE hot-working of iron and steel is an art dating back to antiquity, but until about 25 years ago, relatively few alloying elements were used, and these were present only in small percentages. With the exception of sulphur, the amounts of other elements in steels did not markedly affect their hot-workability. The references in the literature on the effect of other elements on the hot-workability of steel are usually reports of failure of these steels in forging or rolling.¹⁻⁸

With the increased use of alloying elements, and their use in larger amounts, it was observed that many of the new steels were red short in certain critical ranges or at all hot-working temperatures. The stainless steels are particularly difficult to hot-work. The determining of the correct conditions for piercing, rolling and forging of these alloys by experimentation in the mill often results in large losses of these expensive metals. It also is found that the hot-workability limits of many types vary from heat to heat, and hence poor results are obtained on changing to a new heat after a previous one has rolled satisfactorily. To determine the effect on hot-workability of iron to which various elements have been added, it was necessary to devise a method that could be used on small quantities of metal. In such a method, the minimum number of variables should be present, and the procedure should be simple, quick and correlatable with large-scale hot-working operations.

Sauveur,9 in the first Henry Marion Howe lecture in 1924, described the effect of carbon on the ductility of steels in torsion near their critical points. He found that carbon increases the plasticity of gamma iron. In the 1930 Campbell Memorial lecture, 10 he gives the effect of carbon, chromium, and chromium and nickel on the ductility of steels under 2000°F. in torsion. Ellis¹¹ has studied the malleability of steels at various elevated temperatures by means of a single-blow drop-hammer test. In this test the percentage decrease in height of standard cylinders is taken as a measure of their malleability. He has shown that in the lowalloy steels studied, carbon has a greater effect than nickel, chromium and vanadium.

In 1938 the first tests were run on a new quantitative hot-workability test in the laboratories of the Globe Steel Tubes Co. Thum¹² mentioned it in 1940. An illustration of the apparatus was published in January 1942. The effect of a few alloying elements on the hot-workability of metals was shown in a description of the test in 1944. The effect of the test in 1944.

DESCRIPTION OF TEST METHOD

The method adopted after a trial of several others is a rapid twisting of bars to failure in a furnace. The standard-size bar was chosen as $\%_6$ in. It is prepared from larger pieces by forging and cold-

Manuscript received at the office of the Institute Dec. 15, 1944. Issued as T.P. 1932 in METALS TECHNOLOGY, October 1945.

METALS TECHNOLOGY, October 1945.

* Director of Laboratories, Globe Steel Tubes Co., Milwaukee, Wisconsin.

¹ References are at the end of paper.

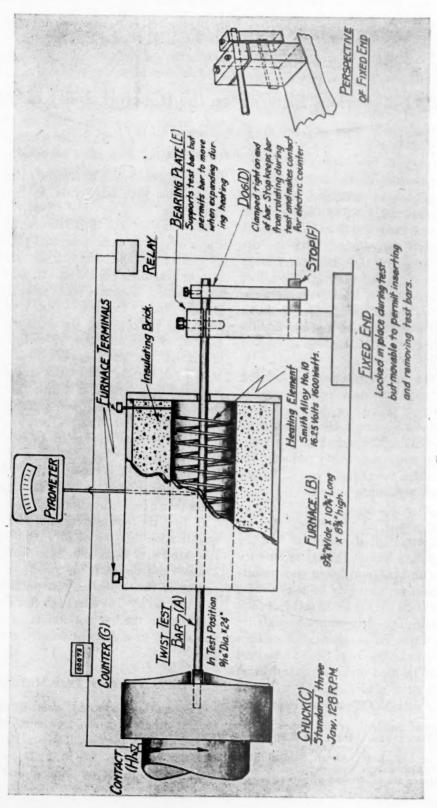


FIG. I.—APPARATUS.

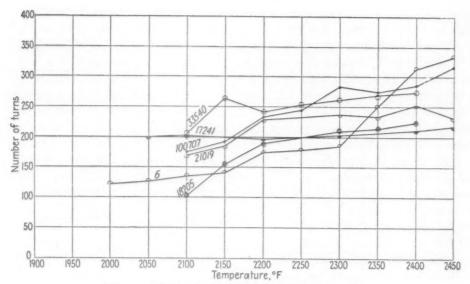


Fig. 2.—Spread of heats of S.A.E. 1010 steels.

	An	alyses				
Heat number	17241	18205	21019	33540	100707	6
V	0.12	0.12	0.12	0.11	0.11	0.16
Mn	0.46	0.52	0.45	0.52	0.47	0.73
5	0.030	0.026	0.025	0.030	0.023	0.014
P	0.025	0.018	0.023	0.022	0.013	0.023
Si	0.178	0.17	0.132	0.20	0.04	0.02

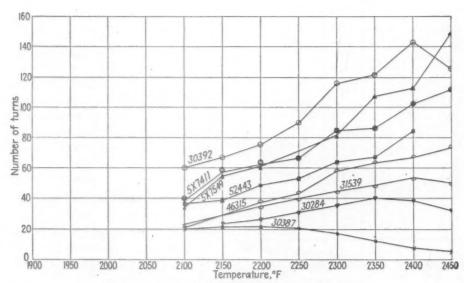


Fig. 3.—Spread of heats of type 304 steels.

			Analys	ses				
Heat number	52443	5X7549 0.04	30392	30387	31539	5X7411	30284	46315
Mn	0.77	0.55	0.50	0.59	1.06	0.54	0.46	0.45
P	0.015	0.013	0.012	0.012	0.014	0.009	0.012	0.012
Si Cr Ni	0.41 17.85 10.72	0.48 18.64 10.50	0.47 17.15 9.94	0.39 20.28 8.45	0.38 18.12 10.12	0.63 18.56 10.58	0.22 18.57 8.53	0.36 18.25 10.70

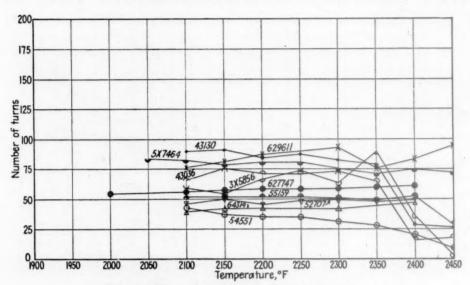


FIG. 4.—SPREAD OF HEATS OF TYPE 321 STEELS.

				Analys	ies					
Heat number		55159	627747	629611	64314	54551	43130	5X7464	43036	52707
C		0.06	0.05	0.05	0.06	0.05	0.05	0.05	0.05	0.05
Mn		1.32	0.75	0.47	1.37	1.08	0.43	0.65	0.45	1.09
S	0.013	0.010	0.009	0.009	0.007	0.007	0.013	0.007	0.010	0.010
P	0.025	0.013	0.016	0.015	0.010	0.023	0.016	0.007	0.014	0.017
Si	0.42	0.66	0.42	0.50	0.46	0.60	0.51	0.57	0.60	0.67
Cr	18.08	17.75	18.65	18.08	18.50	18.25	18.20	17.91	18.35	18.00
Ni	10.42	10.99	11.90	11.82	11.38	10.79	10.54	11.86	10.55	10.56
Ti	0.52	0.38	0.52	0.38	0.45	0.37	0.49	0.38	0.51	0.39

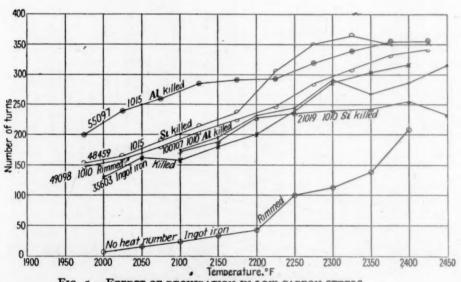


FIG. 5.—EFFECT OF DEOXIDATION IN LOW-CARBON STEELS.

		Analys	ies .				
Heat number		Ingot Iron 35603	1010	1010	1010	1015	1015 55097
C	0.02	0.04	0.12	0.12	O.II	0.13	0.13
Mn	0.005	0.26	0.53	0.45	0.47	0.57	0.47
S	0.026	0.024	0.028	0.025	0.023	0.029	0.028
P	0.000	0.004	0.010	0.023	0.013	0.013	0.013
Si	0.02	0.003	0.01	0.132	0.04	0.26	0.03

drawing to size. A light, centerless grind may be given the finished bars to remove surface imperfections.

Fig. 1 is a diagram of the apparatus. A is the bar inserted in the furnace B. One end is clamped in the chuck C and the other end is held in the heavy dog D. Thus the bar is free to expand through the bearing E, but is kept from rotating on that end while the other is rotated by the chuck. When the torque is applied, the dog makes contact with the stop F and energizes the electrical counter G, which records the number of revolutions made by the chuck by means of the contact at H. When the bar breaks inside the furnace. the dog drops away from and breaks contact with the counter circuit, and an accurate count of the number of twists to failure of the bar under test is recorded.

The bar is soaked at the test temperature for 30 min. The furnace temperature is controlled by a regulator and measured by a pyrometer. The furnace is mounted on a carriage, which may be moved back from the chuck to facilitate easy removal of the broken specimens. The chuck operates at 128 r.p.m. Thus the bar, after accurate heating, is rapidly and uniformly worked by twisting until failure occurs. It is held at temperature in the furnace while being twisted and actually rises slightly in temperature from the working during the test. By running a series of tests on the same heat at different temperatures. curves can be drawn to show the temperature that gives the maximum number of turns and the type of curve for any particular heat. By correlation of these results with mill operations, it is possible to predict whether or not a heat of steel will survive various hot-working operations such as forging, rolling and piercing, and what temperature will give the best results.

Table I shows the number of turns to failure of a low-carbon steel heated from room temperature to 2450°F. in 50°F. intervals. Below 750°F., the bars twisted

outside the furnace as well as inside. At 450°F. and 650°F., the bars broke outside the furnace. Above 2150°F. the ductility rose rapidly. The results of the test on a single heat are very reproducible. Four test samples of a type 304 (18 Cr, 8 Ni) heat were run at each hundred degrees from 2000° to 2400°F. The greatest difference in the 20 samples tested was six turns. The same reproducibility does not apply between different heats of the same class of steels. In Fig. 2 the maximum number of twists for six heats of low-carbon steel in the range from 2100° through 2400°F. varies from 200 to 315. However, all heats of this analysis shown have more than sufficient ductility to hot-work well, and the general shapes of the curves are similar.

Table 1.—Effect of Temperature on the Hot-workability of 0.16 per cent Carbon Steel

Analysis of Steel: C, 0.16 per cent; Mn, 0.73; S, 0.023; P, 0.014; Si, 0.02.

Tem- pera- ture, Deg. F.	Num- ber of Turns	Tem- pera- ture, Deg. F.	Num- ber of Turns	Tem- pera- ture, Deg. F.	Num- ber of Turns
100	20	950	7	1800	85
150	22	1000	7 6	1850	90
200	24	1050	8	1900	104
250	21	1100	9	1950	II2
300	28	1150	12	2000	123
350	26	1200	22	2050	124
400	28	1250	33	3100	132
450	31	1300	35	2150	137
500	18	1350	48	2200	176
550	17	1400	51	2250	178
600	17	1450	43	2300	182
650	23	1500	35	2350	248
700	10	1550	55	2400	314
750	12	1600	63	2450	333
800	9	1650	72		
850	12	1700	77		
900	9	1750	74		

A marked difference in hot-workability is found between heats in some of the high-alloy steels. Fig. 3 shows the tests on eight heats of type 304 (18 Cr, 8 Ni) stainless steels. The maximum number of turns in the range from 2100° through 2400°F. varies from 22 to 143 between the heats. The temperature showing the maximum

number of turns varies from 2150° to 2450°F. This difference in hot-workability between heats is even more pronounced in the curves of Fig. 4 for type 321 (18 Cr, 8 Ni, Ti) steels. The shapes of the curves are quite different, and the temperatures of maximum hot-ductility vary from 2050°F. for heat 5X7464 to 2450°F. for heat 629611. The other heats fall between these limiting temperatures.

Clark 15 has concluded that the maximum forging temperature can be determined from the curves of single heats of various types of steel. It is obvious that such maximums taken from the heats shown in Figs. 3 and 4 would not be applicable to each other. Therefore it is believed that the best temperature for working steels that have critical hot-workability must be determined on each heat. This method has been used successfully for the past seven years in the mill of Globe Steel Tubes Co. for determining the best piercing temperatures for a wide variety of alloy steels.

The following results show the effect of various elements on the hot-workability in about 200 heats of steels and except for heats 363, IL-2720, B-157, B-155, B-156, N-110, C-17099, I-1968, and I-1969, were taken from over 7000 tests of regular commercial heats used for the manufacture of seamless tubing.

EFFECT OF DEOXIDATION AND VARIOUS ELEMENTS ON THE HOT-WORKA-BILITY OF STEELS

Bars were forged and drawn from many steels with varying amounts of a number of elements. These were tested by the method described above. The effects of the individual elements are described in the following pages.

Deoxidation

Although no direct determinations of the oxygen contents of the samples tested were made, several carbon steels made with different deoxidation practices are shown in Fig. 5. The two heats lowest in carbon are ingot irons; the lower is a rimmed heat and the other is aluminum killed. All of the heats show good hot-workability and similar curves except the ingot iron lowest in carbon content. This heat is very low in manganese, and it is believed that the reduction in hot-workability is caused by insufficient manganese to form manganese sulphide with the sulphur in this iron. Apparently deoxidation practice itself does not materially affect the hot-workability of low-carbon steels.

Carbon

Because carbon is the most important element in steels, a detailed study of the hot-workability of steels of different carbon content, both alone and in combination with other elements, was made. Table 2 shows the tests of killed open-hearth straight carbon steels containing from 0.04 to 1.04 per cent carbon. Under about 0.25 per cent carbon, the maximum ductility rises with increasing temperatures. The steels higher in carbon have their maximum ductilities at 2350°F. or lower, and as the carbon increases the ductility falls off rapidly with increase in temperature. The high-carbon steel samples, broken at above 2400°F., show evidence of molten interiors with a shell on the outside. Ellis¹¹ found similar conditions in samples forged at high temperatures.

In the straight chromium stainless steels, the hot-workability decreases with higher carbon content. Fig. 6 shows this effect in types 410, 420, 442 and 443 steels, and Fig. 7 shows the effect in type 446 steels. The low nitrogen of heat 620225 with 0.10 per cent carbon probably accounts for its better hot-ductility than the 0.050 per cent and the 0.08 per cent carbon heats shown.

In the nickel-chromium stainless steels shown in Fig. 8, the low-carbon steels show poorer hot-workability than the ones containing 0.07 and 0.08 per cent carbon. In the lower carbon heats, delta iron is formed, which markedly affects hot-workability.

Manganese

Manganese is necessary in steels to counteract the red-short effect of sulphur. Fig. 9 gives curves for steels containing from 0.005 to 12.88 per cent manganese. There are two ingot irons. The one with 0.26 per cent manganese has a sufficient amount to counteract the sulphur, but the sample with 0.005 per cent manganese shows comparatively low hot-workability.

hot-workability in the type 304 and 321 steels shown in Figs. 10, 11 and 12. However, the nickel content of all of these heats is high. Nickel and manganese tend to be additive in their effect, so that in lower nickel steels it would be expected that manganese would be more effective. The hot-workability is poor in the single heat containing 18 per cent chromium and 8 per cent manganese with no nickel.

Sulphur and Selenium

It is well known that sulphur affects hot-workability adversely. However, no

TABLE 2.—Effect of Carbon on the Hot-workability of Plain Carbon Steel

Composition, Per Cent					t	Number of Turns, Testing Temperature of									
С	Mn	s		P	Si	2000°F.	2050°F.	2100°F.	2150°F.	2200°F.	2250°F.	2300°F.	2350°F.	2400°F	
0.04 0.12 0.13 0.20 0.26	0.38 0.47 0.48	0.033 0.028 0.031	0 0	019	0.03	179 217 204	166 243 231	157 233 270 255	187 140 288 273	201 190 295 259	245 229 312 305	279 259 332 284	302 344 264	320 294 357 288 268	
0.34 0.35 0.40 0.45	0.72 0.54 0.66	0.030 0.038 0.036 0.034 0.042	0 0	014	0.18 0.22 0.16	242		269 125 209 249 258	264 107 219 265 260	309 142 240 262 269	304 145 248 342 317	294 177 225 298	192 216 362	177 181 232 300	
0.76 0.96 1.04	0.34	0.035	0	.019	0.31	189 133 210	145	208 159 198	186	208 153 208	135 147	214 129 196	69 168	162 4 14	

The other steels show that in general manganese improves hot-workability. Heat 3X5921 contains 0.77 per cent manganese and 0.007 per cent sulphur. Because of the lower sulphur content, less manganese is used up in neutralizing the sulphur effect, and therefore it has hot-workability comparable to that of higher manganese steels. The higher sulphur content (0.030 per cent) in heat 83615 lowers its hot-workability. A similar sulphur content of 0.028 per cent but with higher manganese (1.05 per cent) shows much higher hot-workability.

The room-temperature austenitic 12.88 per cent manganese steel shown has much lower hot-workability than the room-temperature ferritic steels.

Manganese above 0.41 per cent seems to give little additional improvement of one previously has determined the quantitative effect of sulphur on the hot-workability of steels.

A heat of steel with resulphurized ingots of different sulphur contents and with sulphur added, both as stick sulphur and as sodium sulphite, was obtained through the courtesy of Mr. B. F. Courtright and Mr. F. W. Forman, of the Wisconsin Steel Co. In this heat containing 0.021 per cent sulphur in the ladle, ingots were resulphurized up to 0.130 per cent. Fig. 13 shows the results of the tests on these steels. The one lowest in sulphur shows much the best hot-workability.

The addition of sulphur as sodium sulphite gives only slightly better hotworkability than corresponding amounts added as elementary sulphur. Ramsey and Graper⁸ conclude that steel with sulphur

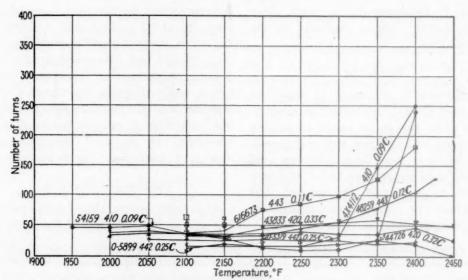


Fig. 6.—Effect of carbon in types 410, 420, 442 and 443 straight chrome steels.

Analyses												
Heat number	54159	4X4112	616673	48259	0-5319	0-5899	44726	43833				
C	0.09	0.09	0.108	0.12	0.25	0.25	0.32	0.33				
Mn	0.36	0.44	0.40	0.33	0.38	0.40	0.39	0.40				
S	0.010	0.008	0.017	0.009	0.018	0.020	0.012	0.017				
P	0.020	0.018	0.022	0.015	0.016	0.015	0.014	0.02				
Si	0.30	0.35	0.35	0.58	0.33	0.31	0.33	0.17				
Cr	12.47	12.71	21.73	21.10	22.28	22.38	13.93	13.67				
Ni	0.20	0.12	0.28									
Cu			1.16	1.18	1.05	0.99						

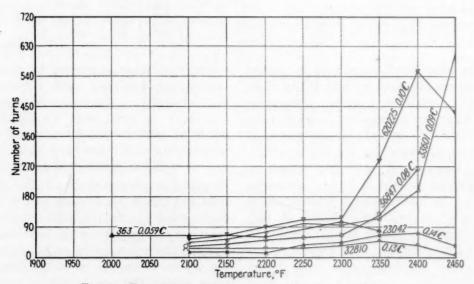


FIG. 7.—EFFECT OF CARBON IN TYPE 446 CHROME STEELS.

	A	nalyses				
Heat number. C. Mn. S.	363 0.059 0.43 0.021	56847 0.08 0.67 0.012 0.014	33601 0.09 0.45 0.011 0.008	620225 0.10 0.42 0.014	32810 0.13 0.51 0.019	23042 0.14 0.58 0.010
Si Cr	0.30 25.88 0.14	0.45 26.10 0.157	0.41 26.72 0.15	0.015 0.27 25.70 0.108	0.030 0.45 25.13 0.129	0.030 0.50 26.01 0.138

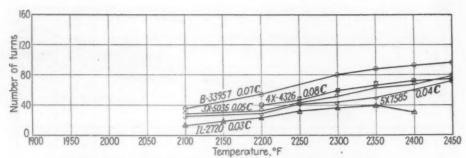


FIG. 8.—EFFECT OF CARBON IN TYPE 304 STEELS.

	Analyses				
Heat number	IL 2720	5X7585	3X5035	B-33957	4X4326
C	0.029	0.04	0.05	0.07	0.08
Mn	I.IO	0.49	0.55	0.50	0.82
S	0.014	0.007	0.007	0.010	0.008
P	O.OII	0.010	0.009	0.011	0.019
Si	0.59	0.42	0.35 -	0.41	0.47
Cr	19.28	18.44	18.24	18.70	19.09
Ni	7.08	10.68	10.68	10.34	10.24

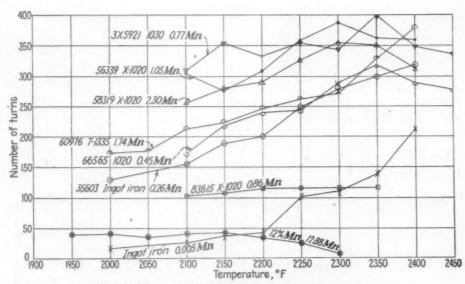


Fig. 9.—Effect of manganese in carbon steels.

				Analyses					
Heat number	Ingot	35603 Ingot Iron	66565	3X5921	83615	56339	60976	58319	12 % Mn
C	0.02	0.04	0.22	0.34	0.23	0.26	0.36	0.25	0.64
Mn	0.005	0.26	0.45	0.77	0.86	1.05	1.74	2.30	12.88
S	0.026	0.024	0.021	0.007	0.031	0.028	0.014	0.017	0.032
P	0.009	0.004	0.014	0.010	0.018	0.021	0.014	0.015	0.017
Si	0.02	0.003	0.08	0.13	0.21	0.23		0.13	0.88
Ni									3.11
Si							0.014		0.88

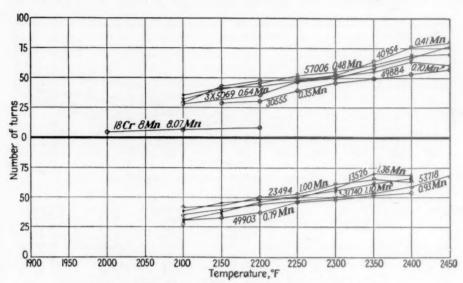


FIG. 10.—EFFECT OF MANGANESE IN TYPE 304 STEELS.

		Analyses				
Heat number 30	2555	40954	57006	3X5069	49884	18 Cr 8 Mn
C 0	. 05	0.06	0.05	0.04	0.06	0.11
	.35	0.41	0.48	0.64	0.70	8.07
	.OII	0.012	0.013	0.006	0.012	0.036
P 0	.012	0.012	. 0.015	0.011	0.016	0.010
Si 0	.41	0.45	0.31	0.37	0.68	0.53
Cr 18	. 15	18.70	18.25	18.70	17.55	17.80
Ni 9	.74	10.50	8.94	10.50	10.68	0.45
Heat number		49903	53718	23494	31740	13526
C		0.05	0.06	0.063	0.06	0.069
Mn		0.79	0.93	1.00	1.10	1.36
S		0.013	0.011	0.006	0.010	0.009
P		0.013	0.024	0.022	0.010	0.031
Si		0.44	0.36	0.21	0.50	0.38
Cr		18.45	19.30	18.16	18.05	
Ni		10.63	10.90	10.35	9.84	
Temperature °F.						

80 80 47556 0.39 Ma 3X6198 273142 4X2003 0.58Mn 20 900 1950 2000 2050 2100 2150 2200 2250 2300 2350 2400 2450 Temperature, °F

FIG. 11.—EFFECT OF MANGANESE IN TYPE 321 STEELS.

	A	nalyses				
47556	615296	4X2003	4X3762 0.06	3X6198	3X6611 0.06	52808
0.39	0.53	0.58	0.70	0.79	0.91	1.01
0.011	0.020	0.018	0.022	0.012	0.024	0.014
18.40	18.24	18.46	17.96	18.00	18.00	18.05 10.82 0.39
	0.05 0.39 0.008 0.011 0.60 18.40	47556 615296 0.05 0.055 0.39 0.53 0.008 0.009 0.011 0.020 0.60 0.52 18.40 18.24 10.53 11.91	0.05 0.055 0.04 0.39 0.53 0.58 0.008 0.009 0.008 0.011 0.020 0.018 0.60 0.52 0.79 18.40 18.24 18.46 10.53 11.91 10.48	47556 615296 4X2003 4X3762 0.05 0.055 0.04 0.06 0.39 0.53 0.58 0.70 0.008 0.009 0.008 0.007 0.011 0.020 0.018 0.022 0.60 0.52 0.79 0.50 18.40 18.24 18.46 17.96 10.53 11.91 10.48 11.48	47556 615296 4X2003 4X3762 3X6198 0.05 0.055 0.04 0.06 0.05 0.39 0.53 0.58 0.70 0.79 0.008 0.009 0.008 0.007 0.008 0.011 0.020 0.018 0.022 0.012 0.60 0.52 0.79 0.50 0.51 18.40 18.24 18.46 17.96 18.00 10.53 11.91 10.48 11.48 11.56	47556 615296 4X2003 4X3762 3X6198 3X6611 0.05 0.055 0.04 0.06 0.05 0.06 0.39 0.53 0.58 0.70 0.79 0.91 0.008 0.009 0.008 0.007 0.008 0.007 0.011 0.020 0.018 0.022 0.012 0.024 0.60 0.52 0.79 0.50 0.51 0.62 18.40 18.24 18.46 17.96 18.00 18.00 10.53 11.91 10.48 11.48 11.56

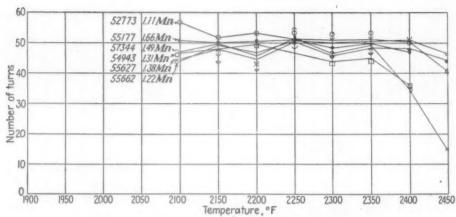


FIG. 12.—EFFECT OF MANGANESE IN TYPE 321 STEELS.

	A	nalyses				
Heat number	52773	55662	54943	55627	57344	55177
C	0.05	0.06	0.05	0.06	0.06	0.05
Mn	I.II	1.22	1.31	1.38	1.49	1.66
S	0.009	0.007	0.009	0.007	0.010	0.008
P	0.020	0.017	0.016	0.017	0.016	0.016
Si	0.50	0.42	0.59	0.59	0.56	0.59
Cr	18.45	18.00	18.50	17.90	18.65	18.40
Ni	10.88	10.94	10.48	10.94	10.75	10.63
Ti	0.38	0.40	0.40	0.39	0.32	0.40

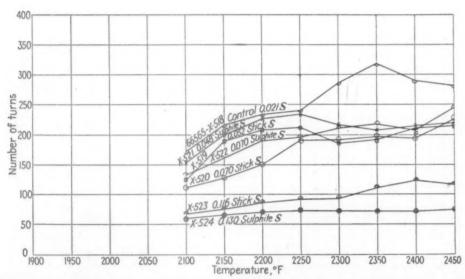


Fig. 13.—Effect of sulphur added as stick sulphur and as sodium sulphite in ingots of a single heat of S.A.E. 1020 steel.

		An	alyses				
Heat number	X-518	X-519	X-520	X-521	X-522	X-523	X-524
C	0.22	0.22	0.23	0.23	0.24	0.24	0.24
Mn	0.45	0.48	0.48	0.46	0.46	0.46	0.44
S	0.021	0.052	0.070	0.048	0.070	0.116	0.130
P	0.014	0.014	0.014	0.014	0.014	0.014	0.014
Si	0.08	0.08	0.08	0.08	0.08	0.08	0.08

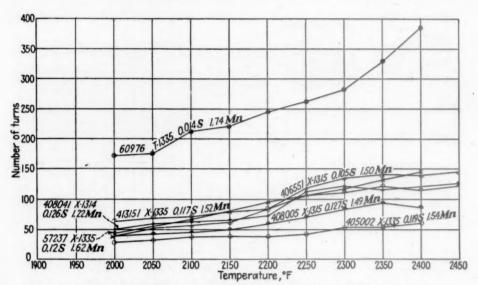


FIG. 14.—EFFECT OF SULPHUR IN S.A.E. X-1314, X-1315 AND X-1335 STEELS.

		An	alyses				
Heat number	408041	406551	408005	413151	405002	57237	60976
C	0.17	0.13	0.19	0.30	0.32	0.33	0.36
Mn	1.22	1.50	1.49	1.52	1.54	1.63	1.74
S	0.126	0.105	0.127	0.117	0.119	0.12	0.014
P	0.022	0.017	0.027	0.025	0.031	0.026	0.014
Si	0.01	0.07	0.11	0.04	0.056	0.20	0.27

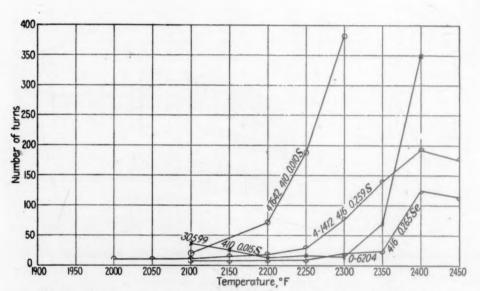


FIG. 15.—EFFECT OF SULPHUR AND SELENIUM IN TYPES 410 AND 416 STEELS.

. A	nalyses			
Heat number	47642	30500	4-1412	0-6204
Mn	0.31	0.44	0.42	0.46
S P	0.010	0.015	0.259	0.017
SiCr	0.33	0.53	0.33	0.28
Se				0.265

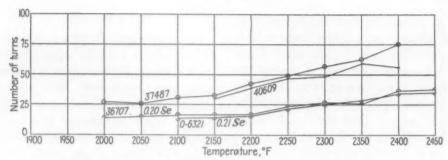


Fig. 16.—Effect of selenium in 303 and 304 steels.

																							,	A	nalyses			
Heat																									36707	37487	0-6321	40609
C					9.				. ,			*			*	Ŕ	*	*		×		×			0.07	0.07	0.04	0.05
Mn					۰						,	4	,		×		*			*					0.60	0.49	1.00	0.73
S		4		*									*		*	×	×		٠	×		*			0.017	0.010	0.016	0.012
P			ò	•					. ,		*				×	×		×		×					0.012	0.014	0.019	0.009
Si	*			6		× :		. ,	. ,					4								,			0.47	0.47	0.66	0.32
Cr																									18.48	18.95	18.55	18.95
N1	ė		è	ė			. ,					0	*			,	×	ĸ	*	8		*			9.43	10.65	9.52	10.58
Se						. 1				*		*		*			*	*			0				0.20		0.210	

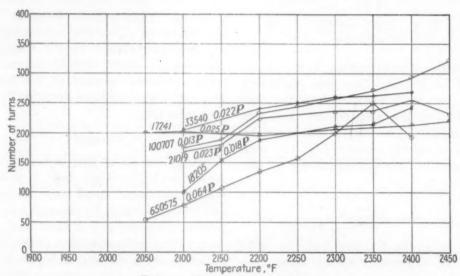


FIG. 17.—EFFECT OF PHOSPHORUS.

	A	nalyses				
Heat number	100707	18205	33540	31010	17241	650575
U.x	O.II	0.12	0.11	0.12	0.12	0.08
Mn	0.47	0.52	0.52	0.45	0.46	0.18
S	0.023	0.026	0.030	0.025	0.030	0.027
P	0.013	0.018	0.022	0.023	0.025	0.064
S1	0.04	0.17	0.20	0.132	0.178	0.01

added as sodium sulphite can be rolled as well as though no sulphur were added. This is not confirmed by the tests shown in Fig. 13, which show that in general the lower the sulphur content of the steel the better its hot-workability. Added sulphite sulphur in no case gives such good results as the low-sulphur control samples.

Fig. 14 gives the results of tests on steels with different sulphur, carbon, and manganese contents. Although manganese is important for reducing sulphur red shortness, the 0.014 per cent sulphur steel is definitely the most ductile at high temperatures.

In Fig. 15, chromium reduces the redshort effect of sulphur and selenium and makes type 416 steels quite hot-workable. In Fig. 16, selenium in the 18-8 type of stainless steel lowers its hot-workability.

Phosphorus

Low-phosphorus steels show normal curves in Fig. 17. One heat containing 0.064 per cent phosphorus shows low ductility at low temperatures and this rises rapidly above 2250°F. and then falls off just as quickly above 2350°F. This may be caused by the low manganese of this heat.

Silicon

Silicon up to 0.20 per cent has little effect in low-carbon steels. Over 1.00 per cent, it decreases hot-workability as shown in Fig. 18. The higher sulphur in heats 1065276 and 1083578 has an added depressing effect on their hot-workability.

In the austenitic chrome, nickel, stainless steels, silicon above 0.50 per cent markedly decreases hot-workability at the higher temperatures, as shown in Fig. 19. This is probably the result of the ferriteforming tendency of this element, which forms a duplex structure and thus reduces the hot-workability.

Chromium

Chromium from about 0.5 per cent up to 27 per cent is a widely used alloying element in steels. It also is used in conjunction with other elements such as nickel, molybdenum and silicon.

Nine steels containing from 0.70 to 26.0 per cent chromium are shown in Fig. 20. Below about 9 per cent, the steels show lower hot-workability with increasing chromium content, but above 9 per cent the ductility increases, especially above 2300°F.

In Fig. 21, a series of 5 per cent chromium steels is shown. Molybdenum, silicon and vanadium have little effect in these steels as compared with heat 57153, which contains no additional alloying elements. Titanium causes a dip in the curves, which again rise at very high temperatures.

Silicon, molybdenum, titanium and columbium all affect the hot-workability at high temperatures of the austenitic, chrome-nickel steels. Here the curves turn down, probably because of the ferrite-forming tendency of these elements. Fig. 22 illustrates this.

Nitrogen

Nitrogen as an alloying element is used most often in chromium steels. It is found also as an impurity in all steels. In carbon and low-alloy steels, the amounts normally present are small and in these quantities do not affect hot-workability. In the higher chromium steels, ductility at high temperatures decreases with increased nitrogen. The effect of 0.058 per cent nitrogen in type 430 steels is evident in Fig. 23. A maximum of 0.035 per cent nitrogen is specified for type 430 piercing rounds, to assure good pierceability.

Fig. 24 shows the effect of nitrogen in type 446 steels.

Nickel

Pure nickel is very ductile at high temperatures. Nickel up to 5 per cent in steels

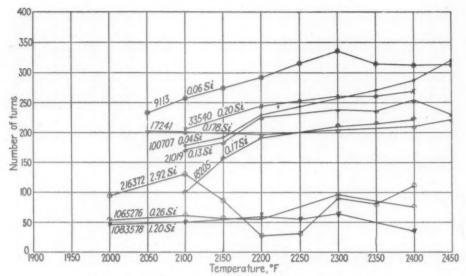


Fig. 18.—Effect of silicon in low-carbon steels.

				Analyse	S				
Heat number		9113 0.12	21019	18205	33540	17241	1065276	0.052	1083578
Mn	0.47	0.51	0.45	0.52	0.52	0.46	0.26	0.37	0.232
P		0.035	0.025	0.026	0.030	0.030	0.043	0.030	0.043
Si	0.04	0.06	0.132	0.17	0.20	0.178	0.26	2.98	1.20

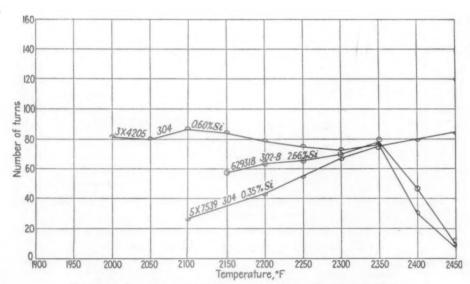


Fig. 19.—Effect of silicon in types 304 and 302-B steels.

													A	2	20	ıl	y	Sé	es		
Heat																			5X7539	3X4205	629318
C	0.1						 	Ċ,		*			*		*		×		0.05	0.05	0.08
Mn.				×	*	×	* 1		. ,	6	,	*		*	*			×	0.54	0.59	1.40
S							. ,				×					×			0.007	0.010	0.010
P																			0.012	0.014	0.021
Si	*	 		×							×					,			0.35	0.60	2.66
Cr		 																	18.56	18.40	18.08
Ni																			10.66	10.48	9.80

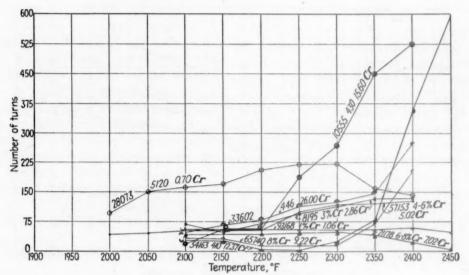


FIG. 20.—EFFECT OF CHROMIUM.

		A	nalyses					
28073 0.21 0.43 0.026 0.018 0.23 0.70	93168 0.15 0.45 0.011 0.014 0.80 1.06	8195 0.11 0.47 0.009 0.013 0.30	57153 0.14 0.28 0.018 0.016 0.16 5.02	21178 0.11 0.38 0.014 0.016 0.69 7.02	65740 0.06 0.42 0.027 0.009 0.74 9.22	54163 0.10 0.34 0.014 0.016 0.25	10555 0.07 0.41 0.013 0.018 0.38	33602 0.08 0.39 0.019 0.014 0.26 26.00
	0.51	0.49		0.55	0.90		0.025	0.15
	0.21 0.43 0.026 0.018 0.23	0.21 0.15 0.43 0.45 0.026 0.011 0.018 0.014 0.23 0.80 0.70 1.06	28073 93168 8195 0.21 0.15 0.11 0.43 0.45 0.47 0.026 0.011 0.009 0.018 0.014 0.013 0.23 0.80 0.30 0.70 1.06 2.86	0.21 0.15 0.11 0.14 0.43 0.45 0.47 0.28 0.026 0.011 0.009 0.018 0.018 0.014 0.013 0.016 0.23 0.80 0.30 0.16 0.70 1.06 2.86 5.02	28073 93168 8195 57153 21178 0.21 0.15 0.11 0.14 0.11 0.43 0.45 0.47 0.28 0.38 0.026 0.011 0.009 0.018 0.014 0.018 0.014 0.013 0.016 0.016 0.23 0.80 0.30 0.16 0.69 0.70 1.06 2.86 5.02 7.02	28073 93168 8195 57153 21178 65740 0.21 0.15 0.11 0.14 0.11 0.06 0.43 0.45 0.47 0.28 0.38 0.42 0.026 0.011 0.009 0.018 0.014 0.027 0.018 0.014 0.013 0.016 0.016 0.009 0.23 0.80 0.30 0.16 0.69 0.74 0.70 1.06 2.86 5.02 7.02 9.22 0.51 0.49 0.55	28073 93168 8195 57153 21178 65740 54163 0.21 0.15 0.11 0.14 0.11 0.06 0.10 0.43 0.45 0.47 0.28 0.38 0.42 0.34 0.026 0.011 0.009 0.018 0.014 0.027 0.014 0.018 0.014 0.013 0.016 0.016 0.009 0.016 0.23 0.80 0.30 0.16 0.69 0.74 0.25 0.70 1.06 2.86 5.02 7.02 9.22 12.37 0.51 0.49 0.55	28073 93168 8195 57153 21178 65740 54163 10555 0.21 0.15 0.11 0.14 0.11 0.06 0.10 0.07 0.43 0.45 0.47 0.28 0.38 0.42 0.34 0.41 0.026 0.011 0.009 0.018 0.014 0.027 0.014 0.013 0.018 0.014 0.013 0.016 0.016 0.009 0.016 0.018 0.23 0.80 0.30 0.16 0.69 0.74 0.25 0.38 0.70 1.06 2.86 5.02 7.02 9.22 12.37 15.60

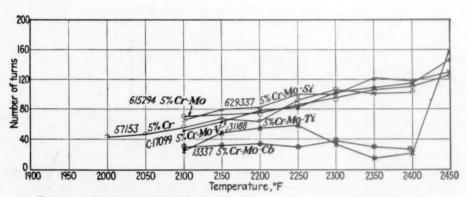


FIG. 21.—EFFECT OF Mo, Si, Ti, Cb, V IN 5 PER CENT CHROMIUM STEELS.

	A	nalyses				
Heat number	57153 0.14 0.28 0.018 0.016 0.16 5.02	615294 0.13 0.37 0.012 0.018 0.20 5.00 0.53	31188 0.09 0.45 0.014 0.011 0.50 5.18	13337 0.058 0.41 0.033 0.008 0.35 5.30	C-17099 0.16 0.56 0.018 0.014 0.20 4.94 0.45	629337 0.13 0.29 0.020 0.015 1.07 5.13 0.55
Ti. Cb. V		0.33	0.39	0.76	0.23	0.33

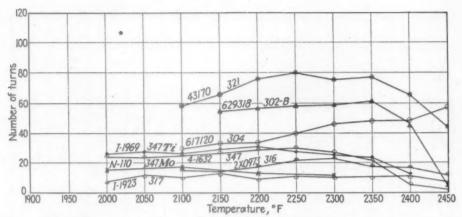


Fig. 22.—Effect of Ti, Cb, Mo, Si, CbTi, CbMo in chrome-nickel stainless steels.

			Analys	es				
Heat number	629318	617120	2X0973	I-1923 0.05	43170	4-1632	I-1969 0.05	N-110 0.05
Mn	1.40	1.37	1,60	4.00	0.45	1.75	2.49	1.76
S	0.010	0.013	0.107	0.009	0.011	0.015	0.010	0.011
P	0.021	0.017	0.015	0.018	0.018	0.015	0.016	0.023
Si	2.66	0.50	0.32	0.29	0.49	0.47	0.60	0.41
Cr	18.08	18.59	18.08	18.18	18.60	19.63	18.35	18.40
N1	9.80	10.44	11.40	12.52	10.74	11.47	10.45	13.39
Mo			2.35	3.39				2.02
Ti					0.45		0.10	
Cb						0.73	0.80	0.70

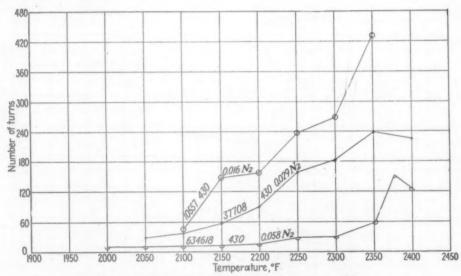


Fig. 23.—Effect of nitrogen in type 430 steels.

														A	2	26	ıl	ys	ies		
Heat :																			10557	37708	634618
C			*					,			,					*			0.08	0.09	O.II
Mn		* 1				×	*		*				*				×		0.44	0.43	0.34
S			*	*	*														0.018	0.013	0.018
P																			0.022	0.013	0.018
Si																			0.38	0.38	0.35
Cr	* *		*		*							*							15.86	15.00	15.60
Ns																			0.016	0.020	0.0575

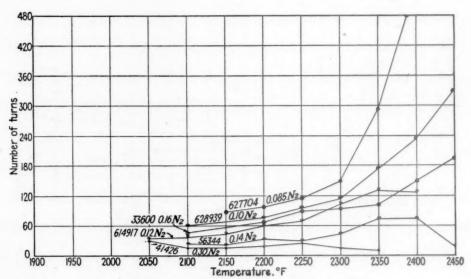


Fig. 24.—Effect of nitrogen in type 446 steels.

	A	nalyses				
Heat number	627704	628939	614917	56344	33600	41426
	0.09	0.09	0.105	0.12	0.10	0.10
	0.37	0.42	0.38	0.64	0.42	0.48
S P	0.014	0.009	0.010	0.005	0.010	0.012
Si.	0.20	0.33	0.36	0.47	0.43	0.38
Cr.	25.10	26.36	26.12	25.65	27.12	26.44
N ₂ .	0.085	0.108	0.125	0.14	0.16	0.30

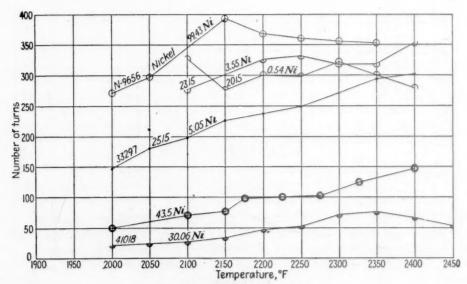


FIG. 25.—EFFECT OF NICKEL.

	A	nalyses				
Heat number	SAE 2015 0.18	SAE 2315 0.16	SAE 2515	41018	43.5 % Ni 0.052	Nickel 0.06
Mn	0.39	0.57	0.51	0.47	0.49	0.26
S P	0.021	0.013	0.009	0.042	0.008	0.005
Si Ni	0.28	3.55	0.18	0.17	0.13	0.05
Pe. Cu.	54	3.33	3.33	000	40.3	0.10

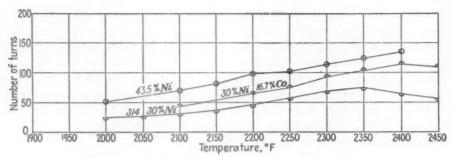


Fig. 26.—Effect of cobalt in high-nickel steels.

													Д		0 /	-7	yses		
												,	6.8	LE	0.6	DO.	7303		
																	Ni-Co Alloy	314	43.5 % Ni
C	 			 													0.040	O.II	0.052
Mn.			9.		,			4	×					÷			0.41	0.47	0.49
S																	0.021	0.042	0.011
P																		0.010	0.008
Si	 			 	,		*			ė							0.08	0.17	0.13
Ni.						*		×		×	ń		8	×		*	30.10	30.06	43.5
Co.																			

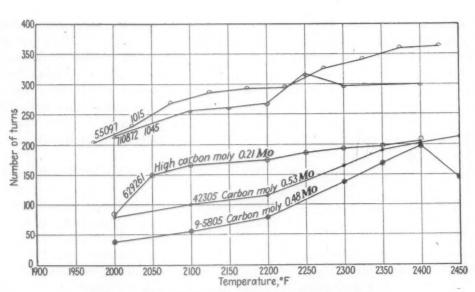


Fig. 27.—Effect of molybdenum in carbon steels.

An	llyses			
	5805 42305	55097	629261	710872
	14 0.12	0.13	0.40	0.45
***********	42 0.48	0.47	1.73	0.84
***************************************	020 0.025	0.028	0.016	0.042
		0.013	0.016	0.026
	.31 0.23 48 0.53	0.03	0.15	0 00

improves hot-workability at all temperatures. Fig. 25 shows high ductility curves for 0.5, 3.5 and 5 per cent nickel steels. The 30 and 43 per cent nickel steels have much lower values but this is probably caused by the formation of austenite rather than from the nickel as an element. Nickel is one of the few elements that improves the hot-workability of steels.

Cobalt

Cobalt is not widely used as an alloying element in steels. Fig. 26 shows a comparison between straight nickel steels and a steel containing 19 per cent cobalt with nickel. The cobalt does not appear to affect the hot-workability of these steels.

Molybdenum

Molybdenum reduces the hot-workability of carbon steels as shown in Fig. 27. Steels of the same carbon content without molybdenum are shown to be better.

In the 5 per cent chromium steels shown in Fig. 28, molybdenum has little effect.

In the 27 per cent chromium steels shown in Fig. 29, the nitrogen spread probably accounts for the variation in the curves. However, the hot-workability of chromium steels with more than 2 per cent molybdenum decreases markedly above 2300°F.

The ferrite-forming tendency of molybdenum in the austenitic chromium-nickel steels lowers the hot-workability of these steels as shown in Fig. 30.

Vanadium

Fig. 31 shows the effect of vanadium in chromium steels and in chromium-nickelcolumbium steels. This element in small amounts seems to have little effect on hot-workability.

Titanium

No titanium-carbon steels were available for determining the effect of titanium alone. Its effect on other steels is to change the type of curve rather than the maximum number of turns. Curves showing this tendency are found in Fig. 32. This element is a ferrite former and hence must be balanced with nickel, manganese and carbon to prevent a duplex structure, and poor hot-workability.

Columbium

Columbium has a marked depressing effect on the hot-workability of 5 per cent chromium-molybdenum steels, and also on the austenitic chromium-nickel stainless steels. In Fig. 33, the comparison of these with similar steels containing no columbium is shown.

Lead

Recently lead has been used in steels to improve machineability. This has raised the question of whether it affects the other properties of these steels. The previous work indicates that little change in such properties occurs from the addition of lead. This work, however, has been confined to these properties at room temperatures.

Fig. 34 shows the detrimental effect of lead on hot-working in steels of low and intermediate carbon. This comparative effect is not so pronounced in the high-sulphur steels shown in Fig. 35. The hot-workability of the similar nonleaded steels is low because of the sulphur. The lead, however, is additive in this direction. Lead seems to have a lowering effect similar to that of sulphur.

Fig. 36 shows the neutralizing effect of chromium on the red-shortness tendency of lead. This is similar to its action on sulphur.

Tin

Through the courtesy of Dr. S. F. Urban and Mr. R. D. Webb, Jr., of the Carnegie Illinois Steel Corporation, a series of killed open-hearth steels contain-

ing various amounts of tin and carbon were made available for hot-workability tests. Individual ingots were given increasing amounts of tin in each carbon-content and 39. In the higher carbon steels shown in Figs. 40 and 41, less difference is found between the low-tin steels and the ones containing greater amounts. However, even

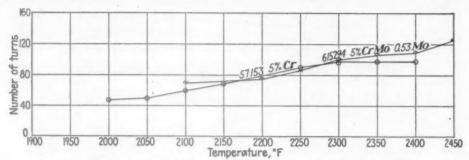


FIG. 28.—EFFECT OF MOLYBDENUM IN 5 PER CENT CHROME STEELS.

																				ai									
Heat	1	11	1	n	1	b	eı	r.		×			ě								*							615294	57153
C		0.	9										0			9	0	9	×				*			0	×	0.13	0.14
Mn.					0		0			0	,	0		0	0				0				*	×				0.37	0.28
S		0				0.0	0		0			à			0		0							*				0.012	0.018
P						2				*														*				0.018	0.016
Si	0				45	0	10				0														۰			0.20	0.16
Cr			a		*		×				6	6			D			0	0	0			*					5.00	5.02
Mo										0		*							*									0.53	

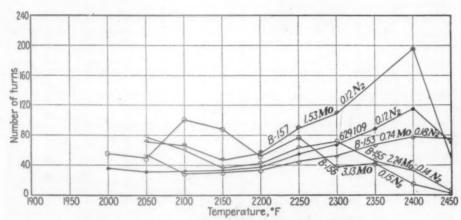


Fig. 29.—Effect of molybdenum in type 446 steels.

	Analyses				
Heat number	629109	B-153	B-157	B-155	B-156
C	0.11	0.12	0.12	0.12	0.12
Mn	0.33	0.43	0.38	0.43	0.43
5	0.010	0.015	0.012	0.012	0.013
**************	0.013	0.009	0.011	0.008	0.008
Si	0.28	0.41	0.39	0.37	0.45
UT	25.80	26.91	26.88	26.84	26.81
Mo		0.74	1.53	2.24	3.13
N1	0 120	0.18	0.12	OTA	0 15

class. Fig. 37 shows the effect of tin in low-carbon steels. Even 0.057 per cent tin markedly lowers the hot-workability, and this decreases further with increased tin content. In the 1025 and 1045 steels, the effect of tin is similar, as shown in Figs. 38

in these steels, increasing tin definitely decreases hot-ductility.

DISCUSSION OF RESULTS

A rapid twist test was devised to study quantitatively the hot-workability effect

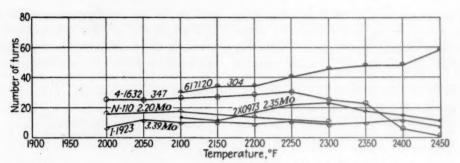


FIG. 30.—EFFECT OF MOLYBDENUM IN CHROME-NICKEL STAINLESS STEELS.

	Analyses				
Heat number	617120	2X0973	I-1923	4-1632	N-110
C	0.074	0.022	0.05	0.07	0.05
Mn	1.37	1.60	4.00	1.75	1.76
D	0.013	0.107	0 009	0.015	0.011
P	0.017	0.015	0.018	0.015	0.023
Si	0.50	0.32	0.29	0.47	0.41
Cr	18.59	18.08	18.18	19.63	18.40
Ni	10.44	11.40	12.52	11.47	13.39
MO		2.35	3.39		2.02
Сь				0.73	0.70

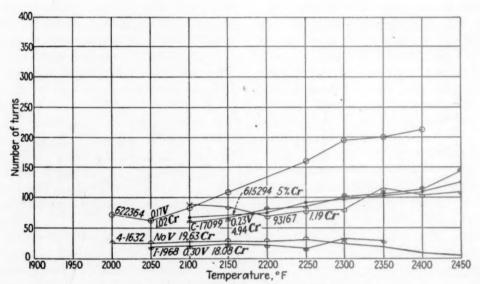


FIG. 31.—EFFECT OF VANADIUM.

	A	nalyses				
Heat number	93167	622364	615294	C-17099	4-1632	I-1968
C	0.13	0.20	0.13	0.16	0.07	0.05
Mn	0.45	0.72	0.37	0.56	1.75	1.98
S	0.014	0.023	0.012	0.018	0.015	0.000
P	0.017	0.017	0.018	0.014	0.015	0.010
Si	0.95	0.26	0.20	0.20	0.47	0.47
Cr	1.19	1.02	5.00	4.94	19.63	18.08
V		0.17		0.23	0.032	0.30
Ni					II.47	10.53
Съ					0.73	0.70

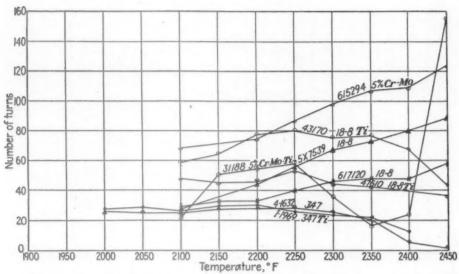


Fig. 32.—Effect of titanium in 5 per cent chrome and chrome-nickel stainless steels

9 43170 0.07 0.45 7 0.011 2 0.018	47610 0.05 0.40 0.011	4-1632 0.07 1.75 0.015	I-1969 0.05 2.49 0.010	615294 0.13 0.37	31188 0.09 0.45
0.45 7 0.011	0.40	1.75 0.015	2.49	0.37	0.45
7 0.011	0.011	0.015			
			0.010	0 010	
2 0.018				0.012	0.014
	0.013	0.015	0.016	0.018	0.011
0.49	0.50	0.47	0.60	0.20	0.50
18.60	18.15	19.63	18.35	5.00	5.18
10.74	10.68	11.47	10.45		
0.45	0.40		0.10	0.53	0.54
		0.73	0.80		0.39
			0.45 0.40	10.74 10.68 11.47 10.45 0.45 0.40 0.10	10.74 10.68 11.47 10.45 0.45 0.40 0.10 0.53

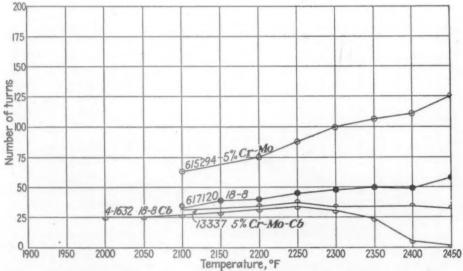


Fig. 33.—Effect of columbium in 5 per cent chrome and chrome-nickel stainless steels

Analyses			
Heat number 615294	13337	617120	4-1632
C 0,13	0.058	0.074	0.07
Mn 0.37	0.41	1.37	1.75
S 0.012	0.033	0.013	0.015
P 0.018	0.008	0.017	0.015
Si 0.20	0.35	0.50	0.47
Cr 5.00	5.30	18.59	19.63
Ni		10.44	11.47
Mo 0.53	0.51		
Cb	0.76		0.73

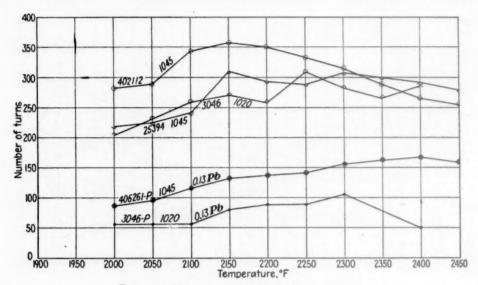


FIG. 34.—EFFECT OF LEAD IN CARBON STEELS.

	Analyses				
Heat number.	3046	3046-P	402112	25394 0.45	406261-P 0.45
Mn	0.48	0.48	0.78	0.84	0.71
SP	0.031	0.031	0.035	0.025	0.032
Si	0.17	0.17	0.29	0.21	0.20
Pb		0.13			0.13

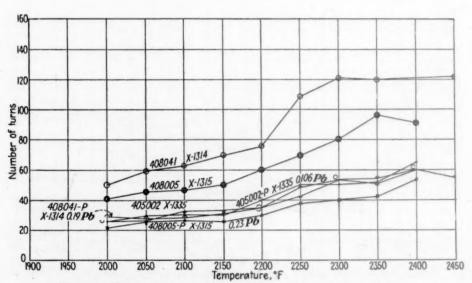


FIG. 35.—EFFECT OF LEAD IN HIGH-SULPHUR MANGANESE STEELS.

		Analyses				
Heat number	408041	408041-P	408005	408005-P	405002	405002-P
Mn.	0.17	0.17	1.40	0.19	0.32	1.53
S	0.126	0.126	0.127	0.127	0.119	0.119
P	0.022	0.022	0.027	0.027	0.031	0.031
Si	0.01	0.01	O.II	O.II	0.056	0.056
Pb		0.19		0.23		0.106

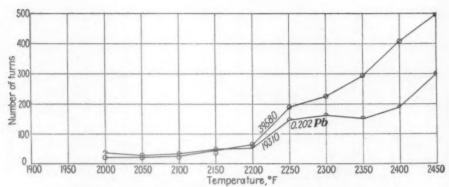


Fig. 36.—Effect of lead in type 430 stainless steels.

													J.	L	121	ai	13	13	e.	s					
Heat 1																								39580	0.086
Mn	*							,																0.43	0.44
S																								0.015	0.014
Si								,,	4									*		* *	*		*	0.42	0.37
Cr																								15.48	17.09
Pb		*	٠	٠	*	*	*	*	*	*	*	*		*		*	+	*	*	÷	*	*	*		0.202

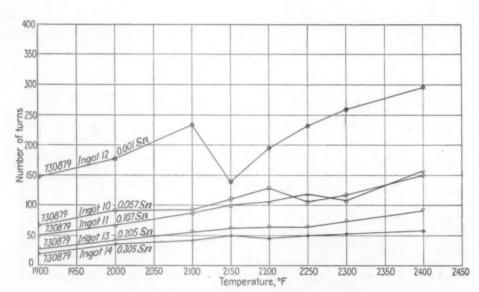


Fig. 37.—Effect of tin in S.A.E. 1010 steels.

	Analyses				
	Ingot 12	Ingot 10	Ingot II	Ingot 13	Ingot 14
C	0.12	O.II	0.12	0.11	0.12
Mn	0.38	0.36	0.37	0.37	0.38
S	0.033	0.033	0.033	0.032	0.034
P	0.019	0.019	0.019	0.019	0.019
Si	0.04	0.05	0.05	0.04	0.04
Sn	100.0	0.057	0.107	0.205	0.304

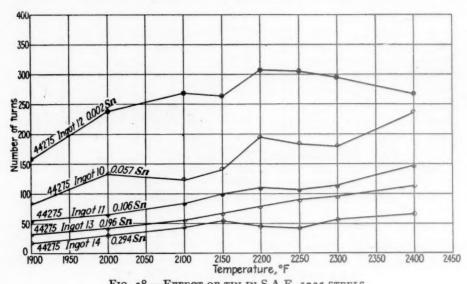


FIG. 38.—EFFECT OF TIN IN S.A.E. 1025 STEELS.

	Analyses				
Ç	Ingot 12 0.26	Ingot 10 0.27	Ingot II	Ingot 13 0.27	Ingot 14 0.26
Mn	0.49	0.49	0.48	0.50	0.48
PSi	0.014	0.012	0.015	0.014	0.012
Sn	0.002	0.057	0.106	0.196	0.294

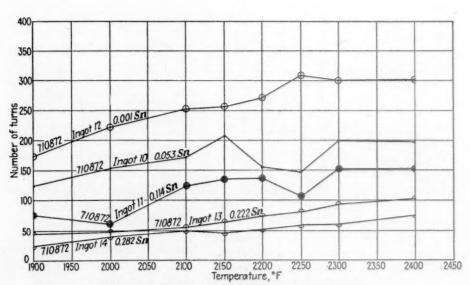


FIG. 39.—EFFECT OF TIN IN S.A.E. 1045 STEELS.

	Analyses				
	Ingot 12	Ingot 10	Inget II	Ingot 13	Ingot 14
C	0.45	0.47	0.48	0.47	0.44
Mn	0.84	0.84	0.86	0.86	0.84
S	0.042	0.042	0.041	0.042	0.041
P	0.026	0.027	0.026	0.027	0.025
Si	0.08	0.07	0.08	0.07	0.07
Sn	0.001	0.053	0.114	0.222	0.282

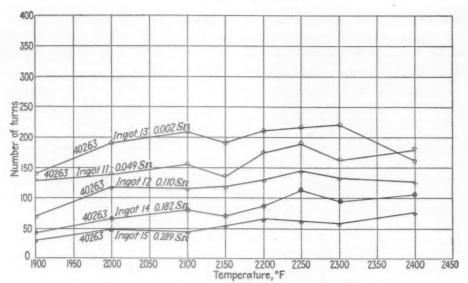


Fig. 40.—Effect of tin in S.A.E. 1075 steels.

	Analyses				
CMn	Ingot 13 0.76 0.84	Ingot 11 0.76 0.81	Ingot 12 0.78 0.80	Ingot 14 0.77 0.83	Ingot 15 0.77 0.85
P.	0.035	0.040	0.039	0.040	0.038
Sn	0.20	0.20	0.20	0.20	0.19

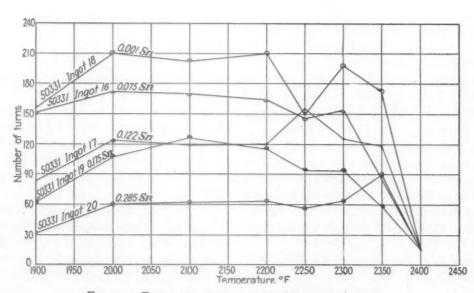


FIG. 41.—EFFECT OF TIN IN I PER CENT CARBON STEELS.

	Analyses				
C	Ingot 18	Ingot 16	Ingot 17	Ingot 19	Ingot 20
Mn	0.44	0.45	0.44	0.45	0.43
P	0.044	0.038	0.039	0.040	0.038
Si	0.22	0.20	0.22	0.21	0.21
Sn	0.001	0.075	0.122	0.175	0.285

of various alloying elements in steels. The test has shown excellent reproducibility on samples taken from a single heat. It has also shown that heats of the same class Manganese and nickel improve the hotworkability of carbon steels. Manganese also neutralizes some of the detrimental effect of sulphur.

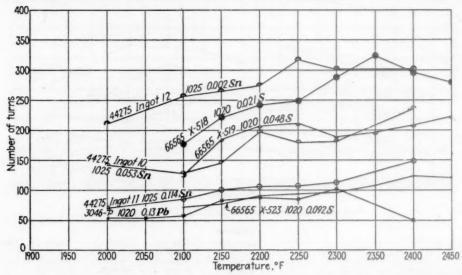


FIG. 42.—COMPARISON OF THE EFFECT OF TIN, LEAD AND SULPHUR IN CARBON STEELS.

		An	alyses				
Heat number	66565 X-518	66565 X-519	66565 X-523	44275 Ingot 12	44275 Ingot 10	44275 Ingot II	3046-P
C	0.22	0.22	0.24	0.26	0.27	0.28	0.20
Mn	0.45	0.48	0.46	0.49	0.49	0.48	0.48
S	0.021	0.052	0.116	0.030	0.037	0.040	0.031
P	0.014	0.014	0.014	0.014	0.012	0.015	0.020
Si	0.08	0.08	0.08	0.19	0.18	0.18	0.17
Sn				0.002	0.057	0.106	0.13

of steels vary considerably in their hotworkabilities. Critical steels must be tested individually to determine the proper conditions for rolling, forging or piercing. For seven years results of the tests have been successfully correlated with mill results on the piercing of rounds for the manufacture of seamless tubing.

Most of the added elements studied tend to decrease the hot-workability of steels. Sulphur, silicon, molybdenum, tin and lead show this effect in carbon steels.

Sulphur, tin and lead have a strikingly similar effect for equal amounts added to steels, as shown in Fig. 42. The decrease in the number of turns and the shape of the curves are very much alike for these elements.

Nitrogen and columbium have a marked depressing effect on the hot-workability of chromium steels.

Oxygen, carbon, phosphorus, cobalt, vanadium and titanium individually have little, if any, effect.

Chromium seems to have an adverse effect up to about 9 per cent, and above this amount it markedly increases the hotworkability. It also has a neutralizing effect on sulphur and lead in high-chromium steels.

The room-temperature austenitic steels have much poorer hot-workability than the room-temperature ferritic steels. Austenitic steels with ferrite-forming elements or with insufficient austenite-forming elements tend to have duplex structures, which have the poorest hot-workability.

CONCLUSIONS

A quantitative, hot-workability test has been devised and used to determine the effect of oxygen, carbon, manganese, sulphur, selenium, phosphorus, silicon, chromium, nitrogen, nickel, cobalt, molybdenum, vanadium, titanium, lead and tin on the hot-workability of steels. These elements have the following effects on the steels studied:

Little or	Beneficial	Detrimental
No Effect	Effect	Effect
Oxygen Carbon Phosphorus Cobalt Vanadium Titanium	Manganese Nickel Chromium (above 9 per cent)	Sulphur Selenium Silicon Nitrogen Molybdenum Columbium Lead Tin Chromium (below 9 per cent)

ACKNOWLEDGMENTS

The data for this paper have been taken from more than 7000 tests made in the laboratories of the Globe Steel Tubes Co. during the past seven years. Almost all of the laboratory staff have had a part in the development of the test, and in the collection and compilation of the data that have made this paper possible. This help is gratefully acknowledged.

REFERENCES

I. A. L. Feild: Effect of Zirconium on Hotrolling Properties of High-sulphur Steels. Trans. A.I.M.E. (1924) 70, 201-238.

. Hamilton: Determining Oxygen in Alloy Steels and Its Effect on Tube Piercing. Trans. A.I.M.E. (1934) 113, 111-125.

3. H. S. Rawdon: Effect of Sulphur and Phosphorus on Forging Steel. Proc. Amer. Soc. Test. Mat. (1934) 34, pt. I, 87-121; (1936) 36, pt. I, 88-91
4. J. Mitchell: Relative Effect of Elements on Alloy Steels. Metal Progress (July

J. W. Halley: Effect of Tin on the Properties of Plain Carbon Steels. Trans.

A.I.M.E. (1943) 154, 374-385.

Keller: The Effect of Tin on the Nature, Notably on the Rolling Characteristics of Siemens-Martin Ingot Steel.

7. J. H. Andrew and J. P. Peile: Effect of Tin as Impurity in Mild Steels. Jnl. Iron and Steel Inst. (1933) 128, 193-204.

8. E. L. Ramsey and L. G. Graper: Observa-

tions in the Making and Use of Sulphitetreated Steels. Trans. A.I.M.E. (1942)

150, 127-130. What is Steel? Trans. 9. A. A.I.M.E. (1924) 70, 3-24.

10. A. Sauveur: Steel at Elevated Temperatures. Trans. Amer. Soc. Steel Treat.

tures. Irans. Amer. Soc. Steel 1133. (1930) 17, 410-448.
W. Ellis: (a) An Investigation into the Effect of Constitution on the Malleability of Steel at High Temperatures. Carnegie Schol. Memoirs (1924) 13, 47-81; (1926) 15, 195-211. (b) Further Experiments on the Forgeability of Steel. Trans. Amer. Soc. Steel Treat. 11. O. Steel. Trans. Amer. Soc. Steel Treat.

(1933) 21, 673-707. 12. E. E. Thum: Critical Points. Metal Pro-

gress (1940) 37, 535.

13. The New House of Science. Globe Steel
Tubes Co., 1942.

14. H. K. Ihrig: A Quantitative Hot Workability Test for Metals. Iron Age (Apr. 20, 1944) 86-89. 15. C. L. Clark: Evaluating Steel Forge-

ability. Iron Age (March 16, 1944) 52-55.

DISCUSSION

(K. L. Fetters presiding)

C. L. CLARK* and J. J. Russ.*-Dr. Ihrig is to be complimented for this very comprehensive paper covering the hot-working of metals as influenced by various elements and, where similar analyses have been considered, his findings are in general agreement with ours.

While it is true, as Dr. Ihrig indicates, that appreciable differences may exist between individual heats of the more highly alloyed steel, it should be further recognized that Dr. Ihrig has selected heats covering the maximum permissible variations in composition and, in certain cases, even compositions somewhat beyond the allowable range. For example, in Fig. 3, eight different heats of type 304 are considered with a total nickel range of 8.43 to 10.72 per cent, and a chromium range of 17.15 to 20.28 per cent. Furthermore, the steel containing the maximum chromium content contains the minimum nickel. While these ranges may be permissible, any given producer of these steels recognizes that the chromium and nickel content must be properly balanced, especially for severe hot-working applications such as the piercing of seamless tubes. In fact, because of this, all tubular specifications permit a maximum nickel content of 11.0 per cent, rather than 10.0 per cent, in type 304 tubes, and we would certainly not consider a steel of this type containing 8.43 nickel, 20.28 chromium as being

^{*} Metallurgical Department, Steel and Tube Division, Timken Roller Bearing Co., Canton, Ohio.

satisfactory for piercing. If the two lowest nickel heats of Fig. 3 be disregarded, the differences in the temperature of maximum twist for the remaining heats is not great or of commercial importance.

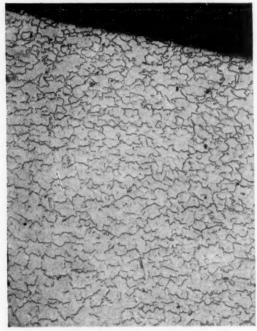


Fig. 43.—Heat 619276, type 430. Twist-tested at 2400°F. \times 35. Electrolytic oxalic acid etch.

This same general criticism applies to many of the other figures, for often, in addition to the variable under consideration, there are other variables that may be equally important. This is illustrated in Fig. 8, which has been included to show the influence of variations in carbon on type 304. Yet the nickel range in this series of heats is from 7.08 to 10.34 per cent and the chromium range from 18.24 to 10.28 per cent.

When Dr. Ihrig says that we have "concluded that the maximum forging temperature can be determined from the curves of single heats of various type steels" (p. 754), we believe he must have misinterpreted certain of our statements. We have always recognized that differences might and do exist between different heats of the same analysis and, in fact, if that were not true the validity of this test would be very much open to question, for no test, to our knowledge, is available that will yield absolutely the same results on different heats

of the same steel. However, we do believe that in the case of the lower alloyed steels produced by a given company, the differences in the temperature of maximum twist from heat to heat of a given analysis are of academic rather than commercial importance as far as hot workability is concerned. If this were not true, the ability of these steels to be forged on a production basis in the past under constant and uniform procedures would not have been possible.

H. K. IHRIG.*—Clark and Russ confirm our conclusions that the rapid hot-twist test is "an ideal procedure for determining proper temperatures for hot processing" of metals. This procedure originated in the Globe Steel Tubes Company's laboratories more than six years ago, and since that time has been used to control the hot piercing and rolling of seamless steel tubing of many different analyses.

Clark and Russ say that "in each case the number of twists required for fracture increases as the temperature is raised, until a critical temperature is reached after which the number of twists decreases." Their Fig. 3, curve D, has no critical maximum temperature; also, in their Fig. 8 the curve for 18-8 continues to rise with temperature. We have found a number of analyses that do not show any critical maximum temperature. Types 410 and 430 straight chrome stainless steels show a marked rise at high temperatures, rather than a falling off. Therefore, their statement that "each steel possesses a critical temperature as far as its ductility (as measured by twists to fracture) is concerned" is not supported by their own data nor by ours.

A sample twist bar of type 430, which had been fractured at 2400°F., was examined microscopically for the intergranular cracks that occur at high temperatures described by the authors. No evidence of any cracks could be found even very close to the actual breaks. The micrograph in Fig. 43 shows the fracture and the area adjacent to it.

In the presentation of their data on the twisting of various steels, no results are shown on the accuracy of reproduction of the test on a single heat or the difference in hot-

^{*} Chemical Engineer and Director of Laboratories, Globe Steel Tubes Co., Milwaukee, Wisconsin.

workability between heats of the same type of steels. It is believed that such data are essential for the use of any proposed test.

Clark and Russ make the statement that "the addition of stabilizing elements, such as

in temperature during hot-working. Why not measure this increase directly in the twist-test furnace?

The authors present no experimental data on either the variability of steels between

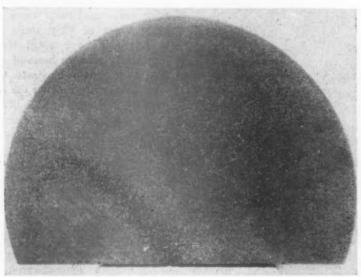


Fig. 44.—Effects of hot mechanical work (hammering) on overheated type 4340 steel. Actual size about $5\frac{1}{2}$ inches diameter.

columbium or titanium, and free-machining additions such as sulphur, selenium or phosphorus, decreases both the temperature of the maximum twist and the number of twists at this temperature" (p. 740). No data are shown for the effect of phosphorus and selenium. In fact, the 18-8 Ti heat in their Fig. 8 contains more than twice as much phosphorus as the 18-8 Cb heat, yet it shows better hotworkability in their twist tests. Our own work shows that phosphorus has little or no effect on the hot-workability of steels.

Clark and Russ give the results of torque tests on each of the steels tested. For each class the values are very much the same and all decrease regularly with increasing temperature. From these curves and work done by us no relationship between the torque values and the hot-workability of a steel can be seen. They also attempt to use the twist-torque ratio as a measure of hot-workability. Since the torque values are almost the same and decrease regularly with temperature, the ratio simply becomes a measure of the number of twists. They also attempt to use the torque values as a measure of the increase

heats or the reproducibility of results on a* single heat to support their conclusions. It has been shown by the writer* that the hotworkability of various heats of the same type of steel shows a wide range of twist-test values and therefore the test must be made on individual heats. Generalization on the factors that affect hot-workability cannot be made by single tests, but must be made only after many heats have been individually tested.

A. O. Schaefer.†—It is a pleasure to offer some comments on these papers even although we cannot submit any additional data, and our comments must consist largely in raising questions.

We have several interesting photographs taken from chrome-nickel-molybdenum steel gun forgings that were overheated before forging (Figs. 44 and 45).

The theory offered by Dr. Clark to explain "burning" seems to be reasonable in view of

^{*} Page 749 this volume and Iron Age (April 20, 1944).

[†] Executive Metallurgical Engineer, The Midvale Co., Nicetown, Philadelphia, Pennsylvania.

the condition revealed by these illustrations. It would appear from a study of these photographs that there is not only a critical or equicohesive temperature, but also a critical rate of deformation.

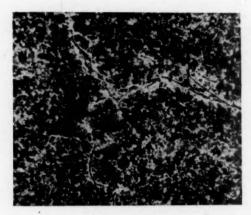


Fig. 45.—Micrograph taken in "dark" or "loose" zone of Figure 44. imes 100. Nital etch.

Most large forgings probably are worked at temperatures below the equicohesive temperature. In fact, it might be said that the temperature for the hot-working of large forgings is not too critical as compared with other factors, such as the thorough soaking at temperature prior to working.

One important factor that must be considered is that too high a temperature of heating for forging may result in finishing the forging at too high a temperature, with a resultant coarse grain structure that is removed by heat-treatment only at increased cost and time.

Furthermore, long experience has shown that finishing at a low temperature is an aid to heat-treatment, particularly in attaining improved ductility in the direction of working. The reverse of this is true to a certain extent, and forgings subjected to transverse testing usually are finished at higher temperatures.

Several questions suggest themselves after a reading of these two excellent papers. The torque reported in inch-pounds by Clark and Russ must represent the maximum torque reached during the period of the test. Is it not possible that the stress-strain curve that might be plotted from this test would be even more indicative of the condition of the metal than the data that have been presented?

The greatest field of usefulness of tests such as those described in the present papers for the manufacturer of forgings by conventional methods probably lies with the alloys that are now being developed for hightemperature applications. These alloys naturally are forged with more difficulty than other types of alloy steels. Manufacturers in this field have noted the difference in forgeability between heats of similar analysis. Mr. Ihrig's data illustrate this very well. Fig. 2 of his paper shows the spread in forgeability of a group of heats of SAE-1010 steel to be relatively small compared with the spread in forgeability between a group of heats of type 304 steel.

This variation in forgeability is extremely important, and no one who has worked with these steels will doubt its reality. However, to be of value to the men in the shop, the tests should be related to some means to indicate how such material may be forged. We should think it advisable to extend the work for groups of heats such as those shown in Fig. 3 to cover repetition of the tests using a variety of test speeds.

Furthermore, we think the stress strain curves should be plotted and compared for all of the determinations made. We should like to ask the speaker if any such thorough analysis of the situation has been made, or if the deductions from the series of curves have been utilized in any way in forging heats of these materials. The method of test is especially useful because it can be performed easily, and we look forward to the future development of increased usefulness for this means of study.

W. O. BINDER.*—The authors of both papers have indicated that a marked variation in hotworkability exists between different heats of steel, especially in some of the high-alloy-content materials. Dr. Ihrig illustrates this point in Figs. 3 and 4 of his paper, which show the spread of results in types 304 and 321 stainless steels. Neither paper, however, has brought out very clearly the influence of deoxidation in hotworkability. In comparing Figs. 10 and 12 of Dr. Ihrig's paper, which show the effect of manganese on the hot ductility of types 304 and 321 stainless steels, with Figs. 3, 4, and 11,

^{*}Union Carbide and Carbon Research Laboratories, Niagara Falls, N. Y.

it is seen that the 1 to 1.5 per cent manganese steels show greater uniformity than the lower manganese steels, especially the type 321 stainless steel. It seems logical to conclude, therefore, that deoxidation and cleanliness play a great part in rendering the steel uniformly hot-workable.

The beneficial influence of 1 to 2 per cent manganese in the production of stainless steels has been observed both experimentally and commercially, although it has not been revealed by the hot-twist test. Manganese, in amounts higher than normally considered necessary for deoxidation, facilitates the hot-rolling of stainless steels, particularly the austenitic grades containing carbide-forming elements such as columbium. These elements cause the formation of ferrite, which is likely to produce difficulty in hot-working. To assist forging and rolling, the practice has been to increase the nickel content somewhat to render the steel austenitic at the working temperatures and to increase the manganese content to between I and 2 per cent. The improvement imparted by manganese is not completely understood, although probably it is connected with its ability to form austenite and to deoxidize the steel.

K. L. Fetters.*—Several of us have seen the testing procedure that Dr. Clark uses, and several of us at one time and another have known the speed at which he operated his testing equipment. Do you know, Dr. Ihrig?†

H. K. IHRIG.—I think it was given in a previous paper in *Iron Age*; 180 r.p.m.

K. L. Fetters.—I think it is important that we have in mind that the rate of deformation in these two tests is quite similar.

There is one use that I know has been made of the results that Dr. Clark has studied or obtained; that is, they have been able to pierce some very high-alloy steels and some graphitic steels, which one might expect would be extremely difficult to do. They have used the torque value because they were able to control the speed of piercing on the piercing mill. I think that has been a very important reason why they have been able to pierce some of these very difficult alloys.

I was very much interested in the discussion on the effect of deoxidation on these steels. That is a part of the study that should be carried much further, although perhaps it has been in either one or both of the authors' laboratories.

I note that in piercing plain carbon steels and low-alloy steels, we find considerable variation from heat to heat, and in many cases the only factor that can be designated is the deoxidation of the respective heats.

Mr. Foley will read Dr. Clark's reply to Dr. Ihrig's discussion of his paper.

C. L. CLARK and J. J. Russ (author's reply). We are indebted to Dr. Ihrig for his discussion of our paper, and while differences of opinion evidently exist, it is apparent that we are in full agreement as to the value of the hot twist test for evaluating the hot-workability of metals.

We still insist that a critical temperature exists for each steel, after which the number of twists to fracture decreases. It is true, as Dr. Ihrig says, that the results presented for certain steels do not show this critical temperature but this is because of the extent of the temperature range investigated. For example, referring to our Fig. 8, the temperature of maximum twist for 18-8 is beyond the maximum temperature of 2450°F. considered in this figure, being 2500°F.

We likewise have examined twist bars of type 430 but, unlike Dr. Ihrig, we have found intergranular cracking in bars twisted at 2500°F. We did use a magnification of 100 diameters, rather than 35 diameters, as we would not expect the cracking to be visible at the lower magnification.

We probably erred in not mentioning the possible reproduction of results on the apparatus. Naturally, in the early days of our work a large number of bars from a given heat were tested at the same temperature and the agreement in both the torque and twist values was excellent. In this same connection, other companies have duplicated our equipment and, for calibration, they have been given heats already tested by us, and in every case the agreement in twist, at any given temperature, has been within two or three turns.

We cannot agree with Dr. Ihrig's comments with respect to the value of the torque char-

^{*} Youngstown Sheet and Tube Co., Youngstown, Ohio.

[†] Dr. Clark was not present at the meeting.

acteristics. While it is true that in all cases the torque values decrease with increasing temperature, they are not of the same order of magnitude, a fact that will be substantiated by anyone who has forged a wide range of alloy steels. To us, the torque values are just as important as the twist values in determining the proper temperature and speed for piercing seamless tubes.

Conclusions we have drawn as to the hotworkability of steels are based on tests from at least five production heats of each analysis over the complete temperature range. For the low and intermediate alloy steels the results are sufficiently uniform to be applicable to all heats, unless certain known variables are present in their composition. We agree, however, that on the highly alloyed steels it may be advisable to conduct the hot twist test on each heat, and this is our standard practice when piercing is concerned.

R. S. ARCHER.*—First I would like to join in the expression of appreciation for both of these papers. They are excellent and very valuable.

Clark and Russ have brought out in an interesting way the application of Jeffries' equicohesive temperature hypothesis to studies of the hot-working characteristics of metals. The extension of the hypothesis into the hotworking range is suggested by an early statement of Jeffries: "The equicohesive temperature of copper has been found to lie above 950°C. for rates of loading producing rupture in about 3 seconds." On this basis they have properly concluded that testing methods should employ rates of deformation comparable with those encountered commercially. It does not follow, however, that the behavior of all metals and alloys in hot-working processes will be affected by rate of deformation in the manner suggested. The equicohesive temperature was concerned chiefly with the properties of nearly pure metals. The grainboundary strength was considered as varying with rate and duration of loading in accordance with the view that the properties of the meal at the boundaries simulate those of the "amorphous cement" postulated by Beilby. The controlling factor was thus the variation

Dr. Ihrig has referred in his paper several times to the three hot-working processes; rolling, forging and tube piercing.

I assume that his actual correlation has been primarily with tube piercing in his own plant, and it is perhaps worth while considering that what steel-mill men commonly refer to as hot-rolling characteristics may include an entirely different phenomenon than that under consideration in these papers.

There are men here, of course, from other mills, and I hope some of them will express opinions in agreement or otherwise with the remarks I am about to make. To the rolling-mill men, in my experience, the criterion of whether a steel rolls well or not is based on the observation of cracking or breaking in the blooming mill, and on the subsequent observation of seams and other defects that result from such breaks.

It is a common expression that certain ingots have "broken during rolling," or that they show rolling-mill or blooming-mill breaks. Observation of many steels of the straight carbon and low-alloy types in my own experience has indicated that by far the great majority of these breaks are in the ingot before it enters the blooming mill, and up to that point, they do not involve this characteristic of hot-workability. They are essentially casting cracks.

They may occur at various stages prior to rolling. They may occur before the ingot is removed from the ingot mold, or they might occur in the soaking pits or during cooling before the ingot is charged into the pits if charging is abnormally delayed, and so on. We are all familiar with these various causes.

It seems that there is a basic difference between this characteristic of certain types of steel, and the characteristics revealed by the hot torsion test. Specifically we might refer to the effect of carbon content.

I believe it is rather a general experience in most of the mills that there is a rather critical

in the strength of the "amorphous phase" with temperature and rate or duration of loading. In some commercial alloys, grain-boundary strength may be affected to a greater extent by other factors, such as the occurrences of fusible material or brittle constituents at the boundaries, so that the effect of rate of deformation may be somewhat different.

^{*} Metallurgical Engineer and Assistant to Vice President, Climax Molybdenum Co., New York, N. Y.

range of carbon content in killed steels at about 0.15 to 0.22 per cent carbon where ingot breaks are most severe. The tendency to show breaks in rolling is less with higher carbon or with lower carbon. This difference becomes most clear if we depart substantially from the range that I mentioned; for example, over 0.30 per cent carbon or under 0.10, we find rolling with fewer breaks, which again we believe is due to the fact that the ingots had fewer breaks when they entered the blooming mill.

I believe no such effect is brought out in the torsion test and it is quite natural it should not be, because it is a different phenomenon.

One of the great values of Dr. Ihrig's paper lies in the tremendous number of tests involved, but I think probably he will agree that there are also a tremendous number of variables involved, so that perhaps still further experience may be needed to arrive at final conclusions.

Referring to Figure 14 of the paper, we find that the lowest or poorest curve on the chart is for an X-1335. In general, it seems to me that the curves would rate X-1335, X-1314, and X-1315 as being rather similar in hotworkability, but the X-1335 would be the lowest curve on the chart.

When we start the subsequent hot-working of finished bars, for example, in forging, we may assume that usually the defects that have resulted from ingot breaks have been removed. We all know, unfortunately, that that is not always true, although the intention is that it shall be true.

Citing specific experience on upset forging, there have been large numbers of heats of X-1335 made into upset forgings for shells with, I believe, excellent results; that is, the hot-working characteristics were quite satisfactory, although not quite as good perhaps as those of a 1045 steel.

There has also been quite a contrary experience in the making of similar forgings of X-1314, which would appear to be inconsistent with the results of these twist tests.

H. B. EMERICK.*—The Jones and Laughlin Steel Corporation recently installed at the Aliquippa Works metallurgical laboratory hot torsion testing equipment very similar

to that described by Clark and Russ. We use a 2-hp., 25-cycle, three-phase, 220-volt special squirrel-cage induction motor, with a Speed-Ranger and single parallel gearhead having a range of 6 to 1, and a torque output varying with the speeds. This type of test offers an excellent means for establishing optimum hot-working temperatures for a large variety of processing operations performed on steels that are particularly heatsensitive. Our work to date has been confined almost entirely to the resulphurized freemachining steels, both bessemer and openhearth, and to straight carbon and low-alloy grades utilized in tube-piercing operations on a Mannesmann seamless mill.

I agree with Dr. Archer that the test probably has no applicability for evaluating the forgeability of unconditioned cast ingots during primary operations. Our experience has been that the breaks and tears that occur in primary rolling are about 95 per cent due to defects existing in the ingots. In a seamless piercing mill, however, where first the bloom is conditioned carefully, rerolled to a round, and in some cases reconditioned in the round, there is a fairly clean surface with which to work. Then, of course, the hot-working temperature becomes a matter of primary importance.

Our main problem to date has been to find a tube to be inserted in the high-temperature furnace that will give a decent life at temperatures above 2300°F. We have used wrought 18-8 stainless, 2-in. o.d., 1-in. i.d., and ½-in. wall, and the life has been very poor with temperatures above 2150°F.; that is, the number of tests that can be run on each tube before it fails is not very great.

We consulted an alloy-casting company in an effort to secure a tube that would give higher life at these upper temperatures, and we now have a trial shipment of 38 per cent Ni, 18 per cent Cr centrifugally cast steel tubes that show some possibilities of giving longer life at temperatures in the neighborhood of 2350°, which is the range in which we are primarily interested.

In the Clark and Russ paper, a great deal of emphasis is placed upon the effect of changes in the deformation rate on the equicohesive temperature. In Dr. Ihrig's paper, the rate of deformation is stated to be 128 r.p.m. As Dr. Fetters has pointed out, this important

^{*}Steel Works Metallurgist, Jones and Laughlin Steel Corp., Alquippa, Pennsylvania.

detail seems to have been overlooked in the Clark-Russ paper.

If this rate of deformation is so important, I wonder about the advisability of standardizing on one rate of deformation for all the various grades described. In Dr. Ihrig's case, for example, how does the particular rate of deformation that he has chosen (128 r.p.m.) relate itself to the actual piercing rates on the mill for various grades and sizes of tubes?

I have one other question for Dr. Ihrig. He made a point, both in the paper and in the discussion, that it is quite possible to obtain different values of maximum twist for various heats of the same grade of steel. I should like some elaboration of how knowledge of the variation in the maximum twist temperature is applied to seamless piercing-mill operation? In other words, if the author finds a heat of a certain grade of steel that shows a temperature of maximum twist 50° or 100° below that of another heat of the same grade, what steps are taken in the seamless mill to apply that knowledge in piercing the respective heats?

K. L. Fetters.—As Mr. Emerick pointed out, each plant has its piercers operating at different speeds, and most of them do not have the benefit of variable-speed mills, or mills that have a wide range of speed. It may be that certain speed ranges in this twist testing would give the better correlations with the particular piercing practice.

F. B. Foley.*—It seems extremely doubtful to me that the kind of test described in these papers by Clark and Russ and by Ihrig is any measure at all of the strength of these materials at these temperatures.

It is doubtful whether any of them have any noteworthy strength of the kind we measure at room temperature. The postulate offered by Clark and Russ to explain certain observed phenomena and based on relative crystal and grain-boundary strength is open to criticism on a number of grounds. First of all, metal undergoing the very rapid type of deformation produced at the high temperatures in these experiments in a short-time high-temperature tensile test is probably not crystalline but amorphous at the time of fracture.

In other words, I suggest that atoms moving as far and as fast as they must move in the metal being subjected to such severe deformation are not able to maintain their position in any fixed crystalline lattice.

The atoms in metals undergoing mechanical work move distances that produce deformation that is measurable by means of instruments of the highest precision, if the loads be relatively very low, or are readily perceived by the unaided eye when loads are relatively very high. When the load is light enough to cause only a little movement of the atoms making up the crystal lattice, the crystallinity of the metal persists and ultimately, after a very long period of time, failure occurs with very little deformation through grain boundaries, which are the weakest points at elevated temperatures because of the normal atomic movement there incident to grain growth.

When the load is high enough to produce continuous flow, the atoms, in the region of stress concentration, are set into motion so that the mass acts as a viscous liquid. Under these conditions the metal loses its crystallinity and there are no grain boundaries through which failure may occur.

Between the two extremes, one in which the load is so low as not to move the atoms effectively within long periods of time, and the other in which the load is so great as to move all of them continuously out of their spheres of crystalline influence, localized decrystallization occurs. This local decrystallization happens in the neighborhood of the grain boundaries where movement of the atoms incident to grain growth tends toward decrystallization and involves layers of atoms at greater and greater depth within the crystals as the stress applied becomes great enough to throw the balance in favor of decrystallization. Under such conditions, there is a mixture of amorphous, so to speak, and crystalline matter. It is to be understood that upon unloading movement stops and crystallinity is completely restored. It is only while the metal is actually in motion that the described conditions prevail, and what determines the nature of the failure is the distance and speed of the movement.

This mechanism of failure suggests itself as a result of the observation of crystalline behavior of steel subjected to hot-working

^{*}Superintendent of Research, The Midvale Co., Nicetown, Philadelphia, Pa.

by rolling, forging and pressing. It is an observed fact that the austenitic grain size of steel that has been hot-worked and not treated subsequently is a function of the temperature at which hot-working ceased. This could result from one of two mechanisms of grainsize alteration. One of these would involve the mechanical "breaking up" by forging or rolling of the large crystals that grew at the temperature to which the steel was initially heated. The other mechanism involves the decrystallization of the metal by the forces applied in hot-working, which results in the destruction of the original large grains. Immediately deformation ceases recrystallization occurs with the formation of grains characteristic of the existing temperature and time. The first of these processes would produce, for one thing, austenitic crystals distorted in the direction of the applied working stresses rather than the equiaxed austenitic grains that actually are found. Only a process such as the second one could result in the equiaxed crystals of a size that decreases as the temperature of final hotworking decreases. This discussion is not concerned with "work lines" produced by drawing out segregates in the direction of hot-working.

The rapid and violent distortion of the metal produced by the method used by these authors must necessarily develop the highest degree of decrystallization and plasticity. Naturally, the metal lends itself more readily to decrystallization the higher the temperature to which it is heated. The test is simply a measure of the ability of the metal to deform readily at high temperatures without rupture. The word "readily" is used advisedly. The readiness with which the metal deforms depends largely on the strength of the intracrystalline cohesive forces at the temperature of testing. The readiness with which the metal fails may be due to weakening of the intercrystalline cohesive forces by what amounts to liquefaction produced by heat intentionally applied for the test and by that resulting from mechanical work.

C. CRUSSARD.*—About this question of equicohesive temperature, I should like to point out some results we obtained in the

metallurgical laboratory of the School of Mines in Paris, showing that resistance to the deformation passes through a maximum with increasing grain size. We found these results in creep tests under constant load. Of course the deformation rates were slower than in the high-temperature twist tests, and I will discuss further the validity of my results for the latter tests. What we found was the following:

Plotting the creep rate (second stage) versus grain size (going from very fine grain to single crystals) the curve passed through a minimum for a grain size about 1-mm. diameter. If the creep rate is minimum, the resistance to deformation is maximum for this grain size. This could be understood easily if we think that creep implies two counteracting phenomena.

First, the larger the grain, the easier the intracrystalline gliding, which explains the increase of creep rate with grain size on the right part of the curve.

Second, the slip process creates near the boundaries a very high distorted zone, which, if the temperature is high enough, can deform as a kind of amorphous layer. This so-called amorphous plasticity has a more important effect; the greater the boundary surface, the finer the grain. This phenomenon explains the left part of the curve.

Of course the grain size for minimum creep rate depends on the temperature and load.

I do not know exactly what the result will be for very high deformation rate as involved in forging processes, but care must be used in applying in this field the results described, because of a new phenomenon we were able to see—the plastic glide at high deformation rates follows different laws than at low rates. We have shown it in the following way:

The first stage of a creep curve under moderate load is a regular parabolic curve, but if the load is high and applied abruptly, the creep goes on in a jerky way and the registered curve is stepwise; that means that the strain-hardening effect is very high under high rates of deformation, almost stopping the creep for a short time, during which a kind of recovery occurs, allowing a new creep to take place, and so on.

These two phenomena (ratio between boundary and intracrystalline creep on one

^{*} School of Mines, Paris, France.

hand and effect of deformation rate on strainhardening on the other) may be sufficient to explain the hot-workability of pure metals, but forging of impure metals like steel imply many other complicated factors.

C. D. PREUSCH.*—Primarily, I had a number of questions but some of them have already been answered. Could the authors give us an idea of what they would consider a satisfactory number of twists for piercing or rolling quality, or for hammer forging, or upsetting?

Some of the data that have been presented do not seem to agree exactly with our mill experience. Of course, many variables enter into this. The matter of metal working is to a great extent an art as yet, but I wonder if Dr. Ihrig could explain some of the contradictions that appear between our mill practice and the twist-test data?

For instance, in Dr. Clark's paper, there is a chart showing poorer workability for 18-8 with 0.23 per cent sulphur than for the 25-12 and 25-20 analyses. Our mill experience has been contrary to this. We have generally found 18-8 with 0.25 per cent sulphur to be reasonably easily workable, whereas 25-20 and 25-12 are more difficult to handle. Also, in our forging operations we found an addition of columbium to 18-8 to be helpful rather than harmful to over-all workability.

We have never been able to work 25-20 at some of the temperatures that appear to be suitable as indicated by the twist-test curves. The curves seem to show that these steels should work satisfactorily at 2300° to 2400°F., whereas our experience indicates better workability at slightly lower temperatures.

There has always been a great deal of discussion among operating men about the effect of soaking time. Has any work been done on that phase of the question by means of the twist test?

Dr. Ihrig has shown the effects of nitrogen, and to some extent, the effect of oxygen on workability. Has any work been done on the effect of hydrogen? Have the effects of manganese over 2 per cent been studied? I refer to the range slightly over 2 per cent but not as high as the Hadfield manganese steels.

Has any work been done with a bend test instead of the twisting test? Rather obviously, a bend test does not have the quantitative possibilities of the twist test, but I wonder whether it might be useful as a rough or convenient guide.

G. H. Boss.*-I would like to ask suggestions concerning a difficulty we experienced recently while hot-flanging boiler plate. This metal, which was from two aluminum-killed open-hearth heats made in the same mill, gave no trouble during rolling by the manufacturer. However, when we tried to hotflange it, cracks similar in appearance to the sort usually associated with copper hot-shortness developed. Numerous short shallow cracks appeared in certain areas, usually where the extension was biaxial; occasionally there was a long crack which cut through the plate. The cracks which, judging by their ragged path, followed old austenitic grain boundaries, all contained the blue oxide of iron. Before burning is suggested, let me say that this metal was never heated above 2000°F. Another company, while flanging sheets from one of the same two heats, had the same difficulty. One of the heats was analyzed with the following results: carbon, 0.12 per cent; manganese, 0.56; phosphorus, 0.000; sulphur, 0.030; copper, 0.12; tin, 0.002; arsenic, 0.004; nickel, 0.06. It is difficult to understand how such an analysis could be troublesome.

In reference to Mr. Foley's hypothesis that metals approach the amorphous state when rapidly hot-worked, may I mention the following? Some years ago I visited a plant making collapsible tubes. The tubes are formed top down from slugs of white-metal alloys a little thicker than a five cent piece. The die, where the slug is placed, is shallow and forms only the top of the tube. The punch, which is shaped like the tube except that the dead end has not been crimped together strikes the slug forming the thick-walled top part of the tube in the die. The metal in the remainder of the slug then forms the tube body around the punch in a sort of impact extrusion process. The metal runs up the punch in ripples. In motion, it looks like a liquid. It is not a true liquid, however,

^{*} Crucible Steel Company of America, Harrison, New Jersey.

^{*} Baldwin Locomotive Works, Philadelphia, Pennsylvania.

as it maintains perfect physical continuity and never splashes; no fluid could run up the wall of the punch body unless it wet the surface, which this does not. Obviously, this low-melting-point alloy has been heated to above its recrystallization temperature by the mechanical working.

R. K. Kulp.*—Some information on Mr. Boss' question regarding the effect of copper on pierceability can be found in a paper by Soler on surface defects. An example is given of contamination of the surface of a tube by a bronze guide roll in the reeling operation. Large amounts of copper, as exemplified by localized contamination in the bronze guide roll, will result in hot-shortness. Copper in limited quantities will not cause surface defects if sufficient nickel is present.

Dr. Archer's comments indicated that the hot twist test is of use primarily in determining the pierceability of a specific type of steel or of an individual heat of steel. Could this same test be used to determine the hotworking characteristics of new analyses of alloy steels? Could data such as optimum temperatures for ingot breakdown be developed by the hot twist test? Have results of accumulated data been used to determine forgeability as well as pierceability of highly alloyed steels?

This method of testing is quite useful because the data that is developed can be applied directly to piercing operations. It is hoped that increased experience with the test will broaden the scope of the application of the data secured from it.

C. L. CLARK and J. J. Russ (authors' reply). We are appreciative of the numerous discussions and regret that we were unable to be present in order to answer from the floor many of the questions that were raised. In order to have our closure as brief as possible, we will attempt to answer the questions without reference to the individuals who raised them, as many can be answered in a more or less general discussion.

All of the results reported were obtained under a testing speed of 180 r.p.m. We have done considerable work on the effect of rate of twist and find in general that increased speeds tend to move the temperature of maximum twist downward but have little effect on the number of twists required for fracture. Likewise, all of the tests reported were confined to rolled or forged bars. Work done on cast bars shows them to generally exhibit the same temperature of maximum twist as wrought bars of the same analysis, but the number of twists to fracture is considerably less. This is probably due to the dendritic formation in the cast bars, especially those of the austenitic grades.

We fully agree that the rate of deformation is of extreme importance in all high-temperature forming operations, and it was entirely for this reason that we have standardized on the twist test, in which the speed can be varied over a wide range, for determining the proper temperature for the various hot-working operations.

In the earlier work it had been planned to continuously record the torque during the entire twisting time but it was found that the torque value did not vary during the test. In other words, the torque value multiplied by the number of twists and divided by the speed of testing gives an accurate indication of the work required for rupture. The uniformity of the torque value over the complete testing-time period has been confirmed by other investigators.

Too broad generalities cannot be drawn as to the relative ease of hot-processing the various austenitic grades of steels without stating which of the hot-forming operations is being considered. Our own experience has definitely shown that types 302 and 304, when properly balanced, will definitely pierce more readily than 303, 321, 347, 309 and 310 and this experience is confirmed by the results from the hot twist tests.

It was not intended to imply that all difficulties concerned with the hot-processing of steel would be eliminated through the determination of the hot twist characteristics for, as it has been stated in the discussion, many of these difficulties may arise in the cast ingots and from other causes. It is believed, however, that defects arising from working the

05.

^{*}Metallurgical Engineer, Electro Metallurgical Co., New York, N. Y.

18 Soler: Trans. A.I.M.E. (1941) 145, 204-

metal either too hot or too cold can be corrected by this procedure.

Because of the relatively short time the hot twist test has been in active use, it is recognized that many factors still remain to be investigated, and among these, of course, are the various practices employed for deoxidation of the steel during melting. It is understood that several companies are now conducting hot twist tests, consequently information should soon be available as to the effect of many variables pertaining to melting practice and chemical composition.

H. K. IHRIG (author's reply).—We agree with Mr. Schaeffer's statement that "manufacturers in this field (high alloy) have noted the difference in forgeability between heats of similar analysis," and, "this variation in forgeability is extremely important, and no one who has worked with these steels will doubt its reality."

We have tried various speeds but have found little differences in the curves or temperatures of maximum hot-workability at different speeds. We believe that the speeds should be fast enough to be of the order of magnitude of large-scale operations.

We have used the twist-test data to a limited extent for our own forging operations, but have correlated them to a much greater extent with our piercing operations, which are more important to us in the manufacture of seamless tubing.

Mr. Binder says, "The authors of both papers have indicated that a marked variation in hot-workability exists between different heats of steel, especially in some of the high-alloy-content materials." We have continually emphasized this experimental fact, but Clark and Russ have drawn conclusions on the hot-workability of steels based on tests of a single or only a few heats of steel.

Mr. Binder raises the question of the influence of deoxidation on the hot-workability. In Fig. 5 we show the effect of silicon and aluminum in the deoxidation of carbon steels. Some work on the effect of manganese in stainless steels is shown in Figs. 10, 11 and 12. It would be interesting to extend this to other steels and with other deoxidizing agents.

Mr. Archer raises the question of the

application of the hot-workability test to the rolling of ingots. It is difficult to obtain cast bars that are representative of large ingots. If the bars are cast individually, the crystalline structures and segregations are not the same as those in the ingots. If bars are cut from different sections of a large ingot, we would expect them to show different hot-workabilities. Such a study might be very informative, however.

In our work we have carefully examined each bar after etching and have tested only the sound bars. The test was designed to test the hot-working properties of steels and not as a detector of defects in them.

Mr. Emerick asks about the type of tube used in the testing furnace, We do not use a tube but merely set the heating coil in a plastic refractory cement. We have never had any difficulty with this part of the apparatus.

He also asks what steps are taken in piercing two heats with different temperatures for maximum twists. In our mill all heats of critical hot-working steels are tested before piercing and the proper piercing temperature as determined by the test for each heat is used on the mill for that heat.

We agree with Mr. Foley that it is doubtful that the twist test is any measure at all of the strength of steels at the temperatures used and that they have any noteworthy strength of the kind we measure at room temperature. Work done several years ago convinced us that torque values were not important. With Mr. Foley, also, we do not agree with the Clark and Russ theory of crystalline and intercrystalline strength at high temperature. In our discussion of their paper we have pointed out several experimental inconsistencies with this theory.

Mr. Preusch asks what we would consider a satisfactory number of twists for piercing or rolling quality. We have correlated thousands of tests with our mill results on the same heats, and from this experience we believe that a heat must show a maximum of about 50 twists for wholly satisfactory piercing in our mill. Between 40 and 50 twists, uncertain results are obtained, usually with poor yields, and with less than 40 twists poor results occur. This would not necessarily be the same on another piercer of different characteristics or operation. For forging and rolling, these

figures would be lower. It is well known that several steels that can be forged and rolled cannot be pierced successfully.

Mr. Preusch's experience with columbium helping the hot-workability of 18-8 steels

years ago but could not correlate the results with our mill operations.

Mr. Kulp asks if the test could be used to determine the hot-working characteristics of new analyses of alloy steels. We have used it

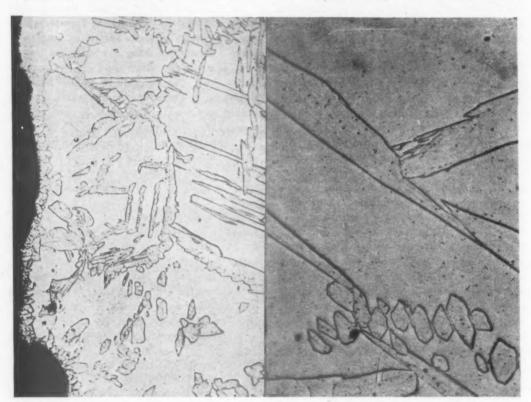


FIG. 46.—TYPE 430 STEEL, 2500°F. X 100.

FIG. 47.—TYPE 430 STEEL, 2500°F. × 500.

is not in accord with our experience or any others that we have heard of. Such steel is much more difficult to pierce than 18-8 without columbium.

We have soaked test bars as long as 8 hr. without showing any marked difference in hot-workability. In larger sections in the mill we have found it advisable to soak critical steels under 1800°F. and then pierce and roll them as soon as they reach their piercing temperatures.

We have not studied the effect of hydrogen because of the lack of a quick and accurate method of hydrogen determination.

We have not done any work with steels containing over 2 per cent manganese except the Hadfield type and the 18 per cent chromium 8 per cent manganese steel shown in Fig. 10.

We ran some hot bend tests a number of

for this purpose many times not only for new alloy steels but for nonferrous metals as well. In every case our mill results checked closely with those of the test.

Clark and Russ, in reply to our discussion of their paper, "still insist that a critical temperature exists for each steel, after which the number of twists to fracture decreases." They offer no experimental evidence to support this insistence. They say that in the example pointed out by us in their Fig. 8 the temperature of maximum twists is 2500°F., but they do not give the data at that temperature or any above it to support their statement. They also do not explain their generalized curve D in their Fig. 3, which shows no maximum.

They believe that the reason we did not detect cracks in the heat of type 430 steel was because it was not examined at high enough magnification. It was shown at 35 diameters to show more of its section, but was examined at higher magnifications also. Micrographs of another heat of type 430 steel are shown in Figs. 46 and 47. No intergranular cracking can be seen. This heat had 785 twists at 2500°F. before breaking.

We note that they have partially agreed with us that the hot-workability characteristics vary from heat to heat of the same type of steel and that critical steels should be tested individually. This would necessitate a change in their conclusions in their present paper and one previously published on this subject.

Clark and Russ in their direct discussion of our paper indicate that we have selected a wide range of analyses in our Fig. 3, some of which were even beyond the allowable range. All of these steels were large commercial heats submitted to Globe Steel Tubes Co. for seamless tubing manufacture. Some were rejected on the basis of their twist tests. Certainly any new proposed test must be tried on other than heats in the middle of any chemistry range and conclusions should not be drawn except on the results obtained from a wide variety of tests. Their 18-8 heat shown in their Table 1 and Fig. 8 is also not within the

allowable range for chromium for type 304 steel.

They say that we have misinterpreted their statements on their conclusions about maximum forging temperatures.

In their conclusions in both their present paper and the one published in *Iron Age*, they say that with a factor of safety of using 50°F. lower temperature than that indicated by the test, heats of any given type of steel may be hot-worked. No mention is made in their papers or in their conclusions that hot-workability varies sufficiently from heat to heat to necessitate individual tests on many steels. The necessity for this has been shown by actual data by us in our papers. Clark and Russ have finally admitted this necessity for high-alloy steels in their reply to our discussion of their paper.

It is gratifying to us to see the interest shown in our hot-workability test as indicated by the large number of discussions and the many interesting points brought out in them. We realize that we have only started work in this interesting field, and that we and others will continue work to answer numerous questions on the effect of variables on the hotworkability of metals with more experimental data.

Institute of Metals Division, Volume 166 Transactions AIME, 1946

TECHNICAL PAPERS AND DISCUSSIONS

Physical Metallurgy

Electron Metallographic Methods and Some Results for Magnesium Alloys. By R. D. Heiden-Reich, C. H. Gerould and R. E. McNulty. (Metals Tech., Apr. 1946, T.P. 1979)

"Shadow cast" Replicas for Use in the Electron Microscope, By Helmut Thielsch. (Metals Tech., Feb. 1946, T.P. 1977, with discussion)

Lamellar and Mosaic Structures—X-ray and Thermodynamic Evidence. By Helmut Thielsch (Metals Tech., Oct. 1945, T.P. 1931, with discussion)

Graphical Methods of Representing Some Conditions of Plasticity. By WILLIAM MARSH BALDWIN, JR. (Metals Tech., Apr. 1946, T.P. 1980, with discussion)

Young's Modulus—Its Metallurgical Aspects. By DAVID J. MACK. (Metals Tech., Dec. 1945, T.P. 1936, with discussion)

Relative Triaxial Deformation Rates. By WILLIAM M. BALDWIN, JR., T. S. HOWALD and A. W. Ross. (Metals Tech., Sept. 1945, T. P. 1808, with discussion)

Diffusion of the Stable Isotopes of Nickel in Copper. By WILLIAM A. JOHNSON. (Metals Tech., June 1946, T.P. 2007, with discussion)

Copper and Copper-rich Alloys

Solubility of Carbon in Molten Copper. By MICHAEL B. BEVER and CARL F. FLOE. (Metals Tech., Sept. 1945, T.P. 1802, with discussion)

Effect of Phosphorus, Arsenic, Sulphur and Selenium on Some Properties of High-purity Copper. By J. S. SMART, JR. and A. A. SMITH, JR. (*Metals Tech.*, Sept. 1945, T.P. 1807, with discussion)

The Effect of Phosphorus on the Properties of Gun Metal—Reducing Conditions. By ROBERT A. COLTON and BLAKE M. LORING. (Metals Tech., June 1946, T.P. 1974, with discussion)

Nickel-antimony-lead-copper Bearing Alloys. By John T. Eash. (Metals Tech., Dec. 1945, T.P. 1937, with discussion)

Physical Properties of Copper-manganese-zinc Alloys Containing 60 Per Cent Copper and 5 to 25 Per Cent Manganese. By R. S. Dean, J. R. Long, T. R. Graham and R. G. Feustel. (Metals Tech., Jan. 1946, T. P. 1956)

Effect of Rolling and Annealing upon the Crystallography, Metallography and Physical Properties of Copper Strip. By William M. Baldwin, Jr. (Metals Tech., April 1942, T.P. 1455)

Aluminum Alloys

Tensile Properties of Aluminum-alloy Sheet at Elevated Temperatures. By Alan E. Flani-Gan, Leslie F. Tedsen and John E. Dorn. (*Metals Tech.*, Dec. 1945, T.P. 1929, with discussion)

Correlation of Mechanical Properties and Corrosion Resistance of 24S-type Aluminum Alloys as Affected by High-temperature Precipitation. By W. D. Robertson. (Metals Tech., Oct. 1945, T.P. 1934, with discussion)

Diffusion in R301 Alloy and Its Effect on the Corrosion Resistance. By L. F. Mondolfo. (Metals Tech., Dec. 1945, T.P. 1940, with discussion)

Magnesium Alloys

- Superheating of Magnesium Alloys. By N. TINER. (Metals Tech., Oct. 1945, T.P. 1935, with discussion)
- Rates of High-temperature Oxidation of Magnesium and Magnesium Alloys. By T. E. LEONTIS and F. N. RHINES. (Metals Tech., June 1946, T.P. 2003, with discussion)
- Properties of Cerium-containing Magnesium Alloys at Room and Elevated Temperatures. By T. E. LEONTIS and J. P. MURPHY. (Metals Tech., Apr. 1946, T.P. 1995, with discussion)
- Susceptibility of Four Magnesium Casting Alloys to Microporosity and Its Effect on the Mechanical Properties. By JAY R. Burns. (Metals Tech., Feb. 1946, T.P. 1955, with discussion)
- Some Properties of Sand-cast Alloys in the Magnesium-rich Corner of the Magnesium-aluminum-zinc System. By R. S. Busk and R. F. Marande. (Metals Tech., June 1946, T.P. 2009, with discussion)

Miscellaneous Metals and Alloys

- Preparation and Properties of Ductile Titanium. By R. S. Dean, J. R. Long, F. S. Wartman and E. L. Anderson. (Metals Tech., Feb. 1946, T.P. 1961)
- Ductile Titanium—Its Fabrication and Physical Properties. By R. S. Dean, J. R. Long, F. S. Wartman and E. T. Hayes. (Metals Tech., Feb. 1946, T.P. 1965)
- Silver-thallium Antifriction Alloys. By F. R. HENSEL. (Metals Tech., Feb. 1946, T.P. 1930, with discussion)
- Vicalloy—A Workable Alloy for Permanent Magnets. By E. A. NESBITT. (Metals Tech., Feb. 1946, T.P. 1973)
- A Study of the Behavior of Rutheniopalladium in Torch Flames, with the Object of Improving Soldering Technique. By R. H. Atkinson and G. P. Gladis. (*Metals Tech.*, Apr. 1946, T.P. 1982, with discussion)
- Effect of Copper and Some Other Metals on the Gold-germanium Eutectic. By ROBERT I. JAFFEE and BRUCE W. GONSER. (Metals Tech., Apr. 1946, T.P. 1998)

Symposia

Symposium on Extrusion

- The Extrusion Process. By W. W. COTTER and W. R. CLARK. (Metals Tech., Sept. 1945, T.P. 1850, with discussion)
- Some Factors Affecting the Rate of Extrusion of Aluminum Alloys. By T. L. FRITZLEN. (Metals Tech., Oct. 1945, T.P. 1851, with discussion)

Symposium on Powder Metallurgy

- Seminar on Sintering. By F. N. RHINES. (Metals Tech., Aug. 1946, T.P. 2043)
- The Pressing Operation in the Fabrication of Articles by Powder Metallurgy. By RICHARD P. SEELIG and JOHN WULFF. (Metals Tech., Aug. 1946, T.P. 2044) With discussion
- Pressing Complicated Shapes from Iron Powders. By CLAUS G. GOETZEL. (Metals Tech., Oct. 1945, T.P. 1920) With discussion
- Hot-pressing of Iron Powders. By Otto H. Henry and J. J. Cordiano. (Metals Tech., Oct. 1945, T.P. 1919) With discussion
- Notes on Copper-base Compacts and Certain Compositions Susceptible to Precipitation-hardening. By F. R. Hensel, E. I. Larsen and E. F. Swazy. (*Metals Tech.*, Aug. 1945, T.P. 1810) With discussion
- Silicide-hardened Copper Compacts for Bearings. By F. R. HENSEL, E. I. LARSEN and E. F. Swazy. (Metals Tech., Feb. 1946, T.P. 1976) With discussion
- A Study of the Physical Properties and Microstructure of Sintered Steels. By George Stern. (Metals Tech., Aug. 1946, T.P. 2045) With discussion
- Nickel-iron Alloys Produced by Powder Metallurgy. By LAURENCE DELISLE and AARON FINGER. (Metals Tech., Aug. 1946, T.P. 2046) With discussion

INDEX

(NOTE: In this index the names of authors of papers and discussions and of men referred to are printed in SMALL CAPITALS, and the titles of papers in italics.)

A

Anelasticity of metals: bibliography, 186
computation of quasi-static modulus defect associated with changes in equilibrium distribution of carbon atoms-among interstitial positions in ferrite, 185

computation of relaxation strengths, thermal, concentration or magnetic, 185

definition, 155

effects, examples: elastic after-effects, 156 frequency variation of elastic moduli, 157 internal friction, 157, 190

elastic after-effects: definition, 155

in iron wires: cold-worked between 20° and 100°C., 195

fully annealed between 250° and 550°C., 211

strained rods and wires, 218
manifestations reported in literature, 155

mathematical formulation: Boltzmann's theory,

relaxation spectrum, 157

physical origins: relaxation centers: grain boundaries, 164, 219

relaxation centers: intra-specimen diffusion, 168

relaxation centers: lattice position, 173
relaxation centers: slip bands, 161, 219
relaxation centers: theories, 160
potential importance, 180

ARCHER, R. S.: Discussion on Hot-working, 782 Austenite. See Steel.

AUSTIN, J. B.: Discussion on Some Factors Affecting Edgewise Growth of Pearlite, 417

B

BARRETT, C. S.: Discussions: on Anelasticity of Metals, 191

on Orientation Changes during Recrystallization in Silicon Ferrite, 371

Battelle Memorial Institute: study of relationship between transformation of steel at constant temperature and transformation during cooling, 442

Bever, M. B.: Discussion on Gaseous Reduction of Magnetite Ore to Sponge Iron, 277

BEVER, M. B., FLOE, C. F. and LIANG, H.: Solubility of Hydrogen in Molten Iron-silicon Alloys, 395; discussion, 404

BINDER, W. O.: Discussion on Hot-working, 780

Blast-furnace process: iron: arrangement of material in furnace, 18

basic features, 17

control: gas flow, 24

larger furnaces not needed, 29 major obstacles, 17

permeability needed in area between walls and center, 22

potentialities of beneficiated raw materials, 35

temperature variations, 23, 34 gas distribution to fit raw materials, 20

gas velocity at various planes, 20 Borax: deoxidizer for low-carbon steels, 106

Boron: alloying element in steel: equilibrium with oxygen, 93

Boss, G. H.: Discussion on Hot-working, 786

Brandt, W. H.: Some Factors Affecting Edgewise Growth of Pearlite, 405; discussion, 417, 418 Discussion on Kinetics of the Decomposition of Austenite, 585

Brooks, W. B.: Discussion on Elastic After-effects in Iron Wires from 20° to 550°C., 220

Brooks, J. G., Kramer, I. R. and Siegel, S.: Factors for the Calculation of Hardenability, 670

BROPHY, G. R. and MILLER, A. J.: An Appraisal of the Pactor Method for Calculating the Hardenability of Steel from Composition. 654; discussion, 668

Bucknall, E. H.: Discussion on Factor Method for Calculating Hardenability of Steel, 665

C

Carnegie-Illinois Steel Corporation: development of a precipitation-hardening stainless steel of the 18-8 type, 313

study of hardenability effects in relation to percentage of martensite, 502

study of relationship between hardenability and percentage of martensite in some lowalloy steels, 627

Carnegie Institute of Technology: study of the boronoxygen equilibrium in liquid iron, 93

CASSIDY, P. R.: Discussion on Relationship between Hardenability and Martensite, 640

CHIPMAN, J.: Discussion on The Boron-oxygen Equilibriumin Liquid Iron, 109

CHIPMAN, J. and GRANT, N. J.: Sulphur Equilibria between Liquid Iron and Slags, 134; discussion, 153

CHIPMAN, J. and WINKLER, T. B.: Equilibrium Study of the Distribution of Phosphorus between Liquid Iron and Basic Slags, 111 CHOU, Y. H. and DERGE, G.: Discussion on Solubility of Hydrogen in Molten Iron-silicon Alloys, 404

CLARK, C. L. and Russ, J. J.: A Laboratory Evaluation of Hot-working Characteristics of Metals, 736; discussion, 777, 781, 787

CLARK, H. T. and FEIGENBAUM, S.: A Radiation Pyrometer for Open-hearth Bath Measurements, 80

Climax Molybdenum Co.: determination of most efficient alloy combinations for hardenability, 643

COMSTOCK, G. P.: The Influence of Titanium on the Hardenability of Steel, 719; discussion, 734

Corson, M. G.: Discussion on Anelasticity of Metals, 189

CRAFTS. W.: Discussions: on Factor Method for Calculating Hardenability of Steel, 663 on The Hardenability Concept, 612

on Most Efficient Alloy Combinations for Hardenability, 652

CRAFTS, W. and LAMONT, J. L.: Addition Method for Calculating Rockwell C Hardness of the Jominy Hardenability Test, 698; discussion, 718

Discussion on Relationship between Hardenability and Martensite, 639

Crucibles: rotating liquid, 93

CRUSSARD, C.: Discussions: on Hol-working, 785 on Kinetics of the Decomposition of Austenite, 590

D

DARKEN, L. S.: Discussion on Equilibrium Relations and Phase Boundaries in Medium-alloy Steels, 546

Derge, G.: The Boron-oxygen Equilibrium in Liquid Iron, 93; discussion, 109

Discussion on Sulphur Equilibria between Liquid Iron and Slags, 152

Derge, G. and Chou, Y. H.: Discussion on Solubility of Hydrogen in Molten Iron-silicon Alloys, 404

DEVRIES, G.: Discussions: On The Influence of Titanium on the Hardenability of Steel, 733

on Relationship between Hardenability and Martensite, 641

DUNN, C. G.: Effect of Original Orientation on Orientation Changes during Recrystallization in Silicon Ferrite, 357; discussion, 371

Some Aspects of Crystal Recovery in Silicon. Ferrite Following Plastic Strains, 373

E

Elastic after-effects. See Anelasticity. EMERICK, H. B.: Discussion on Hot-working, 783

I

FEIGENBAUM, S. and CLARK, H. T.: A Radiation Pyrometer for Open-hearth Bath Measurements, 80

FETTERS, K. L.: Disucssion on Hot-working, 781, 784

Fick, N. C. and Rickett, R. L.: Constitution of Commercial Low-carbon Iron-silicon Alloys, 346; discussion, 356

FLOE, C. F., LIANG, H. and BEVER, M. B.: Solubility of Hydrogen in Molten Iron-silicon Alloys, 395; discussion, 404

FOLEY, F. B.: Discussion on Hot-working, 784

G

Gases: use in reducing magnetite ore to sponge iron, 237

General Electric Co.: study of effect of original orientation on orientation changes during recrystallization in silicon ferrite, 357

study of some aspects of crystal recovery in silicon ferrite following plastic strains, 373

GILLETT, H. W.: Discussion on Relationship between Hardenability and Martensite, 640

Globe Steel Tubes Co.: study of effect of various elements on hot-workability of steel, 749

GORR, W. W., SMITH, R. and WYCHE, E. H.: A Precipitation-hardening Stainless Steel; 313; discussion, 343, 345

Grain growth in steel. See Steel.

Grange, R. A.: Discussions: on Anisothermal Decomposition of Austenite, 440

on Transformation at Constant Temperature and during Cooling, 463

Grange, R. A. and Stewart, H. M.: Temperature Range of Martensite Formation, 467; discussion, 498

GRANT, N. J. and CHIPMAN, J.: Sulphur Equilibria between Liquid Iron and Slags, 134; discussion, 153

GROSSMANN, M. A.: Introduction to Symposium on Hardenability, 599

Toughness and Fracture of Hardened Steels, (Howe Lecture), 39

photograph, 38

Discussions: on Factor Method for Calculating Hardenability of Steel, 665

on Factors for the Calculation of Hardenability, 697

on Hardenability Effects in Relation to the Percentage of Martensite, 511

Gurry, R. W.: data on boron effect in steel compared with experimental results of Derge's tests, 103 et seq.

H

HALLEY, J. W.: Grain-growth Inhibitors in Steel, 224; discussion, 236

Hardenability, See Steel.

HASLEM, M. E. and ZAPFFE, C. A.: Test for Hydrogen Embrittlement Applied to Stainless Wire, 281; discussion, 311

HAWKES, M. F.: Discussion on Temperature Range of Martensite Formation, 490

HODGE, J. M. and OREHOSKI, M. A.: Hardenability

Effects in Relation to the Percentage of

Martensite, 502; discussion, 511, 512

Relationship between Hardenability and Percentage of Martensite in Some Low-alloy Steels, 627; discussion, 642 Hollomon, J. H.: Discussion on Temperature Range of Martensite Formation, 491

HOLLOMON, J. H. and JAFFE, L. D.: The Hardenability Concept, 601; discussion, 616

Hardenability and Quench Cracking, 617; discussion, 625

Discussion on Relationship between Hardenability and Martensile, 638

HOLLOMON, J. H., JAFFE, L. D. and NORTON, M. R.:

Anisothermal Decomposition of Austenite,
419: discussion, 441

HOSTETTER, H. E.: Determination of Most Efficient Alloy Combinations for Hardenability, 643; discussion, 653

Hot-working characteristics of metals: application of equicohesive temperature hypothesis, 736, 782, 785

burning, 746, 779

effect of deformation rate on high-temperature properties, 736

hot twist test, 737

measure of strength doubtful, 784

laboratory evaluation, 736

steel: effect of various elements, 749 hot twist test: results, 738, 749

Howe Memorial Lecture: The Blast-furnace Process and Means of Control, 15

Toughness and Fracture of Hardened Steels, 39 Hydrogen; solubility; in iron-silicon alloys, 395

in metals: partial pressure of monatomic hydrogen, 403, 404

in pure iron, 398

Hydrogen embrittlement of steel: definition, 281 factors controlling, 283

planar-pressure theory, 305

plated wire: zinc plating vs. cadmium plating, 308 relation to hardness and electrical resistivity, 304 removal of gas: factors affecting, 299

stainless wire: result of acid pickling: measurement, 292, 310

result of cathodic charging: measurement, 284

single-bend test, 281

tests: comparison, 281

single bend: apparatus, 281 single bend: stainless wire, 281

Ι

Ideal critical diameter: definition, 643

IHRIG, H. K.: The Effect of Various Elements on the Hot-workability of Steel, 749; discussion, 778, 781, 788

International Nickel Co.: appraisal of factor method for calculating hardenability of steel from composition, 654

Iron: liquid: boron-oxygen equilibrium: comparison
of direct determination with that
from thermal data, 103, 108
determining, 93, 107

rotating crucible used in tests, 93

phosphorus distribution between liquid iron and basic slags in open-hearth furnace: equilibrium studies, 111

sulphur equilibria between liquid iron and slags in basic open-hearth furnace, 134 Iron: pure: hydrogen solubility proportional to temperature, 398

sponge. See Sponge Iron.

Iron-carbon alloys (see also Steel):

pure: bainite formation, 565 martensite formation, 570

pearlite formation: kinetics, 561, 593

Iron ore: reduction to sponge iron: gaseous: bibliography, 271

with carbon monoxide, 240, 250, 262, 270 with hydrogen, 237, 246, 252, 269 with various gases, 244, 269, 271

Iron-silicon alloys (see also Steel):

commercial: 0.01-0.03 carbon: constitution diagram, 349

0.05-0.08 carbon: constitution diagram, 347 low-carbon: constitution diagram used in computing diagram of boundaries in Fe-Si-C system, 354

molten: solubility of hydrogen: function of temperature and composition, 395

solubility of hydrogen: industrial experience, 403, 404

J

JAFFE, L. D.: Discussions: on The Influence of Titanium on the Hardenability of Steel, 733 on Temperature Range of Martensite Formation, 493

JAFFE, L. D. and HOLLOMON, J. H.: The Hardenability Concept, 601; discussion, 616

Hardenability and Quench Cracking, 617; discussion, 625

Discussion on Relationship between Hardenability and Martensile, 638

JAFFE, L. D., NORTON, M. R. and HOLLOMON, J. H.:

Anisothermal Decomposition of Austenite,
419; discussion, 441

Jones and Laughlin Steel Corporation: a radiation pyrometer for open-hearth bath measurements, 80

JOSEPH, T. L.: The Blast-furnace Process and Means of Control (Howe Lecture), 15 photograph, 14

K

KLIER, E. P.: Discussion on Kinetics of the Decomposition of Austenite, 591

KRAMER, I. R.: Discussions: on The Hardenability Concept, 613 on Hardenability Effects in Relation to the

Percentage of Martensite, 512

KRAMER, I. R., SIEGEL, S. and BROOKS, J. G.: Factors for the Calculation of Hardenability, 670 KULP, R. K.: Discussion on Hot-working, 787

T

LAMONT, J. L. and CRAFTS, W.: Addition Method for Calculating Rockwell C Hardness of the Jominy Hardenability Test, 698; discussion, 718

Discussion on Relationship between Hardenability and Martensite, 639

LIANG, H., BEVER, M. B. and FLOE, C. F.: Solubility of Hydrogen in Molten Iron-silicon Alloys, 395; discussion, 404

LORIG, C. H. and MANNING, G. K.: Relationship between Transformation at Constant Temperature and during Cooling, 442; discussion, 465, 466

M

MACK, D. J.: Discussion on Test for Hydrogen Embrittlement Applied to Stainless Wire, 310

Magnets: permanent: Vicalloy, 222

Manning, G. K.: Discussion on Anisothermal Decomposition of Austenite, 439

Manning, G. K. and Lorig, C. H.: Relationship between Transformation at Constant Temperature and during Cooling, 442; discussion, 465, 466

Martensite. See Steel.

Massachusetts Institute of Technology: equilibrium study of distribution of phosphorus between liquid iron and basic slags, 111

study of solubility of hydrogen in molten ironsilicon alloys, 395

McDonald, J. C.: Discussion on Elastic After-effects in Iron Wires from 20° to 550°C., 220

MEHL, R. F.: Discussion on Kinetics of the Decomposition of Austenite, 587

MILLER, A. J. and Brophy, G. R.: An Appraisal of the Factor Method for Calculating the Hardenability of Steel from Composition, 654; discussion, 668

N

Naval Research Laboratory: factors for the calculation of hardenability, 670

Nehrenberg, A. E.: Discussion on Temperature Range of Martensite Formation, 494

NESBITT, E. A.: Vicalloy-a Workable Alloy for Permanent Magnets (abstract), 222

Norris, F. G.: Discussion on The Boron-oxygen Equilibrium in Liquid Iron, 108

NORTON, M. R., HOLLOMON, J. H. and JAFFE, L. D.: Anisothermal Decomposition of Austenite, 419; discussion, 441

0

Open-hearth practice: temperature measurements: bath: pyrometers: radiation, 80 pyrometers: various, 80

Open-hearth process: basic: phosphorus distribution between liquid iron and slags: equilibrium study, 111 sulphur equilibria between liquid iron and

slags, 134

OREHOSKI, M. A. and Hodge, J. M.: Hardenability

Effects in Relation to the Percentage of

Martensite, 502; discussion, 511, 512

Relationship between Hardenability and Percentage of Martensite in Some Low-alloy Steels, 627; discussion, 642

p

Pearlite. See Steel.

Phosphorus: distribution between liquid iron and basic slags in open-hearth furnace: equilibrium studies, 111

Planar-pressure theory of hydrogen embrittlement, 305

Plastic deformation: silicon ferrite. See Steel. 7
PREUSCH, C. D.: Discussion on Hot-working, 786

Pyrometer: radiation: open-end tube, immersion:

construction, 83 development, 82 operation, 87 principle, 81

open-hearth bath measurements, 80

R

Rasorite: deoxidizer for low-carbon steels, 106

READ, T. A.: Discussion on Anelasticity of Metals, 190
RICKETT, R. L. and FICK, N. C.: Constitution of Commercial Low-carbon Iron-silicon Alloys,
346; discussion, 356

ROSENBERG, S. J.: Discussion on Test for Hydrogen Embrittlement Applied to Stainless Wire, 308

Russ, J. J. and Clark, C. L.: A Laboratory Evaluation of Hot-working Characteristics of Metals, 736; discussion, 777, 781, 787

S

Schaefer, A. O.: Discussion on Hot-working, 779 Schmucker, R. A. Jr.: Discussion on The Hardenability Concept, 614

Schwartz, H. A.: Discussion on Solubility of Hydrogen in Molten Iron-silicon Alloys, 403

SIEGEL, S., BROOKS, J. G. and KRAMER, I. R.: Factors for the Calculation of Hardenability, 670

Silicon ferrite. See Steel.

Sims, C. E.: Discussion on Grain-growth Inhibitors in Steel, 235

SKAPSKI, A.: Discussions: on Anelasticity of Metals. . . . 190

on Elastic After-effects in Iron Wires from 20° to 550°C., 219

on Grain-growth Inhibitors in Steel, 235

on Sulphur Equilibria between Liquid Iron and Slags, 150, 152

on Temperature Range of Martensite Formation, 491

Smelting: iron: process: basic features, 17

SMITH, R., WYCHE, E. H. and GORR, W. W.: A Precipitation-hardening Stainless Steel, 313; discussion, 343, 345

Soler, G.: Discussion on Sulphur Equilibria between Liquid Iron and Slags, 152

SOUTHARD, J. C.: Discussion on The Boron-oxygen Equilibrium in Liquid Iron, 108

Specht, O. G., Jr. and Zapffe, C. A.: Low-temperature Gaseous Reduction of Magnetite Ore to Sponge Iron, 237; discussion, 280

Sponge iron: made by low-temperature gaseous reduction of magnetite ore, 237 Steel (See also Iron-silicon Alloys): austenite decomposition: anisothermal: definition, 419 anisothermal: two reactions, 423 single reaction, 419 and isothermal relations, 419 isothermal and anisothermal relations, 419 kinetics: effect of alloys, 572, 591, 594 computation of free energy, 579 general principles, 550 progress small, 589 pure iron-carbon system, 561 nature, 601 time - temperature - transformation curves. 576 bainite: formation, 565, 574, 583 grain growth: inhibitors: aluminum series, 224, 227 inhibitors: titanium series, 224, 230 types, 224 zirconium series, 224, 233 hardenability: addition method of calculating Rockwell C hardness of Jominy test, 698 alloy combinations most economical for attaining certain hardnesses, 643 bainitic, 604, 608, 612, 613 calculating from composition: factor method: appraisal, 654 Grossmann method: appraisal, 654 new determination of factor curves: aluminum, 685 carbon, 673 chromium, 688 comparison with earlier curves, 692 copper, 685 elements that form stable carbides, 685 manganese, 684 molybdenum, 688 nickel, 684 silicon, 684 silicon-killed steels vs. aluminumkilled, 680 titanium, acid-soluble and total. 689, 726 vanadium, 689 zirconium, 689 calculating Rockwell C hardness of Jominy test by addition method, 698 carbon series, 502 concept, 601, 616 effect of composition, 602, 610 effect of titanium: dependent on heat-treatment of steel, and on form and amount of titanium present, 719 effect of titanium: fine-grained steels vs. coarse-grained, 723, 733 effects of alloying elements using three percentages of martensite as criteria: manganese, silicon, nickel and molybdenum, Jominy test: Rockwell C hardness: calculating by addition method, 698 low-alloy: relation to percentage of marten-

site, 627

Steel (See also Iron-milicon Alloys): most efficient alloy combinations: cost: new additions, 643, 652 scrap additions, 649, 652 determining, 643 pearlite growth a factor, 405 pearlitic, 603, 608, 612 quench cracking: prevention by control of composition, 617 relation to percentages of martensite, 502 symposium, 599 hot-workability: critical temperature, 746, 778. 781 effect of deoxidation, 754 effect of various elements: carbon, 754 chromium, 762 cobalt.768 columbium, 768 lead, 768 manganese, 755 molybdenum, 768 nickel, 762 nitrogen, 762 phosphorus, 762 proper balance required, 777 selenium, 755 silicon, 762 sulphur, 755 tin, 768 titanium, 768 vanadium, 768 hot twist test, 738 measure of strength doubtful, 784 rapid twist test, 749 hydrogen embrittlement. See Hydrogen Embrittlement. low-carbon: deoxidation with borax-containing minerals technically sound, 106 martensite: effect on hardenability, 502 formation, 570, 574, 590 measurement: dilatometric vs. metallographic method, 468, 491, 499 temperature range: carbon and lowalloy steels, 467 effect of cobalt, 490 effect of undissolved carbides, 479, estimation from steel composition, 480, 490, 498 percentages at different degrees, 486, 493 quench cracking: effect of austenite grain size, 477 relation to hardenability of low-alloy steels, medium alloy: equilibrium relations: computing: rapid method, 513 pearlite: edgewise growth: calculations: nomenclature, 405, 417 effect of alloying elements, 413 effect of carbon content, 413 extrapolations of ferrite and cementite solubilities, 410 lamellar structure, 408 theory, 406

Steel (See also Iron-silicon Alloy): velocity: calculations: comparison of methods of solution of differential equation and dimensional reasoning, 417 dimensional reasoning, 561, 572, 576 calculations: solution of differential equation, 405 formation, 561, 572, 586 nucleation and growth, 405 phase boundaries: medium alloy, 535, 555 quench cracking: prevention by control of composition, 617 quench-hardened: toughness and fracture: effect of retained austenite, 58 notch-bar impact test, 39 effect of refrigeration of steel, 59 effect of shape of test piece, 40 effect of tempering temperature, 39 factors influencing mode of fracture, 39, 56 ferrite precipitated in grain boundaries, 39, 41 position of weakest plane, 48 scrap: recovery of alloy: cost, 649 silicon. See Iron-silicon Alloys. cold-rolled: recrystallization: effect of original orientation on orientation changes in silicon ferrite, 357 silicon ferrite: cold-rolled: recrystallization: effect of original orientation on orientation changes, 357 theory of high-order twinning, 371 crystal recovery following plastic strains: class 1, removal of dislocations within mosaic blocks, 374 class 2, removal of elastic strains, 374 class 3, removal, etc.; complex lattice type, 379 effect of time and temperature, 388 double lattice type, 377 single-lattice type, 376 class 3, removal of distortions that produce a spread in orientation over regions that are larger than mosaic blocks, 374 effect on rate of growth, 389 precipitation-hardening 18-8 type stainless: (Stainless W): composition, 313, 315 corrosion resistance, 337 development by Carnegie-Illinois Steel Corporation, 313 heat-treatment, 319 metallurgical characteristics, 315 properties, 329 weldability, 340, 344 sulphides: methods of determination, 150 toughness. See Steel, Quench-hardened. transformation: anisothermal decomposition of austenite, 419 at constant temperature: relation to transformation during cooling, 442

cooling tests, 446

during cooling: relation to transformation at

constant temperature, 442

Steel (See also Iron-silicon Alloy): equilibrium relations: history of subject, 587, isokinetic: definition, 420 isothermal: curves, 444 relation to anisothermal decomposition of austenite, 419 kinetics of decomposition of austenite, 550 medium alloy: equilibrium relations: equations: fundamental, 513 equilibrium relations: experiments with alloying elements: chromium, 537 copper, 539 iron-nickel-phosphorus, 545 manganese, 539 molybdenum, 540 nickel, 540 silicon, 541 tungsten, 544 vanadium, 544 welding: titanium recovery, 344 STEWART, H. M. and GRANGE, R. A.: Temperature Range of Martensite Formation, 467; discussion, 498 Sulphur: equilibria between liquid iron and slags in basic open-hearth furnace, 134 TARASOV, L. P.: Discussion on Test for Hydrogen Embrittlement Applied to Stainless Wire. TAYLOR, W. R.: Discussion on Hardenability Effects in Relation to the Percentage of Martensite, 511 THOMAS, R. D., JR: Discussion on A Precipitationhardening Stainless Steel, 344 Timken Roller Bearing Co.: a laboratory evaluation of the hot-working characteristics of

metals, 736

TISDALE, N. F.: Discussion on The Boron-oxygen

Equilibrium in Liquid Iron, 107

Titanium Alloy Manufacturing Co.: study of influ-

ence of titanium on hardenability of steel,
719

Troiano, A. R.: Discussion on Kinetics of the Decomposition of Austenite, 583

U

UDV, M. C.: Discussion on Gaseous Reduction of Magnetite Ore to Sponge Iron, 277

Union Carbide and Carbon Research Laboratories:
addition method for calculating Rockwell
C hardness of the Jominy hardenability
test, 698

University of Minnesota: study of the low-temperature gaseous reduction of magnetite ore to sponge iron, 237

U. S. Bureau of Mines: tests on steel wire plated with cadmium and zinc, for hydrogen embrittlement, 308, 311

U. S. Steel Corporation: study of constitution of lowcarbon iron-silicon alloys, 346

study of the temperature range of martensite formation, 467

1.7

Vicalloy, a workable alloy for permanent magnets, 222

W

- WALTERS, F. M. Jr.: Discussions: on Calculating Rockwell C Hardness of the Jominy Hardenability Test, 718
 - on A Precipitation-hardening Stainless Steel, 343, 344
- Watertown Arsenal Laboratory: study of anelasticity of metals, 155
 - study of equilibrium relations in medium-alloy steels, 513, 535
 - study of hardenability of steel, 601, 617
 - study of kinetics of decomposition of austenite, 550
 - study of relations between isothermal and anisothermal decomposition of austenite,
- Welding steel. See Steel.
- WELLS, C.: Discussion on Hardenability and Quench Cracking, 625
- WEST, W. A.: Elastic After-effects in Iron Wires from 20° to 550°C., 192
- Phase Boundaries in Medium-alloy Steels, 535
- Westinghouse Electric Corporation: study of some factors affecting edgewise growth of pearlite, 405
- WILSON, W.: Discussion on Temperature Range of Martensite Formation, 491

- WINKLER, T. B. and CHIPMAN, J.: Equilibrium Study of the Distribution of Phosphorus between Liquid Iron and Basic Slags, 111
- Wyche, E. H., Smith, R. and Gorr, W. W.: A Precipitation-hardening Stainless Steel, 313; discussion, 343, 345

Z

- ZAPFFE, C. A.: Discussion on Solubility of Hydrogen in Molten Iron-silicon Alloys, 403
- ZAPFFE, C. A. and HASLEM, M. E.: Test for Hydrogen Embrittlement Applied to Stainless Wire, 281; discussion, 311
- Zapffe, C. A. and Specht, O. G. Jr.: Low-temperature Gaseous Reduction of Magnetite Ore to Sponge Iron, 237; discussion, 280
- ZENER, C.: Anelasticity of Metals, 155; discussion, 191 Equilibrium Relations in Medium-alloy Steels, 513; discussion, 548
 - Kinetics of the Decomposition of Austenite, 550; discussion, 592
 - Discussions: on Constitution of Commercial Lowcarbon Iron-silicon Alloys, 354
 - on Elastic After-effects in Iron Wires from 20° to 550°C., 220
 - on Some Factors Affecting Edgewise Growth of Pearlite, 417
 - on Temperature Range of Martensite Formation, 490
 - on Transformation at Constant Temperature and during Cooling, 465